Appendix A Additional Rheological Data for Vibrated Concrete

Additional rheological data was taken on concrete during vibration. The following experiment was performed on a high-flow concrete, design detailed in Table A.3, notably with water-to-cementitious ratio (by mass) of 0.30 and 8.0 fl. oz. of high-range water reducing (superplasticizing) chemical admixture added per every 100 lb. of cement. The slump of this high-flow concrete exceeds 8 inches, and it has a nominal spread of 20 inches or greater (pursuant to ASTM C1611). Again, the rheological properties are measured using the ICAR rheometer.

Table A-1: High-Flow Concrete Mix Design

Type III Portland Cement	718 lb per cubic yard
#7 Aggregate	2085 lb per cubic yard
#2 Sand	1257 lb per cubic yard
Water	216 lb per cubic yard
Sika Air Entraining Admixture 14	1.5 fl. oz/ 100 lb cementitious
Sika Viscocrete 2100 High Range Water Reducer	8.0 fl. oz/ 100 lb cementitious

The rheology is detailed in Figure A.19, where it is demonstrated that vibration reduces (and perhaps eliminates) the yield stress of concrete. From the unvibrated data, the yield stress is 604 Pa. The plastic viscosity is 67 Pa.s. During vibration, the low shear viscosity is 1252 Pa.s.

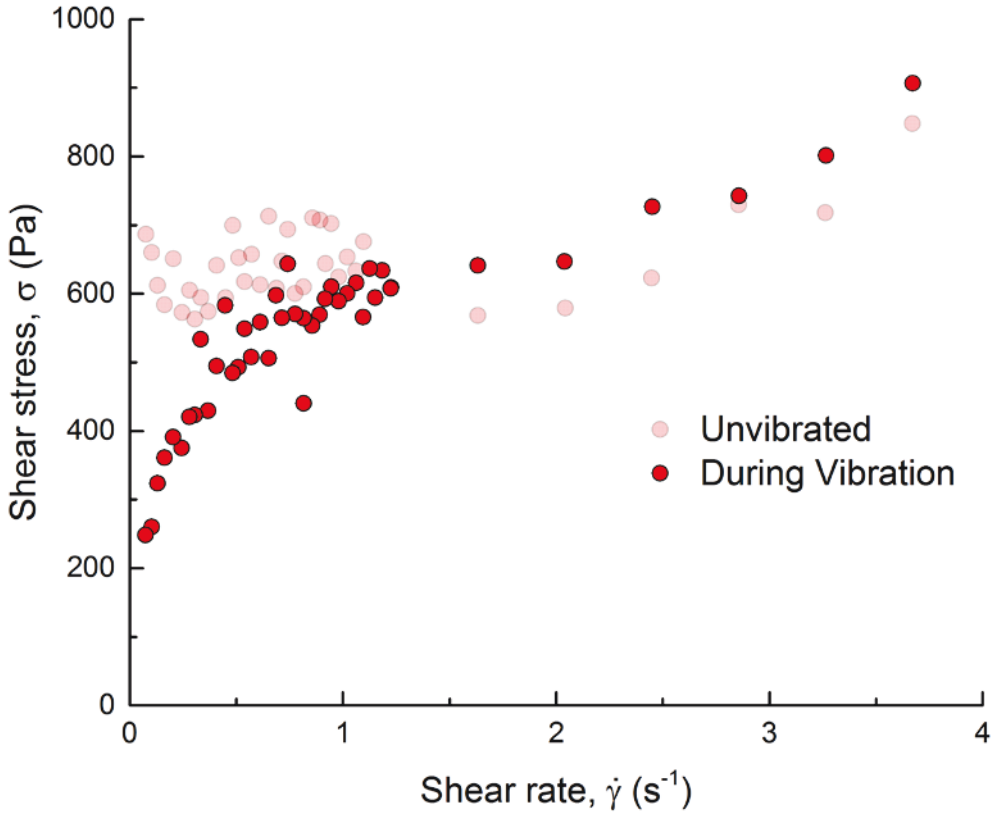

Figure A-1 Rheological measurements of a high-flow concrete, demonstrating a reduction/elimination of yield stress during vibration

Appendix B Measured and Predicted Temperature and Relative Humidity of Internally Instrumented Concrete Crossties, Model Crossties, and Beams

Observed weather in Rantoul, IL

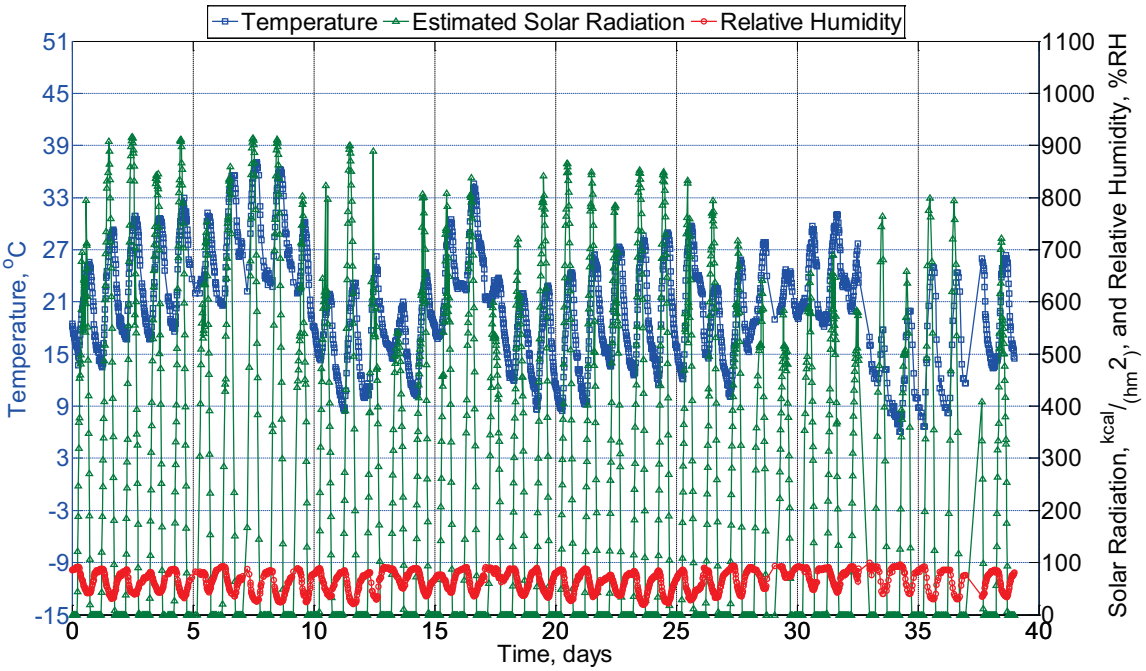

Figure B-1 Temperature and relative humidity collected from weather station KTIP in Rantoul, IL, from September 4, 2013, through October 10, 2013. Solar radiation is estimated over this same timeframe.

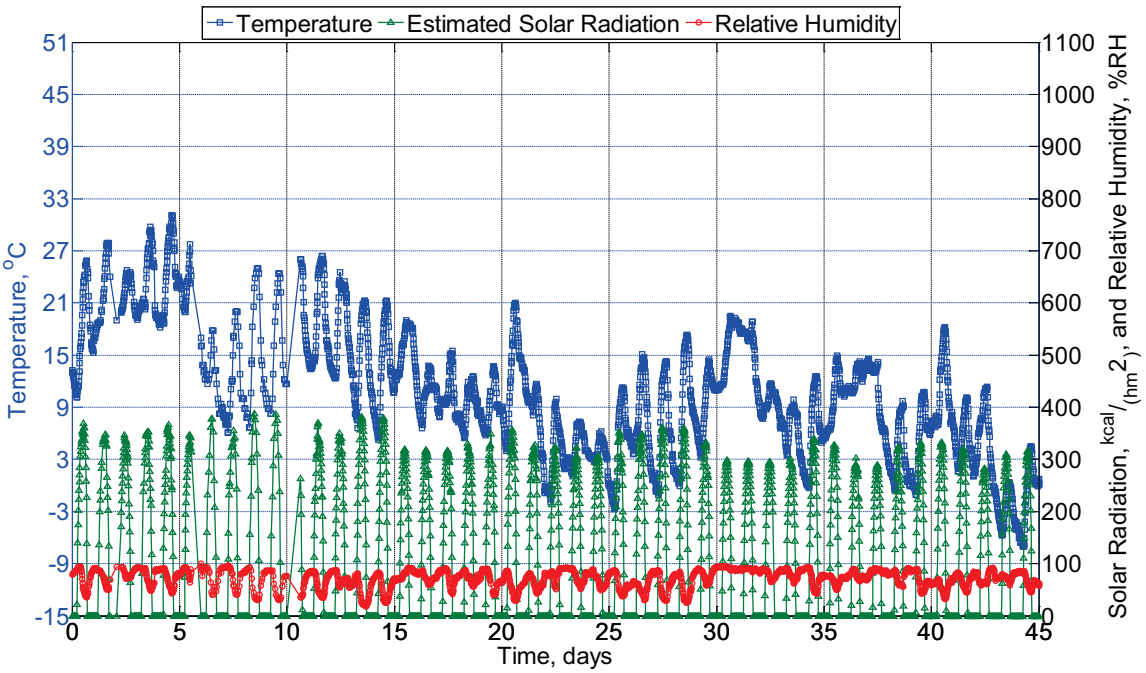

Figure B-2 Temperature and relative humidity collected from weather station KTIP in Rantoul, IL, from October 1, 2013, through November 12, 2013. Solar radiation is estimated over this same timeframe.

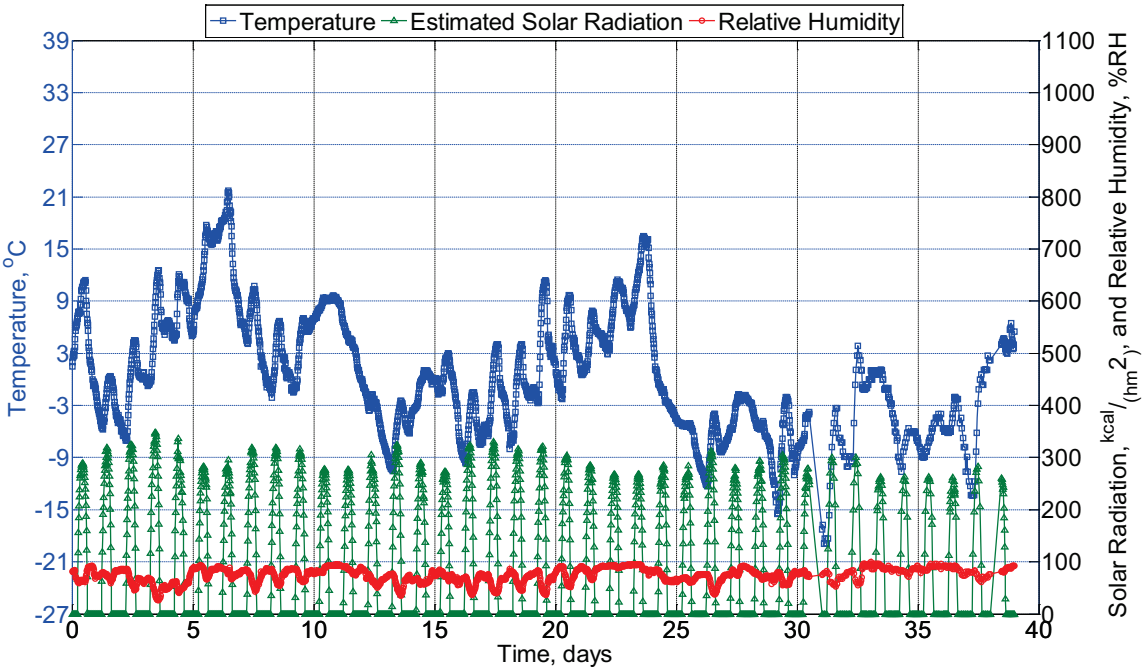

Figure B-3 Temperature and relative humidity collected from weather station KTIP in

Rantoul, IL, from November 12, 2013, through December 18, 2013. Solar radiation is estimated over this same timeframe.

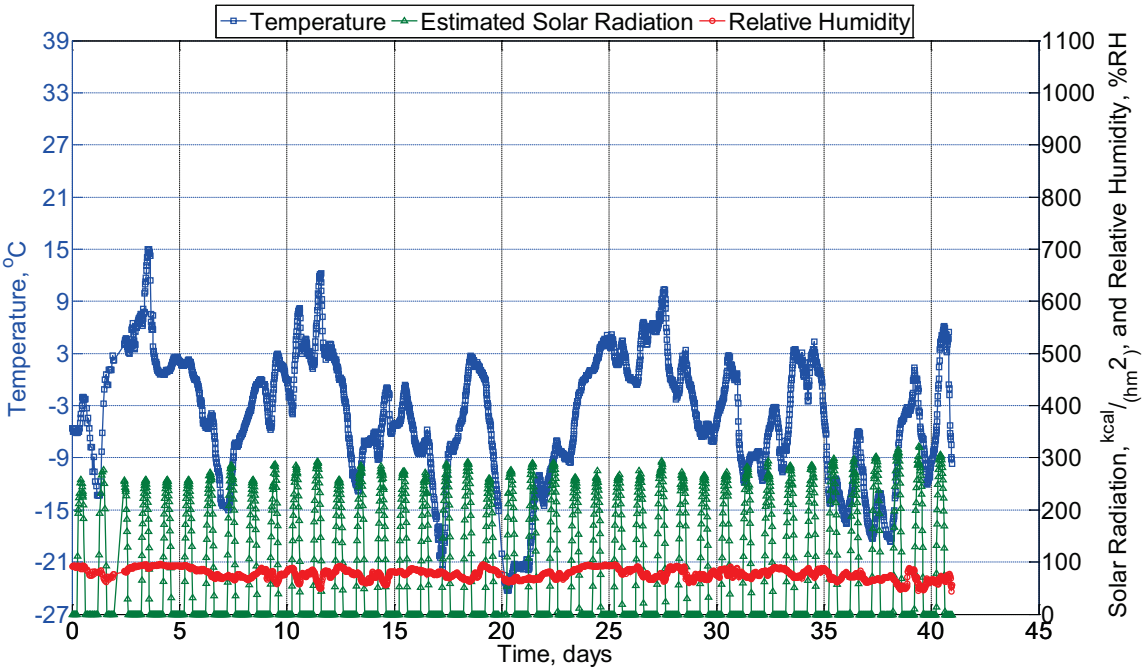

Figure B-4 Temperature and relative humidity collected from weather station KTIP in Rantoul, IL, from December 18, 2013, through January 25, 2014. Solar radiation is estimated over this same timeframe.

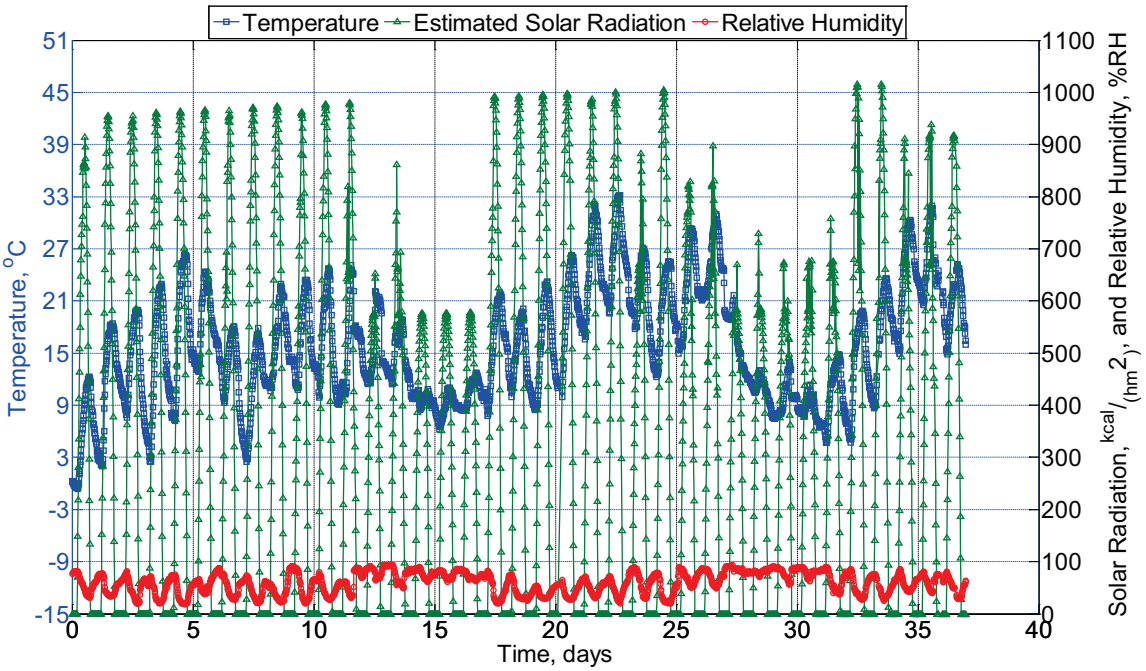

Figure B-5 Temperature and relative humidity collected from weather station KTIP in Rantoul, IL, from April 17, 2014, through May 21, 2014. Solar radiation is estimated over this same timeframe.

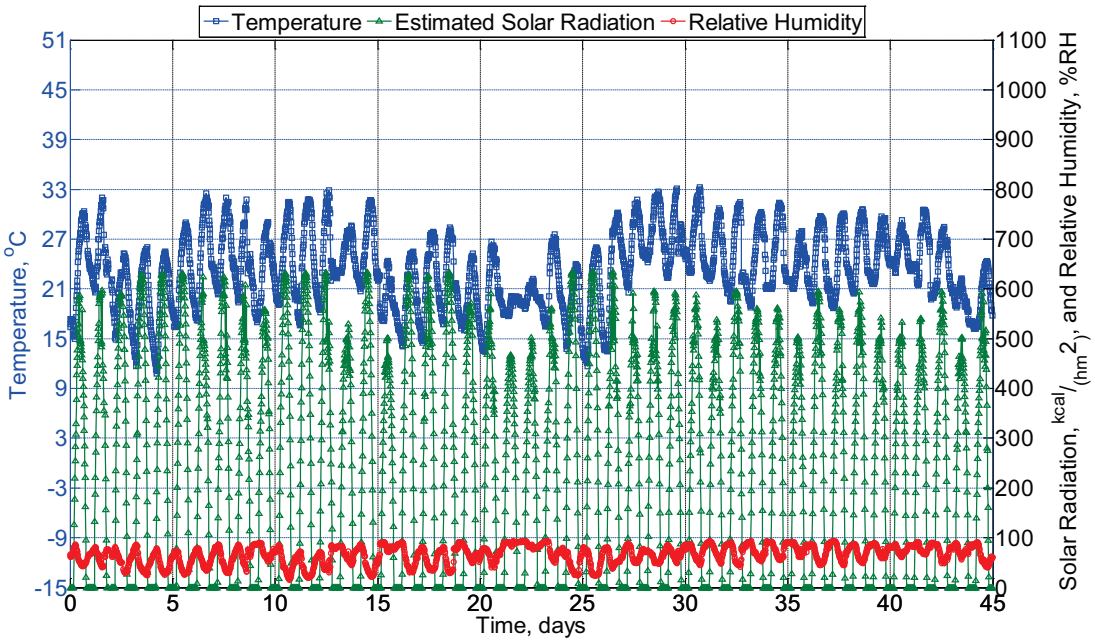

Figure B-6 Temperature and relative humidity collected from weather station KTIP in Rantoul, IL, from May 21, 2014, through July 28, 2014. Solar radiation is estimated over this same timeframe.

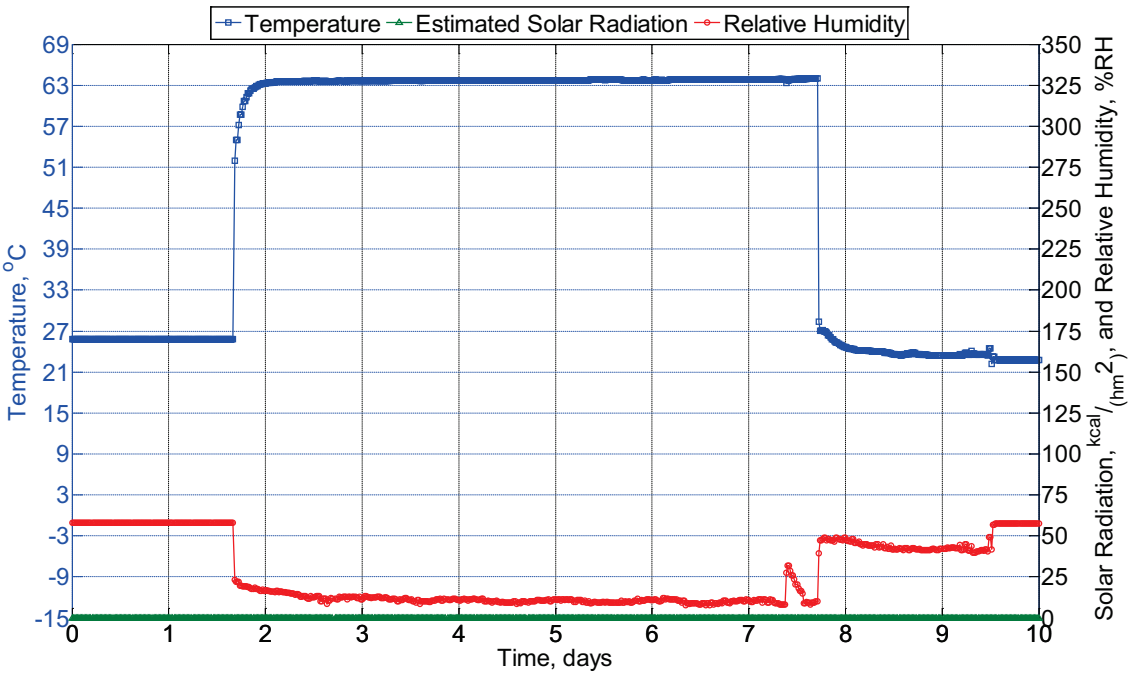

Figure B-7 Temperature and relative humidity applied to three concrete modulus of rupture beams from June 24, 2014, through July 2, 2014, inside an environmentally controlled room (50% RH, 23ºC) and a heating oven (65ºC). No solar radiation is estimated over this same timeframe.

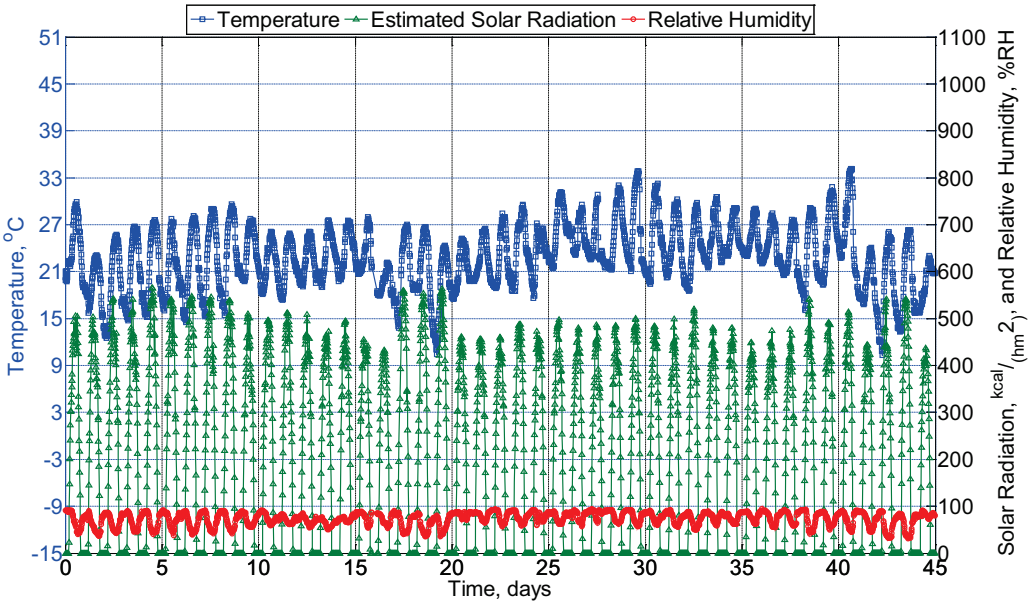

Figure B-8 Temperature and relative humidity collected from weather station KTIP in Rantoul, IL, from July 28, 2014, through September 8, 2014. Solar radiation is estimated over this same timeframe.

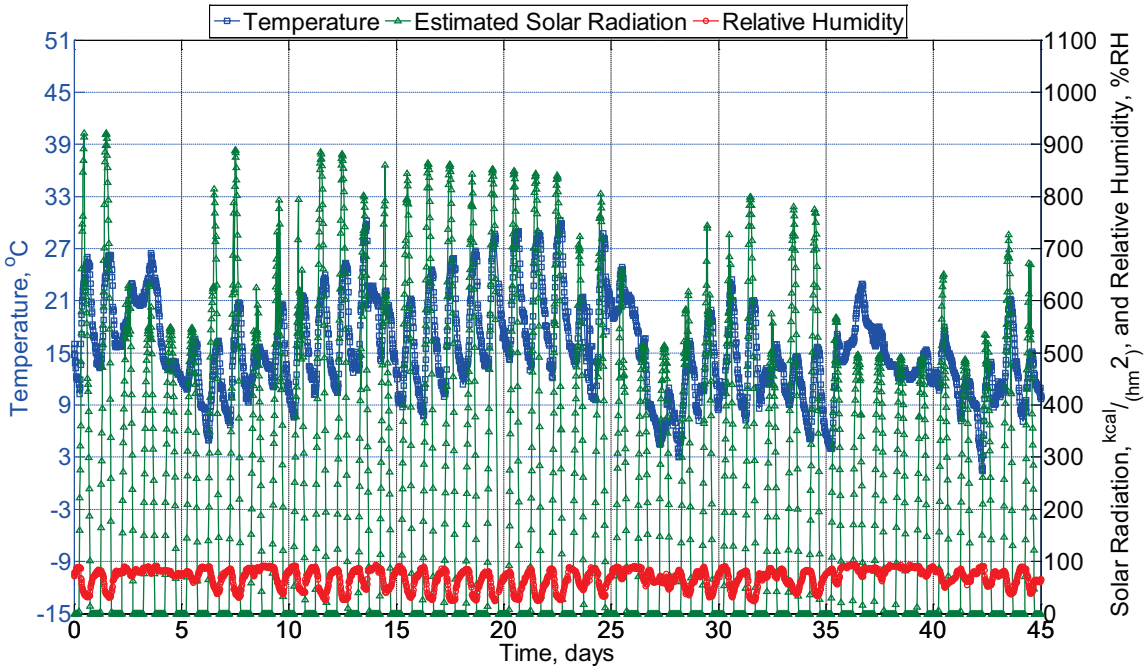

Figure B-9 Temperature and relative humidity collected from weather station KTIP in Rantoul, IL, from September 8, 2014, through October 20, 2014. Solar radiation is estimated over this same timeframe.

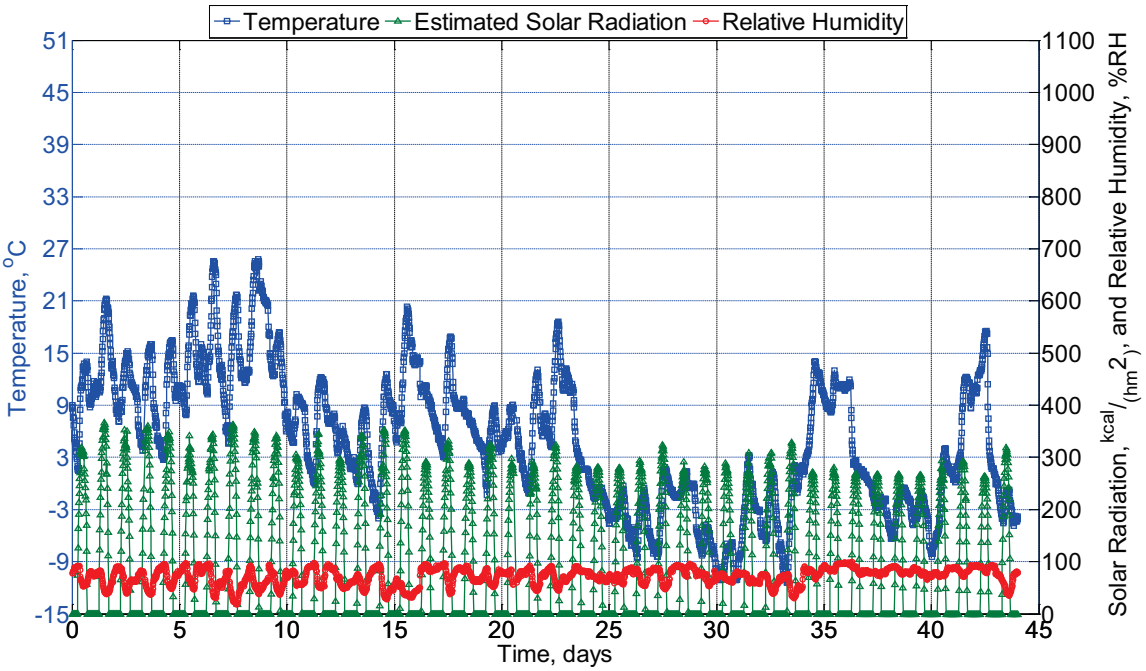

Figure B-10 Temperature and relative humidity collected from weather station KTIP in Rantoul, IL, from October 19, 2014, through November 30, 2014. Solar radiation is estimated over this same timeframe.

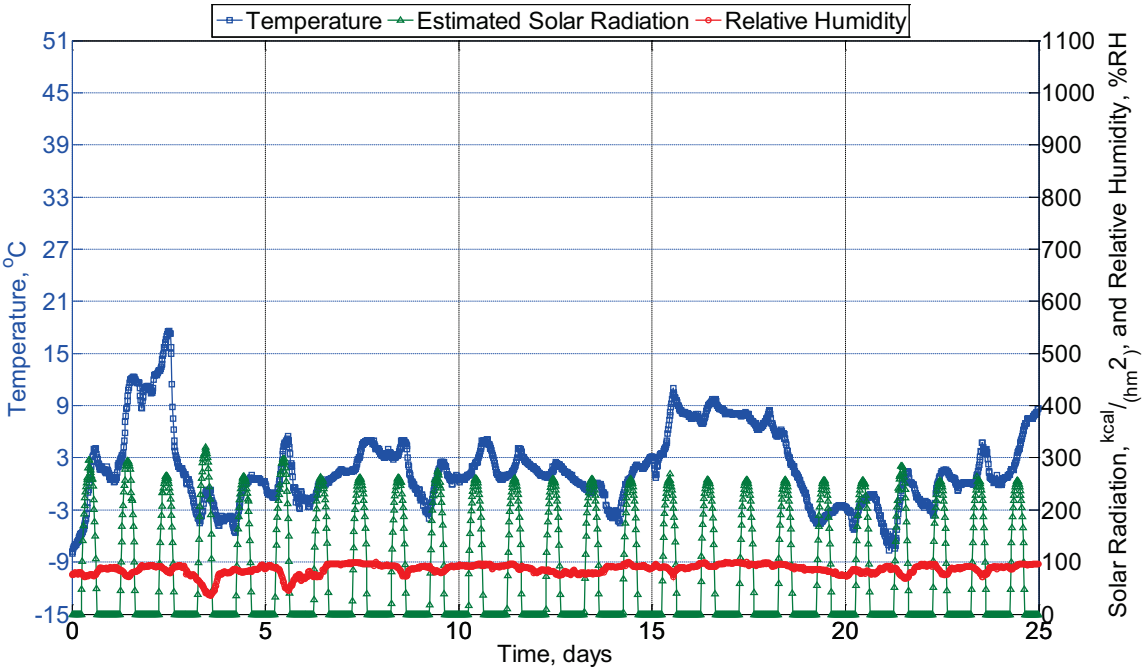

Figure B-11 Temperature and relative humidity collected from weather station KTIP in Rantoul, IL, from November 30, 2014, through December 21, 2014. Solar radiation is estimated over this same timeframe.

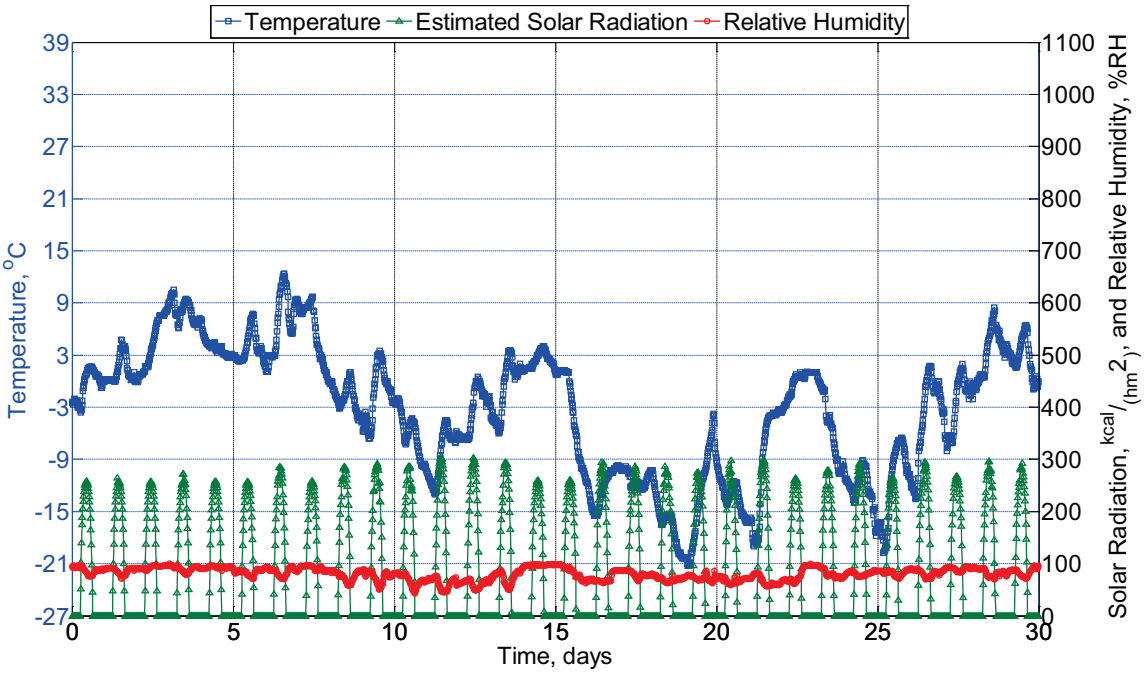

Figure B-12 Temperature and relative humidity collected from weather station KTIP in Rantoul, IL, from December 21, 2014, through January 17, 2015. Solar radiation is estimated over this same timeframe.

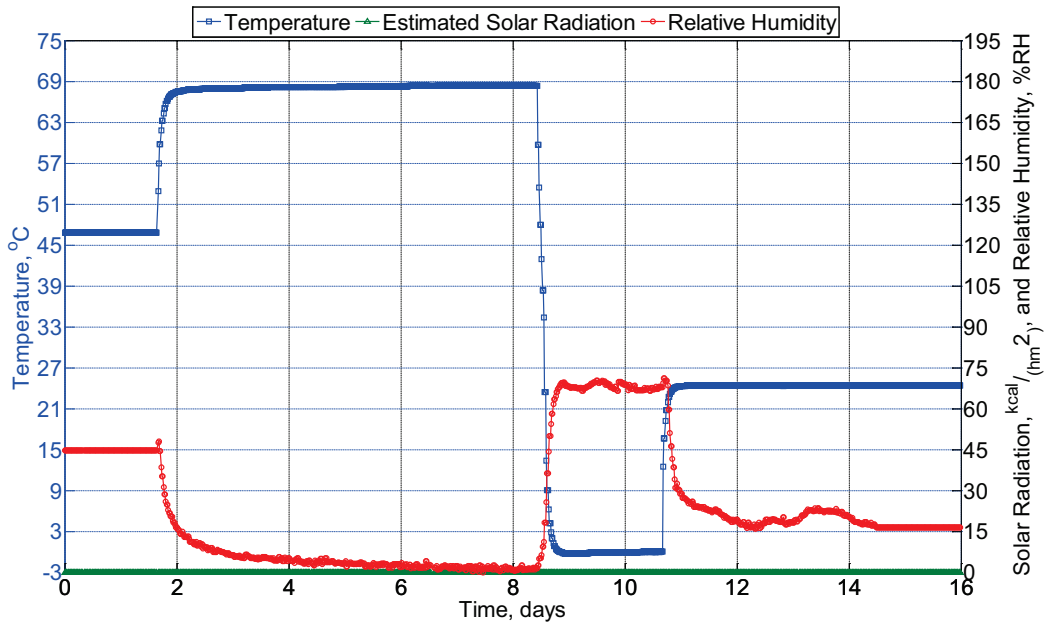

Figure B-13 Temperature and relative humidity applied to three concrete modulus of rupture beams from January 17, 2015, through January 30, 2015, inside a heating oven (65 ºC and 0 ºC) and an environmentally controlled room (50% RH, 23 ºC). No solar radiation is estimated over this same timeframe.

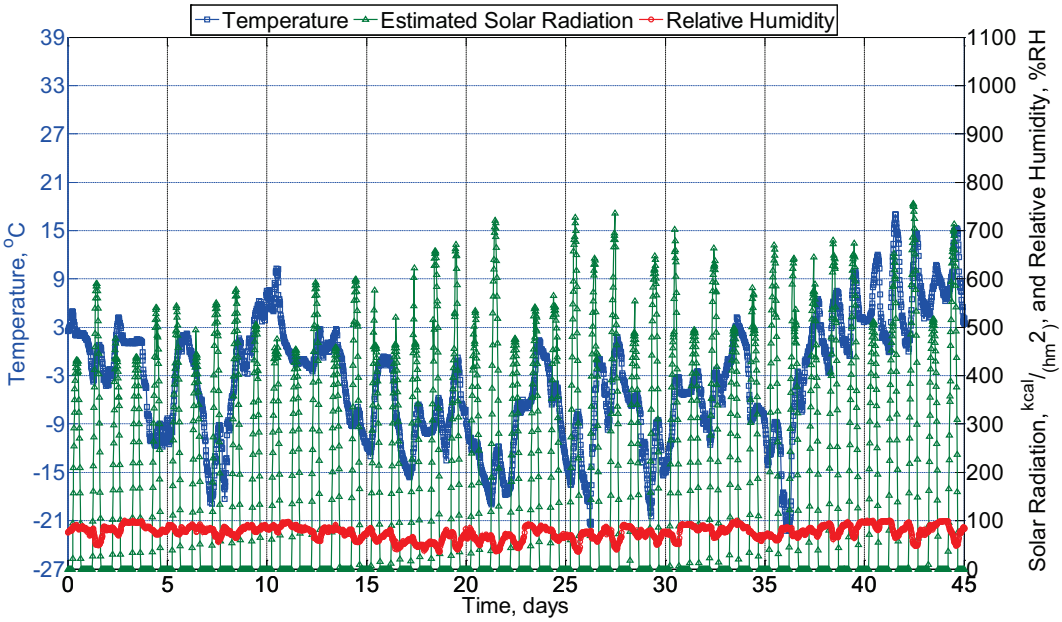

Figure B-14 Temperature and relative humidity collected from weather station KTIP in Rantoul, IL, from January 30, 2015, through March 14, 2015. Solar radiation is estimated over this same timeframe.

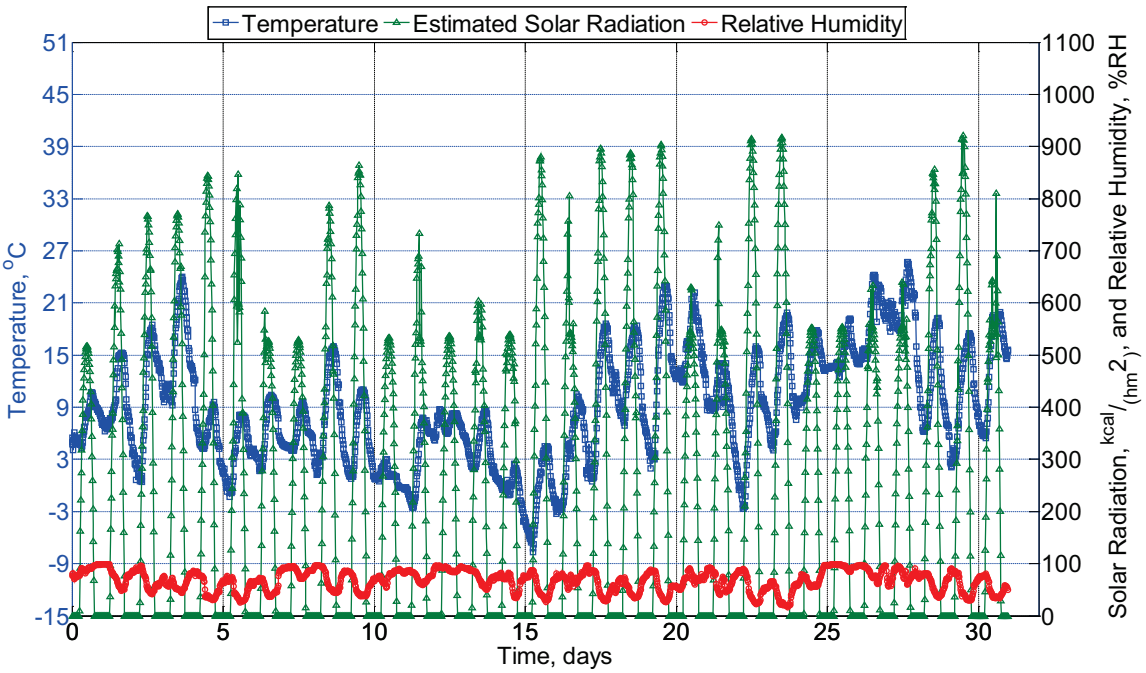

Figure B-15 Temperature and relative humidity collected from weather station KTIP in Rantoul, IL, from March 14, 2015, through April 11, 2015. Solar radiation is estimated over this same timeframe.

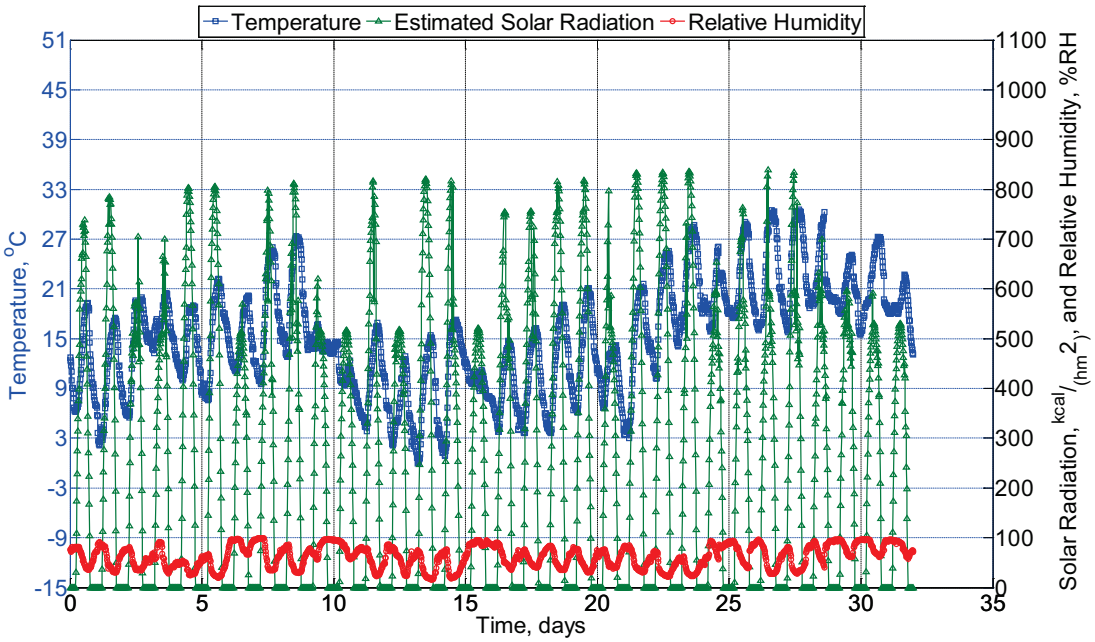

Figure B-16 Temperature and relative humidity collected from weather station KTIP in Rantoul, IL, from April 11, 2015, through May 10, 2015. Solar radiation is estimated over this same timeframe.

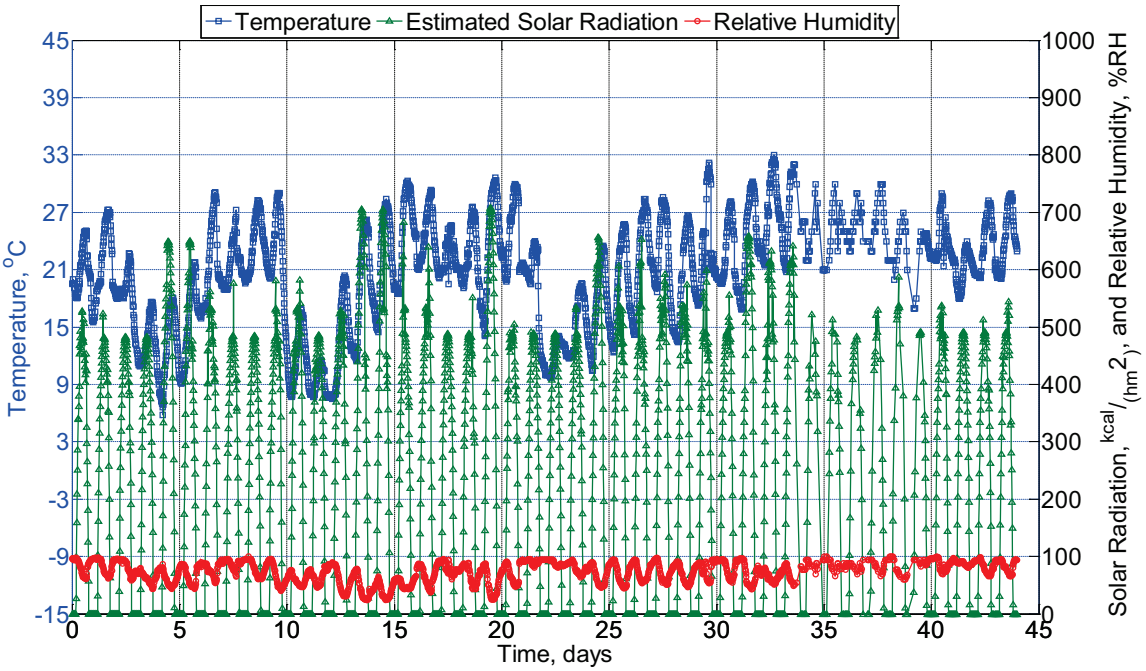

Figure B-17 Temperature and relative humidity collected from weather station KTIP in Rantoul, IL, from May 10, 2015, through June 20, 2015. Solar radiation is estimated over this same timeframe.

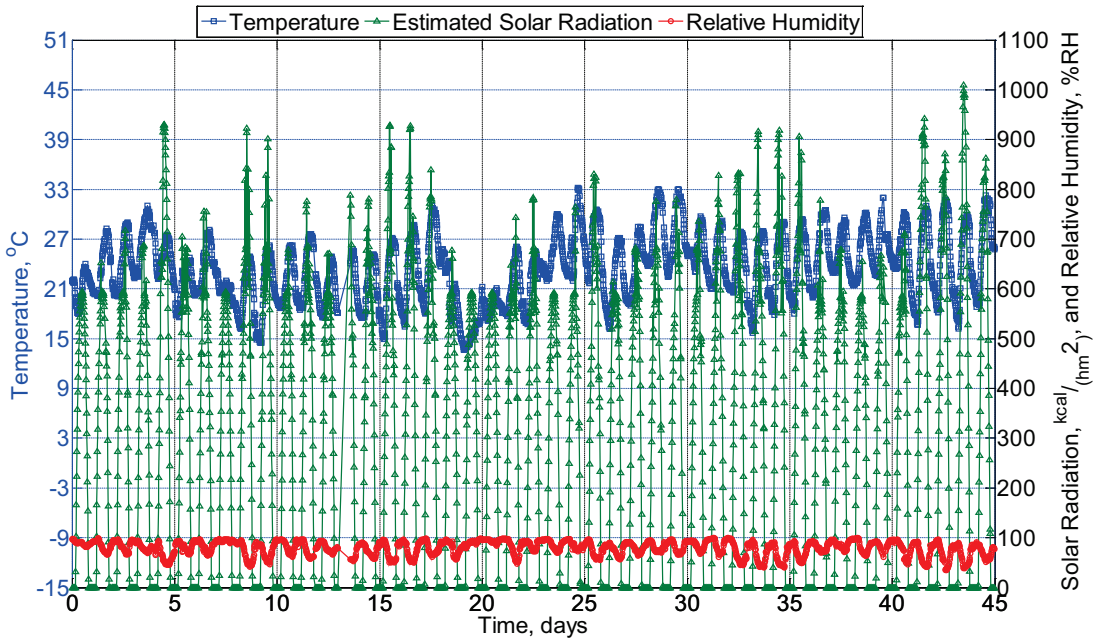

Figure B-18 Temperature and relative humidity collected from weather station KTIP in Rantoul, IL, from June 20, 2015, through August 1, 2015. Solar radiation is estimated over this same timeframe.

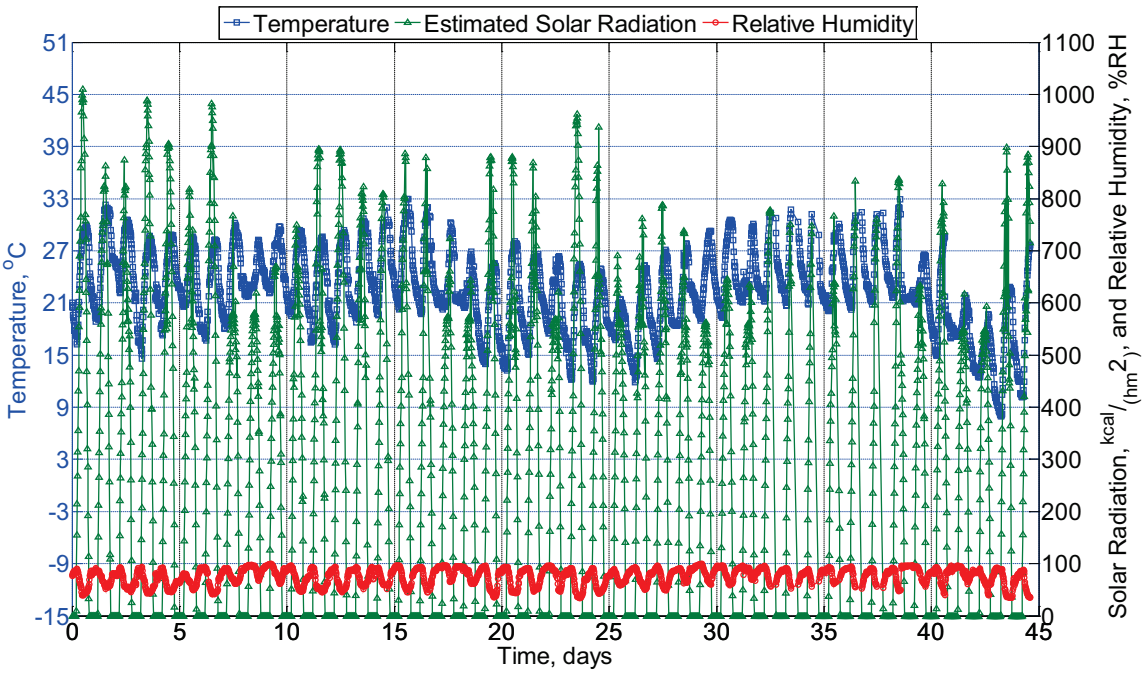

Figure B-19 Temperature and relative humidity collected from weather station KTIP in Rantoul, IL, from August 1, 2015, through September 13, 2015. Solar radiation is estimated over this same timeframe.

Observed weather in Lytton, BC

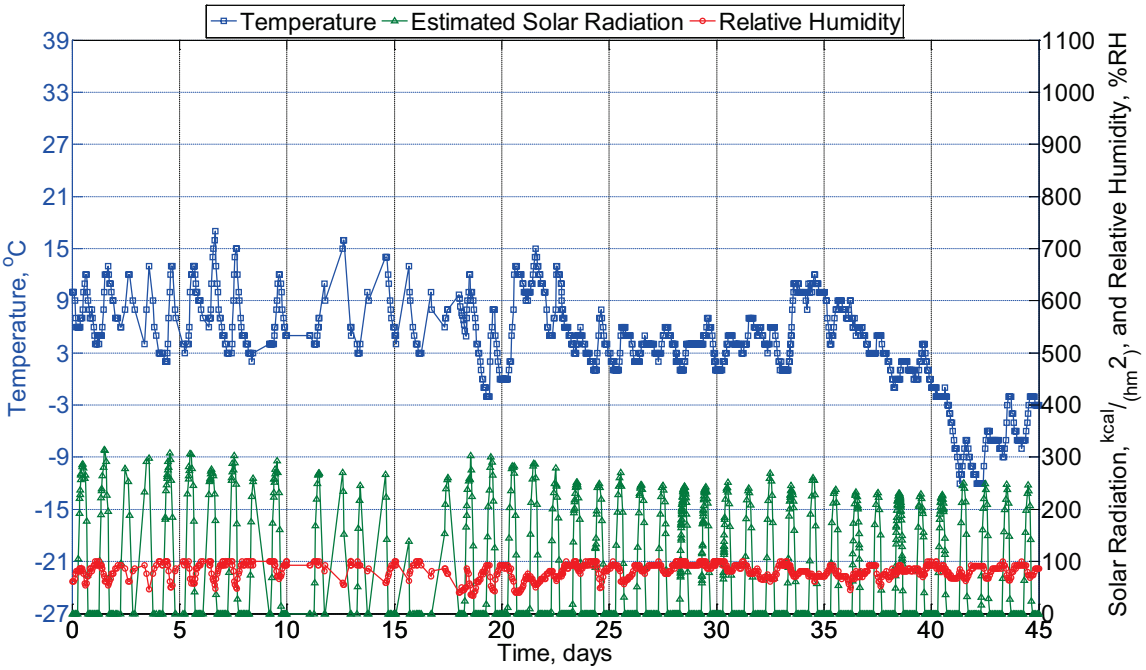

Figure B-20 Temperature and relative humidity collected from weather station CWLY in Lytton, BC, from October 11, 2013, through November 22, 2013. Solar radiation is estimated over this same timeframe.

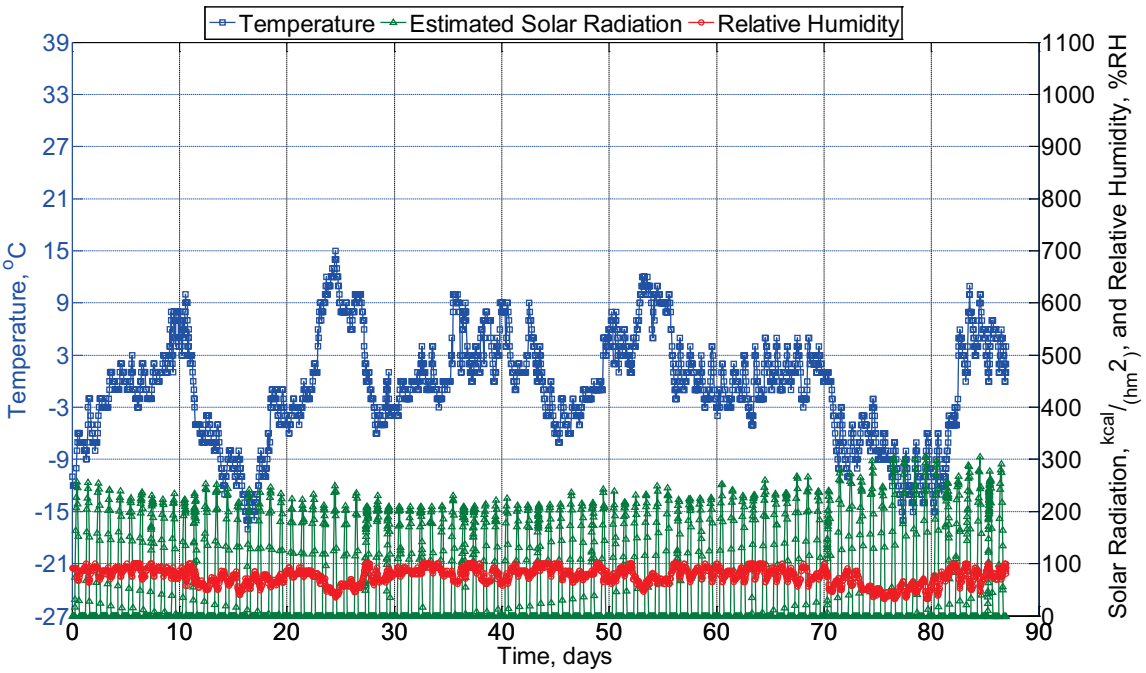

Figure B-21 Temperature and relative humidity collected from weather station CWLY in Lytton, BC, from November 22, 2013, through February 14, 2014. Solar radiation is estimated over this same timeframe.

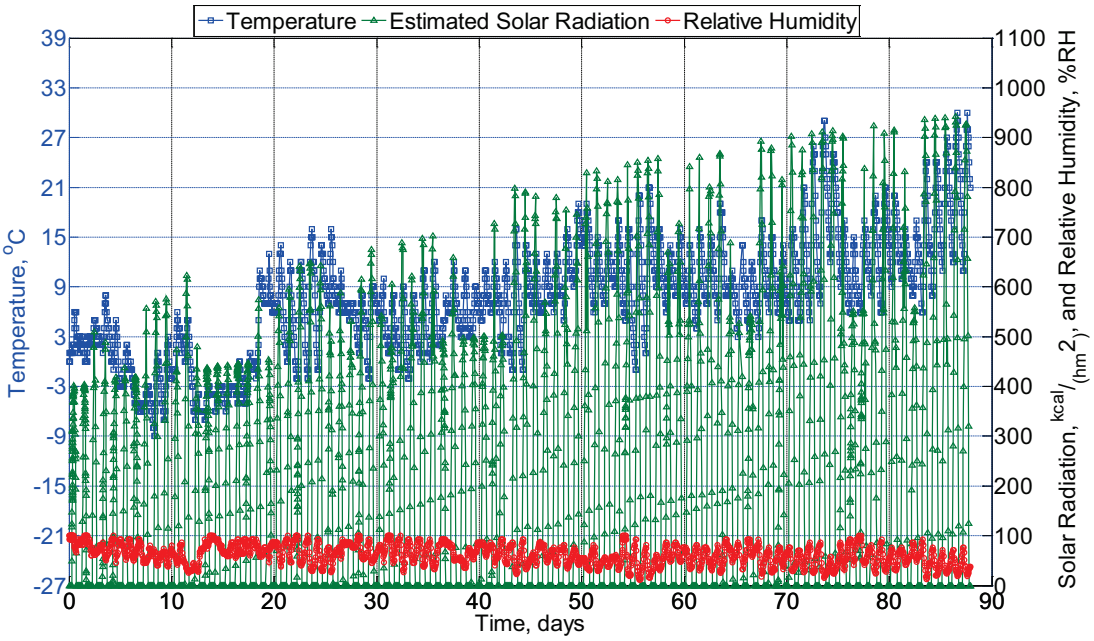

Figure B-22 Temperature and relative humidity collected from weather station CWLY in Lytton, BC, from February 18, 2014, through May 14, 2014. Solar radiation is estimated over this same timeframe.

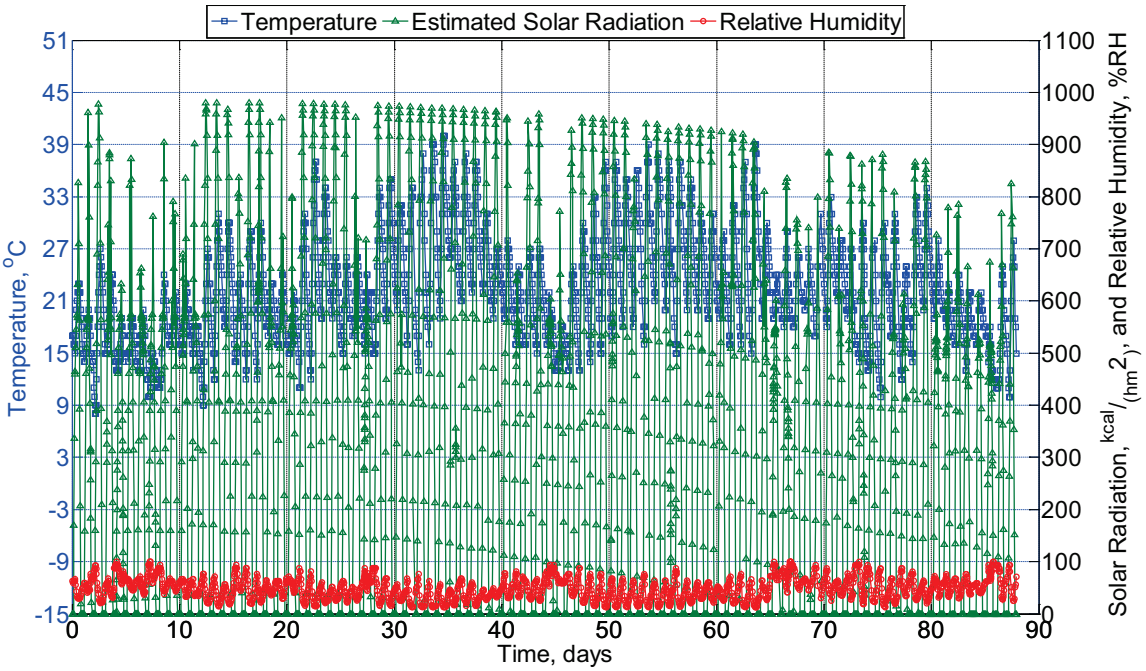

Figure B-23 Temperature and relative humidity collected from weather station CWLY in Lytton, BC, from June 10, 2014, through September 3, 2014. Solar radiation is estimated over this same timeframe.

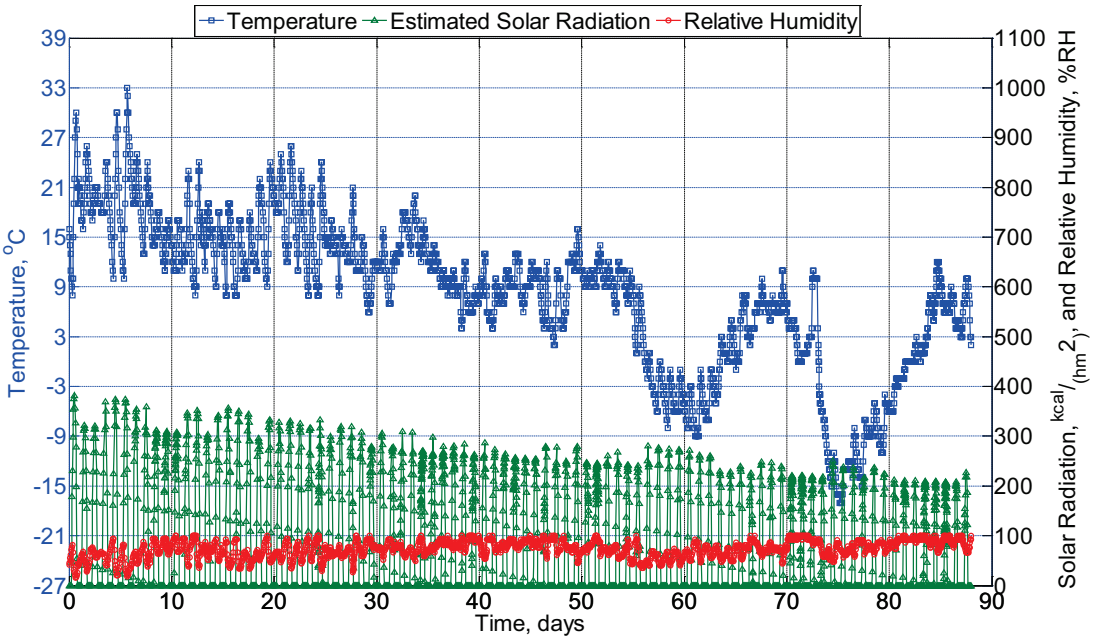

Figure B-24 Temperature and relative humidity collected from weather station CWLY in Lytton, BC, from September 17, 2014, through December 11, 2014. Solar radiation is estimated over this same timeframe.

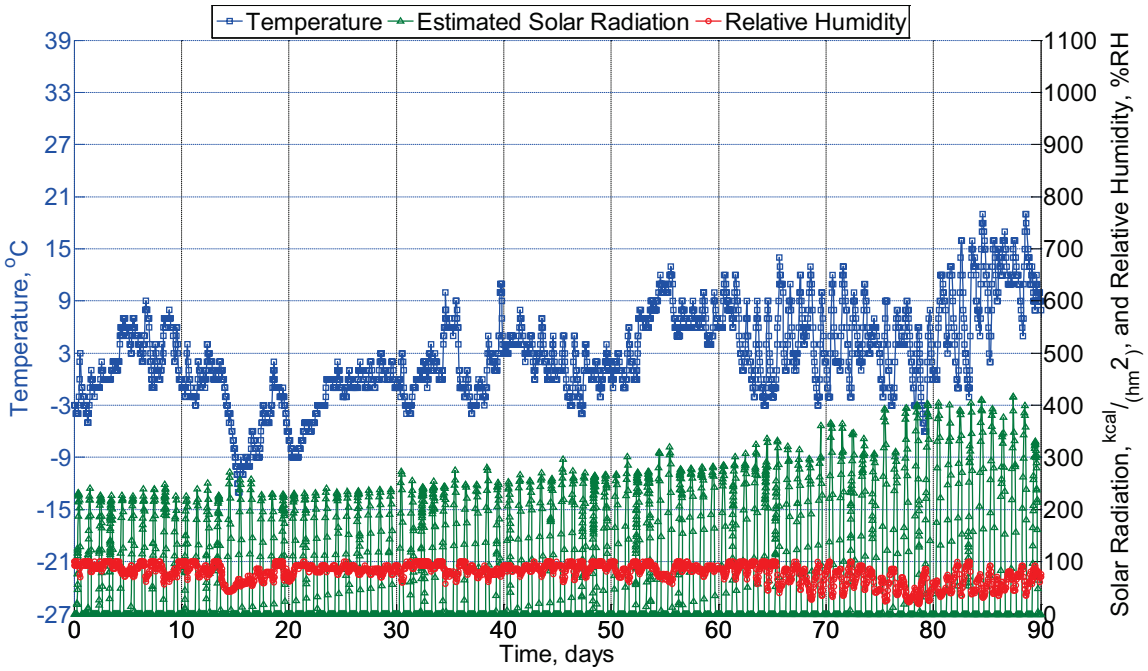

Figure B-25 Temperature and relative humidity collected from weather station CWLY in Lytton, BC, from December 16, 2014, through March 11, 2015. Solar radiation is estimated over this same timeframe.

Measured and predicted internal relative humidity of instrumented modulus of rupture beams

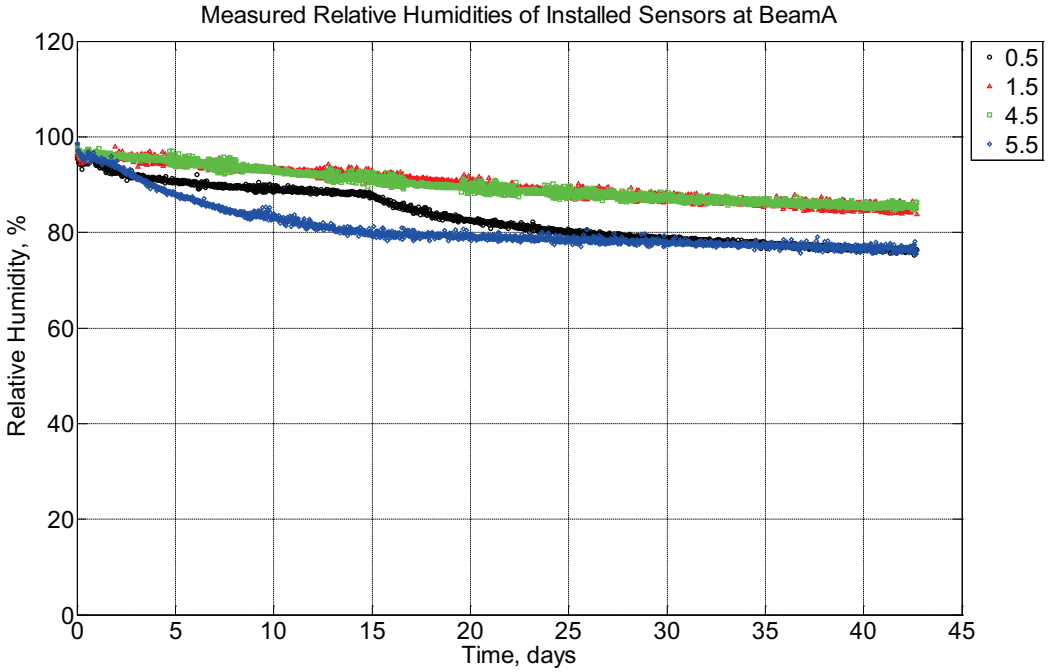

Figure B-26 Measured relative humidity at depths of 0.5 inches (12.7 mm), 1.5 inches (38.1 mm), 4.5 inches (114.3 mm), and 5.5 inches (139.7 mm) from the surface of a modulus of

rupture beam (labeled A) curing inside an environmentally controlled room (50% RH, 23 °C) between January 29, 2014, through March 12, 2014.

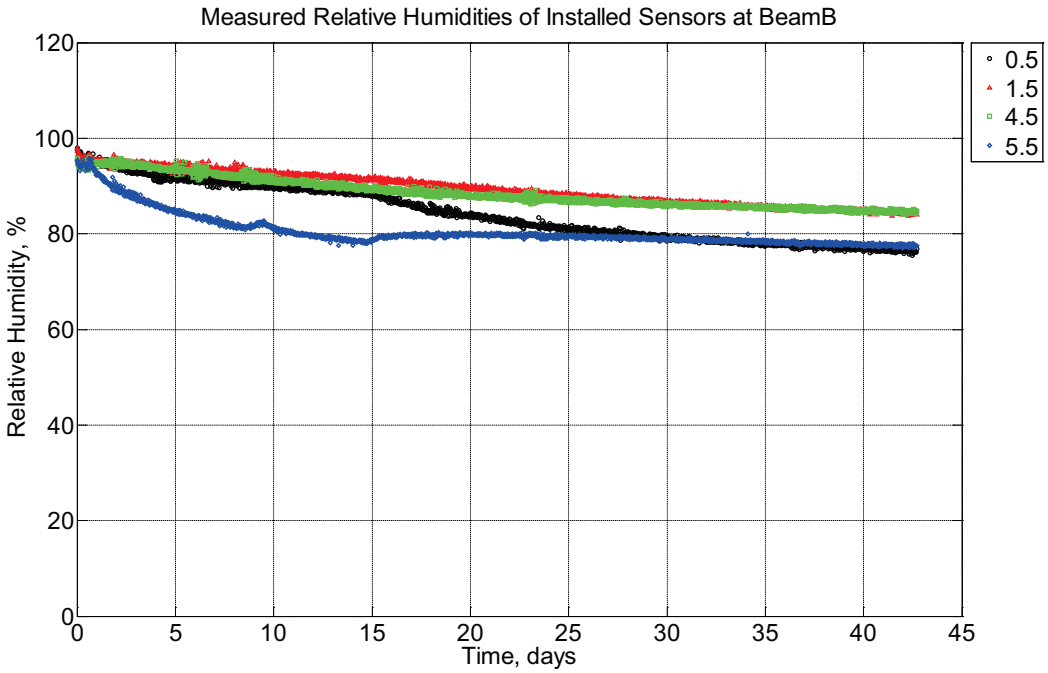

Figure B-27 Measured relative humidity at depths of 0.5 inches (12.7 mm), 1.5 inches (38.1 mm), 4.5 inches (114.3 mm), and 5.5 inches (139.7 mm) from the surface of a modulus of rupture beam (labeled B) curing inside an environmentally controlled room (50% RH, 23 °C) between January 29, 2014, through March 12, 2014.

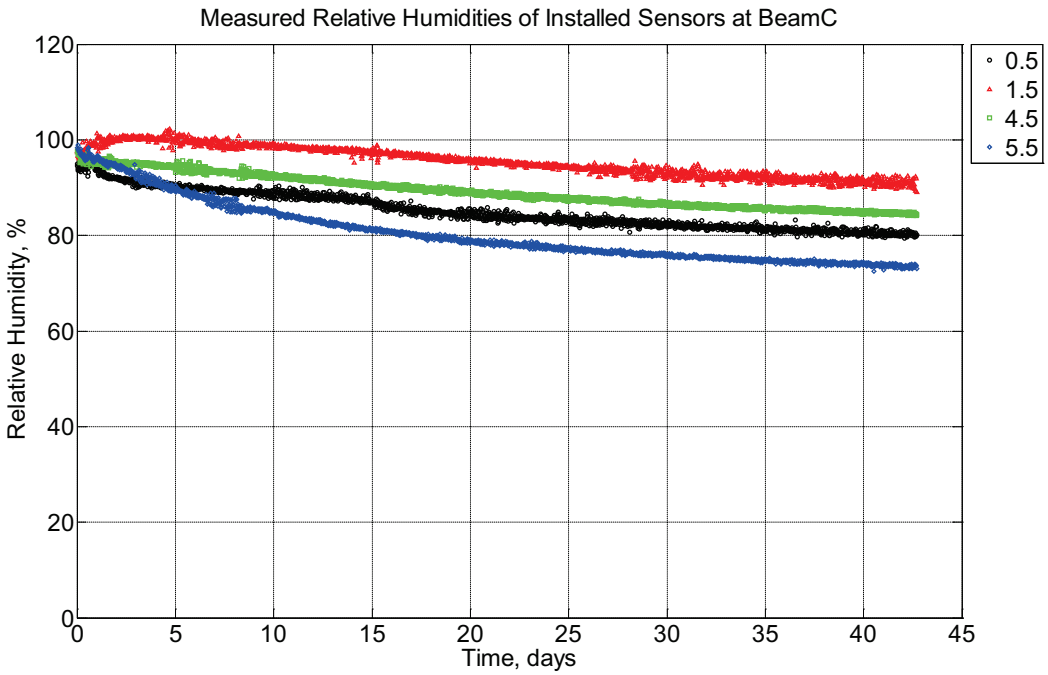

Figure B-28 Measured relative humidity at depths of 0.5 inches (12.7 mm), 1.5 inches (38.1 mm), 4.5 inches (114.3 mm), and 5.5 inches (139.7 mm) from the surface of a modulus of rupture beam (labeled C) curing inside an environmentally controlled room (50% RH, 23 ºC) between January 29, 2014, through March 12, 2014.

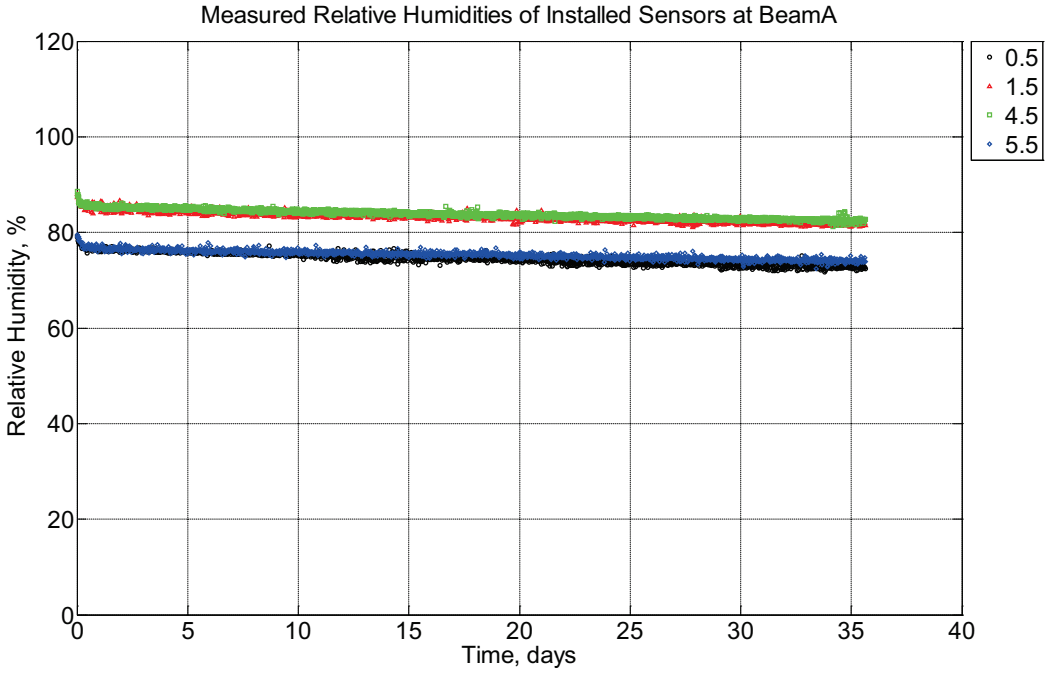

Figure B-29 Measured relative humidity at depths of 0.5 inches (12.7 mm), 1.5 inches (38.1 mm), 4.5 inches (114.3 mm), and 5.5 inches (139.7 mm) from the surface of a modulus of

rupture beam (labeled A) curing inside an environmentally controlled room (50% RH, 23 ºC) between March 12, 2014, through April 17, 2014.

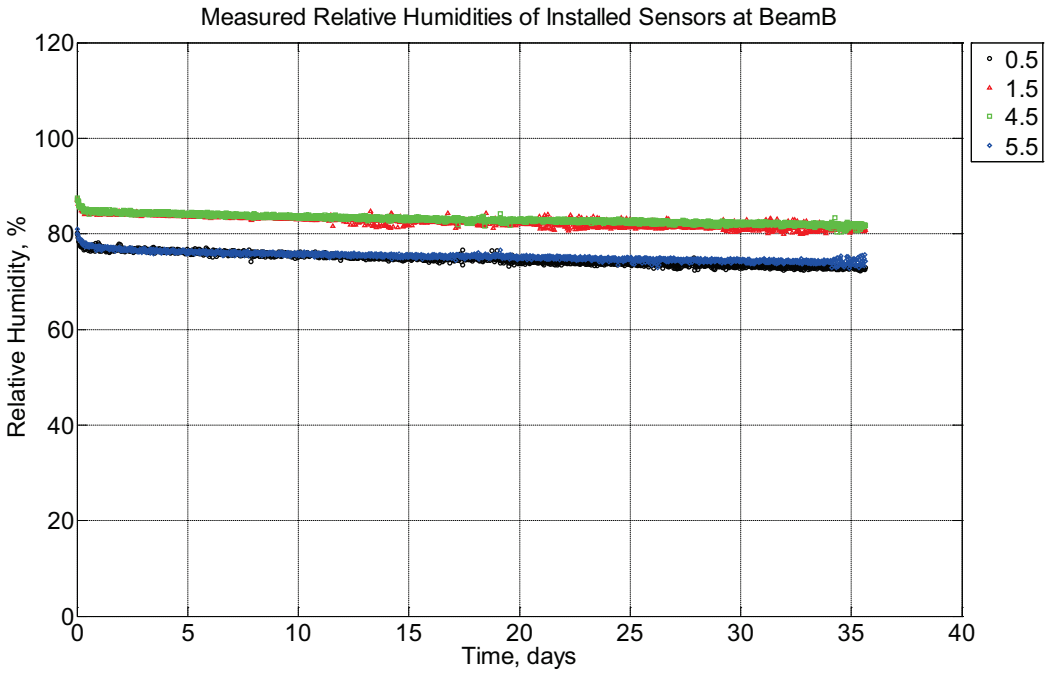

Figure B-30 Measured relative humidity at depths of 0.5 inches (12.7 mm), 1.5 inches (38.1 mm), 4.5 inches (114.3 mm), and 5.5 inches (139.7 mm) from the surface of a modulus of rupture beam (labeled B) curing inside an environmentally controlled room (50% RH, 23 ºC) between March 12, 2014, through April 17, 2014.

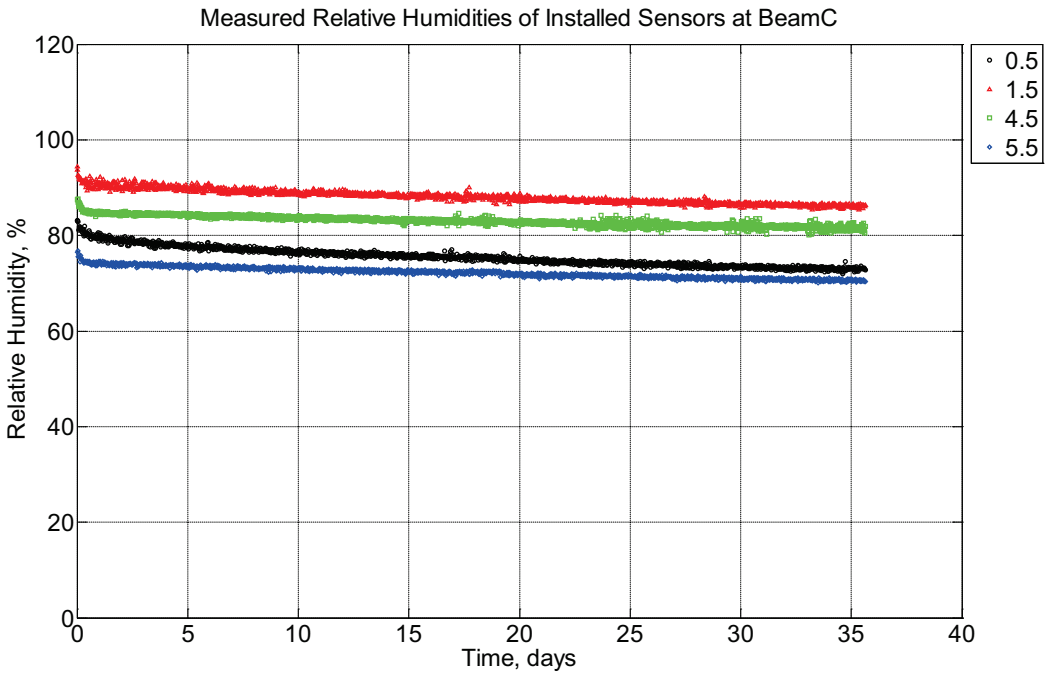

Figure B-31 Measured relative humidity at depths of 0.5 inches (12.7 mm), 1.5 inches (38.1 mm), 4.5 inches (114.3 mm), and 5.5 inches (139.7 mm) from the surface of a modulus of rupture beam (labeled C) curing inside an environmentally controlled room (50% RH, 23 ºC) between March 12, 2014, through April 17, 2014.

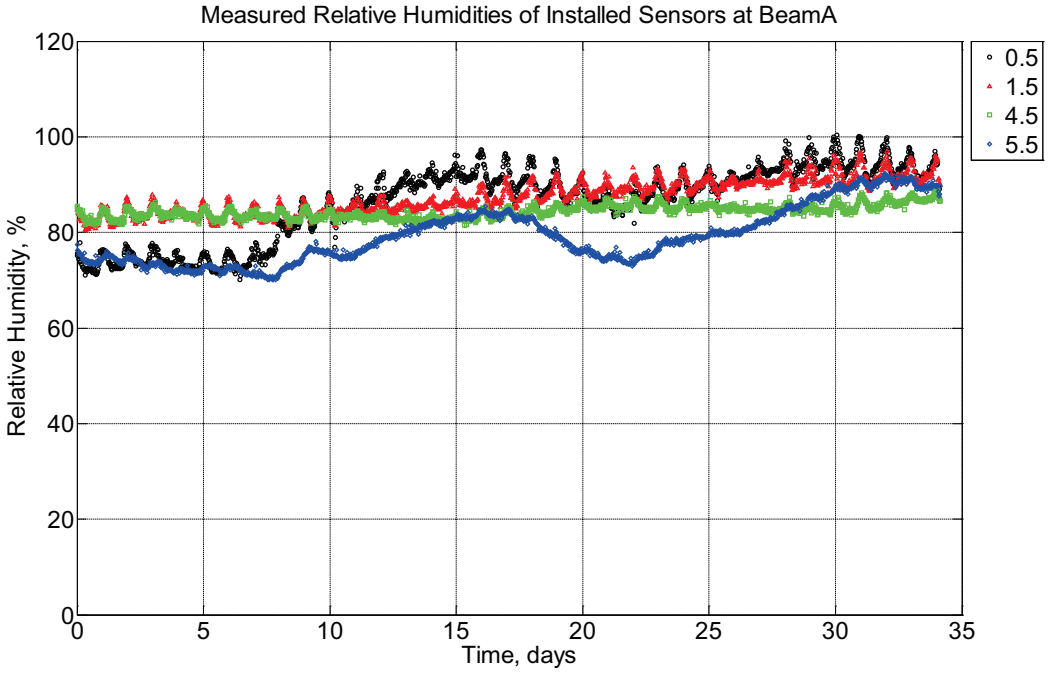

Figure B-32 Measured relative humidity at depths of 0.5 inches (12.7 mm), 1.5 inches (38.1 mm), 4.5 inches (114.3 mm), and 5.5 inches (139.7 mm) from the surface of a modulus of

rupture beam (labeled A) installed in ballast in Rantoul, IL, between April 17, 2014, through May 21, 2014.

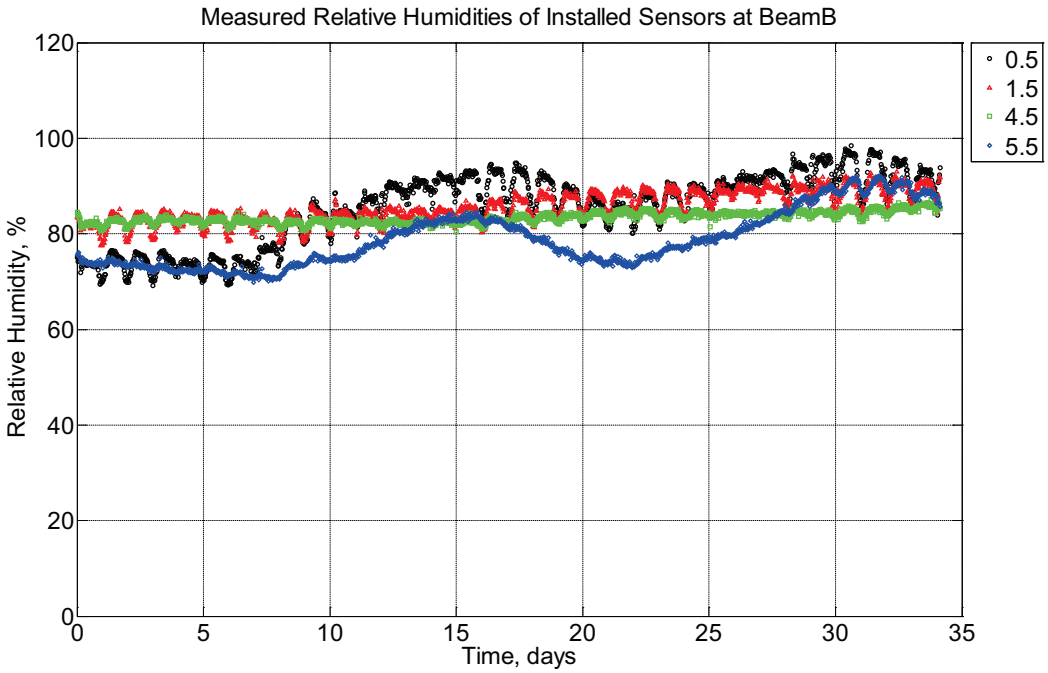

Figure B-33 Measured temperature at depths of 0.5 inches (12.7 mm), 1.5 inches (38.1 mm), 4.5 inches (114.3 mm), and 5.5 inches (139.7 mm) from the surface of a modulus of rupture beam (labeled B) installed in ballast in Rantoul, IL, between April 17, 2014, through May 21, 2014.

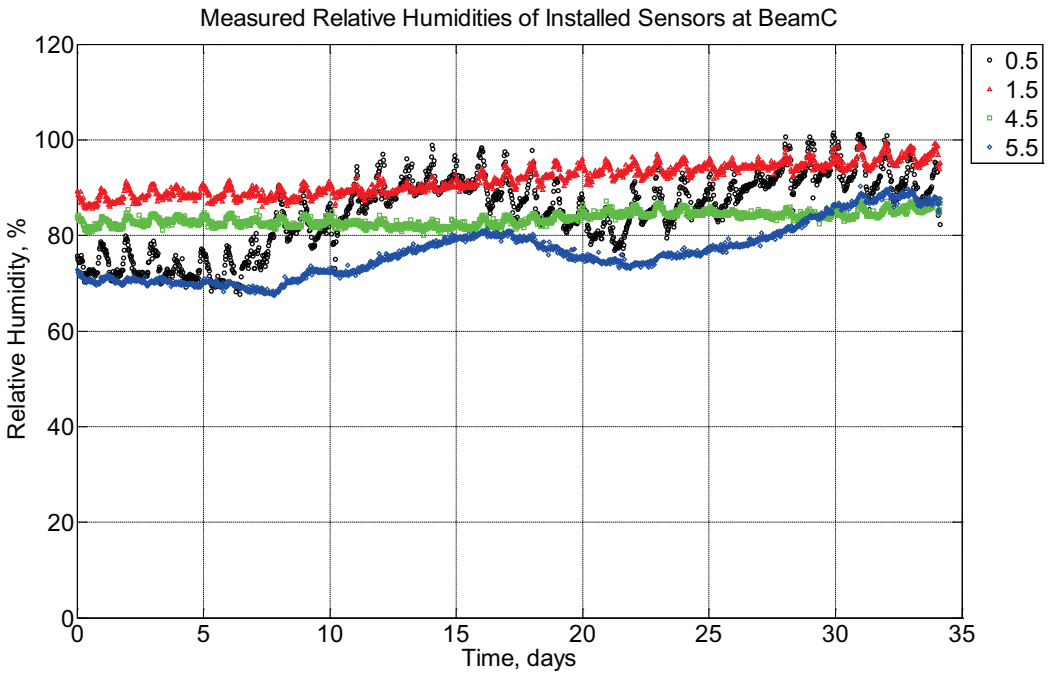

Figure B-34 Measured temperature at depths of 0.5 inches (12.7 mm), 1.5 inches (38.1 mm), 4.5 inches (114.3 mm), and 5.5 inches (139.7 mm) from the surface of a modulus of rupture beam (labeled C) installed in ballast in Rantoul, IL, between April 17, 2014, through May 21, 2014.

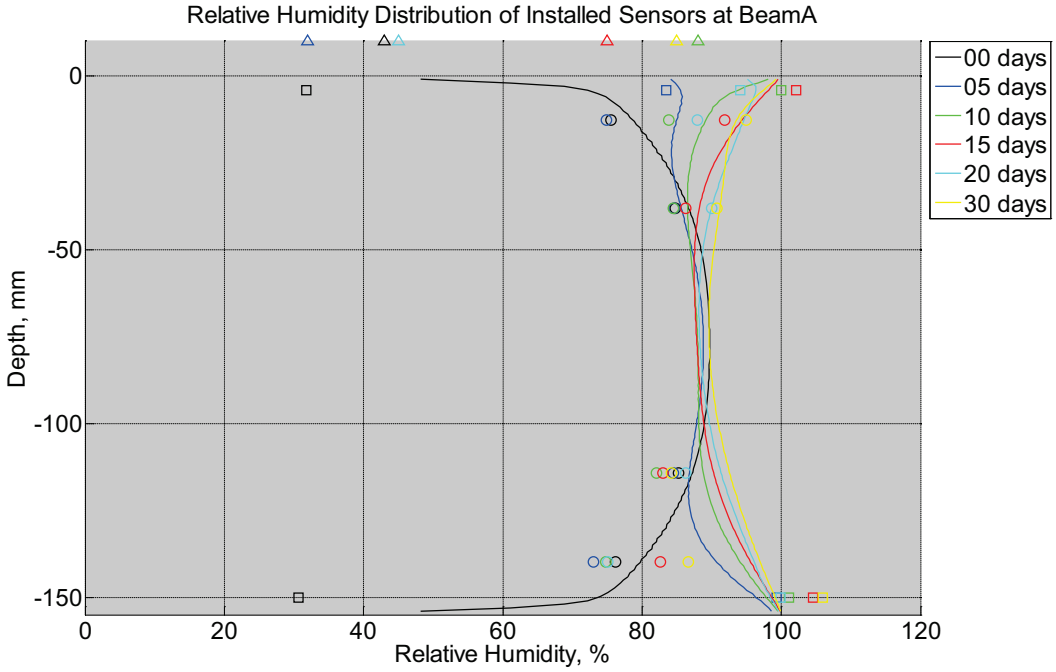

Figure B-35 Measured (markers) and modeled (continuous line) relative humidity profile distribution as a function of depth inside modulus of rupture beam (labeled A) installed in

ballast in Rantoul, IL, between April 17, 2014, through May 21, 2014. Triangular markers denote relative humidity value from KTIP weather station, square markers denote measured relative humidity values from ballast, and circular markers denote measured relative humidity values inside concrete.

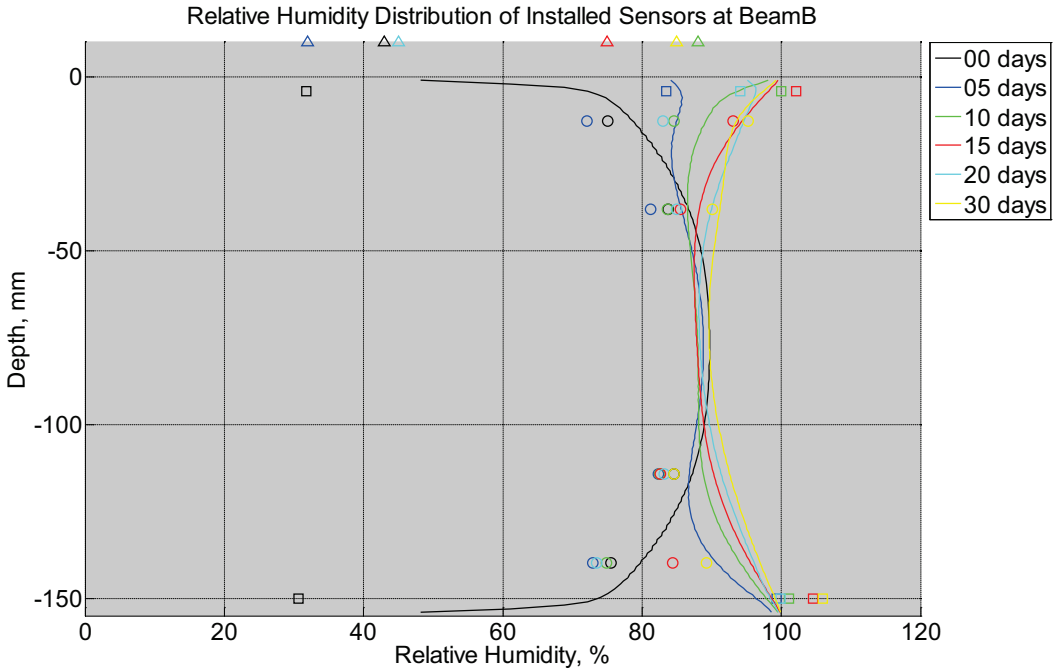

Figure B-36 Measured (markers) and modeled (continuous line) relative humidity profile distribution as a function of depth inside modulus of rupture beam (labeled B) installed in ballast in Rantoul, IL, between April 17, 2014, through May 21, 2014. Triangular markers denote relative humidity value from KTIP weather station, square markers denote measured relative humidity values from ballast, and circular markers denote measured relative humidity values inside concrete.

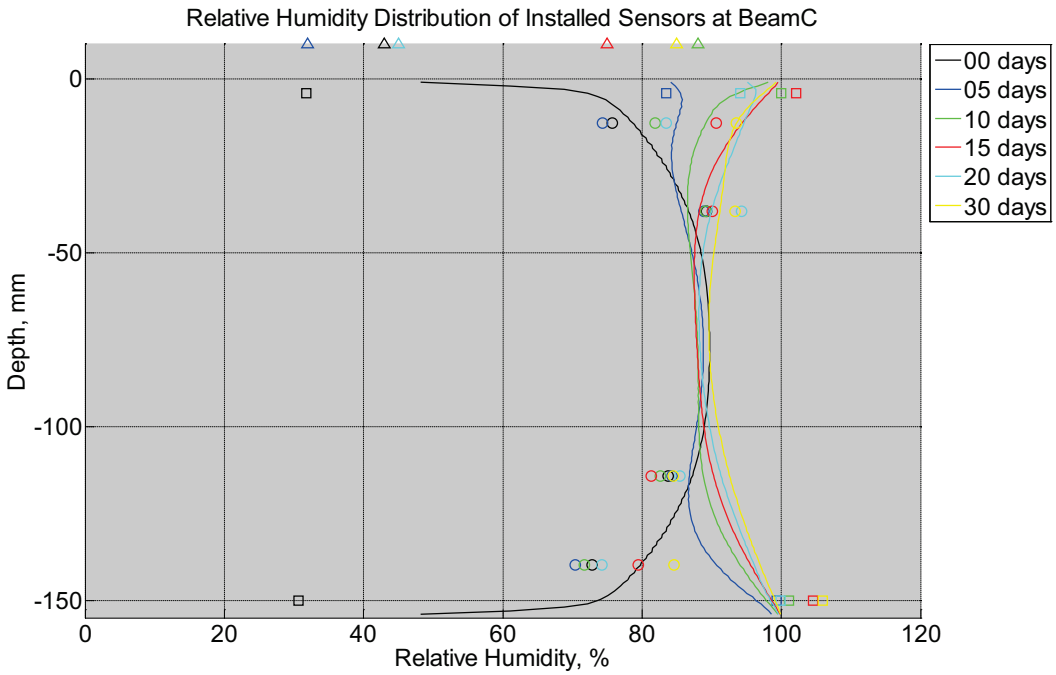

Figure B-37 Measured (markers) and modeled (continuous line) relative humidity profile distribution as a function of depth inside modulus of rupture beam (labeled C) installed in ballast in Rantoul, IL, between April 17, 2014, through May 21, 2014. Triangular markers denote relative humidity value from KTIP weather station, square markers denote measured relative humidity values from ballast, and circular markers denote measured relative humidity values inside concrete.

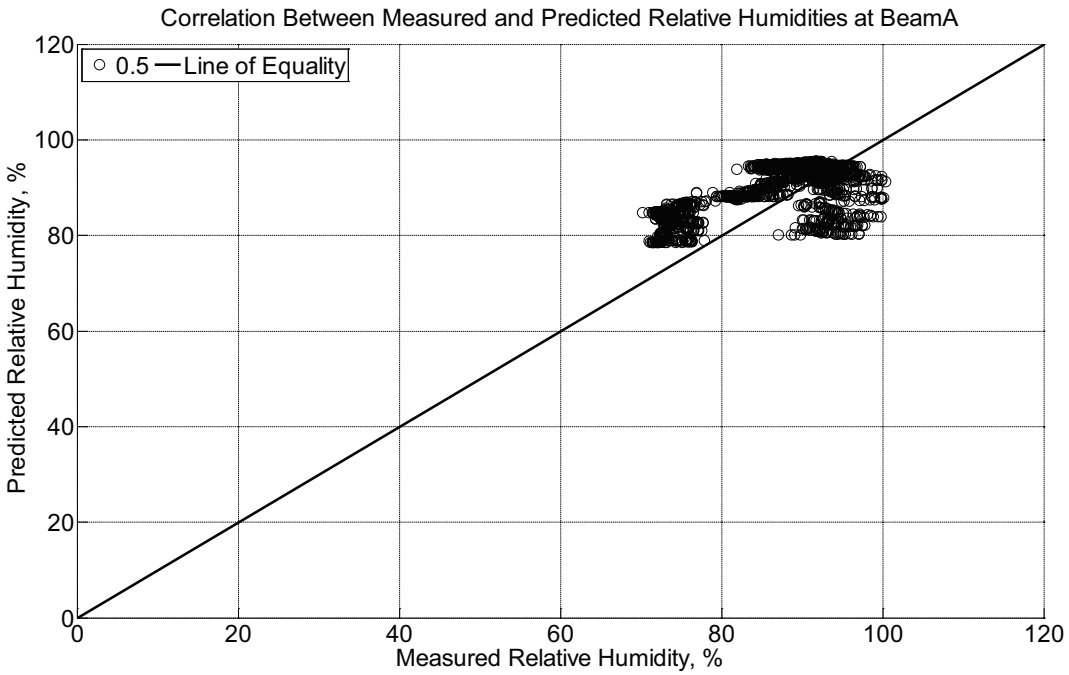

Figure B-38 Correlation between measured and predicted relative humidity values 0.5 inches (12.7 mm) from the surface of a modulus of rupture beam (labeled A) installed in ballast in Rantoul, IL, between April 17, 2014, through May 21, 2014.

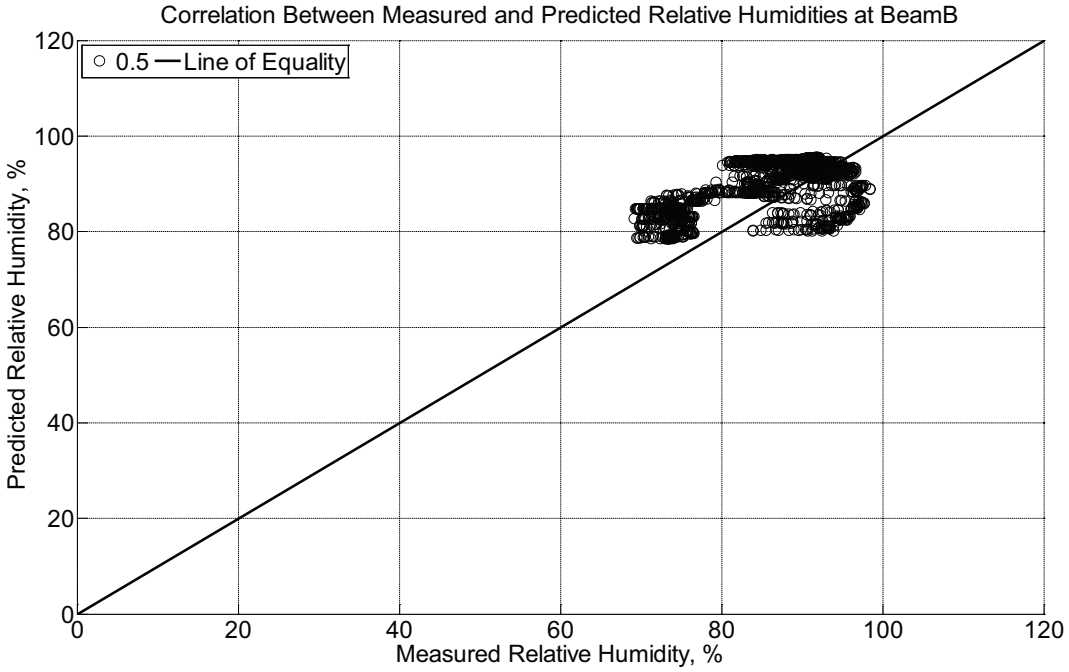

Figure B-39 Correlation between measured and predicted relative humidity values 0.5

inches (12.7 mm) from the surface of a modulus of rupture beam (labeled B) installed in ballast in Rantoul, IL, between April 17, 2014, through May 21, 2014.

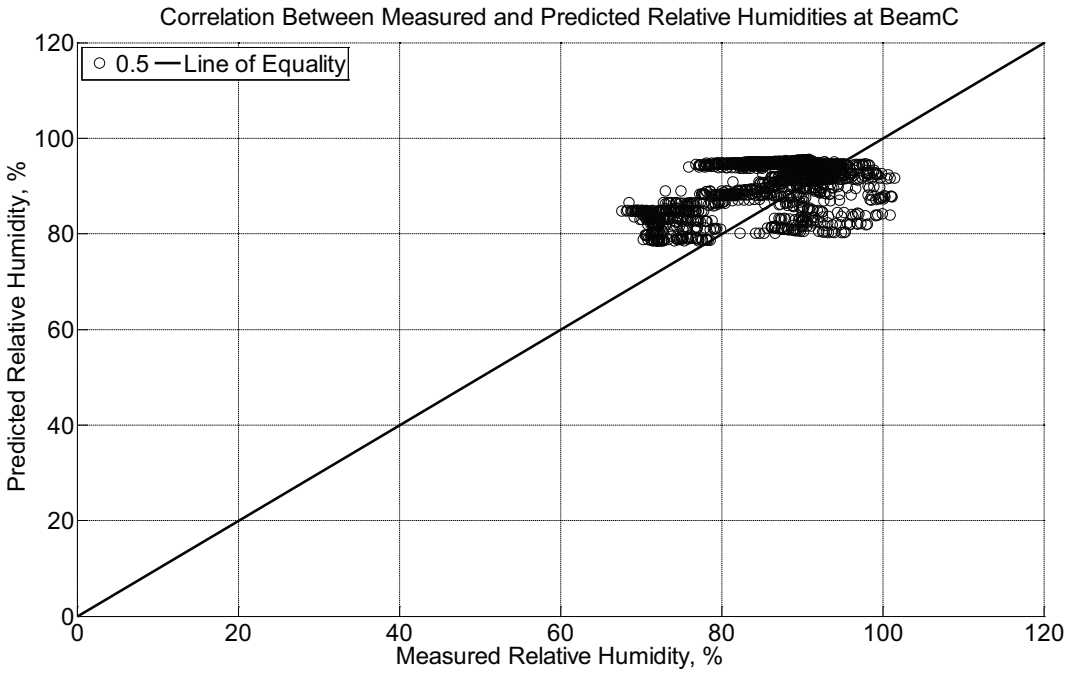

Figure B-40 Correlation between measured and predicted relative humidity values 0.5 inches (12.7 mm) from the surface of a modulus of rupture beam (labeled C) installed in ballast in Rantoul, IL, between April 17, 2014, through May 21, 2014.

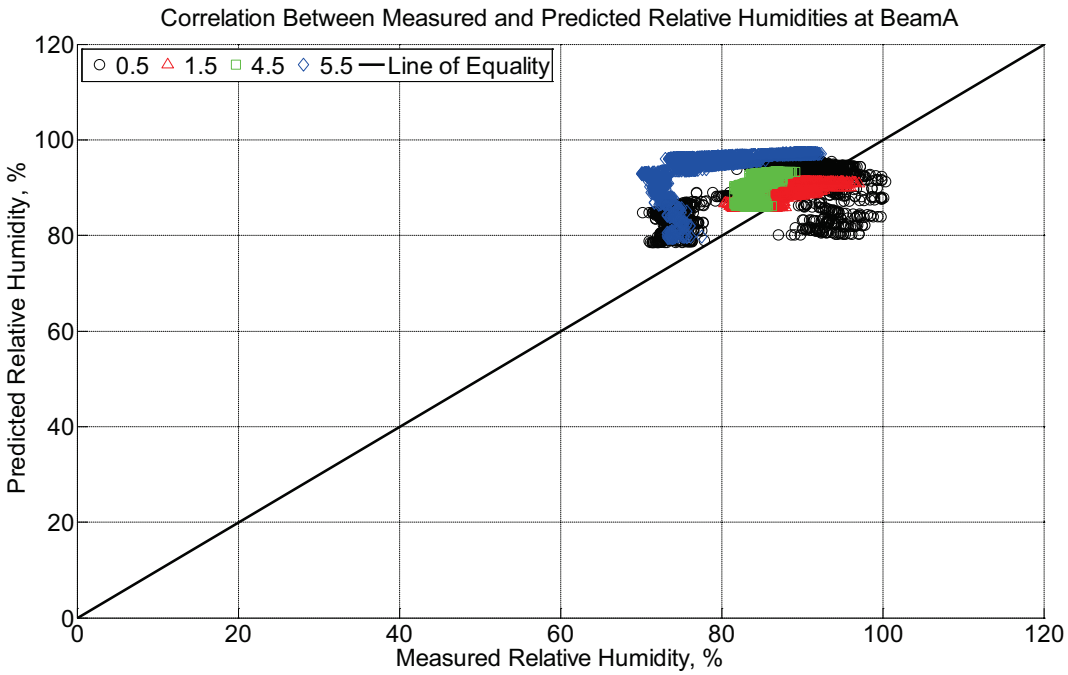

Figure B-41 Correlation between measured and predicted relative humidity values 0.5 inches (12.7 mm), 1.5 inches (38.1 mm), 4.5 inches (114.3 mm), and 5.5 inches (139.7 mm) from the surface of a modulus of rupture beam (labeled A) installed in ballast in Rantoul, IL, between April 17, 2014, through May 21, 2014.

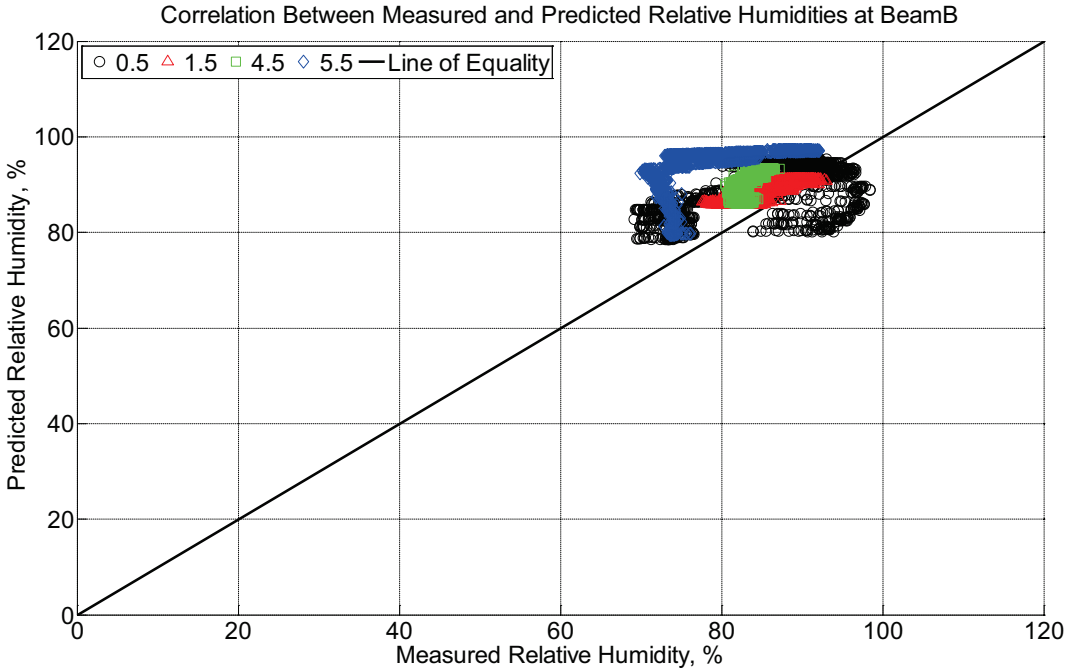

Figure B-42 Correlation between measured and predicted relative humidity values 0.5 inches (12.7 mm), 1.5 inches (38.1 mm), 4.5 inches (114.3 mm), and 5.5 inches (139.7 mm)

from the surface of a modulus of rupture beam (labeled B) installed in ballast in Rantoul, IL, between April 17, 2014, through May 21, 2014.

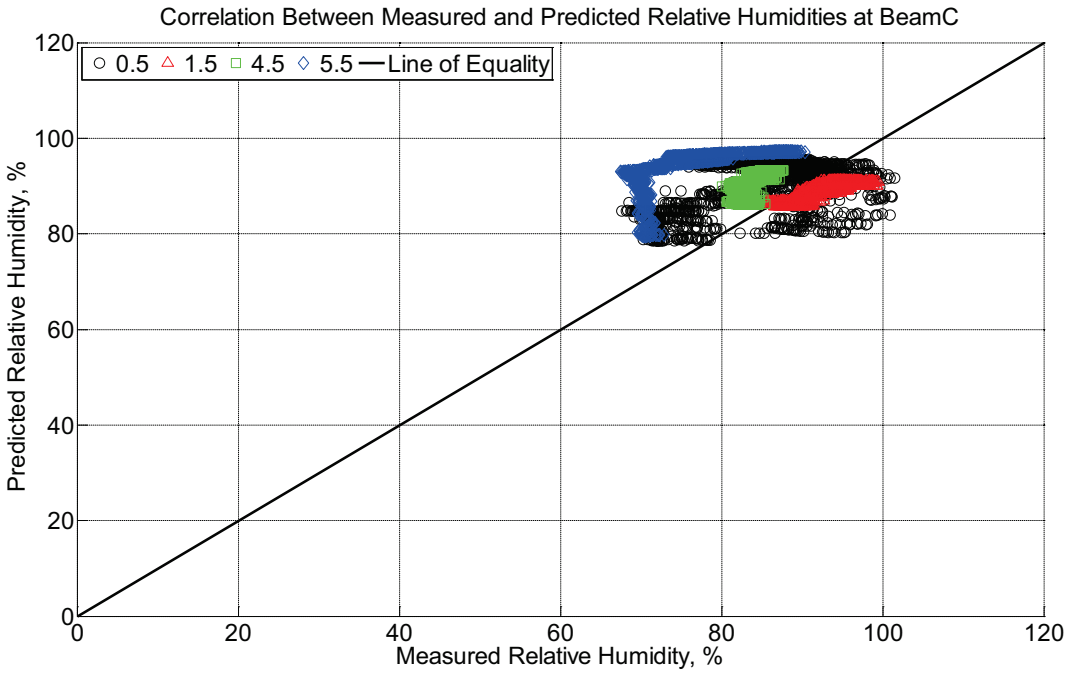

Figure B-43 Correlation between measured and predicted relative humidity values 0.5 inches (12.7 mm), 1.5 inches (38.1 mm), 4.5 inches (114.3 mm), and 5.5 inches (139.7 mm) from the surface of a modulus of rupture beam (labeled C) installed in ballast in Rantoul, IL, between April 17, 2014, through May 21, 2014.

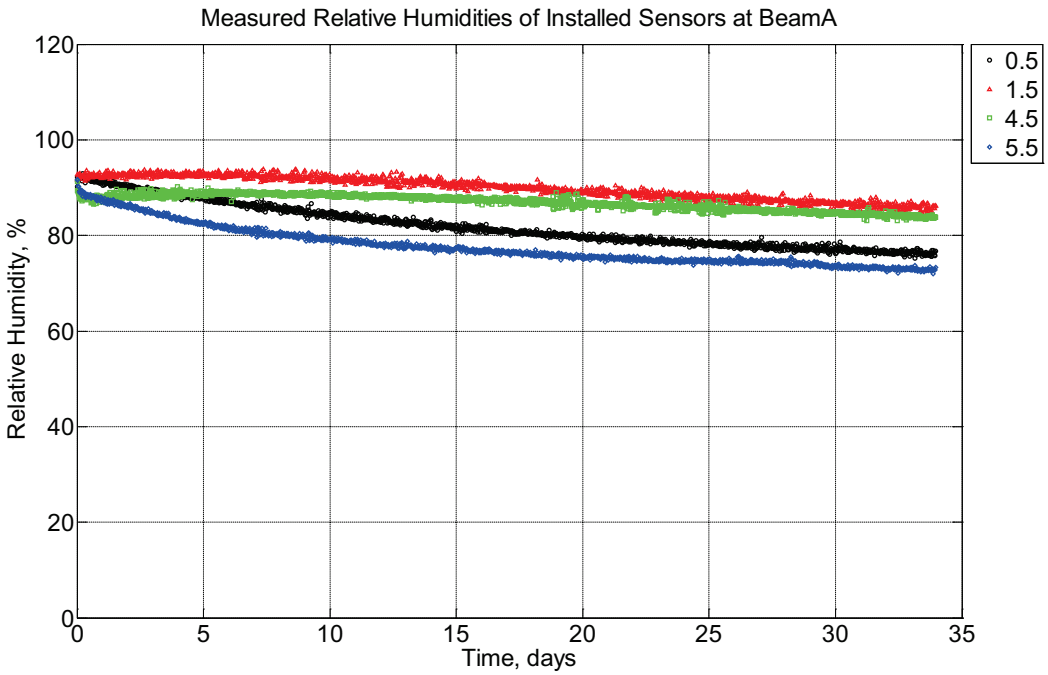

Figure B-44 Measured relative humidity at depths of 0.5 inches (12.7 mm), 1.5 inches (38.1 mm), 4.5 inches (114.3 mm), and 5.5 inches (139.7 mm) from the surface of a modulus of rupture beam (labeled A) located inside an environmentally controlled room (50% RH, 23 ºC) between May 21, 2014, through June 24, 2014.

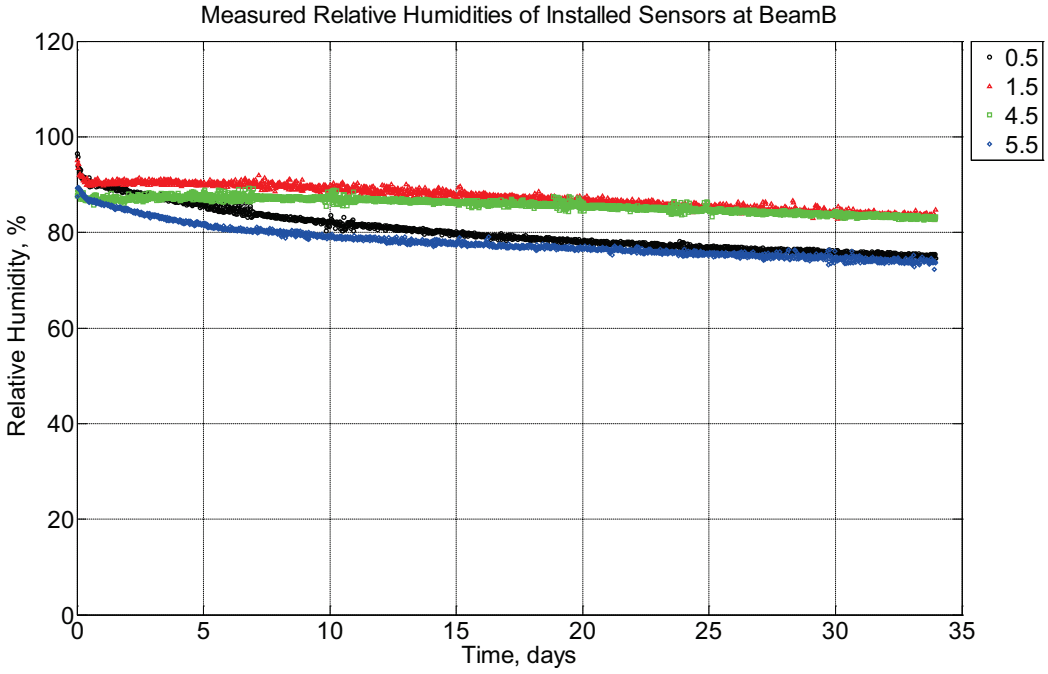

Figure B-45 Measured relative humidity at depths of 0.5 inches (12.7 mm), 1.5 inches (38.1 mm), 4.5 inches (114.3 mm), and 5.5 inches (139.7 mm) from the surface of a modulus of

rupture beam (labeled B) located inside an environmentally controlled room (50% RH, 23 °C) between May 21, 2014, through June 24, 2014.

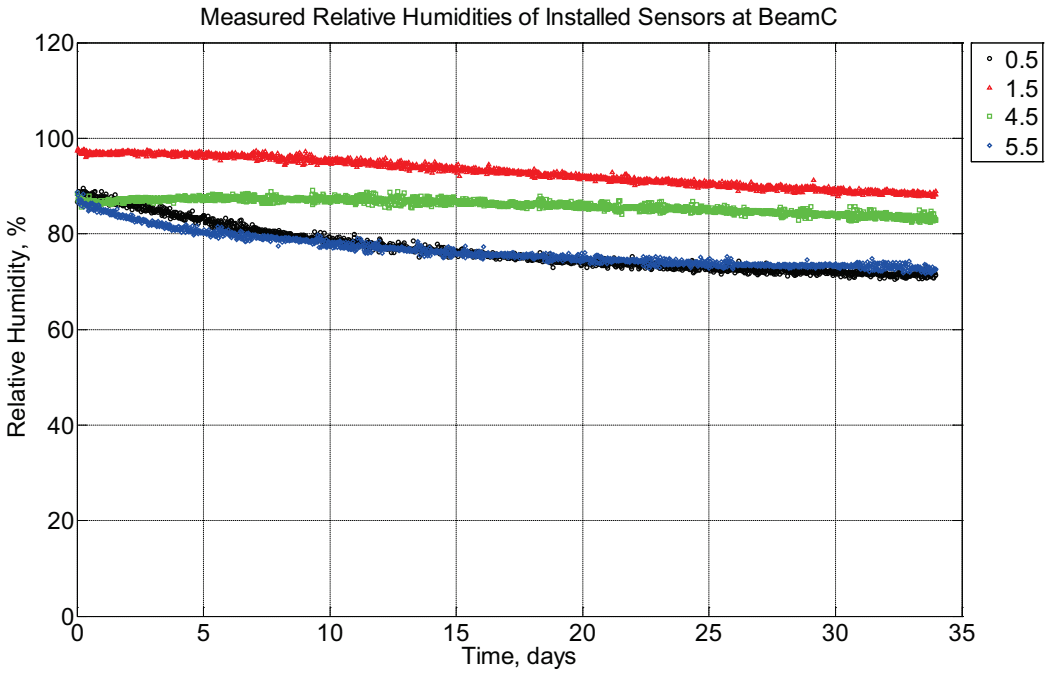

Figure B-46 Measured relative humidity at depths of 0.5 inches (12.7 mm), 1.5 inches (38.1 mm), 4.5 inches (114.3 mm), and 5.5 inches (139.7 mm) from the surface of a modulus of rupture beam (labeled C) located inside an environmentally controlled room (50% RH, 23 °C) between May 21, 2014, through June 24, 2014.

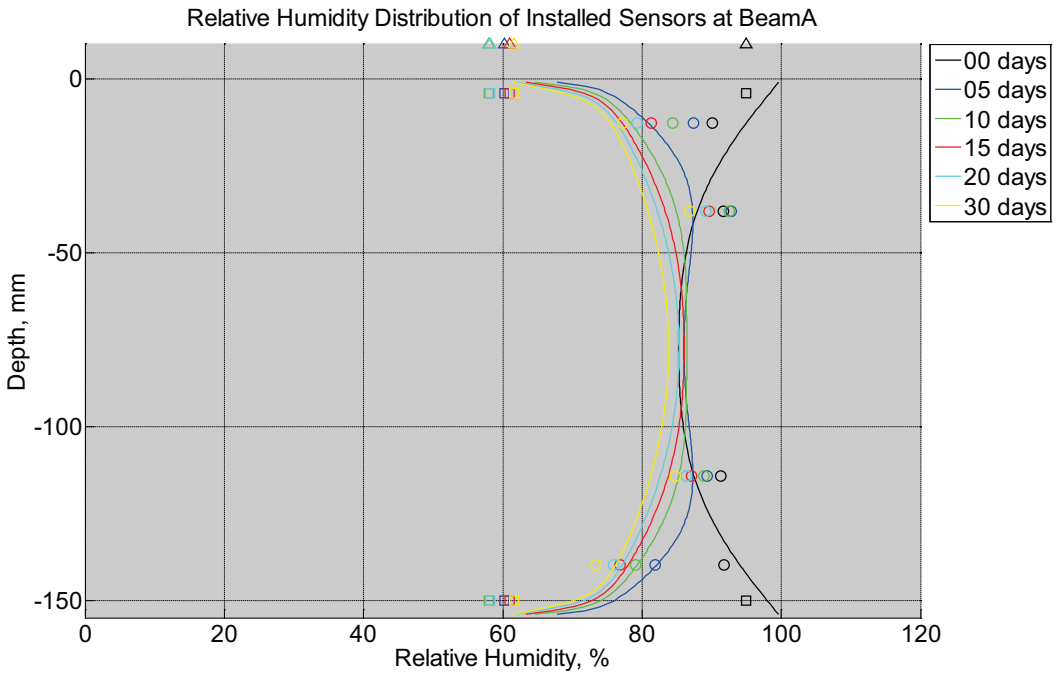

Figure B-47 Measured (markers) and modeled (continuous line) relative humidity profile distribution as a function of depth inside modulus of rupture beam (labeled A) located inside an environmentally controlled room (50% RH, 23 ºC) between May 21, 2014, through June 24, 2014. Triangular markers denote relative humidity value from control panel, square markers denote measured relative humidity values from ambient sensors, and circular markers denote measured relative humidity values inside concrete.

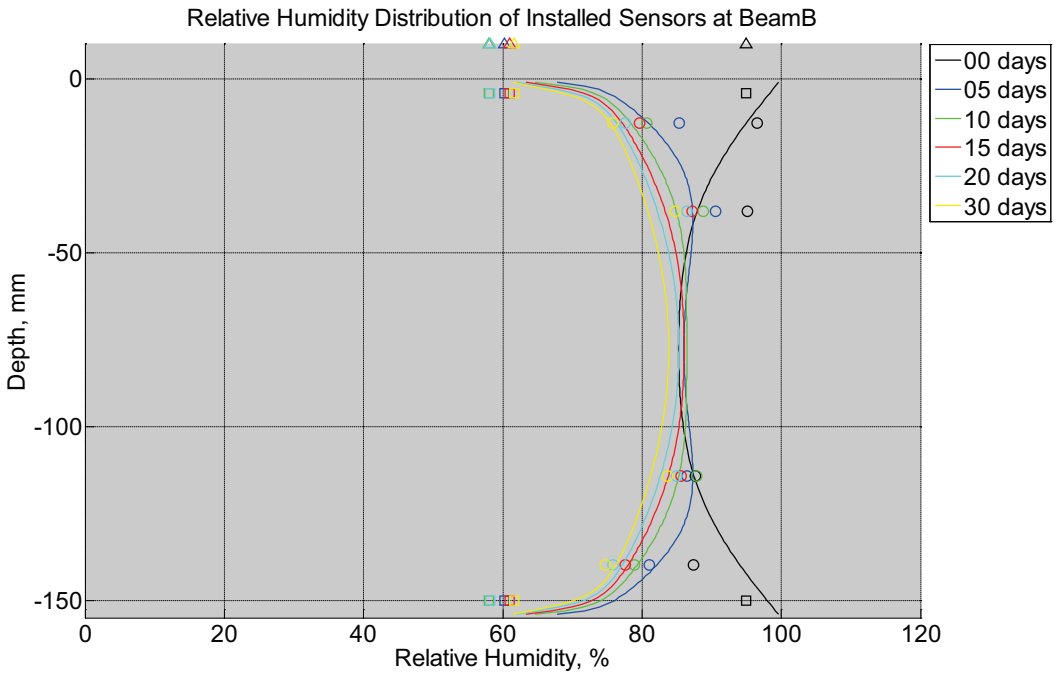

Figure B-48 Measured (markers) and modeled (continuous line) relative humidity profile distribution as a function of depth inside modulus of rupture beam (labeled B) located inside an environmentally controlled room (50% RH, 23 ºC) between May 21, 2014, through June 24, 2014. Triangular markers denote relative humidity value from control panel, square markers denote measured relative humidity values from ambient sensors, and circular markers denote measured relative humidity values inside concrete.

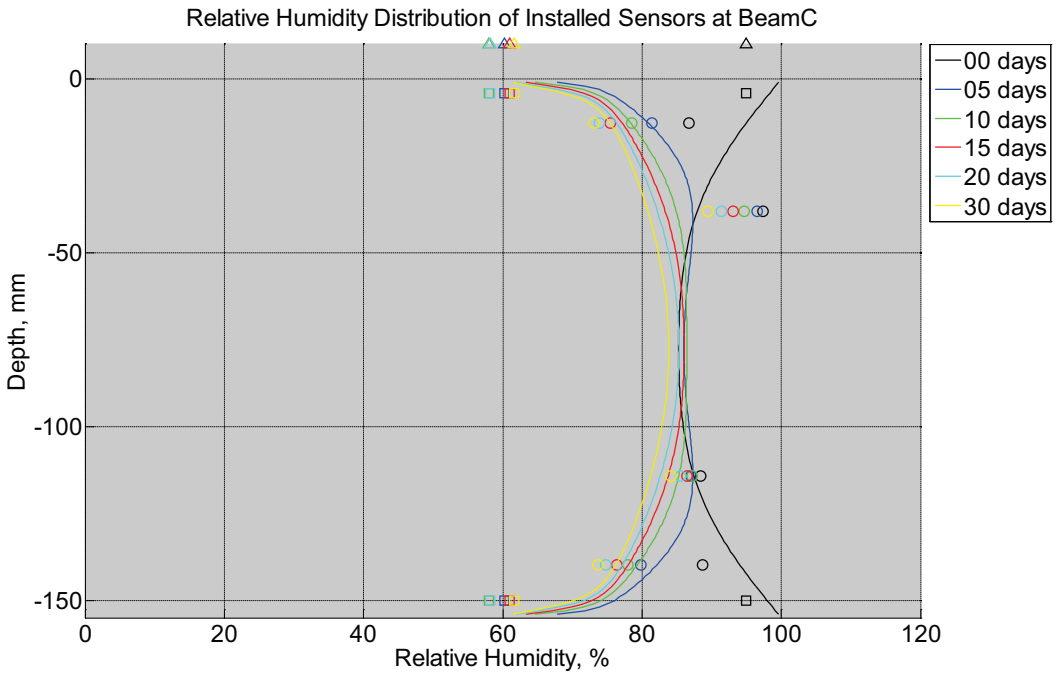

Figure B-49 Measured (markers) and modeled (continuous line) relative humidity profile distribution as a function of depth inside modulus of rupture beam (labeled C) located inside an environmentally controlled room (50% RH, 23 ºC) between May 21, 2014, through June 24, 2014. Triangular markers denote relative humidity value from control panel, square markers denote measured relative humidity values from ambient sensors, and circular markers denote measured relative humidity values inside concrete.

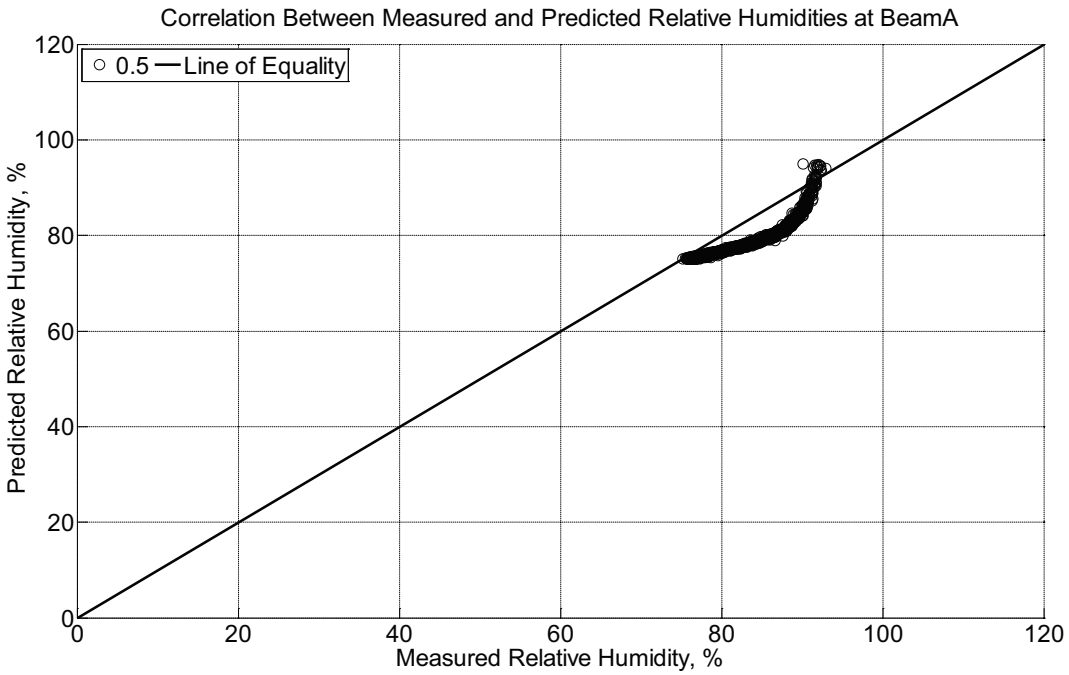

Figure B-50 Correlation between measured and predicted relative humidity values 0.5 inches (12.7 mm) from the surface of a modulus of rupture beam (labeled A) located inside an environmentally controlled room (50% RH, 23 ºC) between May 21, 2014, through June 24, 2014.

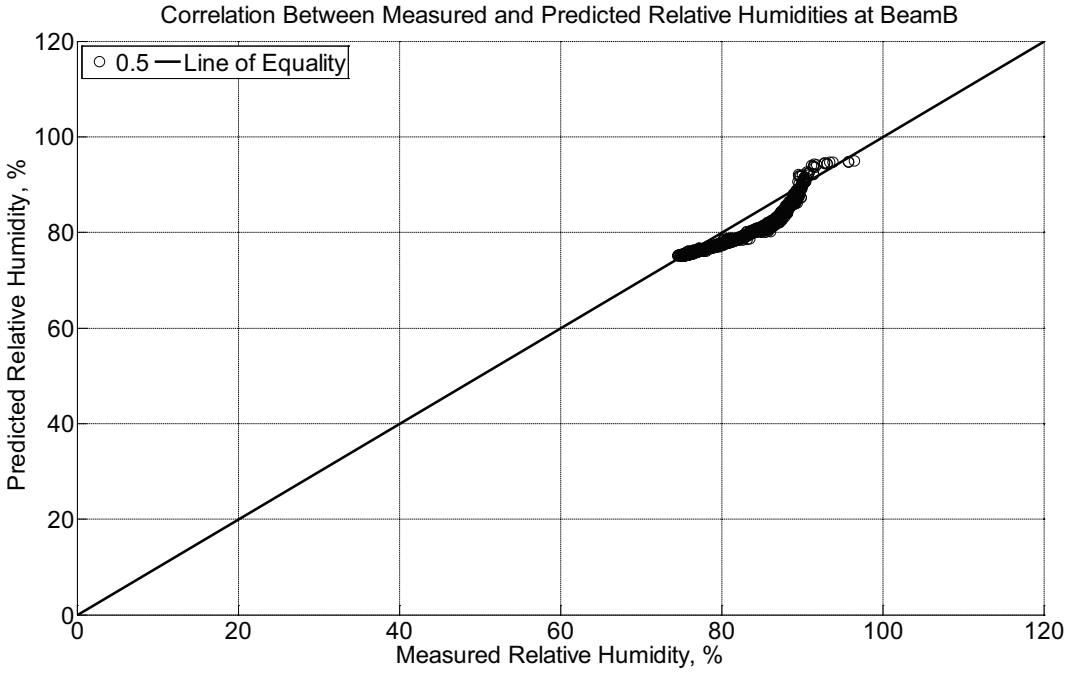

Figure B-51 Correlation between measured and predicted relative humidity values 0.5 inches (12.7 mm) from the surface of a modulus of rupture beam (labeled B) located inside

an environmentally controlled room (50% RH, 23 °C) between May 21, 2014, through June 24, 2014.

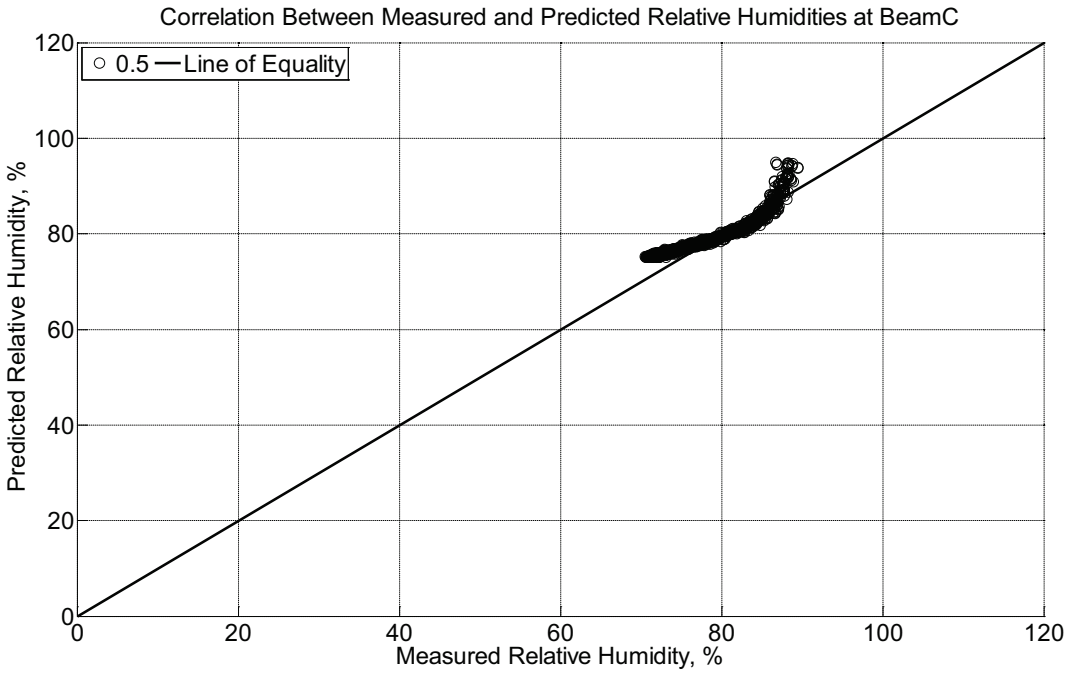

Figure B-52 Correlation between measured and predicted relative humidity values 0.5 inches (12.7 mm) from the surface of a modulus of rupture beam (labeled C) located inside an environmentally controlled room (50% RH, 23 °C) between May 21, 2014, through June 24, 2014.

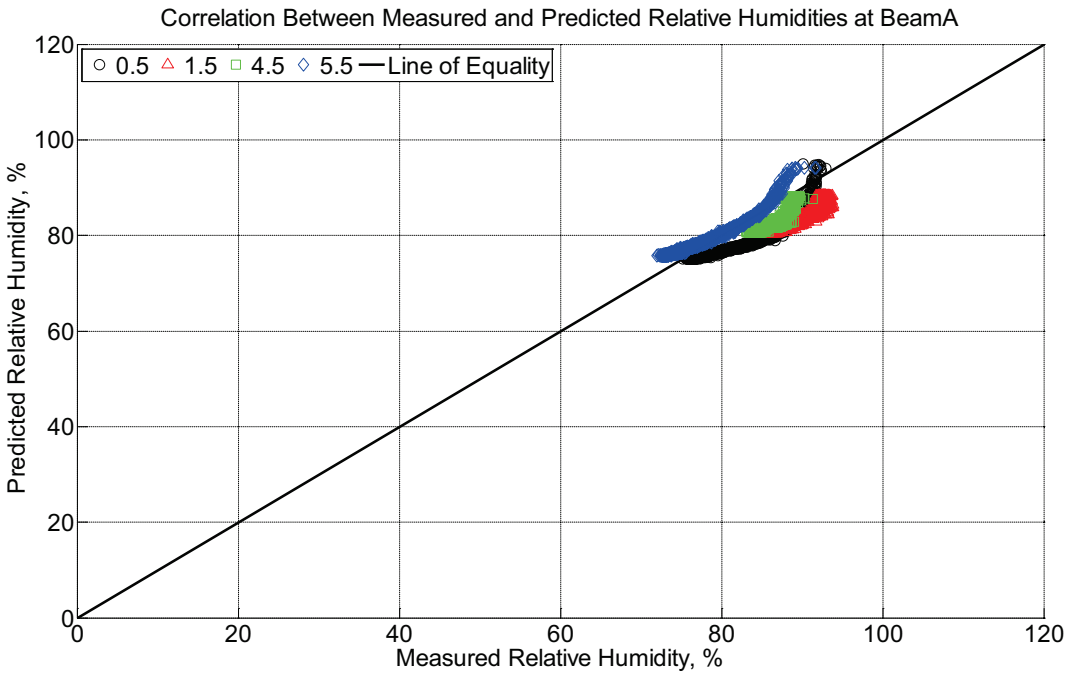

Figure B-53 Correlation between measured and predicted relative humidity values 0.5 inches (12.7 mm), 1.5 inches (38.1 mm), 4.5 inches (114.3 mm), and 5.5 inches (139.7 mm) from the surface of a modulus of rupture beam (labeled A) located inside an environmentally controlled room (50% RH, 23 ºC) between May 21, 2014, through June 24, 2014.

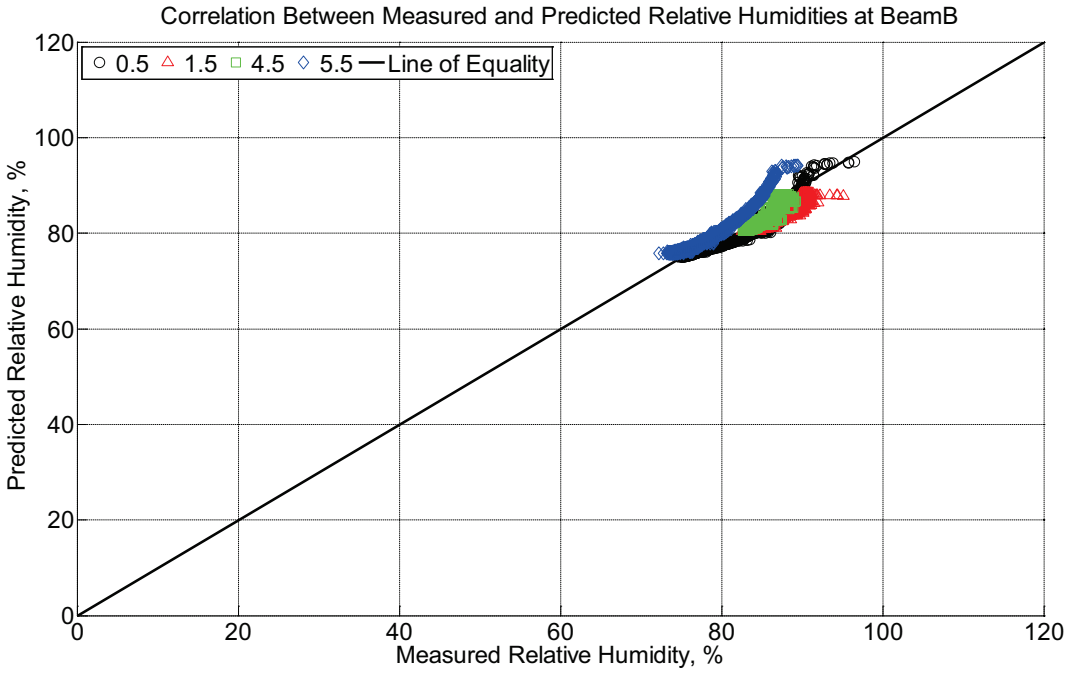

Figure B-54 Correlation between measured and predicted relative humidity values 0.5

inches (12.7 mm), 1.5 inches (38.1 mm), 4.5 inches (114.3 mm), and 5.5 inches (139.7 mm) from the surface of a modulus of rupture beam (labeled A) located inside an environmentally controlled room (50% RH, 23 ºC) between May 21, 2014, through June 24, 2014.

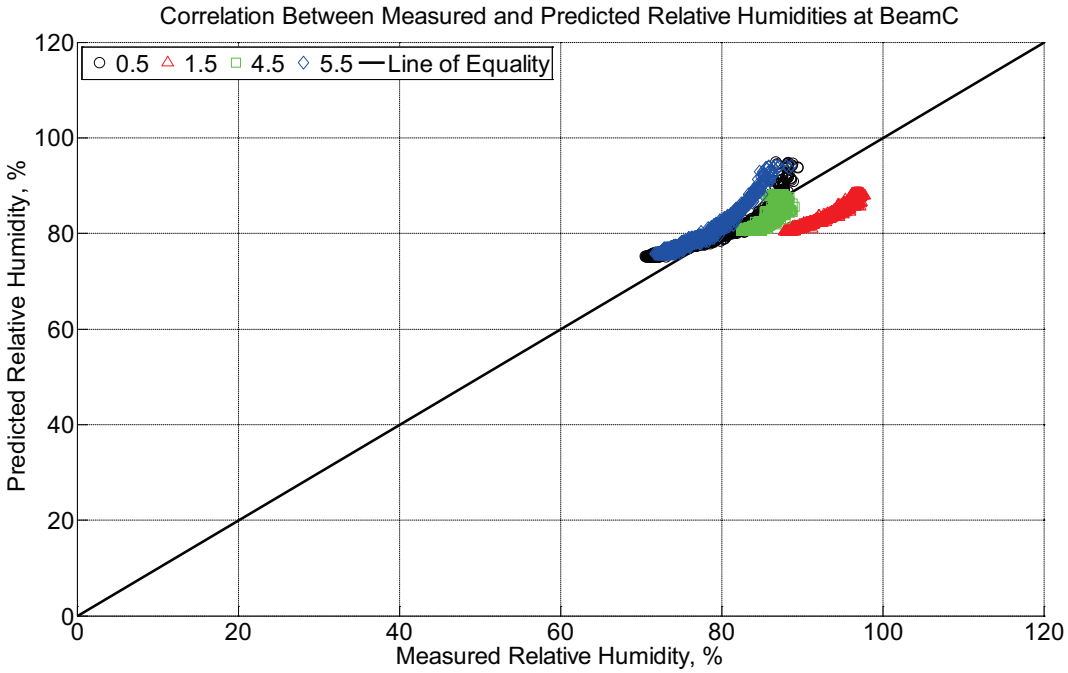

Figure B-55 Correlation between measured and predicted relative humidity values 0.5 inches (12.7 mm), 1.5 inches (38.1 mm), 4.5 inches (114.3 mm), and 5.5 inches (139.7 mm) from the surface of a modulus of rupture beam (labeled A) located inside an environmentally controlled room (50% RH, 23 ºC) between May 21, 2014, through June 24, 2014.

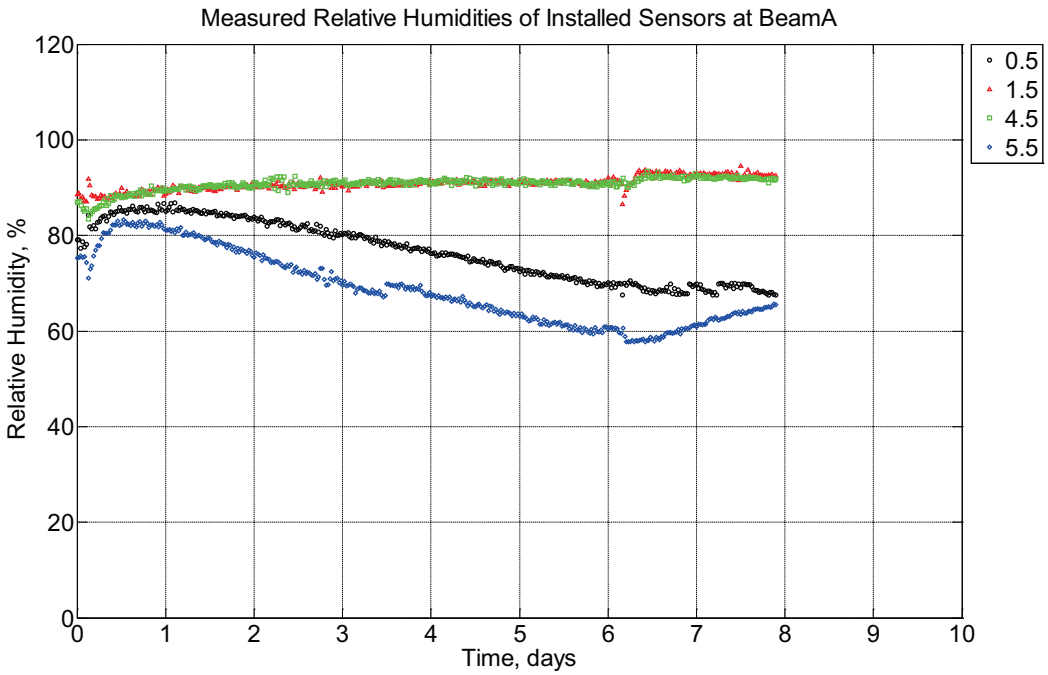

Figure B-56 Measured relative humidity at depths of 0.5 inches (12.7 mm), 1.5 inches (38.1 mm), 4.5 inches (114.3 mm), and 5.5 inches (139.7 mm) from the surface of a modulus of rupture beam (labeled A) located inside an environmentally controlled room (50% RH, 23 ºC) and a heating oven (65 ºC) between June 24, 2014, through July 2, 2014.

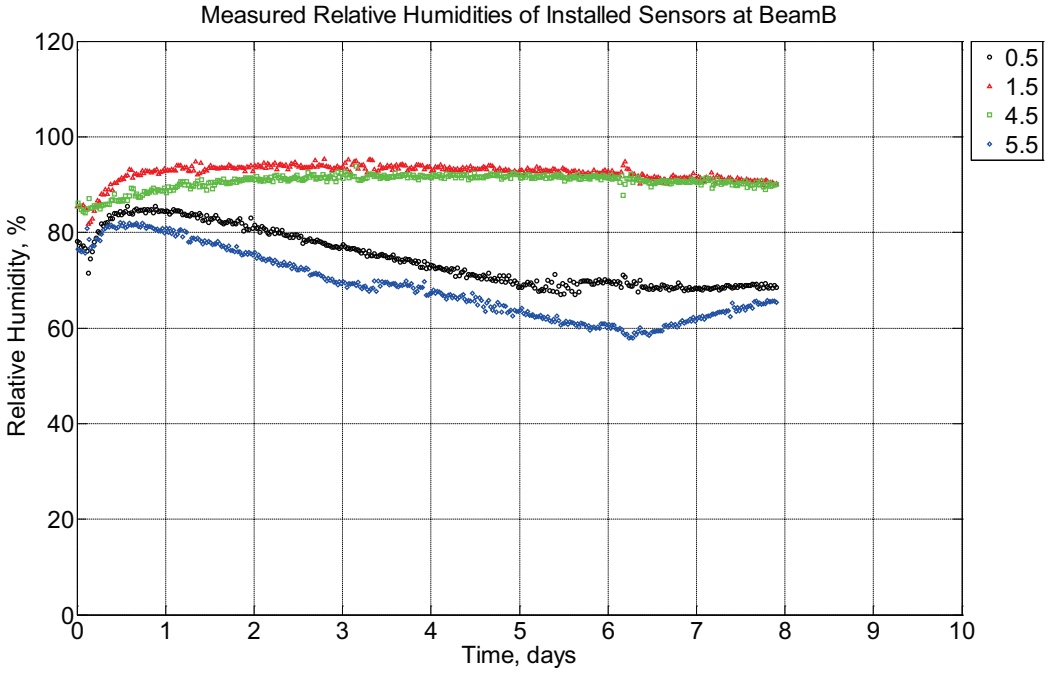

Figure B-57 Measured relative humidity at depths of 0.5 inches (12.7 mm), 1.5 inches (38.1 mm), 4.5 inches (114.3 mm), and 5.5 inches (139.7 mm) from the surface of a modulus of

rupture beam (labeled B) located inside an environmentally controlled room (50% RH, 23 °C) and a heating oven (65 °C) between June 24, 2014, through July 2, 2014.

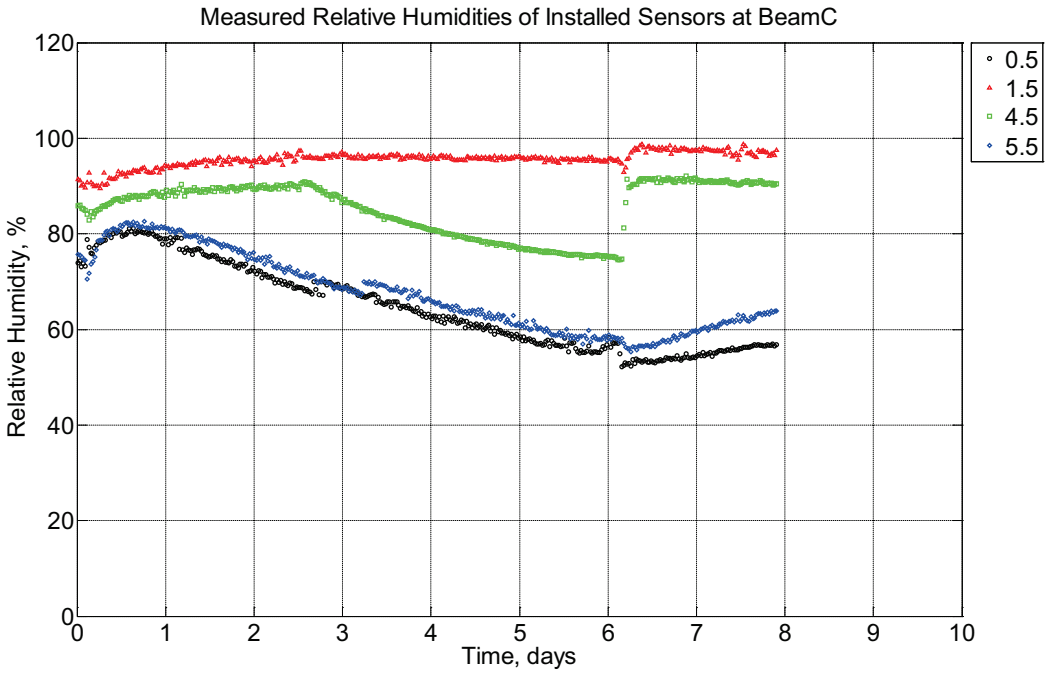

Figure B-58 Measured relative humidity at depths of 0.5 inches (12.7 mm), 1.5 inches (38.1 mm), 4.5 inches (114.3 mm), and 5.5 inches (139.7 mm) from the surface of a modulus of rupture beam (labeled C) located inside an environmentally controlled room (50% RH, 23 °C) and a heating oven (65 °C) between June 24, 2014, through July 2, 2014.

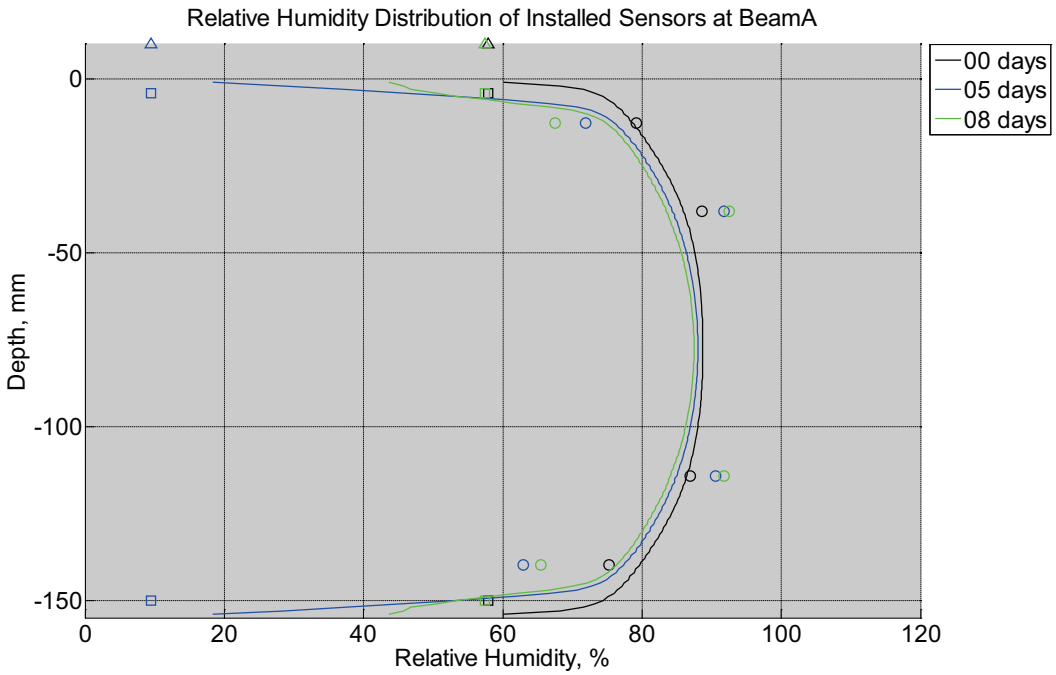

Figure B-59 Measured (markers) and modeled (continuous line) relative humidity profile distribution as a function of depth inside modulus of rupture beam (labeled A) located inside an environmentally controlled room (50% RH, 23 ºC) and a heating oven (65 ºC) between June 24, 2014, through July 2, 2014. Triangular markers denote relative humidity value from control panel, square markers denote measured relative humidity values from ambient sensors, and circular markers denote measured relative humidity values inside concrete.

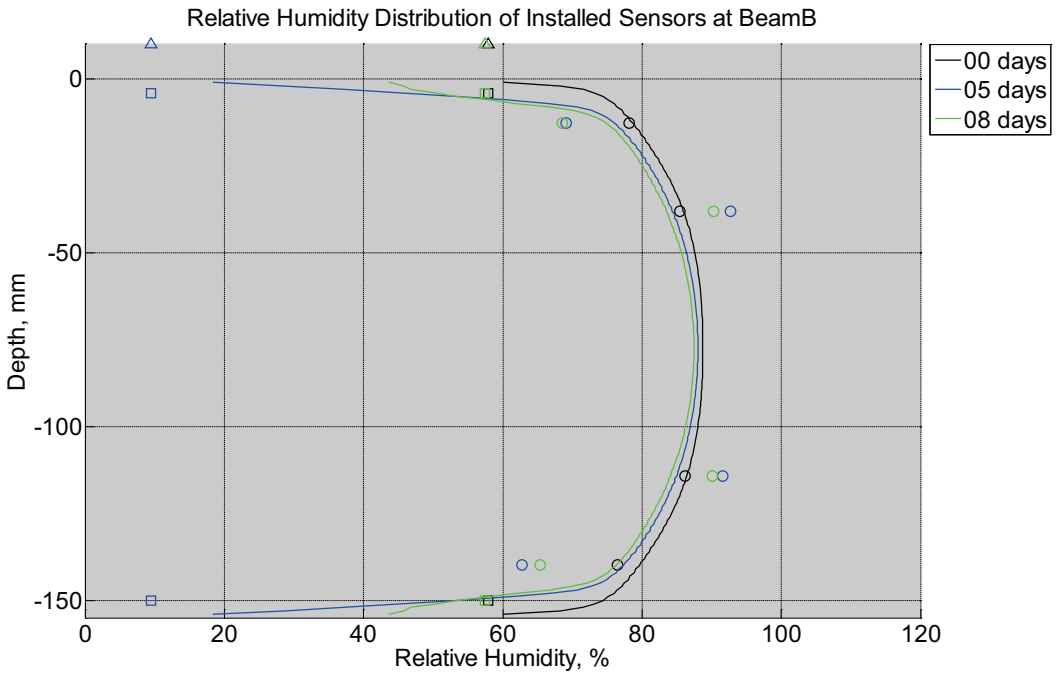

Figure B-60 Measured (markers) and modeled (continuous line) relative humidity profile distribution as a function of depth inside modulus of rupture beam (labeled B) located inside an environmentally controlled room (50% RH, 23 ºC) and a heating oven (65 ºC) between June 24, 2014, through July 2, 2014. Triangular markers denote relative humidity value from control panel, square markers denote measured relative humidity values from ambient sensors, and circular markers denote measured relative humidity values inside concrete.

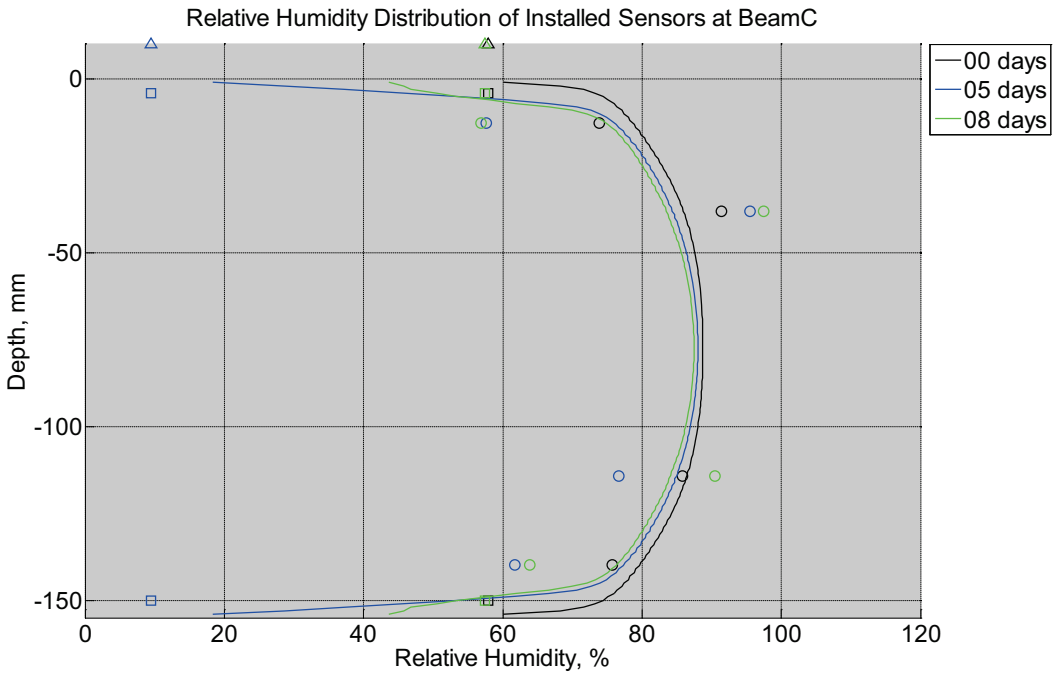

Figure B-61 Measured (markers) and modeled (continuous line) relative humidity profile distribution as a function of depth inside modulus of rupture beam (labeled C) located inside an environmentally controlled room (50% RH, 23 ºC) and a heating oven (65 ºC) between June 24, 2014, through July 2, 2014. Triangular markers denote relative humidity value from control panel, square markers denote measured relative humidity values from ambient sensors, and circular markers denote measured relative humidity values inside concrete.

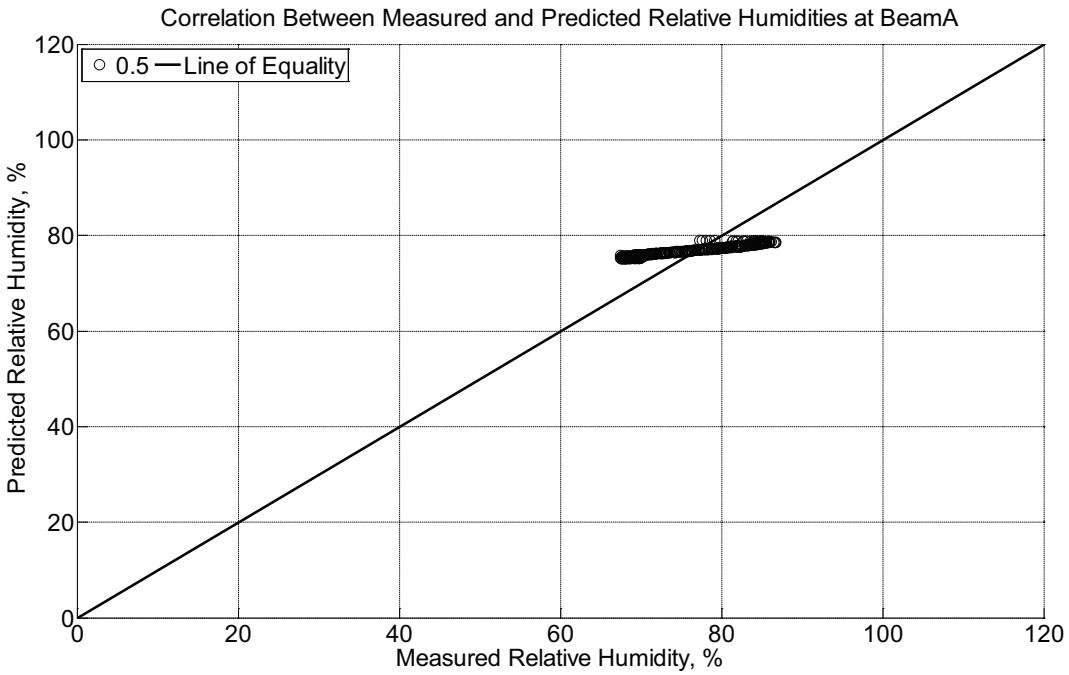

Figure B-62 Correlation between measured and predicted relative humidity values 0.5 inches (12.7 mm) from the surface of a modulus of rupture beam (labeled A) located inside an environmentally controlled room (50% RH, 23 ºC) and a heating oven (65 ºC) between June 24, 2014, through July 2, 2014.

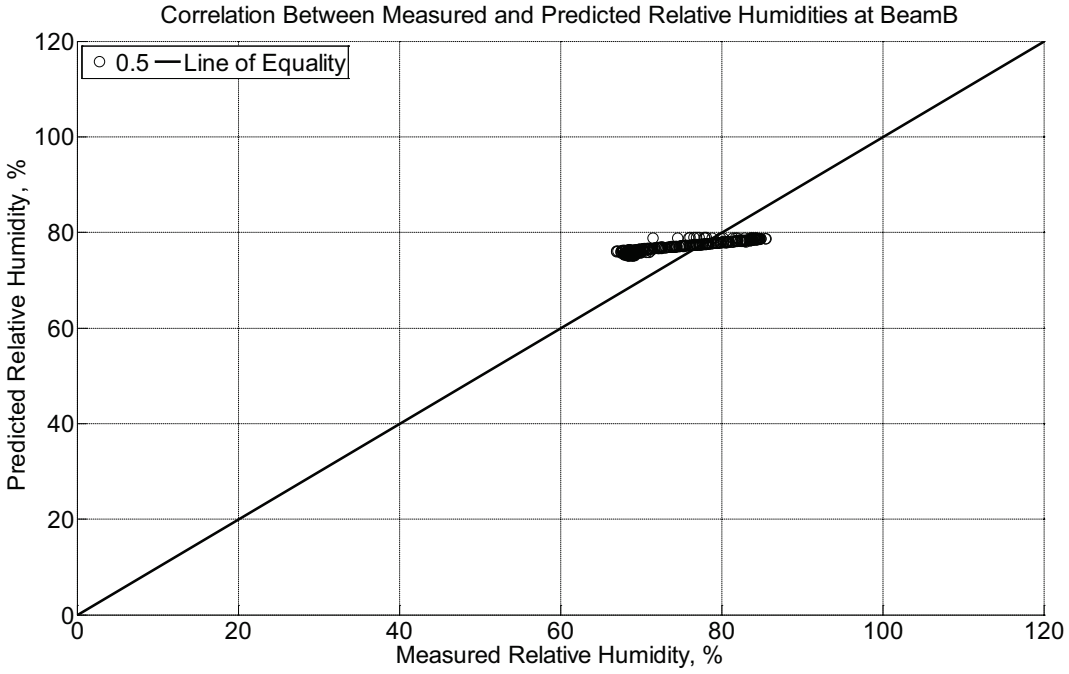

Figure B-63 Correlation between measured and predicted relative humidity values 0.5 inches (12.7 mm) from the surface of a modulus of rupture beam (labeled B) located inside

an environmentally controlled room (50% RH, 23 ºC) and a heating oven (65 ºC) between June 24, 2014, through July 2, 2014.

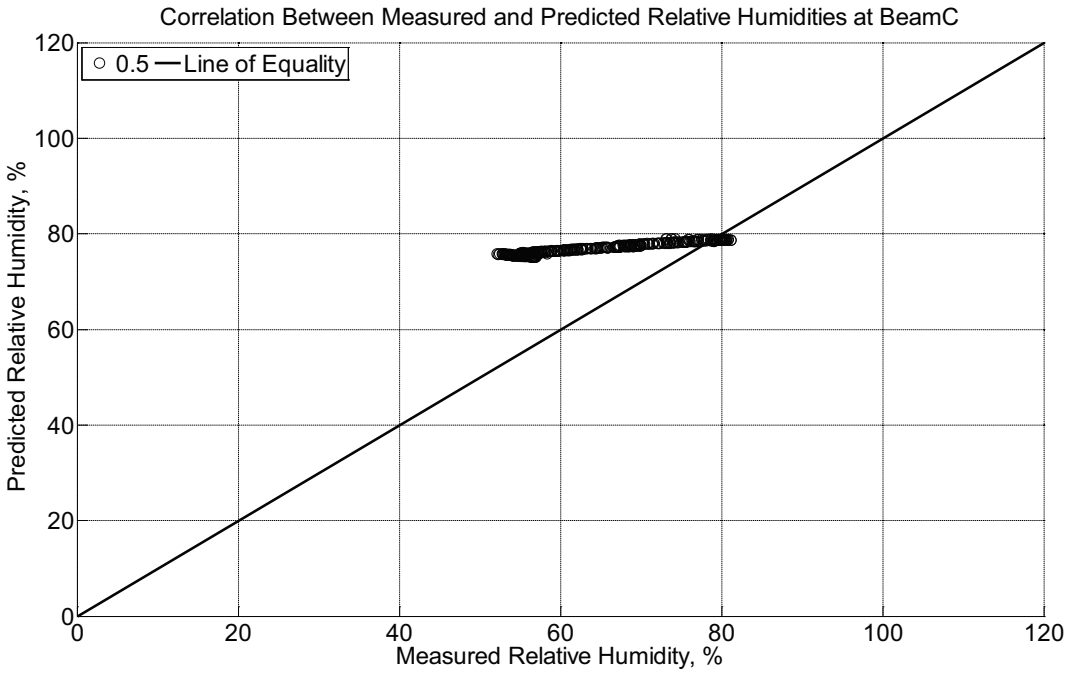

Figure B-64 Correlation between measured and predicted relative humidity values 0.5 inches (12.7 mm) from the surface of a modulus of rupture beam (labeled C) located inside an environmentally controlled room (50% RH, 23 ºC) and a heating oven (65 ºC) between June 24, 2014, through July 2, 2014.

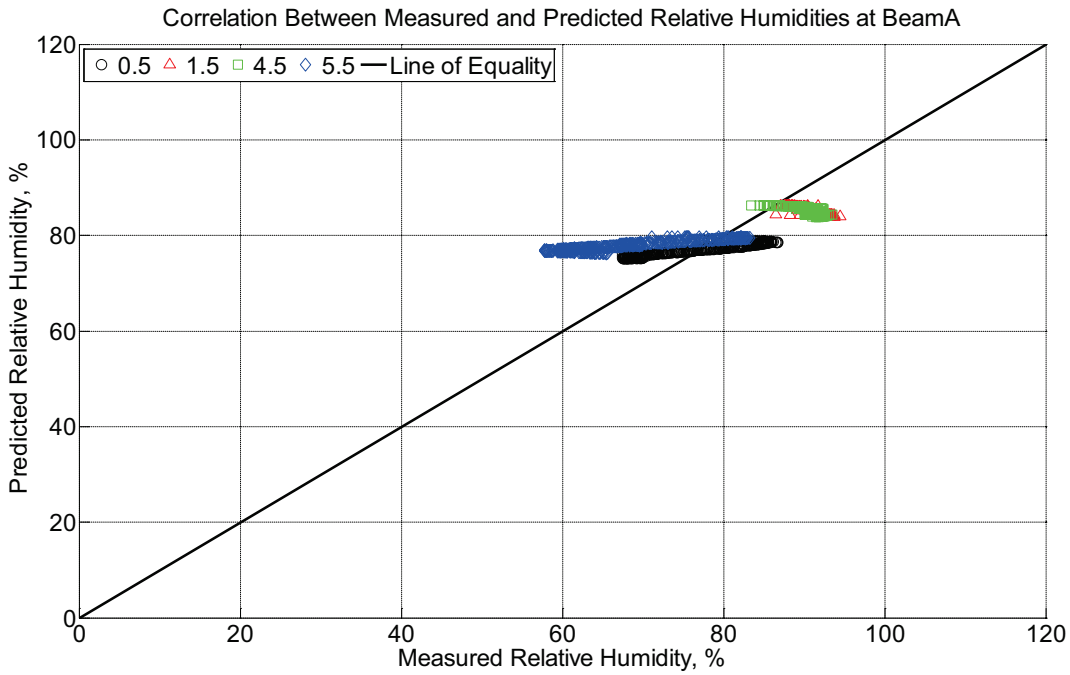

Figure B-65 Correlation between measured and predicted relative humidity values 0.5 inches (12.7 mm), 1.5 inches (38.1 mm), 4.5 inches (114.3 mm), and 5.5 inches (139.7 mm) from the surface of a modulus of rupture beam (labeled A) located inside an environmentally controlled room (50% RH, 23°C) and a heating oven (65°C) between June 24, 2014, through July 2, 2014.

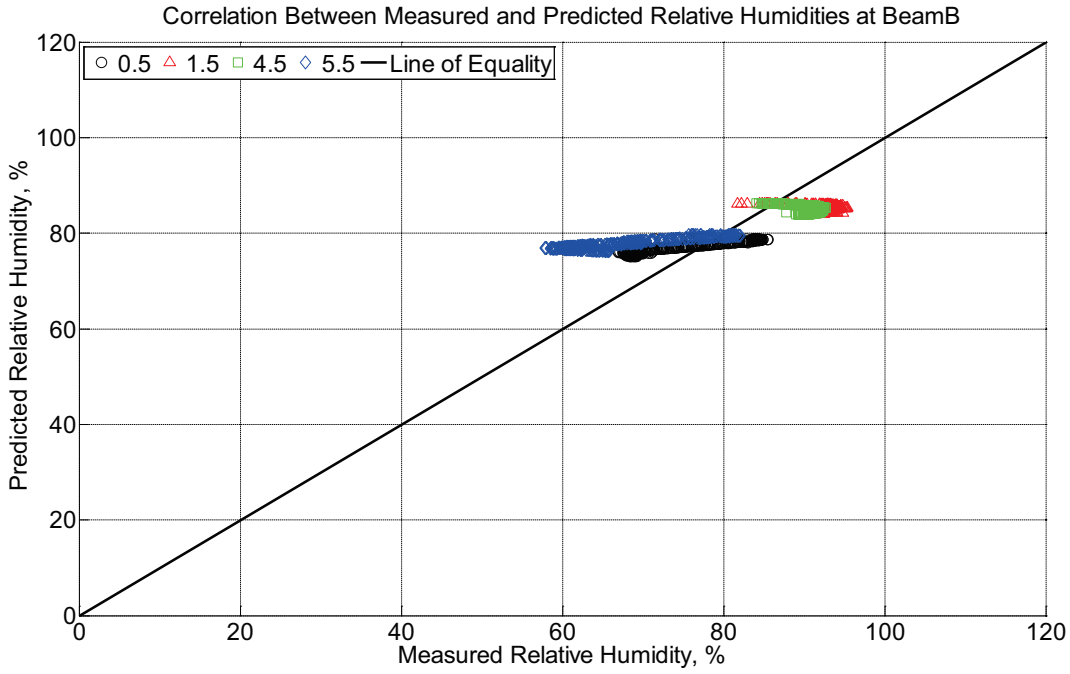

Figure B-66 Correlation between measured and predicted relative humidity values 0.5

inches (12.7 mm), 1.5 inches (38.1 mm), 4.5 inches (114.3 mm), and 5.5 inches (139.7 mm) from the surface of a modulus of rupture beam (labeled B) located inside an environmentally controlled room (50% RH, 23 ºC) and a heating oven (65 ºC) between June 24, 2014, through July 2, 2014.

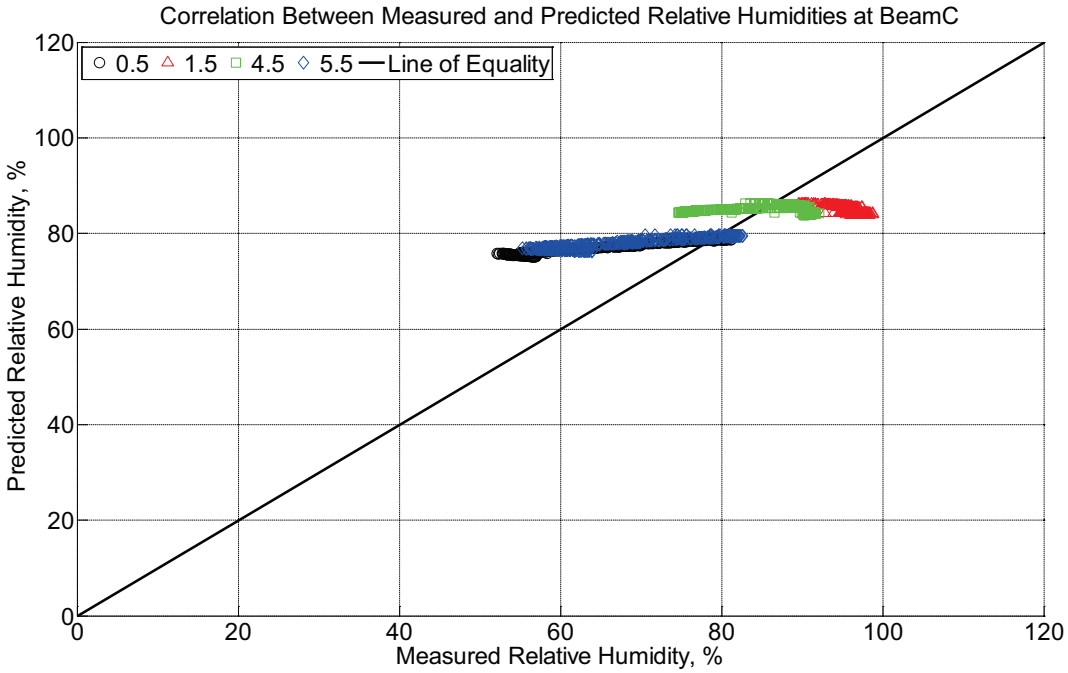

Figure B-67 between measured and predicted relative humidity values 0.5 inches (12.7 mm), 1.5 inches (38.1 mm), 4.5 inches (114.3 mm), and 5.5 inches (139.7 mm) from the surface of a modulus of rupture beam (labeled C) located inside an environmentally controlled room (50% RH, 23 ºC) and a heating oven (65 ºC) between June 24, 2014, through July 2, 2014.

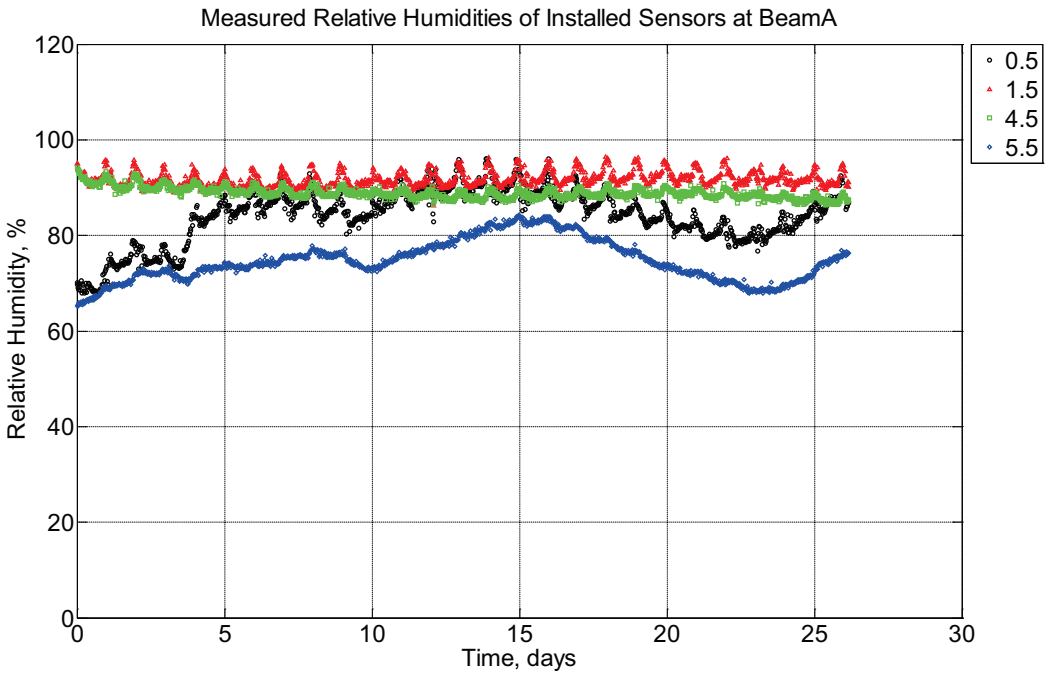

Figure B-68 Measured relative humidity at depths of 0.5 inches (12.7 mm), 1.5 inches (38.1 mm), 4.5 inches (114.3 mm), and 5.5 inches (139.7 mm) from the surface of a modulus of rupture beam (labeled A) installed in ballast in Rantoul, IL, between July 2, 2014, through July 28, 2014.

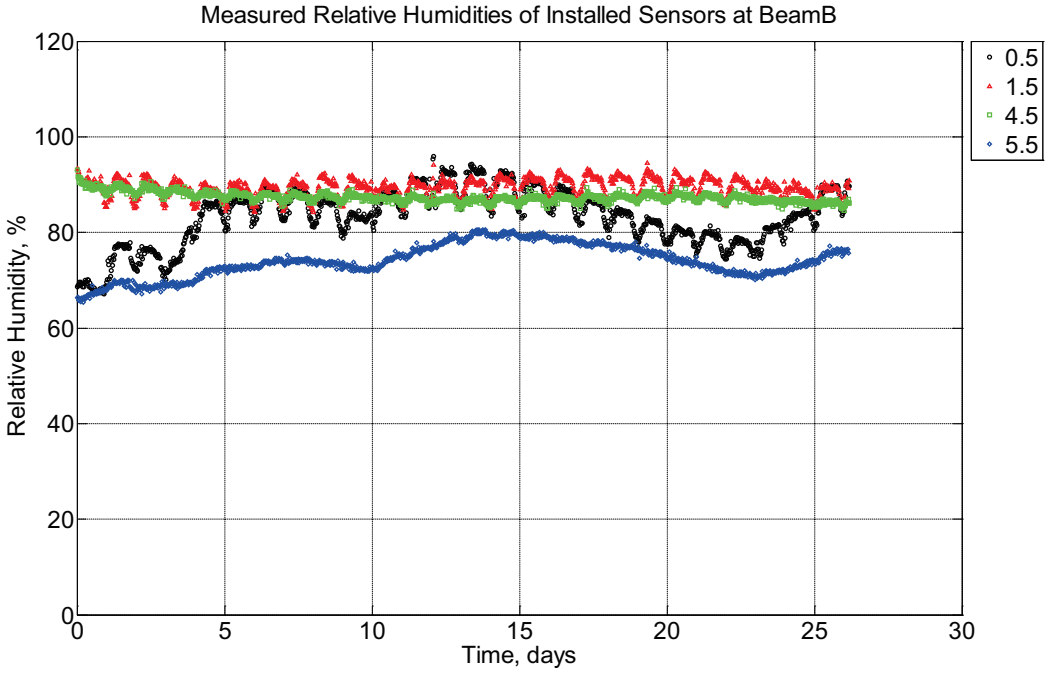

Figure B-69 Measured relative humidity at depths of 0.5 inches (12.7 mm), 1.5 inches (38.1 mm), 4.5 inches (114.3 mm), and 5.5 inches (139.7 mm) from the surface of a modulus of

rupture beam (labeled B) installed in ballast in Rantoul, IL, between July 2, 2014, through July 28, 2014.

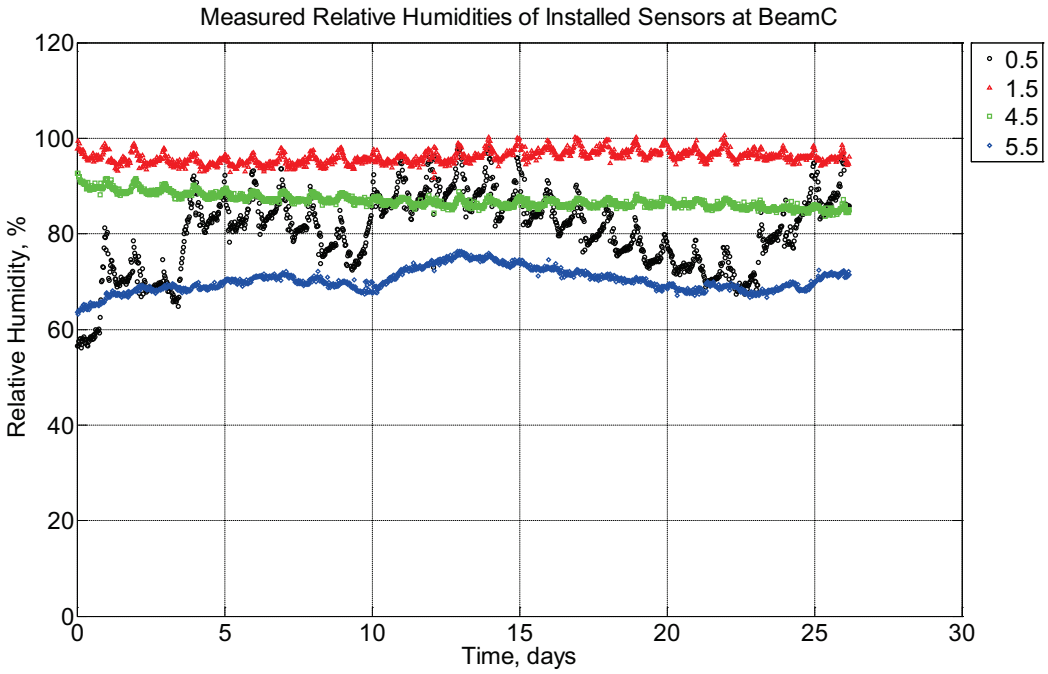

Figure B-70 Measured relative humidity at depths of 0.5 inches (12.7 mm), 1.5 inches (38.1 mm), 4.5 inches (114.3 mm), and 5.5 inches (139.7 mm) from the surface of a modulus of rupture beam (labeled C) installed in ballast in Rantoul, IL, between July 2, 2014, through July 28, 2014.

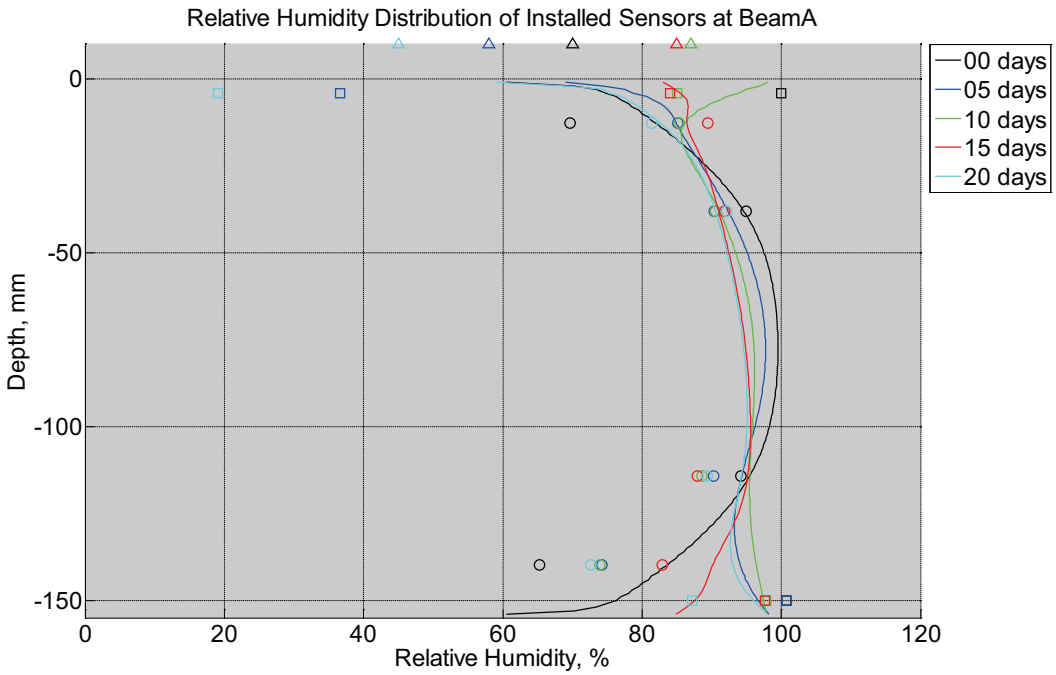

Figure B-71 Measured (markers) and modeled (continuous line) relative humidity profile distribution as a function of depth inside modulus of rupture beam (labeled A) installed in ballast in Rantoul, IL, between July 2, 2014, through July 28, 2014. Triangular markers denote relative humidity value from KTIP weather station, square markers denote measured relative humidity values from ballast, and circular markers denote measured relative humidity values inside concrete.

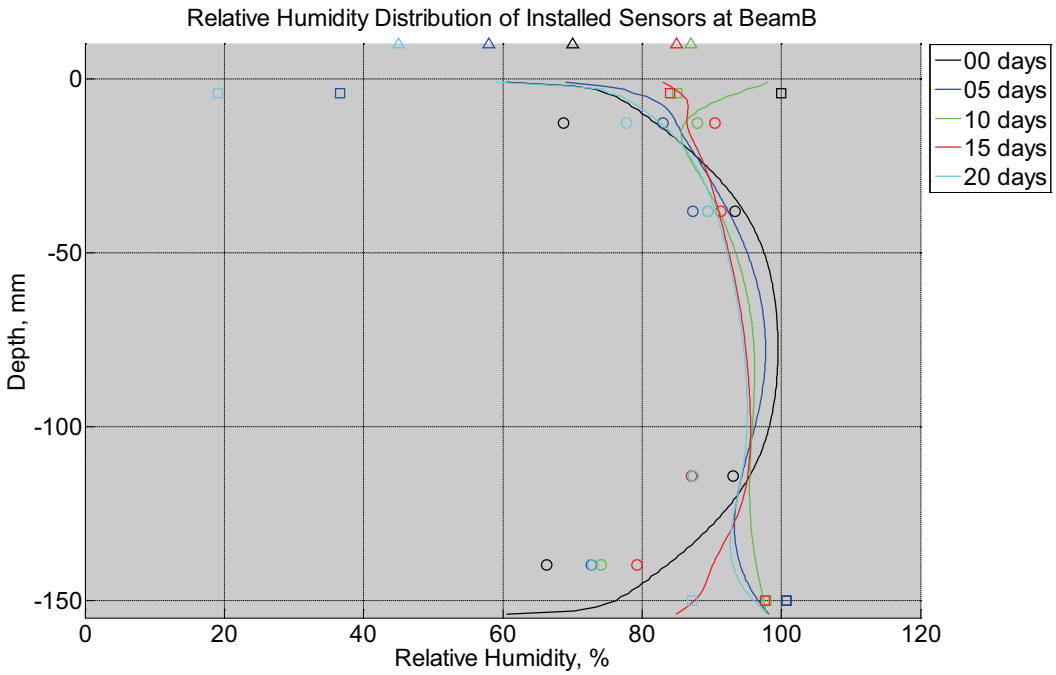

Figure B-72 Measured (markers) and modeled (continuous line) relative humidity profile distribution as a function of depth inside modulus of rupture beam (labeled B) installed in ballast in Rantoul, IL, between July 2, 2014, through July 28, 2014. Triangular markers denote relative humidity value from KTIP weather station, square markers denote measured relative humidity values from ballast, and circular markers denote measured relative humidity values inside concrete.

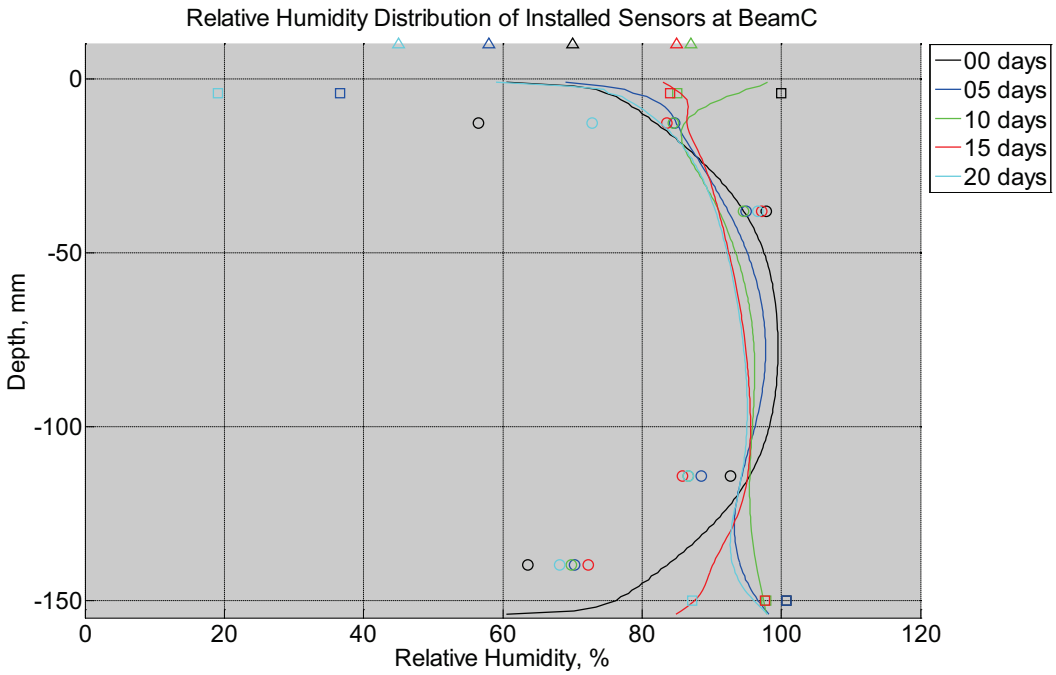

Figure B-73 Measured (markers) and modeled (continuous line) relative humidity profile distribution as a function of depth inside modulus of rupture beam (labeled C) installed in ballast in Rantoul, IL, between July 2, 2014, through July 28, 2014. Triangular markers denote relative humidity value from KTIP weather station, square markers denote measured relative humidity values from ballast, and circular markers denote measured relative humidity values inside concrete.

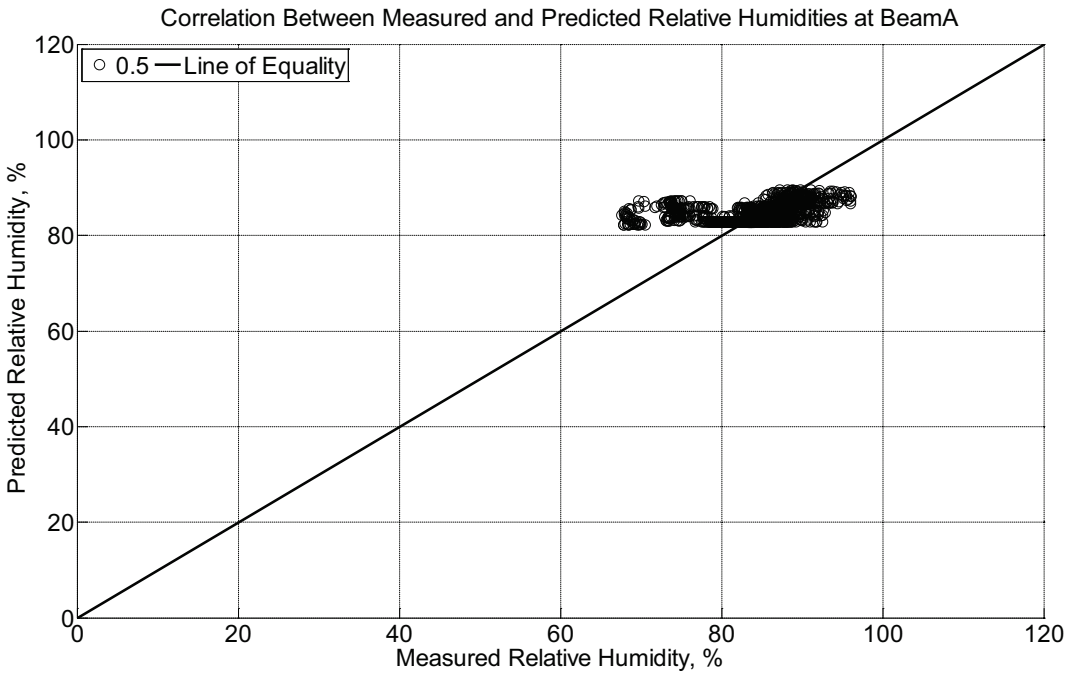

Figure B-74 Correlation between measured and predicted relative humidity values 0.5 inches (12.7 mm) from the surface of a modulus of rupture beam (labeled A) installed in ballast in Rantoul, IL, between July 2, 2014, through July 28, 2014.

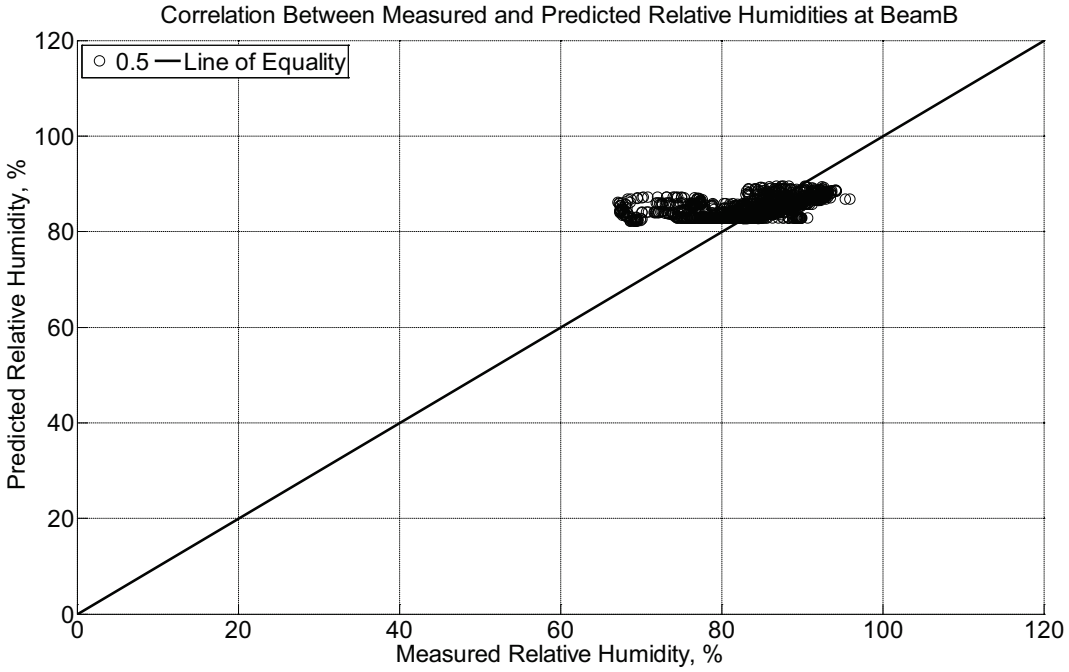

Figure B-75 Correlation between measured and predicted relative humidity values 0.5

inches (12.7 mm) from the surface of a modulus of rupture beam (labeled B) installed in ballast in Rantoul, IL, between July 2, 2014, through July 28, 2014.

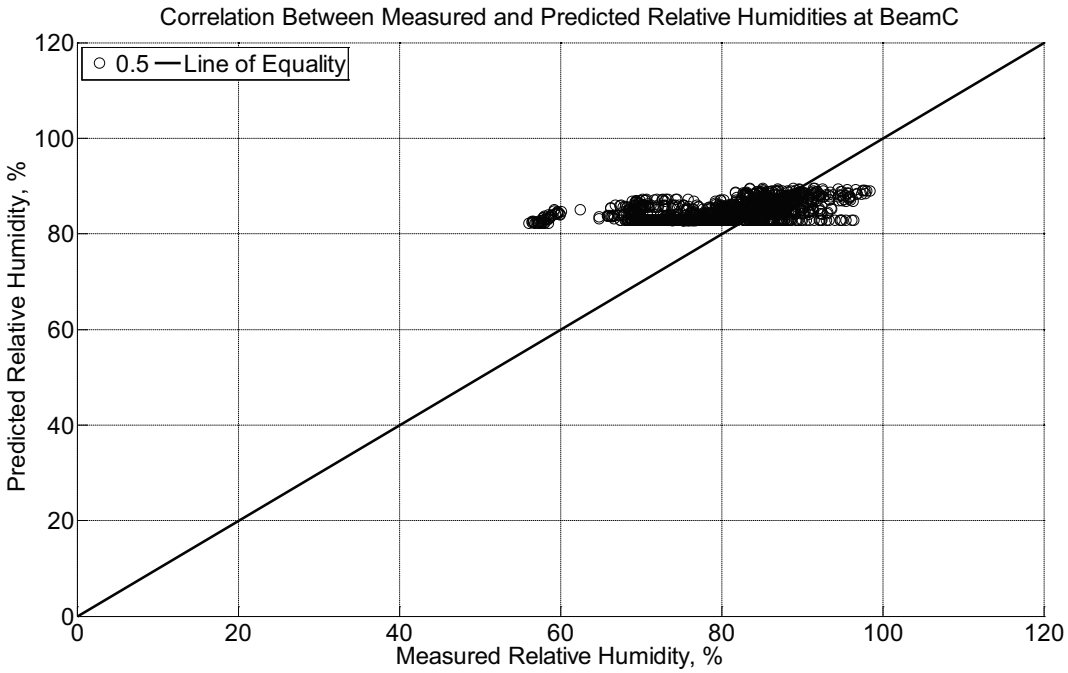

Figure B-76 Correlation between measured and predicted relative humidity values 0.5 inches (12.7 mm) from the surface of a modulus of rupture beam (labeled C) installed in ballast in Rantoul, IL, between July 2, 2014, through July 28, 2014.

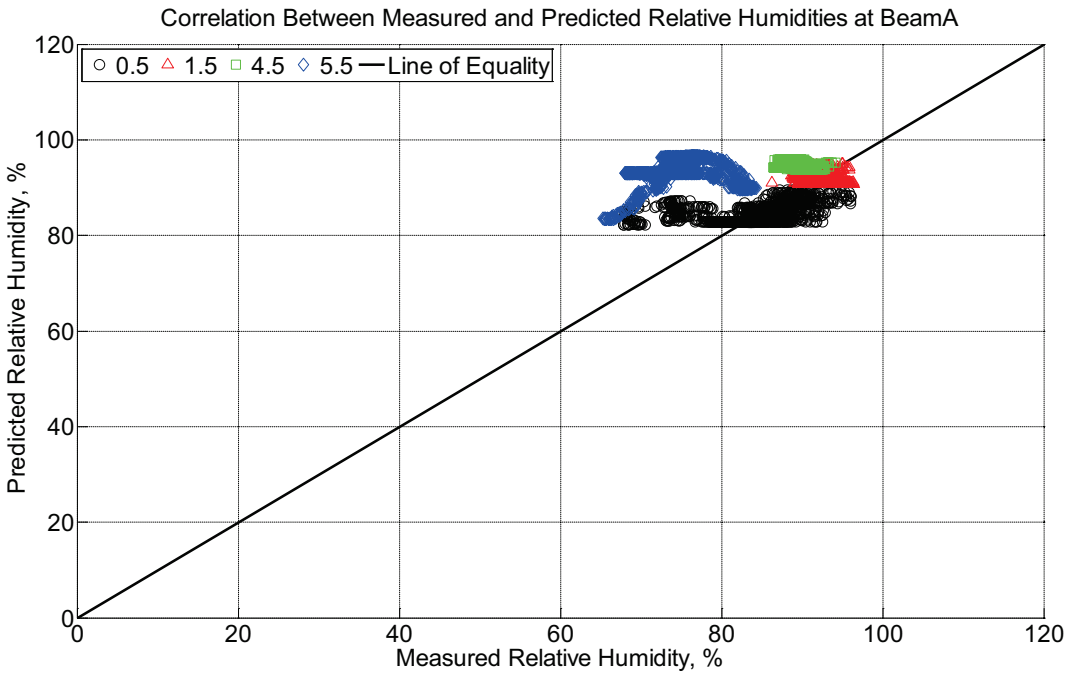

Figure B-77 Correlation between measured and predicted relative humidity values 0.5 inches (12.7 mm), 1.5 inches (38.1 mm), 4.5 inches (114.3 mm), and 5.5 inches (139.7 mm) from the surface of a modulus of rupture beam (labeled A) installed in ballast in Rantoul, IL, between July 2, 2014, through July 28, 2014.

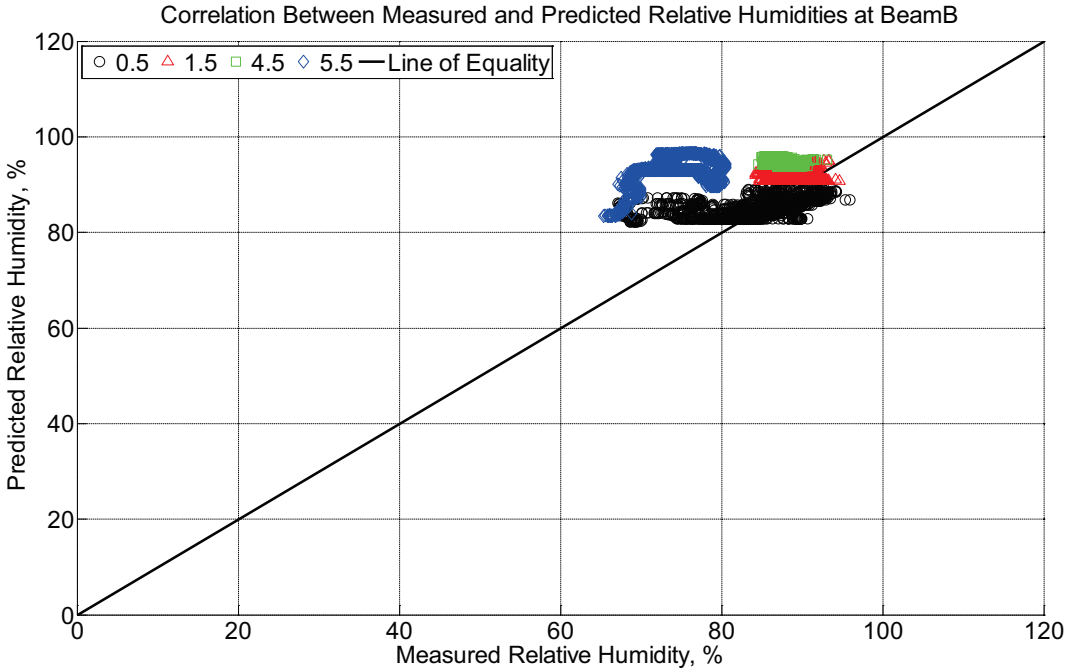

Figure B-78 Correlation between measured and predicted relative humidity values 0.5 inches (12.7 mm), 1.5 inches (38.1 mm), 4.5 inches (114.3 mm), and 5.5 inches (139.7 mm)

from the surface of a modulus of rupture beam (labeled B) installed in ballast in Rantoul, IL, between July 2, 2014, through July 28, 2014.

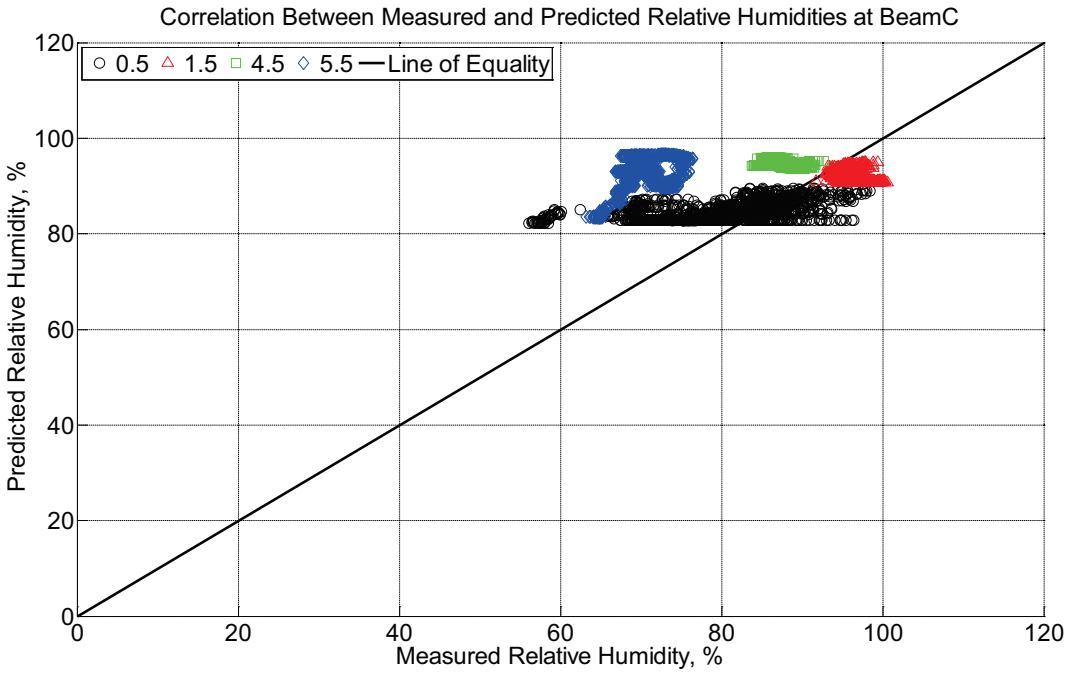

Figure B-79 Correlation between measured and predicted relative humidity values 0.5 inches (12.7 mm), 1.5 inches (38.1 mm), 4.5 inches (114.3 mm), and 5.5 inches (139.7 mm) from the surface of a modulus of rupture beam (labeled C) installed in ballast in Rantoul, IL, between July 2, 2014, through July 28, 2014.

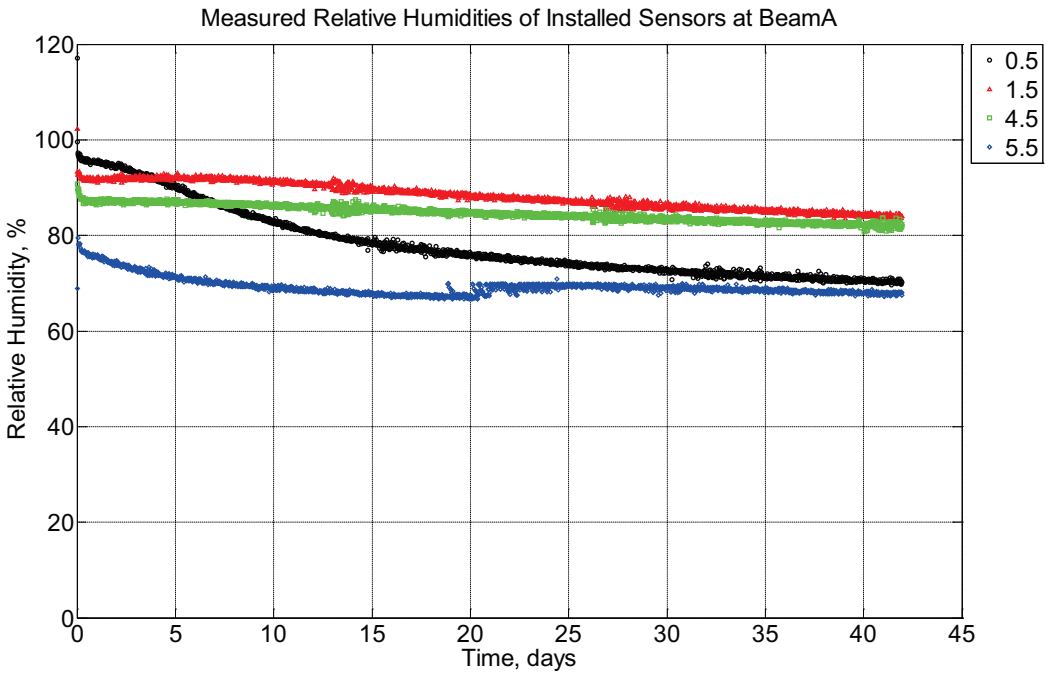

Figure B-80 Measured relative humidity at depths of 0.5 inches (12.7 mm), 1.5 inches (38.1 mm), 4.5 inches (114.3 mm), and 5.5 inches (139.7 mm) from the surface of a modulus of rupture beam (labeled A) located inside an environmentally controlled room (50% RH, 23ºC) between July 29, 2014, through September 9, 2014.

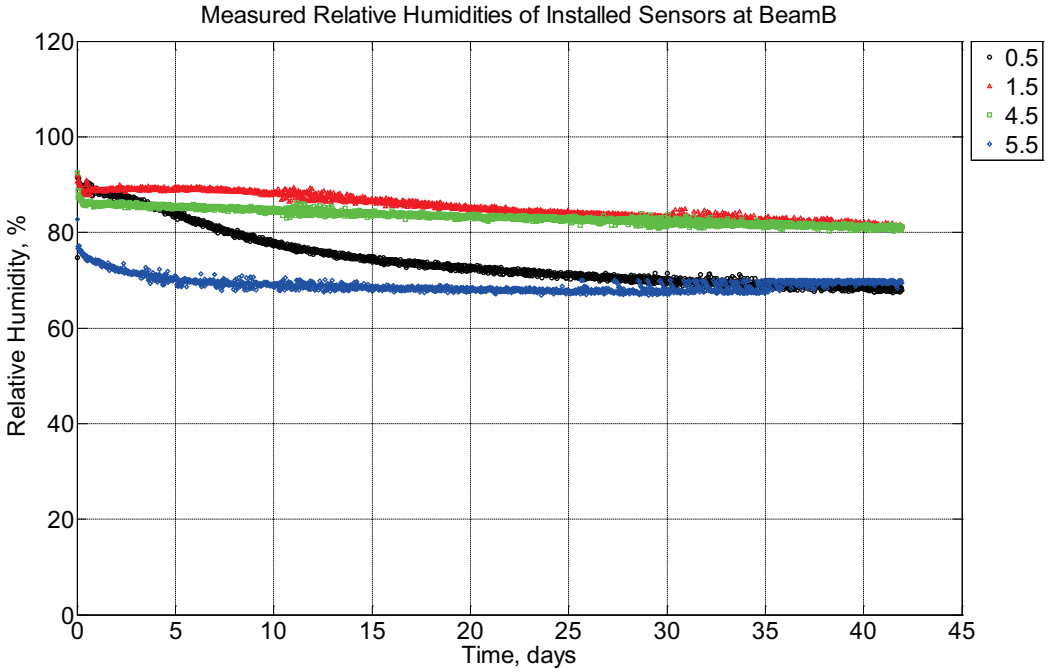

Figure B-81 Measured relative humidity at depths of 0.5 inches (12.7 mm), 1.5 inches (38.1 mm), 4.5 inches (114.3 mm), and 5.5 inches (139.7 mm) from the surface of a modulus of

rupture beam (labeled B) located inside an environmentally controlled room (50% RH, 23 °C) between July 29, 2014, through September 9, 2014.

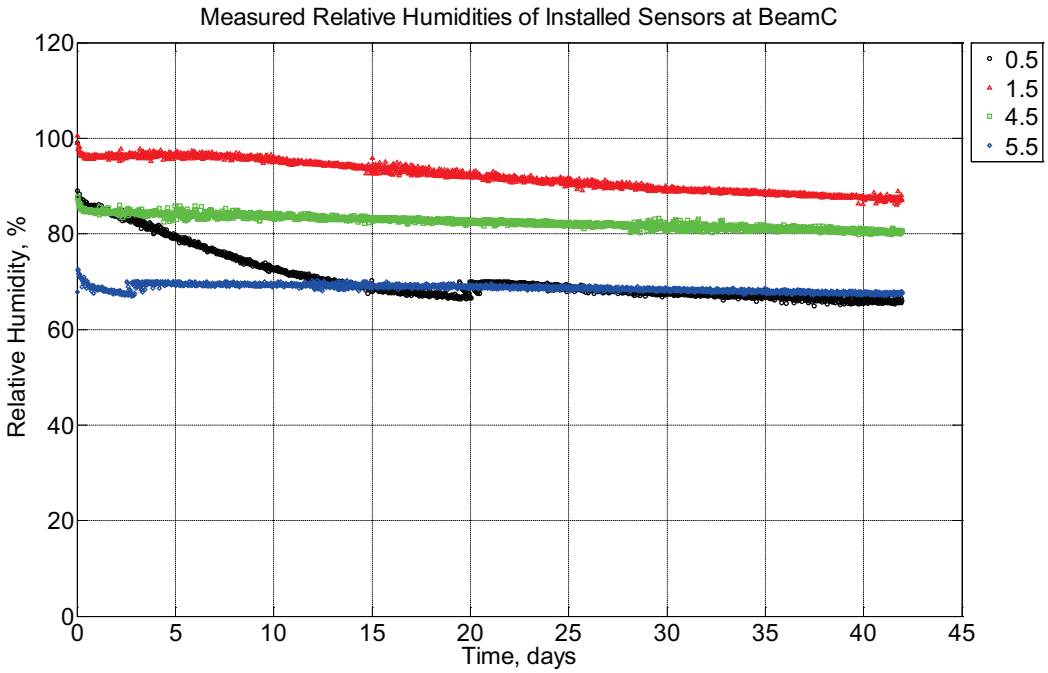

Figure B-82 Measured relative humidity at depths of 0.5 inches (12.7 mm), 1.5 inches (38.1 mm), 4.5 inches (114.3 mm), and 5.5 inches (139.7 mm) from the surface of a modulus of rupture beam (labeled C) located inside an environmentally controlled room (50% RH, 23 °C) between July 29, 2014, through September 9, 2014.

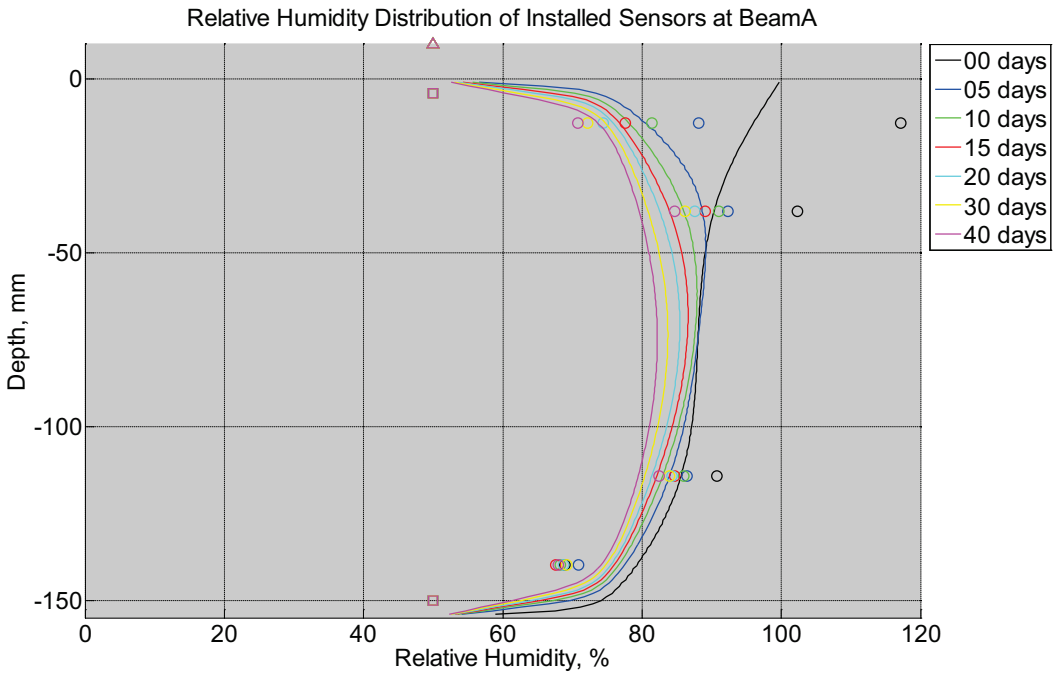

Figure B-83 Measured (markers) and modeled (continuous line) relative humidity profile distribution as a function of depth inside modulus of rupture beam (labeled A) located inside an environmentally controlled room (50% RH, 23 ºC) between July 29, 2014, through September 9, 2014. Triangular markers denote relative humidity value from control panel, square markers denote measured relative humidity values from ambient sensors, and circular markers denote measured relative humidity values inside concrete.

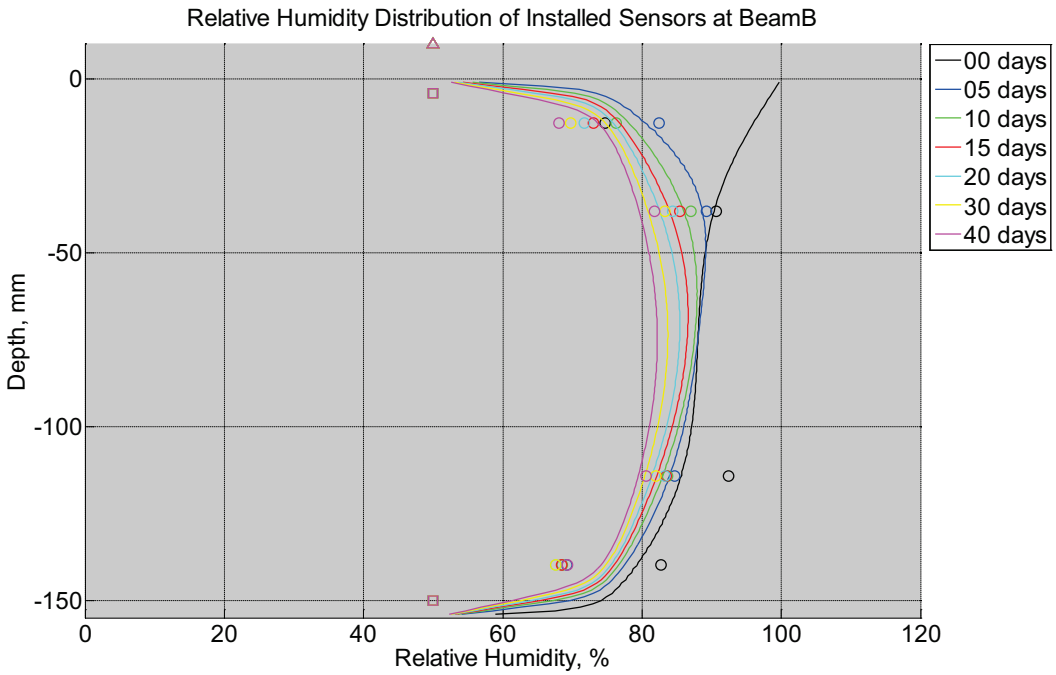

Figure B-84 Measured (markers) and modeled (continuous line) relative humidity profile distribution as a function of depth inside modulus of rupture beam (labeled B) located inside an environmentally controlled room (50% RH, 23 ºC) between July 29, 2014, through September 9, 2014. Triangular markers denote relative humidity value from control panel, square markers denote measured relative humidity values from ambient sensors, and circular markers denote measured relative humidity values inside concrete.

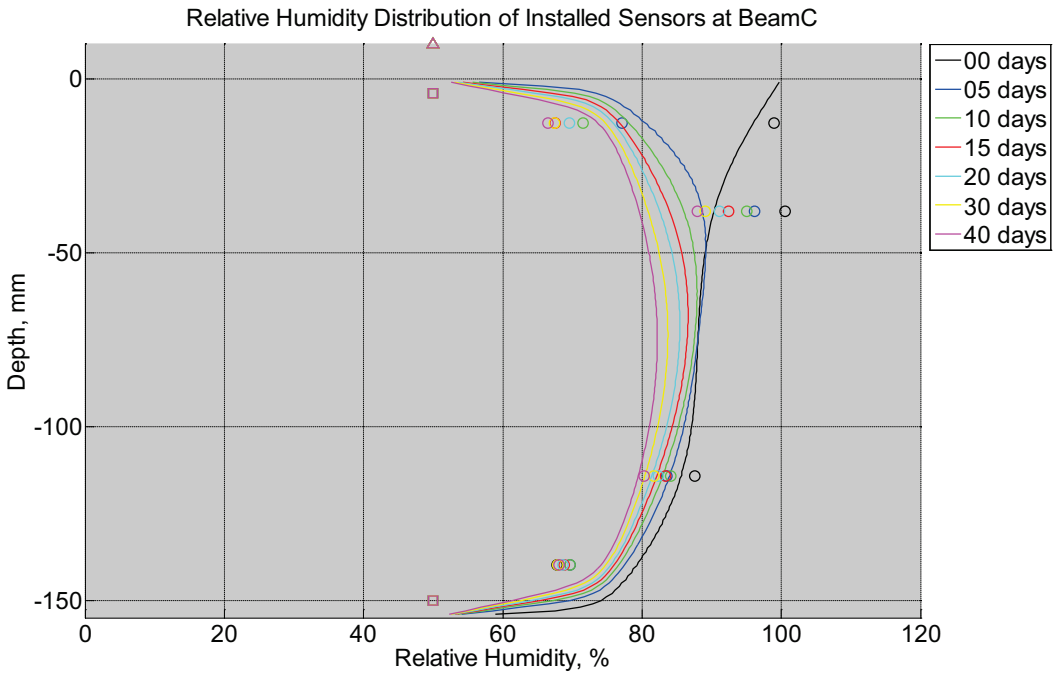

Figure B-85 Measured (markers) and modeled (continuous line) relative humidity profile distribution as a function of depth inside modulus of rupture beam (labeled C) located inside an environmentally controlled room (50% RH, 23 ºC) between July 29, 2014, through September 9, 2014. Triangular markers denote relative humidity value from control panel, square markers denote measured relative humidity values from ambient sensors, and circular markers denote measured relative humidity values inside concrete.

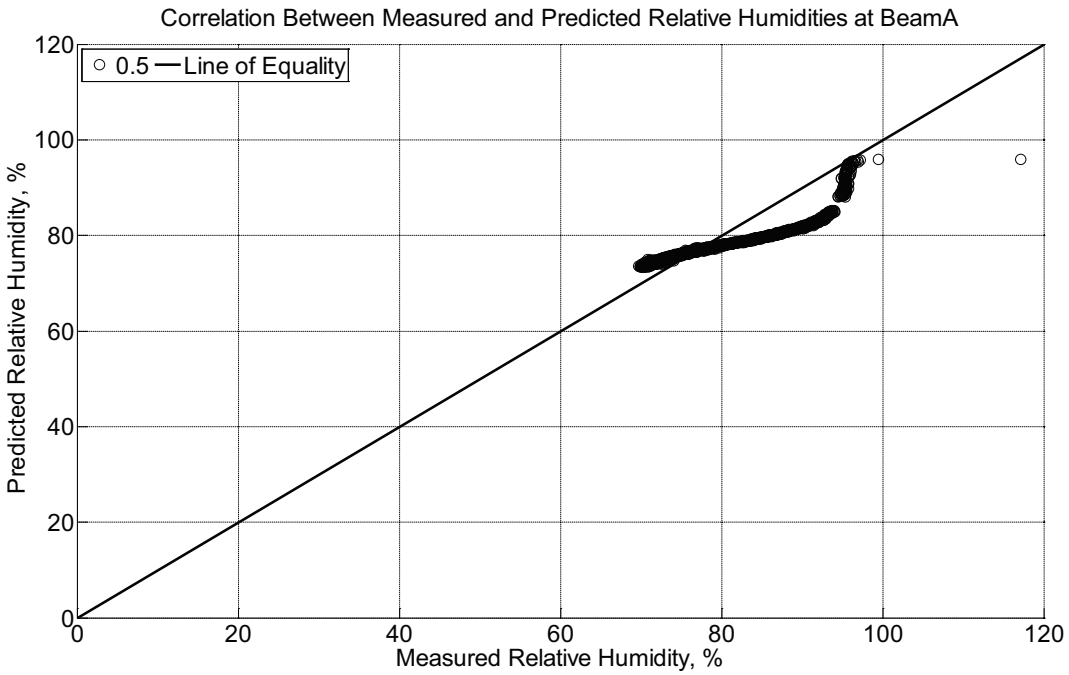

Figure B-86 Correlation between measured and predicted relative humidity values 0.5 inches (12.7 mm) from the surface of a modulus of rupture beam (labeled A) located inside an environmentally controlled room (50% RH, 23 ºC) between July 29, 2014, through September 9, 2014.

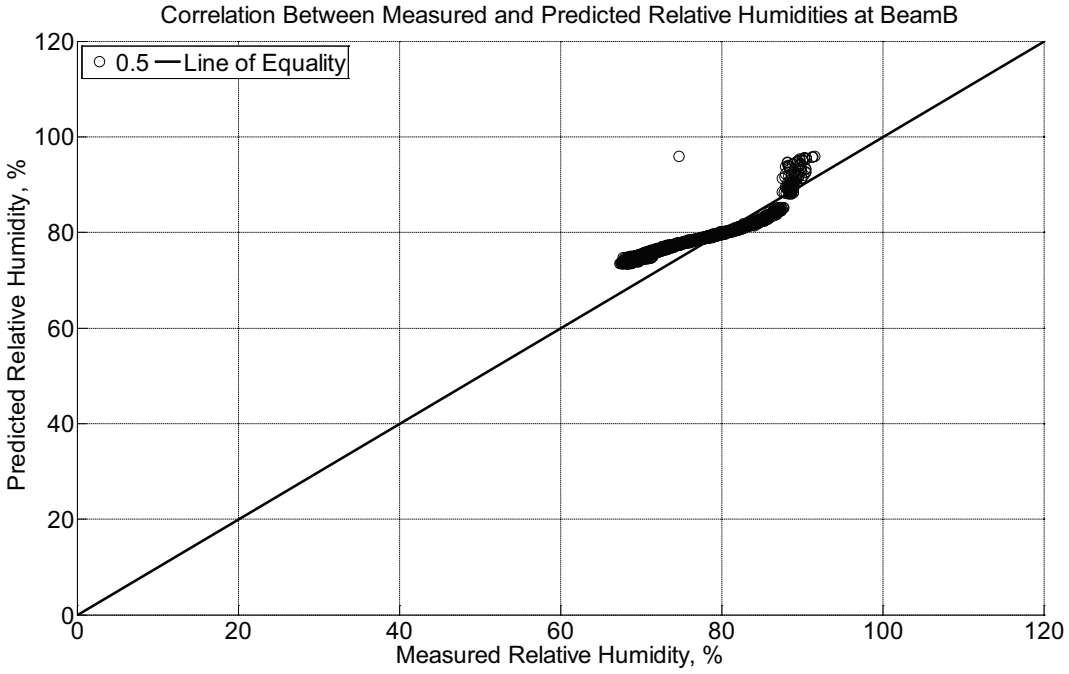

Figure B-87 Correlation between measured and predicted relative humidity values 0.5 inches (12.7 mm) from the surface of a modulus of rupture beam (labeled B) located inside

an environmentally controlled room (50% RH, 23 ºC) between July 29, 2014, through September 9, 2014.

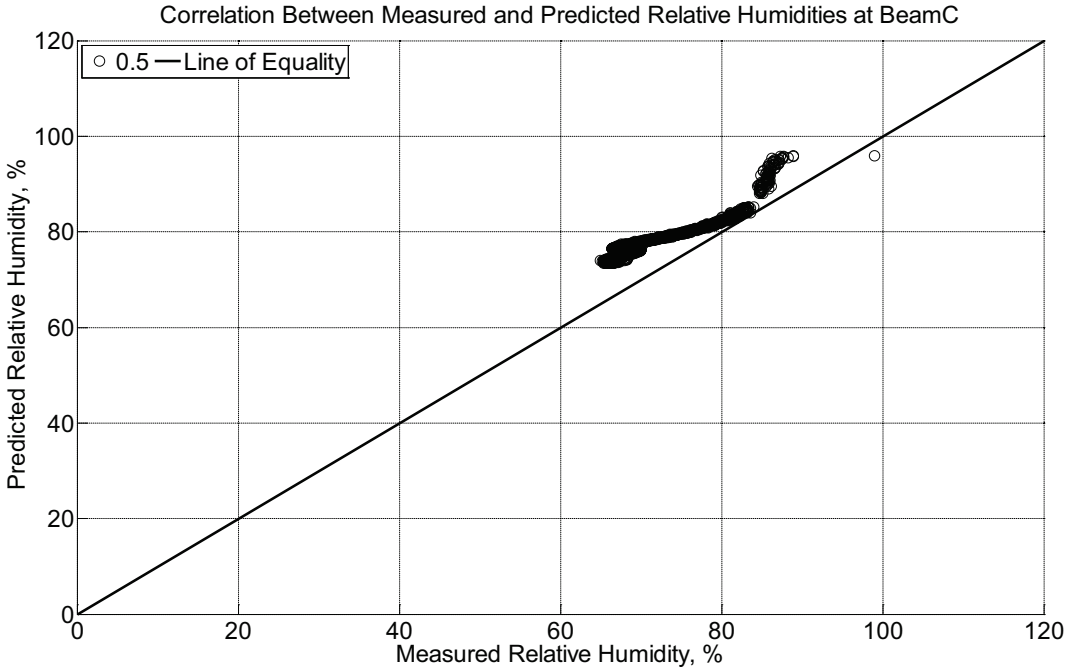

Figure B-88 Correlation between measured and predicted relative humidity values 0.5 inches (12.7 mm) from the surface of a modulus of rupture beam (labeled C) located inside an environmentally controlled room (50% RH, 23 ºC) between July 29, 2014, through September 9, 2014.

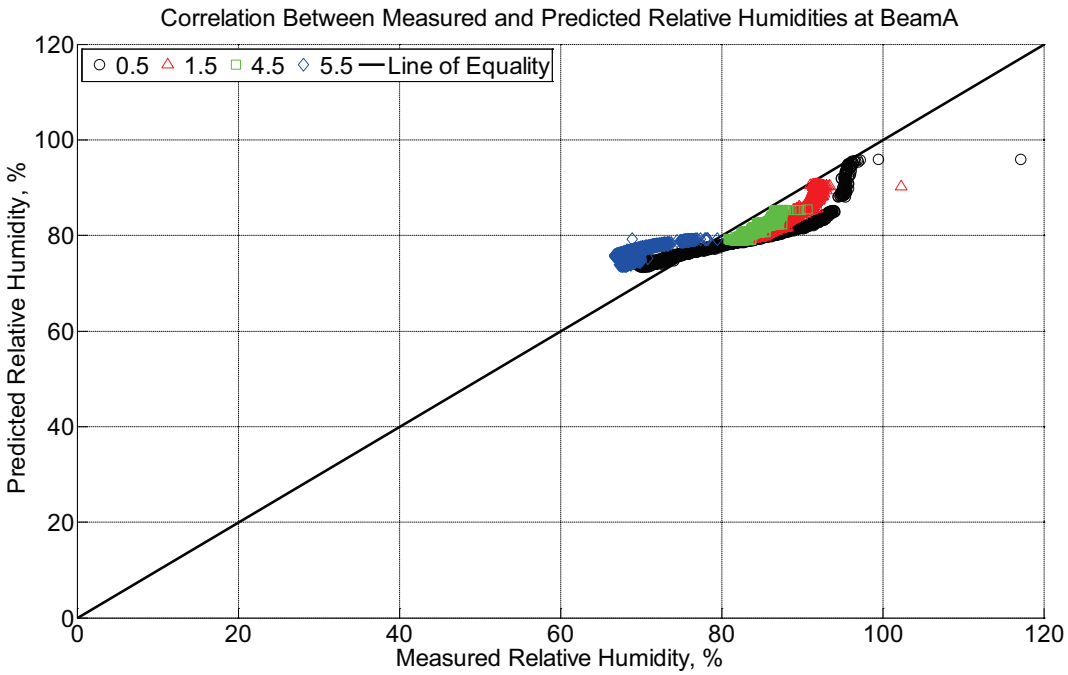

Figure B-89 Correlation between measured and predicted relative humidity values 0.5 inches (12.7 mm), 1.5 inches (38.1 mm), 4.5 inches (114.3 mm), and 5.5 inches (139.7 mm) from the surface of a modulus of rupture beam (labeled A) located inside an environmentally controlled room (50% RH, 23 ºC) between July 29, 2014, through September 9, 2014.

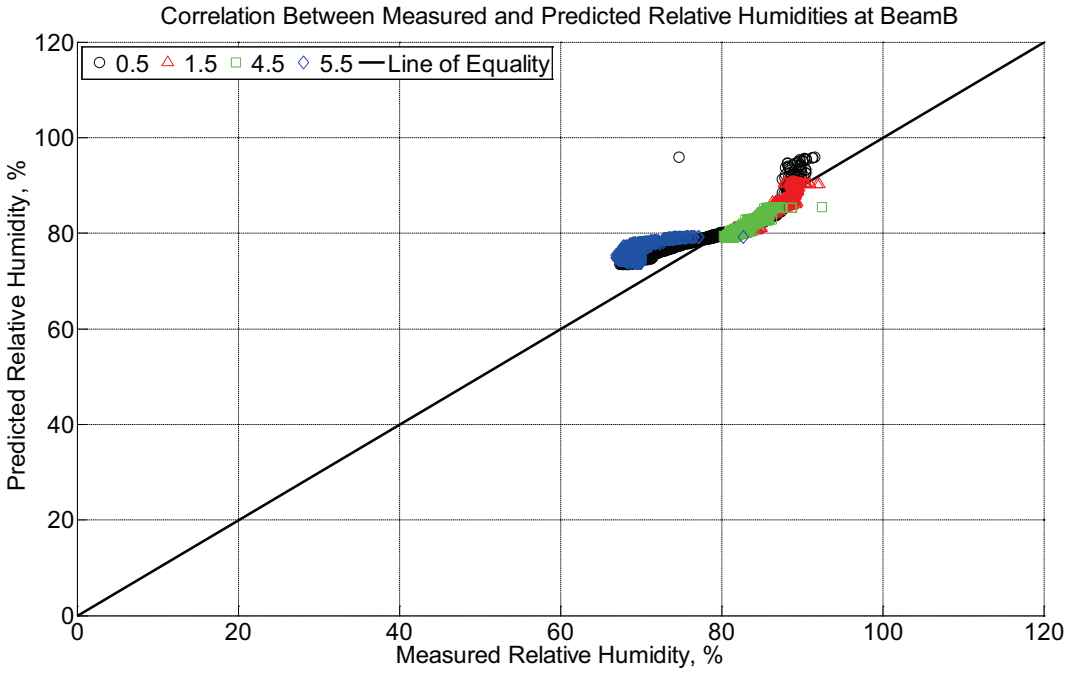

Figure B-90 Correlation between measured and predicted relative humidity values 0.5

inches (12.7 mm), 1.5 inches (38.1 mm), 4.5 inches (114.3 mm), and 5.5 inches (139.7 mm) from the surface of a modulus of rupture beam (labeled B) located inside an environmentally controlled room (50% RH, 23 ºC) between July 29, 2014, through September 9, 2014.

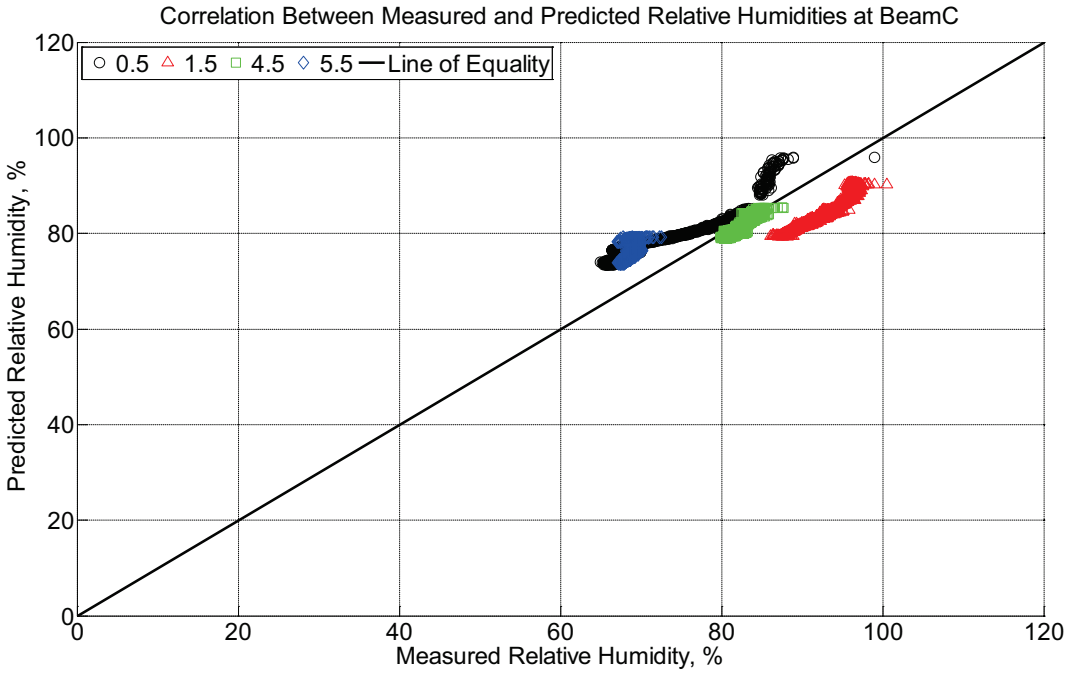

Figure B-91 Correlation between measured and predicted relative humidity values 0.5 inches (12.7 mm), 1.5 inches (38.1 mm), 4.5 inches (114.3 mm), and 5.5 inches (139.7 mm) from the surface of a modulus of rupture beam (labeled C) located inside an environmentally controlled room (50% RH, 23 ºC) between July 29, 2014, through September 9, 2014.

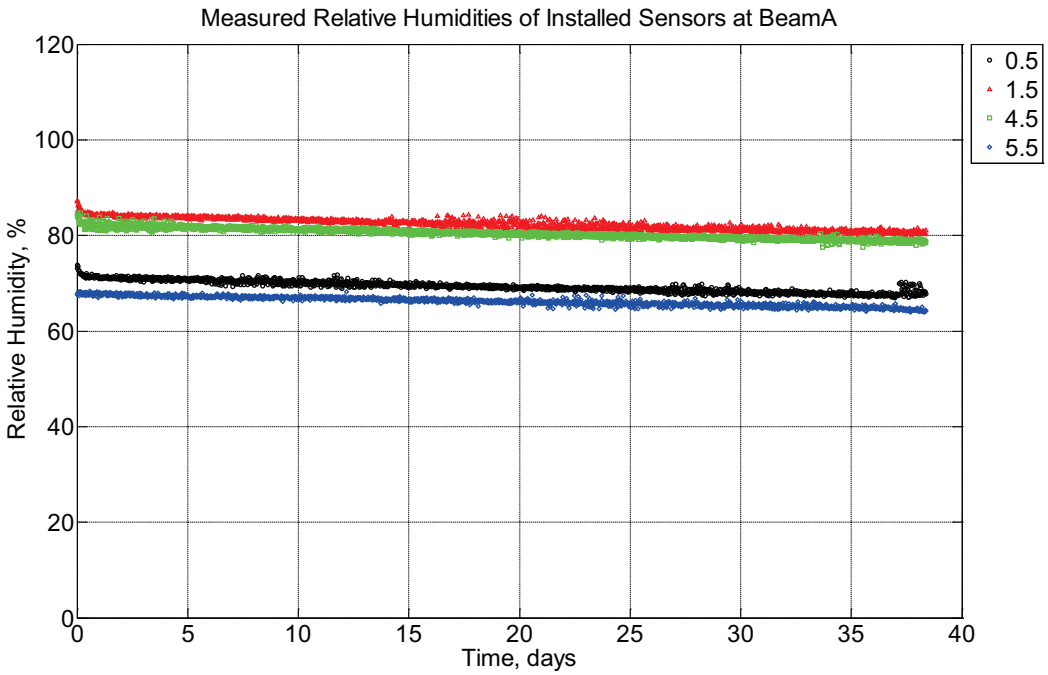

Figure B-92 Measured relative humidity at depths of 0.5 inches (12.7 mm), 1.5 inches (38.1 mm), 4.5 inches (114.3 mm), and 5.5 inches (139.7 mm) from the surface of a modulus of rupture beam (labeled A) located inside an environmentally controlled room (50% RH, 23 ºC) between September 9, 2014, through October 17, 2014.

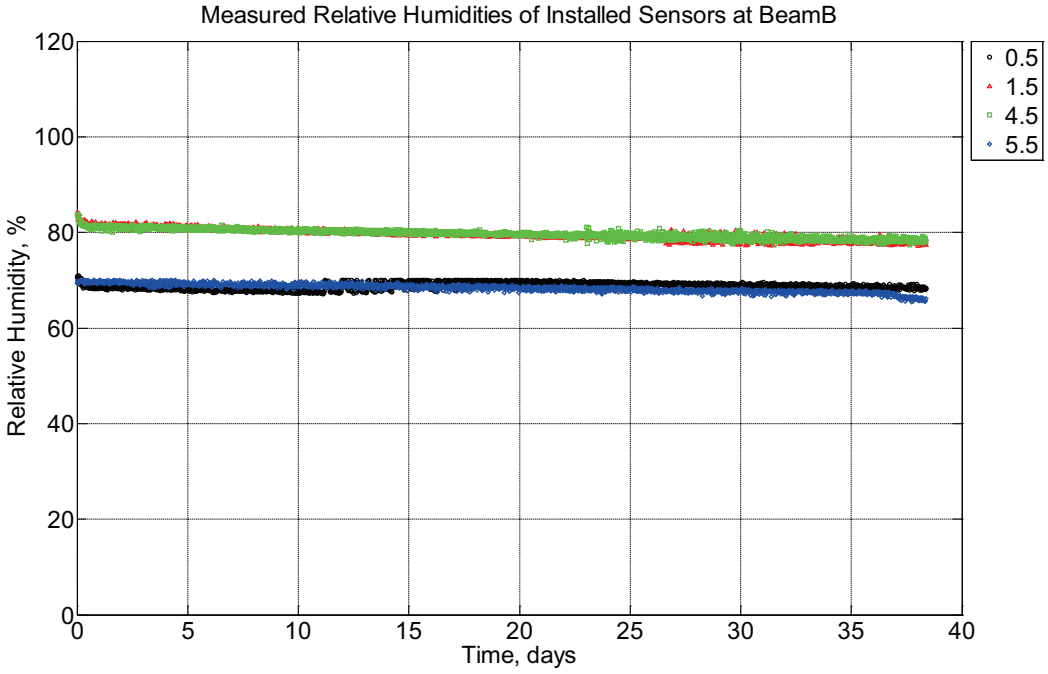

Figure B-93 Measured relative humidity at depths of 0.5 inches (12.7 mm), 1.5 inches (38.1 mm), 4.5 inches (114.3 mm), and 5.5 inches (139.7 mm) from the surface of a modulus of

rupture beam (labeled B) located inside an environmentally controlled room (50% RH, 23 °C) between September 9, 2014, through October 17, 2014.

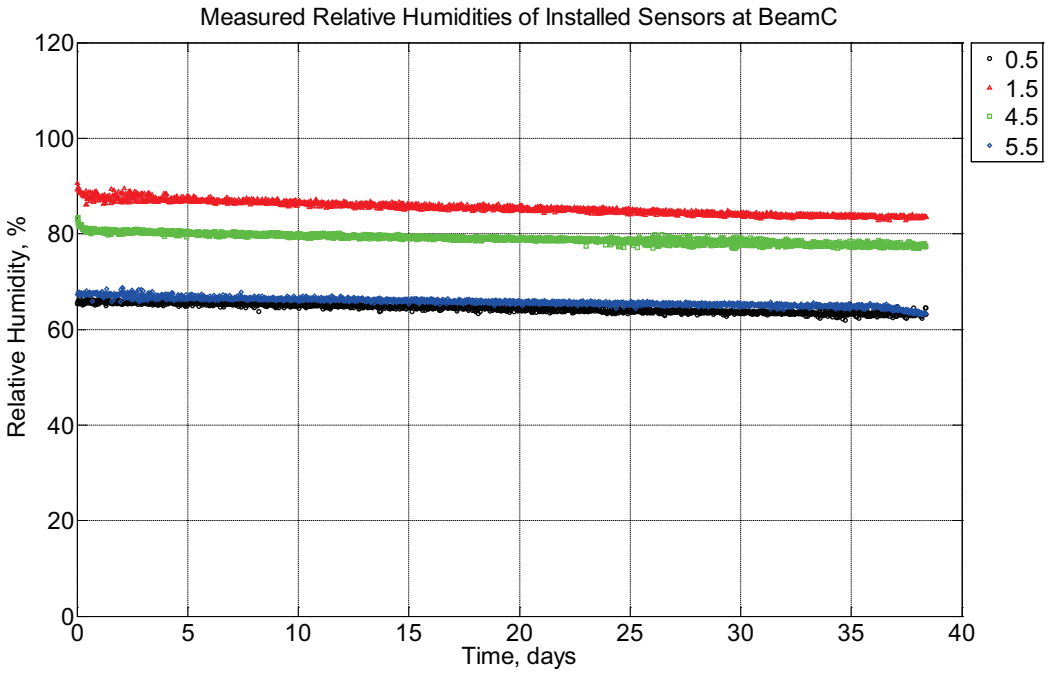

Figure B-94 Measured relative humidity at depths of 0.5 inches (12.7 mm), 1.5 inches (38.1 mm), 4.5 inches (114.3 mm), and 5.5 inches (139.7 mm) from the surface of a modulus of rupture beam (labeled C) located inside an environmentally controlled room (50% RH, 23 °C) between September 9, 2014, through October 17, 2014.

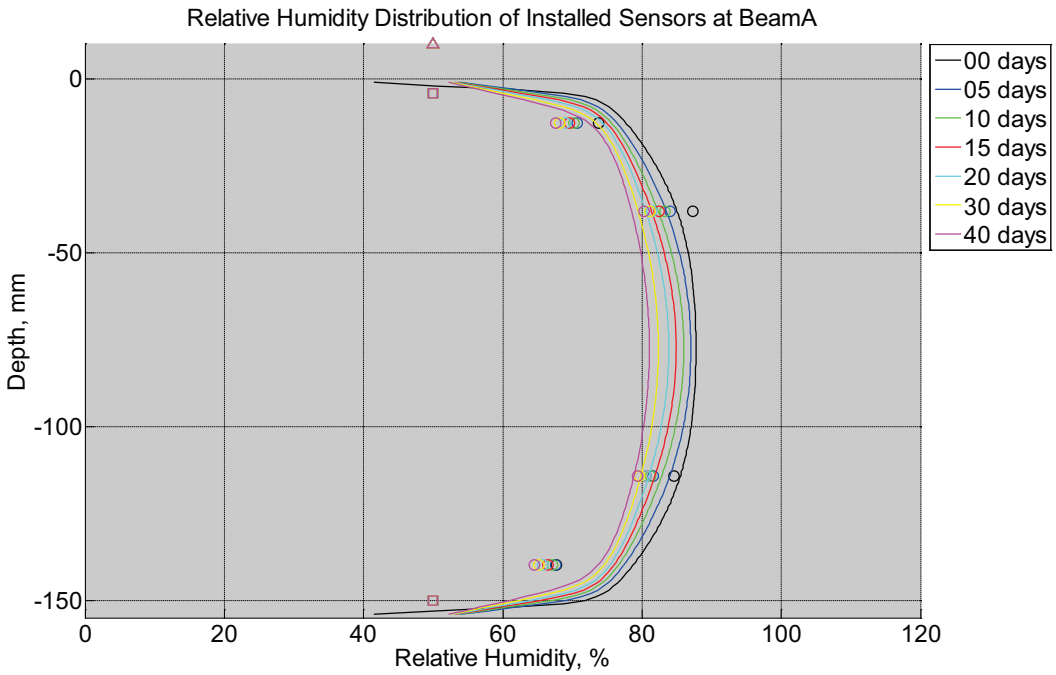

Figure B-95 Measured (markers) and modeled (continuous line) relative humidity profile distribution as a function of depth inside modulus of rupture beam (labeled A) located inside an environmentally controlled room (50% RH, 23 ºC) between September 9, 2014, through October 17, 2014. Triangular markers denote relative humidity value from control panel, square markers denote measured relative humidity values from ambient sensors, and circular markers denote measured relative humidity values inside concrete.

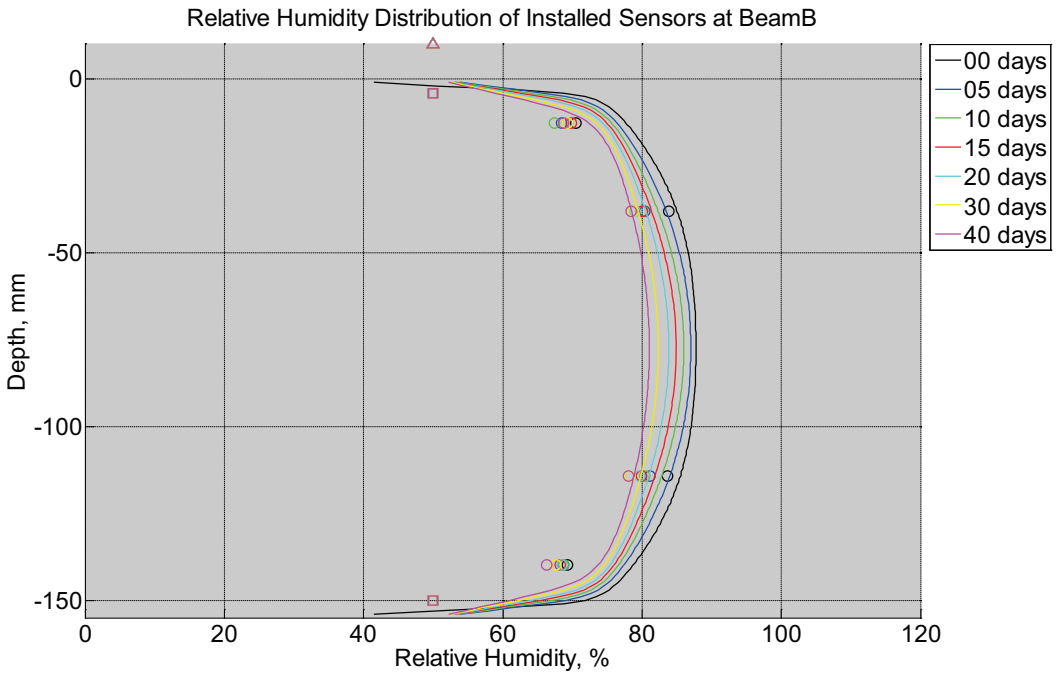

Figure B-96 Measured (markers) and modeled (continuous line) relative humidity profile distribution as a function of depth inside modulus of rupture beam (labeled B) located inside an environmentally controlled room (50% RH, 23 ºC) between September 9, 2014, through October 17, 2014. Triangular markers denote relative humidity value from control panel, square markers denote measured relative humidity values from ambient sensors, and circular markers denote measured relative humidity values inside concrete.

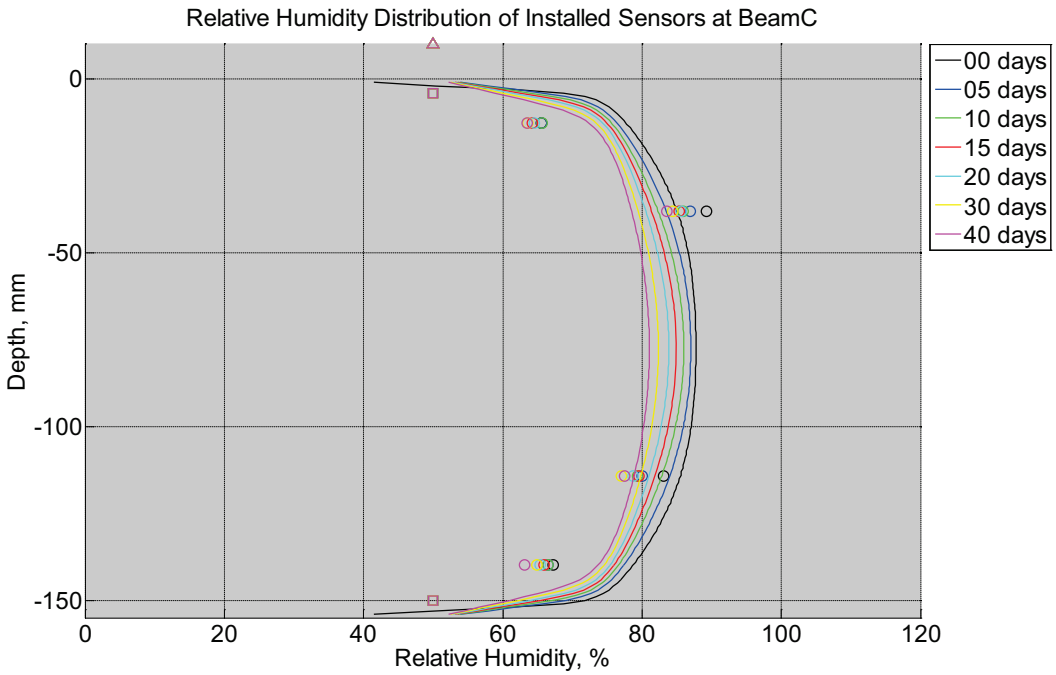

Figure B-97 Measured (markers) and modeled (continuous line) relative humidity profile distribution as a function of depth inside modulus of rupture beam (labeled C) located inside an environmentally controlled room (50% RH, 23 ºC) between September 9, 2014, through October 17, 2014. Triangular markers denote relative humidity value from control panel, square markers denote measured relative humidity values from ambient sensors, and circular markers denote measured relative humidity values inside concrete.

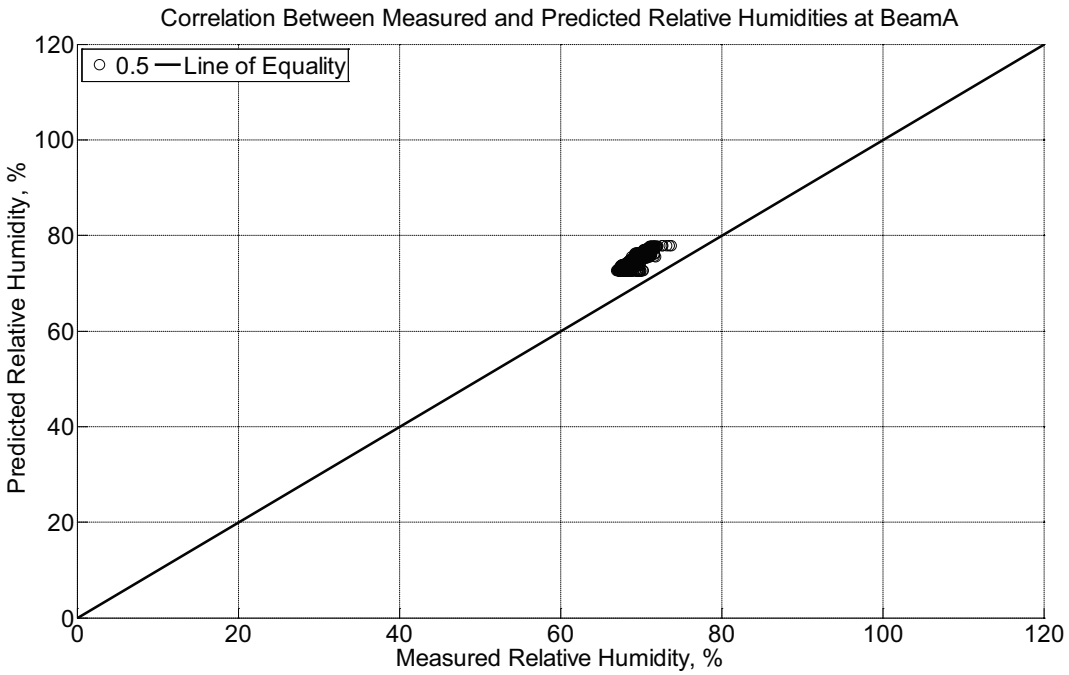

Figure B-98 Correlation between measured and predicted relative humidity values 0.5 inches (12.7 mm) from the surface of a modulus of rupture beam (labeled A) located inside an environmentally controlled room (50% RH, 23 ºC) between September 9, 2014, through October 17, 2014.

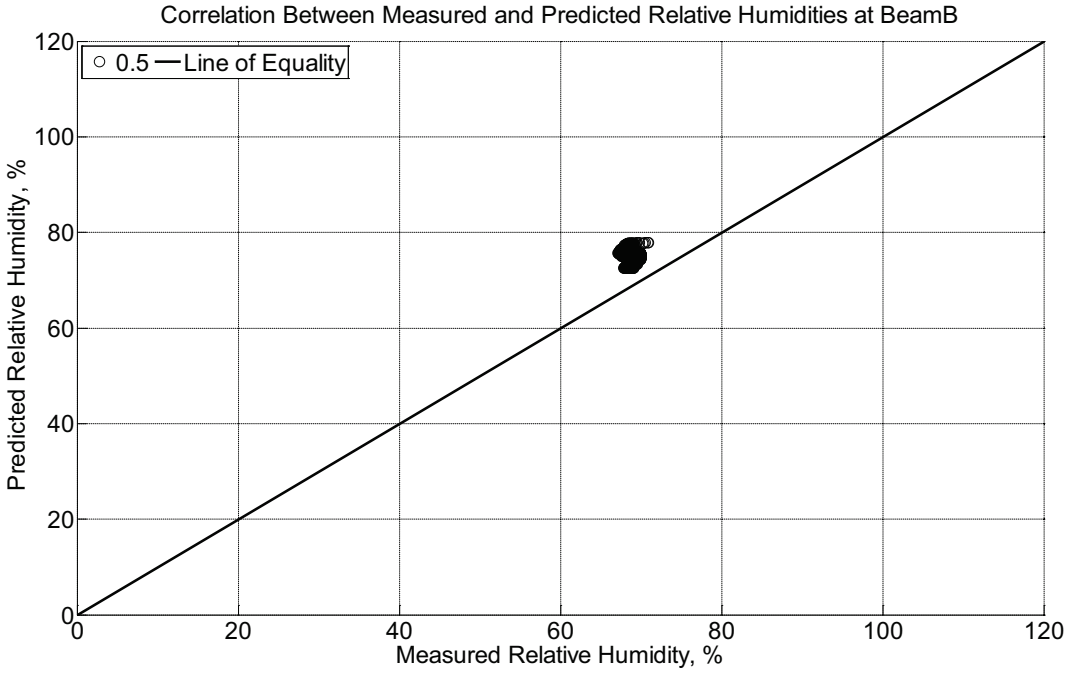

Figure B-99 Correlation between measured and predicted relative humidity values 0.5 inches (12.7 mm) from the surface of a modulus of rupture beam (labeled B) located inside

an environmentally controlled room (50% RH, 23 ºC) between September 9, 2014, through October 17, 2014.

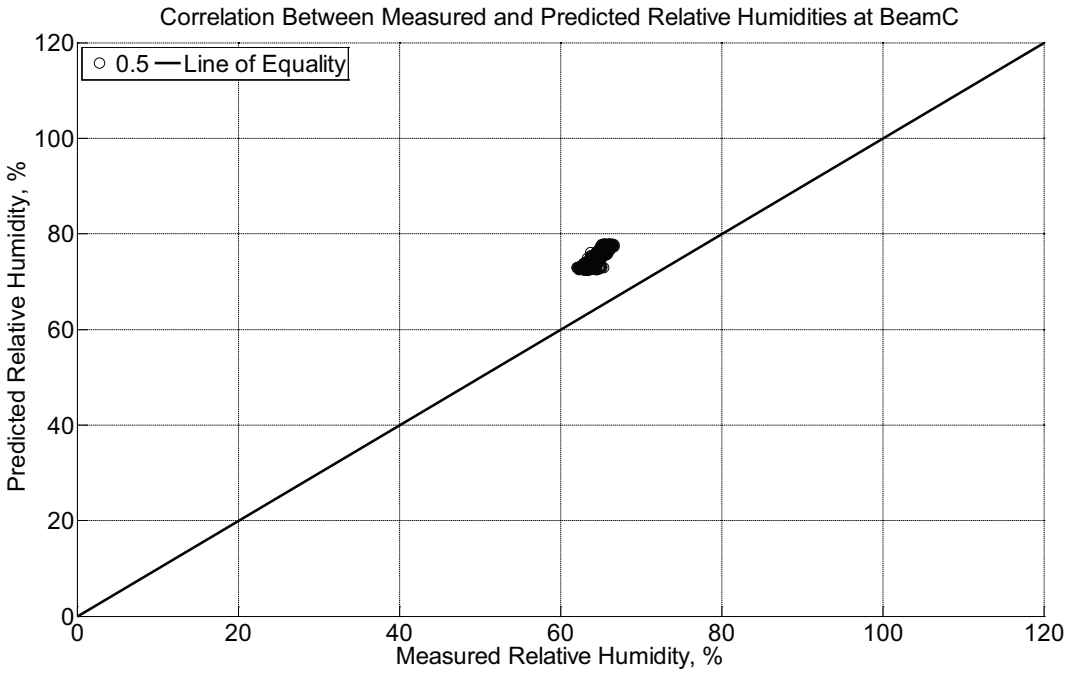

Figure B-100 Correlation between measured and predicted relative humidity values 0.5 inches (12.7 mm) from the surface of a modulus of rupture beam (labeled C) located inside an environmentally controlled room (50% RH, 23 ºC) between September 9, 2014, through October 17, 2014.

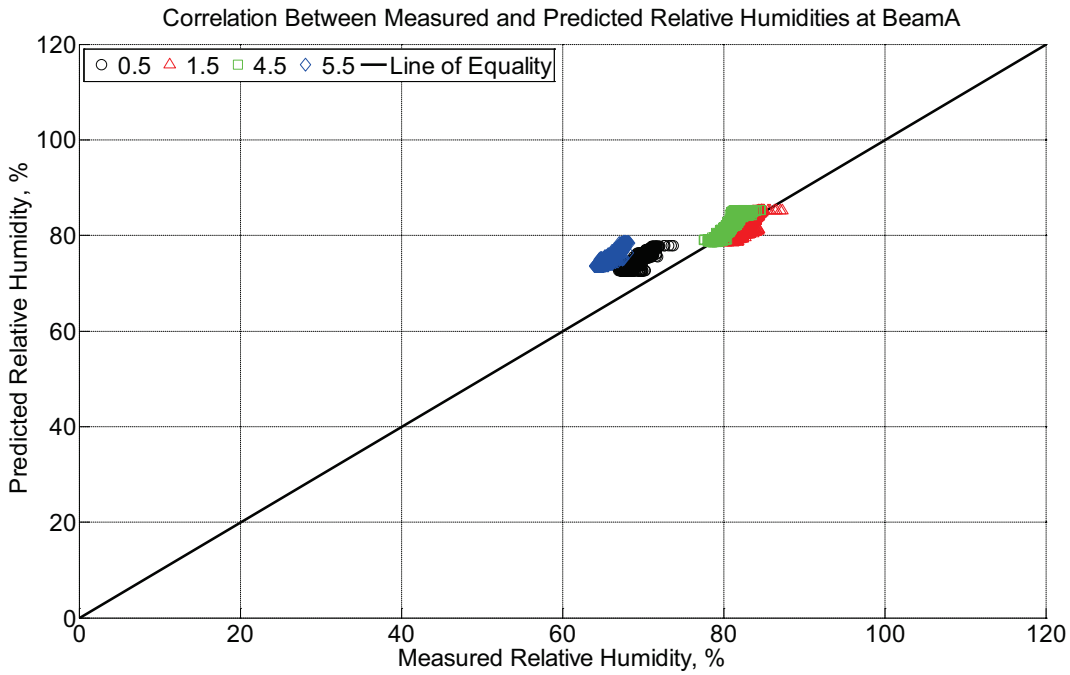

Figure B-101 Correlation between measured and predicted relative humidity values 0.5 inches (12.7 mm), 1.5 inches (38.1 mm), 4.5 inches (114.3 mm), and 5.5 inches (139.7 mm) from the surface of a modulus of rupture beam (labeled A) located inside an environmentally controlled room (50% RH, 23 ºC) between September 9, 2014, through October 17, 2014.

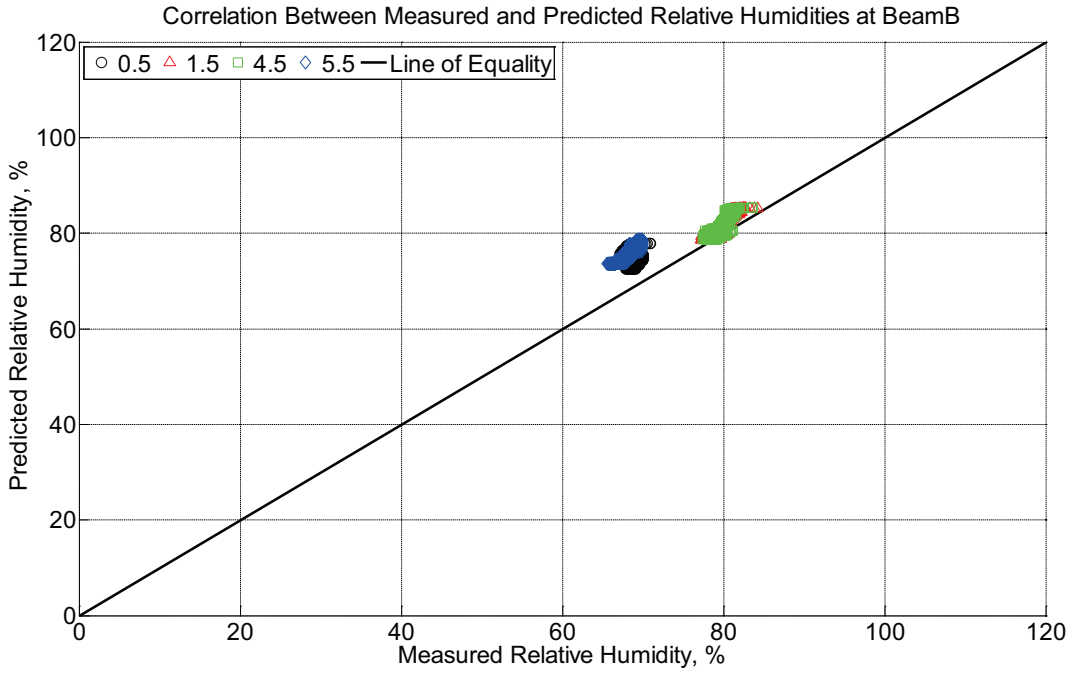

Figure B-102 Correlation between measured and predicted relative humidity values 0.5

inches (12.7 mm), 1.5 inches (38.1 mm), 4.5 inches (114.3 mm), and 5.5 inches (139.7 mm) from the surface of a modulus of rupture beam (labeled B) located inside an environmentally controlled room (50% RH, 23 ºC) between September 9, 2014, through October 17, 2014.

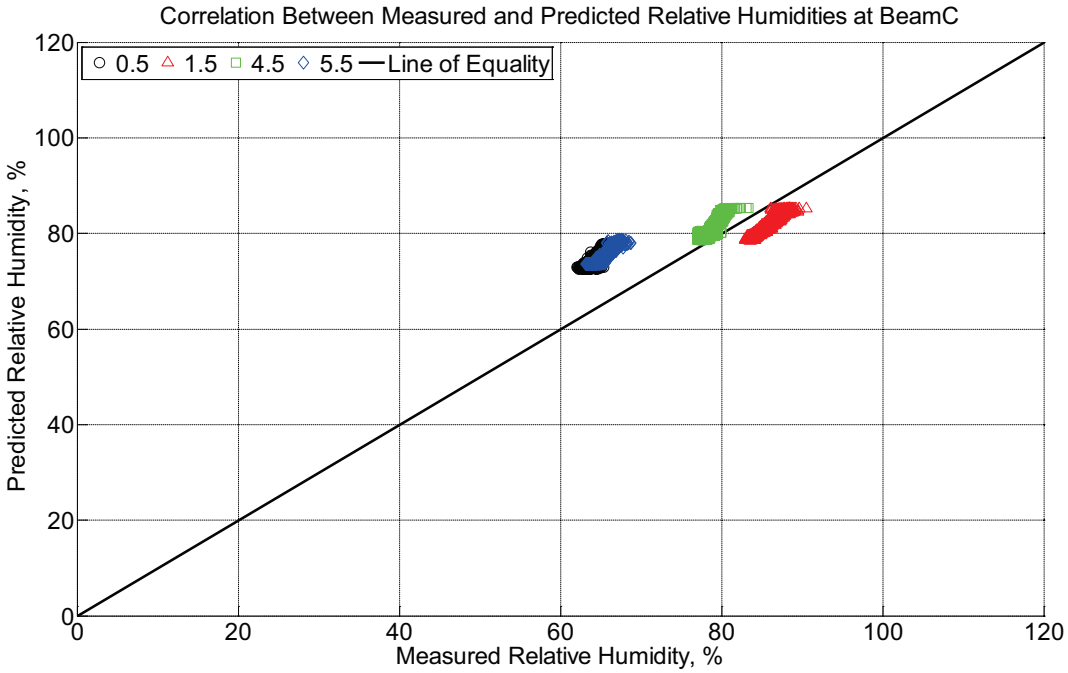

Figure B-103 Correlation between measured and predicted relative humidity values 0.5 inches (12.7 mm), 1.5 inches (38.1 mm), 4.5 inches (114.3 mm), and 5.5 inches (139.7 mm) from the surface of a modulus of rupture beam (labeled C) located inside an environmentally controlled room (50% RH, 23 ºC) between September 9, 2014, through October 17, 2014.

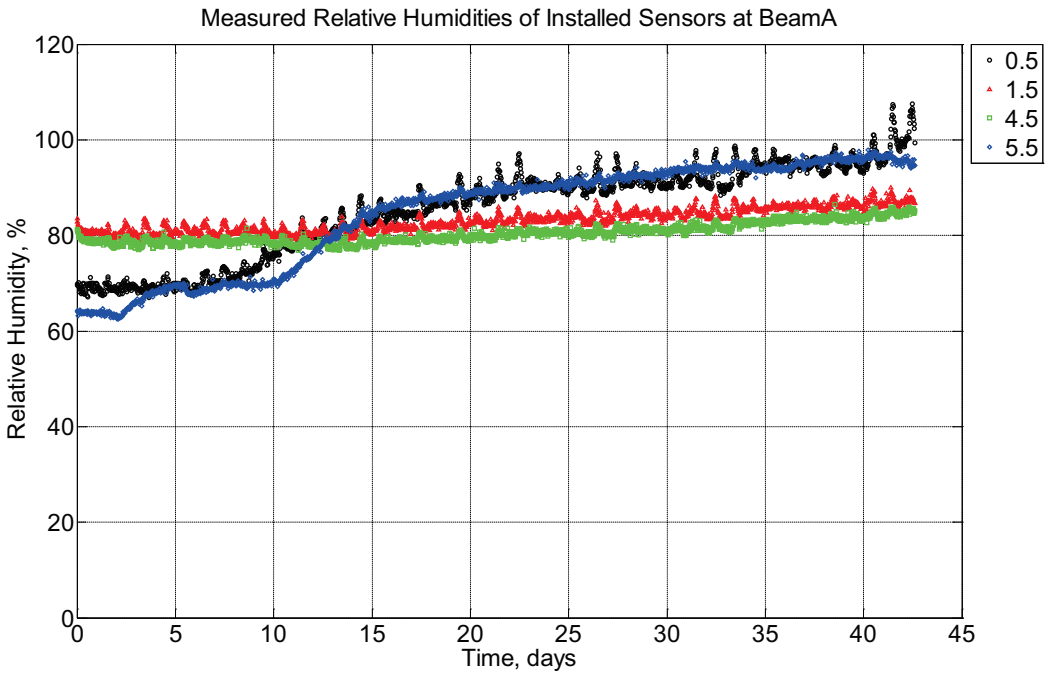

Figure B-104 Measured relative humidity at depths of 0.5 inches (12.7 mm), 1.5 inches (38.1 mm), 4.5 inches (114.3 mm), and 5.5 inches (139.7 mm) from the surface of a modulus of rupture beam (labeled A) installed in ballast in Rantoul, IL, between October 19, 2014, through November 30, 2014.

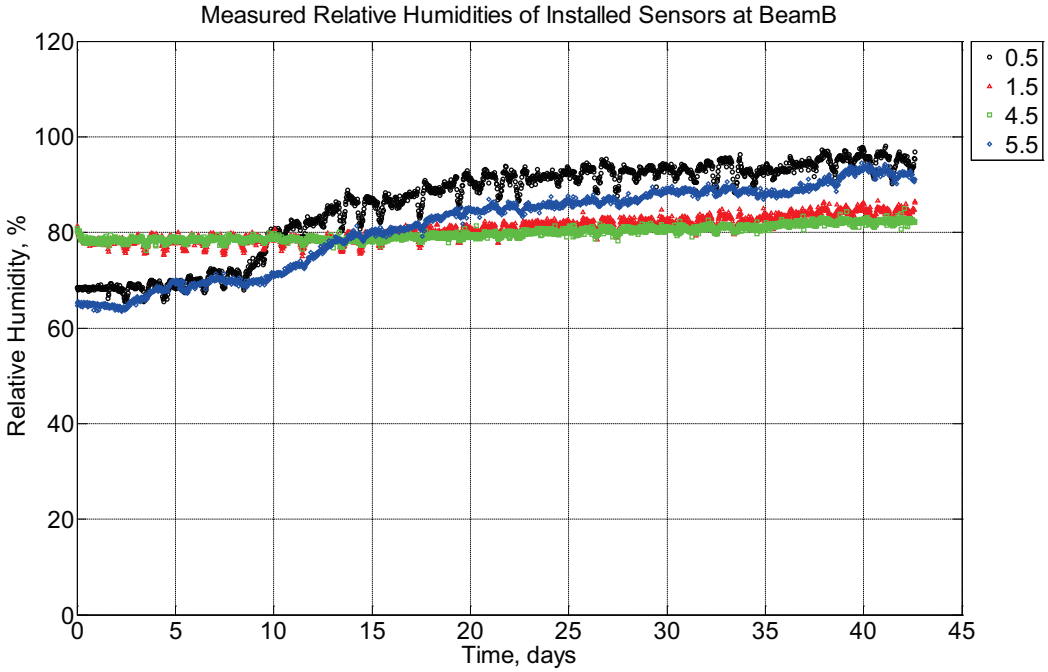

Figure B-105 Measured relative humidity at depths of 0.5 inches (12.7 mm), 1.5 inches (38.1 mm), 4.5 inches (114.3 mm), and 5.5 inches (139.7 mm) from the surface of a modulus of

rupture beam (labeled B) installed in ballast in Rantoul, IL, between October 19, 2014, through November 30, 2014.

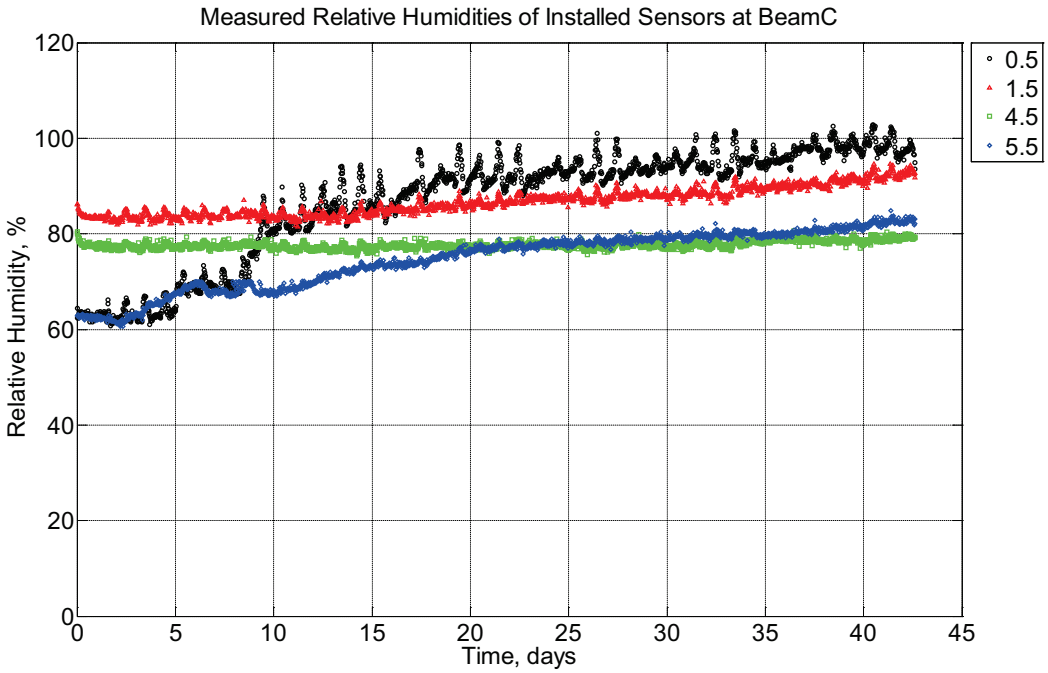

Figure B-106 Measured relative humidity at depths of 0.5 inches (12.7 mm), 1.5 inches (38.1 mm), 4.5 inches (114.3 mm), and 5.5 inches (139.7 mm) from the surface of a modulus of rupture beam (labeled C) installed in ballast in Rantoul, IL, between October 19, 2014, through November 30, 2014.

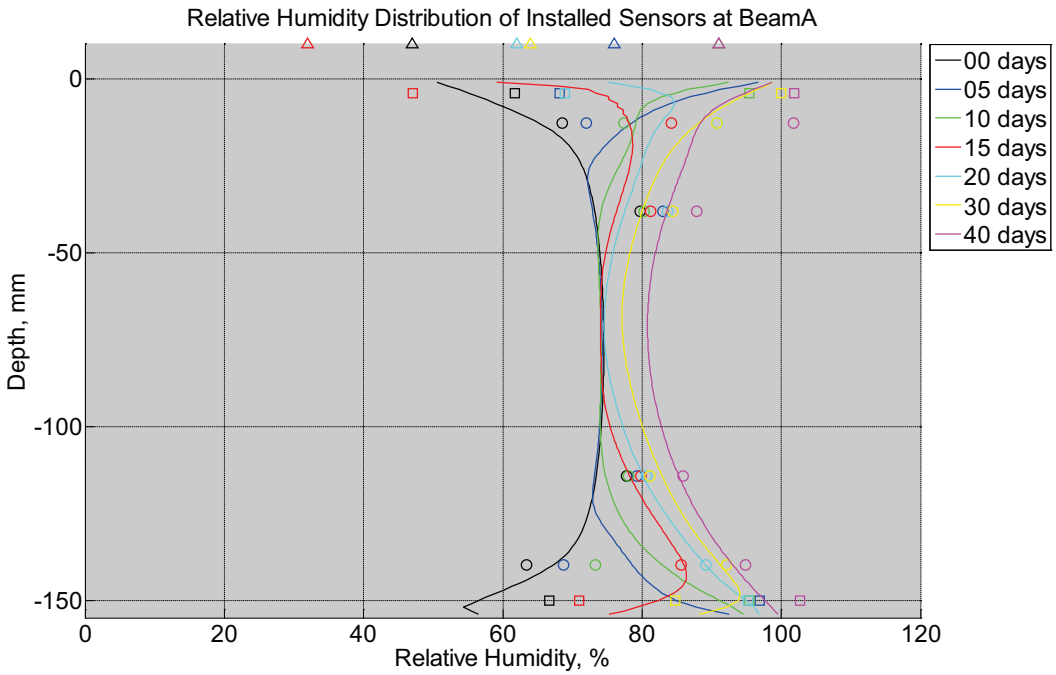

Figure B-107 Measured (markers) and modeled (continuous line) relative humidity profile distribution as a function of depth inside modulus of rupture beam (labeled A) installed in ballast in Rantoul, IL, between October 19, 2014, through November 30, 2014. Triangular markers denote relative humidity value from KTIP weather station, square markers denote measured relative humidity values from ballast, and circular markers denote measured relative humidity values inside concrete.

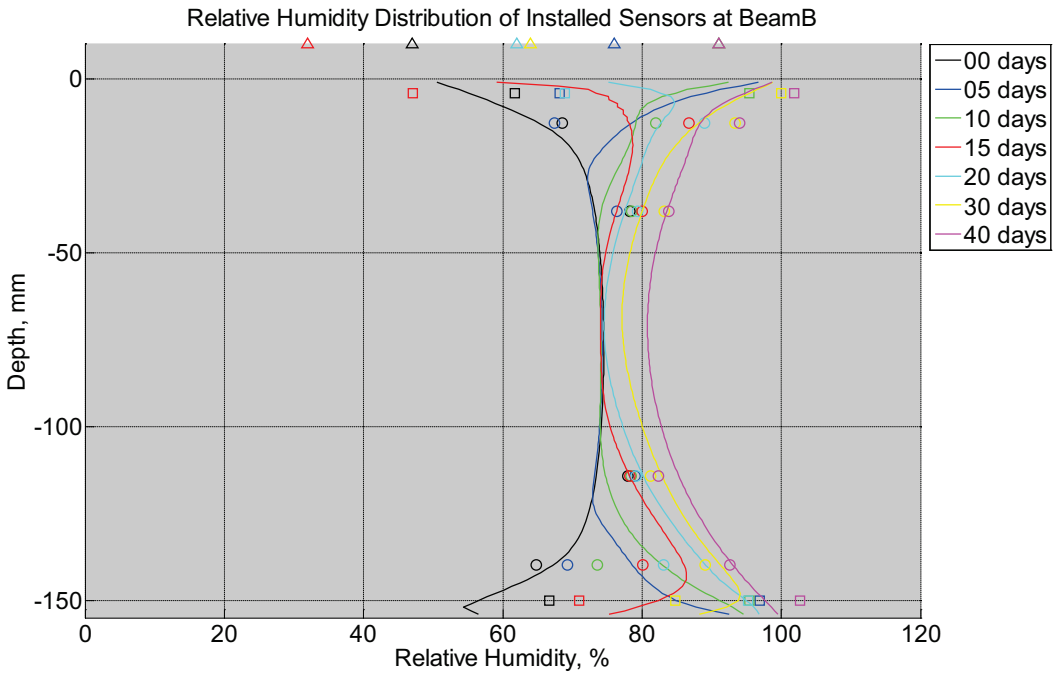

Figure B-108 Measured (markers) and modeled (continuous line) relative humidity profile distribution as a function of depth inside modulus of rupture beam (labeled B) installed in ballast in Rantoul, IL, between October 19, 2014, through November 30, 2014. Triangular markers denote relative humidity value from KTIP weather station, square markers denote measured relative humidity values from ballast, and circular markers denote measured relative humidity values inside concrete.

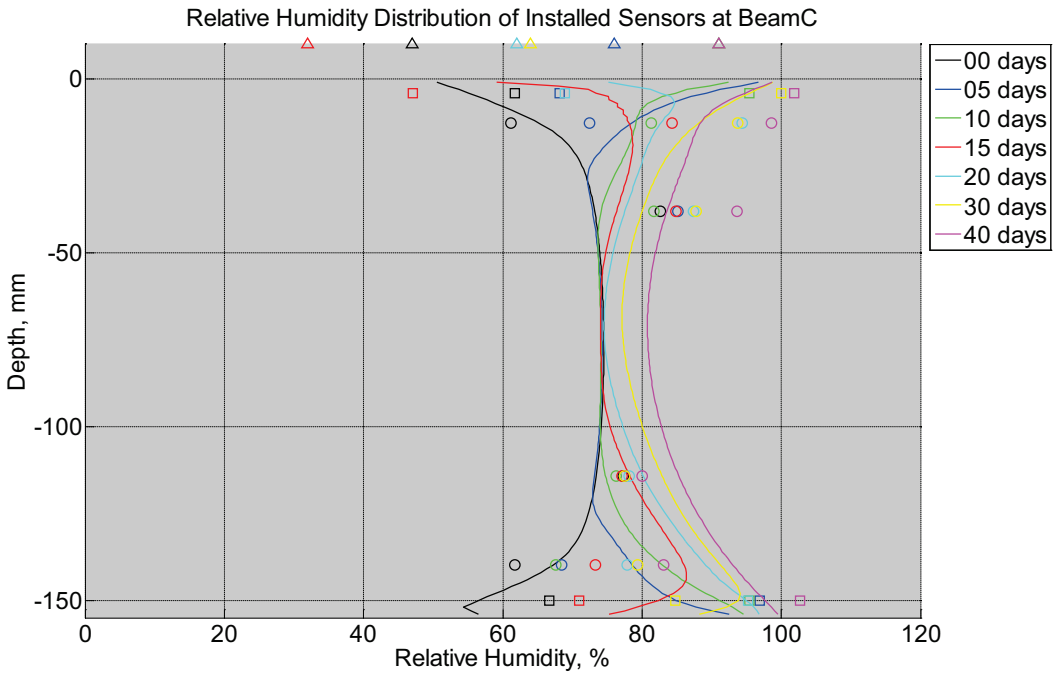

Figure B-109 Measured (markers) and modeled (continuous line) relative humidity profile distribution as a function of depth inside modulus of rupture beam (labeled C) installed in ballast in Rantoul, IL, between October 19, 2014, through November 30, 2014. Triangular markers denote relatieve humidity value from KTIP weather station, square markers denote measured relative humidity values from ballast, and circular markers denote measured relative humidity values inside concrete.

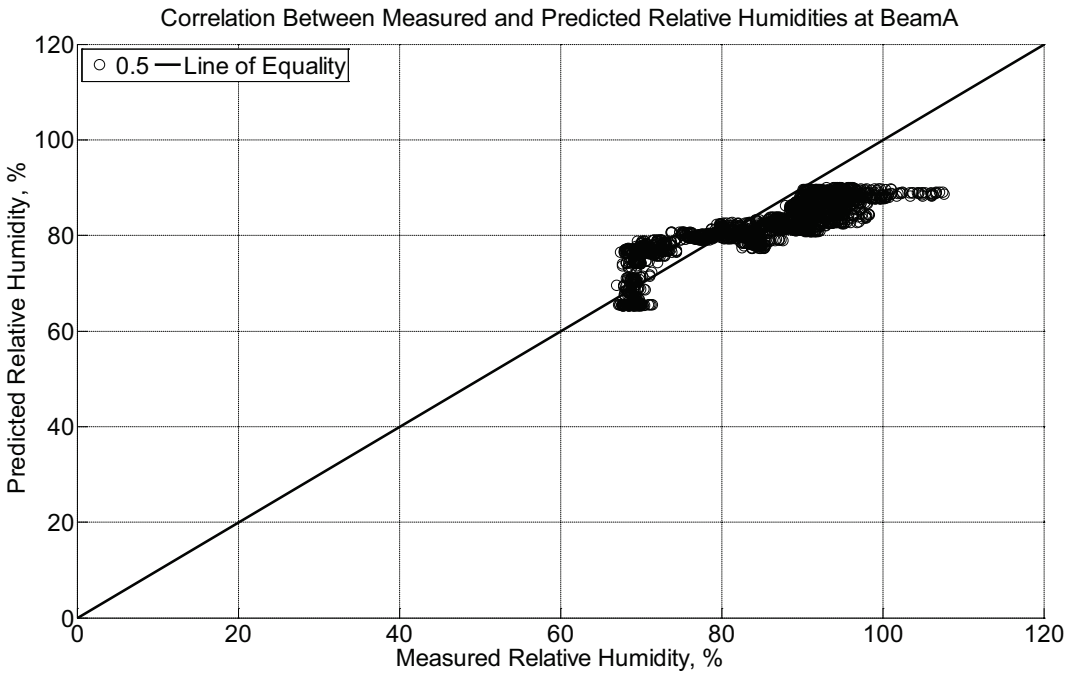

Figure B-110 Correlation between measured and predicted relative humidity values 0.5 inches (12.7 mm) from the surface of a modulus of rupture beam (labeled A) installed in ballast in Rantoul, IL, between October 19, 2014, through November 30, 2014.

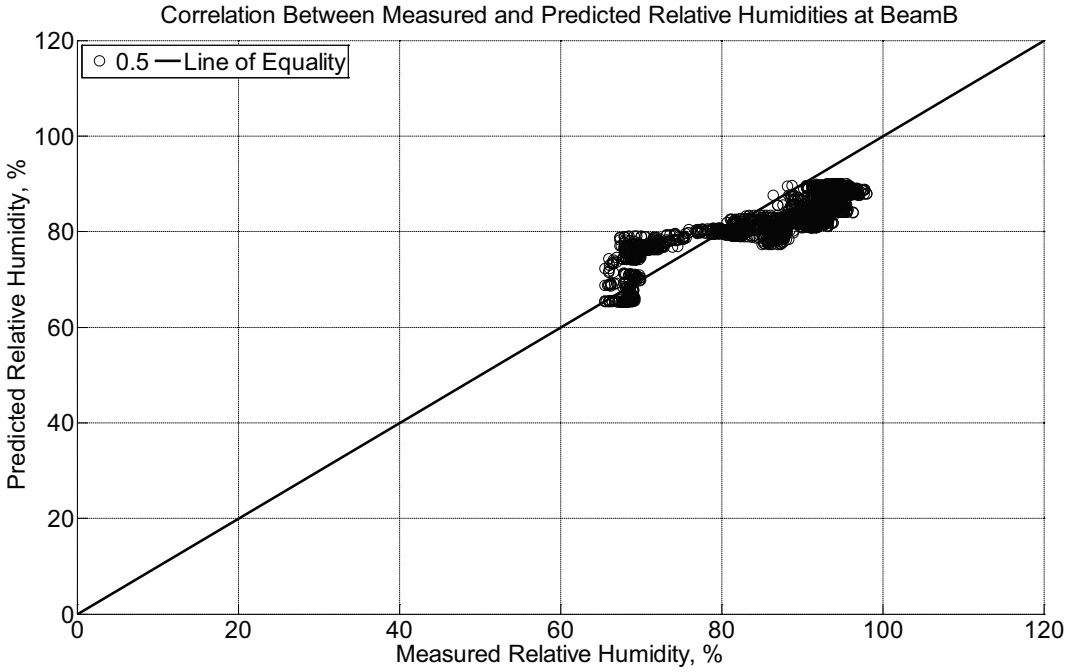

Figure B-111 Correlation between measured and predicted relative humidity values 0.5

inches (12.7 mm) from the surface of a modulus of rupture beam (labeled B) installed in ballast in Rantoul, IL, between October 19, 2014, through November 30, 2014.

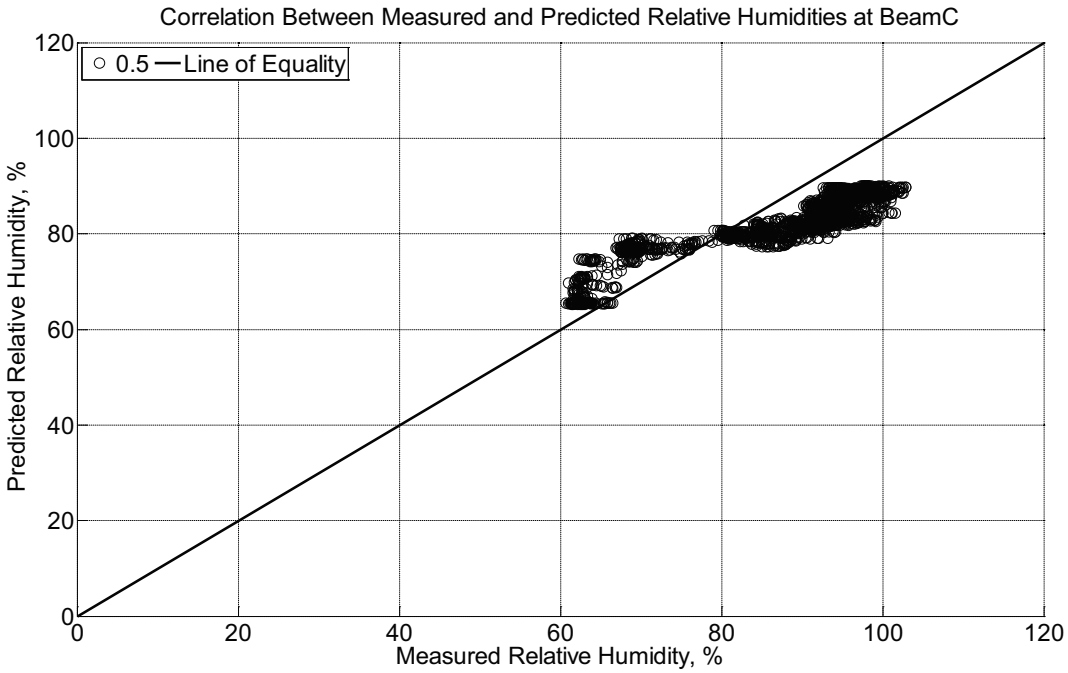

Figure B-112 Correlation between measured and predicted relative humidity values 0.5 inches (12.7 mm) from the surface of a modulus of rupture beam (labeled C) installed in ballast in Rantoul, IL, between October 19, 2014, through November 30, 2014.

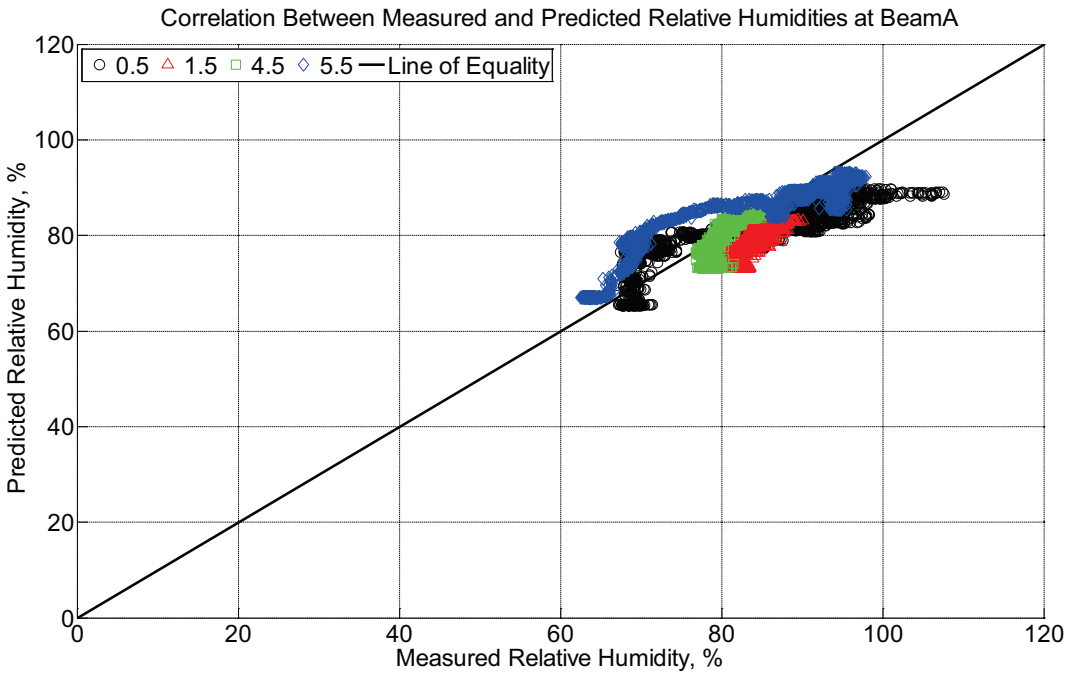

Figure B-113 Correlation between measured and predicted relative humidity values 0.5 inches (12.7 mm), 1.5 inches (38.1 mm), 4.5 inches (114.3 mm), and 5.5 inches (139.7 mm) from the surface of a modulus of rupture beam (labeled A) installed in ballast in Rantoul, IL, between October 19, 2014, through November 30, 2014.

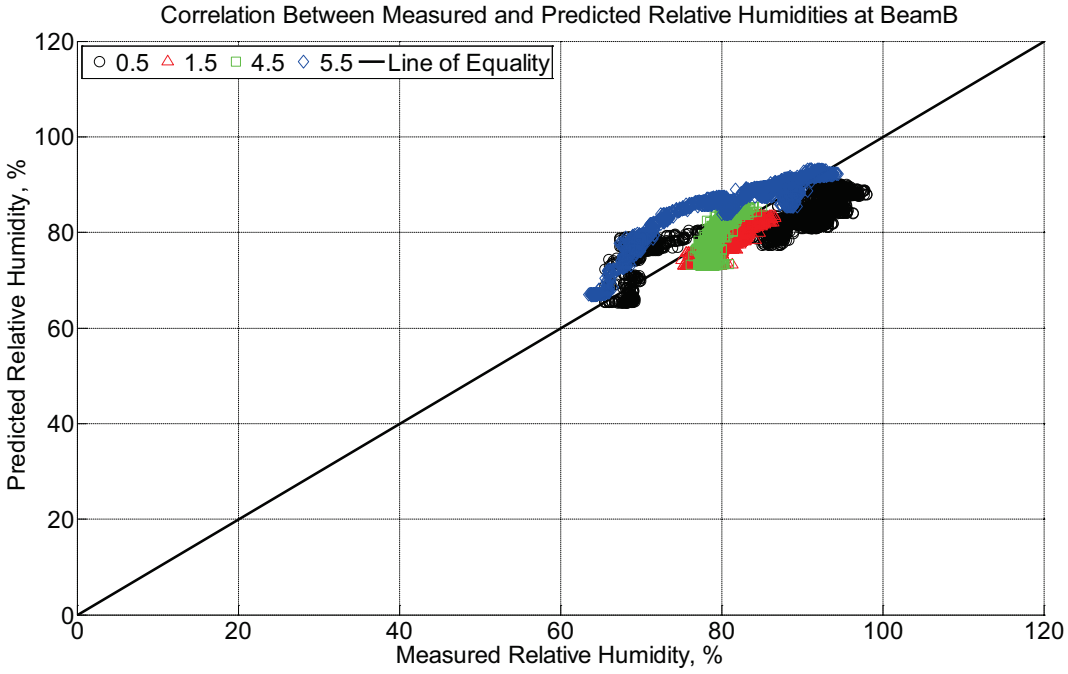

Figure B-114 Correlation between measured and predicted relative humidity values 0.5 inches (12.7 mm), 1.5 inches (38.1 mm), 4.5 inches (114.3 mm), and 5.5 inches (139.7 mm)

from the surface of a modulus of rupture beam (labeled B) installed in ballast in Rantoul, IL, between October 19, 2014, through November 30, 2014.

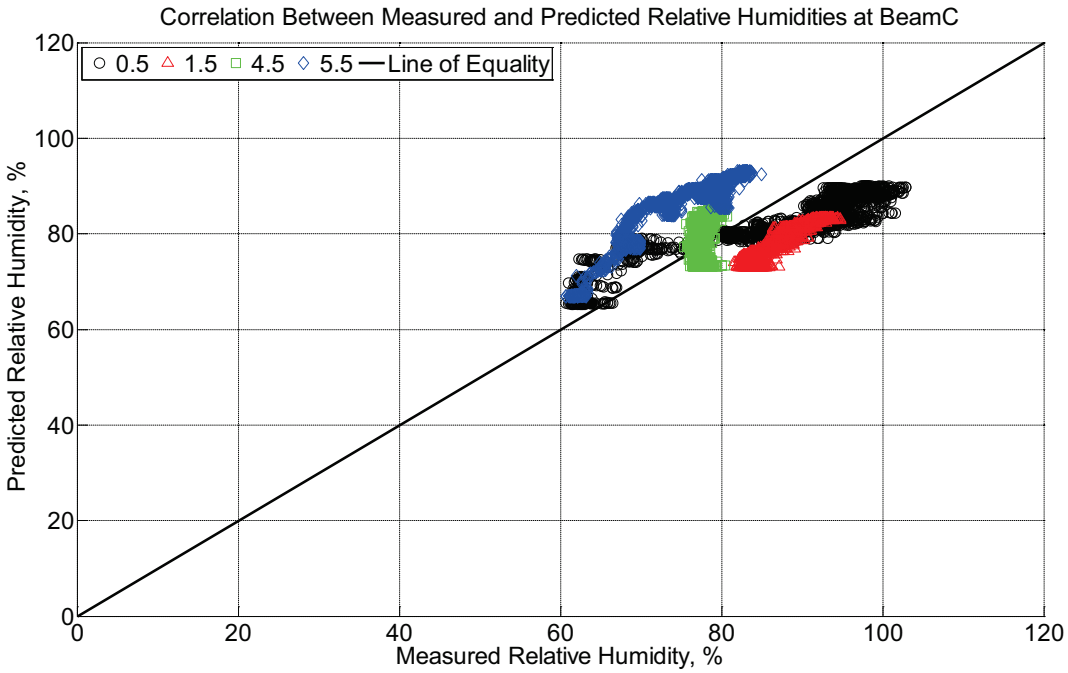

Figure B-115 Correlation between measured and predicted relative humidity values 0.5 inches (12.7 mm), 1.5 inches (38.1 mm), 4.5 inches (114.3 mm), and 5.5 inches (139.7 mm) from the surface of a modulus of rupture beam (labeled C) installed in ballast in Rantoul, IL, between October 19, 2014, through November 30, 2014.

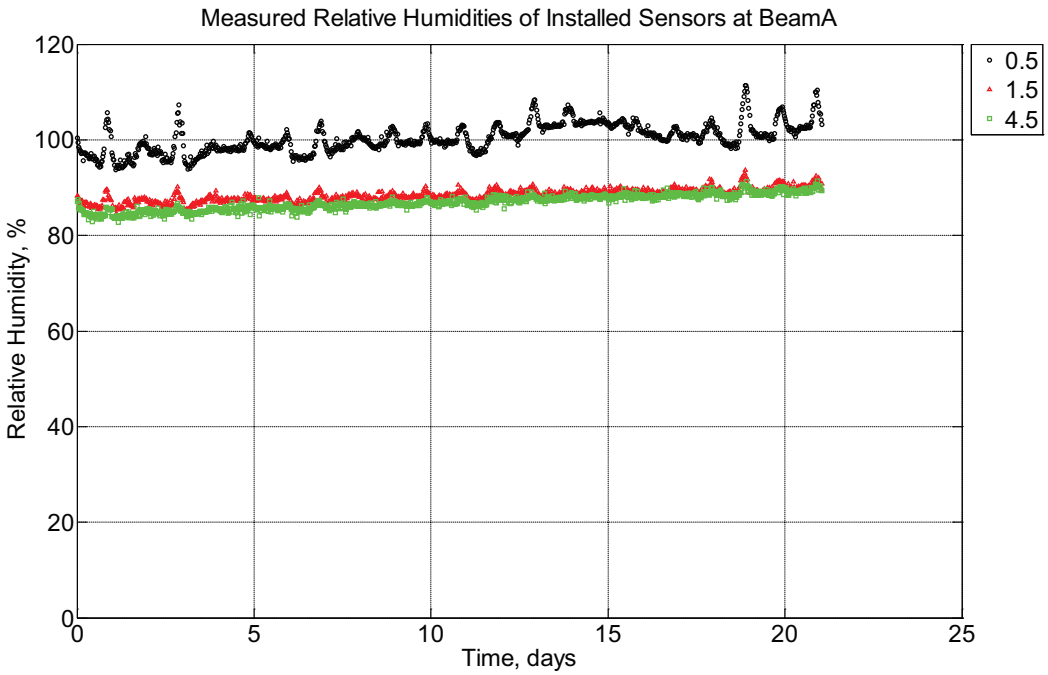

Figure B-116 Measured relative humidity at depths of 0.5 inches (12.7 mm), 1.5 inches (38.1 mm), and 4.5 inches (114.3 mm) from the surface of a modulus of rupture beam (labeled A) installed in ballast in Rantoul, IL, between November 30, 2014, through December 21, 2014.

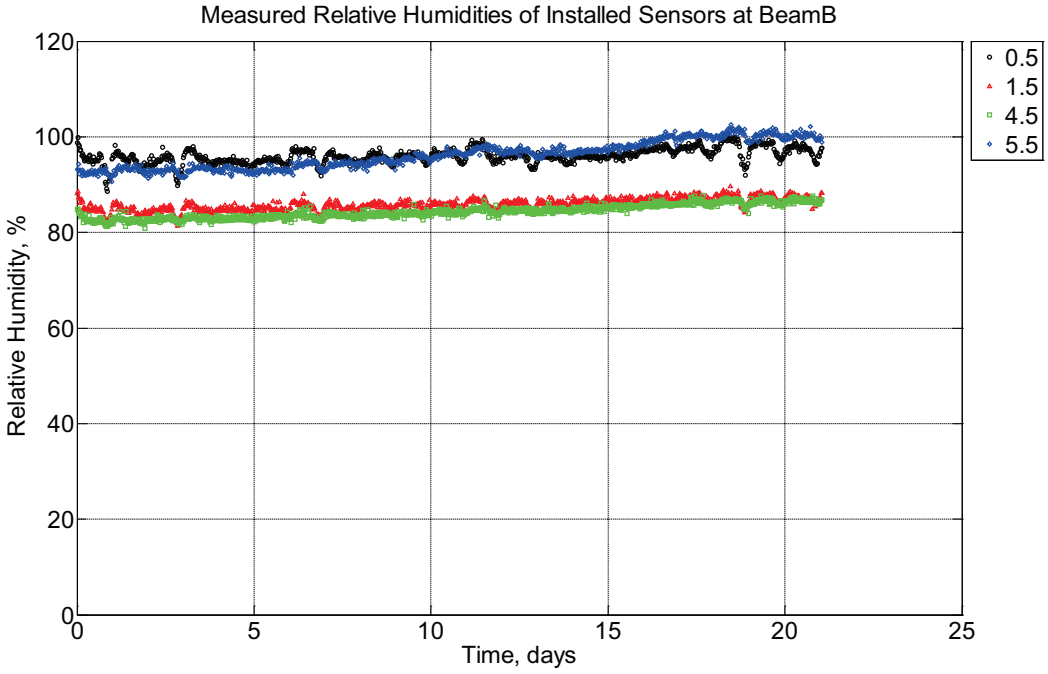

Figure B-117 Measured relative humidity at depths of 0.5 inches (12.7 mm), 1.5 inches (38.1 mm), 4.5 inches (114.3 mm), and 5.5 inches (139.7 mm) from the surface of a modulus of

rupture beam (labeled B) installed in ballast in Rantoul, IL, between November 30, 2014, through December 21, 2014.

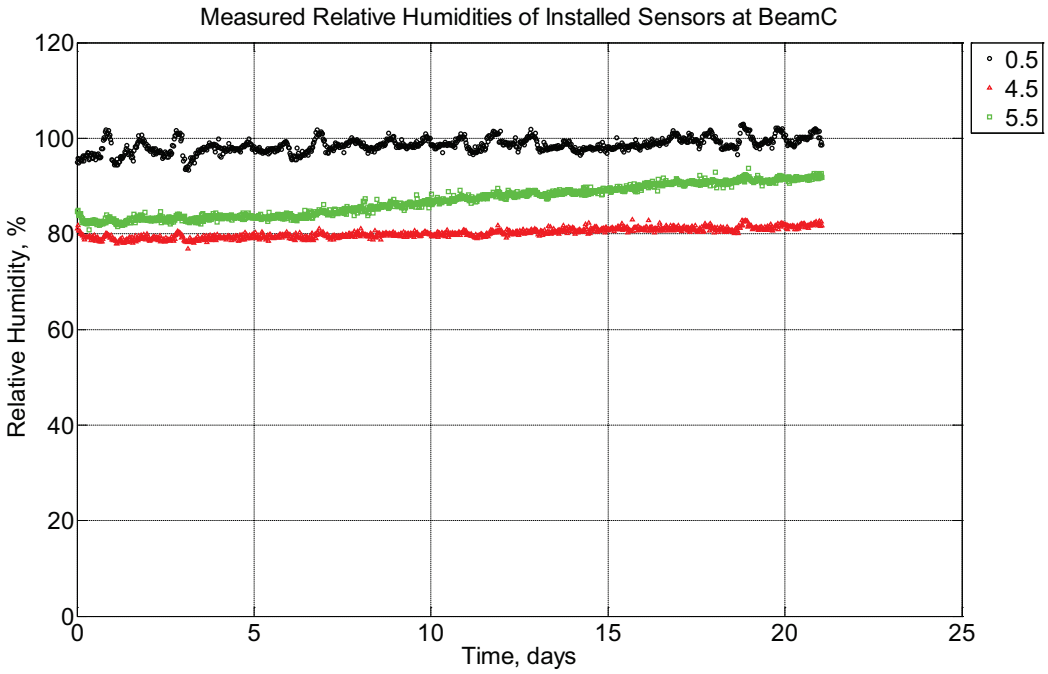

Figure B-118 Measured relative humidity at depths of 0.5 inches (12.7 mm), 4.5 inches (114.3 mm), and 5.5 inches (139.7 mm) from the surface of a modulus of rupture beam (labeled C) installed in ballast in Rantoul, IL, between November 30, 2014, through December 21, 2014.

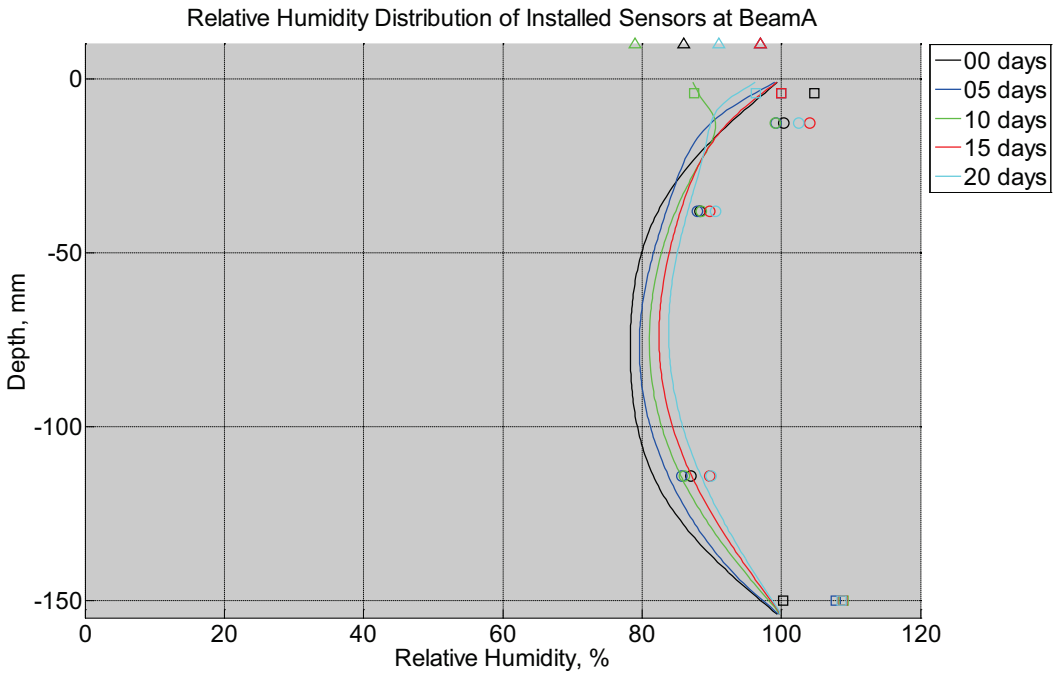

Figure B-119 Measured (markers) and modeled (continuous line) relative humidity profile distribution as a function of depth inside modulus of rupture beam (labeled A) installed in ballast in Rantoul, IL, between November 30, 2014, through December 21, 2014. Triangular markers denote relative humidity value from KTIP weather station, square markers denote measured relative humidity values from ballast, and circular markers denote measured relative humidity values inside concrete.

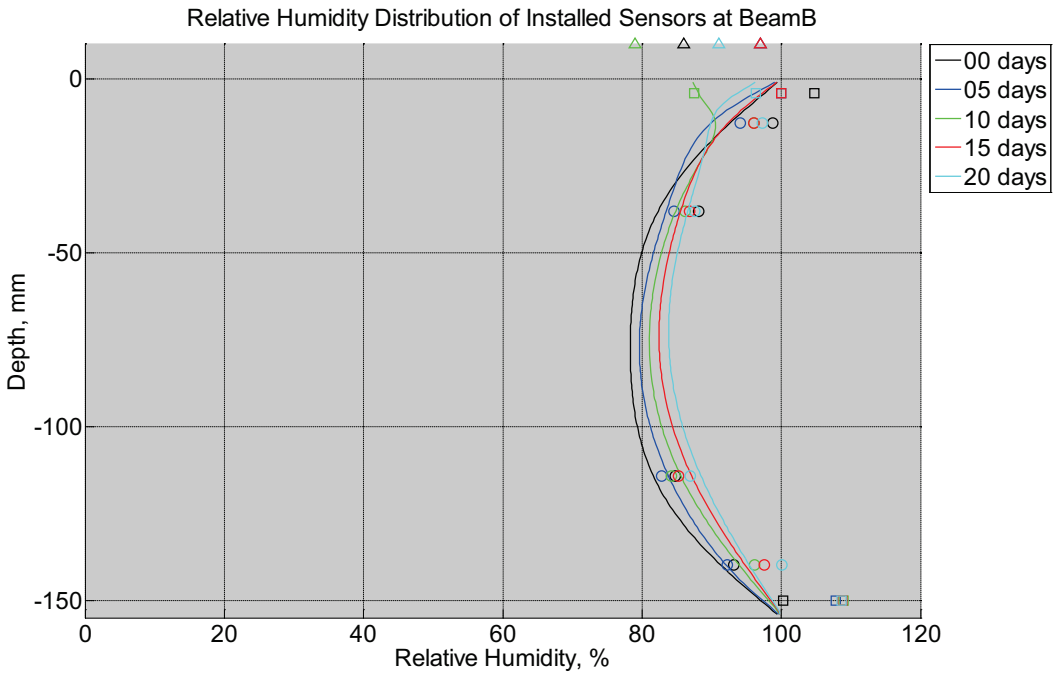

Figure B-120 Measured (markers) and modeled (continuous line) relative humidity profile distribution as a function of depth inside modulus of rupture beam (labeled B) installed in ballast in Rantoul, IL, between November 30, 2014, through December 21, 2014. Triangular markers denote relative humidity value from KTIP weather station, square markers denote measured relative humidity values from ballast, and circular markers denote measured relative humidity values inside concrete.

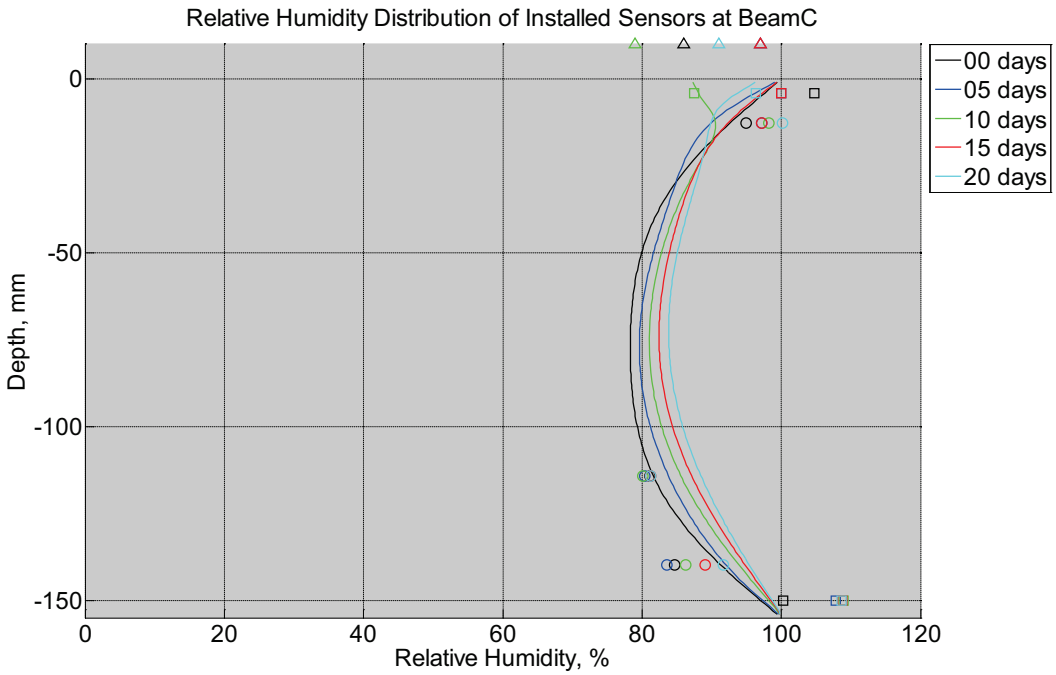

Figure B-121 Measured (markers) and modeled (continuous line) relative humidity profile distribution as a function of depth inside modulus of rupture beam (labeled C) installed in ballast in Rantoul, IL, between November 30, 2014, through December 21, 2014. Triangular markers denote relative humidity value from KTIP weather station, square markers denote measured relative humidity values from ballast, and circular markers denote measured relative humidity values inside concrete.

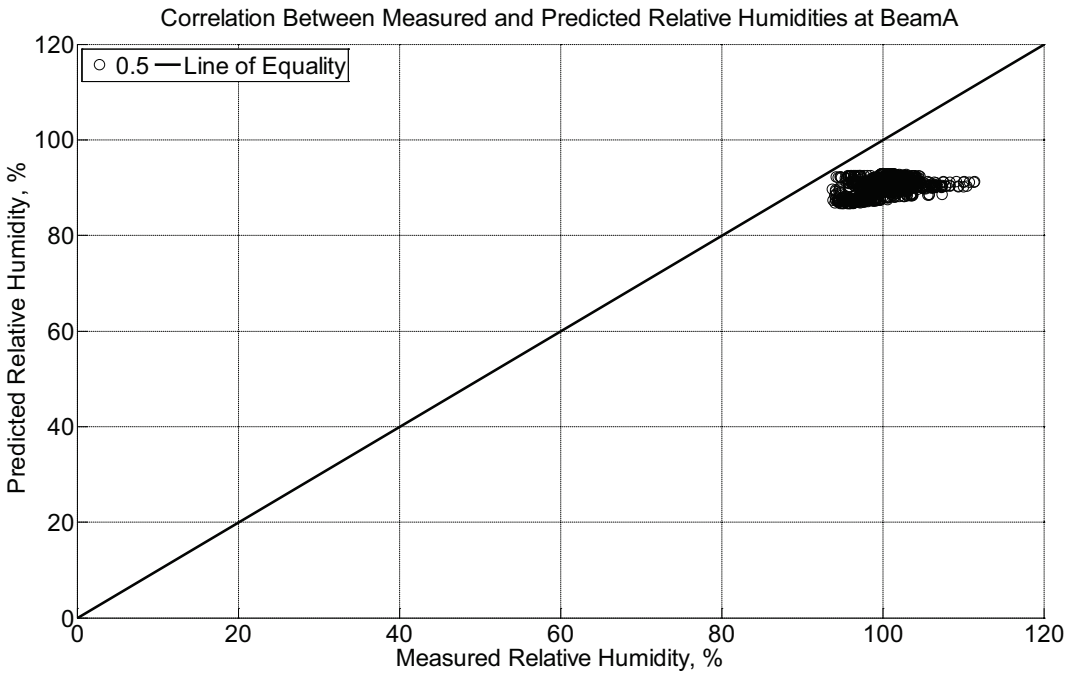

Figure B-122 Correlation between measured and predicted relative humidity values 0.5 inches (12.7 mm) from the surface of a modulus of rupture beam (labeled A) installed in ballast in Rantoul, IL, between November 30, 2014, through December 21, 2014.

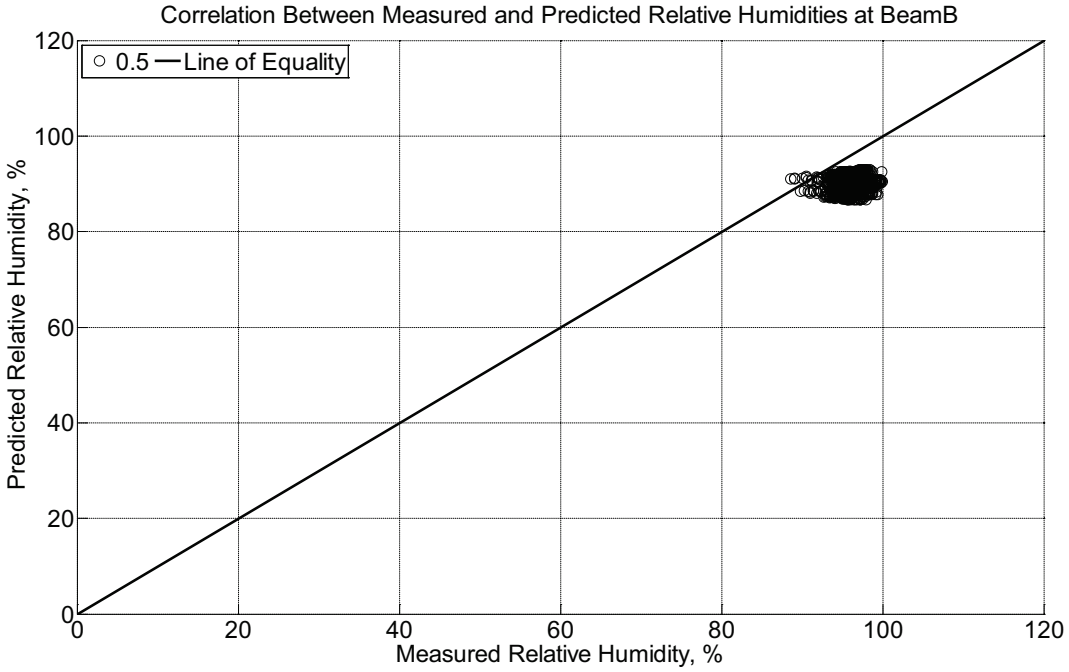

Figure B-123 Correlation between measured and predicted relative humidity values 0.5

inches (12.7 mm) from the surface of a modulus of rupture beam (labeled B) installed in ballast in Rantoul, IL, between November 30, 2014, through December 21, 2014.

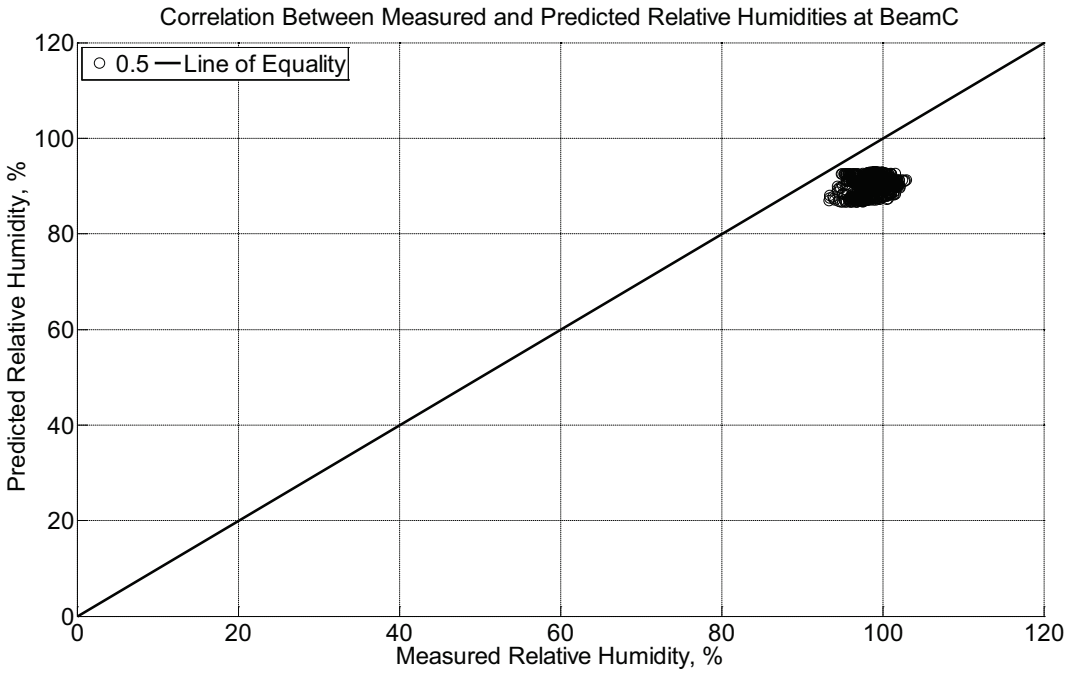

Figure B-124 Correlation between measured and predicted relative humidity values 0.5 inches (12.7 mm) from the surface of a modulus of rupture beam (labeled C) installed in ballast in Rantoul, IL, between November 30, 2014, through December 21, 2014.

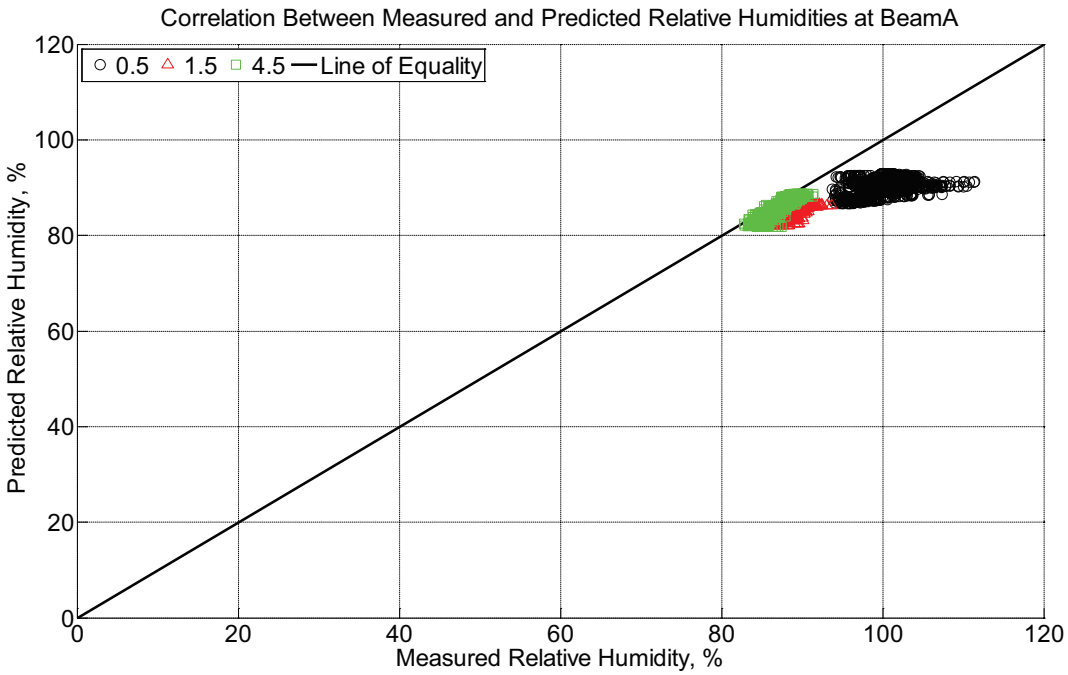

Figure B-125 Correlation between measured and predicted relative humidity values 0.5 inches (12.7 mm), 1.5 inches (38.1 mm), and 4.5 inches (114.3 mm) from the surface of a modulus of rupture beam (labeled A) installed in ballast in Rantoul, IL, between November 30, 2014, through December 21, 2014.

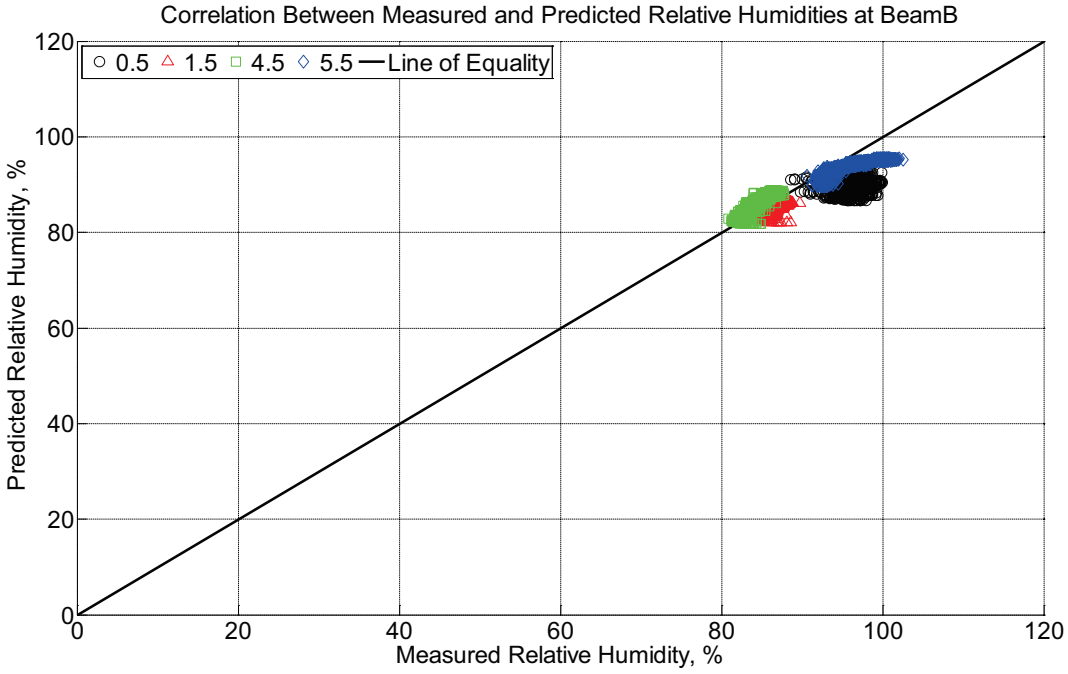

Figure B-126 Correlation between measured and predicted relative humidity values 0.5 inches (12.7 mm), 1.5 inches (38.1 mm), 4.5 inches (114.3 mm), and 5.5 inches (139.7 mm)

from the surface of a modulus of rupture beam (labeled B) installed in ballast in Rantoul, IL, between November 30, 2014, through December 21, 2014.

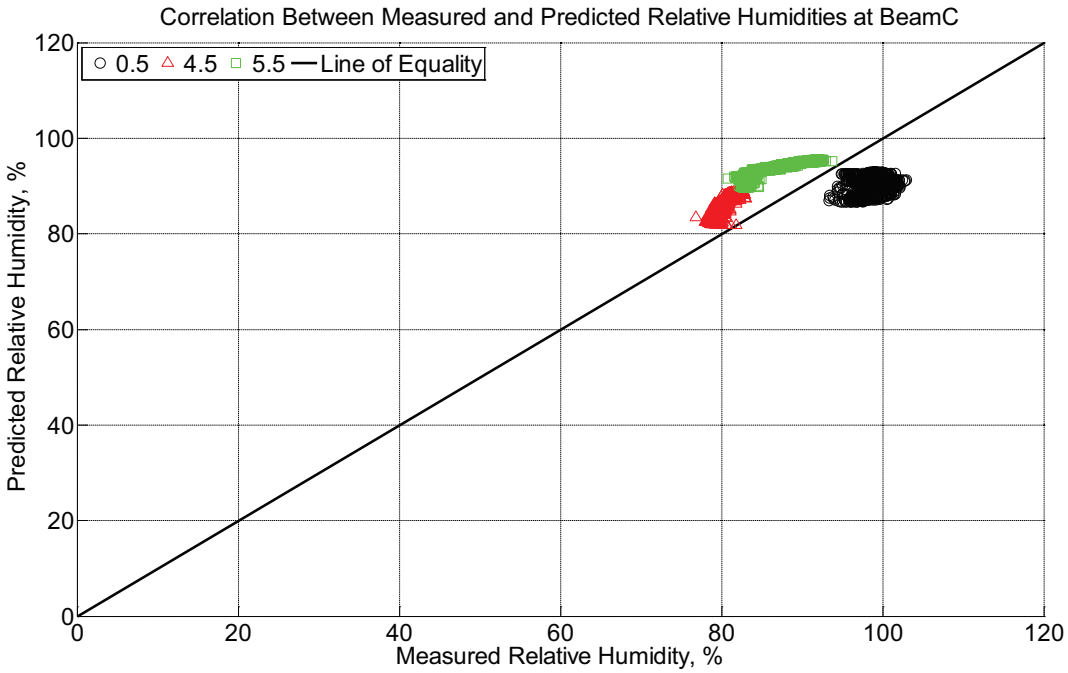

Figure B-127 Correlation between measured and predicted relative humidity values 0.5 inches (12.7 mm), 4.5 inches (114.3 mm), and 5.5 inches (139.7 mm) from the surface of a modulus of rupture beam (labeled C) installed in ballast in Rantoul, IL, between November 30, 2014, through December 21, 2014.

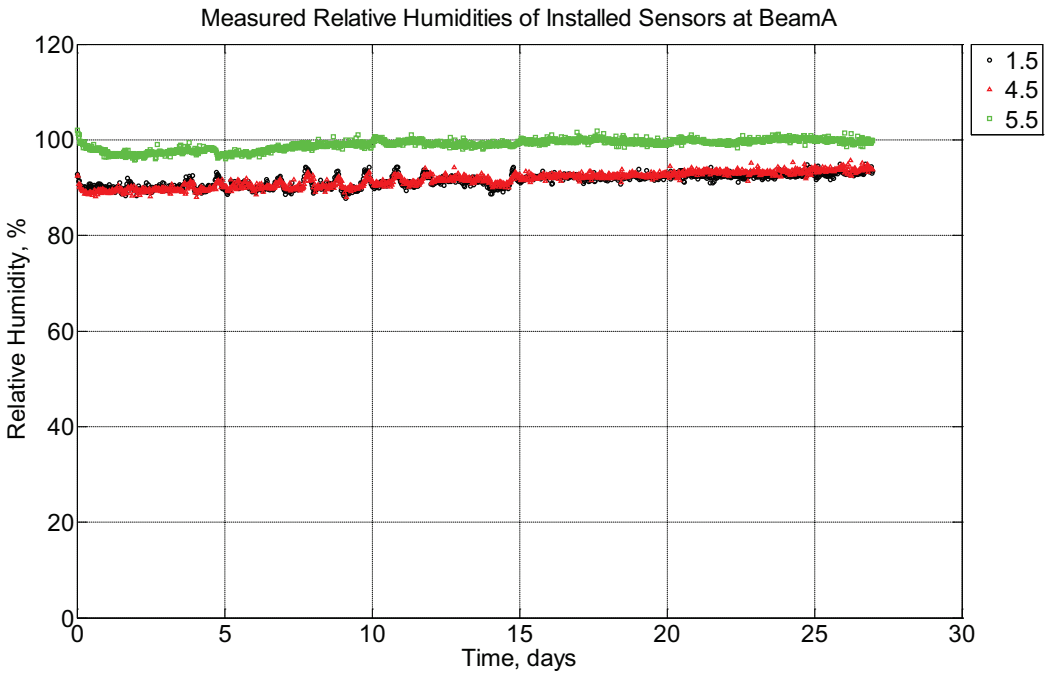

Figure B-128 Measured relative humidity at depths of 1.5 inches (38.1 mm), 4.5 inches (114.3 mm), and 5.5 inches (139.7 mm) from the surface of a modulus of rupture beam (labeled A) installed in ballast in Rantoul, IL, between December 21, 2014, through January 17, 2015.

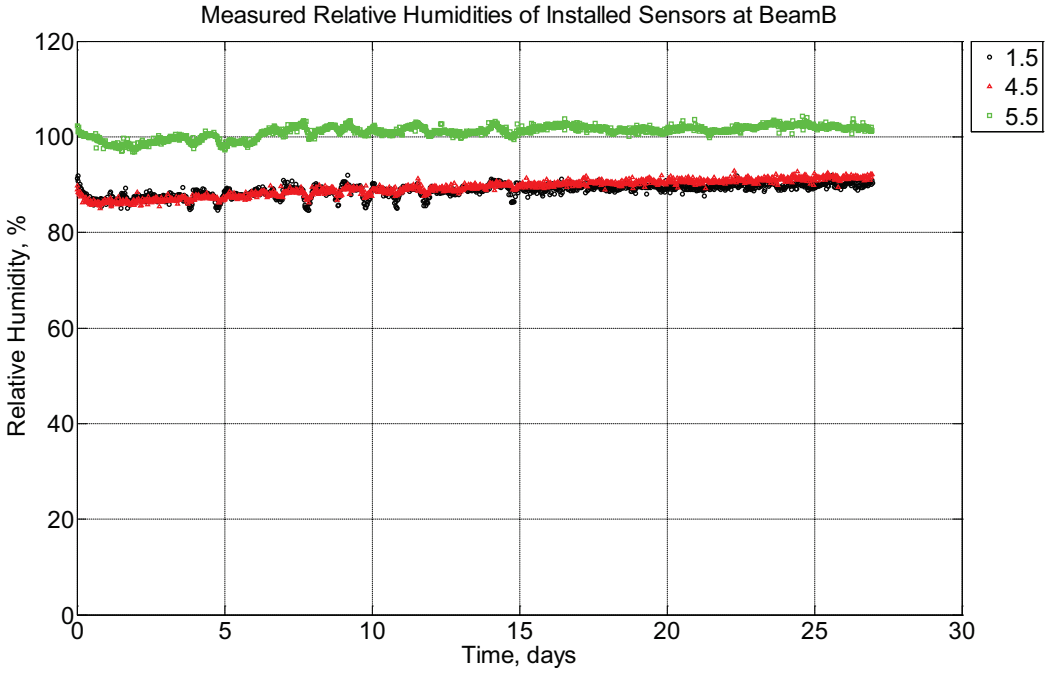

Figure B-129 Measured relative humidity at depths of 1.5 inches (38.1 mm), 4.5 inches (114.3 mm), and 5.5 inches (139.7 mm) from the surface of a modulus of rupture beam

(labeled B) installed in ballast in Rantoul, IL, between December 21, 2014, through January 17, 2015.

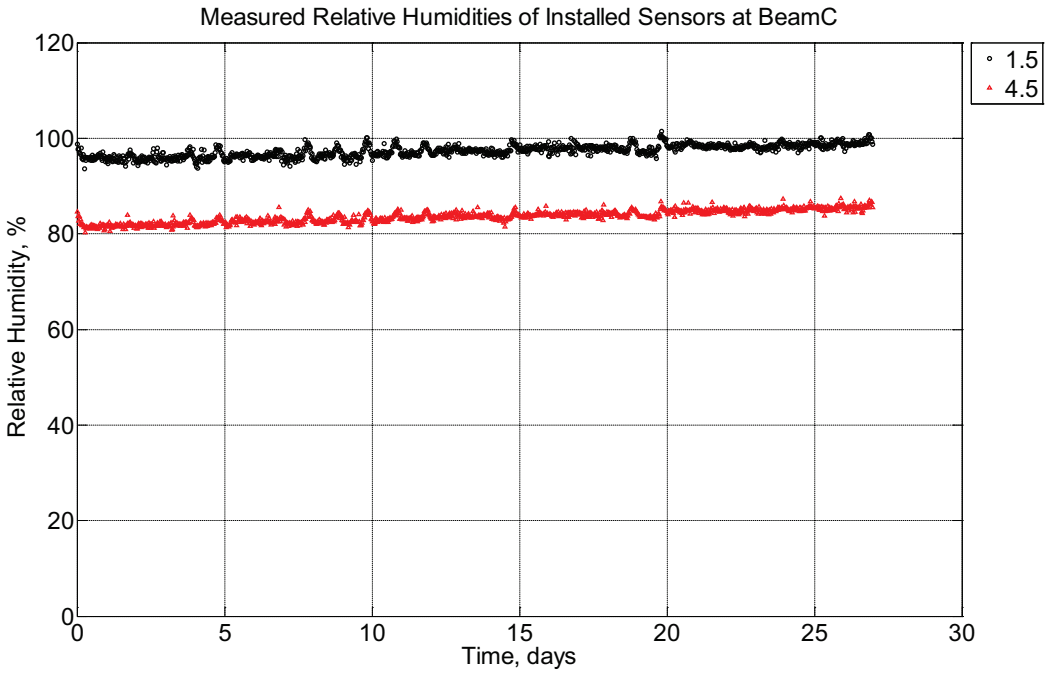

Figure B-130 Measured relative humidity at depths of 1.5 inches (38.1 mm) and 4.5 inches (114.3 mm) from the surface of a modulus of rupture beam (labeled C) installed in ballast in Rantoul, IL, between December 21, 2014, through January 17, 2015.

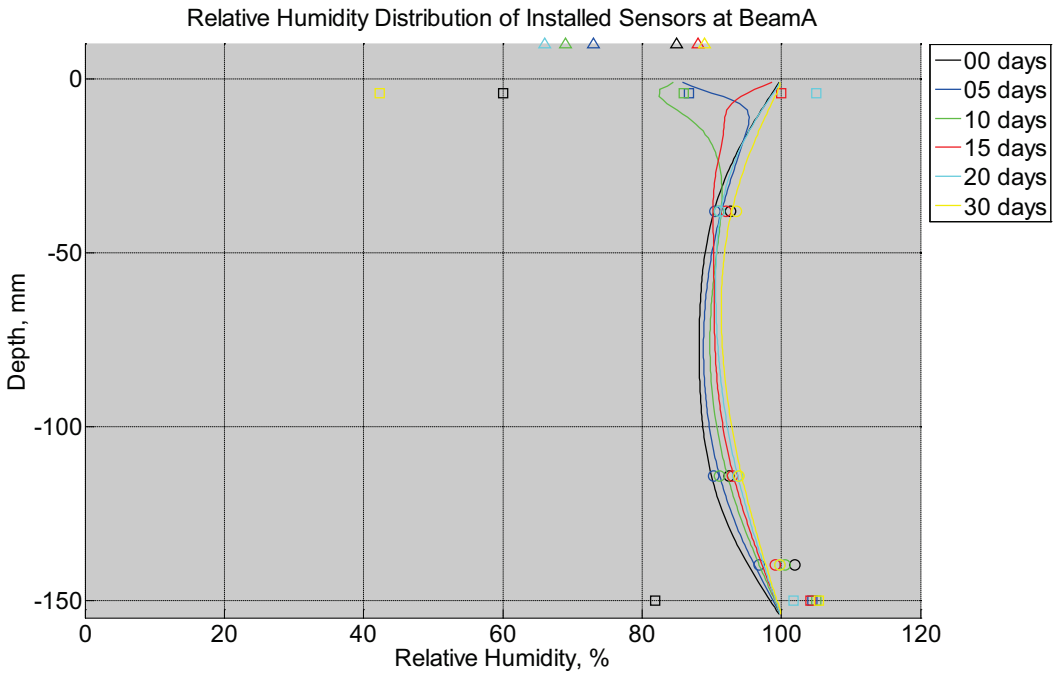

Figure B-131 Measured (markers) and modeled (continuous line) relative humidity profile distribution as a function of depth inside modulus of rupture beam (labeled A) installed in ballast in Rantoul, IL, between December 21, 2014, through January 17, 2015. Triangular markers denote relative humidity value from KTIP weather station, square markers denote measured relative humidity values from ballast, and circular markers denote measured relative humidity values inside concrete.

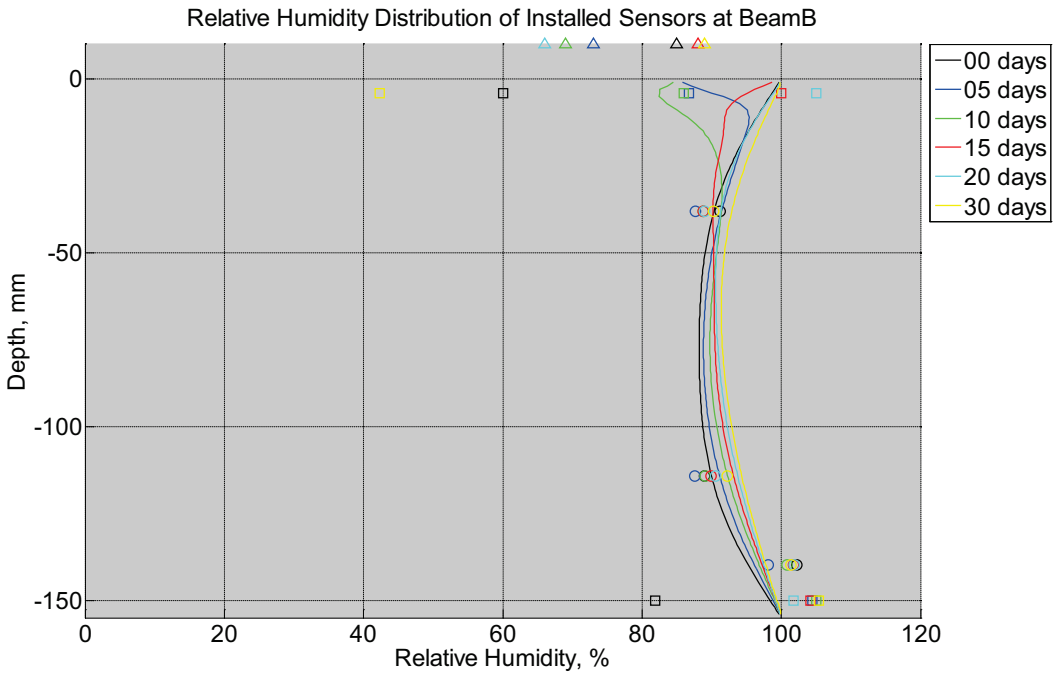

Figure B-132 Measured (markers) and modeled (continuous line) relative humidity profile distribution as a function of depth inside modulus of rupture beam (labeled B) installed in ballast in Rantoul, IL, between December 21, 2014, through January 17, 2015. Triangular markers denote relative humidity value from KTIP weather station, square markers denote measured relative humidity values from ballast, and circular markers denote measured relative humidity values inside concrete.

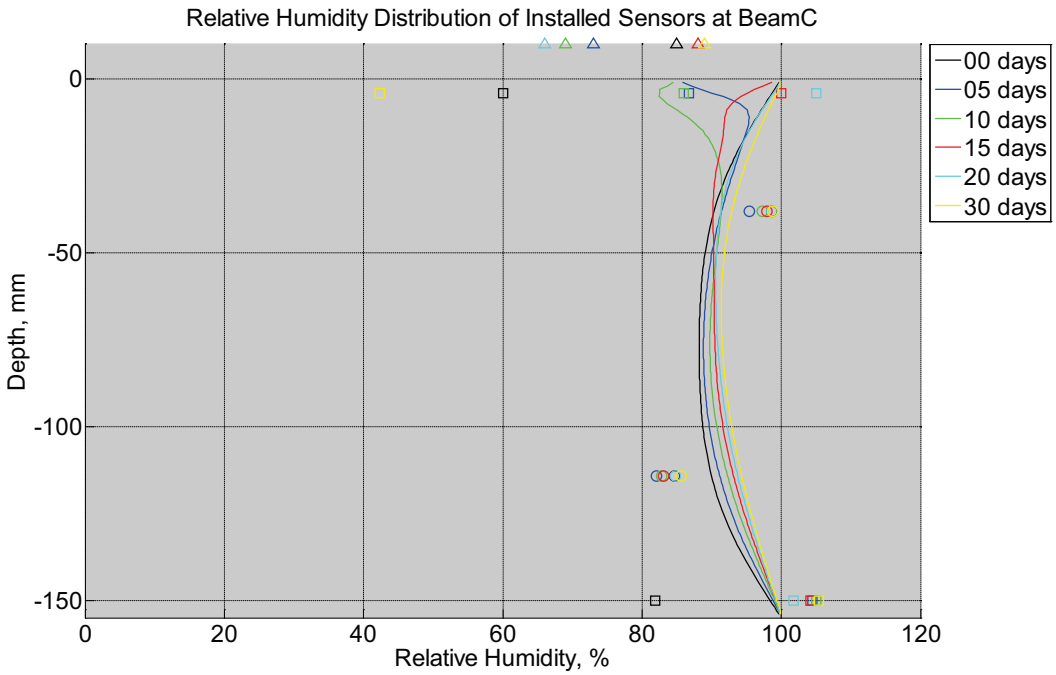

Figure B-133 Measured (markers) and modeled (continuous line) relative humidity profile distribution as a function of depth inside modulus of rupture beam (labeled C) installed in ballast in Rantoul, IL, between December 21, 2014, through January 17, 2015. Triangular markers denote relative humidity value from KTIP weather station, square markers denote measured relative humidity values from ballast, and circular markers denote measured relative humidity values inside concrete.

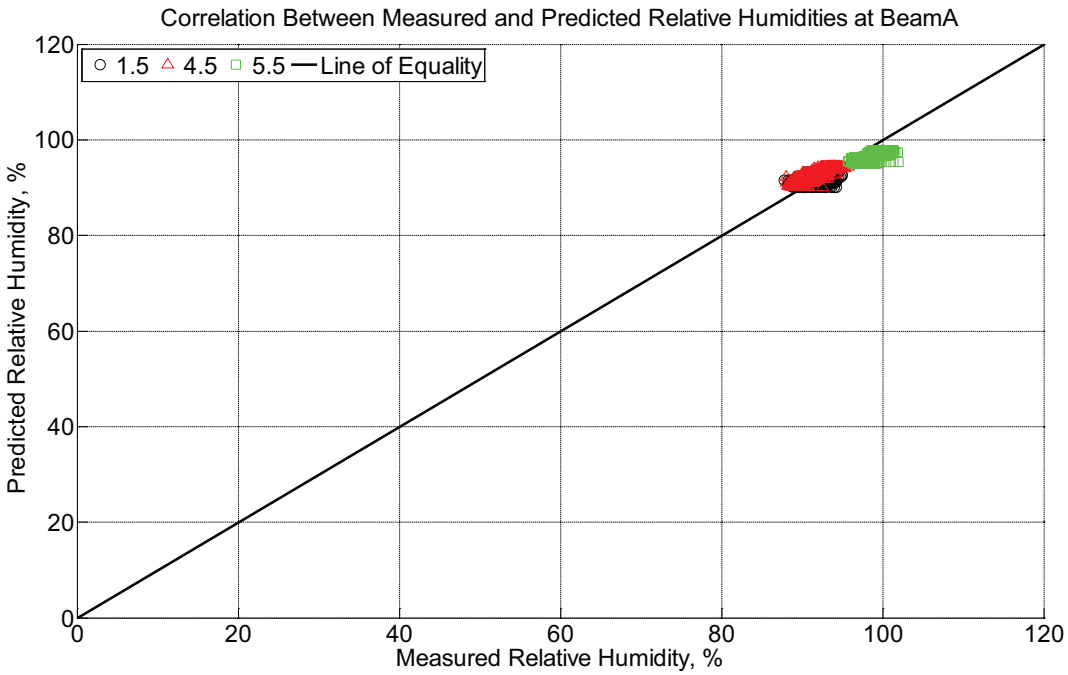

Figure B-134 Correlation between measured and predicted relative humidity values 1.5 inches (38.1 mm), 4.5 inches (114.3 mm), and 5.5 inches (139.7 mm) from the surface of a modulus of rupture beam (labeled A) installed in ballast in Rantoul, IL, between December 21, 2014, through January 17, 2015.

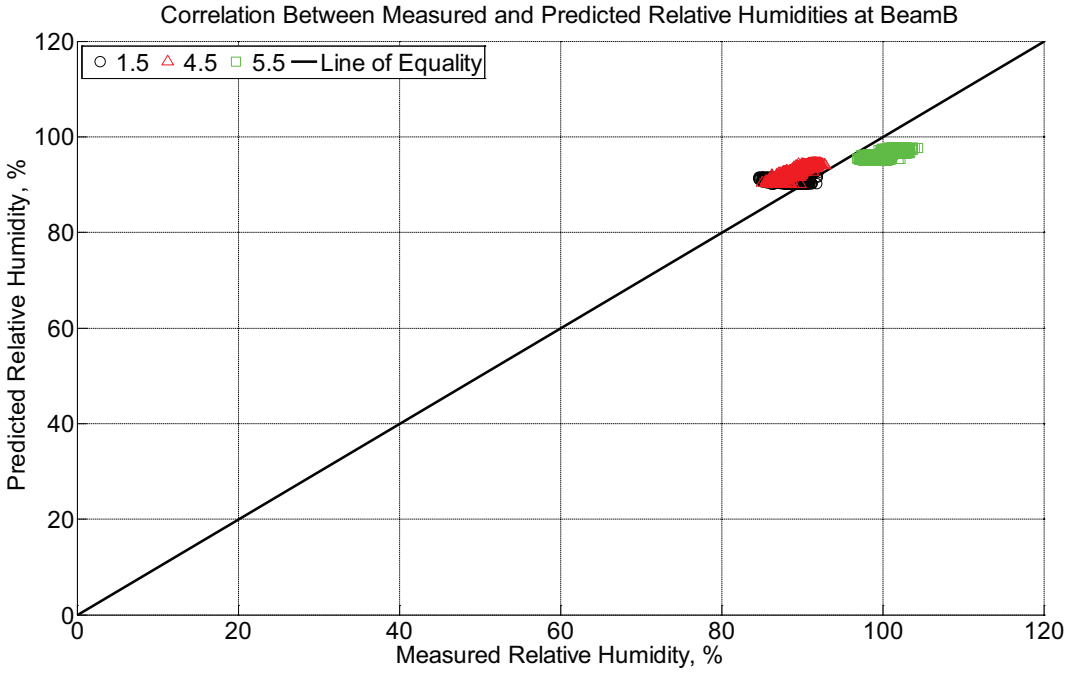

Figure B-135 Correlation between measured and predicted relative humidity values 1.5 inches (38.1 mm), 4.5 inches (114.3 mm), and 5.5 inches (139.7 mm) from the surface of a

modulus of rupture beam (labeled B) installed in ballast in Rantoul, IL, between December 21, 2014, through January 17, 2015.

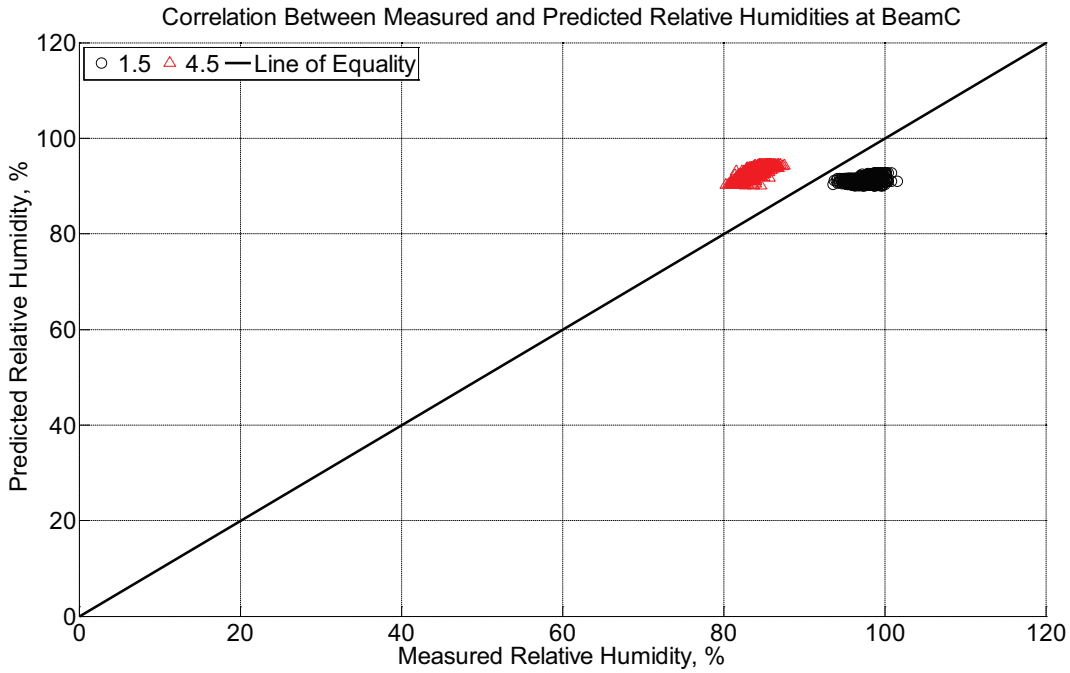

Figure B-136 Correlation between measured and predicted relative humidity values 1.5 inches (38.1 mm) and 4.5 inches (114.3 mm) from the surface of a modulus of rupture beam (labeled C) installed in ballast in Rantoul, IL, between December 21, 2014, through January 17, 2015.

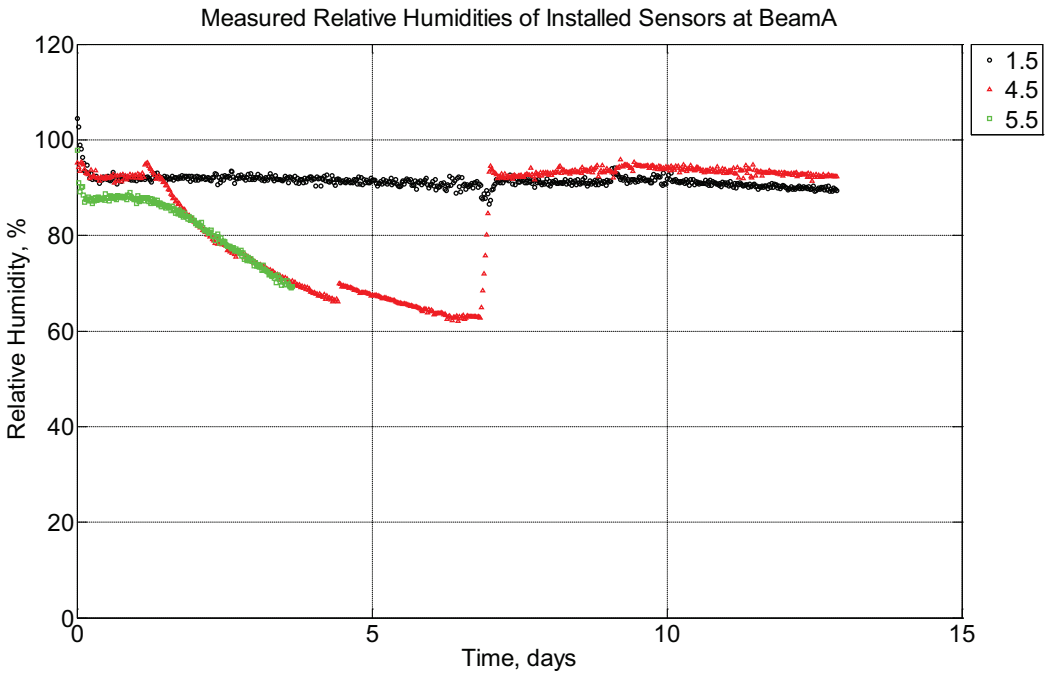

Figure B-137 Measured relative humidity at depths of 1.5 inches (38.1 mm), 4.5 inches (114.3 mm), and 5.5 inches (139.7 mm) from the surface of a modulus of rupture beam (labeled A) located inside a heating oven (65ºC and 0ºC) and an environmentally controlled room (50% RH, 23ºC) between January 17, 2015, through January 30, 2015.

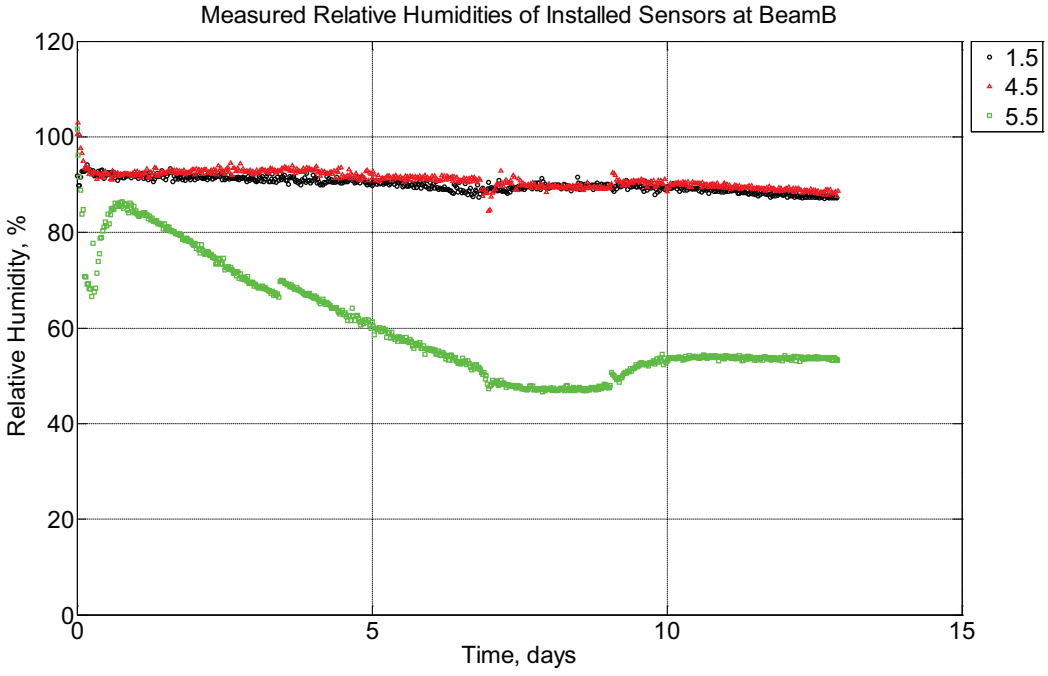

Figure B-138 Measured relative humidity at depths of 1.5 inches (38.1 mm), 4.5 inches (114.3 mm), and 5.5 inches (139.7 mm) from the surface of a modulus of rupture beam

(labeled B) located inside a heating oven (65ºC and 0ºC) and an environmentally controlled room (50% RH, 23ºC) between January 17, 2015, through January 30, 2015.

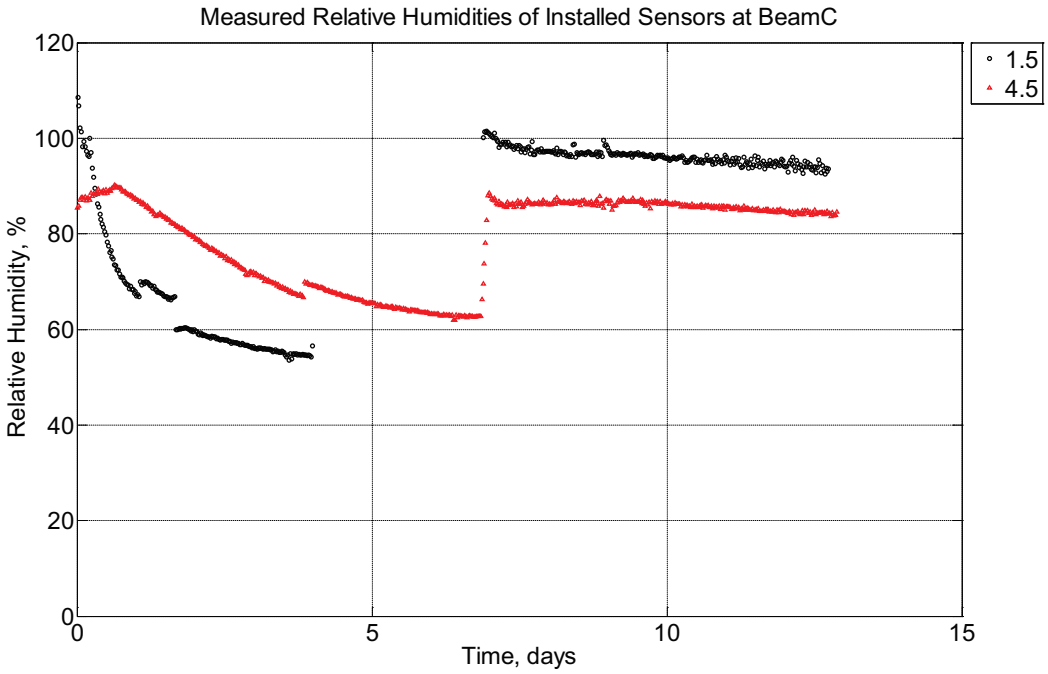

Figure B-139 Measured relative humidity at depths of 1.5 inches (38.1 mm) and 4.5 inches (114.3 mm) from the surface of a modulus of rupture beam (labeled C) located inside a heating oven (65ºC and 0ºC) and an environmentally controlled room (50% RH, 23ºC) between January 17, 2015, through January 30, 2015.

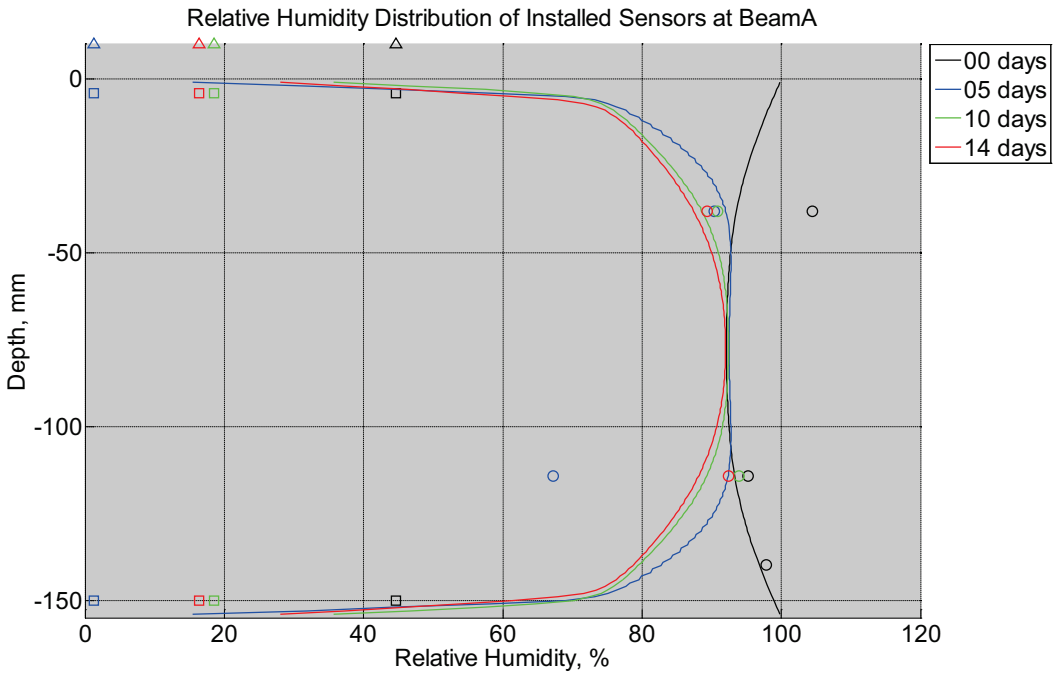

Figure B-140 Measured (markers) and modeled (continuous line) relative humidity profile distribution as a function of depth inside modulus of rupture beam (labeled A) located inside a heating oven (65ºC and 0ºC) and an environmentally controlled room (50% RH, 23ºC) between January 17, 2015, through January 30, 2015. Triangular markers denote relative humidity value from control panel, square markers denote measured relative humidity values from ambient sensors, and circular markers denote measured relative humidity values inside concrete.

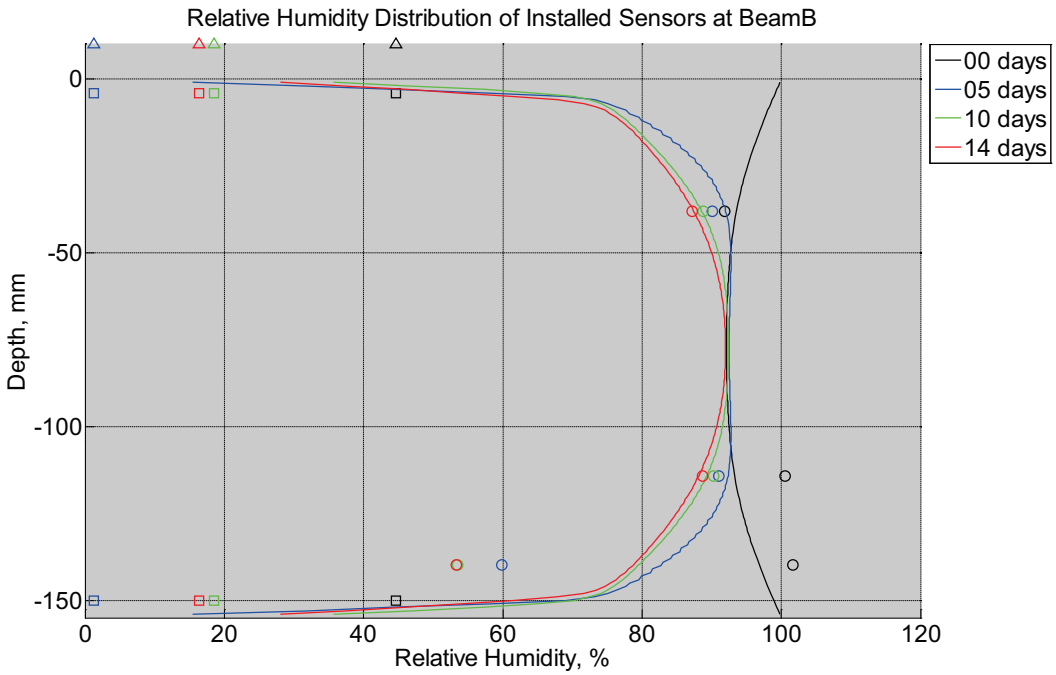

Figure B-141 Measured (markers) and modeled (continuous line) relative humidity profile distribution as a function of depth inside modulus of rupture beam (labeled B) located inside a heating oven (65ºC and 0ºC) and an environmentally controlled room (50% RH, 23ºC) between January 17, 2015, through January 30, 2015. Triangular markers denote relative humidity value from control panel, square markers denote measured relative humidity values from ambient sensors, and circular markers denote measured relative humidity values inside concrete.

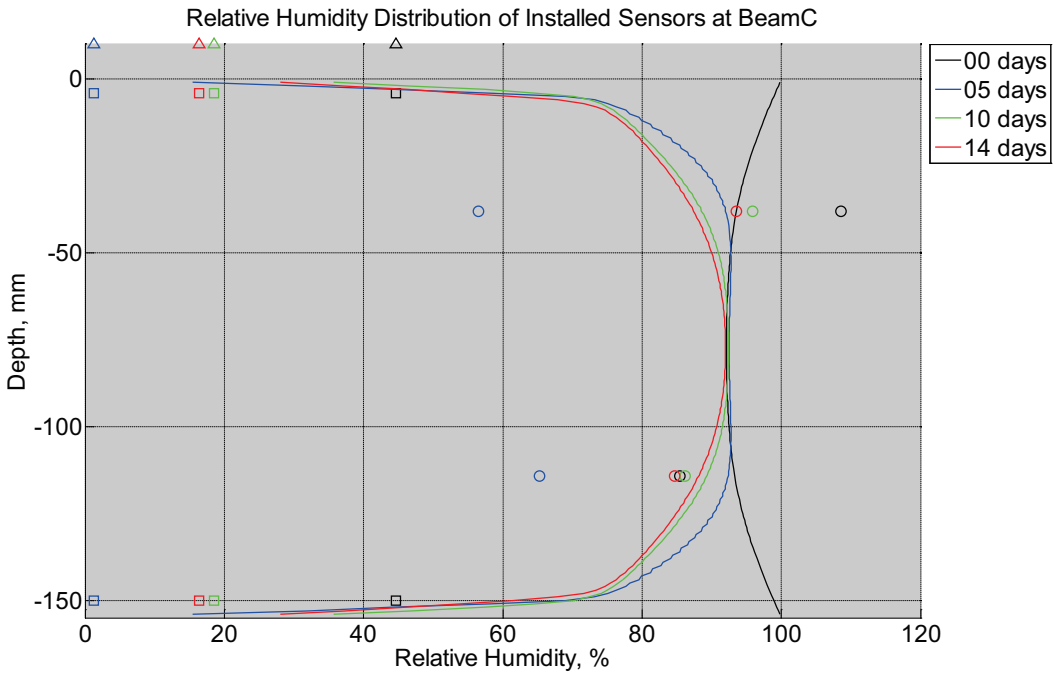

Figure B-142 Measured (markers) and modeled (continuous line) relative humidity profile distribution as a function of depth inside modulus of rupture beam (labeled C) located inside a heating oven (65ºC and 0ºC) and an environmentally controlled room (50% RH, 23ºC) between January 17, 2015, through January 30, 2015. Triangular markers denote relative humidity value from control panel, square markers denote measured relative humidity values from ambient sensors, and circular markers denote measured relative humidity values inside concrete.

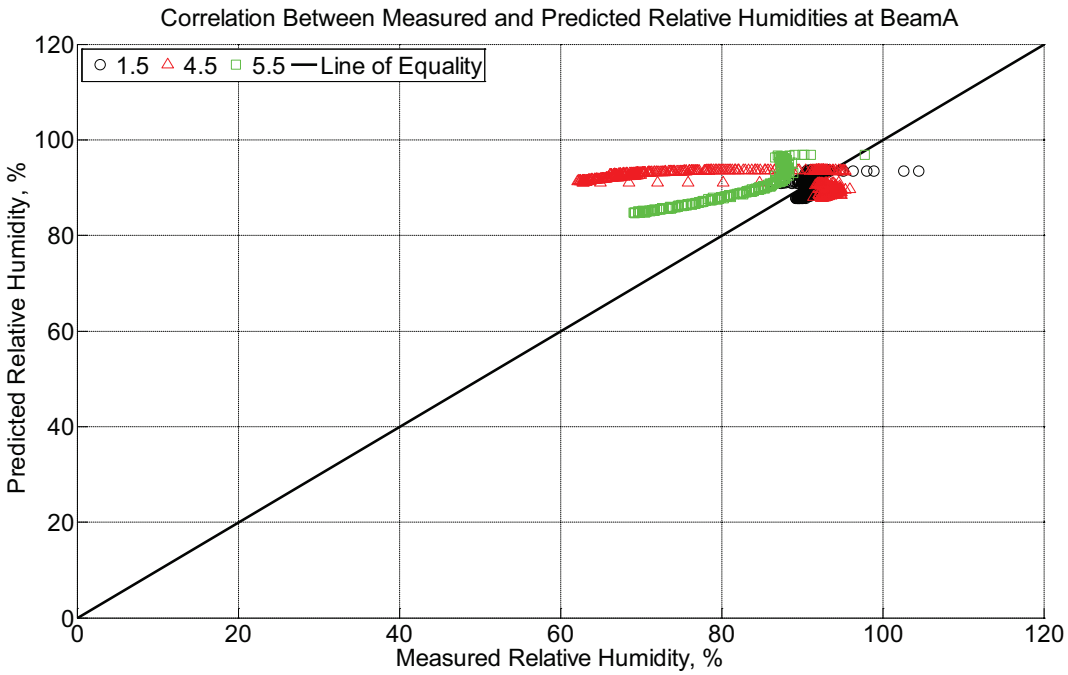

Figure B-143 Correlation between measured and predicted relative humidity values 1.5 inches (38.1 mm), 4.5 inches (114.3 mm), and 5.5 inches (139.7 mm) from the surface of a modulus of rupture beam (labeled A) located inside a heating oven (65ºC and 0ºC) and an environmentally controlled room (50% RH, 23ºC) between January 17, 2015, through January 30, 2015.

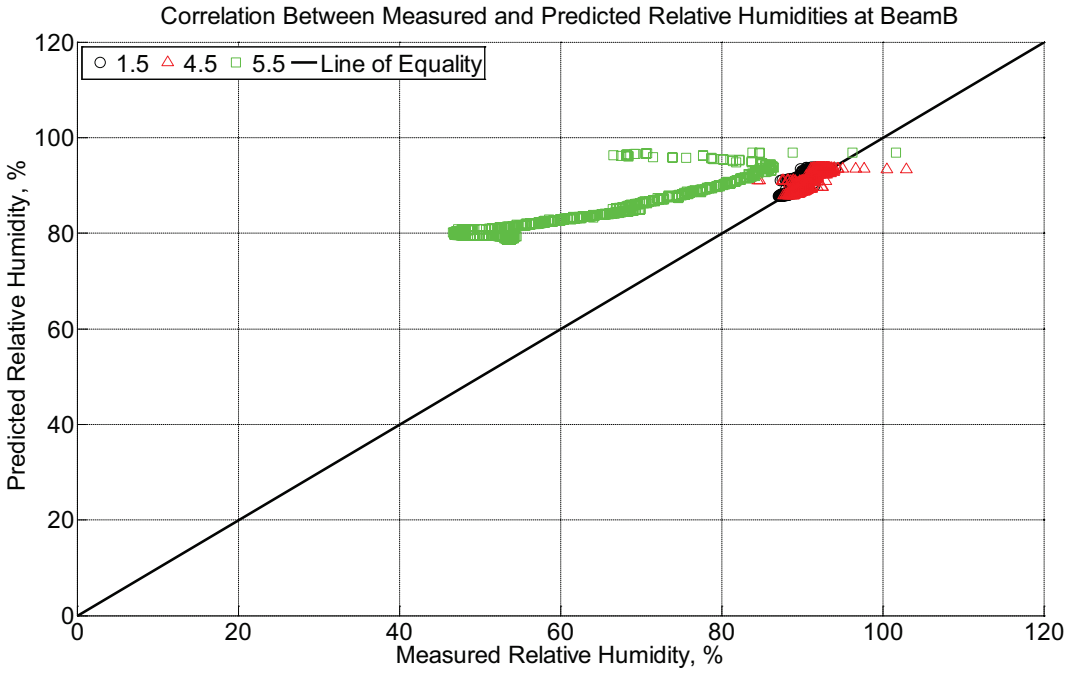

Figure B-144 Correlation between measured and predicted relative humidity values 1.5

inches (38.1 mm), 4.5 inches (114.3 mm), and 5.5 inches (139.7 mm) from the surface of a modulus of rupture beam (labeled B) located inside a heating oven (65ºC and 0ºC) and an environmentally controlled room (50% RH, 23ºC) between January 17, 2015, through January 30, 2015.

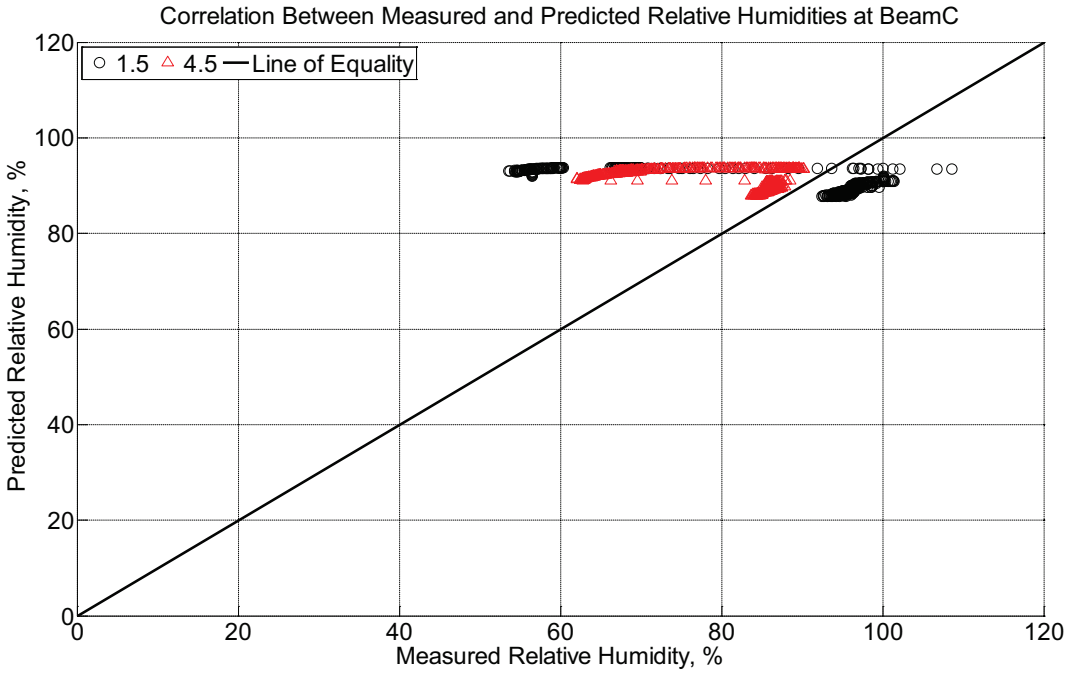

Figure B-145 Correlation between measured and predicted relative humidity values 1.5 inches (38.1 mm) and 4.5 inches (114.3 mm) from the surface of a modulus of rupture beam (labeled C) located inside a heating oven (65ºC and 0ºC) and an environmentally controlled room (50% RH, 23ºC) between January 17, 2015, through January 30, 2015.

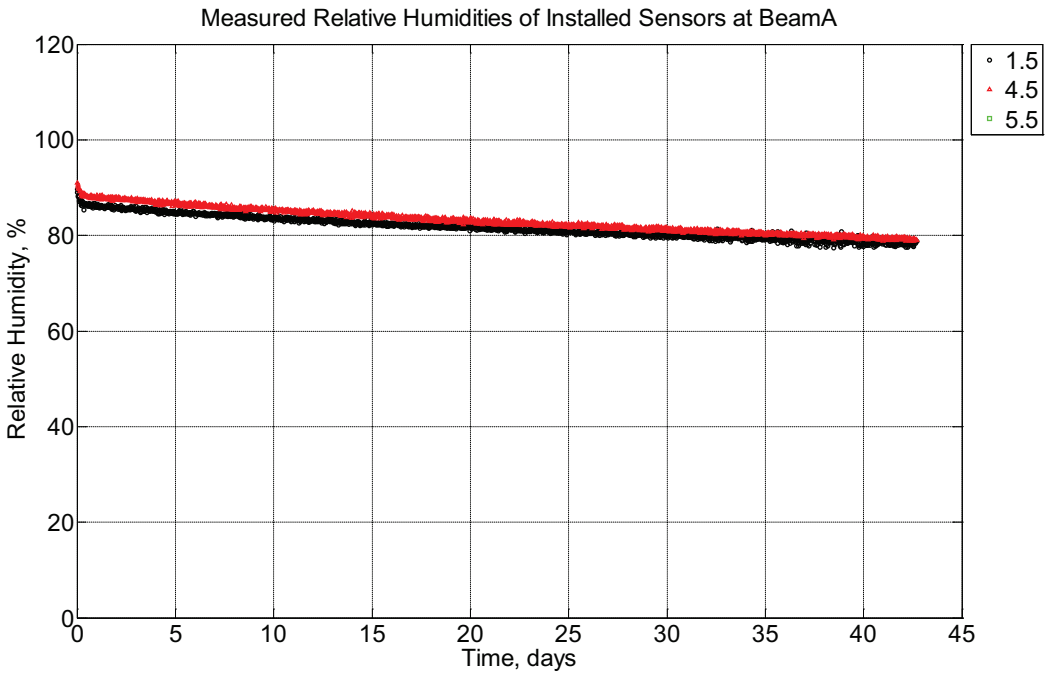

Figure B-146 Measured relative humidity at depths of 1.5 inches (38.1 mm), 4.5 inches (114.3 mm), and 5.5 inches (139.7 mm) from the surface of a modulus of rupture beam (labeled A) located inside an environmentally controlled room (50% RH, 23ºC) between February 5, 2015, through March 20, 2015.

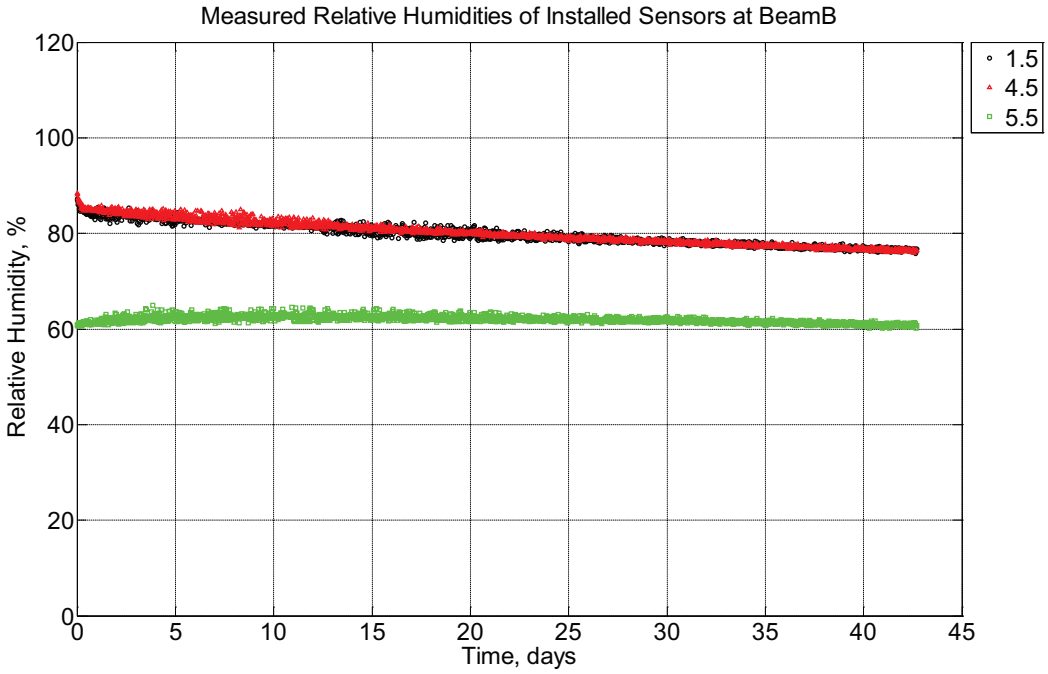

Figure B-147 Measured relative humidity at depths of 1.5 inches (38.1 mm), 4.5 inches (114.3 mm), and 5.5 inches (139.7 mm) from the surface of a modulus of rupture beam

(labeled B) located inside an environmentally controlled room (50% RH, 23°C) between February 5, 2015, through March 20, 2015.

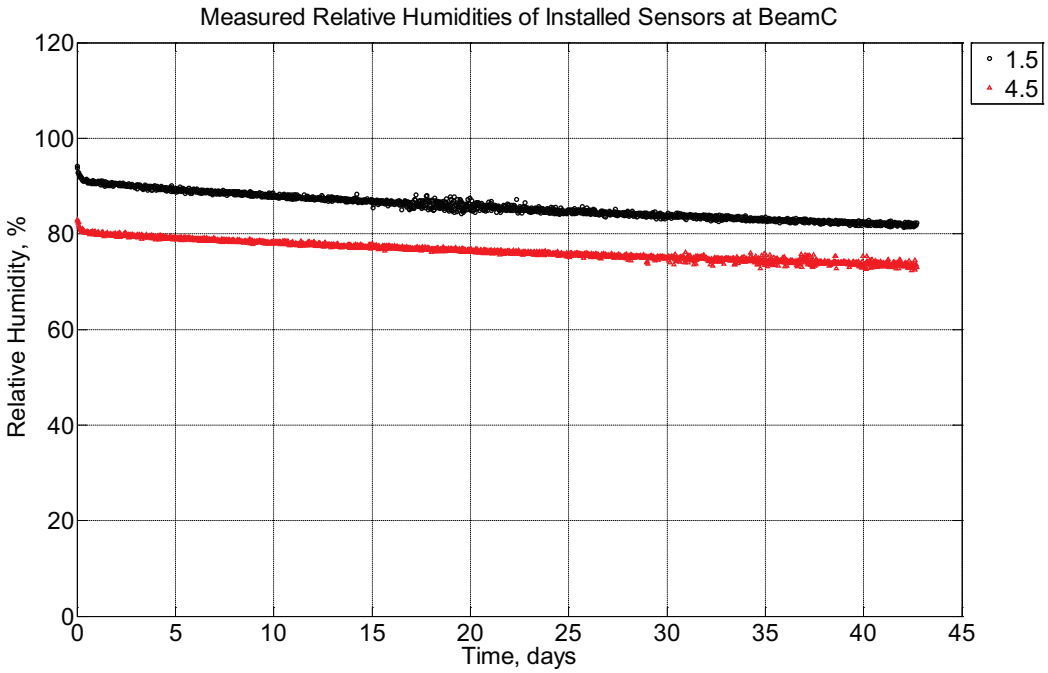

Figure B-148 Measured relative humidity at depths of 1.5 inches (38.1 mm) and 4.5 inches (114.3 mm) from the surface of a modulus of rupture beam (labeled C) located inside an environmentally controlled room (50% RH, 23°C) between February 5, 2015, through March 20, 2015.

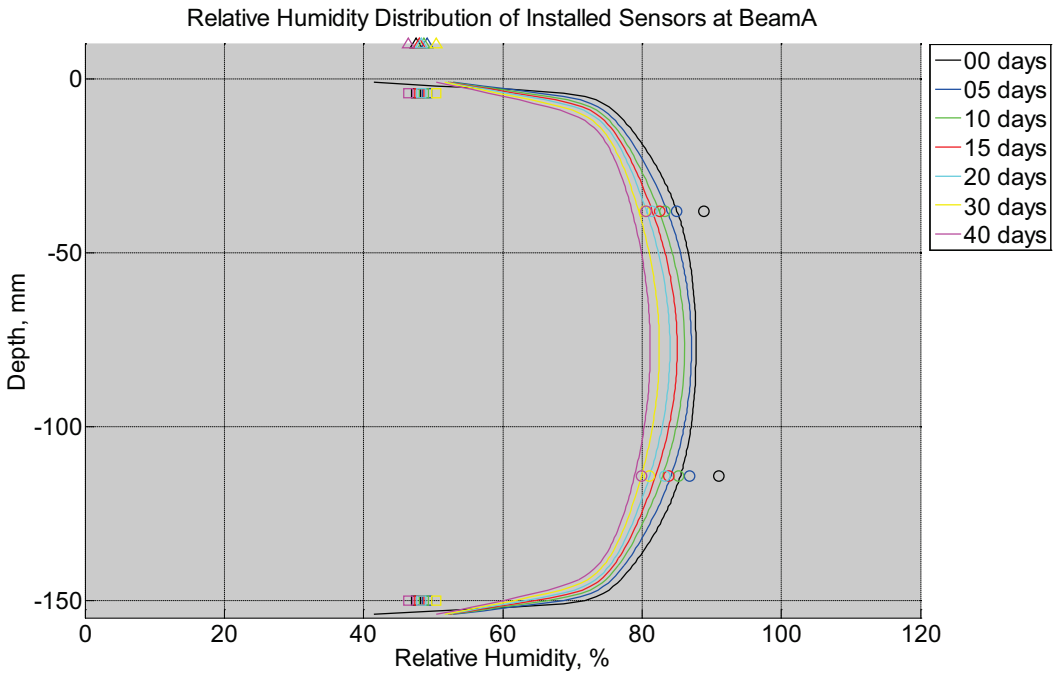

Figure B-149 Measured (markers) and modeled (continuous line) relative humidity profile distribution as a function of depth inside modulus of rupture beam (labeled A) located inside an environmentally controlled room (50% RH, 23°C) between February 5, 2015, through March 20, 2015. Triangular markers denote relative humidity value from control panel, square markers denote measured relative humidity values from ambient sensors, and circular markers denote measured relative humidity values inside concrete.

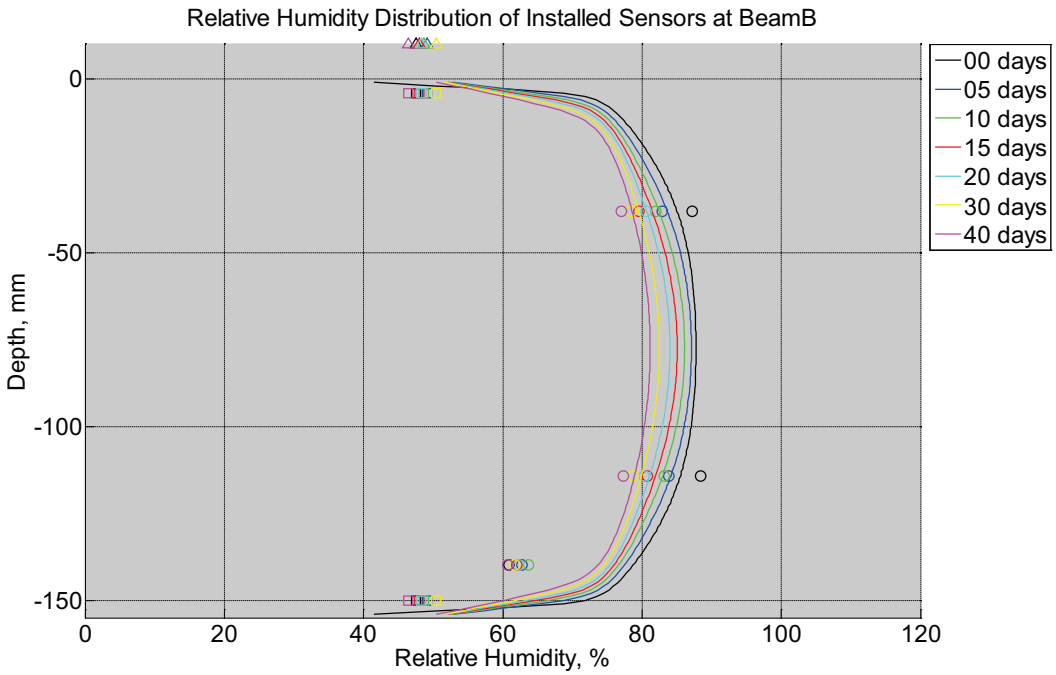

Figure B-150 Measured (markers) and modeled (continuous line) relative humidity profile distribution as a function of depth inside modulus of rupture beam (labeled B) located inside an environmentally controlled room (50% RH, 23°C) between February 5, 2015, through March 20, 2015. Triangular markers denote relative humidity value from control panel, square markers denote measured relative humidity values from ambient sensors, and circular markers denote measured relative humidity values inside concrete.

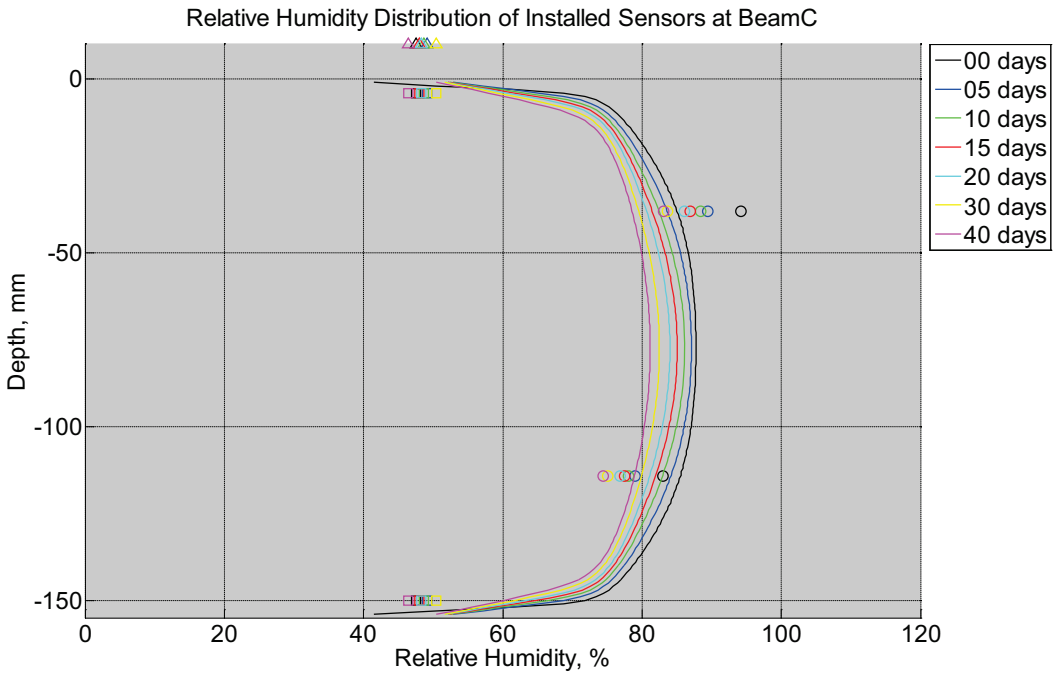

Figure B-151 Measured (markers) and modeled (continuous line) relative humidity profile distribution as a function of depth inside modulus of rupture beam (labeled C) located inside an environmentally controlled room (50% RH, 23°C) between February 5, 2015, through March 20, 2015. Triangular markers denote relative humidity value from control panel, square markers denote measured relative humidity values from ambient sensors, and circular markers denote measured relative humidity values inside concrete.

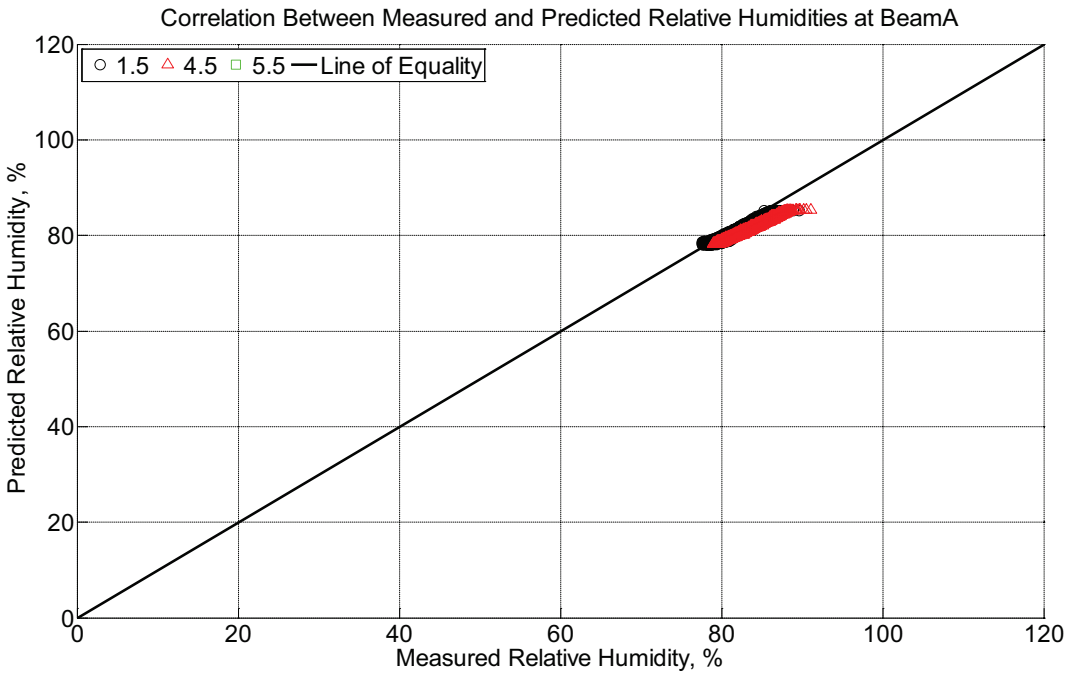

Figure B-152 Correlation between measured and predicted relative humidity values 1.5 inches (38.1 mm), 4.5 inches (114.3 mm), and 5.5 inches (139.7 mm) from the surface of a modulus of rupture beam (labeled A) located inside an environmentally controlled room (50% RH, 23°C) between February 5, 2015, through March 20, 2015.

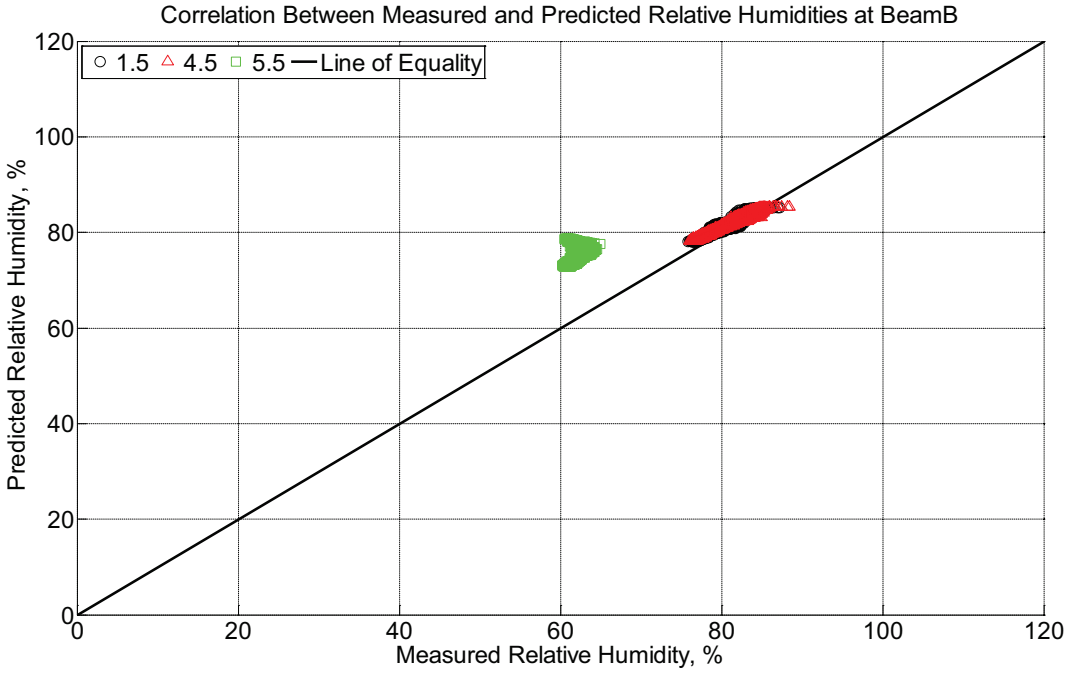

Figure B-153 Correlation between measured and predicted relative humidity values 1.5 inches (38.1 mm), 4.5 inches (114.3 mm), and 5.5 inches (139.7 mm) from the surface of a

modulus of rupture beam (labeled B) located inside an environmentally controlled room (50% RH, 23°C) between February 5, 2015, through March 20, 2015.

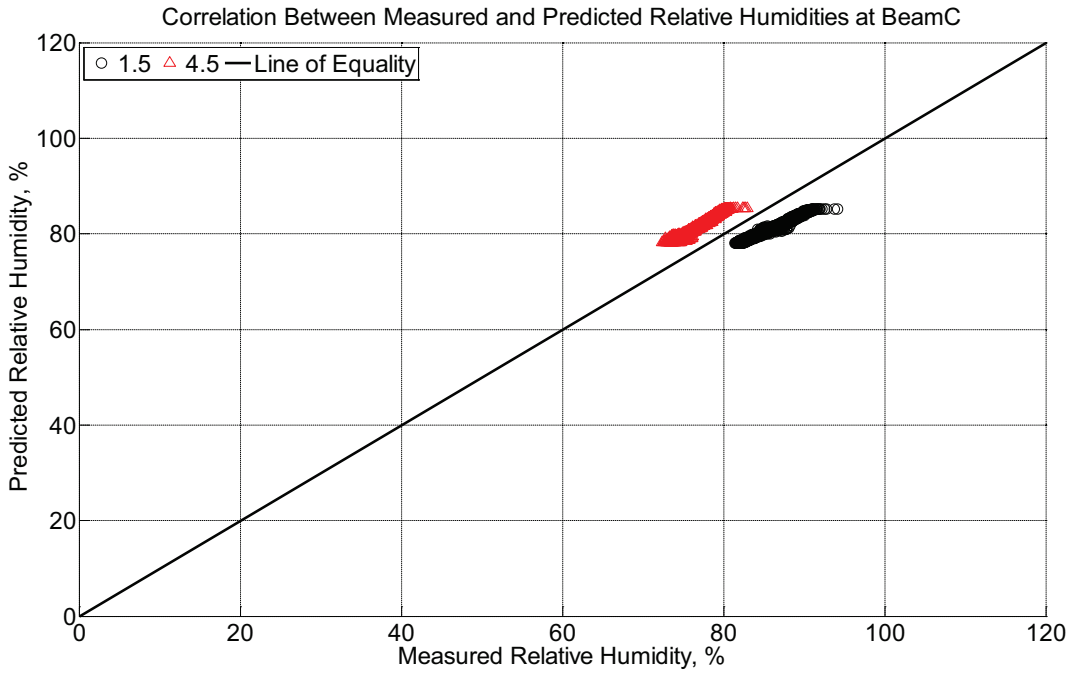

Figure B-154 Correlation between measured and predicted relative humidity values 1.5 inches (38.1 mm) and 4.5 inches (114.3 mm) from the surface of a modulus of rupture beam (labeled C) located inside an environmentally controlled room (50% RH, 23°C) between February 5, 2015, through March 20, 2015.

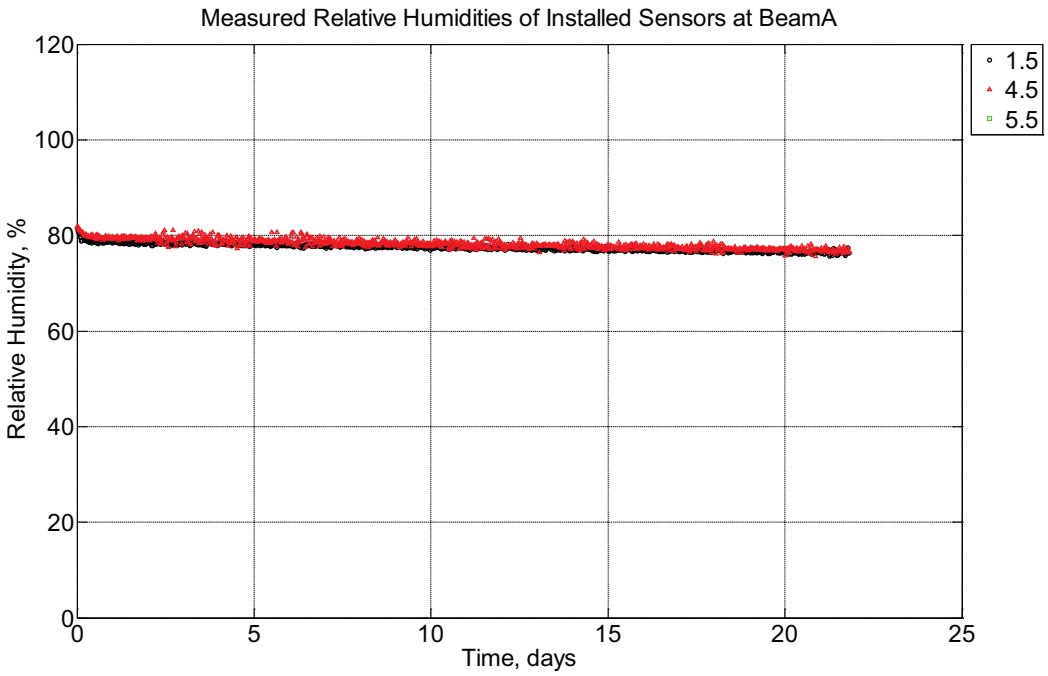

Figure B-155 Measured relative humidity at depths of 1.5 inches (38.1 mm), 4.5 inches (114.3 mm), and 5.5 inches (139.7 mm) from the surface of a modulus of rupture beam (labeled A) located inside an environmentally controlled room (50% RH, 23ºC) between March 20, 2015, through April 11, 2015.

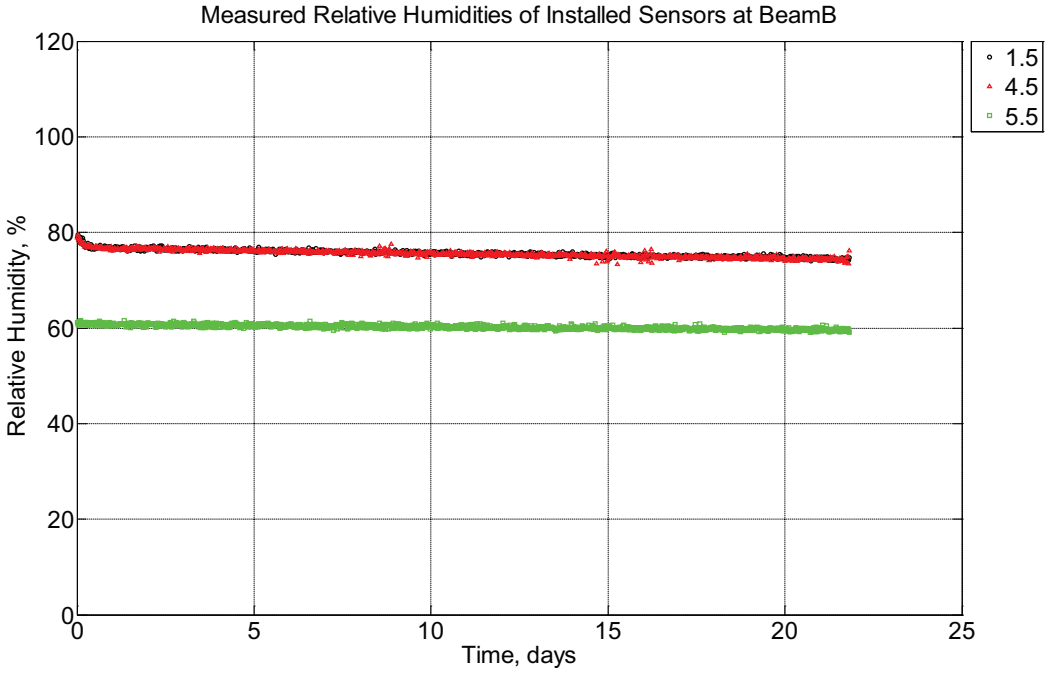

Figure B-156 Measured relative humidity at depths of 1.5 inches (38.1 mm), 4.5 inches (114.3 mm), and 5.5 inches (139.7 mm) from the surface of a modulus of rupture beam

(labeled B) located inside an environmentally controlled room (50% RH, 23°C) between March 20, 2015, through April 11, 2015.

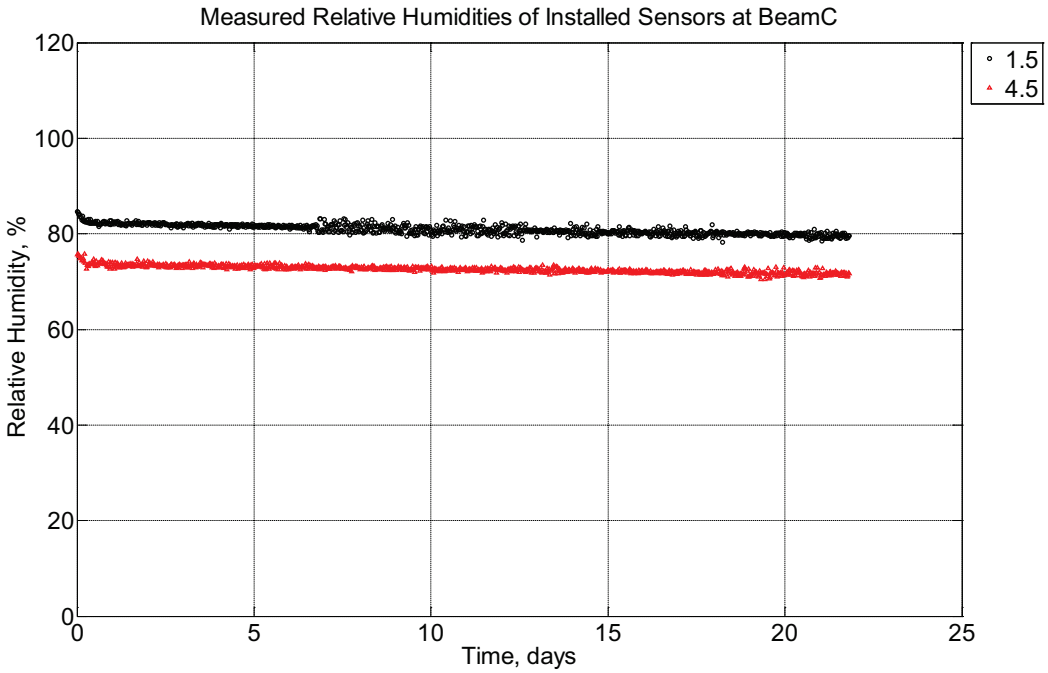

Figure B-157 Measured relative humidity at depths of 1.5 inches (38.1 mm) and 4.5 inches (114.3 mm) from the surface of a modulus of rupture beam (labeled C) located inside an environmentally controlled room (50% RH, 23°C) between March 20, 2015, through April 11, 2015.

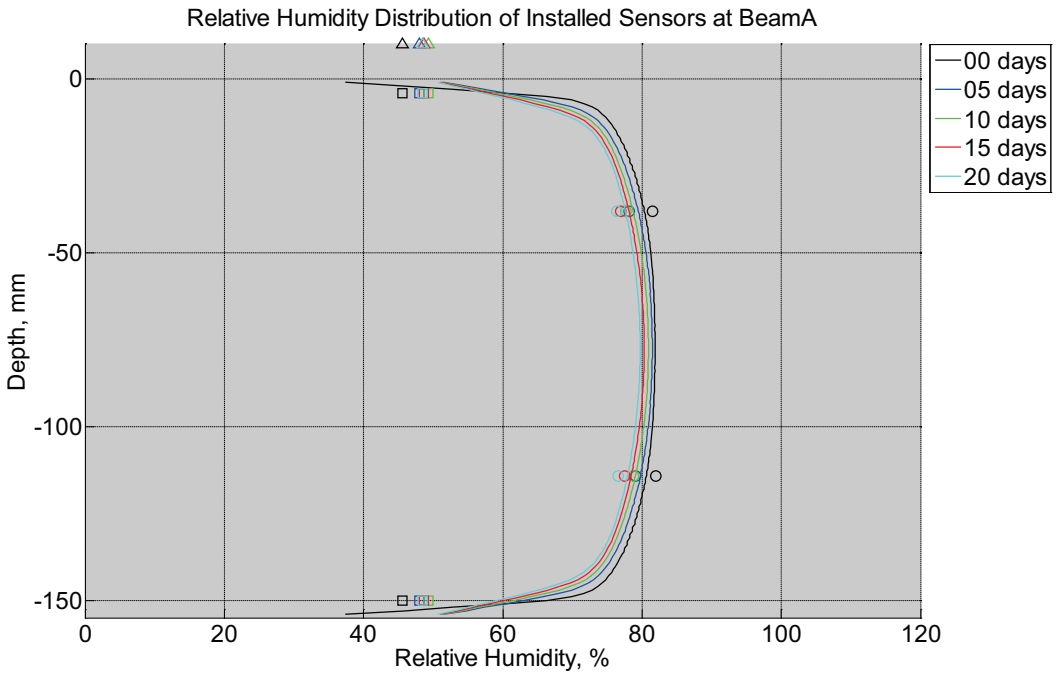

Figure B-158 Measured (markers) and modeled (continuous line) relative humidity profile distribution as a function of depth inside modulus of rupture beam (labeled A) located inside an environmentally controlled room (50% RH, 23°C) between March 20, 2015, through April 11, 2015. Triangular markers denote relative humidity value from control panel, square markers denote measured relative humidity values from ambient sensors, and circular markers denote measured relative humidity values inside concrete.

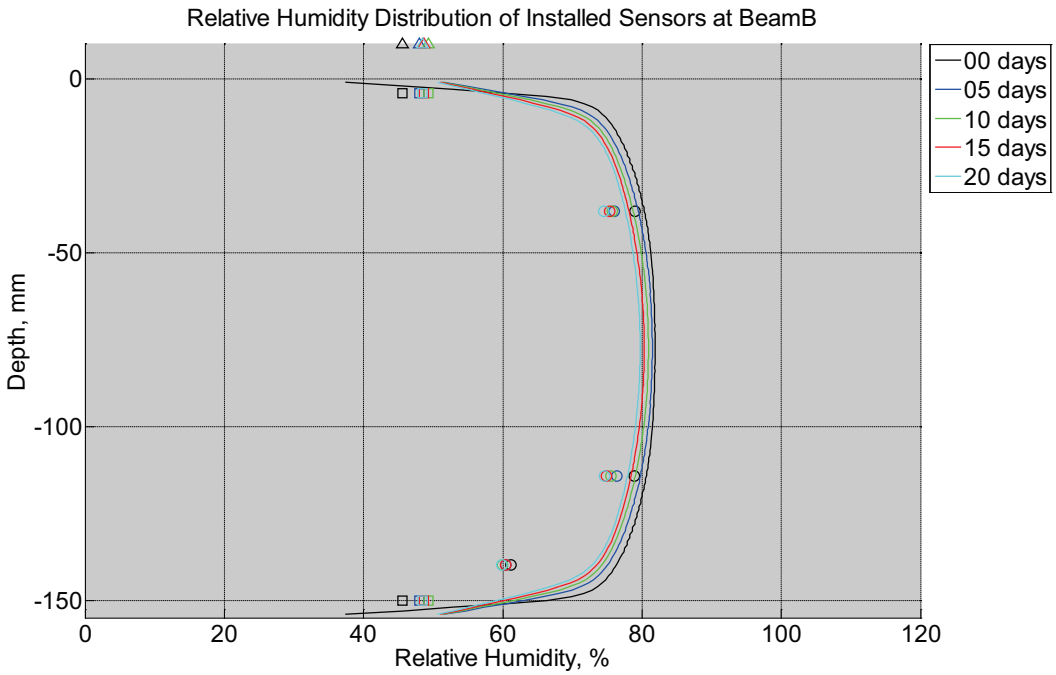

Figure B-159 Measured (markers) and modeled (continuous line) relative humidity profile distribution as a function of depth inside modulus of rupture beam (labeled B) located inside an environmentally controlled room (50% RH, 23ºC) between March 20, 2015, through April 11, 2015. Triangular markers denote relative humidity value from control panel, square markers denote measured relative humidity values from ambient sensors, and circular markers denote measured relative humidity values inside concrete.

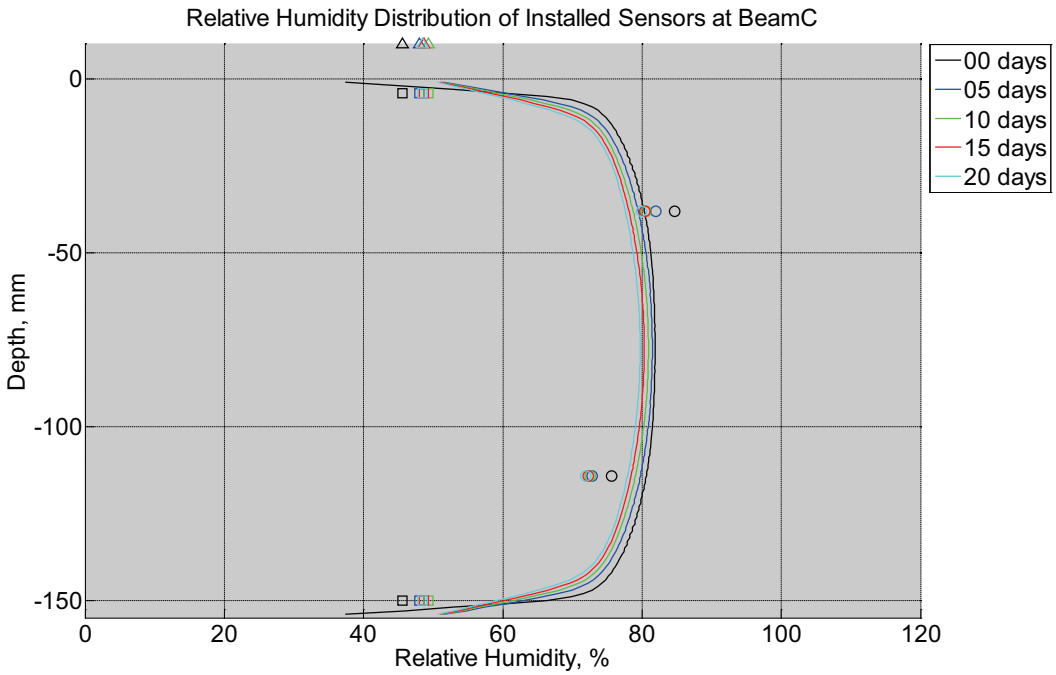

Figure B-160 Measured (markers) and modeled (continuous line) relative humidity profile distribution as a function of depth inside modulus of rupture beam (labeled C) located inside an environmentally controlled room (50% RH, 23°C) between March 20, 2015, through April 11, 2015. Triangular markers denote relative humidity value from control panel, square markers denote measured relative humidity values from ambient sensors, and circular markers denote measured relative humidity values inside concrete.

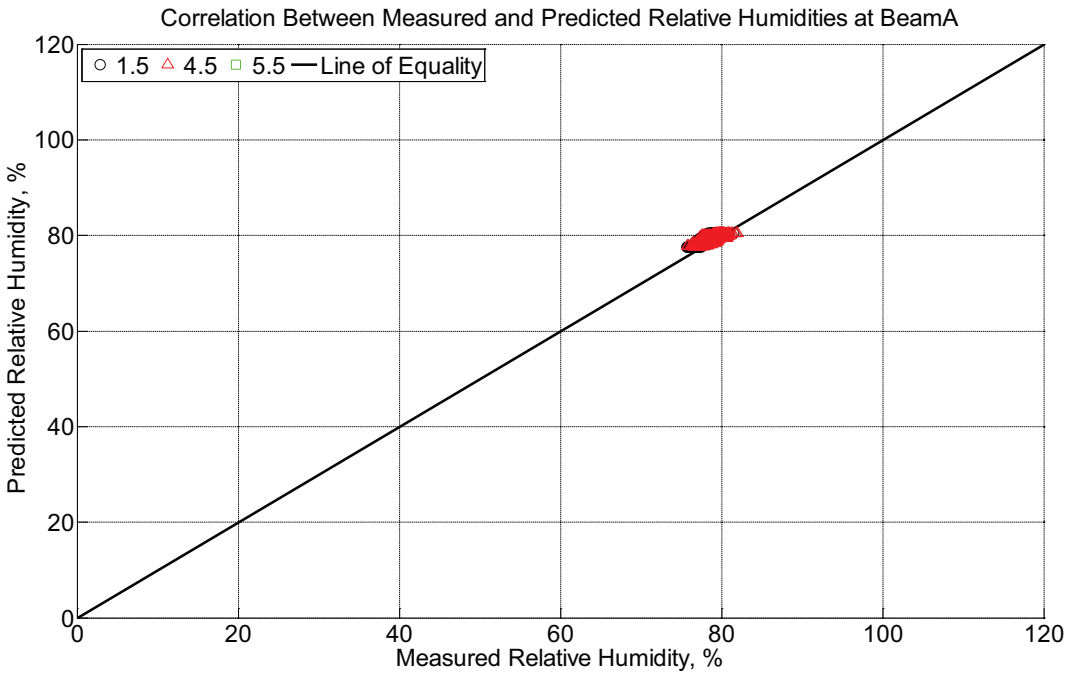

Figure B-161 Correlation between measured and predicted relative humidity values 1.5 inches (38.1 mm), 4.5 inches (114.3 mm), and 5.5 inches (139.7 mm) from the surface of a modulus of rupture beam (labeled A) located inside an environmentally controlled room (50% RH, 23ºC) between March 20, 2015, through April 11, 2015.

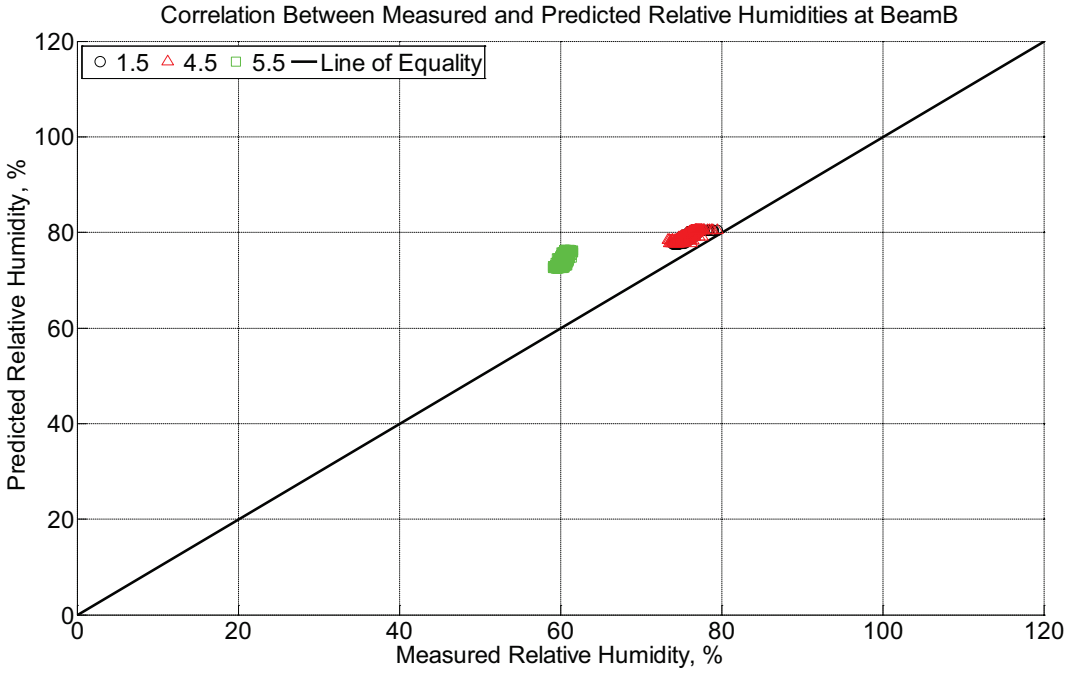

Figure B-162 Correlation between measured and predicted relative humidity values 1.5 inches (38.1 mm), 4.5 inches (114.3 mm), and 5.5 inches (139.7 mm) from the surface of a

modulus of rupture beam (labeled B) located inside an environmentally controlled room (50% RH, 23°C) between March 20, 2015, through April 11, 2015.

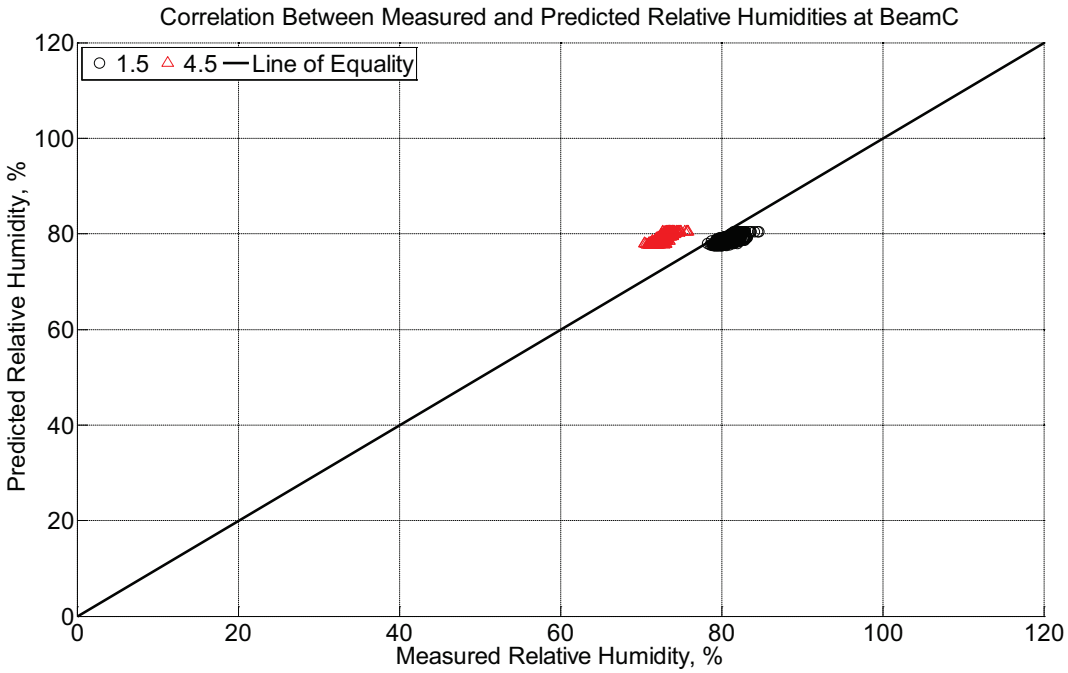

Figure B-163 Correlation between measured and predicted relative humidity values 1.5 inches (38.1 mm) and 4.5 inches (114.3 mm) from the surface of a modulus of rupture beam (labeled C) located inside an environmentally controlled room (50% RH, 23°C) between March 20, 2015, through April 11, 2015.

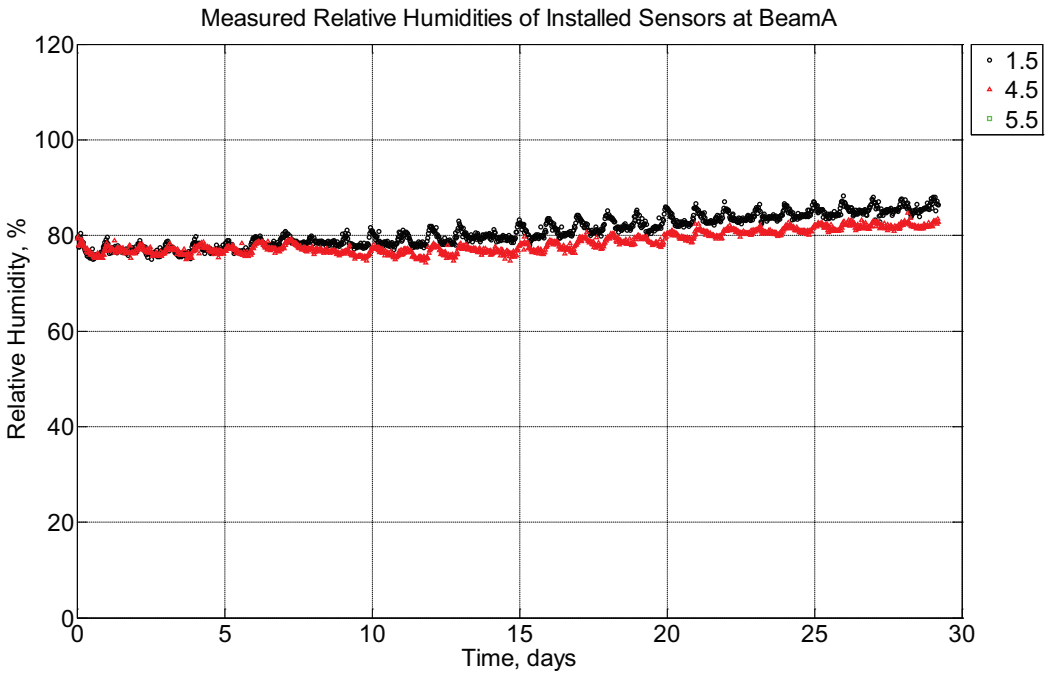

Figure B-164 Measured relative humidity at depths of 1.5 inches (38.1 mm), 4.5 inches (114.3 mm), and 5.5 inches (139.7 mm) from the surface of a modulus of rupture beam (labeled A) installed in ballast in Rantoul, IL, between April 11, 2015, through May 10, 2015.

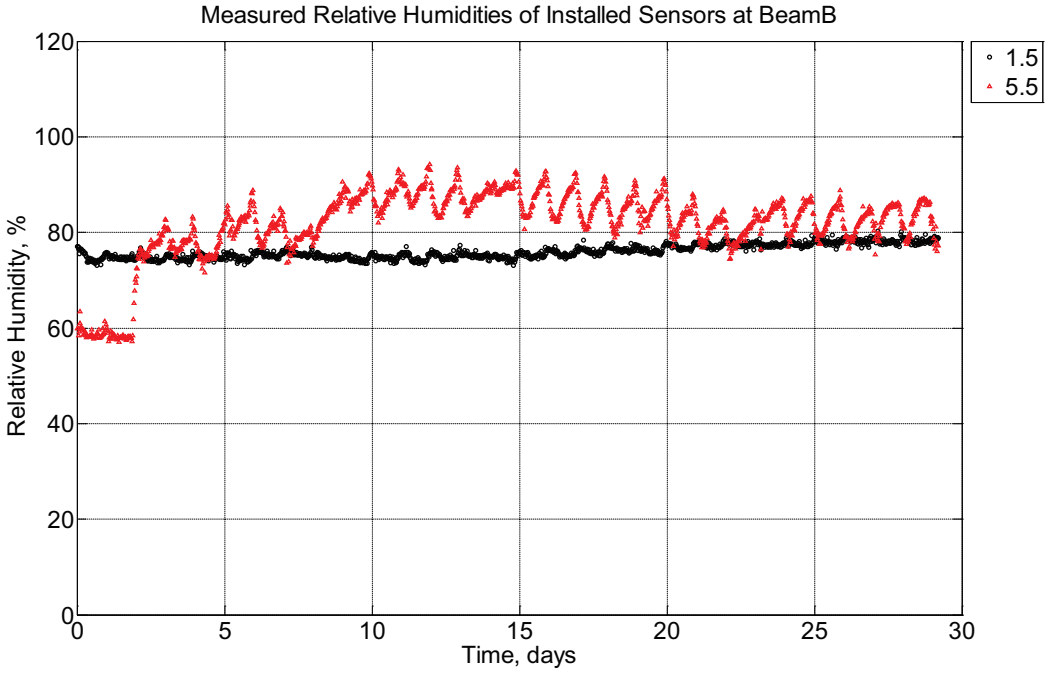

Figure B-165 Measured relative humidity at depths of 1.5 inches (38.1 mm) and 5.5 inches

(139.7 mm) from the surface of a modulus of rupture beam (labeled B) installed in ballast in Rantoul, IL, between April 11, 2015, through May 10, 2015.

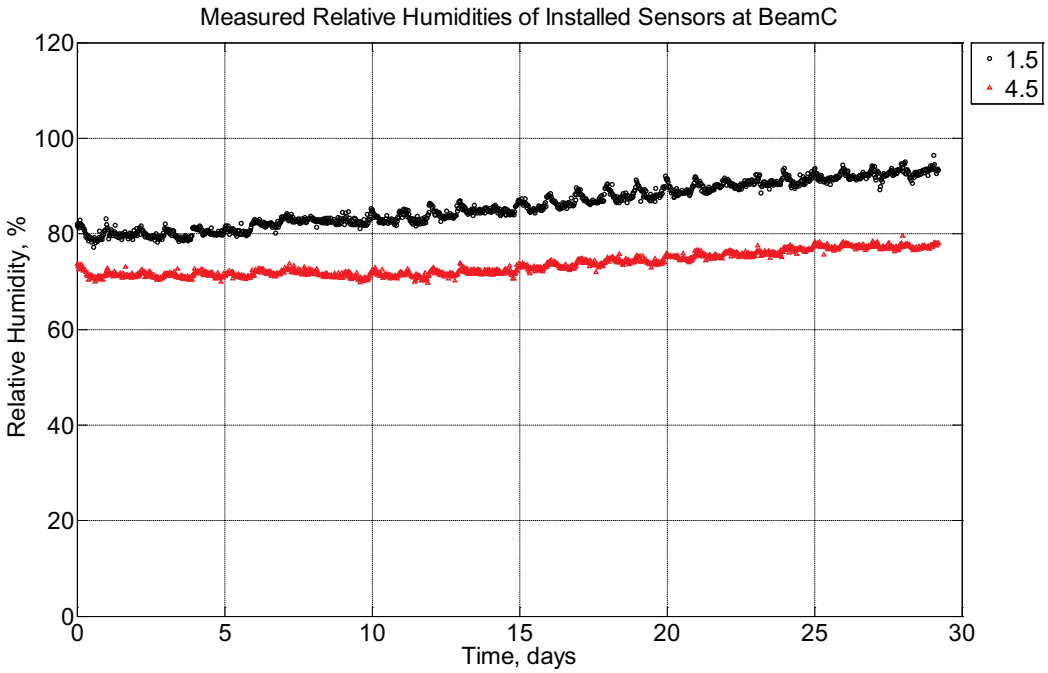

Figure B-166 Measured relative humidity at depths of 1.5 inches (38.1 mm) and 4.5 inches (114.3 mm) from the surface of a modulus of rupture beam (labeled C) installed in ballast in Rantoul, IL, between April 11, 2015, through May 10, 2015.

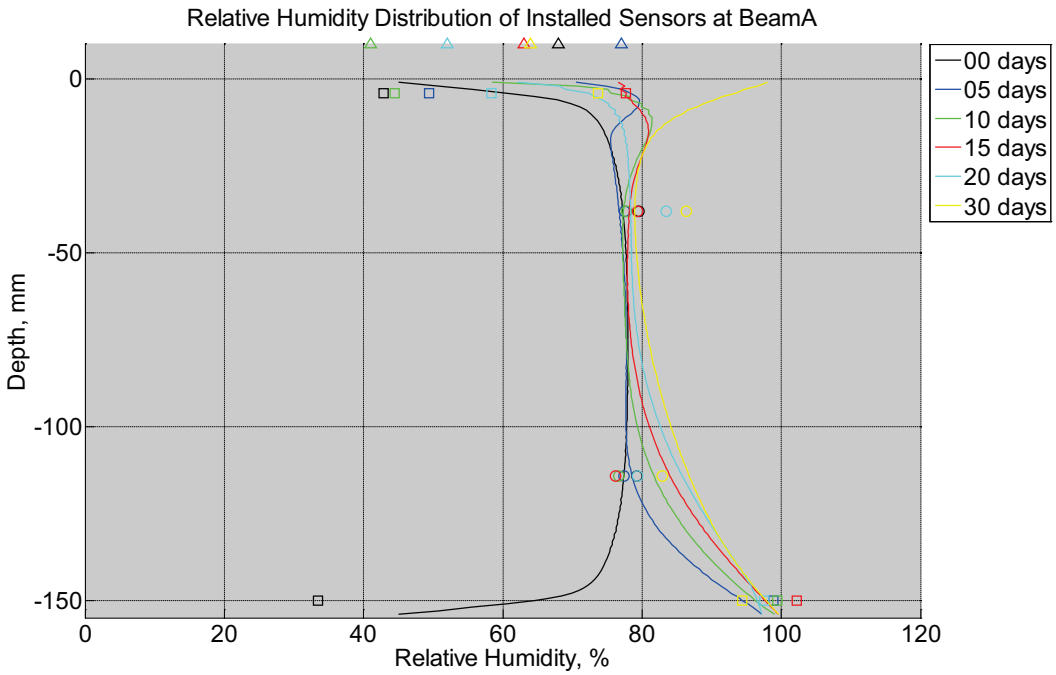

Figure B-167 Measured (markers) and modeled (continuous line) relative humidity distribution as a function of depth inside modulus of rupture beam (labeled A) installed in ballast in Rantoul, IL, between April 11, 2015, through May 10, 2015. Triangular markers denote relative humidity value from KTIP weather station, square markers denote measured relative humidity values from ballast, and circular markers denote measured relative humidity values inside concrete.

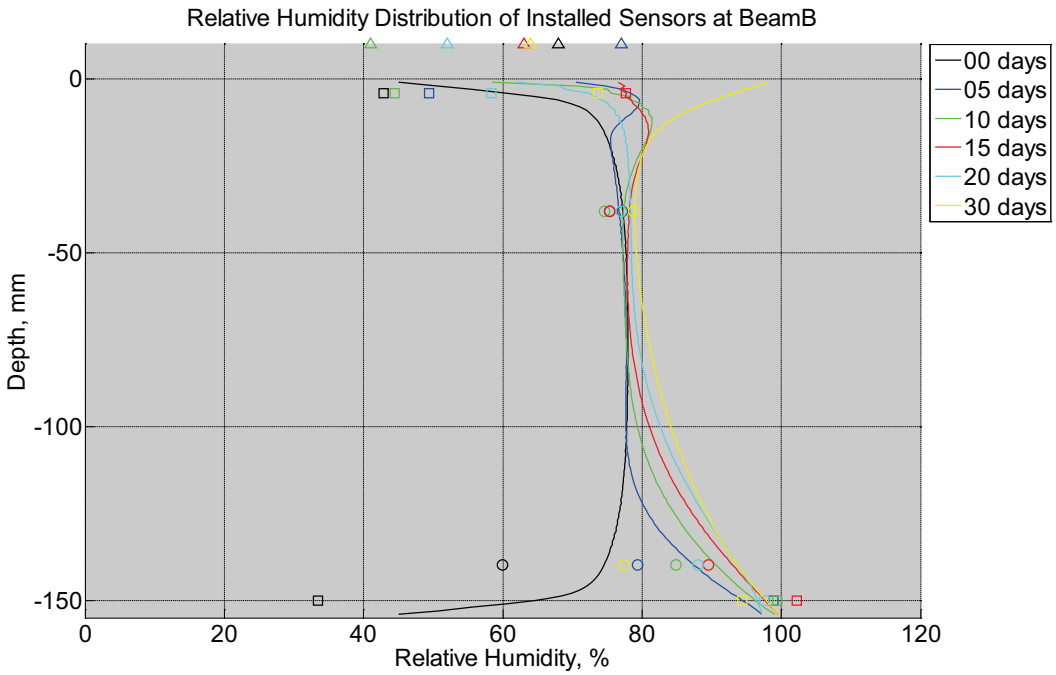

Figure B-168 Measured (markers) and modeled (continuous line) relative humidity distribution as a function of depth inside modulus of rupture beam (labeled B) installed in ballast in Rantoul, IL, between April 11, 2015, through May 10, 2015. Triangular markers denote relative humidity value from KTIP weather station, square markers denote measured relative humidity values from ballast, and circular markers denote measured relative humidity values inside concrete.

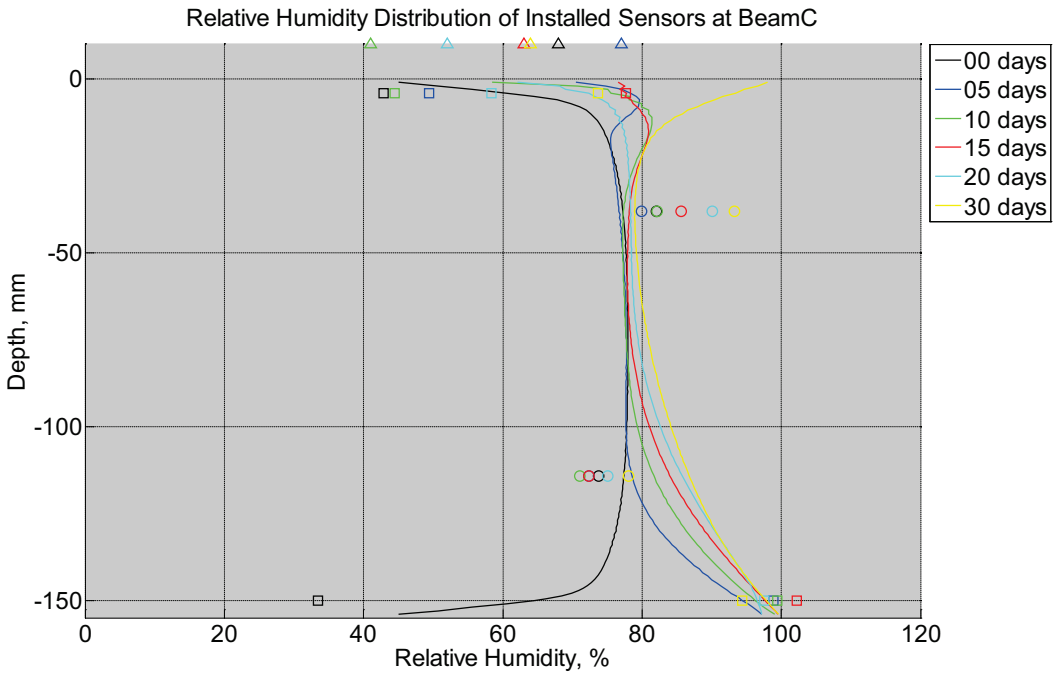

Figure B-169 Measured (markers) and modeled (continuous line) relative humidity distribution as a function of depth inside modulus of rupture beam (labeled C) installed in ballast in Rantoul, IL, between April 11, 2015, through May 10, 2015. Triangular markers denote relative humidity value from KTIP weather station, square markers denote measured relative humidity values from ballast, and circular markers denote measured relative humidity values inside concrete.

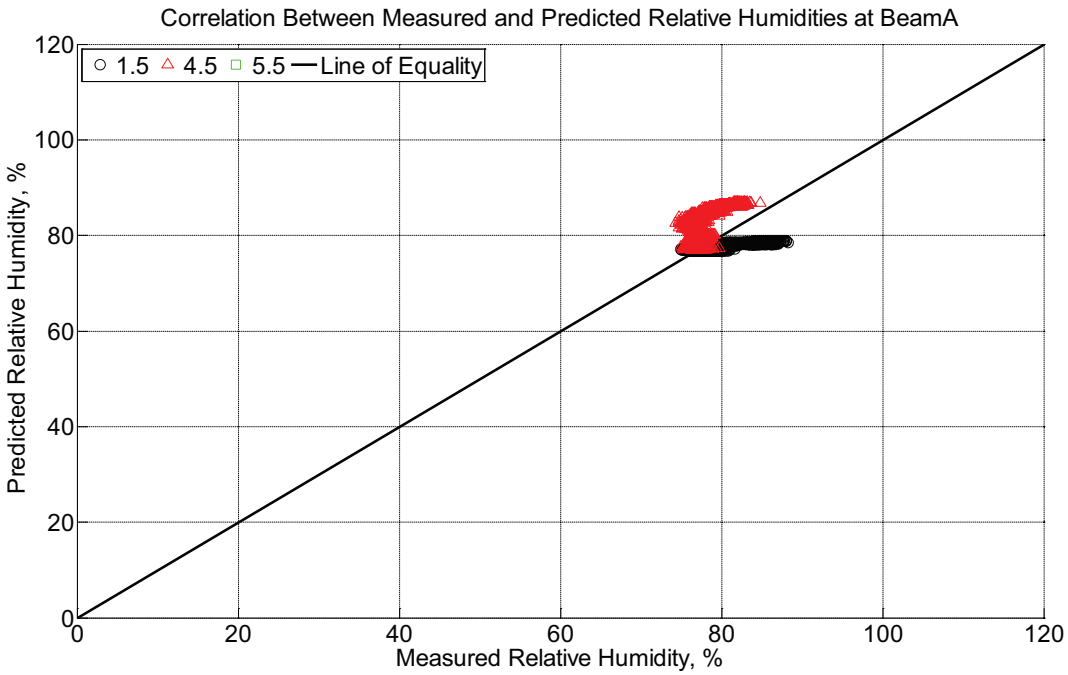

Figure B-170 Correlation between measured and predicted relative humidity values 1.5 inches (38.1 mm), 4.5 inches (114.3 mm), and 5.5 inches (139.7 mm) from the surface of a modulus of rupture beam (labeled A) installed in ballast in Rantoul, IL, between April 11, 2015, through May 10, 2015.

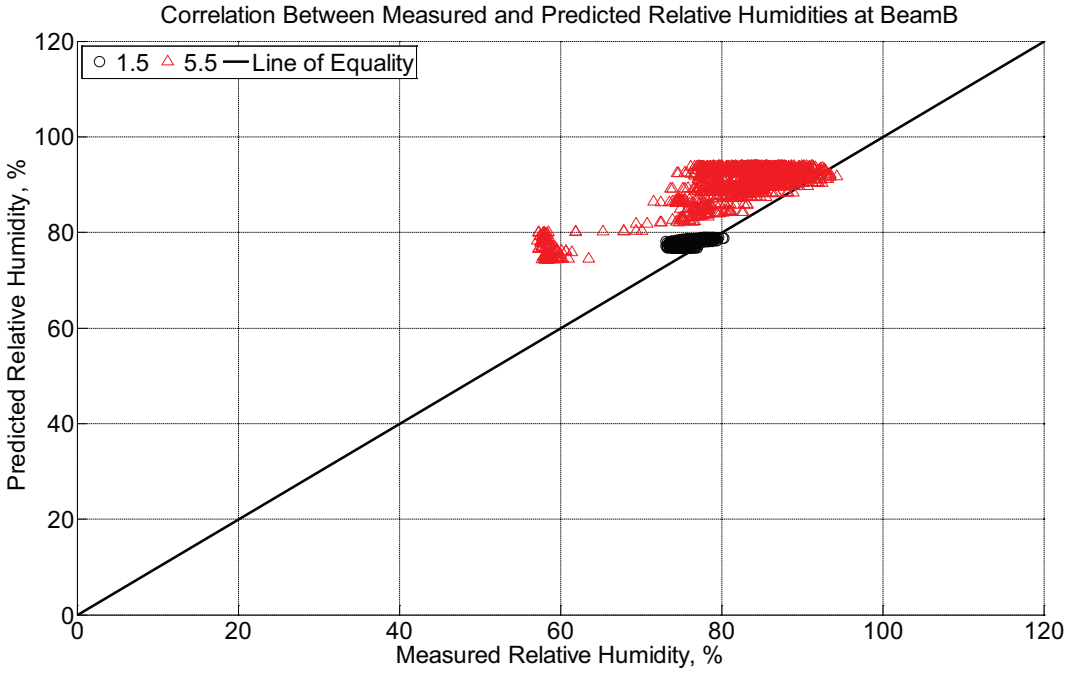

Figure B-171 Correlation between measured and predicted relative humidity values 1.5 inches (38.1 mm) and 5.5 inches (139.7 mm) from the surface of a modulus of rupture beam

(labeled B) installed in ballast in Rantoul, IL, between April 11, 2015, through May 10, 2015.

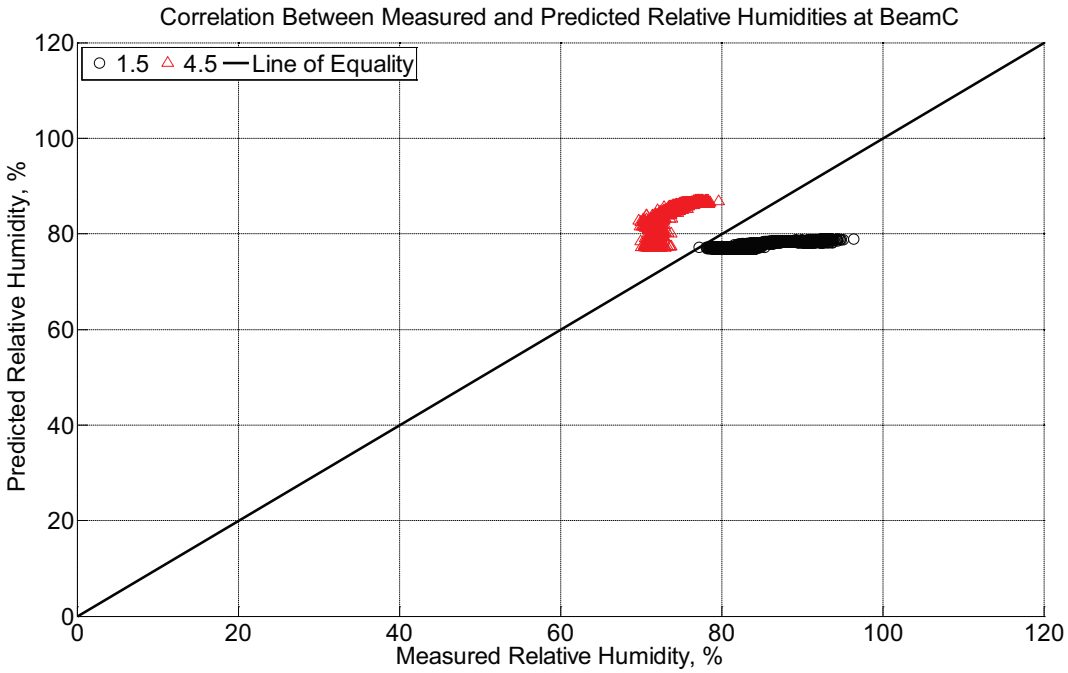

Figure B-172 Correlation between measured and predicted relative humidity values 1.5 inches (38.1 mm) and 4.5 inches (114.3 mm) from the surface of a modulus of rupture beam (labeled C) installed in ballast in Rantoul, IL, between April 11, 2015, through May 10, 2015.

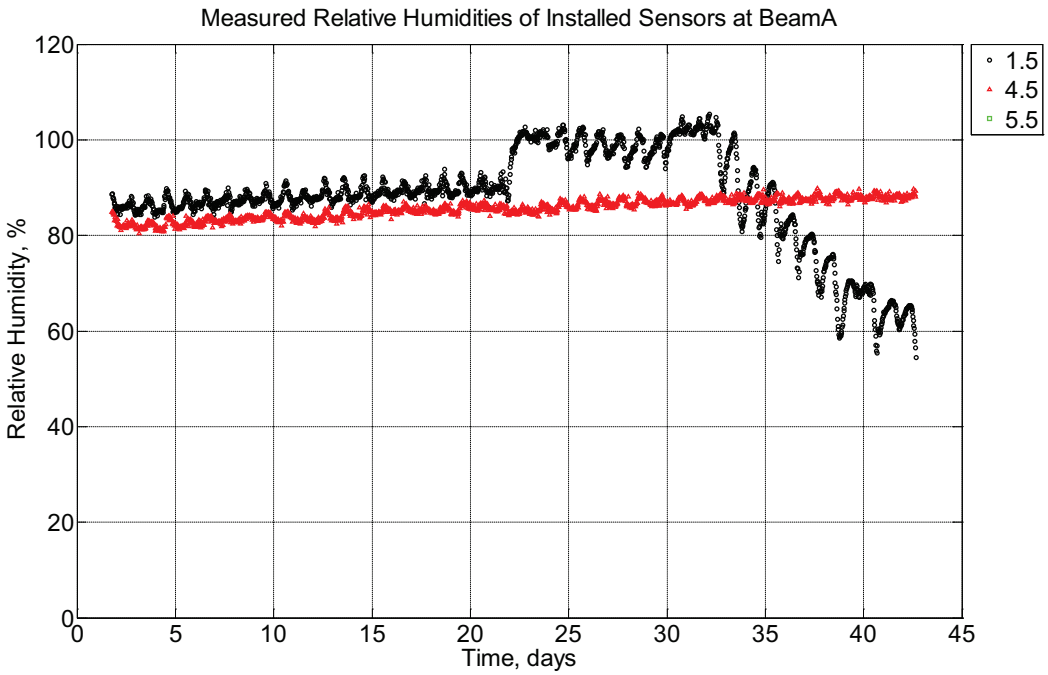

Figure B-173 Measured relative humidity at depths of 1.5 inches (38.1 mm), 4.5 inches (114.3 mm), and 5.5 inches (139.7 mm) from the surface of a modulus of rupture beam (labeled A) installed in ballast in Rantoul, IL, between May 10, 2015, through June 20, 2015.

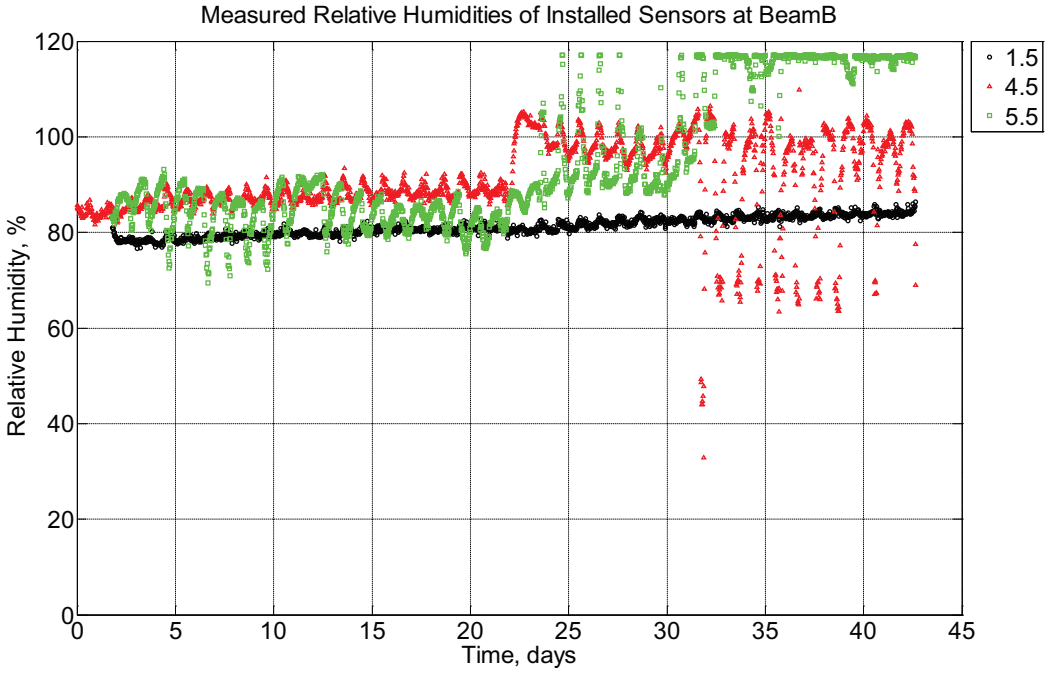

Figure B-174 Measured relative humidity at depths of 1.5 inches (38.1 mm), 4.5 inches (114.3 mm), and 5.5 inches (139.7 mm) from the surface of a modulus of rupture beam

(labeled B) installed in ballast in Rantoul, IL, between May 10, 2015, through June 20, 2015.

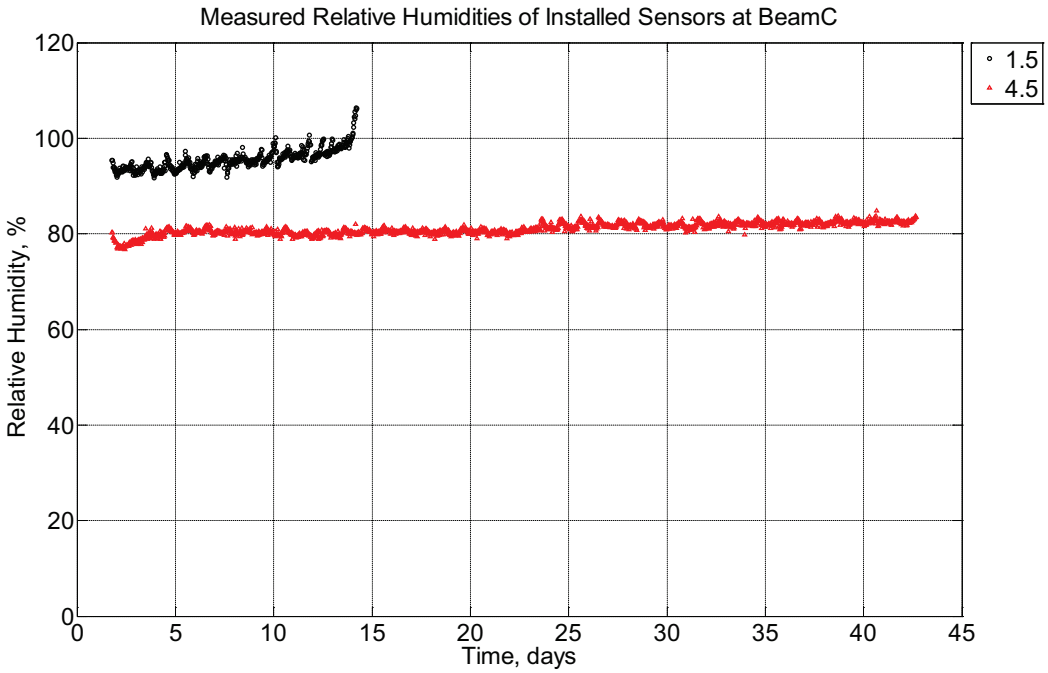

Figure B-175 Measured relative humidity at depths of 1.5 inches (38.1 mm) and 4.5 inches (114.3 mm), from the surface of a modulus of rupture beam (labeled C) installed in ballast in Rantoul, IL, between May 10, 2015, through June 20, 2015.

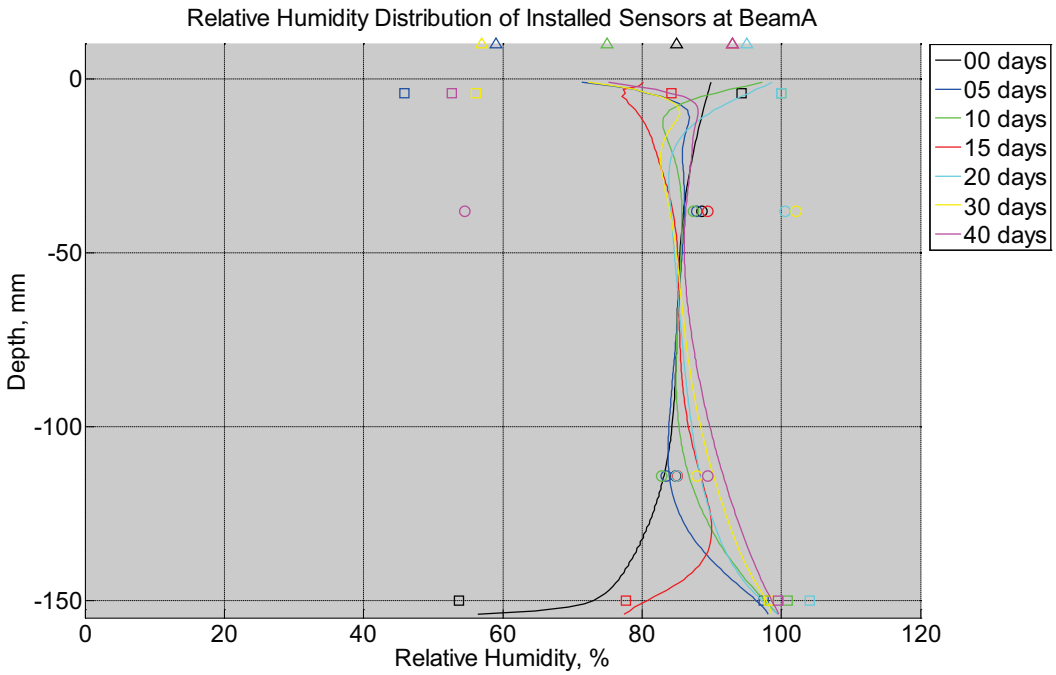

Figure B-176 Measured (markers) and modeled (continuous line) relative humidity distribution as a function of depth inside modulus of rupture beam (labeled A) installed in ballast in Rantoul, IL, between May 10, 2015, through June 20, 2015. Triangular markers denote relative humidity value from KTIP weather station, square markers denote measured relative humidity values from ballast, and circular markers denote measured relative humidity values inside concrete.

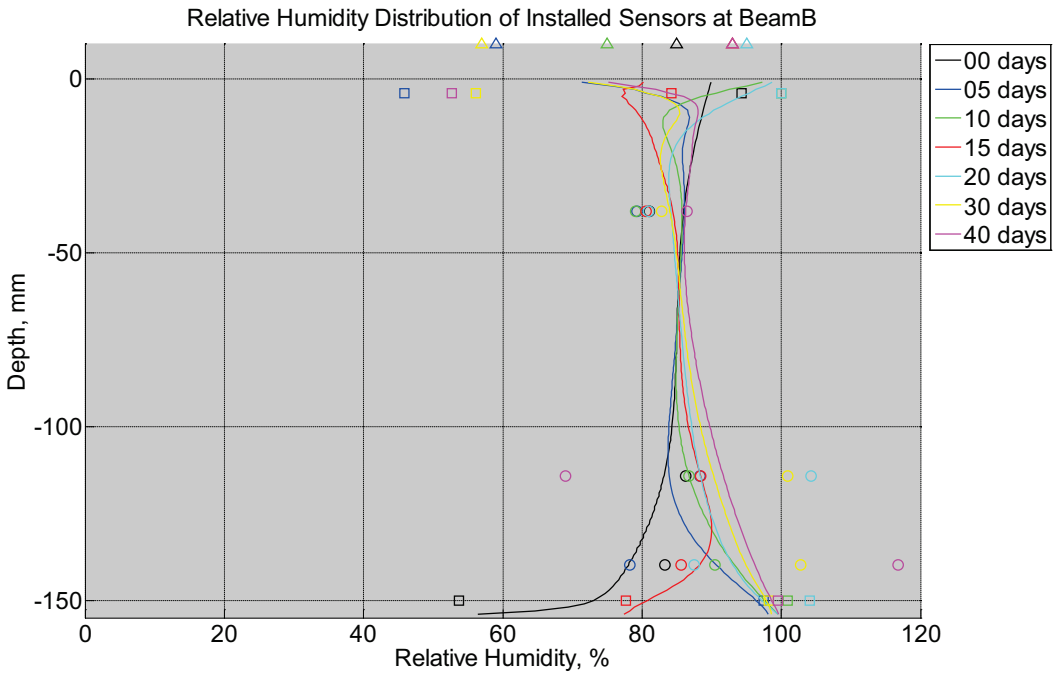

Figure B-177 Measured (markers) and modeled (continuous line) relative humidity distribution as a function of depth inside modulus of rupture beam (labeled B) installed in ballast in Rantoul, IL, between May 10, 2015, through June 20, 2015. Triangular markers denote relative humidity value from KTIP weather station, square markers denote measured relative humidity values from ballast, and circular markers denote measured relative humidity values inside concrete.

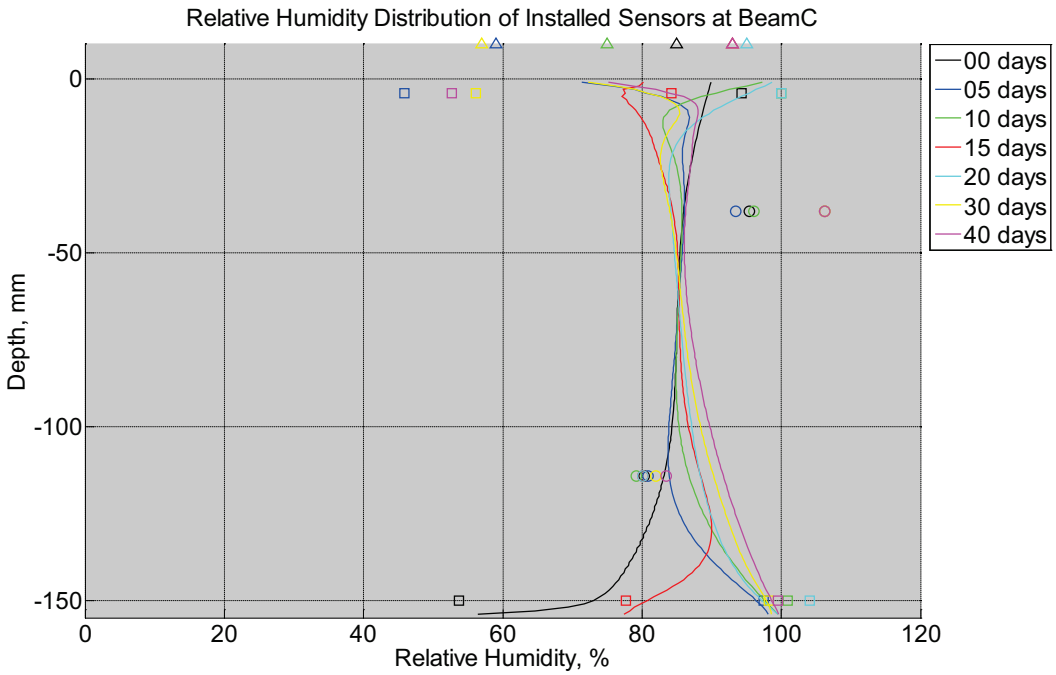

Figure B-178 Measured (markers) and modeled (continuous line) relative humidity distribution as a function of depth inside modulus of rupture beam (labeled C) installed in ballast in Rantoul, IL, between May 10, 2015, through June 20, 2015. Triangular markers denote relative humidity value from KTIP weather station, square markers denote measured relative humidity values from ballast, and circular markers denote measured relative humidity values inside concrete.

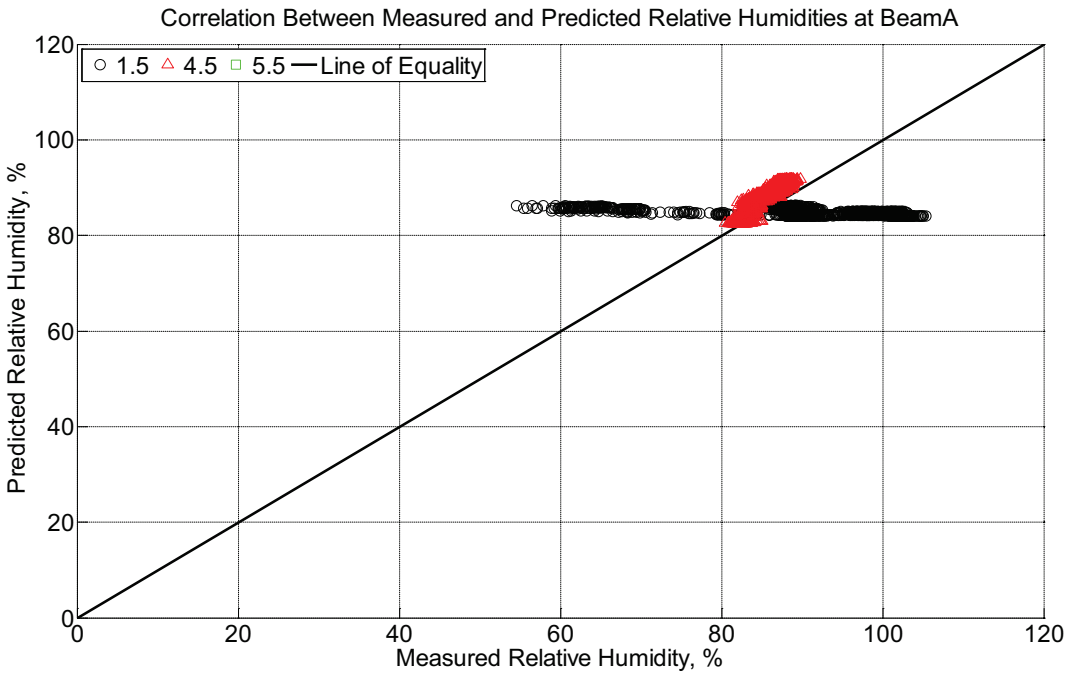

Figure B-179 Correlation between measured and predicted relative humidity values 1.5 inches (38.1 mm), 4.5 inches (114.3 mm), and 5.5 inches (139.7 mm) from the surface of a modulus of rupture beam (labeled A) installed in ballast in Rantoul, IL, between May 10, 2015, through June 20, 2015.

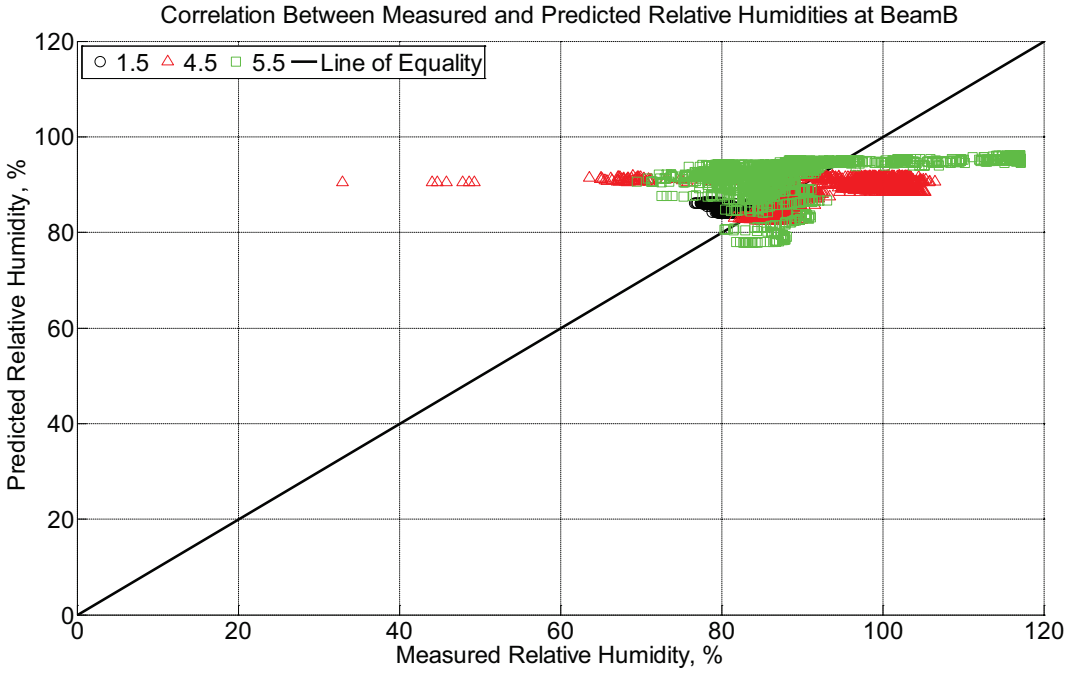

Figure B-180 Correlation between measured and predicted relative humidity values 1.5 inches (38.1 mm), 4.5 inches (114.3 mm), and 5.5 inches (139.7 mm) from the surface of a

modulus of rupture beam (labeled B) installed in ballast in Rantoul, IL, between May 10, 2015, through June 20, 2015.

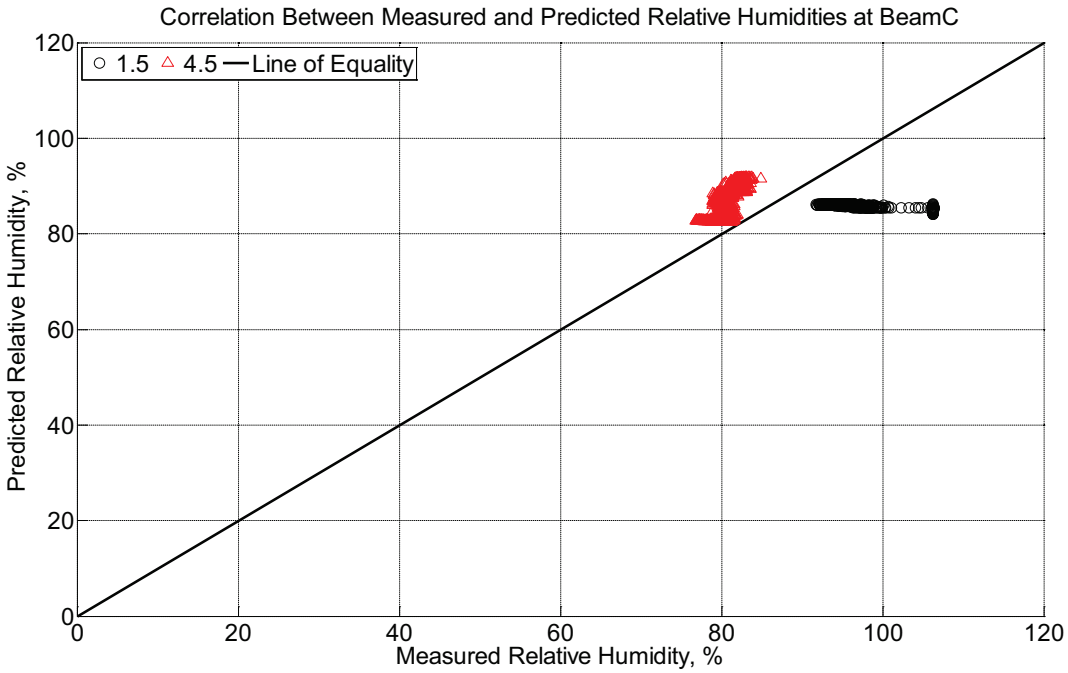

Figure B-181 Correlation between measured and predicted relative humidity values 1.5 inches (38.1 mm) and 4.5 inches (114.3 mm) from the surface of a modulus of rupture beam (labeled C) installed in ballast in Rantoul, IL, between May 10, 2015, through June 20, 2015.

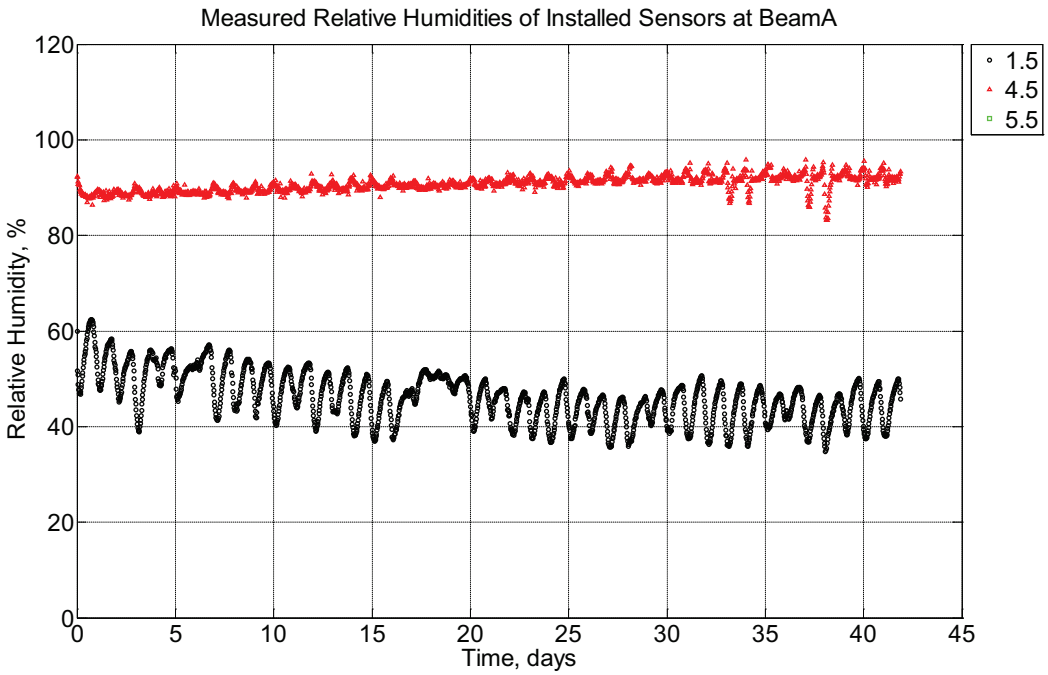

Figure B-182 Measured relative humidity at depths of 1.5 inches (38.1 mm), 4.5 inches (114.3 mm), and 5.5 inches (139.7 mm) from the surface of a modulus of rupture beam (labeled A) installed in ballast in Rantoul, IL, between June 20, 2015, through August 1, 2015.

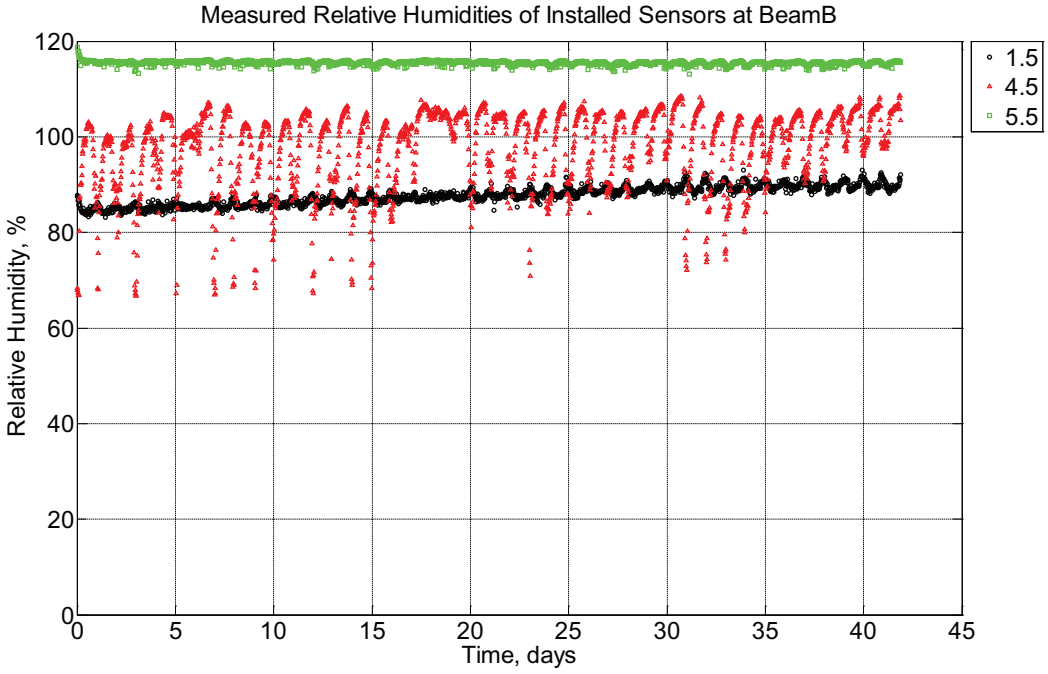

Figure B-183 Measured relative humidity at depths of 1.5 inches (38.1 mm), 4.5 inches (114.3 mm), and 5.5 inches (139.7 mm) from the surface of a modulus of rupture beam

(labeled B) installed in ballast in Rantoul, IL, between June 20, 2015, through August 1, 2015.

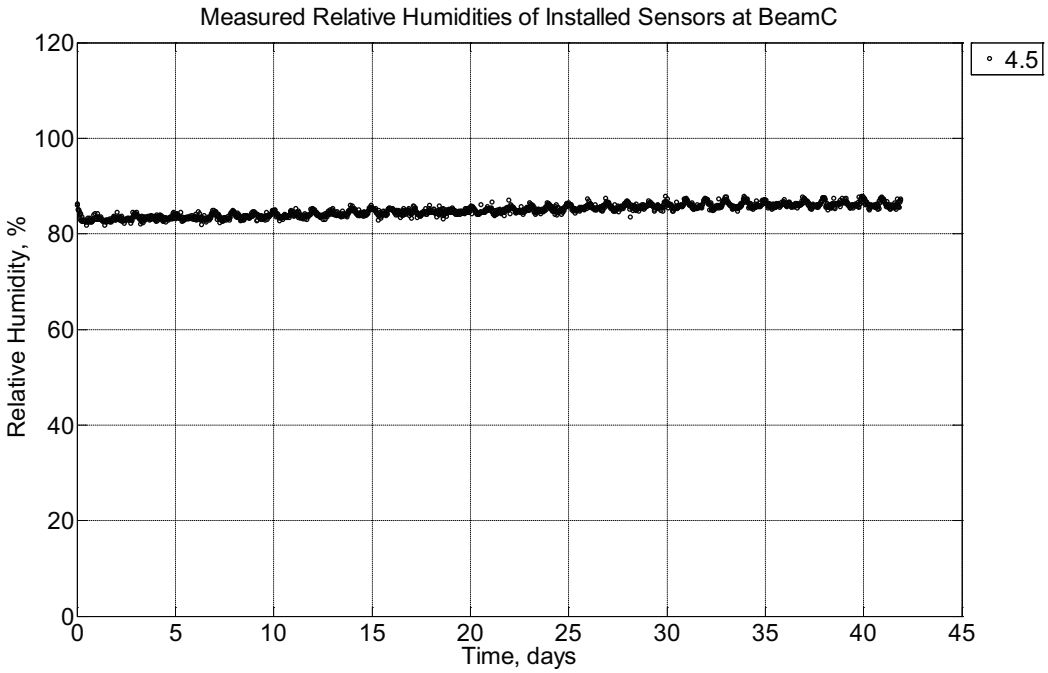

Figure B-184 Measured relative humidity at depths of 4.5 inches (114.3 mm) from the surface of a modulus of rupture beam (labeled C) installed in ballast in Rantoul, IL, between June 20, 2015, through August 1, 2015.

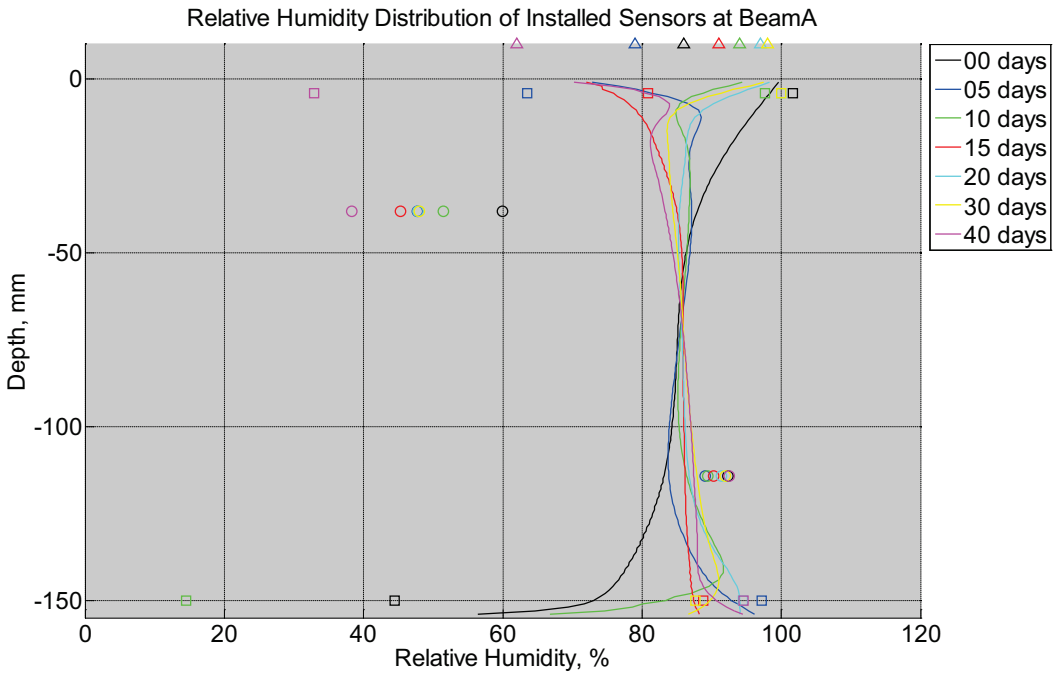

Figure B-185 Measured (markers) and modeled (continuous line) relative humidity distribution as a function of depth inside modulus of rupture beam (labeled A) installed in ballast in Rantoul, IL, between June 20, 2015, through August 1, 2015. Triangular markers denote relative humidity value from KTIP weather station, square markers denote measured relative humidity values from ballast, and circular markers denote measured relative humidity values inside concrete.

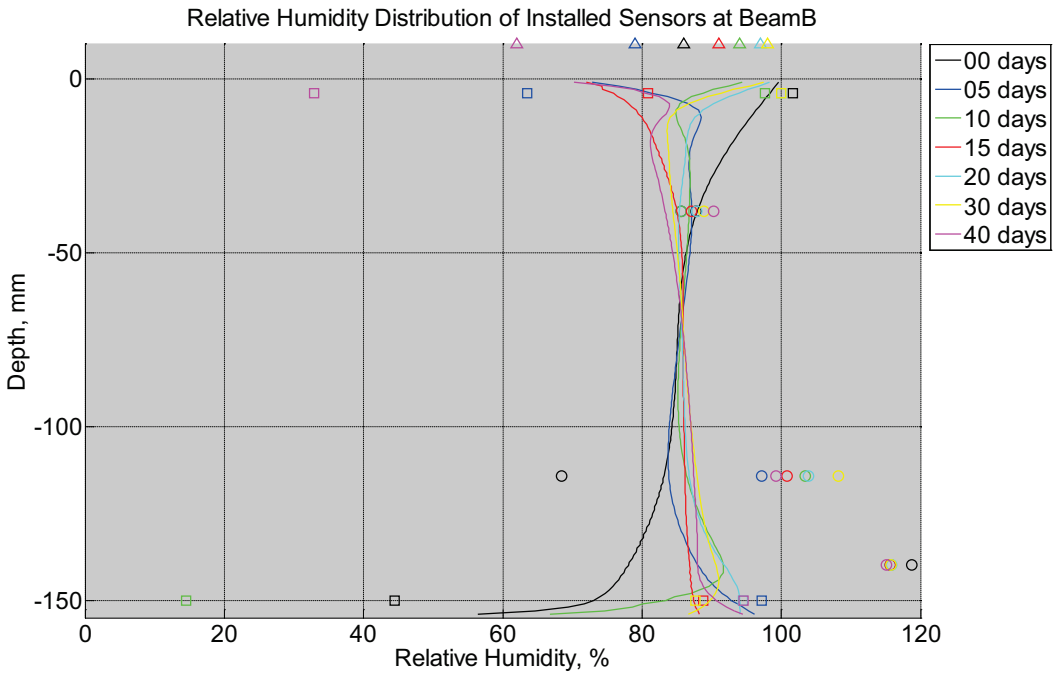

Figure B-186 Measured (markers) and modeled (continuous line) relative humidity distribution as a function of depth inside modulus of rupture beam (labeled B) installed in ballast in Rantoul, IL, between June 20, 2015, through August 1, 2015. Triangular markers denote relative humidity value from KTIP weather station, square markers denote measured relative humidity values from ballast, and circular markers denote measured relative humidity values inside concrete.

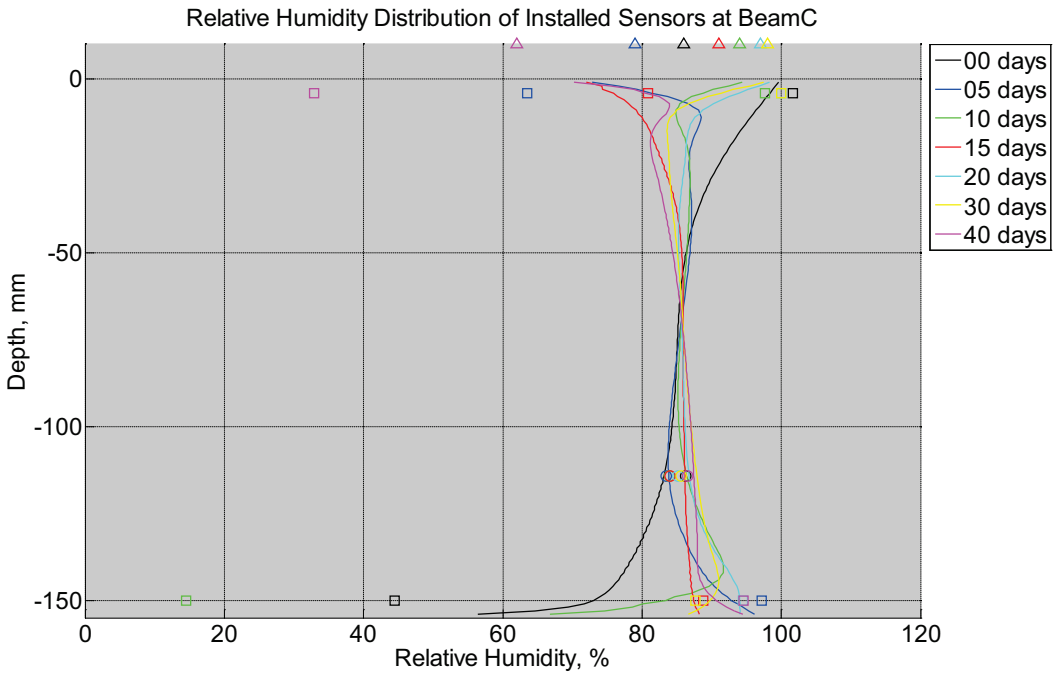

Figure B-187 Measured (markers) and modeled (continuous line) relative humidity distribution as a function of depth inside modulus of rupture beam (labeled C) installed in ballast in Rantoul, IL, between June 20, 2015, through August 1, 2015. Triangular markers denote relative humidity value from KTIP weather station, square markers denote measured relative humidity values from ballast, and circular markers denote measured relative humidity values inside concrete.

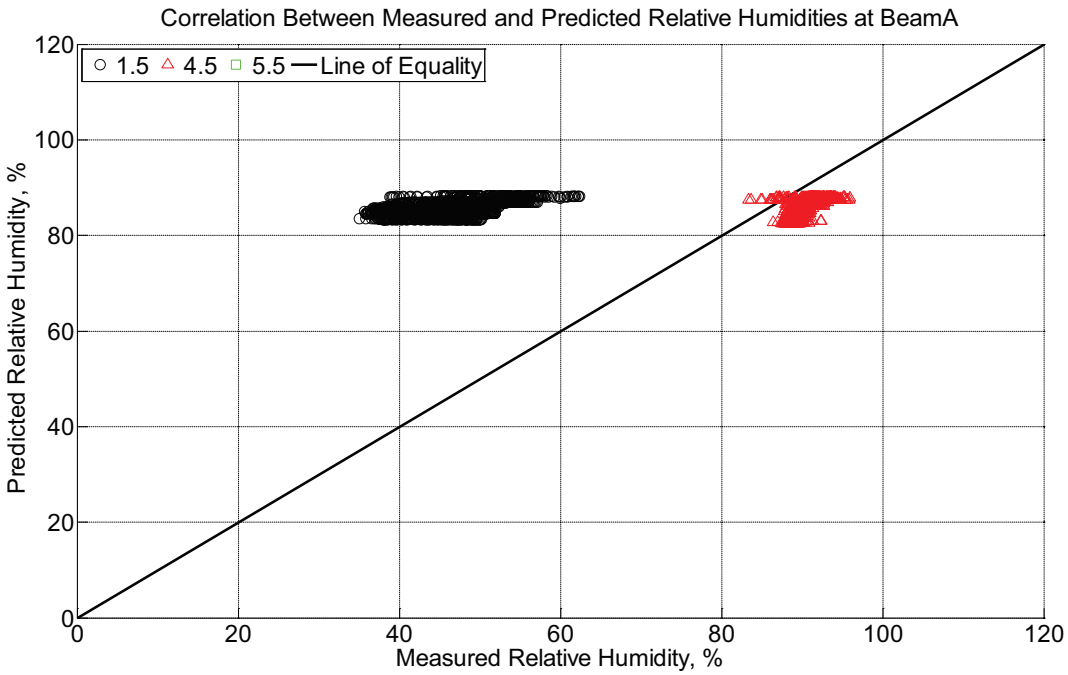

Figure B-188 Correlation between measured and predicted relative humidity values 1.5 inches (38.1 mm), 4.5 inches (114.3 mm), and 5.5 inches (139.7 mm) from the surface of a modulus of rupture beam (labeled A) installed in ballast in Rantoul, IL, between June 20, 2015, through August 1, 2015.

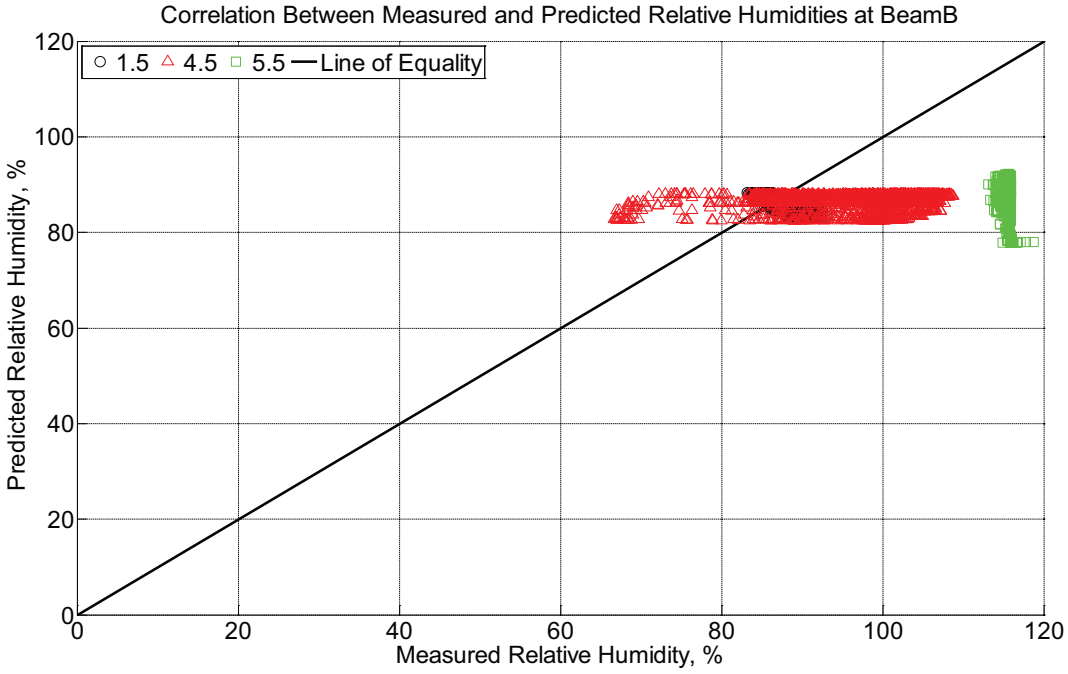

Figure B-189 Correlation between measured and predicted relative humidity values 1.5 inches (38.1 mm), 4.5 inches (114.3 mm), and 5.5 inches (139.7 mm) from the surface of a

modulus of rupture beam (labeled B) installed in ballast in Rantoul, IL, between June 20, 2015, through August 1, 2015.

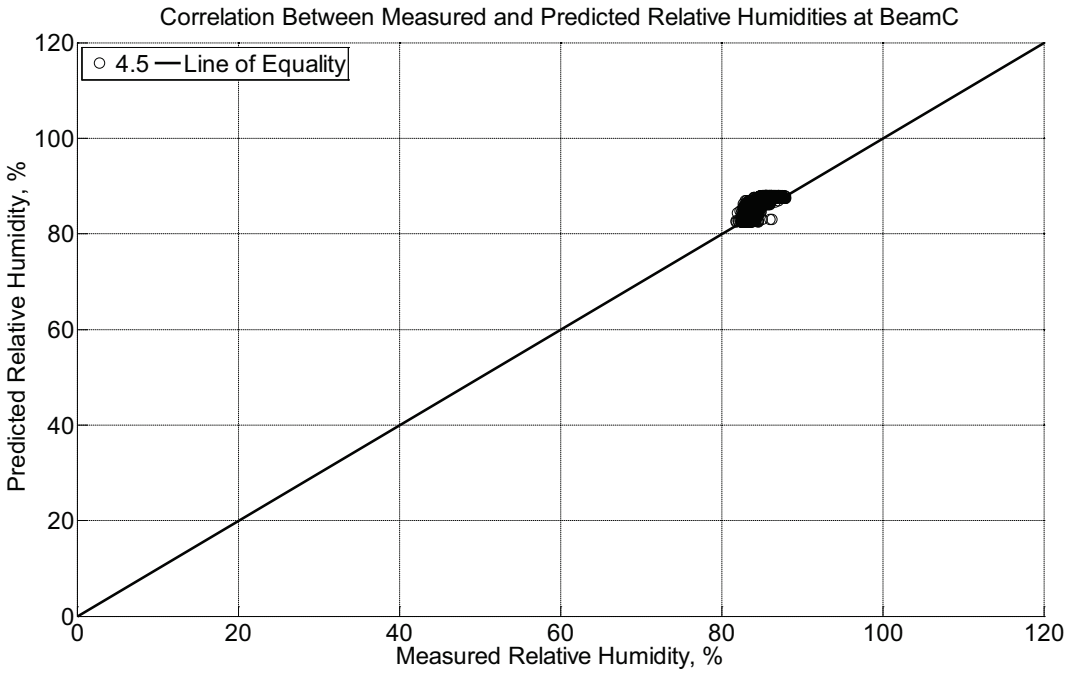

Figure B-190 Correlation between measured and predicted relative humidity values 4.5 inches (114.3 mm) from the surface of a modulus of rupture beam (labeled C) installed in ballast in Rantoul, IL, between June 20, 2015, through August 1, 2015.

Measured and predicted internal temperature of instrumented modulus of rupture beams

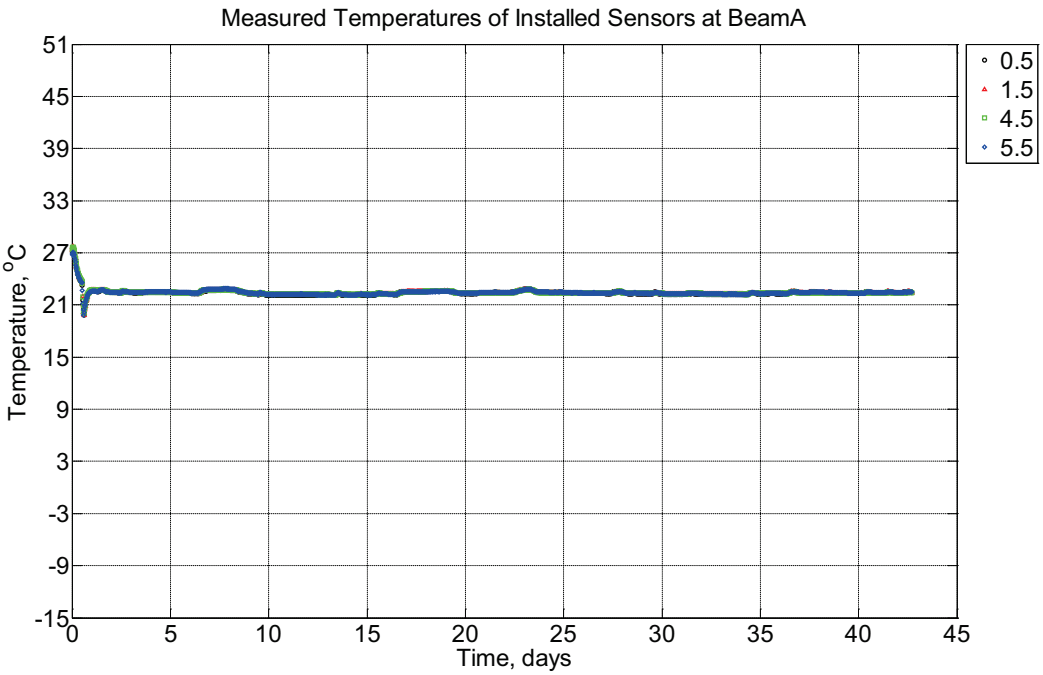

Figure B-191 Measured temperature at depths of 0.5 inches (12.7 mm), 1.5 inches (38.1 mm), 4.5 inches (114.3 mm), and 5.5 inches (139.7 mm) from the surface of a modulus of rupture beam (labeled A) curing inside an environmentally controlled room (50% RH, 23ºC) between January 29, 2014, through March 12, 2014.

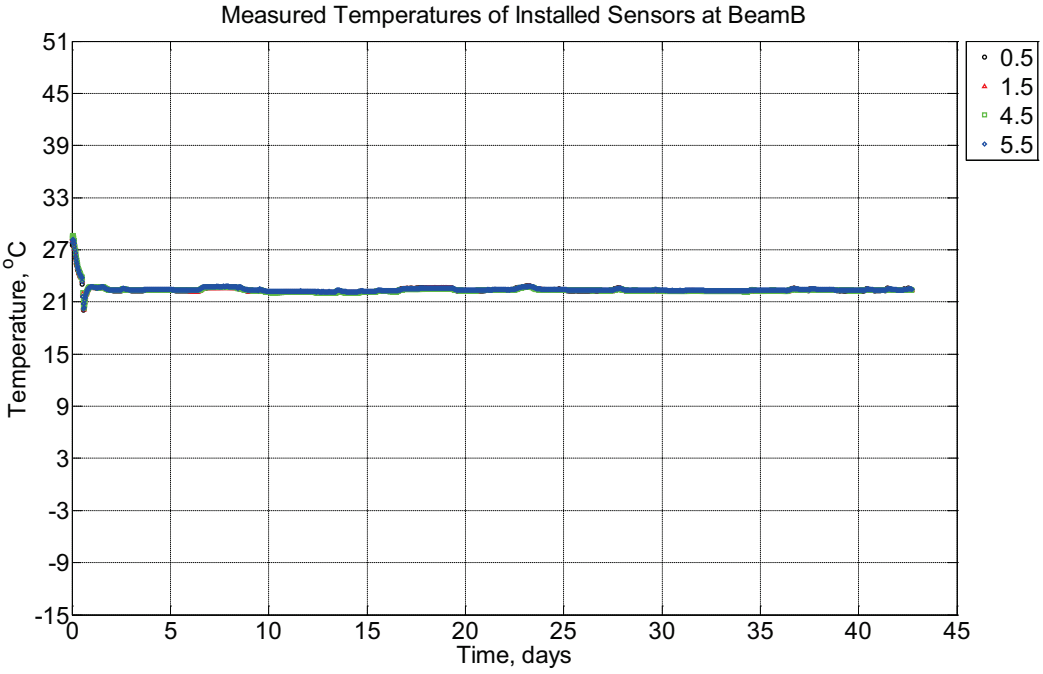

Figure B-192 Measured temperature at depths of 0.5 inches (12.7 mm), 1.5 inches (38.1 mm), 4.5 inches (114.3 mm), and 5.5 inches (139.7 mm) from the surface of a modulus of

rupture beam (labeled B) curing inside an environmentally controlled room (50% RH, 23°C) between January 29, 2014, through March 12, 2014.

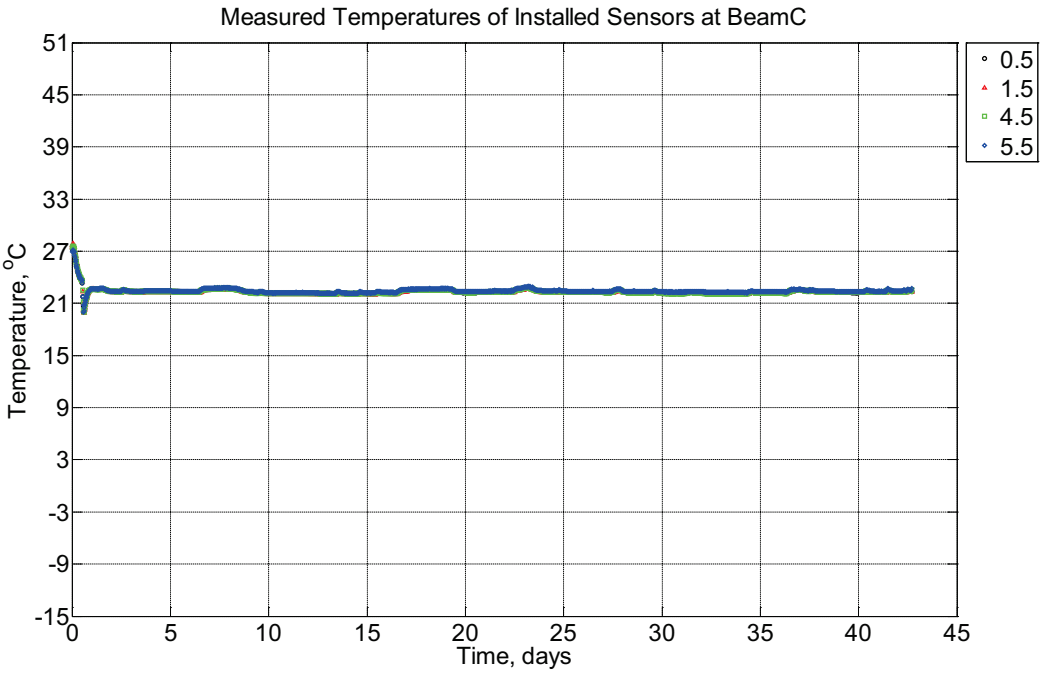

Figure B-193 Measured temperature at depths of 0.5 inches (12.7 mm), 1.5 inches (38.1 mm), 4.5 inches (114.3 mm), and 5.5 inches (139.7 mm) from the surface of a modulus of rupture beam (labeled C) curing inside an environmentally controlled room (50% RH, 23°C) between January 29, 2014, through March 12, 2014.

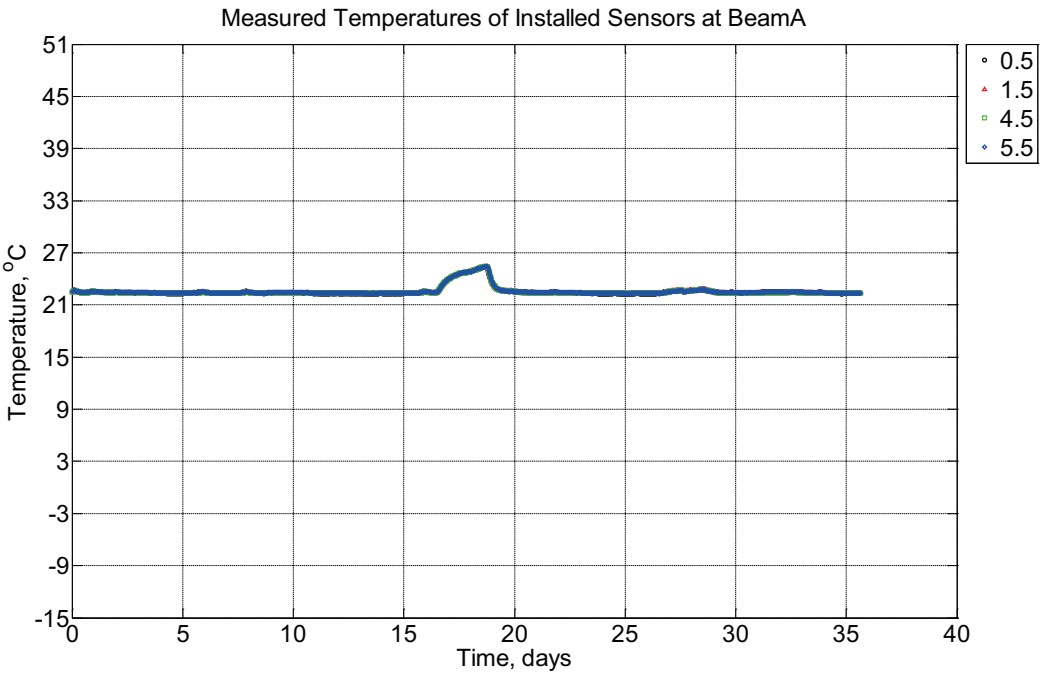

Figure B-194 Measured temperature at depths of 0.5 inches (12.7 mm), 1.5 inches (38.1 mm), 4.5 inches (114.3 mm), and 5.5 inches (139.7 mm) from the surface of a modulus of rupture beam (labeled A) curing inside an environmentally controlled room (50% RH, 23°C) between March 12, 2014, through April 17, 2014.

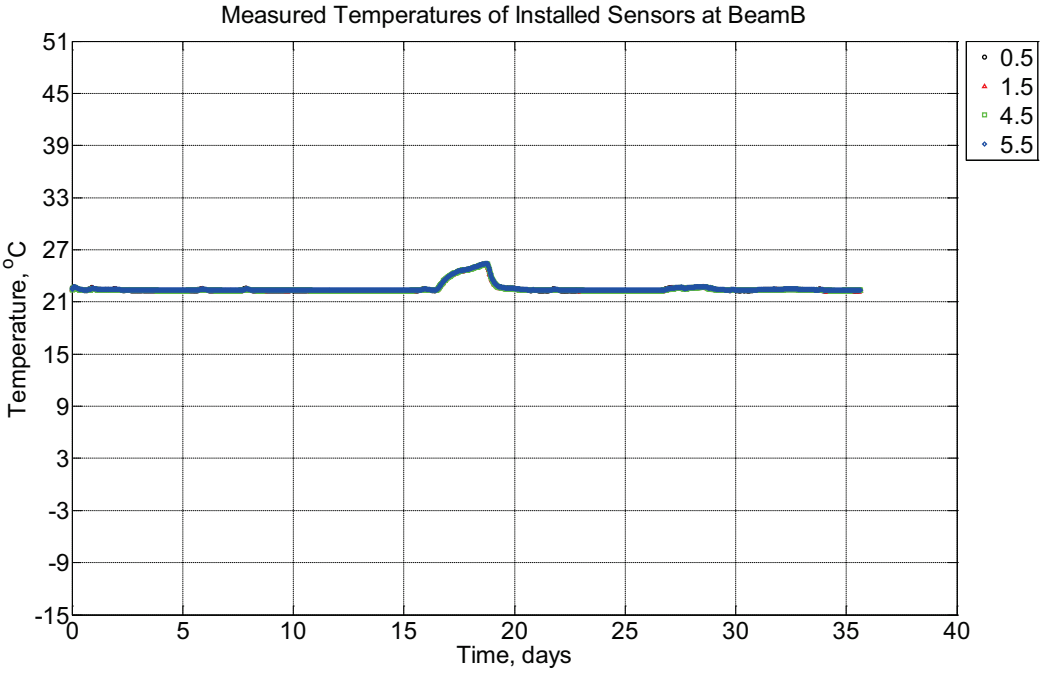

Figure B-195 Measured temperature at depths of 0.5 inches (12.7 mm), 1.5 inches (38.1 mm), 4.5 inches (114.3 mm), and 5.5 inches (139.7 mm) from the surface of a modulus of

rupture beam (labeled B) curing inside an environmentally controlled room (50% RH, 23°C) between March 12, 2014, through April 17, 2014.

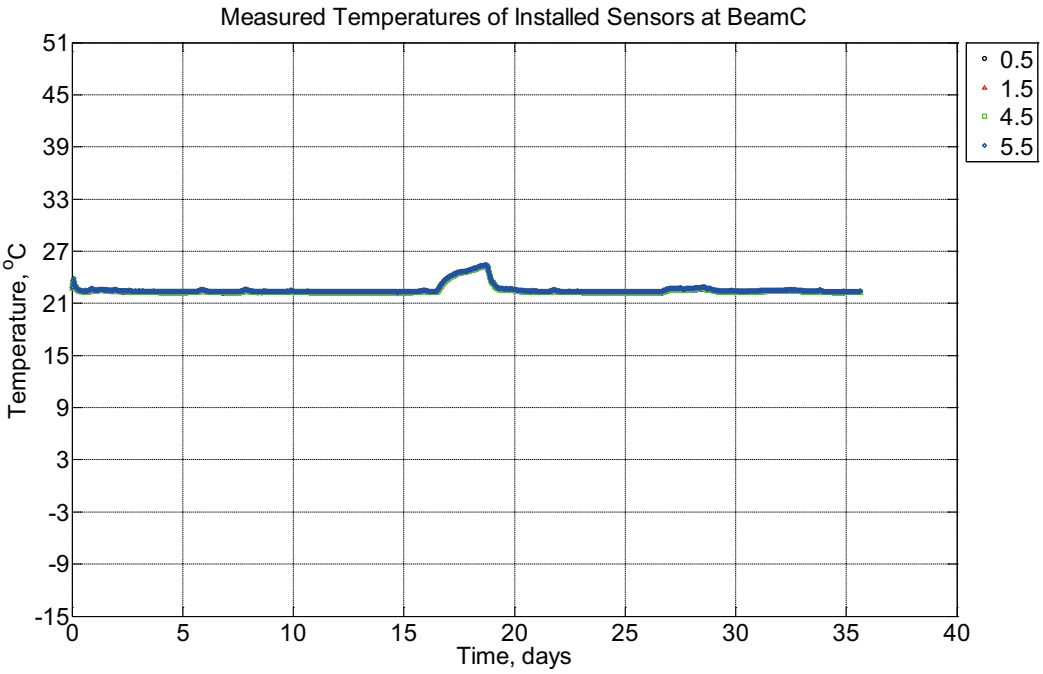

Figure B-196 Measured temperature at depths of 0.5 inches (12.7 mm), 1.5 inches (38.1 mm), 4.5 inches (114.3 mm), and 5.5 inches (139.7 mm) from the surface of a modulus of rupture beam (labeled C) located inside an environmentally controlled room (50% RH, 23°C) between March 12, 2014, through April 17, 2014.

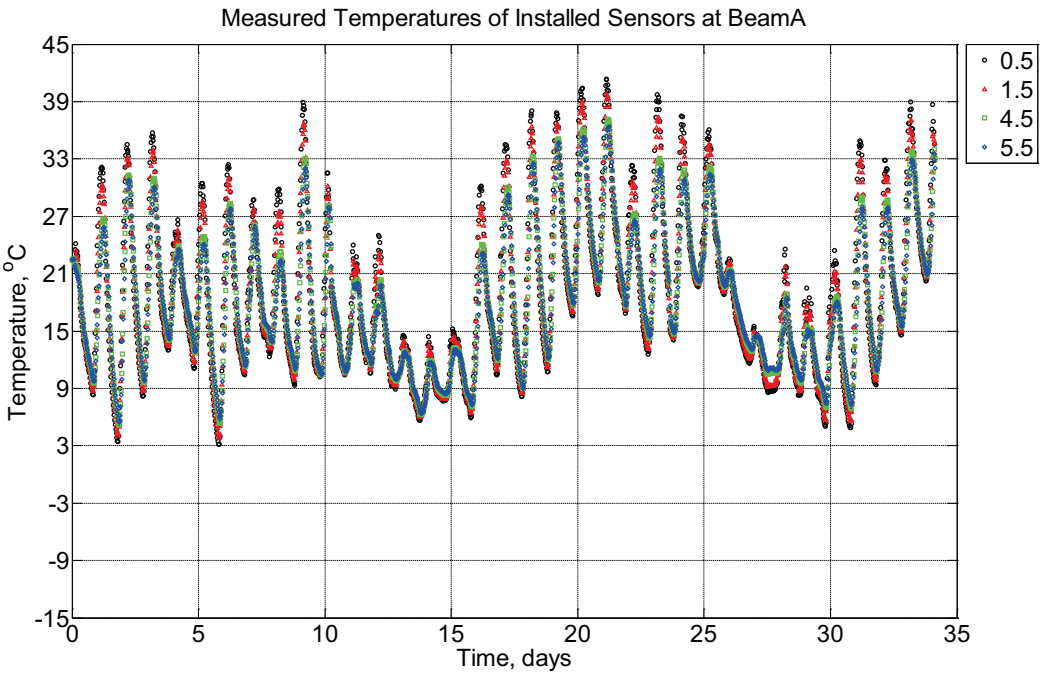

Figure B-197 Measured temperature at depths of 0.5 inches (12.7 mm), 1.5 inches (38.1 mm), 4.5 inches (114.3 mm), and 5.5 inches (139.7 mm) from the surface of a modulus of rupture beam (labeled A) installed in ballast in Rantoul, IL, between April 17, 2014, through May 21, 2014.

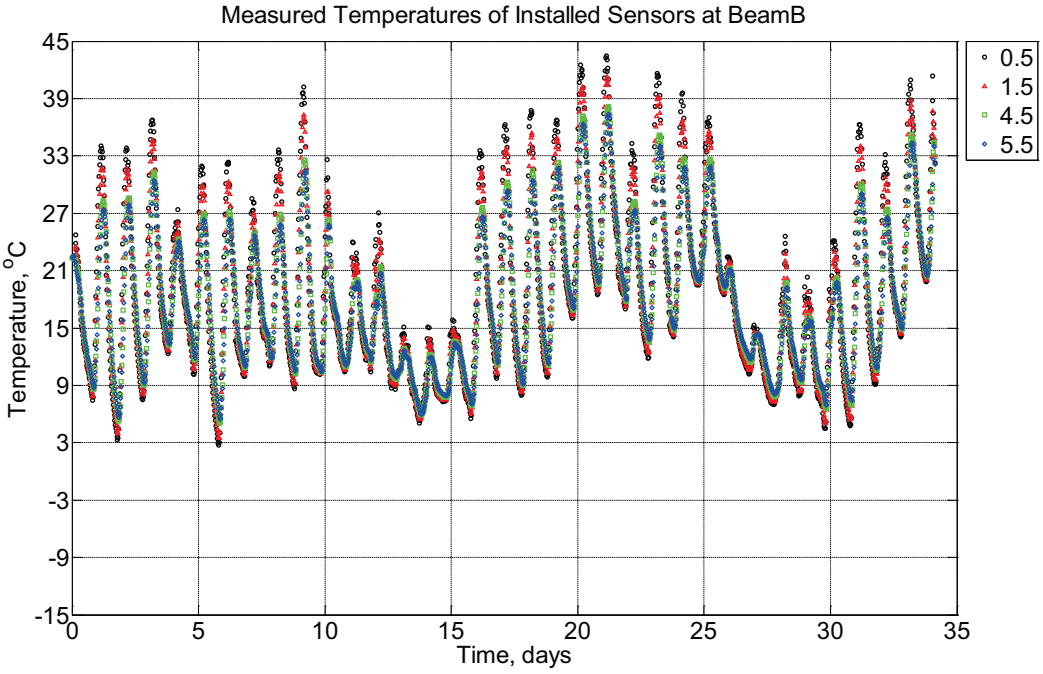

Figure B-198 Measured temperature at depths of 0.5 inches (12.7 mm), 1.5 inches (38.1 mm), 4.5 inches (114.3 mm), and 5.5 inches (139.7 mm) from the surface of a modulus of

rupture beam (labeled B) installed in ballast in Rantoul, IL, between April 17, 2014, through May 21, 2014.

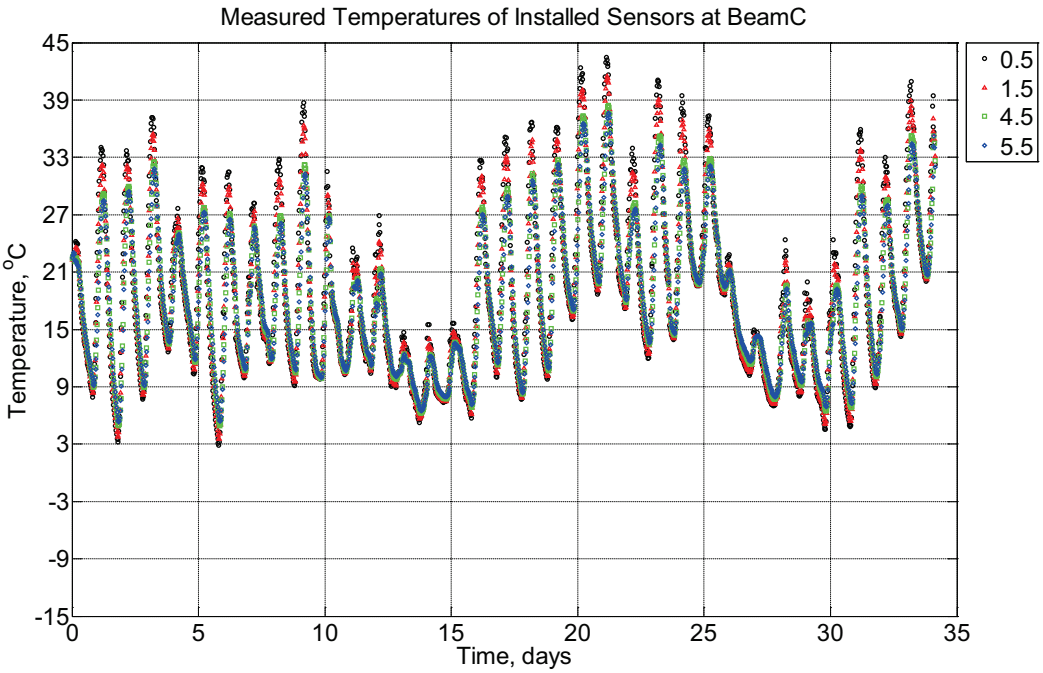

Figure B-199 Measured temperature at depths of 0.5 inches (12.7 mm), 1.5 inches (38.1 mm), 4.5 inches (114.3 mm), and 5.5 inches (139.7 mm) from the surface of a modulus of rupture beam (labeled C) installed in ballast in Rantoul, IL, between April 17, 2014, through May 21, 2014.

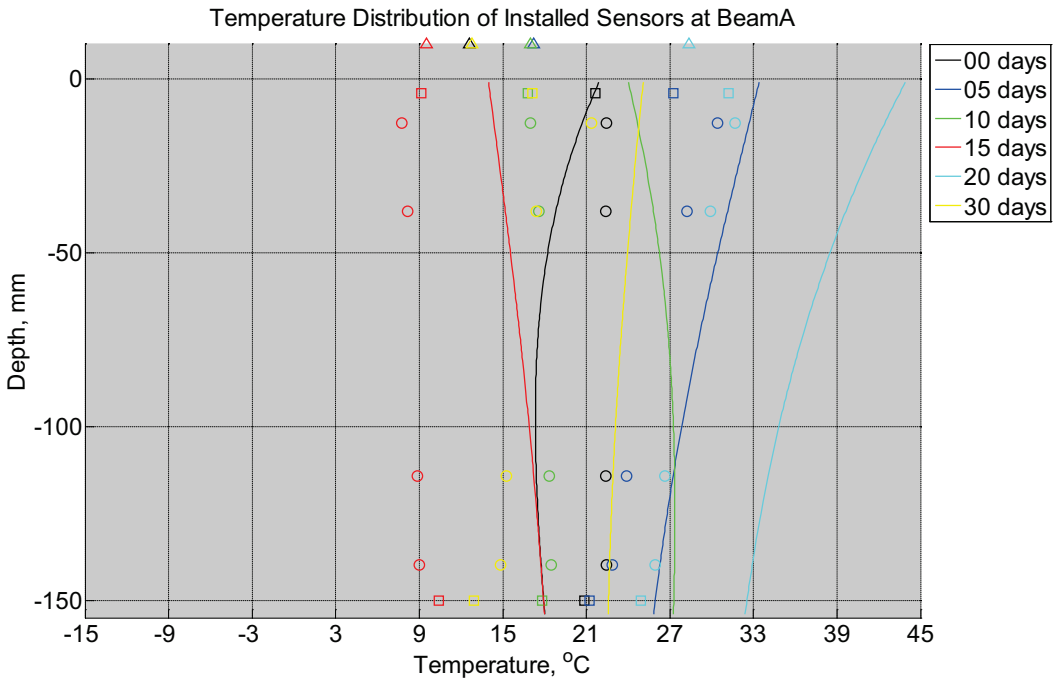

Figure B-200 Measured (markers) and modeled (continuous line) temperature profile distribution as a function of depth inside modulus of rupture beam (labeled A) installed in ballast in Rantoul, IL, between April 17, 2014, through May 21, 2014. Triangular markers denote temperature value from KTIP weather station, square markers denote measured temperature values from ballast, and circular markers denote measured temperature values inside concrete.

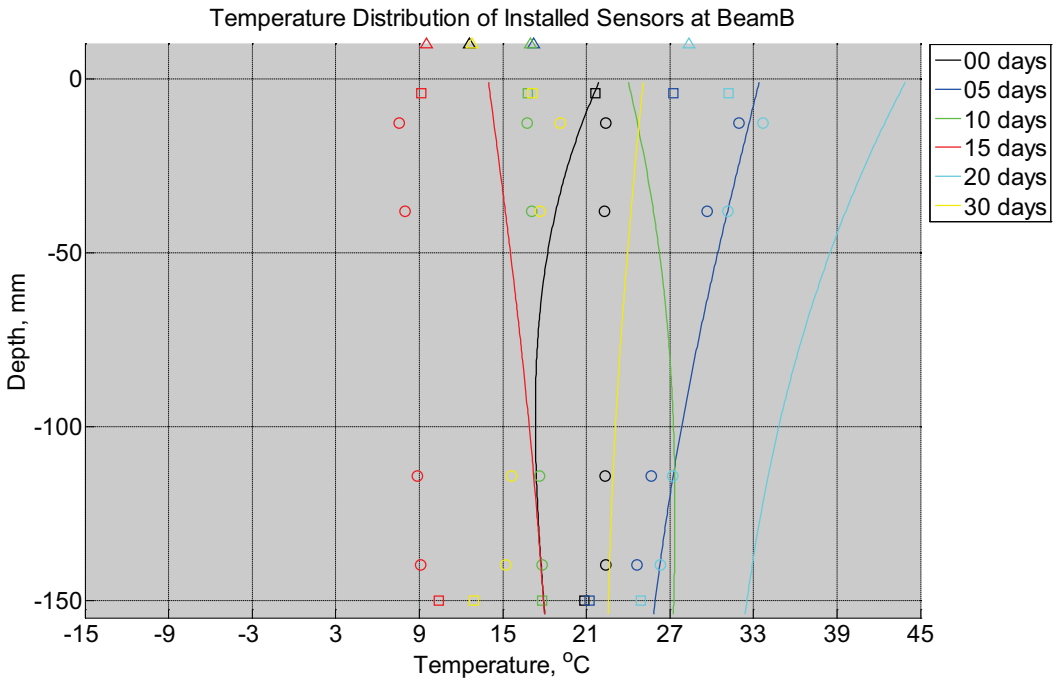

Figure B-201 Measured (markers) and modeled (continuous line) temperature profile distribution as a function of depth inside modulus of rupture beam (labeled B) installed in ballast in Rantoul, IL, between April 17, 2014, through May 21, 2014. Triangular markers denote temperature value from KTIP weather station, square markers denote measured temperature values from ballast, and circular markers denote measured temperature values inside concrete.

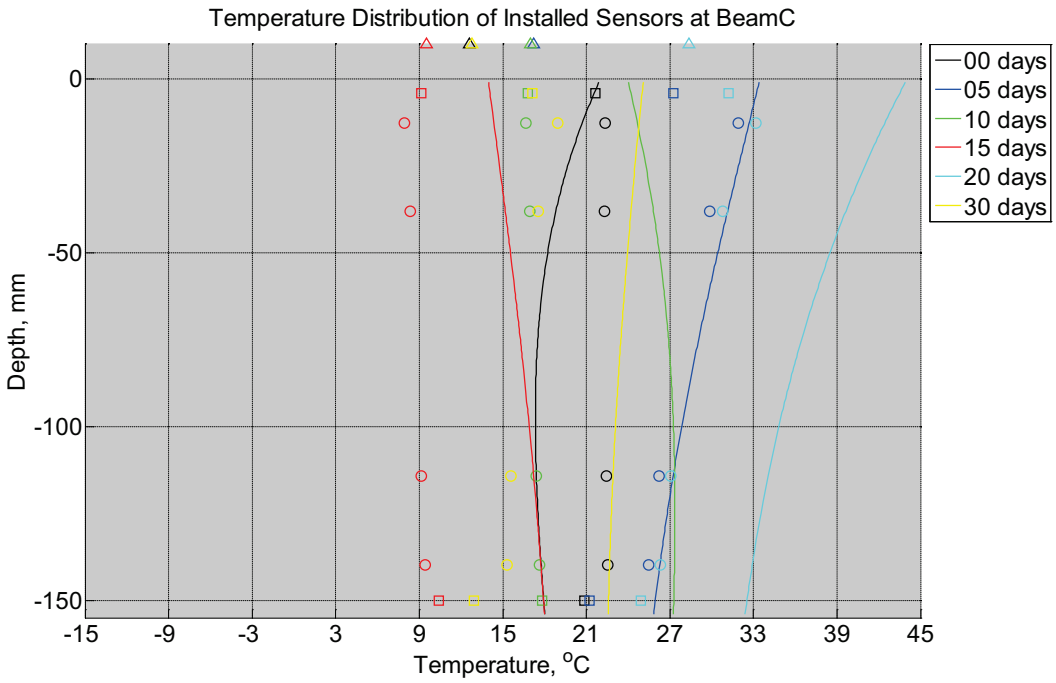

Figure B-202 Measured (markers) and modeled (continuous line) temperature profile distribution as a function of depth inside modulus of rupture beam (labeled C) installed in ballast in Rantoul, IL, between April 17, 2014, through May 21, 2014. Triangular markers denote temperature value from KTIP weather station, square markers denote measured temperature values from ballast, and circular markers denote measured temperature values inside concrete.

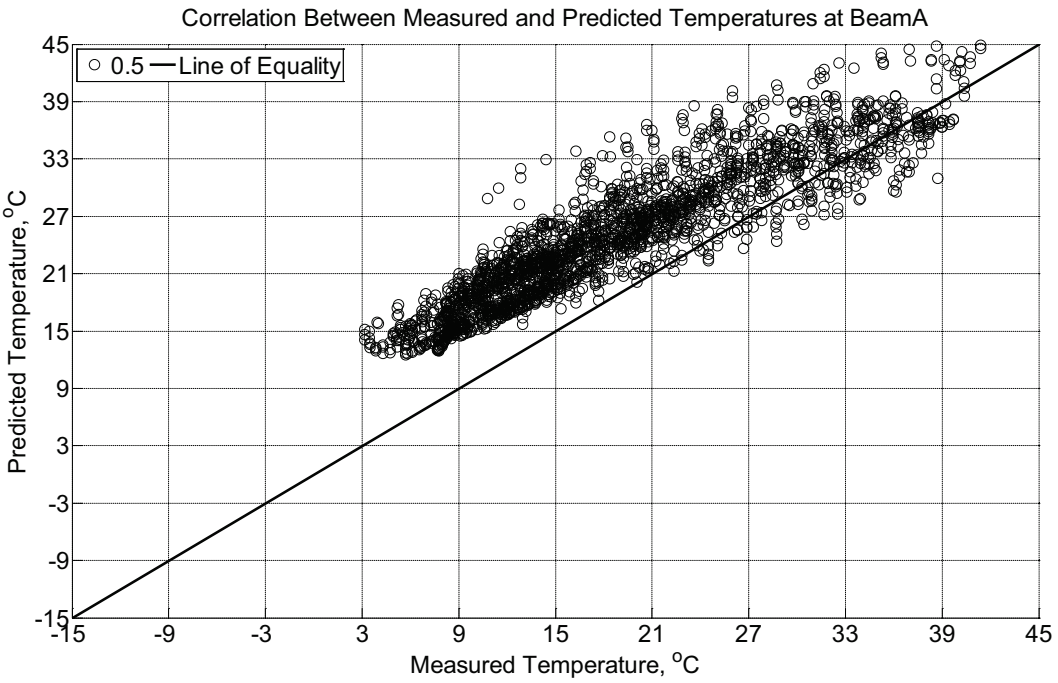

Figure B-203 Correlation between measured and predicted temperature values 0.5 inches (12.7 mm) from the surface of a modulus of rupture beam (labeled A) installed in ballast in Rantoul, IL, between April 17, 2014, through May 21, 2014.

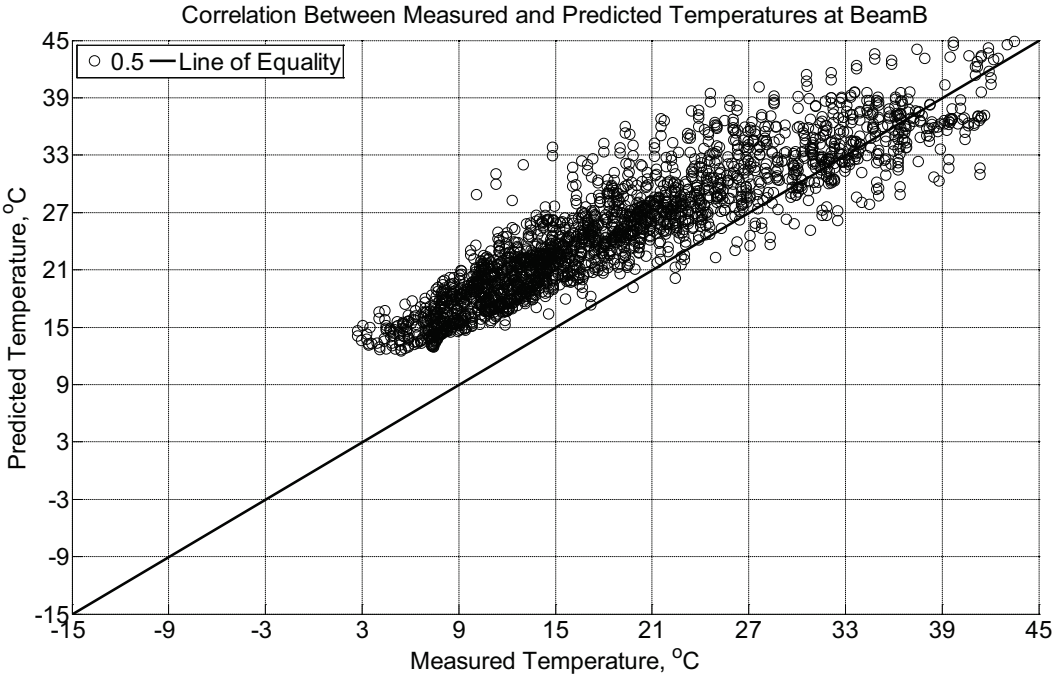

Figure B-204 Correlation between measured and predicted temperature values 0.5 inches

(12.7 mm) from the surface of a modulus of rupture beam (labeled B) installed in ballast in Rantoul, IL, between April 17, 2014, through May 21, 2014.

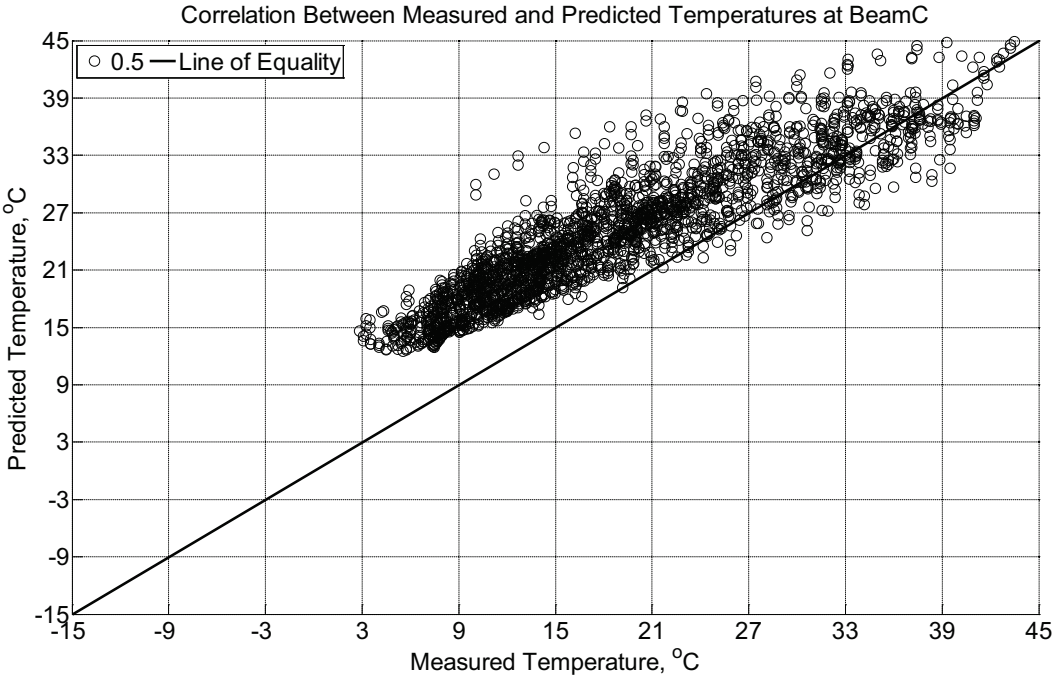

Figure B-205 Correlation between measured and predicted temperature values 0.5 inches (12.7 mm) from the surface of a modulus of rupture beam (labeled C) installed in ballast in Rantoul, IL, between April 17, 2014, through May 21, 2014.

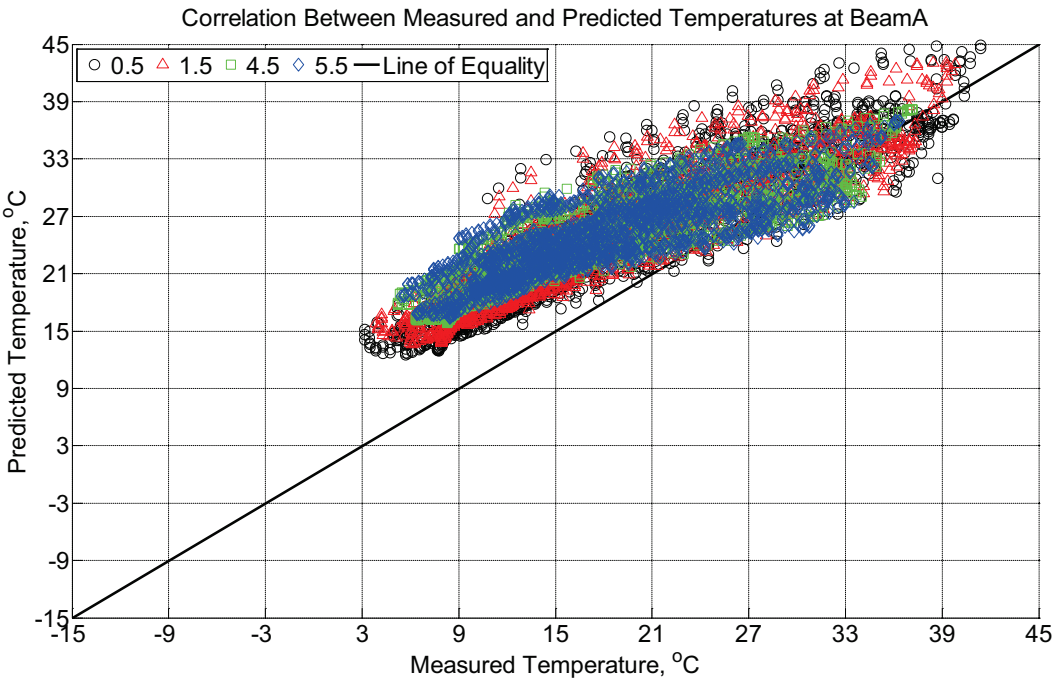

Figure B-206 Correlation between measured and predicted temperature values 0.5 inches (12.7 mm), 1.5 inches (38.1 mm), 4.5 inches (114.3 mm), and 5.5 inches (139.7 mm) from the surface of a modulus of rupture beam (labeled A) installed in ballast in Rantoul, IL, between April 17, 2014, through May 21, 2014.

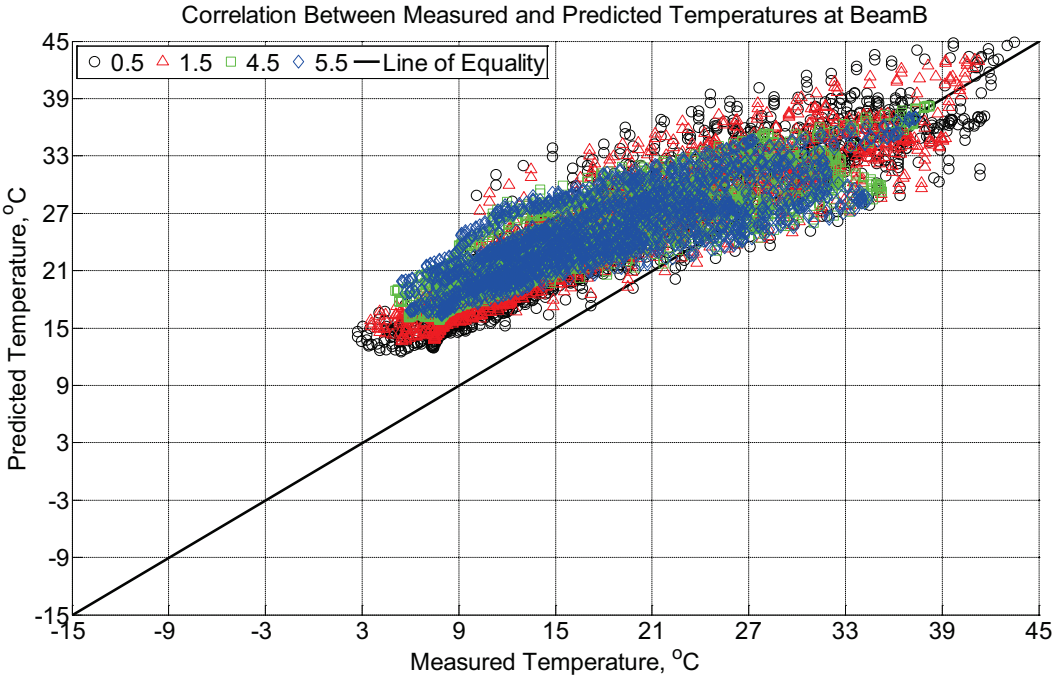

Figure B-207 Correlation between measured and predicted temperature values 0.5 inches (12.7 mm), 1.5 inches (38.1 mm), 4.5 inches (114.3 mm), and 5.5 inches (139.7 mm) from the

surface of a modulus of rupture beam (labeled B) installed in ballast in Rantoul, IL, between April 17, 2014, through May 21, 2014.

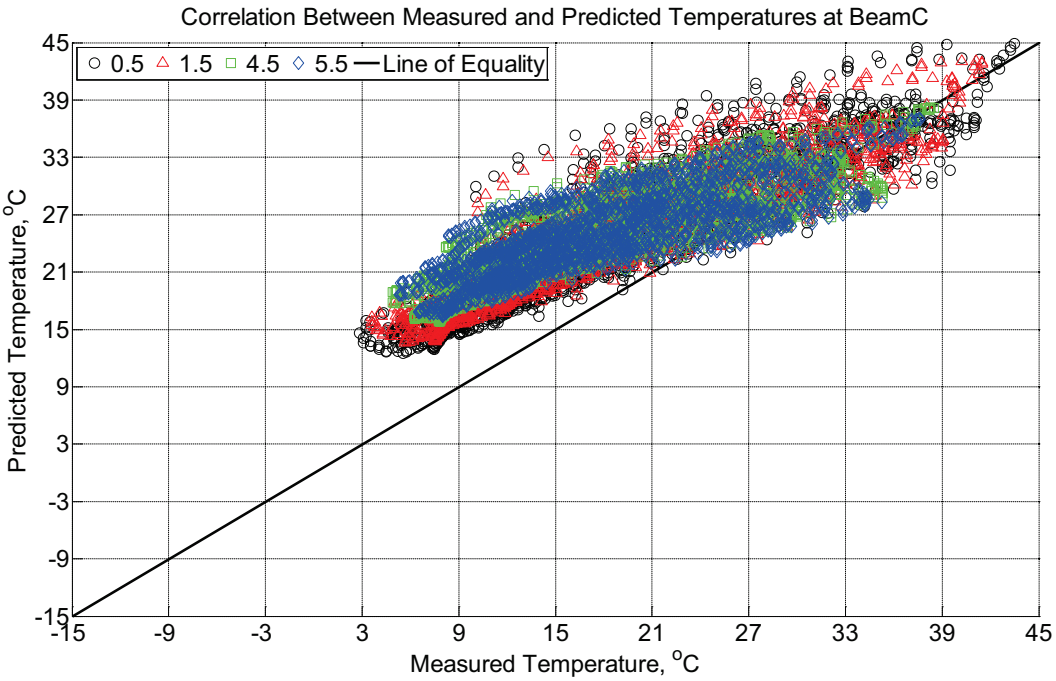

Figure B-208 Correlation between measured and predicted temperature values 0.5 inches (12.7 mm), 1.5 inches (38.1 mm), 4.5 inches (114.3 mm), and 5.5 inches (139.7 mm) from the surface of a modulus of rupture beam (labeled C) installed in ballast in Rantoul, IL, between April 17, 2014, through May 21, 2014.

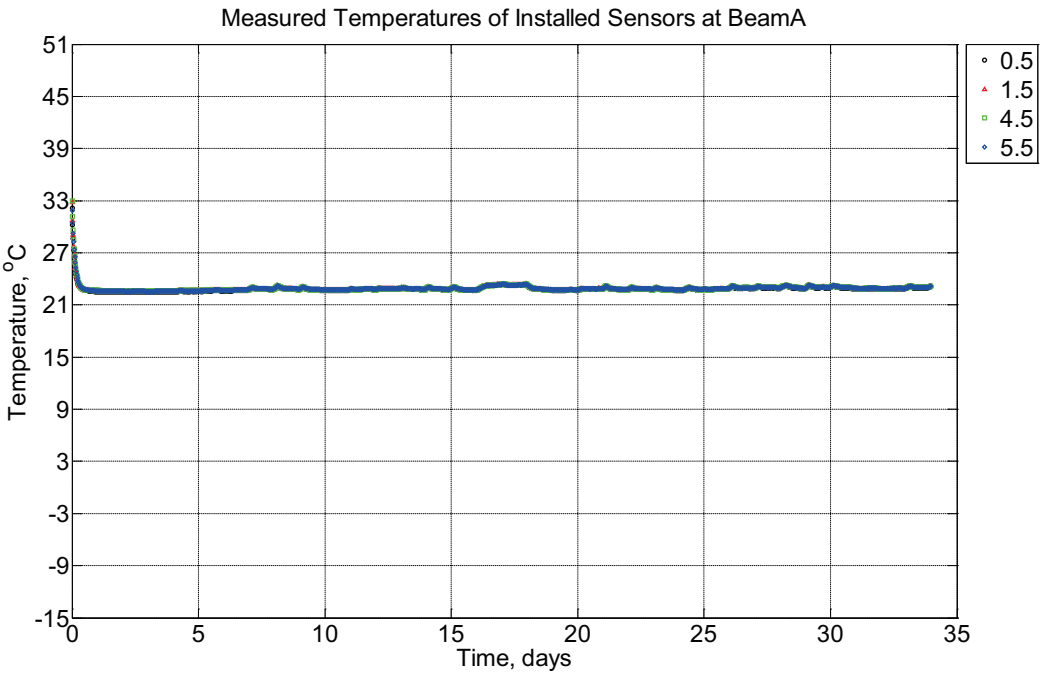

Figure B-209 Measured temperature at depths of 0.5 inches (12.7 mm), 1.5 inches (38.1 mm), 4.5 inches (114.3 mm), and 5.5 inches (139.7 mm) from the surface of a modulus of rupture beam (labeled A) located inside an environmentally controlled room (50% RH, 23°C) between May 21, 2014, through June 24, 2014.

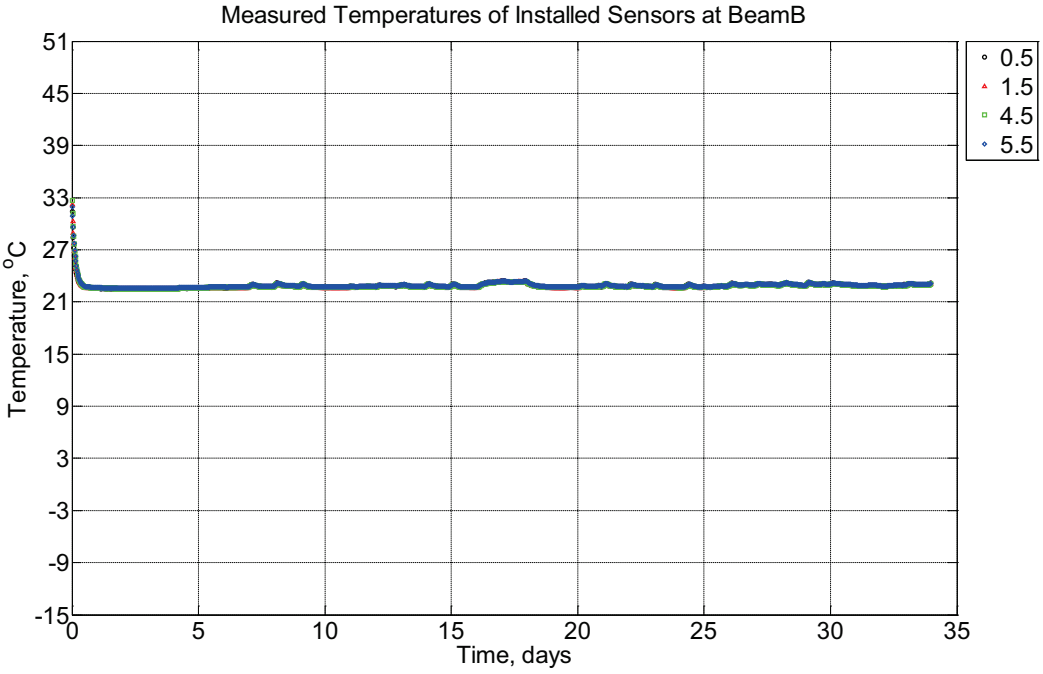

Figure B-210 Measured temperature at depths of 0.5 inches (12.7 mm), 1.5 inches (38.1 mm), 4.5 inches (114.3 mm), and 5.5 inches (139.7 mm) from the surface of a modulus of

rupture beam (labeled B) located inside an environmentally controlled room (50% RH, 23°C) between May 21, 2014, through June 24, 2014.

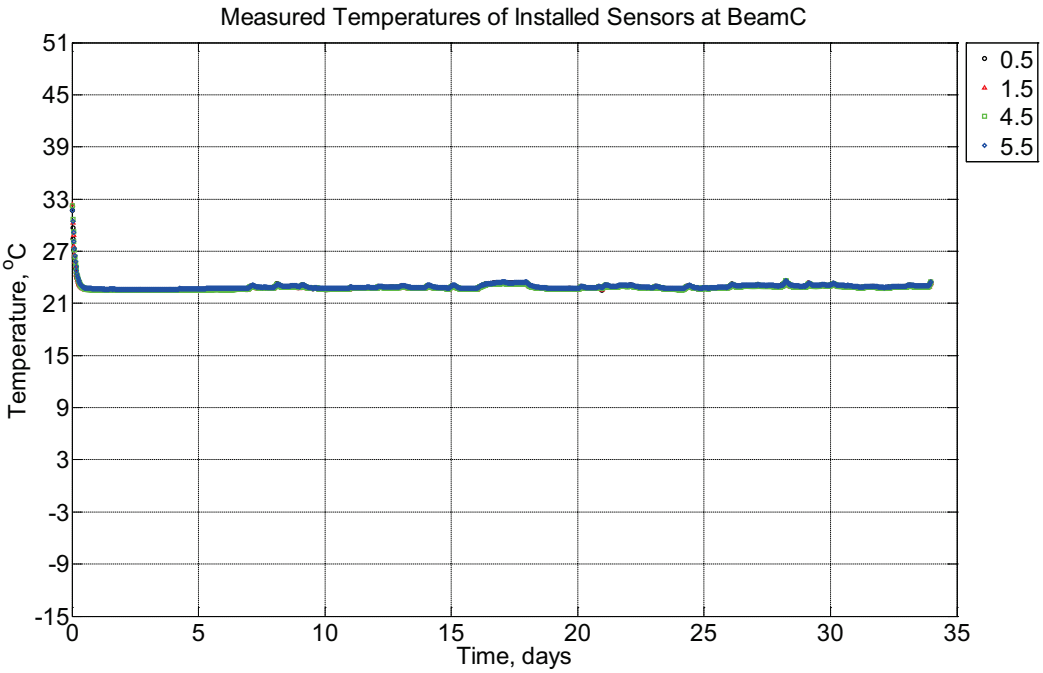

Figure B-211 Measured temperature at depths of 0.5 inches (12.7 mm), 1.5 inches (38.1 mm), 4.5 inches (114.3 mm), and 5.5 inches (139.7 mm) from the surface of a modulus of rupture beam (labeled C) located inside an environmentally controlled room (50% RH, 23°C) between May 21, 2014, through June 24, 2014.

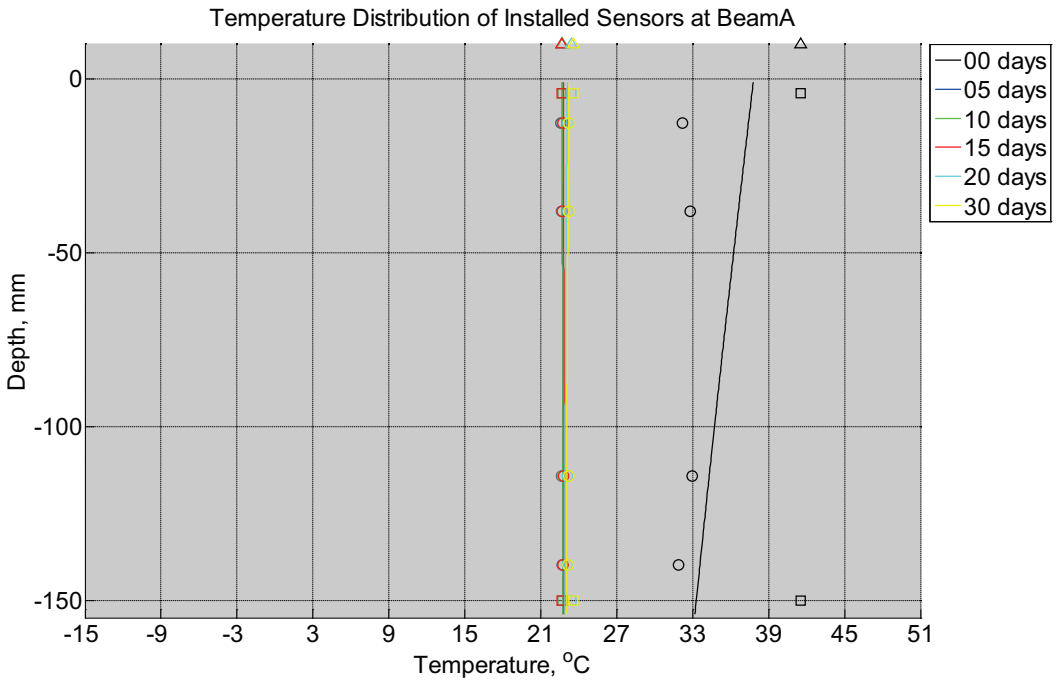

Figure B-212 Measured (markers) and modeled (continuous line) temperature profile distribution as a function of depth inside modulus of rupture beam (labeled A) located inside an environmentally controlled room (50% RH, 23ºC) between May 21, 2014, through June 24, 2014. Triangular markers denote temperature value from control panel, square markers denote measured temperature values from ambient sensors, and circular markers denote measured temperature values inside concrete.

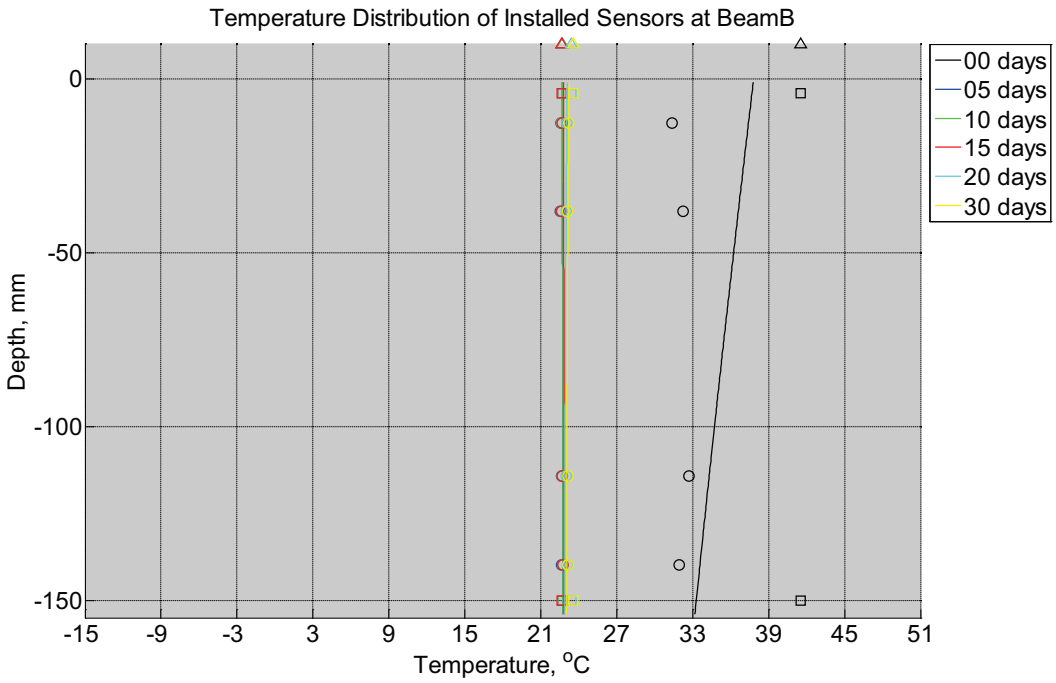

Figure B-213 Measured (markers) and modeled (continuous line) temperature profile distribution as a function of depth inside modulus of rupture beam (labeled B) located inside an environmentally controlled room (50% RH, 23ºC) between May 21, 2014, through June 24, 2014. Triangular markers denote temperature value from control panel, square markers denote measured temperature values from ambient sensors, and circular markers denote measured temperature values inside concrete.

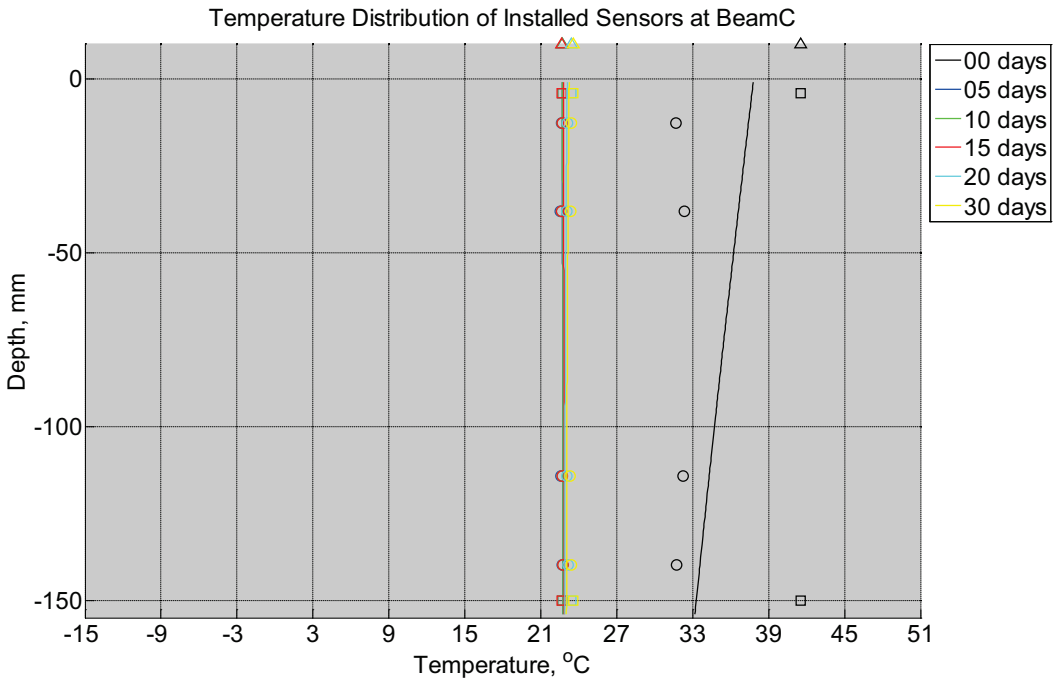

Figure B-214 Measured (markers) and modeled (continuous line) temperature profile distribution as a function of depth inside modulus of rupture beam (labeled C) located inside an environmentally controlled room (50% RH, 23ºC) between May 21, 2014, through June 24, 2014. Triangular markers denote temperature value from control panel, square markers denote measured temperature values from ambient sensors, and circular markers denote measured temperature values inside concrete.

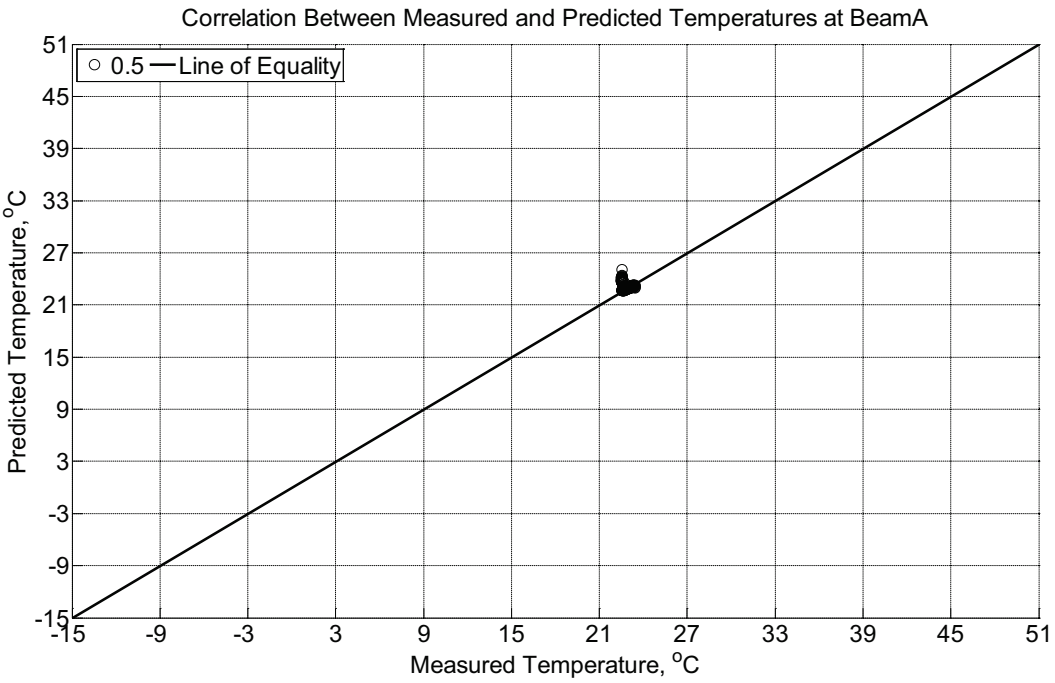

Figure B-215 Correlation between measured and predicted temperature values 0.5 inches (12.7 mm) from the surface of a modulus of rupture beam (labeled A) located inside an environmentally controlled room (50% RH, 23ºC) between May 21, 2014, through June 24, 2014.

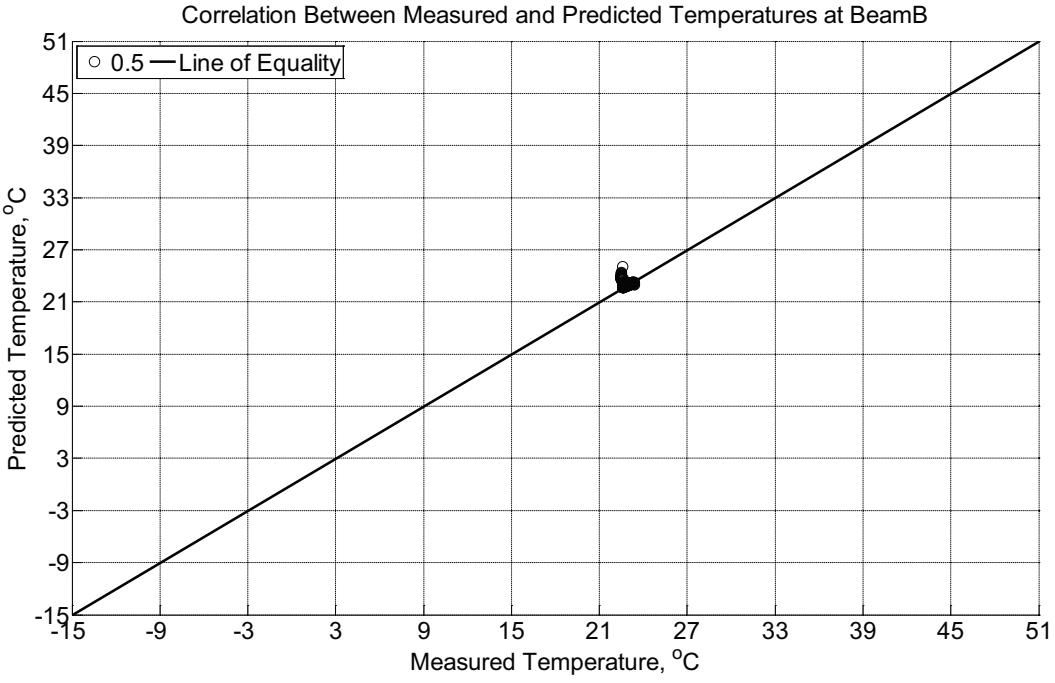

Figure B-216 Correlation between measured and predicted temperature values 0.5 inches (12.7 mm) from the surface of a modulus of rupture beam (labeled B) located inside an

environmentally controlled room (50% RH, 23°C) between May 21, 2014, through June 24, 2014.

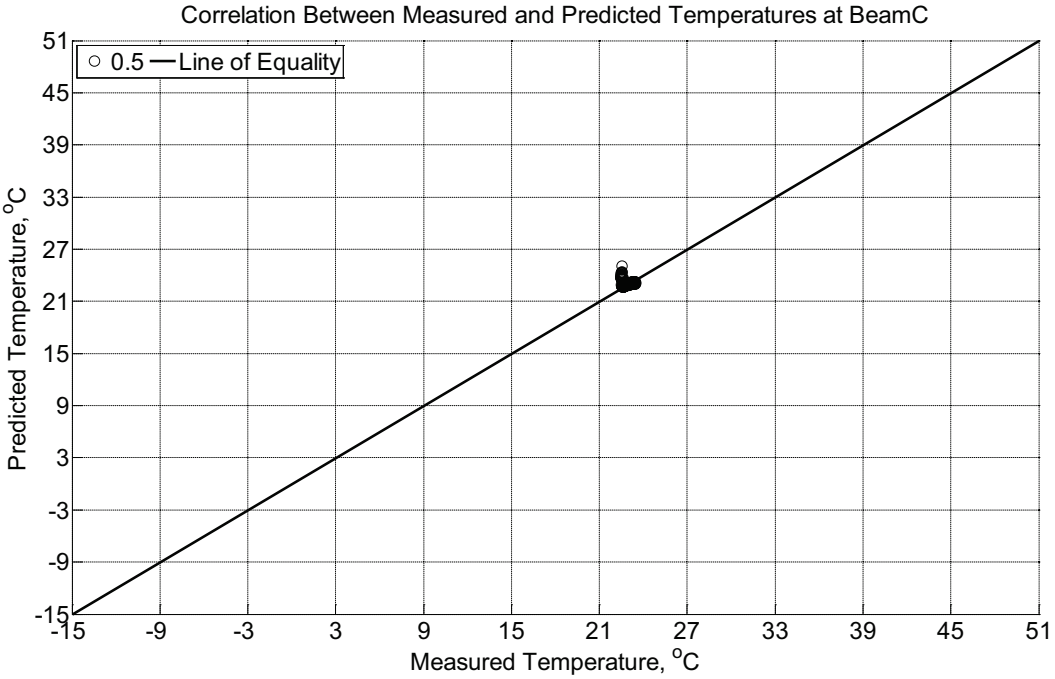

Figure B-217 Correlation between measured and predicted temperature values 0.5 inches (12.7 mm) from the surface of a modulus of rupture beam (labeled C) located inside an environmentally controlled room (50% RH, 23°C) between May 21, 2014, through June 24, 2014.

Figure B-218 Correlation between measured and predicted temperature values 0.5 inches (12.7 mm), 1.5 inches (38.1 mm), 4.5 inches (114.3 mm), and 5.5 inches (139.7 mm) from the surface of a modulus of rupture beam (labeled A) located inside an environmentally controlled room (50% RH, 23°C) between May 21, 2014, through June 24, 2014

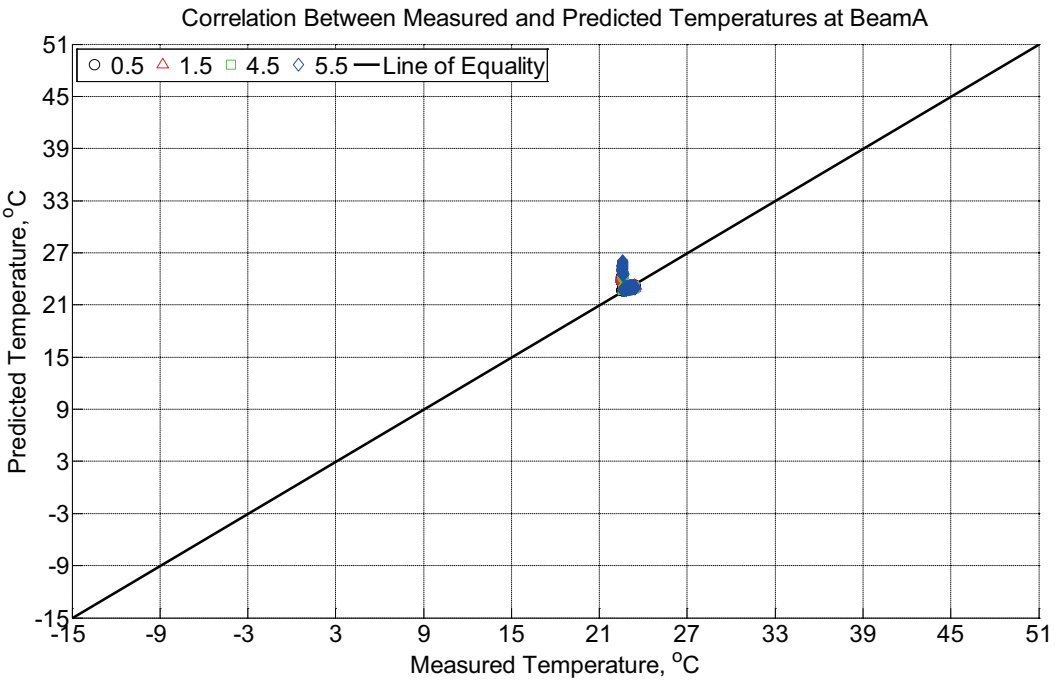

Figure B-219 Correlation between measured and predicted temperature values 0.5 inches (12.7 mm), 1.5 inches (38.1 mm), 4.5 inches (114.3 mm), and 5.5 inches (139.7 mm) from the surface of a modulus of rupture beam (labeled A) located inside an environmentally controlled room (50% RH, 23°C) between May 21, 2014, through June 24, 2014.

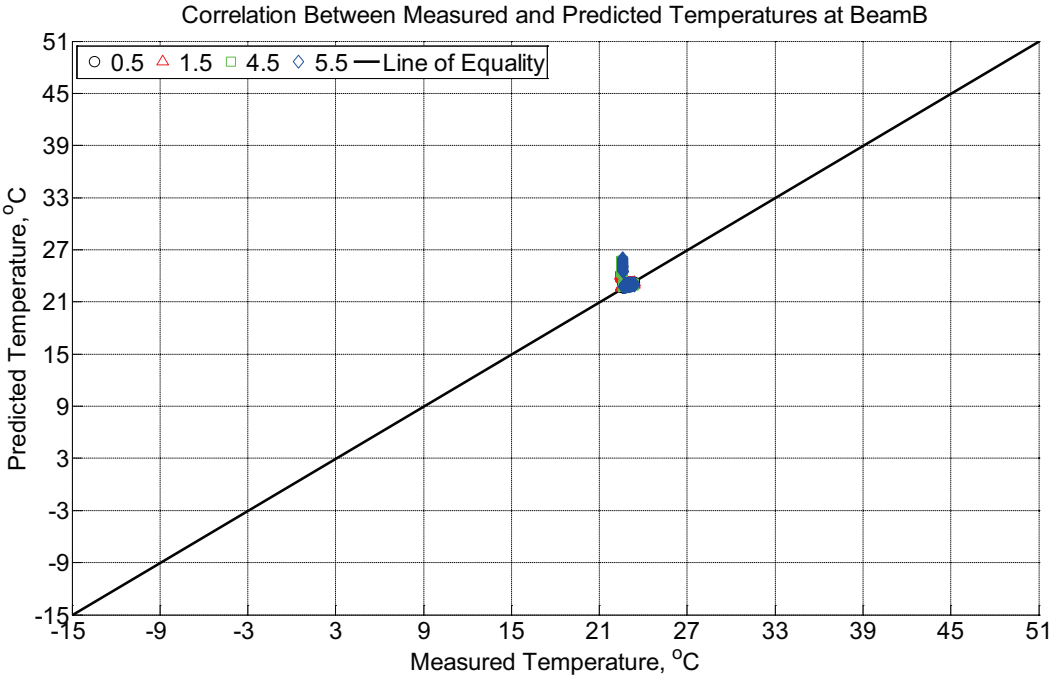

Figure B-220 Correlation between measured and predicted temperature values 0.5 inches (12.7 mm), 1.5 inches (38.1 mm), 4.5 inches (114.3 mm), and 5.5 inches (139.7 mm) from the

surface of a modulus of rupture beam (labeled A) located inside an environmentally controlled room (50% RH, 23°C) between May 21, 2014, through June 24, 2014.

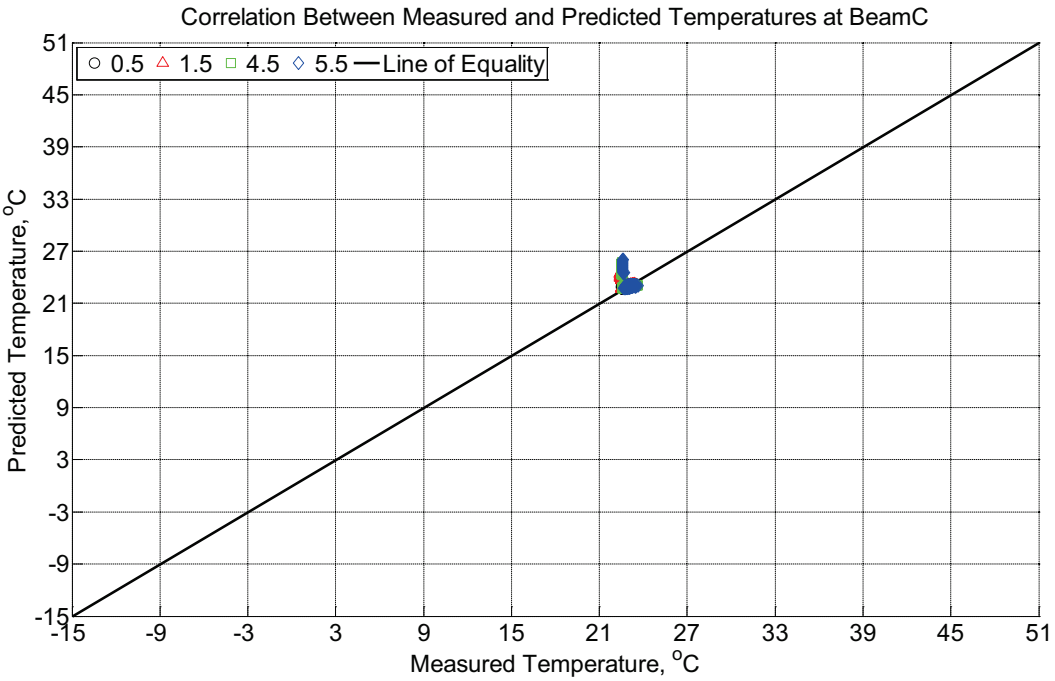

Figure B-221 Correlation between measured and predicted temperature values 0.5 inches (12.7 mm), 1.5 inches (38.1 mm), 4.5 inches (114.3 mm), and 5.5 inches (139.7 mm) from the surface of a modulus of rupture beam (labeled A) located inside an environmentally controlled room (50% RH, 23°C) between May 21, 2014, through June 24, 2014.

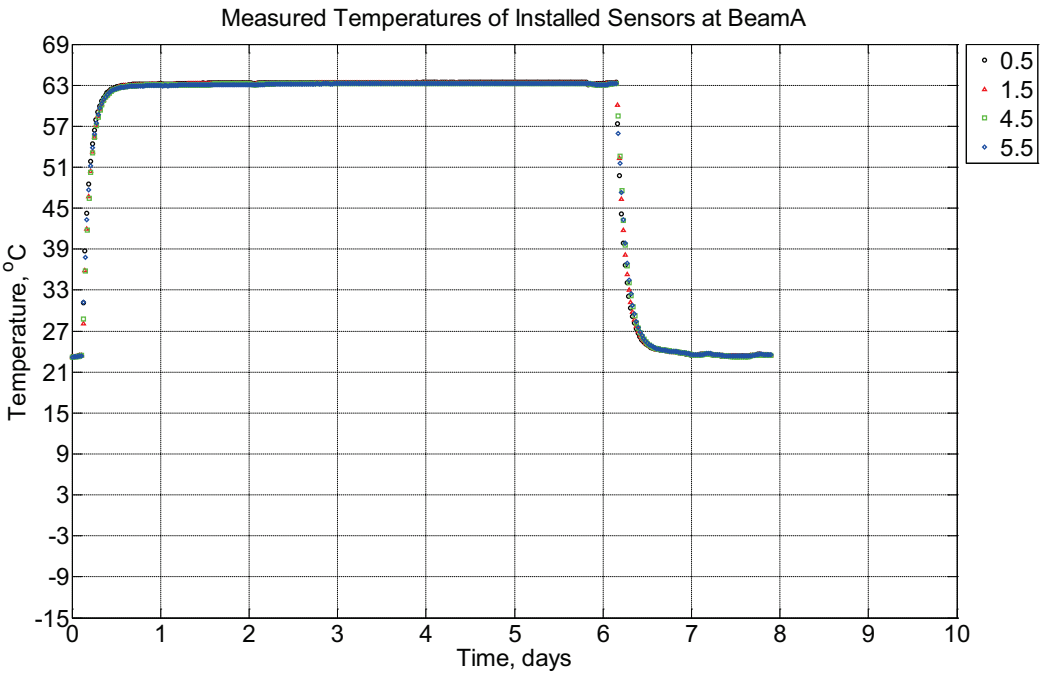

Figure B-222 Measured temperature at depths of 0.5 inches (12.7 mm), 1.5 inches (38.1 mm), 4.5 inches (114.3 mm), and 5.5 inches (139.7 mm) from the surface of a modulus of rupture beam (labeled A) located inside an environmentally controlled room (50% RH, 23ºC) and a heating oven (65ºC) between June 24, 2014, through July 2, 2014.

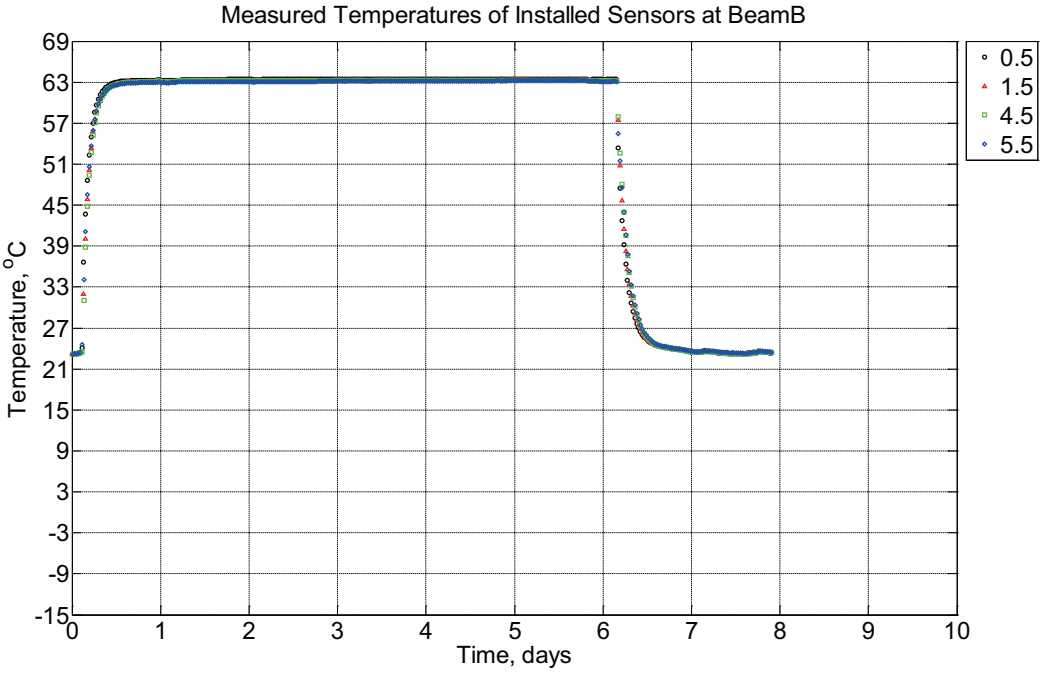

Figure B-223 Measured temperature at depths of 0.5 inches (12.7 mm), 1.5 inches (38.1 mm), 4.5 inches (114.3 mm), and 5.5 inches (139.7 mm) from the surface of a modulus of

rupture beam (labeled B) located inside an environmentally controlled room (50% RH, 23°C) and a heating oven (65°C) between June 24, 2014, through July 2, 2014.

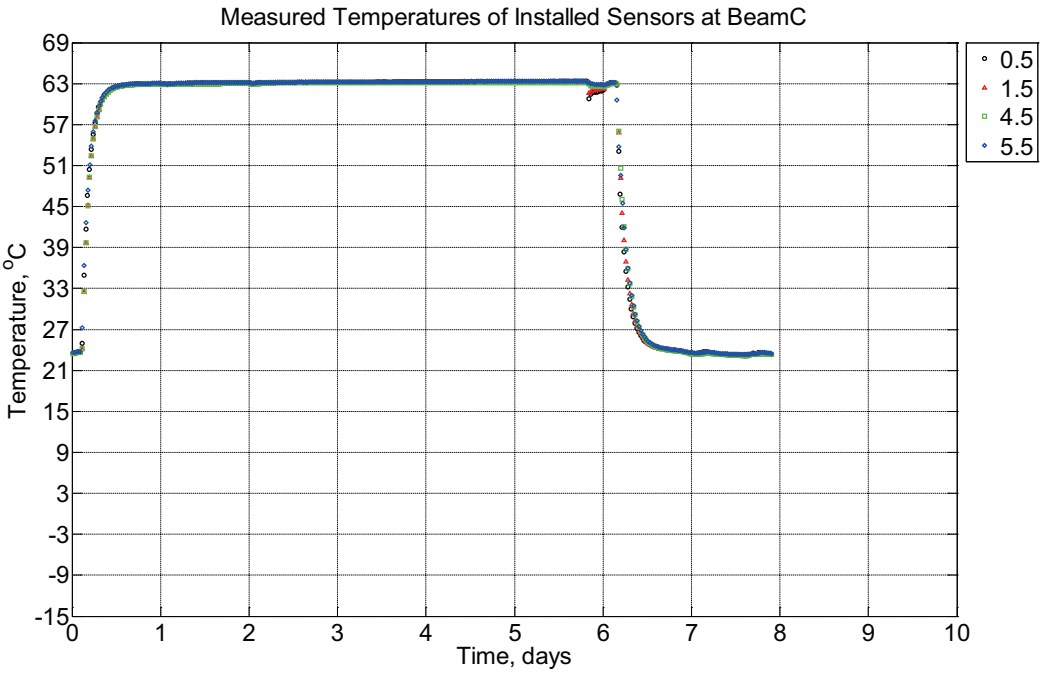

Figure B-224 Measured temperature at depths of 0.5 inches (12.7 mm), 1.5 inches (38.1 mm), 4.5 inches (114.3 mm), and 5.5 inches (139.7 mm) from the surface of a modulus of rupture beam (labeled C) located inside an environmentally controlled room (50% RH, 23°C) and a heating oven (65°C) between June 24, 2014, through July 2, 2014.

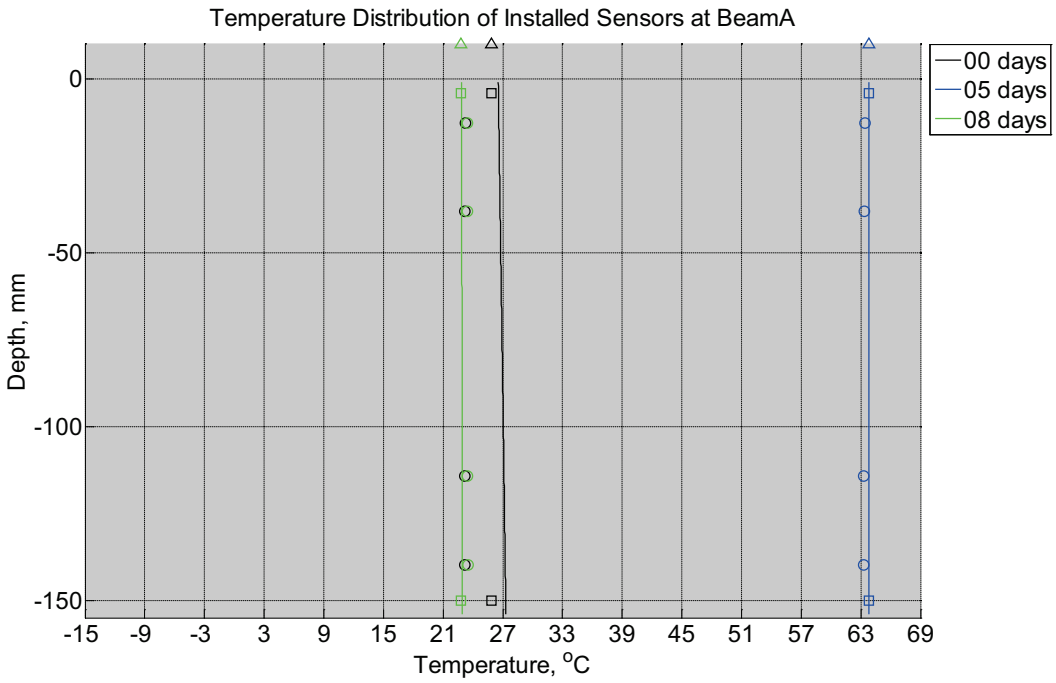

Figure B-225 Measured (markers) and modeled (continuous line) temperature profile distribution as a function of depth inside modulus of rupture beam (labeled A) located inside an environmentally controlled room (50% RH, 23ºC) and a heating oven (65ºC) between June 24, 2014, through July 2, 2014. Triangular markers denote temperature value from control panel, square markers denote measured temperature values from ambient sensors, and circular markers denote measured temperature values inside concrete.

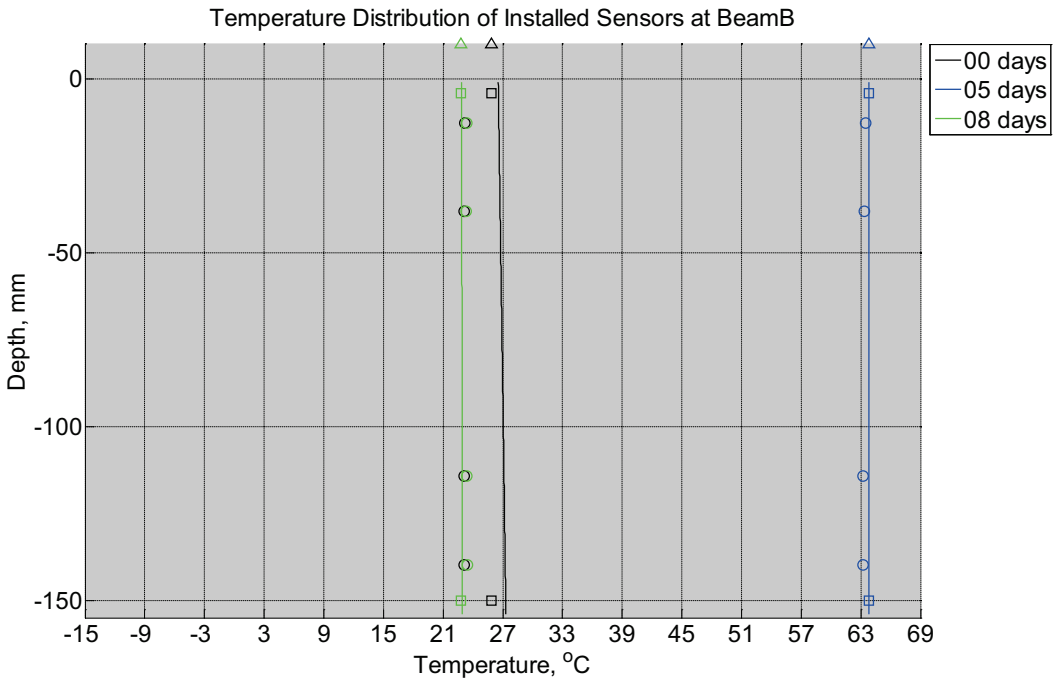

Figure B-226 Measured (markers) and modeled (continuous line) temperature profile distribution as a function of depth inside modulus of rupture beam (labeled B) located inside an environmentally controlled room (50% RH, 23ºC) and a heating oven (65ºC) between June 24, 2014, through July 2, 2014. Triangular markers denote temperature value from control panel, square markers denote measured temperature values from ambient sensors, and circular markers denote measured temperature values inside concrete.

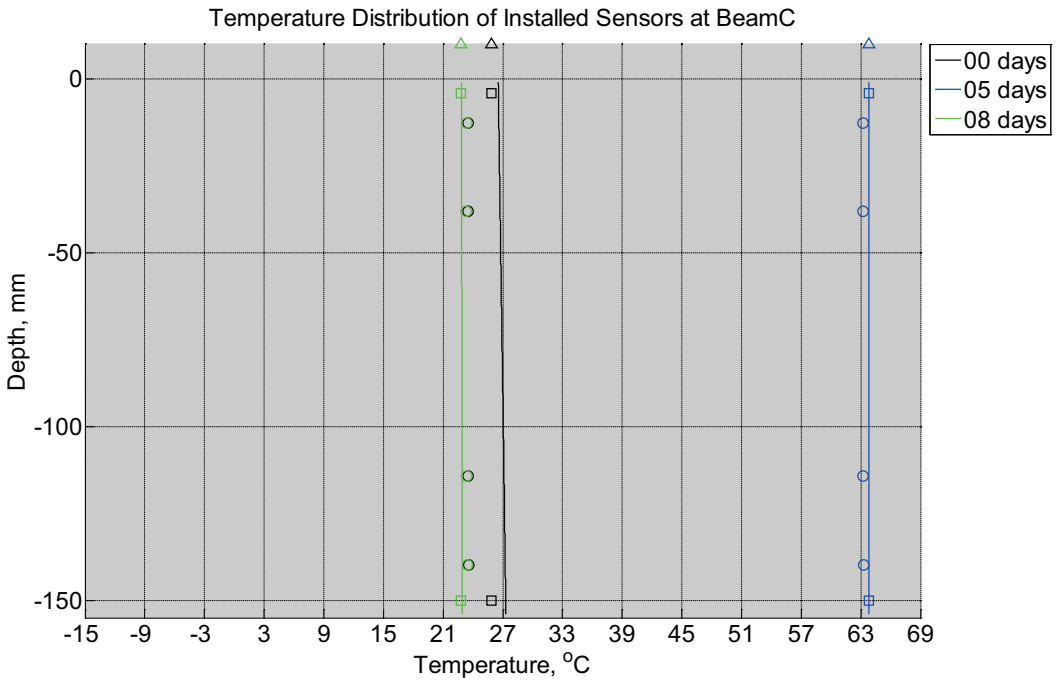

Figure B-227 Measured (markers) and modeled (continuous line) temperature profile distribution as a function of depth inside modulus of rupture beam (labeled C) located inside an environmentally controlled room (50% RH, 23ºC) and a heating oven (65ºC) between June 24, 2014, through July 2, 2014. Triangular markers denote temperature value from control panel, square markers denote measured temperature values from ambient sensors, and circular markers denote measured temperature values inside concrete.

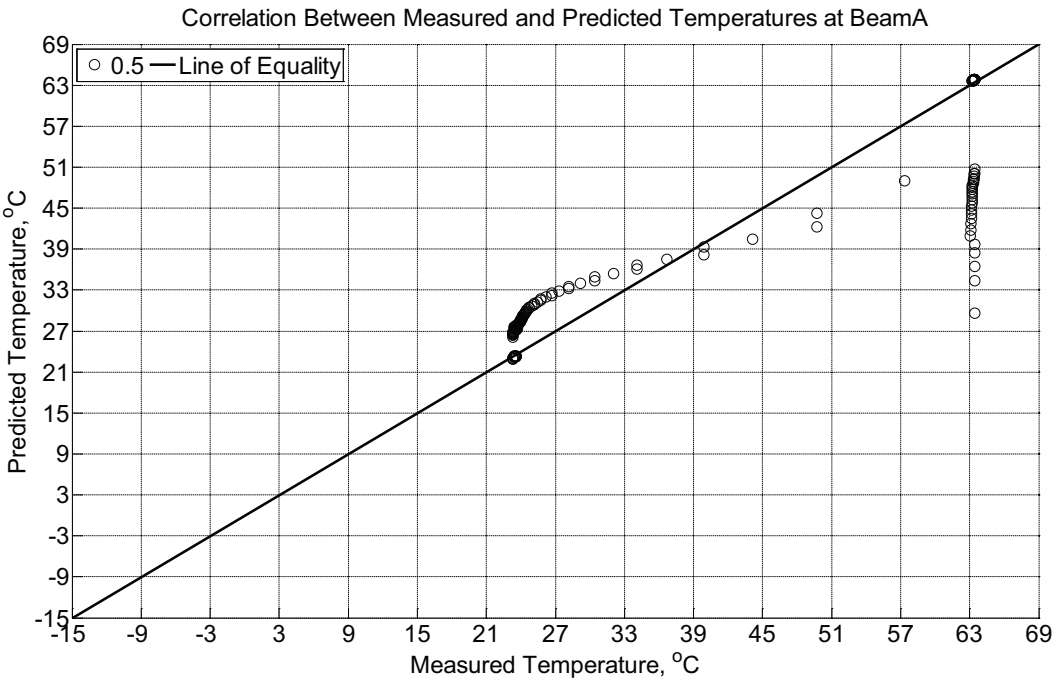

Figure B-228 Correlation between measured and predicted temperature values 0.5 inches (12.7 mm) from the surface of a modulus of rupture beam (labeled A) located inside an environmentally controlled room (50% RH, 23ºC) and a heating oven (65ºC) between June 24, 2014, through July 2, 2014.

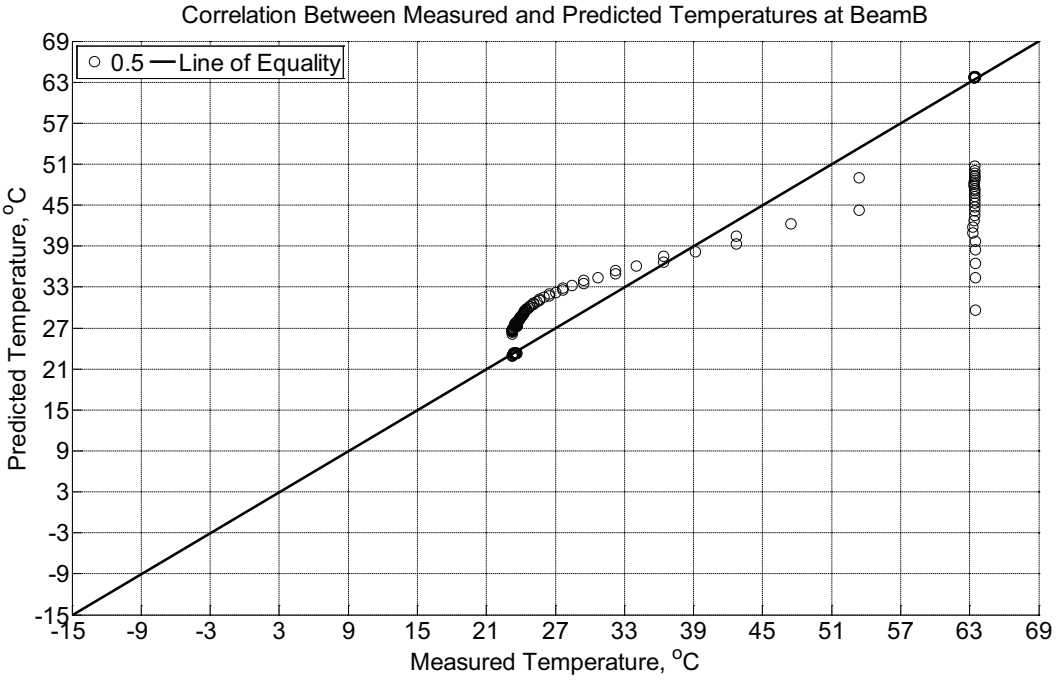

Figure B-229 Correlation between measured and predicted temperature values 0.5 inches (12.7 mm) from the surface of a modulus of rupture beam (labeled B) located inside an

environmentally controlled room (50% RH, 23°C) and a heating oven (65°C) between June 24, 2014, through July 2, 2014.

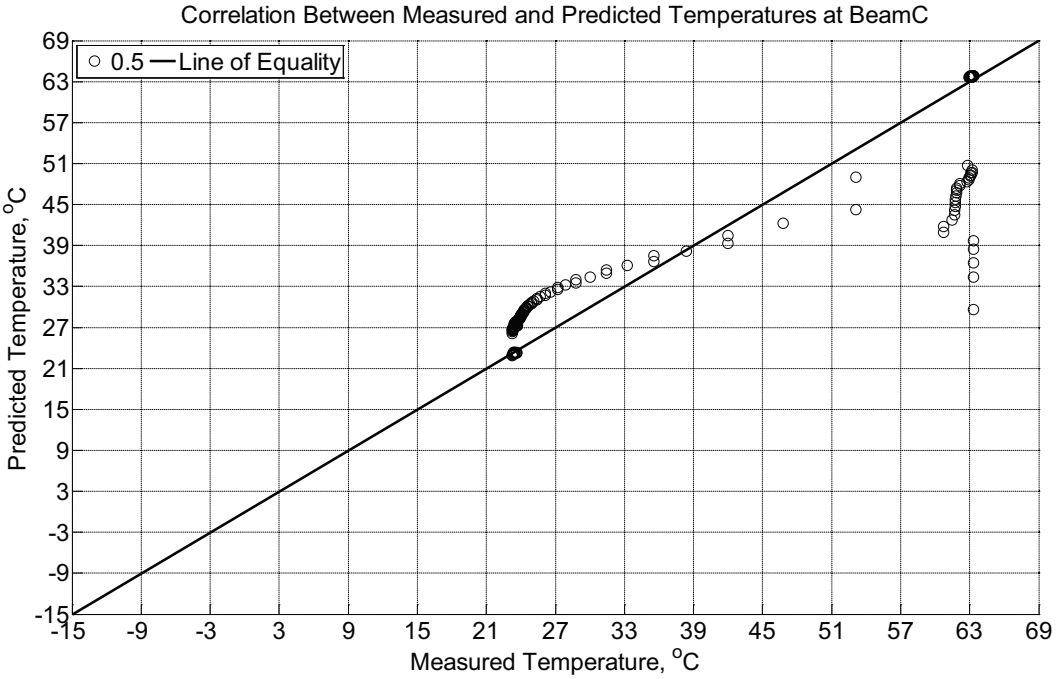

Figure B-230 Correlation between measured and predicted temperature values 0.5 inches (12.7 mm) from the surface of a modulus of rupture beam (labeled C) located inside an environmentally controlled room (50% RH, 23°C) and a heating oven (65°C) between June 24, 2014, through July 2, 2014.

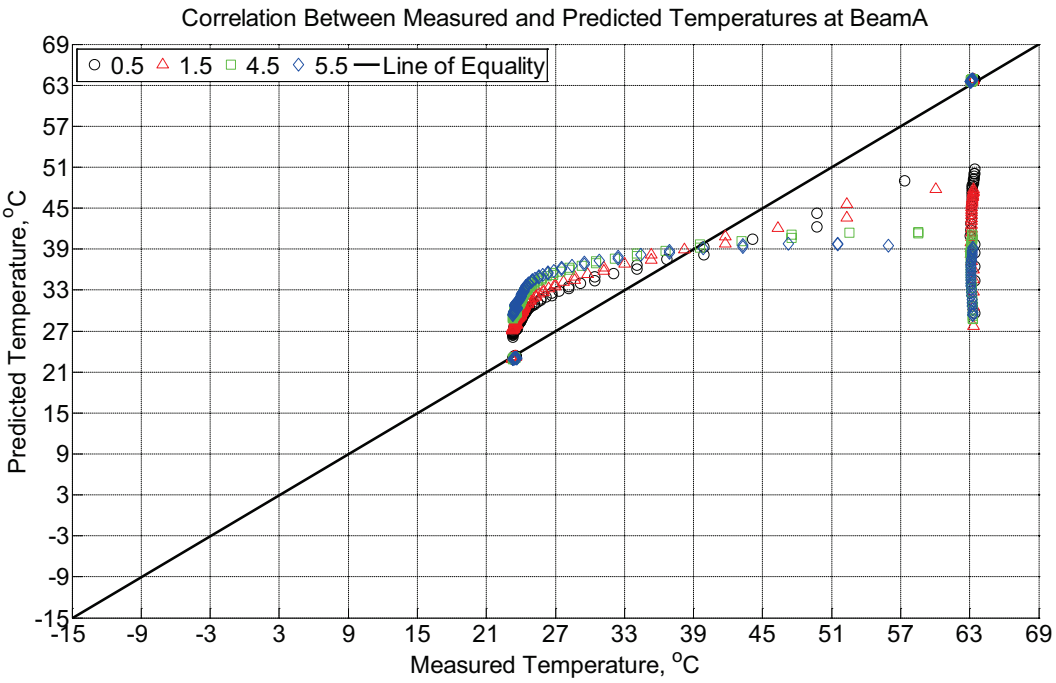

Figure B-231 Correlation between measured and predicted temperature values 0.5 inches (12.7 mm), 1.5 inches (38.1 mm), 4.5 inches (114.3 mm), and 5.5 inches (139.7 mm) from the surface of a modulus of rupture beam (labeled A) located inside an environmentally controlled room (50% RH, 23ºC) and a heating oven (65ºC) between June 24, 2014, through July 2, 2014.

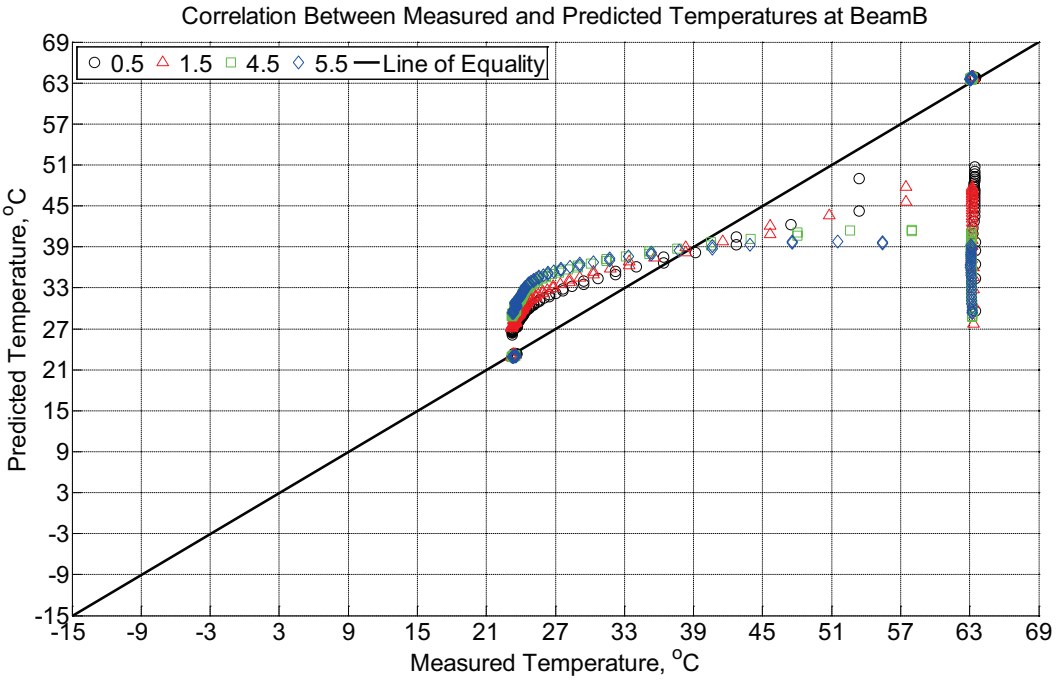

Figure B-232 Correlation between measured and predicted temperature values 0.5 inches

(12.7 mm), 1.5 inches (38.1 mm), 4.5 inches (114.3 mm), and 5.5 inches (139.7 mm) from the surface of a modulus of rupture beam (labeled B) located inside an environmentally controlled room (50% RH, 23ºC) and a heating oven (65ºC) between June 24, 2014, through July 2, 2014.

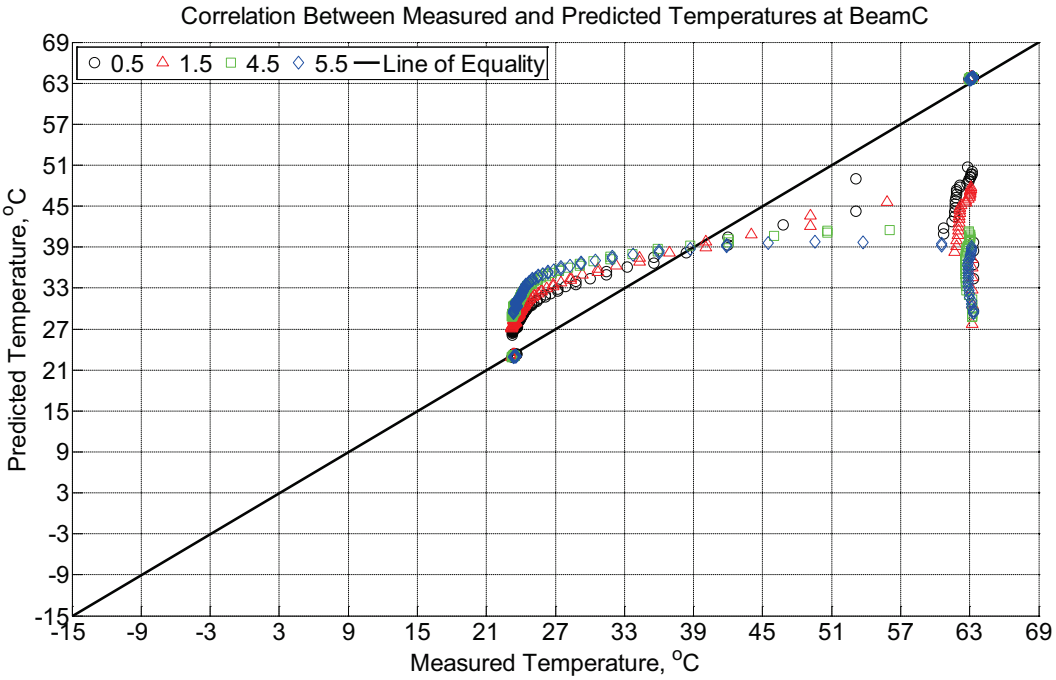

Figure B-233 Correlation between measured and predicted temperature values 0.5 inches (12.7 mm), 1.5 inches (38.1 mm), 4.5 inches (114.3 mm), and 5.5 inches (139.7 mm) from the surface of a modulus of rupture beam (labeled C) located inside an environmentally controlled room (50% RH, 23ºC) and a heating oven (65ºC) between June 24, 2014, through July 2, 2014.

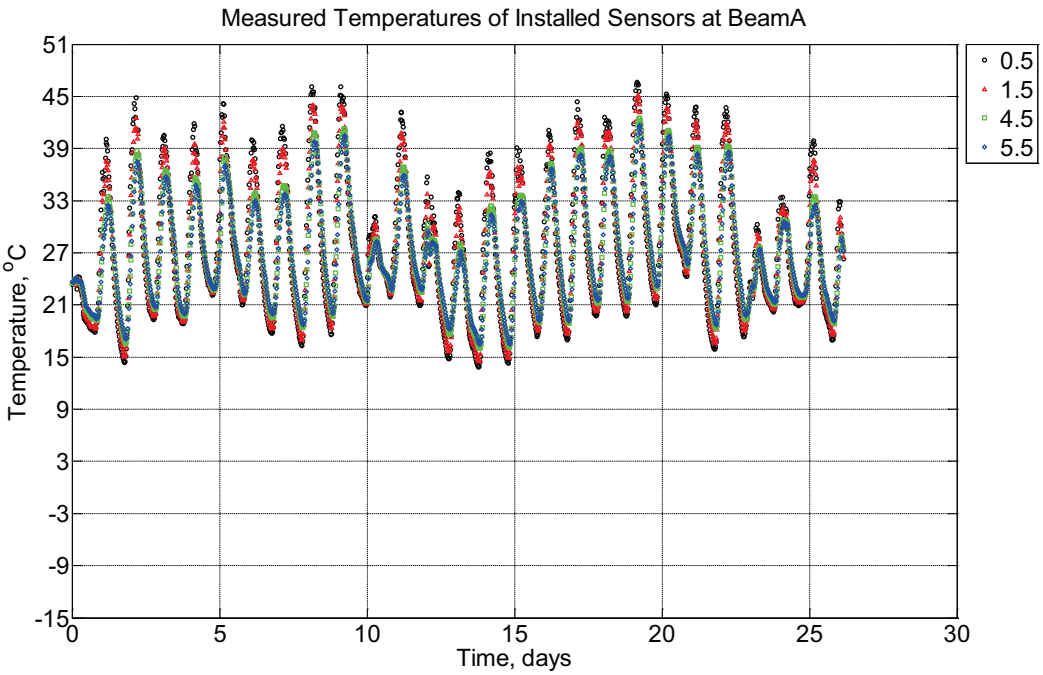

Figure B-234 Measured temperature at depths of 0.5 inches (12.7 mm), 1.5 inches (38.1 mm), 4.5 inches (114.3 mm), and 5.5 inches (139.7 mm) from the surface of a modulus of rupture beam (labeled A) installed in ballast in Rantoul, IL, between July 2, 2014, through July 28, 2014.

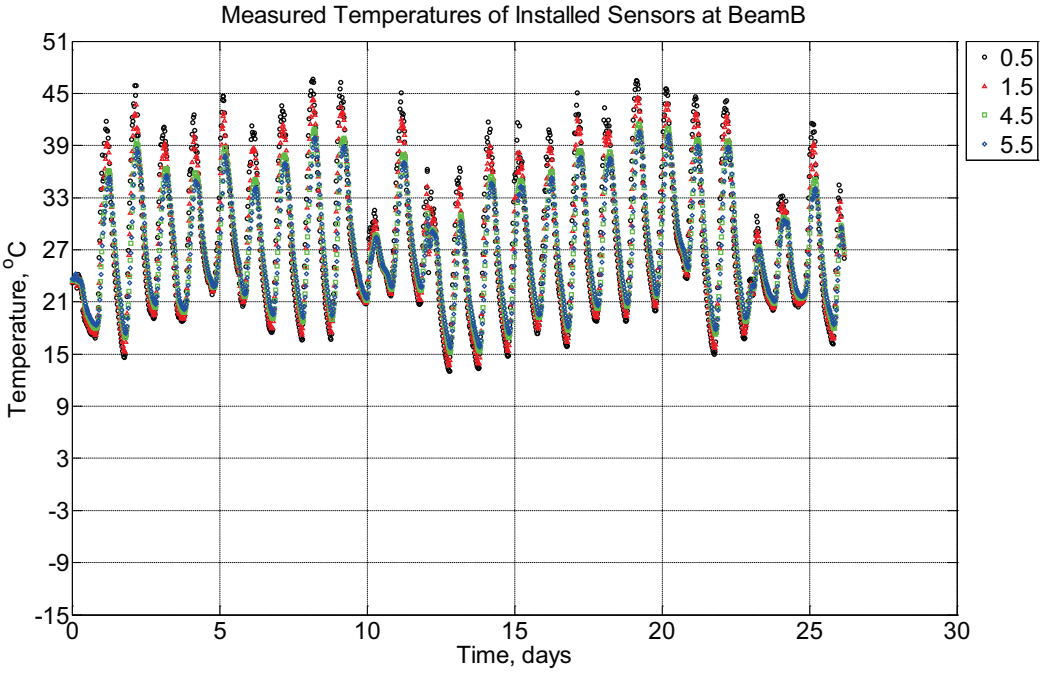

Figure B-235 Measured temperature at depths of 0.5 inches (12.7 mm), 1.5 inches (38.1 mm), 4.5 inches (114.3 mm), and 5.5 inches (139.7 mm) from the surface of a modulus of

rupture beam (labeled B) installed in ballast in Rantoul, IL, between July 2, 2014, through July 28, 2014.

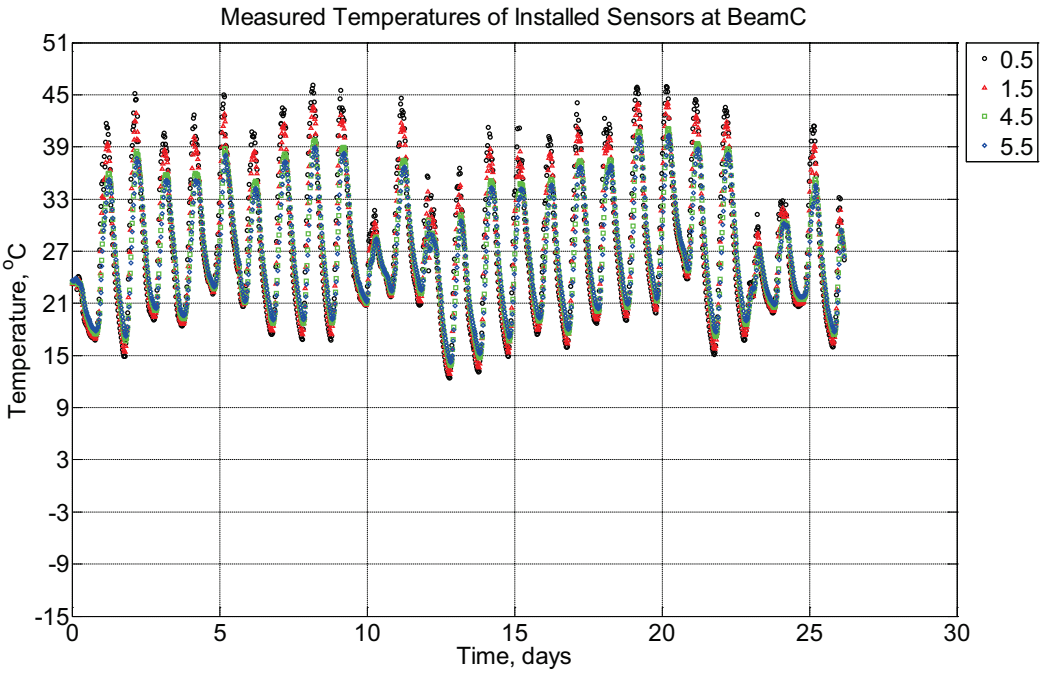

Figure B-236 Measured temperature at depths of 0.5 inches (12.7 mm), 1.5 inches (38.1 mm), 4.5 inches (114.3 mm), and 5.5 inches (139.7 mm) from the surface of a modulus of rupture beam (labeled C) installed in ballast in Rantoul, IL, between July 2, 2014, through July 28, 2014.

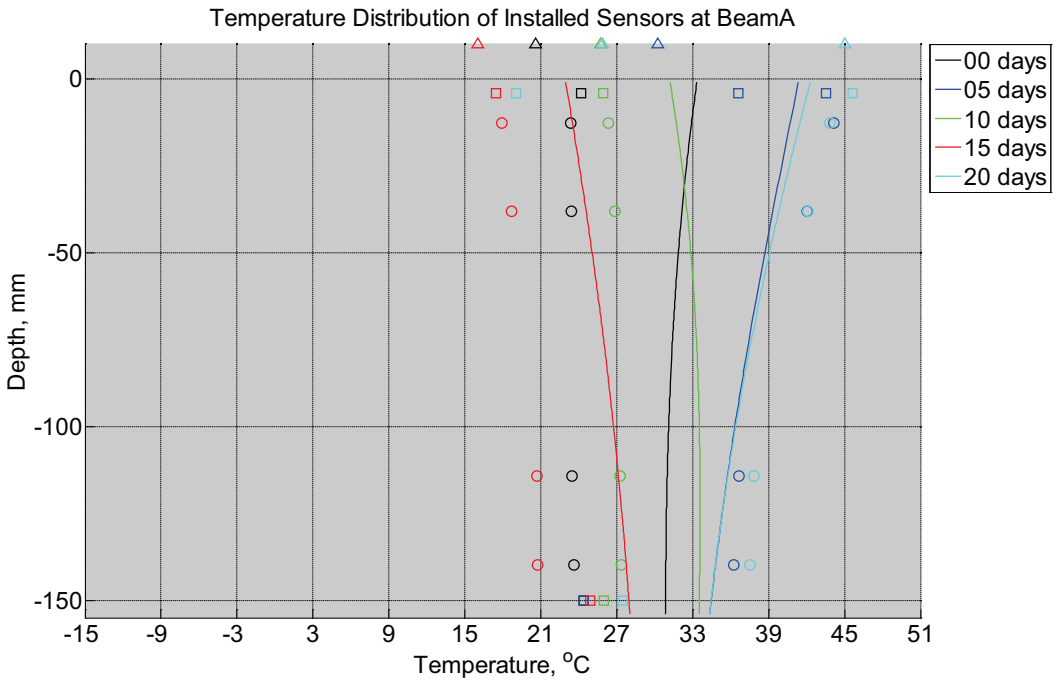

Figure B-237 Measured (markers) and modeled (continuous line) temperature profile distribution as a function of depth inside modulus of rupture beam (labeled A) installed in ballast in Rantoul, IL, between July 2, 2014, through July 28, 2014. Triangular markers denote temperature value from KTIP weather station, square markers denote measured temperature values from ballast, and circular markers denote measured temperature values inside concrete.

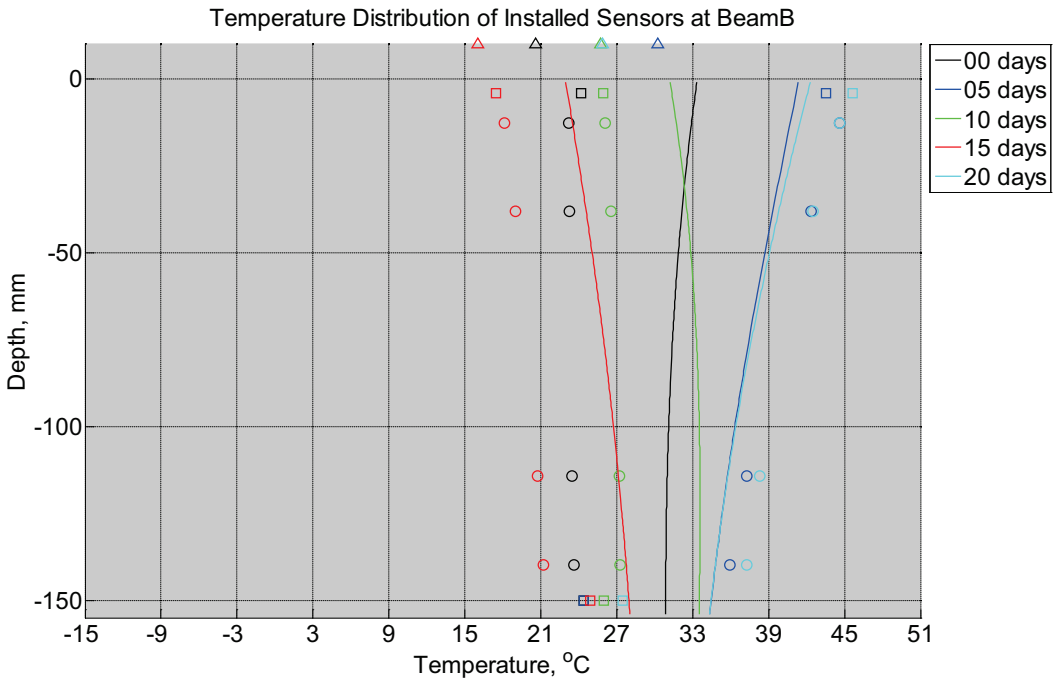

Figure B-238 Measured (markers) and modeled (continuous line) temperature profile distribution as a function of depth inside modulus of rupture beam (labeled B) installed in ballast in Rantoul, IL, between July 2, 2014, through July 28, 2014. Triangular markers denote temperature value from KTIP weather station, square markers denote measured temperature values from ballast, and circular markers denote measured temperature values inside concrete.

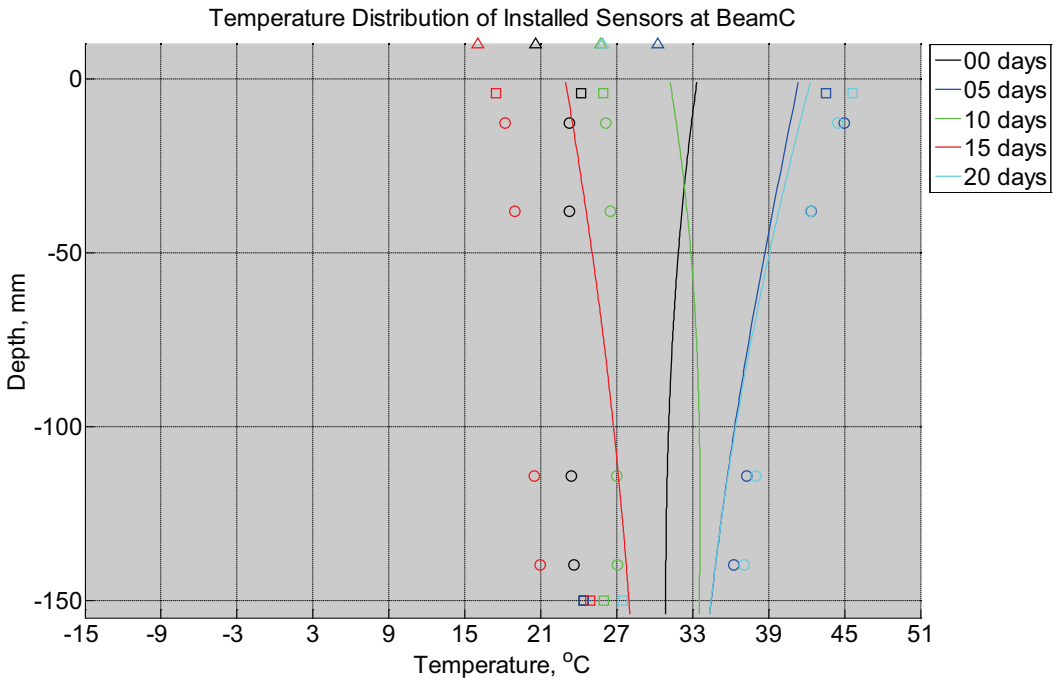

Figure B-239 Measured (markers) and modeled (continuous line) temperature profile distribution as a function of depth inside modulus of rupture beam (labeled C) installed in ballast in Rantoul, IL, between July 2, 2014, through July 28, 2014. Triangular markers denote temperature value from KTIP weather station, square markers denote measured temperature values from ballast, and circular markers denote measured temperature values inside concrete.

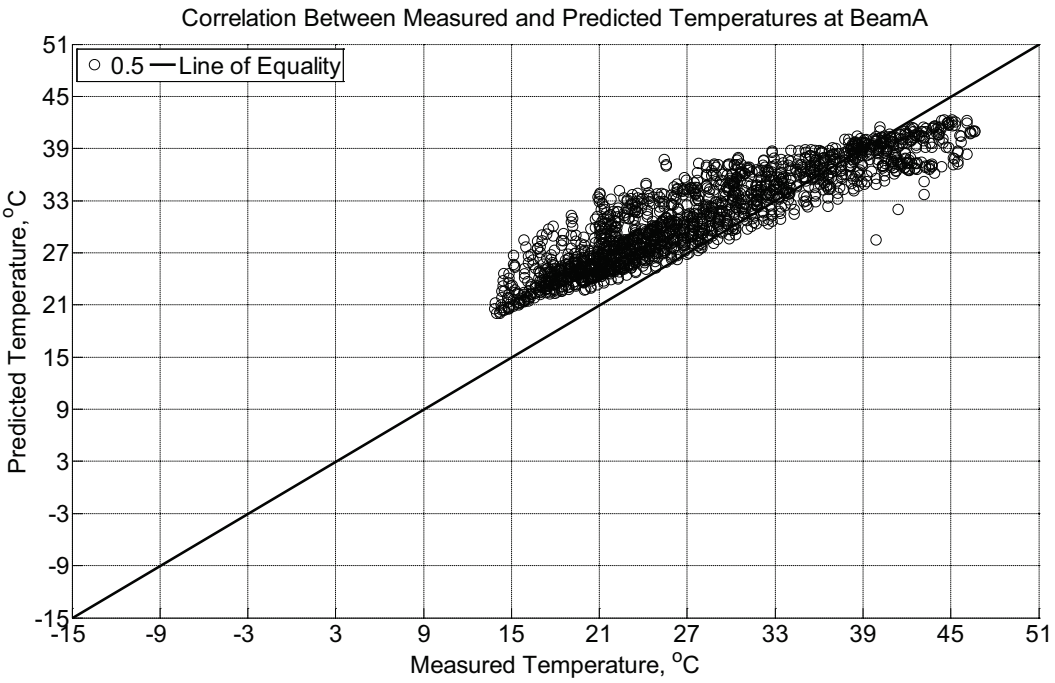

Figure B-240 Correlation between measured and predicted temperature values 0.5 inches (12.7 mm) from the surface of a modulus of rupture beam (labeled A) installed in ballast in Rantoul, IL, between July 2, 2014, through July 28, 2014.

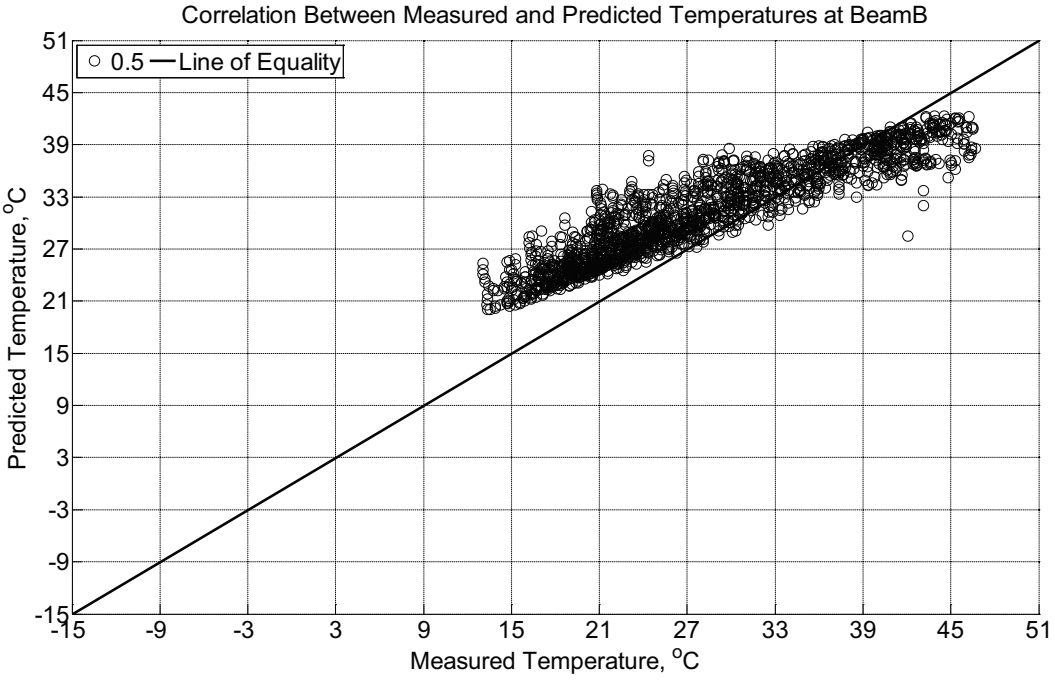

Figure B-241 Correlation between measured and predicted temperature values 0.5 inches

(12.7 mm) from the surface of a modulus of rupture beam (labeled B) installed in ballast in Rantoul, IL, between July 2, 2014, through July 28, 2014.

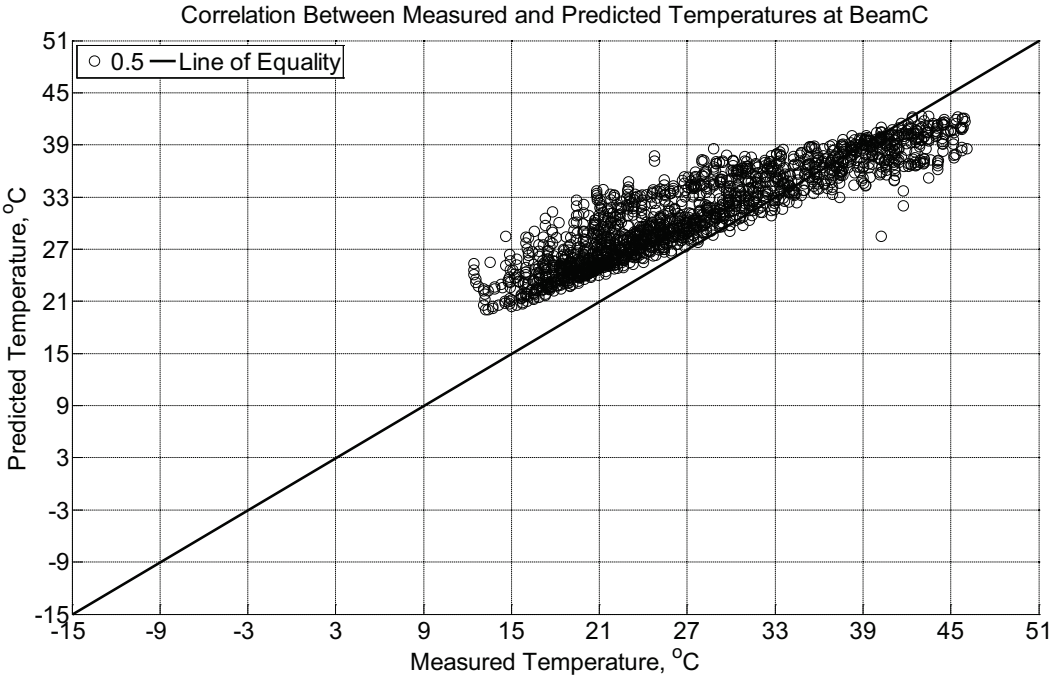

Figure B-242 Correlation between measured and predicted temperature values 0.5 inches (12.7 mm) from the surface of a modulus of rupture beam (labeled C) installed in ballast in Rantoul, IL, between July 2, 2014, through July 28, 2014.

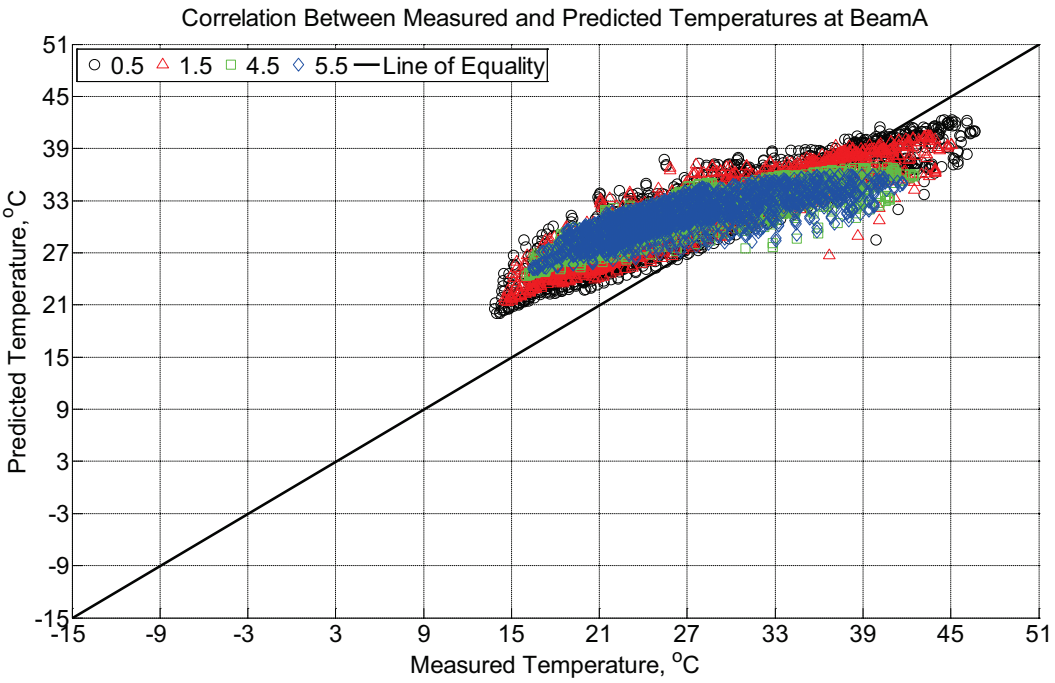

Figure B-243 Correlation between measured and predicted temperature values 0.5 inches (12.7 mm), 1.5 inches (38.1 mm), 4.5 inches (114.3 mm), and 5.5 inches (139.7 mm) from the surface of a modulus of rupture beam (labeled A) installed in ballast in Rantoul, IL, between July 2, 2014, through July 28, 2014.

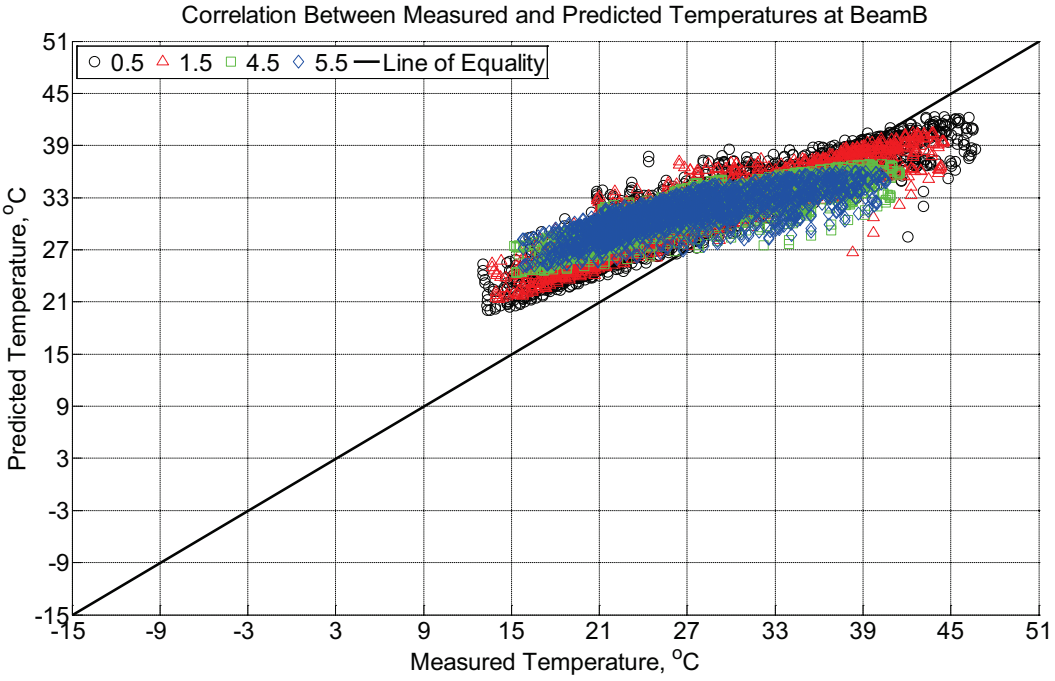

Figure B-244 Correlation between measured and predicted temperature values 0.5 inches (12.7 mm), 1.5 inches (38.1 mm), 4.5 inches (114.3 mm), and 5.5 inches (139.7 mm) from the

surface of a modulus of rupture beam (labeled B) installed in ballast in Rantoul, IL, between July 2, 2014, through July 28, 2014.

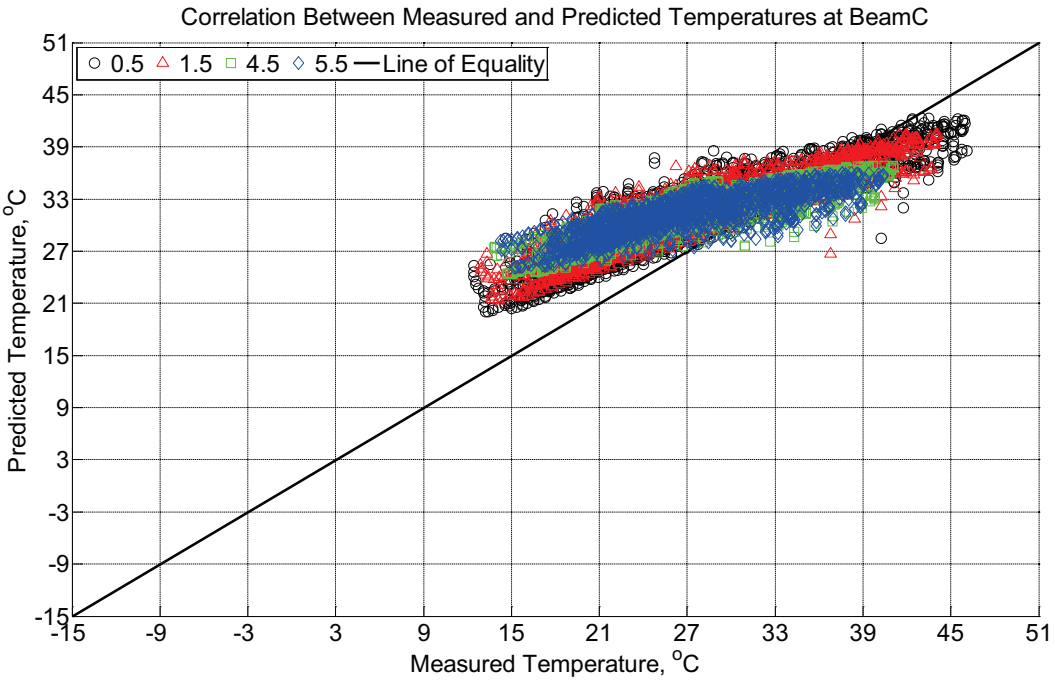

Figure B-245 Correlation between measured and predicted temperature values 0.5 inches (12.7 mm), 1.5 inches (38.1 mm), 4.5 inches (114.3 mm), and 5.5 inches (139.7 mm) from the surface of a modulus of rupture beam (labeled C) installed in ballast in Rantoul, IL, between July 2, 2014, through July 28, 2014.

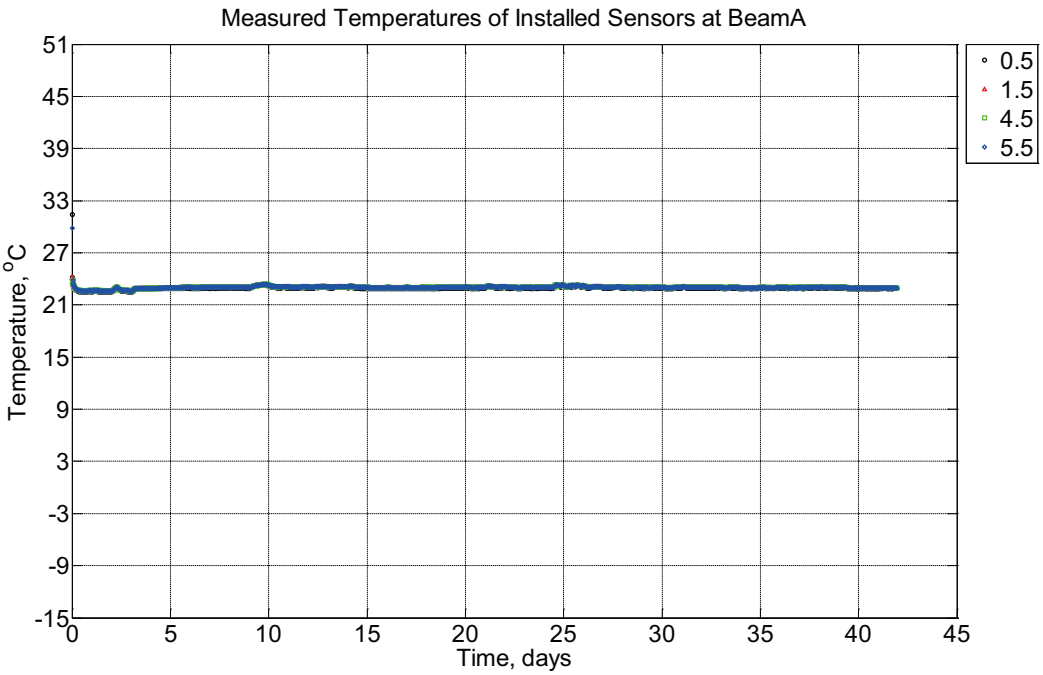

Figure B-246 Measured temperature at depths of 0.5 inches (12.7 mm), 1.5 inches (38.1 mm), 4.5 inches (114.3 mm), and 5.5 inches (139.7 mm) from the surface of a modulus of rupture beam (labeled A) located inside an environmentally controlled room (50% RH, 23°C) between July 29, 2014, through September 9, 2014.

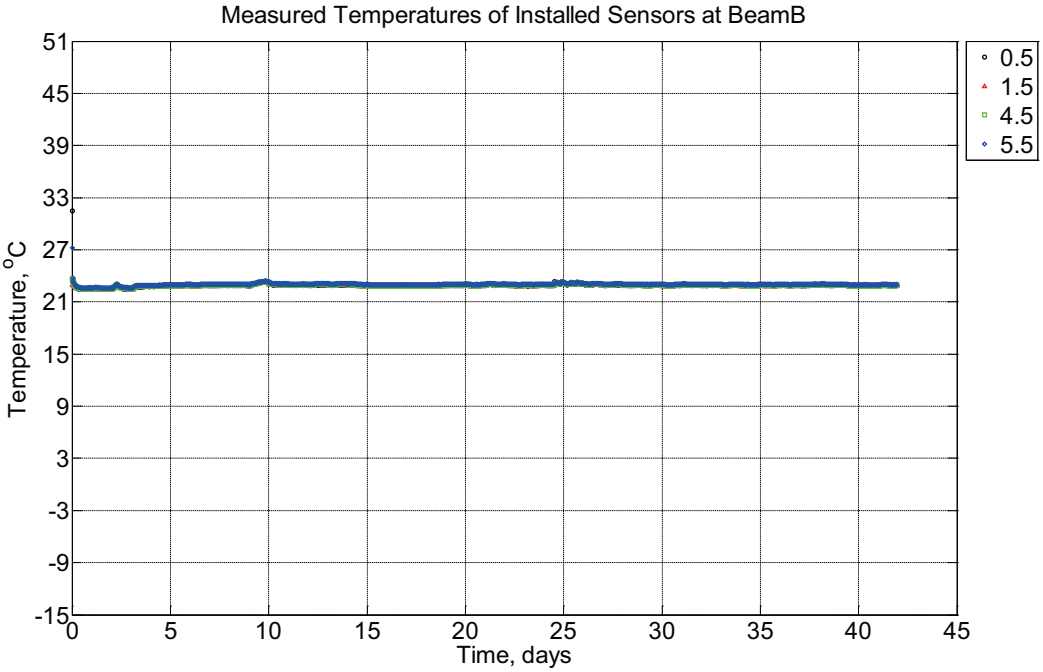

Figure B-247 Measured temperature at depths of 0.5 inches (12.7 mm), 1.5 inches (38.1 mm), 4.5 inches (114.3 mm), and 5.5 inches (139.7 mm) from the surface of a modulus of

rupture beam (labeled B) located inside an environmentally controlled room (50% RH, 23°C) between July 29, 2014, through September 9, 2014.

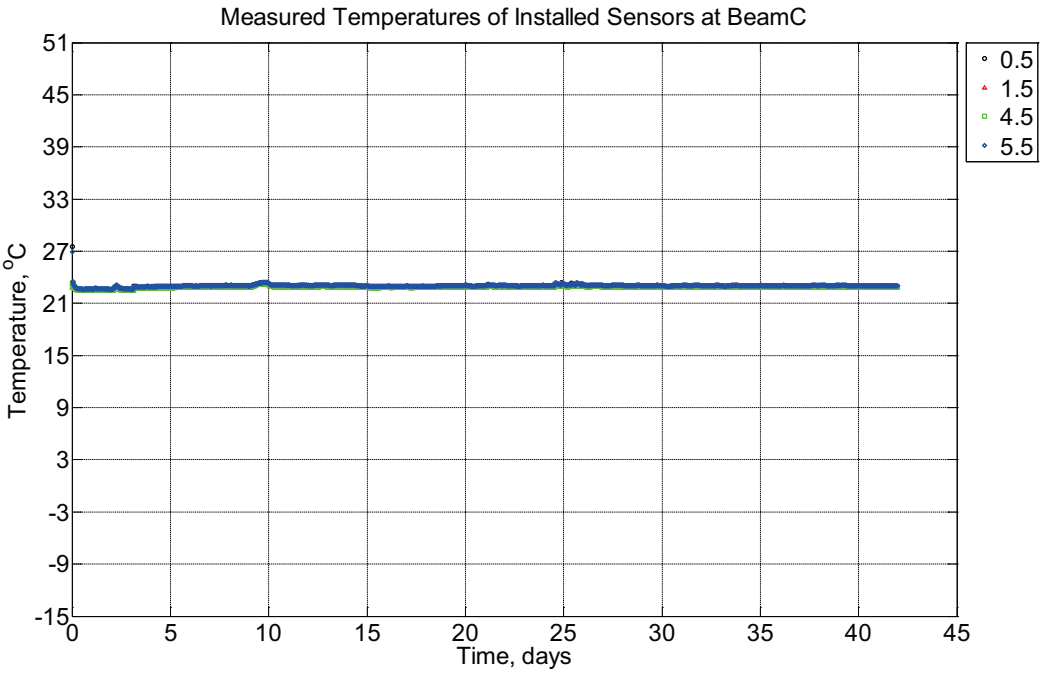

Figure B-248 Measured temperature at depths of 0.5 inches (12.7 mm), 1.5 inches (38.1 mm), 4.5 inches (114.3 mm), and 5.5 inches (139.7 mm) from the surface of a modulus of rupture beam (labeled C) located inside an environmentally controlled room (50% RH, 23°C) between July 29, 2014, through September 9, 2014.

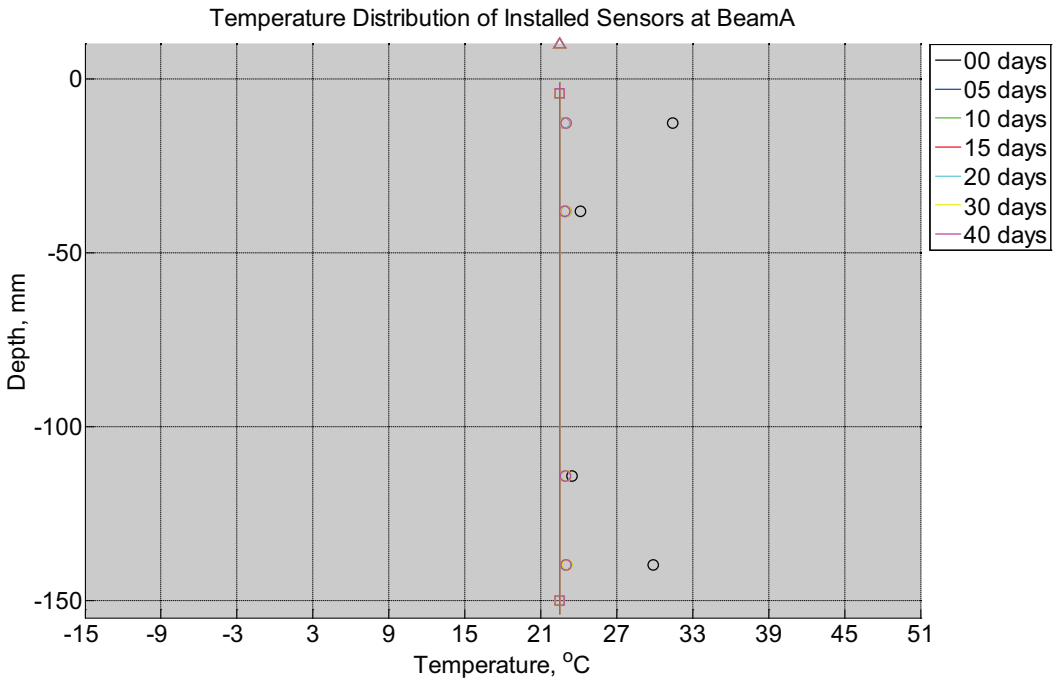

Figure B-249 Measured (markers) and modeled (continuous line) temperature profile distribution as a function of depth inside modulus of rupture beam (labeled A) located inside an environmentally controlled room (50% RH, 23ºC) between July 29, 2014, through September 9, 2014. Triangular markers denote temperature value from control panel, square markers denote measured temperature values from ambient sensors, and circular markers denote measured temperature values inside concrete.

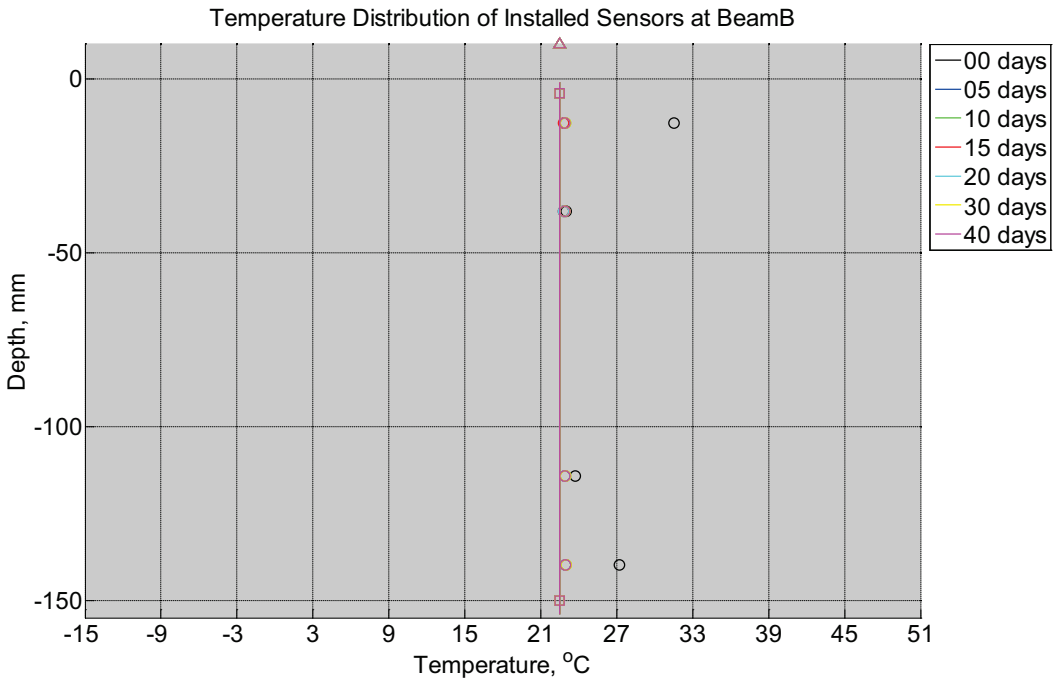

Figure B-250 Measured (markers) and modeled (continuous line) temperature profile distribution as a function of depth inside modulus of rupture beam (labeled B) located inside an environmentally controlled room (50% RH, 23ºC) between July 29, 2014, through September 9, 2014. Triangular markers denote temperature value from control panel, square markers denote measured temperature values from ambient sensors, and circular markers denote measured temperature values inside concrete.

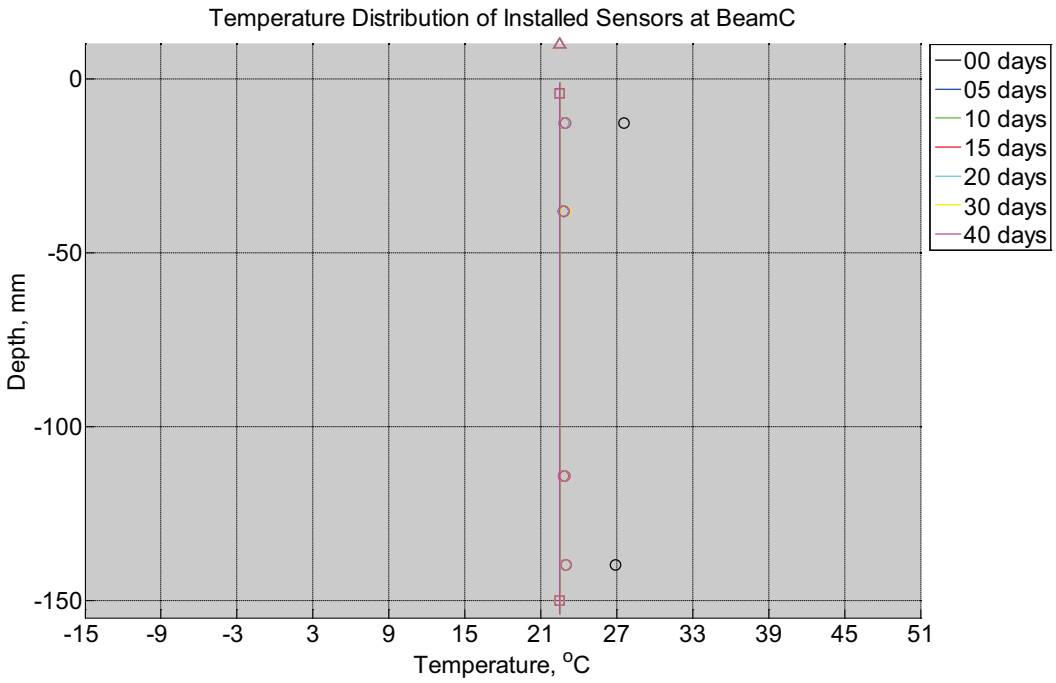

Figure B-251 Measured (markers) and modeled (continuous line) temperature profile distribution as a function of depth inside modulus of rupture beam (labeled C) located inside an environmentally controlled room (50% RH, 23ºC) between July 29, 2014, through September 9, 2014. Triangular markers denote temperature value from control panel, square markers denote measured temperature values from ambient sensors, and circular markers denote measured temperature values inside concrete.

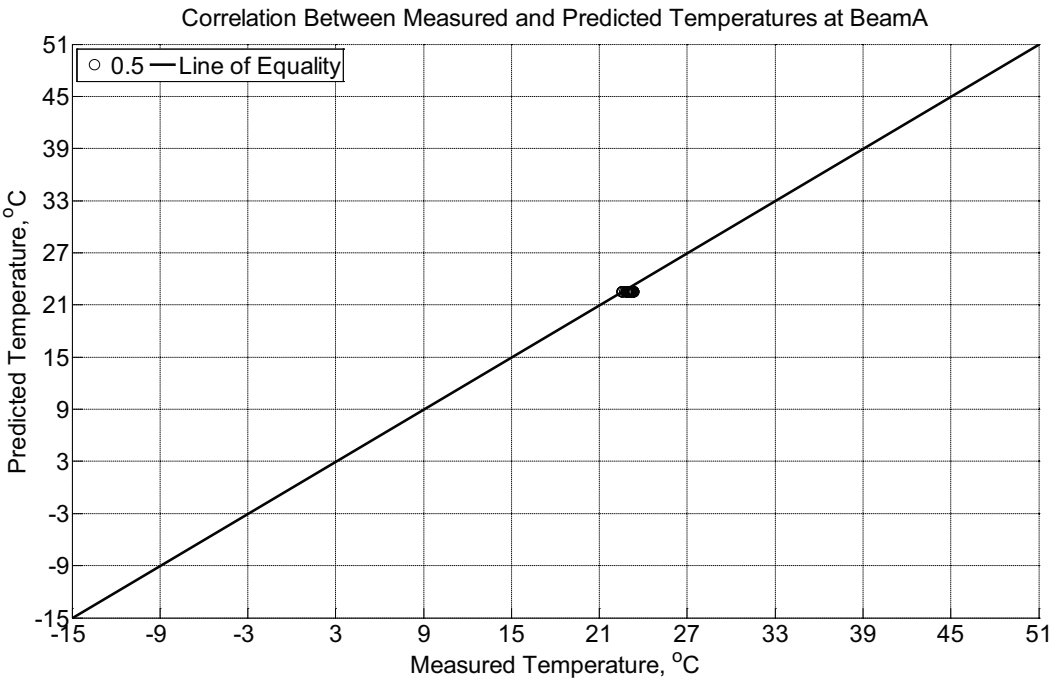

Figure B-252 Correlation between measured and predicted temperature values 0.5 inches (12.7 mm) from the surface of a modulus of rupture beam (labeled A) located inside an environmentally controlled room (50% RH, 23°C) between July 29, 2014, through September 9, 2014.

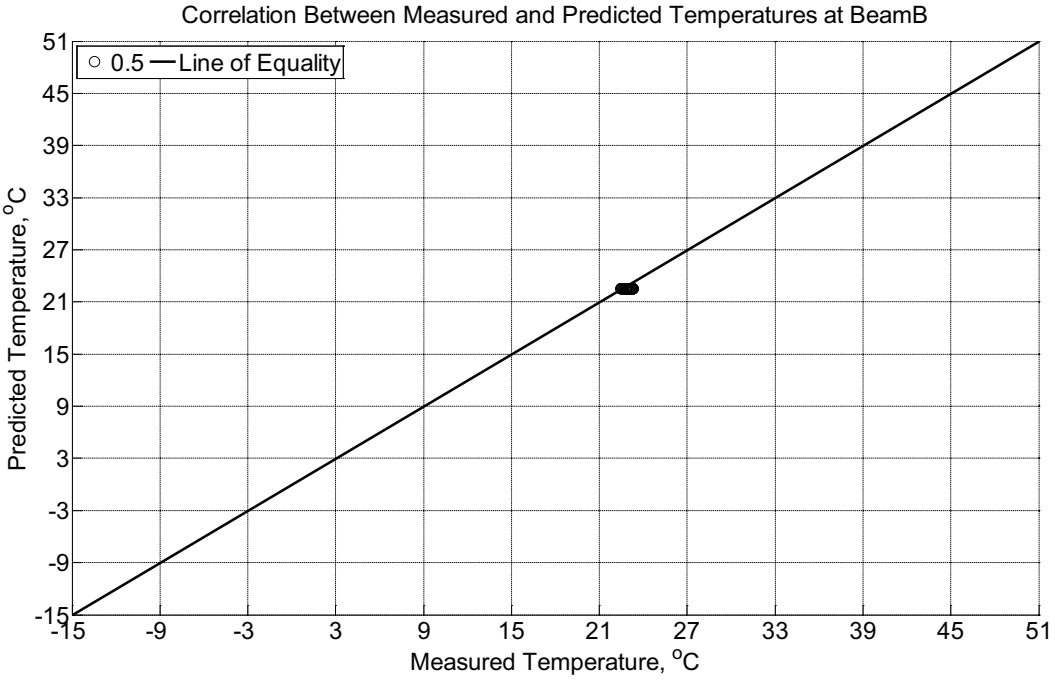

Figure B-253 Correlation between measured and predicted temperature values 0.5 inches (12.7 mm) from the surface of a modulus of rupture beam (labeled B) located inside an

environmentally controlled room (50% RH, 23°C) between July 29, 2014, through September 9, 2014.

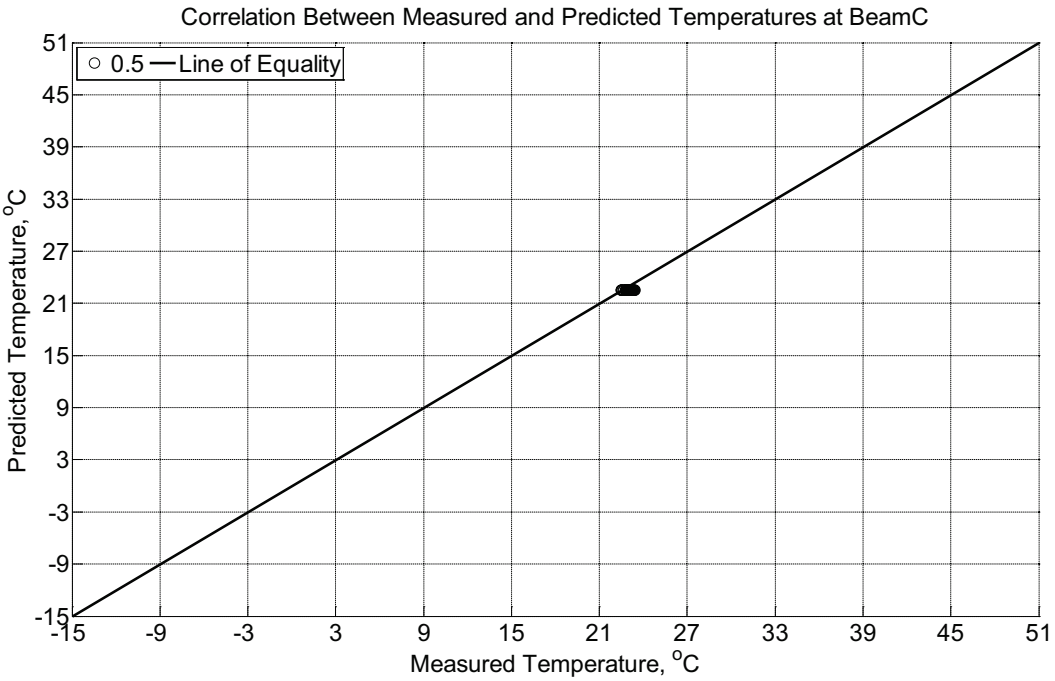

Figure B-254 Correlation between measured and predicted temperature values 0.5 inches (12.7 mm) from the surface of a modulus of rupture beam (labeled C) located inside an environmentally controlled room (50% RH, 23°C) between July 29, 2014, through September 9, 2014.

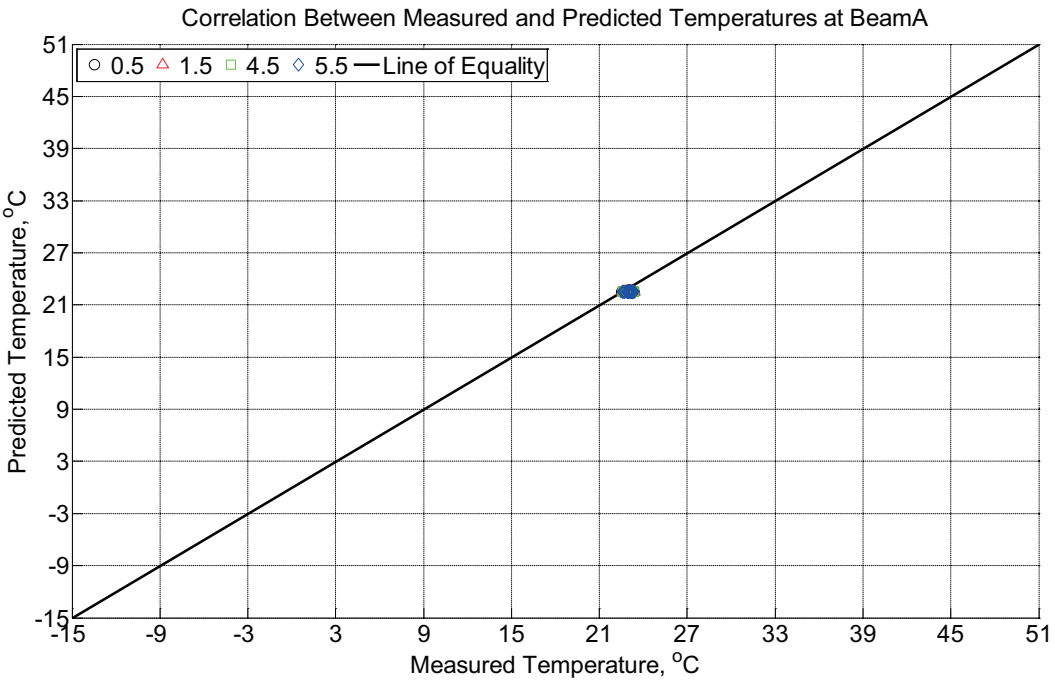

Figure B-255 Correlation between measured and predicted temperature values 0.5 inches (12.7 mm), 1.5 inches (38.1 mm), 4.5 inches (114.3 mm), and 5.5 inches (139.7 mm) from the surface of a modulus of rupture beam (labeled A) located inside an environmentally controlled room (50% RH, 23ºC) between July 29, 2014, through September 9, 2014.

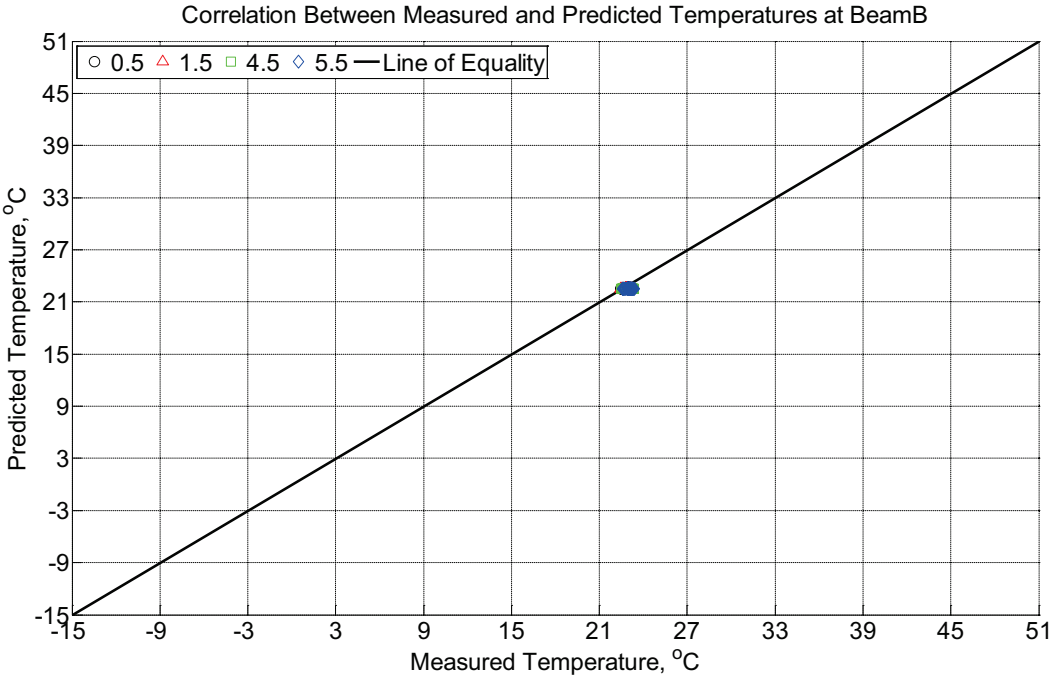

Figure B-256 Correlation between measured and predicted temperature values 0.5 inches (12.7 mm), 1.5 inches (38.1 mm), 4.5 inches (114.3 mm), and 5.5 inches (139.7 mm) from the

surface of a modulus of rupture beam (labeled B) located inside an environmentally controlled room (50% RH, 23°C) between July 29, 2014, through September 9, 2014.

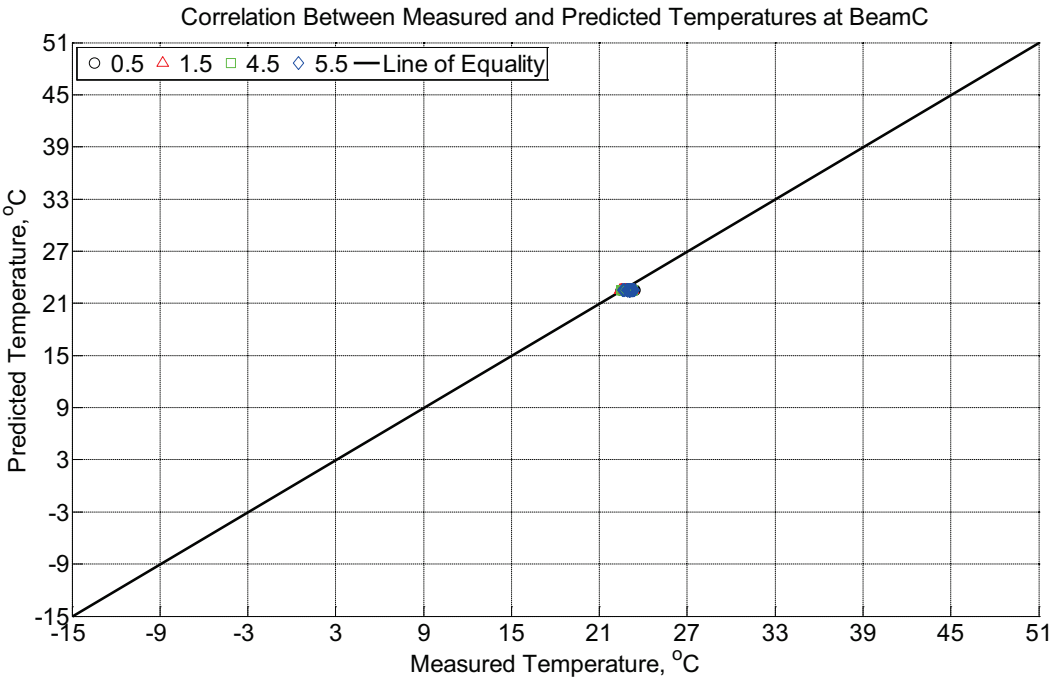

Figure B-257 Correlation between measured and predicted temperature values 0.5 inches (12.7 mm), 1.5 inches (38.1 mm), 4.5 inches (114.3 mm), and 5.5 inches (139.7 mm) from the surface of a modulus of rupture beam (labeled C) located inside an environmentally controlled room (50% RH, 23°C) between July 29, 2014, through September 9, 2014.

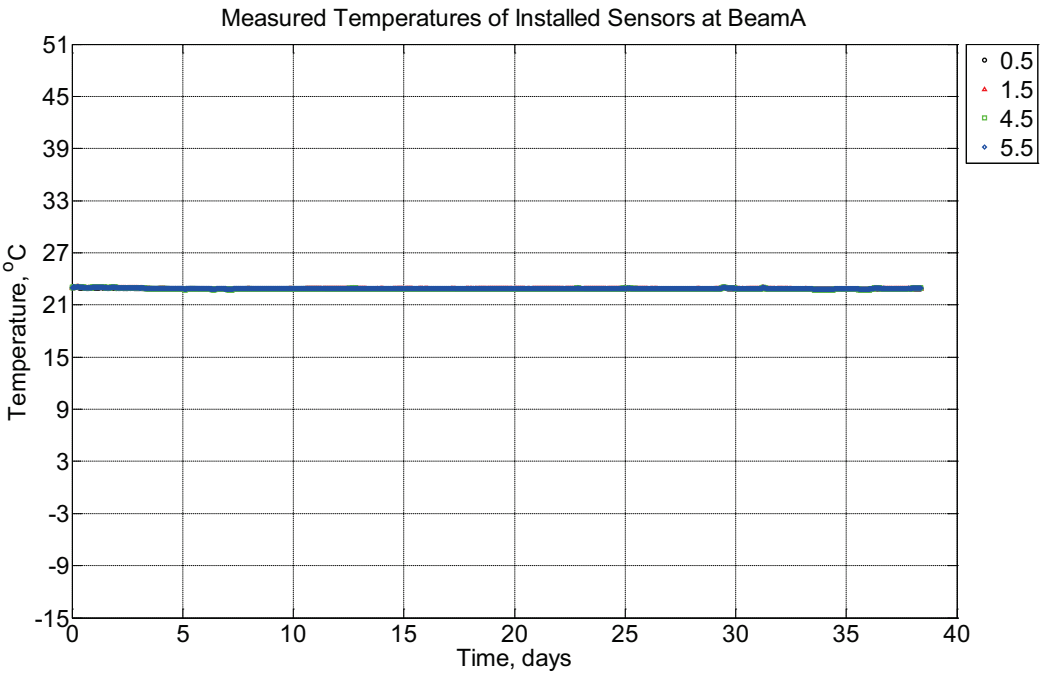

Figure B-258 Measured temperature at depths of 0.5 inches (12.7 mm), 1.5 inches (38.1 mm), 4.5 inches (114.3 mm), and 5.5 inches (139.7 mm) from the surface of a modulus of rupture beam (labeled A) located inside an environmentally controlled room (50% RH, 23ºC) between September 9, 2014, through October 17, 2014.

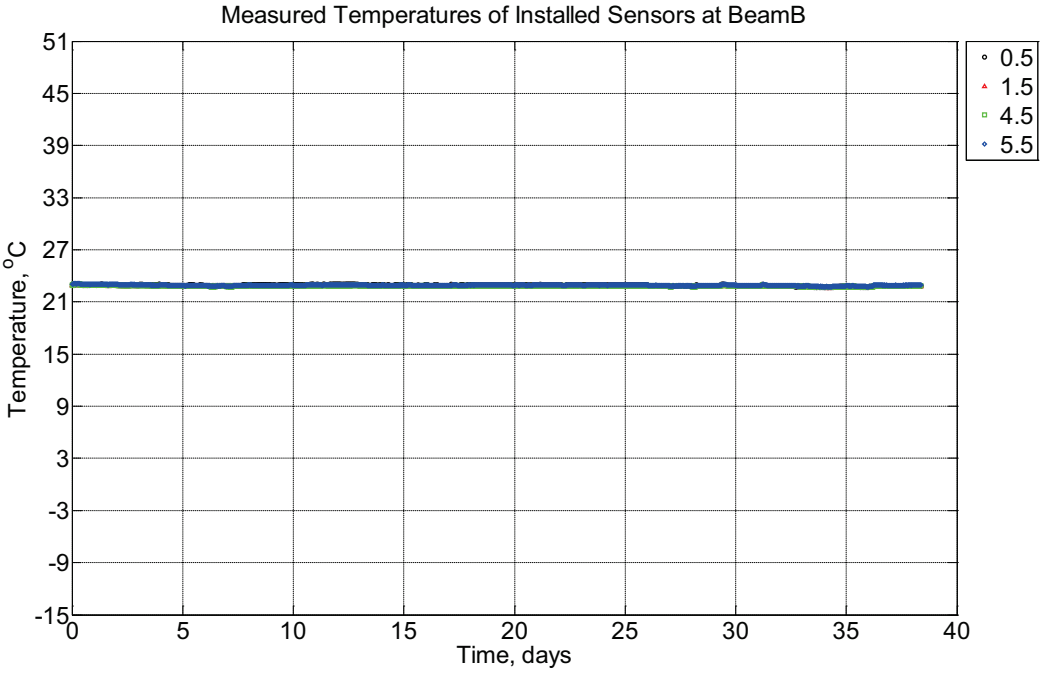

Figure B-259 Measured temperature at depths of 0.5 inches (12.7 mm), 1.5 inches (38.1 mm), 4.5 inches (114.3 mm), and 5.5 inches (139.7 mm) from the surface of a modulus of

rupture beam (labeled B) located inside an environmentally controlled room (50% RH, 23°C) between September 9, 2014, through October 17, 2014.

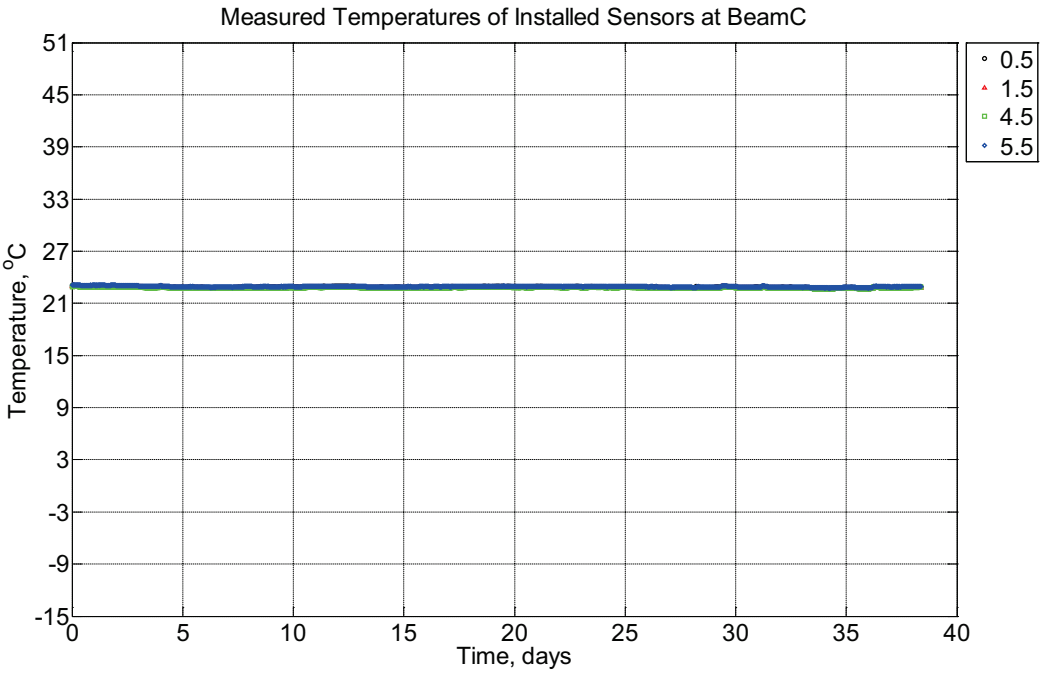

Figure B-260 Measured temperature at depths of 0.5 inches (12.7 mm), 1.5 inches (38.1 mm), 4.5 inches (114.3 mm), and 5.5 inches (139.7 mm) from the surface of a modulus of rupture beam (labeled C) located inside an environmentally controlled room (50% RH, 23°C) between September 9, 2014, through October 17, 2014.

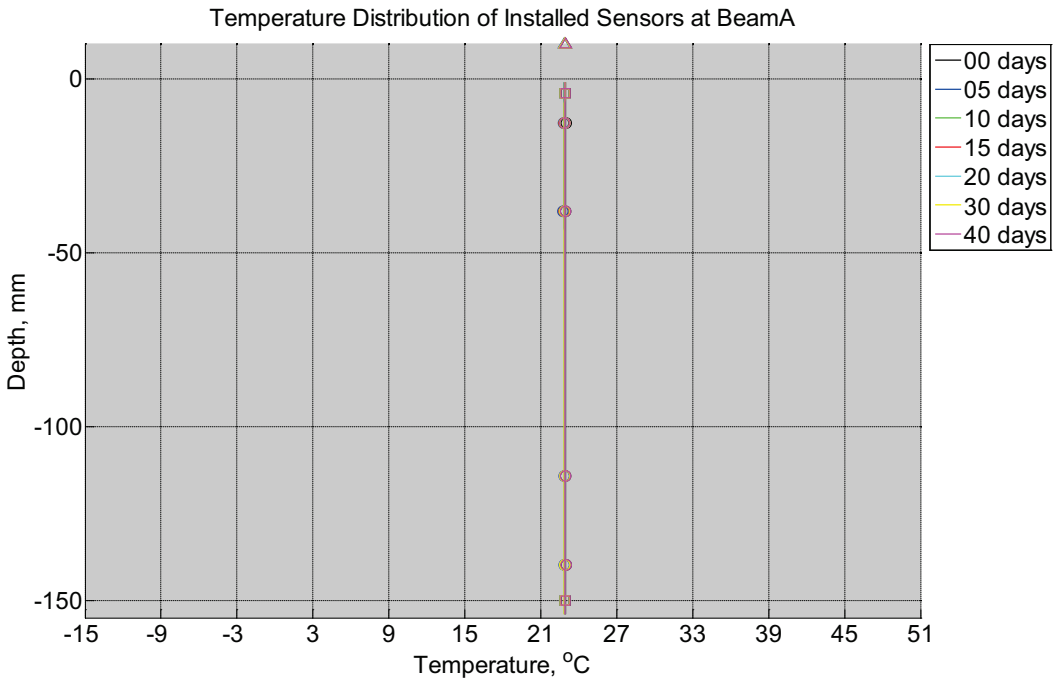

Figure B-261 Measured (markers) and modeled (continuous line) temperature profile distribution as a function of depth inside modulus of rupture beam (labeled A) located inside an environmentally controlled room (50% RH, 23°C) between September 9, 2014, through October 17, 2014. Triangular markers denote temperature value from control panel, square markers denote measured temperature values from ambient sensors, and circular markers denote measured temperature values inside concrete.

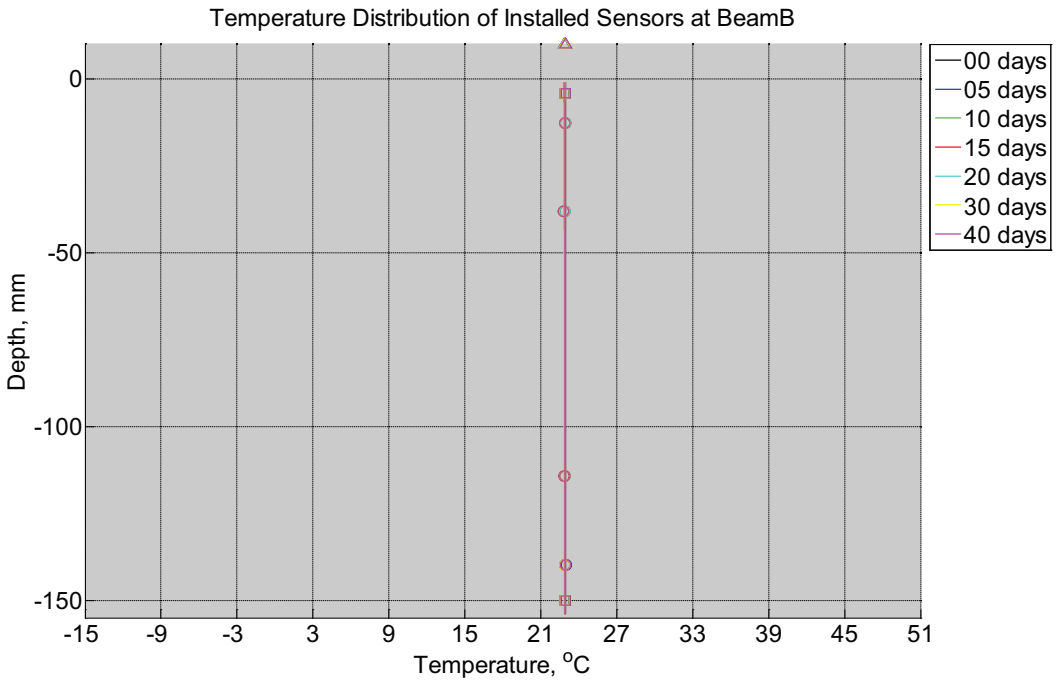

Figure B-262 Measured (markers) and modeled (continuous line) temperature profile distribution as a function of depth inside modulus of rupture beam (labeled B) located inside an environmentally controlled room (50% RH, 23°C) between September 9, 2014, through October 17, 2014. Triangular markers denote temperature value from control panel, square markers denote measured temperature values from ambient sensors, and circular markers denote measured temperature values inside concrete.

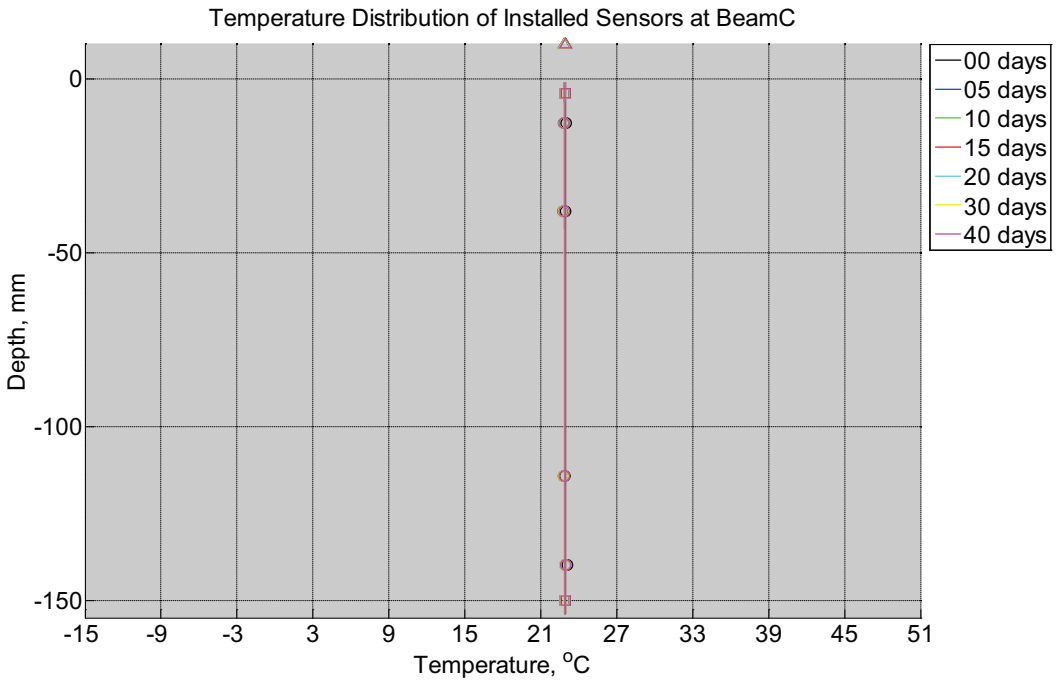

Figure B-263 Measured (markers) and modeled (continuous line) temperature profile distribution as a function of depth inside modulus of rupture beam (labeled C) located inside an environmentally controlled room (50% RH, 23°C) between September 9, 2014, through October 17, 2014. Triangular markers denote temperature value from control panel, square markers denote measured temperature values from ambient sensors, and circular markers denote measured temperature values inside concrete.

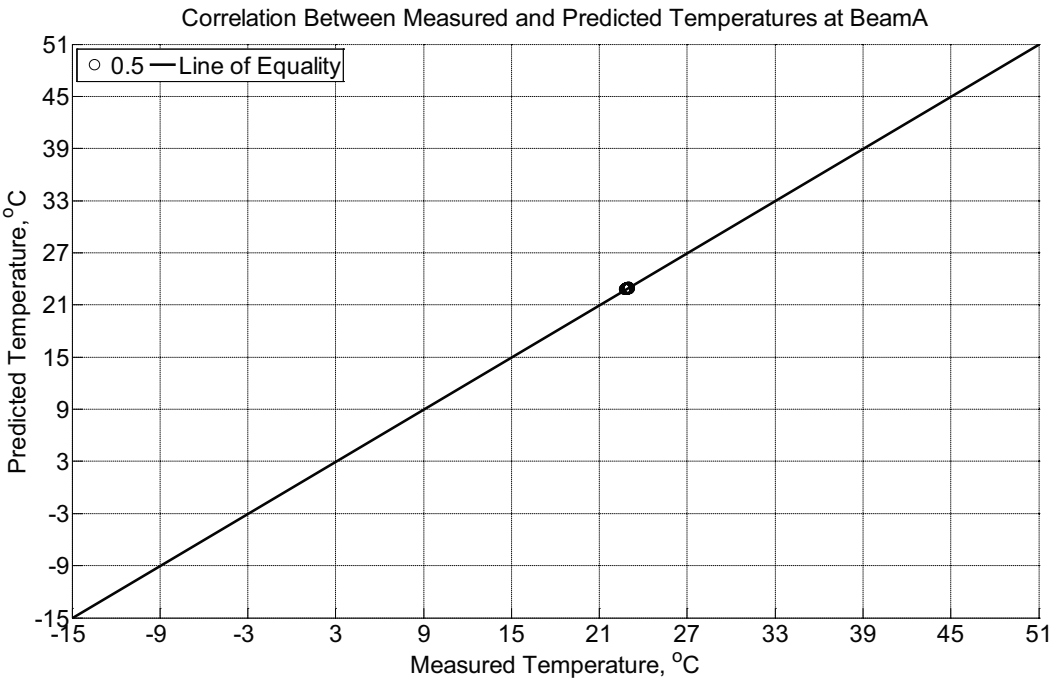

Figure B-264 Correlation between measured and predicted temperature values 0.5 inches (12.7 mm) from the surface of a modulus of rupture beam (labeled A) located inside an environmentally controlled room (50% RH, 23ºC) between September 9, 2014, through October 17, 2014.

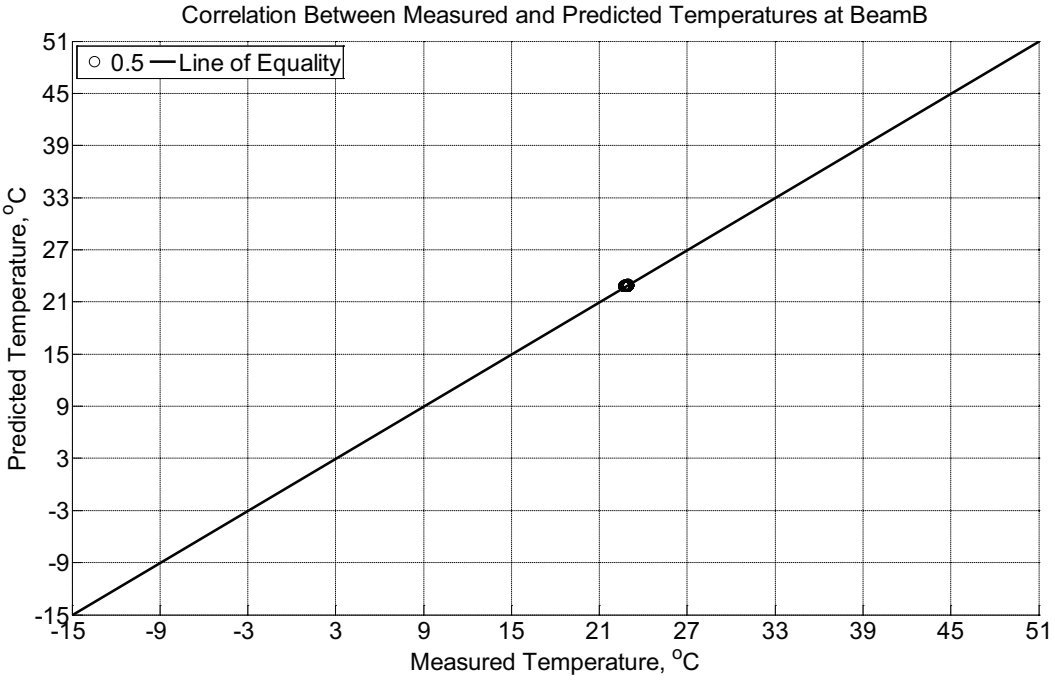

Figure B-265 Correlation between measured and predicted temperature values 0.5 inches (12.7 mm) from the surface of a modulus of rupture beam (labeled B) located inside an

environmentally controlled room (50% RH, 23°C) between September 9, 2014, through October 17, 2014.

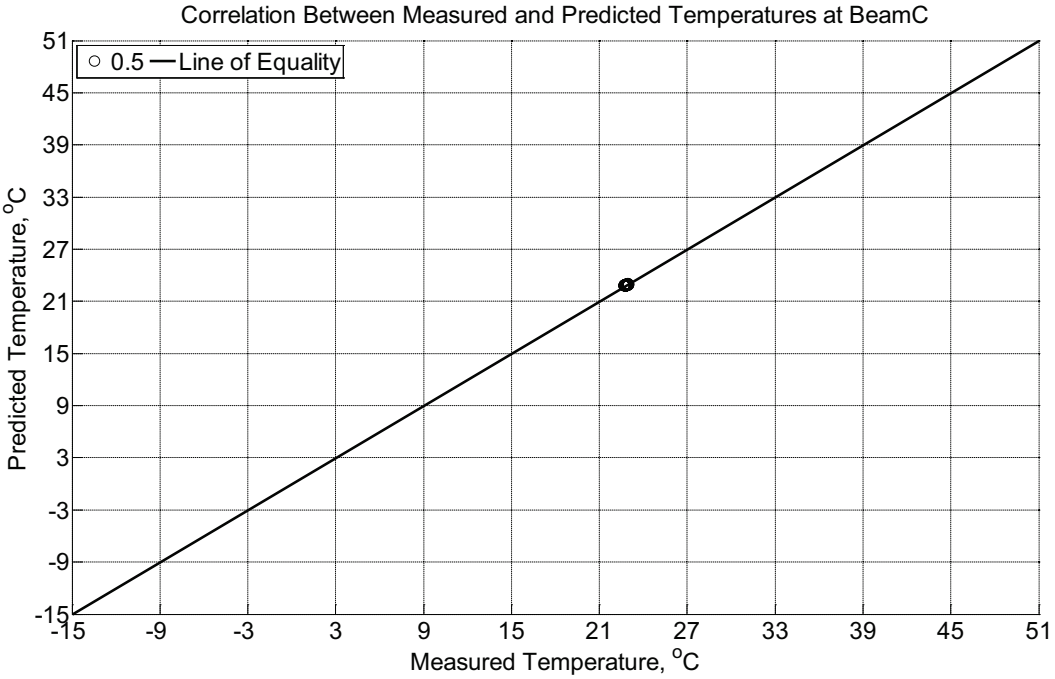

Figure B-266 Correlation between measured and predicted temperature values 0.5 inches (12.7 mm) from the surface of a modulus of rupture beam (labeled C) located inside an environmentally controlled room (50% RH, 23°C) between September 9, 2014, through October 17, 2014.

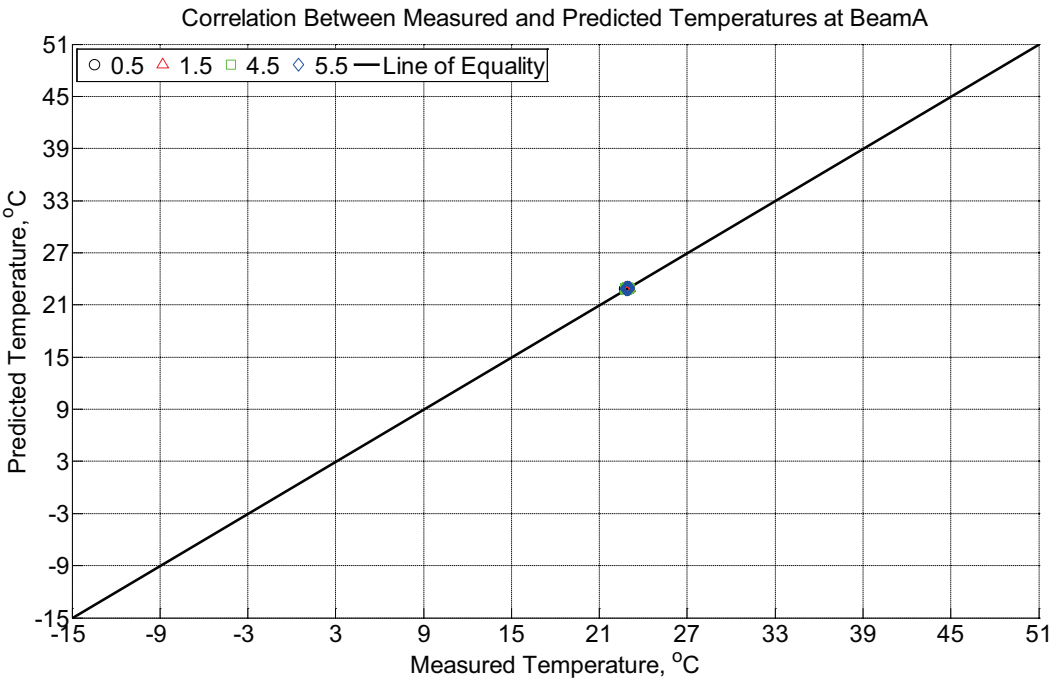

Figure B-267 Correlation between measured and predicted temperature values 0.5 inches (12.7 mm), 1.5 inches (38.1 mm), 4.5 inches (114.3 mm), and 5.5 inches (139.7 mm) from the surface of a modulus of rupture beam (labeled A) located inside an environmentally controlled room (50% RH, 23ºC) between September 9, 2014, through October 17, 2014.

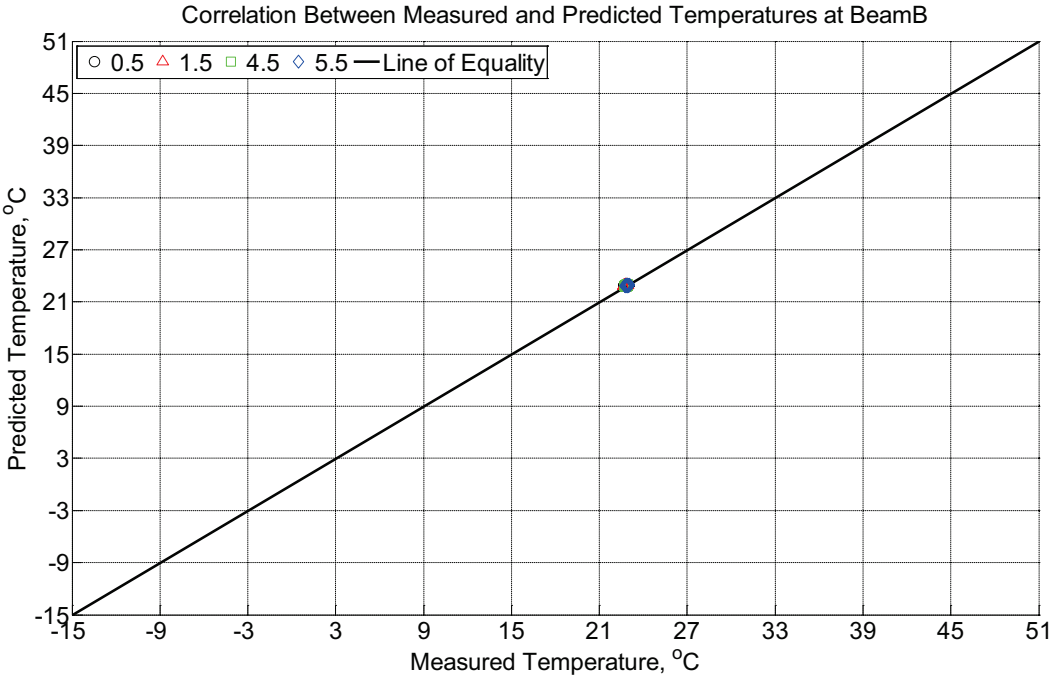

Figure B-268 Correlation between measured and predicted temperature values 0.5 inches (12.7 mm), 1.5 inches (38.1 mm), 4.5 inches (114.3 mm), and 5.5 inches (139.7 mm) from the

surface of a modulus of rupture beam (labeled B) located inside an environmentally controlled room (50% RH, 23°C) between September 9, 2014, through October 17, 2014.

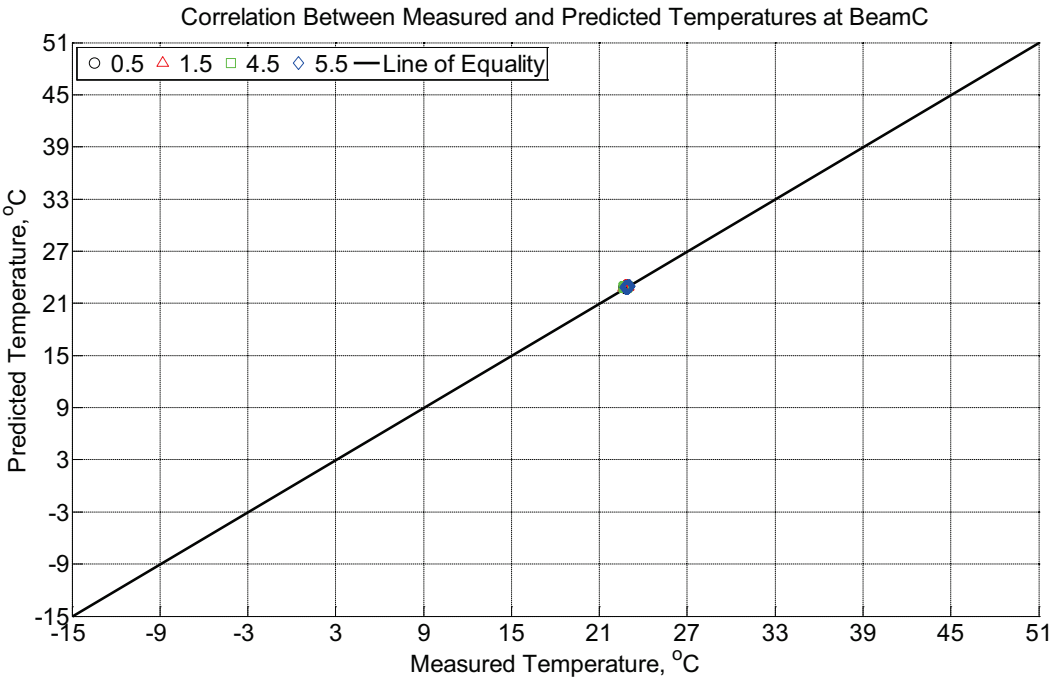

Figure B-269 Correlation between measured and predicted temperature values 0.5 inches (12.7 mm), 1.5 inches (38.1 mm), 4.5 inches (114.3 mm), and 5.5 inches (139.7 mm) from the surface of a modulus of rupture beam (labeled C) located inside an environmentally controlled room (50% RH, 23°C) between September 9, 2014, through October 17, 2014.

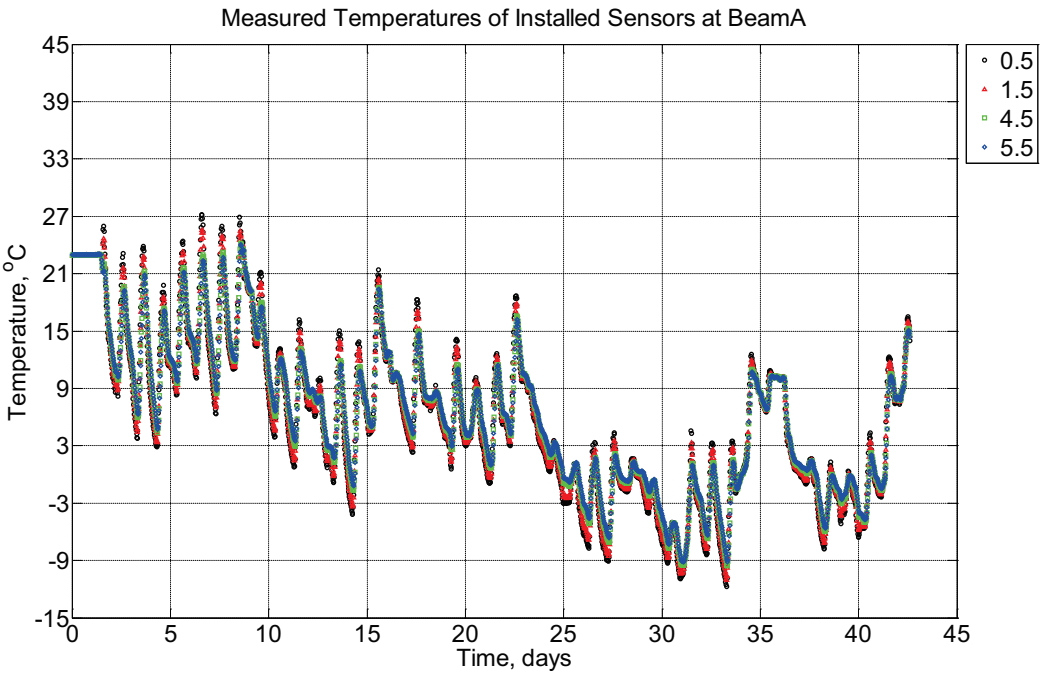

Figure B-270 Measured temperature at depths of 0.5 inches (12.7 mm), 1.5 inches (38.1 mm), 4.5 inches (114.3 mm), and 5.5 inches (139.7 mm) from the surface of a modulus of rupture beam (labeled A) installed in ballast in Rantoul, IL, between October 19, 2014, through November 30, 2014.

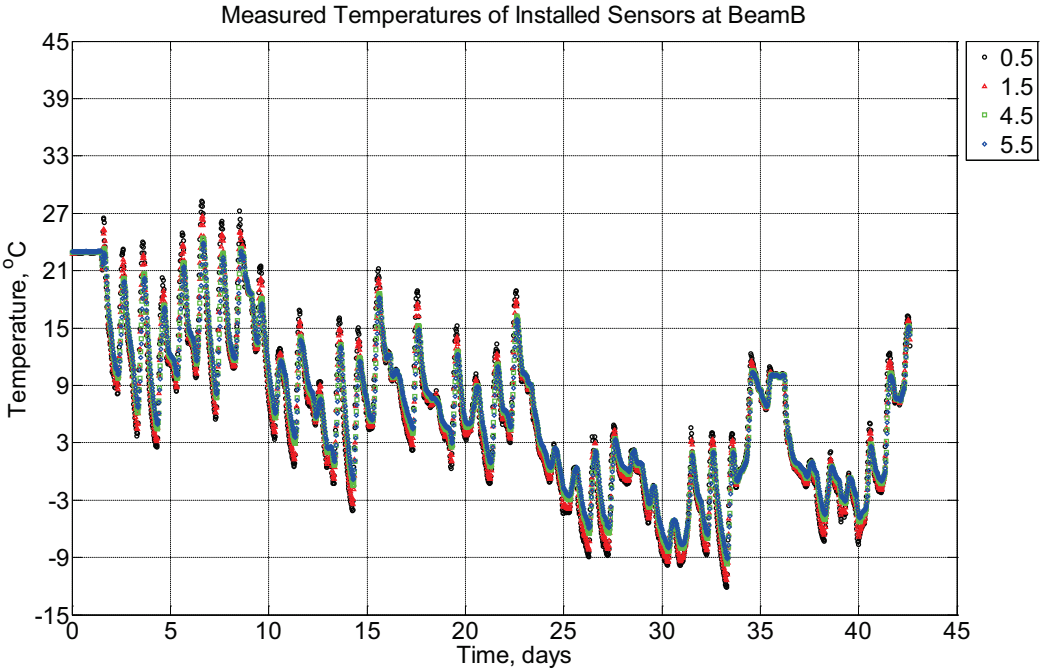

Figure B-271 Measured temperature at depths of 0.5 inches (12.7 mm), 1.5 inches (38.1 mm), 4.5 inches (114.3 mm), and 5.5 inches (139.7 mm) from the surface of a modulus of

rupture beam (labeled B) installed in ballast in Rantoul, IL, between October 19, 2014, through November 30, 2014.

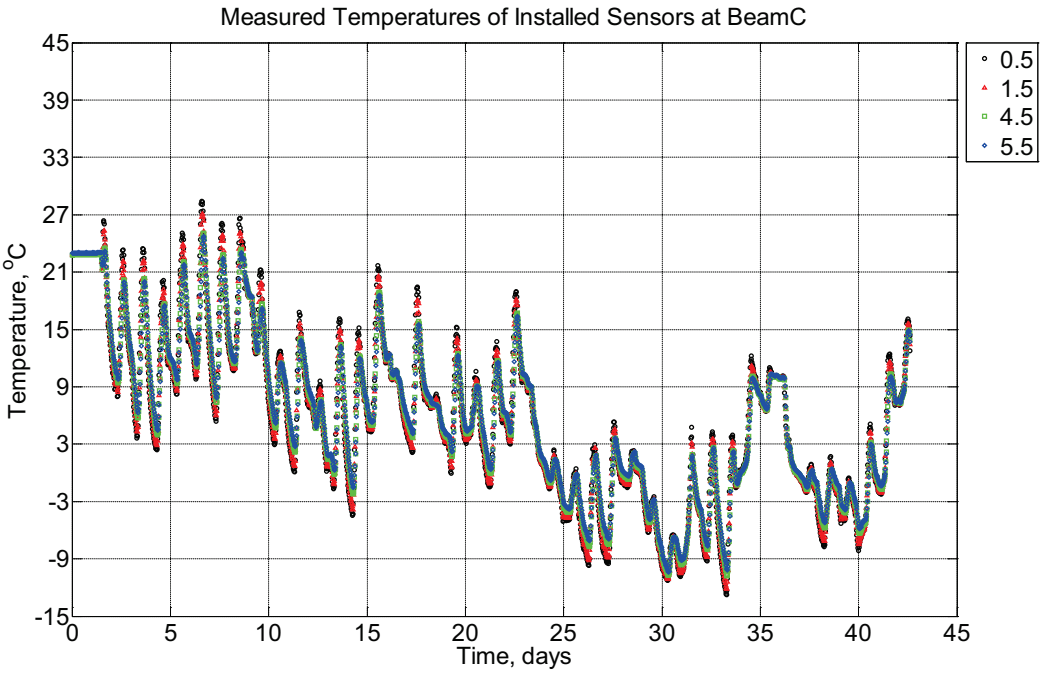

Figure B-272 Measured temperature at depths of 0.5 inches (12.7 mm), 1.5 inches (38.1 mm), 4.5 inches (114.3 mm), and 5.5 inches (139.7 mm) from the surface of a modulus of rupture beam (labeled C) installed in ballast in Rantoul, IL, between October 19, 2014, through November 30, 2014.

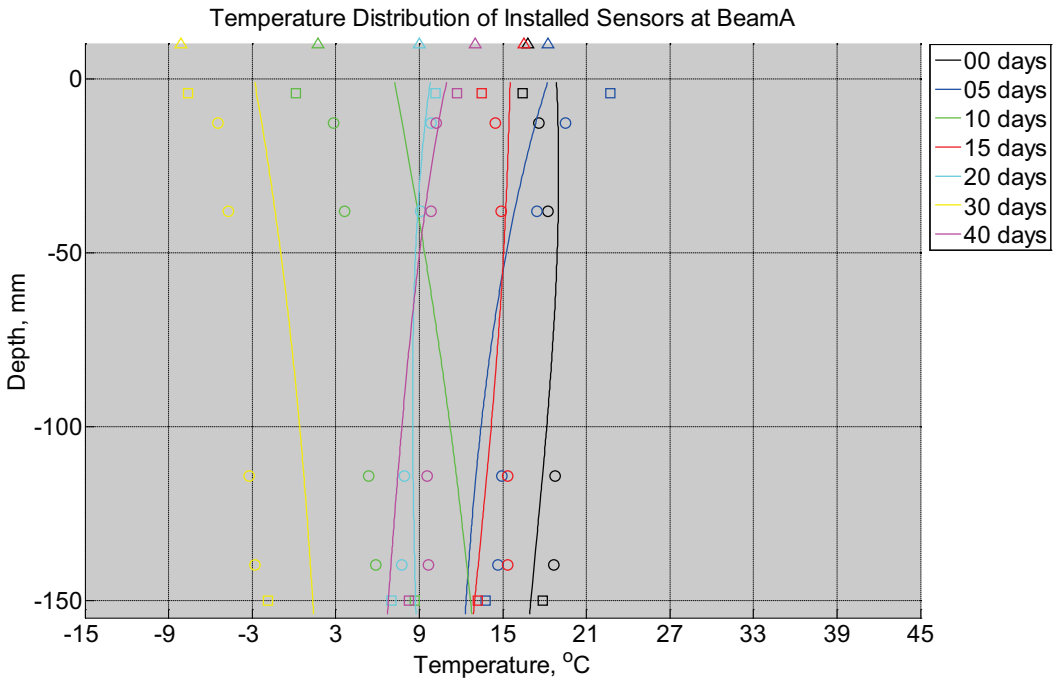

Figure B-273 Measured (markers) and modeled (continuous line) temperature profile distribution as a function of depth inside modulus of rupture beam (labeled A) installed in ballast in Rantoul, IL, between October 19, 2014, through November 30, 2014. Triangular markers denote temperature value from KTIP weather station, square markers denote measured temperature values from ballast, and circular markers denote measured temperature values inside concrete.

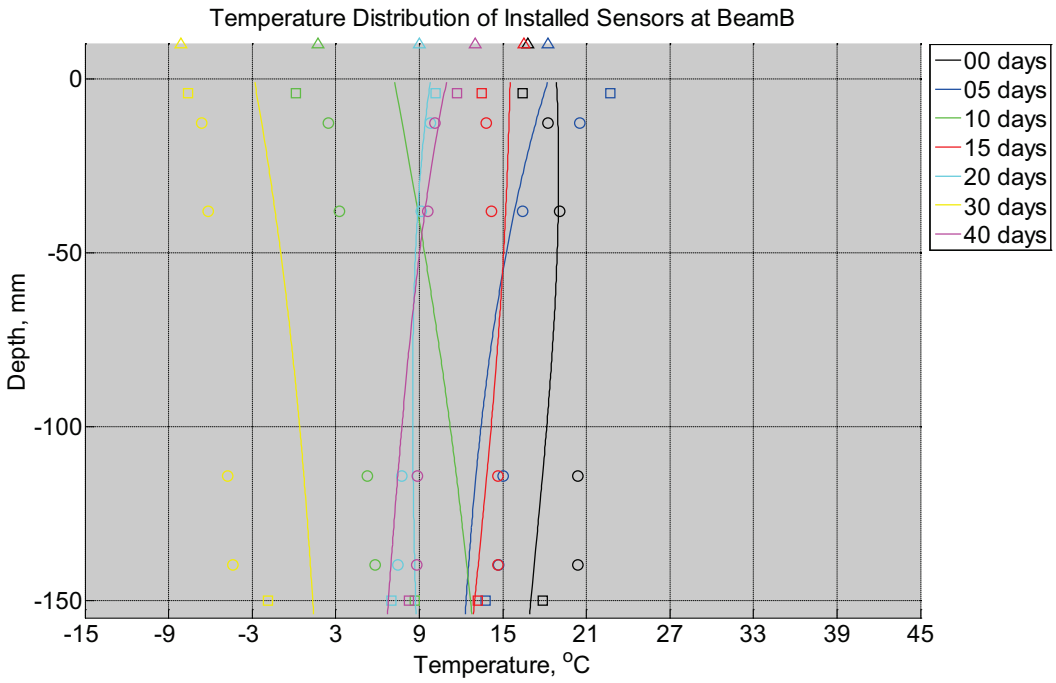

Figure B-274. Measured (markers) and modeled (continuous line) temperature profile distribution as a function of depth inside modulus of rupture beam (labeled B) installed in ballast in Rantoul, IL, between October 19, 2014, through November 30, 2014. Triangular markers denote temperature value from KTIP weather station, square markers denote measured temperature values from ballast, and circular markers denote measured temperature values inside concrete.

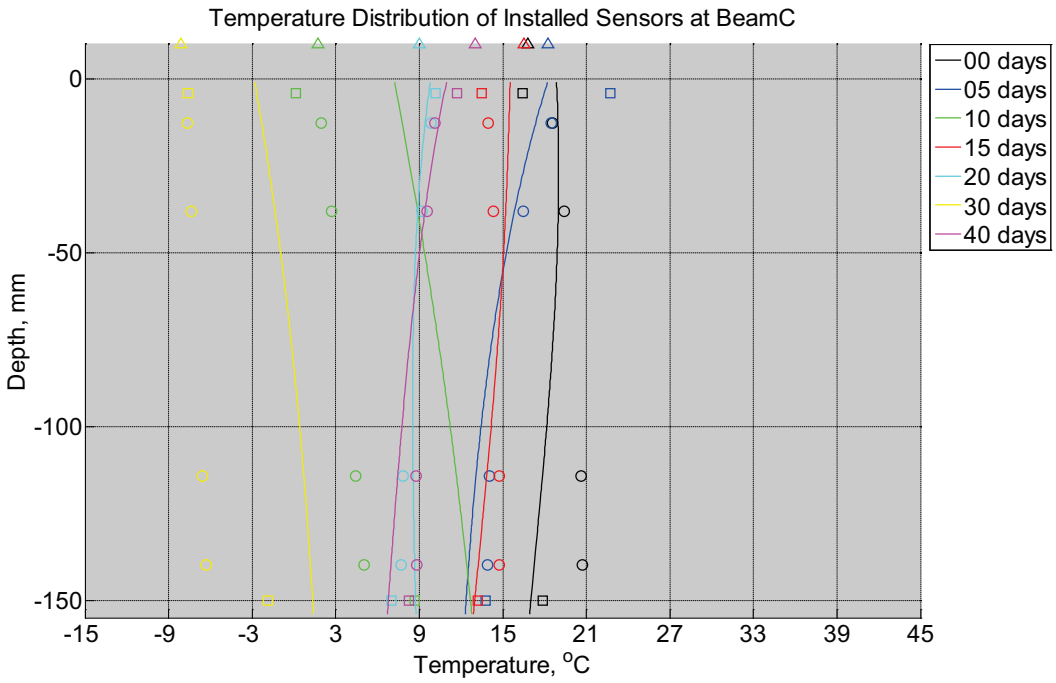

Figure B-275 Measured (markers) and modeled (continuous line) temperature profile distribution as a function of depth inside modulus of rupture beam (labeled C) installed in ballast in Rantoul, IL, between October 19, 2014, through November 30, 2014. Triangular markers denote temperature value from KTIP weather station, square markers denote measured temperature values from ballast, and circular markers denote measured temperature values inside concrete.

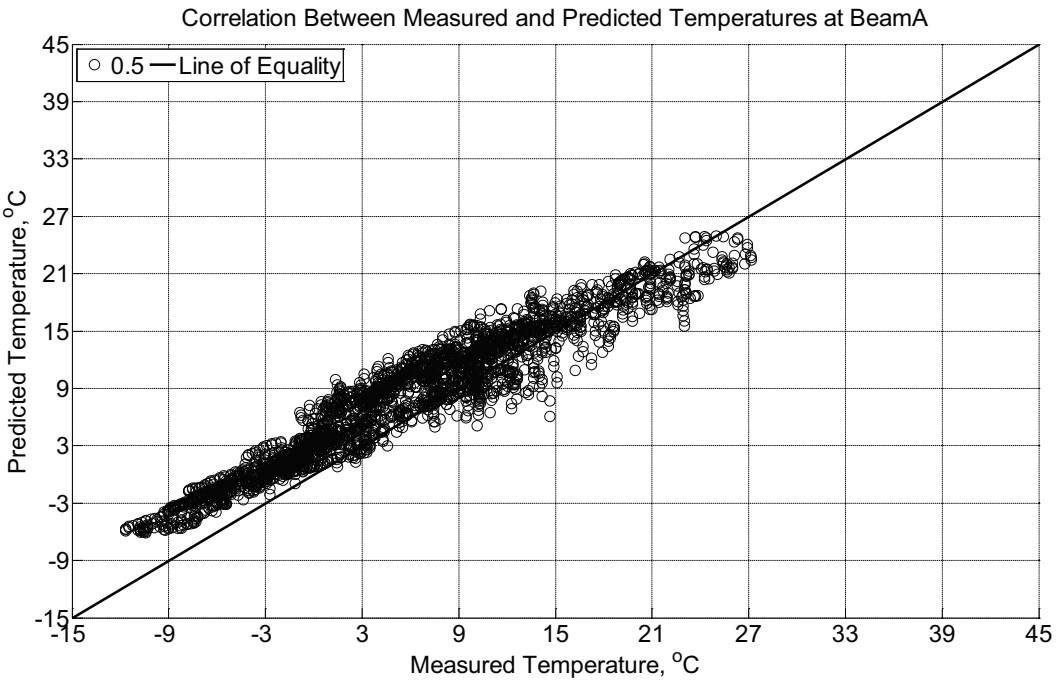

Figure B-276 Correlation between measured and predicted temperature values 0.5 inches (12.7 mm) from the surface of a modulus of rupture beam (labeled A) installed in ballast in Rantoul, IL, between October 19, 2014, through November 30, 2014.

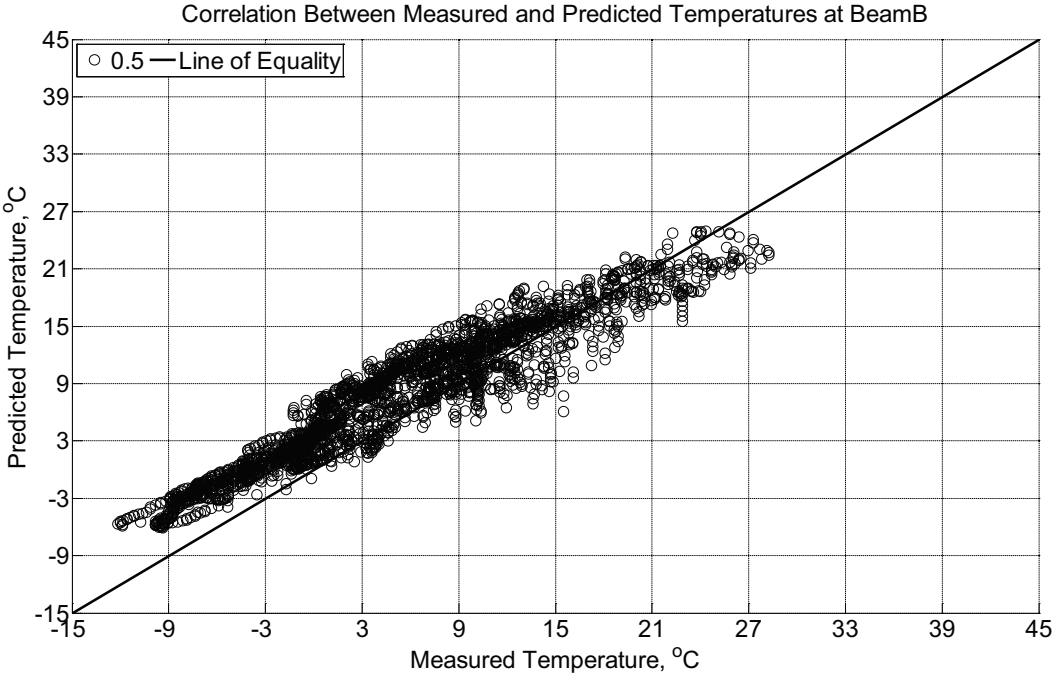

Figure B-277 Correlation between measured and predicted temperature values 0.5 inches

(12.7 mm) from the surface of a modulus of rupture beam (labeled B) installed in ballast in Rantoul, IL, between October 19, 2014, through November 30, 2014.

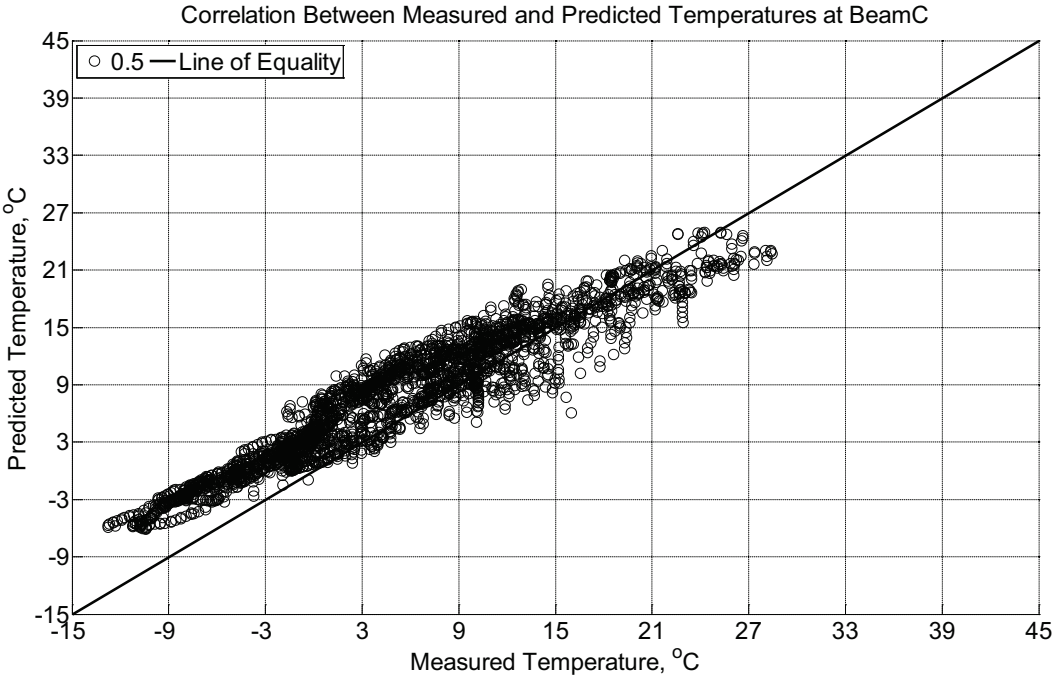

Figure B-278 Correlation between measured and predicted temperature values 0.5 inches (12.7 mm) from the surface of a modulus of rupture beam (labeled C) installed in ballast in Rantoul, IL, between October 19, 2014, through November 30, 2014.

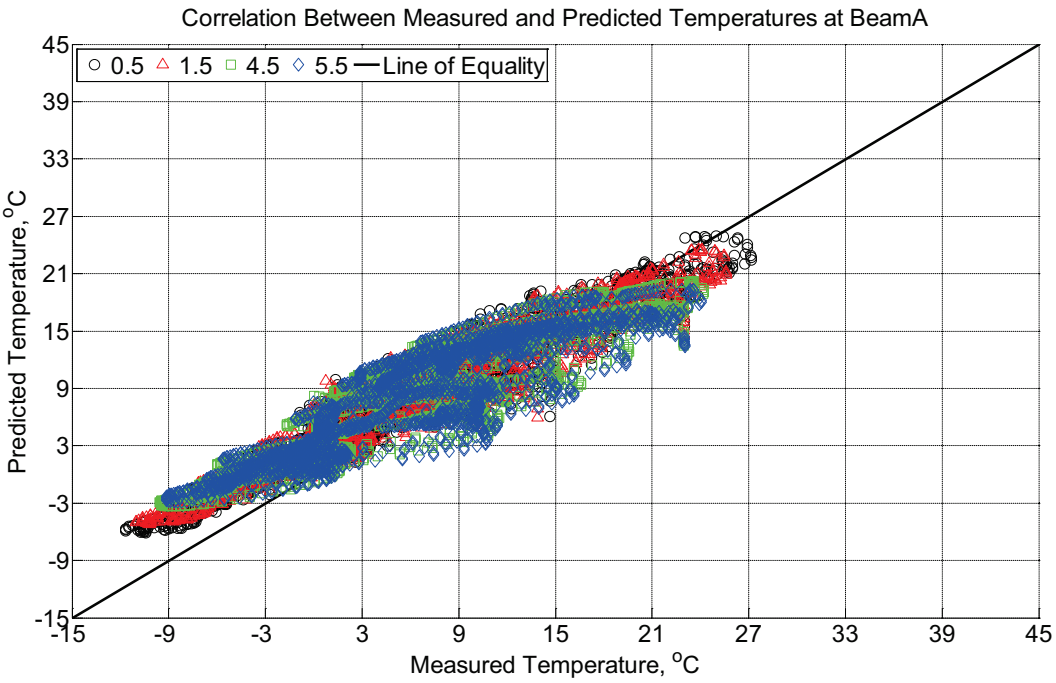

Figure B-279 Correlation between measured and predicted temperature values 0.5 inches (12.7 mm), 1.5 inches (38.1 mm), 4.5 inches (114.3 mm), and 5.5 inches (139.7 mm) from the surface of a modulus of rupture beam (labeled A) installed in ballast in Rantoul, IL, between October 19, 2014, through November 30, 2014.

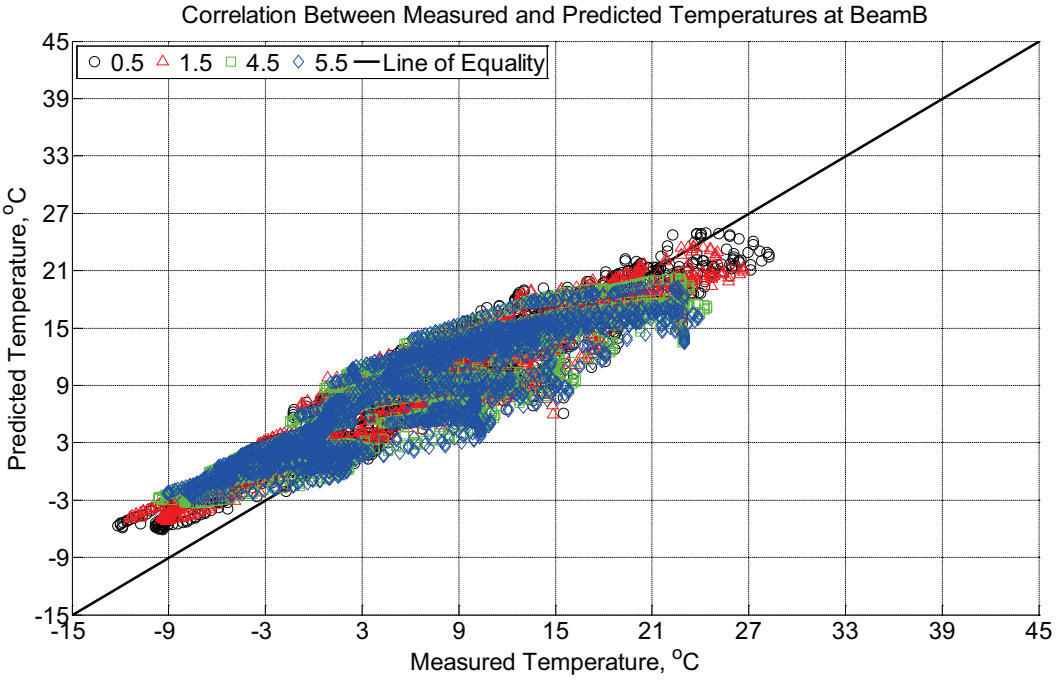

Figure B-280 Correlation between measured and predicted temperature values 0.5 inches (12.7 mm), 1.5 inches (38.1 mm), 4.5 inches (114.3 mm), and 5.5 inches (139.7 mm) from the

surface of a modulus of rupture beam (labeled B) installed in ballast in Rantoul, IL, between October 19, 2014, through November 30, 2014.

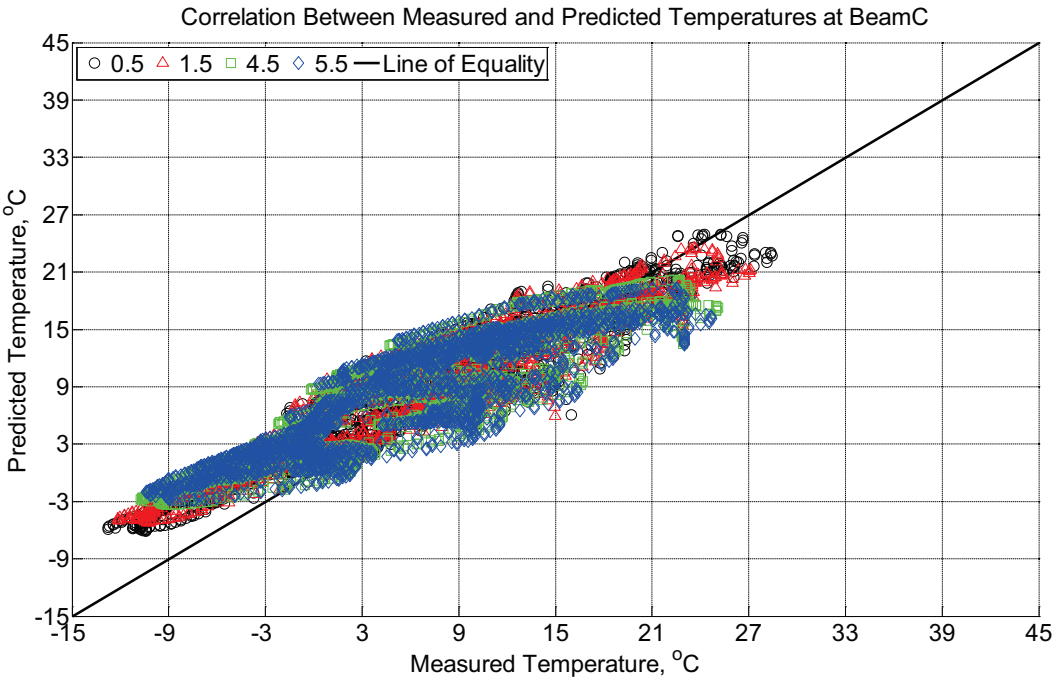

Figure B-281 Correlation between measured and predicted temperature values 0.5 inches (12.7 mm), 1.5 inches (38.1 mm), 4.5 inches (114.3 mm), and 5.5 inches (139.7 mm) from the surface of a modulus of rupture beam (labeled C) installed in ballast in Rantoul, IL, between October 19, 2014, through November 30, 2014.

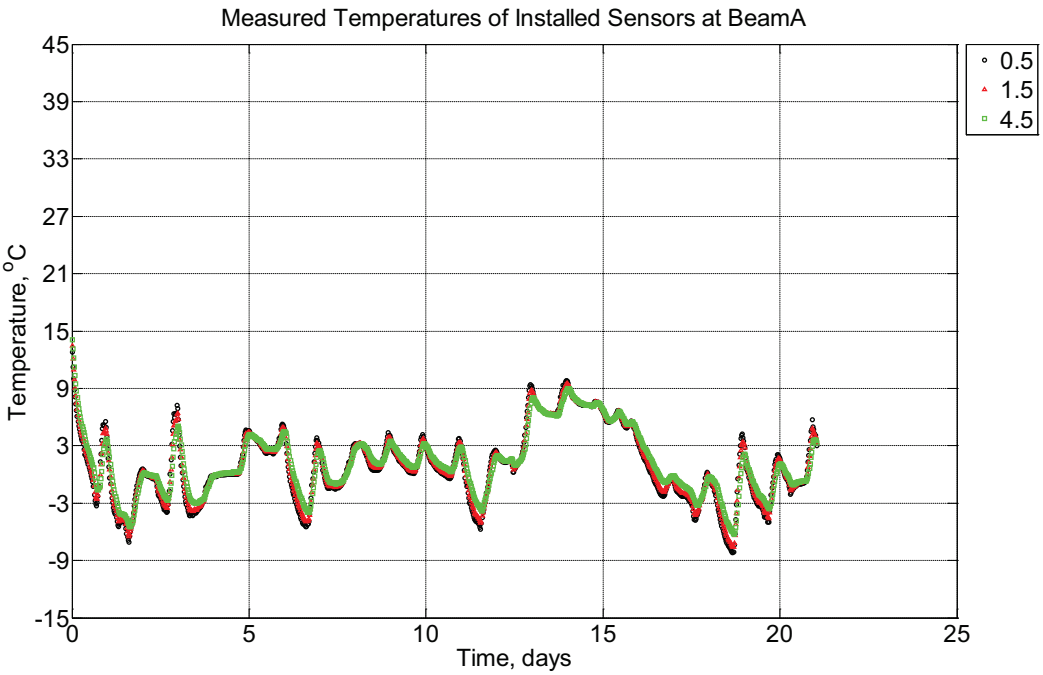

Figure B-282 Measured temperature at depths of 0.5 inches (12.7 mm), 1.5 inches (38.1 mm), and 4.5 inches (114.3 mm) from the surface of a modulus of rupture beam (labeled A) installed in ballast in Rantoul, IL, between November 30, 2014, through December 21, 2014.

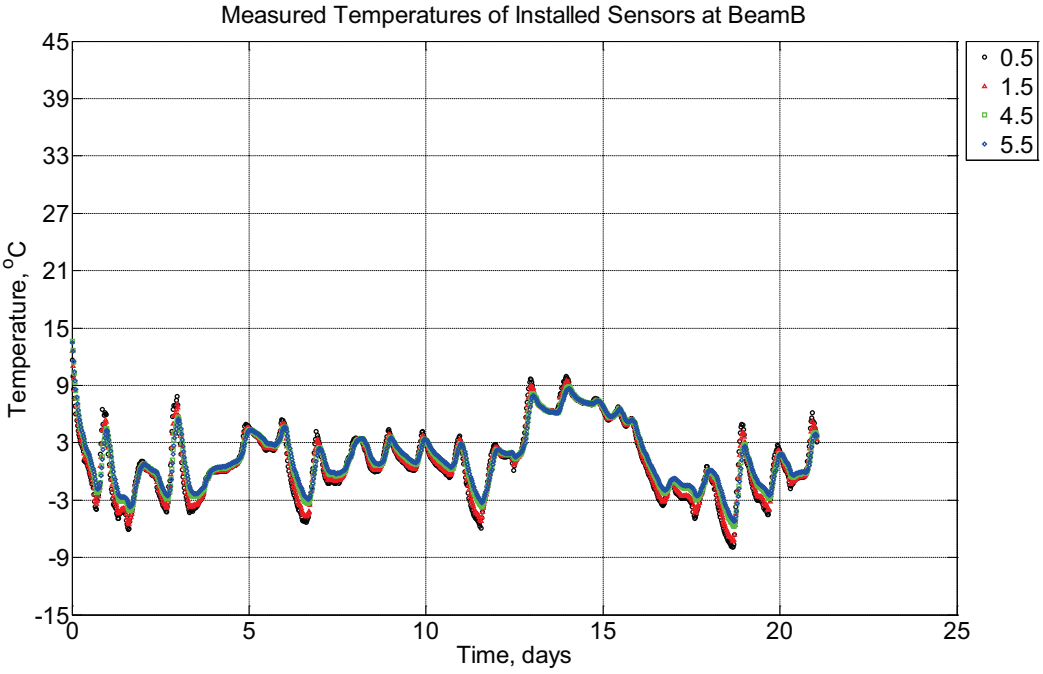

Figure B-283 Measured temperature at depths of 0.5 inches (12.7 mm), 1.5 inches (38.1 mm), 4.5 inches (114.3 mm), and 5.5 inches (139.7 mm) from the surface of a modulus of

rupture beam (labeled B) installed in ballast in Rantoul, IL, between November 30, 2014, through December 21, 2014.

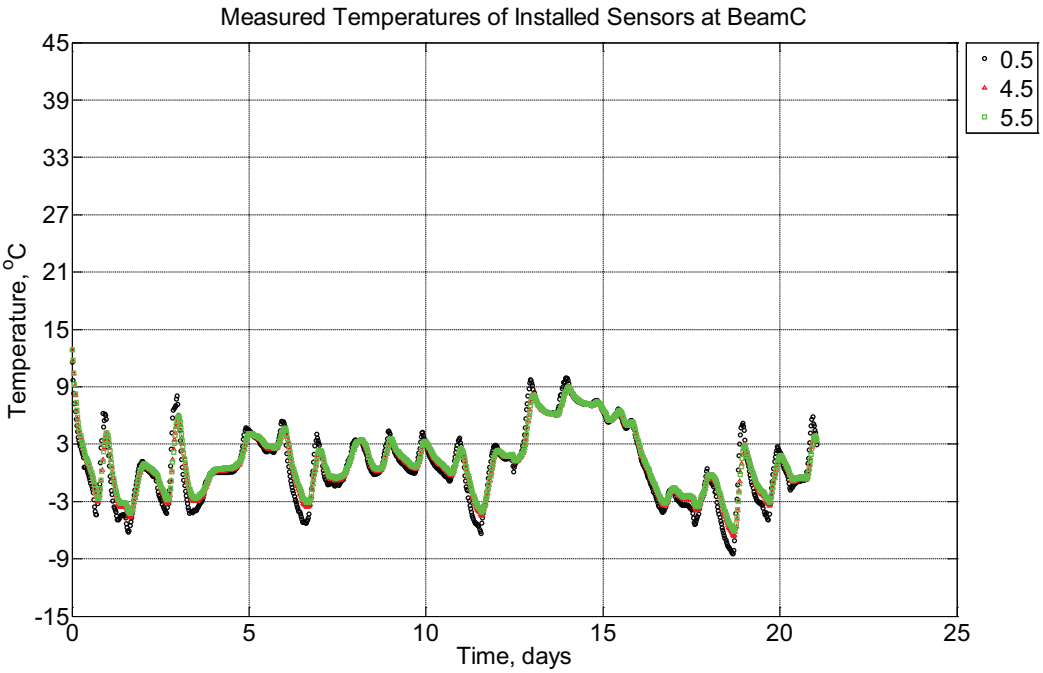

Figure B-284 Measured temperature at depths of 0.5 inches (12.7 mm), 4.5 inches (114.3 mm), and 5.5 inches (139.7 mm) from the surface of a modulus of rupture beam (labeled C) installed in ballast in Rantoul, IL, between November 30, 2014, through December 21, 2014.

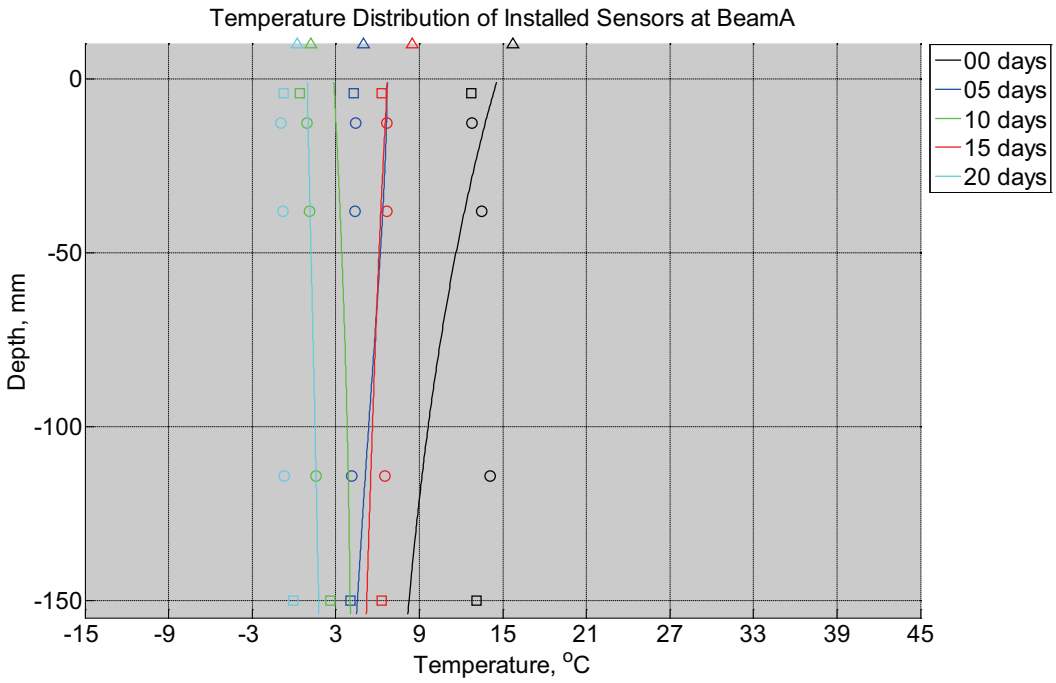

Figure B-285 Measured (markers) and modeled (continuous line) temperature profile distribution as a function of depth inside modulus of rupture beam (labeled A) installed in ballast in Rantoul, IL, between November 30, 2014, through December 21, 2014. Triangular markers denote temperature value from KTIP weather station, square markers denote measured temperature values from ballast, and circular markers denote measured temperature values inside concrete.

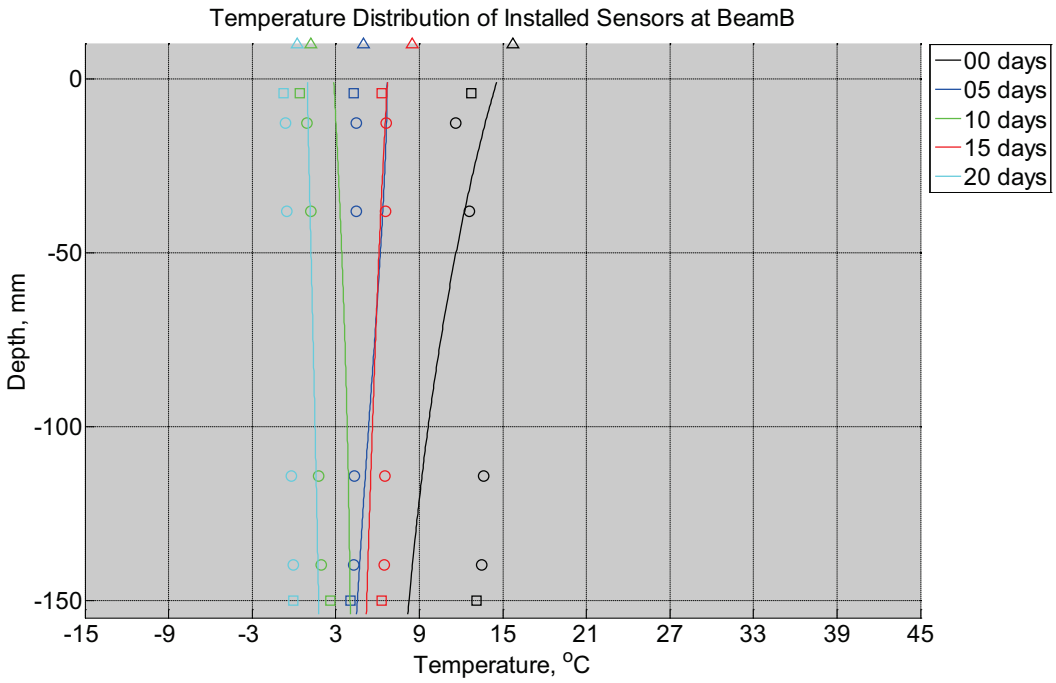

Figure B-286 Measured (markers) and modeled (continuous line) temperature profile distribution as a function of depth inside modulus of rupture beam (labeled B) installed in ballast in Rantoul, IL, between November 30, 2014, through December 21, 2014. Triangular markers denote temperature value from KTIP weather station, square markers denote measured temperature values from ballast, and circular markers denote measured temperature values inside concrete.

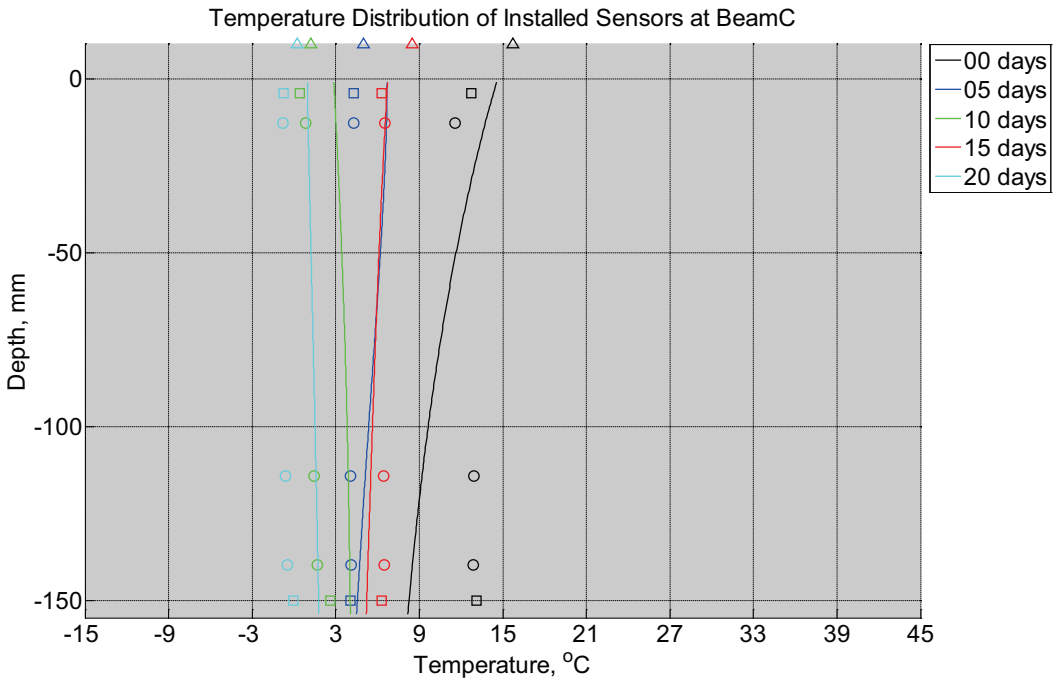

Figure B-287 Measured (markers) and modeled (continuous line) temperature profile distribution as a function of depth inside modulus of rupture beam (labeled C) installed in ballast in Rantoul, IL, between November 30, 2014, through December 21, 2014. Triangular markers denote temperature value from KTIP weather station, square markers denote measured temperature values from ballast, and circular markers denote measured temperature values inside concrete.

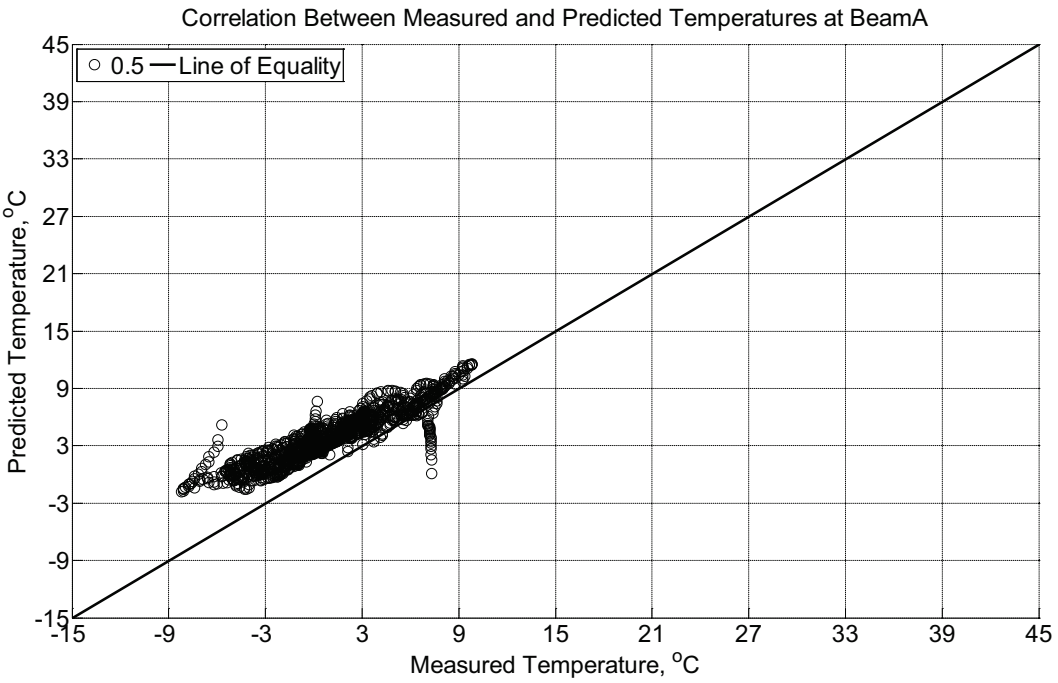

Figure B-288 Correlation between measured and predicted temperature values 0.5 inches (12.7 mm) from the surface of a modulus of rupture beam (labeled A) installed in ballast in Rantoul, IL, between November 30, 2014, through December 21, 2014.

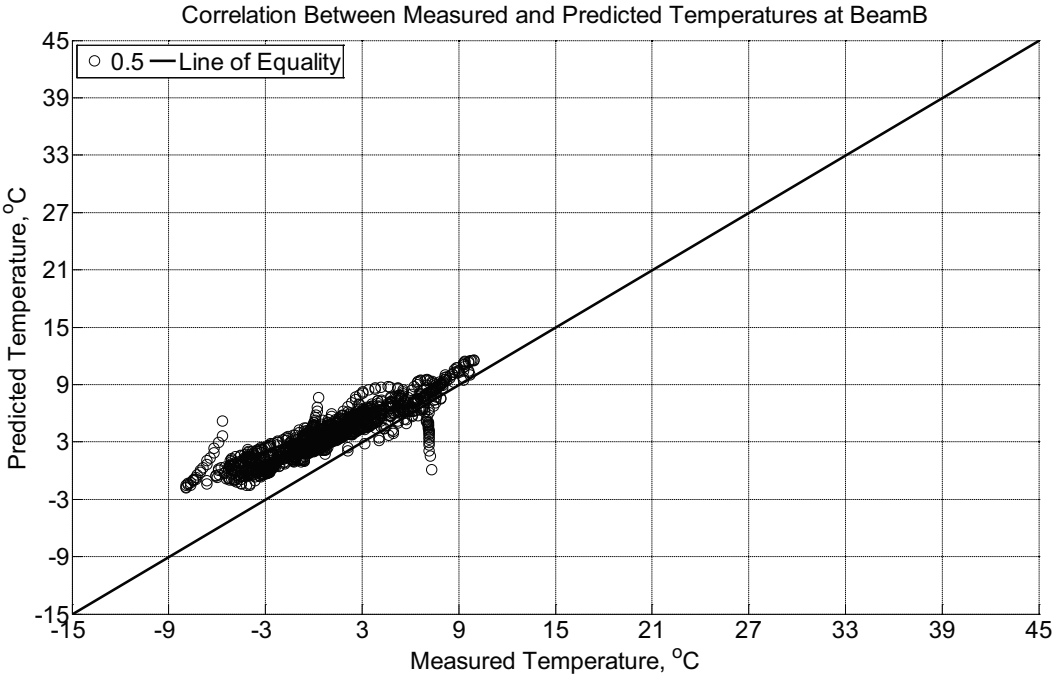

Figure B-289 Correlation between measured and predicted temperature values 0.5 inches

(12.7 mm) from the surface of a modulus of rupture beam (labeled B) installed in ballast in Rantoul, IL, between November 30, 2014, through December 21, 2014.

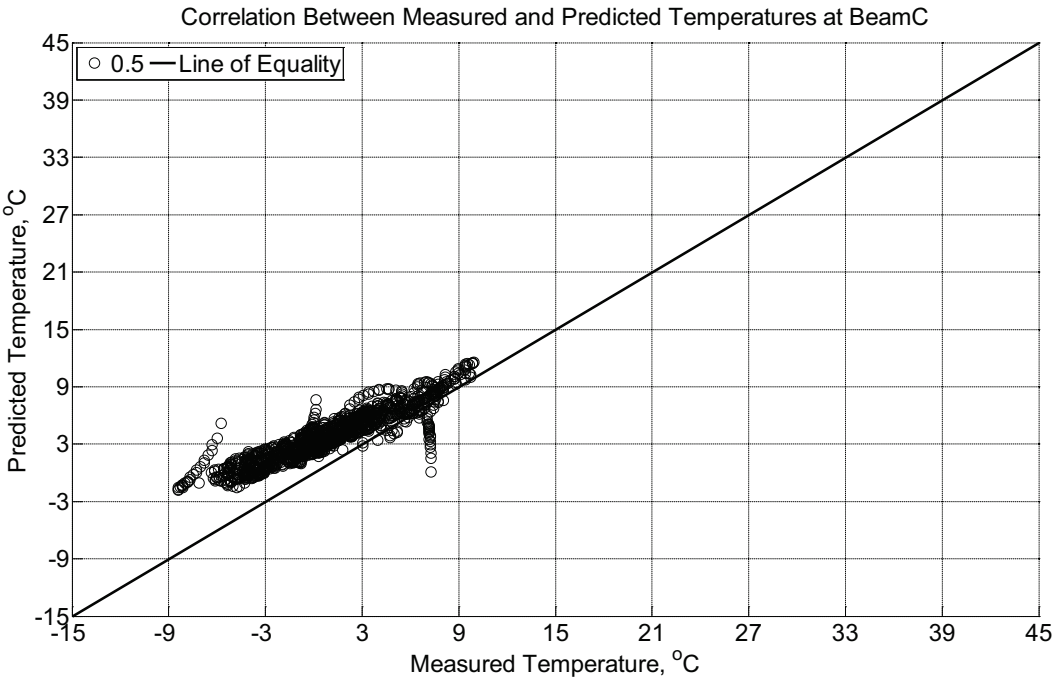

Figure B-290 Correlation between measured and predicted temperature values 0.5 inches (12.7 mm) from the surface of a modulus of rupture beam (labeled C) installed in ballast in Rantoul, IL, between November 30, 2014, through December 21, 2014.

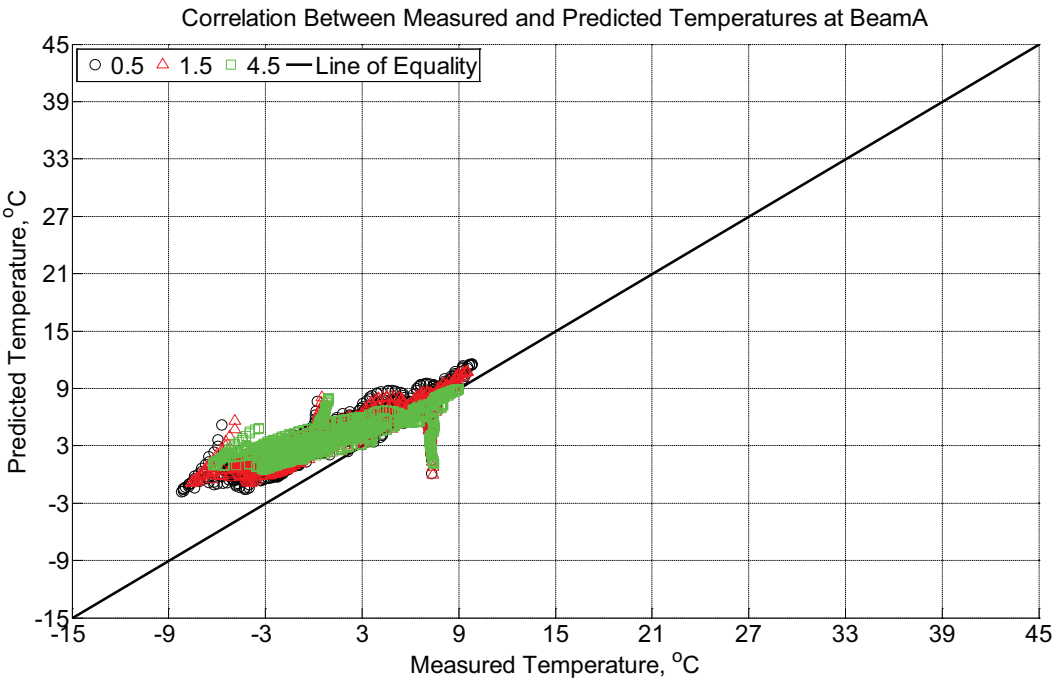

Figure B-291 Correlation between measured and predicted temperature values 0.5 inches (12.7 mm), 1.5 inches (38.1 mm), and 4.5 inches (114.3 mm) from the surface of a modulus of rupture beam (labeled A) installed in ballast in Rantoul, IL, between November 30, 2014, through December 21, 2014.

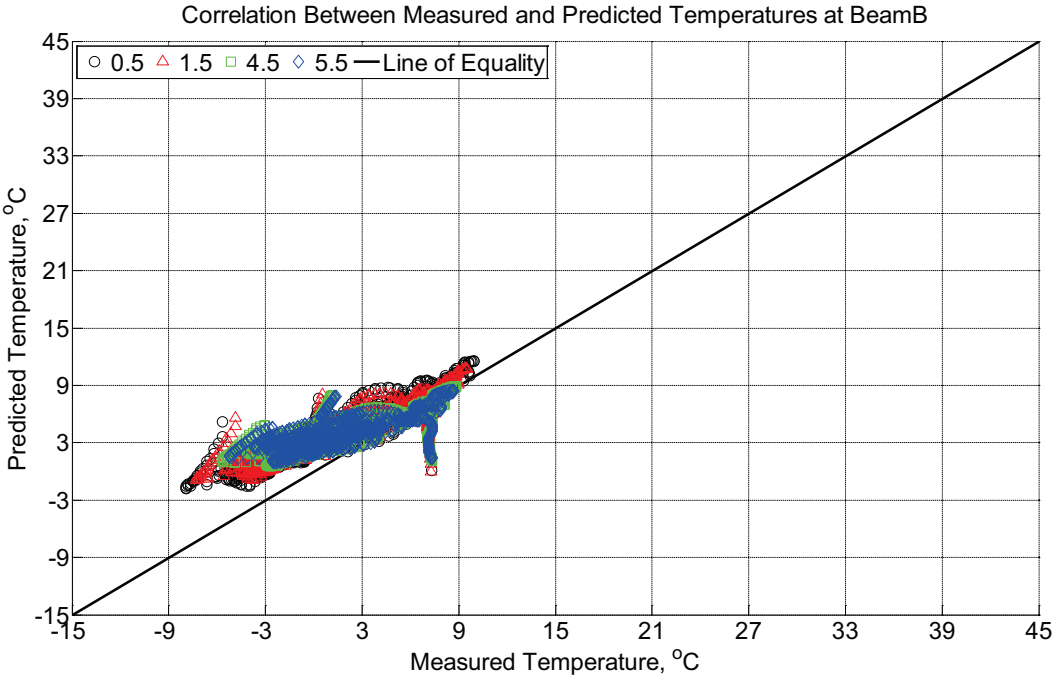

Figure B-292 Correlation between measured and predicted temperature values 0.5 inches (12.7 mm), 1.5 inches (38.1 mm), 4.5 inches (114.3 mm), and 5.5 inches (139.7 mm) from the

surface of a modulus of rupture beam (labeled B) installed in ballast in Rantoul, IL, between November 30, 2014, through December 21, 2014.

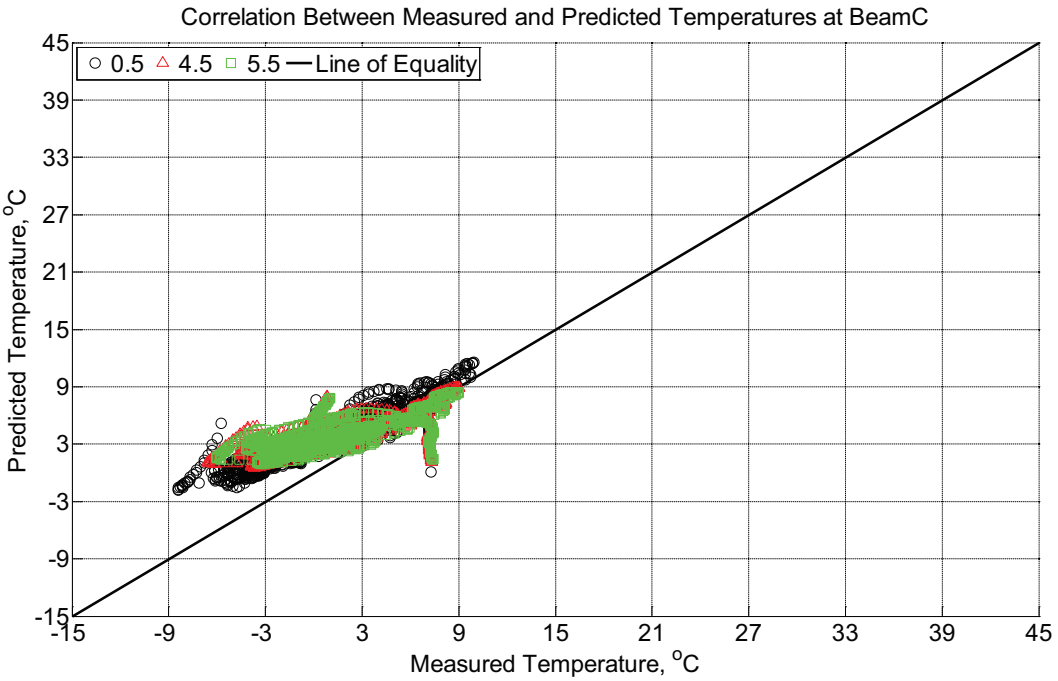

Figure B-293 Correlation between measured and predicted temperature values 0.5 inches (12.7 mm), 4.5 inches (114.3 mm), and 5.5 inches (139.7 mm) from the surface of a modulus of rupture beam (labeled C) installed in ballast in Rantoul, IL, between November 30, 2014, through December 21, 2014.

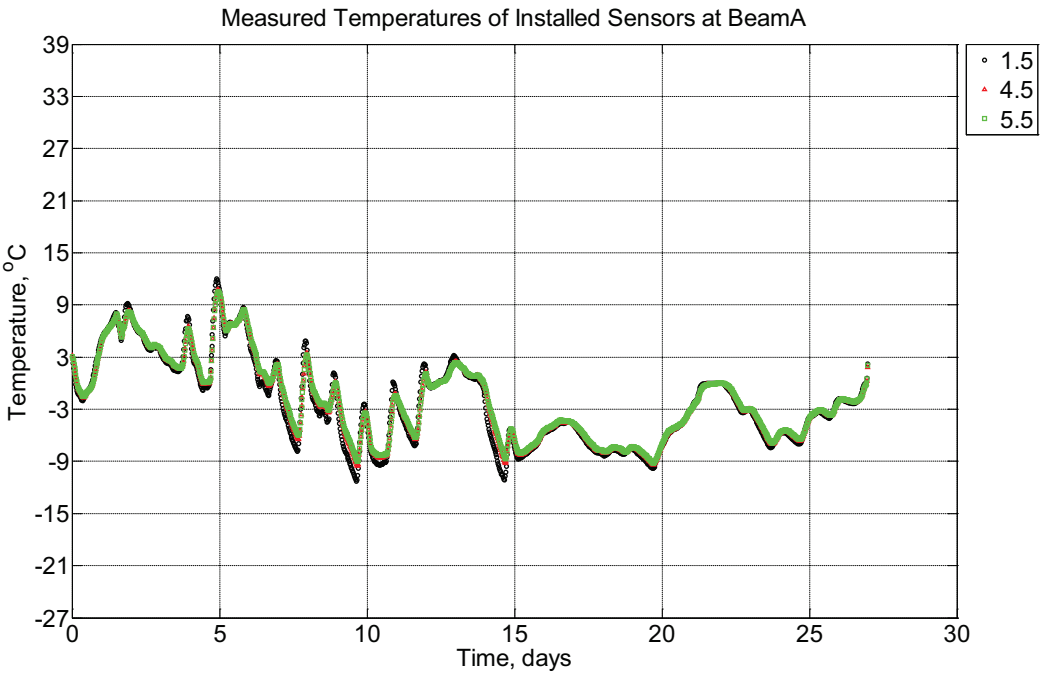

Figure B-294 Measured temperature at depths of 1.5 inches (38.1 mm), 4.5 inches (114.3 mm), and 5.5 inches (139.7 mm) from the surface of a modulus of rupture beam (labeled A) installed in ballast in Rantoul, IL, between December 21, 2014, through January 17, 2015.

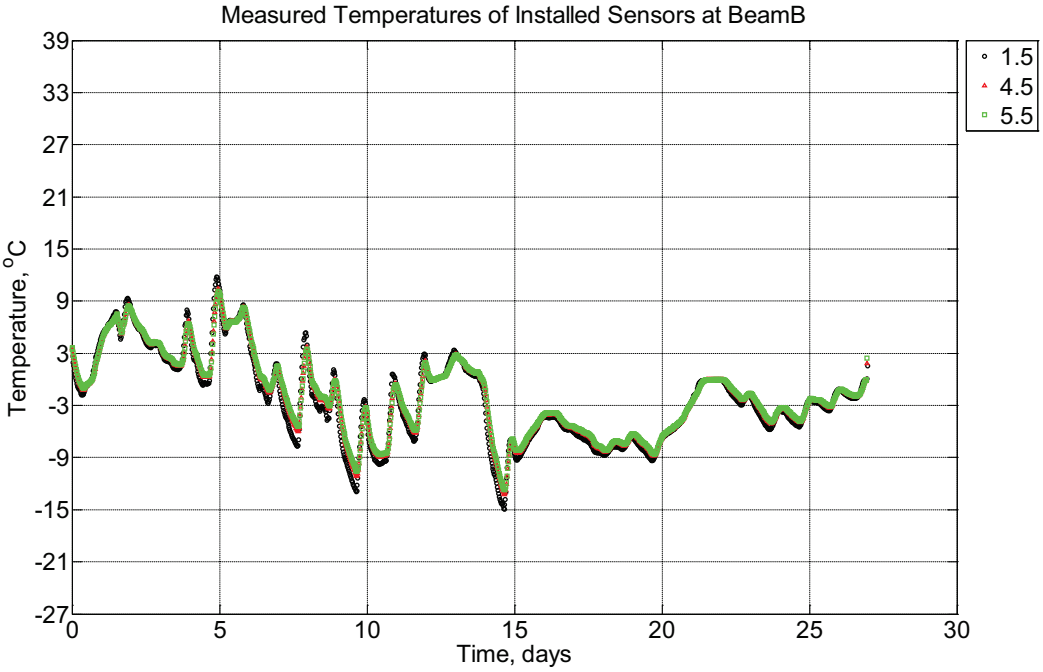

Figure B-295 Measured temperature at depths of 1.5 inches (38.1 mm), 4.5 inches (114.3

mm), and 5.5 inches (139.7 mm) from the surface of a modulus of rupture beam (labeled B) installed in ballast in Rantoul, IL, between December 21, 2014, through January 17, 2015.

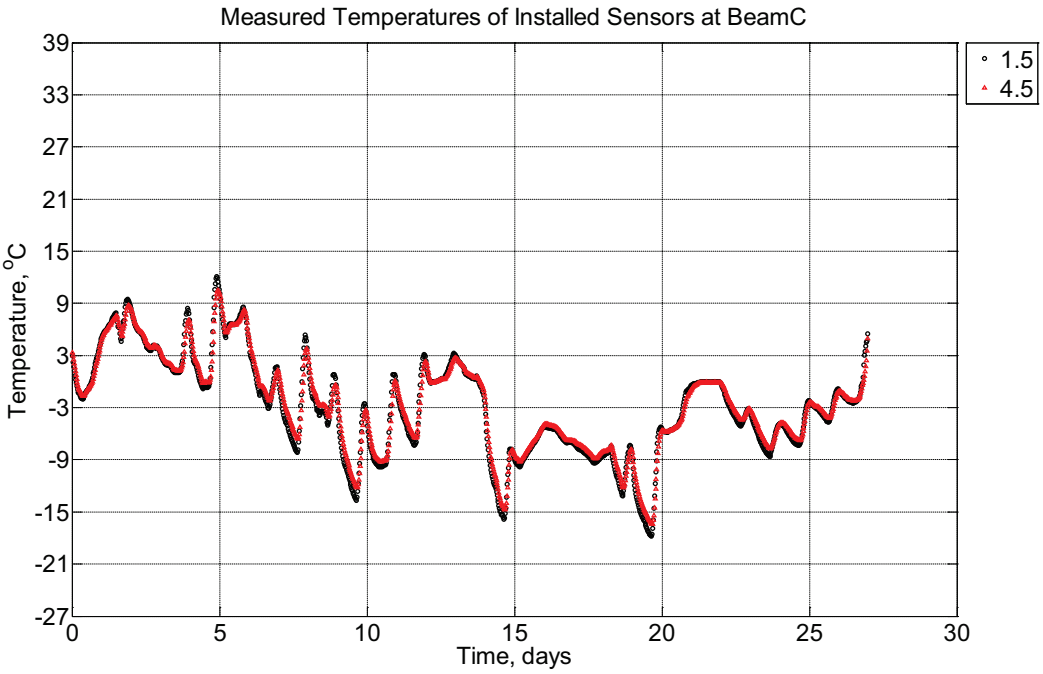

Figure B-296 Measured temperature at depths of 1.5 inches (38.1 mm) and 4.5 inches (114.3 mm) from the surface of a modulus of rupture beam (labeled C) installed in ballast in Rantoul, IL, between December 21, 2014, through January 17, 2015.

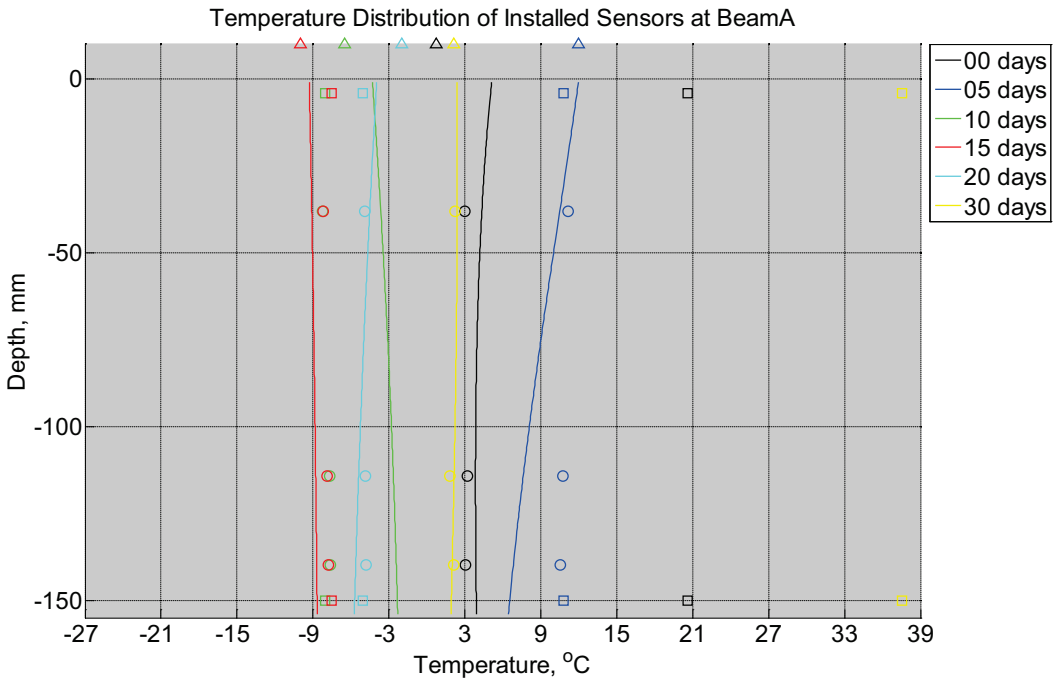

Figure B-297 Measured (markers) and modeled (continuous line) temperature profile distribution as a function of depth inside modulus of rupture beam (labeled A) installed in ballast in Rantoul, IL, between December 21, 2014, through January 17, 2015. Triangular markers denote temperature value from KTIP weather station, square markers denote measured temperature values from ballast, and circular markers denote measured temperature values inside concrete.

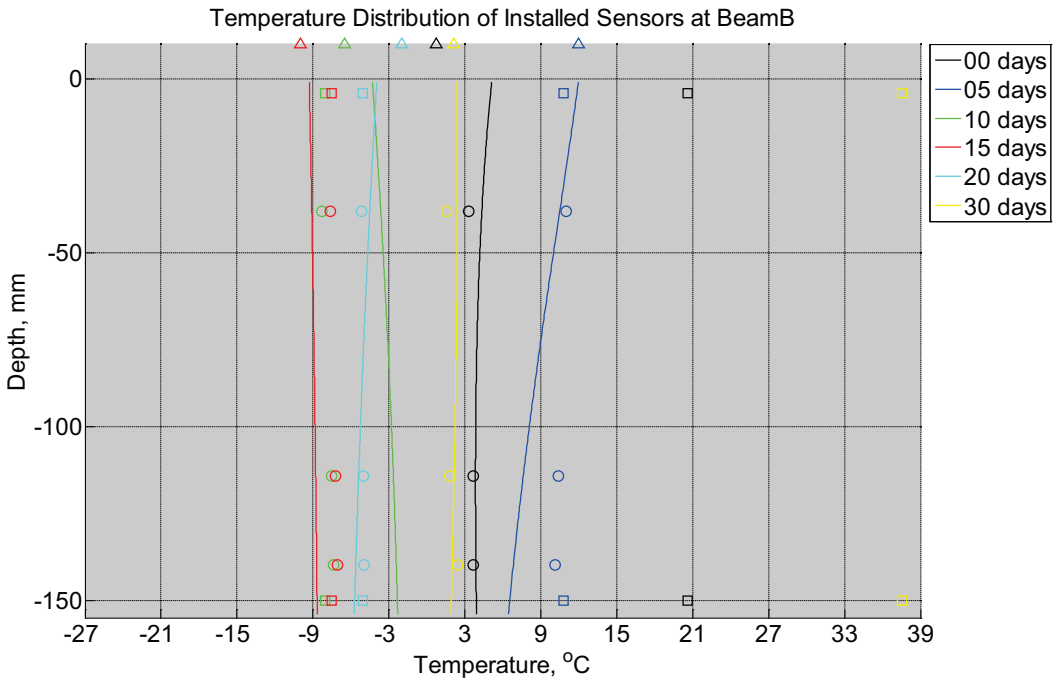

Figure B-298 Measured (markers) and modeled (continuous line) temperature profile distribution as a function of depth inside modulus of rupture beam (labeled B) installed in ballast in Rantoul, IL, between December 21, 2014, through January 17, 2015. Triangular markers denote temperature value from KTIP weather station, square markers denote measured temperature values from ballast, and circular markers denote measured temperature values inside concrete.

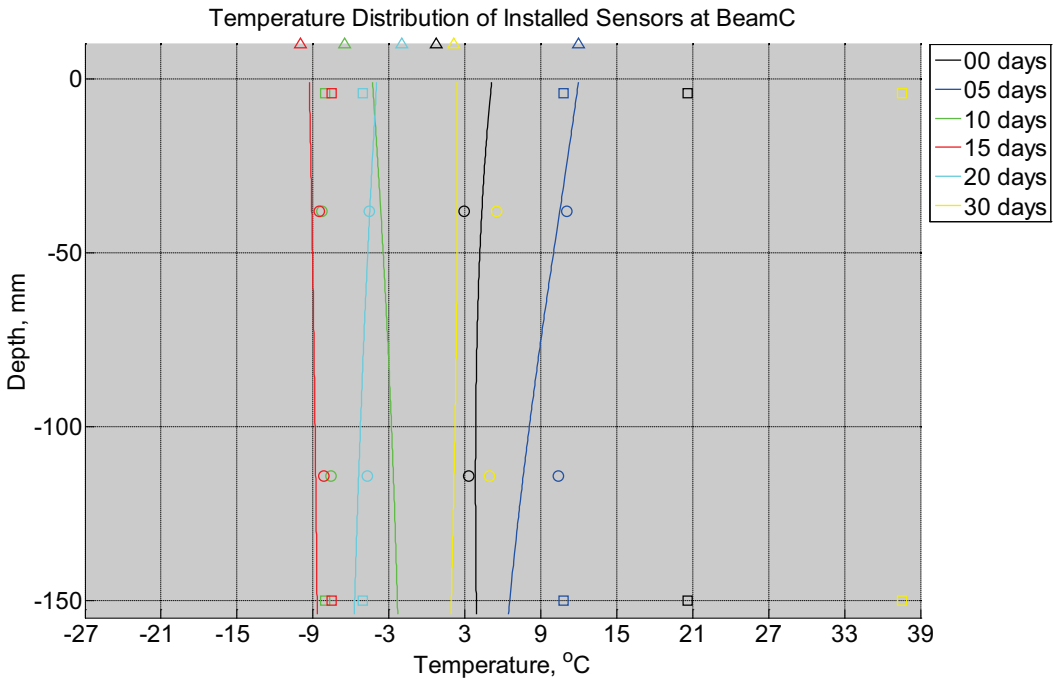

Figure B-299 Measured (markers) and modeled (continuous line) temperature profile distribution as a function of depth inside modulus of rupture beam (labeled C) installed in ballast in Rantoul, IL, between December 21, 2014, through January 17, 2015. Triangular markers denote temperature value from KTIP weather station, square markers denote measured temperature values from ballast, and circular markers denote measured temperature values inside concrete.

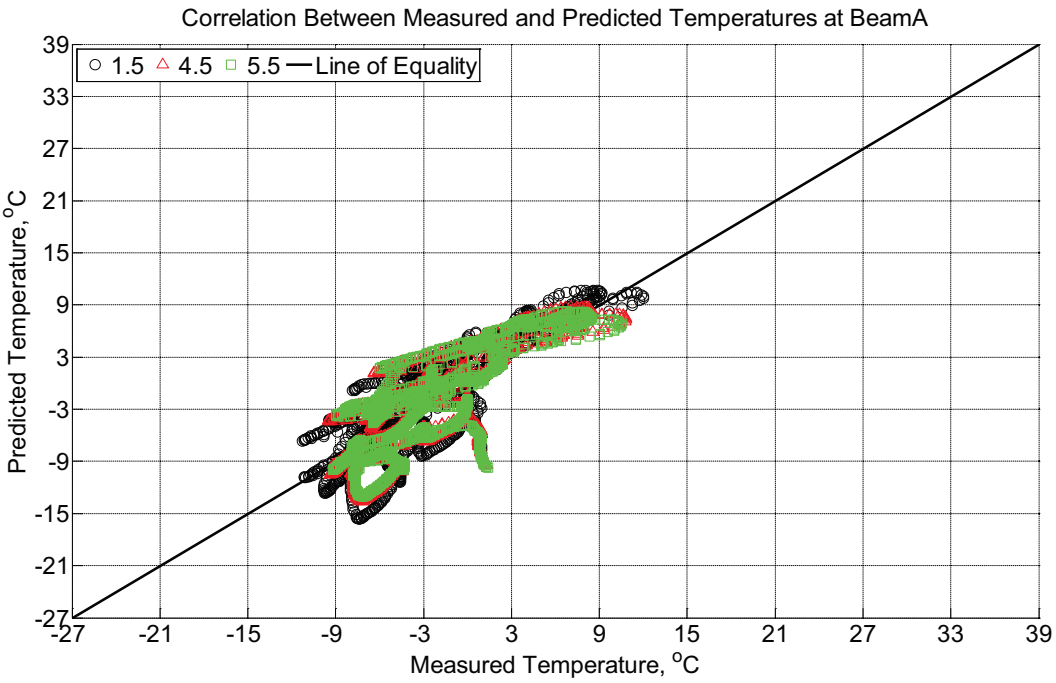

Figure B-300 Correlation between measured and predicted temperature values 1.5 inches (38.1 mm), 4.5 inches (114.3 mm), and 5.5 inches (139.7 mm) from the surface of a modulus of rupture beam (labeled A) installed in ballast in Rantoul, IL, between December 21, 2014, through January 17, 2015.

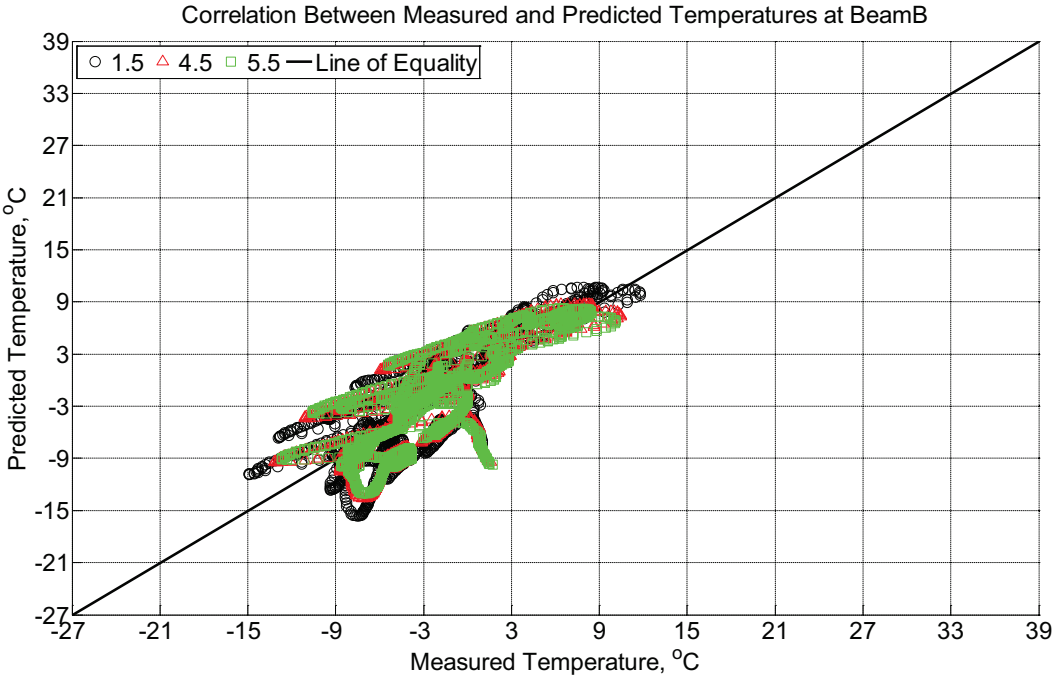

Figure B-301 Correlation between measured and predicted temperature values 1.5 inches (38.1 mm), 4.5 inches (114.3 mm), and 5.5 inches (139.7 mm) from the surface of a modulus

of rupture beam (labeled B) installed in ballast in Rantoul, IL, between December 21, 2014, through January 17, 2015.

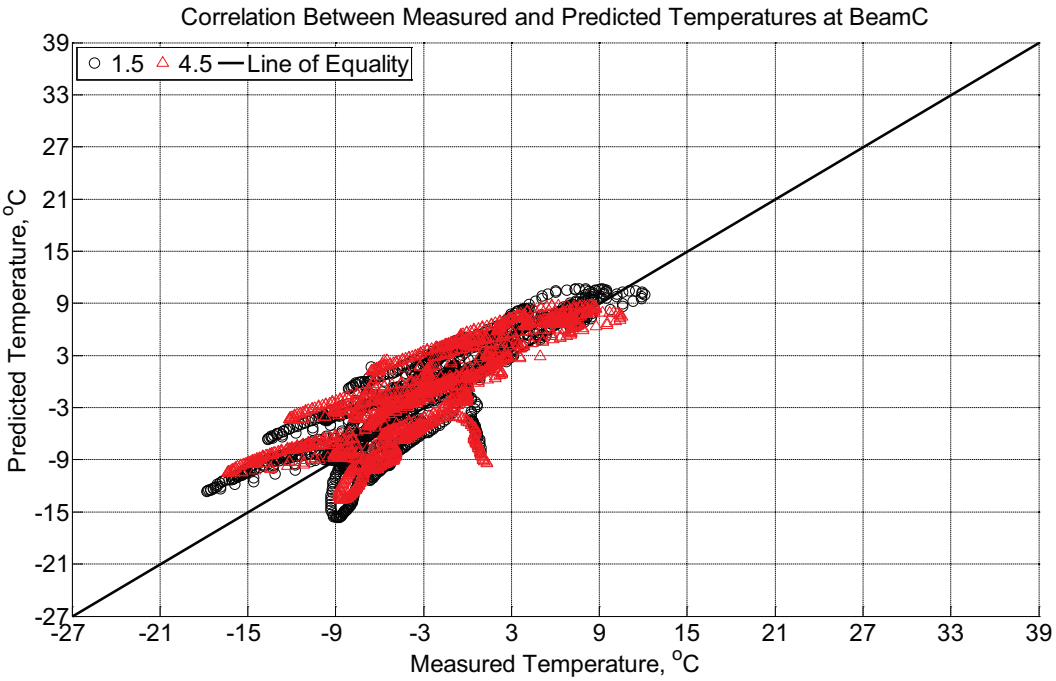

Figure B-302 Correlation between measured and predicted temperature values 1.5 inches (38.1 mm) and 4.5 inches (114.3 mm) from the surface of a modulus of rupture beam (labeled C) installed in ballast in Rantoul, IL, between December 21, 2014, through January 17, 2015.

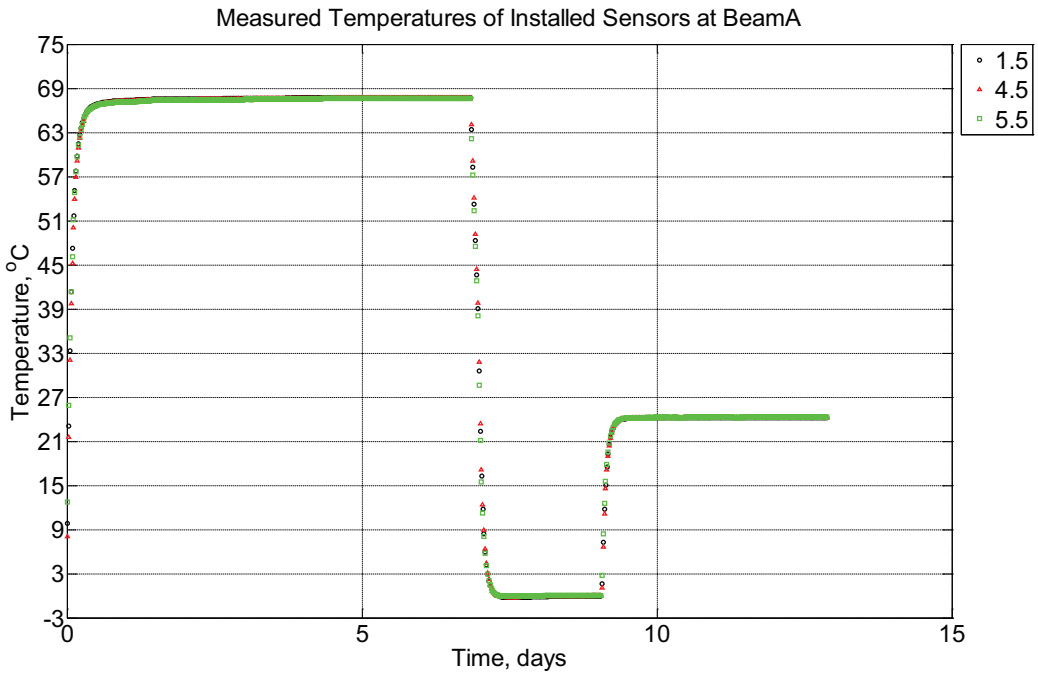

Figure B-303 Measured temperature at depths of 1.5 inches (38.1 mm), 4.5 inches (114.3 mm), and 5.5 inches (139.7 mm) from the surface of a modulus of rupture beam (labeled A) located inside a heating oven (65°C and 0°C) and an environmentally controlled room (50% RH, 23°C) between January 17, 2015, through January 30, 2015.

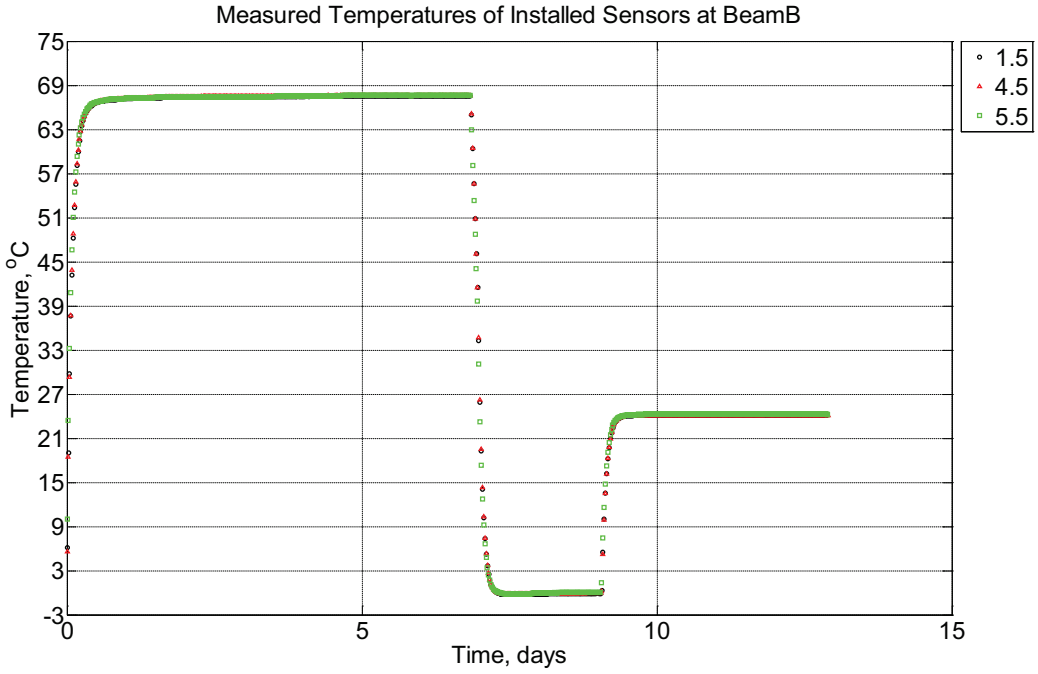

Figure B-304 Measured temperature at depths of 1.5 inches (38.1 mm), 4.5 inches (114.3 mm), and 5.5 inches (139.7 mm) from the surface of a modulus of rupture beam (labeled B)

located inside a heating oven (65°C and 0°C) and an environmentally controlled room (50% RH, 23°C) between January 17, 2015, through January 30, 2015.

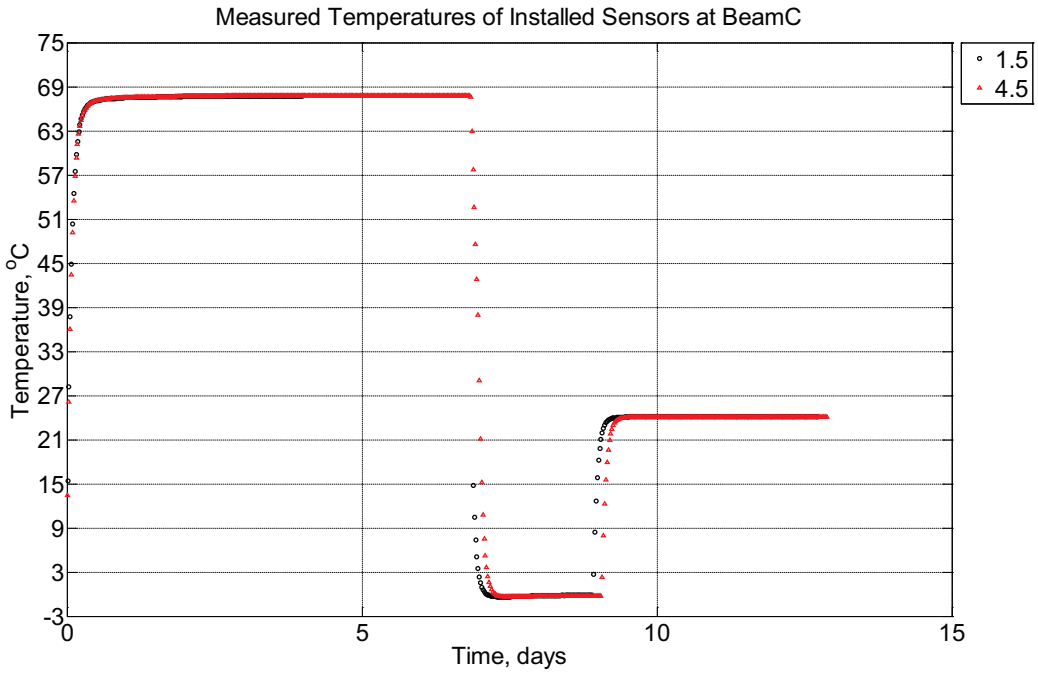

Figure B-305 Measured temperature at depths of 1.5 inches (38.1 mm) and 4.5 inches (114.3 mm) from the surface of a modulus of rupture beam (labeled C) located inside a heating oven (65°C and 0°C) and an environmentally controlled room (50% RH, 23°C) between January 17, 2015, through January 30, 2015.

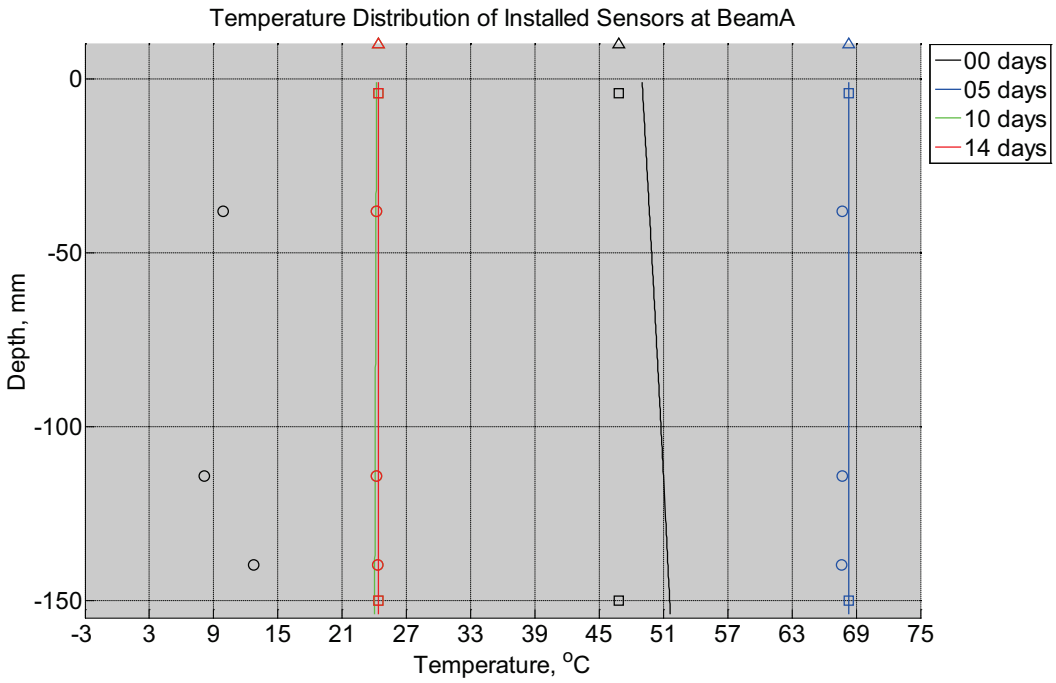

Figure B-306 Measured (markers) and modeled (continuous line) temperature profile distribution as a function of depth inside modulus of rupture beam (labeled A) located inside a heating oven (65ºC and 0ºC) and an environmentally controlled room (50% RH, 23ºC) between January 17, 2015, through January 30, 2015. Triangular markers denote temperature value from control panel, square markers denote measured temperature values from ambient sensors, and circular markers denote measured temperature values inside concrete.

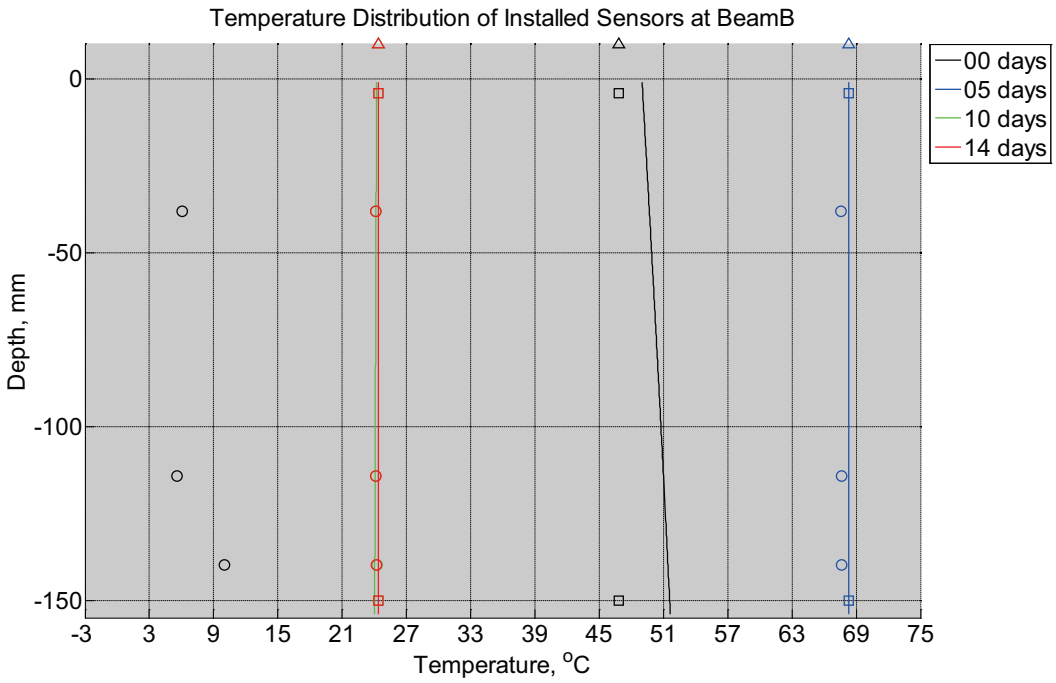

Figure B-307 Measured (markers) and modeled (continuous line) temperature profile distribution as a function of depth inside modulus of rupture beam (labeled B) located inside a heating oven (65ºC and 0ºC) and an environmentally controlled room (50% RH, 23ºC) between January 17, 2015, through January 30, 2015. Triangular markers denote temperature value from control panel, square markers denote measured temperature values from ambient sensors, and circular markers denote measured temperature values inside concrete.

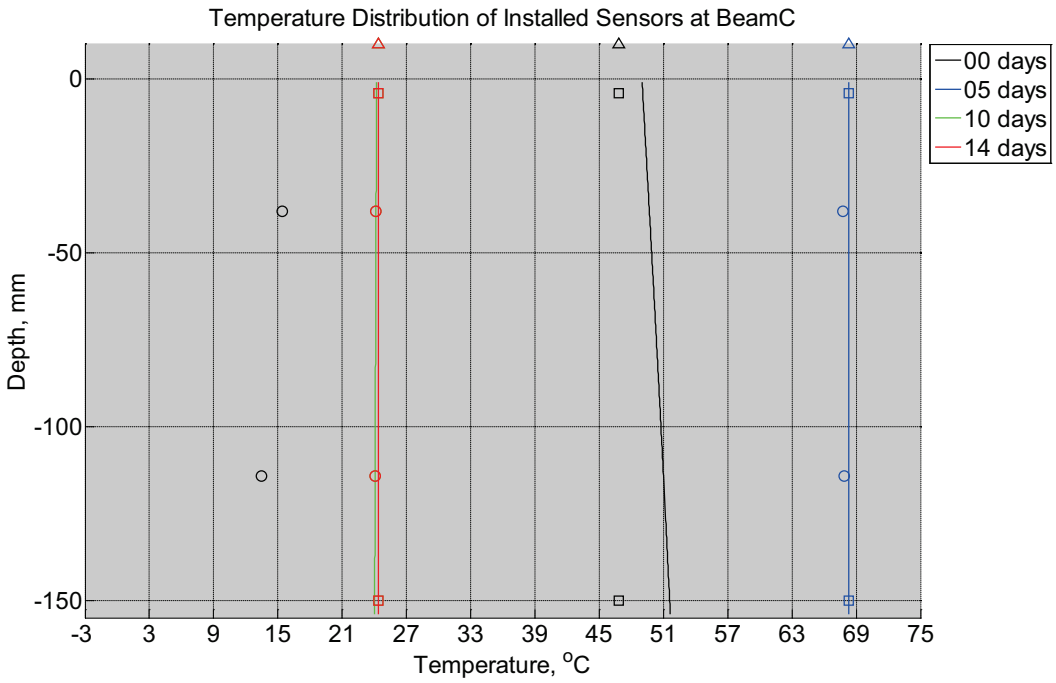

Figure B-308 Measured (markers) and modeled (continuous line) temperature profile distribution as a function of depth inside modulus of rupture beam (labeled C) located inside a heating oven (65ºC and 0ºC) and an environmentally controlled room (50% RH, 23ºC) between January 17, 2015, through January 30, 2015. Triangular markers denote temperature value from control panel, square markers denote measured temperature values from ambient sensors, and circular markers denote measured temperature values inside concrete.

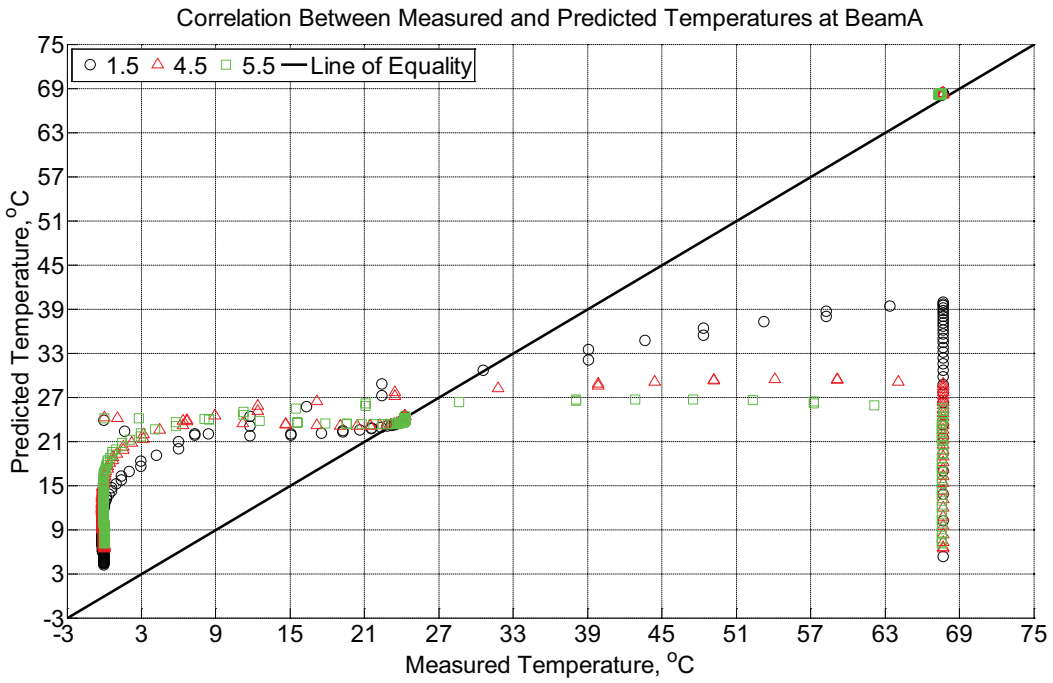

Figure B-309 Correlation between measured and predicted temperature values 1.5 inches (38.1 mm), 4.5 inches (114.3 mm), and 5.5 inches (139.7 mm) from the surface of a modulus of rupture beam (labeled A) located inside a heating oven (65ºC and 0ºC) and an environmentally controlled room (50% RH, 23ºC) between January 17, 2015, through January 30, 2015.

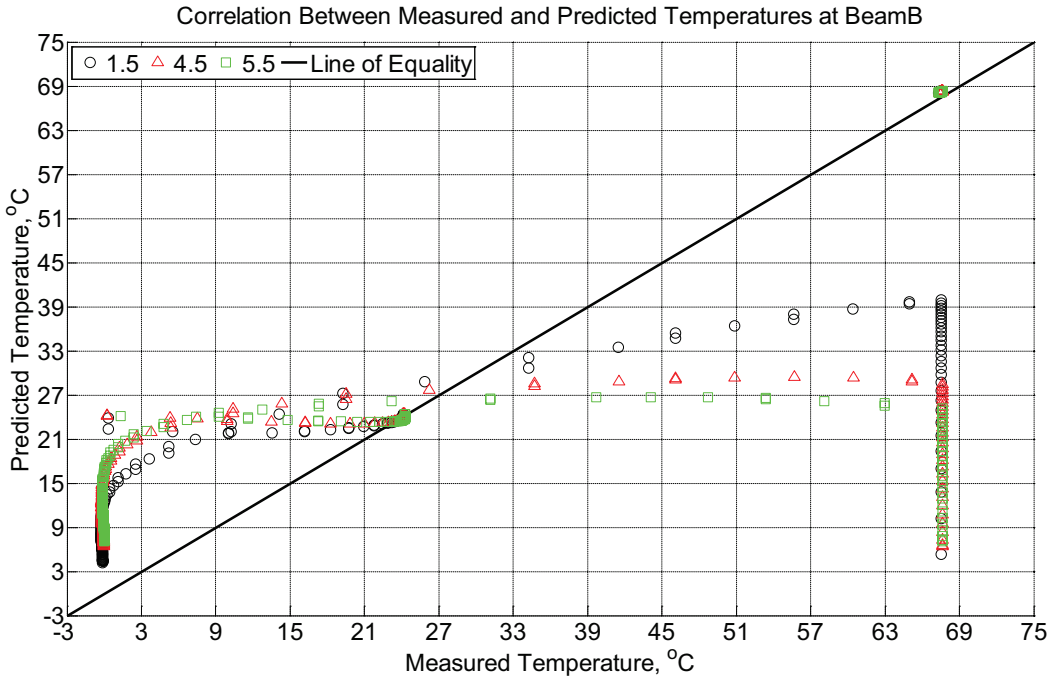

Figure B-310 Correlation between measured and predicted temperature values 1.5 inches

(38.1 mm), 4.5 inches (114.3 mm), and 5.5 inches (139.7 mm) from the surface of a modulus of rupture beam (labeled B) located inside a heating oven (65ºC and 0ºC) and an environmentally controlled room (50% RH, 23ºC) between January 17, 2015, through January 30, 2015.

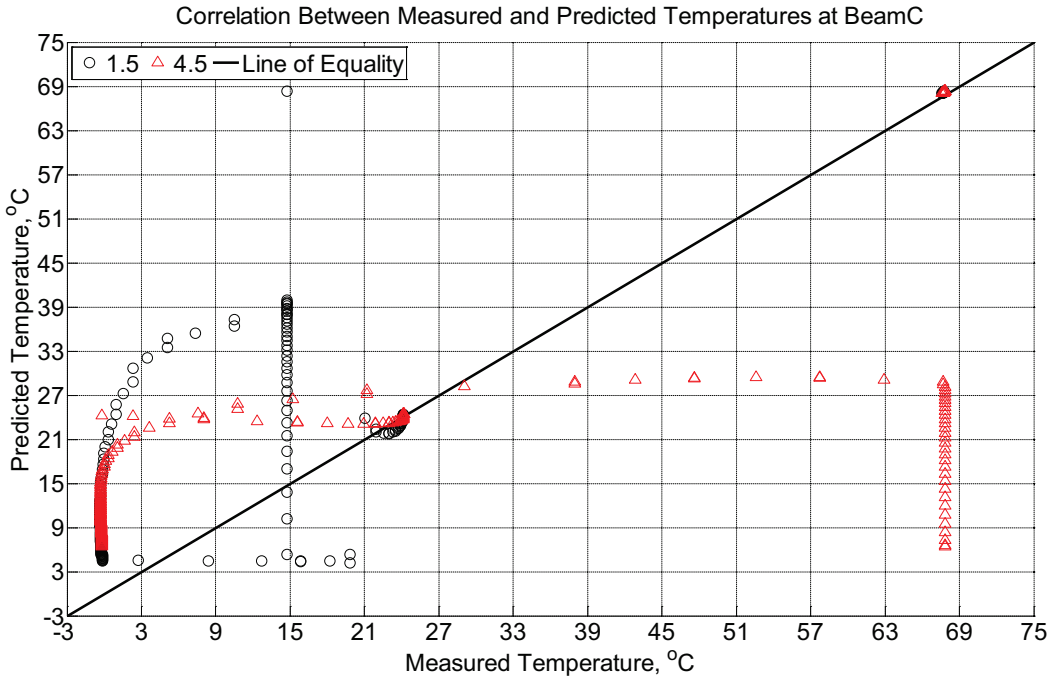

Figure B-311 Correlation between measured and predicted temperature values 1.5 inches (38.1 mm) and 4.5 inches (114.3 mm) from the surface of a modulus of rupture beam (labeled C) located inside a heating oven (65ºC and 0ºC) and an environmentally controlled room (50% RH, 23ºC) between January 17, 2015, through January 30, 2015.

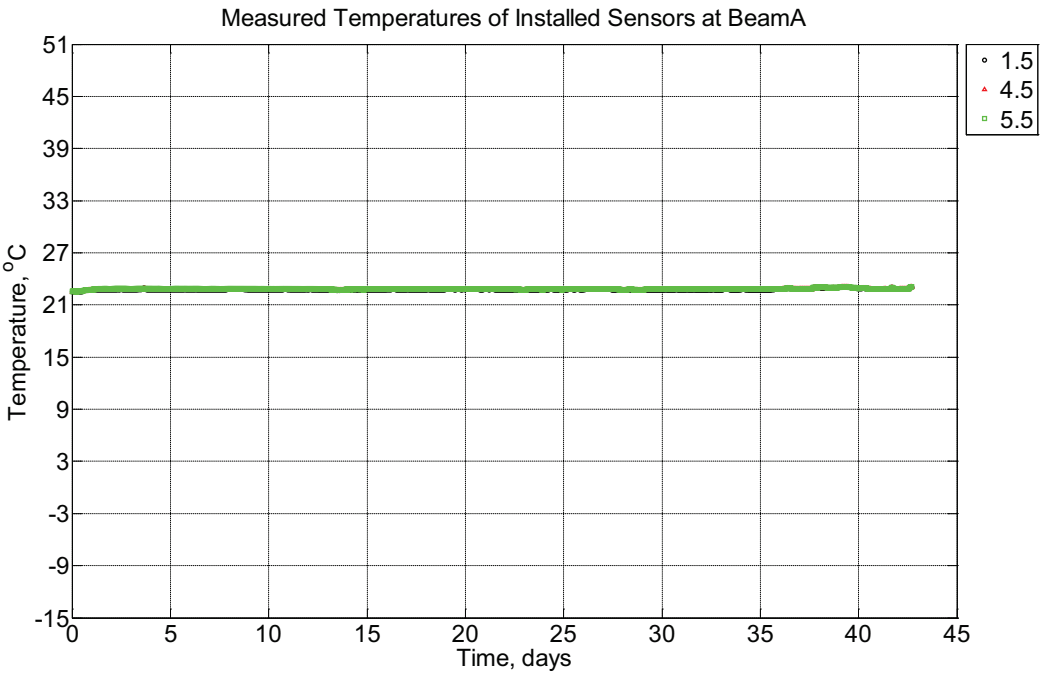

Figure B-312 Measured temperature at depths of 1.5 inches (38.1 mm), 4.5 inches (114.3 mm), and 5.5 inches (139.7 mm) from the surface of a modulus of rupture beam (labeled A) located inside an environmentally controlled room (50% RH, 23ºC) between February 5, 2015, through March 20, 2015.

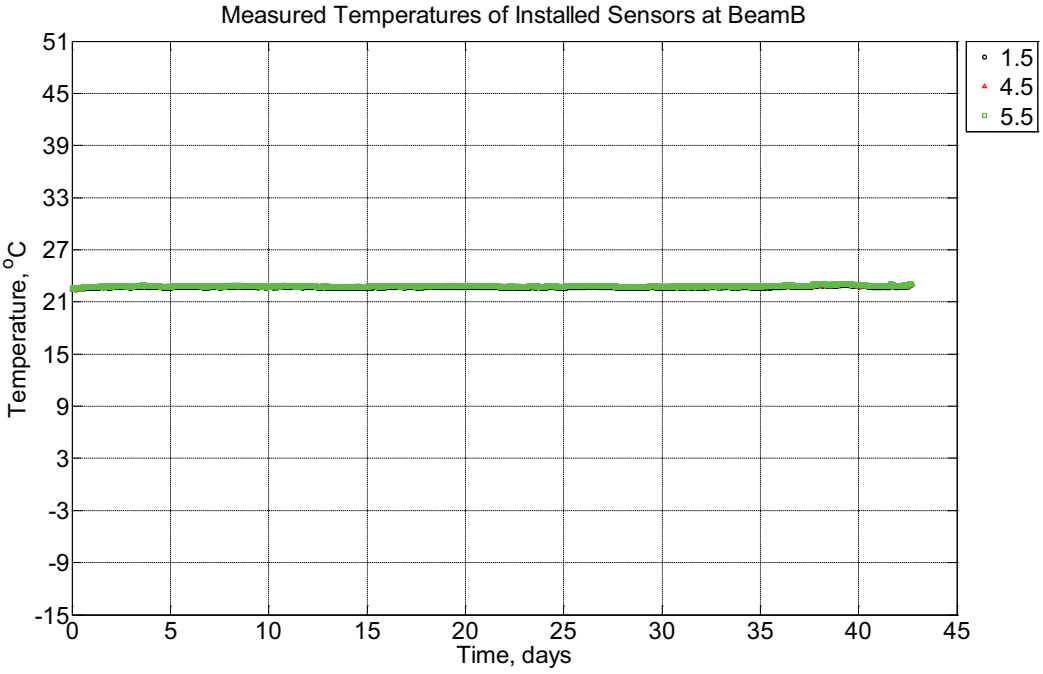

Figure B-313 Measured temperature at depths of 1.5 inches (38.1 mm), 4.5 inches (114.3 mm), and 5.5 inches (139.7 mm) from the surface of a modulus of rupture beam (labeled B)

located inside an environmentally controlled room (50% RH, 23°C) between February 5, 2015, through March 20, 2015.

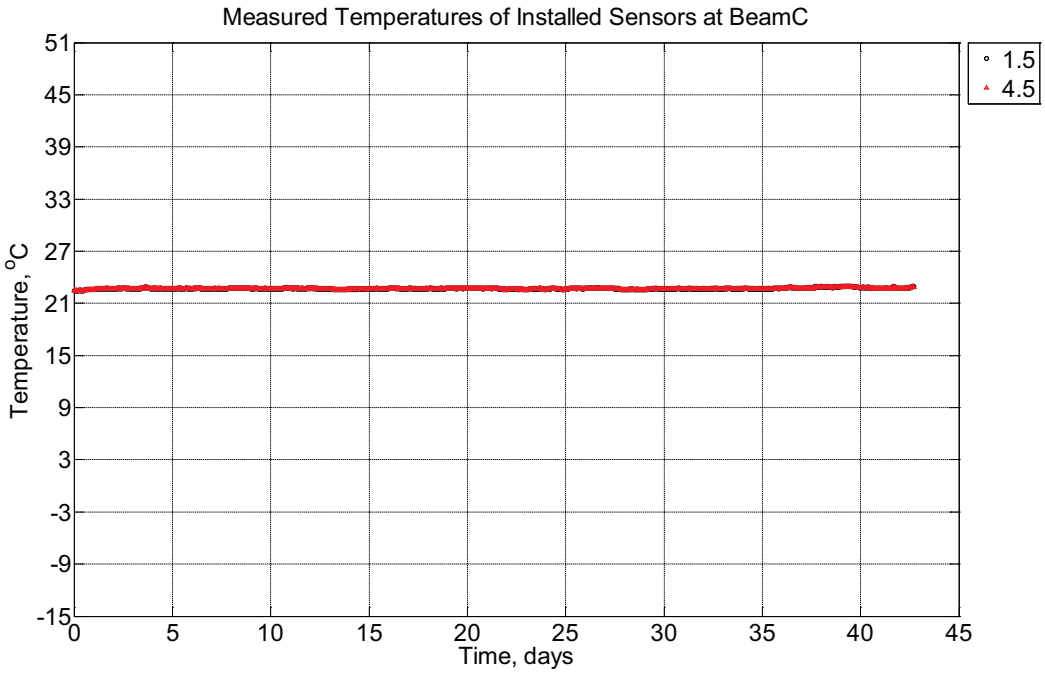

Figure B-314 Measured temperature at depths of 1.5 inches (38.1 mm) and 4.5 inches (114.3 mm) from the surface of a modulus of rupture beam (labeled C) located inside an environmentally controlled room (50% RH, 23°C) between February 5, 2015, through March 20, 2015.

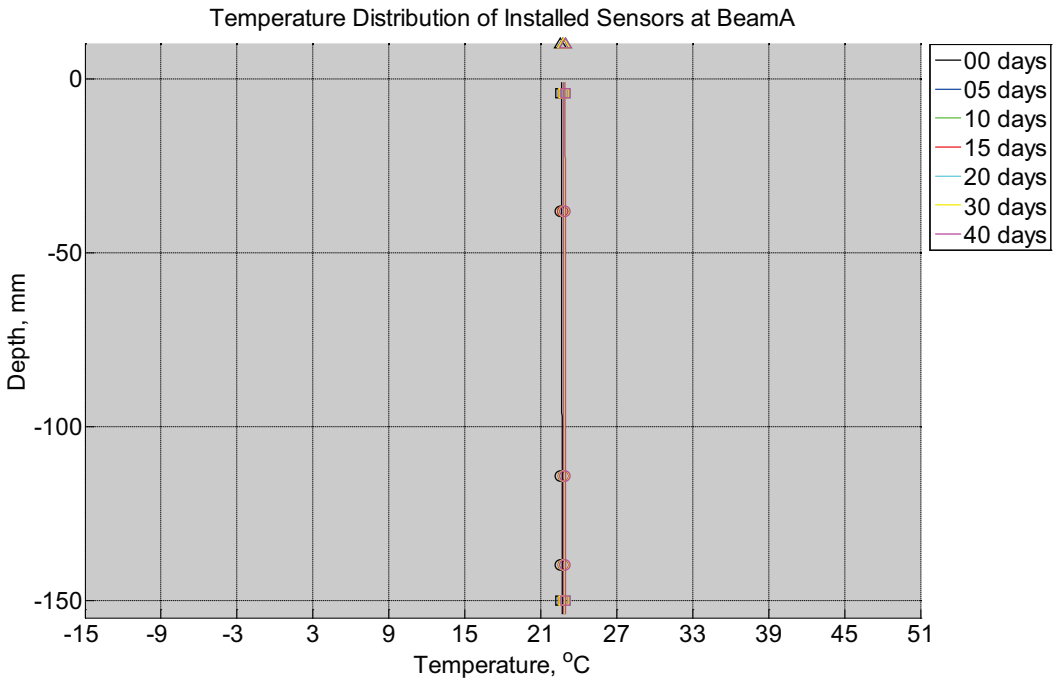

Figure B-315 Measured (markers) and modeled (continuous line) temperature profile distribution as a function of depth inside modulus of rupture beam (labeled A) located inside an environmentally controlled room (50% RH, 23°C) between February 5, 2015, through March 20, 2015. Triangular markers denote temperature value from control panel, square markers denote measured temperature values from ambient sensors, and circular markers denote measured temperature values inside concrete.

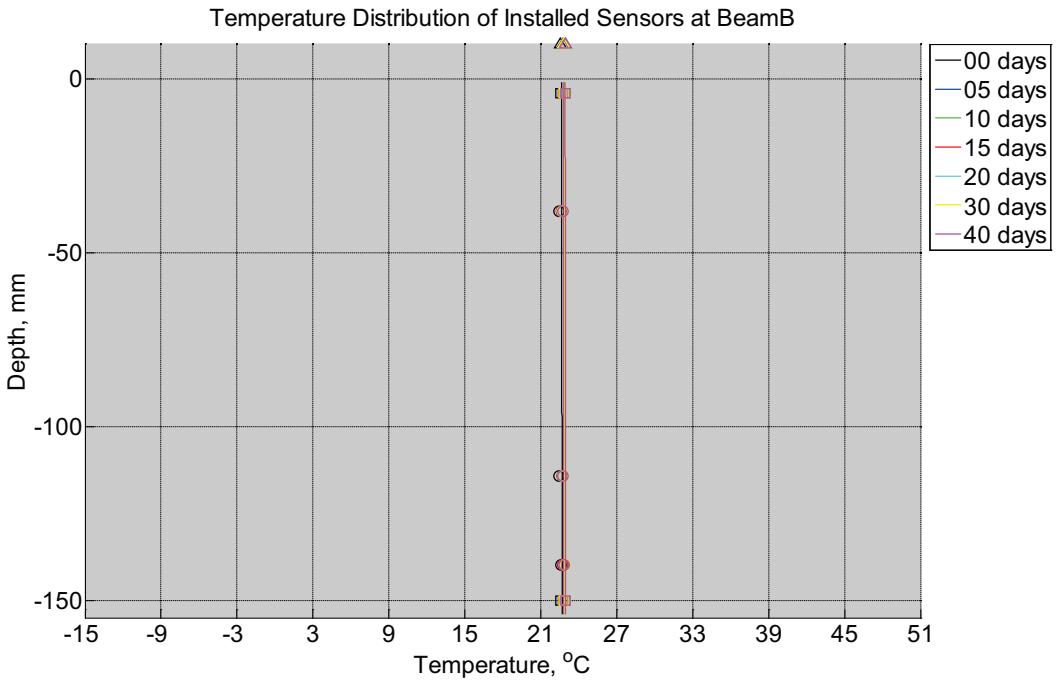

Figure B-316 Measured (markers) and modeled (continuous line) temperature profile distribution as a function of depth inside modulus of rupture beam (labeled B) located inside an environmentally controlled room (50% RH, 23°C) between February 5, 2015, through March 20, 2015. Triangular markers denote temperature value from control panel, square markers denote measured temperature values from ambient sensors, and circular markers denote measured temperature values inside concrete.

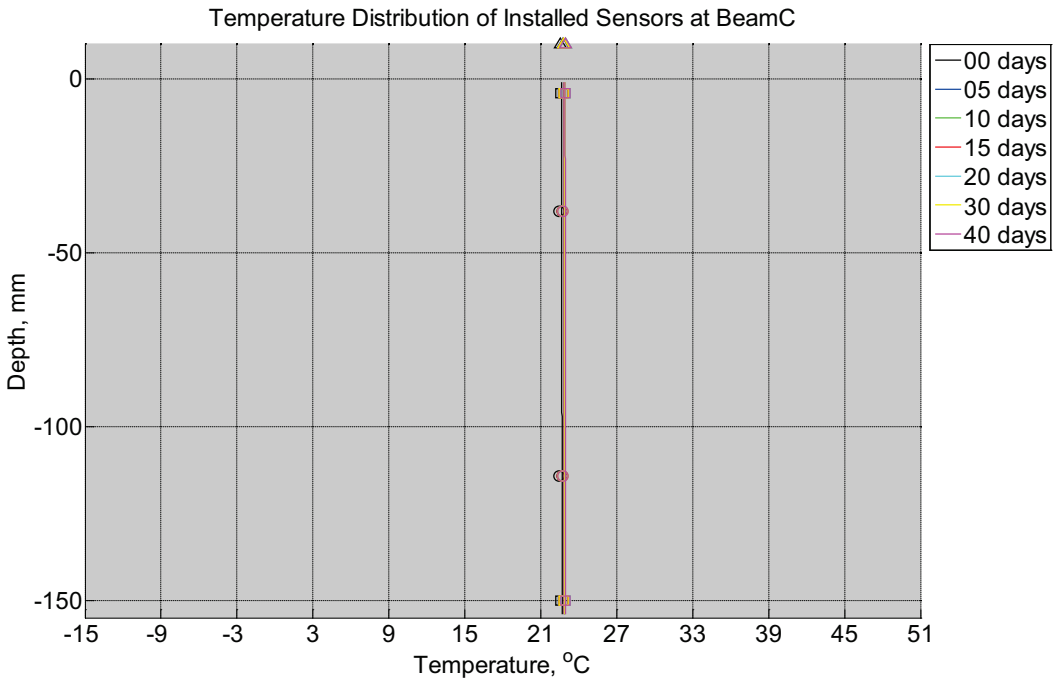

Figure B-317 Measured (markers) and modeled (continuous line) temperature profile distribution as a function of depth inside modulus of rupture beam (labeled C) located inside an environmentally controlled room (50% RH, 23°C) between February 5, 2015, through March 20, 2015. Triangular markers denote temperature value from control panel, square markers denote measured temperature values from ambient sensors, and circular markers denote measured temperature values inside concrete.

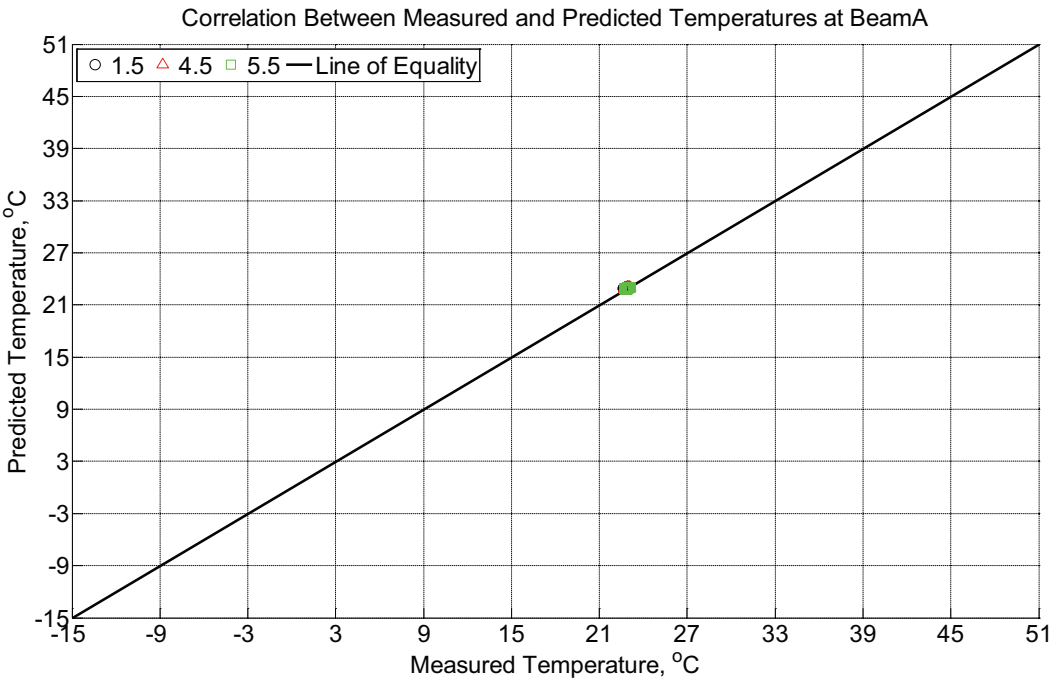

Figure B-318 Correlation between measured and predicted temperature values 1.5 inches (38.1 mm), 4.5 inches (114.3 mm), and 5.5 inches (139.7 mm) from the surface of a modulus of rupture beam (labeled A) located inside an environmentally controlled room (50% RH, 23ºC) between February 5, 2015, through March 20, 2015.

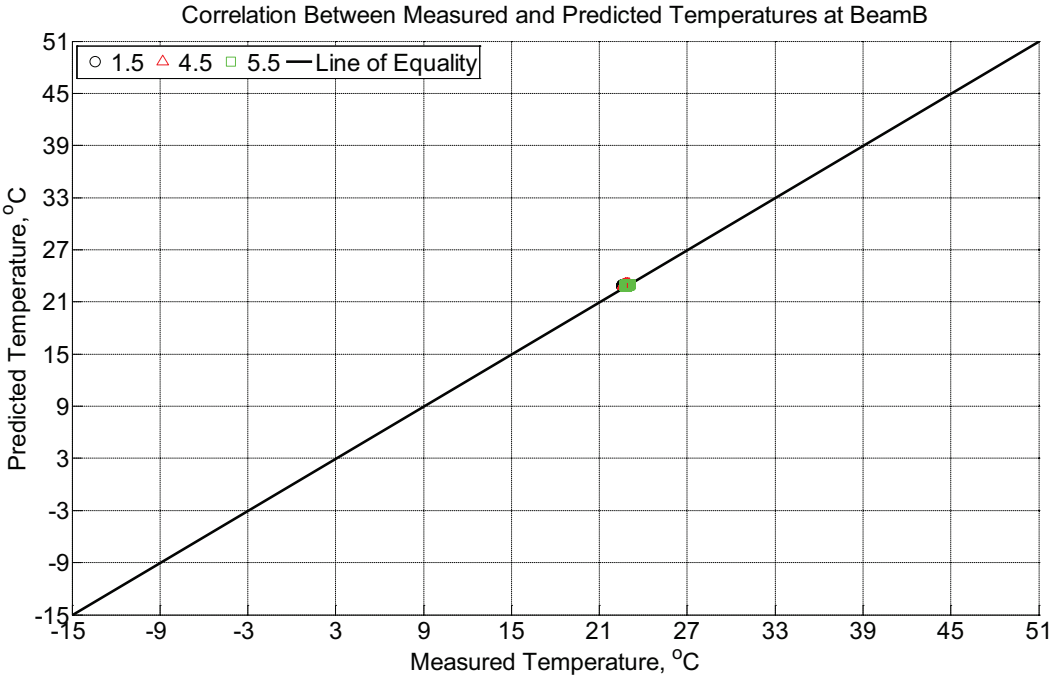

Figure B-319 Correlation between measured and predicted temperature values 1.5 inches (38.1 mm), 4.5 inches (114.3 mm), and 5.5 inches (139.7 mm) from the surface of a modulus

of rupture beam (labeled B) located inside an environmentally controlled room (50% RH, 23°C) between February 5, 2015, through March 20, 2015.

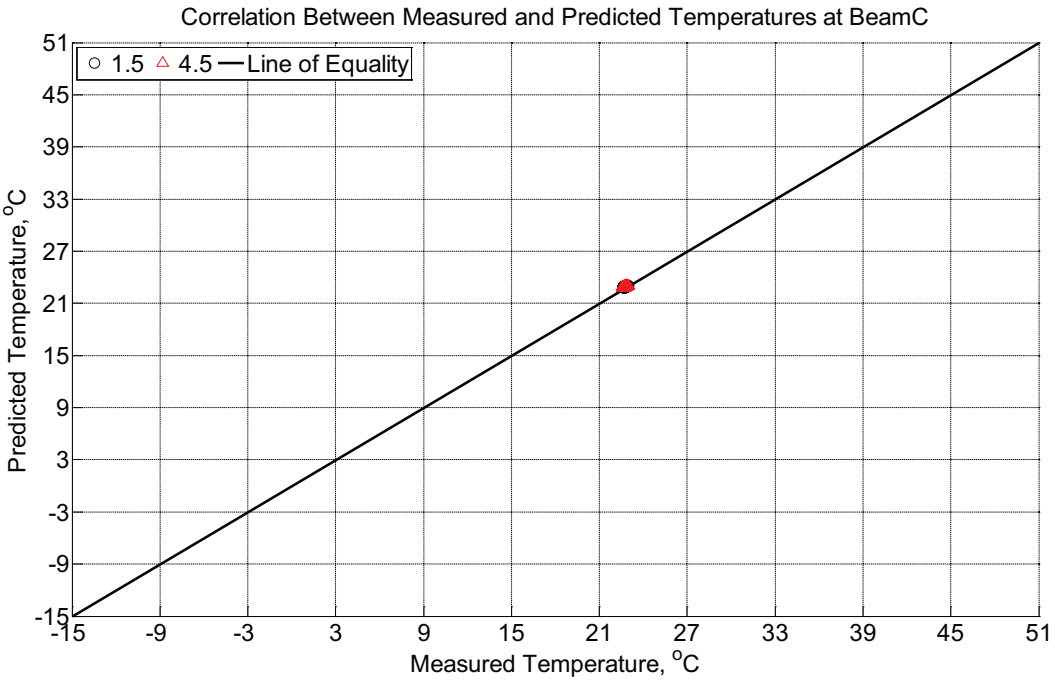

Figure B-320 Correlation between measured and predicted temperature values 1.5 inches (38.1 mm) and 4.5 inches (114.3 mm) from the surface of a modulus of rupture beam (labeled C) located inside an environmentally controlled room (50% RH, 23°C) between February 5, 2015, through March 20, 2015.

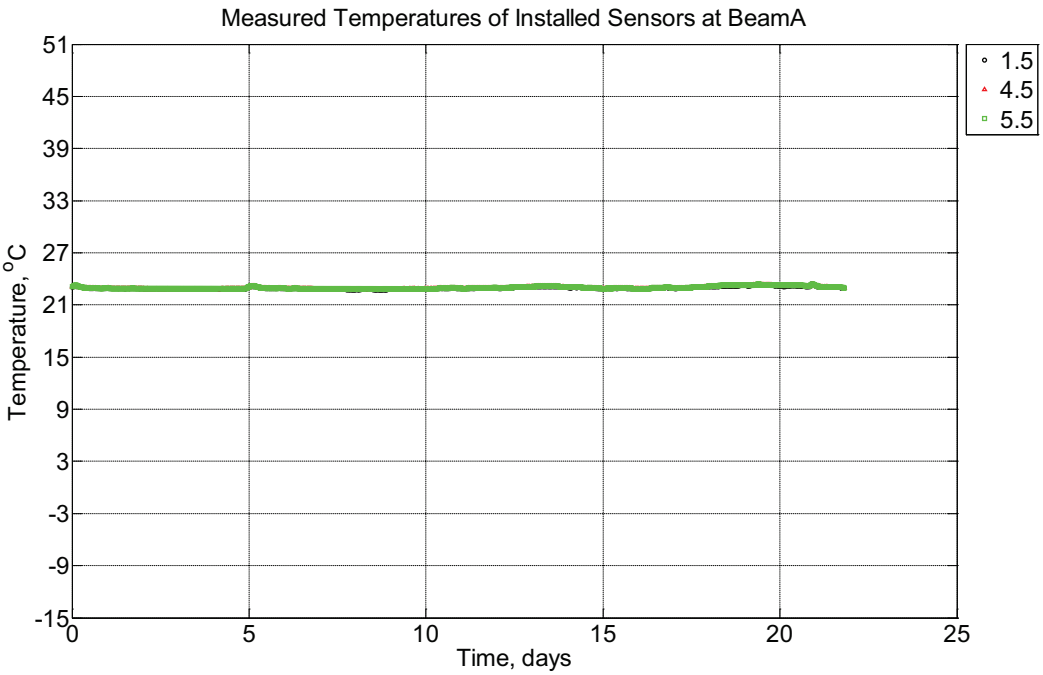

Figure B-321 Measured temperature at depths of 1.5 inches (38.1 mm), 4.5 inches (114.3 mm), and 5.5 inches (139.7 mm) from the surface of a modulus of rupture beam (labeled A) located inside an environmentally controlled room (50% RH, 23ºC) between March 20, 2015, through April 11, 2015.

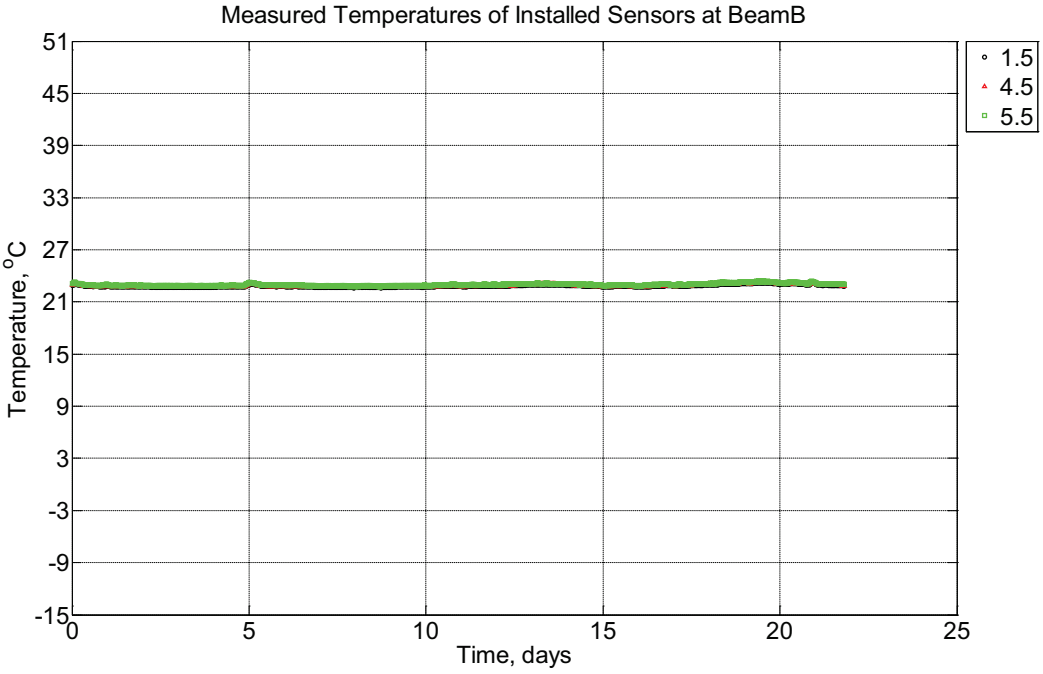

Figure B-322 Measured temperature at depths of 1.5 inches (38.1 mm), 4.5 inches (114.3 mm), and 5.5 inches (139.7 mm) from the surface of a modulus of rupture beam (labeled B)

located inside an environmentally controlled room (50% RH, 23°C) between March 20, 2015, through April 11, 2015.

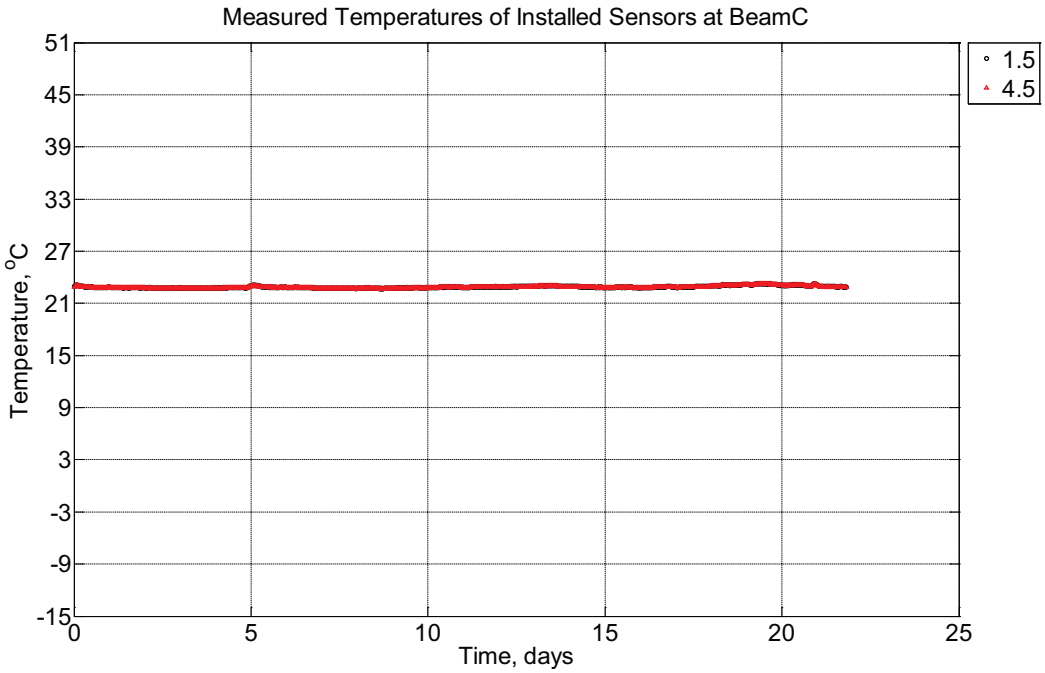

Figure B-323 Measured temperature at depths of 1.5 inches (38.1 mm) and 4.5 inches (114.3 mm) from the surface of a modulus of rupture beam (labeled C) located inside an environmentally controlled room (50% RH, 23°C) between March 20, 2015, through April 11, 2015.

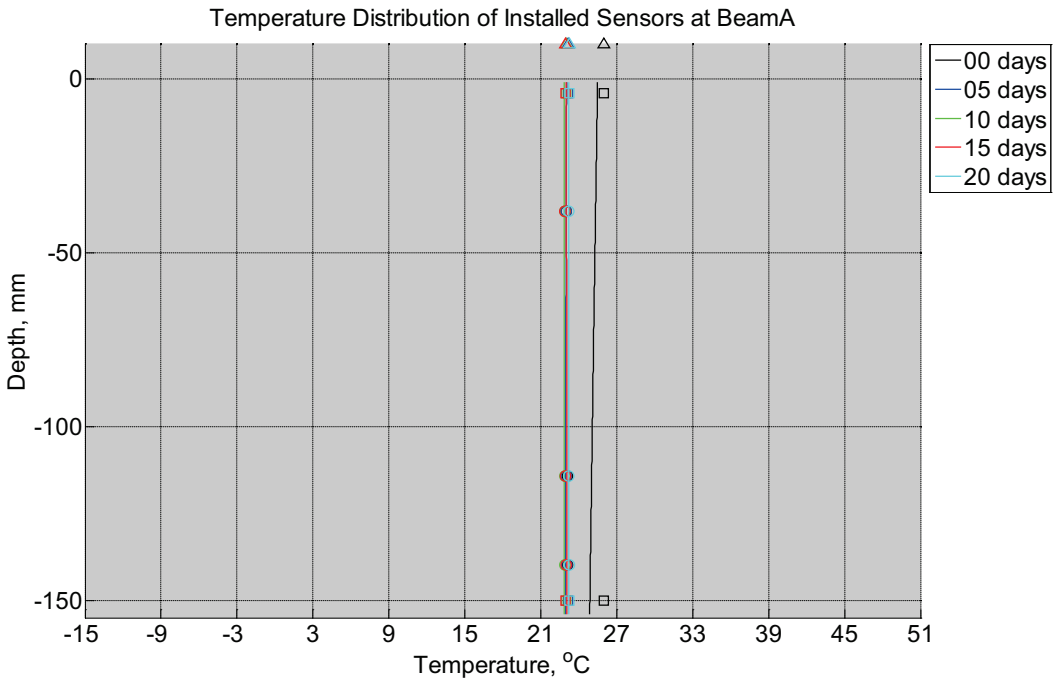

Figure B-324 Measured (markers) and modeled (continuous line) temperature profile distribution as a function of depth inside modulus of rupture beam (labeled A) located inside an environmentally controlled room (50% RH, 23°C) between March 20, 2015, through April 11, 2015. Triangular markers denote temperature value from control panel, square markers denote measured temperature values from ambient sensors, and circular markers denote measured temperature values inside concrete.

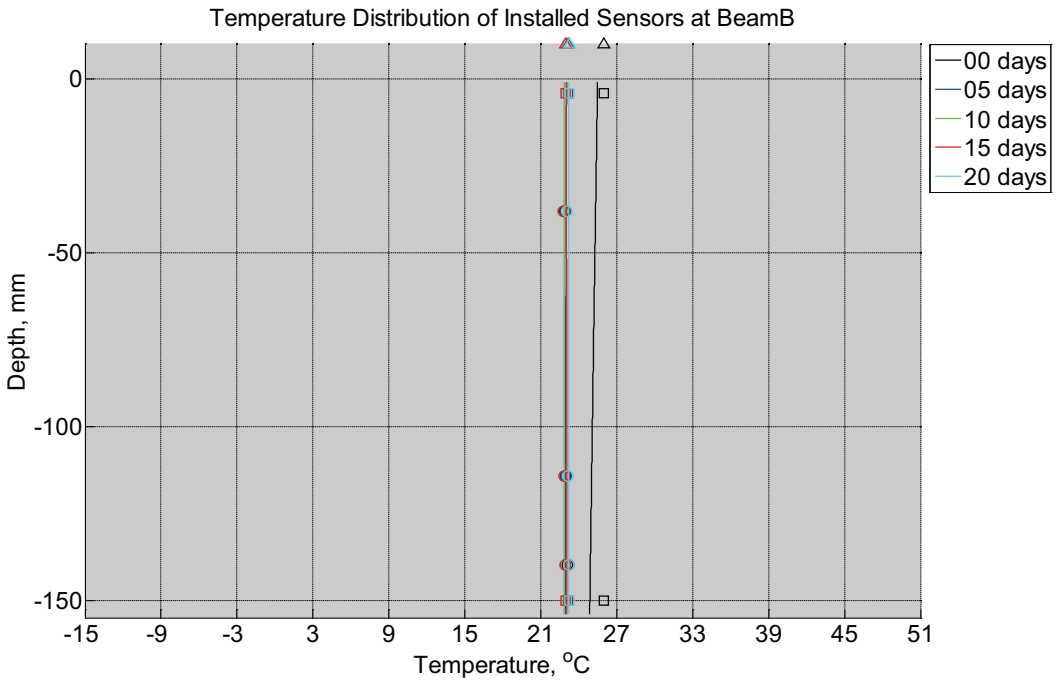

Figure B-325 Measured (markers) and modeled (continuous line) temperature profile distribution as a function of depth inside modulus of rupture beam (labeled B) located inside an environmentally controlled room (50% RH, 23°C) between March 20, 2015, through April 11, 2015. Triangular markers denote temperature value from control panel, square markers denote measured temperature values from ambient sensors, and circular markers denote measured temperature values inside concrete.

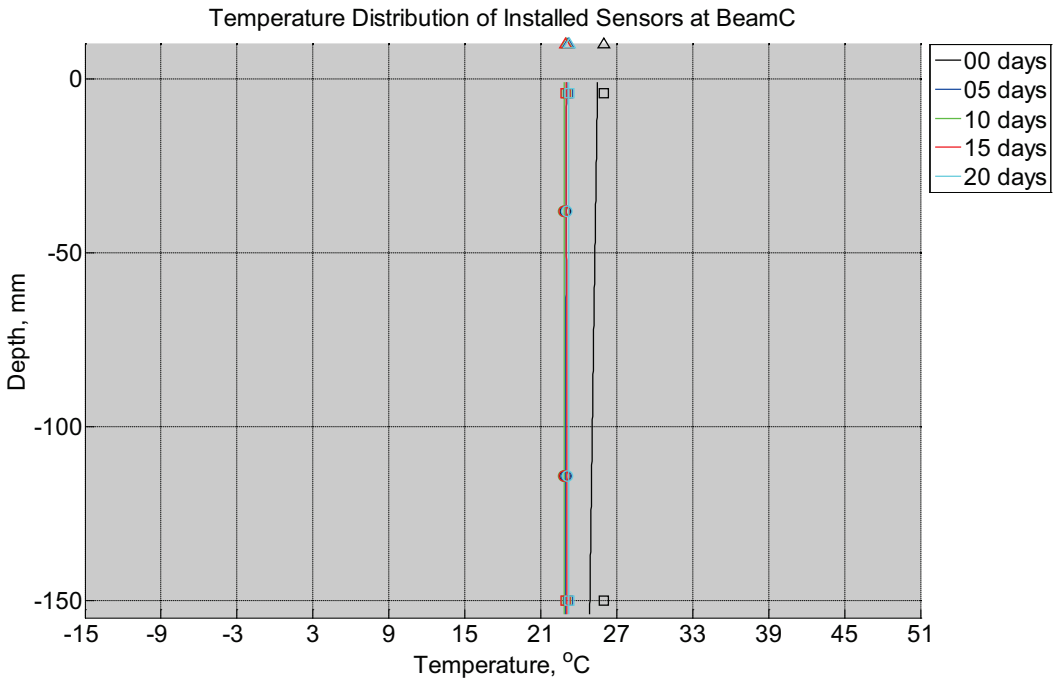

Figure B-326 Measured (markers) and modeled (continuous line) temperature profile distribution as a function of depth inside modulus of rupture beam (labeled C) located inside an environmentally controlled room (50% RH, 23°C) between March 20, 2015, through April 11, 2015. Triangular markers denote temperature value from control panel, square markers denote measured temperature values from ambient sensors, and circular markers denote measured temperature values inside concrete.

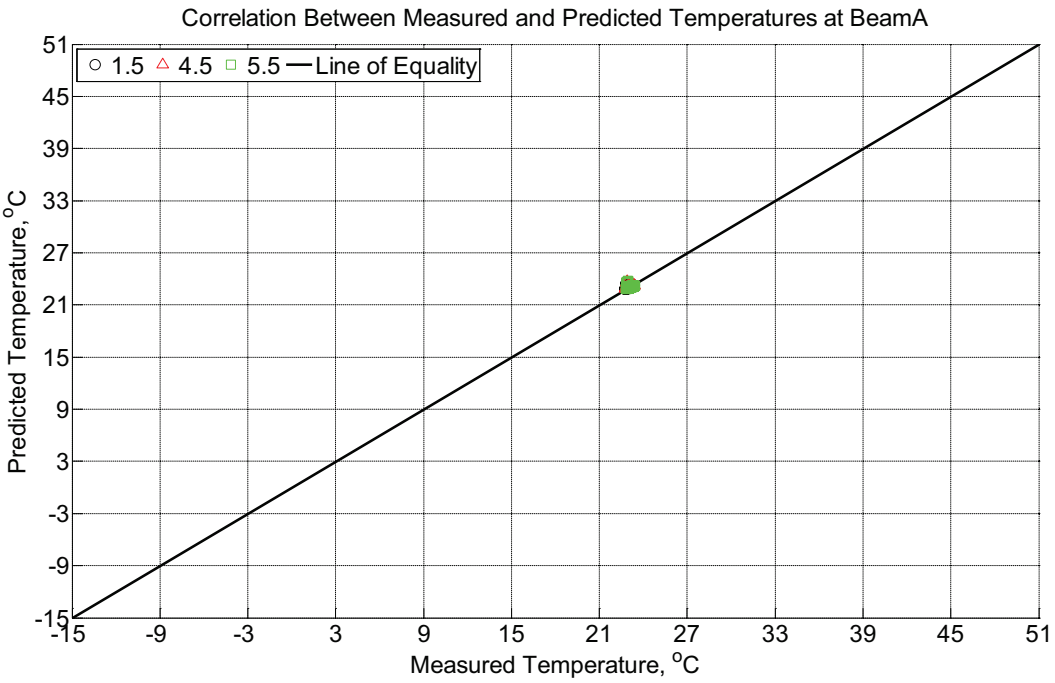

Figure B-327 Correlation between measured and predicted temperature values 1.5 inches (38.1 mm), 4.5 inches (114.3 mm), and 5.5 inches (139.7 mm) from the surface of a modulus of rupture beam (labeled A) located inside an environmentally controlled room (50% RH, 23°C) between March 20, 2015, through April 11, 2015.

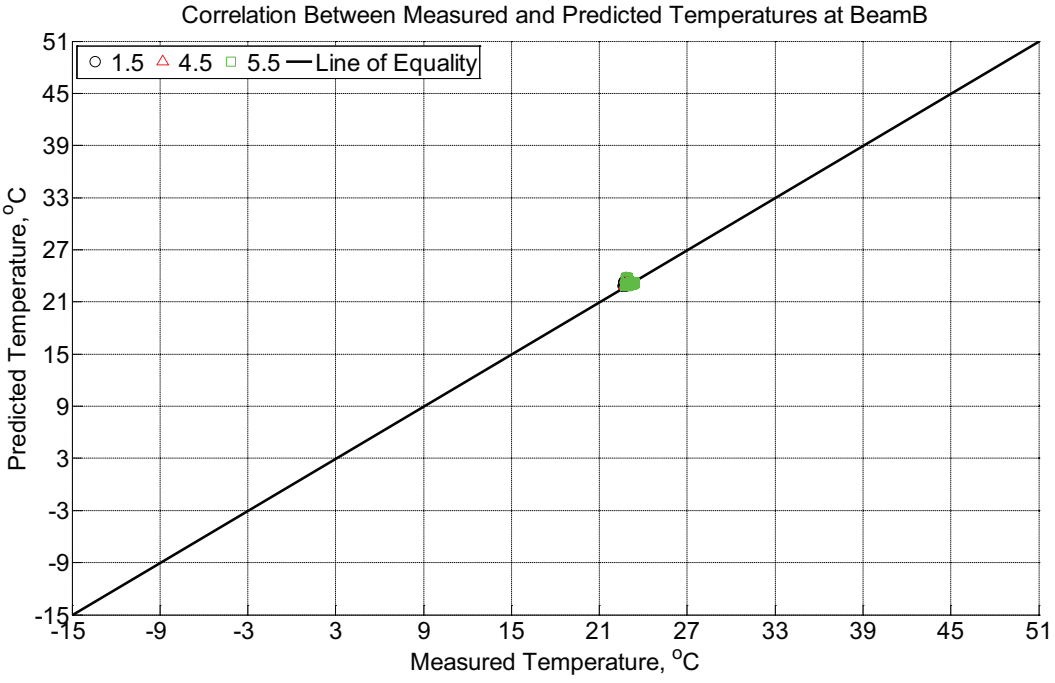

Figure B-328 Correlation between measured and predicted temperature values 1.5 inches (38.1 mm), 4.5 inches (114.3 mm), and 5.5 inches (139.7 mm) from the surface of a modulus

of rupture beam (labeled B) located inside an environmentally controlled room (50% RH, 23°C) between March 20, 2015, through April 11, 2015.

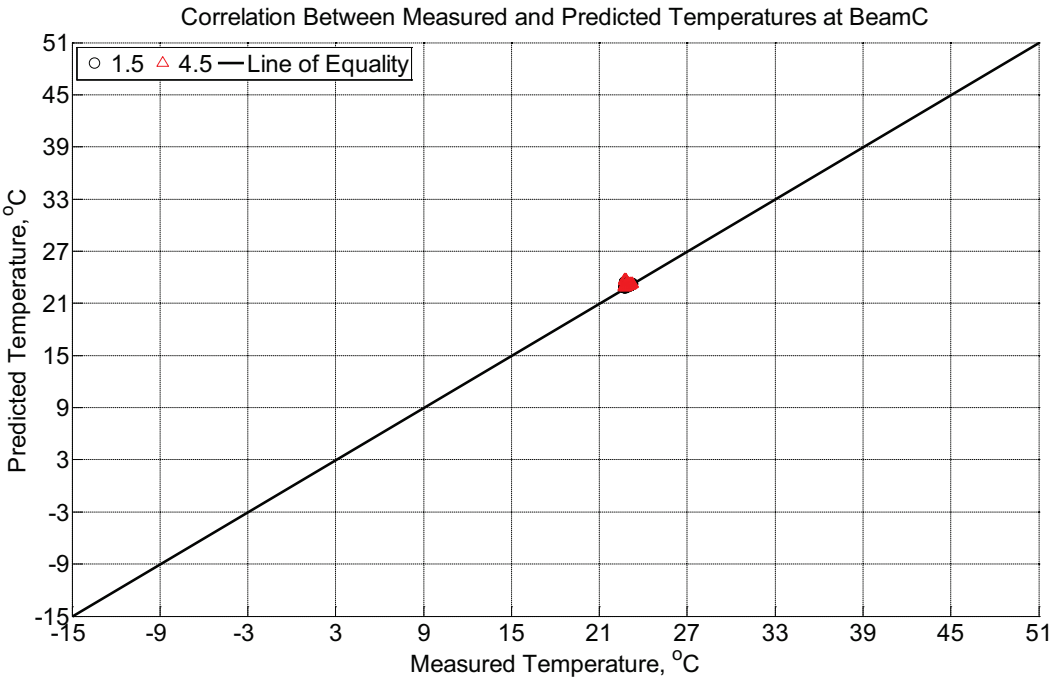

Figure B-329 Correlation between measured and predicted temperature values 1.5 inches (38.1 mm) and 4.5 inches (114.3 mm) from the surface of a modulus of rupture beam (labeled C) located inside an environmentally controlled room (50% RH, 23°C) between March 20, 2015, through April 11, 2015.

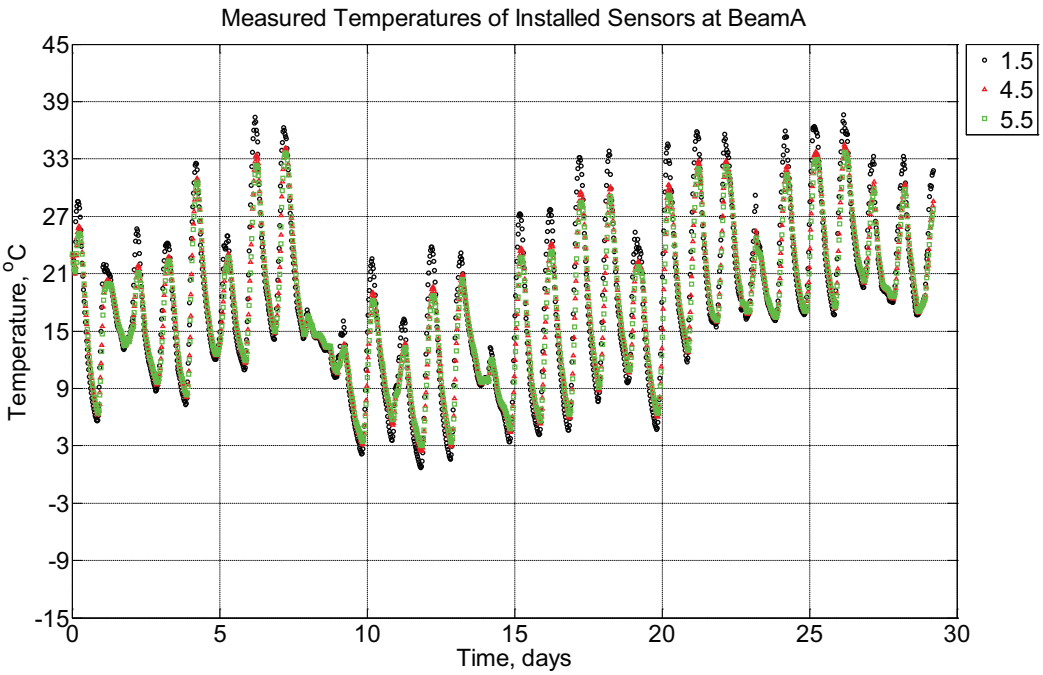

Figure B-330 Measured temperature at depths of 1.5 inches (38.1 mm), 4.5 inches (114.3 mm), and 5.5 inches (139.7 mm) from the surface of a modulus of rupture beam (labeled A) installed in ballast in Rantoul, IL, between April 11, 2015, through May 10, 2015.

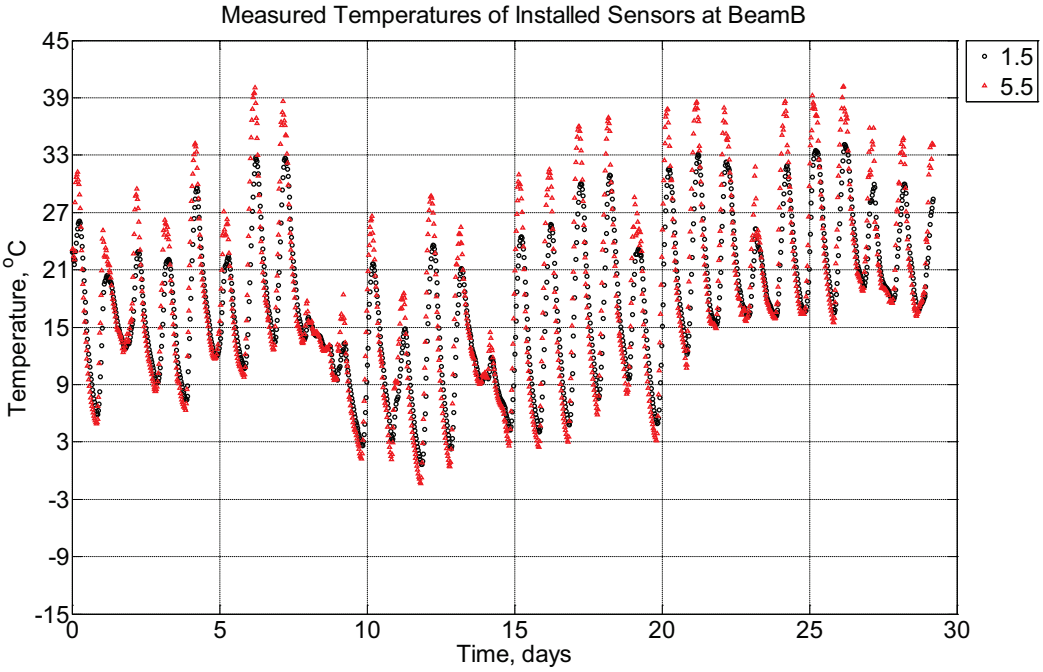

Figure B-331 Measured temperature at depths of 1.5 inches (38.1 mm) and 5.5 inches

(139.7 mm) from the surface of a modulus of rupture beam (labeled B) installed in ballast in Rantoul, IL, between April 11, 2015, through May 10, 2015.

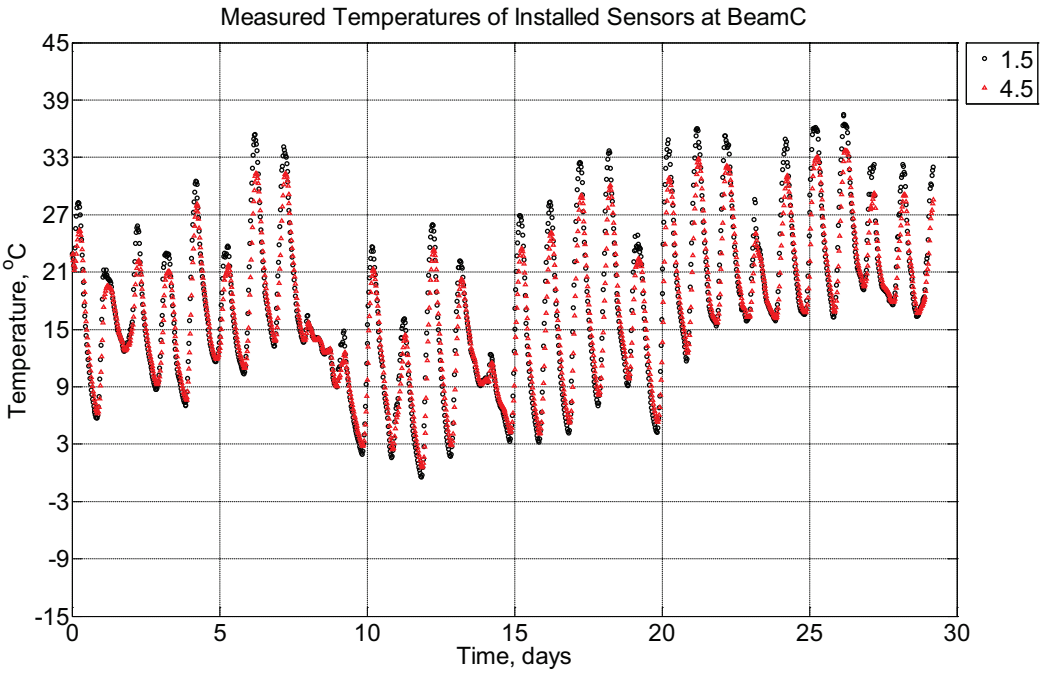

Figure B-332 Measured temperature at depths of 1.5 inches (38.1 mm) and 4.5 inches (114.3 mm from the surface of a modulus of rupture beam (labeled C) installed in ballast in Rantoul, IL, between April 11, 2015, through May 10, 2015.

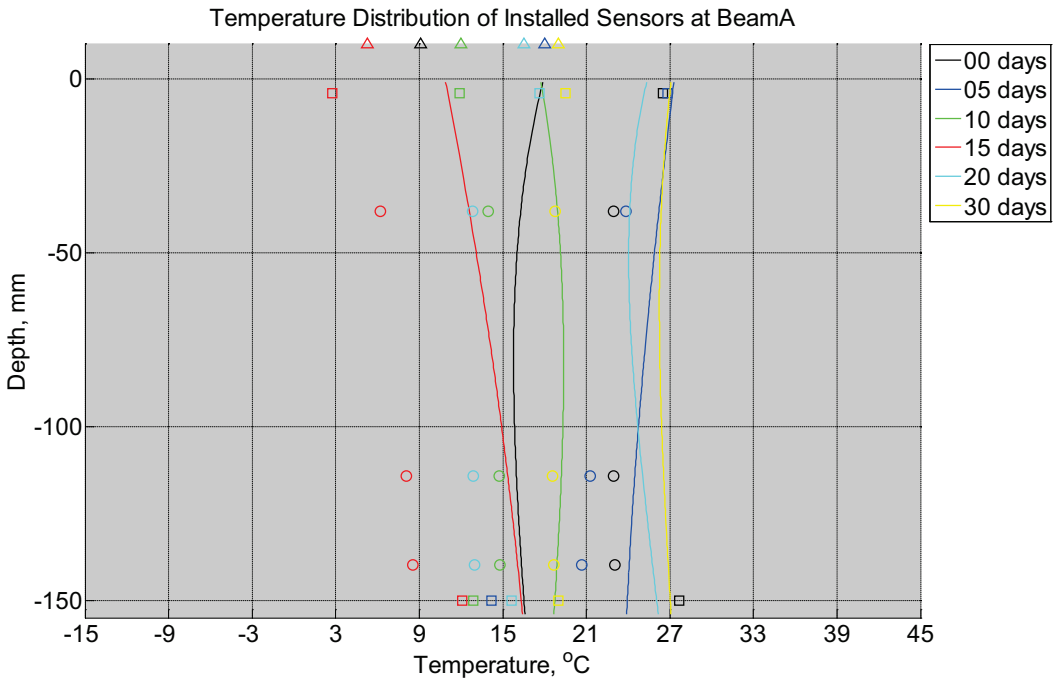

Figure B-333 Measured (markers) and modeled (continuous line) temperature distribution as a function of depth inside modulus of rupture beam (labeled A) installed in ballast in Rantoul, IL, between April 11, 2015, through May 10, 2015. Triangular markers denote temperature value from KTIP weather station, square markers denote measured temperature values from ballast, and circular markers denote measured temperature values inside concrete.

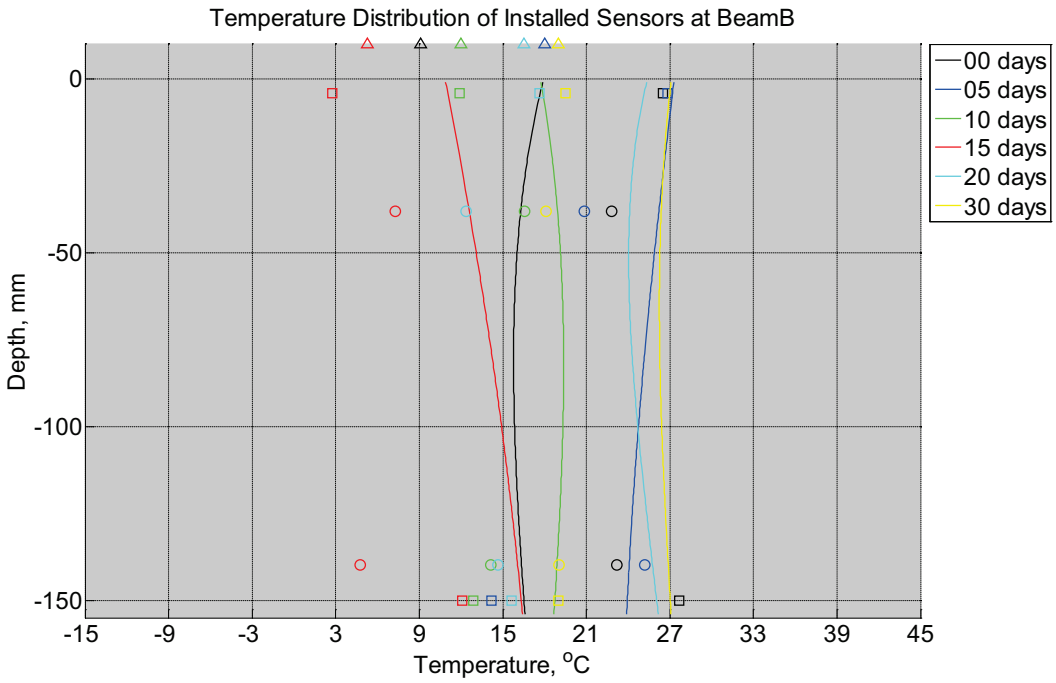

Figure B-334 Measured (markers) and modeled (continuous line) temperature distribution as a function of depth inside modulus of rupture beam (labeled B) installed in ballast in Rantoul, IL, between April 11, 2015, through May 10, 2015. Triangular markers denote temperature value from KTIP weather station, square markers denote measured temperature values from ballast, and circular markers denote measured temperature values inside concrete.

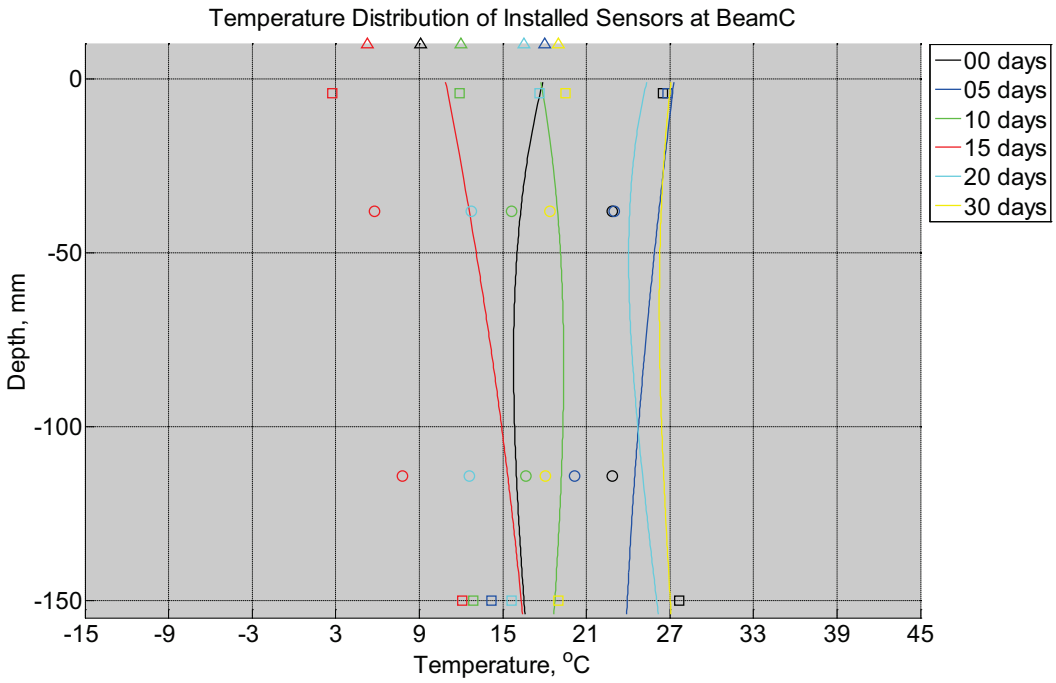

Figure B-335 Measured (markers) and modeled (continuous line) temperature distribution as a function of depth inside modulus of rupture beam (labeled C) installed in ballast in Rantoul, IL, between April 11, 2015, through May 10, 2015. Triangular markers denote temperature value from KTIP weather station, square markers denote measured temperature values from ballast, and circular markers denote measured temperature values inside concrete.

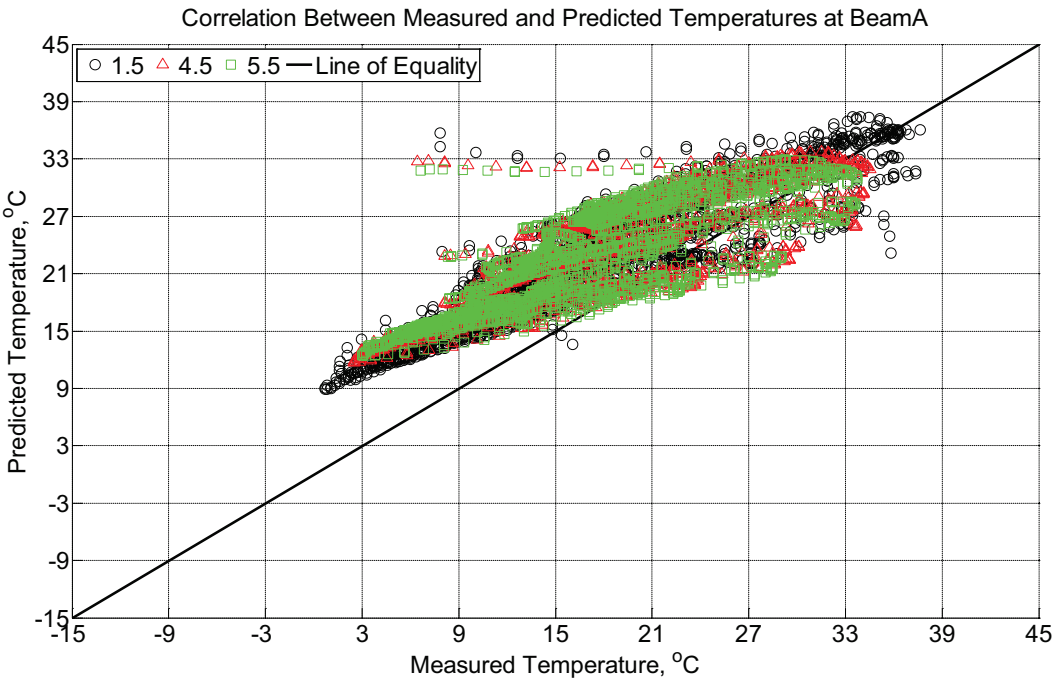

Figure B-336 Correlation between measured and predicted temperature values 1.5 inches (38.1 mm), 4.5 inches (114.3 mm), and 5.5 inches (139.7 mm) from the surface of a modulus of rupture beam (labeled A) installed in ballast in Rantoul, IL, between April 11, 2015, through May 10, 2015.

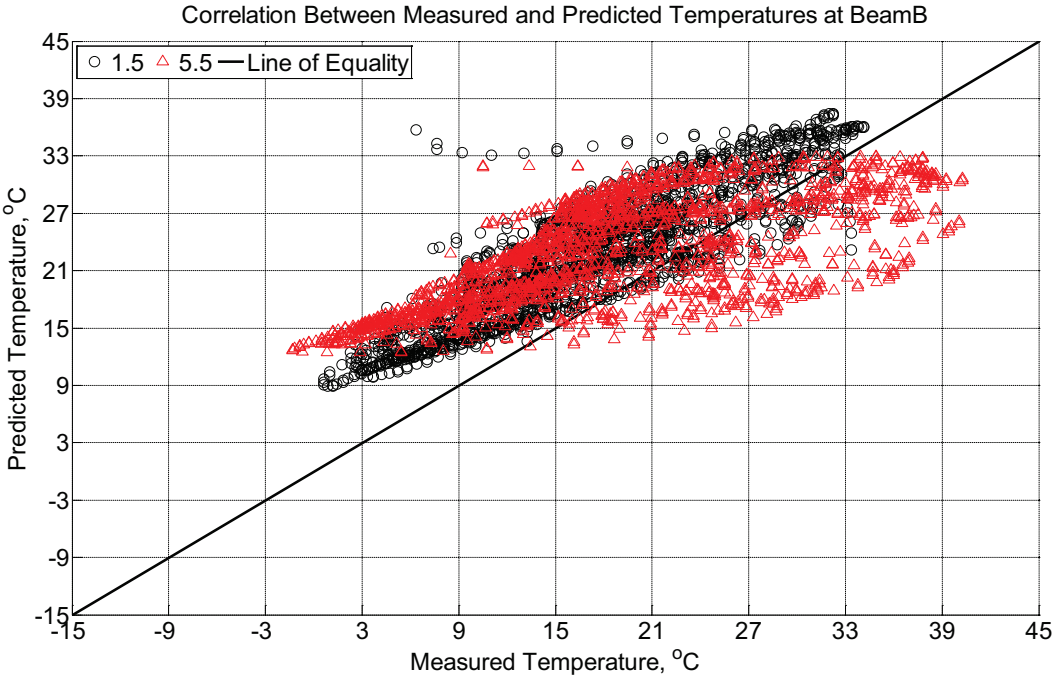

Figure B-337 Correlation between measured and predicted temperature values 1.5 inches (38.1 mm) and 5.5 inches (139.7 mm) from the surface of a modulus of rupture beam

(labeled B) installed in ballast in Rantoul, IL, between April 11, 2015, through May 10, 2015.

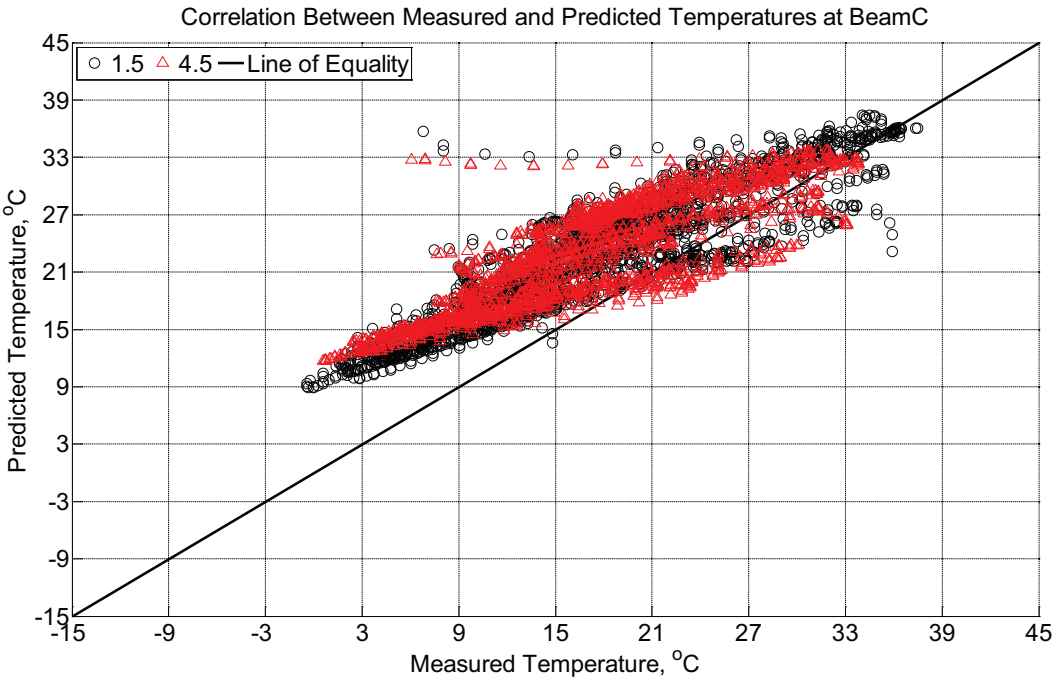

Figure B-338 Correlation between measured and predicted temperature values 1.5 inches (38.1 mm) and 4.5 inches (114.3 mm) from the surface of a modulus of rupture beam (labeled C) installed in ballast in Rantoul, IL, between April 11, 2015, through May 10, 2015.

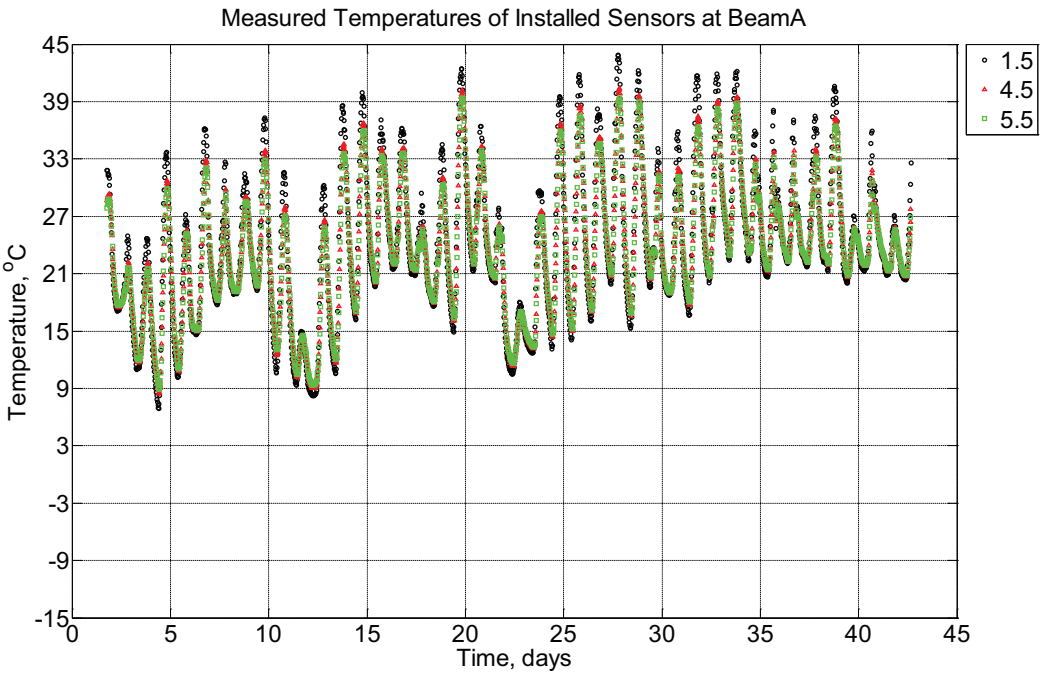

Figure B-339 Measured temperature at depths of 1.5 inches (38.1 mm), 4.5 inches (114.3 mm), and 5.5 inches (139.7 mm) from the surface of a modulus of rupture beam (labeled A) installed in ballast in Rantoul, IL, between May 10, 2015, through June 20, 2015.

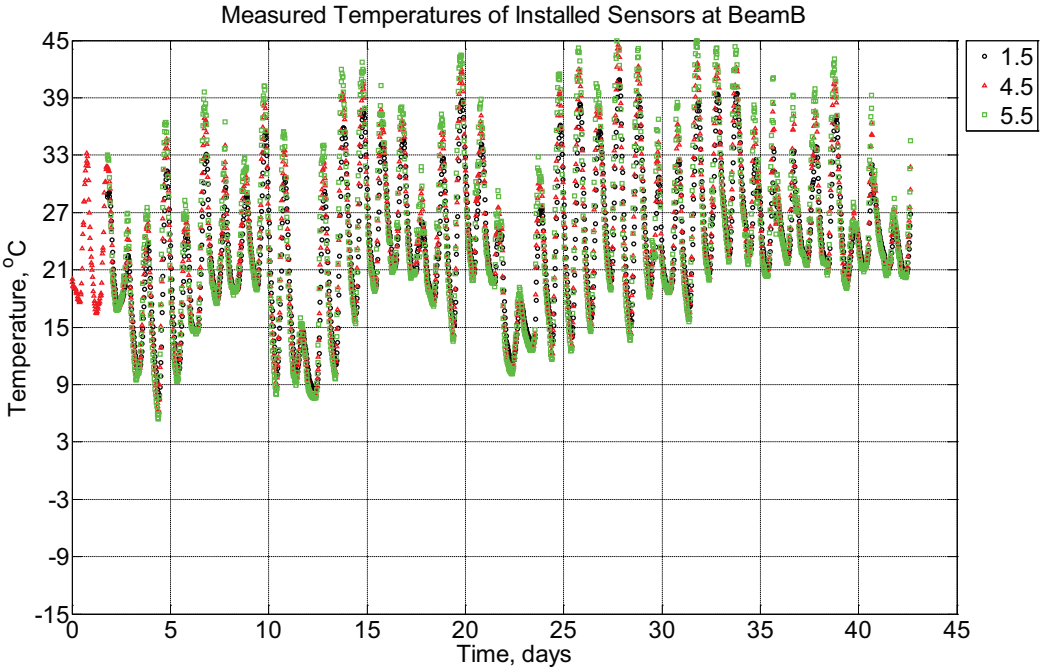

Figure B-340 Measured temperature at depths of 1.5 inches (38.1 mm), 4.5 inches (114.3

mm), and 5.5 inches (139.7 mm) from the surface of a modulus of rupture beam (labeled B) installed in ballast in Rantoul, IL, between May 10, 2015, through June 20, 2015.

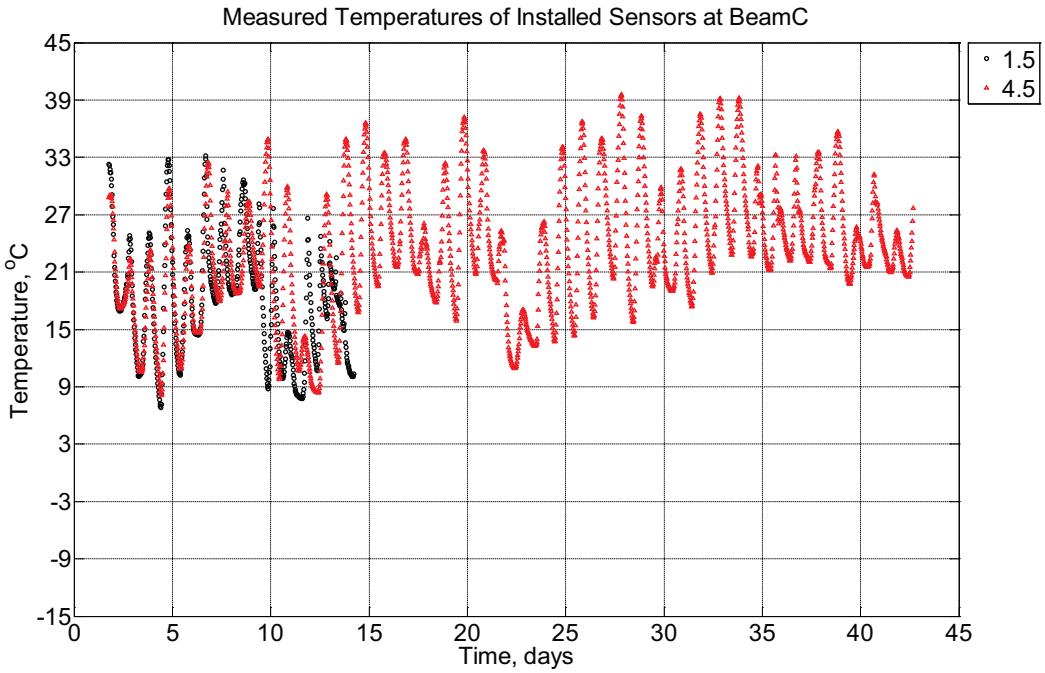

Figure B-341 Measured temperature at depths of 1.5 inches (38.1 mm) and 4.5 inches (114.3 mm), from the surface of a modulus of rupture beam (labeled C) installed in ballast in Rantoul, IL, between May 10, 2015, through June 20, 2015.

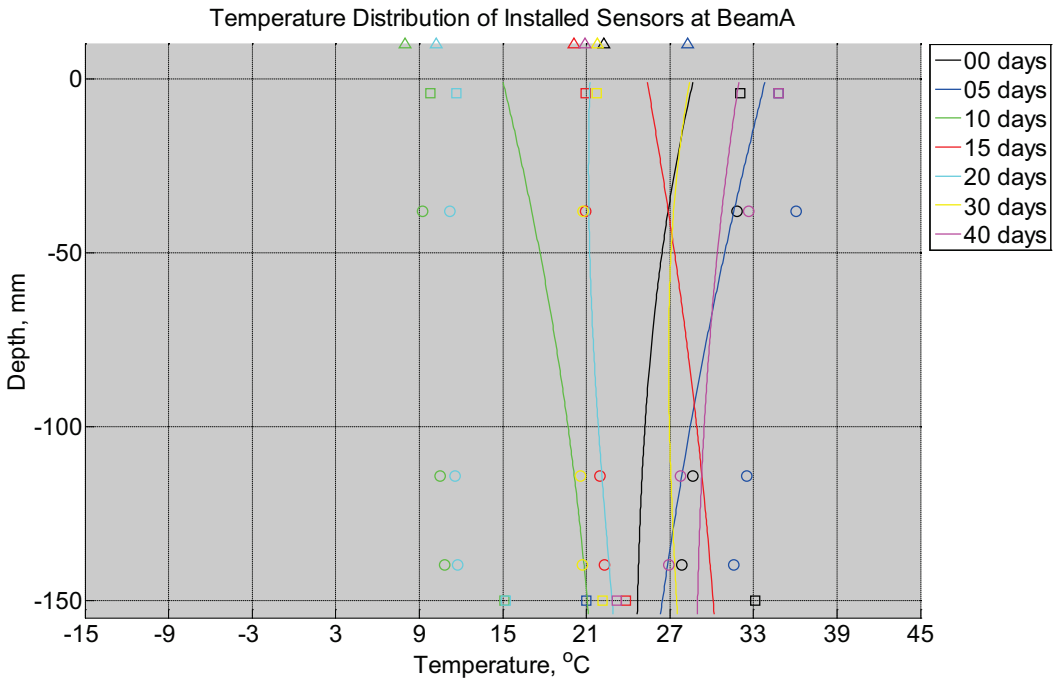

Figure B-342 Measured (markers) and modeled (continuous line) temperature distribution as a function of depth inside modulus of rupture beam (labeled A) installed in ballast in Rantoul, IL, between May 10, 2015, through June 20, 2015. Triangular markers denote temperature value from KTIP weather station, square markers denote measured temperature values from ballast, and circular markers denote measured temperature values inside concrete.

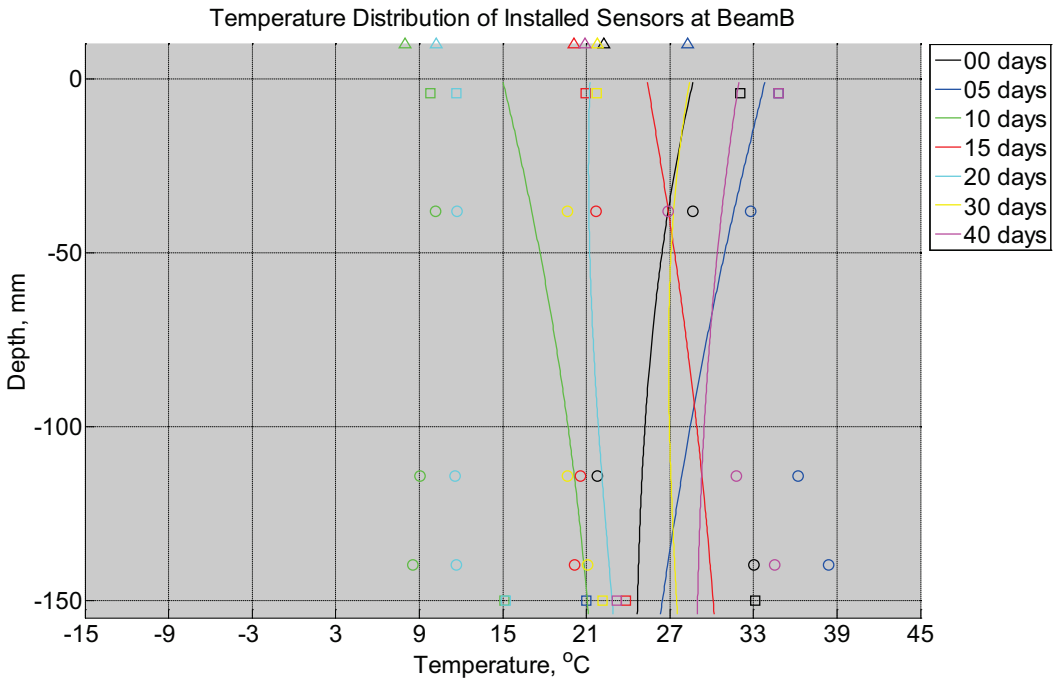

Figure B-343 Measured (markers) and modeled (continuous line) temperature distribution as a function of depth inside modulus of rupture beam (labeled A) installed in ballast in Rantoul, IL, between May 10, 2015, through June 20, 2015. Triangular markers denote temperature value from KTIP weather station, square markers denote measured temperature values from ballast, and circular markers denote measured temperature values inside concrete.

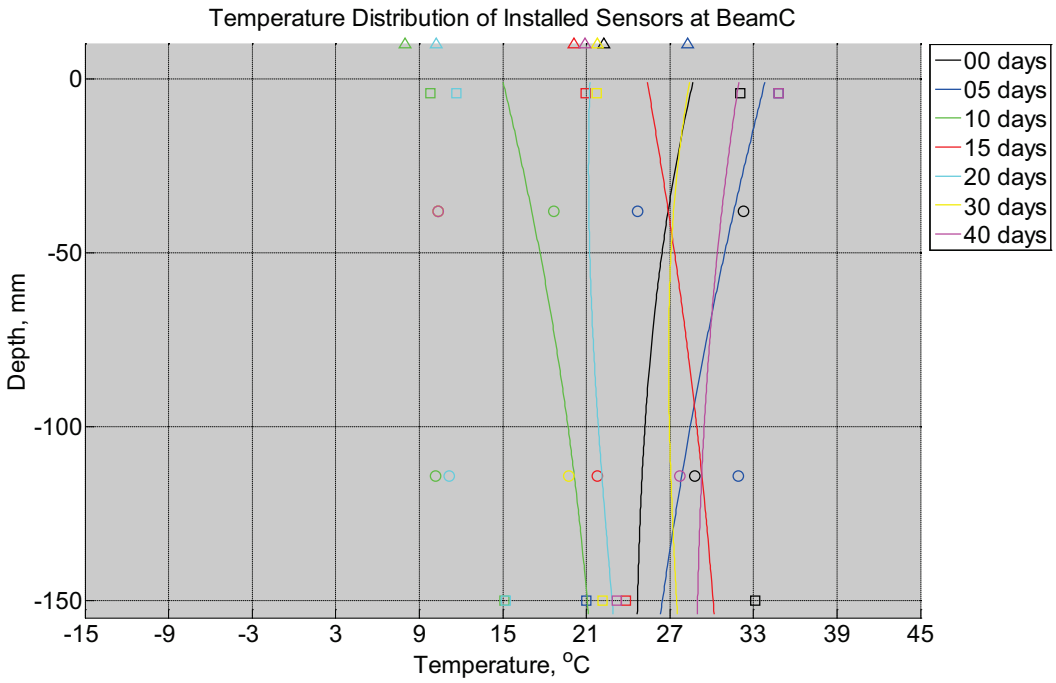

Figure B-344 Measured (markers) and modeled (continuous line) temperature distribution as a function of depth inside modulus of rupture beam (labeled A) installed in ballast in Rantoul, IL, between May 10, 2015, through June 20, 2015. Triangular markers denote temperature value from KTIP weather station, square markers denote measured temperature values from ballast, and circular markers denote measured temperature values inside concrete.

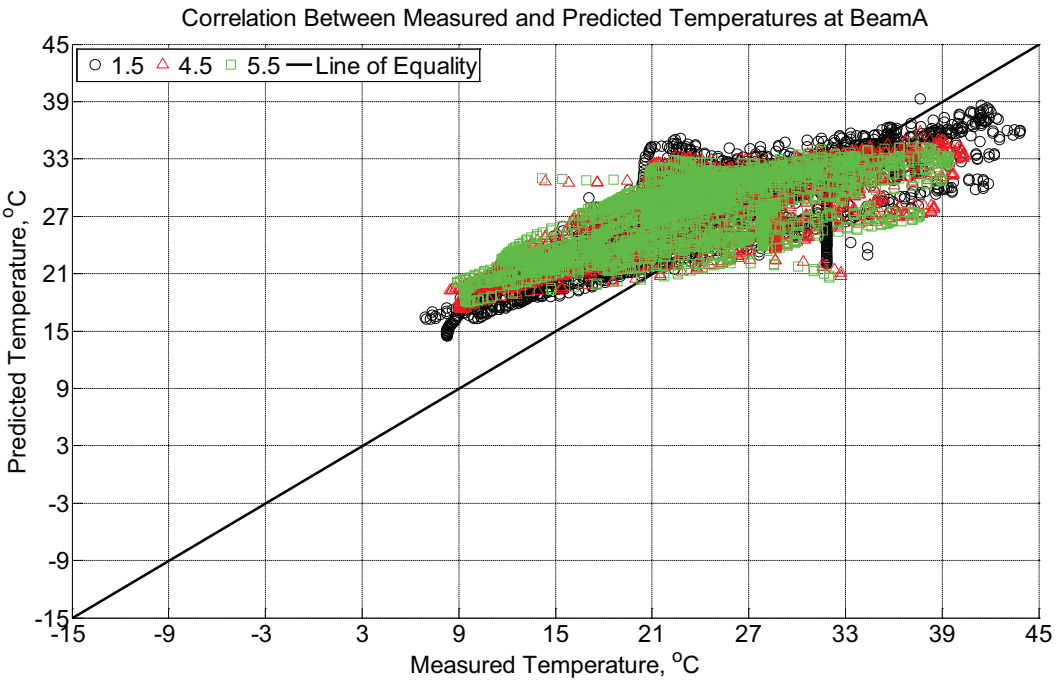

Figure B-345 Correlation between measured and predicted temperature values 1.5 inches (38.1 mm), 4.5 inches (114.3 mm), and 5.5 inches (139.7 mm) from the surface of a modulus of rupture beam (labeled A) installed in ballast in Rantoul, IL, between A May 10, 2015, through June 20, 2015.

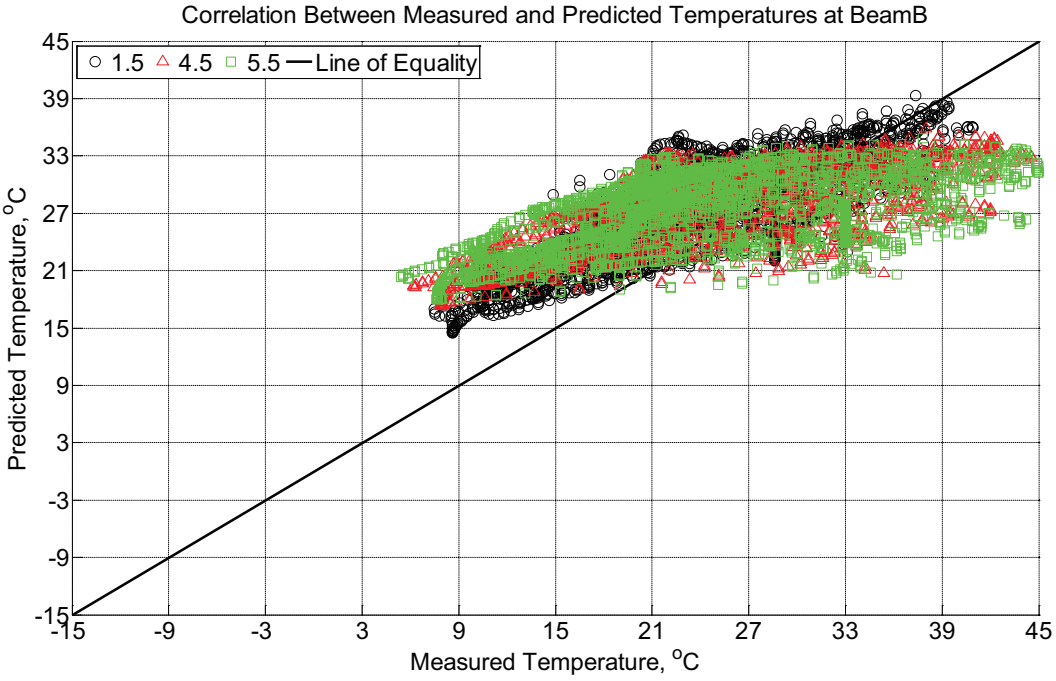

Figure B-346 Correlation between measured and predicted temperature values 1.5 inches (38.1 mm), 4.5 inches (114.3 mm), and 5.5 inches (139.7 mm) from the surface of a modulus

of rupture beam (labeled B) installed in ballast in Rantoul, IL, between A May 10, 2015, through June 20, 2015.

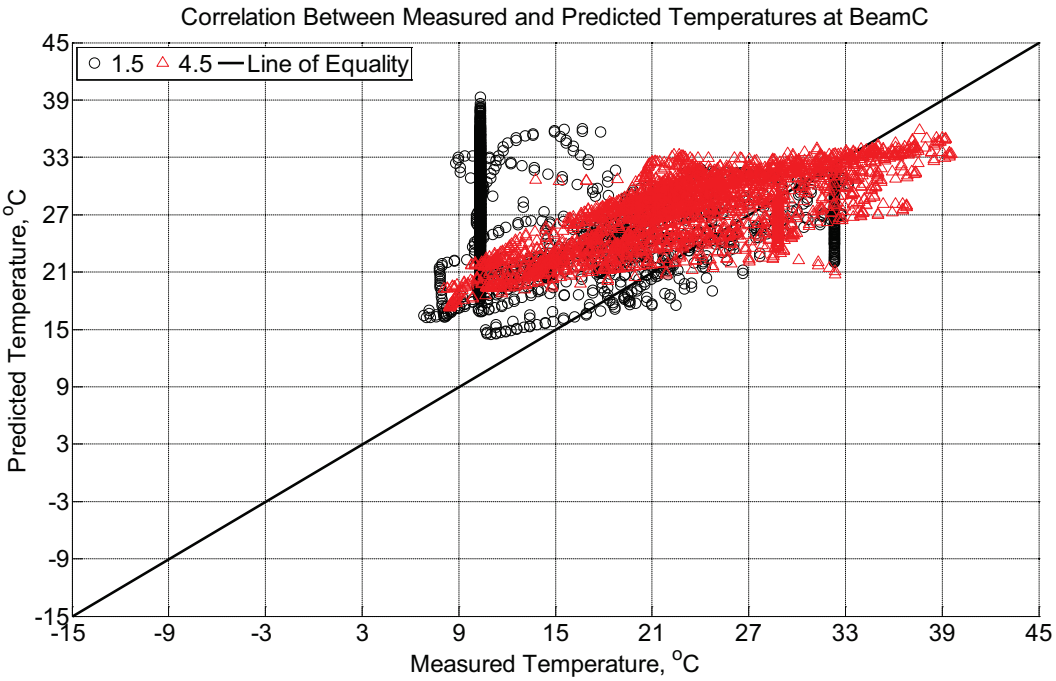

Figure B-347 Correlation between measured and predicted temperature values 1.5 inches (38.1 mm) and 4.5 inches (114.3 mm) from the surface of a modulus of rupture beam (labeled C) installed in ballast in Rantoul, IL, between A May 10, 2015, through June 20, 2015.

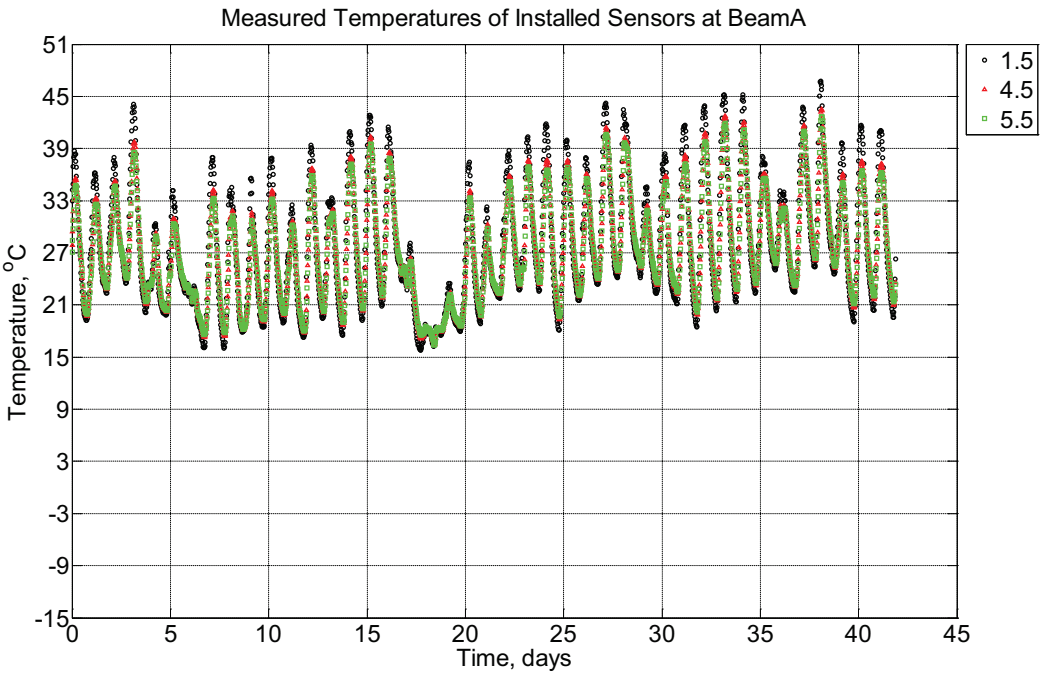

Figure B-348 Measured temperature at depths of 1.5 inches (38.1 mm), 4.5 inches (114.3 mm), and 5.5 inches (139.7 mm) from the surface of a modulus of rupture beam (labeled A) installed in ballast in Rantoul, IL, between June 20, 2015, through August 1, 2015.

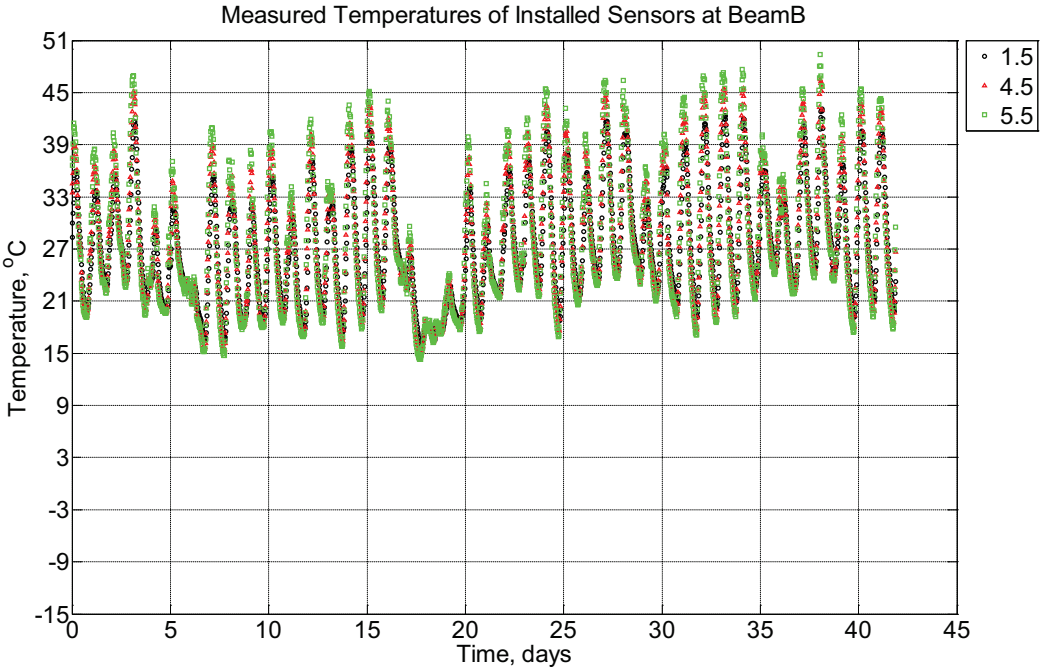

Figure B-349 Measured temperature at depths of 1.5 inches (38.1 mm), 4.5 inches (114.3

mm), and 5.5 inches (139.7 mm) from the surface of a modulus of rupture beam (labeled B) installed in ballast in Rantoul, IL, between June 20, 2015, through August 1, 2015.

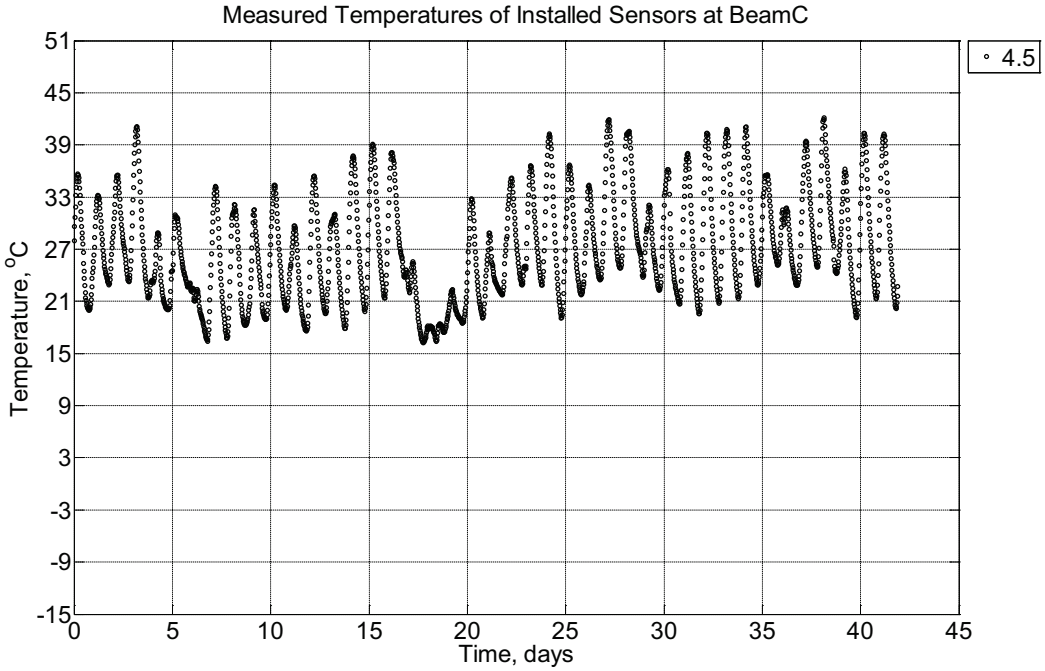

Figure B-350 Measured temperature at depths of 4.5 inches (114.3 mm) from the surface of a modulus of rupture beam (labeled C) installed in ballast in Rantoul, IL, between June 20, 2015, through August 1, 2015.

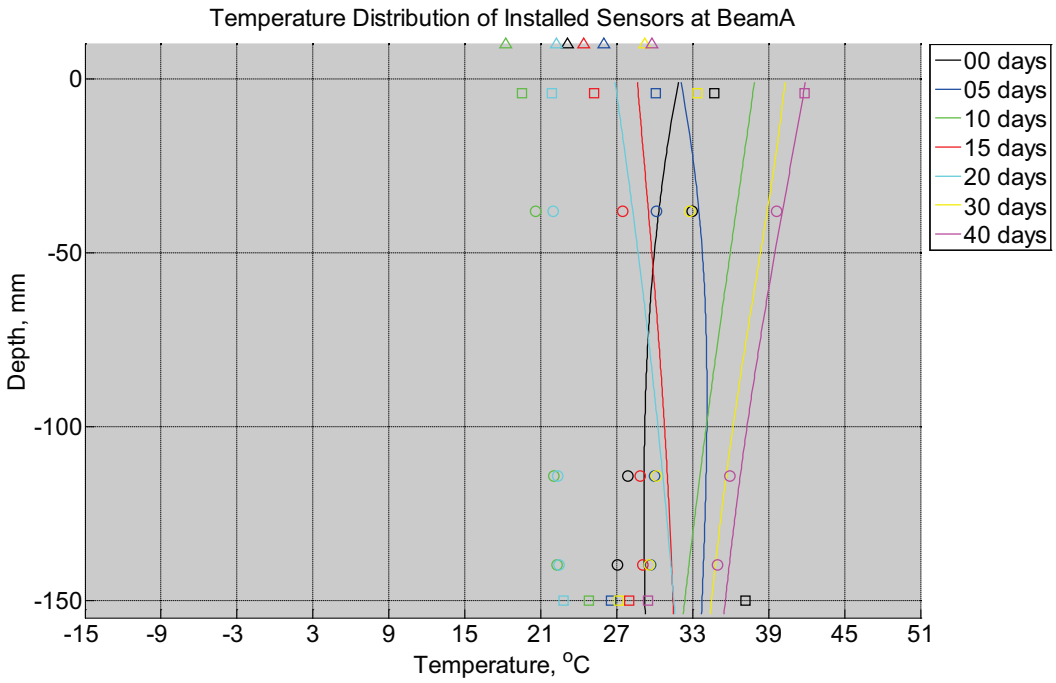

Figure B-351 Measured (markers) and modeled (continuous line) temperature distribution as a function of depth inside modulus of rupture beam (labeled A) installed in ballast in Rantoul, IL, between June 20, 2015, through August 1, 2015. Triangular markers denote temperature value from KTIP weather station, square markers denote measured temperature values from ballast, and circular markers denote measured temperature values inside concrete.

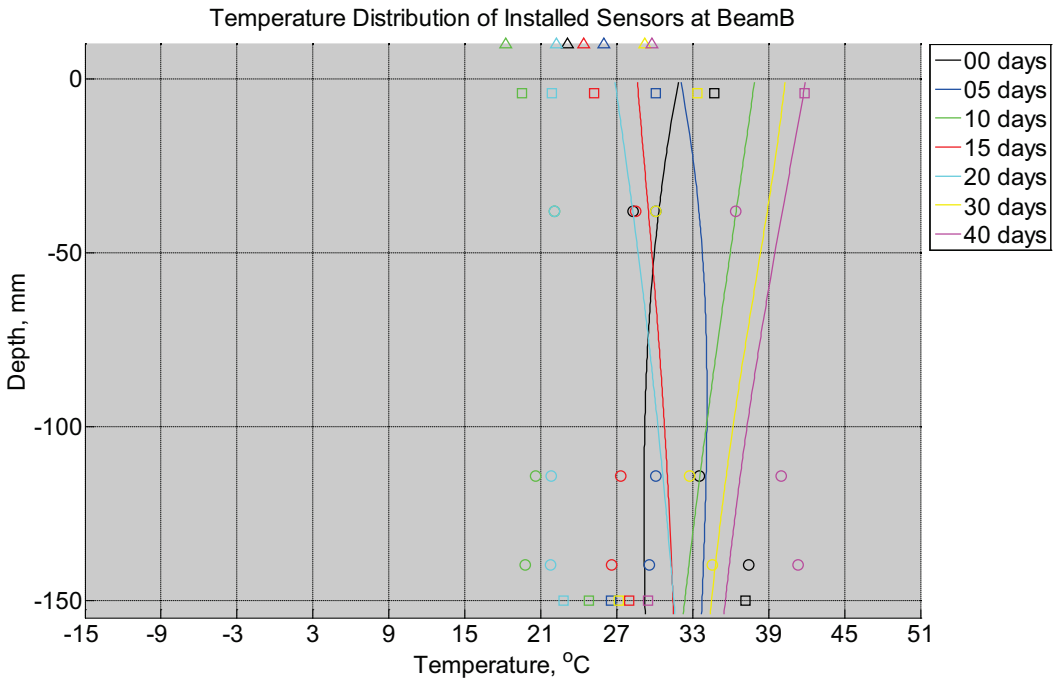

Figure B-352 Measured (markers) and modeled (continuous line) temperature distribution as a function of depth inside modulus of rupture beam (labeled B) installed in ballast in Rantoul, IL, between June 20, 2015, through August 1, 2015. Triangular markers denote temperature value from KTIP weather station, square markers denote measured temperature values from ballast, and circular markers denote measured temperature values inside concrete.

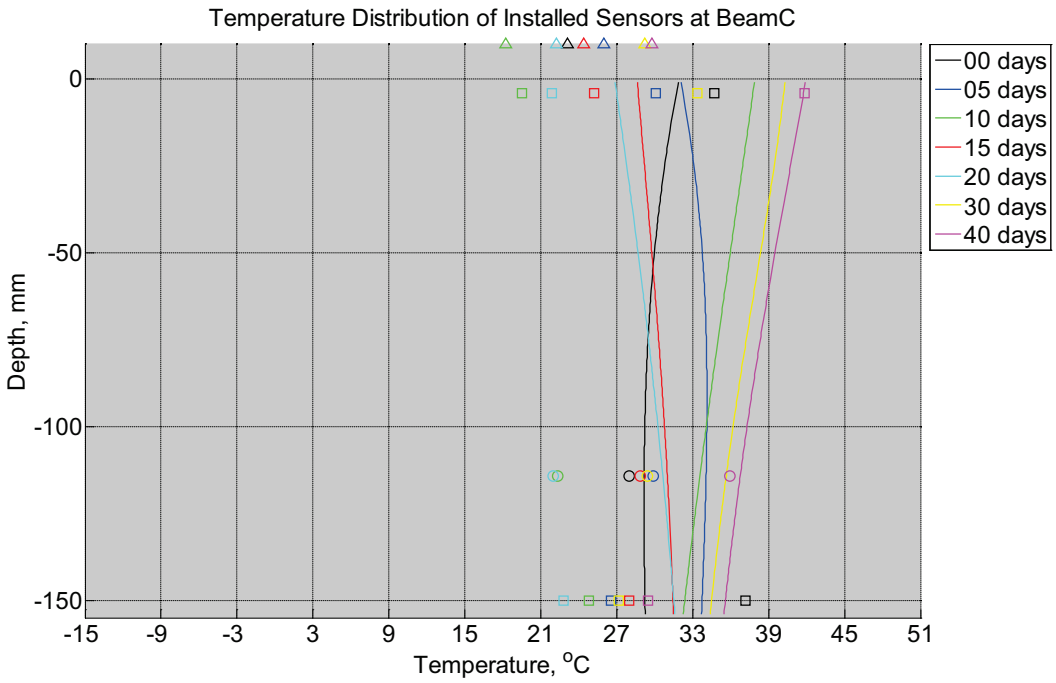

Figure B-353 Measured (markers) and modeled (continuous line) temperature distribution as a function of depth inside modulus of rupture beam (labeled C) installed in ballast in Rantoul, IL, between June 20, 2015, through August 1, 2015. Triangular markers denote temperature value from KTIP weather station, square markers denote measured temperature values from ballast, and circular markers denote measured temperature values inside concrete.

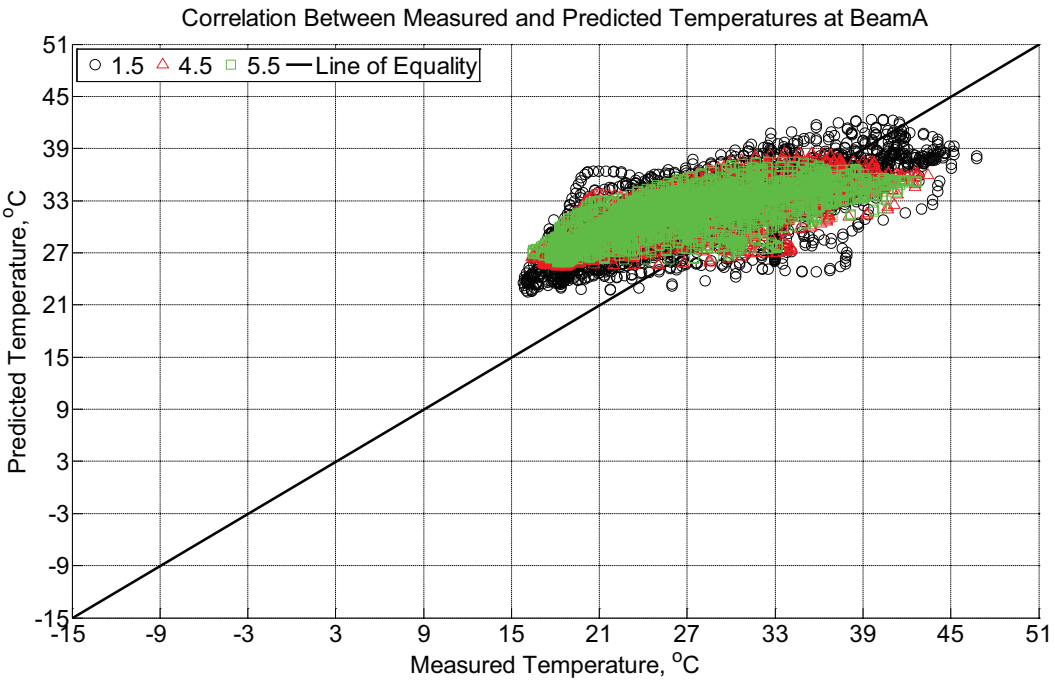

Figure B-354 Correlation between measured and predicted temperature values 1.5 inches (38.1 mm), 4.5 inches (114.3 mm), and 5.5 inches (139.7 mm) from the surface of a modulus of rupture beam (labeled A) installed in ballast in Rantoul, IL, between June 20, 2015, through August 1, 2015.

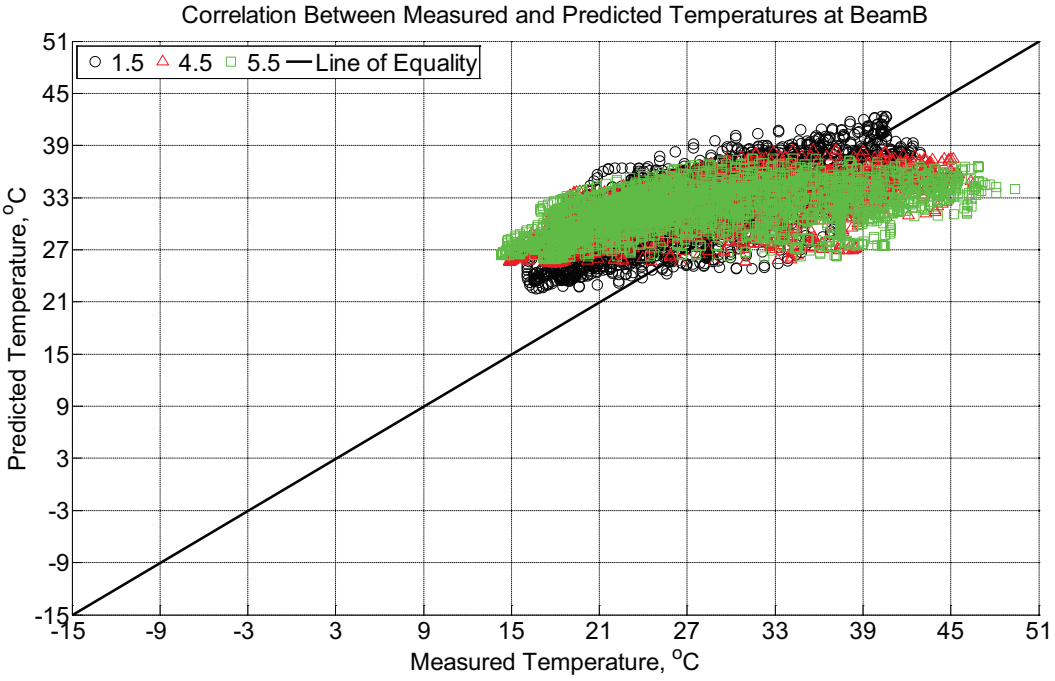

Figure B-355 Correlation between measured and predicted temperature values 1.5 inches (38.1 mm), 4.5 inches (114.3 mm), and 5.5 inches (139.7 mm) from the surface of a modulus

of rupture beam (labeled B) installed in ballast in Rantoul, IL, between June 20, 2015, through August 1, 2015.

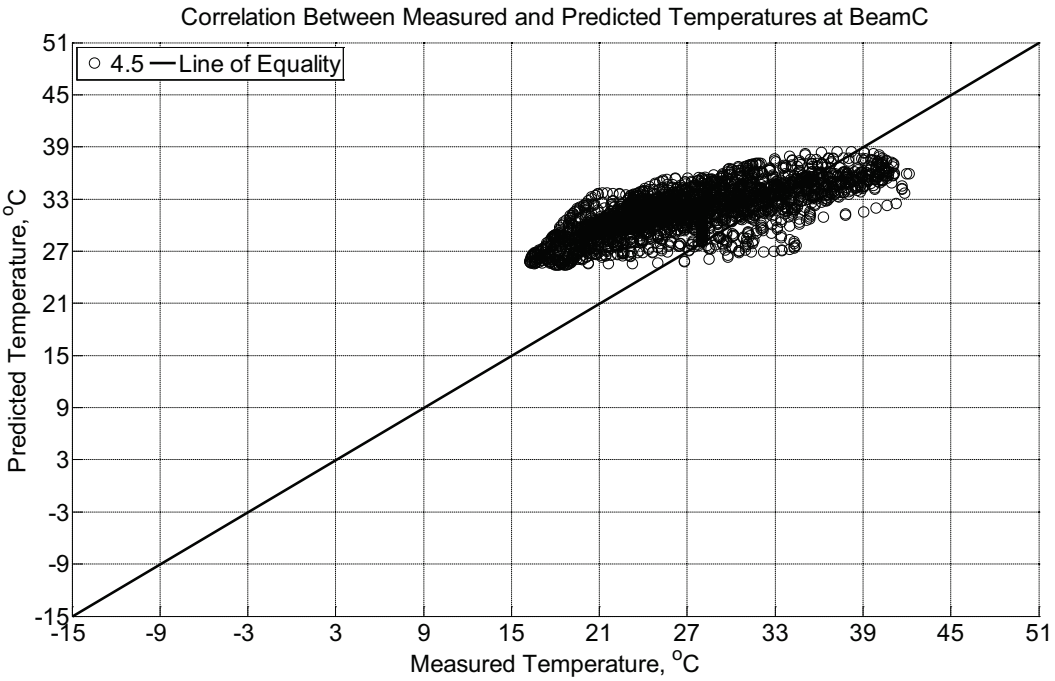

Figure B-356 Correlation between measured and predicted temperature values 4.5 inches (114.3 mm) from the surface of a modulus of rupture beam (labeled C) installed in ballast in Rantoul, IL, between June 20, 2015, through August 1, 2015.

Measured and predicted internal relative humidity of instrumented concrete crossties located in Champaign and Rantoul, IL

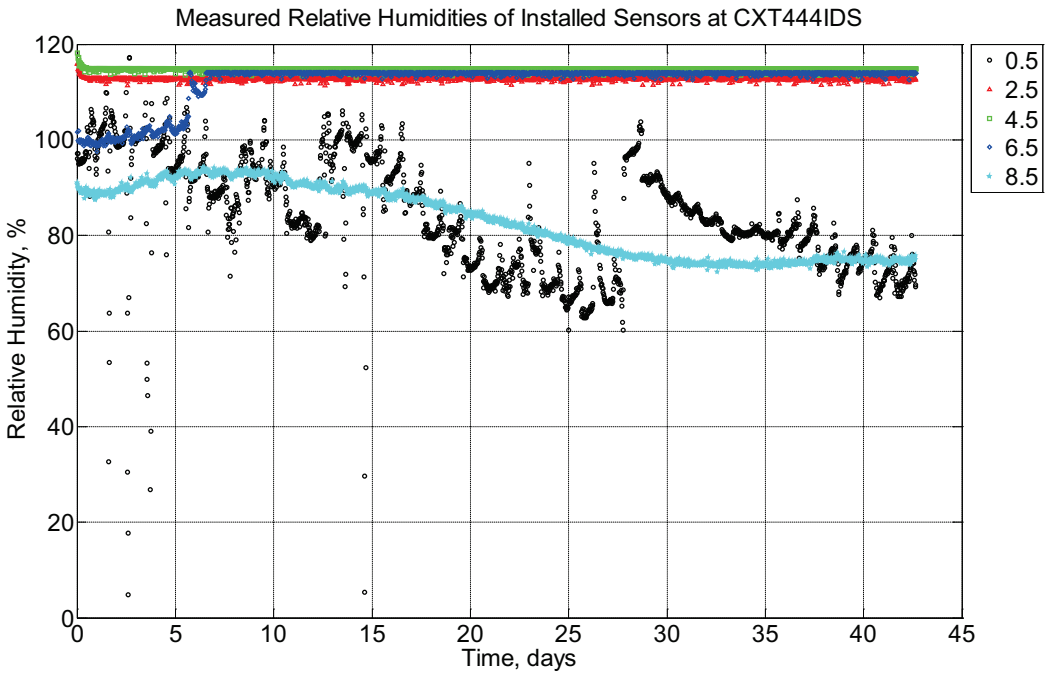

Figure B-357 Measured relative humidity at depths of 0.5 inches (12.7 mm), 2.5 inches (63.5 mm), 4.5 inches (114.3 mm), 6.5 inches (139.7 mm), and 8.5 inches (215.9 mm) from the surface of a concrete crosstie (labeled CXT444IDS) without a polyurethane pad nor rail as transported from Tucson, AZ, to Champaign, IL, between July 23, 2013, through September 4, 2013.

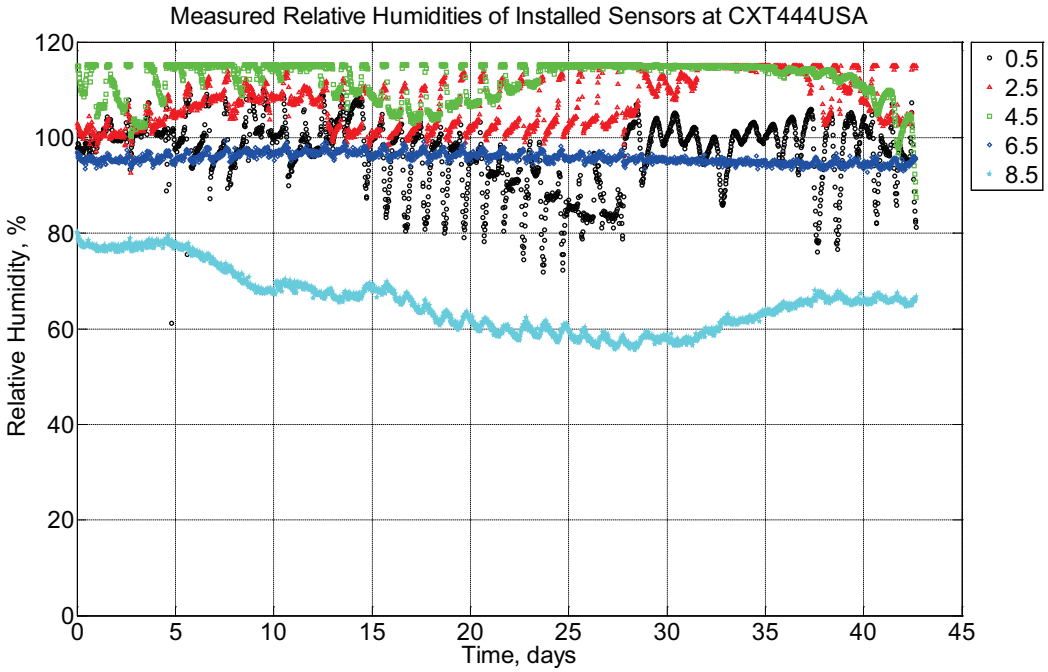

Figure B-358 Measured relative humidity at depths of 0.5 inches (12.7 mm), 2.5 inches (63.5

mm), 4.5 inches (114.3 mm), 6.5 inches (139.7 mm), and 8.5 inches (215.9 mm) from the surface of a concrete crosstie (labeled CXT444USA) without a polyurethane pad nor rail as transported from Tucson, AZ, to Champaign, IL, between July 23, 2013, through September 4, 2013.

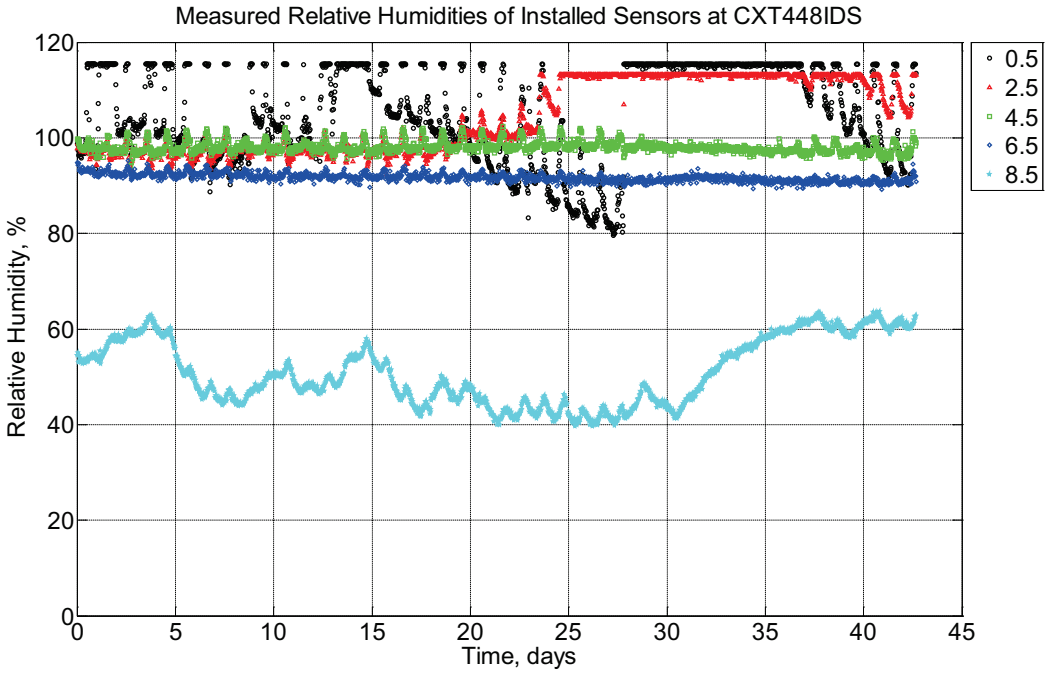

Figure B-359 Measured relative humidity at depths of 0.5 inches (12.7 mm), 2.5 inches (63.5 mm), 4.5 inches (114.3 mm), 6.5 inches (139.7 mm), and 8.5 inches (215.9 mm) from the surface of a concrete crosstie (labeled CXT448IDS) without a polyurethane pad nor rail as transported from Tucson, AZ, to Champaign, IL between July 23, 2013, through September 4, 2013.

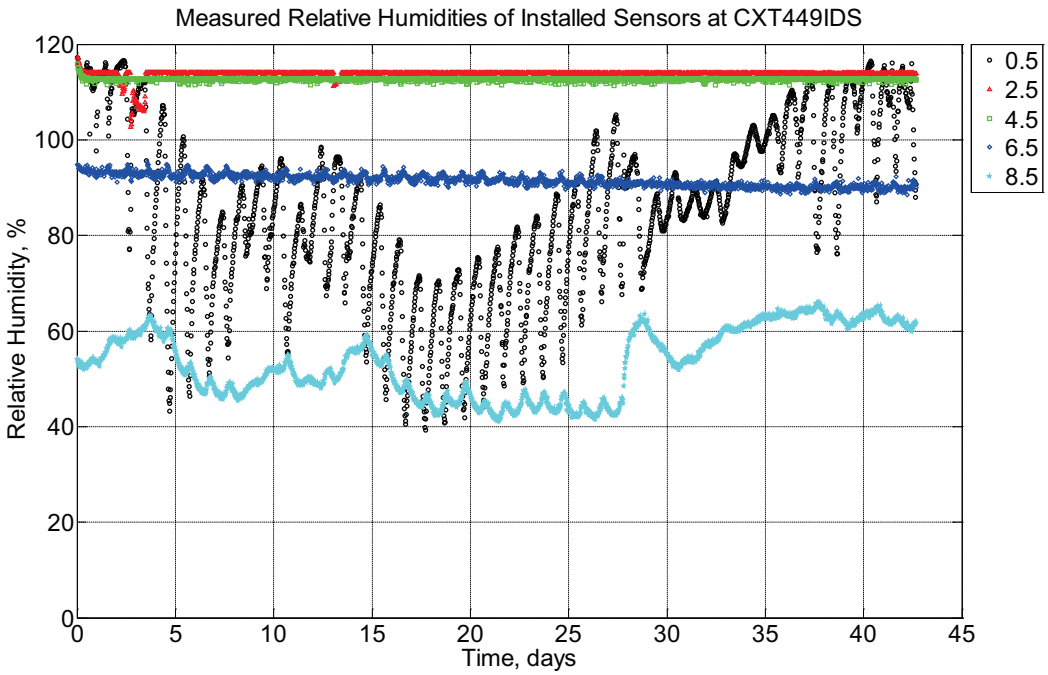

Figure B-360 Measured relative humidity at depths of 0.5 inches (12.7 mm), 2.5 inches (63.5 mm), 4.5 inches (114.3 mm), 6.5 inches (139.7 mm), and 8.5 inches (215.9 mm) from the surface of a concrete crosstie (labeled CXT449IDS) without a polyurethane pad nor rail as transported from Tucson, AZ, to Champaign, IL, between July 23, 2013, through September 4, 2013.

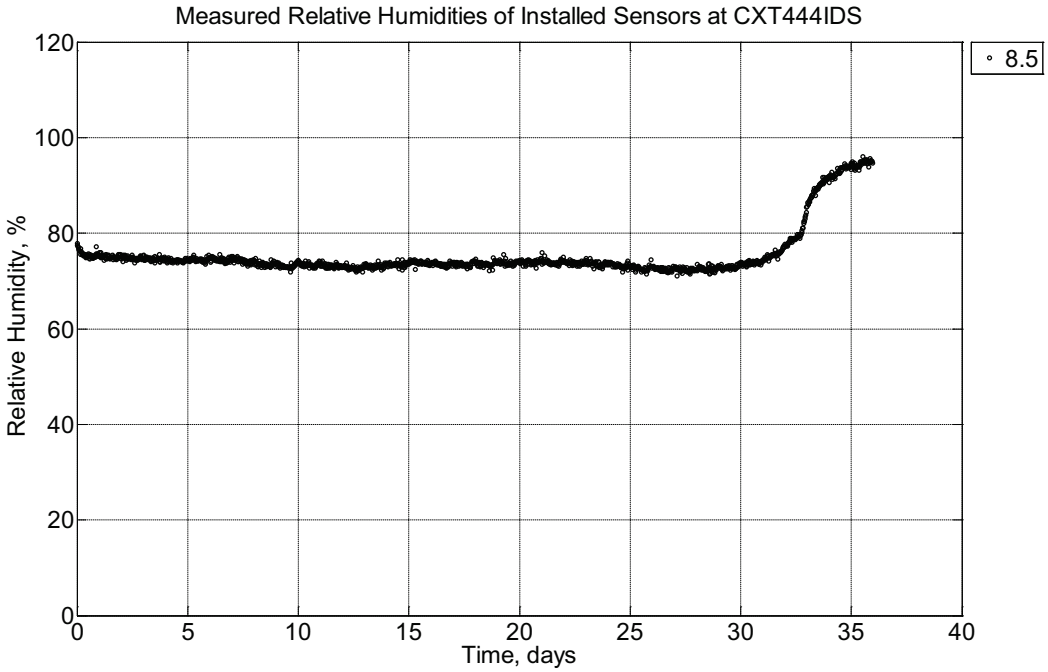

Figure B-361 Measured relative humidity at a depth of 8.5 inches (215.9 mm) from the

surface of a concrete crosstie (labeled CXT444IDS) without a polyurethane pad nor rail located in Champaign, IL, between September 4, 2013, through October 10, 2013.

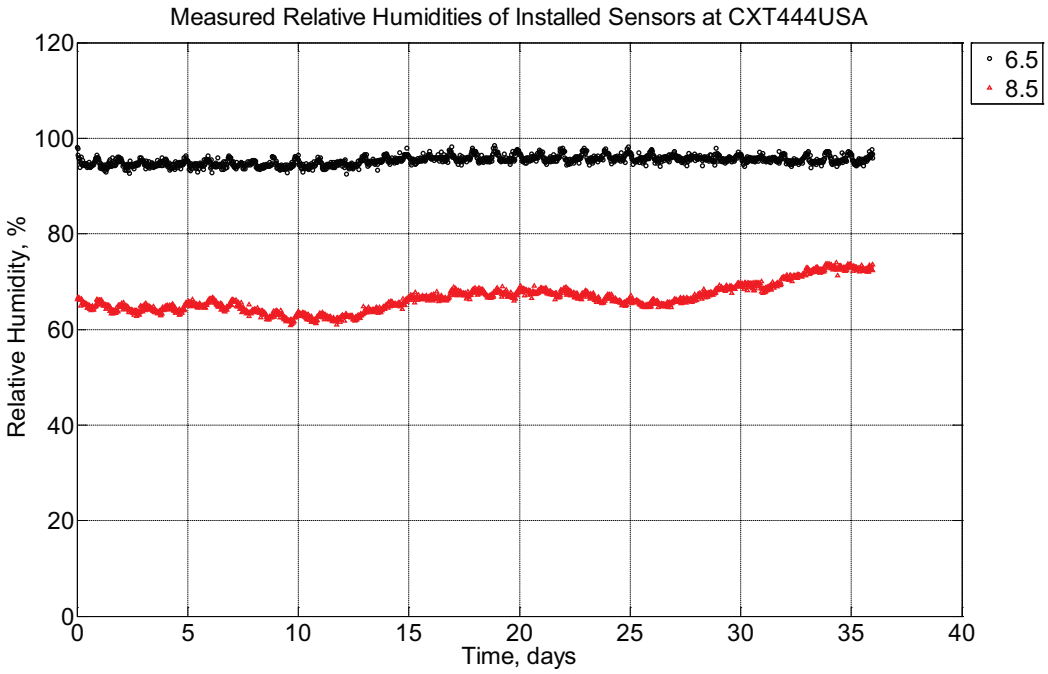

Figure B-362 Measured relative humidity at depths of 6.5 inches (139.7 mm) and 8.5 inches (215.9 mm) from the surface of a concrete crosstie (labeled CXT444USA) without a polyurethane pad nor rail located in Champaign, IL, between September 4, 2013, through October 10, 2013.

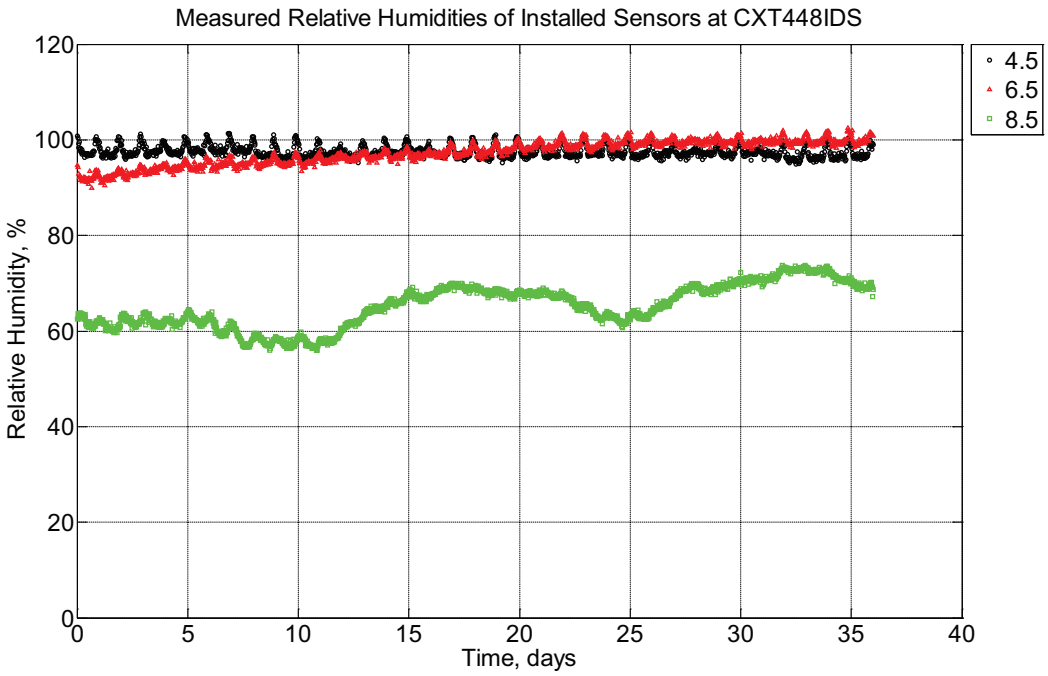

Figure B-363 Measured relative humidity at depths of 4.5 inches (114.3 mm), 6.5 inches (139.7 mm), and 8.5 inches (215.9 mm) from the surface of a concrete crosstie (labeled CXT448IDS) without a polyurethane pad nor rail located in Champaign, IL, between September 4, 2013, through October 10, 2013.

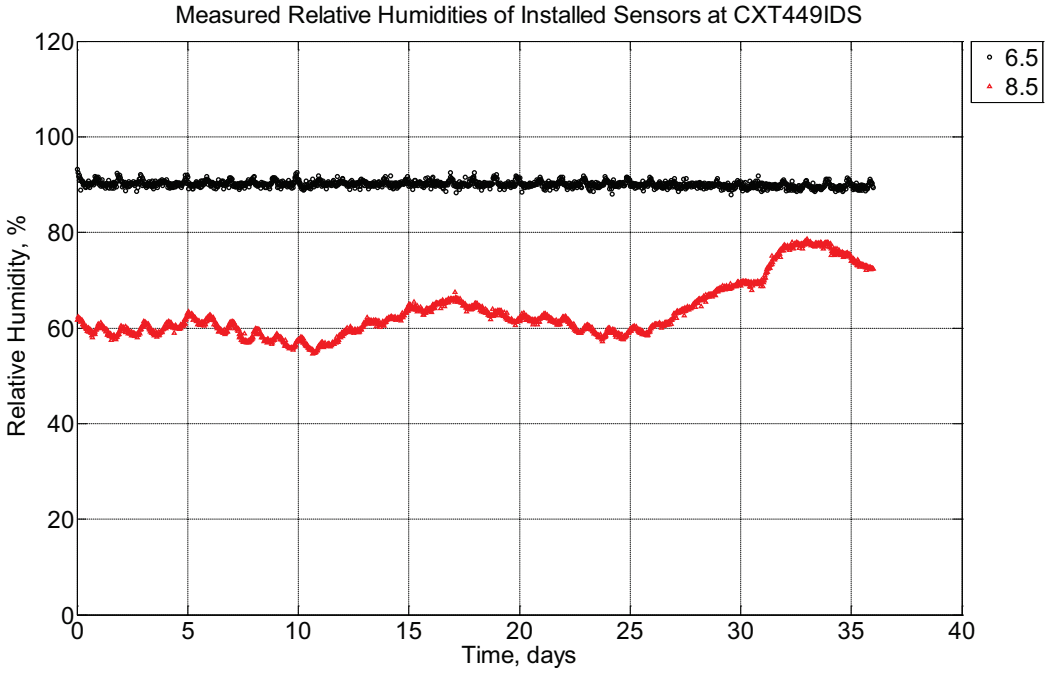

Figure B-364 Measured relative humidity at depths of 6.5 inches (139.7 mm) and 8.5 inches (215.9 mm) from the surface of a concrete crosstie (labeled CXT449IDS) without a

polyurethane pad nor rail located in Champaign, IL, between September 4, 2013, through October 10, 2013.

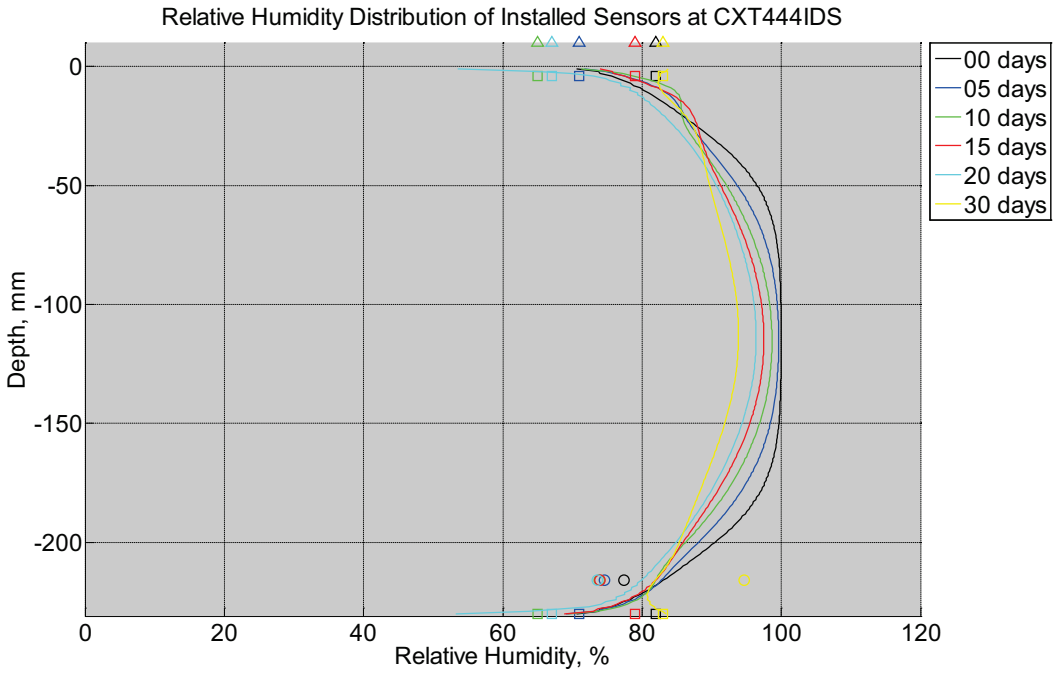

Figure B-365 Measured (markers) and modeled (continuous line) relative humidity profile distribution as a function of depth inside a concrete crosstie (labeled CXT444IDS) without a polyurethane pad nor rail located in Champaign, IL, between September 4, 2013, through October 10, 2013. Triangular markers denote relative humidity value from KTIP weather station, square markers denote measured relative humidity values from ambient sensors, and circular markers denote measured relative humidity values inside concrete.

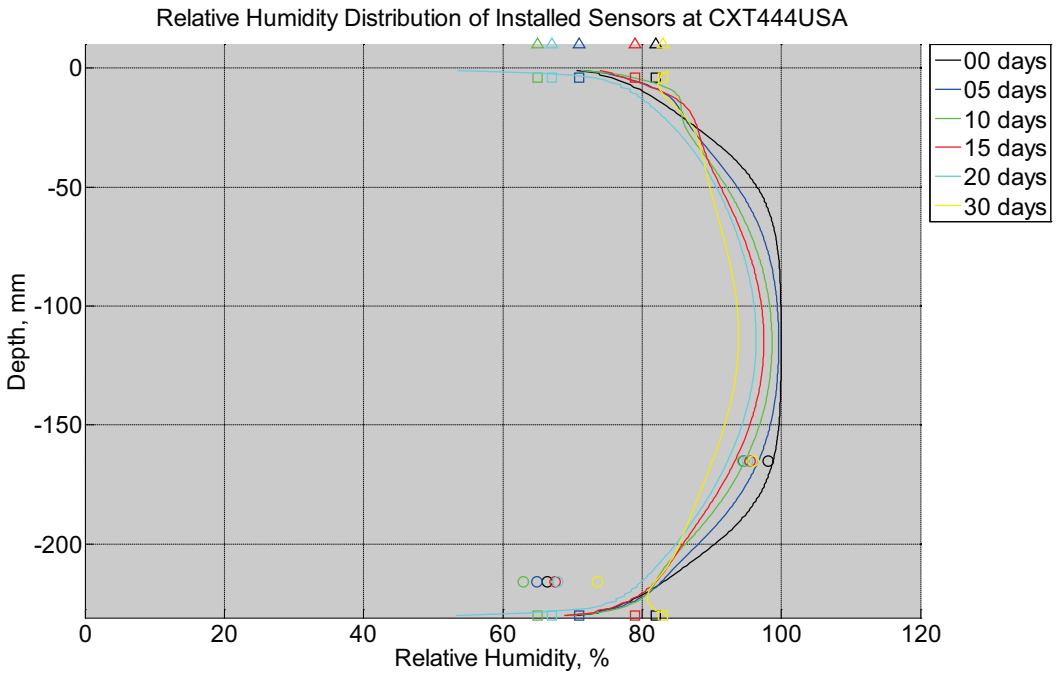

Figure B-366 Measured (markers) and modeled (continuous line) relative humidity profile distribution as a function of depth inside a concrete crosstie (labeled CXT444USA) without a polyurethane pad nor rail located in Champaign, IL, between September 4, 2013, through October 10, 2013. Triangular markers denote relative humidity value from KTIP weather station, square markers denote measured relative humidity values from ambient sensors, and circular markers denote measured relative humidity values inside concrete.

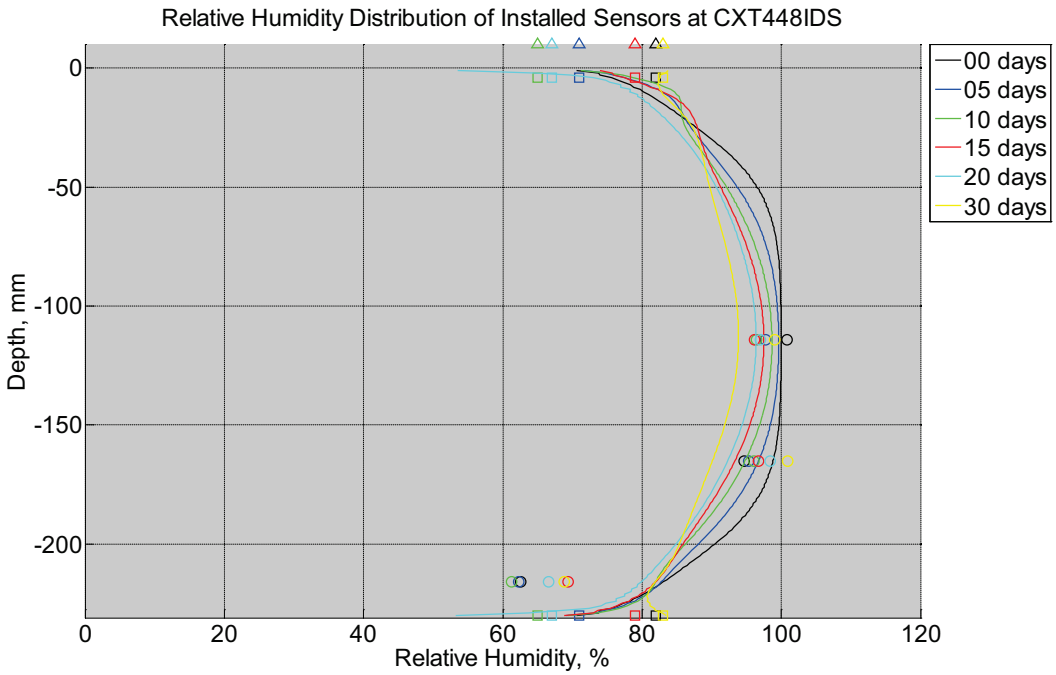

Figure B-367 Measured (markers) and modeled (continuous line) relative humidity profile distribution as a function of depth inside a concrete crosstie (labeled CXT448IDS) without a polyurethane pad nor rail located in Champaign, IL, between September 4, 2013, through October 10, 2013. Triangular markers denote relative humidity value from KTIP weather station, square markers denote measured relative humidity values from ambient sensors, and circular markers denote measured relative humidity values inside concrete.

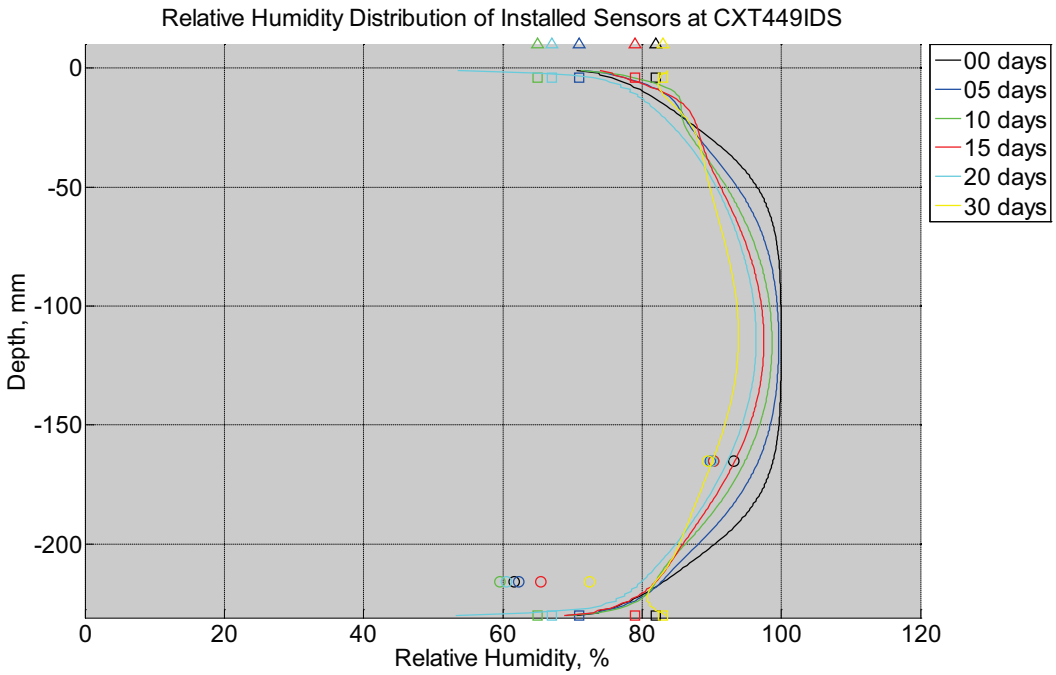

Figure B-368 Measured (markers) and modeled (continuous line) relative humidity profile distribution as a function of depth inside a concrete crosstie (labeled CXT449IDS) without a polyurethane pad nor rail located in Champaign, IL, between September 4, 2013, through October 10, 2013. Triangular markers denote relative humidity value from KTIP weather station, square markers denote measured relative humidity values from ambient sensors, and circular markers denote measured relative humidity values inside concrete.

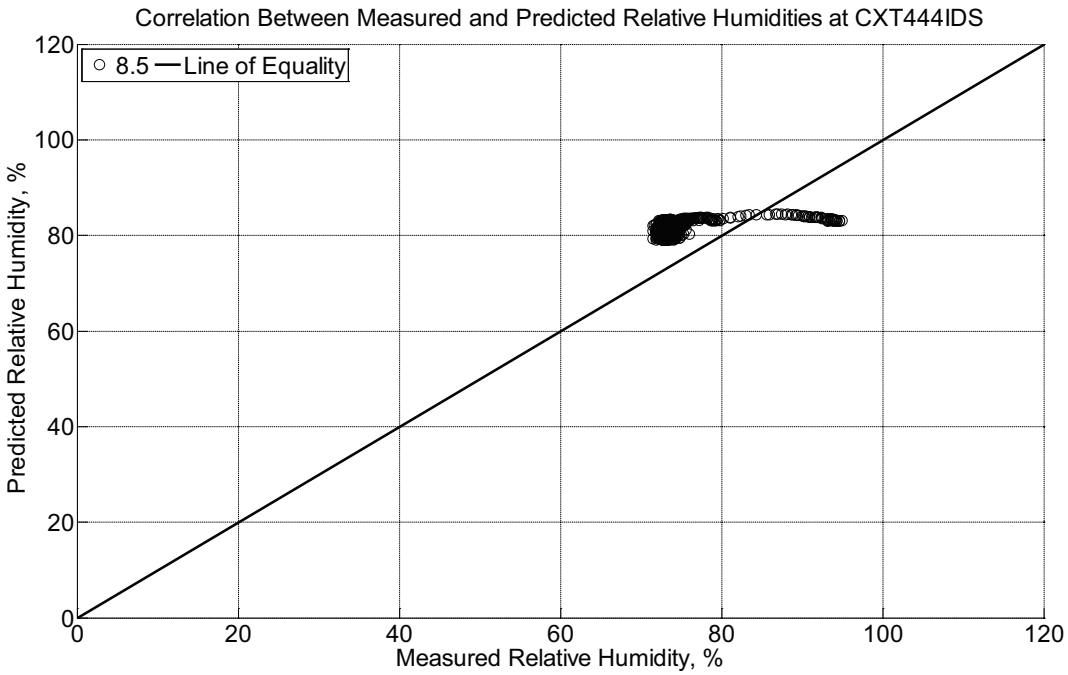

Figure B-369 Correlation between measured and predicted relative humidity values 8.5 inches (215.9 mm) from the surface of a concrete crosstie (labeled CXT444IDS) without a polyurethane pad nor rail located in Champaign, IL, between September 4, 2013, through October 10, 2013.

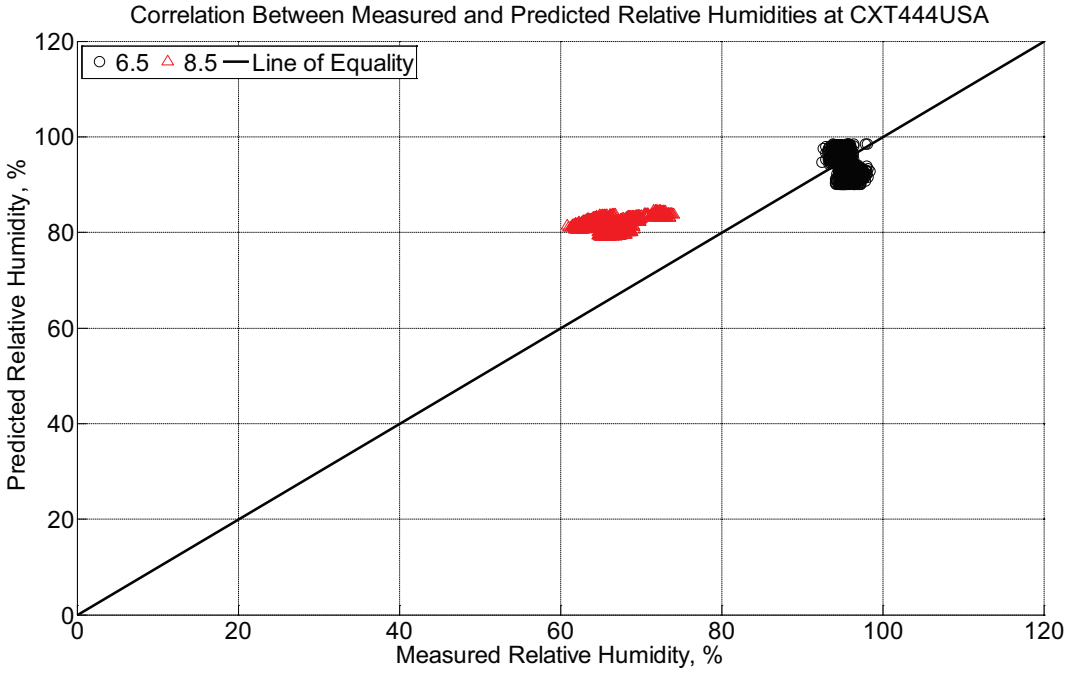

Figure B-370 Correlation between measured and predicted relative humidity values 6.5 inches (139.7 mm) and 8.5 inches (215.9 mm) from the surface of a concrete crosstie

(labeled CXT444USA) without a polyurethane pad nor rail located in Champaign, IL, between September 4, 2013, through October 10, 2013.

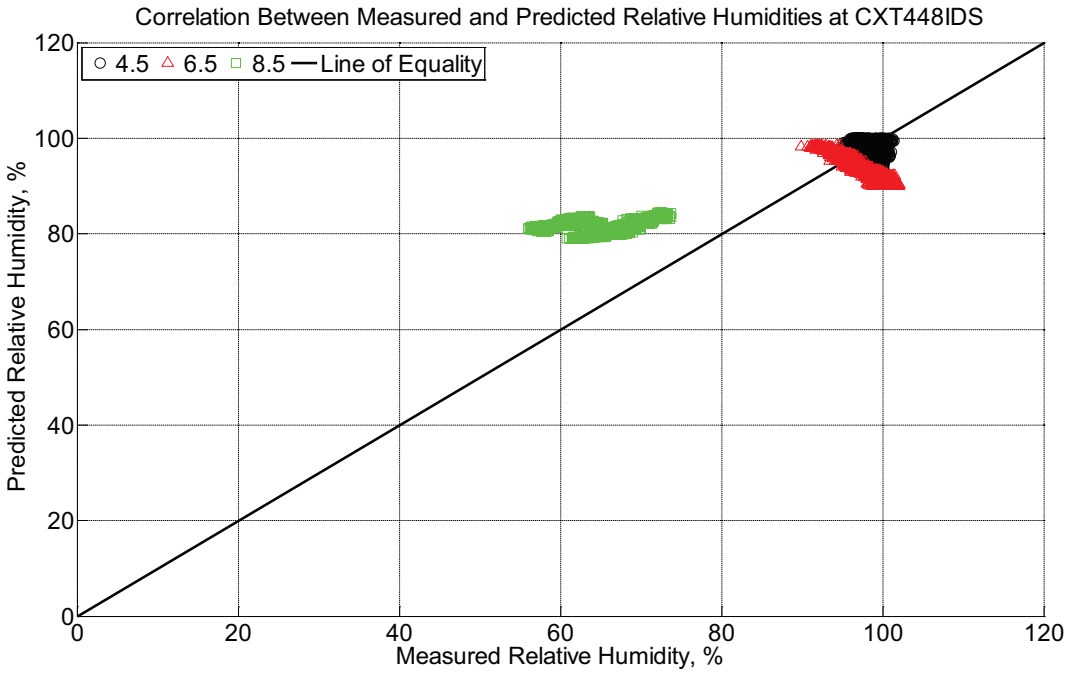

Figure B-371 Correlation between measured and predicted relative humidity values 4.5 inches (114.3 mm), 6.5 inches (139.7 mm), and 8.5 inches (215.9 mm) from the surface of a concrete crosstie (labeled CXT448IDS) without a polyurethane pad nor rail located in Champaign, IL, between September 4, 2013, through October 10, 2013.

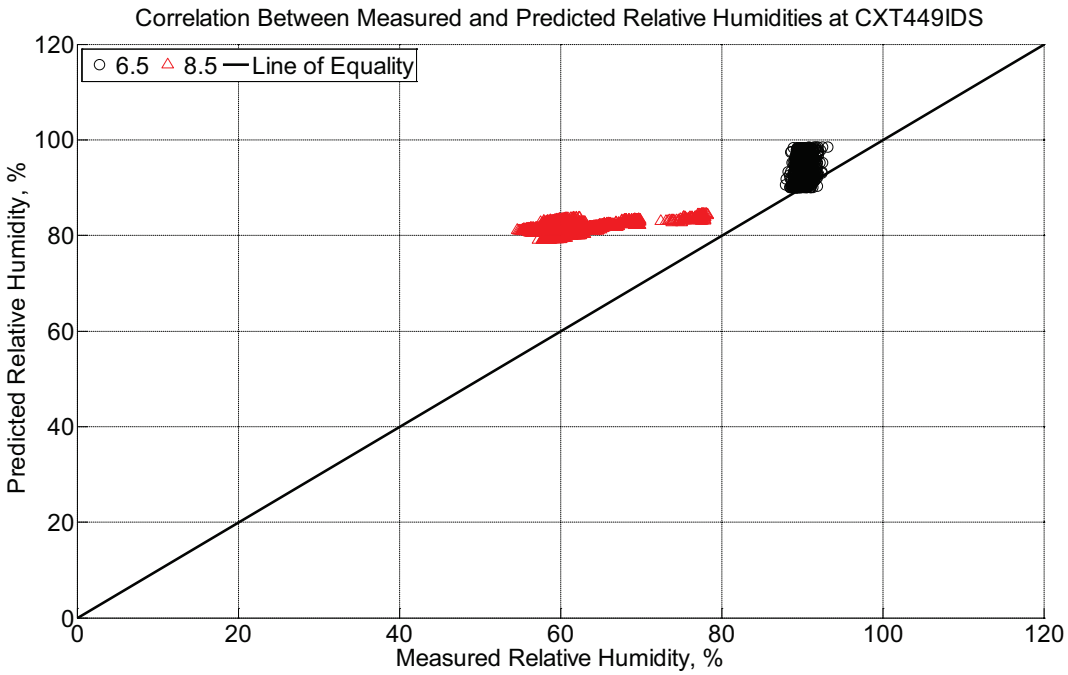

Figure B-372 Correlation between measured and predicted relative humidity values 6.5 inches (139.7 mm) and 8.5 inches (215.9 mm) from the surface of a concrete crosstie (labeled CXT449IDS) without a polyurethane pad nor rail located in Champaign, IL, between September 4, 2013, through October 10, 2013.

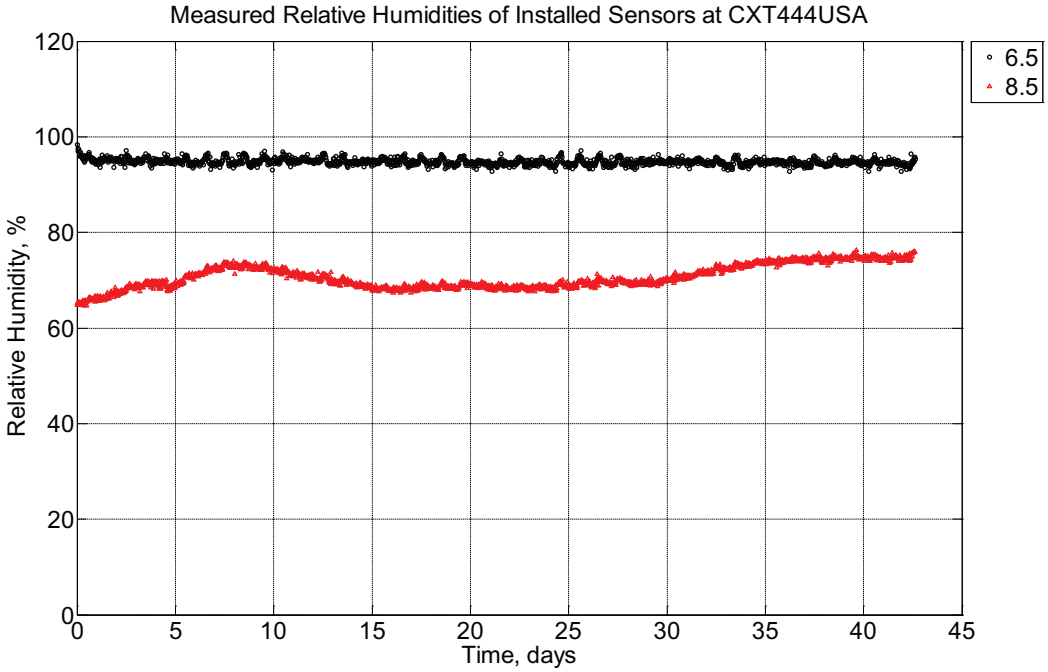

Figure B-373 Measured relative humidity at depths of 6.5 inches (139.7 mm) and 8.5 inches (215.9 mm) from the surface of a concrete crosstie (labeled CXT444USA) without a

polyurethane pad nor rail located in Champaign, IL, between October 1, 2013, through November 12, 2013.

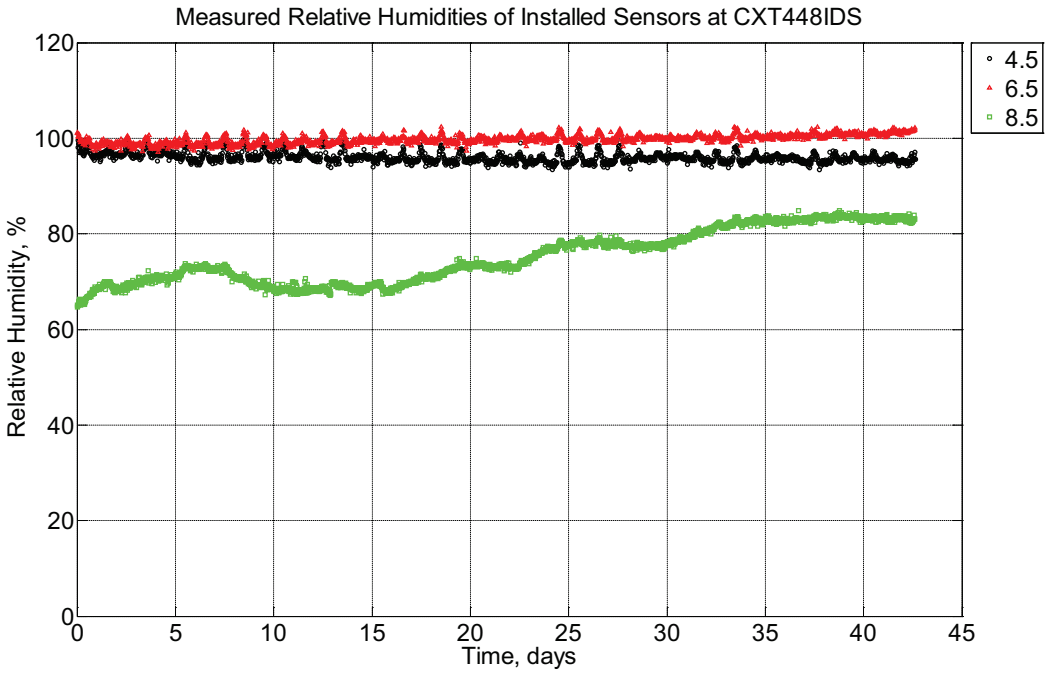

Figure B-374 Measured relative humidity at depths of 4.5 inches (114.3 mm), 6.5 inches (139.7 mm), and 8.5 inches (215.9 mm) from the surface of a concrete crosstie (labeled CXT448IDS) without a polyurethane pad nor rail located in Champaign, IL, between October 1, 2013, through November 12, 2013.

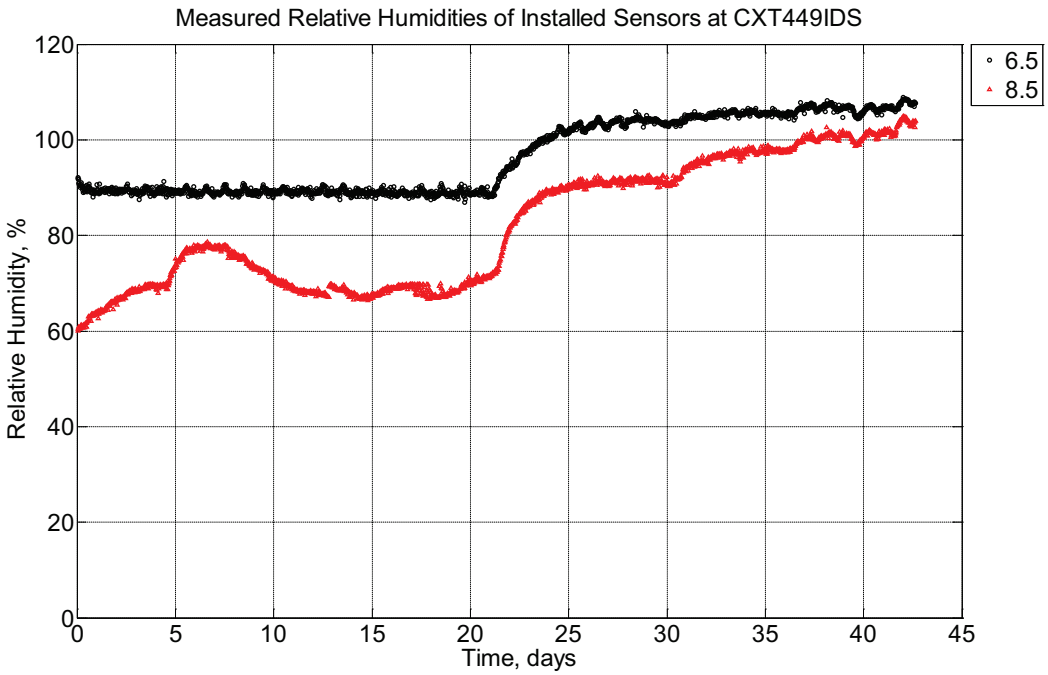

Figure B-375 Measured relative humidity at depths of 6.5 inches (139.7 mm) and 8.5 inches (215.9 mm) from the surface of a concrete crosstie (labeled CXT449IDS) without a polyurethane pad nor rail located in Champaign, IL, between October 1, 2013, through November 12, 2013.

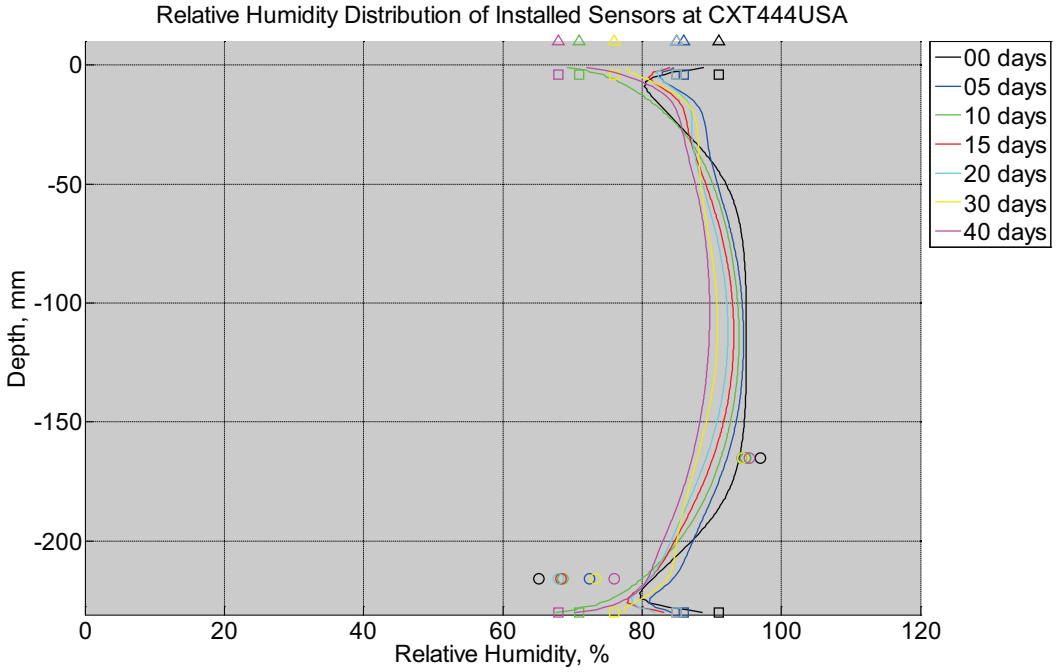

Figure B-376 Measured (markers) and modeled (continuous line) relative humidity profile distribution as a function of depth inside a concrete crosstie (labeled CXT444USA) without

a polyurethane pad nor rail located in Champaign, IL, between October 1, 2013, through November 12, 2013. Triangular markers denote relative humidity value from KTIP weather station, square markers denote measured relative humidity values from ambient sensors, and circular markers denote measured relative humidity values inside concrete.

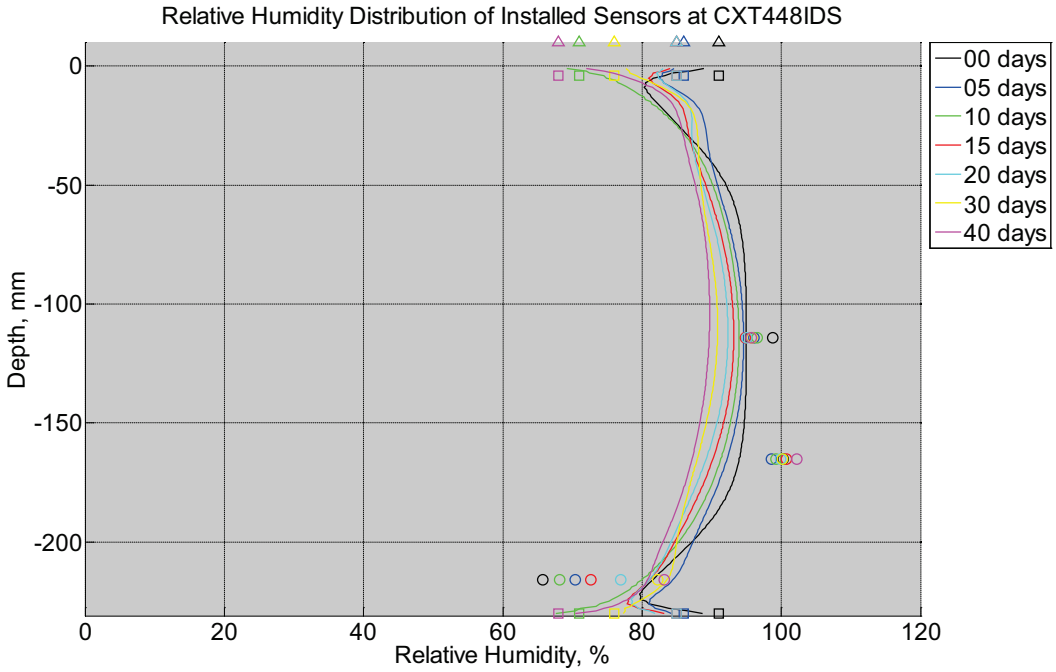

Figure B-377 Measured (markers) and modeled (continuous line) relative humidity profile distribution as a function of depth inside a concrete crosstie (labeled CXT448IDS) without a polyurethane pad nor rail located in Champaign, IL, between October 1, 2013, through November 12, 2013. Triangular markers denote relative humidity value from KTIP weather station, square markers denote measured relative humidity values from ambient sensors, and circular markers denote measured relative humidity values inside concrete.

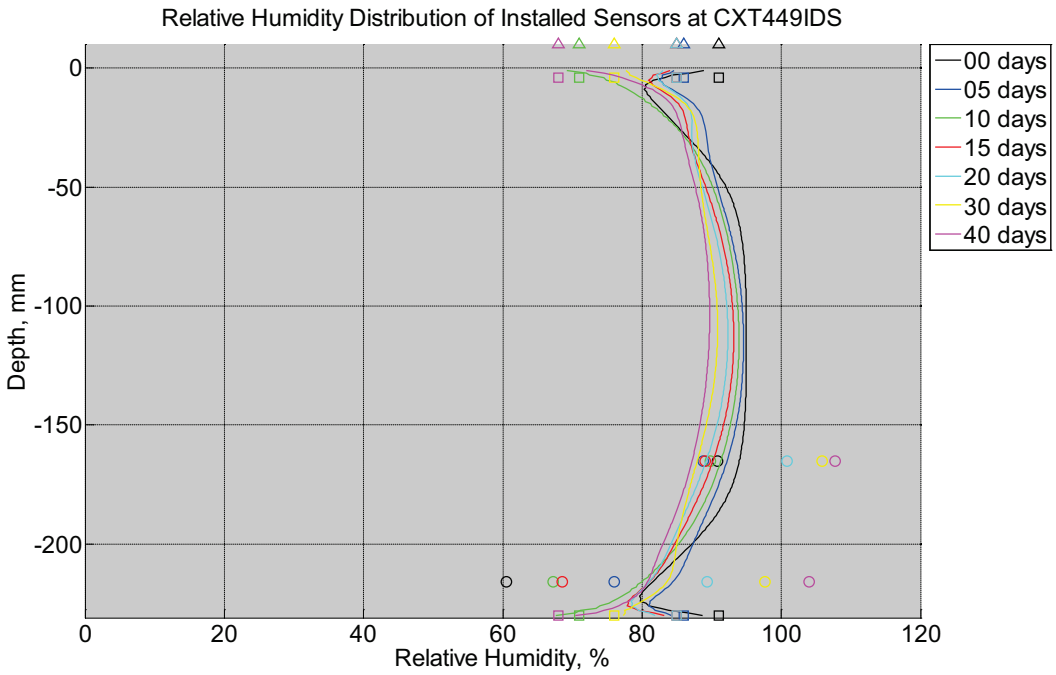

Figure B-378 Measured (markers) and modeled (continuous line) relative humidity profile distribution as a function of depth inside a concrete crosstie (labeled CXT449IDS) without a polyurethane pad nor rail located in Champaign, IL, between October 1, 2013, through November 12, 2013. Triangular markers denote relative humidity value from KTIP weather station, square markers denote measured relative humidity values from ambient sensors, and circular markers denote measured relative humidity values inside concrete.

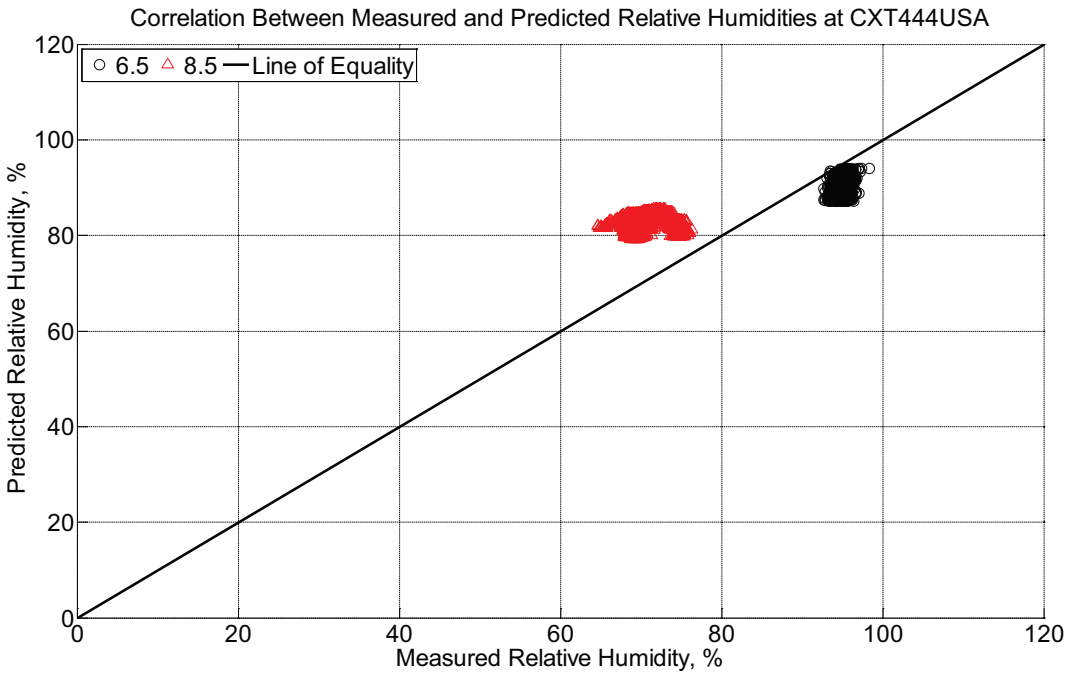

Figure B-379 Correlation between measured and predicted relative humidity values 6.5 inches (139.7 mm) and 8.5 inches (215.9 mm) from the surface of a concrete crosstie (labeled CXT444USA) without a polyurethane pad nor rail located in Champaign, IL, between October 1, 2013, through November 12, 2013.

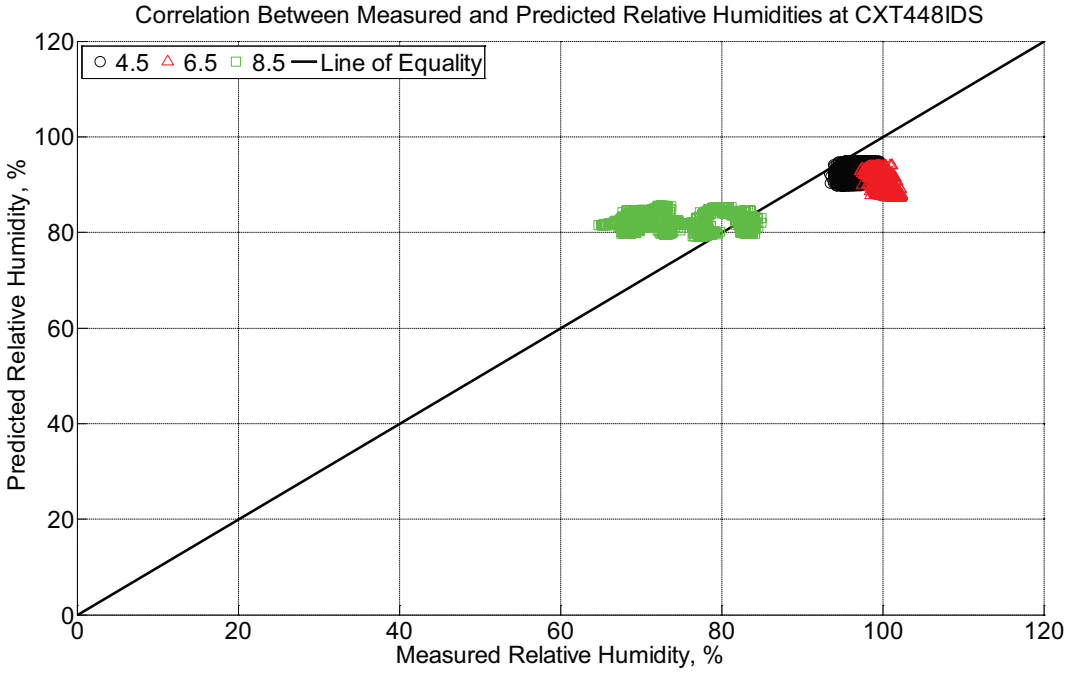

Figure B-380 Correlation between measured and predicted relative humidity values 4.5 inches (114.3 mm), 6.5 inches (139.7 mm), and 8.5 inches (215.9 mm) from the surface of a

concrete crosstie (labeled CXT448IDS) without a polyurethane pad nor rail located in Champaign, IL, between October 1, 2013, through November 12, 2013.

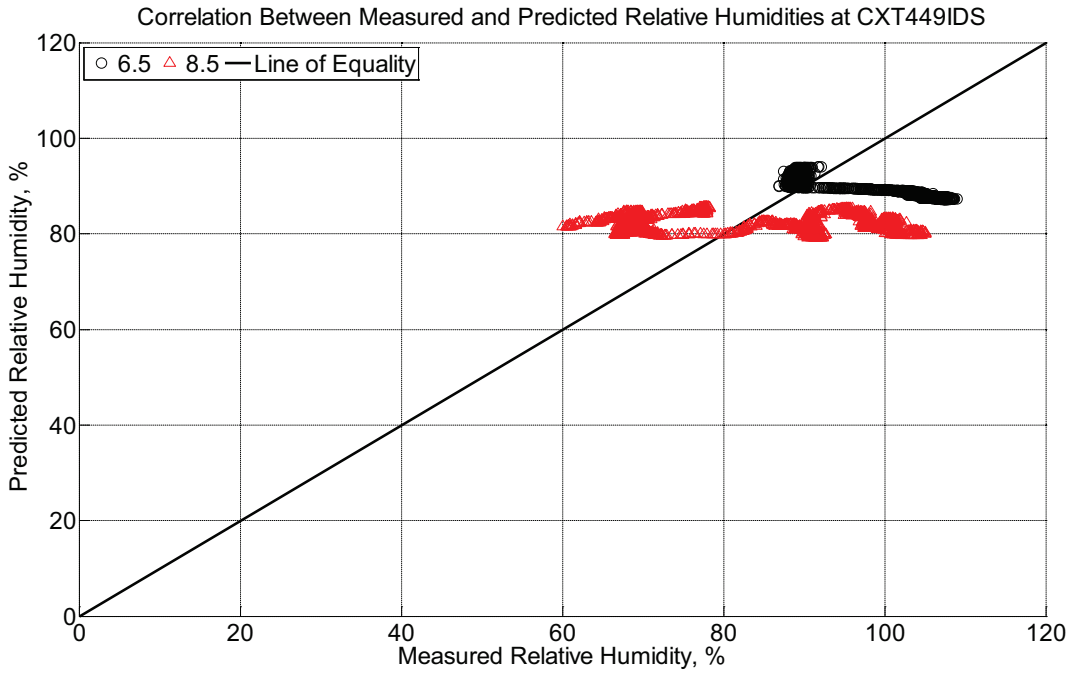

Figure B-381 Correlation between measured and predicted relative humidity values 6.5 inches (139.7 mm) and 8.5 inches (215.9 mm) from the surface of a concrete crosstie (labeled CXT449IDS) without a polyurethane pad nor rail located in Champaign, IL, between October 1, 2013, through November 12, 2013.

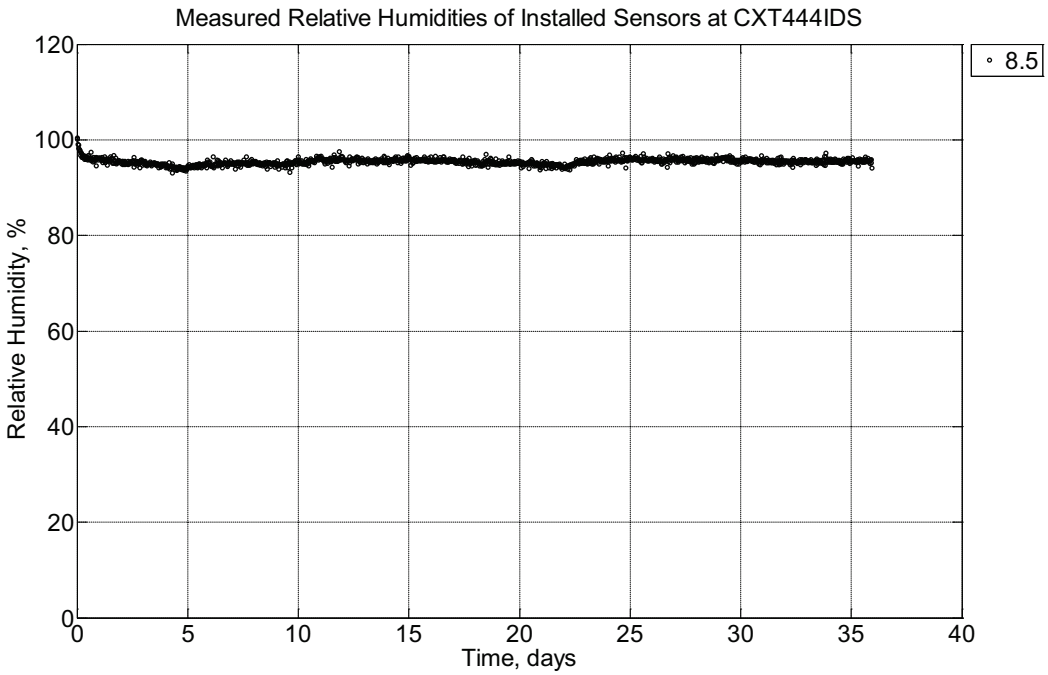

Figure B-382 Measured relative humidity at a depth of 8.5 inches (215.9 mm) from the surface of a concrete crosstie (labeled CXT444IDS) without a polyurethane pad nor rail located in Champaign, IL, between November 12, 2013, through December 18, 2013.

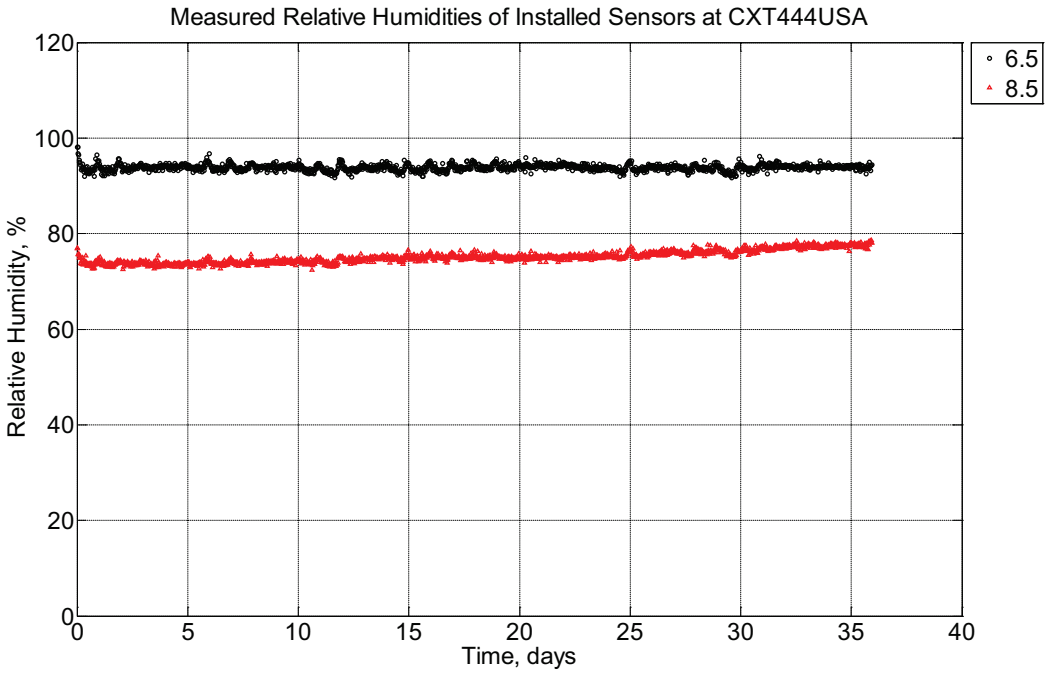

Figure B-383 Measured relative humidity at depths of 6.5 inches (139.7 mm) and 8.5 inches (215.9 mm) from the surface of a concrete crosstie (labeled CXT444USA) without a

polyurethane pad nor rail located in Champaign, IL, between November 12, 2013, through December 18, 2013.

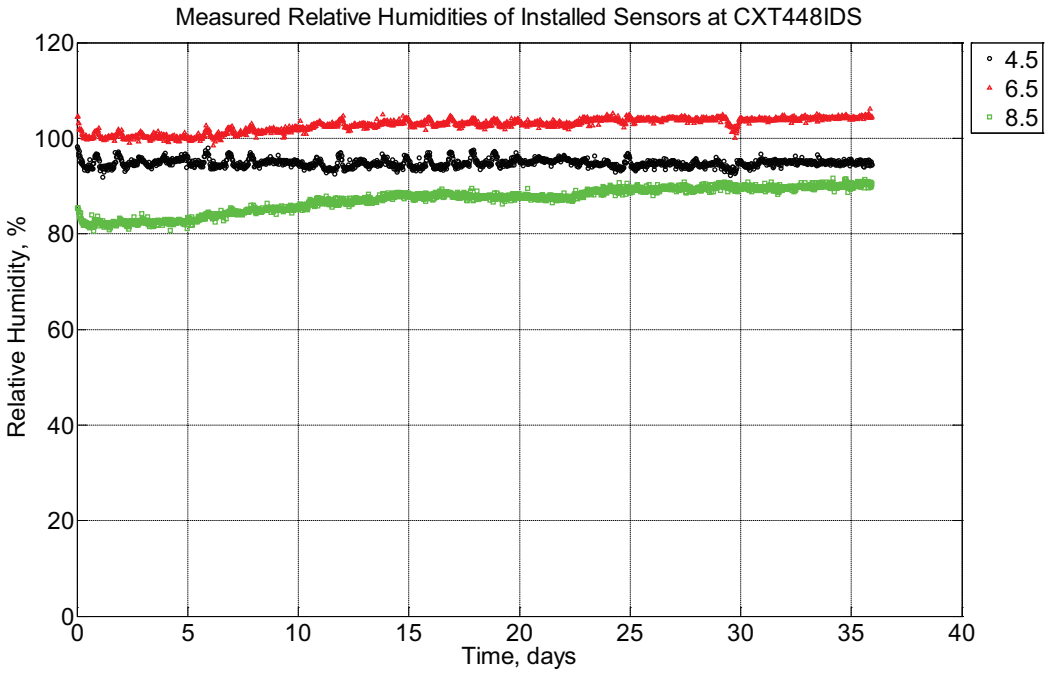

Figure B-384 Measured relative humidity at depths of 4.5 inches (114.3 mm), 6.5 inches (139.7 mm), and 8.5 inches (215.9 mm) from the surface of a concrete crosstie (labeled CXT448IDS) without a polyurethane pad nor rail located in Champaign, IL, between November 12, 2013, through December 18, 2013.

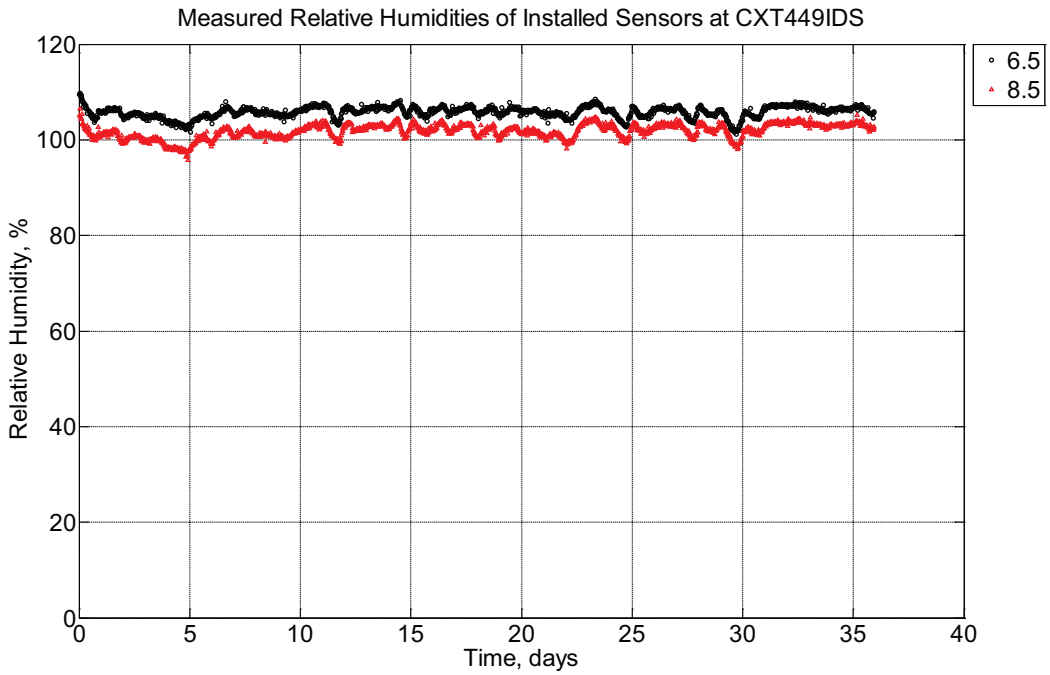

Figure B-385 Measured relative humidity at depths of 6.5 inches (139.7 mm) and 8.5 inches (215.9 mm) from the surface of a concrete crosstie (labeled CXT449IDS) without a polyurethane pad nor rail located in Champaign, IL, between November 12, 2013, through December 18, 2013.

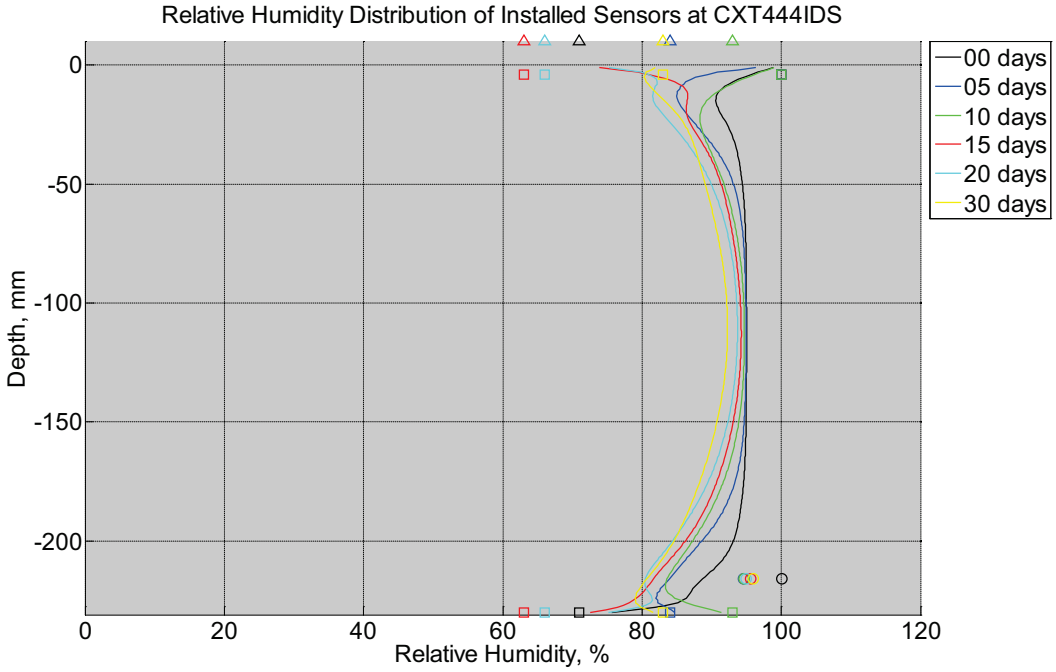

Figure B-386 Measured (markers) and modeled (continuous line) relative humidity profile distribution as a function of depth inside a concrete crosstie (labeled CXT444IDS) without

a polyurethane pad nor rail located in Champaign, IL, between November 12, 2013, through December 18, 2013. Triangular markers denote relative humidity value from KTIP weather station, square markers denote measured relative humidity values from ambient sensors, and circular markers denote measured relative humidity values inside concrete.

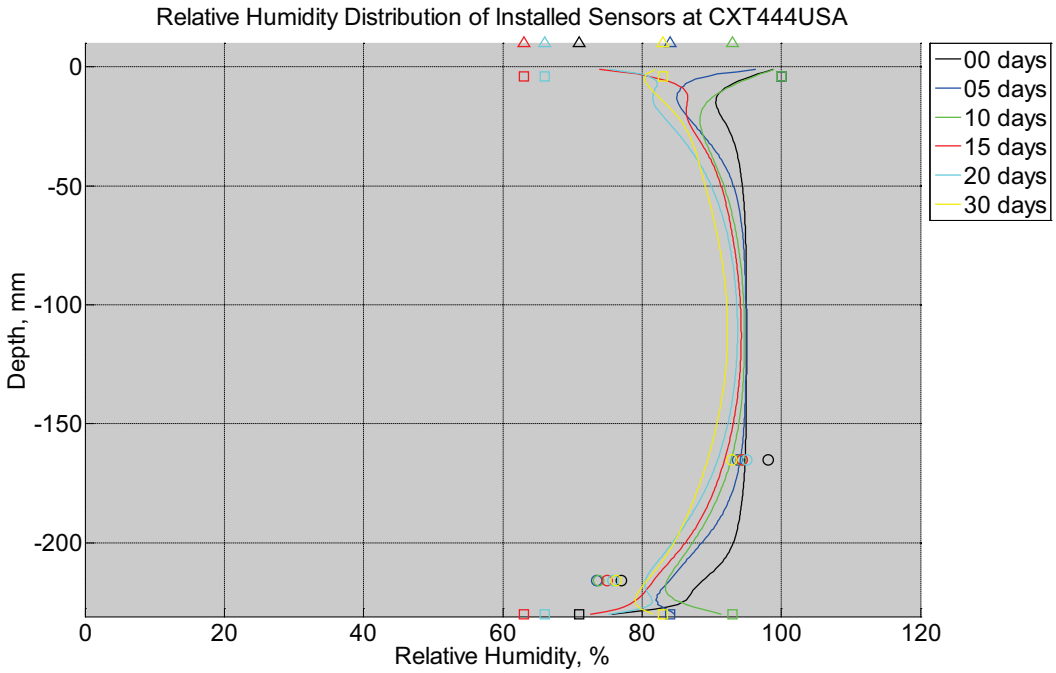

Figure B-387 Measured (markers) and modeled (continuous line) relative humidity profile distribution as a function of depth inside a concrete crosstie (labeled CXT444USA) without a polyurethane pad nor rail located in Champaign, IL, between November 12, 2013, through December 18, 2013. Triangular markers denote relative humidity value from KTIP weather station, square markers denote measured relative humidity values from ambient sensors, and circular markers denote measured relative humidity values inside concrete.

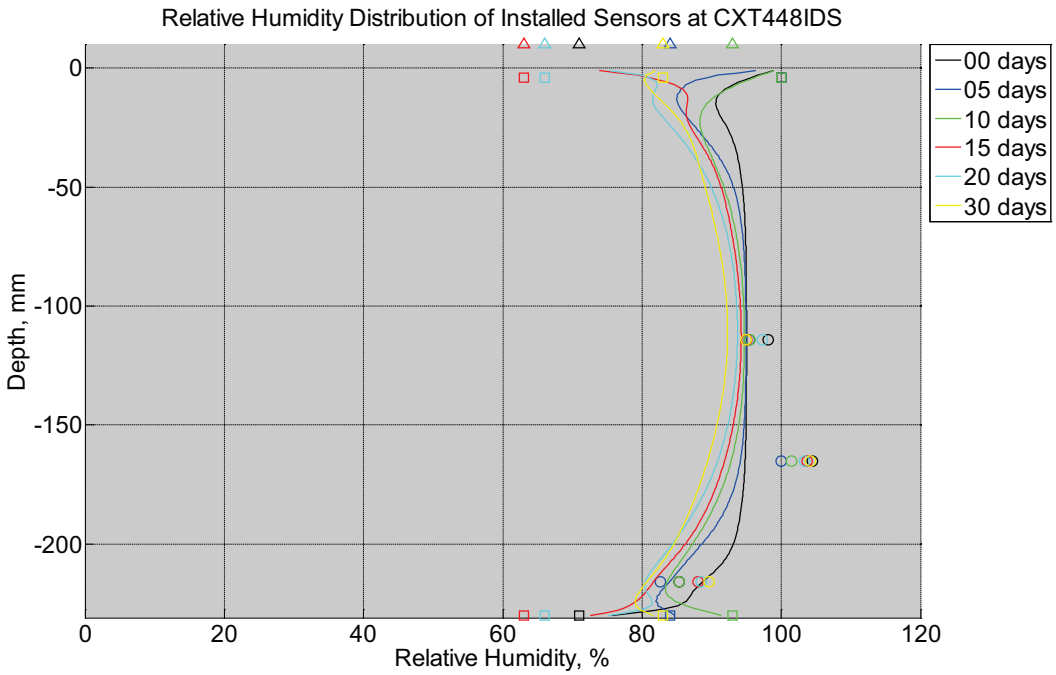

Figure B-388 Measured (markers) and modeled (continuous line) relative humidity profile distribution as a function of depth inside a concrete crosstie (labeled CXT448IDS) without a polyurethane pad nor rail located in Champaign, IL, between November 12, 2013, through December 18, 2013. Triangular markers denote relative humidity value from KTIP weather station, square markers denote measured relative humidity values from ambient sensors, and circular markers denote measured relative humidity values inside concrete.

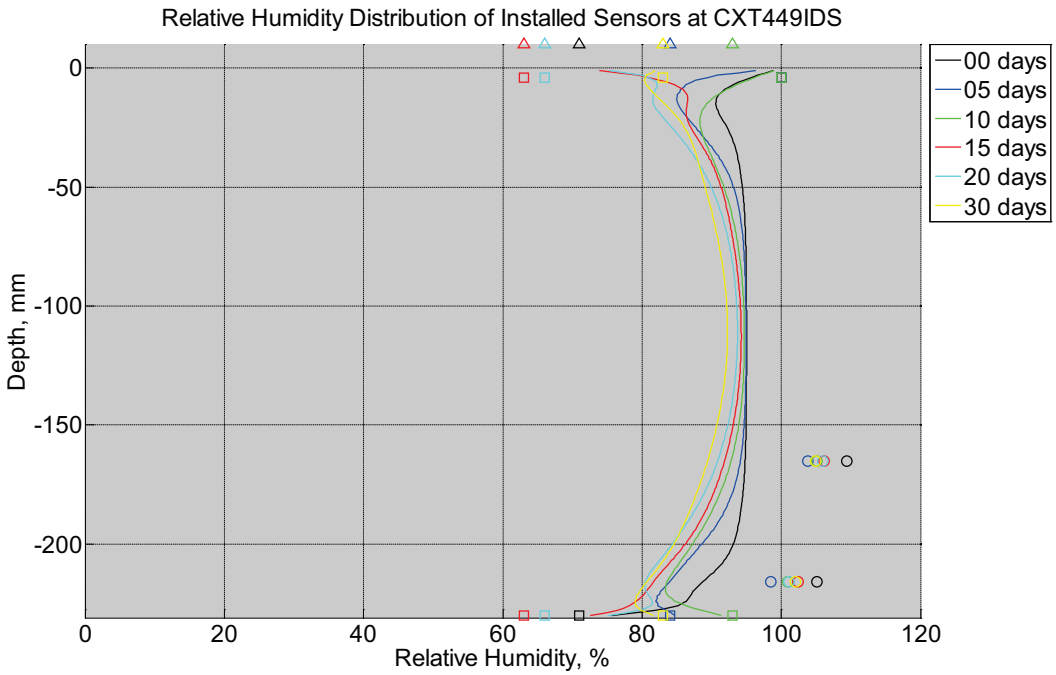

Figure B-389 Measured (markers) and modeled (continuous line) relative humidity profile distribution as a function of depth inside a concrete crosstie (labeled CXT449IDS) without a polyurethane pad nor rail located in Champaign, IL, between November 12, 2013, through December 18, 2013. Triangular markers denote relative humidity value from KTIP weather station, square markers denote measured relative humidity values from ambient sensors, and circular markers denote measured relative humidity values inside concrete.

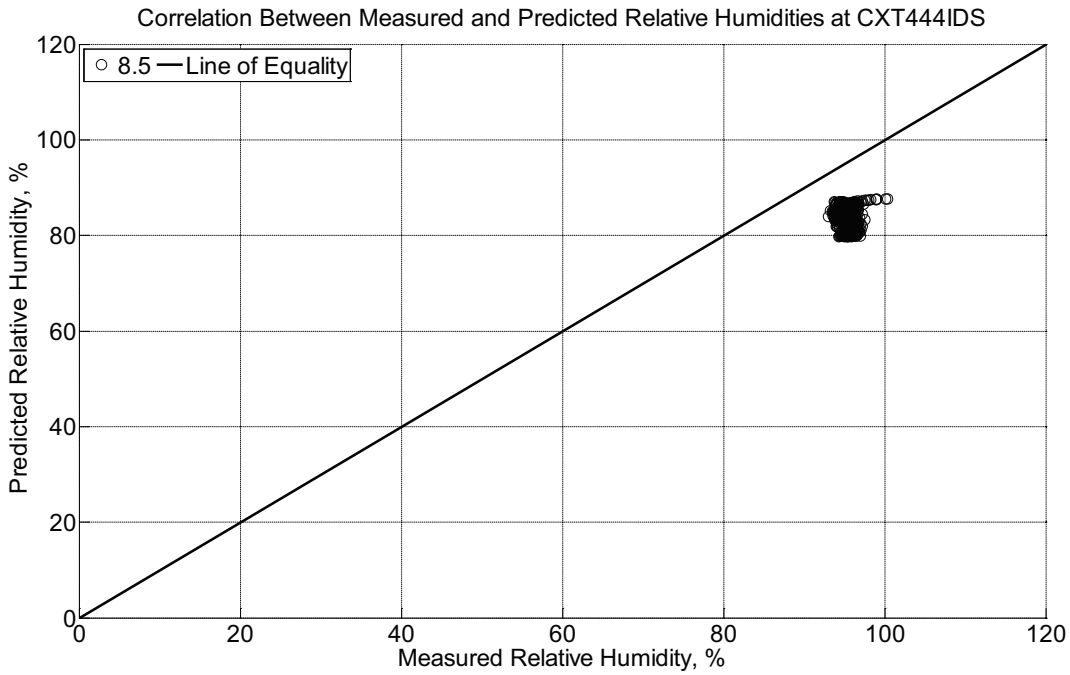

Figure B-390 Correlation between measured and predicted relative humidity values 8.5 inches (215.9 mm) from the surface of a concrete crosstie (labeled CXT444IDS) without a polyurethane pad nor rail located in Champaign, IL, between November 12, 2013, through December 18, 2013.

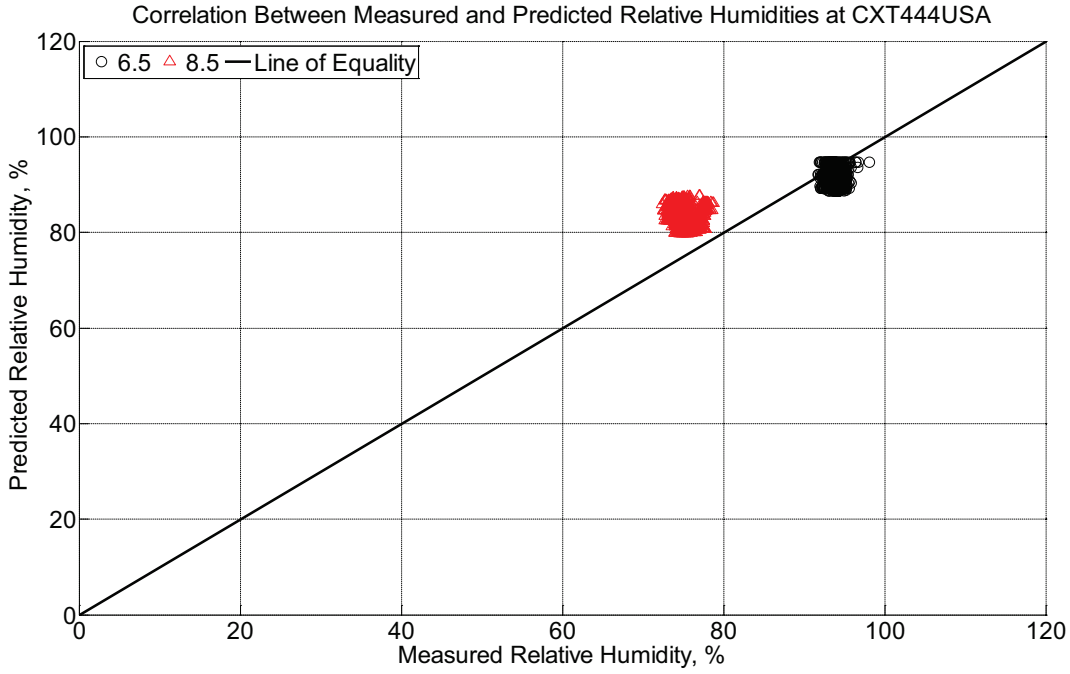

Figure B-391 Correlation between measured and predicted relative humidity values 6.5 inches (139.7 mm) and 8.5 inches (215.9 mm) from the surface of a concrete crosstie

(labeled CXT444USA) without a polyurethane pad nor rail located in Champaign, IL, between November 12, 2013, through December 18, 2013.

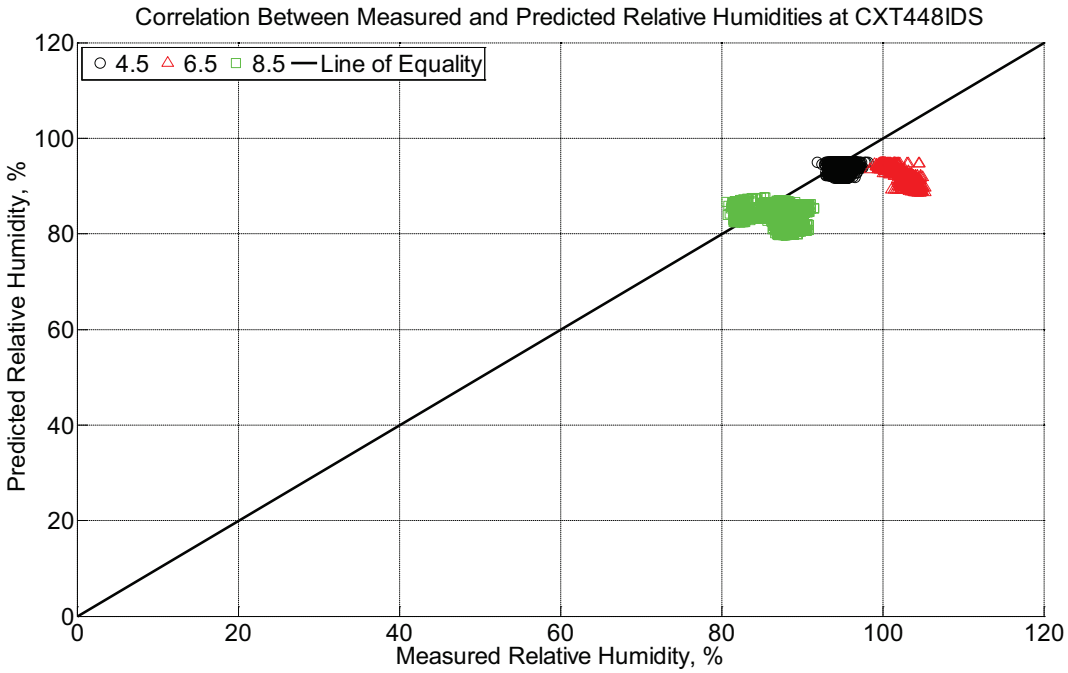

Figure B-392 Correlation between measured and predicted relative humidity values 4.5 inches (114.3 mm), 6.5 inches (139.7 mm), and 8.5 inches (215.9 mm) from the surface of a concrete crosstie (labeled CXT448IDS) without a polyurethane pad nor rail located in Champaign, IL, between November 12, 2013, through December 18, 2013.

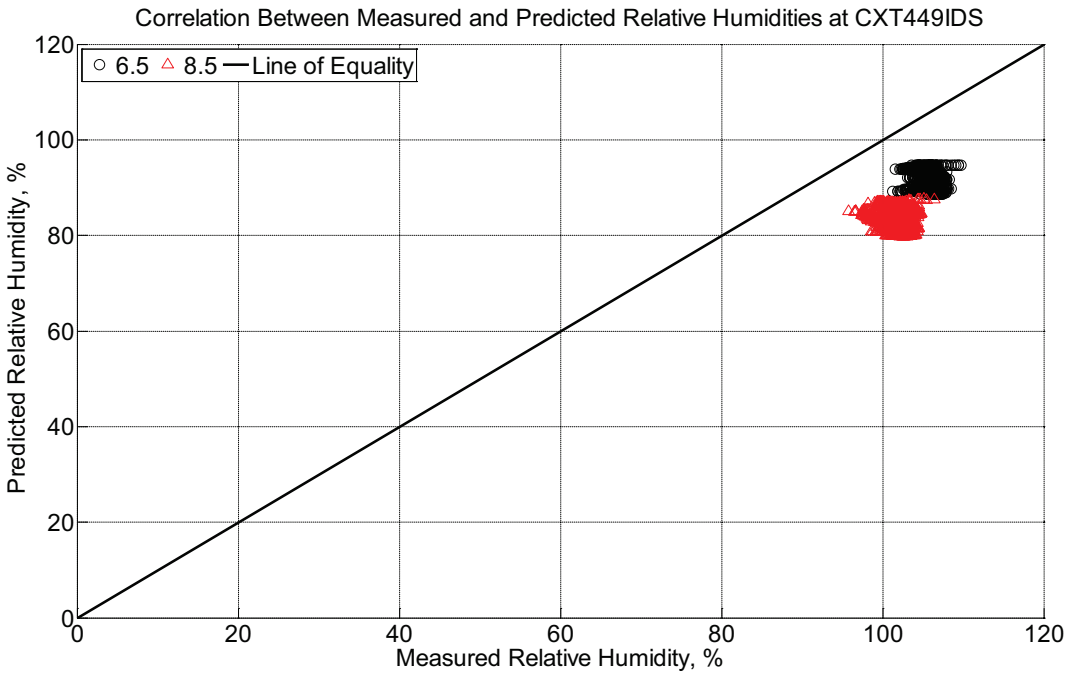

Figure B-393 Correlation between measured and predicted relative humidity values 6.5 inches (139.7 mm) and 8.5 inches (215.9 mm) from the surface of a concrete crosstie (labeled CXT449IDS) without a polyurethane pad nor rail located in Champaign, IL, between November 12, 2013, through December 18, 2013.

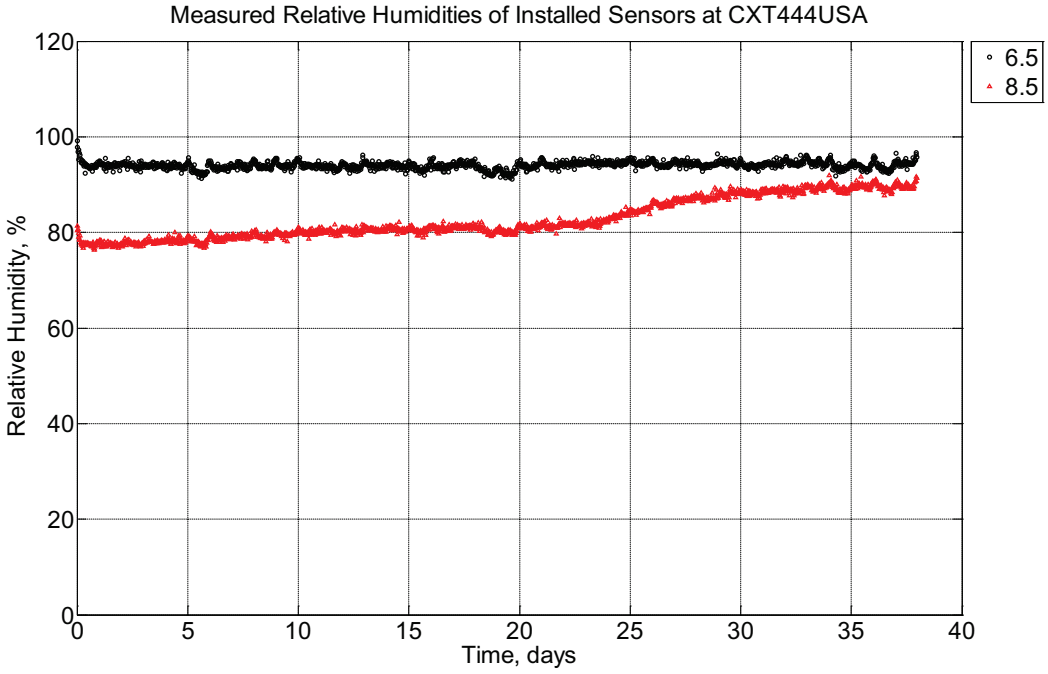

Figure B-394 Measured relative humidity at depths of 6.5 inches (139.7 mm) and 8.5 inches (215.9 mm) from the surface of a concrete crosstie (labeled CXT444USA) without a

polyurethane pad nor rail located in Champaign, IL, between December 18, 2013, through January 25, 2014.

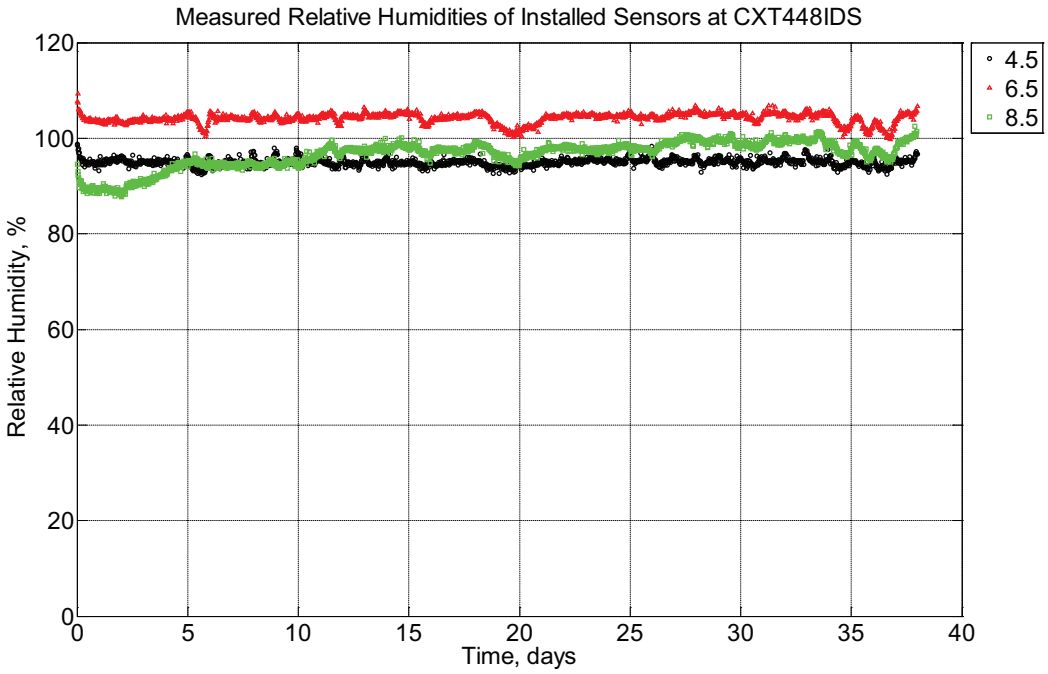

Figure B-395 Measured relative humidity at depths of 4.5 inches (114.3 mm), 6.5 inches (139.7 mm), and 8.5 inches (215.9 mm) from the surface of a concrete crosstie (labeled CXT448IDS) without a polyurethane pad nor rail located in Champaign, IL, between December 18, 2013, through January 25, 2014.

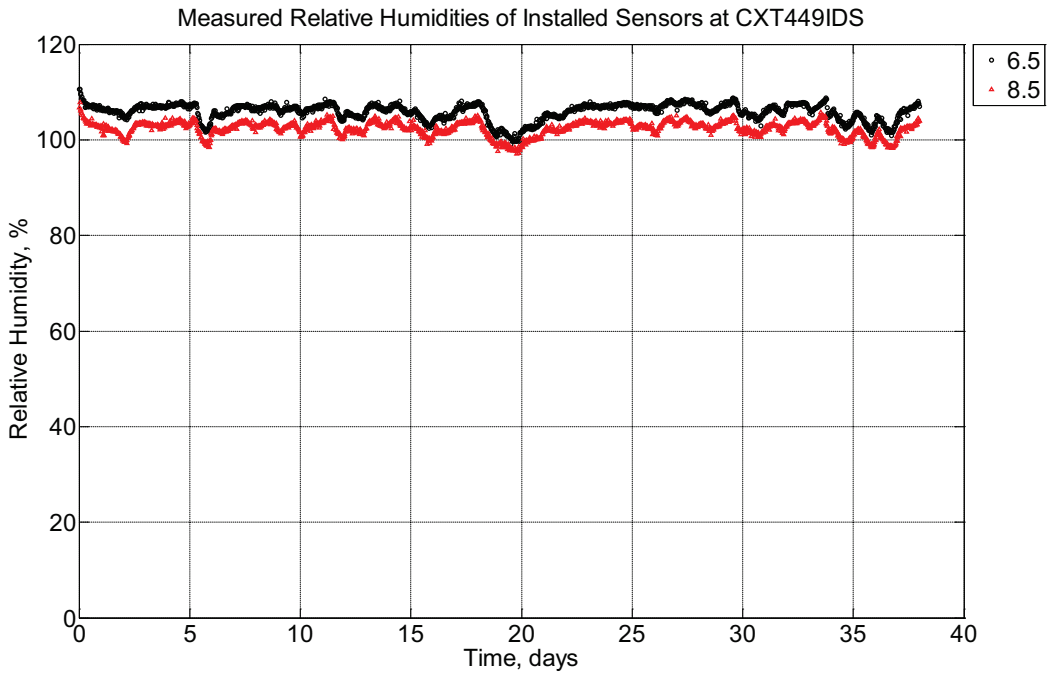

Figure B-396 Measured relative humidity at depths of 6.5 inches (139.7 mm) and 8.5 inches (215.9 mm) from the surface of a concrete crosstie (labeled CXT449IDS) without a polyurethane pad nor rail located in Champaign, IL, between December 18, 2013, through January 25, 2014.

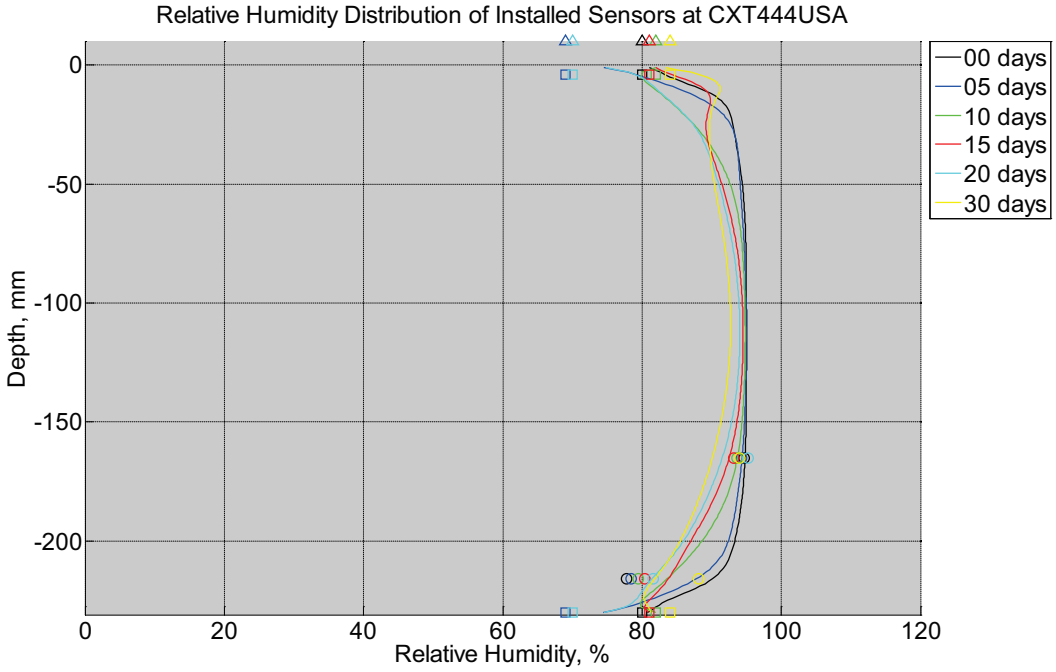

Figure B-397 Measured (markers) and modeled (continuous line) relative humidity profile distribution as a function of depth inside a concrete crosstie (labeled CXT444USA) without

a polyurethane pad nor rail located in Champaign, IL, between December 18, 2013, through January 25, 2014. Triangular markers denote relative humidity value from KTIP weather station, square markers denote measured relative humidity values from ambient sensors, and circular markers denote measured relative humidity values inside concrete.

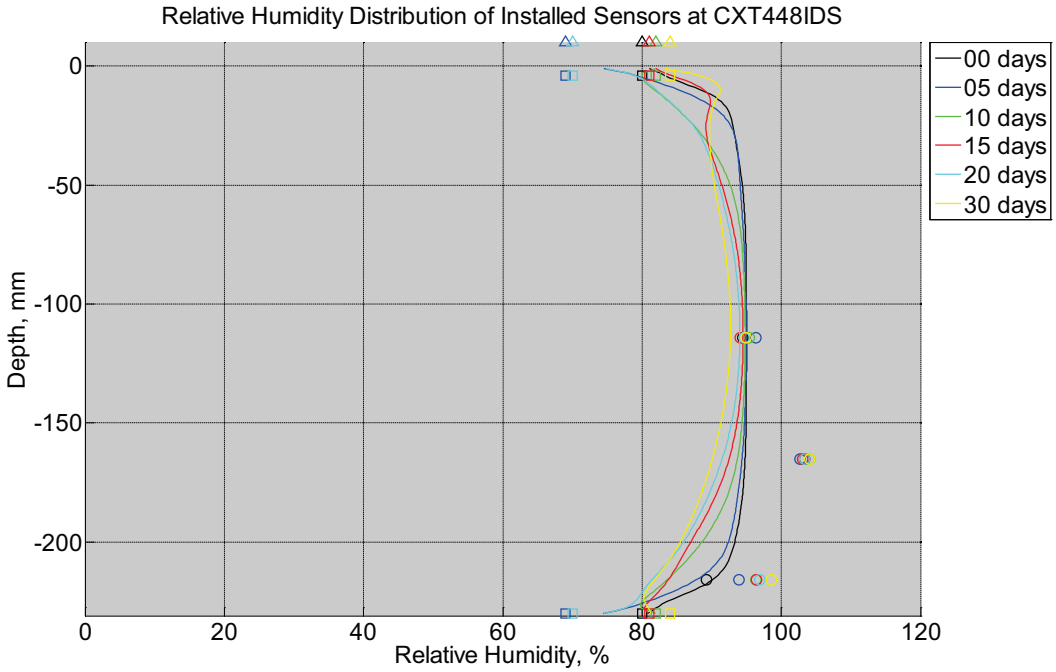

Figure B-398 Measured (markers) and modeled (continuous line) relative humidity profile distribution as a function of depth inside a concrete crosstie (labeled CXT448IDS) without a polyurethane pad nor rail located in Champaign, IL, between December 18, 2013, through January 25, 2014. Triangular markers denote relative humidity value from KTIP weather station, square markers denote measured relative humidity values from ambient sensors, and circular markers denote measured relative humidity values inside concrete.

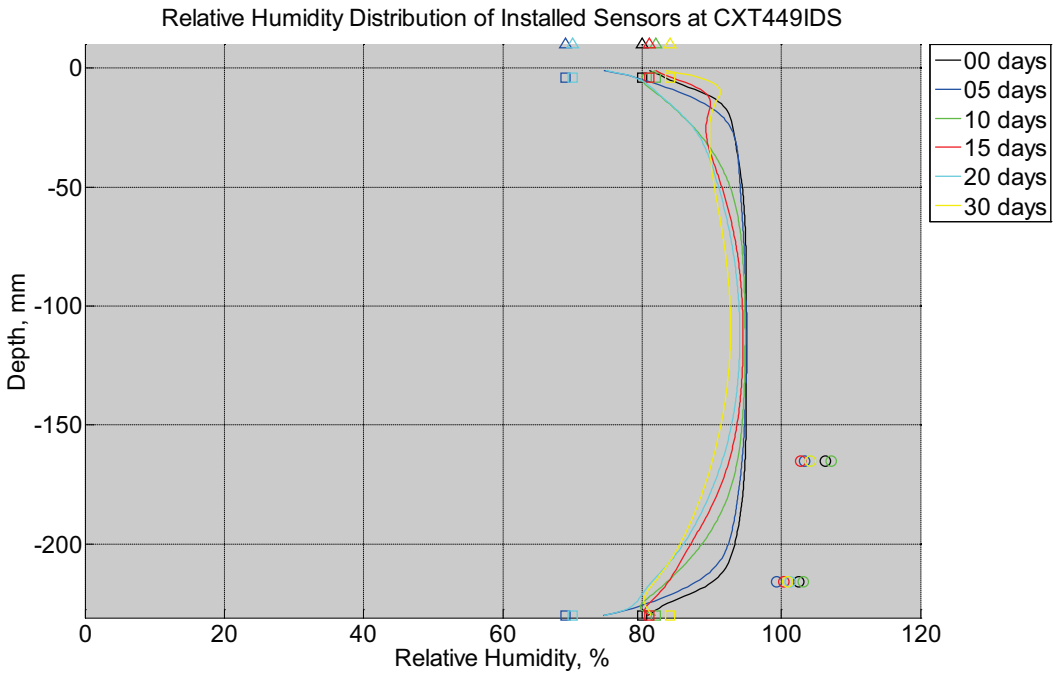

Figure B-399 Measured (markers) and modeled (continuous line) relative humidity profile distribution as a function of depth inside a concrete crosstie (labeled CXT449IDS) without a polyurethane pad nor rail located in Champaign, IL, between December 18, 2013, through January 25, 2014. Triangular markers denote relative humidity value from KTIP weather station, square markers denote measured relative humidity values from ambient sensors, and circular markers denote measured relative humidity values inside concrete.

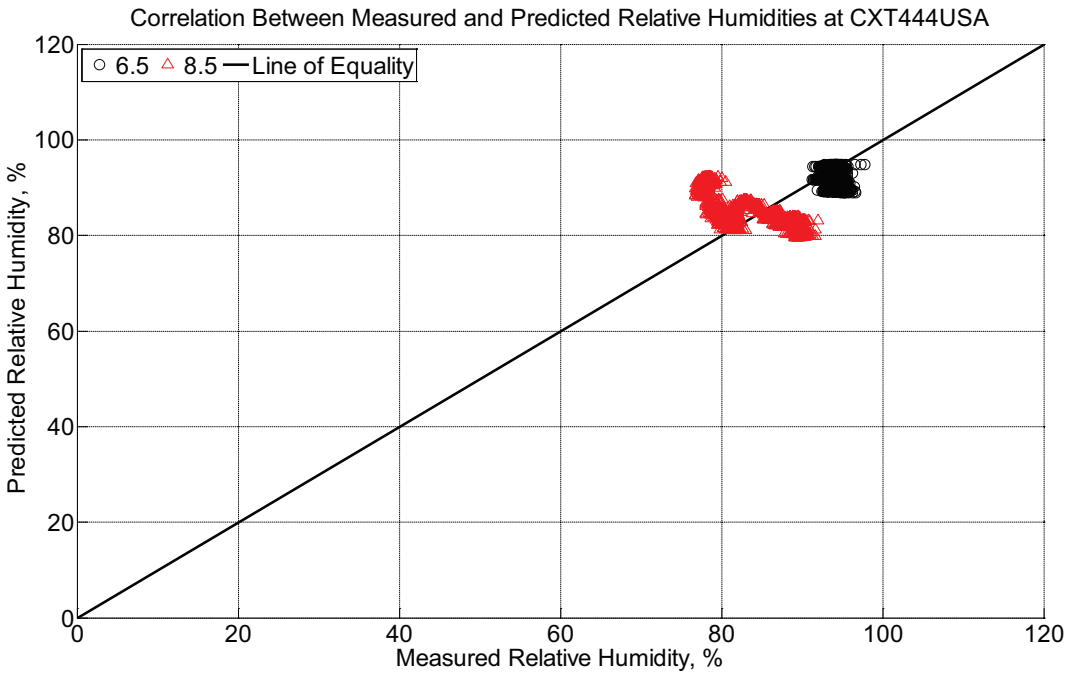

Figure B-400 Correlation between measured and predicted relative humidity values 6.5 inches (139.7 mm) and 8.5 inches (215.9 mm) from the surface of a concrete crosstie (labeled CXT444USA) without a polyurethane pad nor rail located in Champaign, IL, between December 18, 2013, through January 25, 2014.

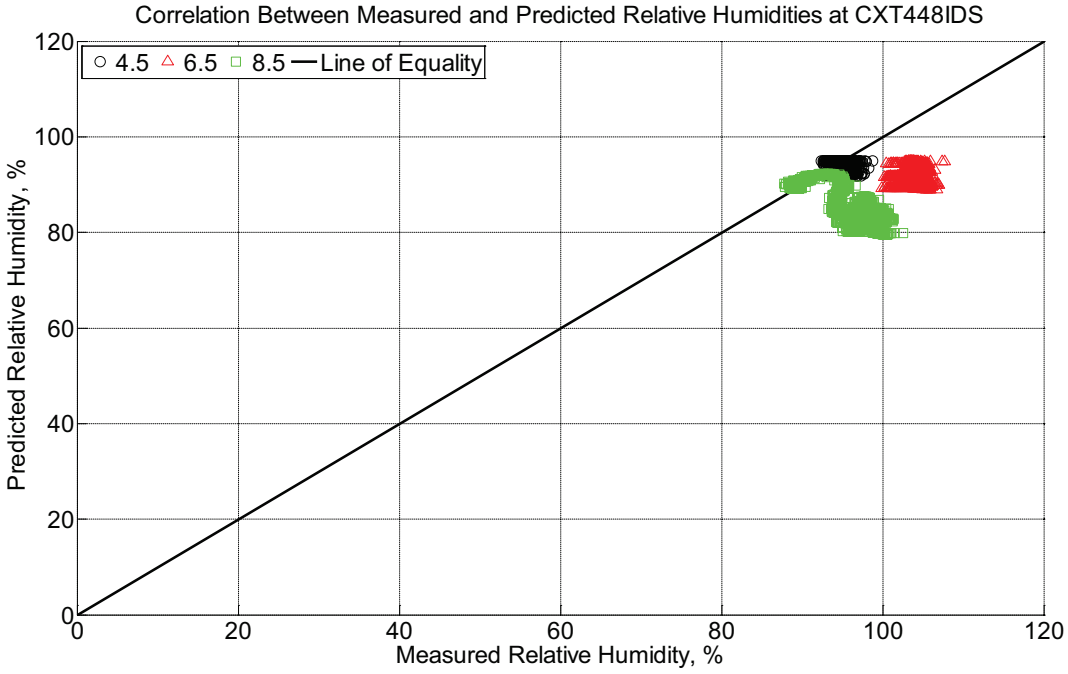

Figure B-401 Correlation between measured and predicted relative humidity values 4.5 inches (114.3 mm), 6.5 inches (139.7 mm), and 8.5 inches (215.9 mm) from the surface of a

concrete crosstie (labeled CXT448IDS) without a polyurethane pad nor rail located in Champaign, IL, between December 18, 2013, through January 25, 2014.

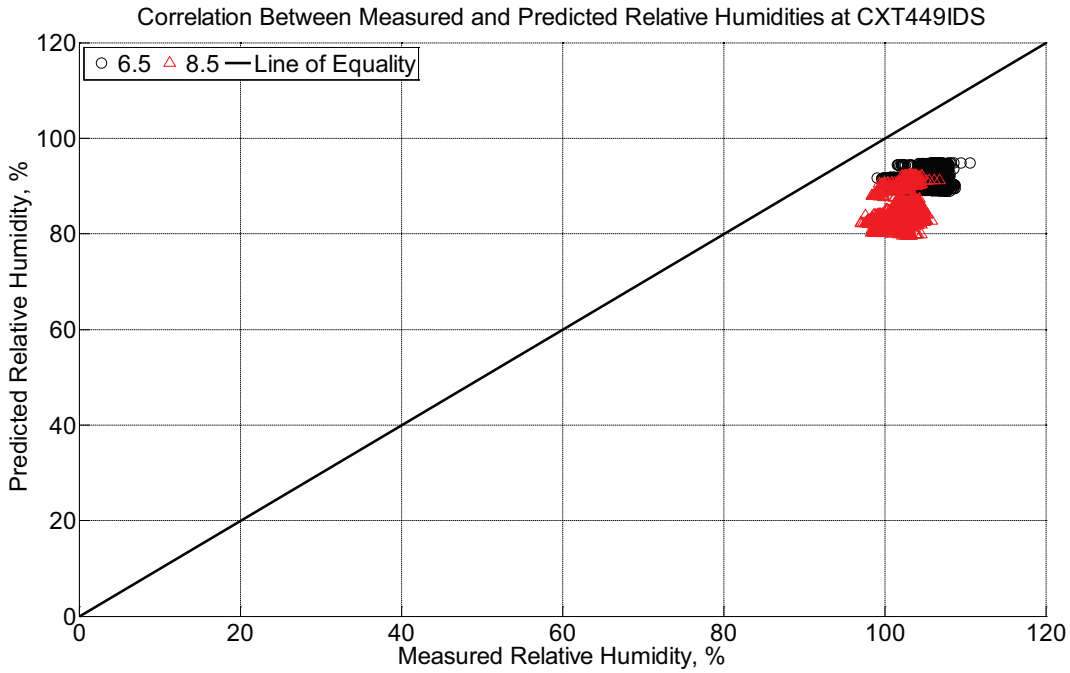

Figure B-402 Correlation between measured and predicted relative humidity values 6.5 inches (139.7 mm) and 8.5 inches (215.9 mm) from the surface of a concrete crosstie (labeled CXT449IDS) without a polyurethane pad nor rail located in Champaign, IL, between December 18, 2013, through January 25, 2014.

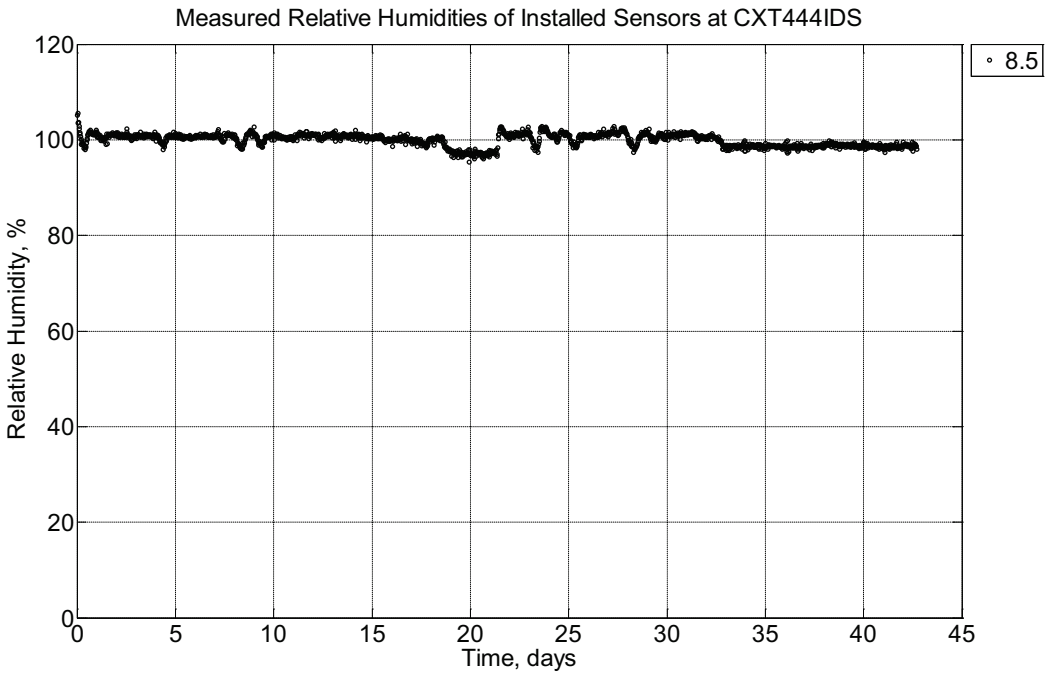

Figure B-403 Measured relative humidity at a depth of 8.5 inches (215.9 mm) from the surface of a concrete crosstie (labeled CXT444IDS) without a polyurethane pad nor rail located in Champaign, IL, between February 2, 2014, through March 17, 2014. At days 19-21, the instrumented crossties are moved inside of the Newmark Civil Engineering Laboratory. At days 21-33, the instrumented crossties are located outside in Rantoul, IL. At days 33-43, the instrumented crossties are moved inside the Materials Testing Laboratory at the Advanced Transportation Research Laboratory (ATREL) in Rantoul, IL.

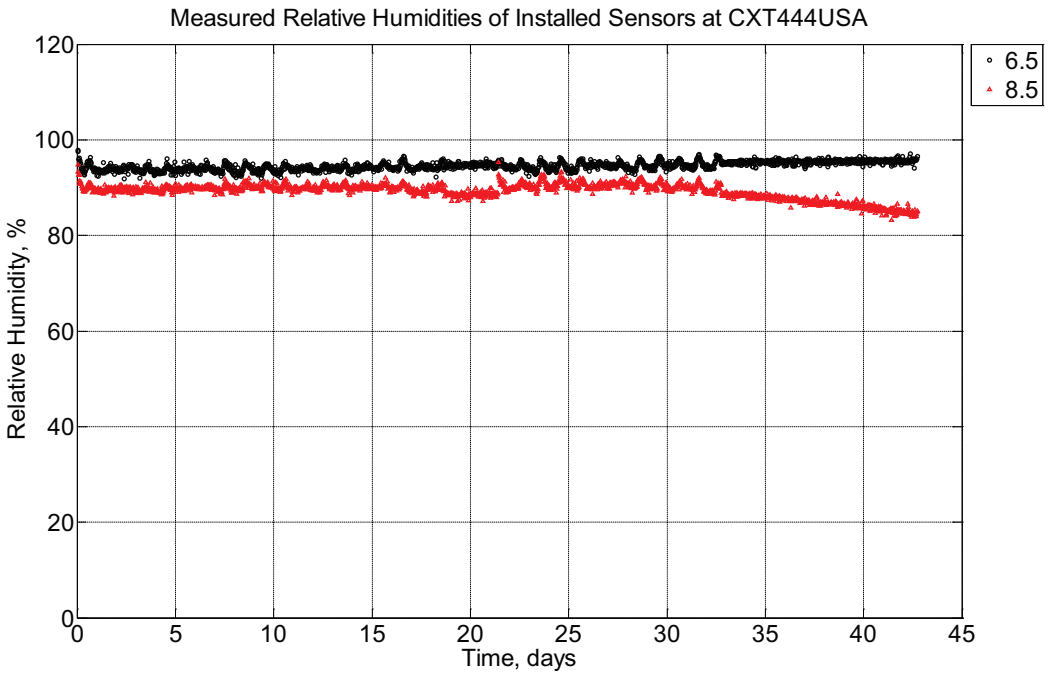

Figure B-404 Measured relative humidity at depths of 6.5 inches (139.7 mm) and 8.5 inches (215.9 mm) from the surface of a concrete crosstie (labeled CXT444USA) without a polyurethane pad nor rail located in Champaign, IL, between February 2, 2014, through March 17, 2014. At days 19-21, the instrumented crossties are moved inside of the Newmark Civil Engineering Laboratory. At days 21-33, the instrumented crossties are located outside in Rantoul, IL. At days 33-43, the instrumented crossties are moved inside the Materials Testing Laboratory at the Advanced Transportation Research Laboratory (ATREL) in Rantoul, IL.

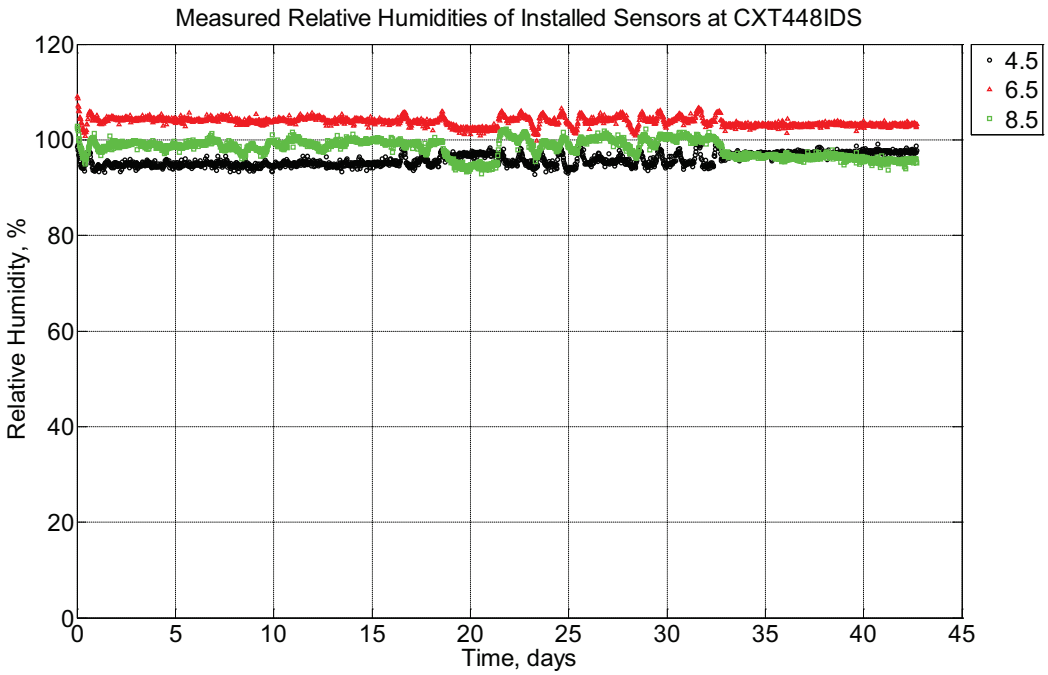

Figure B-405 Measured relative humidity at depths of 4.5 inches (114.3 mm), 6.5 inches (139.7 mm), and 8.5 inches (215.9 mm) from the surface of a concrete crosstie (labeled CXT448IDS) without a polyurethane pad nor rail located in Champaign, IL, between February 2, 2014, through March 17, 2014. At days 19-21, the instrumented crossties are moved inside of the Newmark Civil Engineering Laboratory. At days 21-33, the instrumented crossties are located outside in Rantoul, IL. At days 33-43, the instrumented crossties are moved inside the Materials Testing Laboratory at the Advanced Transportation Research Laboratory (ATREL) in Rantoul, IL.

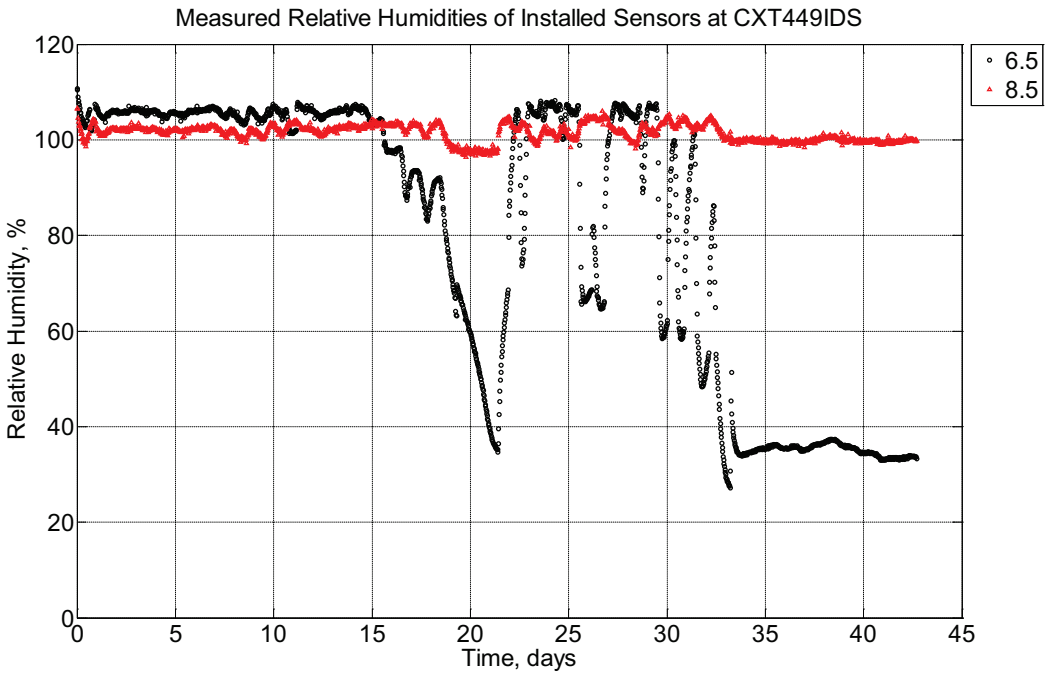

Figure B-406 Measured relative humidity at depths of 6.5 inches (139.7 mm) and 8.5 inches (215.9 mm) from the surface of a concrete crosstie (labeled CXT449IDS) without a polyurethane pad nor rail located in Champaign, IL, between February 2, 2014, through March 17, 2014. At days 19-21, the instrumented crossties are moved inside of the Newmark Civil Engineering Laborary. At days 21-33, the instrumented crossties are located outside in Rantoul, IL. At days 33-43, the instrumented crossties are moved inside the Materials Testing Laboratory at the Advanced Transportation Research Laboratory (ATREL) in Rantoul, IL.

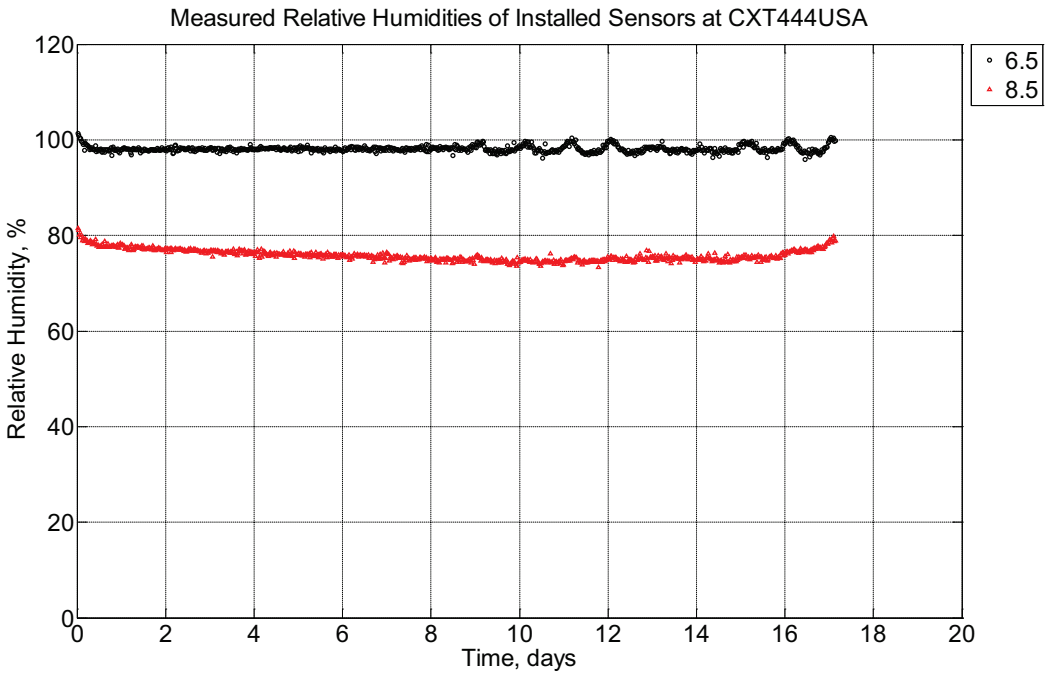

Figure B-407 Measured relative humidity at depths of 6.5 inches (139.7 mm) and 8.5 inches (215.9 mm) from the surface of a concrete crosstie (labeled CXT444USA) without a polyurethane pad nor rail located in Rantoul, IL, between March 31, 2014, through April 17, 2014. At days 1-9, the instrumented crossties are inside the Materials Testing Laboratory at the Advanced Transportation Research Laboratory (ATREL) in Rantoul, IL. At days 9-17, the instrumented crossties are moved outside and into model ballast in Rantoul, IL.

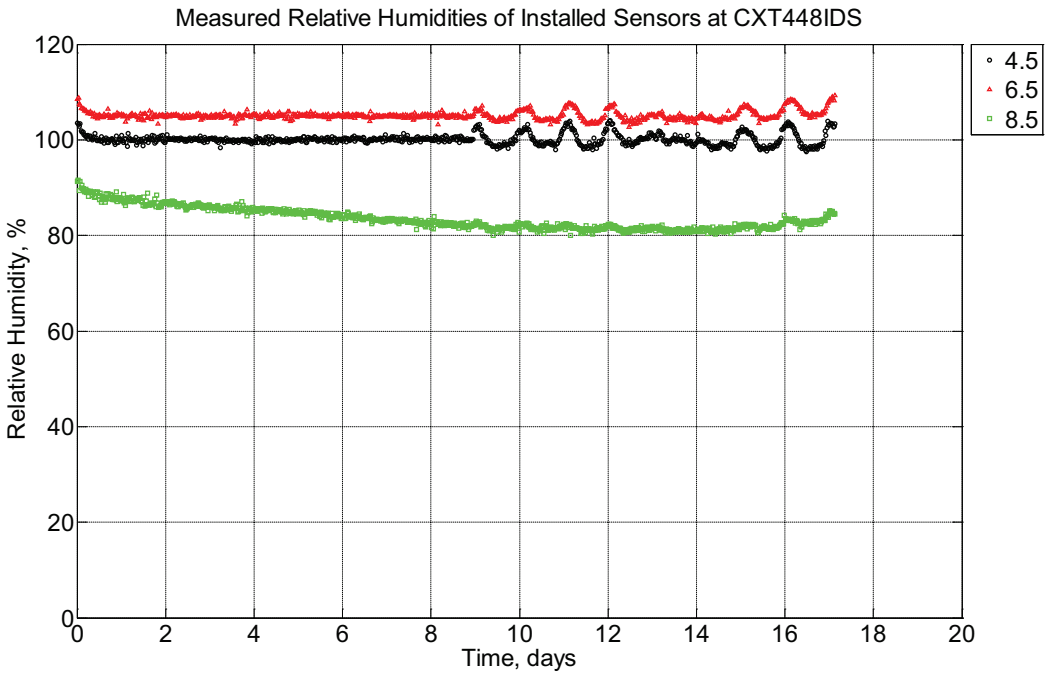

Figure B-408 Measured relative humidity at depths of 4.5 inches (114.3 mm), 6.5 inches (139.7 mm), and 8.5 inches (215.9 mm) from the surface of a concrete crosstie (labeled CXT448IDS) without a polyurethane pad nor rail located in Rantoul, IL, between March 31, 2014, through April 17, 2014. At days 1-9, the instrumented crossties are inside the Materials Testing Laboratory at the Advanced Transportation Research Laboratory (ATREL) in Rantoul, IL. At days 9-17, the instrumented crossties are moved outside and into model ballast in Rantoul, IL.

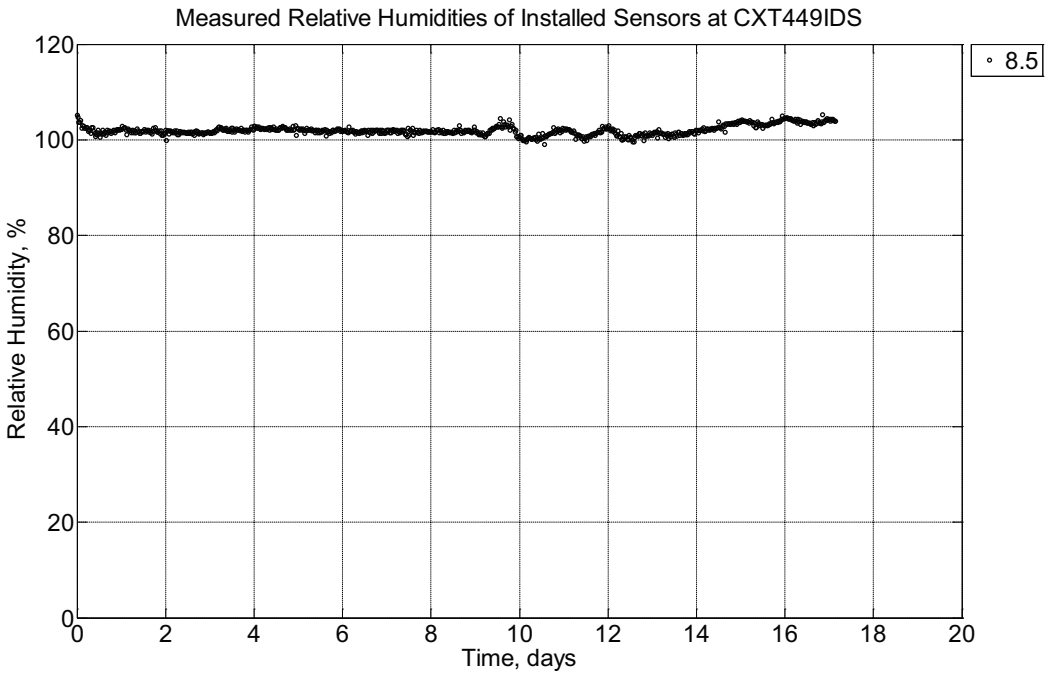

Figure B-409 Measured temperature at a depth of 8.5 inches (215.9 mm) from the surface of a concrete crosstie (labeled CXT449IDS) without a polyurethane pad nor rail located in Rantoul, IL, between March 31, 2014, through April 17, 2014. At days 1-9, the instrumented crossties are inside the Materials Testing Laboratory at the Advanced Transportation Research Laboratory (ATREL) in Rantoul, IL. At days 9-17, the instrumented crossties are moved outside and into model ballast in Rantoul, IL.

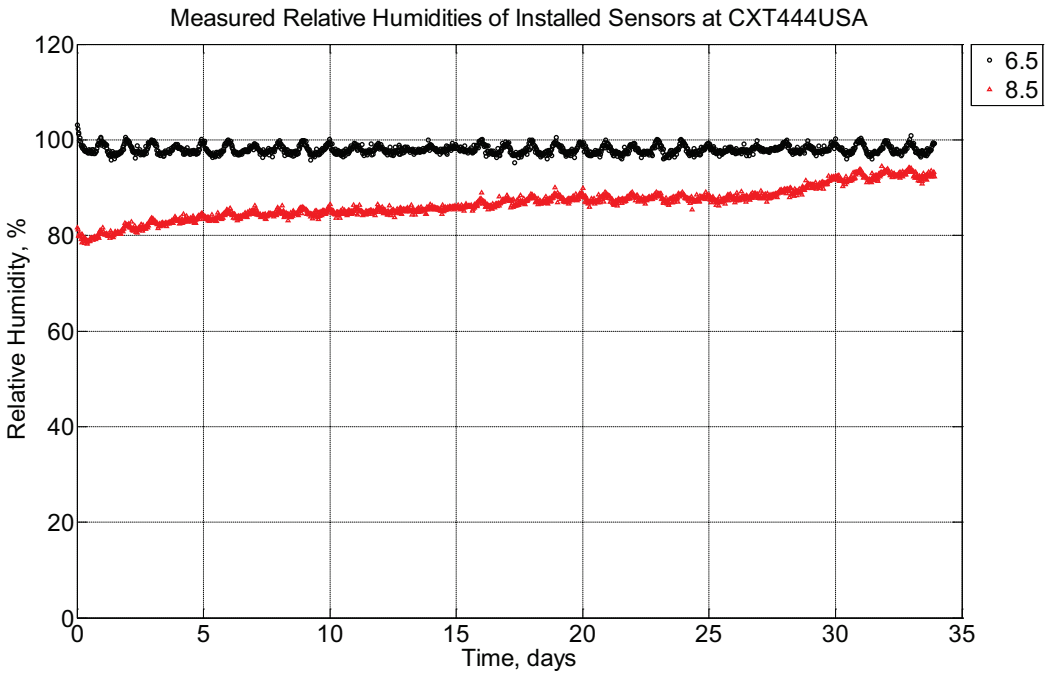

Figure B-410 Measured relative humidity at depths of 6.5 inches (139.7 mm) and 8.5 inches (215.9 mm) from the surface of a concrete crosstie (labeled CXT444USA) without a polyurethane pad nor rail installed in ballast in Rantoul, IL, between April 17, 2014, through May 21, 2014.

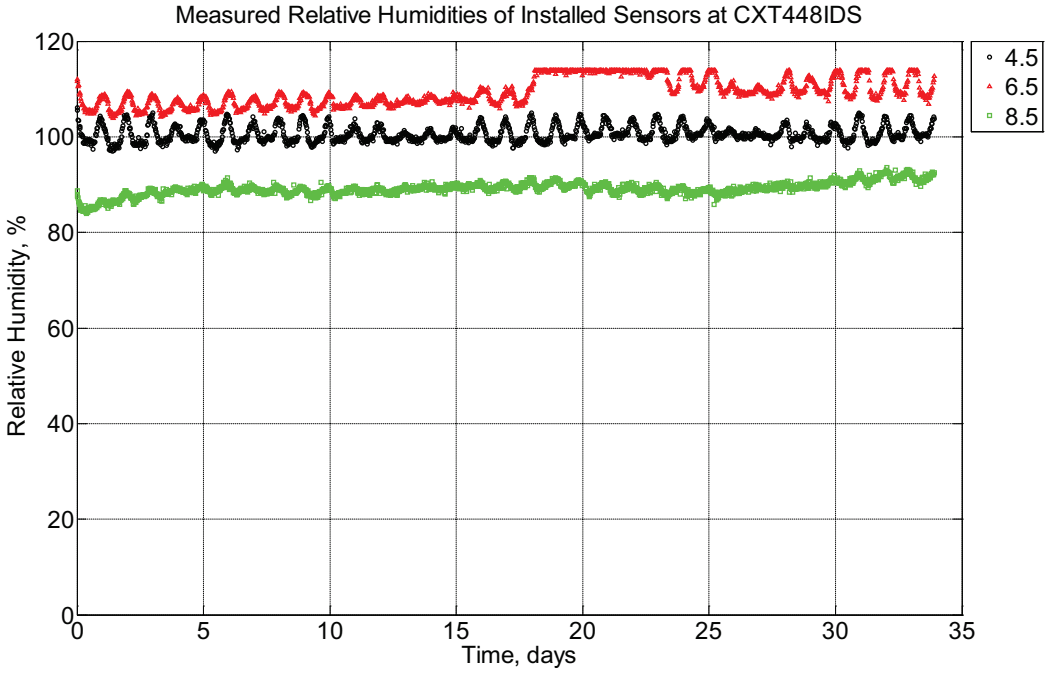

Figure B-411 Measured relative humidity at depths of 4.5 inches (114.3 mm), 6.5 inches (139.7 mm), and 8.5 inches (215.9 mm) from the surface of a concrete crosstie (labeled

CXT448IDS) without a polyurethane pad nor rail installed in ballast in Rantoul, IL, between April 17, 2014, through May 21, 2014.

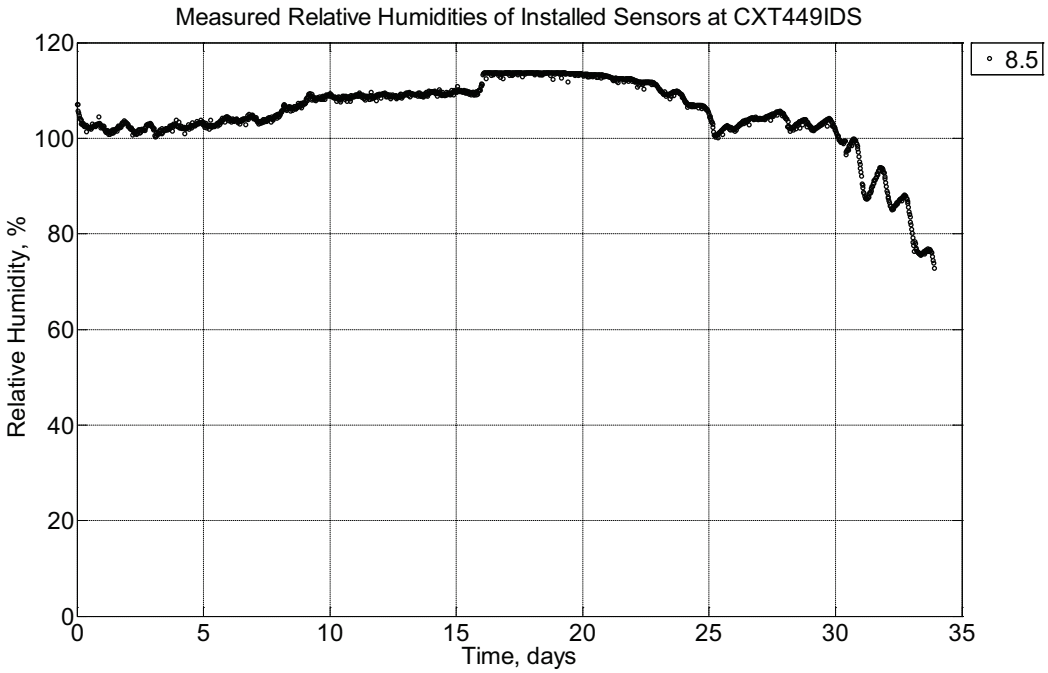

Figure B-412 Measured relative humidity at a depth of 8.5 inches (215.9 mm) from the surface of a concrete crosstie (labeled CXT449IDS) without a polyurethane pad nor rail installed in ballast in Rantoul, IL, between April 17, 2014, through May 21, 2014.

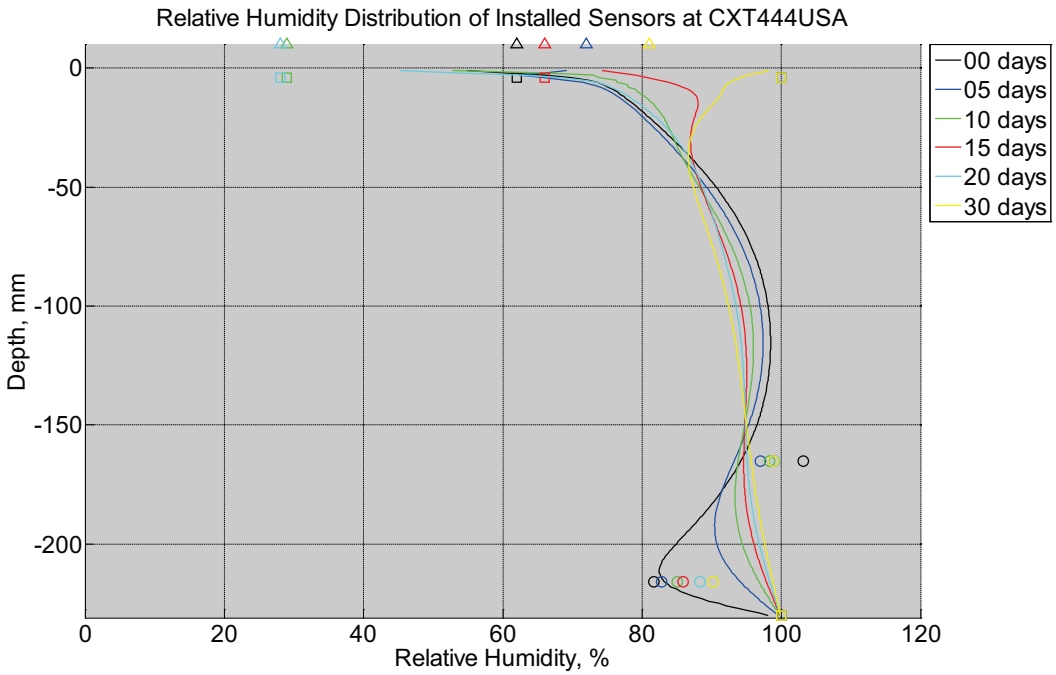

Figure B-413 Measured (markers) and modeled (continuous line) relative humidity profile distribution as a function of depth inside a concrete crosstie (labeled CXT444USA) without a polyurethane pad nor rail installed in ballast in Rantoul, IL, between April 17, 2014, through May 21, 2014. Triangular markers denote relative humidity value from KTIP weather station, square markers denote measured relative humidity values from ballast, and circular markers denote measured relative humidity values inside concrete.

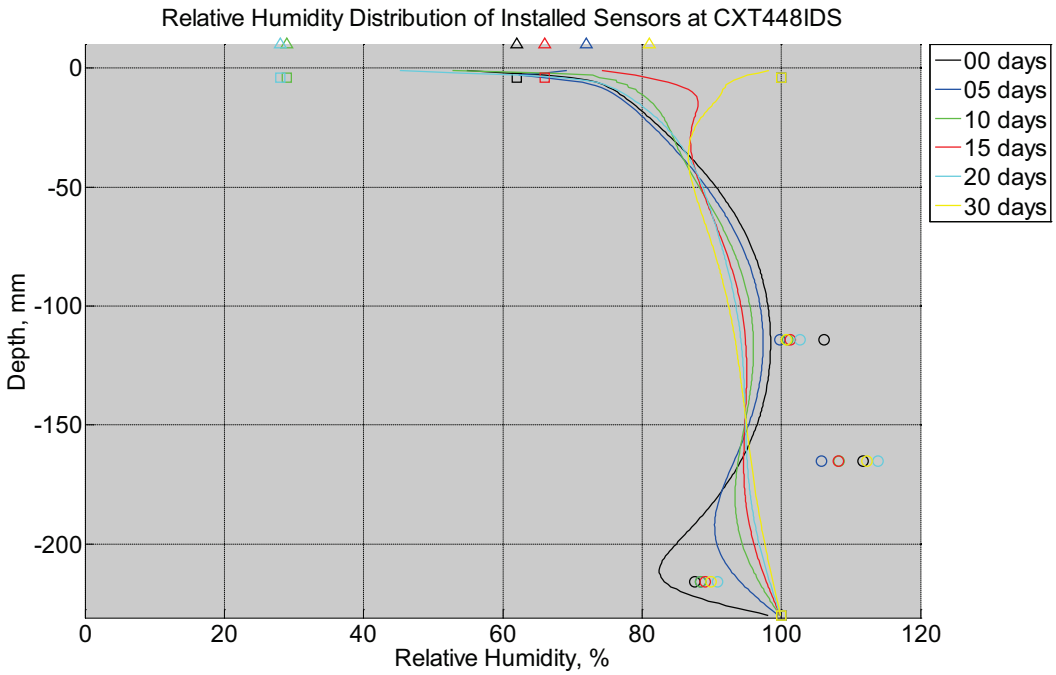

Figure B-414 Measured (markers) and modeled (continuous line) relative humidity profile distribution as a function of depth inside a concrete crosstie (labeled CXT448IDS) without a polyurethane pad nor rail installed in ballast in Rantoul, IL, between April 17, 2014, through May 21, 2014. Triangular markers denote relative humidity value from KTIP weather station, square markers denote measured relative humidity values from ballast, and circular markers denote measured relative humidity values inside concrete.

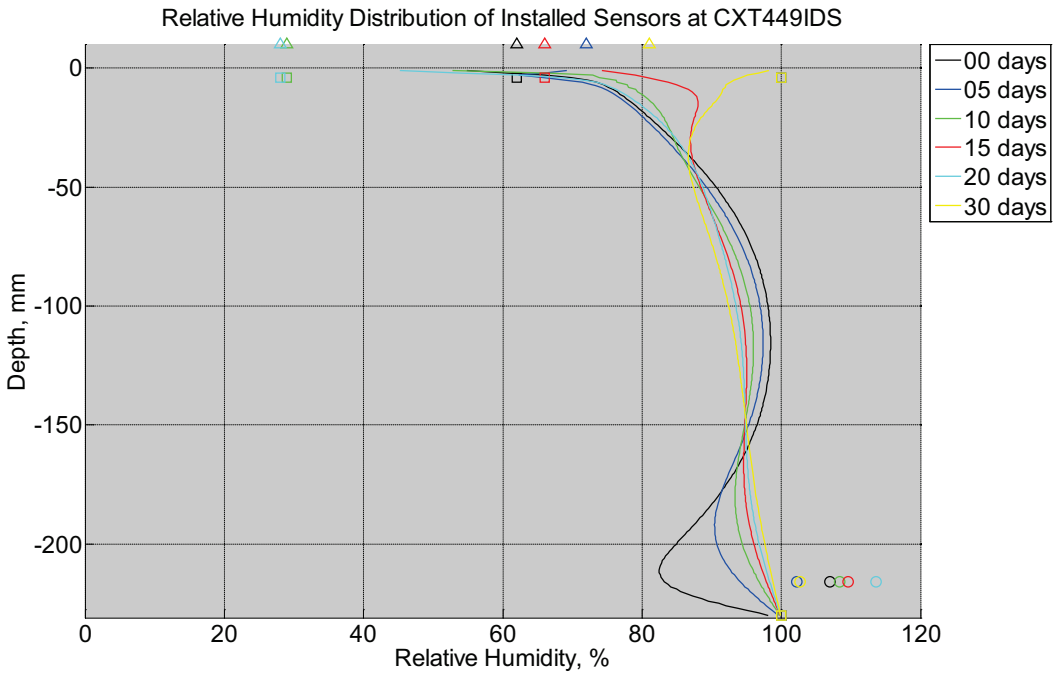

Figure B-415 Measured (markers) and modeled (continuous line) relative humidity profile distribution as a function of depth inside a concrete crosstie (labeled CXT449IDS) without a polyurethane pad nor rail installed in ballast in Rantoul, IL, between April 17, 2014, through May 21, 2014. Triangular markers denote relative humidity value from KTIP weather station, square markers denote measured relative humidity values from ballast, and circular markers denote measured relative humidity values inside concrete.

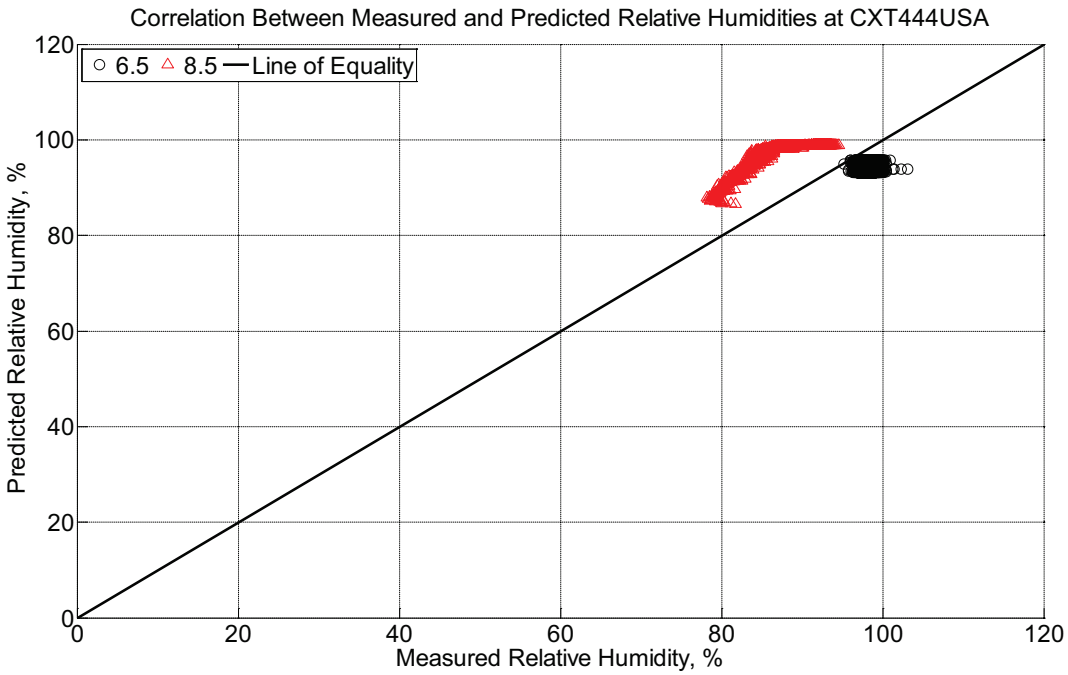

Figure B-416 Correlation between measured and predicted relative humidity values 6.5 inches (139.7 mm) and 8.5 inches (215.9 mm) from the surface of a concrete crosstie (labeled CXT444USA) without a polyurethane pad nor rail installed in ballast in Rantoul, IL, between April 17, 2014, through May 21, 2014.

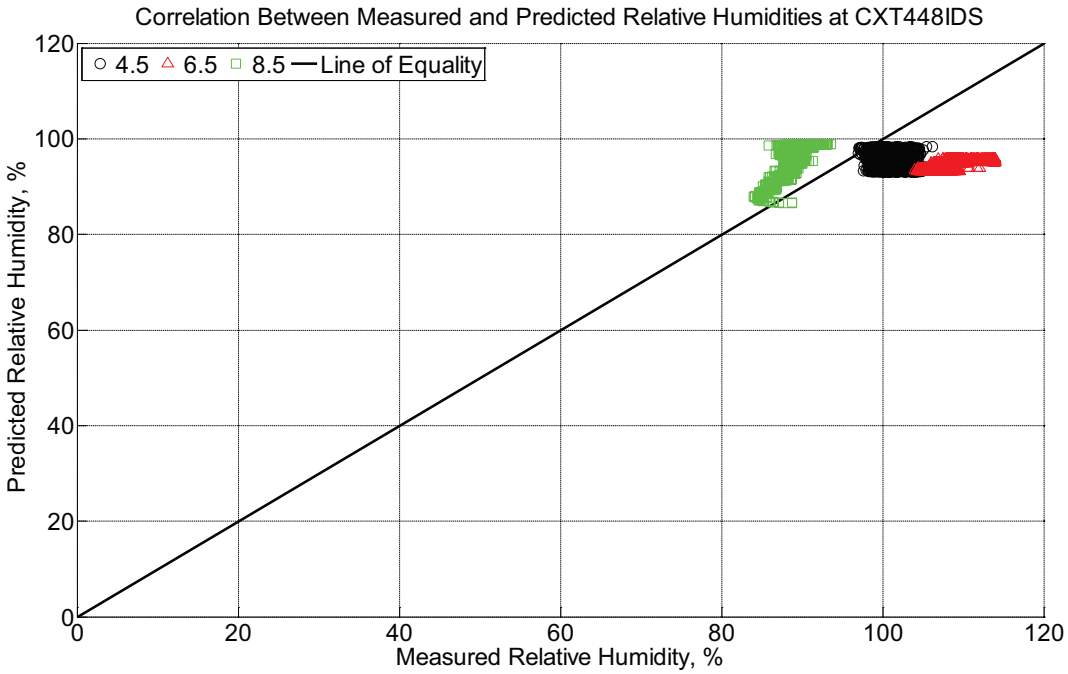

Figure B-417 Correlation between measured and predicted relative humidity values 4.5 inches (114.3 mm), 6.5 inches (139.7 mm), and 8.5 inches (215.9 mm) from the surface of a

concrete crosstie (labeled CXT448IDS) without a polyurethane pad nor rail installed in ballast in Rantoul, IL, between April 17, 2014, through May 21, 2014.

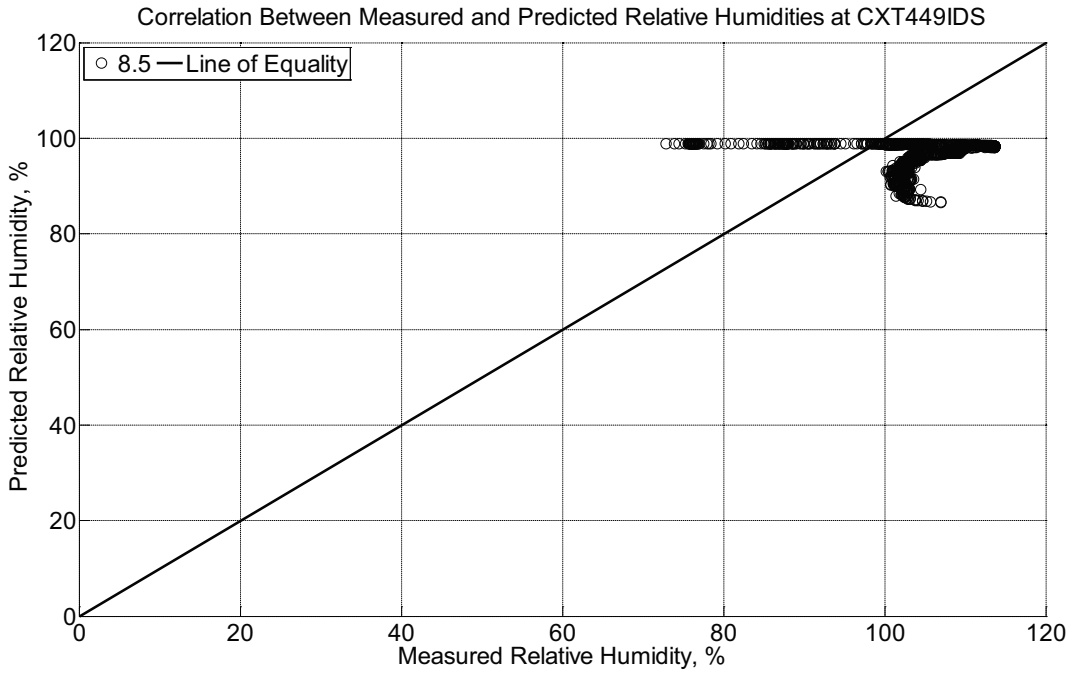

Figure B-418 Correlation between measured and predicted relative humidity values 8.5 inches (215.9 mm) from the surface of a concrete crosstie (labeled CXT449IDS) without a polyurethane pad nor rail installed in ballast in Rantoul, IL, between April 17, 2014, through May 21, 2014.

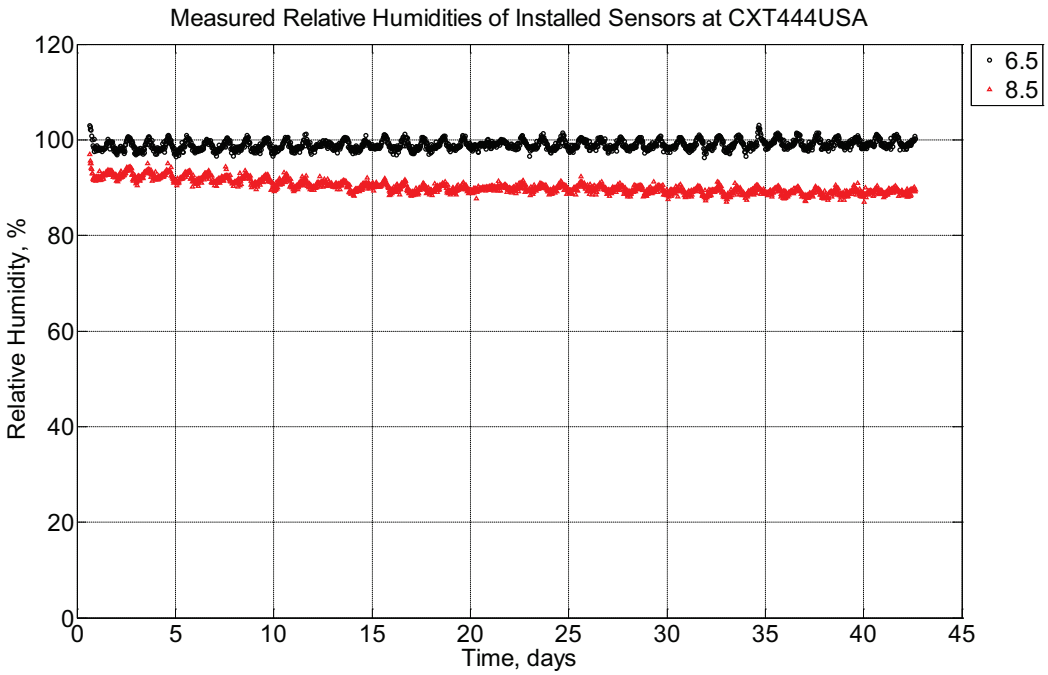

Figure B-419 Measured relative humidity at depths of 6.5 inches (139.7 mm) and 8.5 inches (215.9 mm) from the surface of a concrete crosstie (labeled CXT444USA) without a polyurethane pad nor rail installed in ballast in Rantoul, IL, between May 21, 2014, through July 2, 2014.

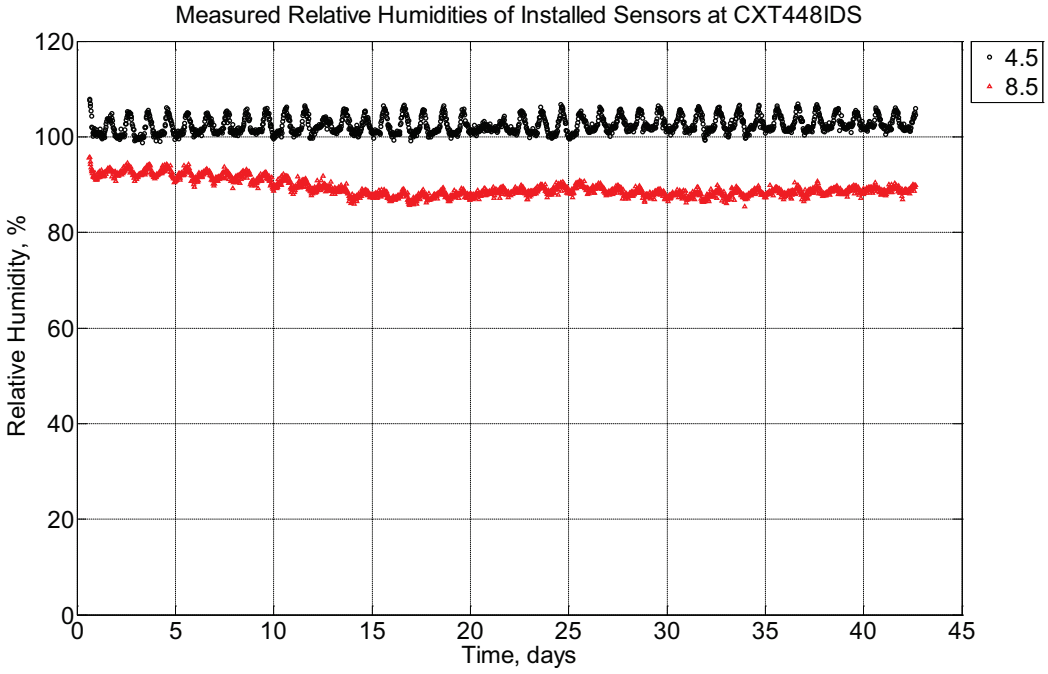

Figure B-420 Measured relative humidity at depths of 4.5 inches (114.3 mm) and 8.5 inches (215.9 mm) from the surface of a concrete crosstie (labeled CXT448IDS) without a

polyurethane pad nor rail installed in ballast in Rantoul, IL, between May 21, 2014, through July 2, 2014.

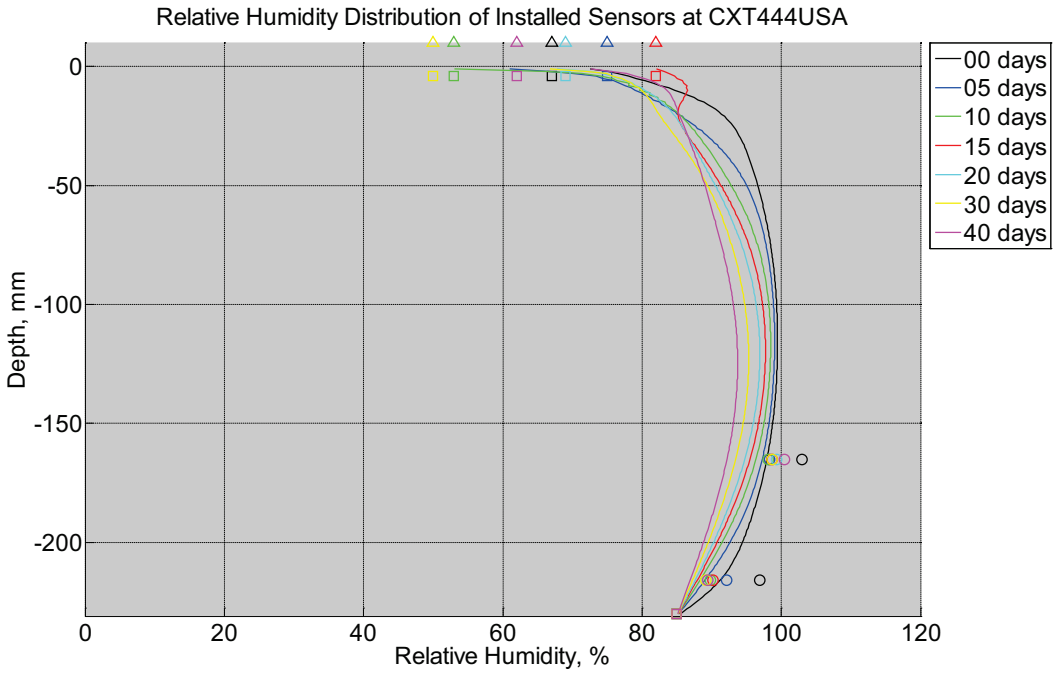

Figure B-421 Measured (markers) and modeled (continuous line) relative humidity profile distribution as a function of depth inside a concrete crosstie (labeled CXT444USA) without a polyurethane pad nor rail installed in ballast in Rantoul, IL, between May 21, 2014, through July 2, 2014. Triangular markers denote relative humidity value from KTIP weather station, square markers denote measured relative humidity values from ballast, and circular markers denote measured relative humidity values inside concrete.

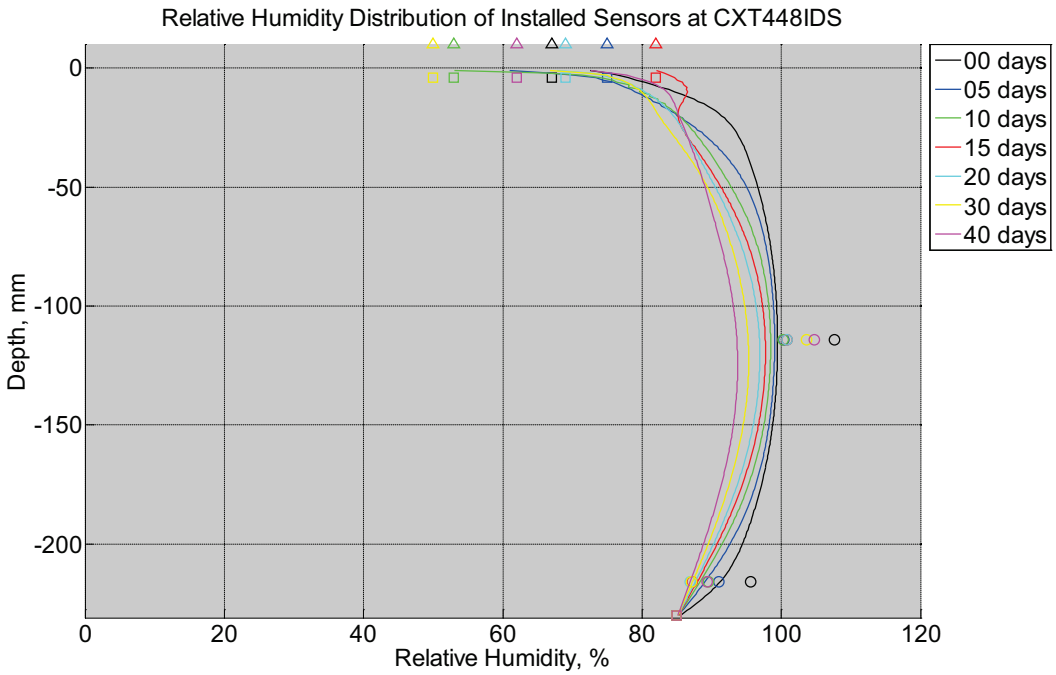

Figure B-422 Measured (markers) and modeled (continuous line) relative humidity profile distribution as a function of depth inside a concrete crosstie (labeled CXT448IDS) without a polyurethane pad nor rail installed in ballast in Rantoul, IL, between May 21, 2014, through July 2, 2014. Triangular markers denote relative humidity value from KTIP weather station, square markers denote measured relative humidity values from ballast, and circular markers denote measured relative humidity values inside concrete.

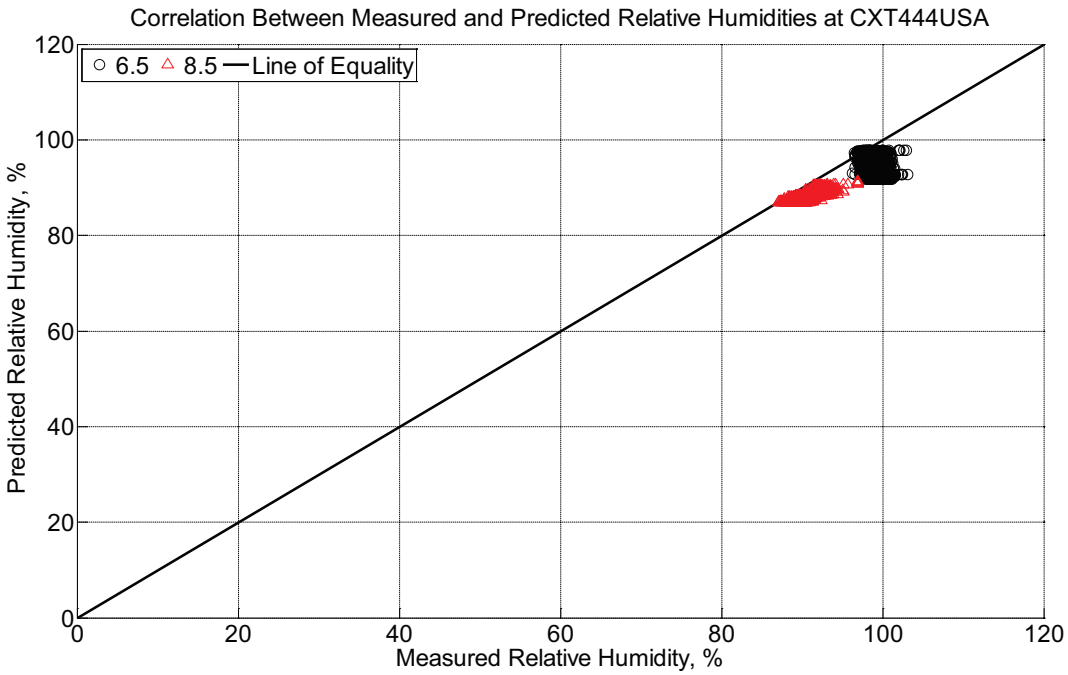

Figure B-423 Correlation between measured and predicted relative humidity values 6.5 inches (139.7 mm) and 8.5 inches (215.9 mm) from the surface of a concrete crosstie (labeled CXT444USA) without a polyurethane pad nor rail installed in ballast in Rantoul, IL, between May 21, 2014, through July 2, 2014.

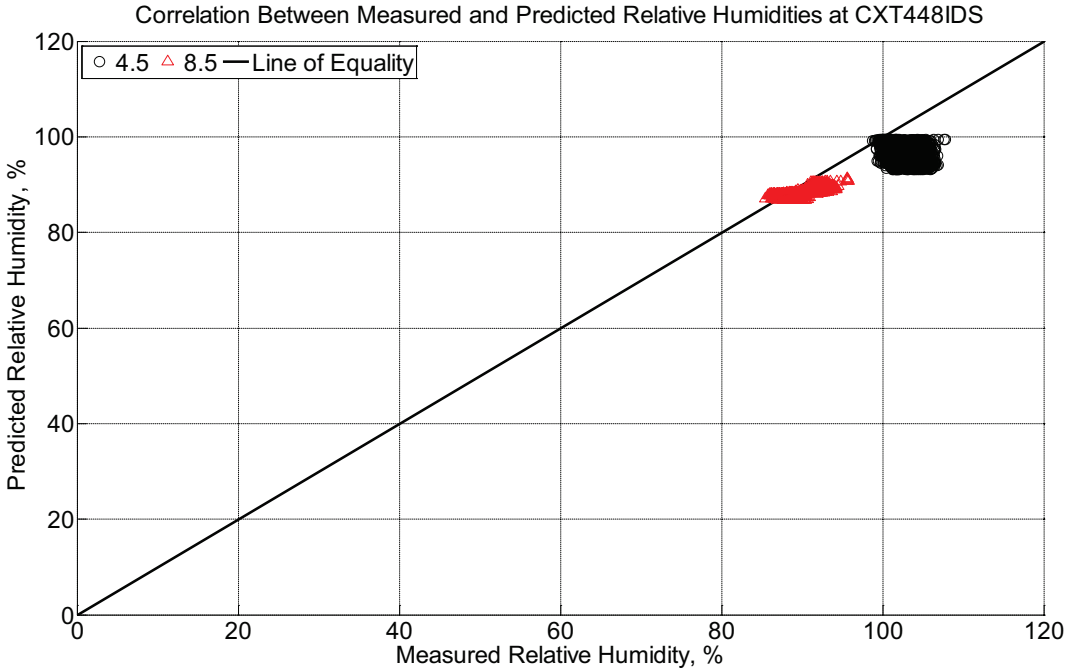

Figure B-424 Correlation between measured and predicted relative humidity values 4.5 inches (114.3 mm) and 8.5 inches (215.9 mm) from the surface of a concrete crosstie

(labeled CXT448IDS) without a polyurethane pad nor rail installed in ballast in Rantoul, IL, between May 21, 2014, through July 2, 2014.

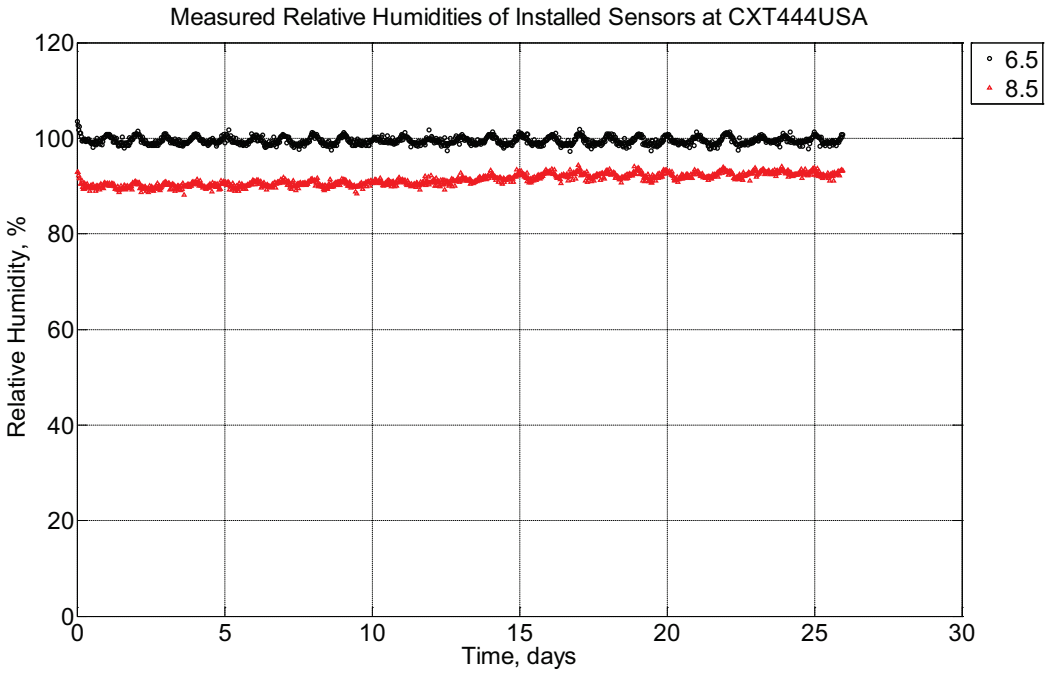

Figure B-425 Measured relative humidity at depths of 6.5 inches (139.7 mm) and 8.5 inches (215.9 mm) from the surface of a concrete crosstie (labeled CXT444USA) installed in ballast in Rantoul, IL, between July 2, 2014, through July 28, 2014. An 8 mm thick polyurethane pad and 12 in (30.48 cm) length 136 lb/yd (67.5 kg/m) section of steel rail are additionally installed atop the concrete crosstie.

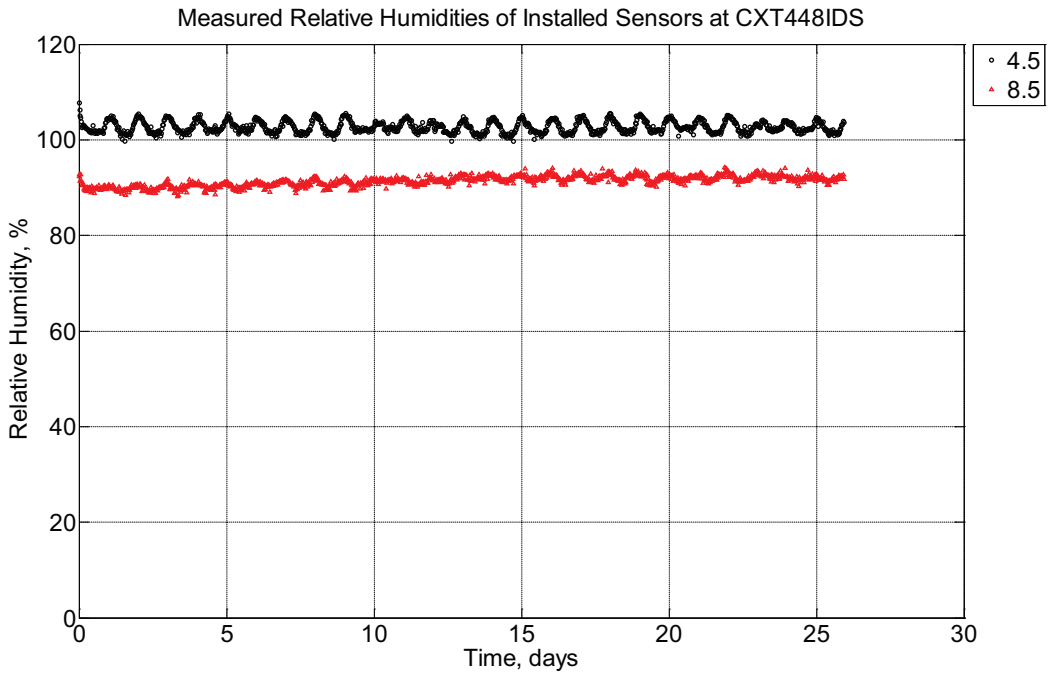

Figure B-426 Measured relative humidity at depths of 4.5 inches (114.3 mm) and 8.5 inches (215.9 mm) from the surface of a concrete crosstie (labeled CXT448IDS) installed in ballast in Rantoul, IL, between July 2, 2014, through July 28, 2014. An 8 mm thick polyurethane pad and 12 in (30.48 cm) length 136 lb/yd (67.5 kg/m) section of steel rail are additionally installed atop the concrete crosstie.

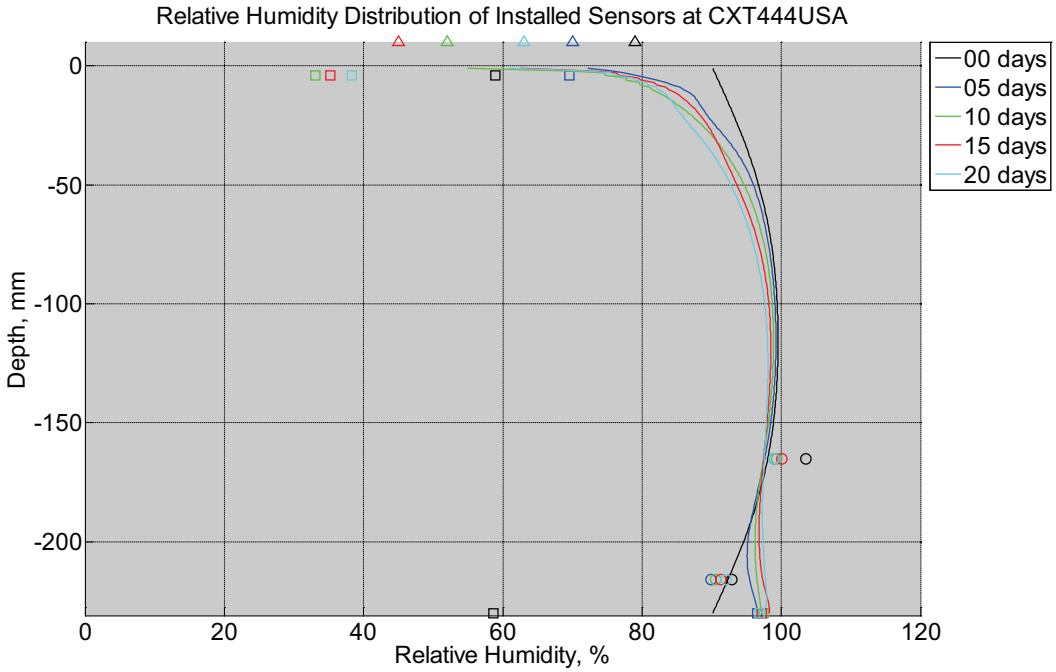

Figure B-427 Measured (markers) and modeled (continuous line) relative humidity profile

distribution as a function of depth inside a concrete crosstie (labeled CXT444USA) installed in ballast in Rantoul, IL, between July 2, 2014, through July 28, 2014. An 8 mm thick polyurethane pad and 12 in (30.48 cm) length 136 lb/yd (67.5 kg/m) section of steel rail are additionally installed atop the concrete crosstie. The model does not incorporate a polyurethane pad nor steel rail line. Triangular markers denote relative humidity value from KTIP weather station, square markers denote measured relative humidity values from ballast, and circular markers denote measured relative humidity values inside concrete.

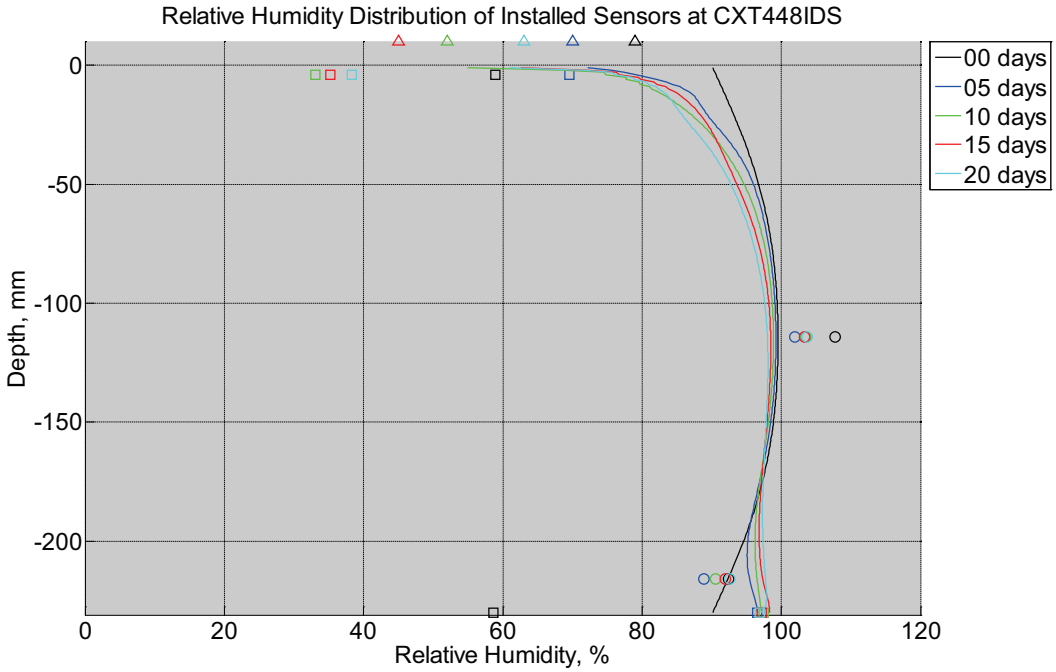

Figure B-428 Measured (markers) and modeled (continuous line) relative humidity profile distribution as a function of depth inside a concrete crosstie (labeled CXT448IDS) installed in ballast in Rantoul, IL, between July 2, 2014, through July 28, 2014. An 8 mm thick polyurethane pad and 12 in (30.48 cm) length 136 lb/yd (67.5 kg/m) section of steel rail are additionally installed atop the concrete crosstie. The model does not incorporate a polyurethane pad nor steel rail line. Triangular markers denote relative humidity value from KTIP weather station, square markers denote measured relative humidity values from ballast, and circular markers denote measured relative humidity values inside concrete.

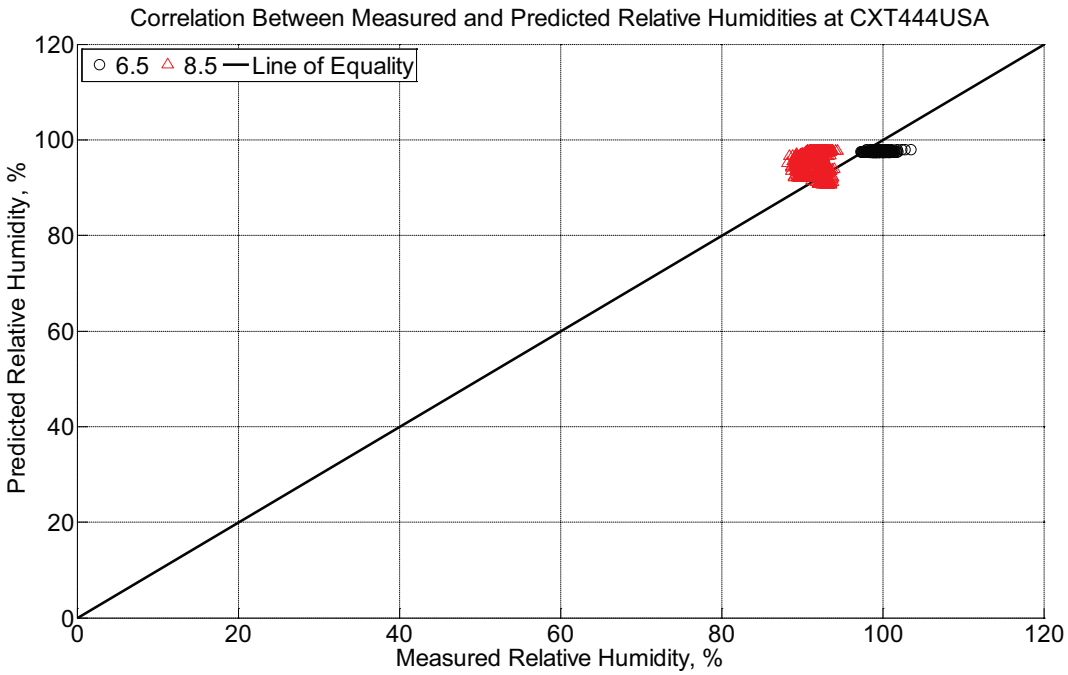

Figure B-429 Correlation between measured and predicted relative humidity values 6.5 inches (139.7 mm) and 8.5 inches (215.9 mm) from the surface of a concrete crosstie (labeled CXT444USA) installed in ballast in Rantoul, IL, between July 2, 2014, through July 28, 2014. An 8 mm thick polyurethane pad and 12 in (30.48 cm) length 136 lb/yd (67.5 kg/m) section of steel rail are additionally installed atop the concrete crosstie. The model does not incorporate a polyurethane pad nor steel rail line.

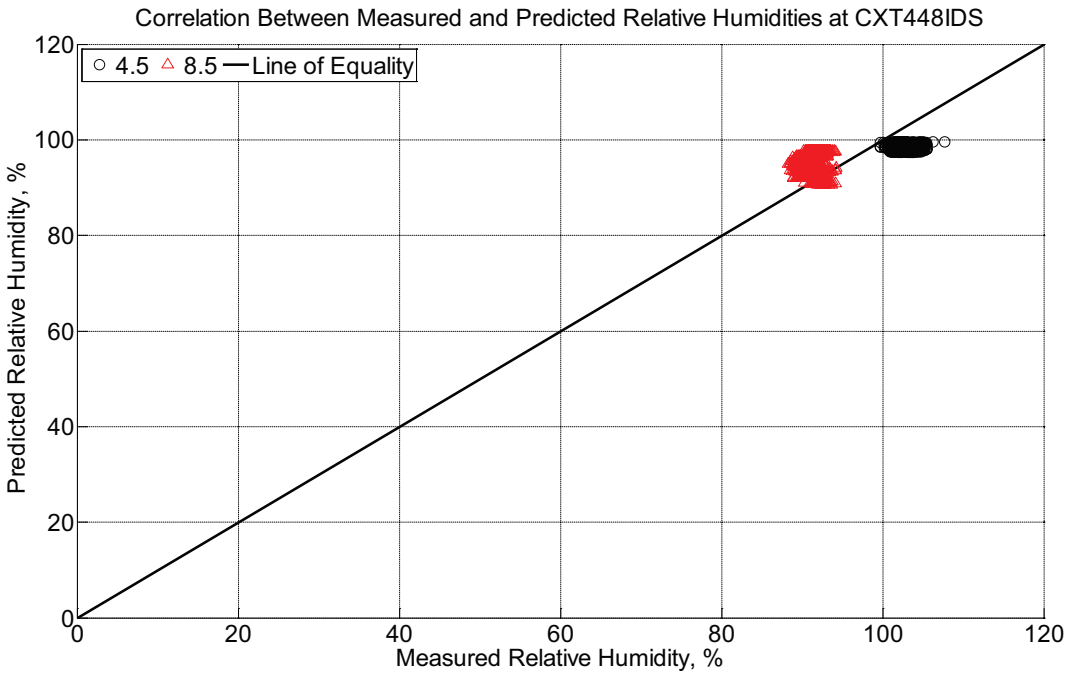

Figure B-430 Correlation between measured and predicted relative humidity values 4.5 inches (114.3 mm) and 8.5 inches (215.9 mm) from the surface of a concrete crosstie (labeled CXT448IDS) installed in ballast in Rantoul, IL, between July 2, 2014, through July 28, 2014. An 8 mm thick polyurethane pad and 12 in (30.48 cm) length 136 lb/yd (67.5 kg/m) section of steel rail are additionally installed atop the concrete crosstie. The model does not incorporate a polyurethane pad nor steel rail line.

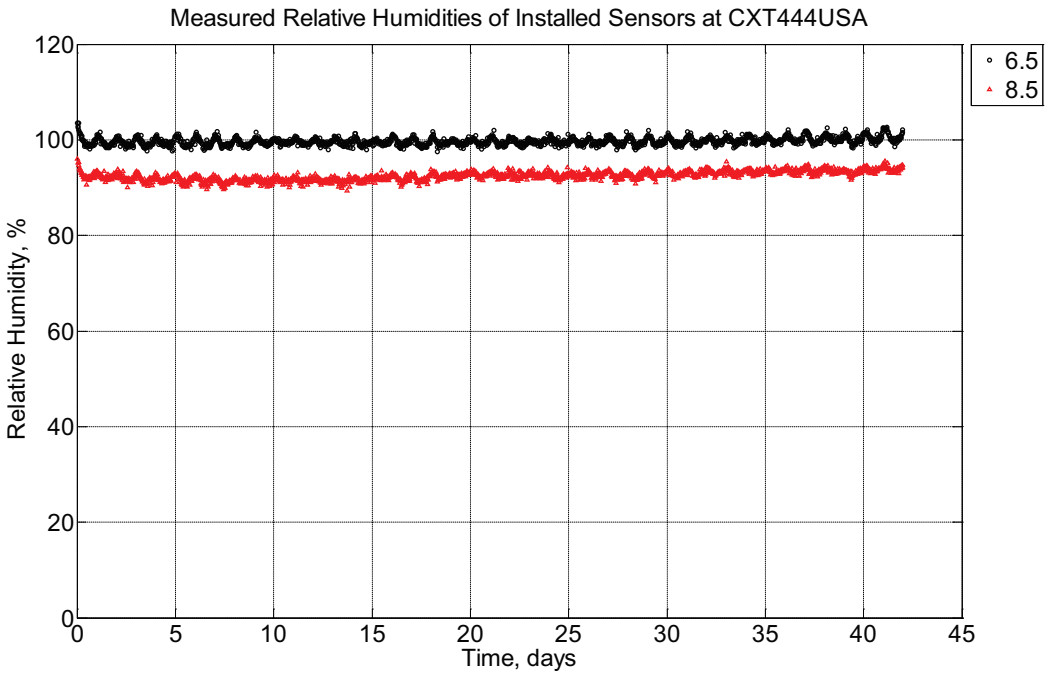

Figure B-431 Measured relative humidity at depths of 6.5 inches (139.7 mm) and 8.5 inches (215.9 mm) from the surface of a concrete crosstie (labeled CXT444USA) installed in ballast in Rantoul, IL, between July 28, 2014, through September 8, 2014. An 8 mm thick polyurethane pad and 12 in (30.48 cm) length 136 lb/yd (67.5 kg/m) section of steel rail are additionally installed atop the concrete crosstie.

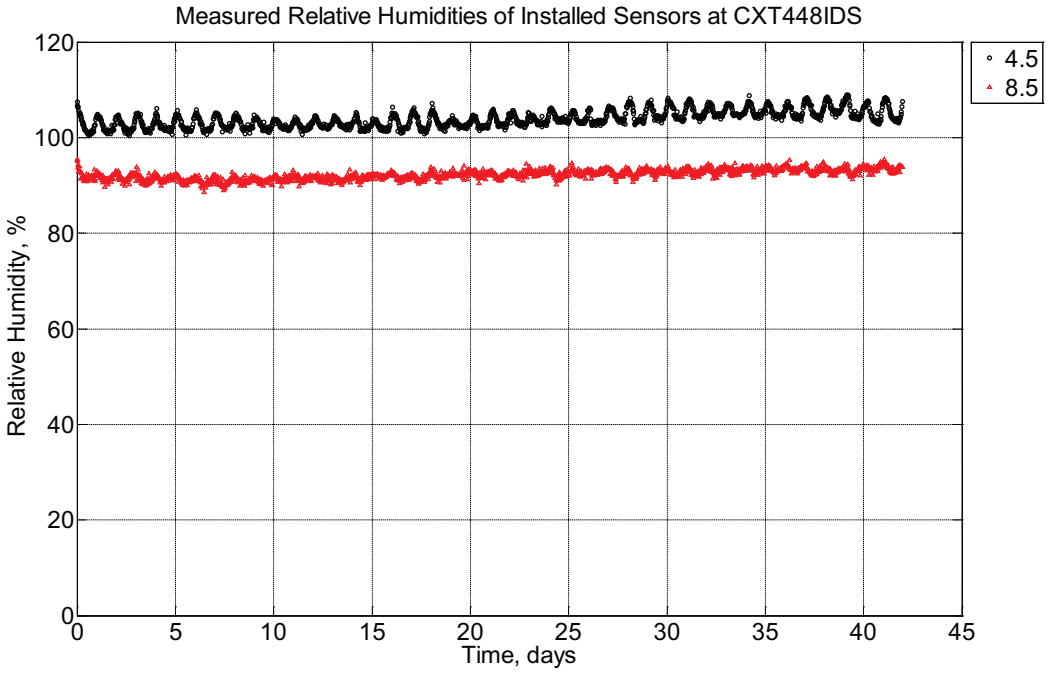

Figure B-432 Measured relative humidity at depths of 4.5 inches (114.3 mm) and 8.5 inches

(215.9 mm) from the surface of a concrete crosstie (labeled CXT448IDS) installed in ballast in Rantoul, IL, between July 28, 2014, through September 8, 2014. An 8 mm thick polyurethane pad and 12 in (30.48 cm) length 136 lb/yd (67.5 kg/m) section of steel rail are additionally installed atop the concrete crosstie.

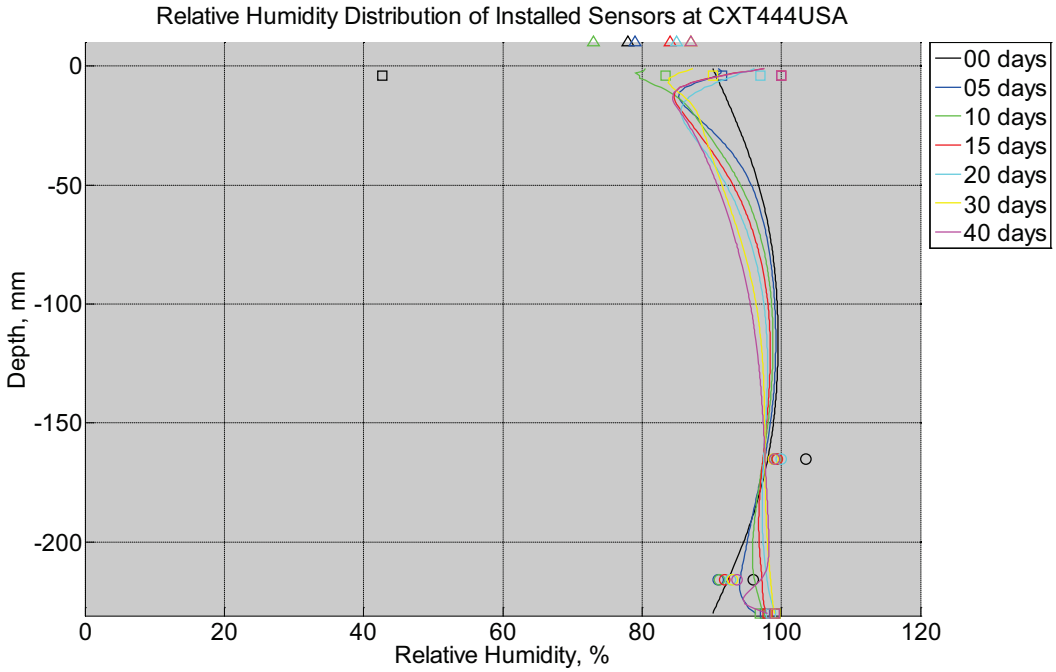

Figure B-433 Measured (markers) and modeled (continuous line) relative humidity profile distribution as a function of depth inside a concrete crosstie (labeled CXT444USA) installed in ballast in Rantoul, IL, between July 28, 2014, through September 8, 2014. An 8 mm thick polyurethane pad and 12 in (30.48 cm) length 136 lb/yd (67.5 kg/m) section of steel rail are additionally installed atop the concrete crosstie. The model does not incorporate a polyurethane pad nor steel rail line. Triangular markers denote relative humidity value from KTIP weather station, square markers denote measured relative humidity values from ballast, and circular markers denote measured relative humidity values inside concrete.

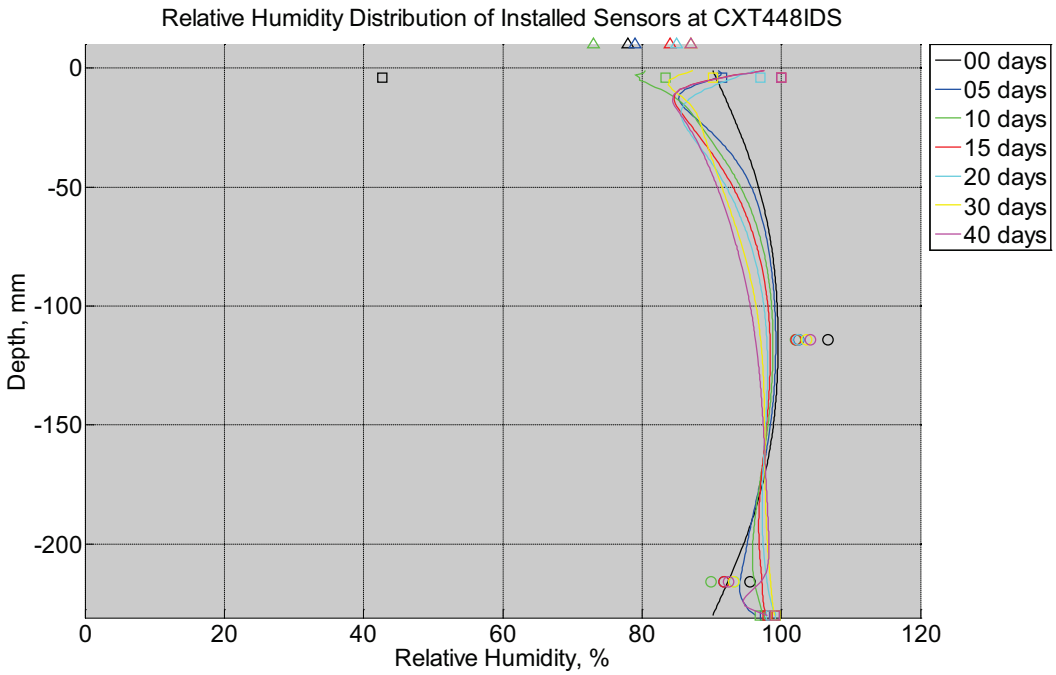

Figure B-434 Measured (markers) and modeled (continuous line) relative humidity profile distribution as a function of depth inside a concrete crosstie (labeled CXT448IDS) installed in ballast in Rantoul, IL, between July 28, 2014, through September 8, 2014. An 8 mm thick polyurethane pad and 12 in (30.48 cm) length 136 lb/yd (67.5 kg/m) section of steel rail are additionally installed atop the concrete crosstie. The model does not incorporate a polyurethane pad nor steel rail line. Triangular markers denote relative humidity value from KTIP weather station, square markers denote measured relative humidity values from ballast, and circular markers denote measured relative humidity values inside concrete.

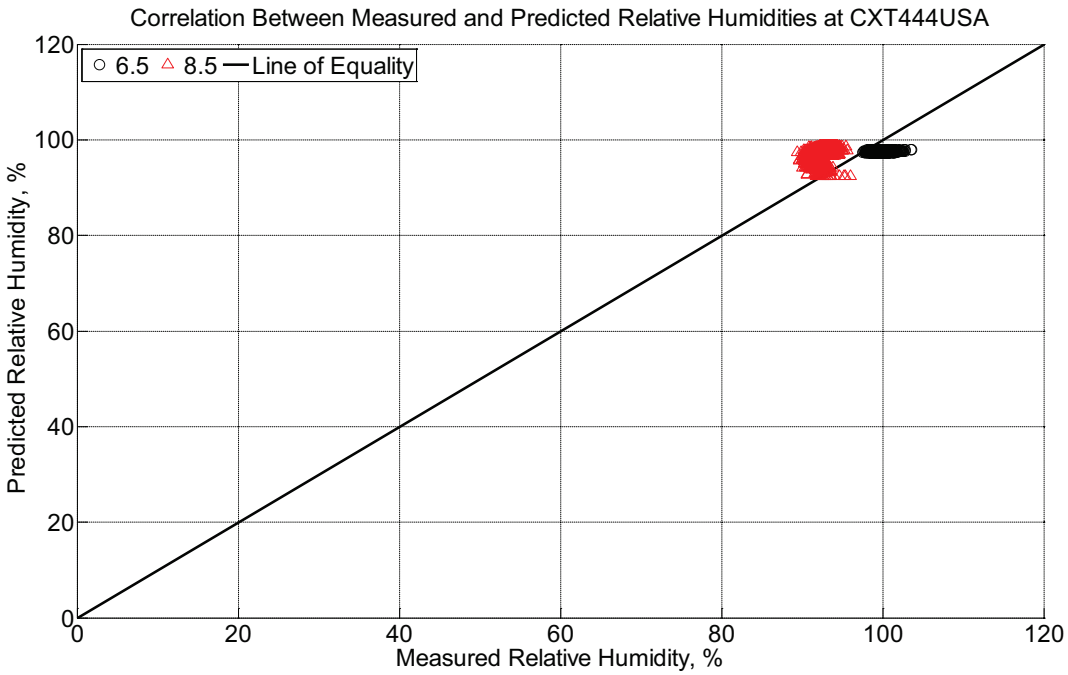

Figure B-435 Correlation between measured and predicted relative humidity values 6.5 inches (139.7 mm) and 8.5 inches (215.9 mm) from the surface of a concrete crosstie (labeled CXT444USA) installed in ballast in Rantoul, IL, between July 28, 2014, through September 8, 2014. An 8 mm thick polyurethane pad and 12 in (30.48 cm) length 136 lb/yd (67.5 kg/m) section of steel rail are additionally installed atop the concrete crosstie. The model does not incorporate a polyurethane pad nor steel rail line.

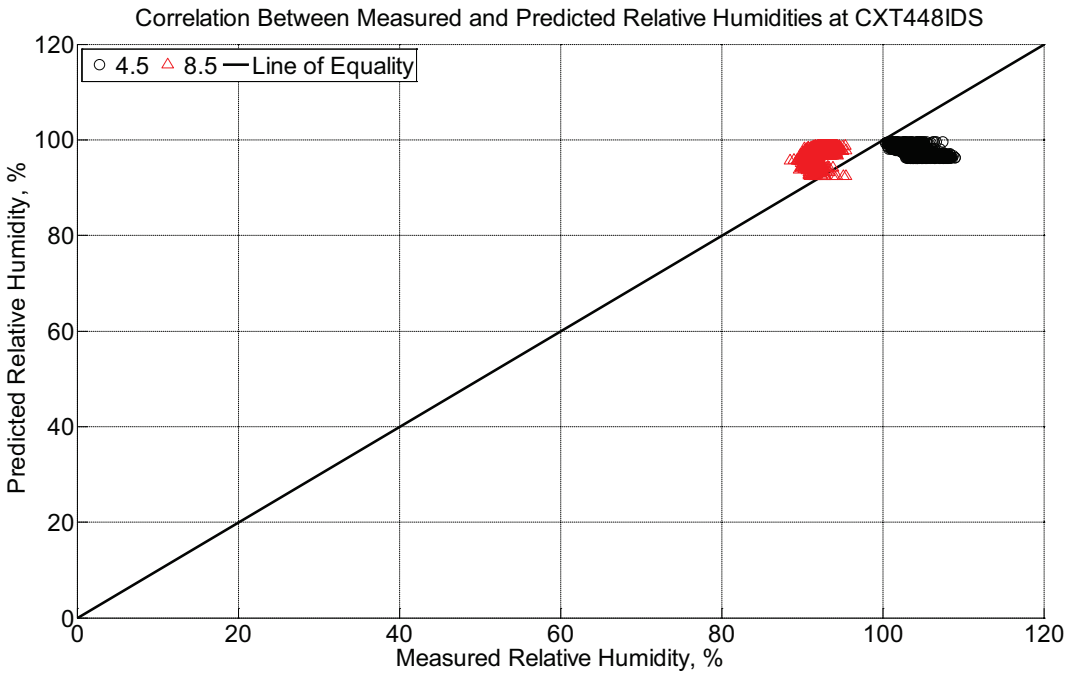

Figure B-436 Correlation between measured and predicted relative humidity values 4.5 inches (114.3 mm) and 8.5 inches (215.9 mm) from the surface of a concrete crosstie (labeled CXT448IDS) installed in ballast in Rantoul, IL, between July 28, 2014, through September 8, 2014. An 8 mm thick polyurethane pad and 12 in (30.48 cm) length 136 lb/yd (67.5 kg/m) section of steel rail are additionally installed atop the concrete crosstie. The model does not incorporate a polyurethane pad nor steel rail line.

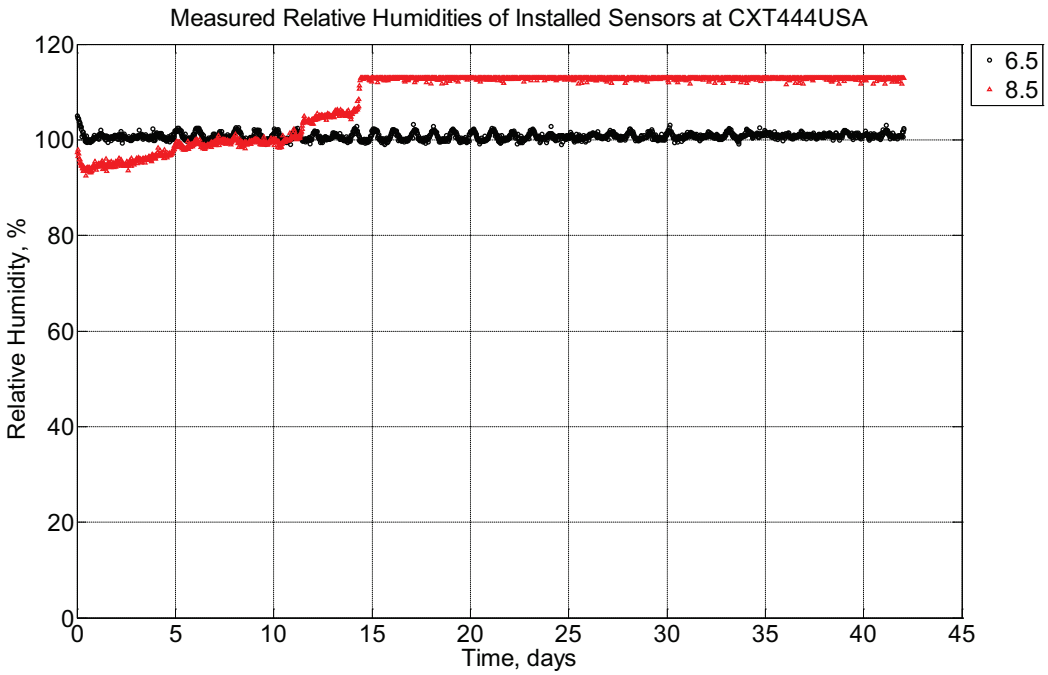

Figure B-437 Measured relative humidity at depths of 6.5 inches (139.7 mm) and 8.5 inches (215.9 mm) from the surface of a concrete crosstie (labeled CXT444USA) installed in ballast in Rantoul, IL, between September 8, 2014, through October 20, 2014. An 8 mm thick polyurethane pad and 12 in (30.48 cm) length 136 lb/yd (67.5 kg/m) section of steel rail are additionally installed atop the concrete crosstie.

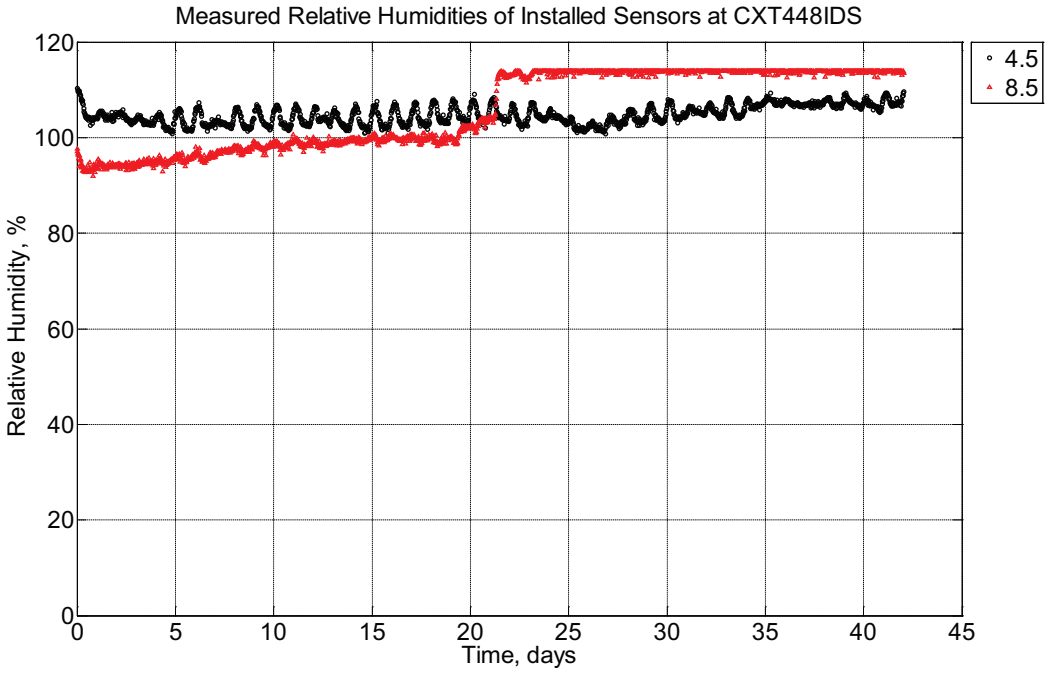

Figure B-438 Measured relative humidity at depths of 4.5 inches (114.3 mm) and 8.5 inches

(215.9 mm) from the surface of a concrete crosstie (labeled CXT448IDS) installed in ballast in Rantoul, IL, between September 8, 2014, through October 20, 2014. An 8 mm thick polyurethane pad and 12 in (30.48 cm) length 136 lb/yd (67.5 kg/m) section of steel rail are additionally installed atop the concrete crosstie.

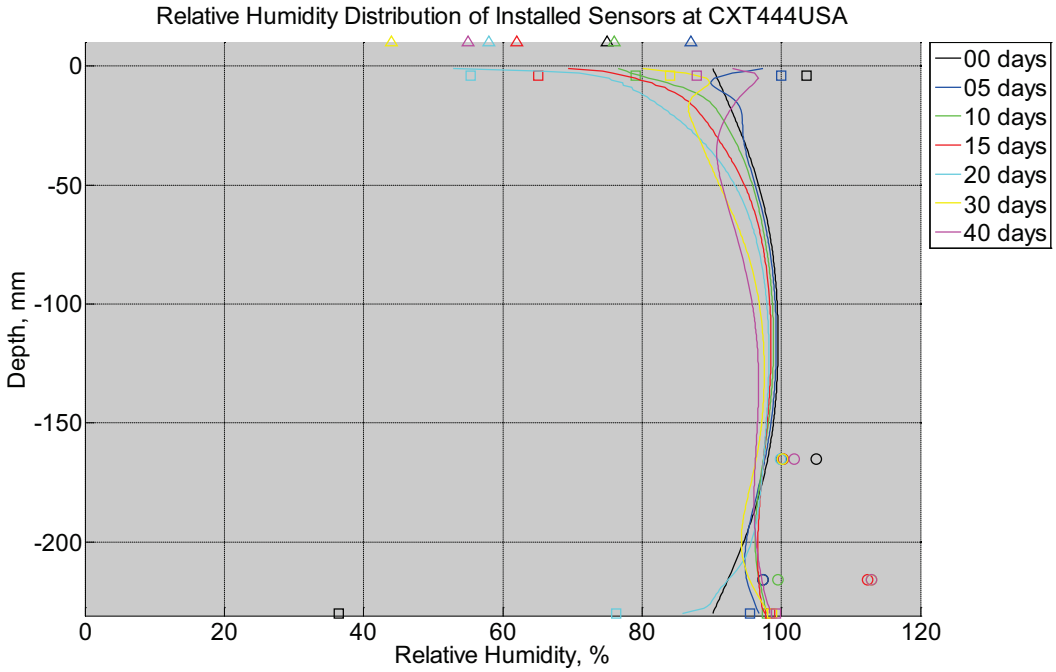

Figure B-439 Measured (markers) and modeled (continuous line) relative humidity profile distribution as a function of depth inside a concrete crosstie (labeled CXT444USA) installed in ballast in Rantoul, IL, between September 8, 2014, through October 20, 2014. An 8 mm thick polyurethane pad and 12 in (30.48 cm) length 136 lb/yd (67.5 kg/m) section of steel rail are additionally installed atop the concrete crosstie. The model does not incorporate a polyurethane pad nor steel rail line. Triangular markers denote relative humidity value from KTIP weather station, square markers denote measured relative humidity values from ballast, and circular markers denote measured relative humidity values inside concrete.

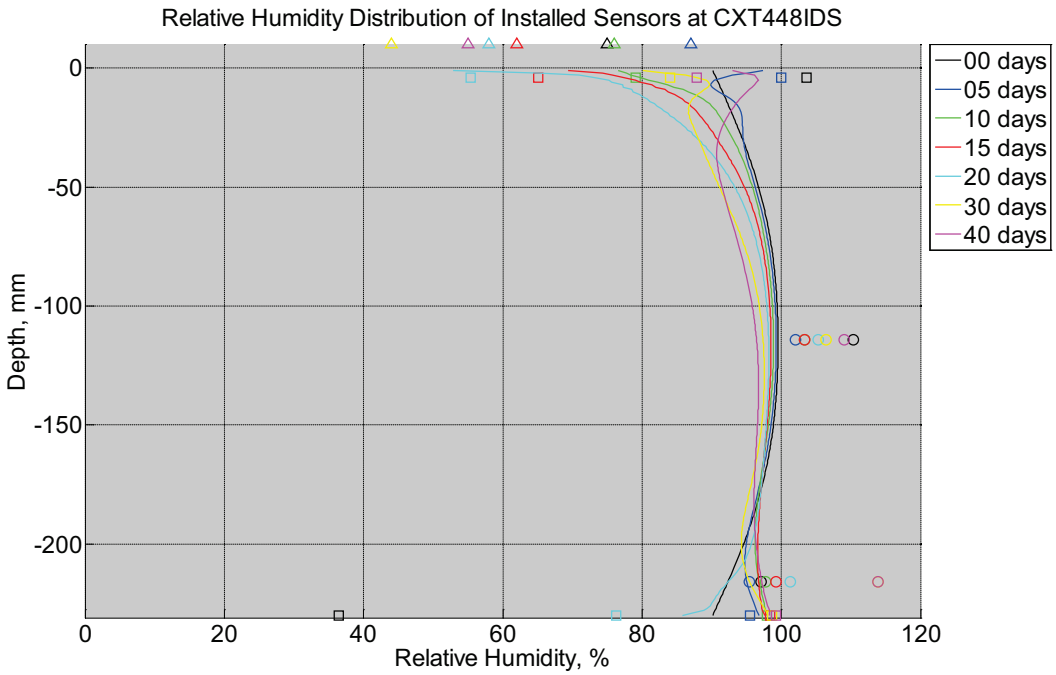

Figure B-440 Measured (markers) and modeled (continuous line) relative humidity profile distribution as a function of depth inside a concrete crosstie (labeled CXT448IDS) installed in ballast in Rantoul, IL, between September 8, 2014, through October 20, 2014. An 8 mm thick polyurethane pad and 12 in (30.48 cm) length 136 lb/yd (67.5 kg/m) section of steel rail are additionally installed atop the concrete crosstie. The model does not incorporate a polyurethane pad nor steel rail line. Triangular markers denote relative humidity value from KTIP weather station, square markers denote measured relative humidity values from ballast, and circular markers denote measured relative humidity values inside concrete.

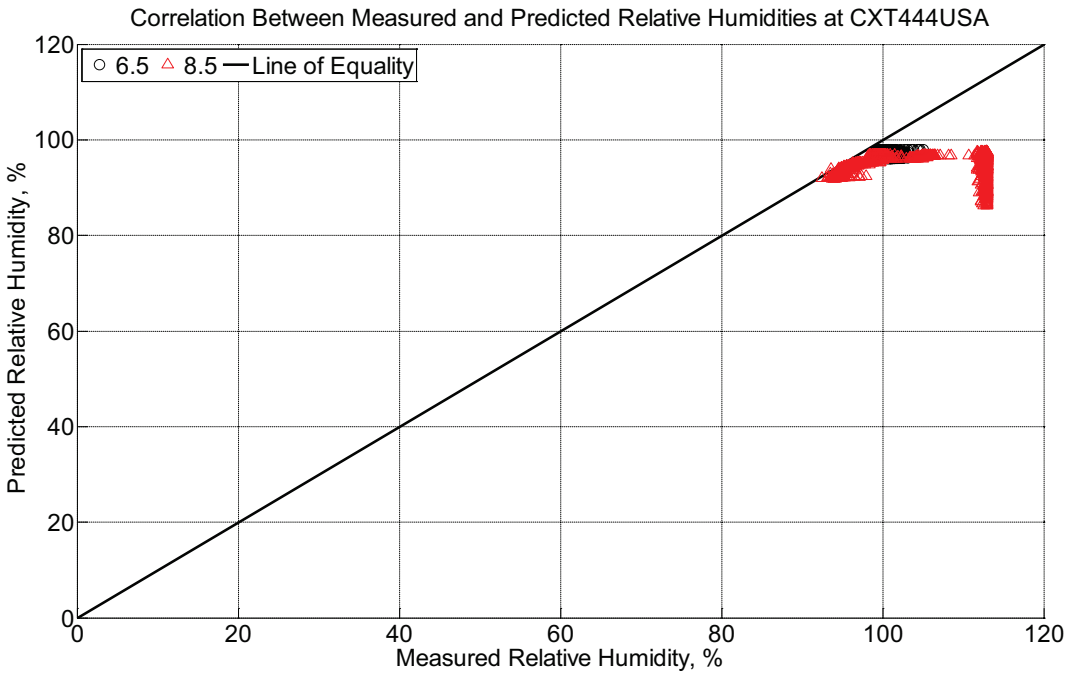

Figure B-441 Correlation between measured and predicted relative humidity values 6.5 inches (139.7 mm) and 8.5 inches (215.9 mm) from the surface of a concrete crosstie (labeled CXT444USA) installed in ballast in Rantoul, IL, between September 8, 2014, through October 20, 2014. An 8 mm thick polyurethane pad and 12 in (30.48 cm) length 136 lb/yd (67.5 kg/m) section of steel rail are additionally installed atop the concrete crosstie. The model does not incorporate a polyurethane pad nor steel rail line.

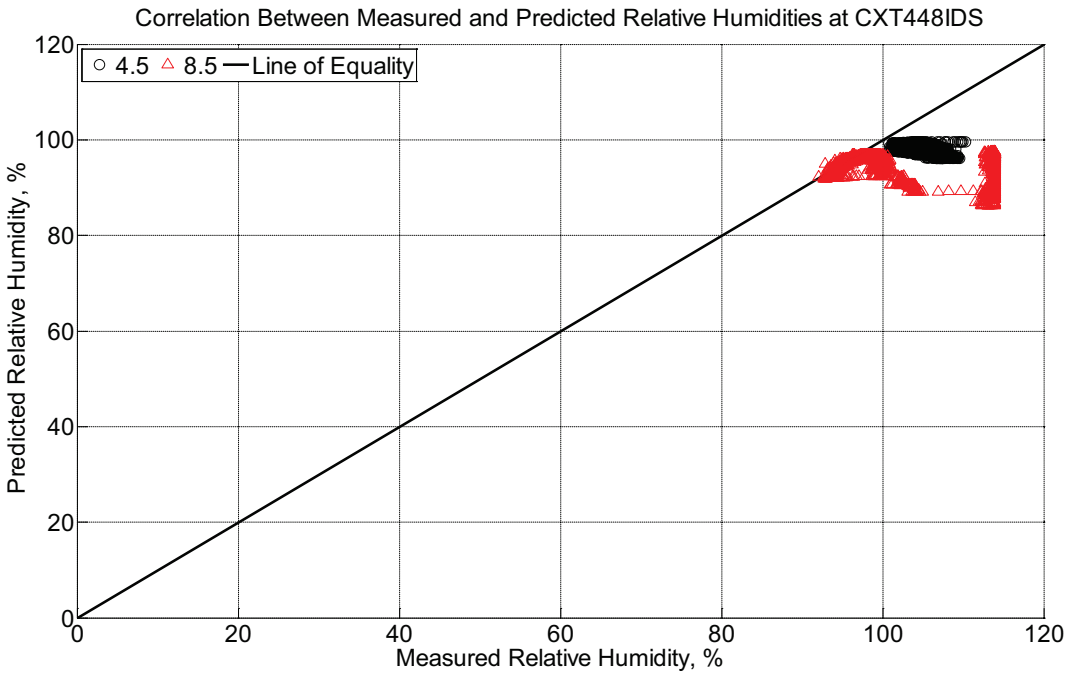

Figure B-442 Correlation between measured and predicted relative humidity values 4.5 inches (114.3 mm) and 8.5 inches (215.9 mm) from the surface of a concrete crosstie (labeled CXT448IDS) installed in ballast in Rantoul, IL, between September 8, 2014, through October 20, 2014. An 8 mm thick polyurethane pad and 12 in (30.48 cm) length 136 lb/yd (67.5 kg/m) section of steel rail are additionally installed atop the concrete crosstie. The model does not incorporate a polyurethane pad nor steel rail line.

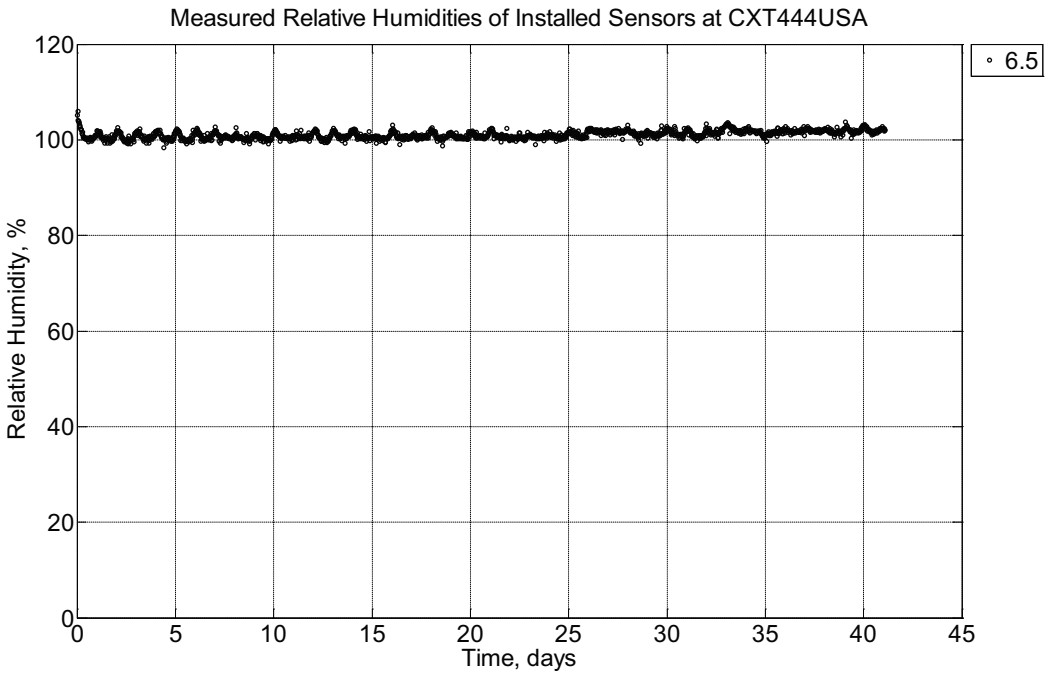

Figure B-443 Measured relative humidity at a depth of 6.5 inches (139.7 mm) from the surface of a concrete crosstie (labeled CXT444USA) installed in ballast in Rantoul, IL, between October 20, 2014, through November 30, 2014. An 8 mm thick polyurethane pad and 12 in (30.48 cm) length 136 lb/yd (67.5 kg/m) section of steel rail are additionally installed atop the concrete crosstie.

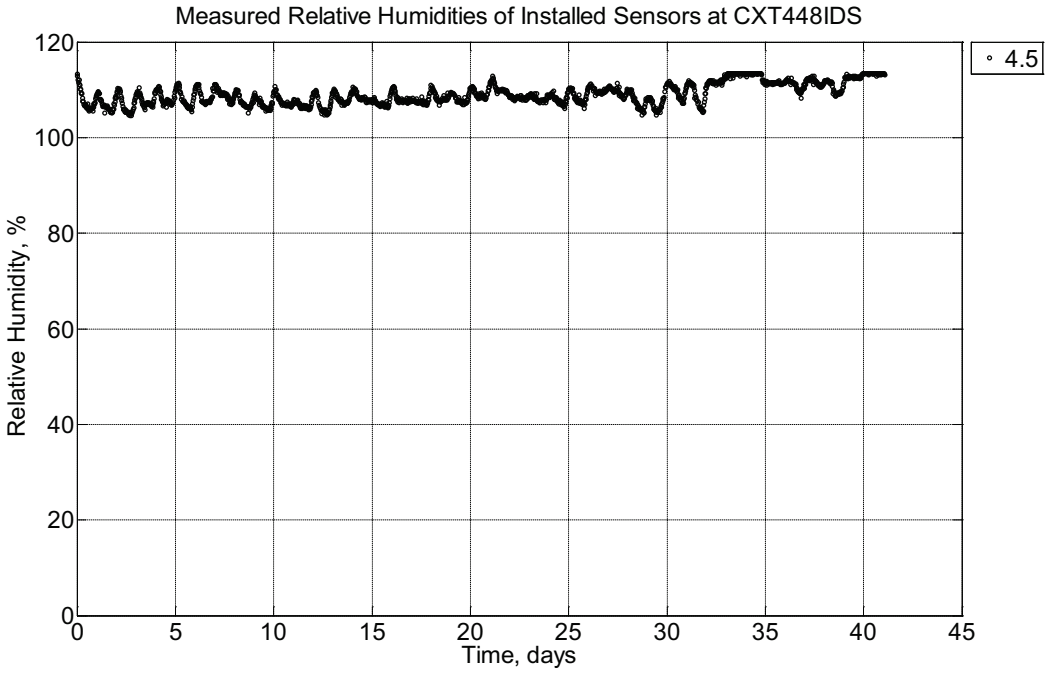

Figure B-444 Measured relative humidity at a depth of 4.5 inches (114.3 mm) from the

surface of a concrete crosstie (labeled CXT448IDS) installed in ballast in Rantoul, IL, between October 20, 2014, through November 30, 2014. An 8 mm thick polyurethane pad and 12 in (30.48 cm) length 136 lb/yd (67.5 kg/m) section of steel rail are additionally installed atop the concrete crosstie.

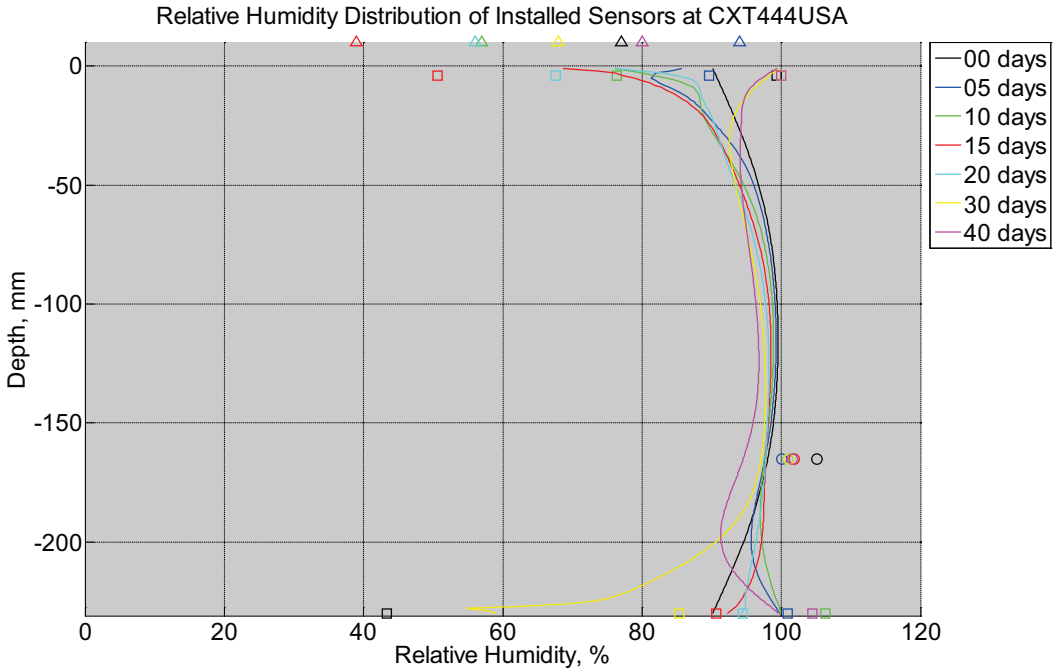

Figure B-445 Measured (markers) and modeled (continuous line) relative humidity profile distribution as a function of depth inside a concrete crosstie (labeled CXT444USA) installed in ballast in Rantoul, IL, between October 20, 2014, through November 30, 2014. An 8 mm thick polyurethane pad and 12 in (30.48 cm) length 136 lb/yd (67.5 kg/m) section of steel rail are additionally installed atop the concrete crosstie. The model does not incorporate a polyurethane pad nor steel rail line. Triangular markers denote relative humidity value from KTIP weather station, square markers denote measured relative humidity values from ballast, and circular markers denote measured relative humidity values inside concrete.

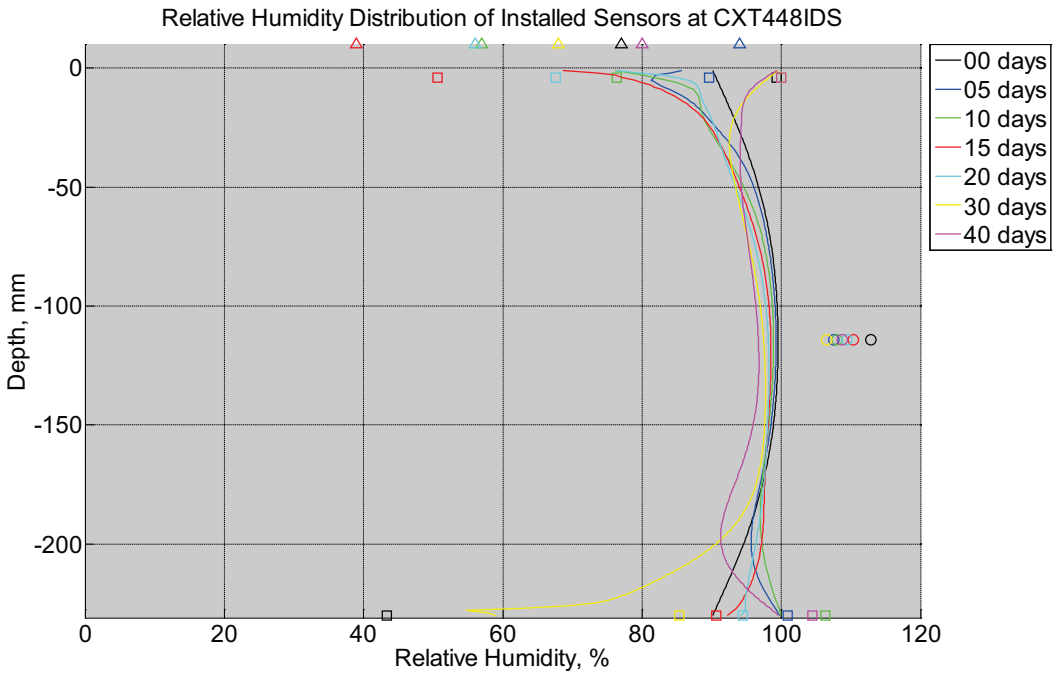

Figure B-446 Measured (markers) and modeled (continuous line) relative humidity profile distribution as a function of depth inside a concrete crosstie (labeled CXT448IDS) installed in ballast in Rantoul, IL, between October 20, 2014, through November 30, 2014. An 8 mm thick polyurethane pad and 12 in (30.48 cm) length 136 lb/yd (67.5 kg/m) section of steel rail are additionally installed atop the concrete crosstie. The model does not incorporate a polyurethane pad nor steel rail line. Triangular markers denote relative humidity value from KTIP weather station, square markers denote measured relative humidity values from ballast, and circular markers denote measured relative humidity values inside concrete.

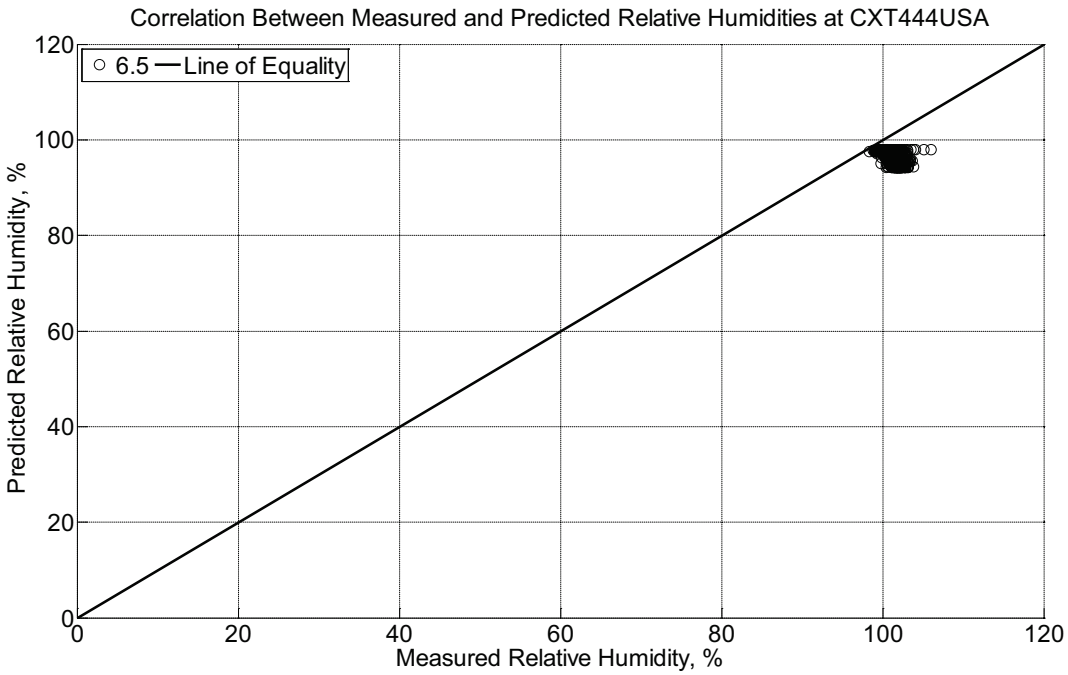

Figure B-447 Correlation between measured and predicted relative humidity values 6.5 inches (139.7 mm) from the surface of a concrete crosstie (labeled CXT444USA) installed in ballast in Rantoul, IL, between October 20, 2014, through November 30, 2014. An 8 mm thick polyurethane pad and 12 in (30.48 cm) length 136 lb/yd (67.5 kg/m) section of steel rail are additionally installed atop the concrete crosstie. The model does not incorporate a polyurethane pad nor steel rail line.

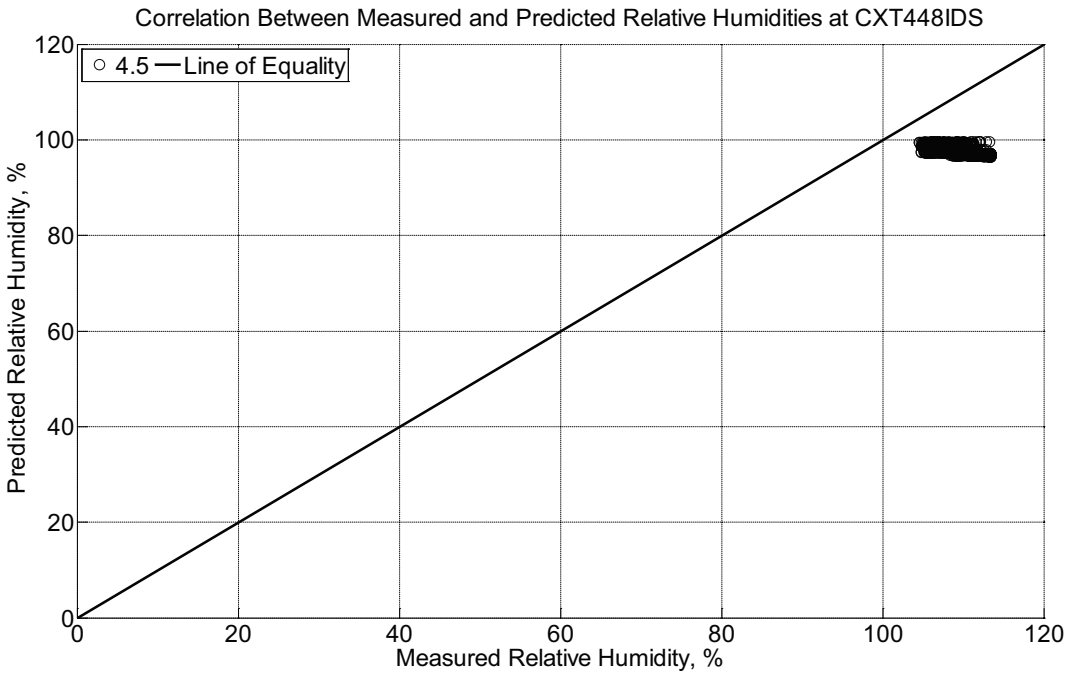

Figure B-448 Correlation between measured and predicted relative humidity values 4.5 inches (114.3 mm) from the surface of a concrete crosstie (labeled CXT448IDS) installed in ballast in Rantoul, IL, between October 20, 2014, through November 30, 2014. An 8 mm thick polyurethane pad and 12 in (30.48 cm) length 136 lb/yd (67.5 kg/m) section of steel rail are additionally installed atop the concrete crosstie. The model does not incorporate a polyurethane pad nor steel rail line.

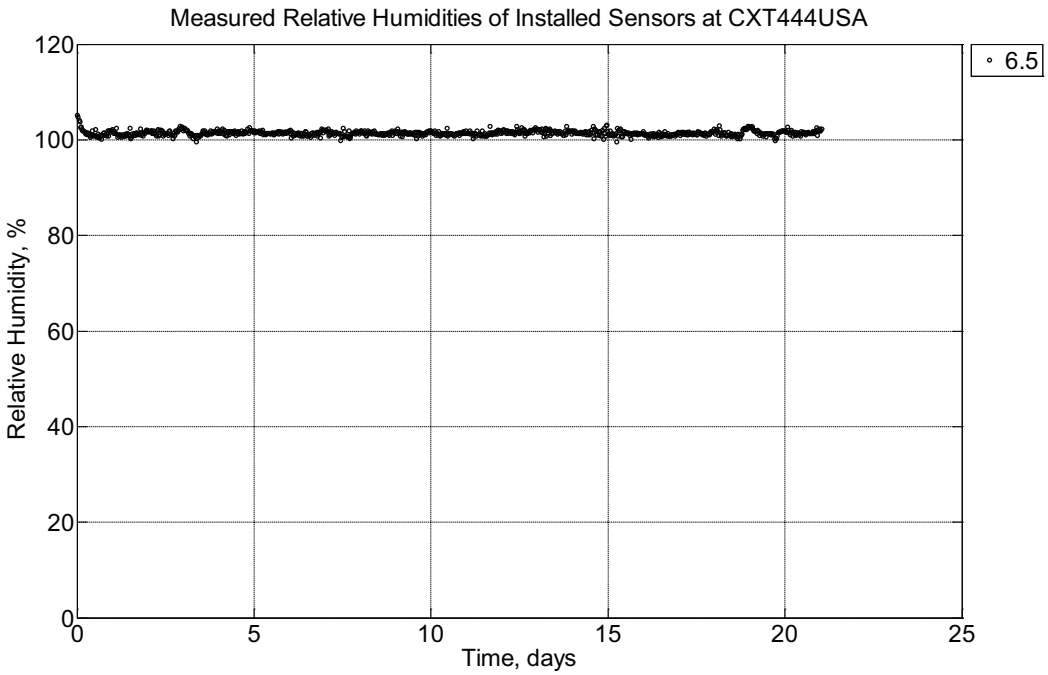

Figure B-449 Measured relative humidity at a depth of 6.5 inches (139.7 mm) from the surface of a concrete crosstie (labeled CXT444USA) installed in ballast in Rantoul, IL, between November 30, 2014, through December 21, 2014. An 8 mm thick polyurethane pad and 12 in (30.48 cm) length 136 lb/yd (67.5 kg/m) section of steel rail are additionally installed atop the concrete crosstie.

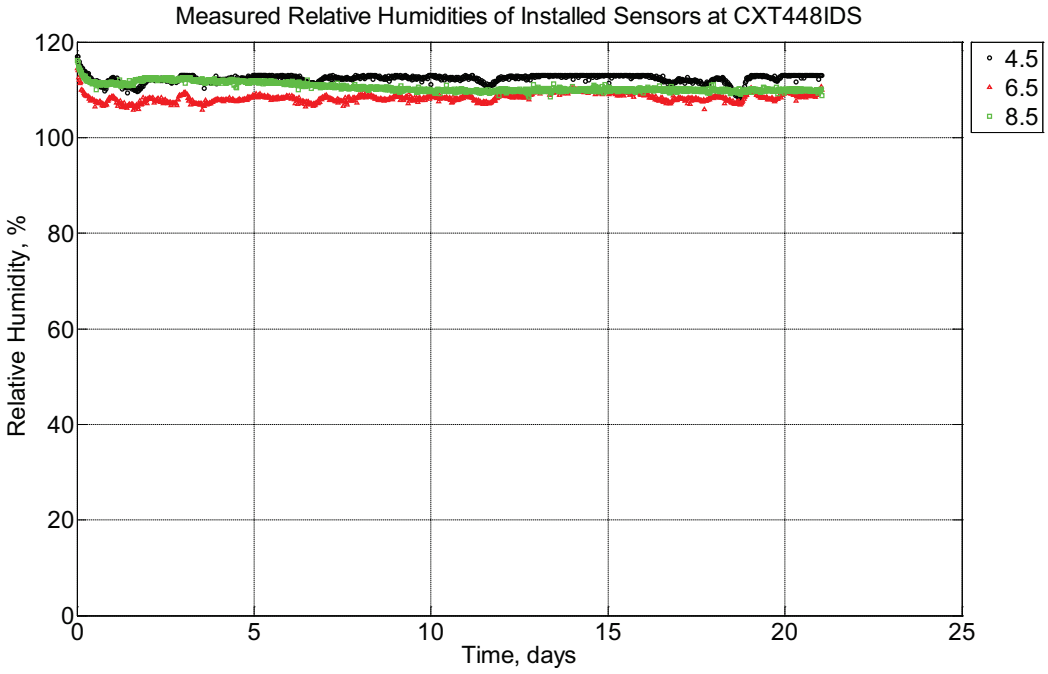

Figure B-450 Measured relative humidity at depths of 4.5 inches (114.3 mm), 6.5 inches

(139.7 mm), and 8.5 inches (215.9 mm) from the surface of a concrete crosstie (labeled CXT448IDS) installed in ballast in Rantoul, IL, between November 30, 2014, through December 21, 2014. An 8 mm thick polyurethane pad and 12 in (30.48 cm) length 136 lb/yd (67.5 kg/m) section of steel rail are additionally installed atop the concrete crosstie.

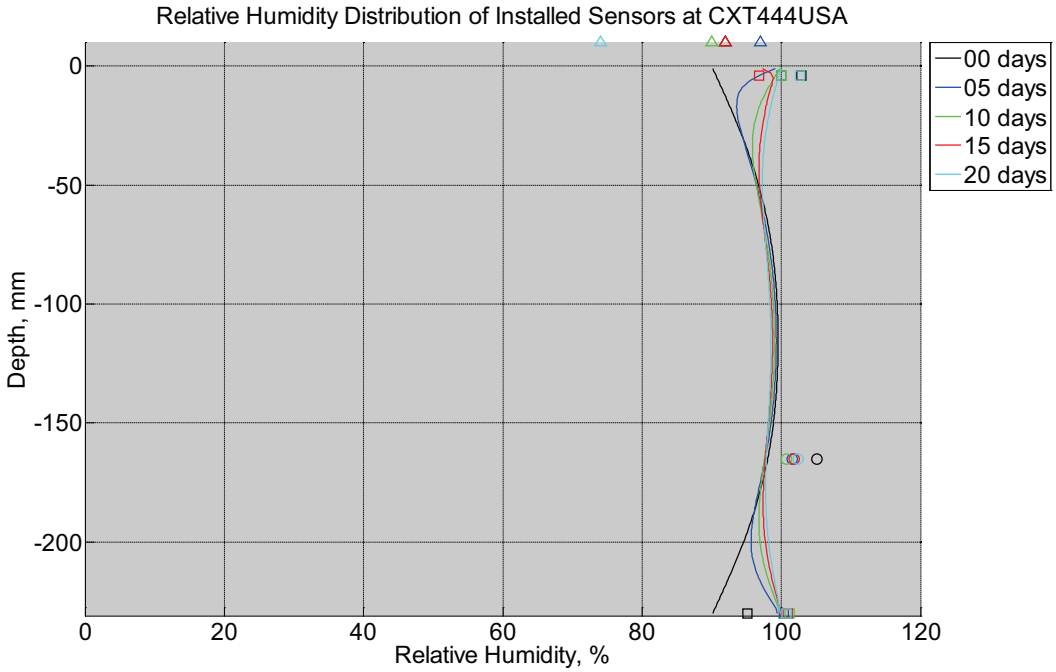

Figure B-451 Measured (markers) and modeled (continuous line) relative humidity profile distribution as a function of depth inside a concrete crosstie (labeled CXT444USA) installed in ballast in Rantoul, IL, between November 30, 2014, through December 21, 2014. An 8 mm thick polyurethane pad and 12 in (30.48 cm) length 136 lb/yd (67.5 kg/m) section of steel rail are additionally installed atop the concrete crosstie. The model does not incorporate a polyurethane pad nor steel rail line. Triangular markers denote relative humidity value from KTIP weather station, square markers denote measured relative humidity values from ballast, and circular markers denote measured relative humidity values inside concrete.

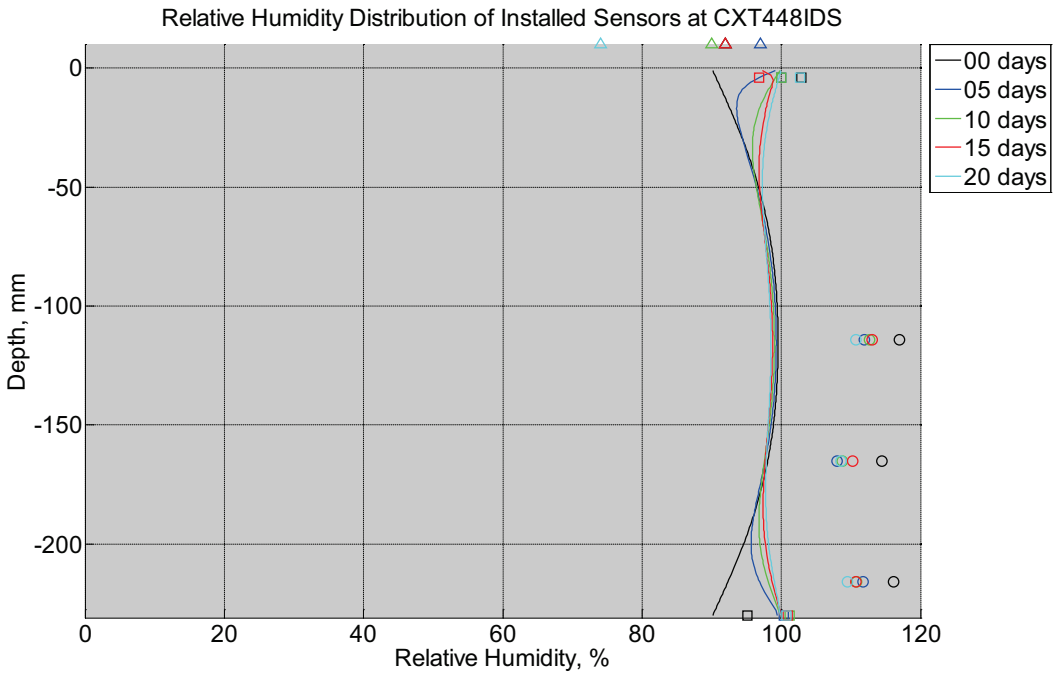

Figure B-452 Measured (markers) and modeled (continuous line) relative humidity profile distribution as a function of depth inside a concrete crosstie (labeled CXT448IDS) installed in ballast in Rantoul, IL, between November 30, 2014, through December 21, 2014. An 8 mm thick polyurethane pad and 12 in (30.48 cm) length 136 lb/yd (67.5 kg/m) section of steel rail are additionally installed atop the concrete crosstie. The model does not incorporate a polyurethane pad nor steel rail line. Triangular markers denote relative humidity value from KTIP weather station, square markers denote measured relative humidity values from ballast, and circular markers denote measured relative humidity values inside concrete.

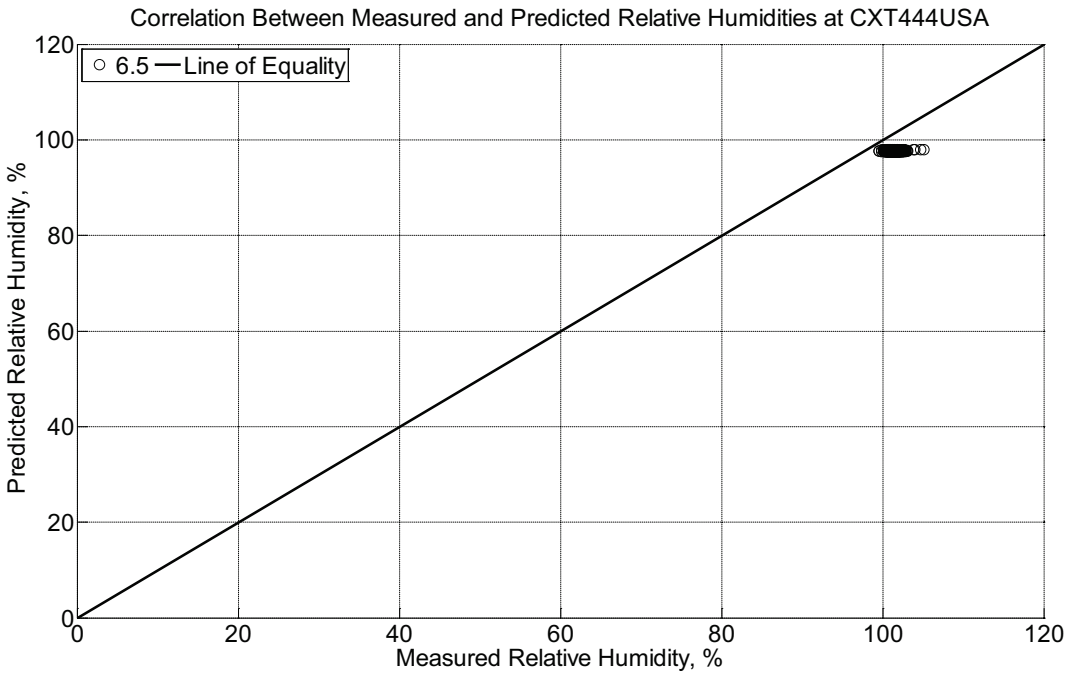

Figure B-453 Correlation between measured and predicted relative humidity values 6.5 inches (139.7 mm) from the surface of a concrete crosstie (labeled CXT444USA) installed in ballast in Rantoul, IL, between October 20, 2014, through November 30, 2014. An 8 mm thick polyurethane pad and 12 in (30.48 cm) length 136 lb/yd (67.5 kg/m) section of steel rail are additionally installed atop the concrete crosstie. The model does not incorporate a polyurethane pad nor steel rail line.

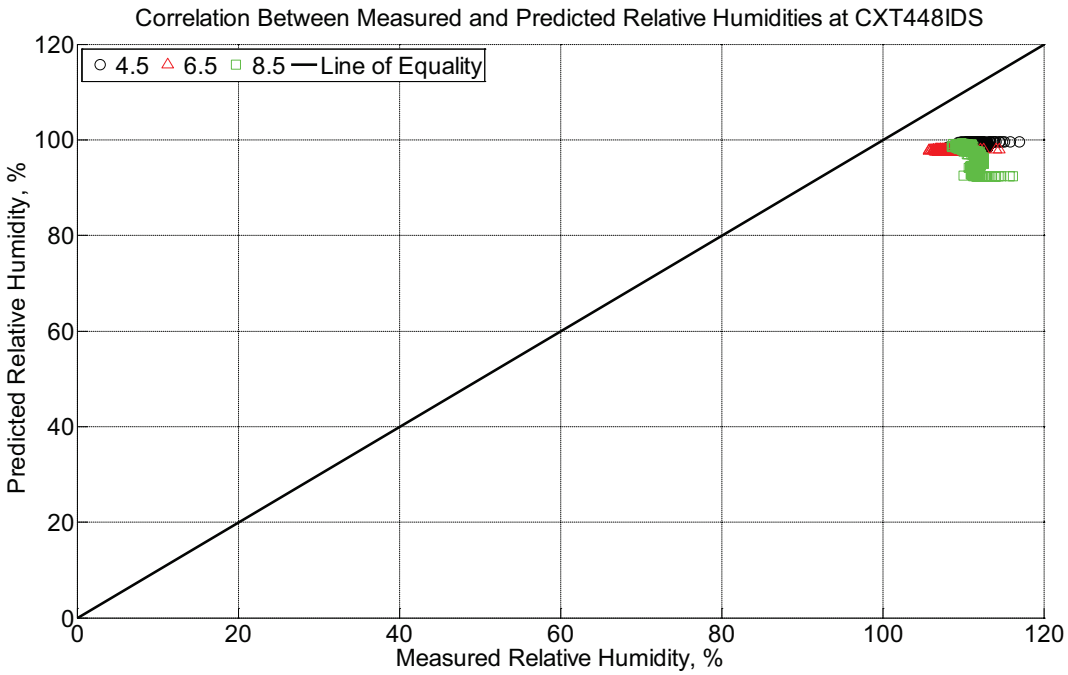

Figure B-454 Correlation between measured and predicted relative humidity values 4.5 inches (114.3 mm), 6.5 inches (139.7 mm), and 8.5 inches (215.9 mm) from the surface of a concrete crosstie (labeled CXT448IDS) installed in ballast in Rantoul, IL, between November 30, 2014, through December 21, 2014. An 8 mm thick polyurethane pad and 12 in (30.48 cm) length 136 lb/yd (67.5 kg/m) section of steel rail are additionally installed atop the concrete crosstie. The model does not incorporate a polyurethane pad nor steel rail line.

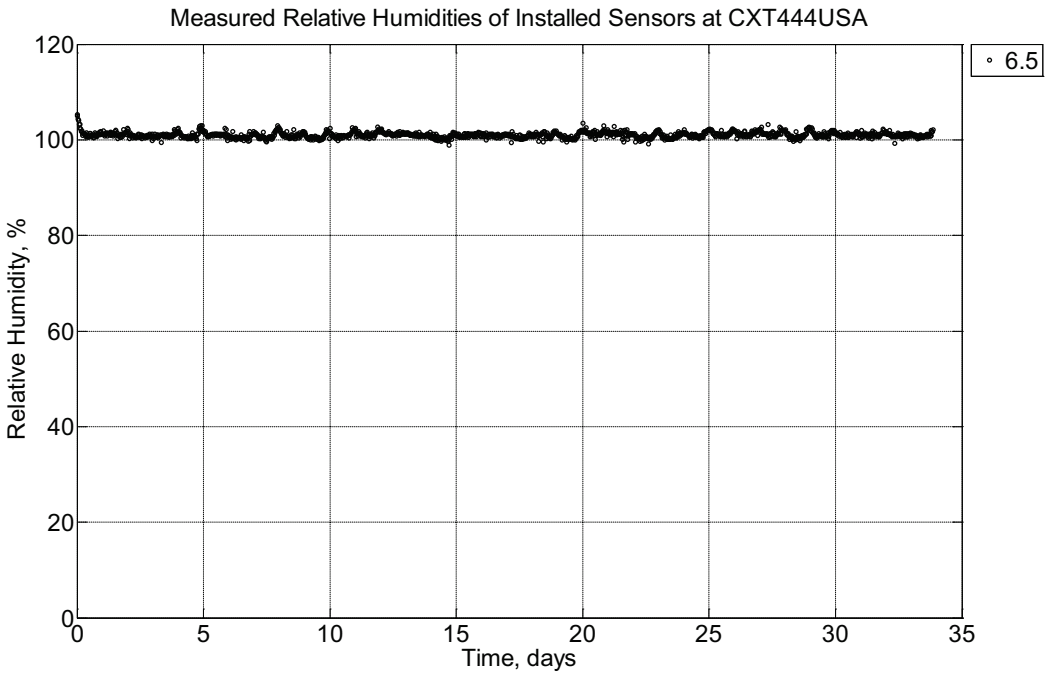

Figure B-455 Measured relative humidity at a depth of 6.5 inches (139.7 mm) from the surface of a concrete crosstie (labeled CXT444USA) installed in ballast in Rantoul, IL, between December 21, 2014, through January 24, 2015. An 8 mm thick polyurethane pad and 12 in (30.48 cm) length 136 lb/yd (67.5 kg/m) section of steel rail are additionally installed atop the concrete crosstie.

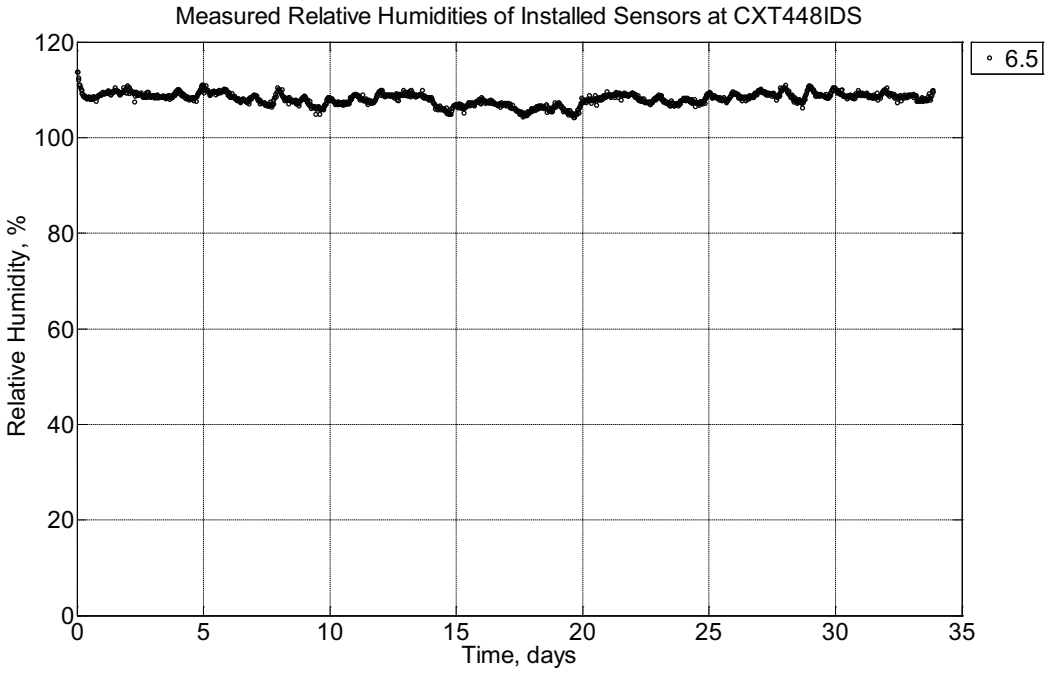

Figure B-456 Measured relative humidity at depths of 6.5 inches (139.7 mm) from the

surface of a concrete crosstie (labeled CXT448IDS) installed in ballast in Rantoul, IL, between December 21, 2014, through January 24, 2015. An 8 mm thick polyurethane pad and 12 in (30.48 cm) length 136 lb/yd (67.5 kg/m) section of steel rail are additionally installed atop the concrete crosstie.

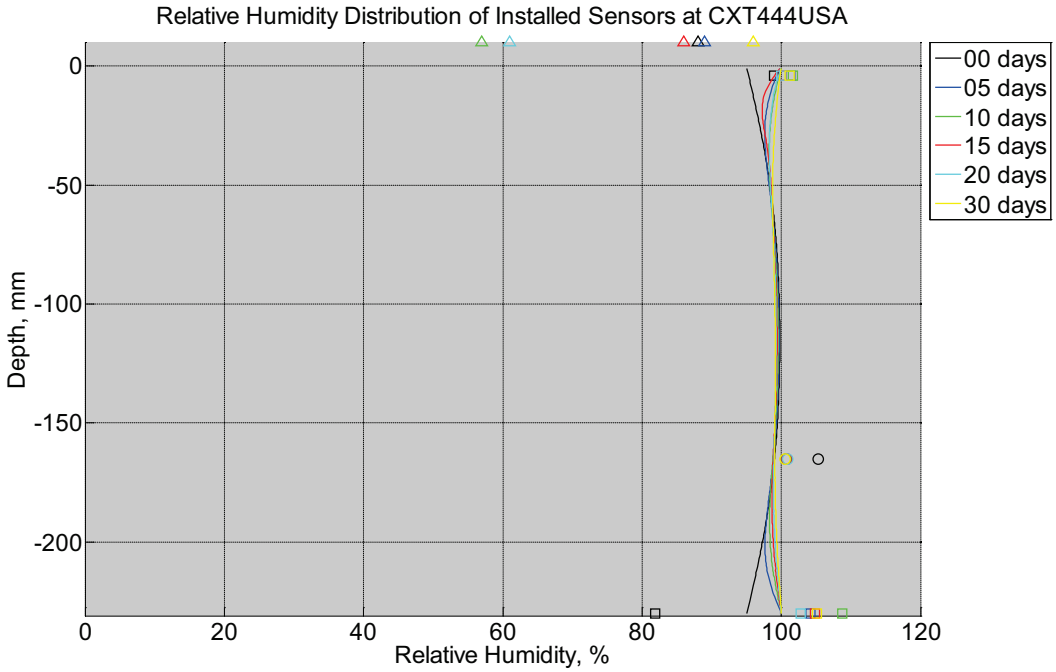

Figure B-457 Measured (markers) and modeled (continuous line) relative humidity profile distribution as a function of depth inside a concrete crosstie (labeled CXT444USA) installed in ballast in Rantoul, IL, between December 21, 2014, through January 24, 2015. An 8 mm thick polyurethane pad and 12 in (30.48 cm) length 136 lb/yd (67.5 kg/m) section of steel rail are additionally installed atop the concrete crosstie. The model does not incorporate a polyurethane pad nor steel rail line. Triangular markers denote relative humidity value from KTIP weather station, square markers denote measured relative humidity values from ballast, and circular markers denote measured relative humidity values inside concrete.

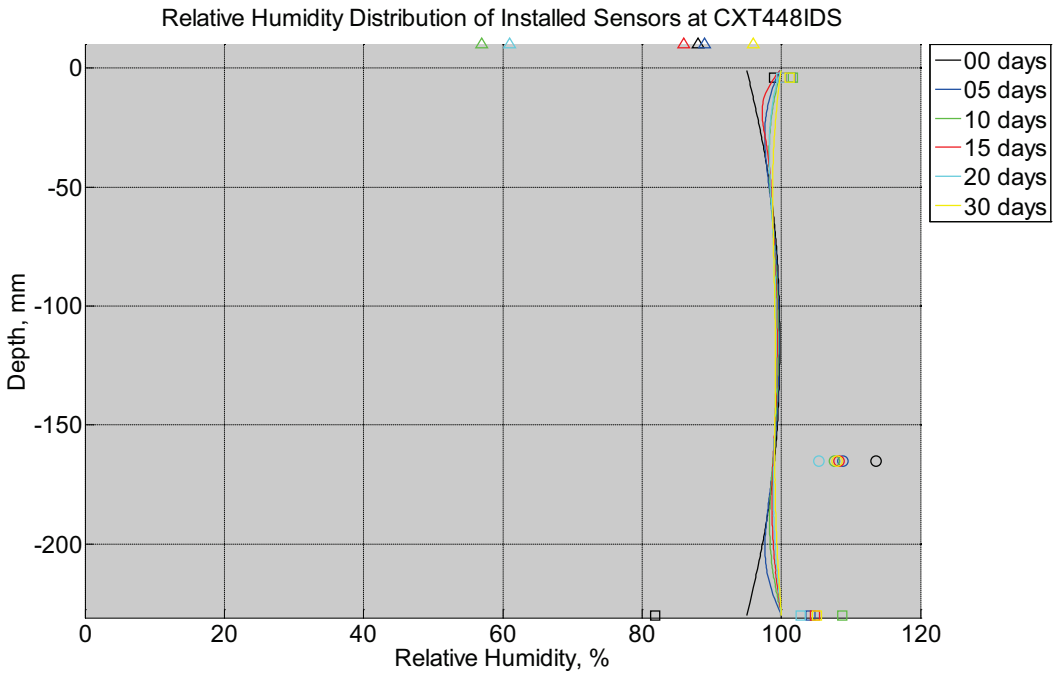

Figure B-458 Measured (markers) and modeled (continuous line) relative humidity profile distribution as a function of depth inside a concrete crosstie (labeled CXT448IDS) installed in ballast in Rantoul, IL, between December 21, 2014, through January 24, 2015. An 8 mm thick polyurethane pad and 12 in (30.48 cm) length 136 lb/yd (67.5 kg/m) section of steel rail are additionally installed atop the concrete crosstie. The model does not incorporate a polyurethane pad nor steel rail line. Triangular markers denote relative humidity value from KTIP weather station, square markers denote measured relative humidity values from ballast, and circular markers denote measured relative humidity values inside concrete.

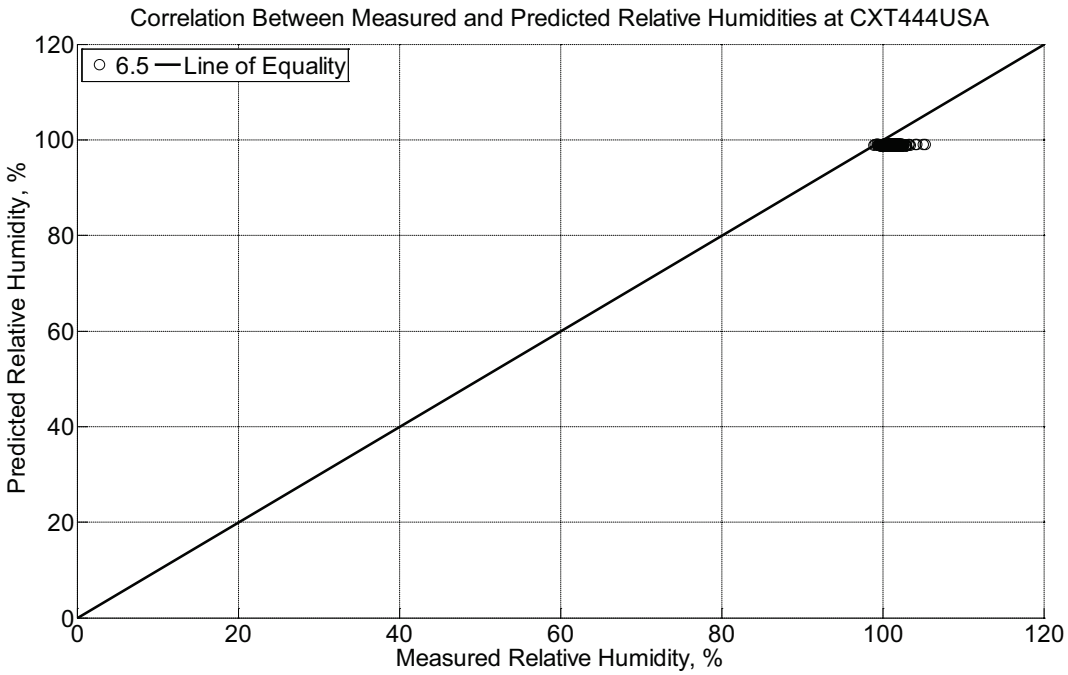

Figure B-459 Correlation between measured and predicted relative humidity values 6.5 inches (139.7 mm) from the surface of a concrete crosstie (labeled CXT444USA) installed in ballast in Rantoul, IL, between December 21, 2014, through January 24, 2015. An 8 mm thick polyurethane pad and 12 in (30.48 cm) length 136 lb/yd (67.5 kg/m) section of steel rail are additionally installed atop the concrete crosstie. The model does not incorporate a polyurethane pad nor steel rail line.

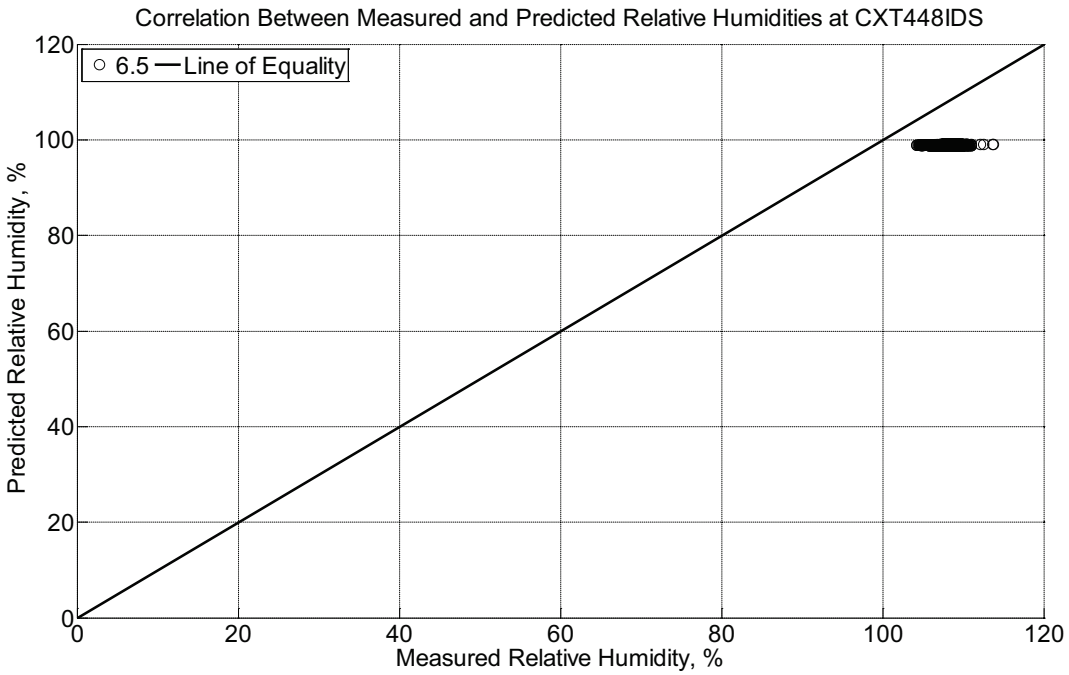

Figure B-460 Correlation between measured and predicted relative humidity values 6.5 inches (139.7 mm) from the surface of a concrete crosstie (labeled CXT448IDS) installed in ballast in Rantoul, IL, between December 21, 2014, through January 24, 2015. An 8 mm thick polyurethane pad and 12 in (30.48 cm) length 136 lb/yd (67.5 kg/m) section of steel rail are additionally installed atop the concrete crosstie. The model does not incorporate a polyurethane pad nor steel rail line.

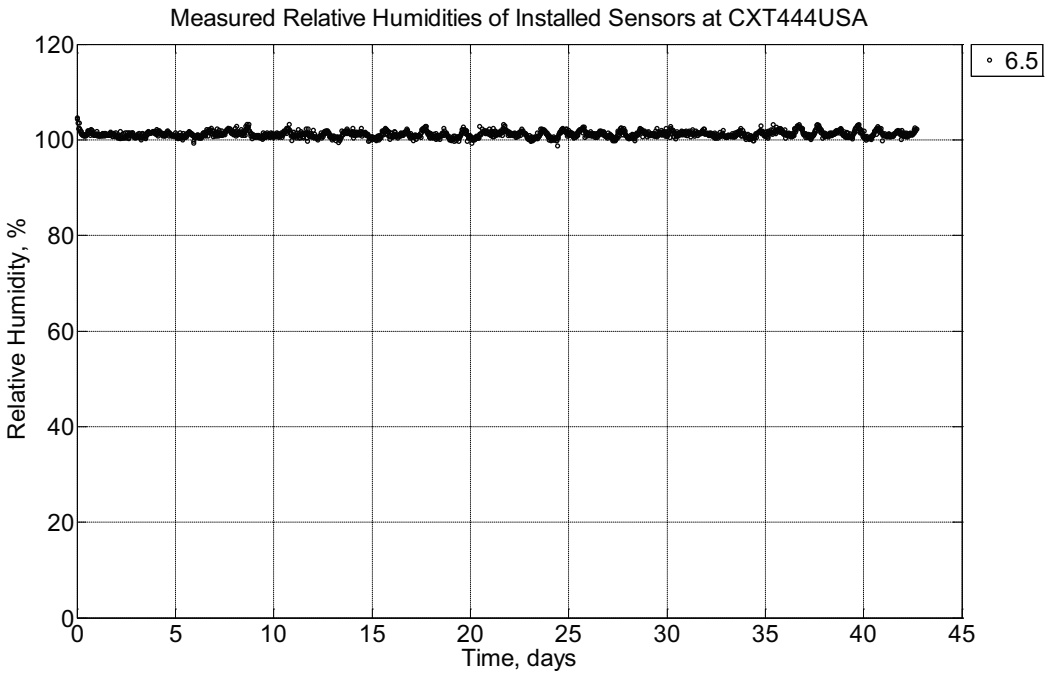

Figure B-461 Measured relative humidity at a depth of 6.5 inches (139.7 mm) from the surface of a concrete crosstie (labeled CXT444USA) installed in ballast in Rantoul, IL, between January 30, 2015, through March 14, 2015. An 8 mm thick polyurethane pad and 12 in (30.48 cm) length 136 lb/yd (67.5 kg/m) section of steel rail are additionally installed atop the concrete crosstie.

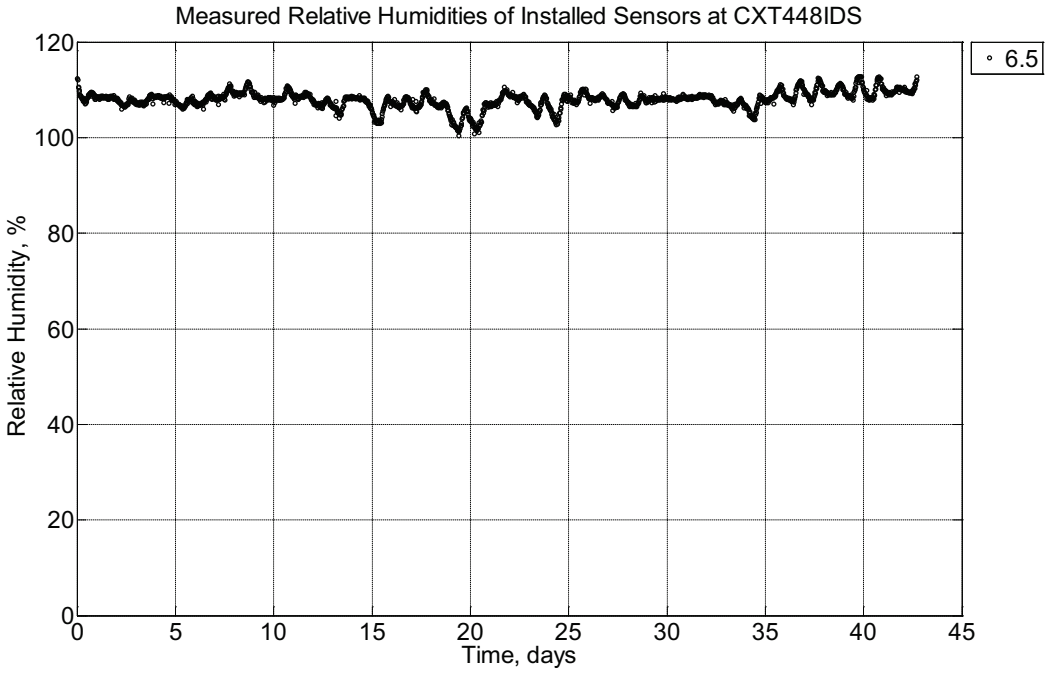

Figure B-462 Measured relative humidity at depths of 6.5 inches (139.7 mm) from the

surface of a concrete crosstie (labeled CXT448IDS) installed in ballast in Rantoul, IL, between January 30, 2015, through March 14, 2015. An 8 mm thick polyurethane pad and 12 in (30.48 cm) length 136 lb/yd (67.5 kg/m) section of steel rail are additionally installed atop the concrete crosstie.

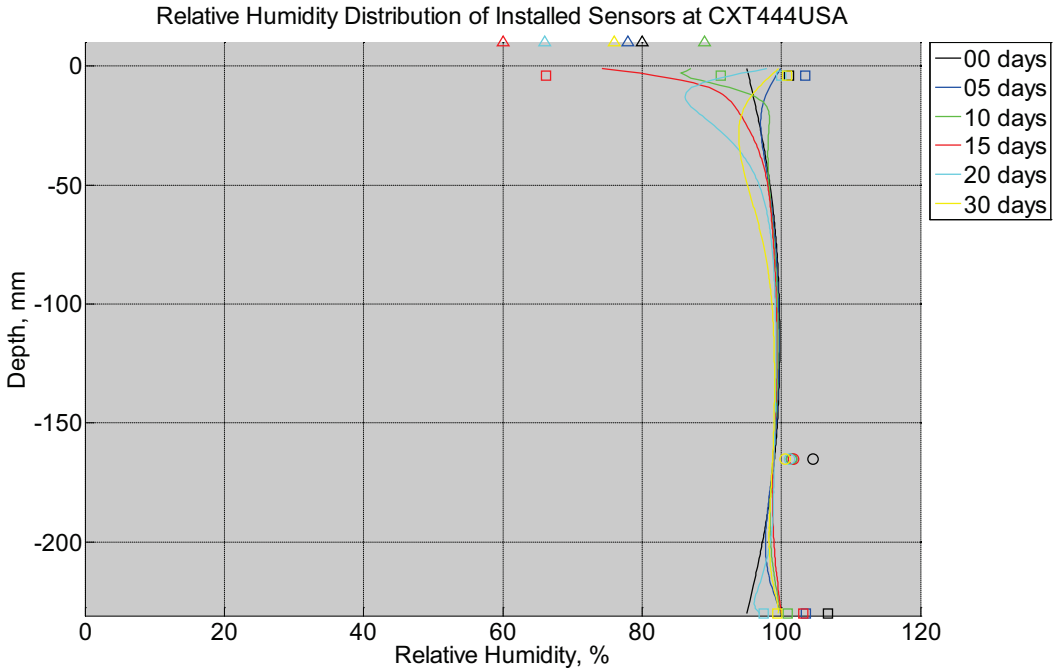

Figure B-463 Measured (markers) and modeled (continuous line) relative humidity profile distribution as a function of depth inside a concrete crosstie (labeled CXT444USA) installed in ballast in Rantoul, IL, between January 30, 2015, through March 14, 2015. An 8 mm thick polyurethane pad and 12 in (30.48 cm) length 136 lb/yd (67.5 kg/m) section of steel rail are additionally installed atop the concrete crosstie. The model does not incorporate a polyurethane pad nor steel rail line. Triangular markers denote relative humidity value from KTIP weather station, square markers denote measured relative humidity values from ballast, and circular markers denote measured relative humidity values inside concrete.

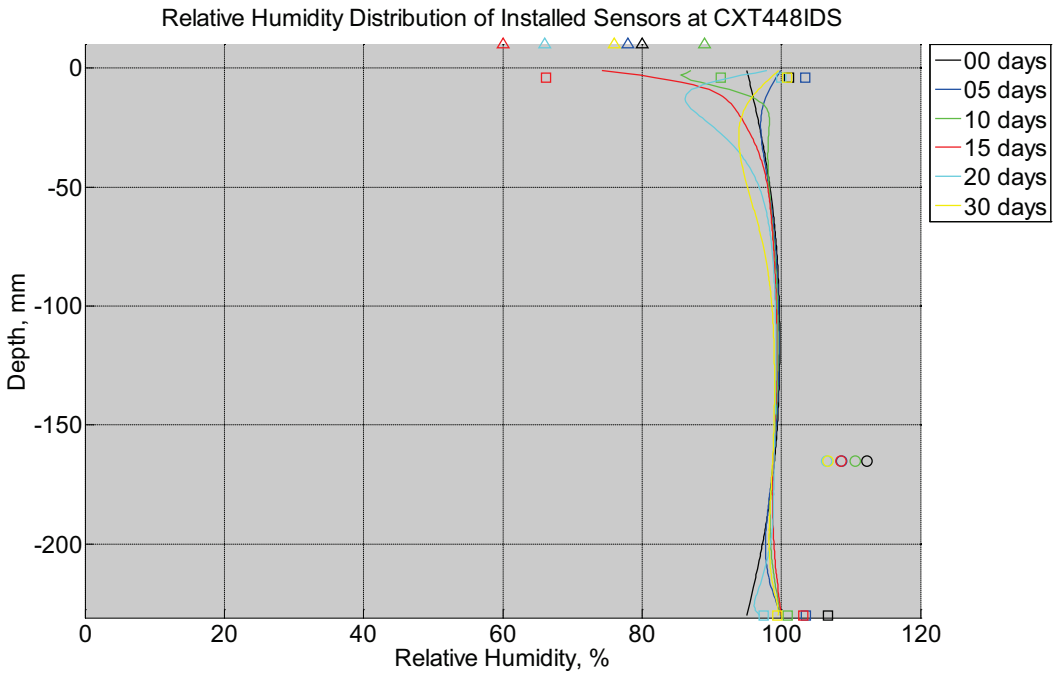

Figure B-464 Measured (markers) and modeled (continuous line) relative humidity profile distribution as a function of depth inside a concrete crosstie (labeled CXT448IDS) installed in ballast in Rantoul, IL, between January 30, 2015, through March 14, 2015. An 8 mm thick polyurethane pad and 12 in (30.48 cm) length 136 lb/yd (67.5 kg/m) section of steel rail are additionally installed atop the concrete crosstie. The model does not incorporate a polyurethane pad nor steel rail line. Triangular markers denote relative humidity value from KTIP weather station, square markers denote measured relative humidity values from ballast, and circular markers denote measured relative humidity values inside concrete.

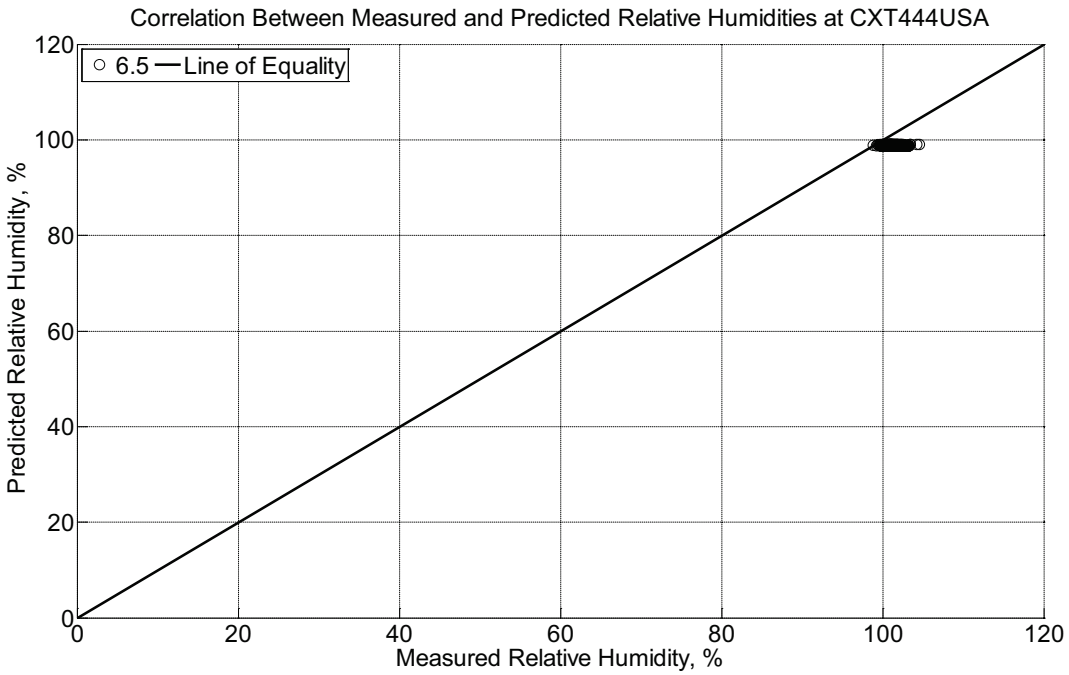

Figure B-465 Correlation between measured and predicted relative humidity values 6.5 inches (139.7 mm) from the surface of a concrete crosstie (labeled CXT444USA) installed in ballast in Rantoul, IL, between January 30, 2015, through March 14, 2015. An 8 mm thick polyurethane pad and 12 in (30.48 cm) length 136 lb/yd (67.5 kg/m) section of steel rail are additionally installed atop the concrete crosstie. The model does not incorporate a polyurethane pad nor steel rail line.

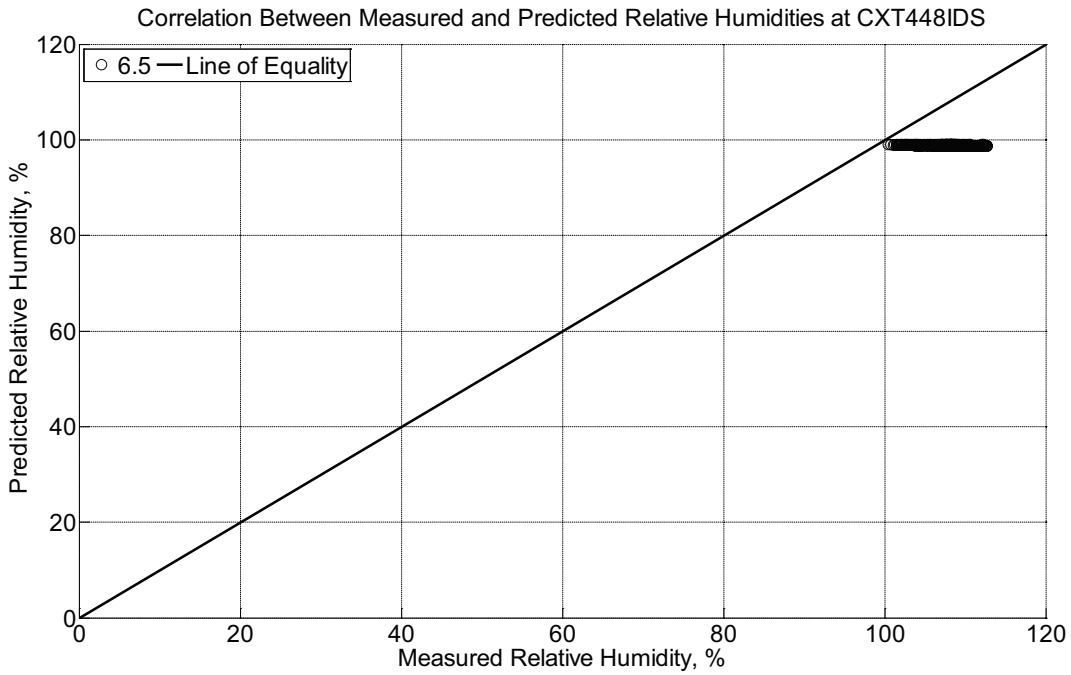

Figure B-466 Correlation between measured and predicted relative humidity values 6.5 inches (139.7 mm) from the surface of a concrete crosstie (labeled CXT448IDS) installed in ballast in Rantoul, IL, between January 30, 2015, through March 14, 2015. An 8 mm thick polyurethane pad and 12 in (30.48 cm) length 136 lb/yd (67.5 kg/m) section of steel rail are additionally installed atop the concrete crosstie. The model does not incorporate a polyurethane pad nor steel rail line.

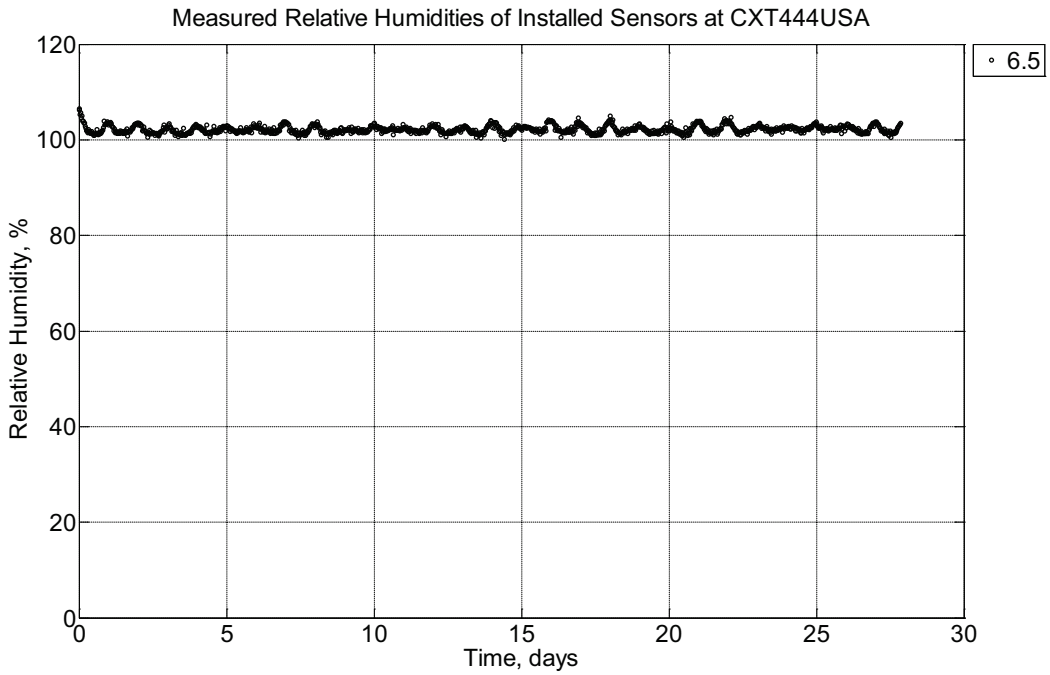

Figure B-467 Measured relative humidity at a depth of 6.5 inches (139.7 mm) from the surface of a concrete crosstie (labeled CXT444USA) installed in ballast in Rantoul, IL, between March 14, 2015, through April 11, 2015. An 8 mm thick polyurethane pad and 12 in (30.48 cm) length 136 lb/yd (67.5 kg/m) section of steel rail are additionally installed atop the concrete crosstie.

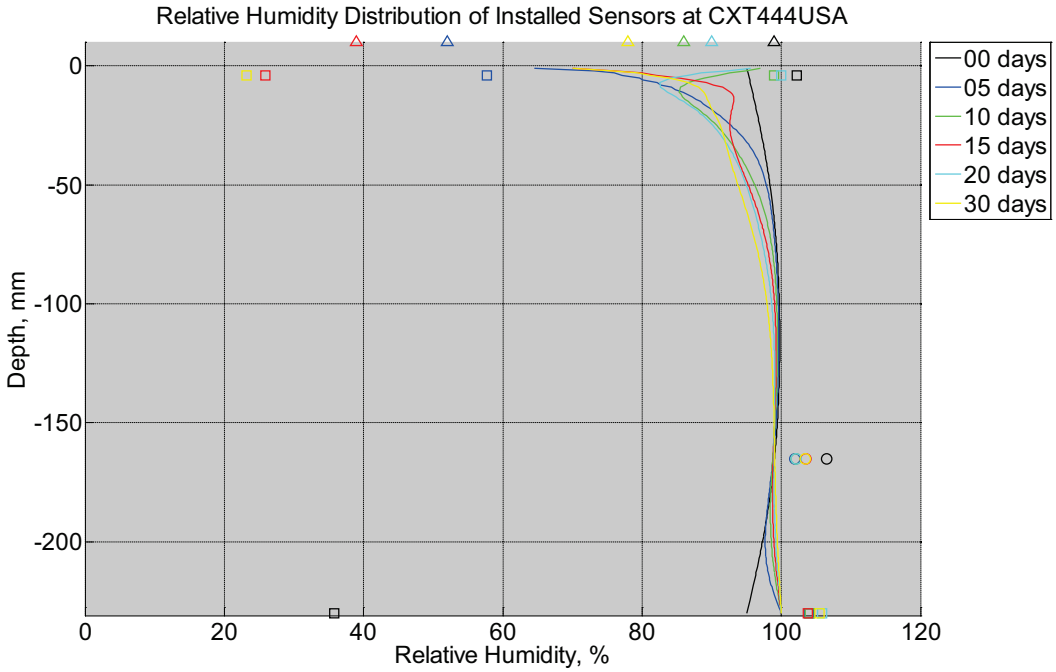

Figure B-468 Measured (markers) and modeled (continuous line) relative humidity profile

distribution as a function of depth inside a concrete crosstie (labeled CXT444USA) installed in ballast in Rantoul, IL, between March 14, 2015, through April 11, 2015. An 8 mm thick polyurethane pad and 12 in (30.48 cm) length 136 lb/yd (67.5 kg/m) section of steel rail are additionally installed atop the concrete crosstie. The model does not incorporate a polyurethane pad nor steel rail line. Triangular markers denote relative humidity value from KTIP weather station, square markers denote measured relative humidity values from ballast, and circular markers denote measured relative humidity values inside concrete.

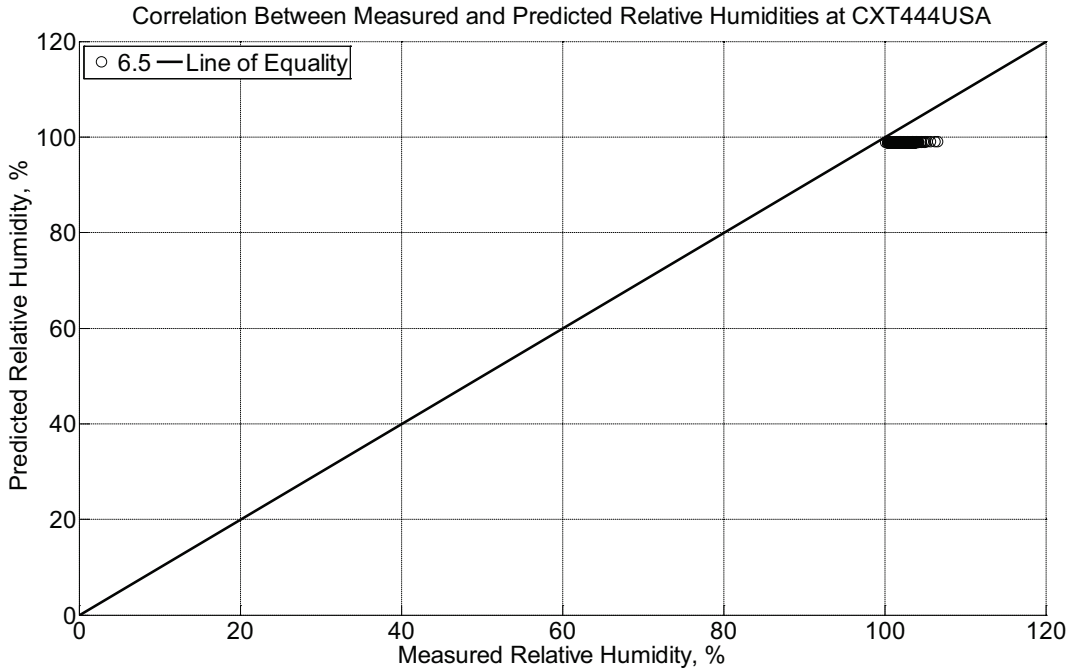

Figure B-469 Correlation between measured and predicted relative humidity values 6.5 inches (139.7 mm) from the surface of a concrete crosstie (labeled CXT444USA) installed in ballast in Rantoul, IL, between March 14, 2015, through April 11, 2015. An 8 mm thick polyurethane pad and 12 in (30.48 cm) length 136 lb/yd (67.5 kg/m) section of steel rail are additionally installed atop the concrete crosstie. The model does not incorporate a polyurethane pad nor steel rail line.

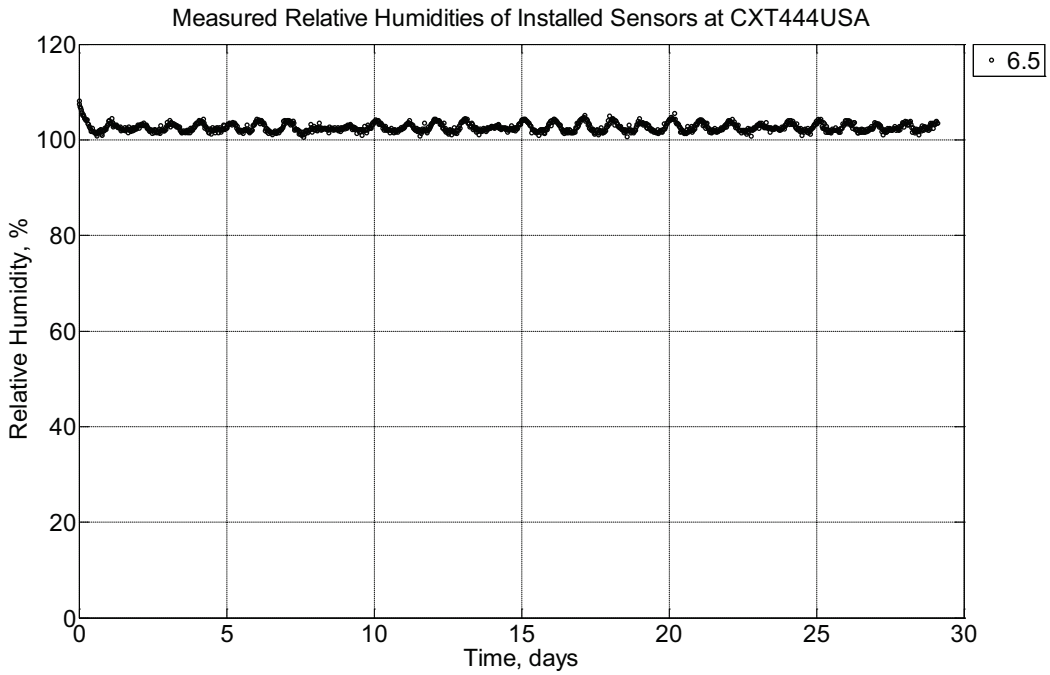

Figure B-470 Measured relative humidity at a depth of 6.5 inches (139.7 mm) from the surface of a concrete crosstie (labeled CXT444USA) installed in ballast in Rantoul, IL, between April 11, 2015, through May 10, 2015. An 8 mm thick polyurethane pad and 12 in (30.48 cm) length 136 lb/yd (67.5 kg/m) section of steel rail are additionally installed atop the concrete crosstie.

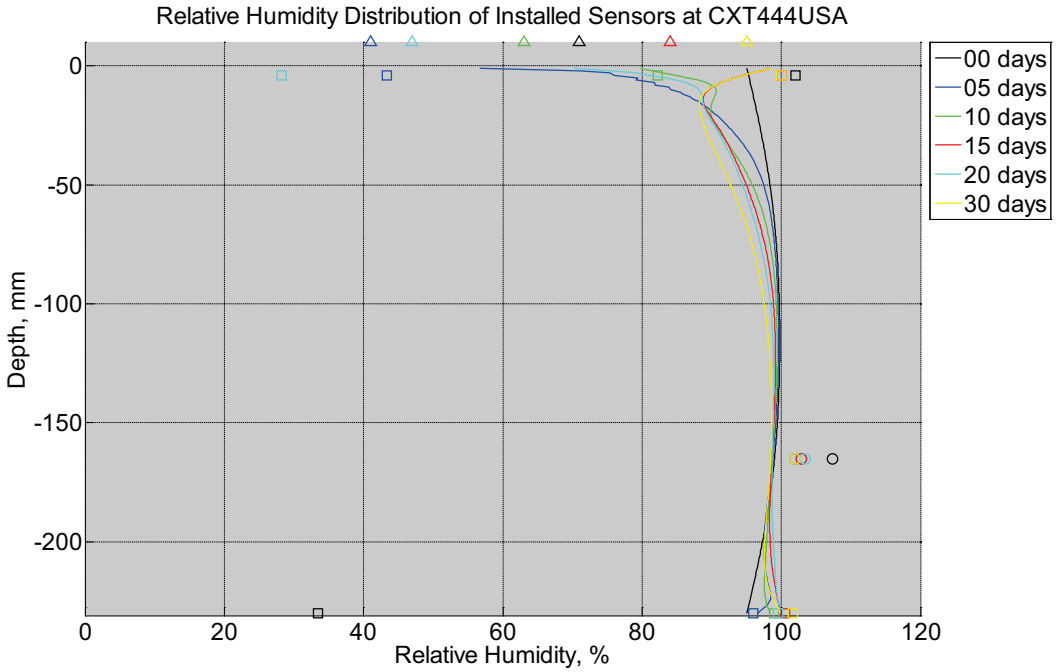

Figure B-471 Measured (markers) and modeled (continuous line) relative humidity profile

distribution as a function of depth inside a concrete crosstie (labeled CXT444USA) installed in ballast in Rantoul, IL, between April 11, 2015, through May 10, 2015. An 8 mm thick polyurethane pad and 12 in (30.48 cm) length 136 lb/yd (67.5 kg/m) section of steel rail are additionally installed atop the concrete crosstie. The model does not incorporate a polyurethane pad nor steel rail line. Triangular markers denote relative humidity value from KTIP weather station, square markers denote measured relative humidity values from ballast, and circular markers denote measured relative humidity values inside concrete.

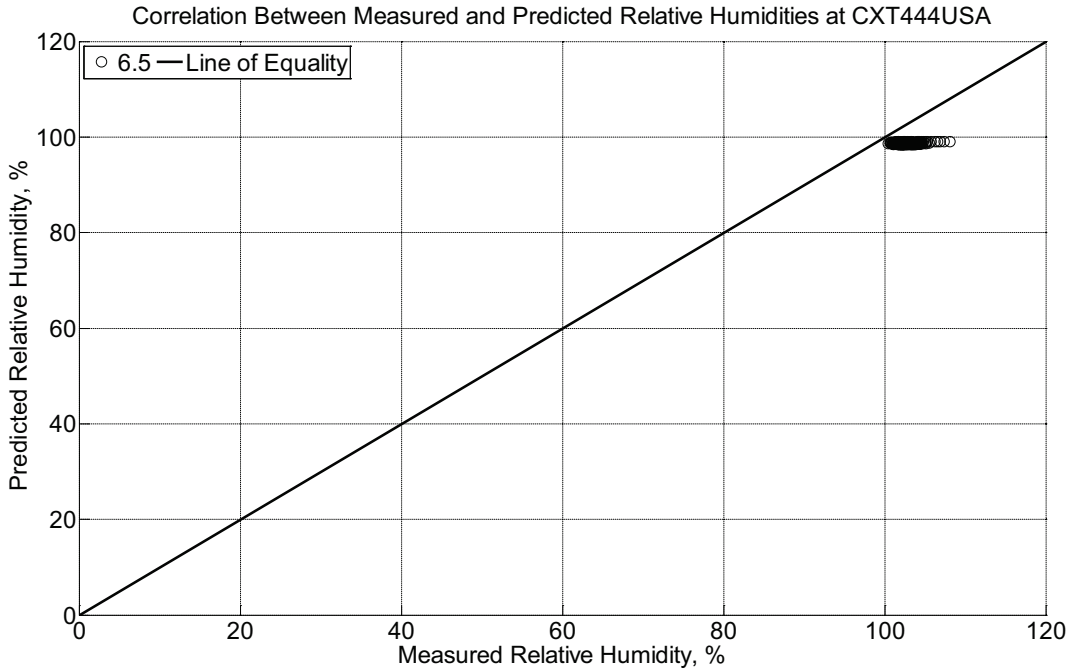

Figure B-472 Correlation between measured and predicted relative humidity values 6.5 inches (139.7 mm) from the surface of a concrete crosstie (labeled CXT444USA) installed in ballast in Rantoul, IL, between April 11, 2015, through May 10, 2015. An 8 mm thick polyurethane pad and 12 in (30.48 cm) length 136 lb/yd (67.5 kg/m) section of steel rail are additionally installed atop the concrete crosstie. The model does not incorporate a polyurethane pad nor steel rail line.

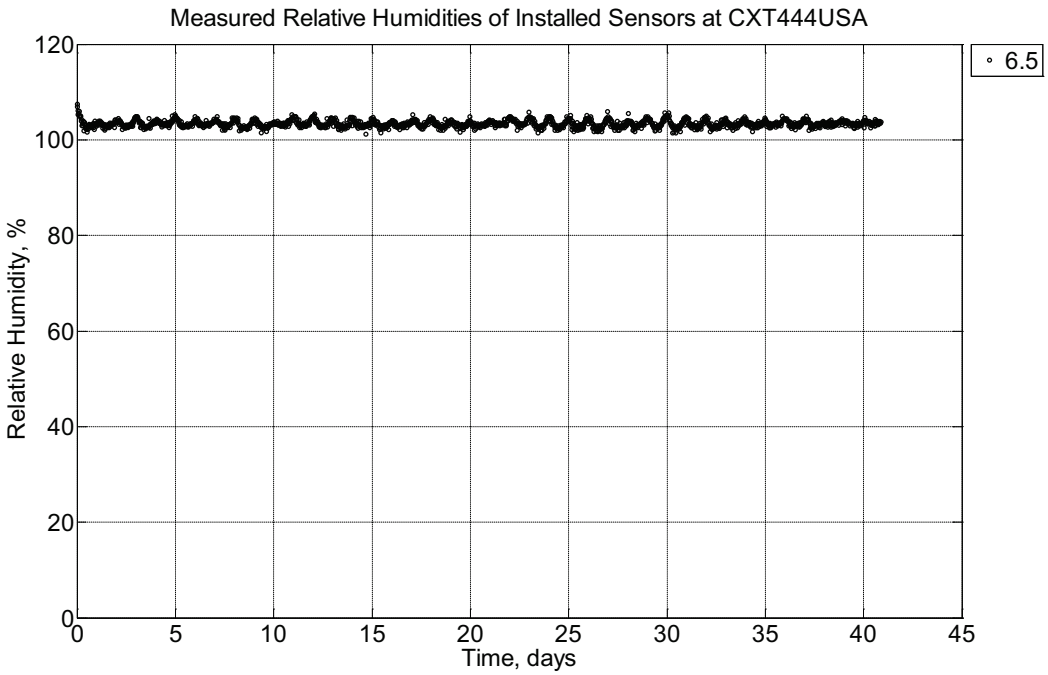

Figure B-473 Measured relative humidity at a depth of 6.5 inches (139.7 mm) from the surface of a concrete crosstie (labeled CXT444USA) installed in ballast in Rantoul, IL, between May 10, 2015, through June 20, 2015. An 8 mm thick polyurethane pad and 12 in (30.48 cm) length 136 lb/yd (67.5 kg/m) section of steel rail are additionally installed atop the concrete crosstie. A breathable water-resistant canvas tarp is additionally installed over the concrete crosstie and immediate ballast area.

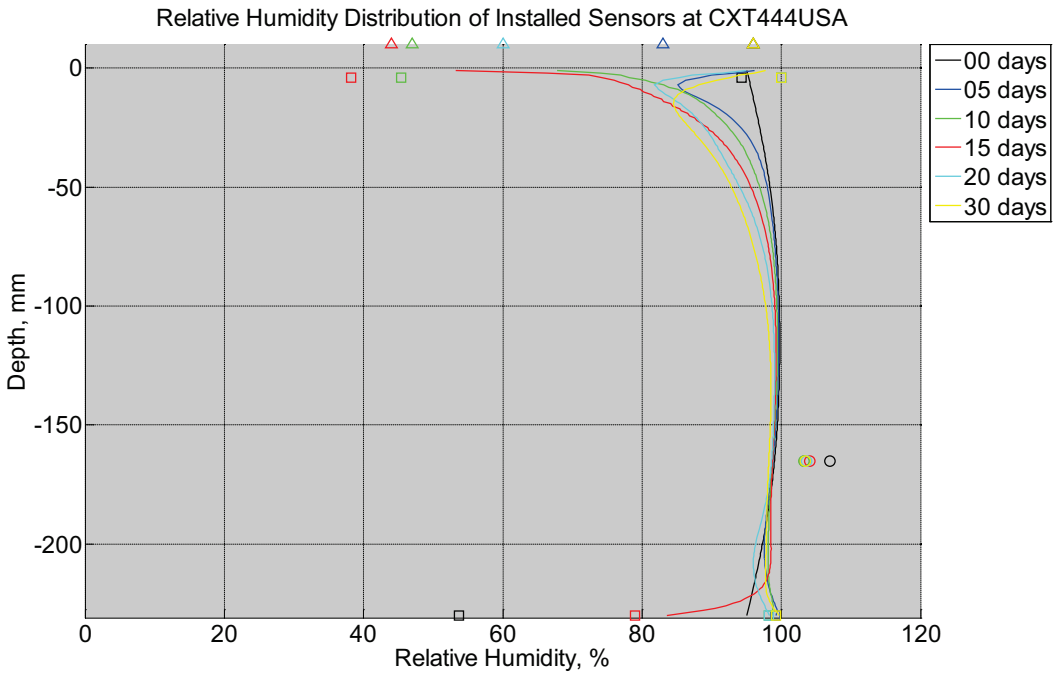

Figure B-474 Measured (markers) and modeled (continuous line) relative humidity profile distribution as a function of depth inside a concrete crosstie (labeled CXT444USA) installed in ballast in Rantoul, IL, between May 10, 2015, through June 20, 2015. An 8 mm thick polyurethane pad and 12 in (30.48 cm) length 136 lb/yd (67.5 kg/m) section of steel rail are additionally installed atop the concrete crosstie. A breathable water-resistant canvas tarp is additionally installed over the concrete crosstie and immediate ballast area. The model does not incorporate a polyurethane pad nor steel rail line. Triangular markers denote relative humidity value from KTIP weather station, square markers denote measured relative humidity values from ballast, and circular markers denote measured relative humidity values inside concrete.

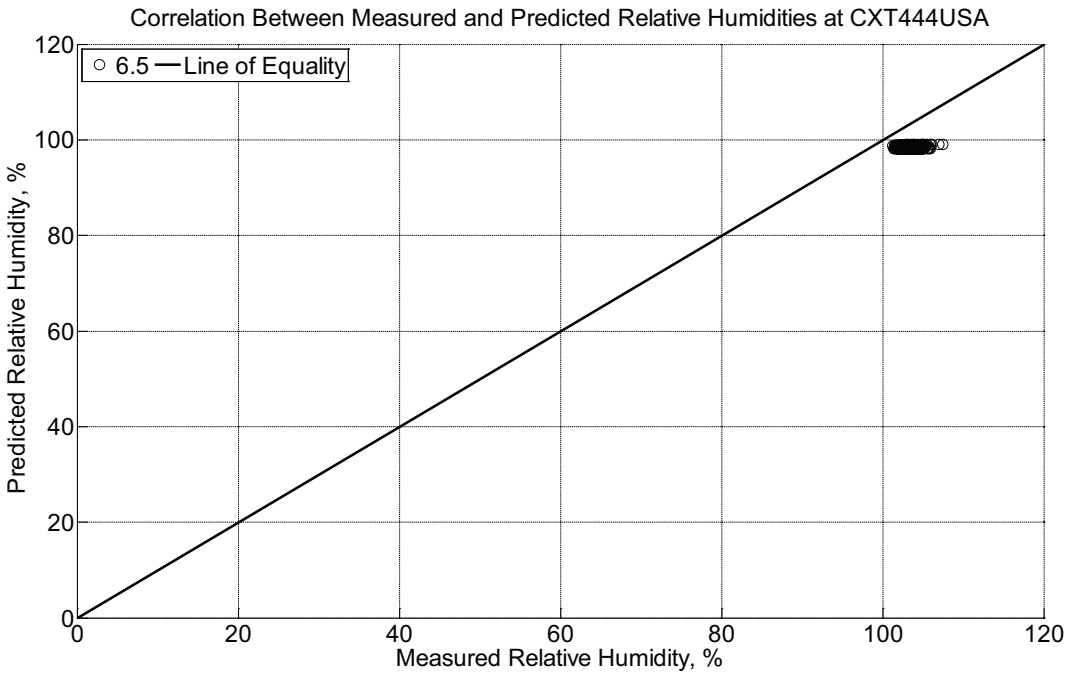

Figure B-475 Correlation between measured and predicted relative humidity values 6.5 inches (139.7 mm) from the surface of a concrete crosstie (labeled CXT444USA) installed in ballast in Rantoul, IL, between May 10, 2015, through June 20, 2015. An 8 mm thick polyurethane pad and 12 in (30.48 cm) length 136 lb/yd (67.5 kg/m) section of steel rail are additionally installed atop the concrete crosstie. A breathable water-resistant canvas tarp is additionally installed over the concrete crosstie and immediate ballast area. The model does not incorporate a polyurethane pad nor steel rail line.

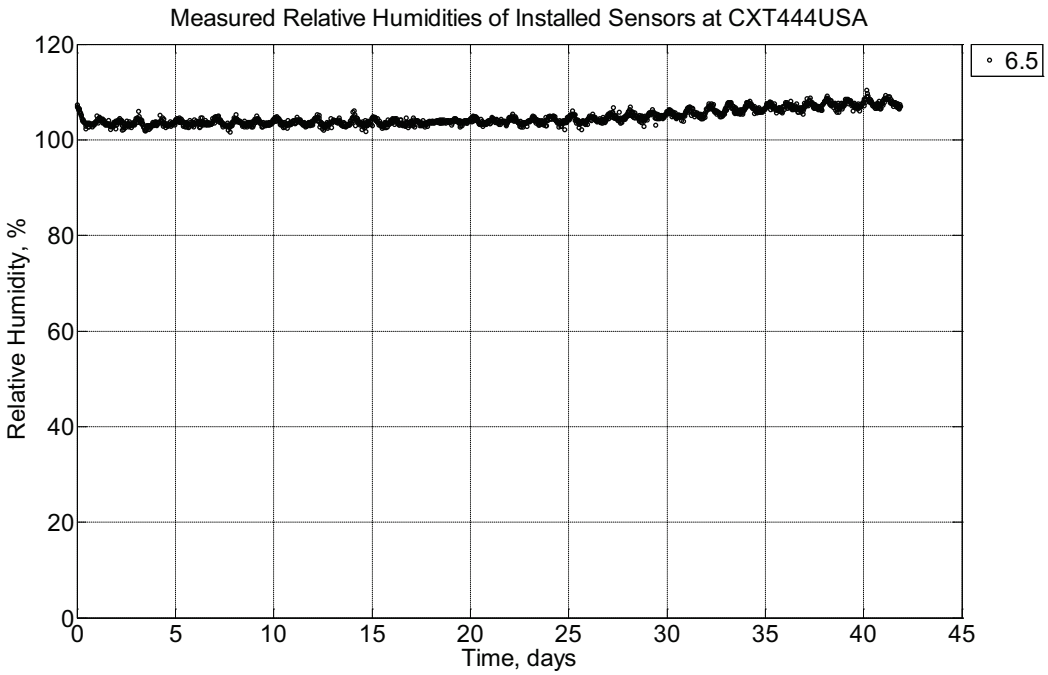

Figure B-476 Measured relative humidity at a depth of 6.5 inches (139.7 mm) from the surface of a concrete crosstie (labeled CXT444USA) installed in ballast in Rantoul, IL, between June 20, 2015, through August 1, 2015. An 8 mm thick polyurethane pad and 12 in (30.48 cm) length 136 lb/yd (67.5 kg/m) section of steel rail are additionally installed atop the concrete crosstie. A breathable water-resistant canvas tarp is additionally installed over the concrete crosstie and immediate ballast area.

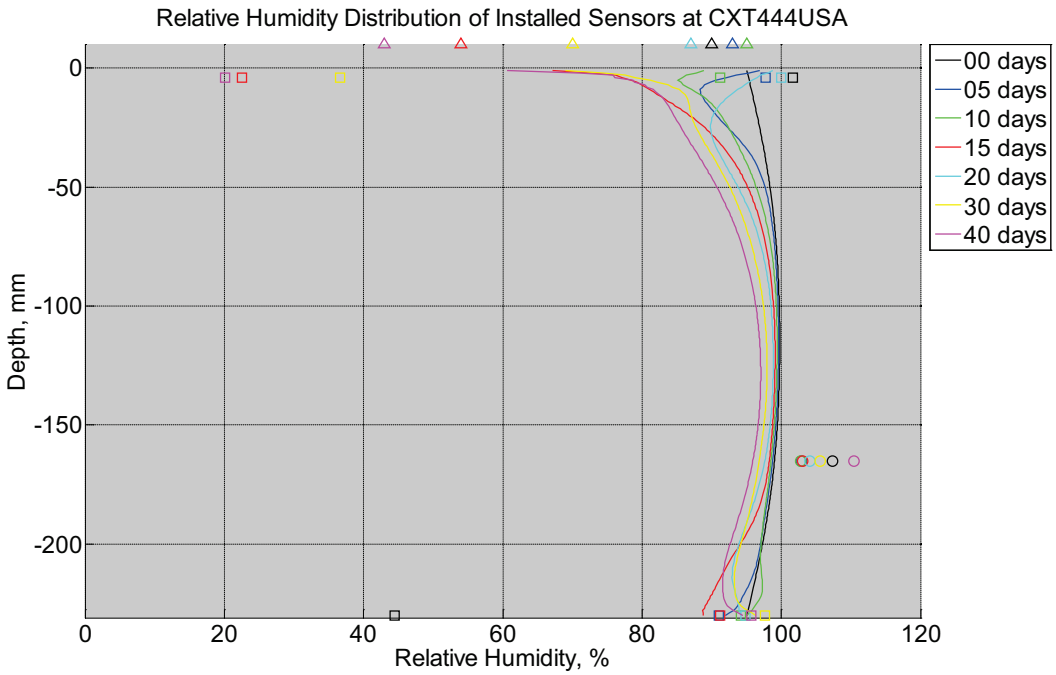

Figure B-477 Measured (markers) and modeled (continuous line) relative humidity profile distribution as a function of depth inside a concrete crosstie (labeled CXT444USA) installed in ballast in Rantoul, IL, between June 20, 2015, through August 1, 2015. An 8 mm thick polyurethane pad and 12 in (30.48 cm) length 136 lb/yd (67.5 kg/m) section of steel rail are additionally installed atop the concrete crosstie. A breathable water-resistant canvas tarp is additionally installed over the concrete crosstie and immediate ballast area. The model does not incorporate a polyurethane pad nor steel rail line. Triangular markers denote relative humidity value from KTIP weather station, square markers denote measured relative humidity values from ballast, and circular markers denote measured relative humidity values inside concrete.

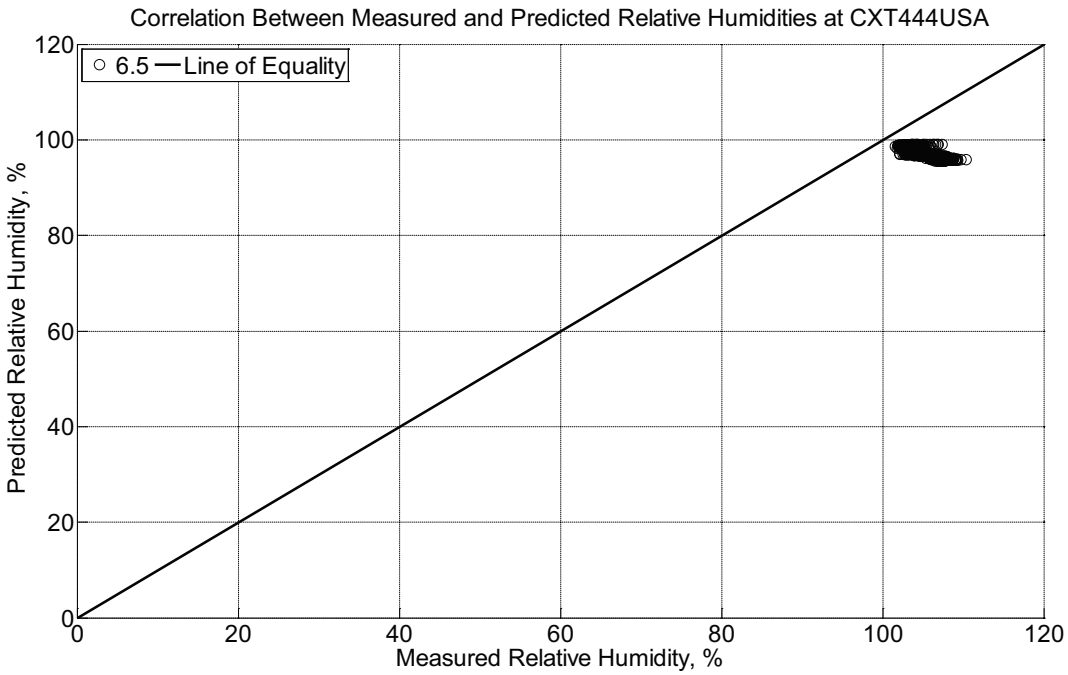

Figure B-478 Correlation between measured and predicted relative humidity values 6.5 inches (139.7 mm) from the surface of a concrete crosstie (labeled CXT444USA) installed in ballast in Rantoul, IL, between June 20, 2015, through August 1, 2015. An 8 mm thick polyurethane pad and 12 in (30.48 cm) length 136 lb/yd (67.5 kg/m) section of steel rail are additionally installed atop the concrete crosstie. A breathable water-resistant canvas tarp is additionally installed over the concrete crosstie and immediate ballast area. The model does not incorporate a polyurethane pad nor steel rail line.

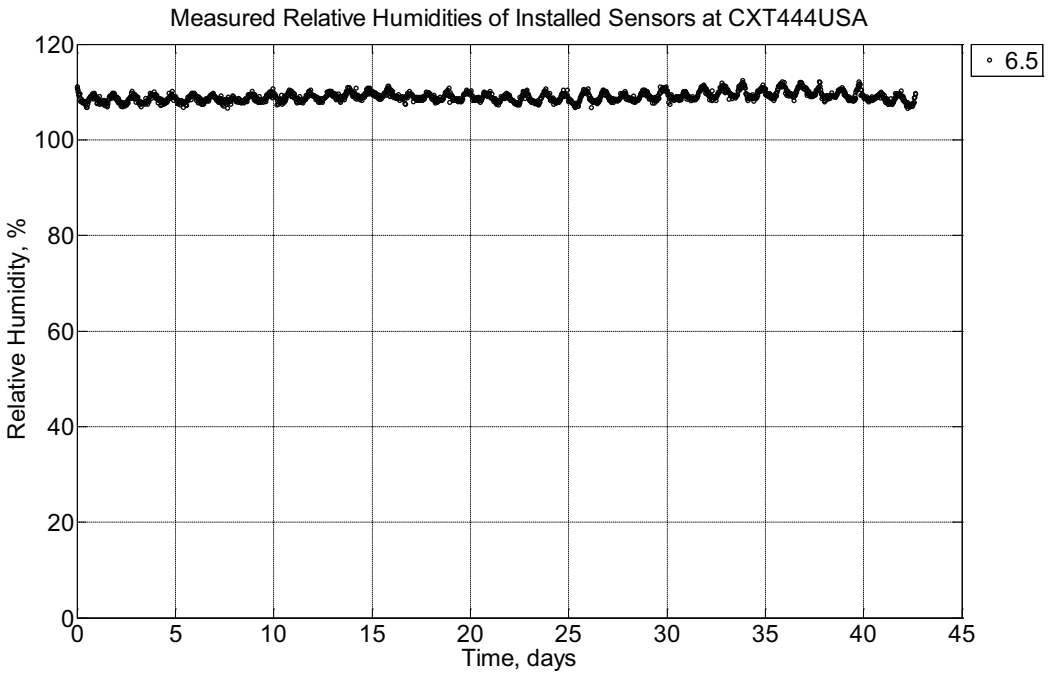

Figure B-479 Measured relative humidity at a depth of 6.5 inches (139.7 mm) from the surface of a concrete crosstie (labeled CXT444USA) installed in ballast in Rantoul, IL, between August 1, 2015, through September 13, 2015. An 8 mm thick polyurethane pad and 12 in (30.48 cm) length 136 lb/yd (67.5 kg/m) section of steel rail are additionally installed atop the concrete crosstie. A breathable water-resistant canvas tarp is additionally installed over the concrete crosstie and immediate ballast area.

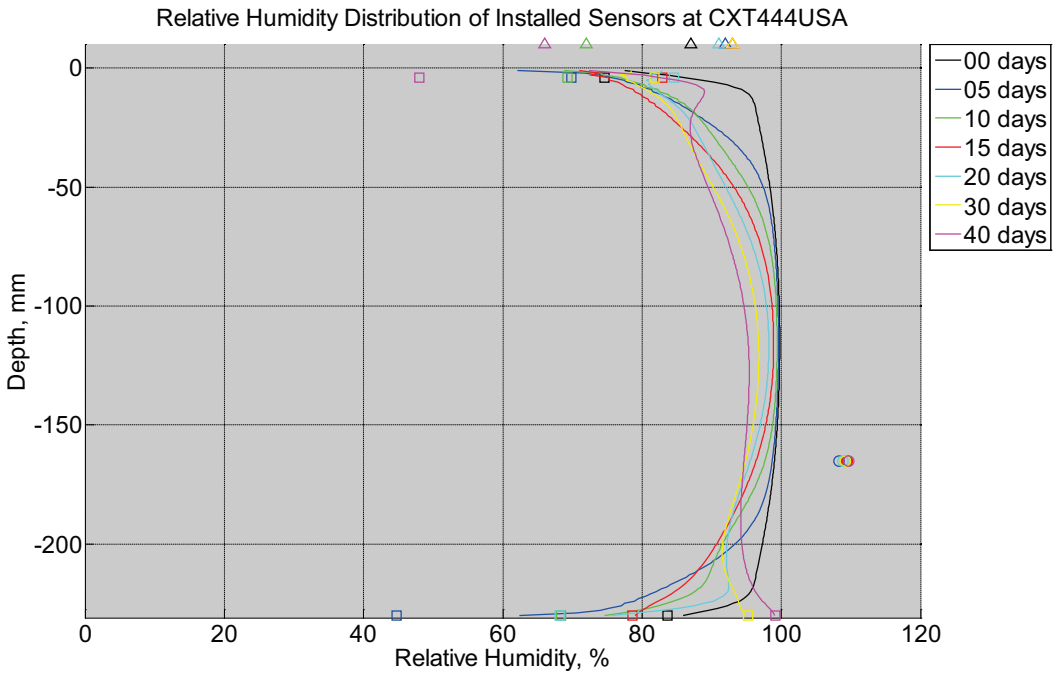

Figure B-480 Measured (markers) and modeled (continuous line) relative humidity profile distribution as a function of depth inside a concrete crosstie (labeled CXT444USA) installed in ballast in Rantoul, IL, between August 1, 2015, through September 13, 2015. An 8 mm thick polyurethane pad and 12 in (30.48 cm) length 136 lb/yd (67.5 kg/m) section of steel rail are additionally installed atop the concrete crosstie. A breathable water-resistant canvas tarp is additionally installed over the concrete crosstie and immediate ballast area. The model does not incorporate a polyurethane pad nor steel rail line. Triangular markers denote relative humidity value from KTIP weather station, square markers denote measured relative humidity values from ballast, and circular markers denote measured relative humidity values inside concrete.

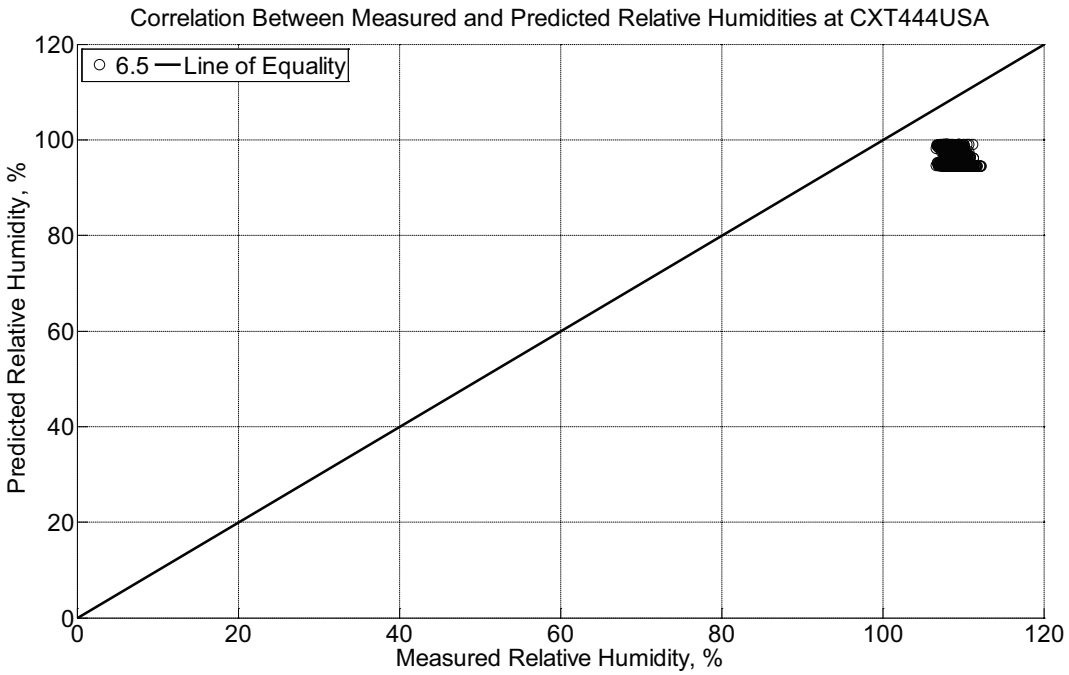

Figure B-481 Correlation between measured and predicted relative humidity values 6.5 inches (139.7 mm) from the surface of a concrete crosstie (labeled CXT444USA) installed in ballast in Rantoul, IL, between August 1, 2015, through September 13, 2015. An 8 mm thick polyurethane pad and 12 in (30.48 cm) length 136 lb/yd (67.5 kg/m) section of steel rail are additionally installed atop the concrete crosstie. A breathable water-resistant canvas tarp is additionally installed over the concrete crosstie and immediate ballast area. The model does not incorporate a polyurethane pad nor steel rail line.

Measured and predicted internal temperature of instrumented concrete crossties located in Champaign and Rantoul, IL

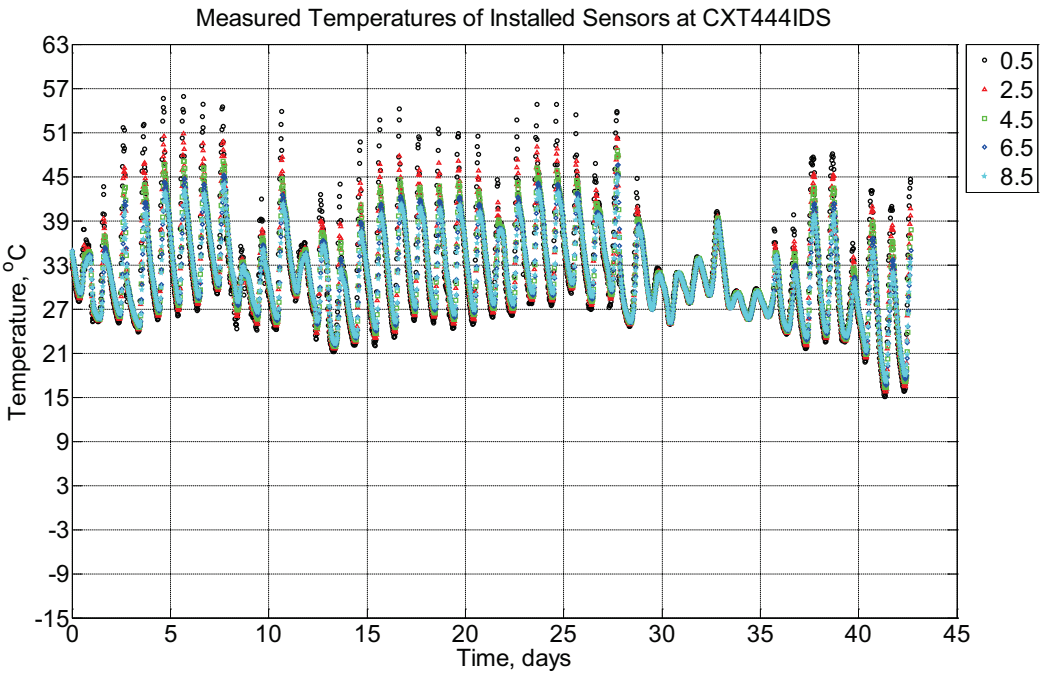

Figure B-482 Measured temperature at depths of 0.5 inches (12.7 mm), 2.5 inches (63.5 mm), 4.5 inches (114.3 mm), 6.5 inches (139.7 mm), and 8.5 inches (215.9 mm) from the surface of a concrete crosstie (labeled CXT444IDS) without a polyurethane pad nor rail as transported from Tucson, AZ, to Champaign, IL, between July 23, 2013, through September 4, 2013.

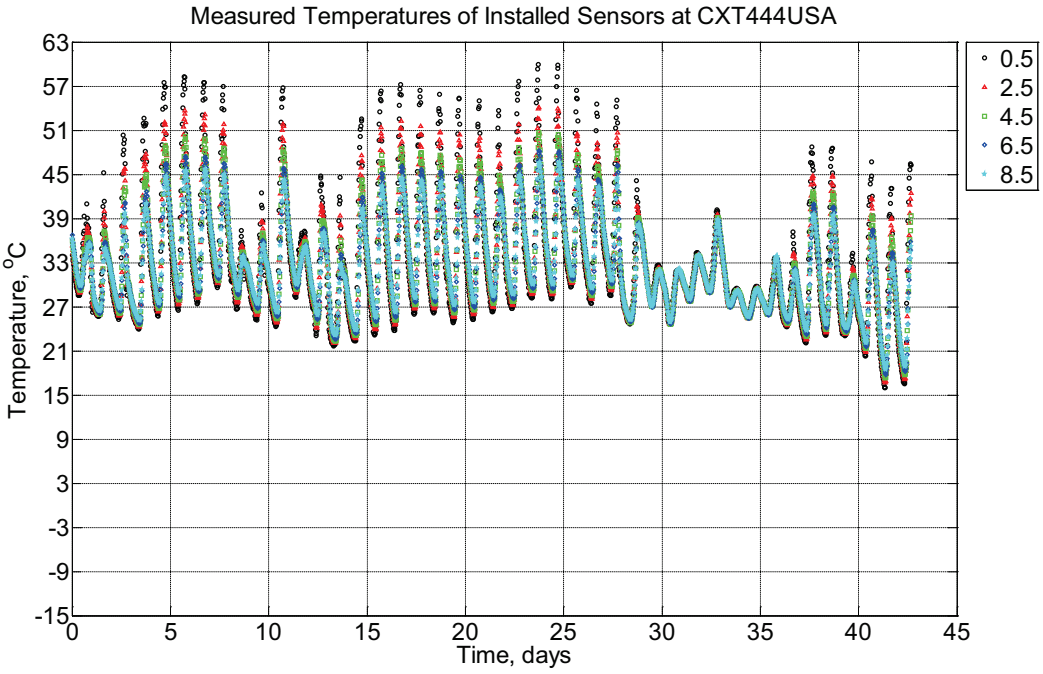

Figure B-483 Measured temperature at depths of 0.5 inches (12.7 mm), 2.5 inches (63.5

mm), 4.5 inches (114.3 mm), 6.5 inches (139.7 mm), and 8.5 inches (215.9 mm) from the surface of a concrete crosstie (labeled CXT444USA) without a polyurethane pad nor rail as transported from Tucson, AZ, to Champaign, IL, between July 23, 2013, through September 4, 2013.

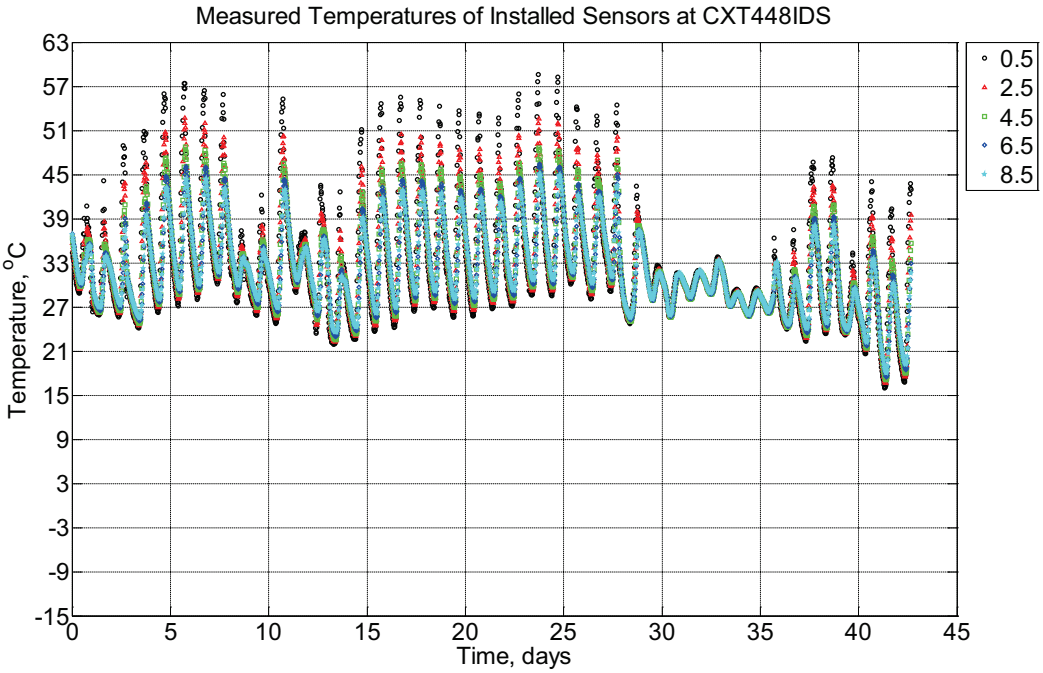

Figure B-484 Measured temperature at depths of 0.5 inches (12.7 mm), 2.5 inches (63.5 mm), 4.5 inches (114.3 mm), 6.5 inches (139.7 mm), and 8.5 inches (215.9 mm) from the surface of a concrete crosstie (labeled CXT448IDS) without a polyurethane pad nor rail as transported from Tucson, AZ, to Champaign, IL, between July 23, 2013, through September 4, 2013.

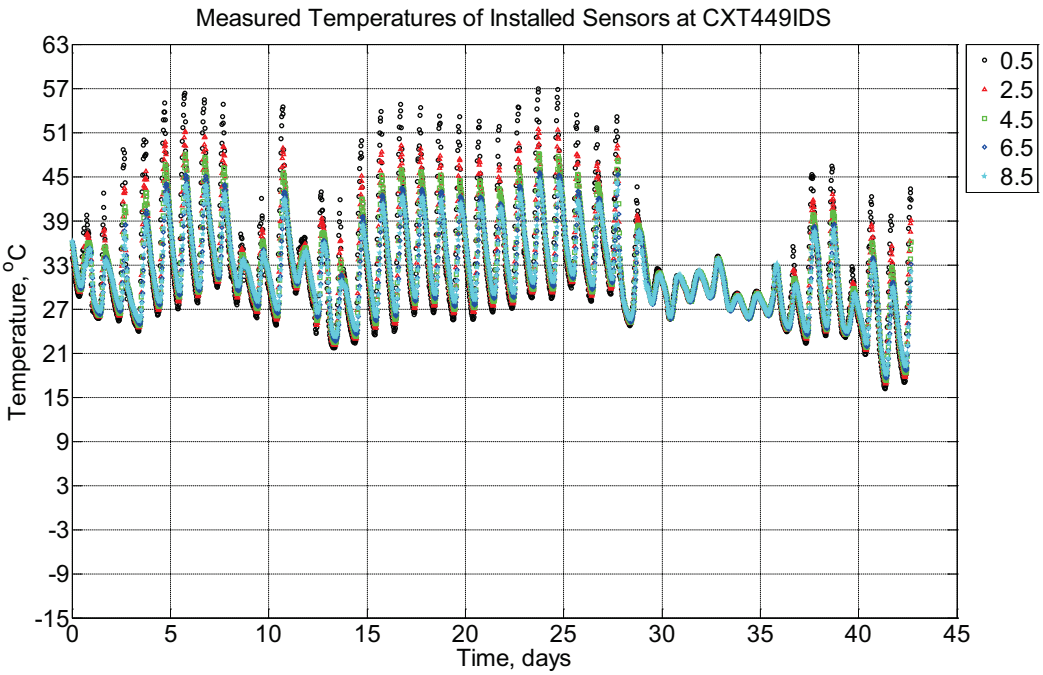

Figure B-485 Measured temperature at depths of 0.5 inches (12.7 mm), 2.5 inches (63.5 mm), 4.5 inches (114.3 mm), 6.5 inches (139.7 mm), and 8.5 inches (215.9 mm) from the surface of a concrete crosstie (labeled CXT449IDS) without a polyurethane pad nor rail as transported from Tucson, AZ, to Champaign, IL, between July 23, 2013, through September 4, 2013.

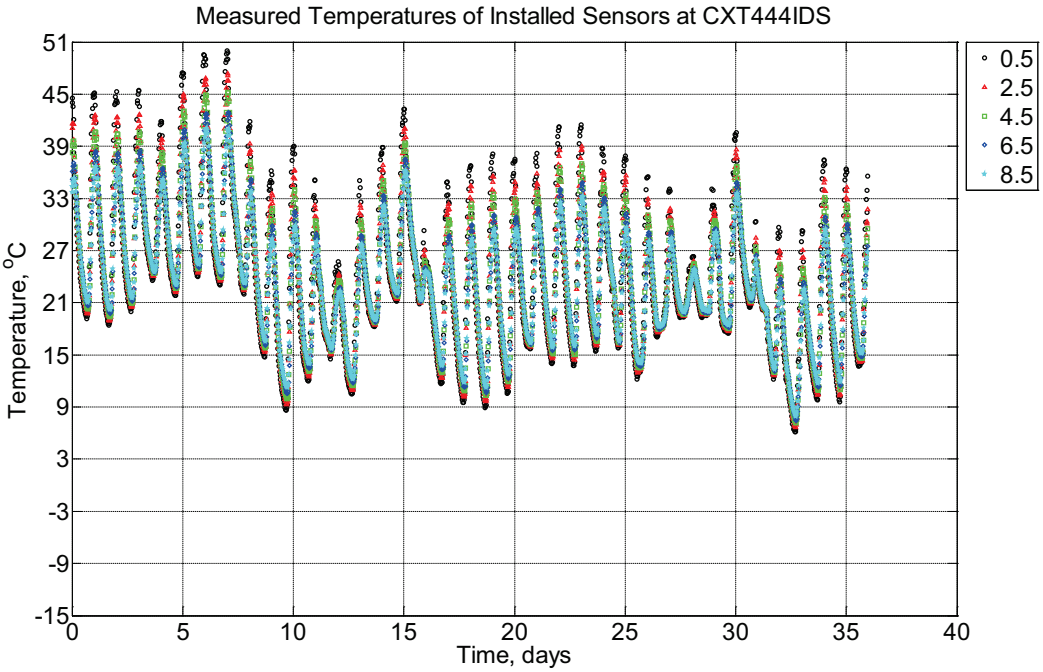

Figure B-486 Measured temperature at depths of 0.5 inches (12.7 mm), 2.5 inches (63.5

mm), 4.5 inches (114.3 mm), 6.5 inches (139.7 mm), and 8.5 inches (215.9 mm) from the surface of a concrete crosstie (labeled CXT444IDS) without a polyurethane pad nor rail located in Champaign, IL, between September 4, 2013, through October 10, 2013.

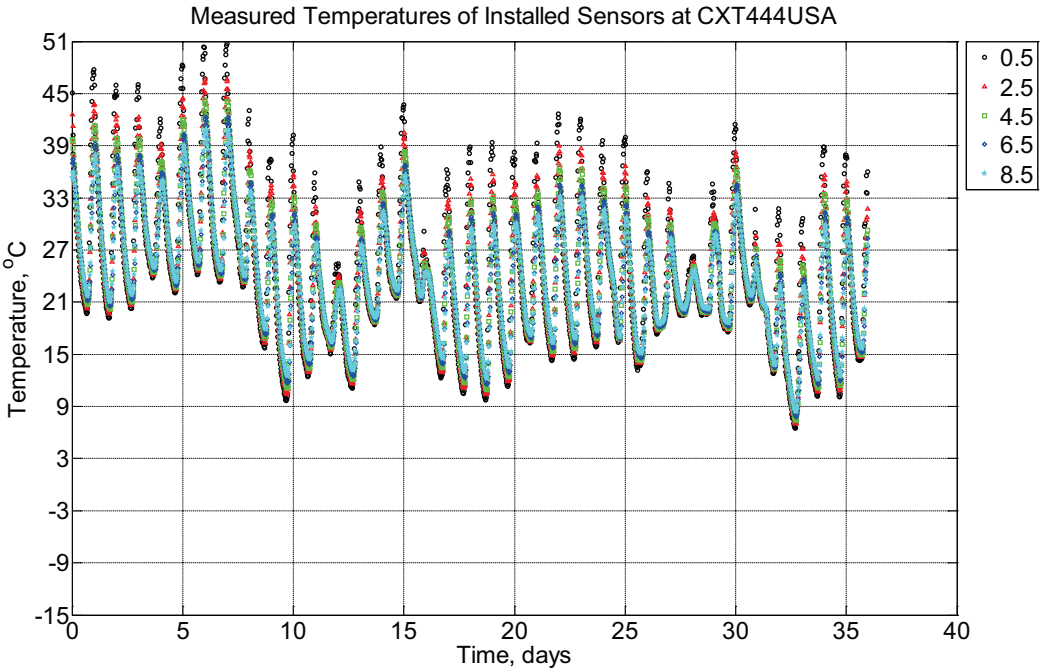

Figure B-487 Measured temperature at depths of 0.5 inches (12.7 mm), 2.5 inches (63.5 mm), 4.5 inches (114.3 mm), 6.5 inches (139.7 mm), and 8.5 inches (215.9 mm) from the surface of a concrete crosstie (labeled CXT444USA) without a polyurethane pad nor rail located in Champaign, IL, between September 4, 2013, through October 10, 2013.

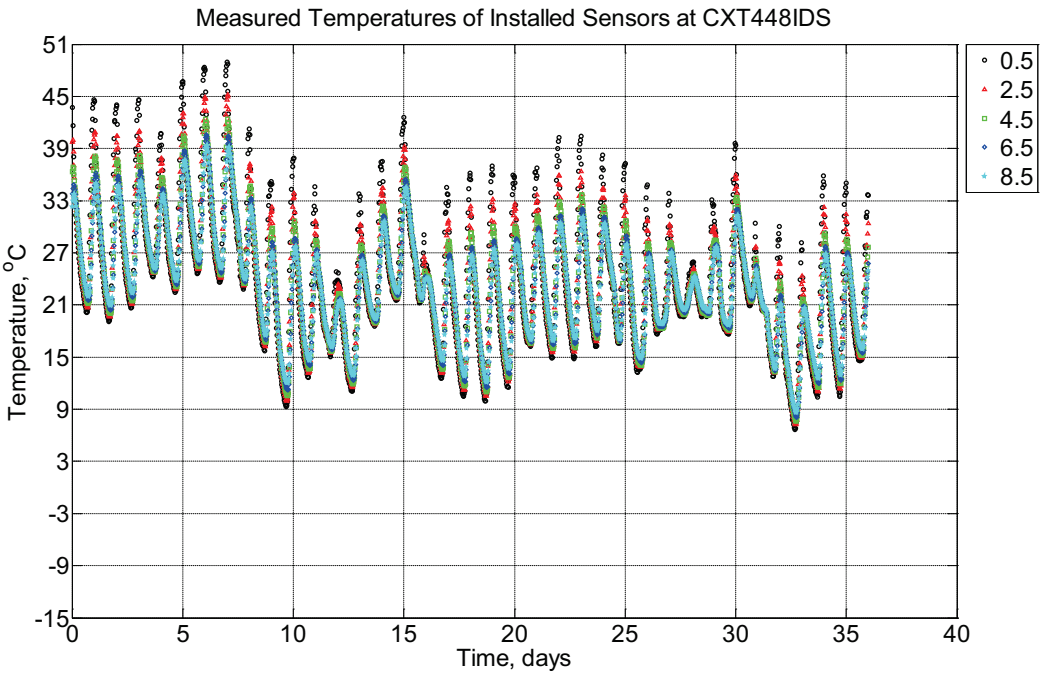

Figure B-488 Measured temperature at depths of 0.5 inches (12.7 mm), 2.5 inches (63.5 mm), 4.5 inches (114.3 mm), 6.5 inches (139.7 mm), and 8.5 inches (215.9 mm) from the surface of a concrete crosstie (labeled CXT448IDS) without a polyurethane pad nor rail located in Champaign, IL, between September 4, 2013, through October 10, 2013.

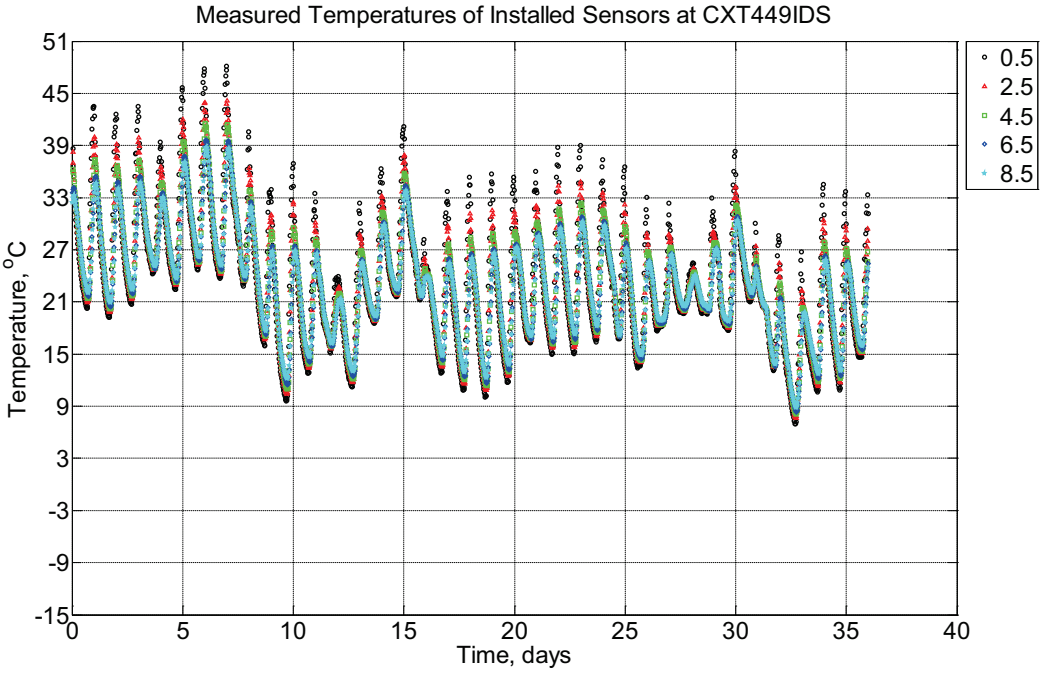

Figure B-489 Measured temperature at depths of 0.5 inches (12.7 mm), 2.5 inches (63.5 mm), 4.5 inches (114.3 mm), 6.5 inches (139.7 mm), and 8.5 inches (215.9 mm) from the

surface of a concrete crosstie (labeled CXT449IDS) without a polyurethane pad nor rail located in Champaign, IL, between September 4, 2013, through October 10, 2013.

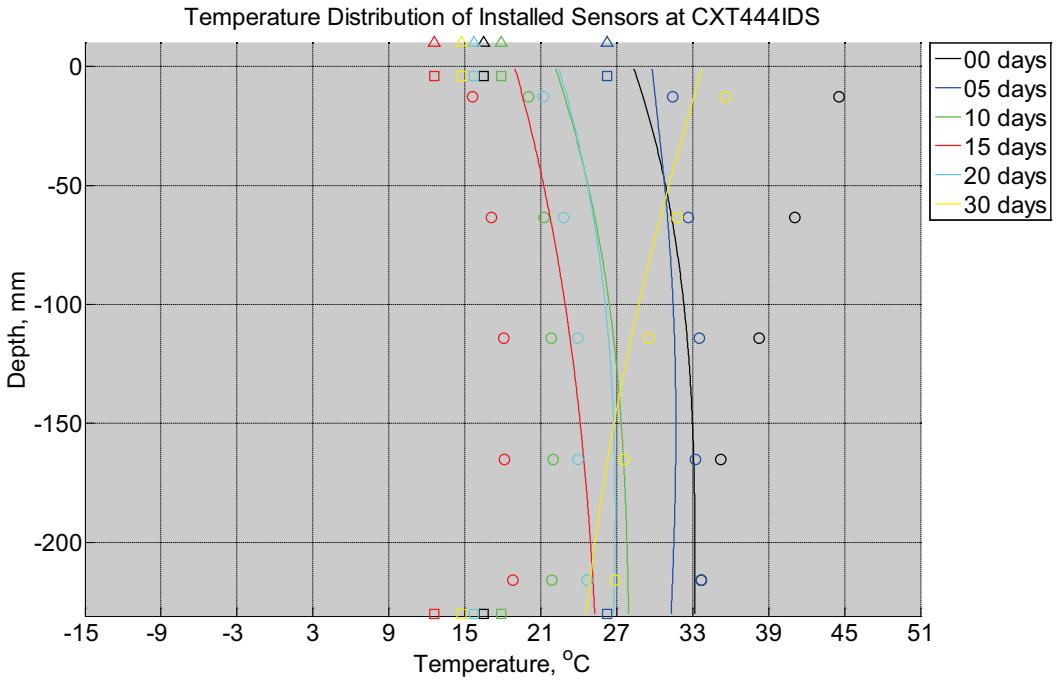

Figure B-490 Measured (markers) and modeled (continuous line) temperature profile distribution as a function of depth inside a concrete crosstie (labeled CXT444IDS) without a polyurethane pad nor rail located in Champaign, IL, between September 4, 2013, through October 10, 2013. Triangular markers denote temperature value from KTIP weather station, square markers denote measured temperature values from ambient sensors, and circular markers denote measured temperature values inside concrete.

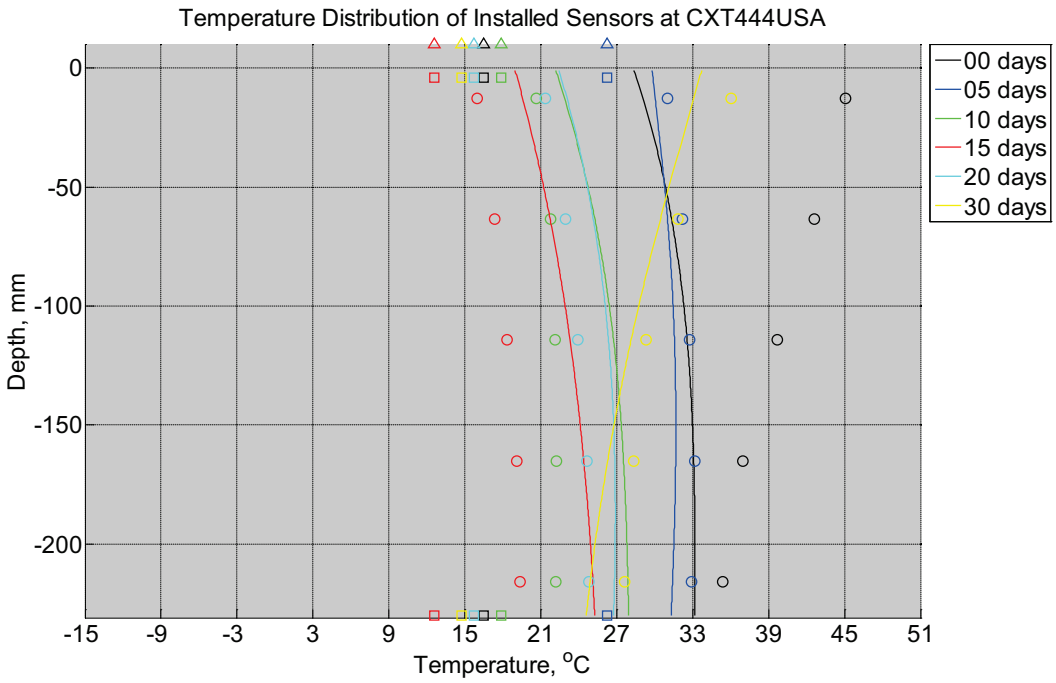

Figure B-491 Measured (markers) and modeled (continuous line) temperature profile distribution as a function of depth inside a concrete crosstie (labeled CXT444USA) without a polyurethane pad nor rail located in Champaign, IL, between September 4, 2013, through October 10, 2013. Triangular markers denote temperature value from KTIP weather station, square markers denote measured temperature values from ambient sensors, and circular markers denote measured temperature values inside concrete.

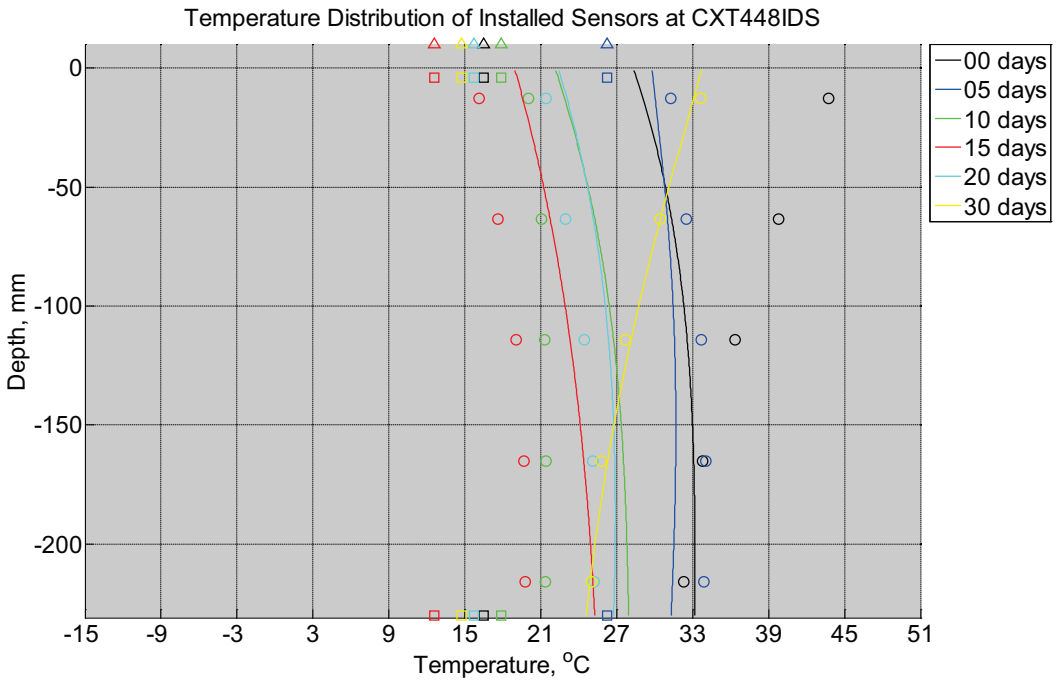

Figure B-492 Measured (markers) and modeled (continuous line) temperature profile distribution as a function of depth inside a concrete crosstie (labeled CXT448IDS) without a polyurethane pad nor rail located in Champaign, IL, between September 4, 2013, through October 10, 2013. Triangular markers denote temperature value from KTIP weather station, square markers denote measured temperature values from ambient sensors, and circular markers denote measured temperature values inside concrete.

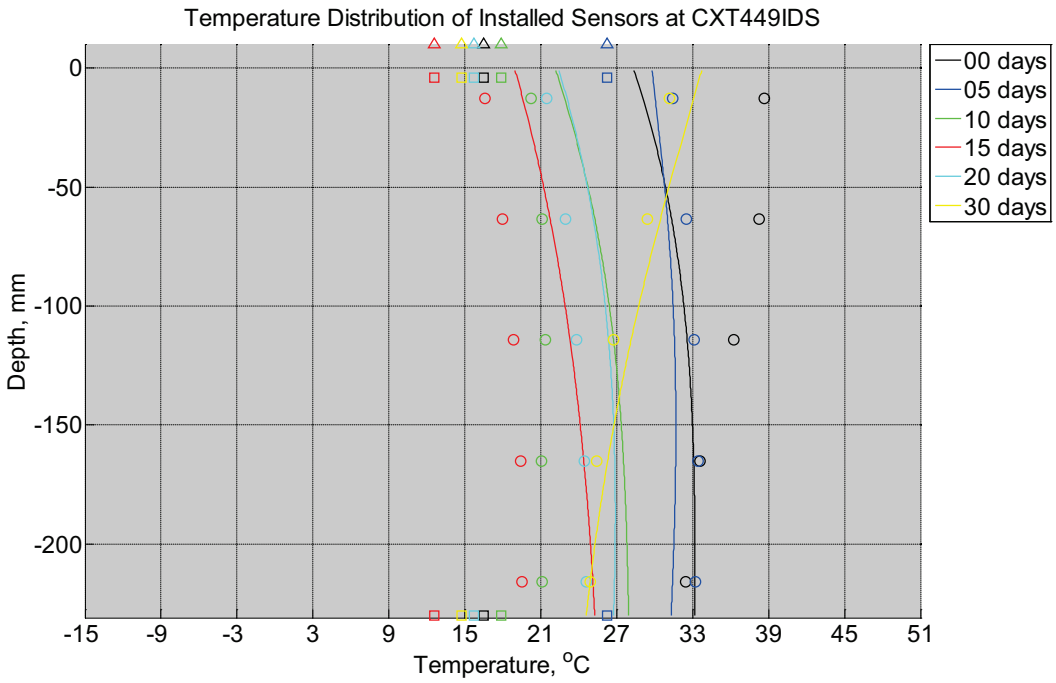

Figure B-493 Measured (markers) and modeled (continuous line) temperature profile distribution as a function of depth inside a concrete crosstie (labeled CXT449IDS) without a polyurethane pad nor rail located in Champaign, IL, between September 4, 2013, through October 10, 2013. Triangular markers denote temperature value from KTIP weather station, square markers denote measured temperature values from ambient sensors, and circular markers denote measured temperature values inside concrete.

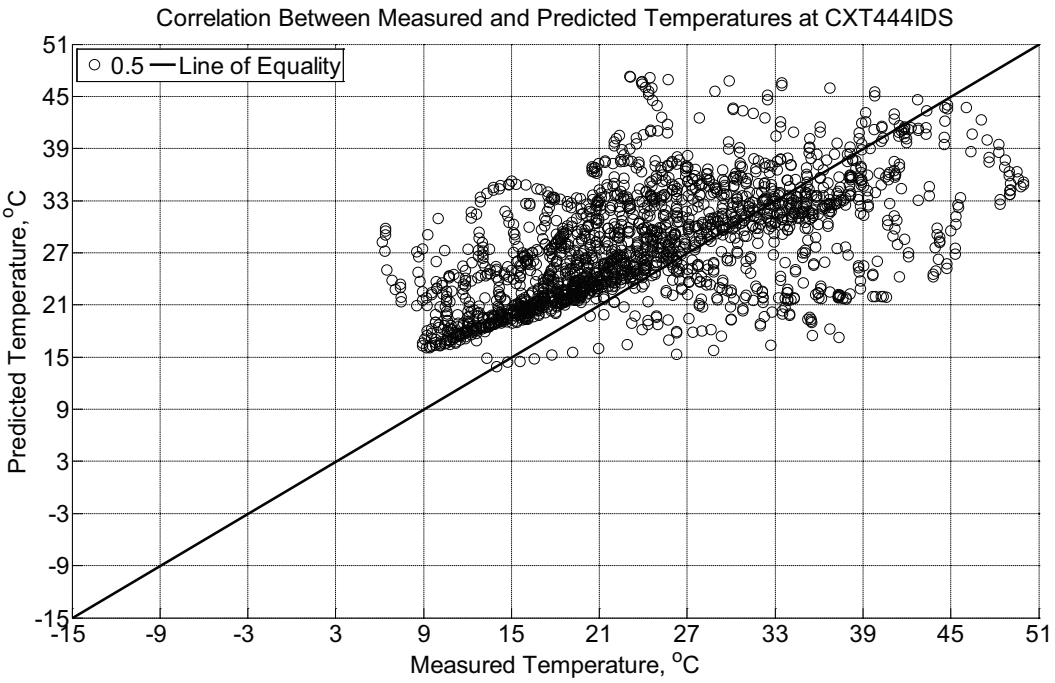

Figure B-494 Correlation between measured and predicted temperature values 0.5 inches (12.7 mm) from the surface of a concrete crosstie (labeled CXT444IDS) without a polyurethane pad nor rail located in Champaign, IL, between September 4, 2013, through October 10, 2013.

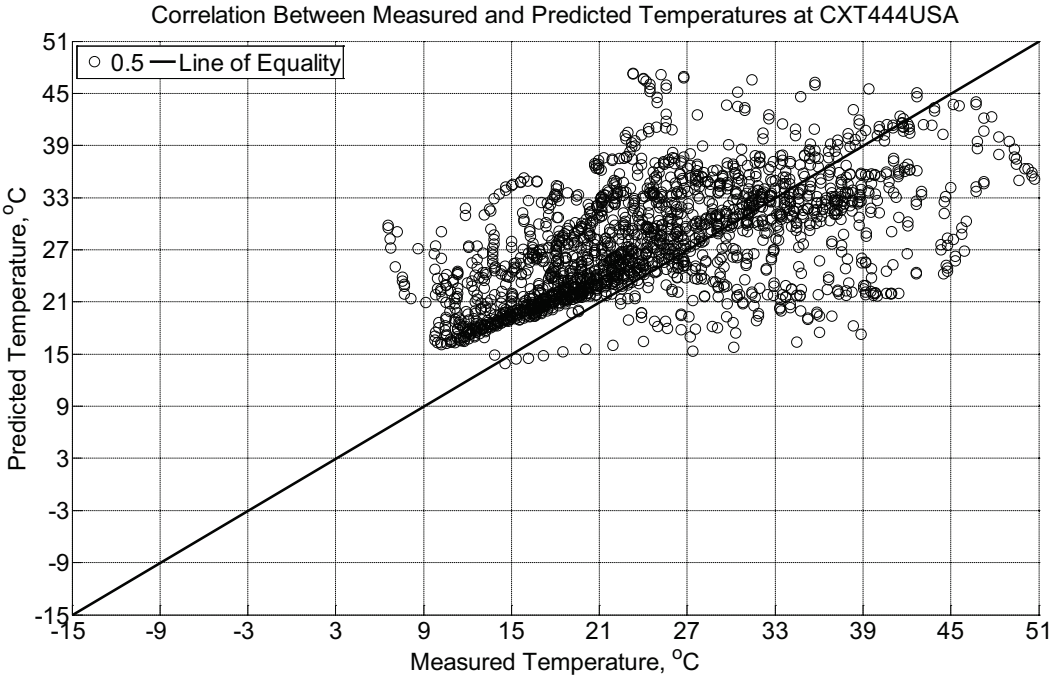

Figure B-495 Correlation between measured and predicted temperature values 0.5 inches (12.7 mm) from the surface of a concrete crosstie (labeled CXT444USA) without a

polyurethane pad nor rail located in Champaign, IL, between September 4, 2013, through October 10, 2013.

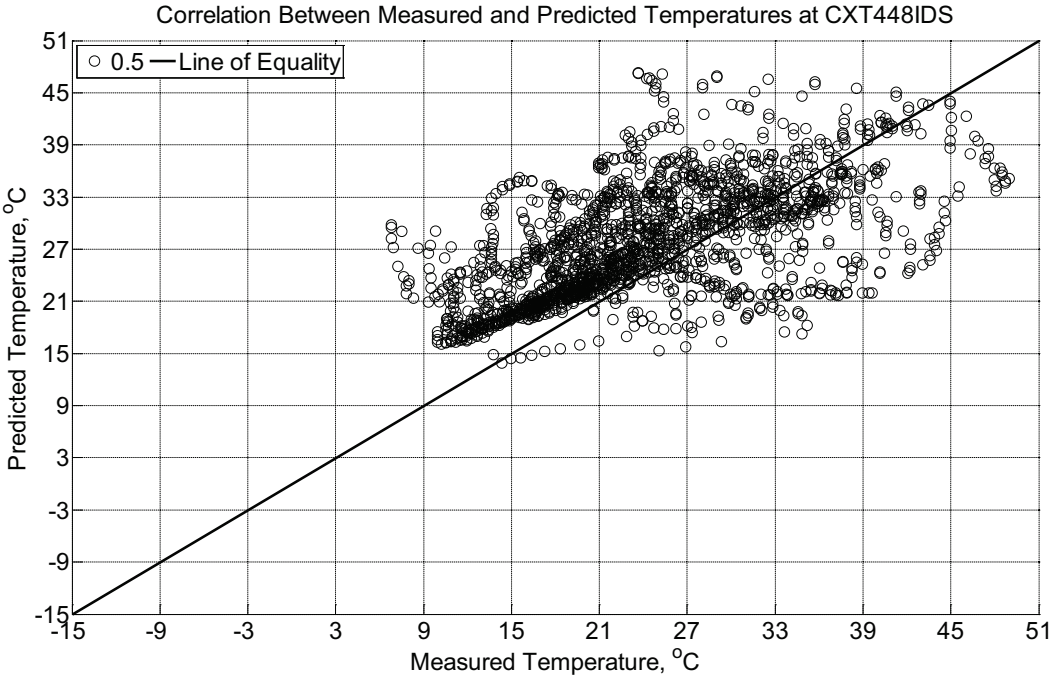

Figure B-496 Correlation between measured and predicted temperature values 0.5 inches (12.7 mm) from the surface of a concrete crosstie (labeled CXT448IDS) without a polyurethane pad nor rail located in Champaign, IL, between September 4, 2013, through October 10, 2013.

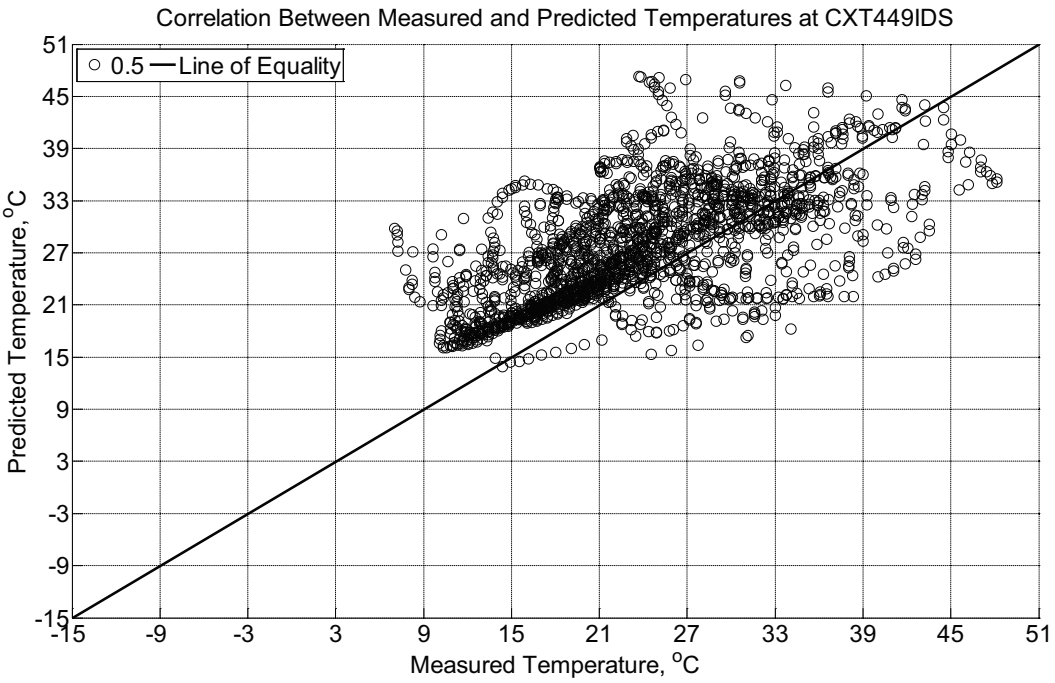

Figure B-497 Correlation between measured and predicted temperature values 0.5 inches (12.7 mm) from the surface of a concrete crosstie (labeled CXT449IDS) without a polyurethane pad nor rail located in Champaign, IL, between September 4, 2013, through October 10, 2013.

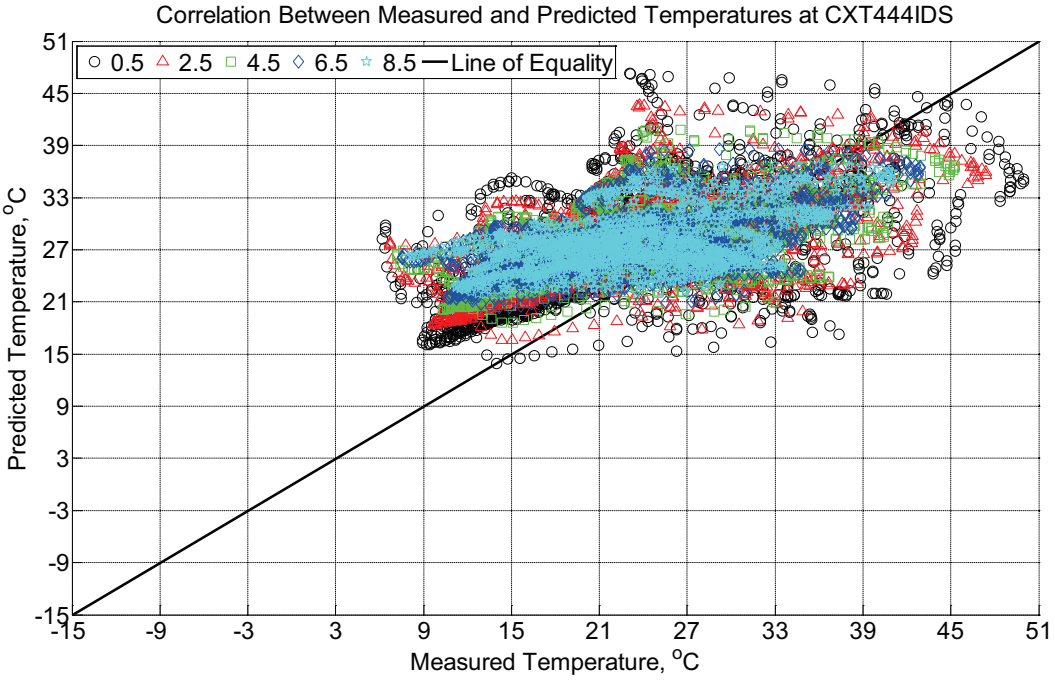

Figure B-498 Correlation between measured and predicted temperature values 0.5 inches (12.7 mm), 2.5 inches (63.5 mm), 4.5 inches (114.3 mm), 6.5 inches (139.7 mm), and 8.5

inches (215.9 mm) from the surface of a concrete crosstie (labeled CXT444IDS) without a polyurethane pad nor rail located in Champaign, IL, between September 4, 2013, through October 10, 2013.

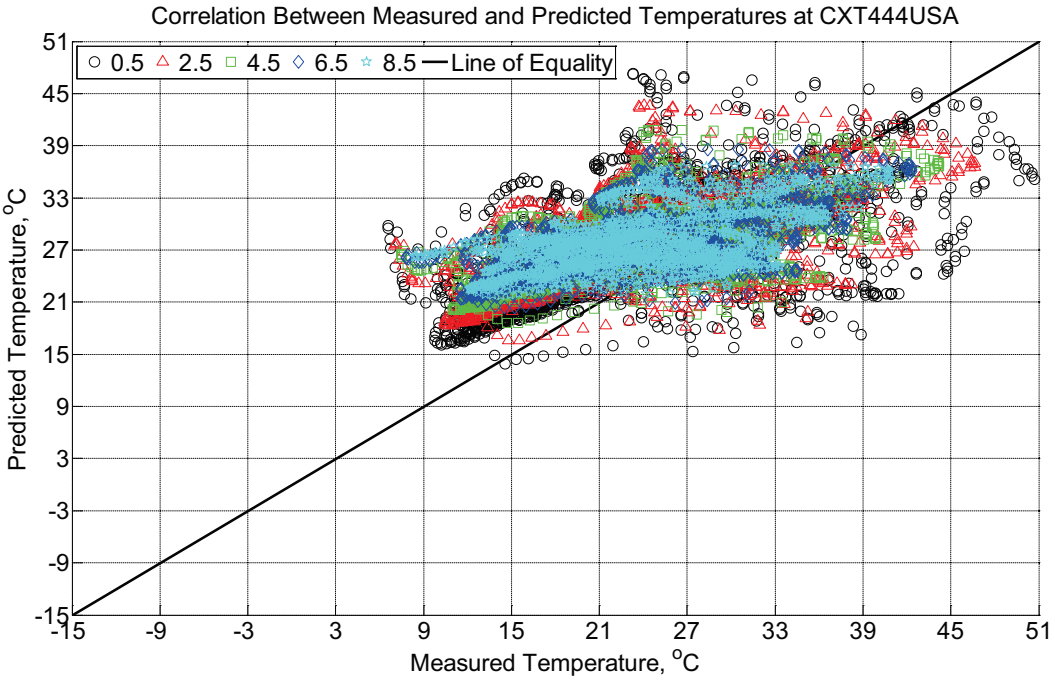

Figure B-499 Correlation between measured and predicted temperature values 0.5 inches (12.7 mm), 2.5 inches (63.5 mm), 4.5 inches (114.3 mm), 6.5 inches (139.7 mm), and 8.5 inches (215.9 mm) from the surface of a concrete crosstie (labeled CXT444USA) without a polyurethane pad nor rail located in Champaign, IL, between September 4, 2013, through October 10, 2013.

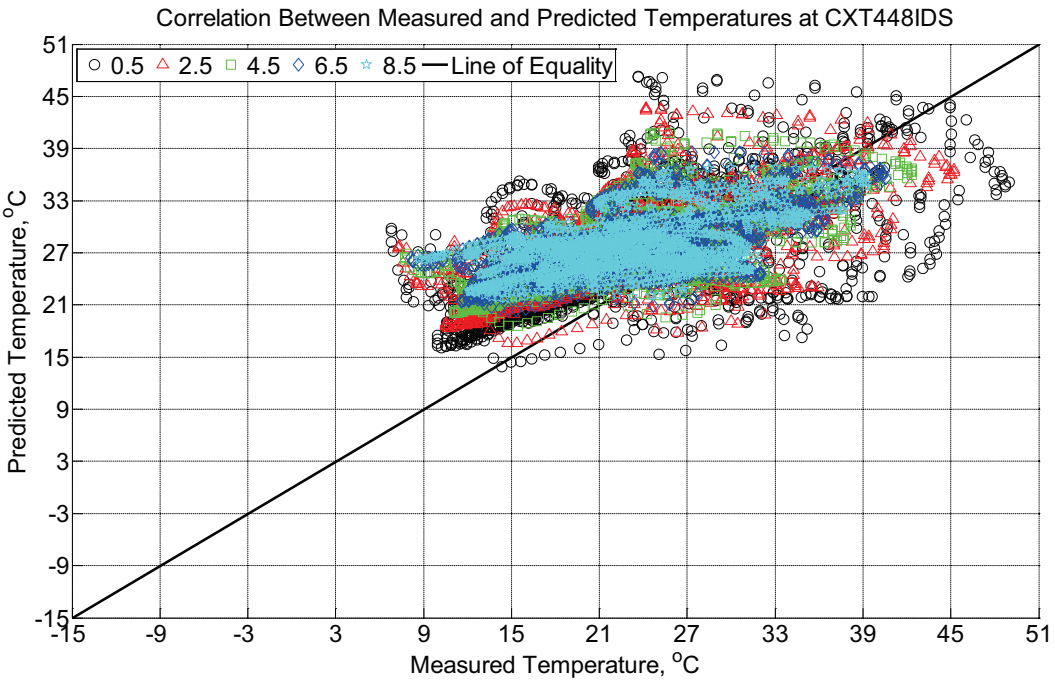

Figure B-500 Correlation between measured and predicted temperature values 0.5 inches (12.7 mm), 2.5 inches (63.5 mm), 4.5 inches (114.3 mm), 6.5 inches (139.7 mm), and 8.5 inches (215.9 mm) from the surface of a concrete crosstie (labeled CXT448IDS) without a polyurethane pad nor rail located in Champaign, IL, between September 4, 2013, through October 10, 2013.

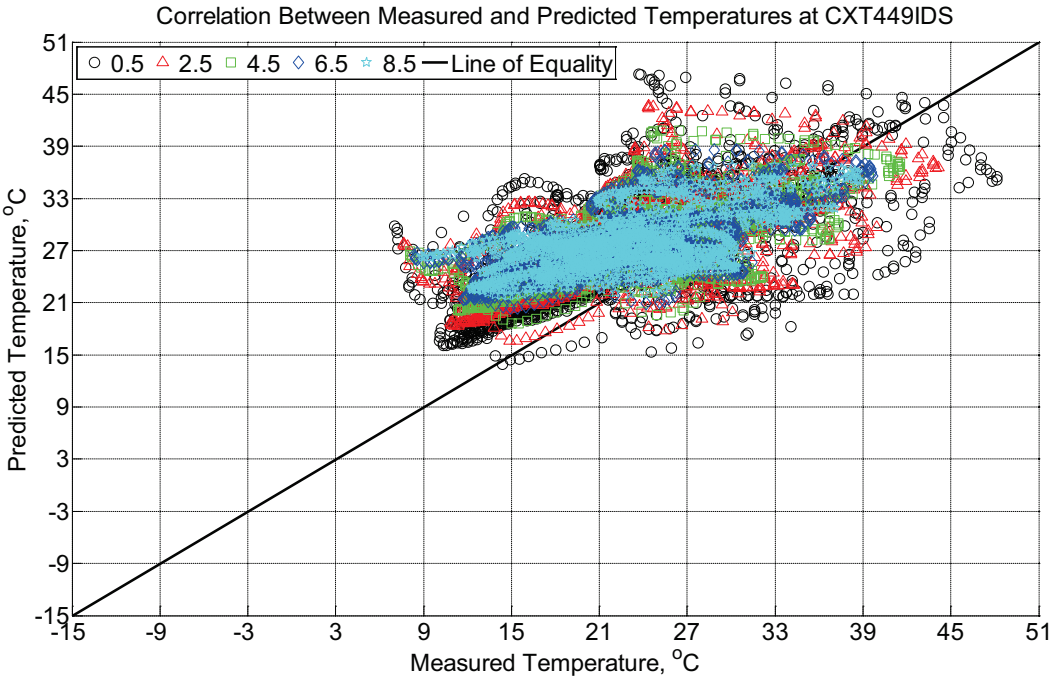

Figure B-501 Correlation between measured and predicted temperature values 0.5 inches

(12.7 mm), 2.5 inches (63.5 mm), 4.5 inches (114.3 mm), 6.5 inches (139.7 mm), and 8.5 inches (215.9 mm) from the surface of a concrete crosstie (labeled CXT449IDS) without a polyurethane pad nor rail located in Champaign, IL, between September 4, 2013, through October 10, 2013.

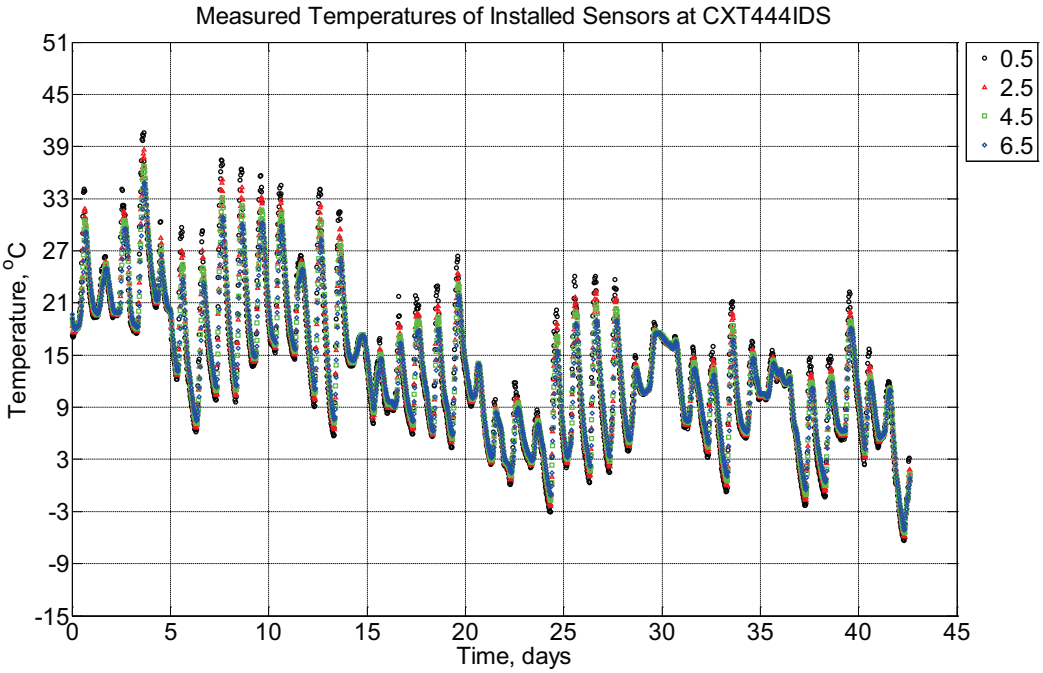

Figure B-502 Measured temperature at depths of 0.5 inches (12.7 mm), 2.5 inches (63.5 mm), 4.5 inches (114.3 mm), and 6.5 inches (139.7 mm) from the surface of a concrete crosstie (labeled CXT444IDS) without a polyurethane pad nor rail located in Champaign, IL, between October 1, 2013, through November 12, 2013.

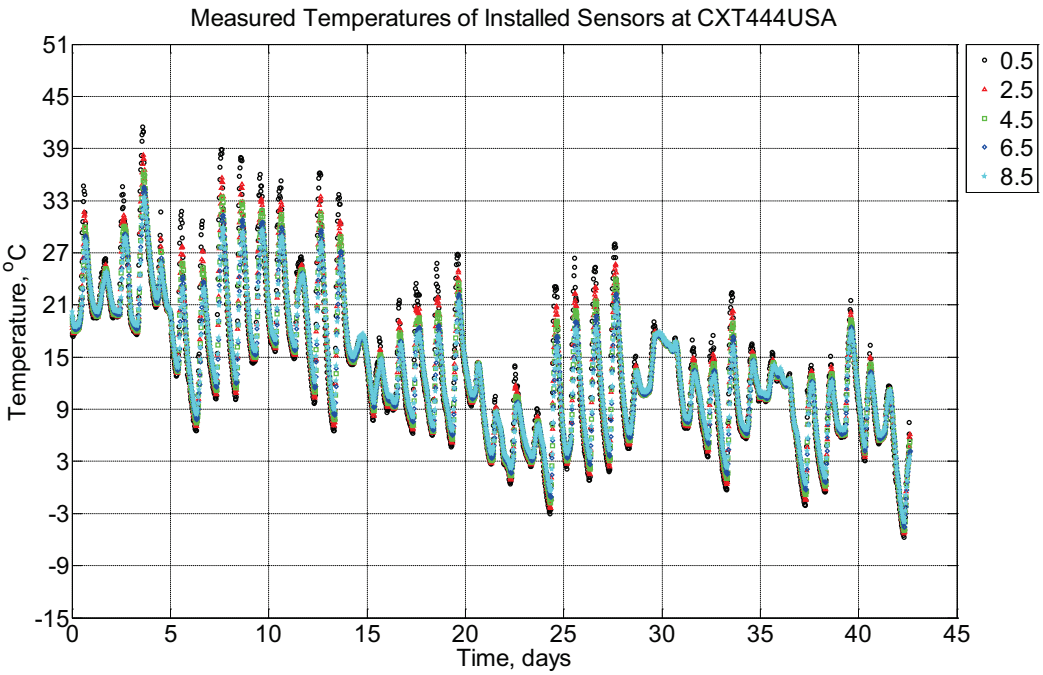

Figure B-503 Measured temperature at depths of 0.5 inches (12.7 mm), 2.5 inches (63.5 mm), 4.5 inches (114.3 mm), 6.5 inches (139.7 mm), and 8.5 inches (215.9 mm) from the surface of a concrete crosstie (labeled CXT444USA) without a polyurethane pad nor rail located in Champaign, IL, between October 1, 2013, through November 12, 2013.

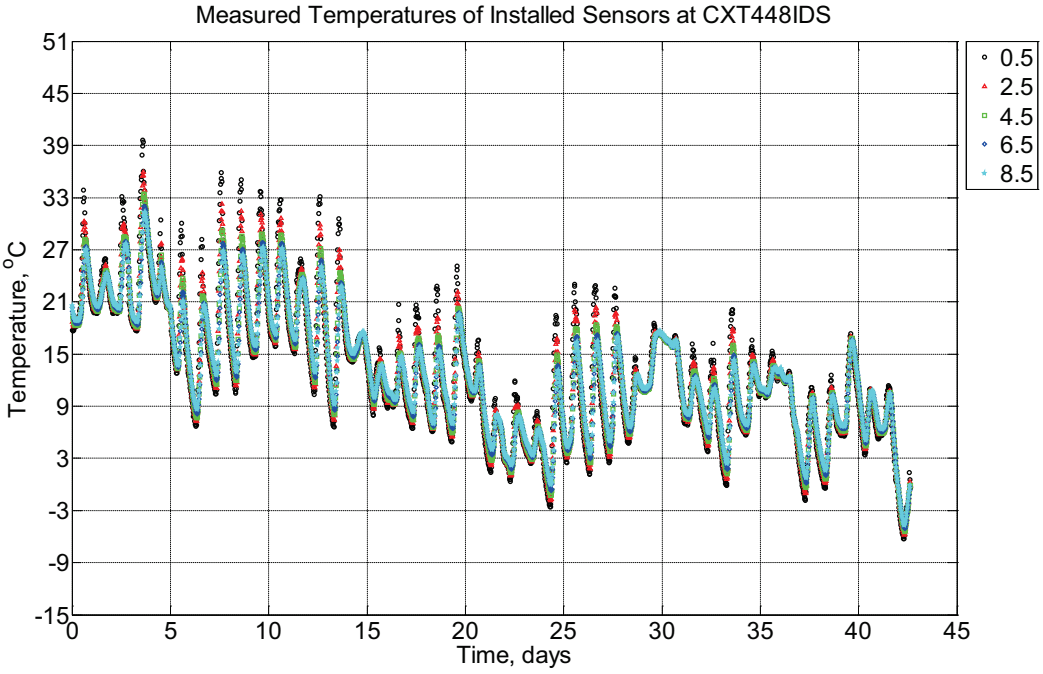

Figure B-504 Measured temperature at depths of 0.5 inches (12.7 mm), 2.5 inches (63.5 mm), 4.5 inches (114.3 mm), 6.5 inches (139.7 mm), and 8.5 inches (215.9 mm) from the

surface of a concrete crosstie (labeled CXT448IDS) without a polyurethane pad nor rail located in Champaign, IL, between October 1, 2013, through November 12, 2013.

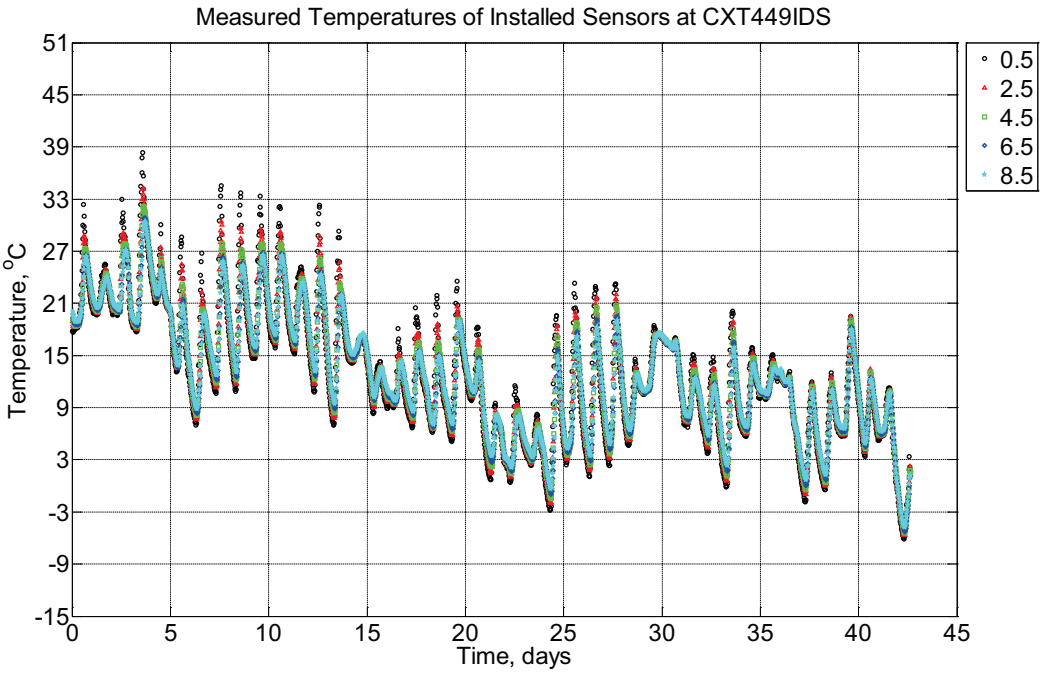

Figure B-505 Measured temperature at depths of 0.5 inches (12.7 mm), 2.5 inches (63.5 mm), 4.5 inches (114.3 mm), 6.5 inches (139.7 mm), and 8.5 inches (215.9 mm) from the surface of a concrete crosstie (labeled CXT449IDS) without a polyurethane pad nor rail located in Champaign, IL, between October 1, 2013, through November 12, 2013.

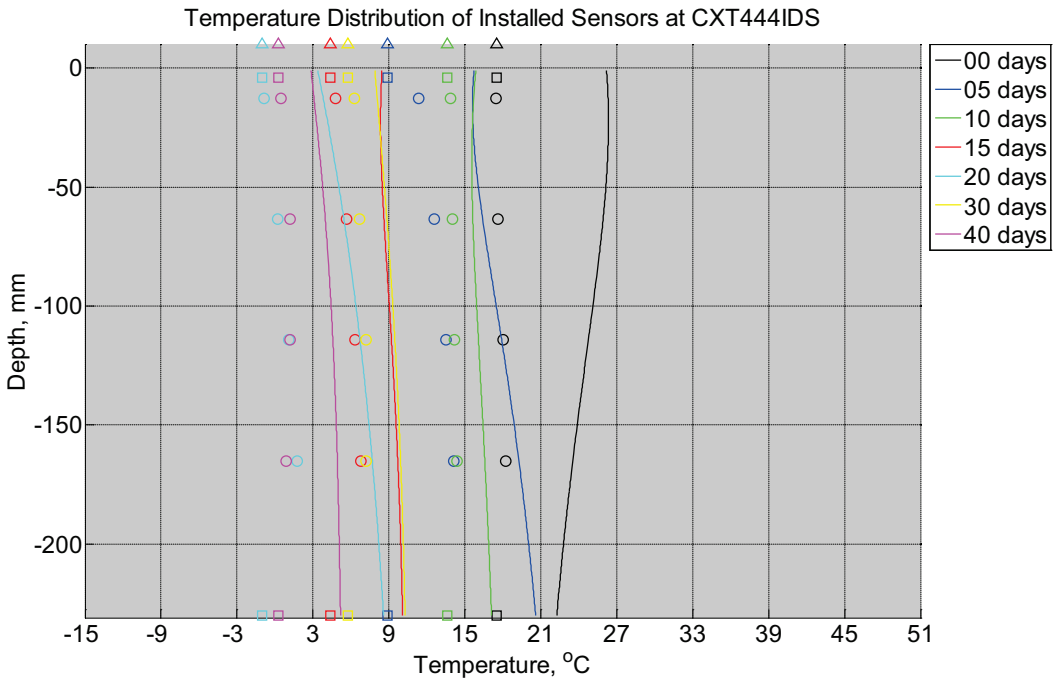

Figure B-506 Measured (markers) and modeled (continuous line) temperature profile distribution as a function of depth inside a concrete crosstie (labeled CXT444IDS) without a polyurethane pad nor rail located in Champaign, IL, between October 1, 2013, through November 12, 2013. Triangular markers denote temperature value from KTIP weather station, square markers denote measured temperature values from ambient sensors, and circular markers denote measured temperature values inside concrete.

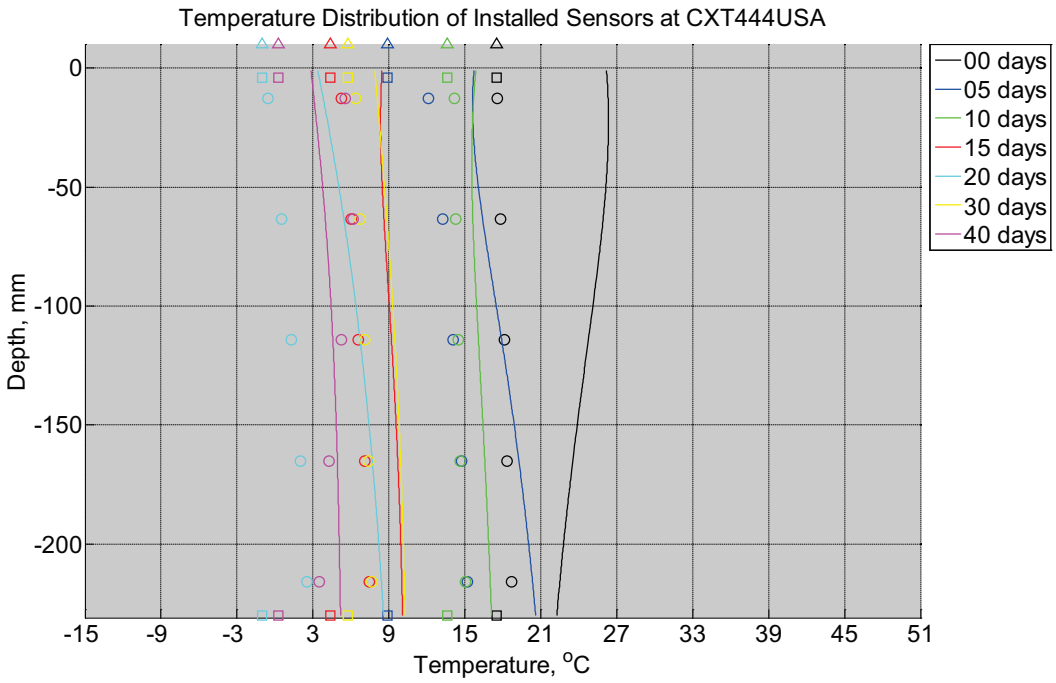

Figure B-507 Measured (markers) and modeled (continuous line) temperature profile distribution as a function of depth inside a concrete crosstie (labeled CXT444USA) without a polyurethane pad nor rail located in Champaign, IL, between October 1, 2013, through November 12, 2013. Triangular markers denote temperature value from KTIP weather station, square markers denote measured temperature values from ambient sensors, and circular markers denote measured temperature values inside concrete.

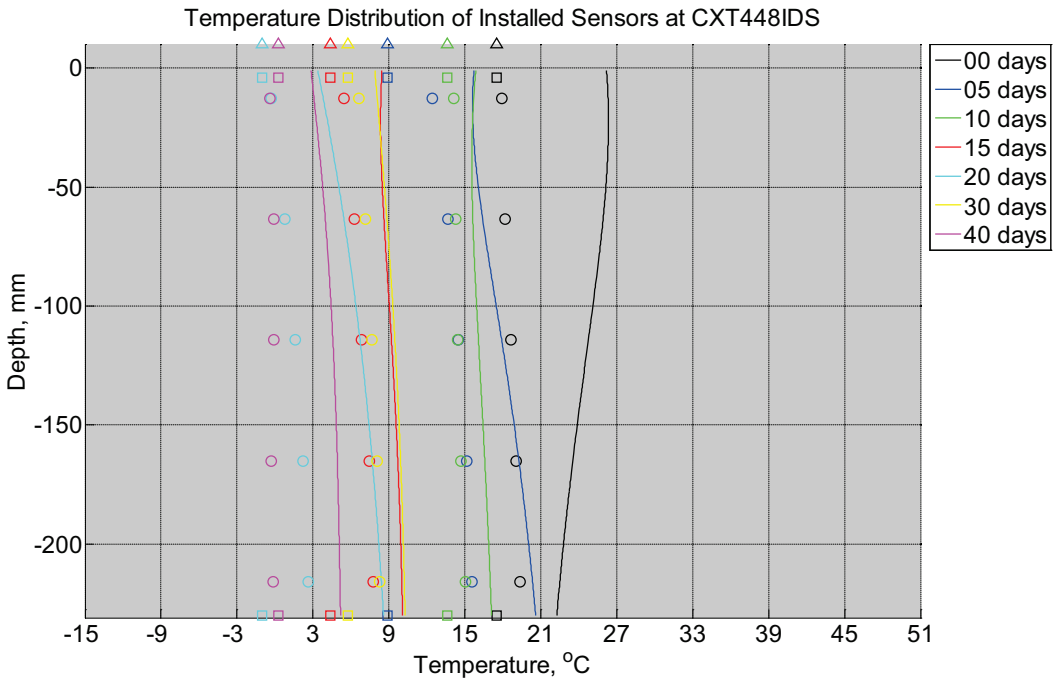

Figure B-508 Measured (markers) and modeled (continuous line) temperature profile distribution as a function of depth inside a concrete crosstie (labeled CXT448IDS) without a polyurethane pad nor rail located in Champaign, IL, between October 1, 2013, through November 12, 2013. Triangular markers denote temperature value from KTIP weather station, square markers denote measured temperature values from ambient sensors, and circular markers denote measured temperature values inside concrete.

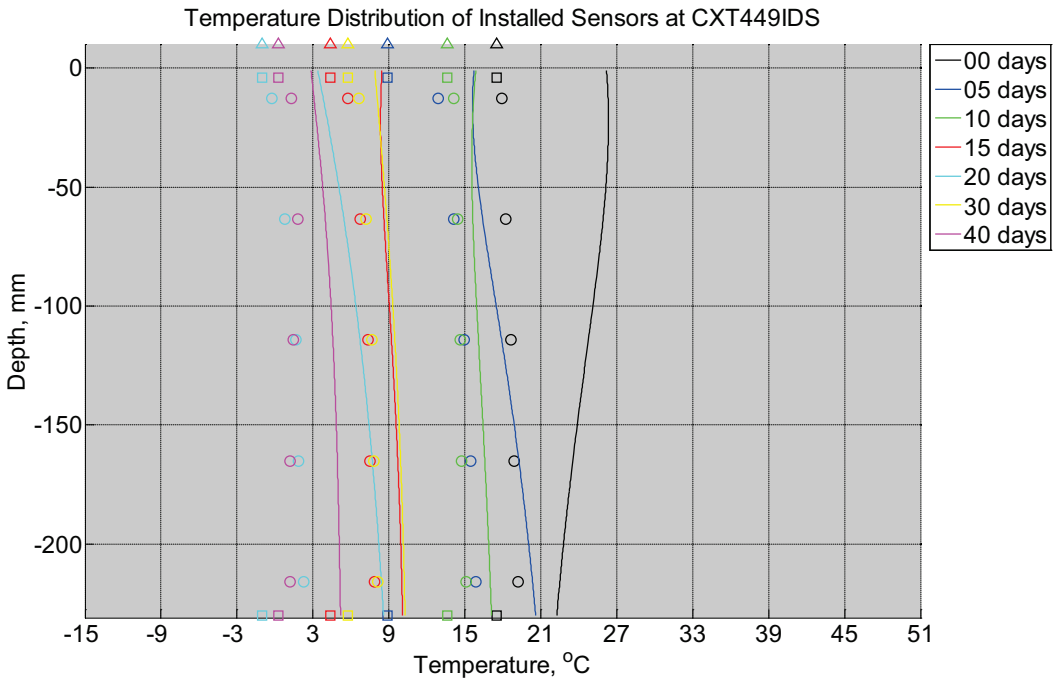

Figure B-509 Measured (markers) and modeled (continuous line) temperature profile distribution as a function of depth inside a concrete crosstie (labeled CXT449IDS) without a polyurethane pad nor rail located in Champaign, IL, between October 1, 2013, through November 12, 2013. Triangular markers denote temperature value from KTIP weather station, square markers denote measured temperature values from ambient sensors, and circular markers denote measured temperature values inside concrete.

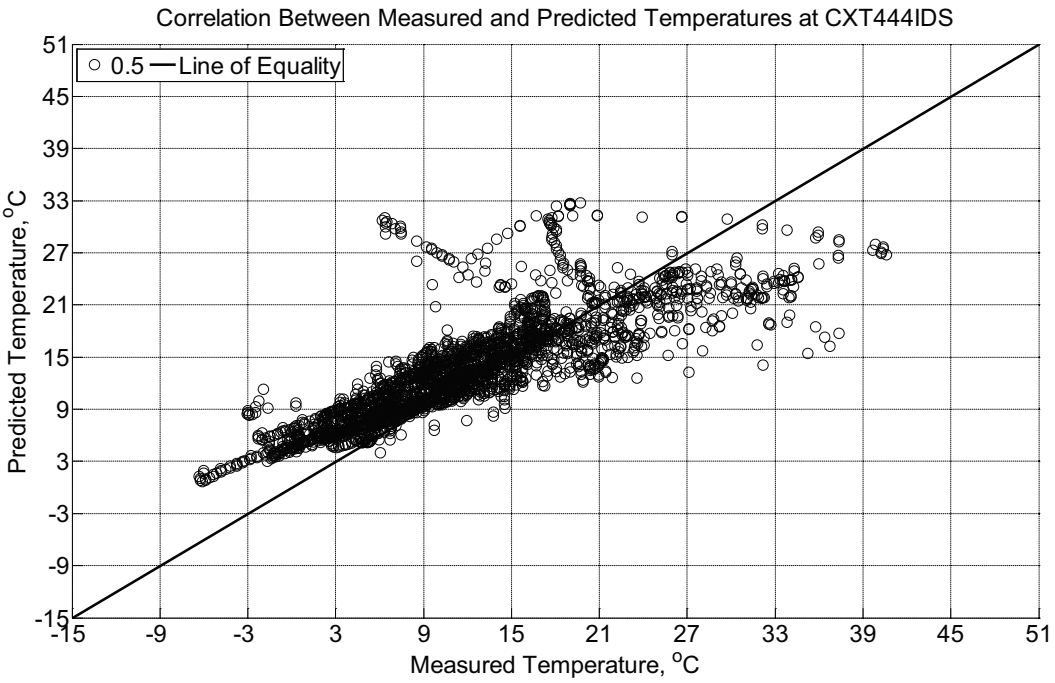

Figure B-510 Correlation between measured and predicted temperature values 0.5 inches (12.7 mm) from the surface of a concrete crosstie (labeled CXT444IDS) without a polyurethane pad nor rail located in Champaign, IL, between October 1, 2013, through November 12, 2013.

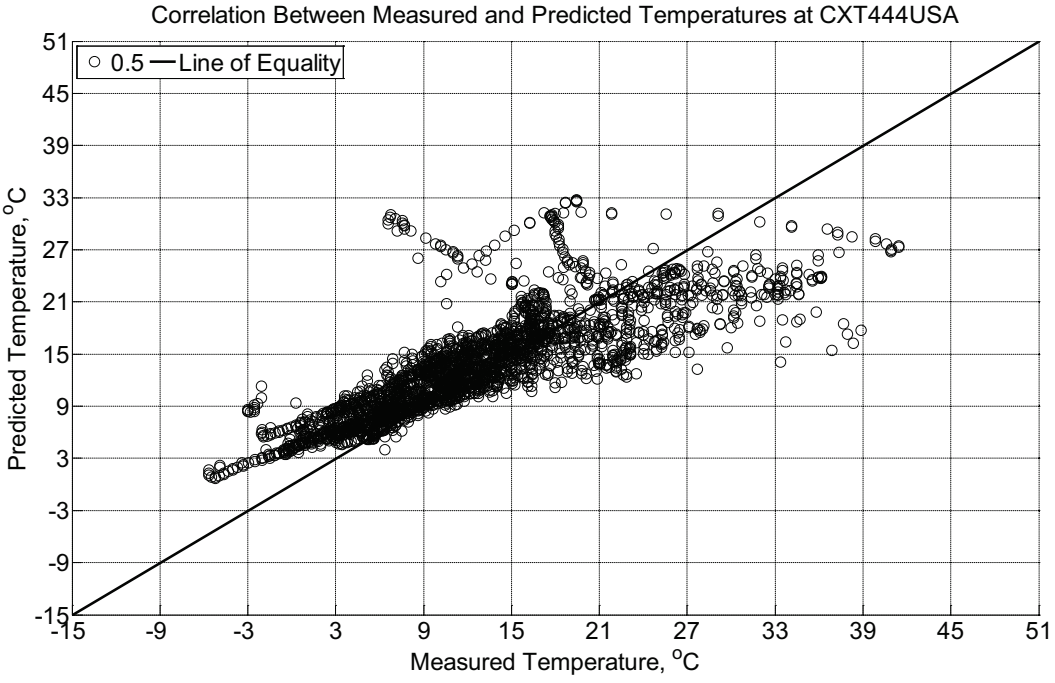

Figure B-511 Correlation between measured and predicted temperature values 0.5 inches (12.7 mm) from the surface of a concrete crosstie (labeled CXT444USA) without a

polyurethane pad nor rail located in Champaign, IL, between October 1, 2013, through November 12, 2013.

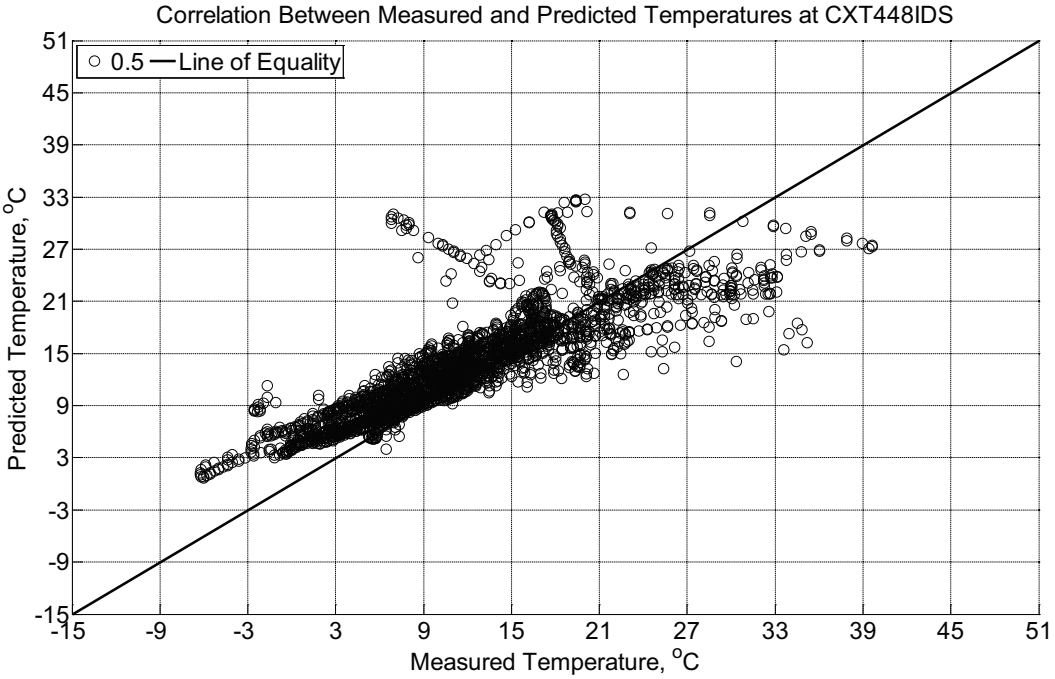

Figure B-512 Correlation between measured and predicted temperature values 0.5 inches (12.7 mm) from the surface of a concrete crosstie (labeled CXT448IDS) without a polyurethane pad nor rail located in Champaign, IL, between October 1, 2013, through November 12, 2013.

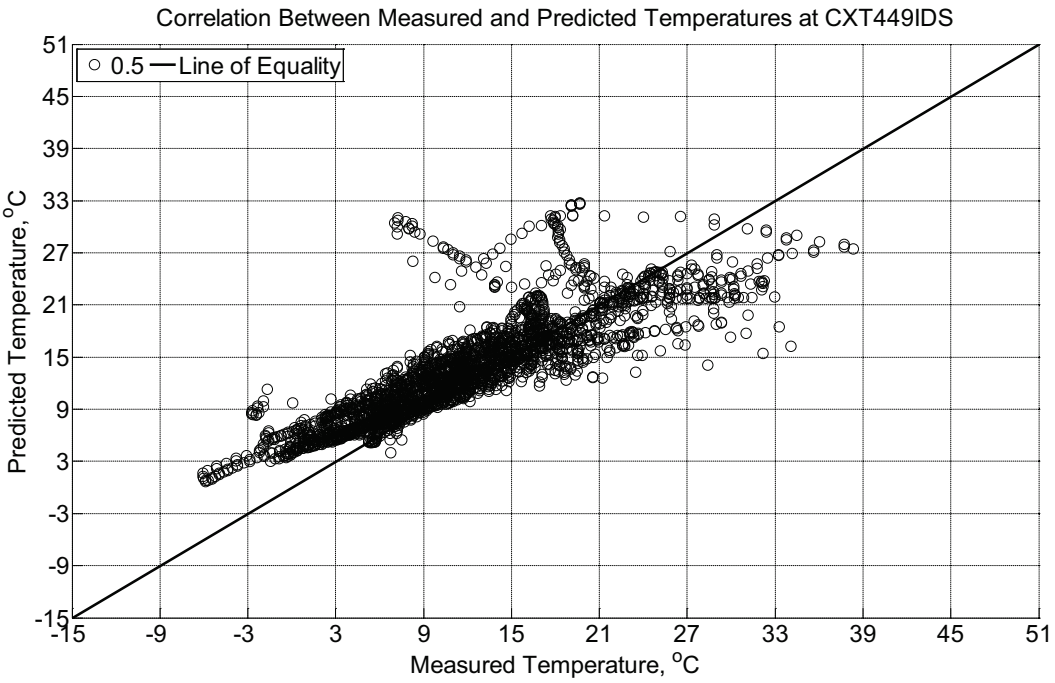

Figure B-513 Correlation between measured and predicted temperature values 0.5 inches (12.7 mm) from the surface of a concrete crosstie (labeled CXT449IDS) without a polyurethane pad nor rail located in Champaign, IL, between October 1, 2013, through November 12, 2013.

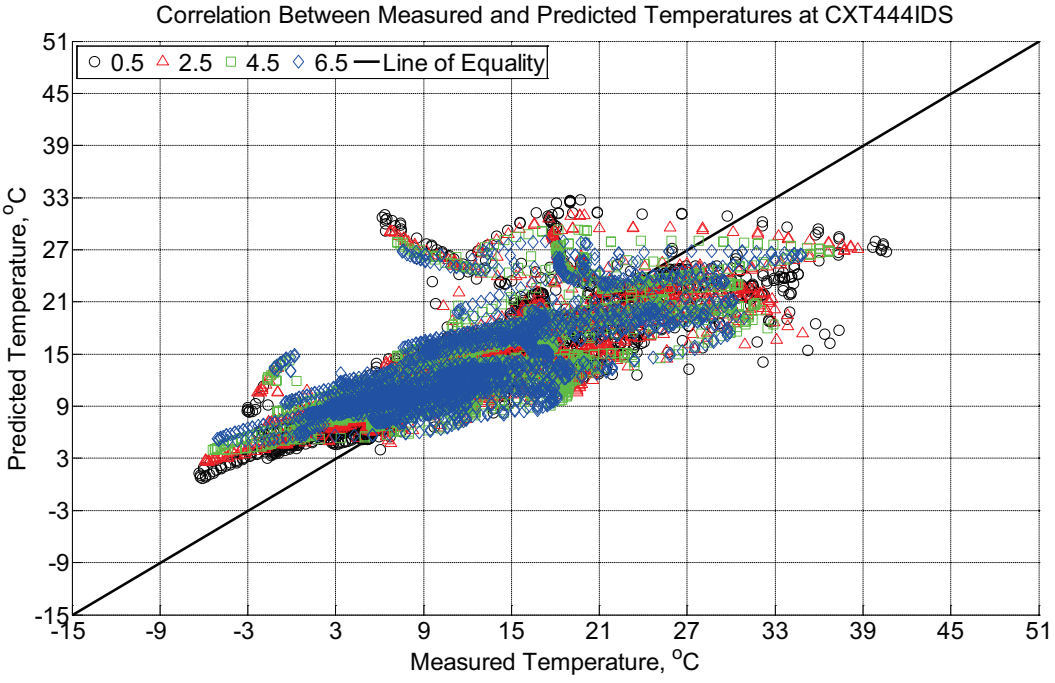

Figure B-514 Correlation between measured and predicted temperature values 0.5 inches (12.7 mm), 2.5 inches (63.5 mm), 4.5 inches (114.3 mm), and 6.5 inches (139.7 mm) from the

surface of a concrete crosstie (labeled CXT444IDS) without a polyurethane pad nor rail located in Champaign, IL, between October 1, 2013, through November 12, 2013.

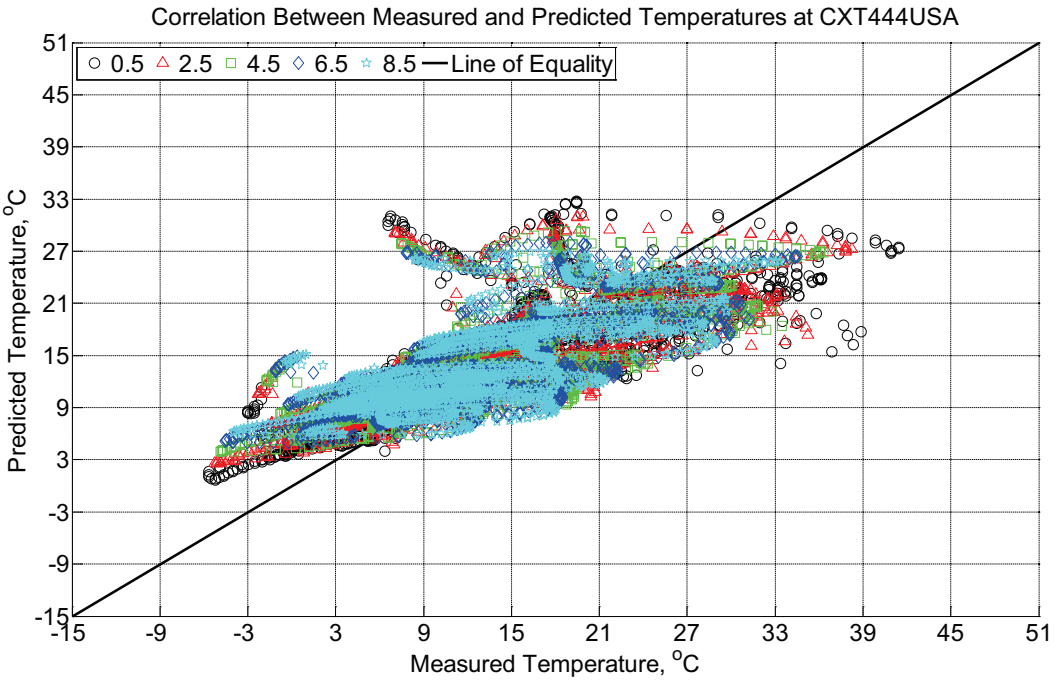

Figure B-515 Correlation between measured and predicted temperature values 0.5 inches (12.7 mm), 2.5 inches (63.5 mm), 4.5 inches (114.3 mm), 6.5 inches (139.7 mm), and 8.5 inches (215.9 mm) from the surface of a concrete crosstie (labeled CXT444USA) without a polyurethane pad nor rail located in Champaign, IL, between October 1, 2013, through November 12, 2013.

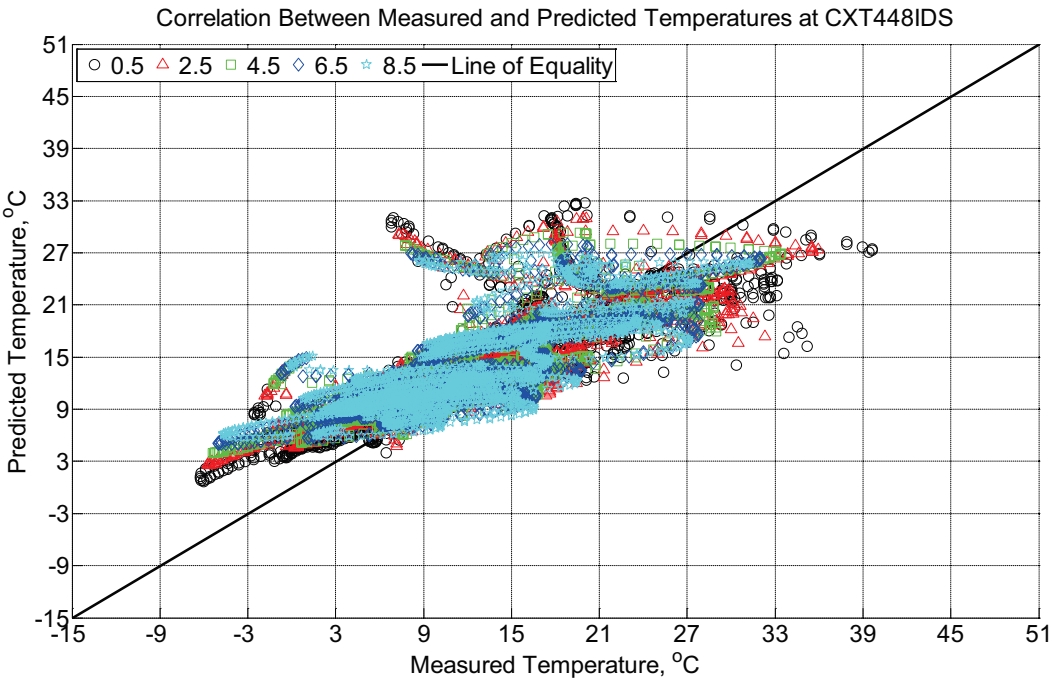

Figure B-516 Correlation between measured and predicted temperature values 0.5 inches (12.7 mm), 2.5 inches (63.5 mm), 4.5 inches (114.3 mm), 6.5 inches (139.7 mm), and 8.5 inches (215.9 mm) from the surface of a concrete crosstie (labeled CXT448IDS) without a polyurethane pad nor rail located in Champaign, IL, between October 1, 2013, through November 12, 2013.

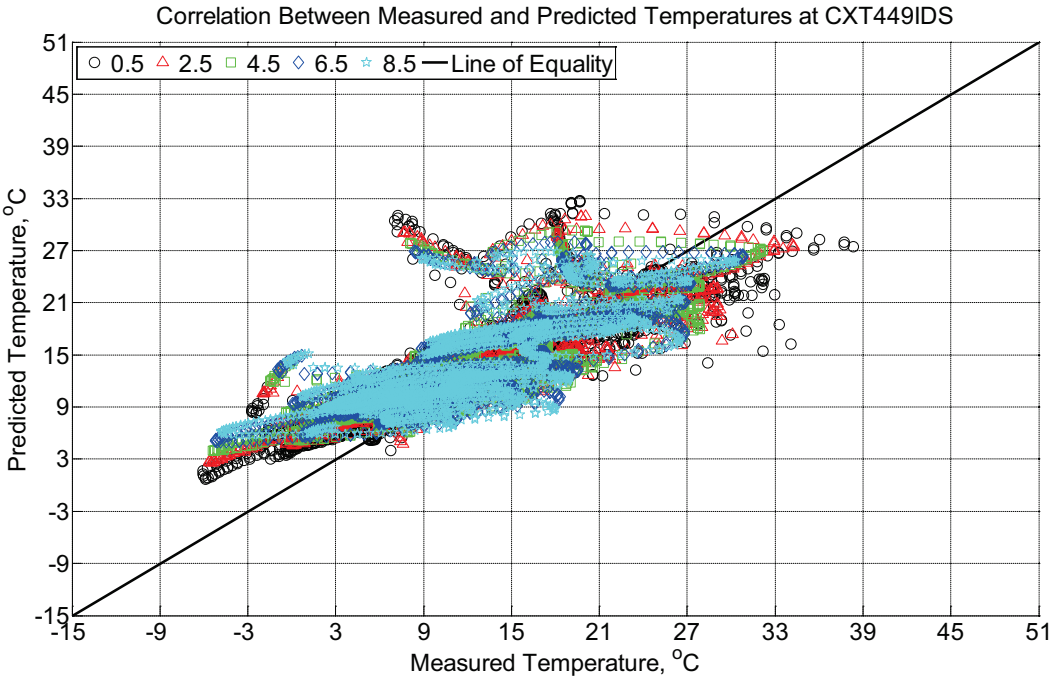

Figure B-517 Correlation between measured and predicted temperature values 0.5 inches

(12.7 mm), 2.5 inches (63.5 mm), 4.5 inches (114.3 mm), 6.5 inches (139.7 mm), and 8.5 inches (215.9 mm) from the surface of a concrete crosstie (labeled CXT449IDS) without a polyurethane pad nor rail located in Champaign, IL, between October 1, 2013, through November 12, 2013.

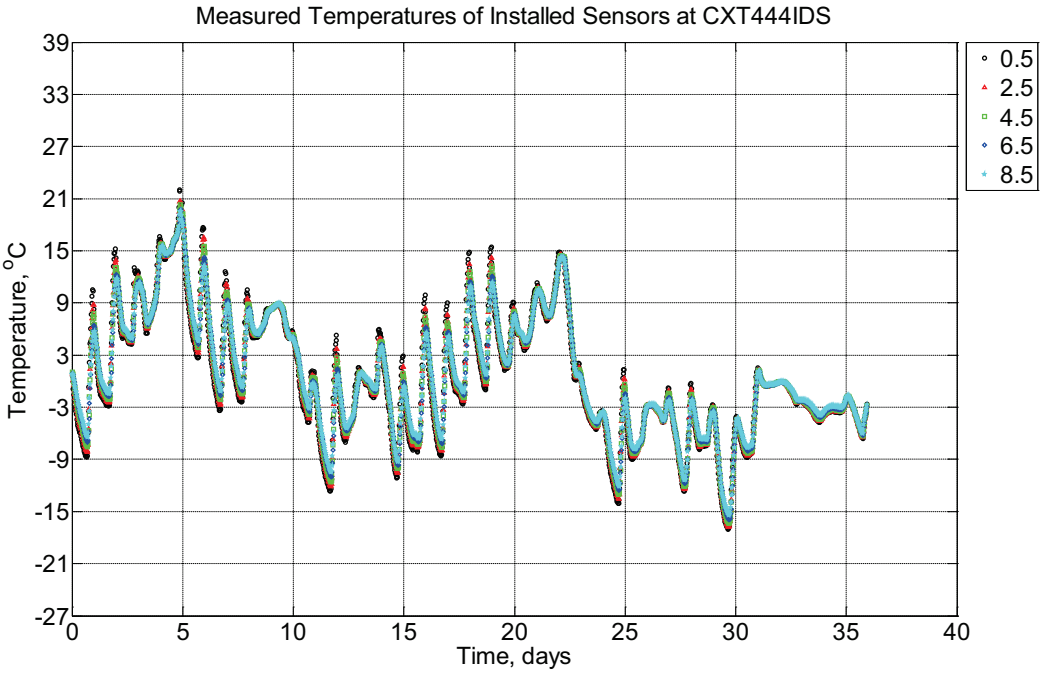

Figure B-518 Measured temperature at depths of 0.5 inches (12.7 mm), 2.5 inches (63.5 mm), 4.5 inches (114.3 mm), 6.5 inches (139.7 mm), and 8.5 inches (215.9 mm) from the surface of a concrete crosstie (labeled CXT444IDS) without a polyurethane pad nor rail located in Champaign, IL, between November 12, 2013, through December 18, 2013.

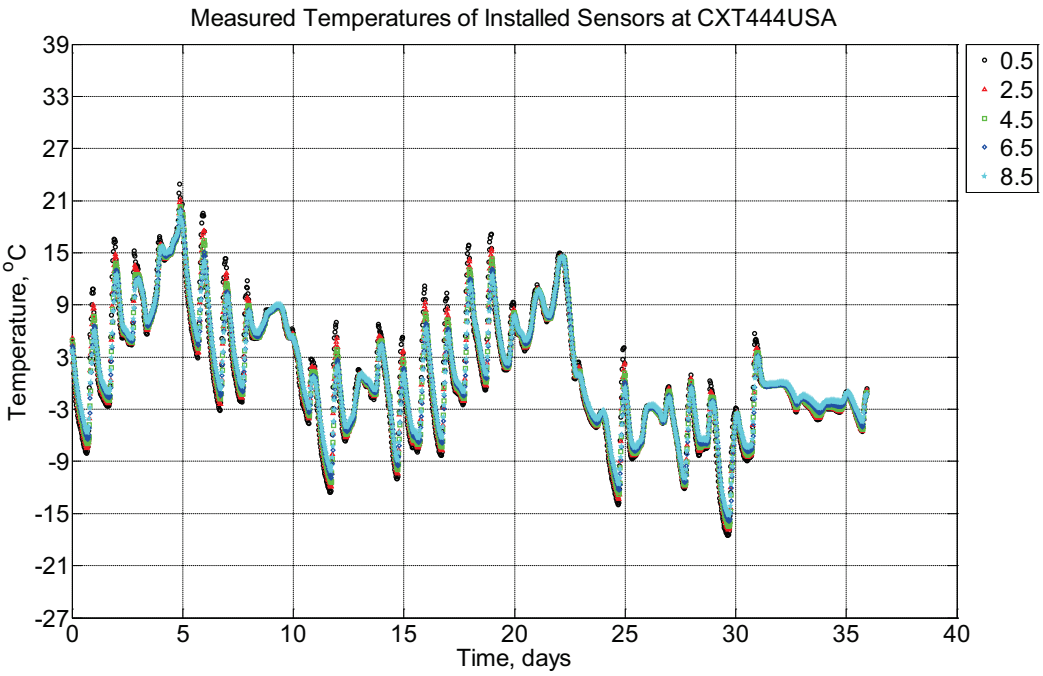

Figure B-519 Measured temperature at depths of 0.5 inches (12.7 mm), 2.5 inches (63.5 mm), 4.5 inches (114.3 mm), 6.5 inches (139.7 mm), and 8.5 inches (215.9 mm) from the surface of a concrete crosstie (labeled CXT444USA) without a polyurethane pad nor rail located in Champaign, IL, between November 12, 2013, through December 18, 2013.

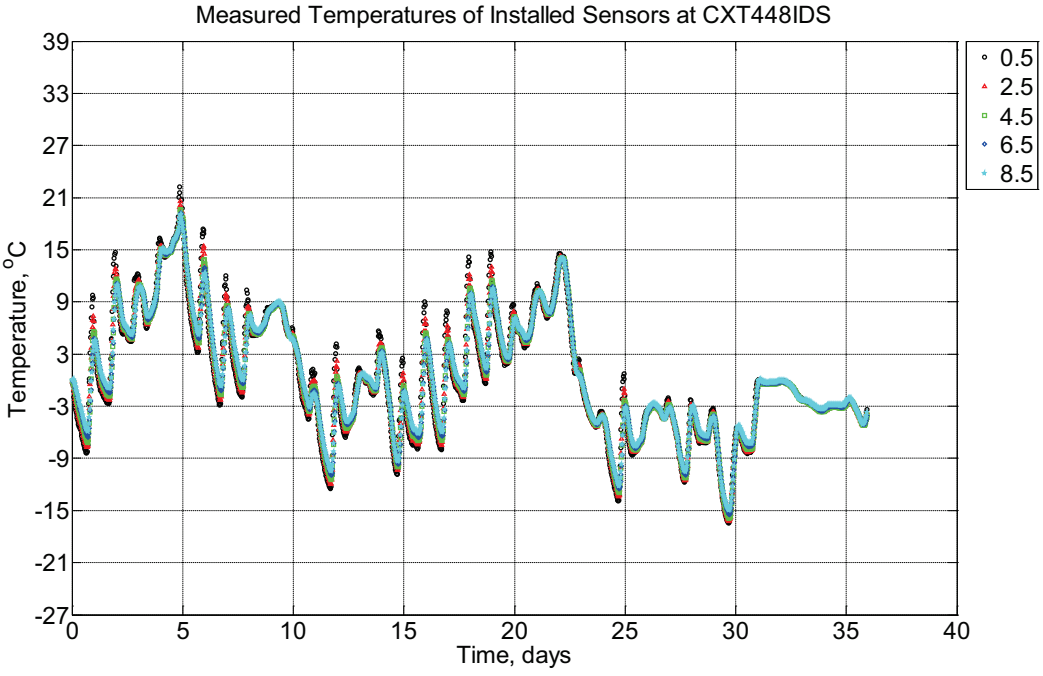

Figure B-520 Measured temperature at depths of 0.5 inches (12.7 mm), 2.5 inches (63.5 mm), 4.5 inches (114.3 mm), 6.5 inches (139.7 mm), and 8.5 inches (215.9 mm) from the

surface of a concrete crosstie (labeled CXT448IDS) without a polyurethane pad nor rail located in Champaign, IL, between November 12, 2013, through December 18, 2013.

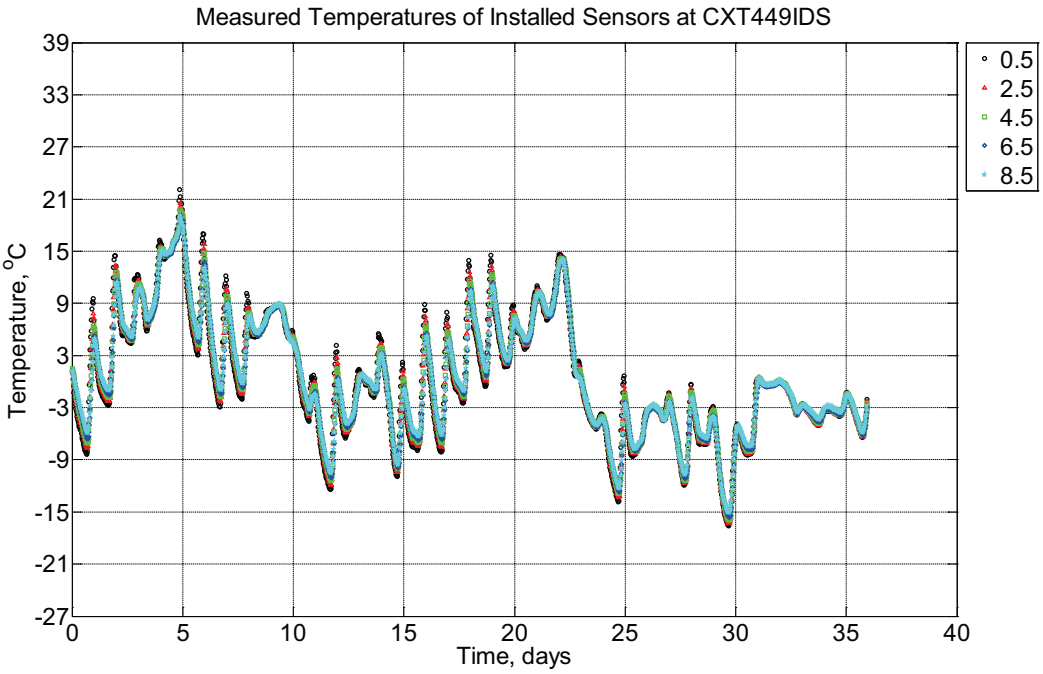

Figure B-521 Measured temperature at depths of 0.5 inches (12.7 mm), 2.5 inches (63.5 mm), 4.5 inches (114.3 mm), 6.5 inches (139.7 mm), and 8.5 inches (215.9 mm) from the surface of a concrete crosstie (labeled CXT449IDS) without a polyurethane pad nor rail located in Champaign, IL, between November 12, 2013, through December 18, 2013.

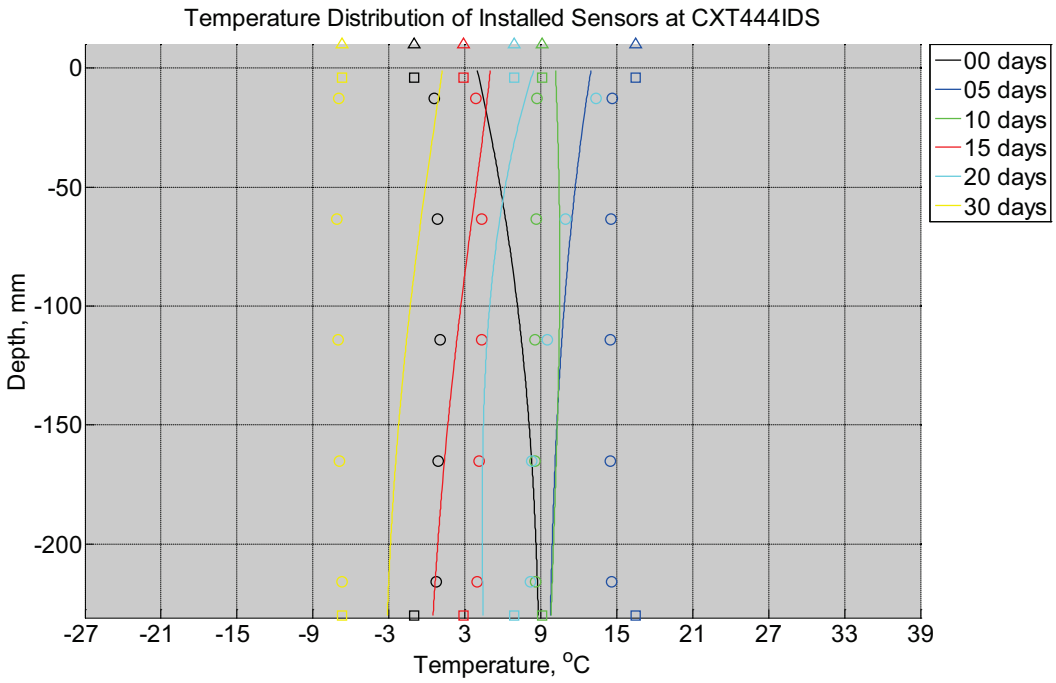

Figure B-522 Measured (markers) and modeled (continuous line) temperature profile distribution as a function of depth inside a concrete crosstie (labeled CXT444IDS) without a polyurethane pad nor rail located in Champaign, IL, between November 12, 2013, through December 18, 2013. Triangular markers denote temperature value from KTIP weather station, square markers denote measured temperature values from ambient sensors, and circular markers denote measured temperature values inside concrete.

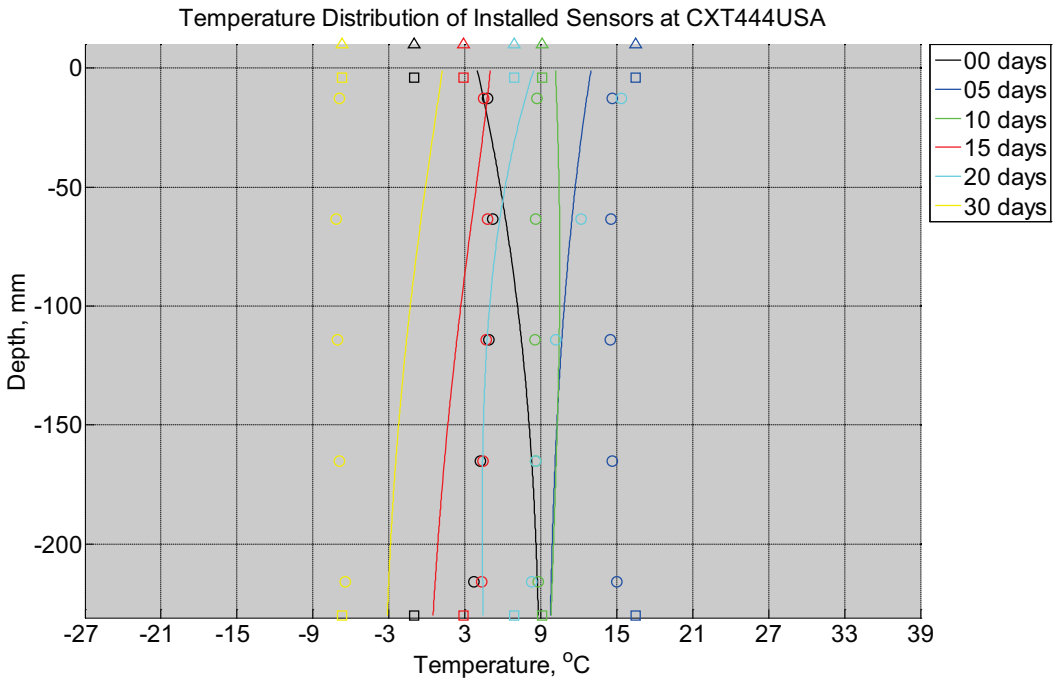

Figure B-523 Measured (markers) and modeled (continuous line) temperature profile distribution as a function of depth inside a concrete crosstie (labeled CXT444USA) without a polyurethane pad nor rail located in Champaign, IL, between November 12, 2013, through December 18, 2013. Triangular markers denote temperature value from KTIP weather station, square markers denote measured temperature values from ambient sensors, and circular markers denote measured temperature values inside concrete.

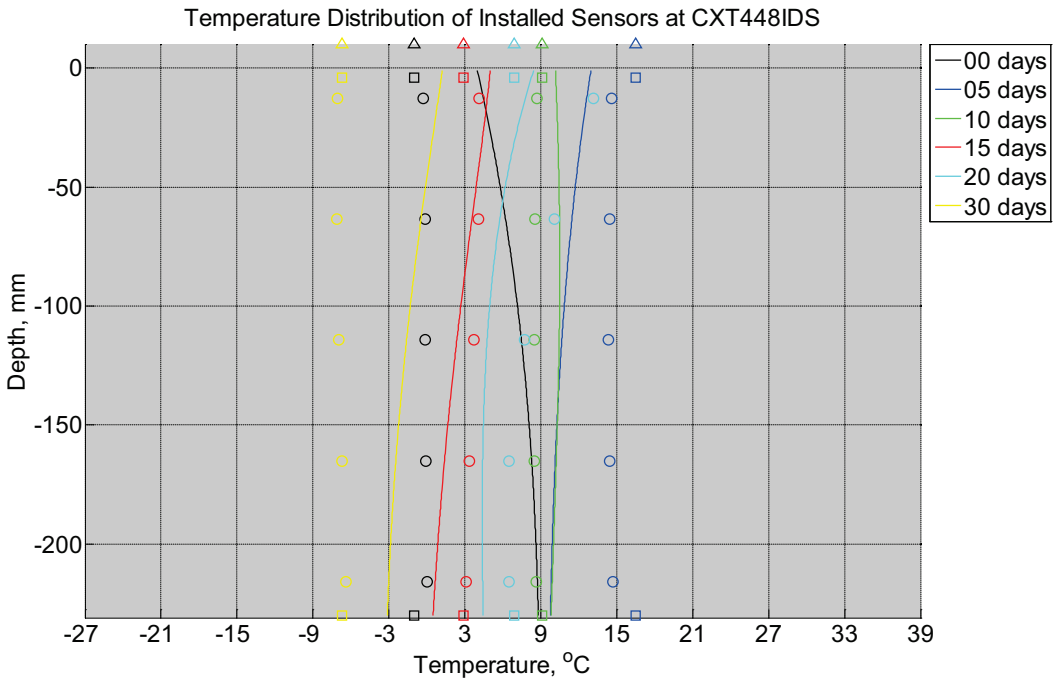

Figure B-524 Measured (markers) and modeled (continuous line) temperature profile distribution as a function of depth inside a concrete crosstie (labeled CXT448IDS) without a polyurethane pad nor rail located in Champaign, IL, between November 12, 2013, through December 18, 2013. Triangular markers denote temperature value from KTIP weather station, square markers denote measured temperature values from ambient sensors, and circular markers denote measured temperature values inside concrete.

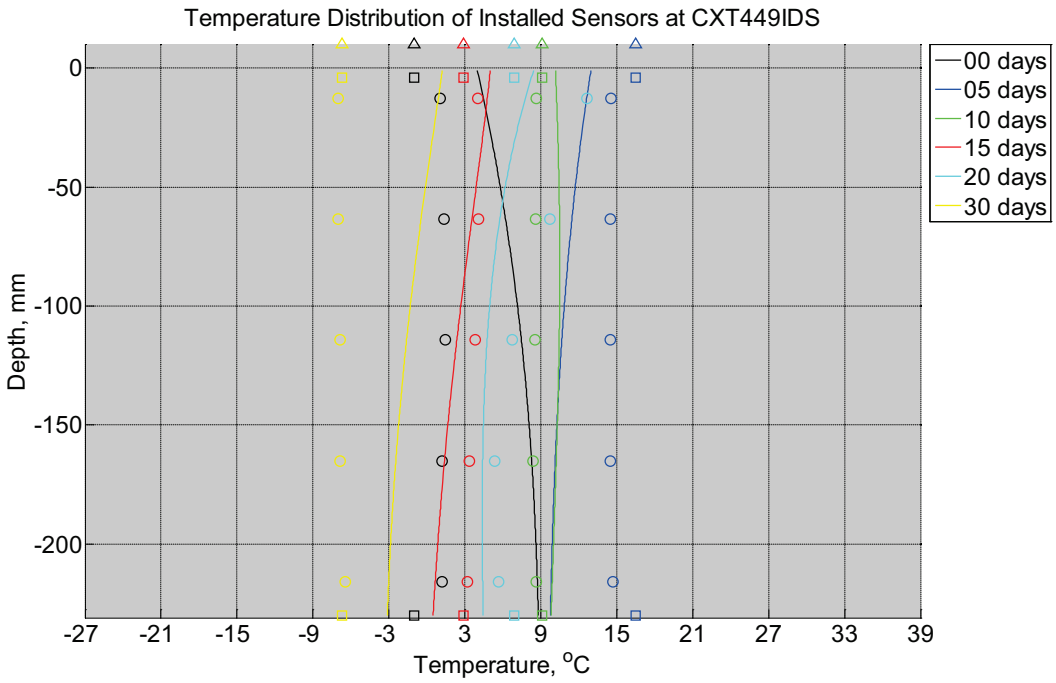

Figure B-525 Measured (markers) and modeled (continuous line) temperature profile distribution as a function of depth inside a concrete crosstie (labeled CXT449IDS) without a polyurethane pad nor rail located in Champaign, IL, between November 12, 2013, through December 18, 2013. Triangular markers denote temperature value from KTIP weather station, square markers denote measured temperature values from ambient sensors, and circular markers denote measured temperature values inside concrete.

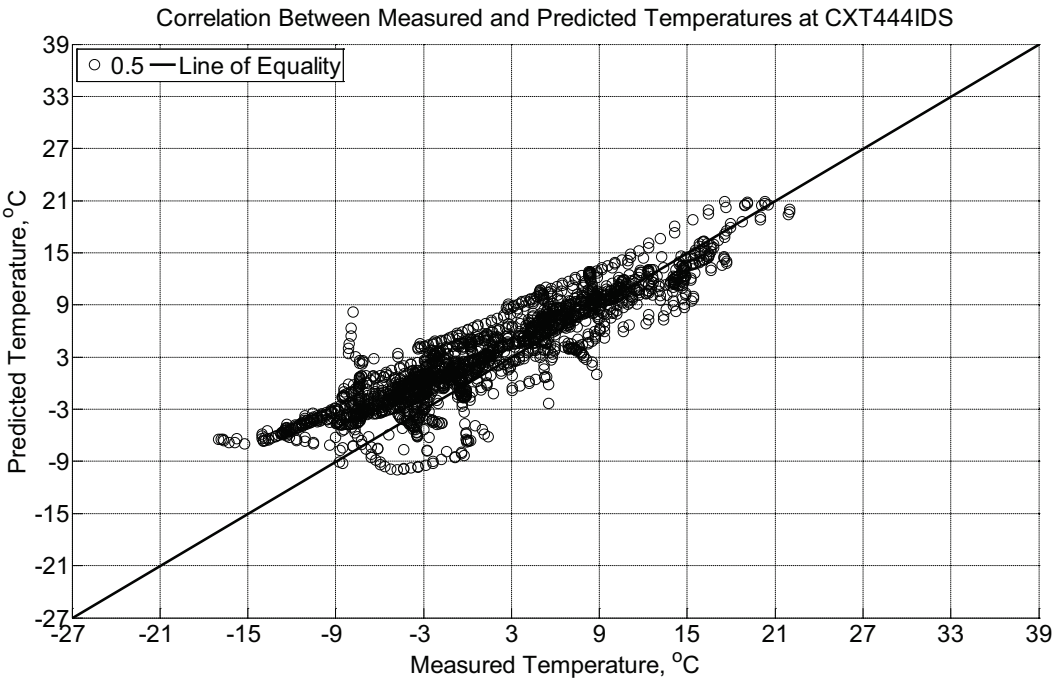

Figure B-526 Correlation between measured and predicted temperature values 0.5 inches (12.7 mm) from the surface of a concrete crosstie (labeled CXT444IDS) without a polyurethane pad nor rail located in Champaign, IL, between November 12, 2013, through December 18, 2013.

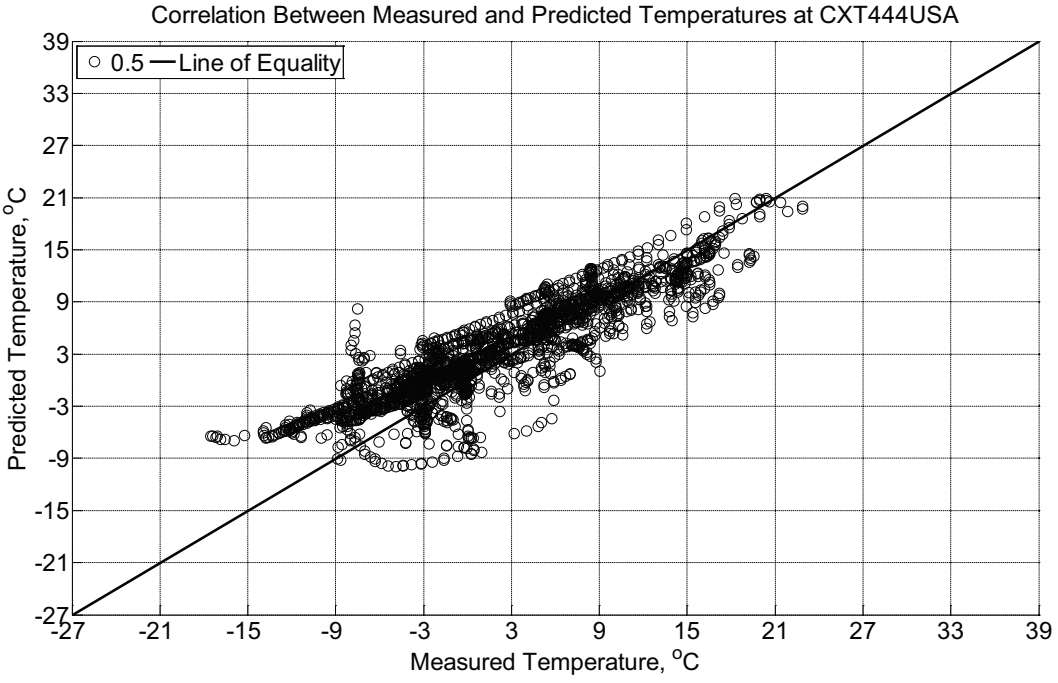

Figure B-527 Correlation between measured and predicted temperature values 0.5 inches (12.7 mm) from the surface of a concrete crosstie (labeled CXT444USA) without a

polyurethane pad nor rail located in Champaign, IL, between November 12, 2013, through December 18, 2013.

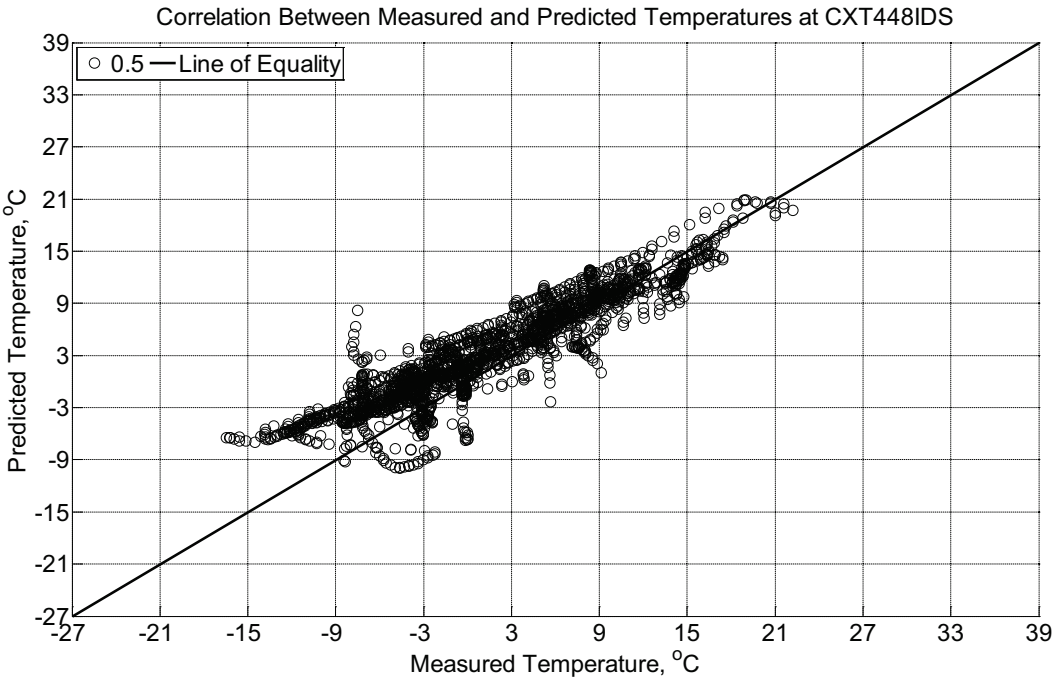

Figure B-528 Correlation between measured and predicted temperature values 0.5 inches (12.7 mm) from the surface of a concrete crosstie (labeled CXT448IDS) without a polyurethane pad nor rail located in Champaign, IL, between November 12, 2013, through December 18, 2013.

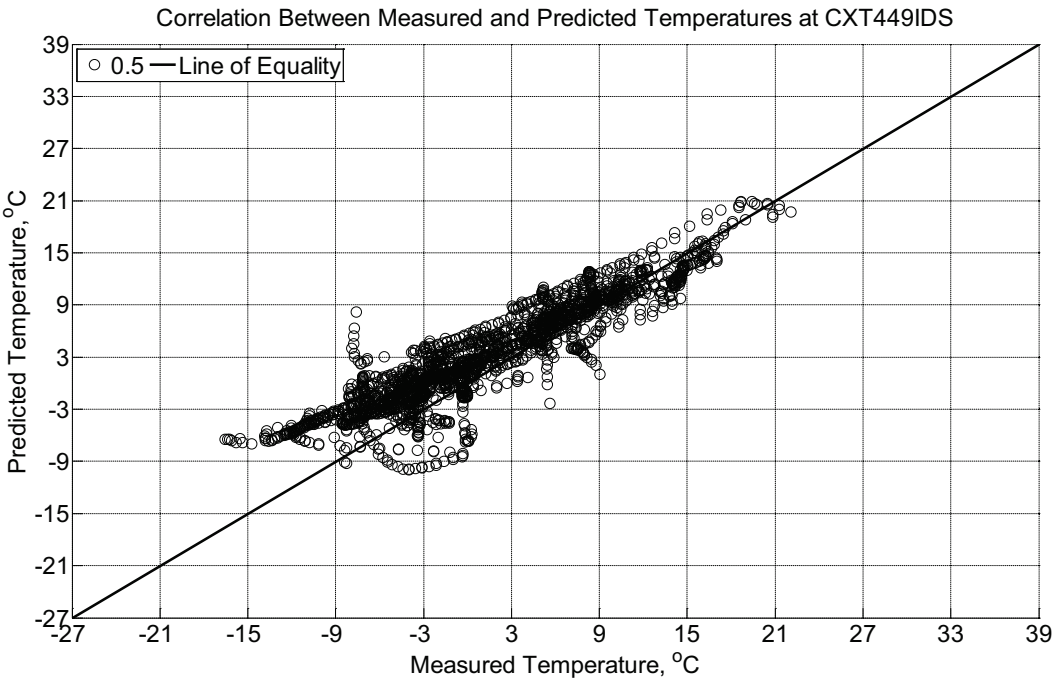

Figure B-529 Correlation between measured and predicted temperature values 0.5 inches (12.7 mm) from the surface of a concrete crosstie (labeled CXT449IDS) without a polyurethane pad nor rail located in Champaign, IL, between November 12, 2013, through December 18, 2013.

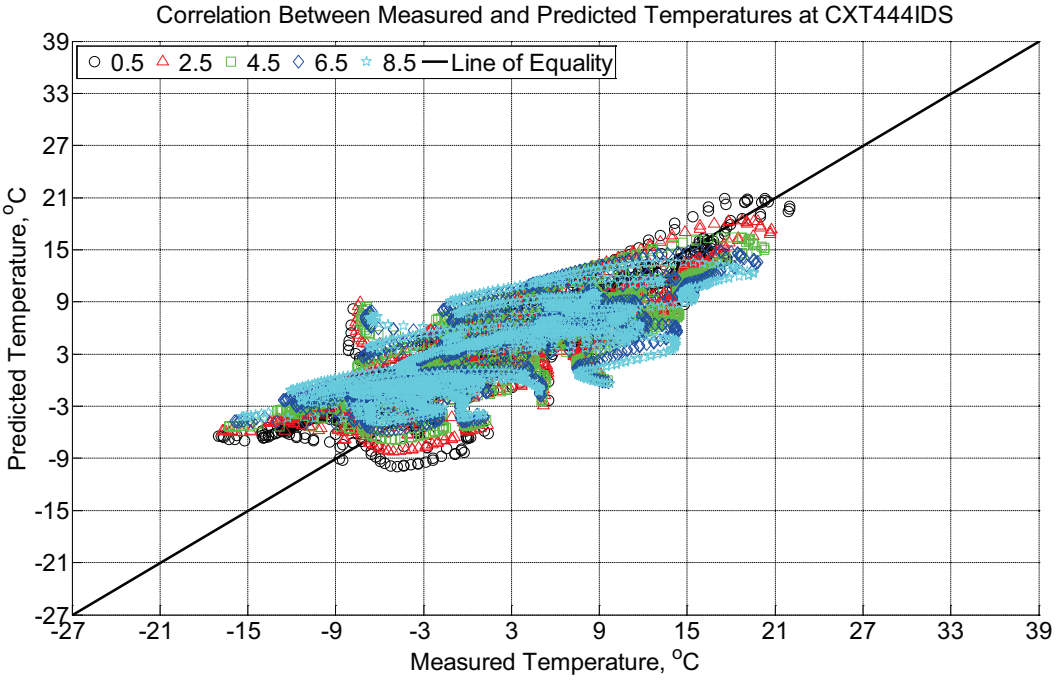

Figure B-530 Correlation between measured and predicted temperature values 0.5 inches (12.7 mm), 2.5 inches (63.5 mm), 4.5 inches (114.3 mm), 6.5 inches (139.7 mm), and 8.5

inches (215.9 mm) from the surface of a concrete crosstie (labeled CXT444IDS) without a polyurethane pad nor rail located in Champaign, IL, between November 12, 2013, through December 18, 2013.

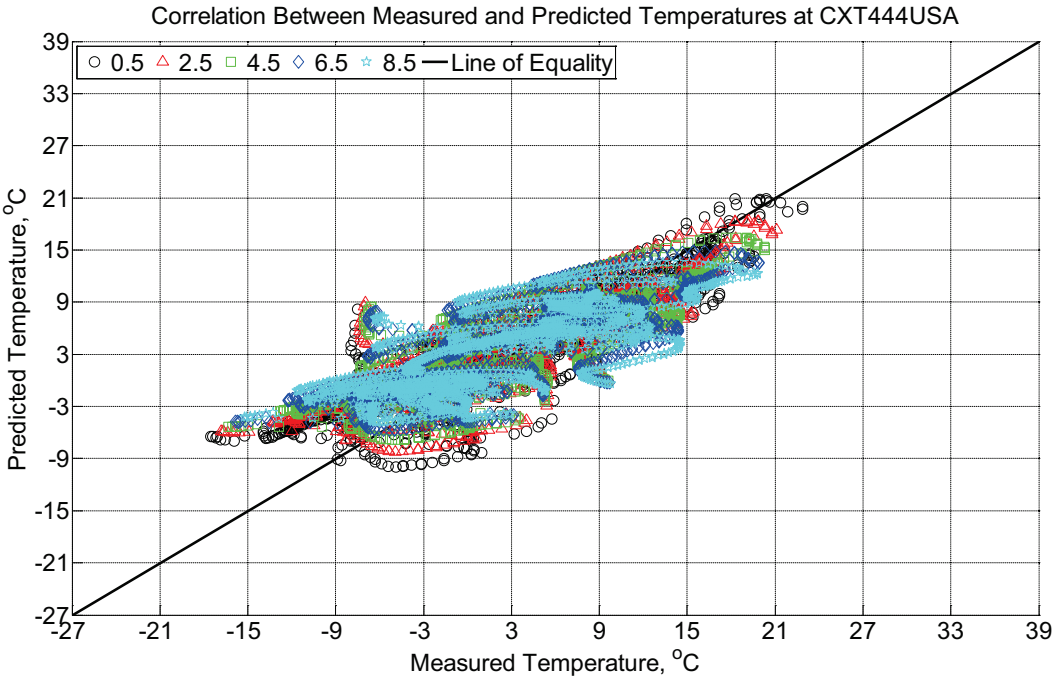

Figure B-531 Correlation between measured and predicted temperature values 0.5 inches (12.7 mm), 2.5 inches (63.5 mm), 4.5 inches (114.3 mm), 6.5 inches (139.7 mm), and 8.5 inches (215.9 mm) from the surface of a concrete crosstie (labeled CXT444USA) without a polyurethane pad nor rail located in Champaign, IL, between November 12, 2013, through December 18, 2013.

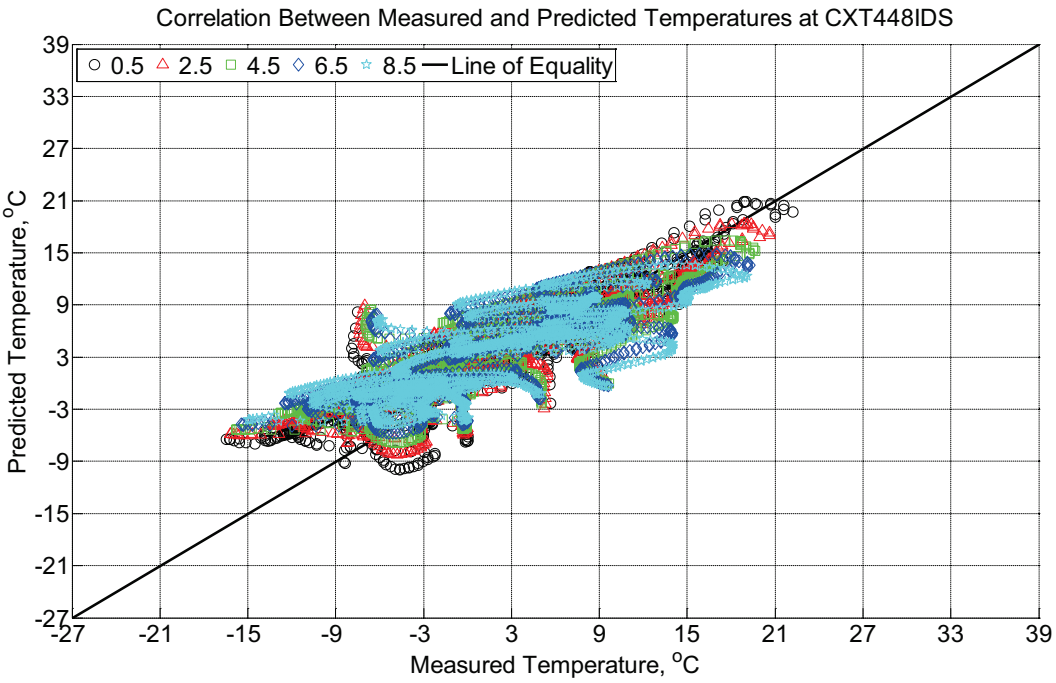

Figure B-532 Correlation between measured and predicted temperature values 0.5 inches (12.7 mm), 2.5 inches (63.5 mm), 4.5 inches (114.3 mm), 6.5 inches (139.7 mm), and 8.5 inches (215.9 mm) from the surface of a concrete crosstie (labeled CXT448IDS) without a polyurethane pad nor rail located in Champaign, IL, between November 12, 2013, through December 18, 2013.

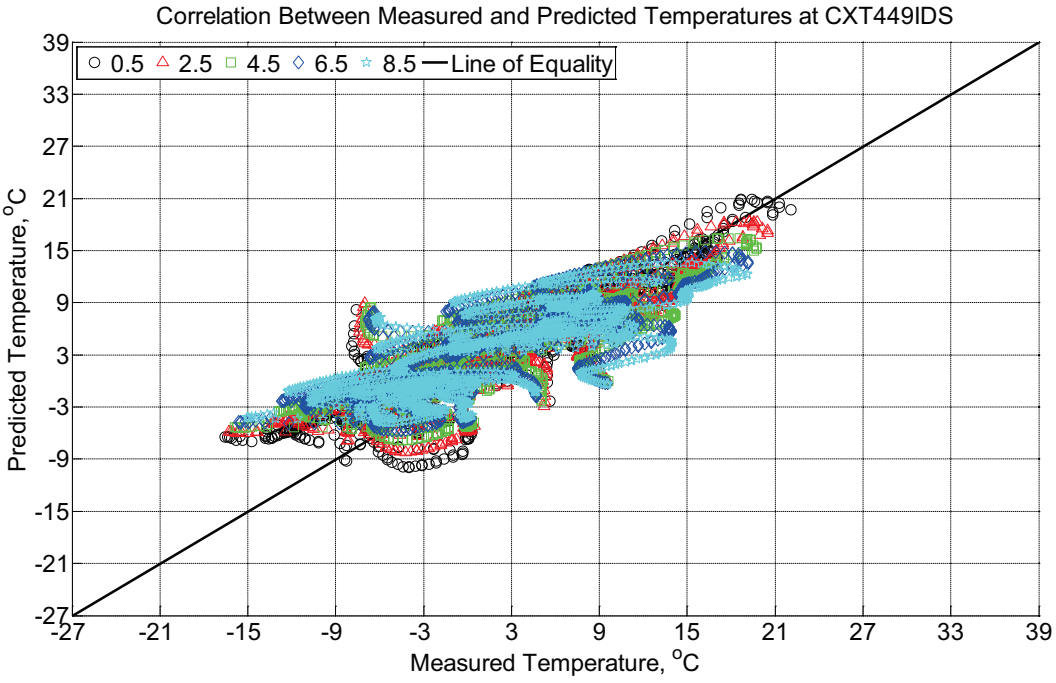

Figure B-533 Correlation between measured and predicted temperature values 0.5 inches

(12.7 mm), 2.5 inches (63.5 mm), 4.5 inches (114.3 mm), 6.5 inches (139.7 mm), and 8.5 inches (215.9 mm) from the surface of a concrete crosstie (labeled CXT449IDS) without a polyurethane pad nor rail located in Champaign, IL, between November 12, 2013, through December 18, 2013.

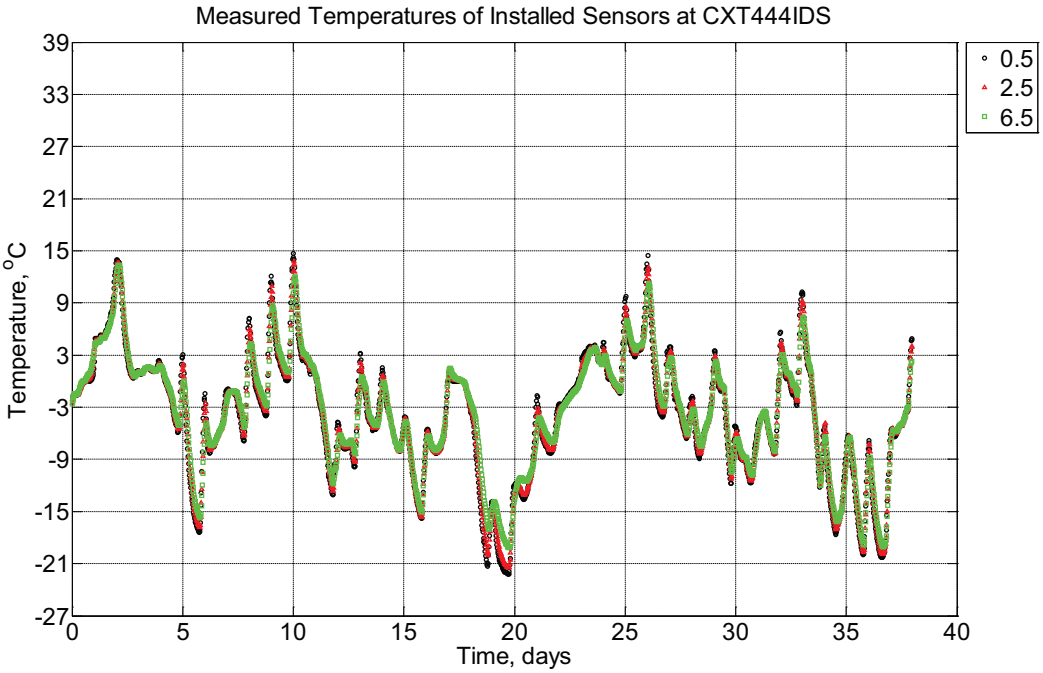

Figure B-534 Measured temperature at depths of 0.5 inches (12.7 mm), 2.5 inches (63.5 mm), and 6.5 inches (139.7 mm) from the surface of a concrete crosstie (labeled CXT444IDS) without a polyurethane pad nor rail located in Champaign, IL, between December 18, 2013, through January 25, 2014.

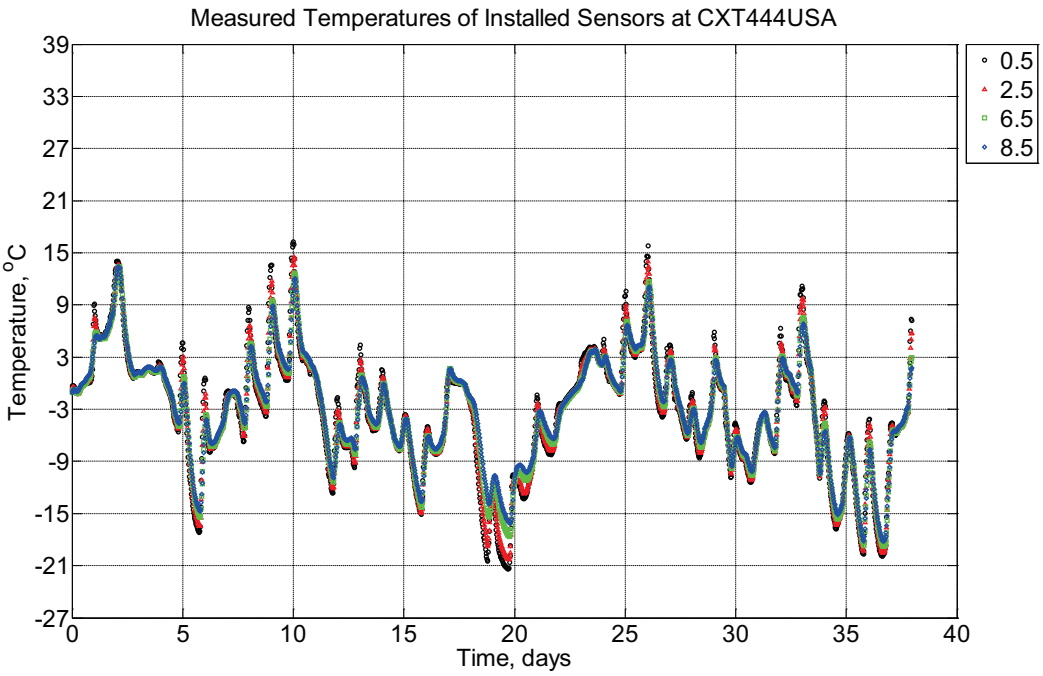

Figure B-535 Measured temperature at depths of 0.5 inches (12.7 mm), 2.5 inches (63.5 mm), 6.5 inches (139.7 mm), and 8.5 inches (215.9 mm) from the surface of a concrete crosstie (labeled CXT444USA) without a polyurethane pad nor rail located in Champaign, IL, between December 18, 2013, through January 25, 2014.

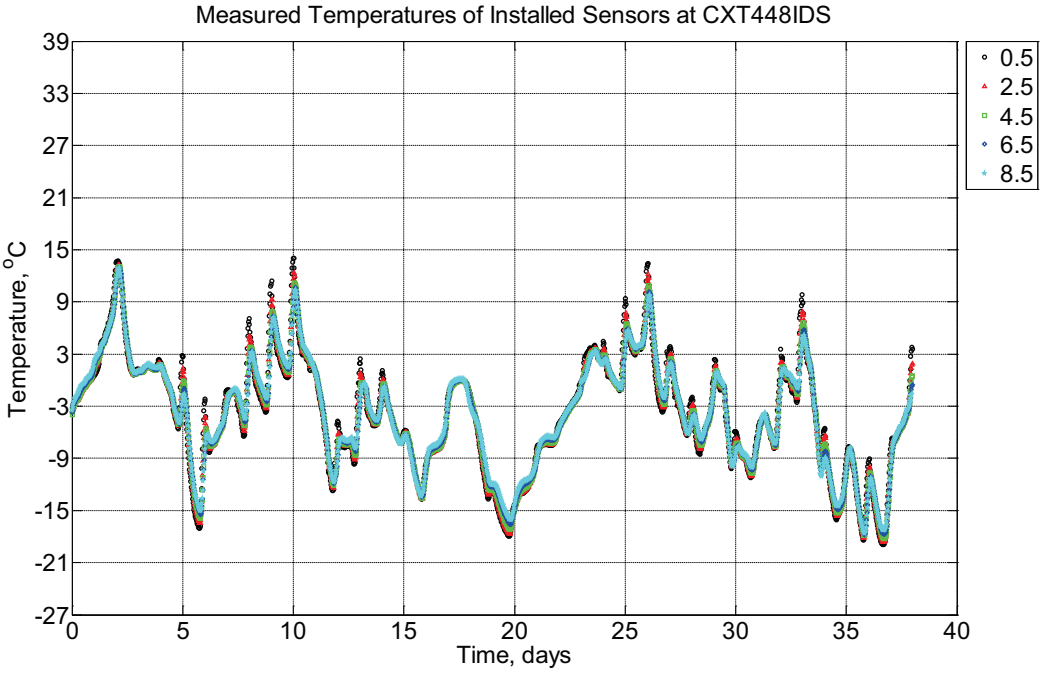

Figure B-536 Measured temperature at depths of 0.5 inches (12.7 mm), 2.5 inches (63.5 mm), 4.5 inches (114.3 mm), 6.5 inches (139.7 mm), and 8.5 inches (215.9 mm) from the

surface of a concrete crosstie (labeled CXT448IDS) without a polyurethane pad nor rail located in Champaign, IL, between December 18, 2013, through January 25, 2014.

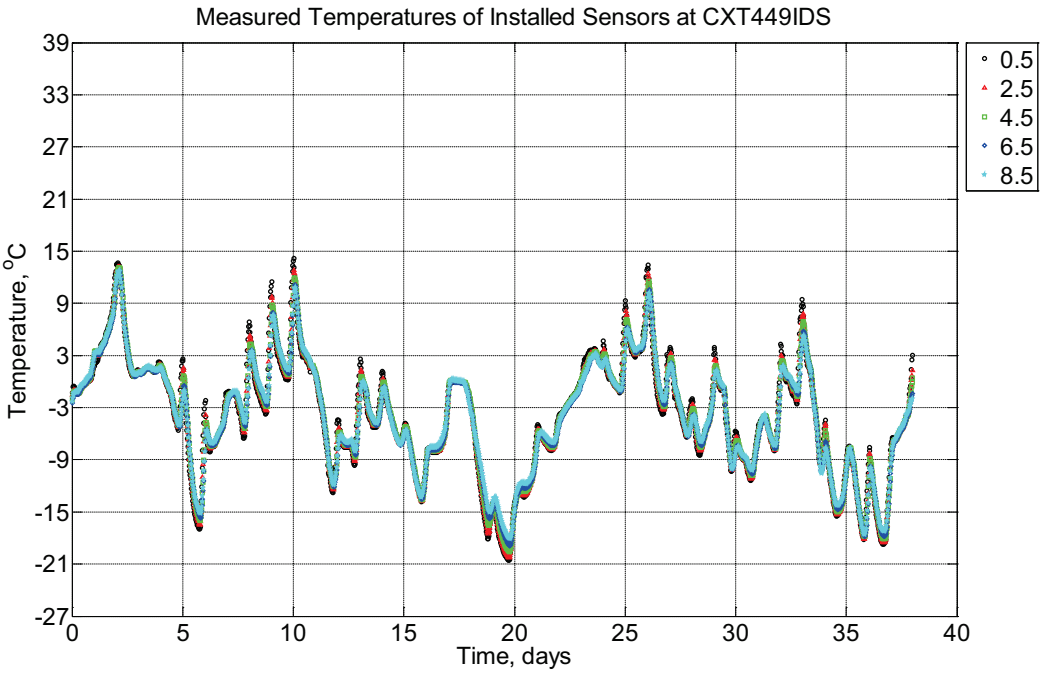

Figure B-537 Measured temperature at depths of 0.5 inches (12.7 mm), 2.5 inches (63.5 mm), 4.5 inches (114.3 mm), 6.5 inches (139.7 mm), and 8.5 inches (215.9 mm) from the surface of a concrete crosstie (labeled CXT449IDS) without a polyurethane pad nor rail located in Champaign, IL, between December 18, 2013, through January 25, 2014.

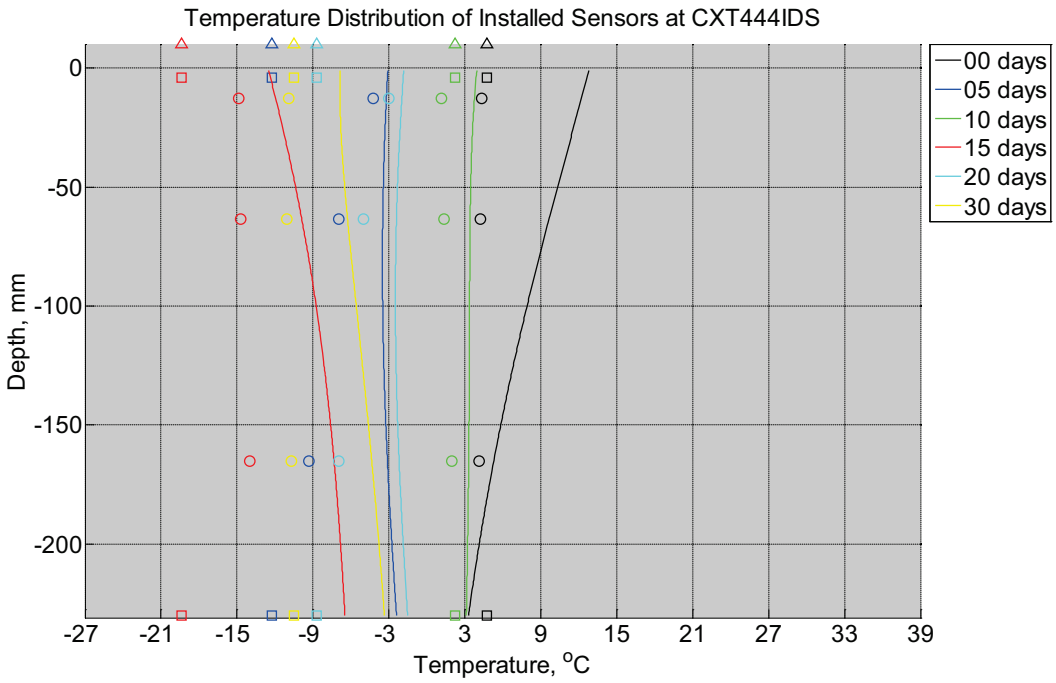

Figure B-538 Measured (markers) and modeled (continuous line) temperature profile distribution as a function of depth inside a concrete crosstie (labeled CXT444IDS) without a polyurethane pad nor rail located in Champaign, IL, between December 18, 2013, through January 25, 2014. Triangular markers denote temperature value from KTIP weather station, square markers denote measured temperature values from ambient sensors, and circular markers denote measured temperature values inside concrete.

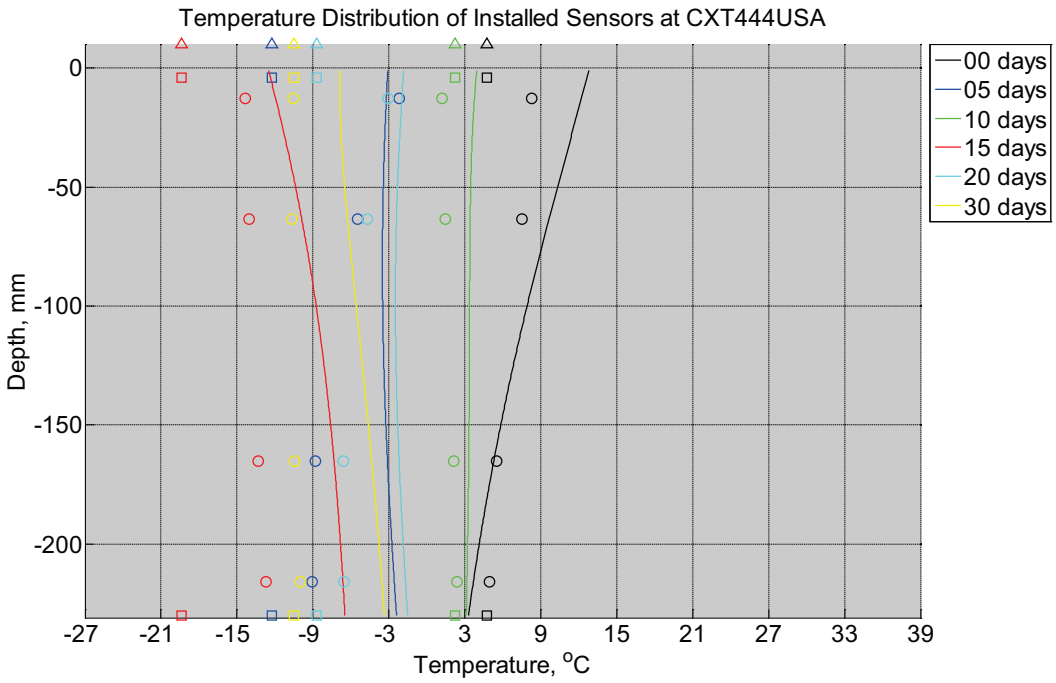

Figure B-539 Measured (markers) and modeled (continuous line) temperature profile distribution as a function of depth inside a concrete crosstie (labeled CXT444USA) without a polyurethane pad nor rail located in Champaign, IL, between December 18, 2013, through January 25, 2014. Triangular markers denote temperature value from KTIP weather station, square markers denote measured temperature values from ambient sensors, and circular markers denote measured temperature values inside concrete.

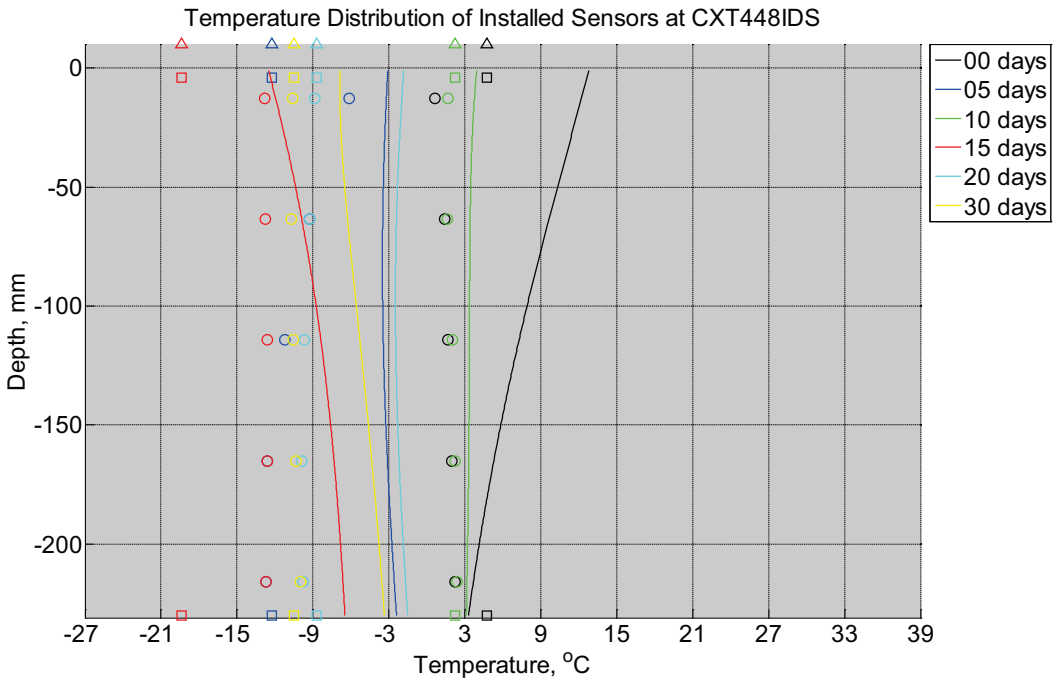

Figure B-540 Measured (markers) and modeled (continuous line) temperature profile distribution as a function of depth inside a concrete crosstie (labeled CXT448IDS) without a polyurethane pad nor rail located in Champaign, IL, between December 18, 2013, through January 25, 2014. Triangular markers denote temperature value from KTIP weather station, square markers denote measured temperature values from ambient sensors, and circular markers denote measured temperature values inside concrete.

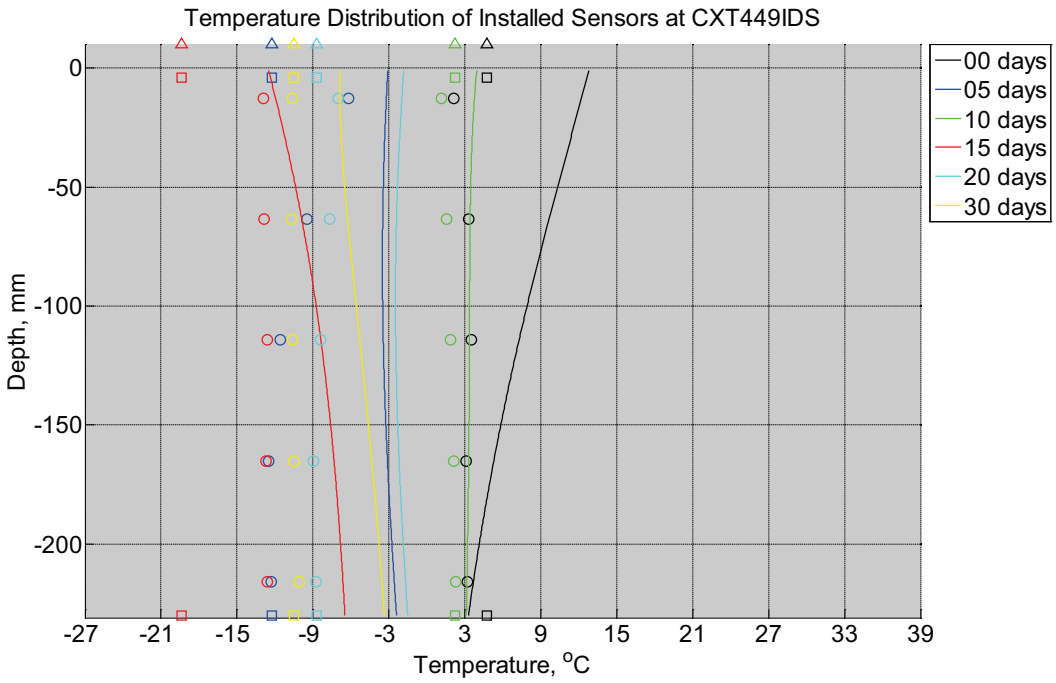

Figure B-541 Measured (markers) and modeled (continuous line) temperature profile distribution as a function of depth inside a concrete crosstie (labeled CXT449IDS) without a polyurethane pad nor rail located in Champaign, IL, between December 18, 2013, through January 25, 2014. Triangular markers denote temperature value from KTIP weather station, square markers denote measured temperature values from ambient sensors, and circular markers denote measured temperature values inside concrete.

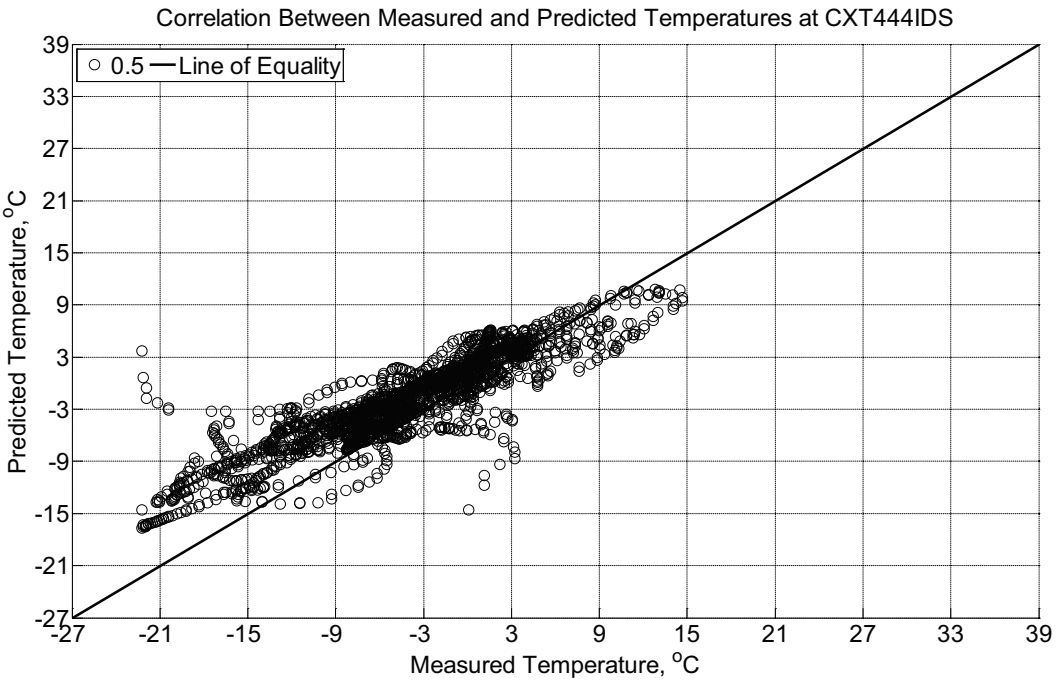

Figure B-542 Correlation between measured and predicted temperature values 0.5 inches (12.7 mm) from the surface of a concrete crosstie (labeled CXT444IDS) without a polyurethane pad nor rail located in Champaign, IL, between December 18, 2013, through January 25, 2014.

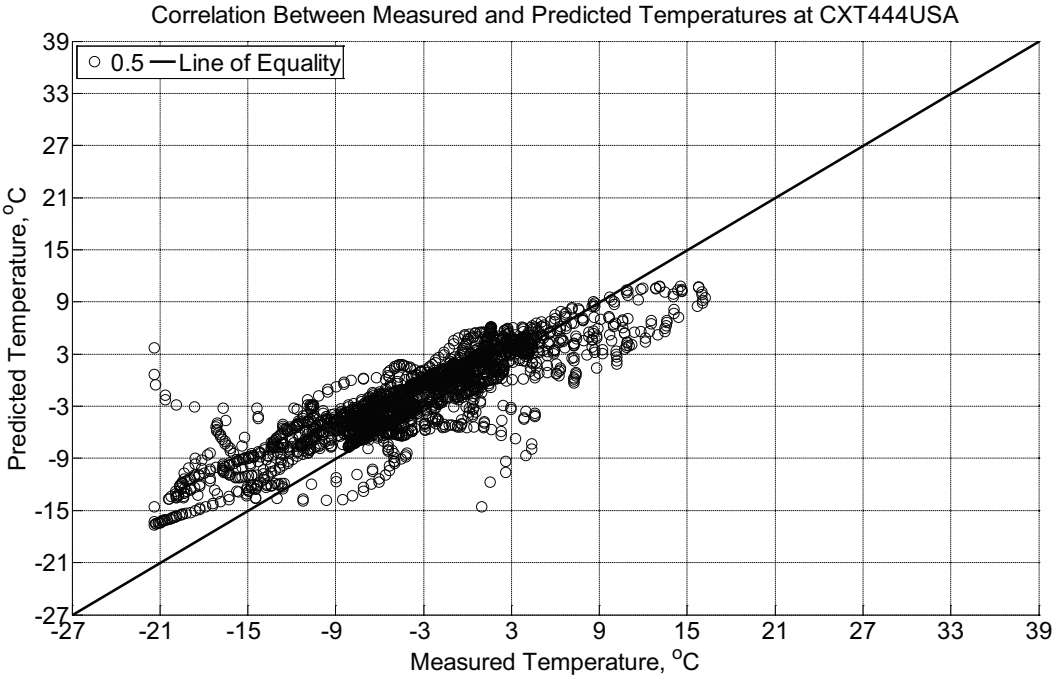

Figure B-543 Correlation between measured and predicted temperature values 0.5 inches (12.7 mm) from the surface of a concrete crosstie (labeled CXT444IDS) without a

polyurethane pad nor rail located in Champaign, IL, between December 18, 2013, through January 25, 2014.

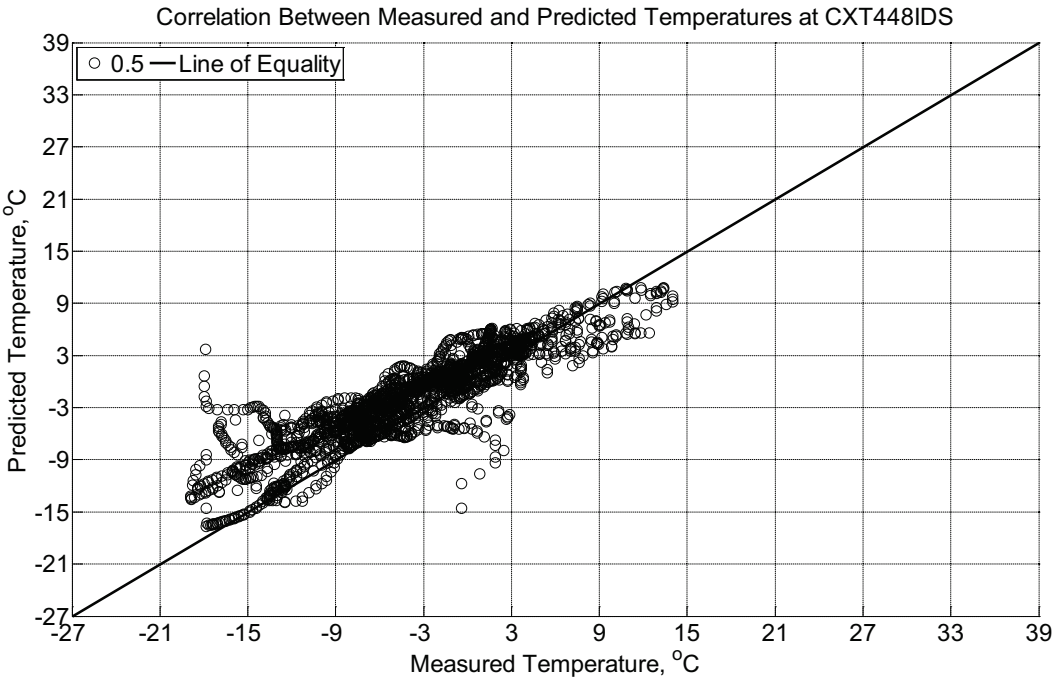

Figure B-544 Correlation between measured and predicted temperature values 0.5 inches (12.7 mm) from the surface of a concrete crosstie (labeled CXT444IDS) without a polyurethane pad nor rail located in Champaign, IL, between December 18, 2013, through January 25, 2014.

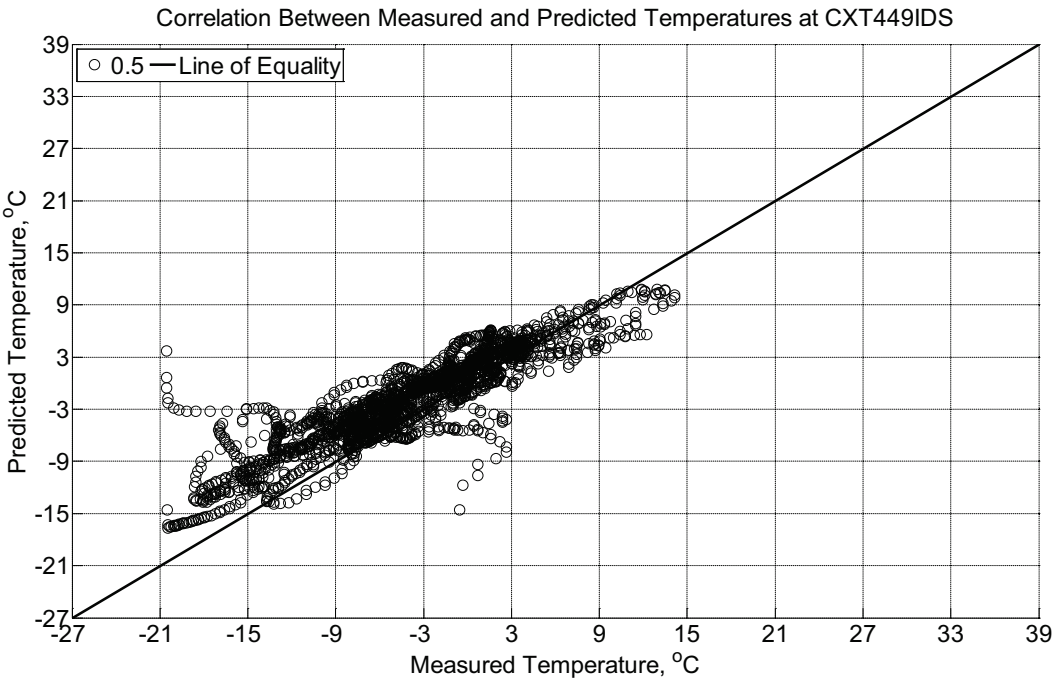

Figure B-545 Correlation between measured and predicted temperature values 0.5 inches (12.7 mm) from the surface of a concrete crosstie (labeled CXT444IDS) without a polyurethane pad nor rail located in Champaign, IL, between December 18, 2013, through January 25, 2014.

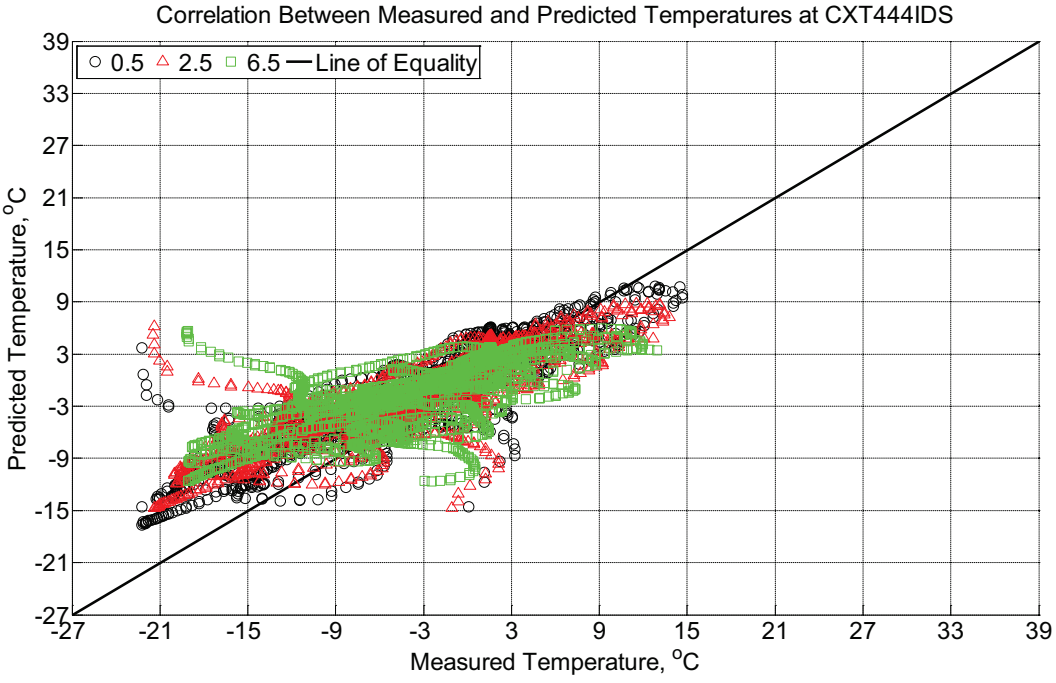

Figure B-546 Correlation between measured and predicted temperature values 0.5 inches (12.7 mm), 2.5 inches (63.5 mm), and 6.5 inches (139.7 mm) from the surface of a concrete

crosstie (labeled CXT444IDS) without a polyurethane pad nor rail located in Champaign, IL, between December 18, 2013, through January 25, 2014.

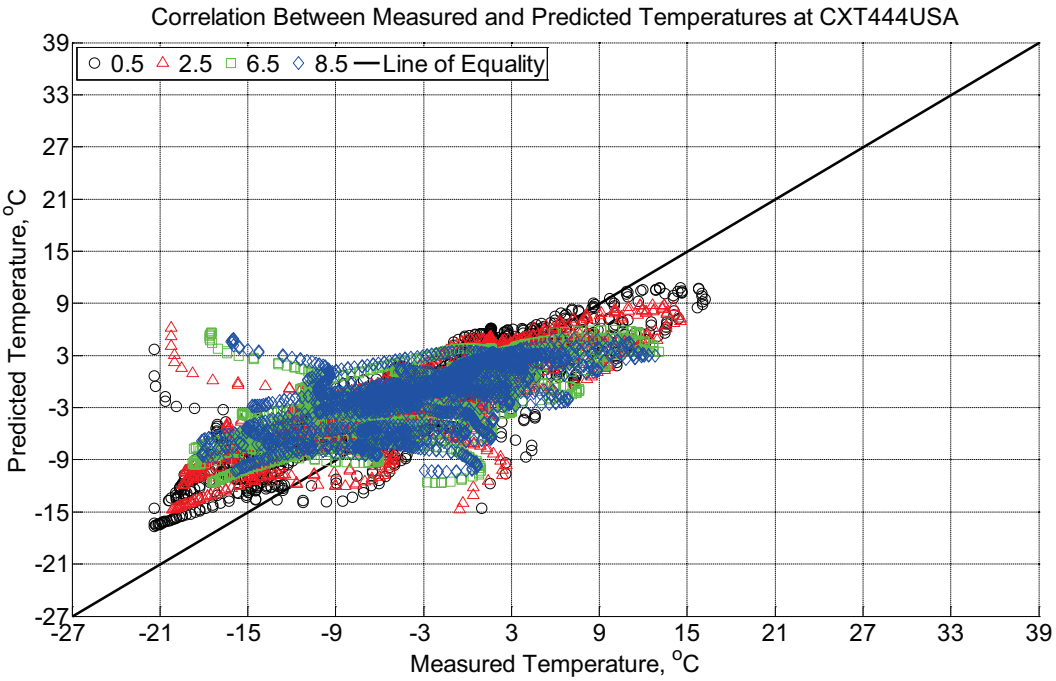

Figure B-547 Correlation between measured and predicted temperature values 0.5 inches (12.7 mm), 2.5 inches (63.5 mm), 6.5 inches (139.7 mm), and 8.5 inches (215.9 mm) from the surface of a concrete crosstie (labeled CXT444USA) without a polyurethane pad nor rail located in Champaign, IL, between December 18, 2013, through January 25, 2014.

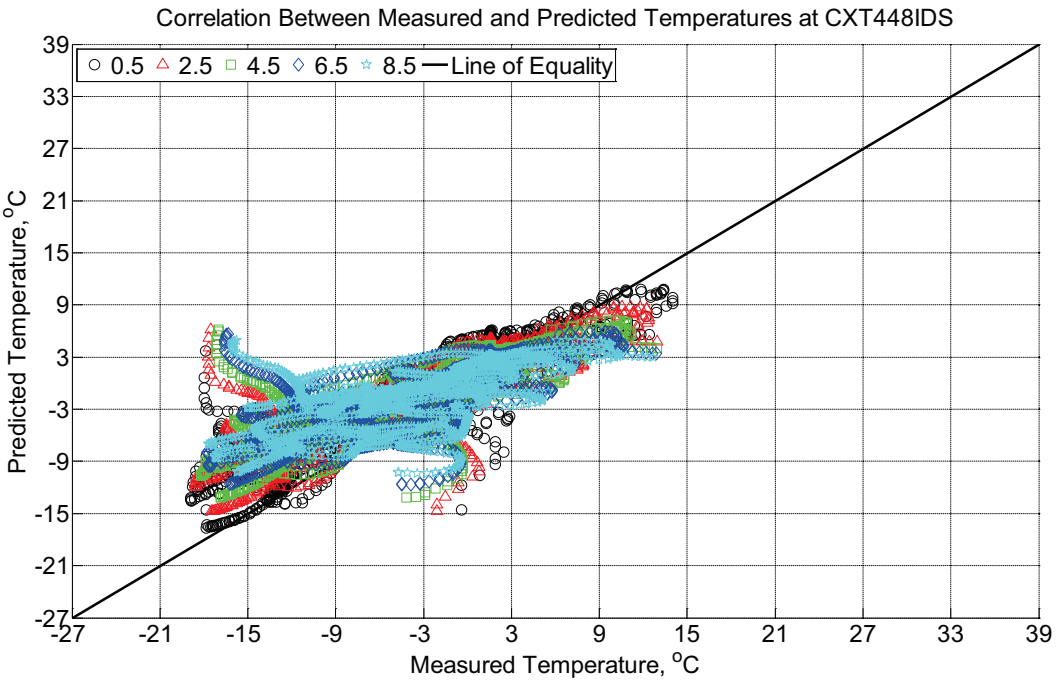

Figure B-548 Correlation between measured and predicted temperature values 0.5 inches (12.7 mm), 2.5 inches (63.5 mm), 4.5 inches (114.3 mm), 6.5 inches (139.7 mm), and 8.5 inches (215.9 mm) from the surface of a concrete crosstie (labeled CXT448IDS) without a polyurethane pad nor rail located in Champaign, IL, between December 18, 2013, through January 25, 2014.

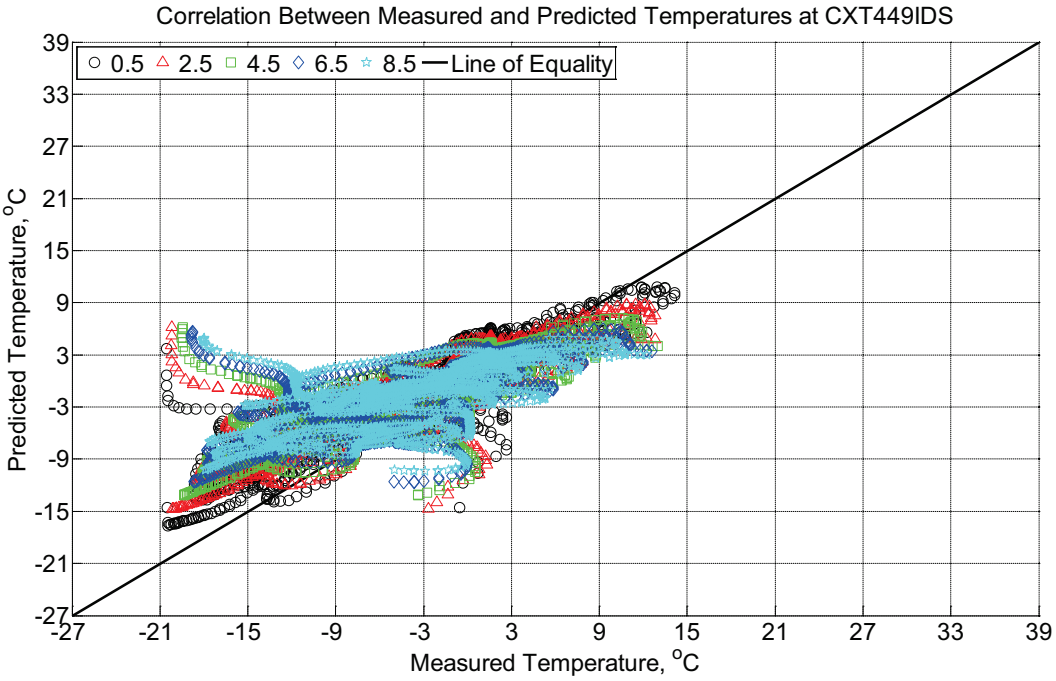

Figure B-549 Correlation between measured and predicted temperature values 0.5 inches

(12.7 mm), 2.5 inches (63.5 mm), 4.5 inches (114.3 mm), 6.5 inches (139.7 mm), and 8.5 inches (215.9 mm) from the surface of a concrete crosstie (labeled CXT449IDS) without a polyurethane pad nor rail located in Champaign, IL, between December 18, 2013, through January 25, 2014.

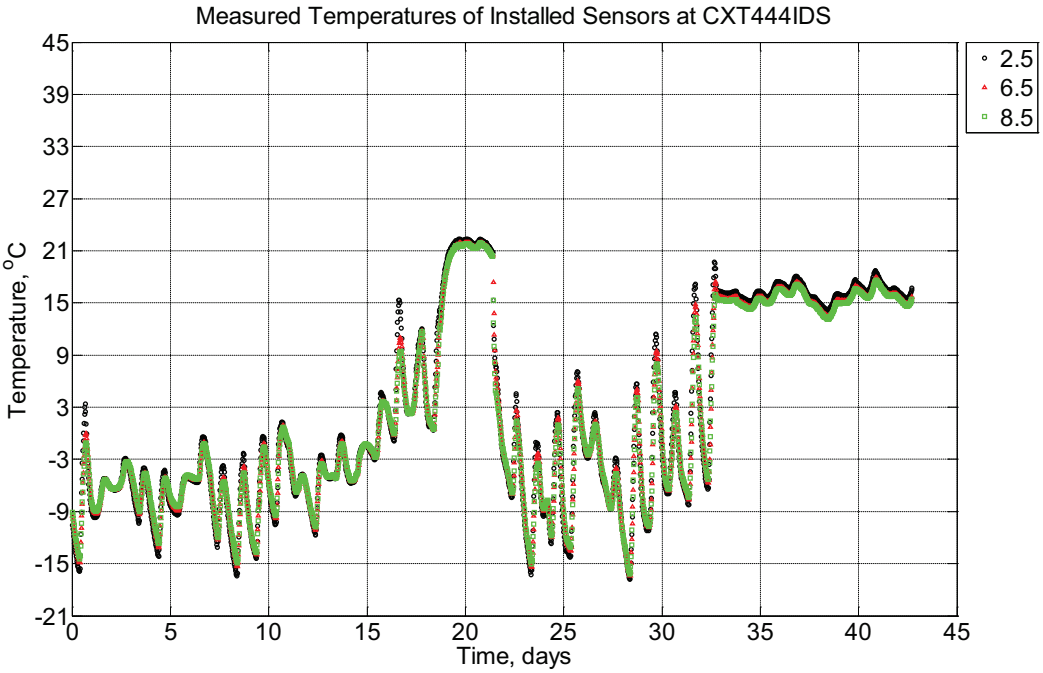

Figure B-550 Measured temperature at depths of 2.5 inches (63.5 mm), 6.5 inches (139.7 mm), and 8.5 inches (215.9 mm) from the surface of a concrete crosstie (labeled CXT444IDS) without a polyurethane pad nor rail located in Champaign, IL, between February 2, 2014, through March 17, 2014. At days 19-21, the instrumented crossties are moved inside of the Newmark Civil Engineering Laboratory. At days 21-33, the instrumented crossties are located outside in Rantoul, IL. At days 33-43, the instrumented crossties are moved inside the Materials Testing Laboratory at the Advanced Transportation Research Laboratory (ATREL) in Rantoul, IL.

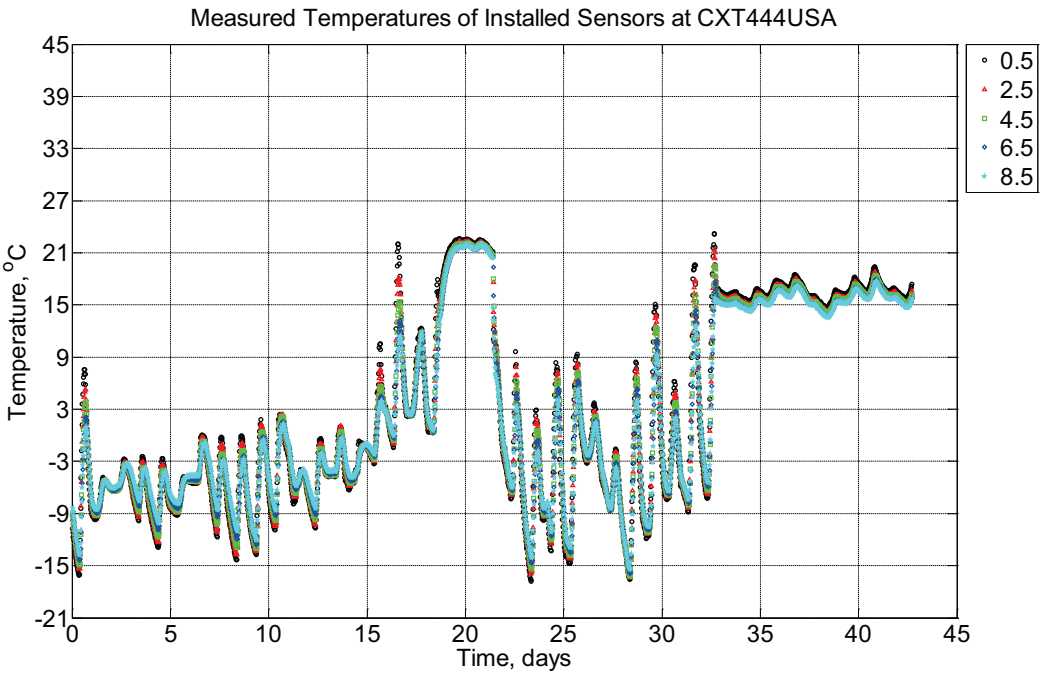

Figure B-551 Measured temperature at depths of 0.5 inches (12.7 mm), 2.5 inches (63.5 mm), 4.5 inches (114.3 mm), 6.5 inches (139.7 mm), and 8.5 inches (215.9 mm) from the surface of a concrete crosstie (labeled CXT444USA) without a polyurethane pad nor rail located in Champaign, IL, between February 2, 2014, through March 17, 2014. At days 19-21, the instrumented crossties are moved inside of the Newmark Civil Engineering Laboratory. At days 21-33, the instrumented crossties are located outside in Rantoul, IL. At days 33-43, the instrumented crossties are moved inside the Materials Testing Laboratory at the Advanced Transportation Research Laboratory (ATREL) in Rantoul, IL.

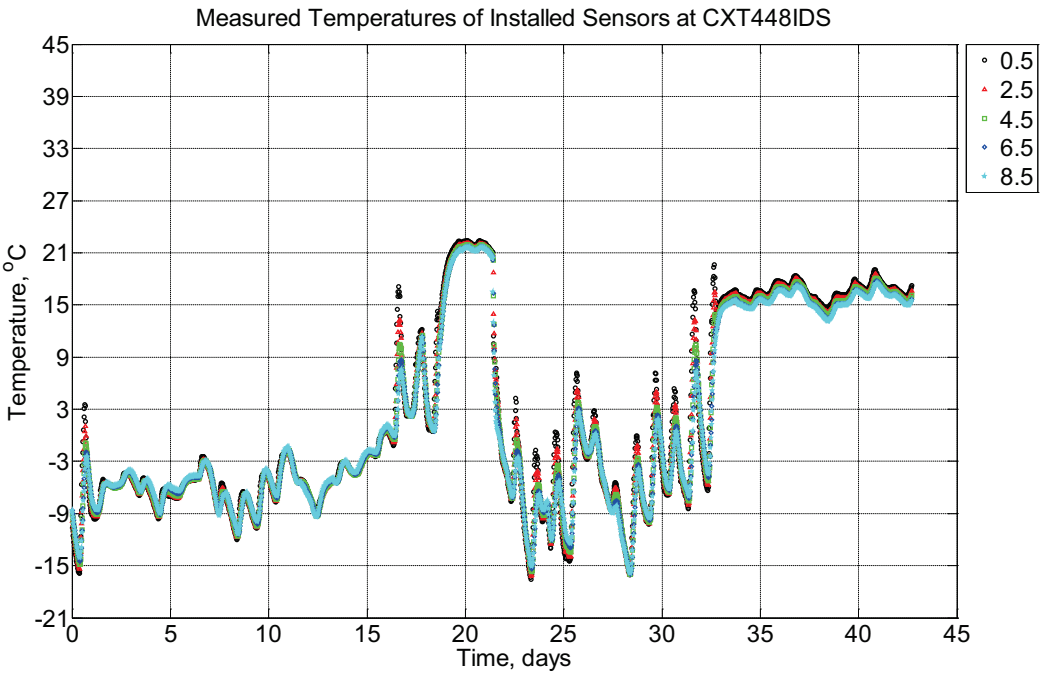

Figure B-552 Measured temperature at depths of 0.5 inches (12.7 mm), 2.5 inches (63.5 mm), 4.5 inches (114.3 mm), 6.5 inches (139.7 mm), and 8.5 inches (215.9 mm) from the surface of a concrete crosstie (labeled CXT448IDS) without a polyurethane pad nor rail located in Champaign, IL, between February 2, 2014, through March 17, 2014. At days 19-21, the instrumented crossties are moved inside of the Newmark Civil Engineering Laboratory. At days 21-33, the instrumented crossties are located outside in Rantoul, IL. At days 33-43, the instrumented crossties are moved inside the Materials Testing Laboratory at the Advanced Transportation Research Laboratory (ATREL) in Rantoul, IL.

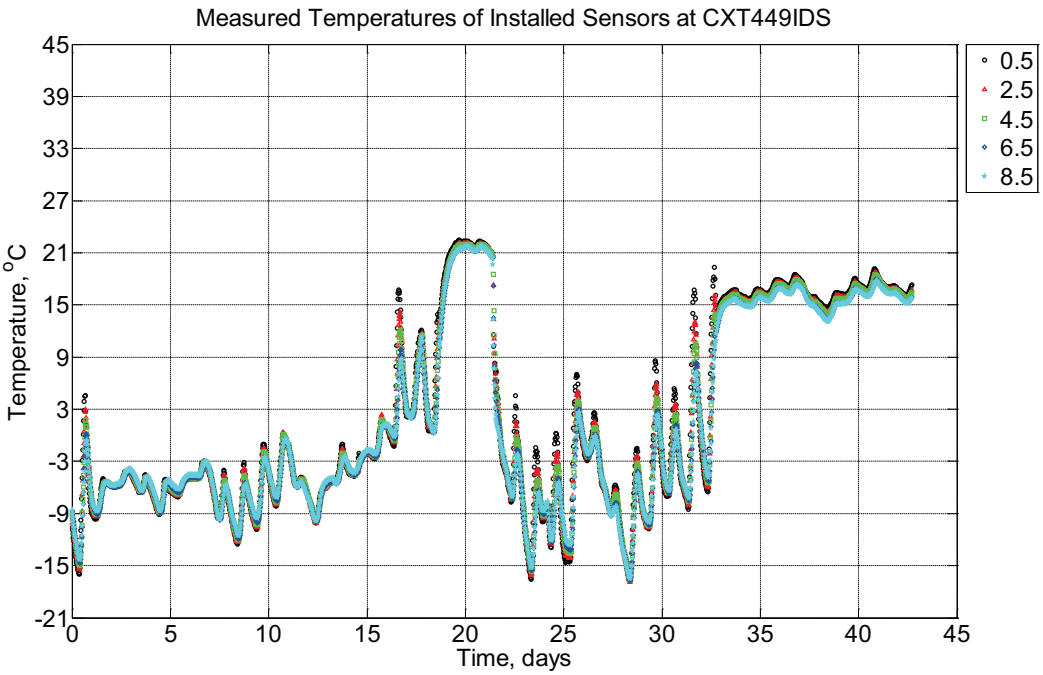

Figure B-553 Measured temperature at depths of 0.5 inches (12.7 mm), 2.5 inches (63.5 mm), 4.5 inches (114.3 mm), 6.5 inches (139.7 mm), and 8.5 inches (215.9 mm) from the surface of a concrete crosstie (labeled CXT449IDS) without a polyurethane pad nor rail located in Champaign, IL, between February 2, 2014, through March 17, 2014. At days 19-21, the instrumented crossties are moved inside of the Newmark Civil Engineering Laborary. At days 21-33, the instrumented crossties are located outside in Rantoul, IL. At days 33-43, the instrumented crossties are moved inside the Materials Testing Laboratory at the Advanced Transportation Research Laboratory (ATREL) in Rantoul, IL.

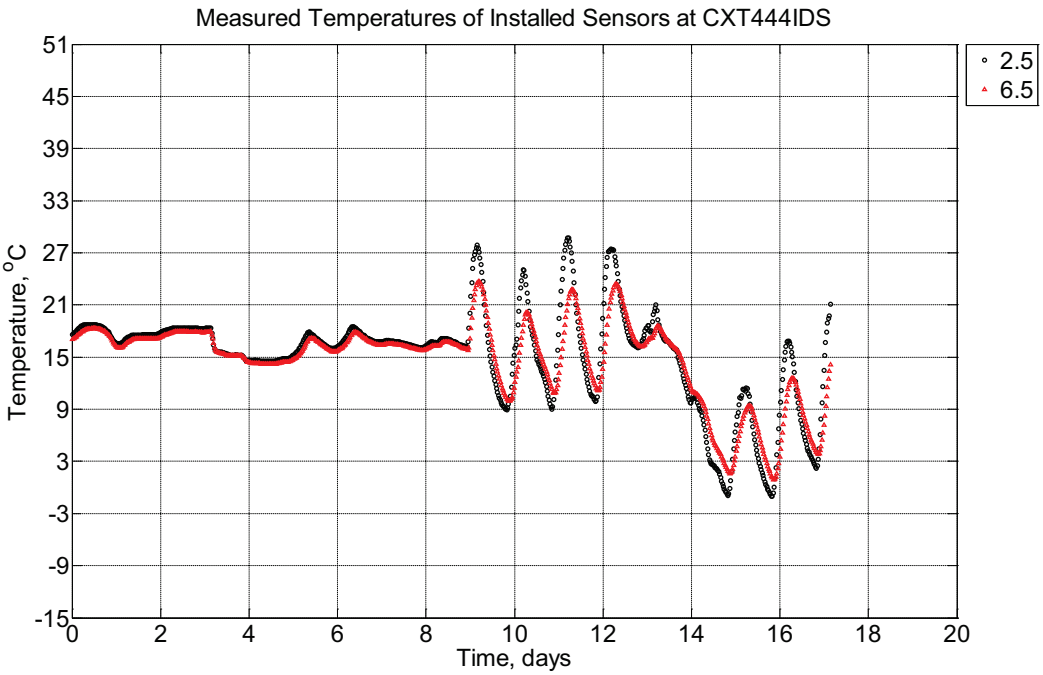

Figure B-554 Measured temperature at depths of 2.5 inches (63.5 mm) and 6.5 inches (139.7 mm) from the surface of a concrete crosstie (labeled CXT444IDS) without a polyurethane pad nor rail located in Rantoul, IL, between March 31, 2014, through April 17, 2014. At days 1-9, the instrumented crossties are inside the Materials Testing Laboratory at the Advanced Transportation Research Laboratory (ATREL) in Rantoul, IL. At days 9-17, the instrumented crossties are moved outside and into model ballast in Rantoul, IL.

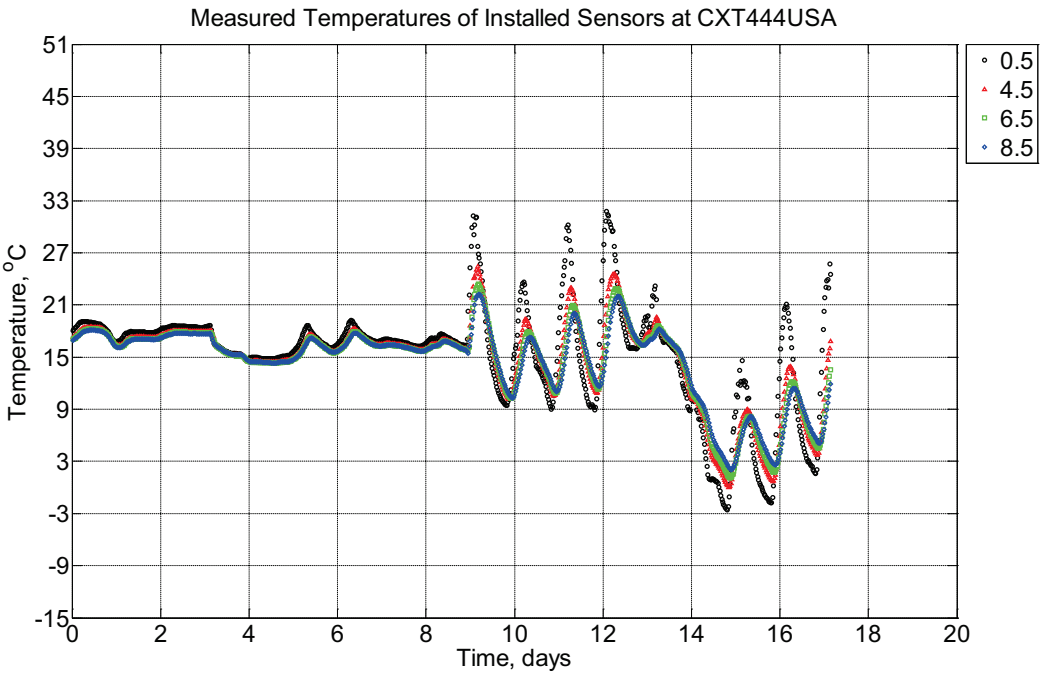

Figure B-555 Measured temperature at depths of 0.5 inches (12.7 mm), 4.5 inches (114.3 mm), 6.5 inches (139.7 mm), and 8.5 inches (215.9 mm) from the surface of a concrete crosstie (labeled CXT444USA) without a polyurethane pad nor rail located in Rantoul, IL, between March 31, 2014, through April 17, 2014. At days 1-9, the instrumented crossties are inside the Materials Testing Laboratory at the Advanced Transportation Research Laboratory (ATREL) in Rantoul, IL. At days 9-17, the instrumented crossties are moved outside and into model ballast in Rantoul, IL.

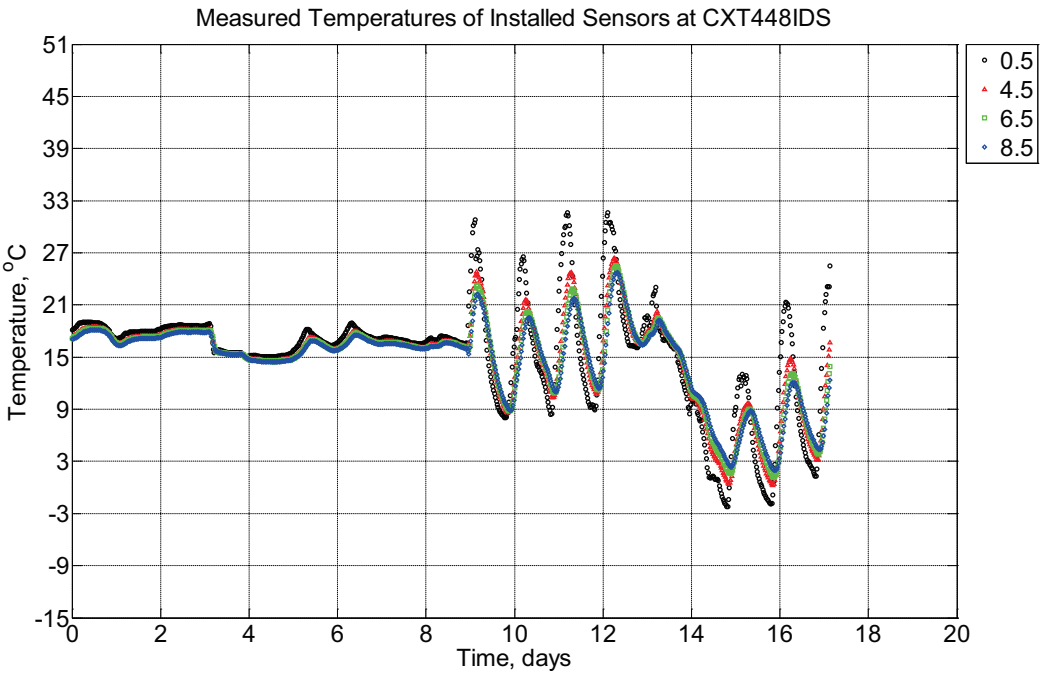

Figure B-556 Measured temperature at depths of 0.5 inches (12.7 mm), 4.5 inches (114.3 mm), 6.5 inches (139.7 mm), and 8.5 inches (215.9 mm) from the surface of a concrete crosstie (labeled CXT448IDS) without a polyurethane pad nor rail located in Rantoul, IL, between March 31, 2014, through April 17, 2014. At days 1-9, the instrumented crossties are inside the Materials Testing Laboratory at the Advanced Transportation Research Laboratory (ATREL) in Rantoul, IL. At days 9-17, the instrumented crossties are moved outside and into model ballast in Rantoul, IL.

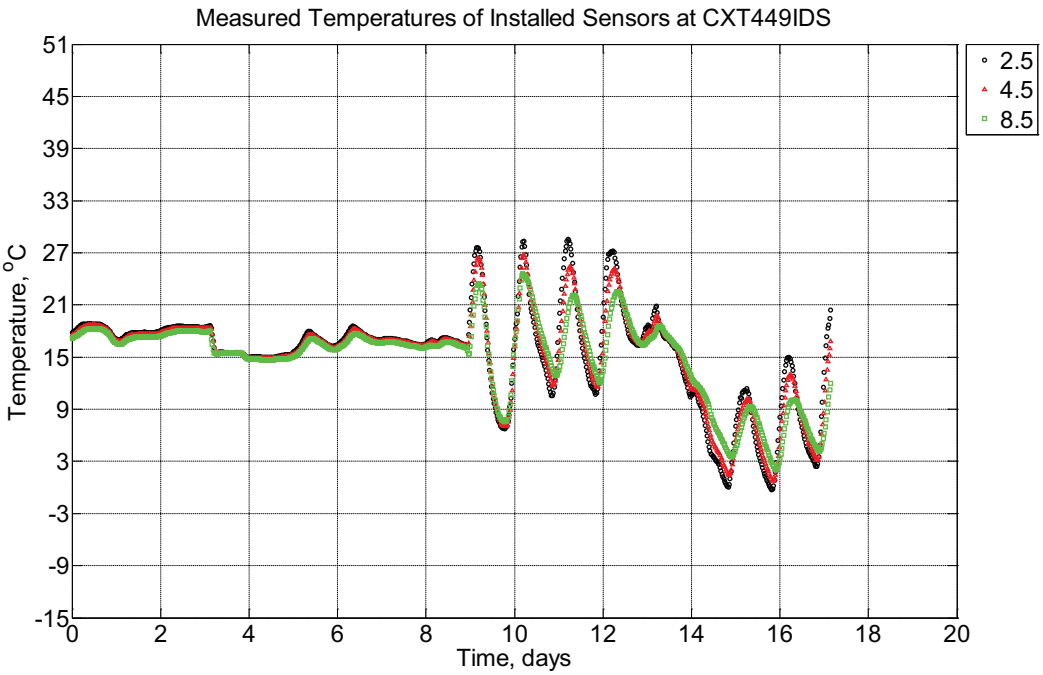

Figure B-557 Measured temperature at depths of 2.5 inches (63.5 mm), 4.5 inches (114.3 mm), and 8.5 inches (215.9 mm) from the surface of a concrete crosstie (labeled CXT449IDS) without a polyurethane pad nor rail located in Rantoul, IL, between March 31, 2014, through April 17, 2014. At days 1-9, the instrumented crossties are inside the Materials Testing Laboratory at the Advanced Transportation Research Laboratory (ATREL) in Rantoul, IL. At days 9-17, the instrumented crossties are moved outside and into model ballast in Rantoul, IL.

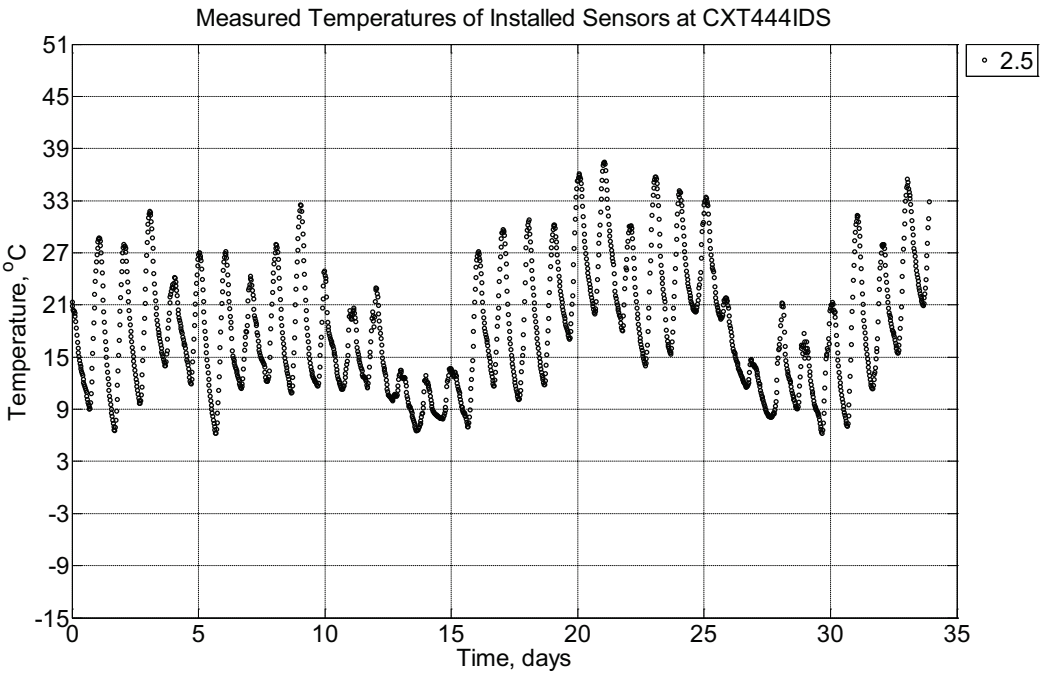

Figure B-558 Measured temperature at a depth of 2.5 inches (63.5 mm) from the surface of a concrete crosstie (labeled CXT444IDS) without a polyurethane pad nor rail installed in ballast in Rantoul, IL, between April 17, 2014, through May 21, 2014.

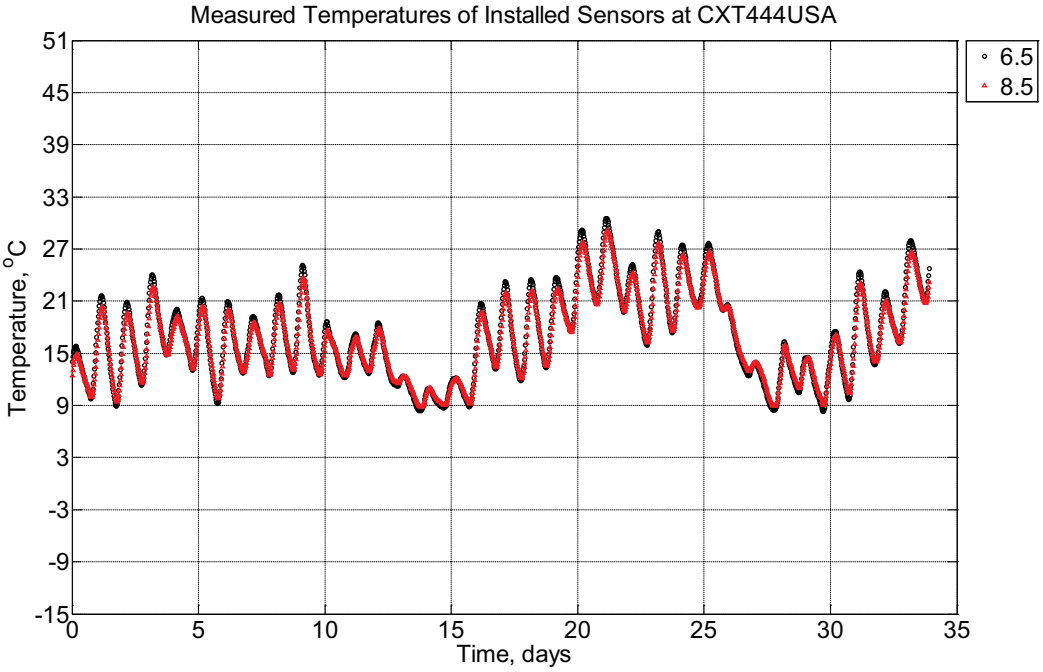

Figure B-559 Measured temperature at depths of 6.5 inches (139.7 mm) and 8.5 inches (215.9 mm) from the surface of a concrete crosstie (labeled CXT444USA) without a

polyurethane pad nor rail installed in ballast in Rantoul, IL, between April 17, 2014, through May 21, 2014.

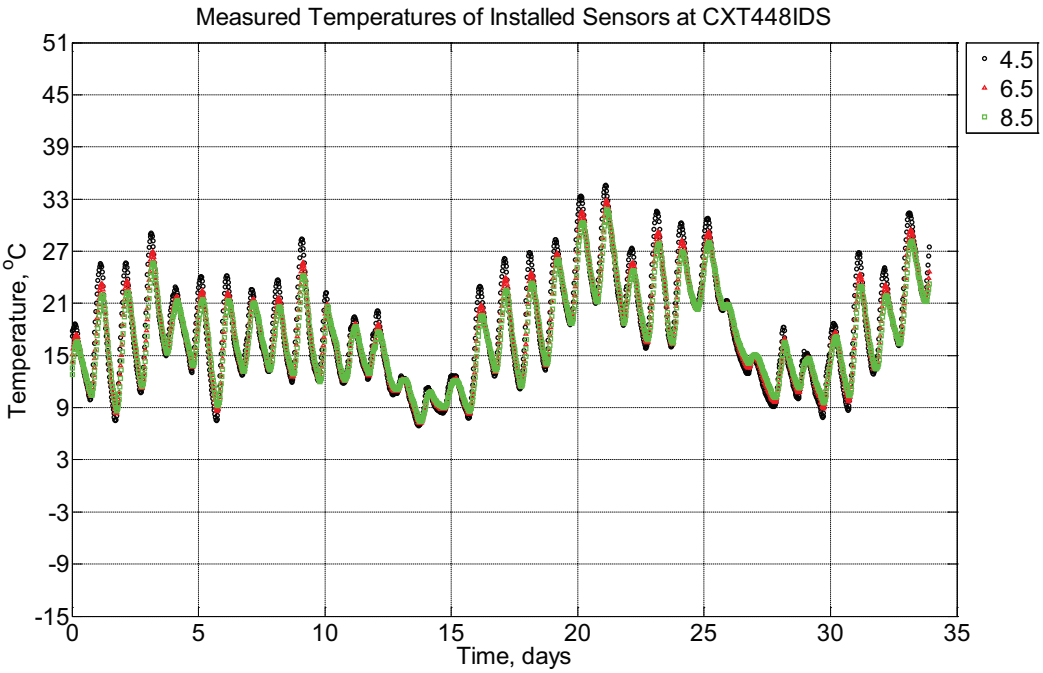

Figure B-560 Measured temperature at depths of 4.5 inches (114.3 mm), 6.5 inches (139.7 mm), and 8.5 inches (215.9 mm) from the surface of a concrete crosstie (labeled CXT448IDS) without a polyurethane pad nor rail installed in ballast in Rantoul, IL, between April 17, 2014, through May 21, 2014.

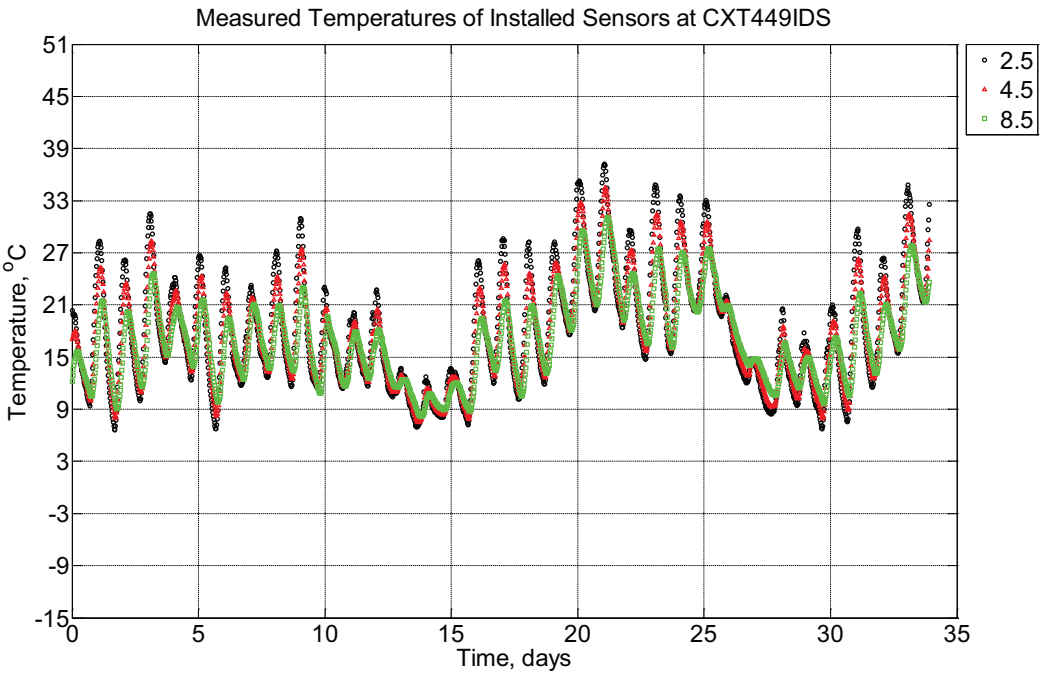

Figure B-561 Measured temperature at depths of 2.5 inches (63.5 mm), 4.5 inches (114.3 mm), and 8.5 inches (215.9 mm) from the surface of a concrete crosstie (labeled CXT449IDS) without a polyurethane pad nor rail installed in ballast in Rantoul, IL, between April 17, 2014, through May 21, 2014.

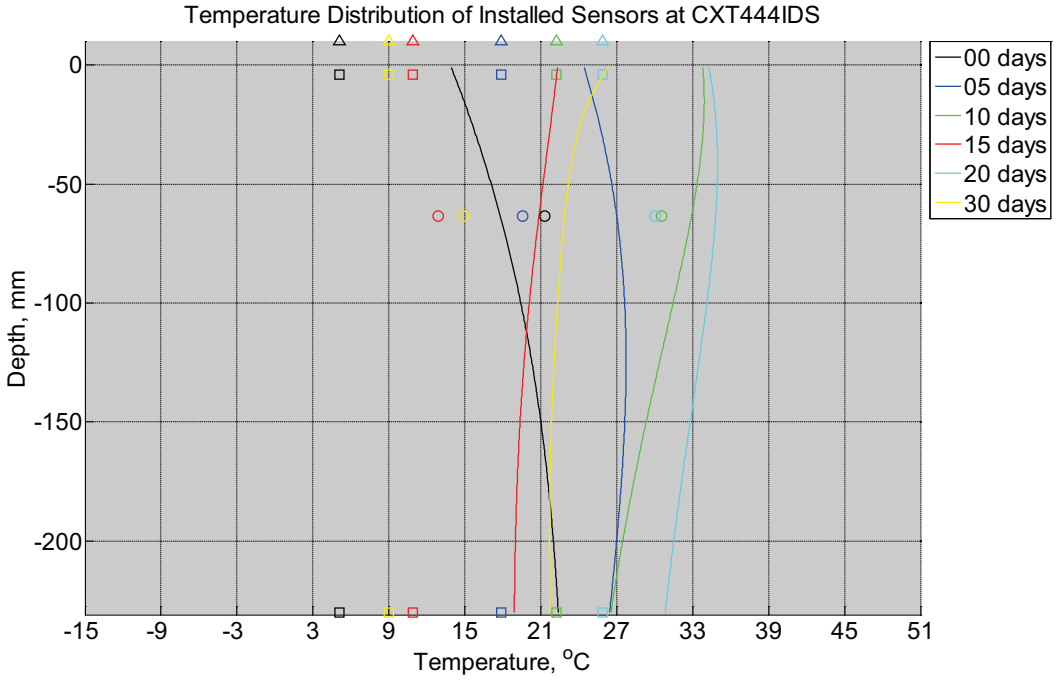

Figure B-562 Measured (markers) and modeled (continuous line) temperature profile distribution as a function of depth inside a concrete crosstie (labeled CXT444IDS) without

a polyurethane pad nor rail installed in ballast in Rantoul, IL, between April 17, 2014, through May 21, 2014. Triangular markers denote temperature value from KTIP weather station, square markers denote measured temperature values from ballast, and circular markers denote measured temperature values inside concrete.

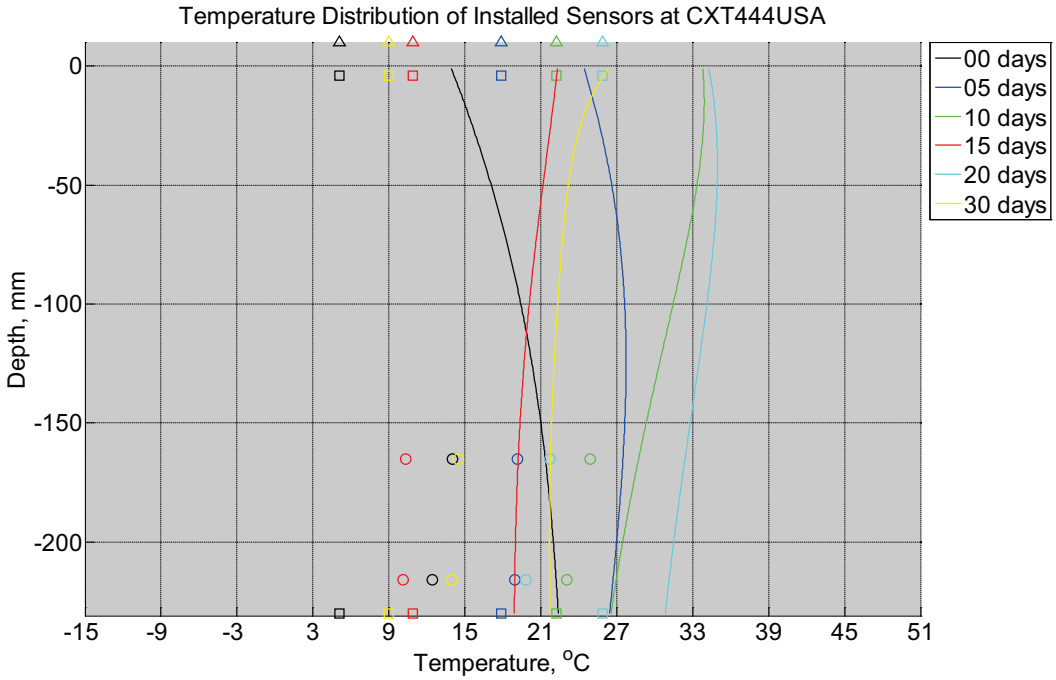

Figure B-563 Measured (markers) and modeled (continuous line) temperature profile distribution as a function of depth inside a concrete crosstie (labeled CXT444USA) without a polyurethane pad nor rail installed in ballast in Rantoul, IL, between April 17, 2014, through May 21, 2014. Triangular markers denote temperature value from KTIP weather station, square markers denote measured temperature values from ballast, and circular markers denote measured temperature values inside concrete.

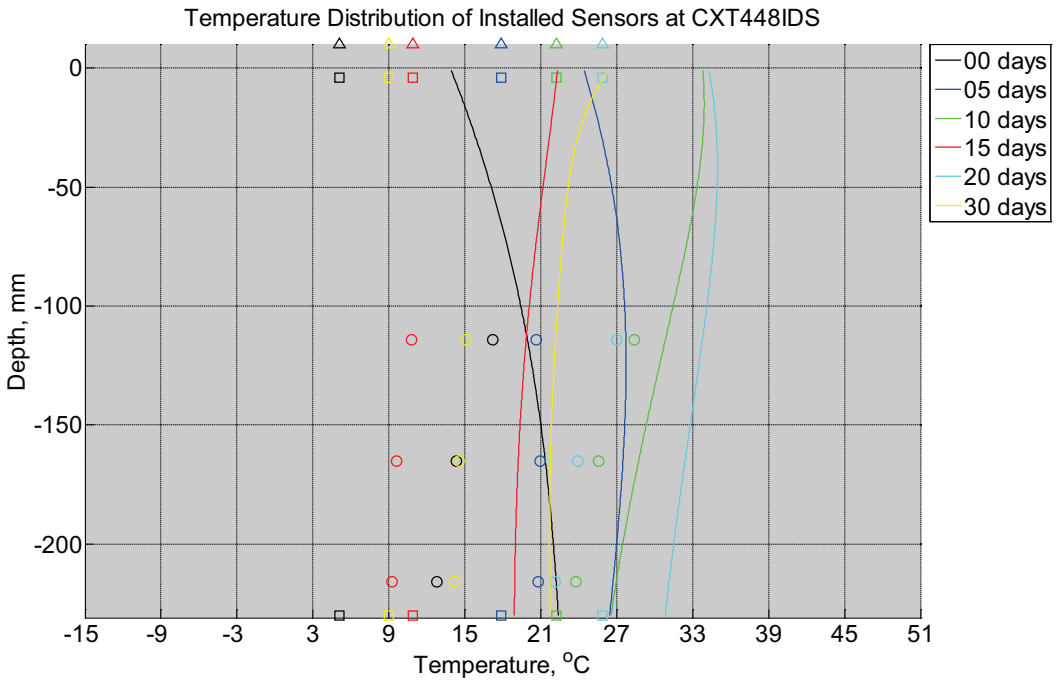

Figure B-564 Measured (markers) and modeled (continuous line) temperature profile distribution as a function of depth inside a concrete crosstie (labeled CXT448IDS) without a polyurethane pad nor rail installed in ballast in Rantoul, IL, between April 17, 2014, through May 21, 2014. Triangular markers denote temperature value from KTIP weather station, square markers denote measured temperature values from ballast, and circular markers denote measured temperature values inside concrete.

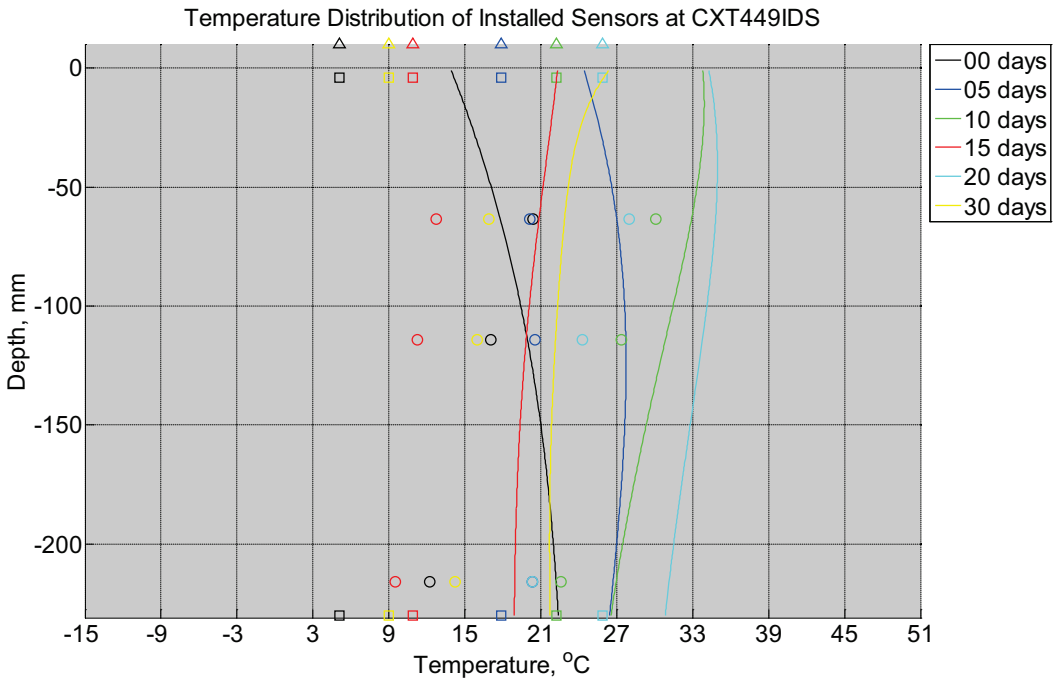

Figure B-565 Measured (markers) and modeled (continuous line) temperature profile distribution as a function of depth inside a concrete crosstie (labeled CXT449IDS) without a polyurethane pad nor rail installed in ballast in Rantoul, IL, between April 17, 2014, through May 21, 2014. Triangular markers denote temperature value from KTIP weather station, square markers denote measured temperature values from ballast, and circular markers denote measured temperature values inside concrete.

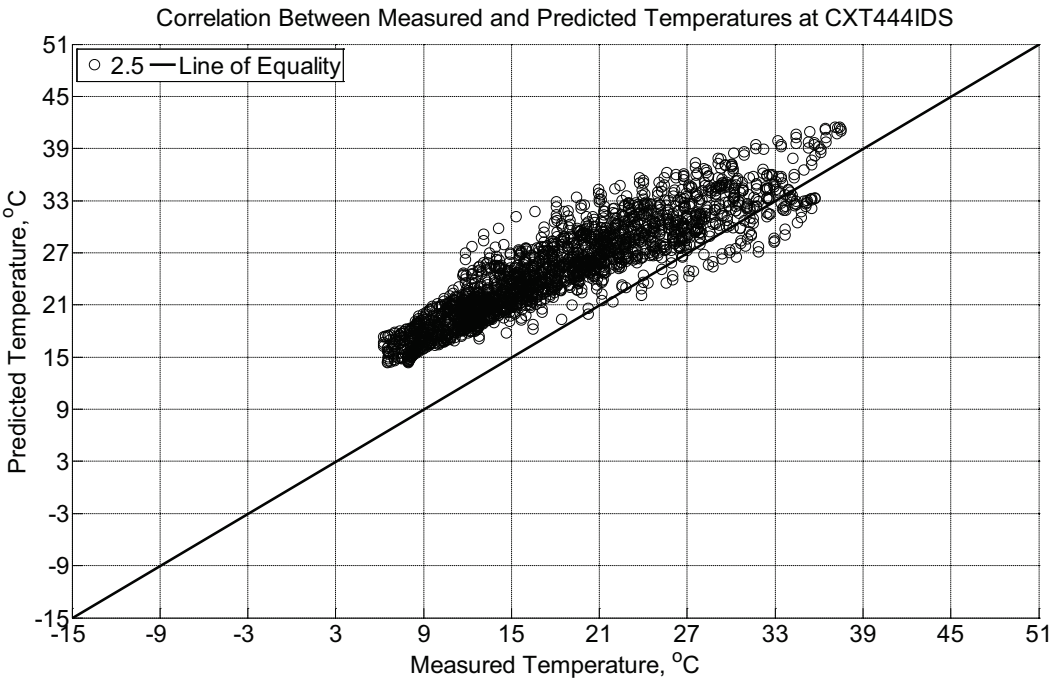

Figure B-566 Correlation between measured and predicted temperature values 2.5 inches (63.5 mm) from the surface of a concrete crosstie (labeled CXT444IDS) without a polyurethane pad nor rail installed in ballast in Rantoul, IL, between April 17, 2014, through May 21, 2014.

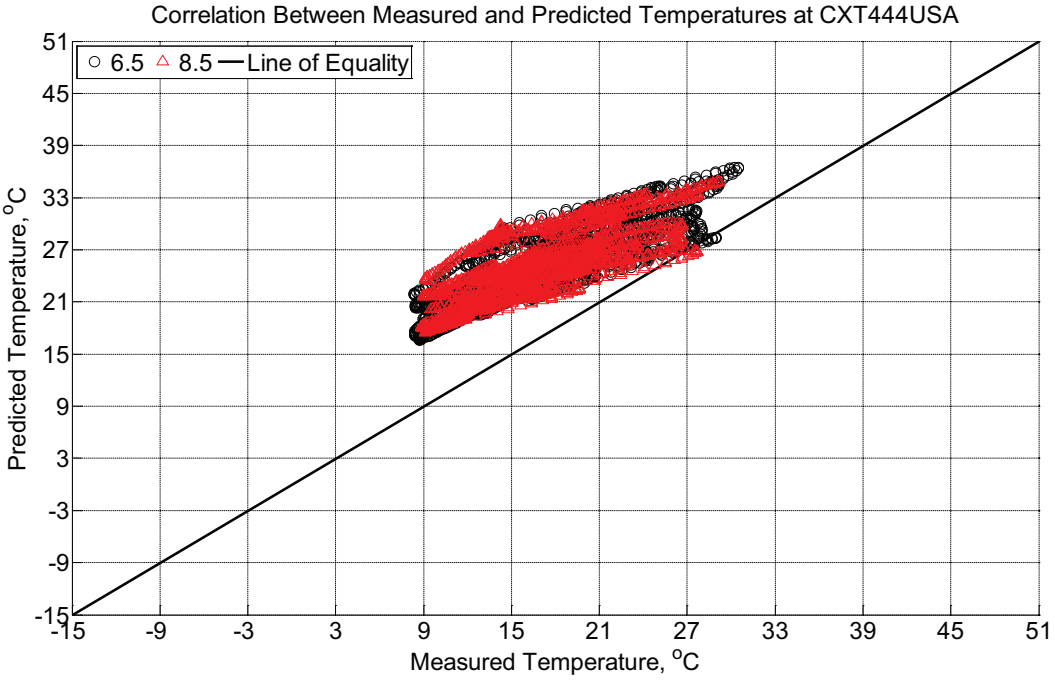

Figure B-567 Correlation between measured and predicted temperature values 6.5 inches (139.7 mm) and 8.5 inches (215.9 mm) from the surface of a concrete crosstie (labeled

CXT444USA) without a polyurethane pad nor rail installed in ballast in Rantoul, IL, between April 17, 2014, through May 21, 2014.

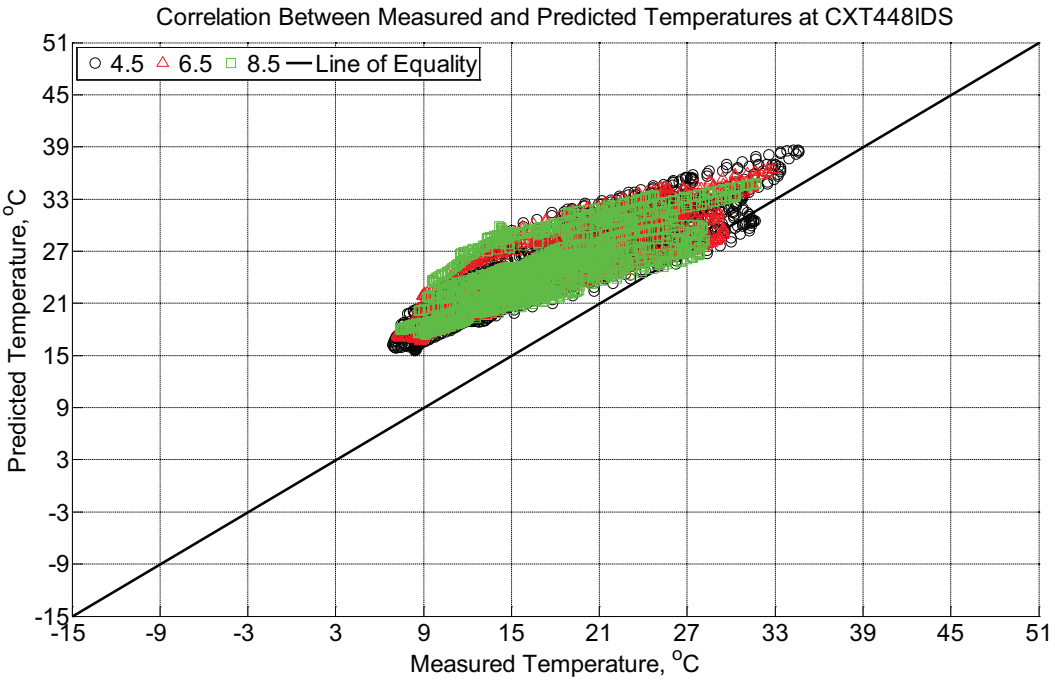

Figure B-568 Correlation between measured and predicted temperature values 4.5 inches (114.3 mm), 6.5 inches (139.7 mm), and 8.5 inches (215.9 mm) from the surface of a concrete crosstie (labeled CXT448IDS) without a polyurethane pad nor rail installed in ballast in Rantoul, IL, between April 17, 2014, through May 21, 2014.

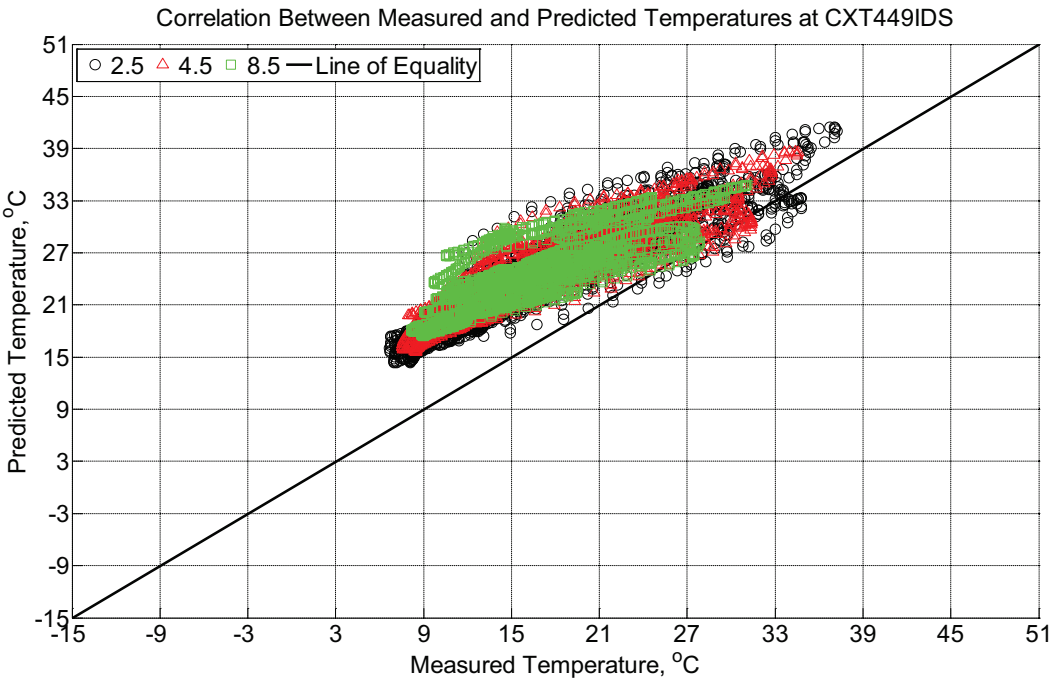

Figure B-569 Correlation between measured and predicted temperature values 2.5 inches (63.5 mm), 4.5 inches (114.3 mm), and 8.5 inches (215.9 mm) from the surface of a concrete crosstie (labeled CXT449IDS) without a polyurethane pad nor rail installed in ballast in Rantoul, IL, between April 17, 2014, through May 21, 2014.

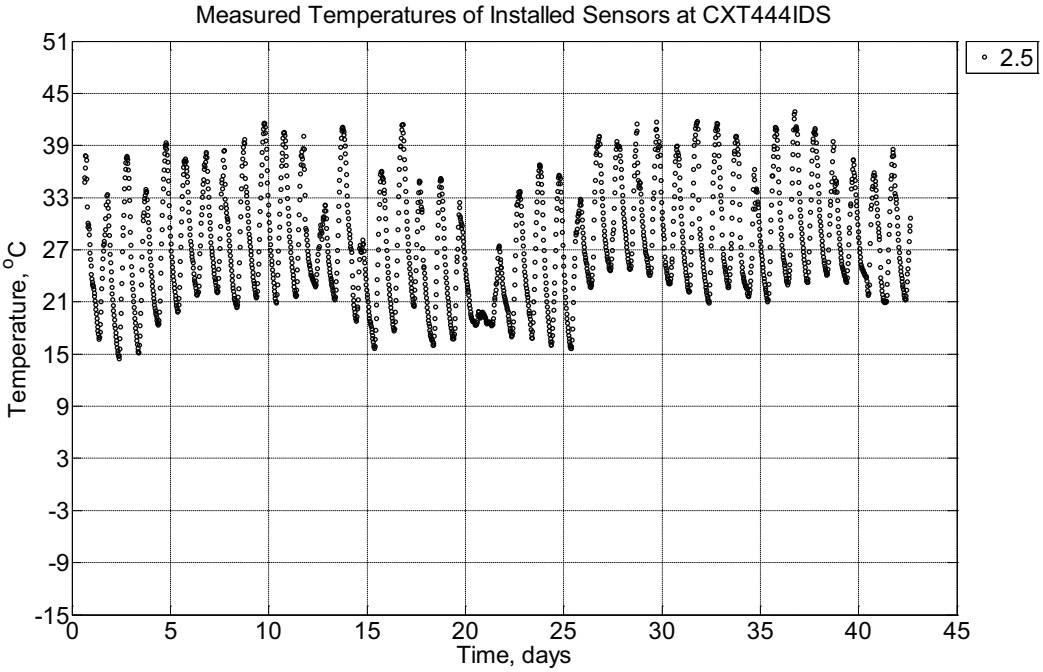

Figure B-570 Measured temperature at a depth of 2.5 inches (63.5 mm) from the surface of a concrete crosstie (labeled CXT444IDS) without a polyurethane pad nor rail without a

polyurethane pad nor rail installed in ballast in Rantoul, IL, between May 21, 2014, through July 2, 2014.

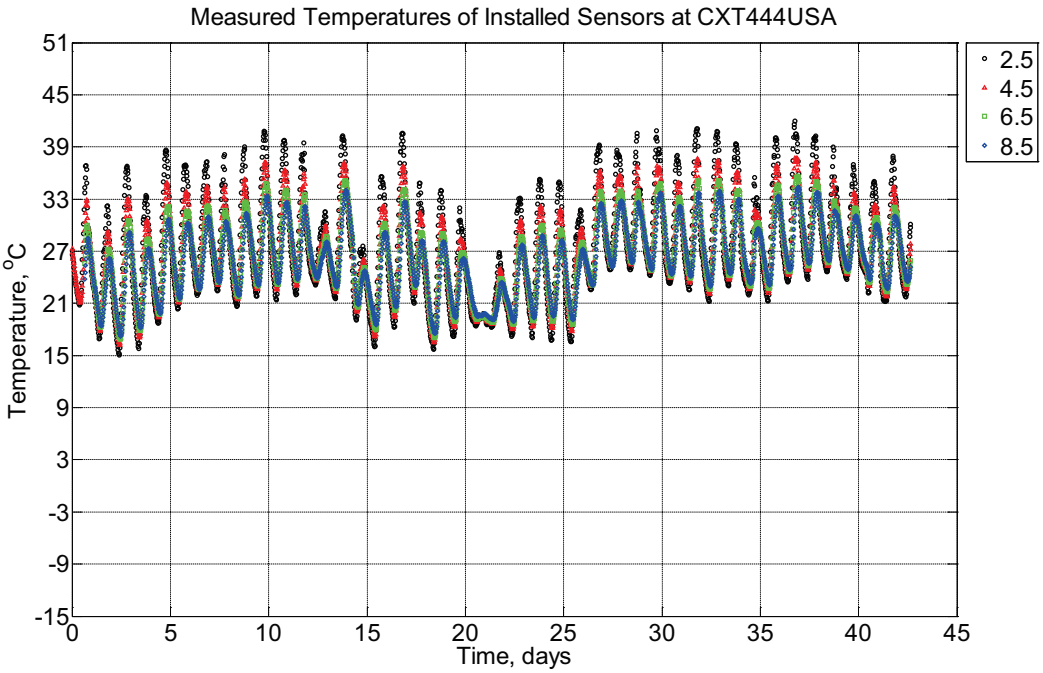

Figure B-571 Measured temperature at depths of 2.5 inches (63.5 mm), 4.5 inches (114.3 mm), 6.5 inches (139.7 mm), and 8.5 inches (215.9 mm) from the surface of a concrete crosstie (labeled CXT444USA) without a polyurethane pad nor rail installed in ballast in Rantoul, IL, between May 21, 2014, through July 2, 2014.

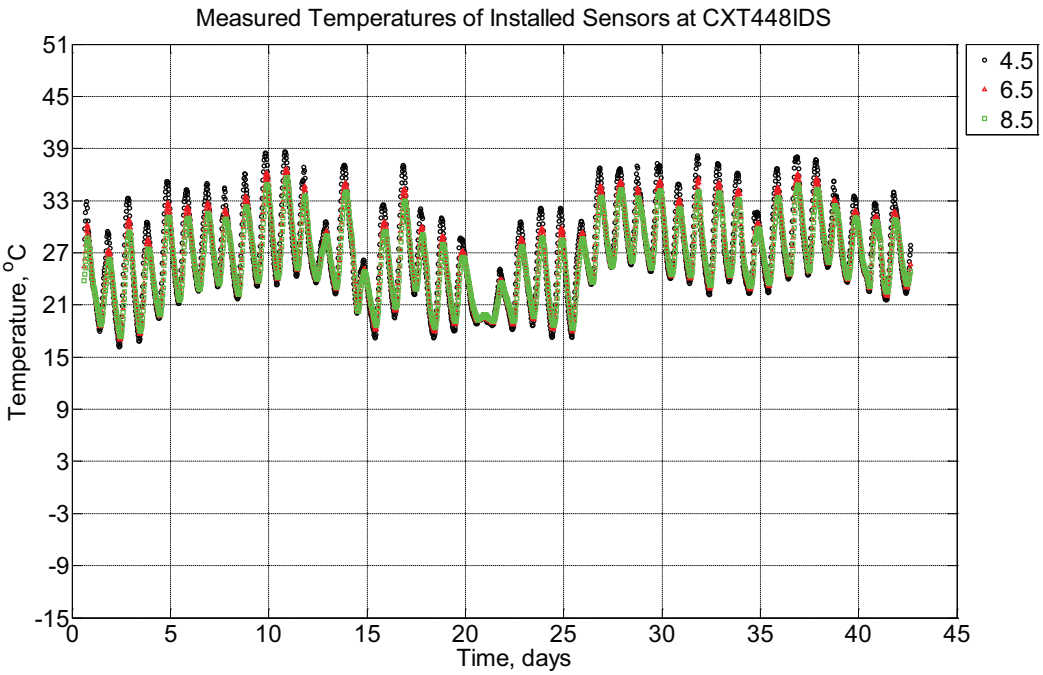

Figure B-572 Measured temperature at depths of 4.5 inches (114.3 mm), 6.5 inches (139.7 mm), and 8.5 inches (215.9 mm) from the surface of a concrete crosstie (labeled CXT448IDS) without a polyurethane pad nor rail installed in ballast in Rantoul, IL, between May 21, 2014, through July 2, 2014.

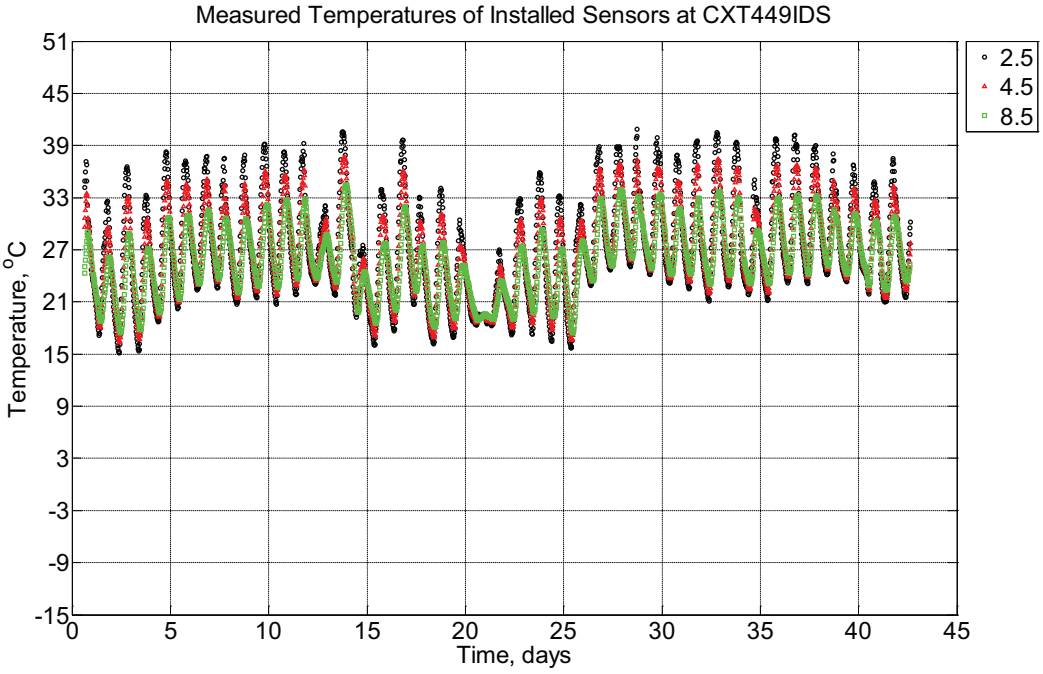

Figure B-573 Measured temperature at depths of 2.5 inches (63.5 mm), 4.5 inches (114.3 mm), and 8.5 inches (215.9 mm) from the surface of a concrete crosstie (labeled

CXT449IDS) without a polyurethane pad nor rail installed in ballast in Rantoul, IL, between May 21, 2014, through July 2, 2014.

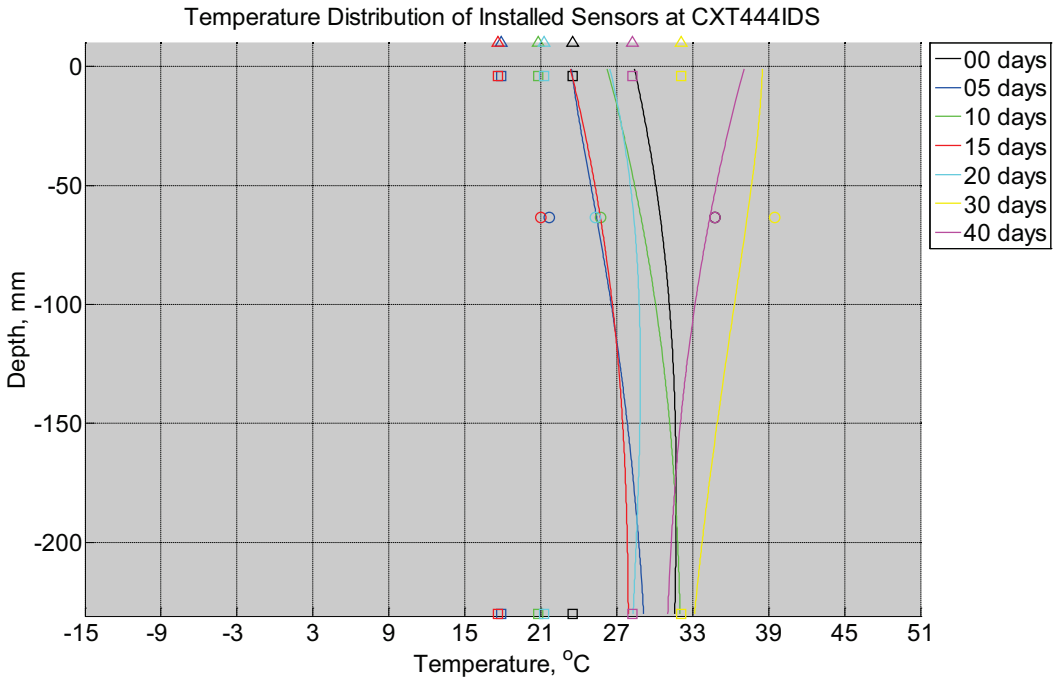

Figure B-574 Measured (markers) and modeled (continuous line) temperature profile distribution as a function of depth inside a concrete crosstie (labeled CXT444IDS) without a polyurethane pad nor rail installed in ballast in Rantoul, IL, between May 21, 2014, through July 2, 2014. Triangular markers denote temperature value from KTIP weather station, square markers denote measured temperature values from ballast, and circular markers denote measured temperature values inside concrete.

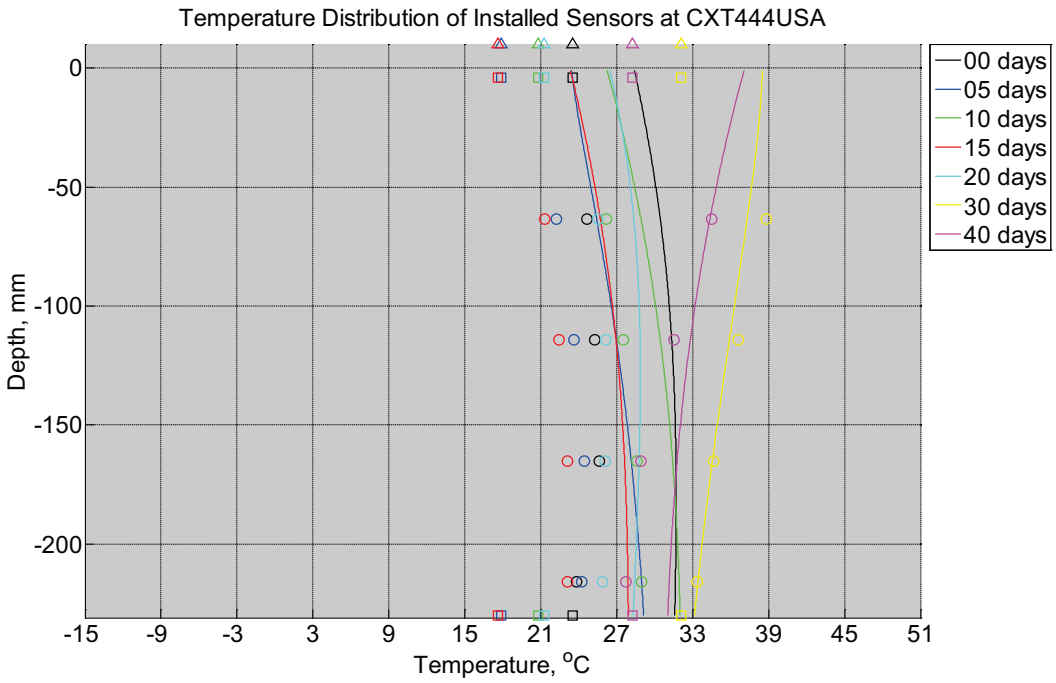

Figure B-575 Measured (markers) and modeled (continuous line) temperature profile distribution as a function of depth inside a concrete crosstie (labeled CXT444USA) without a polyurethane pad nor rail installed in ballast in Rantoul, IL, between May 21, 2014, through July 2, 2014. Triangular markers denote temperature value from KTIP weather station, square markers denote measured temperature values from ballast, and circular markers denote measured temperature values inside concrete.

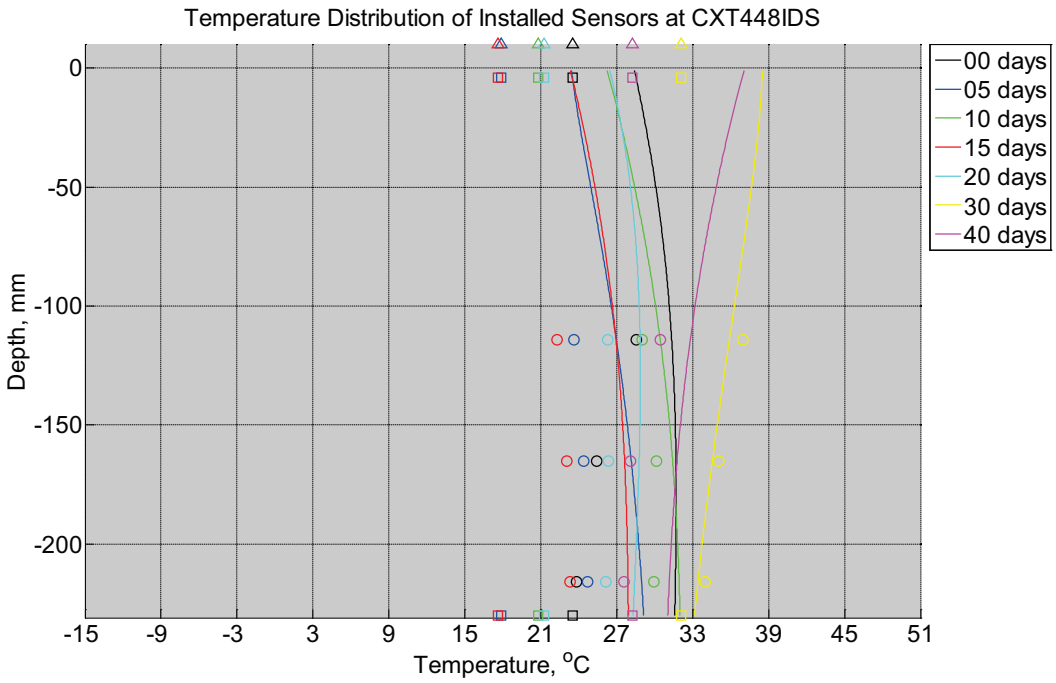

Figure B-576 Measured (markers) and modeled (continuous line) temperature profile distribution as a function of depth inside a concrete crosstie (labeled CXT448IDS) without a polyurethane pad nor rail installed in ballast in Rantoul, IL, between May 21, 2014, through July 2, 2014. Triangular markers denote temperature value from KTIP weather station, square markers denote measured temperature values from ballast, and circular markers denote measured temperature values inside concrete.

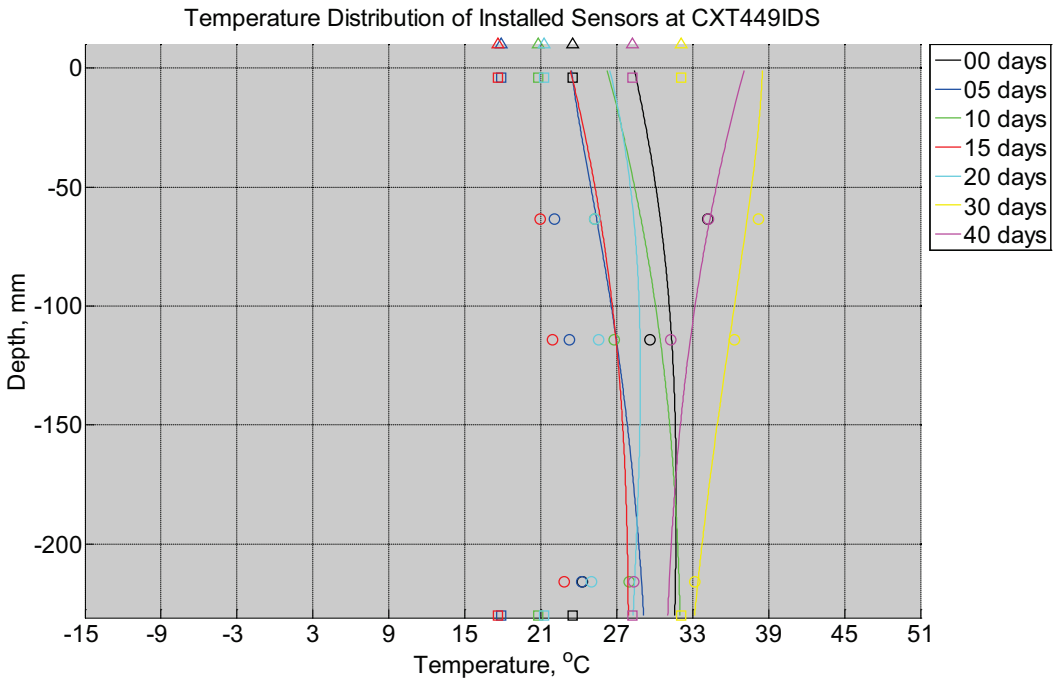

Figure B-577 Measured (markers) and modeled (continuous line) temperature profile distribution as a function of depth inside a concrete crosstie (labeled CXT449IDS) without a polyurethane pad nor rail installed in ballast in Rantoul, IL, between May 21, 2014, through July 2, 2014. Triangular markers denote temperature value from KTIP weather station, square markers denote measured temperature values from ballast, and circular markers denote measured temperature values inside concrete.

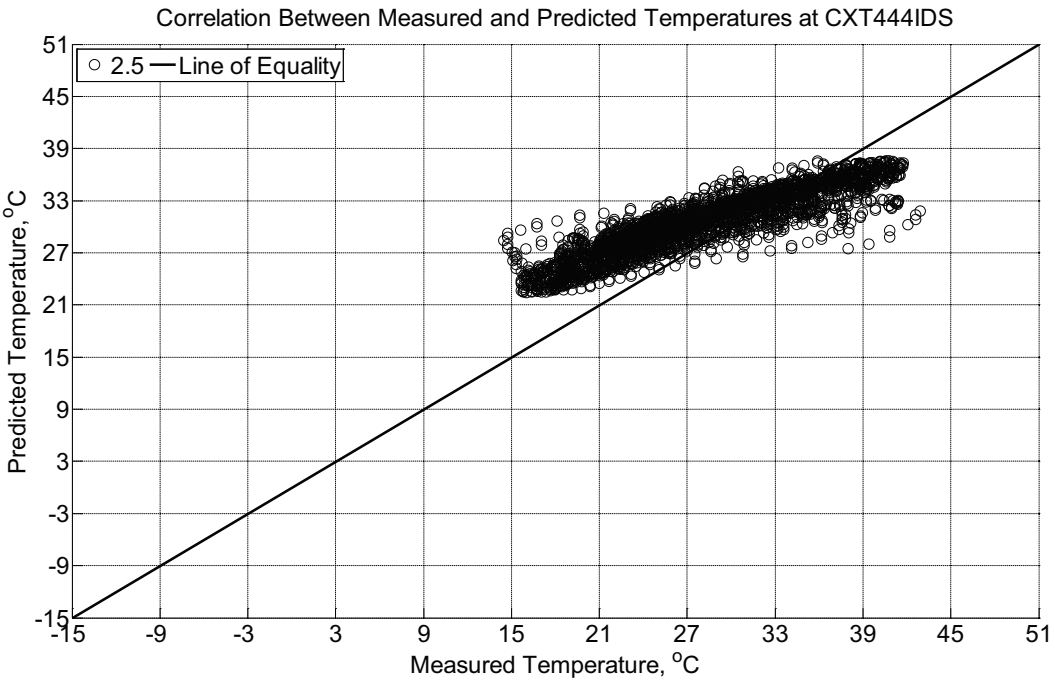

Figure B-578 Correlation between measured and predicted temperature values 2.5 inches (63.5 mm) from the surface of a concrete crosstie (labeled CXT444IDS) without a polyurethane pad nor rail installed in ballast in Rantoul, IL, between May 21, 2014, through July 2, 2014.

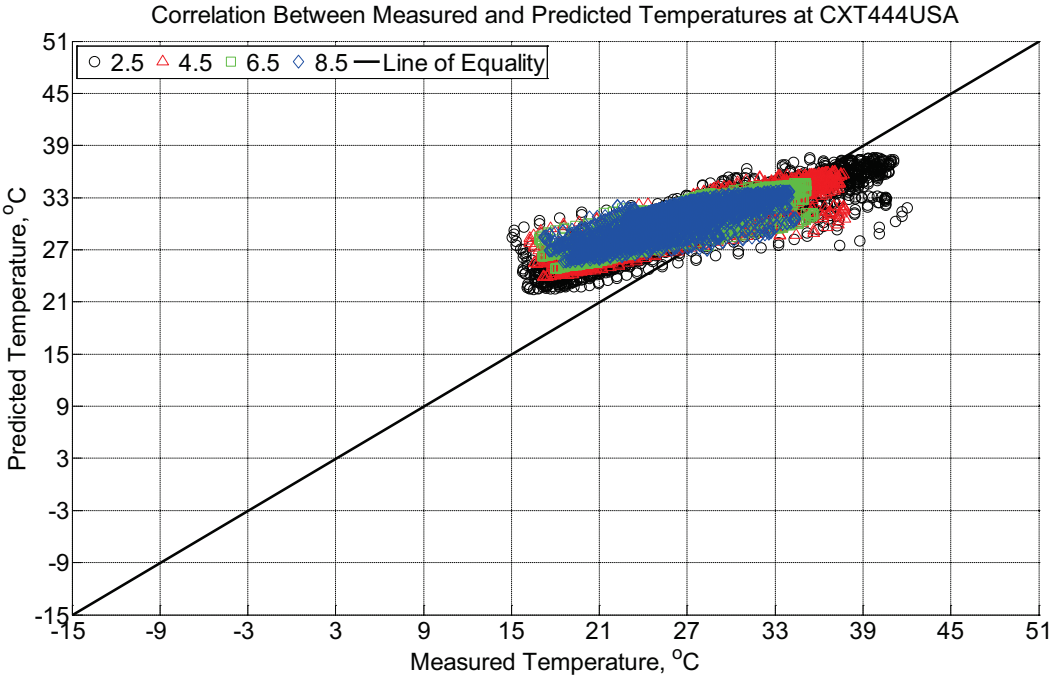

Figure B-579 Correlation between measured and predicted temperature values 2.5 inches (63.5 mm), 4.5 inches (114.3 mm), 6.5 inches (139.7 mm), and 8.5 inches (215.9 mm) from

the surface of a concrete crosstie (labeled CXT444USA) without a polyurethane pad nor rail installed in ballast in Rantoul, IL, between May 21, 2014, through July 2, 2014.

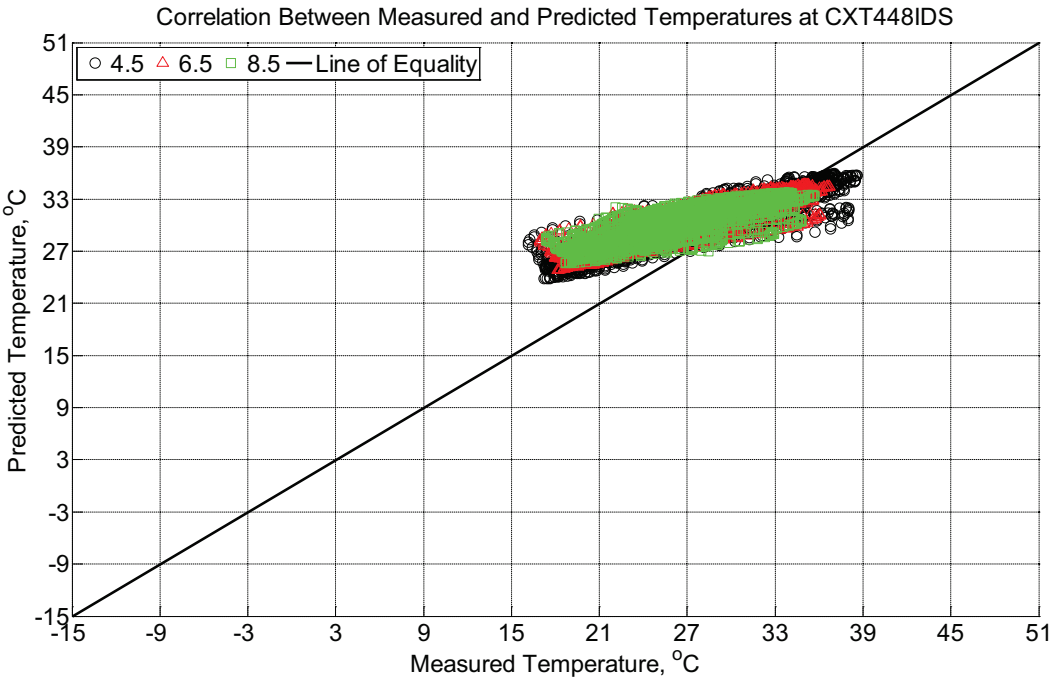

Figure B-580 Correlation between measured and predicted temperature values 4.5 inches (114.3 mm), 6.5 inches (139.7 mm), and 8.5 inches (215.9 mm) from the surface of a concrete crosstie (labeled CXT448IDS) without a polyurethane pad nor rail installed in ballast in Rantoul, IL, between May 21, 2014, through July 2, 2014.

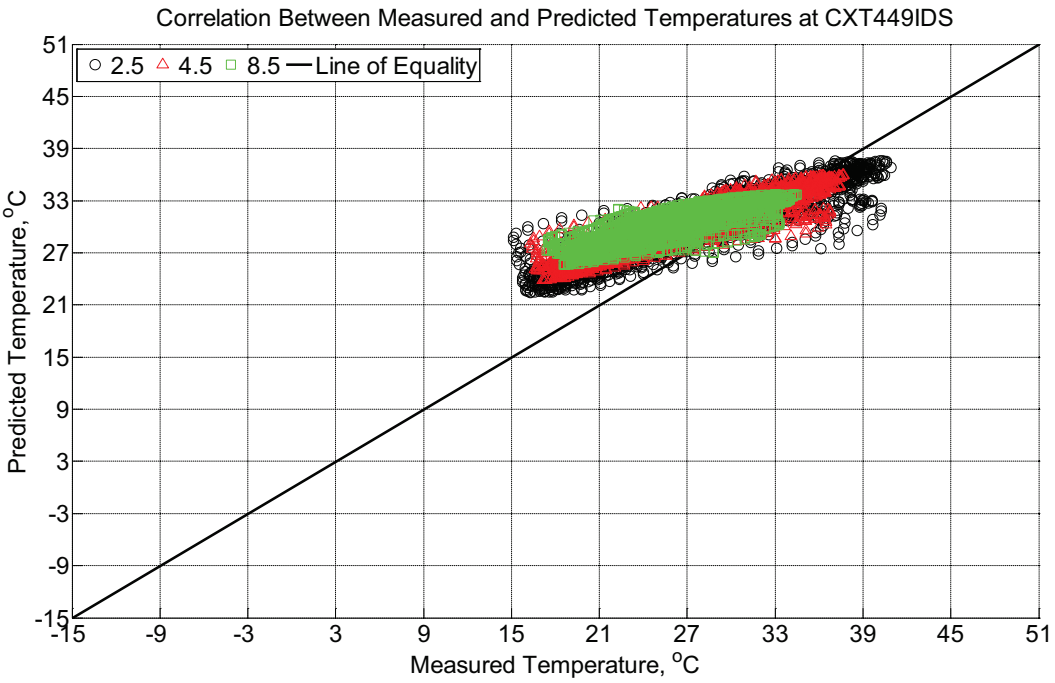

Figure B-581 Correlation between measured and predicted temperature values 2.5 inches (63.5 mm), 4.5 inches (114.3 mm), and 8.5 inches (215.9 mm) from the surface of a concrete crosstie (labeled CXT449IDS) without a polyurethane pad nor rail installed in ballast in Rantoul, IL, between May 21, 2014, through July 2, 2014.

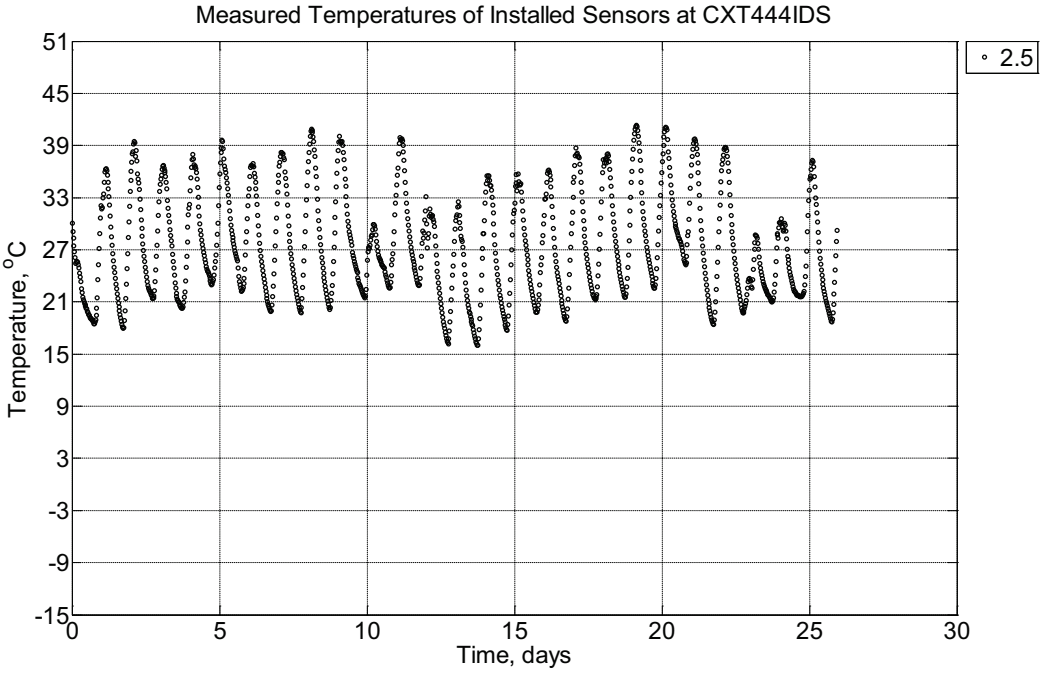

Figure B-582 Measured temperature at a depth of 2.5 inches (63.5 mm) from the surface of

a concrete crosstie (labeled CXT444IDS) without a polyurethane pad nor rail installed in ballast in Rantoul, IL, between July 2, 2014, through July 28, 2014.

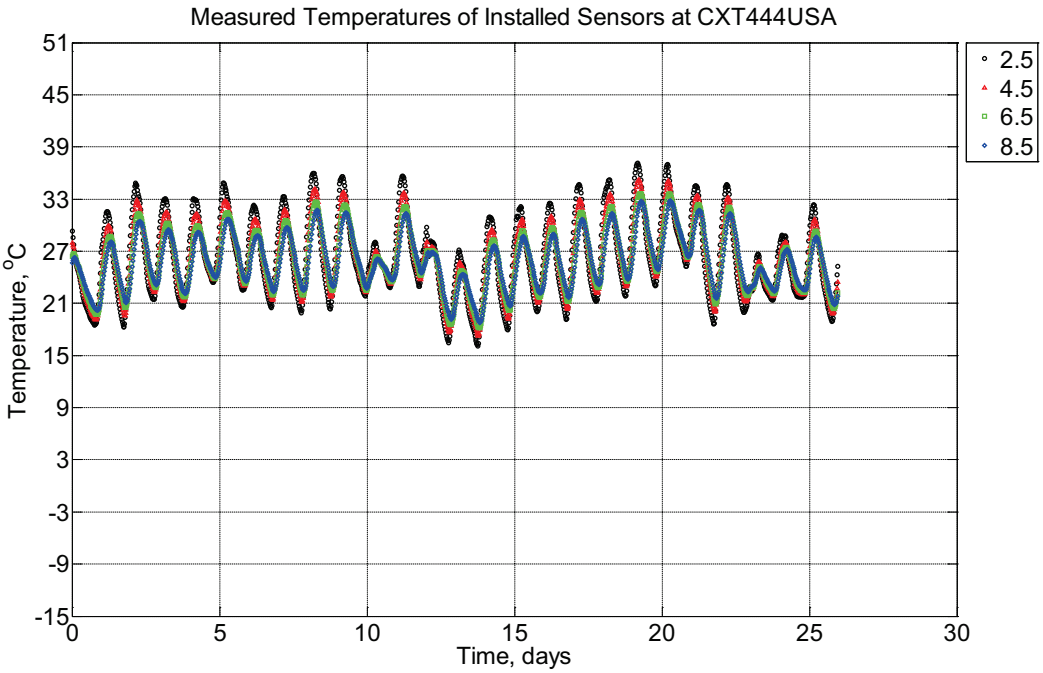

Figure B-583 Measured temperature at depths of 2.5 inches (63.5 mm), 4.5 inches (114.3 mm), 6.5 inches (139.7 mm), and 8.5 inches (215.9 mm) from the surface of a concrete crosstie (labeled CXT444USA) installed in ballast in Rantoul, IL, between July 2, 2014, through July 28, 2014. An 8 mm thick polyurethane pad and 12 in (30.48 cm) length 136 lb/yd (67.5 kg/m) section of steel rail are additionally installed atop the concrete crosstie.

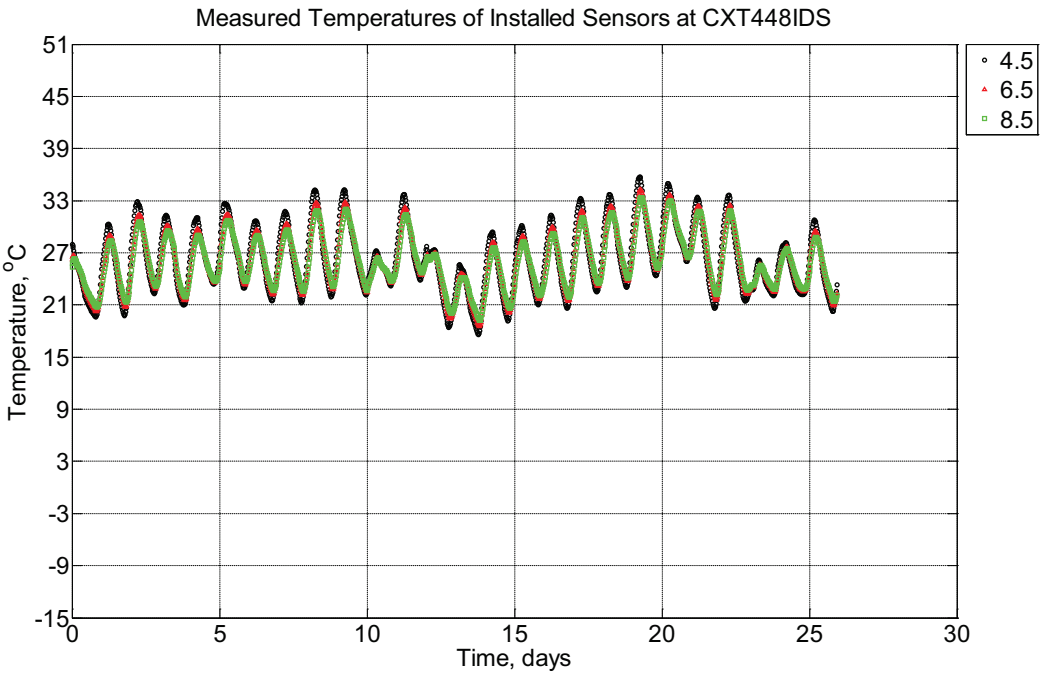

Figure B-584 Measured temperature at depths of 4.5 inches (114.3 mm), 6.5 inches (139.7 mm), and 8.5 inches (215.9 mm) from the surface of a concrete crosstie (labeled CXT448IDS) installed in ballast in Rantoul, IL, between July 2, 2014, through July 28, 2014. An 8 mm thick polyurethane pad and 12 in (30.48 cm) length 136 lb/yd (67.5 kg/m) section of steel rail are additionally installed atop the concrete crosstie.

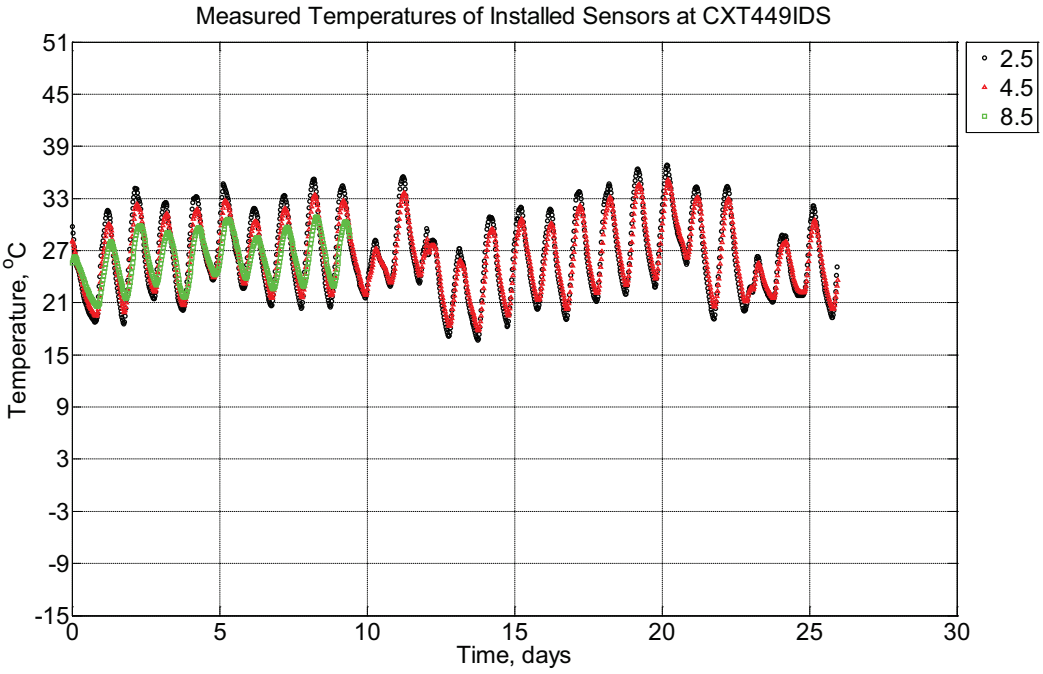

Figure B-585 Measured temperature at depths of 2.5 inches (63.5 mm), 4.5 inches (114.3

mm), and 8.5 inches (215.9 mm) from the surface of a concrete crosstie (labeled CXT449IDS) installed in ballast in Rantoul, IL, between July 2, 2014, through July 28, 2014. An 8 mm thick polyurethane pad and 12 in (30.48 cm) length 136 lb/yd (67.5 kg/m) section of steel rail are additionally installed atop the concrete crosstie.

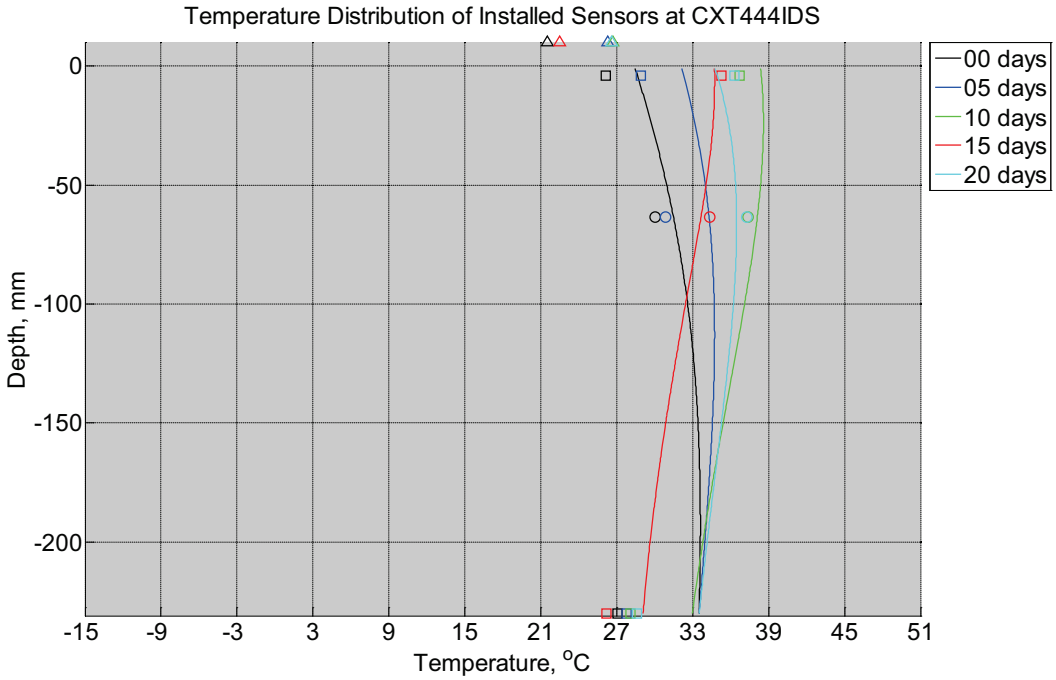

Figure B-586 Measured (markers) and modeled (continuous line) temperature profile distribution as a function of depth inside a concrete crosstie (labeled CXT444IDS) without a polyurethane pad nor rail installed in ballast in Rantoul, IL, between July 2, 2014, through July 28, 2014. Triangular markers denote temperature value from KTIP weather station, square markers denote measured temperature values from ballast, and circular markers denote measured temperature values inside concrete.

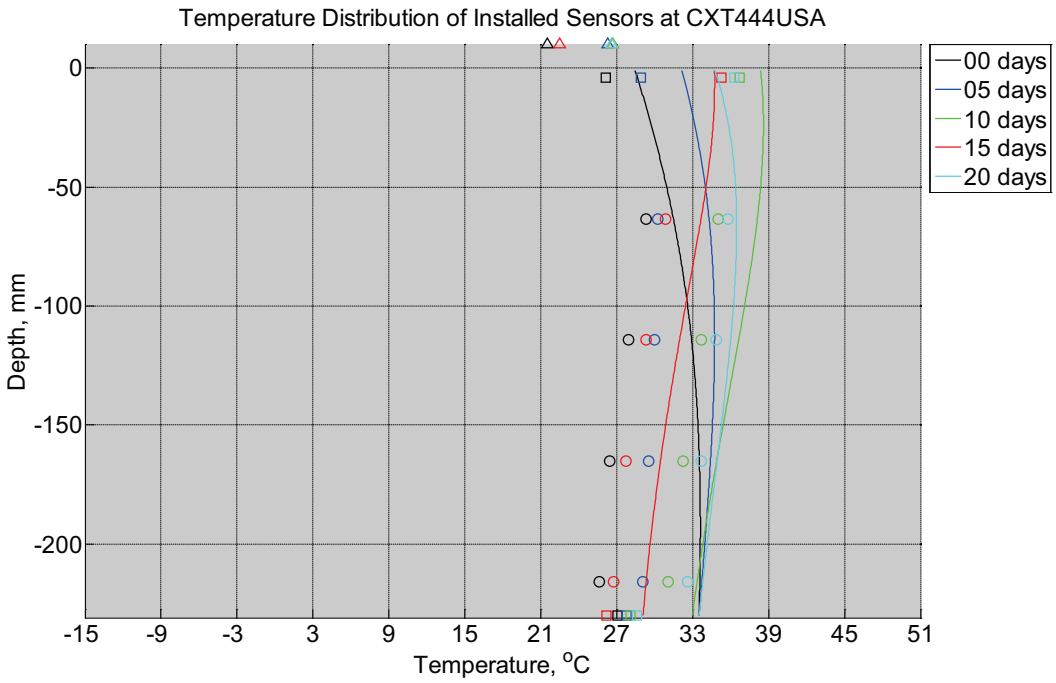

Figure B-587 Measured (markers) and modeled (continuous line) temperature profile distribution as a function of depth inside a concrete crosstie (labeled CXT444USA) installed in ballast in Rantoul, IL, between July 2, 2014, through July 28, 2014. An 8 mm thick polyurethane pad and 12 in (30.48 cm) length 136 lb/yd (67.5 kg/m) section of steel rail are additionally installed atop the model concrete crosstie. The model does not incorporate a polyurethane pad nor steel rail line. Triangular markers denote temperature value from KTIP weather station, square markers denote measured temperature values from ballast, and circular markers denote measured temperature values inside concrete.

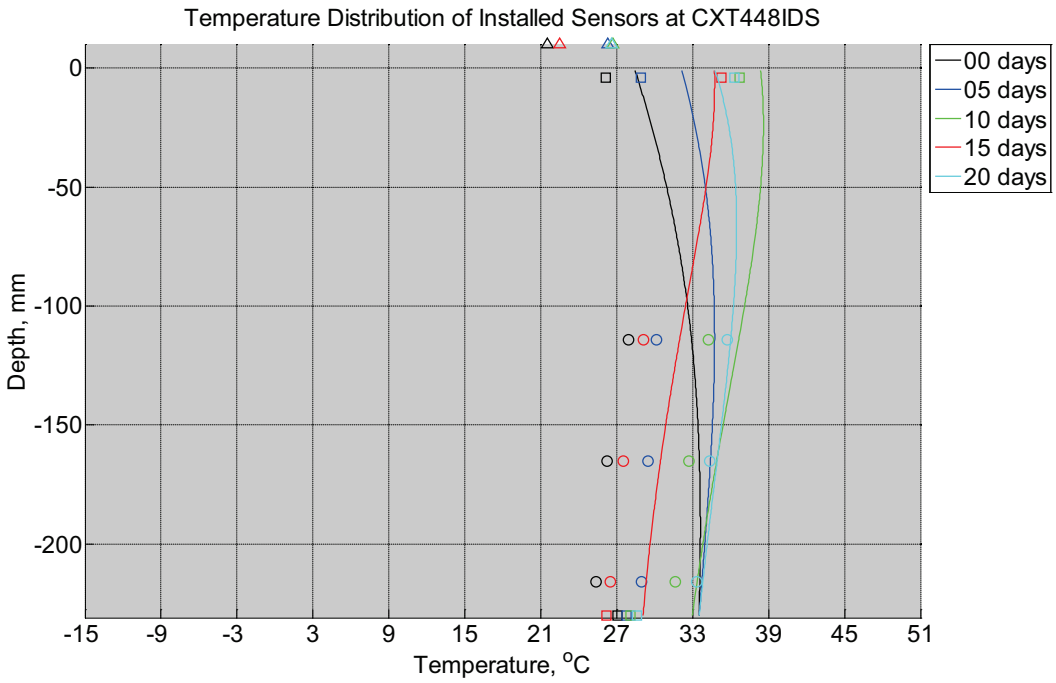

Figure B-588 Measured (markers) and modeled (continuous line) temperature profile distribution as a function of depth inside a concrete crosstie (labeled CXT448IDS) installed in ballast in Rantoul, IL, between July 2, 2014, through July 28, 2014. An 8 mm thick polyurethane pad and 12 in (30.48 cm) length 136 lb/yd (67.5 kg/m) section of steel rail are additionally installed atop the model concrete crosstie. The model does not incorporate a polyurethane pad nor steel rail line. Triangular markers denote temperature value from KTIP weather station, square markers denote measured temperature values from ballast, and circular markers denote measured temperature values inside concrete.

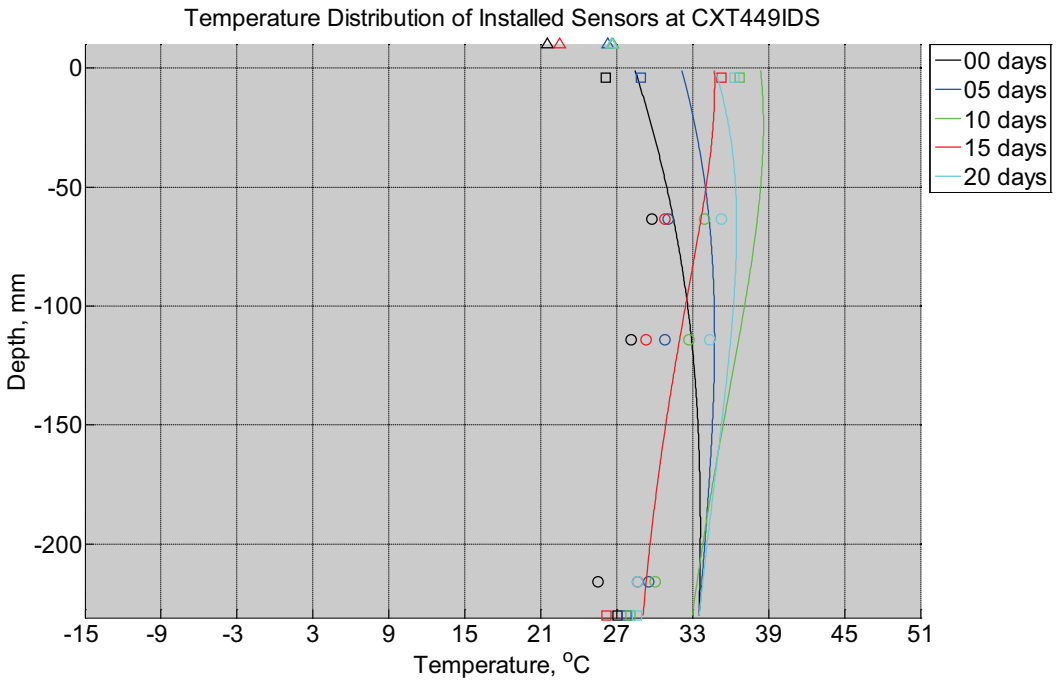

Figure B-589 Measured (markers) and modeled (continuous line) temperature profile distribution as a function of depth inside a concrete crosstie (labeled CXT449IDS) installed in ballast in Rantoul, IL, between July 2, 2014, through July 28, 2014. An 8 mm thick polyurethane pad and 12 in (30.48 cm) length 136 lb/yd (67.5 kg/m) section of steel rail are additionally installed atop the model concrete crosstie. The model does not incorporate a polyurethane pad nor steel rail line. Triangular markers denote temperature value from KTIP weather station, square markers denote measured temperature values from ballast, and circular markers denote measured temperature values inside concrete.

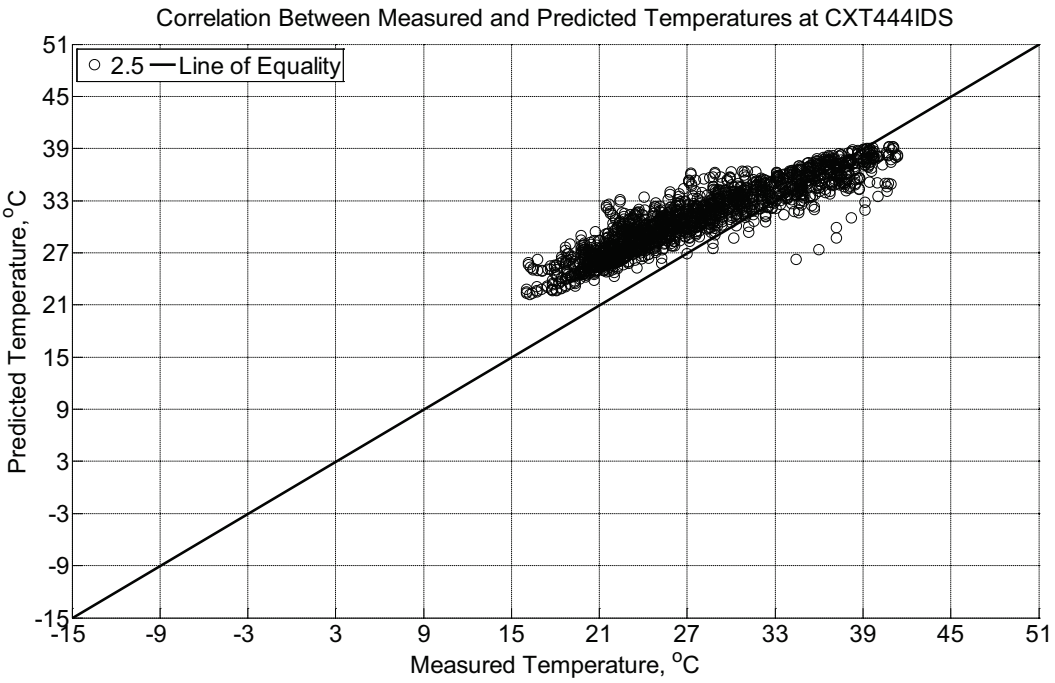

Figure B-590 Correlation between measured and predicted temperature values 2.5 inches (63.5 mm) from the surface of a concrete crosstie (labeled CXT444IDS) without a polyurethane pad nor rail installed in ballast in Rantoul, IL, between July 2, 2014, through July 28, 2014.

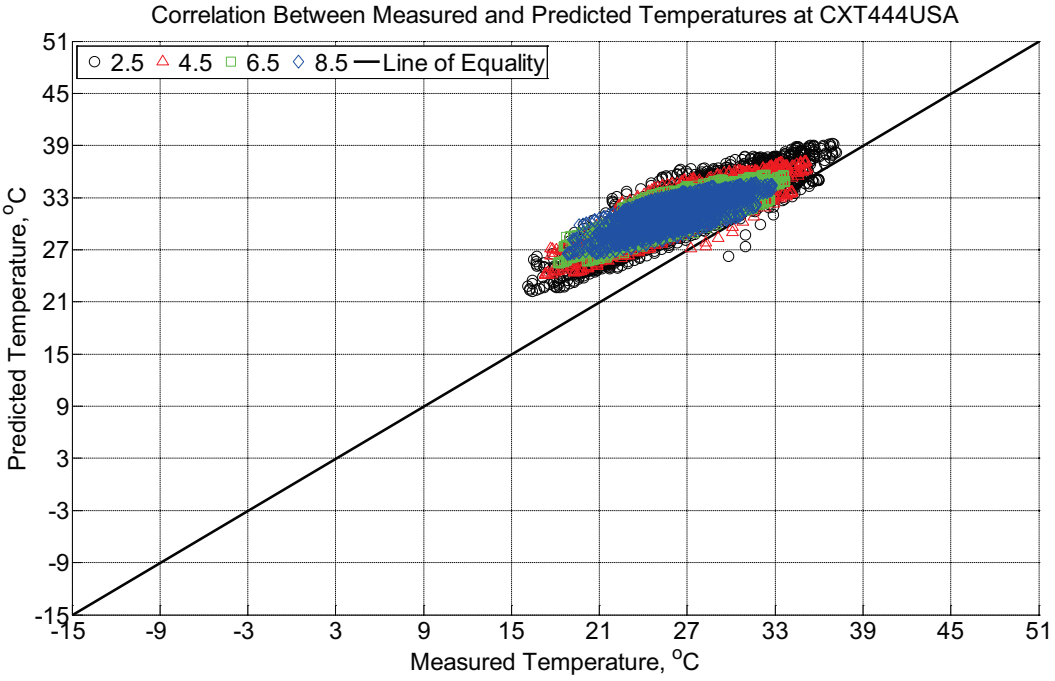

Figure B-591 Correlation between measured and predicted temperature values 2.5 inches (63.5 mm), 4.5 inches (114.3 mm), 6.5 inches (139.7 mm), and 8.5 inches (215.9 mm) from

the surface of a concrete crosstie (labeled CXT444USA) installed in ballast in Rantoul, IL, between July 2, 2014, through July 28, 2014. An 8 mm thick polyurethane pad and 12 in (30.48 cm) length 136 lb/yd (67.5 kg/m) section of steel rail are additionally installed atop the concrete crosstie. The model does not incorporate a polyurethane pad nor steel rail line.

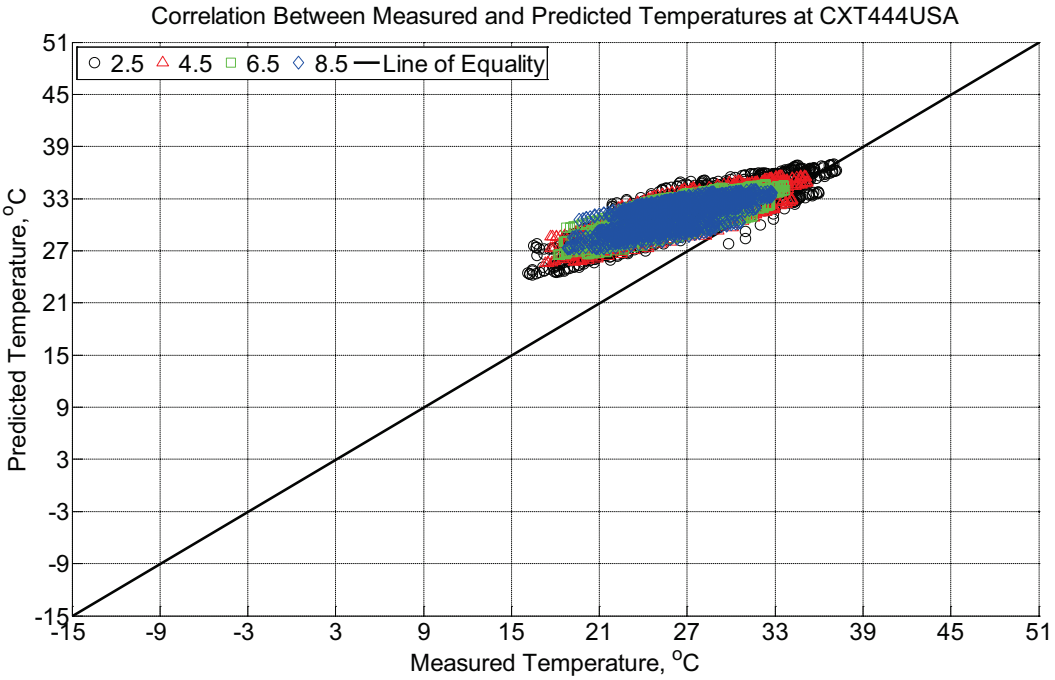

Figure B-592 Correlation between measured and predicted temperature values 2.5 inches (63.5 mm), 4.5 inches (114.3 mm), 6.5 inches (139.7 mm), and 8.5 inches (215.9 mm) from the surface of a concrete crosstie (labeled CXT444USA) installed in ballast in Rantoul, IL, between July 2, 2014, through July 28, 2014. An 8 mm thick polyurethane pad and 12 in (30.48 cm) length 136 lb/yd (67.5 kg/m) section of steel rail are additionally installed atop the concrete crosstie. The model incorporates a 1 mm thick polyurethane pad and 1 mm thick steel rail line.

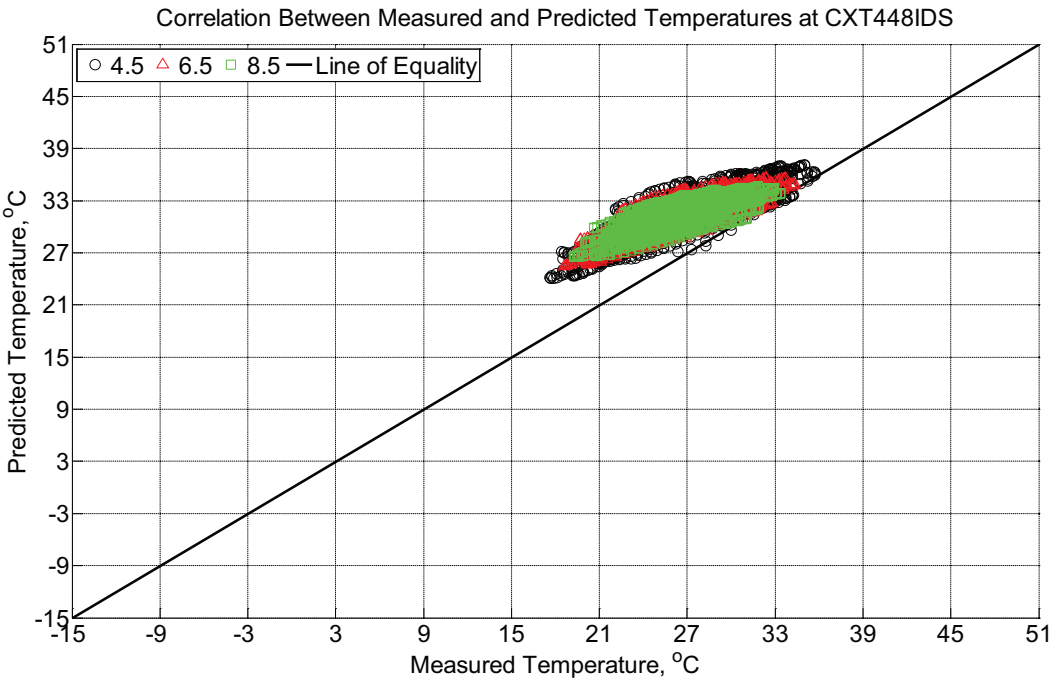

Figure B-593 Correlation between measured and predicted temperature values 4.5 inches (114.3 mm), 6.5 inches (139.7 mm), and 8.5 inches (215.9 mm) from the surface of a concrete crosstie (labeled CXT448IDS) installed in ballast in Rantoul, IL, between July 2, 2014, through July 28, 2014. An 8 mm thick polyurethane pad and 12 in (30.48 cm) length 136 lb/yd (67.5 kg/m) section of steel rail are additionally installed atop the concrete crosstie. The model does not incorporate a polyurethane pad nor steel rail line.

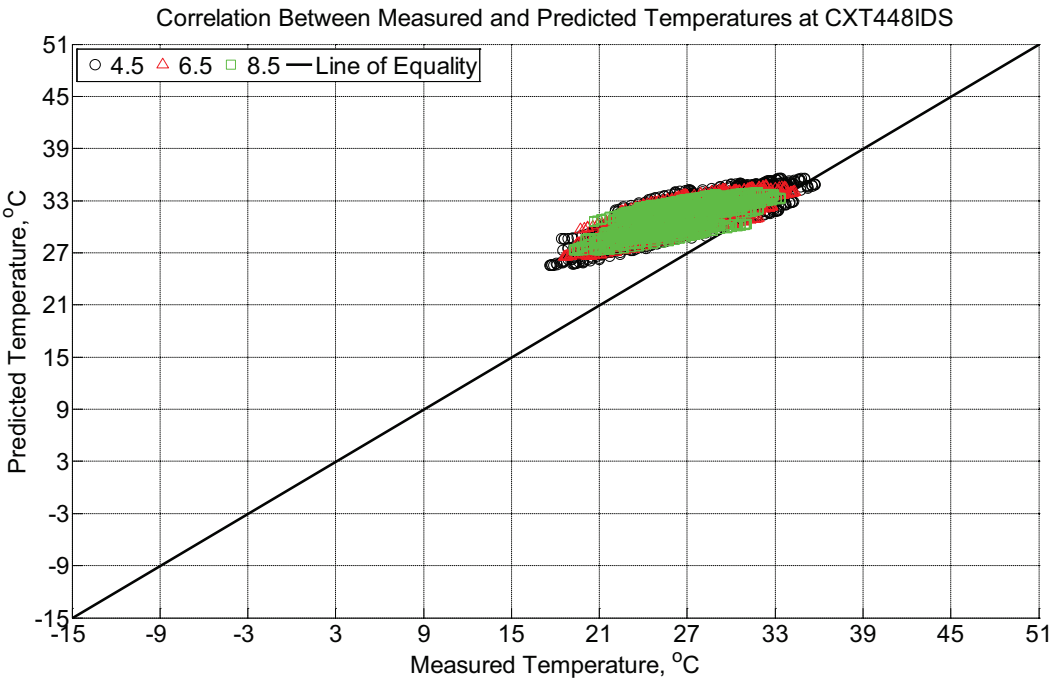

Figure B-594 Correlation between measured and predicted temperature values 4.5 inches (114.3 mm), 6.5 inches (139.7 mm), and 8.5 inches (215.9 mm) from the surface of a concrete crosstie (labeled CXT448IDS) installed in ballast in Rantoul, IL, between July 2, 2014, through July 28, 2014. An 8 mm thick polyurethane pad and 12 in (30.48 cm) length 136 lb/yd (67.5 kg/m) section of steel rail are additionally installed atop the concrete crosstie. The model incorporates a 1 mm thick polyurethane pad and 1 mm thick steel rail line.

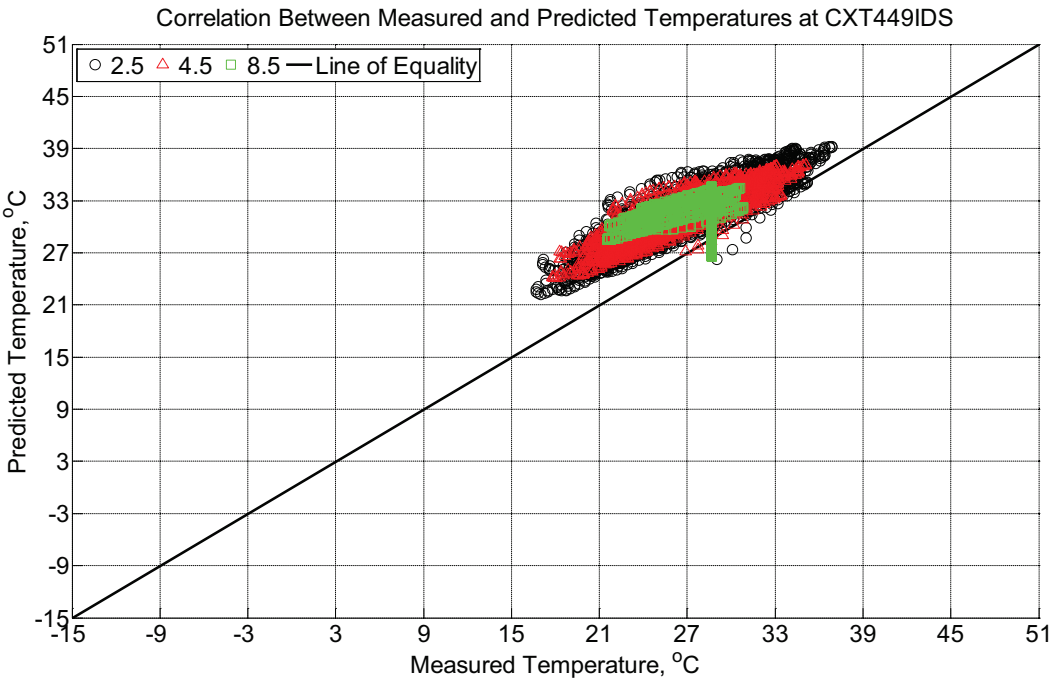

Figure B-595 Correlation between measured and predicted temperature values 2.5 inches (63.5 mm), 4.5 inches (114.3 mm), and 8.5 inches (215.9 mm) from the surface of a concrete crosstie (labeled CXT449IDS) installed in ballast in Rantoul, IL, between July 2, 2014, through July 28, 2014. An 8 mm thick polyurethane pad and 12 in (30.48 cm) length 136 lb/yd (67.5 kg/m) section of steel rail are additionally installed atop the concrete crosstie. The model does not incorporate a polyurethane pad nor steel rail line.

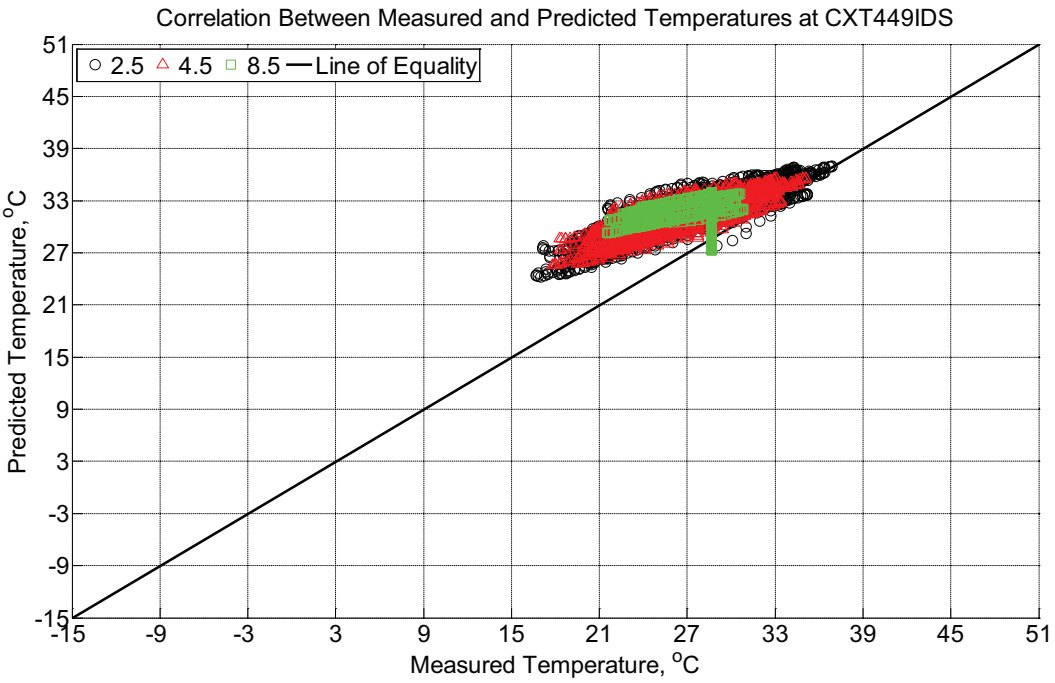

Figure B-596 Correlation between measured and predicted temperature values 2.5 inches (63.5 mm), 4.5 inches (114.3 mm), and 8.5 inches (215.9 mm) from the surface of a concrete crosstie (labeled CXT449IDS) installed in ballast in Rantoul, IL, between July 2, 2014, through July 28, 2014. An 8 mm thick polyurethane pad and 12 in (30.48 cm) length 136 lb/yd (67.5 kg/m) section of steel rail are additionally installed atop the concrete crosstie. The model incorporates a 1 mm thick polyurethane pad and 1 mm thick steel rail line.

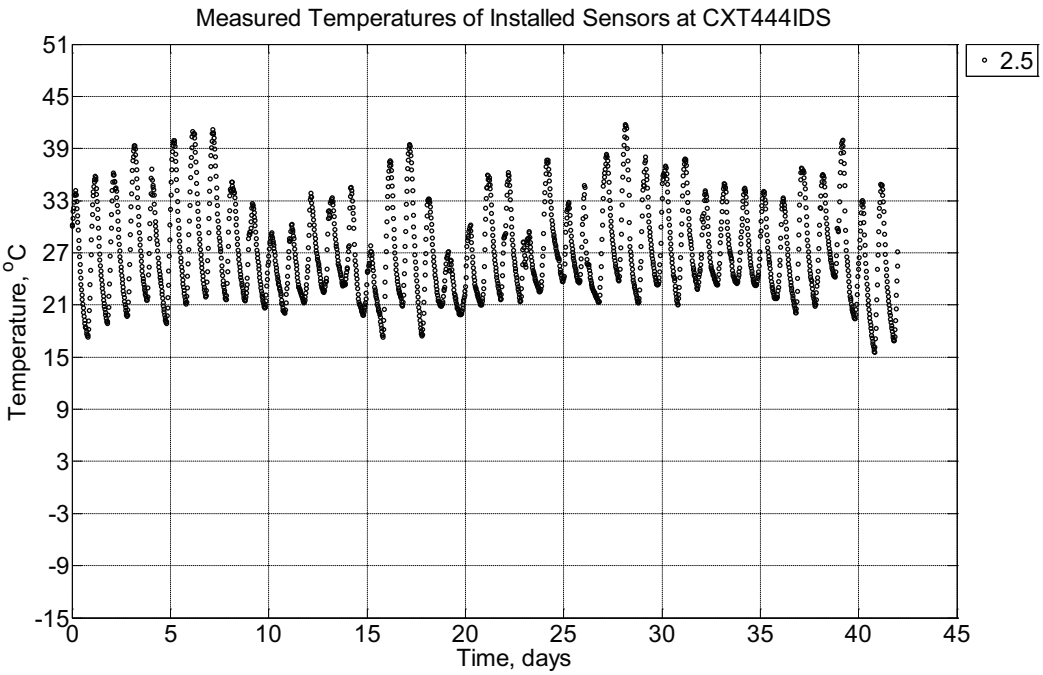

Figure B-597 Measured temperature at a depth of 2.5 inches (63.5 mm) from the surface of a concrete crosstie (labeled CXT444IDS) without a polyurethane pad nor rail installed in ballast in Rantoul, IL, between July 28, 2014, through September 8, 2014.

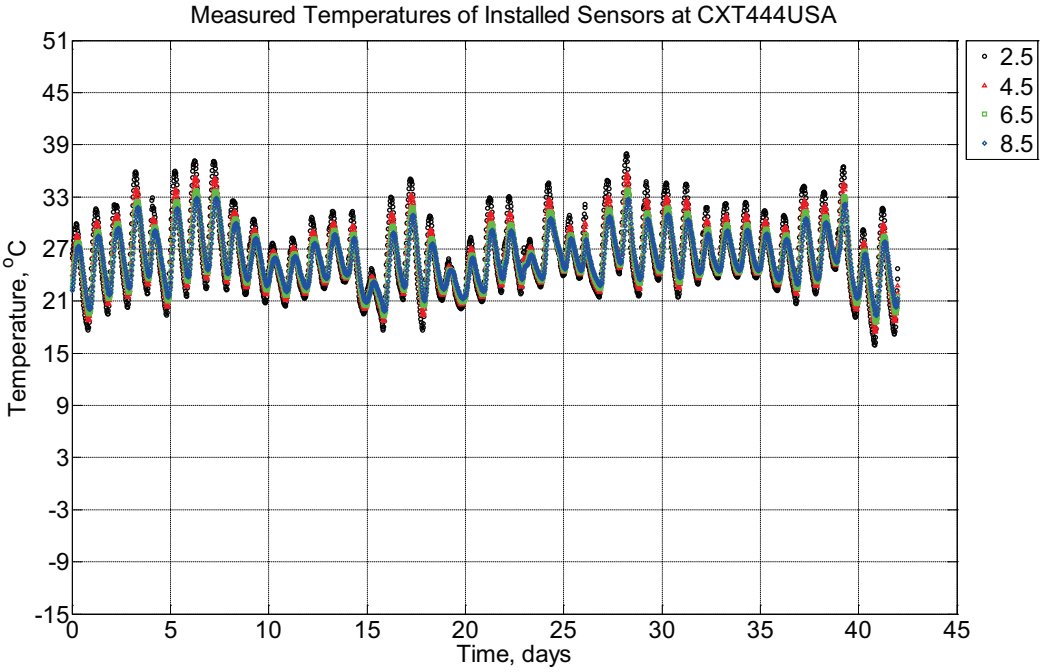

Figure B-598 Measured temperature at depths of 2.5 inches (63.5 mm), 4.5 inches (114.3 mm), 6.5 inches (139.7 mm), and 8.5 inches (215.9 mm) from the surface of a concrete crosstie (labeled CXT444USA) installed in ballast in Rantoul, IL, between July 28, 2014,

through September 8, 2014. An 8 mm thick polyurethane pad and 12 in (30.48 cm) length 136 lb/yd (67.5 kg/m) section of steel rail are additionally installed atop the concrete crosstie.

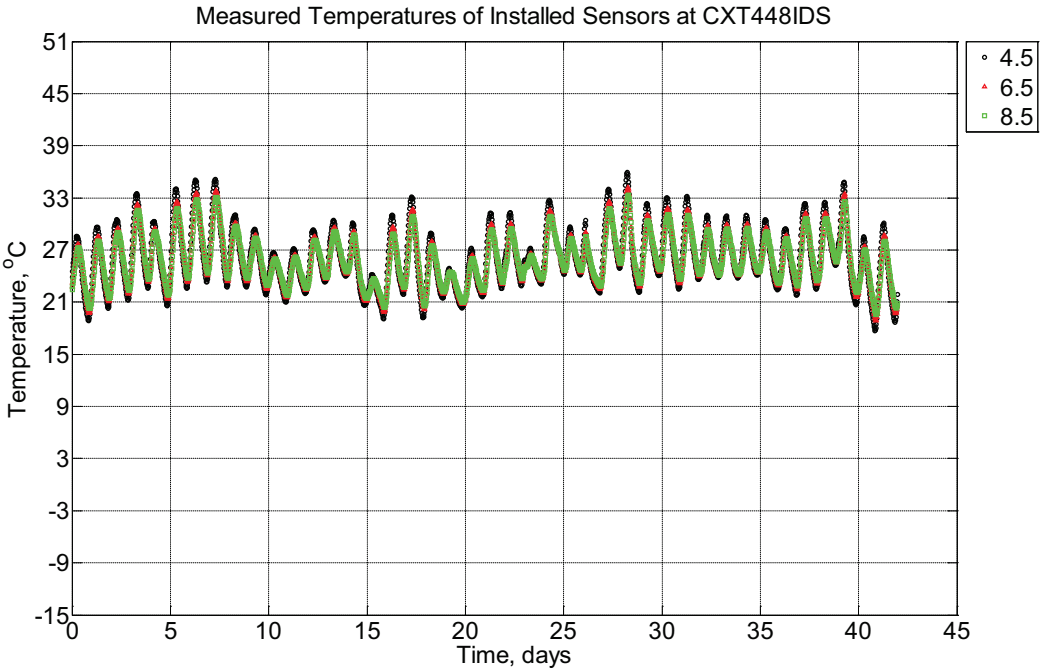

Figure B-599 Measured temperature at depths of 4.5 inches (114.3 mm), 6.5 inches (139.7 mm), and 8.5 inches (215.9 mm) from the surface of a concrete crosstie (labeled CXT448IDS) installed in ballast in Rantoul, IL, between July 28, 2014, through September 8, 2014. An 8 mm thick polyurethane pad and 12 in (30.48 cm) length 136 lb/yd (67.5 kg/m) section of steel rail are additionally installed atop the concrete crosstie.

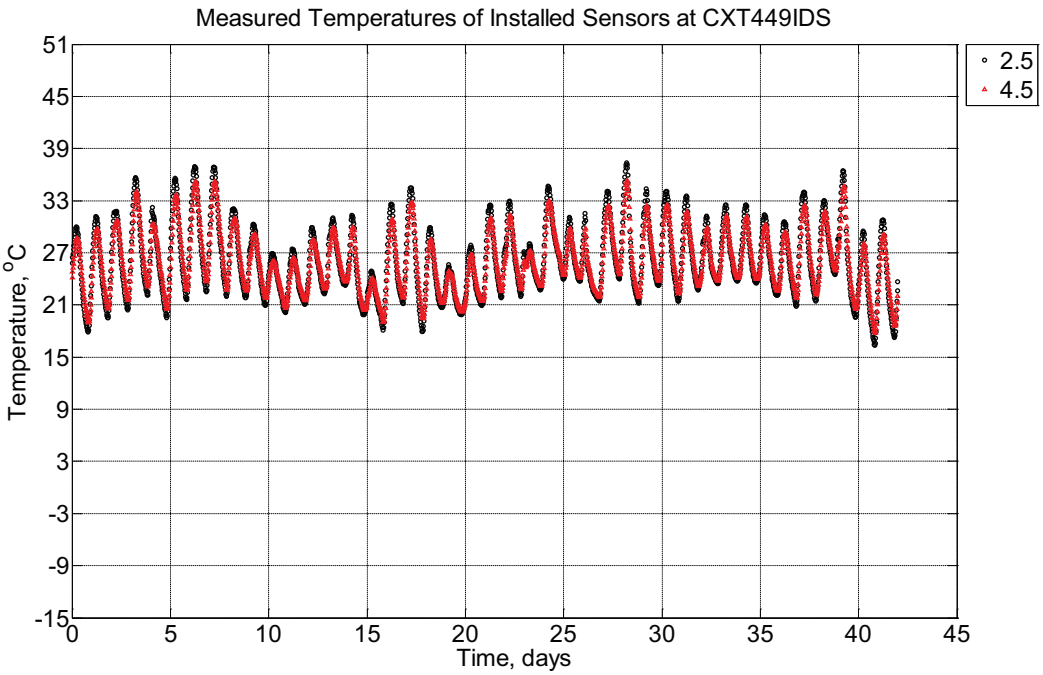

Figure B-600 Measured temperature at depths of 2.5 inches (63.5 mm) and 4.5 inches (114.3 mm) from the surface of a concrete crosstie (labeled CXT449IDS) installed in ballast in Rantoul, IL, between July 28, 2014, through September 8, 2014. An 8 mm thick polyurethane pad and 12 in (30.48 cm) length 136 lb/yd (67.5 kg/m) section of steel rail are additionally installed atop the concrete crosstie.

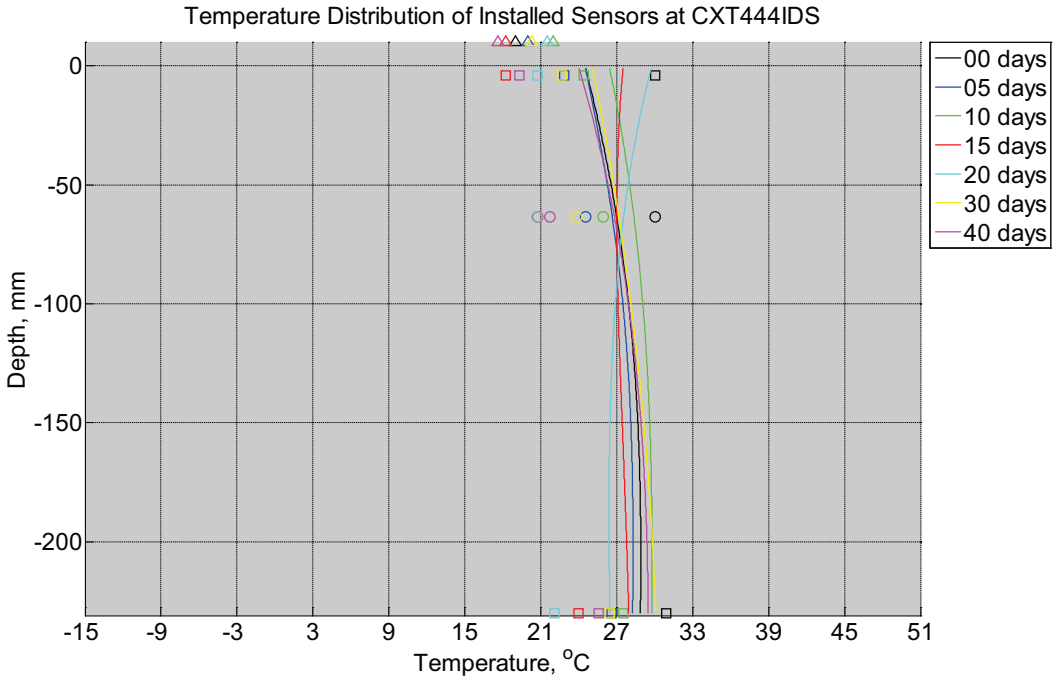

Figure B-601 Measured (markers) and modeled (continuous line) temperature profile

distribution as a function of depth inside a concrete crosstie (labeled CXT444IDS) without a polyurethane pad nor rail installed in ballast in Rantoul, IL, between July 28, 2014, through September 8, 2014. Triangular markers denote temperature value from KTIP weather station, square markers denote measured temperature values from ballast, and circular markers denote measured temperature values inside concrete.

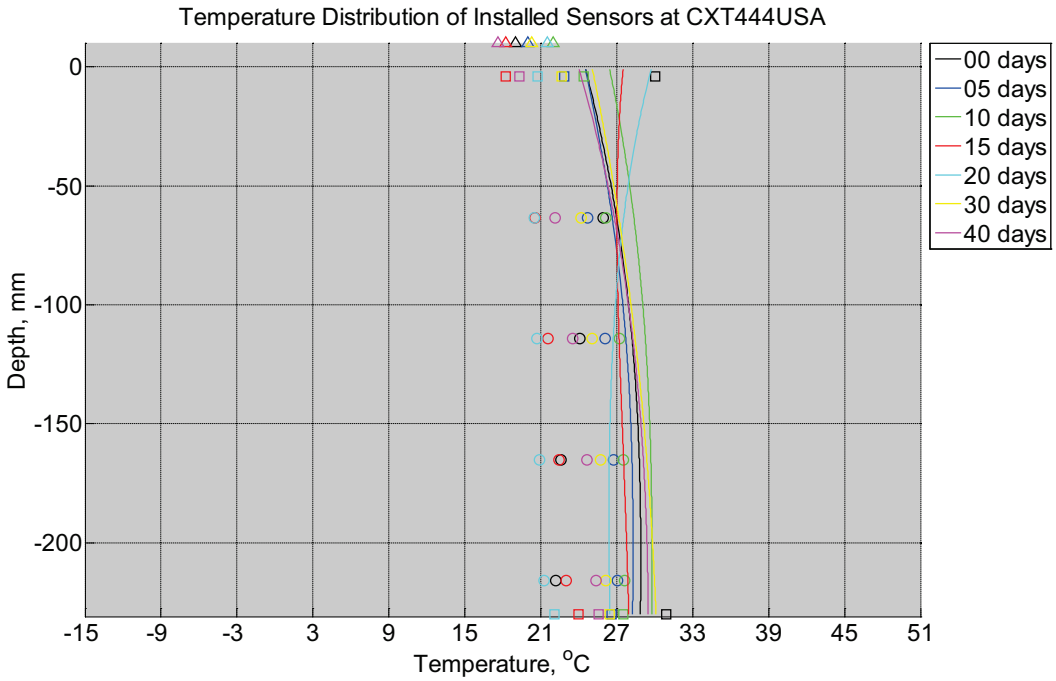

Figure B-602 Measured (markers) and modeled (continuous line) temperature profile distribution as a function of depth inside a concrete crosstie (labeled CXT444USA) installed in ballast in Rantoul, IL, between July 28, 2014, through September 8, 2014. An 8 mm thick polyurethane pad and 12 in (30.48 cm) length 136 lb/yd (67.5 kg/m) section of steel rail are additionally installed atop the model concrete crosstie. The model does not incorporate a polyurethane pad nor steel rail line. Triangular markers denote temperature value from KTIP weather station, square markers denote measured temperature values from ballast, and circular markers denote measured temperature values inside concrete.

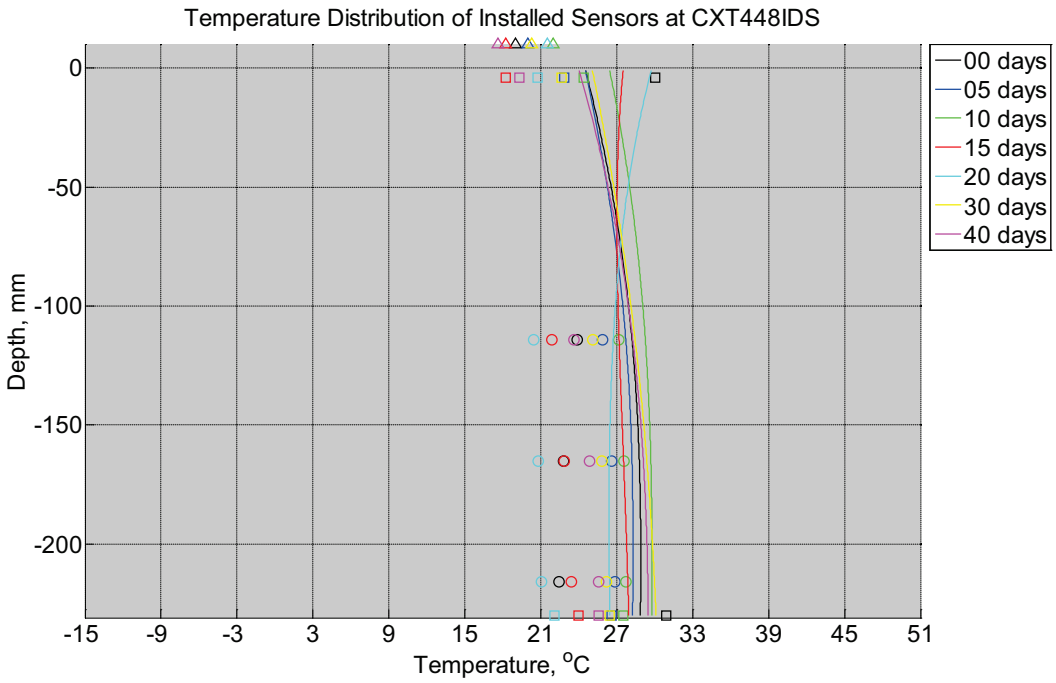

Figure B-603 Measured (markers) and modeled (continuous line) temperature profile distribution as a function of depth inside a concrete crosstie (labeled CXT448IDS) installed in ballast in Rantoul, IL, between July 28, 2014, through September 8, 2014. An 8 mm thick polyurethane pad and 12 in (30.48 cm) length 136 lb/yd (67.5 kg/m) section of steel rail are additionally installed atop the model concrete crosstie. The model does not incorporate a polyurethane pad nor steel rail line. Triangular markers denote temperature value from KTIP weather station, square markers denote measured temperature values from ballast, and circular markers denote measured temperature values inside concrete.

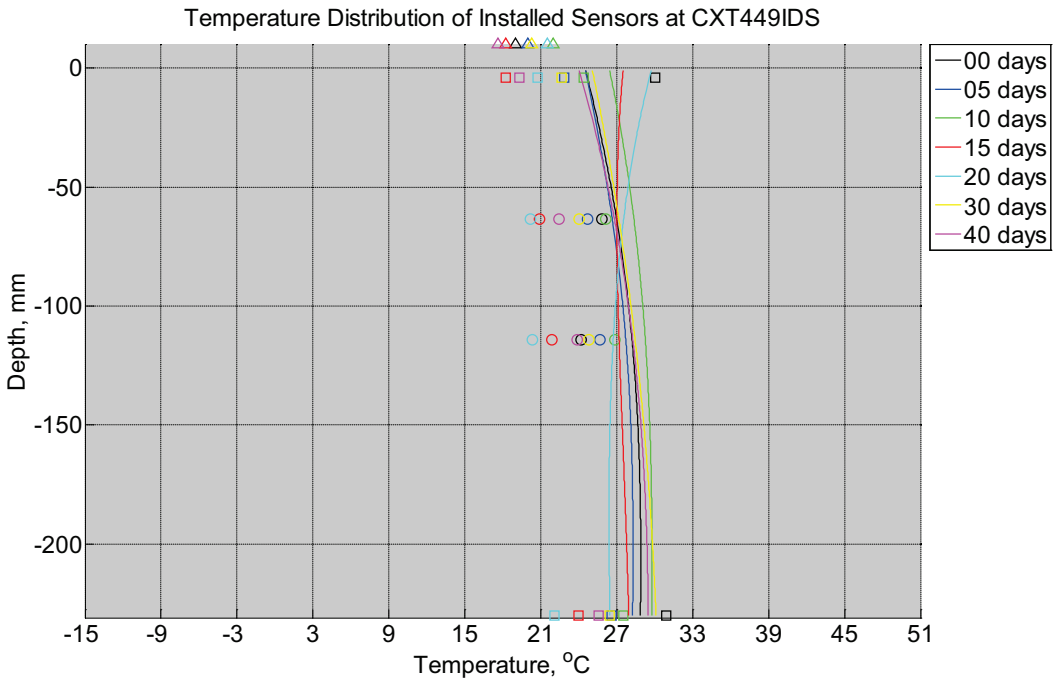

Figure B-604 Measured (markers) and modeled (continuous line) temperature profile distribution as a function of depth inside a concrete crosstie (labeled CXT449IDS) installed in ballast in Rantoul, IL, between July 28, 2014, through September 8, 2014. An 8 mm thick polyurethane pad and 12 in (30.48 cm) length 136 lb/yd (67.5 kg/m) section of steel rail are additionally installed atop the model concrete crosstie. The model does not incorporate a polyurethane pad nor steel rail line. Triangular markers denote temperature value from KTIP weather station, square markers denote measured temperature values from ballast, and circular markers denote measured temperature values inside concrete.

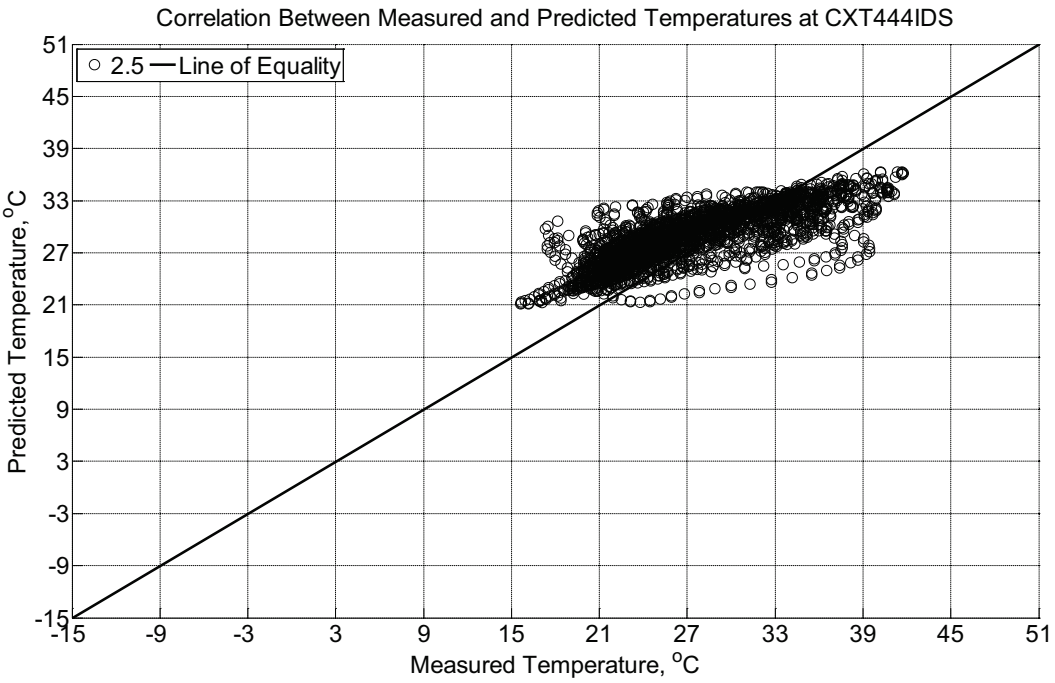

Figure B-605 Correlation between measured and predicted temperature values 2.5 inches (63.5 mm) from the surface of a concrete crosstie (labeled CXT444IDS) without a polyurethane pad nor rail installed in ballast in Rantoul, IL, between July 28, 2014, through September 8, 2014.

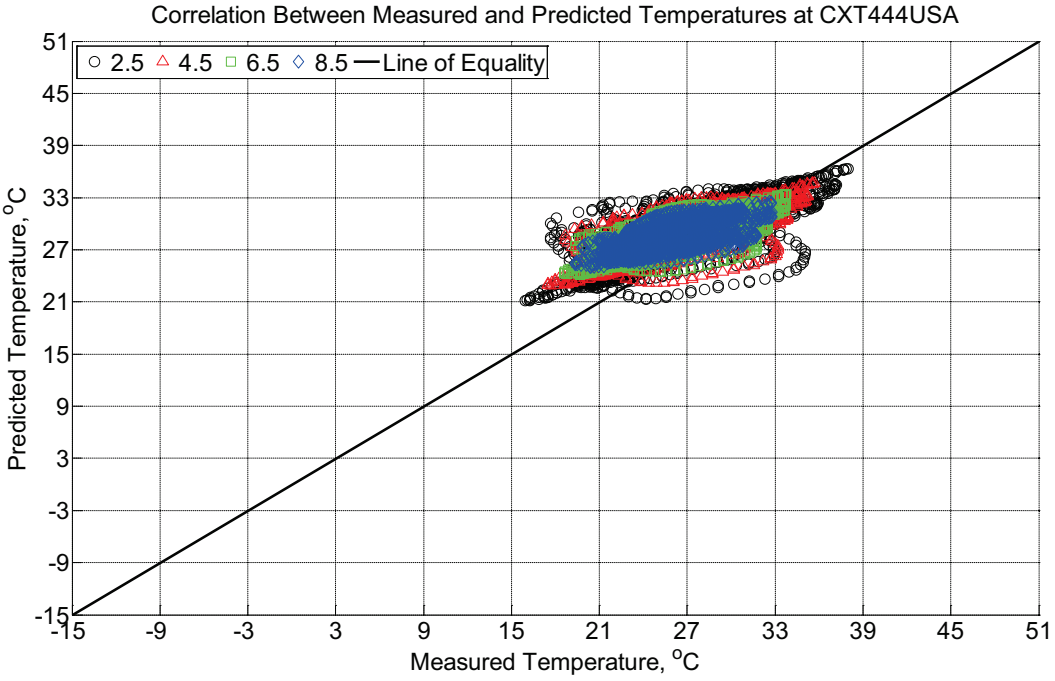

Figure B-606 Correlation between measured and predicted temperature values 2.5 inches (63.5 mm), 4.5 inches (114.3 mm), 6.5 inches (139.7 mm), and 8.5 inches (215.9 mm) from

the surface of a concrete crosstie (labeled CXT444USA) installed in ballast in Rantoul, IL, between July 28, 2014, through September 8, 2014. An 8 mm thick polyurethane pad and 12 in (30.48 cm) length 136 lb/yd (67.5 kg/m) section of steel rail are additionally installed atop the concrete crosstie. The model does not incorporate a polyurethane pad nor steel rail line.

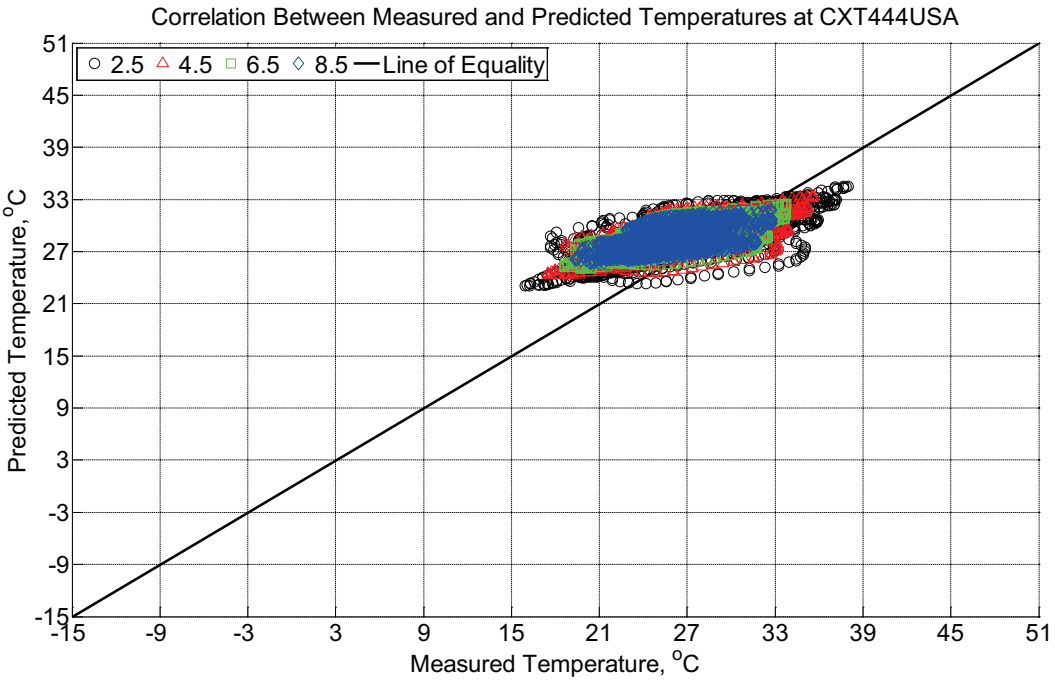

Figure B-607 Correlation between measured and predicted temperature values 2.5 inches (63.5 mm), 4.5 inches (114.3 mm), 6.5 inches (139.7 mm), and 8.5 inches (215.9 mm) from the surface of a concrete crosstie (labeled CXT444USA) installed in ballast in Rantoul, IL, between July 28, 2014, through September 8, 2014. An 8 mm thick polyurethane pad and 12 in (30.48 cm) length 136 lb/yd (67.5 kg/m) section of steel rail are additionally installed atop the concrete crosstie. The model incorporates a 1 mm thick polyurethane pad and 1 mm thick steel rail line.

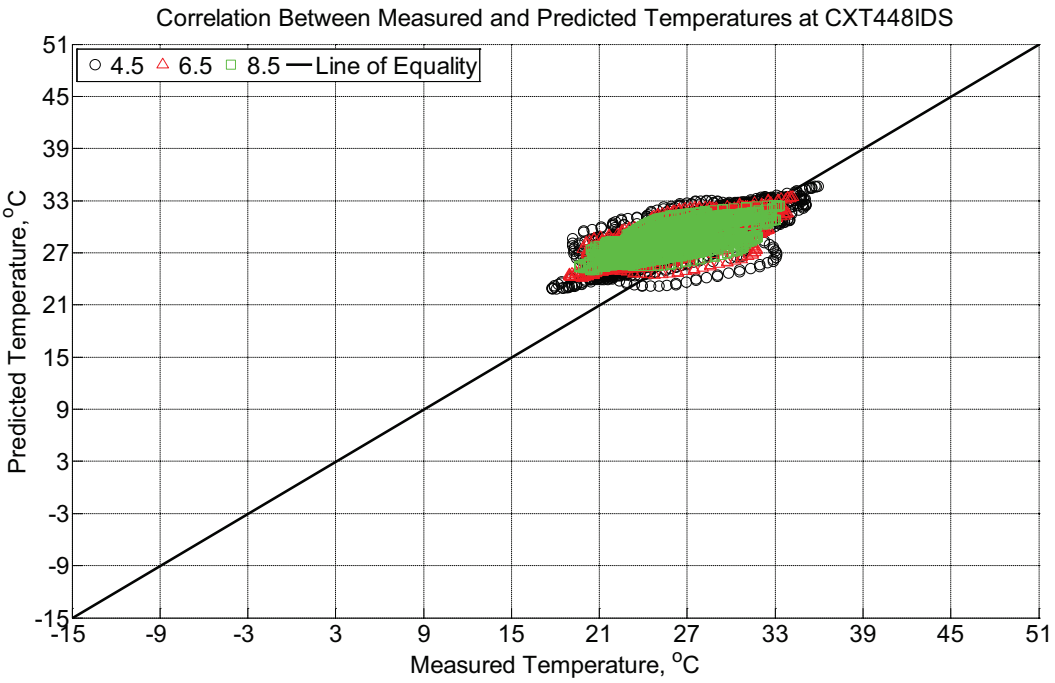

Figure B-608 Correlation between measured and predicted temperature values 4.5 inches (114.3 mm), 6.5 inches (139.7 mm), and 8.5 inches (215.9 mm) from the surface of a concrete crosstie (labeled CXT448IDS) installed in ballast in Rantoul, IL, between July 28, 2014, through September 8, 2014. An 8 mm thick polyurethane pad and 12 in (30.48 cm) length 136 lb/yd (67.5 kg/m) section of steel rail are additionally installed atop the concrete crosstie. The model does not incorporate a polyurethane pad nor steel rail line.

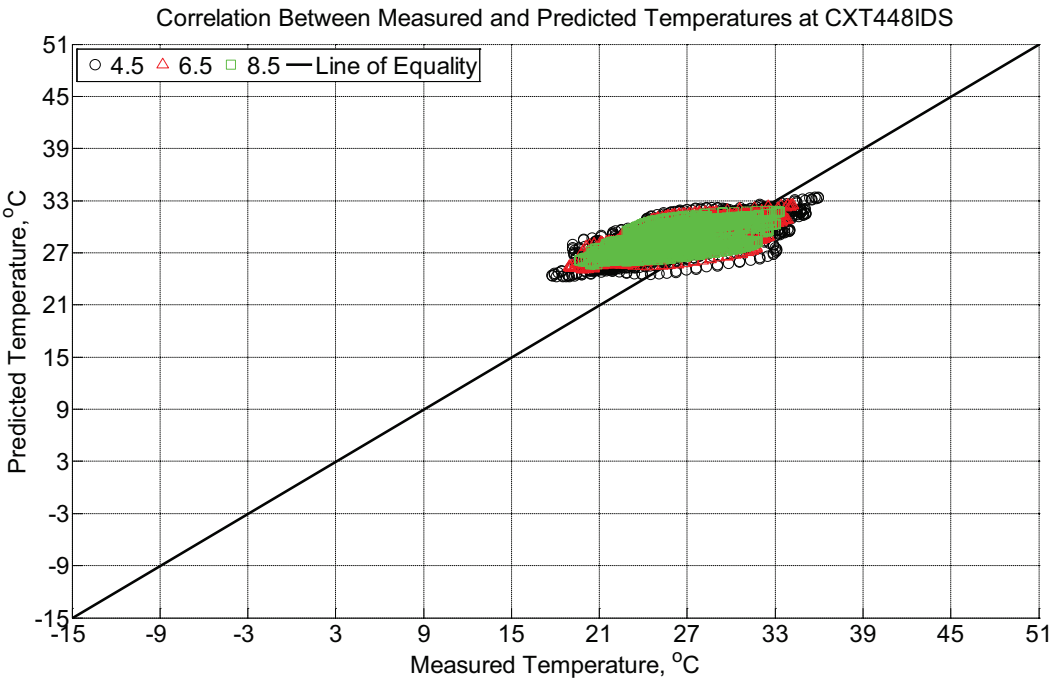

Figure B-609 Correlation between measured and predicted temperature values 4.5 inches (114.3 mm), 6.5 inches (139.7 mm), and 8.5 inches (215.9 mm) from the surface of a concrete crosstie (labeled CXT448IDS) installed in ballast in Rantoul, IL, between July 28, 2014, through September 8, 2014. An 8 mm thick polyurethane pad and 12 in (30.48 cm) length 136 lb/yd (67.5 kg/m) section of steel rail are additionally installed atop the concrete crosstie. The model incorporates a 1 mm thick polyurethane pad and 1 mm thick steel rail line.

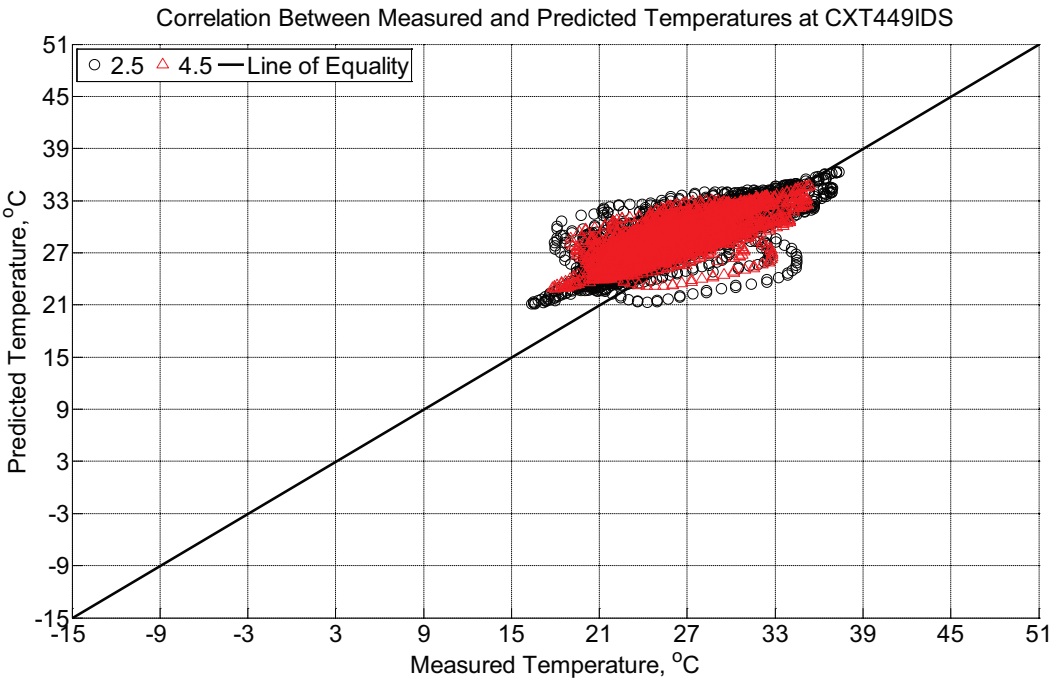

Figure B-610 Correlation between measured and predicted temperature values 2.5 inches (63.5 mm), 4.5 inches (114.3 mm), and 8.5 inches (215.9 mm) from the surface of a concrete crosstie (labeled CXT449IDS) installed in ballast in Rantoul, IL, between July 28, 2014, through September 8, 2014. An 8 mm thick polyurethane pad and 12 in (30.48 cm) length 136 lb/yd (67.5 kg/m) section of steel rail are additionally installed atop the concrete crosstie. The model does not incorporate a polyurethane pad nor steel rail line.

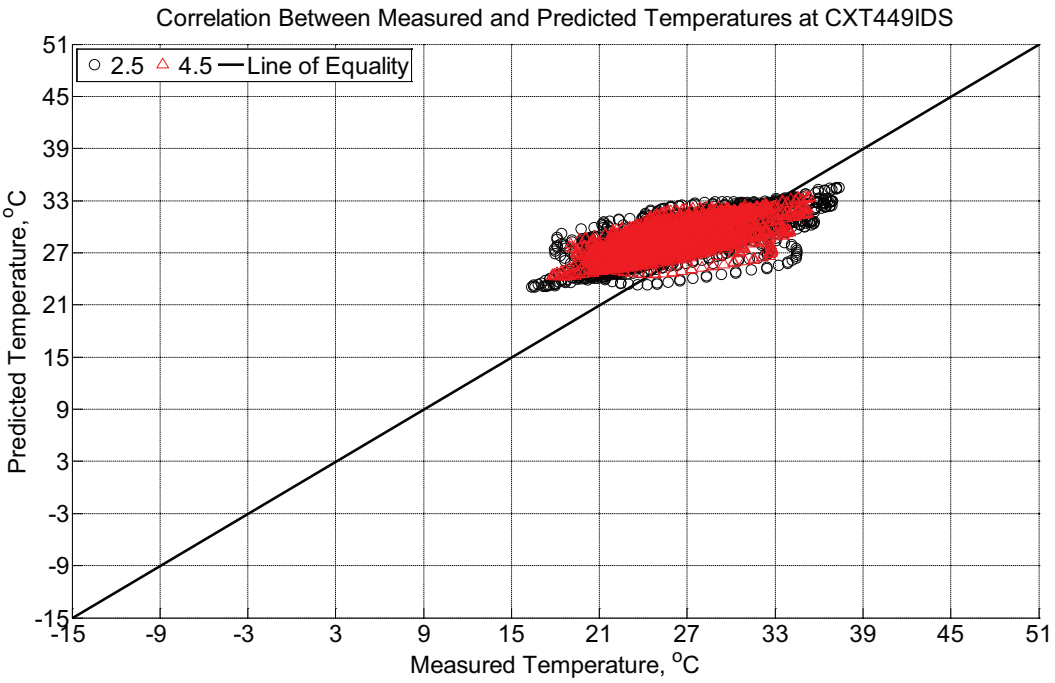

Figure B-611 Correlation between measured and predicted temperature values 2.5 inches (63.5 mm), 4.5 inches (114.3 mm), and 8.5 inches (215.9 mm) from the surface of a concrete crosstie (labeled CXT449IDS) installed in ballast in Rantoul, IL, between July 28, 2014, through September 8, 2014. An 8 mm thick polyurethane pad and 12 in (30.48 cm) length 136 lb/yd (67.5 kg/m) section of steel rail are additionally installed atop the concrete crosstie. The model incorporates a 1 mm thick polyurethane pad and 1 mm thick steel rail line.

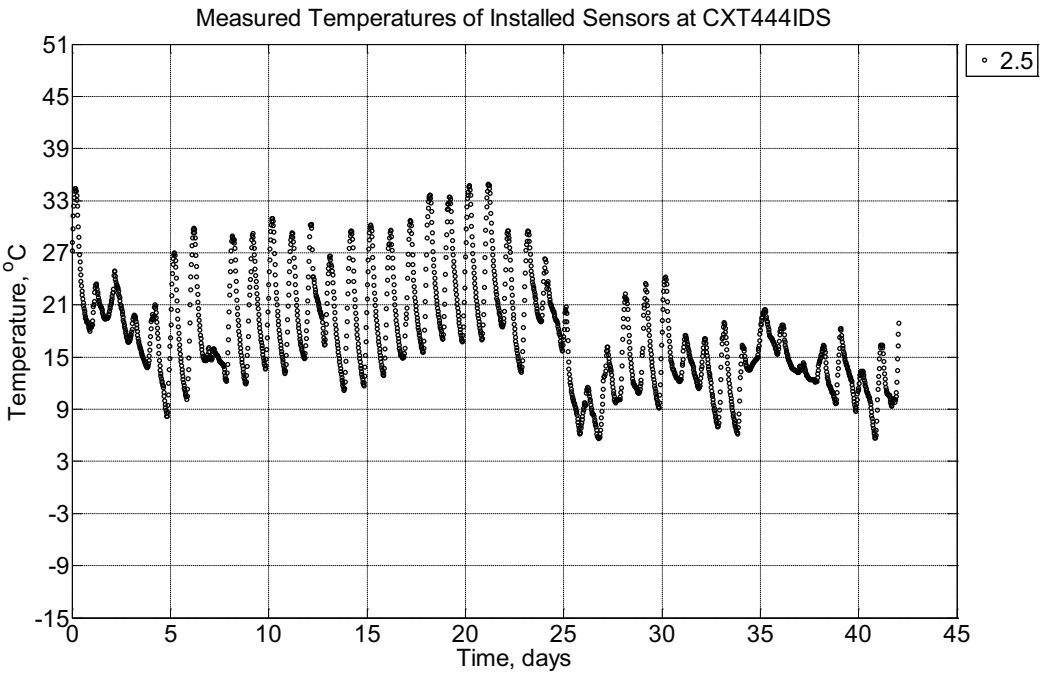

Figure B-612 Measured temperature at a depth of 2.5 inches (63.5 mm) from the surface of a concrete crosstie (labeled CXT444IDS) without a polyurethane pad nor rail installed in ballast in Rantoul, IL, between September 8, 2014, through October 20, 2014.

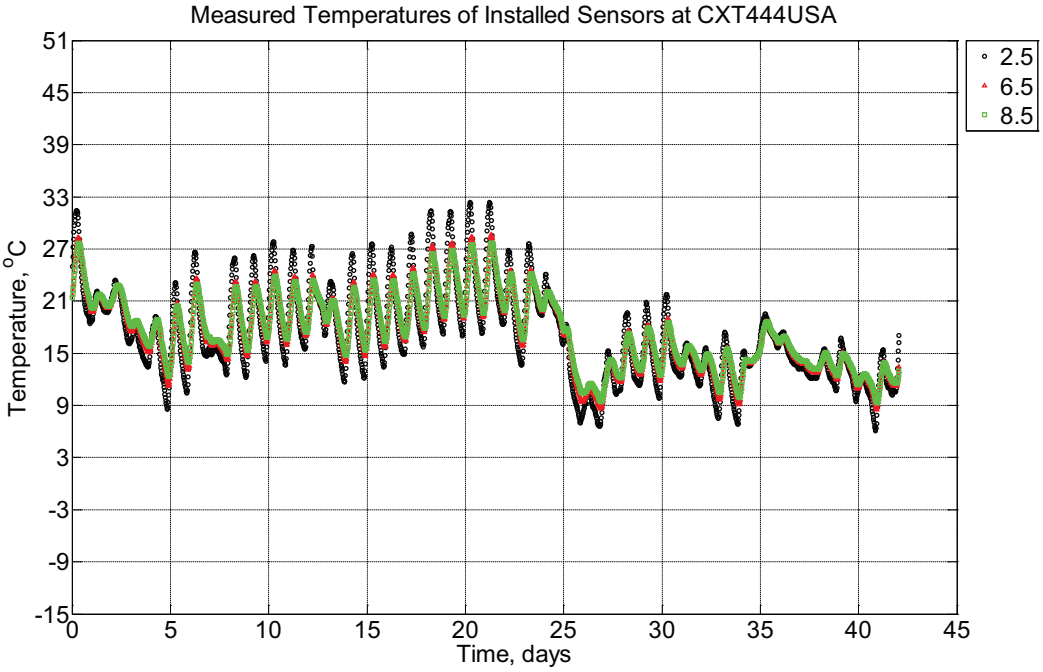

Figure B-613 Measured temperature at depths of 2.5 inches (63.5 mm), 6.5 inches (139.7 mm), and 8.5 inches (215.9 mm) from the surface of a concrete crosstie (labeled CXT444USA) installed in ballast in Rantoul, IL, between September 8, 2014, through

October 20, 2014. An 8 mm thick polyurethane pad and 12 in (30.48 cm) length 136 lb/yd (67.5 kg/m) section of steel rail are additionally installed atop the concrete crosstie.

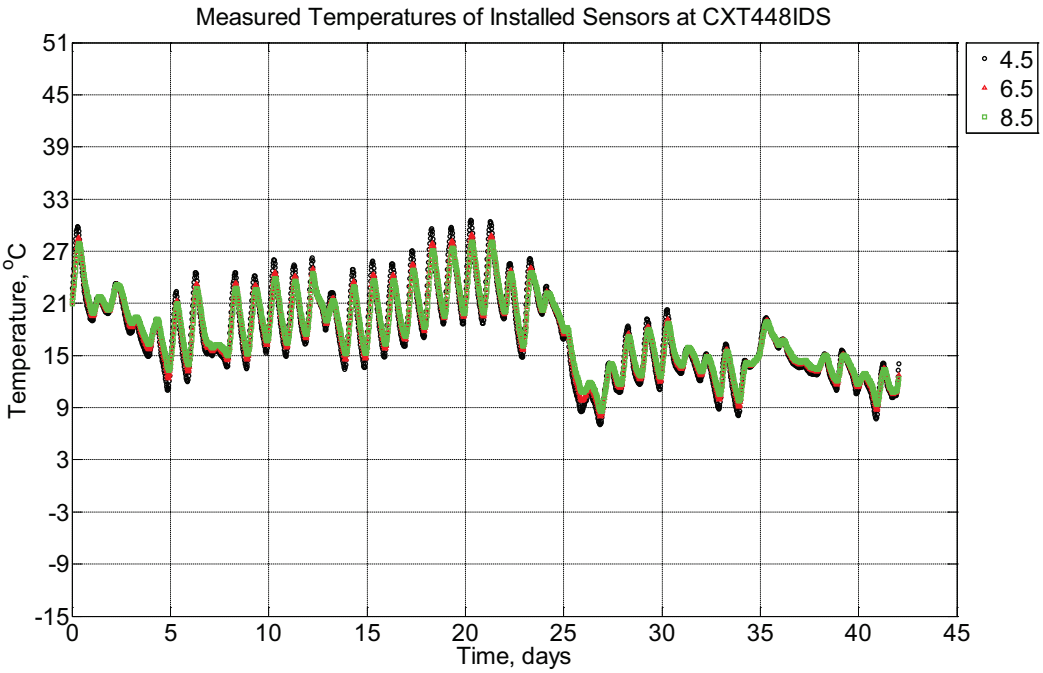

Figure B-614 Measured temperature at depths of 4.5 inches (114.3 mm), 6.5 inches (139.7 mm), and 8.5 inches (215.9 mm) from the surface of a concrete crosstie (labeled CXT448IDS) installed in ballast in Rantoul, IL, between September 8, 2014, through October 20, 2014. An 8 mm thick polyurethane pad and 12 in (30.48 cm) length 136 lb/yd (67.5 kg/m) section of steel rail are additionally installed atop the concrete crosstie.

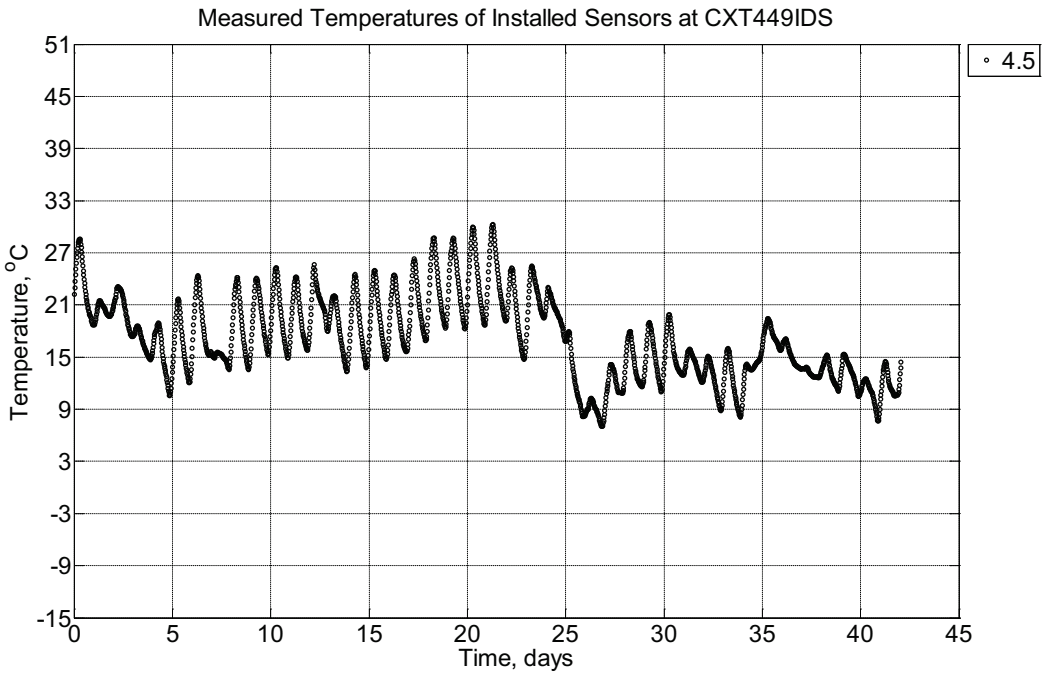

Figure B-615 Measured temperature at a depth of 4.5 inches (114.3 mm) from the surface of a concrete crosstie (labeled CXT449IDS) installed in ballast in Rantoul, IL, between September 8, 2014, through October 20, 2014. An 8 mm thick polyurethane pad and 12 in (30.48 cm) length 136 lb/yd (67.5 kg/m) section of steel rail are additionally installed atop the concrete crosstie.

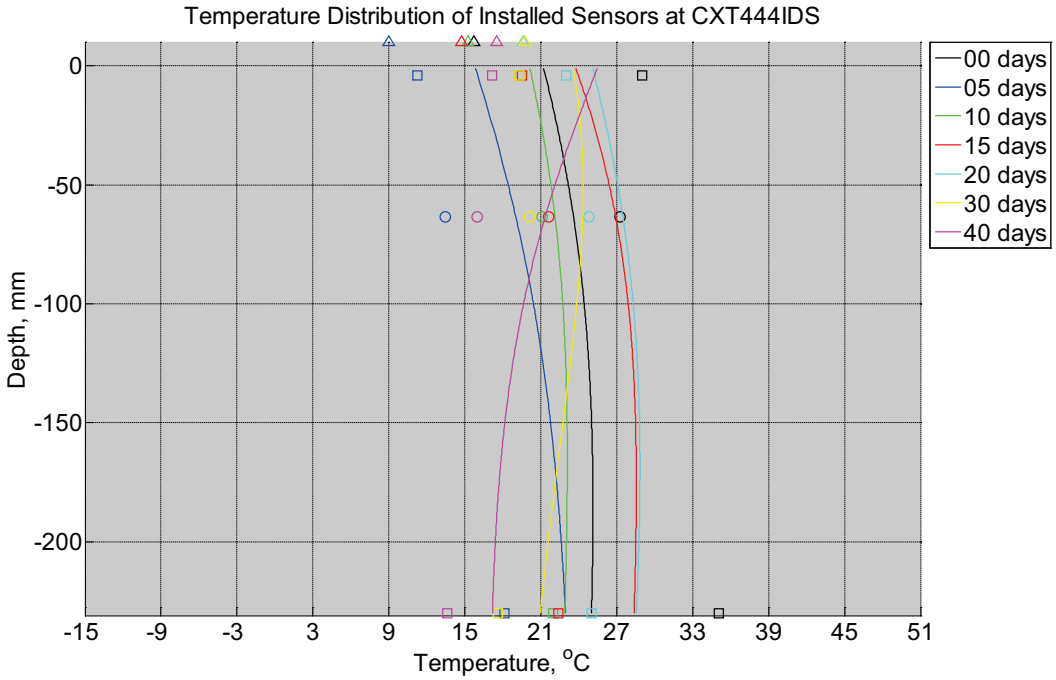

Figure B-616 Measured (markers) and modeled (continuous line) temperature profile

distribution as a function of depth inside a concrete crosstie (labeled CXT444IDS) without a polyurethane pad nor rail installed in ballast in Rantoul, IL, between September 8, 2014, through October 20, 2014. Triangular markers denote temperature value from KTIP weather station, square markers denote measured temperature values from ballast, and circular markers denote measured temperature values inside concrete.

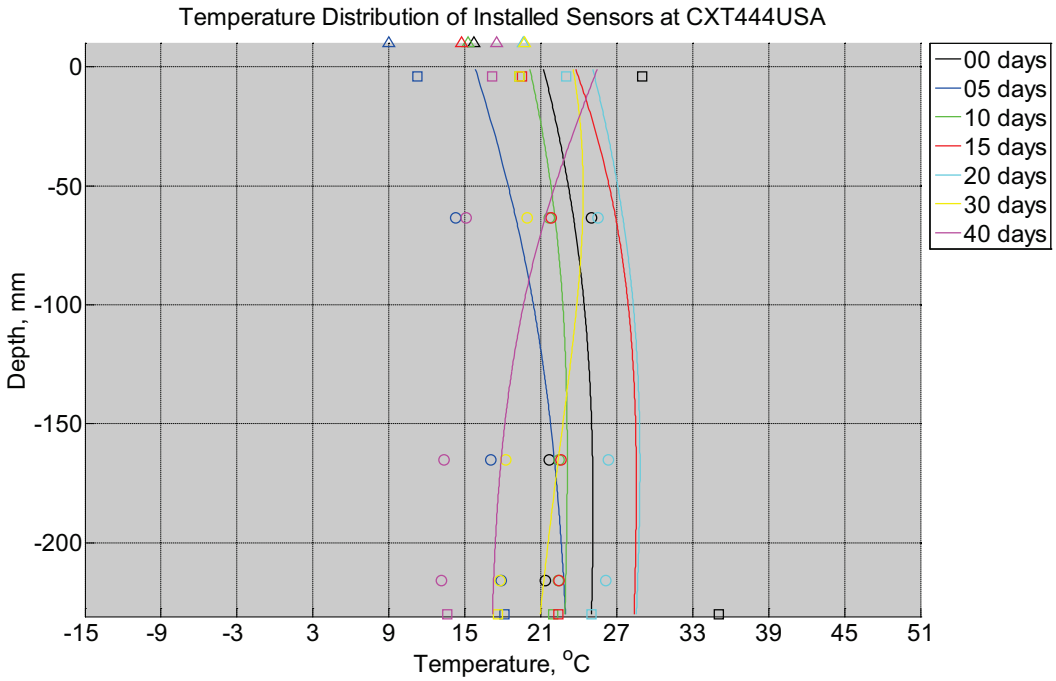

Figure B-617 Measured (markers) and modeled (continuous line) temperature profile distribution as a function of depth inside a concrete crosstie (labeled CXT444USA) installed in ballast in Rantoul, IL, between September 8, 2014, through October 20, 2014. An 8 mm thick polyurethane pad and 12 in (30.48 cm) length 136 lb/yd (67.5 kg/m) section of steel rail are additionally installed atop the model concrete crosstie. The model does not incorporate a polyurethane pad nor steel rail line. Triangular markers denote temperature value from KTIP weather station, square markers denote measured temperature values from ballast, and circular markers denote measured temperature values inside concrete.

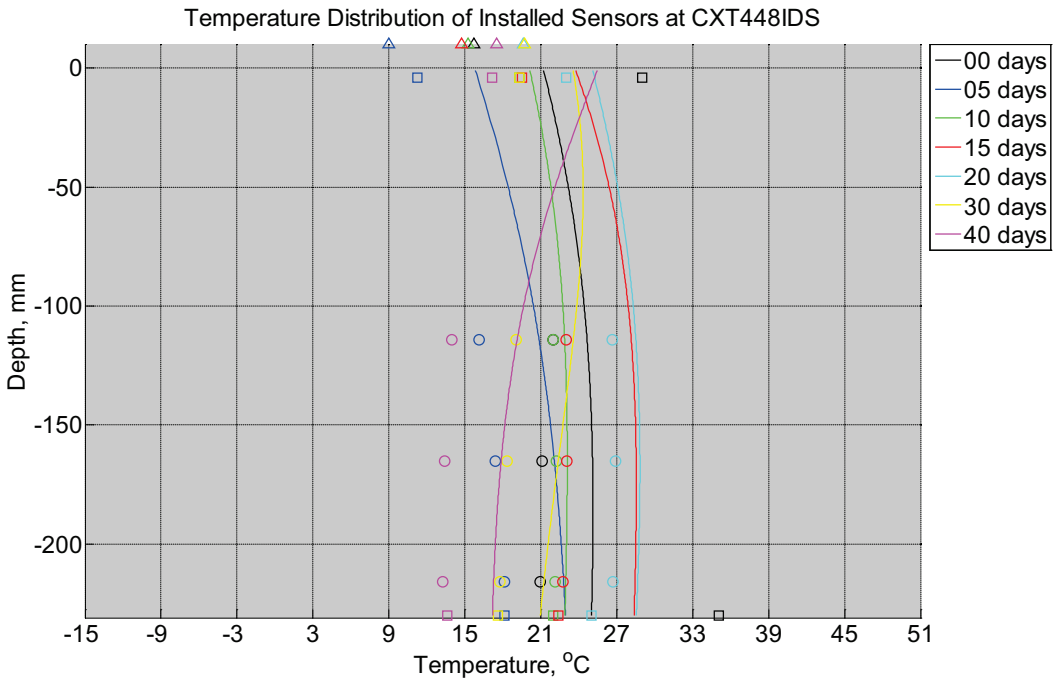

Figure B-618 Measured (markers) and modeled (continuous line) temperature profile distribution as a function of depth inside a concrete crosstie (labeled CXT448IDS) installed in ballast in Rantoul, IL, between September 8, 2014, through October 20, 2014. An 8 mm thick polyurethane pad and 12 in (30.48 cm) length 136 lb/yd (67.5 kg/m) section of steel rail are additionally installed atop the model concrete crosstie. The model does not incorporate a polyurethane pad nor steel rail line. Triangular markers denote temperature value from KTIP weather station, square markers denote measured temperature values from ballast, and circular markers denote measured temperature values inside concrete.

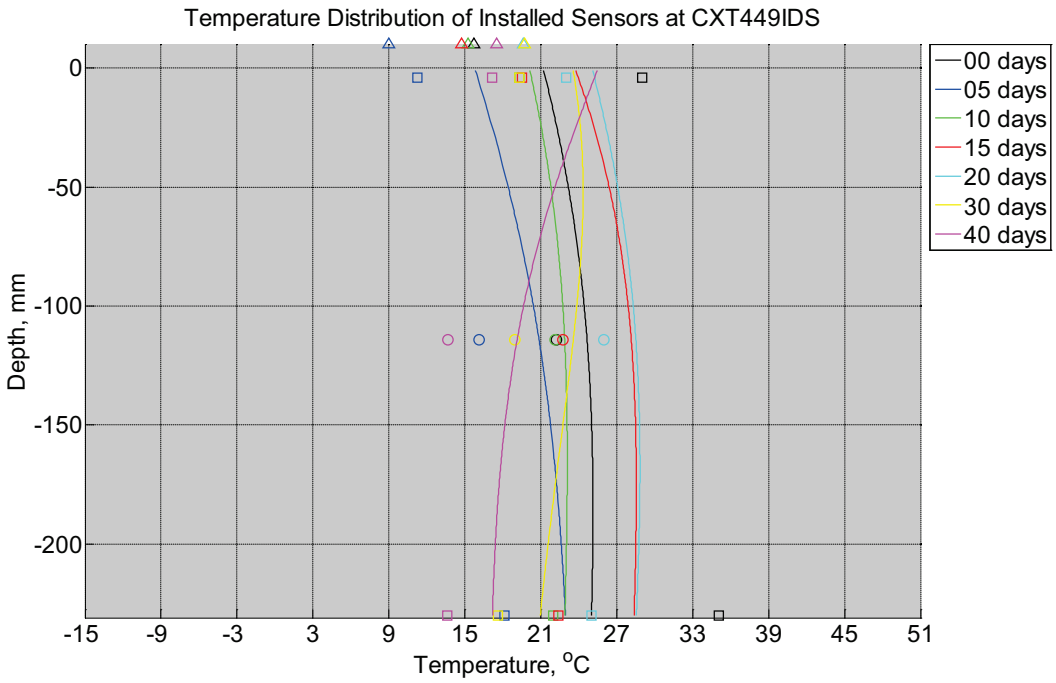

Figure B-619 Measured (markers) and modeled (continuous line) temperature profile distribution as a function of depth inside a concrete crosstie (labeled CXT449IDS) installed in ballast in Rantoul, IL, between September 8, 2014, through October 20, 2014. An 8 mm thick polyurethane pad and 12 in (30.48 cm) length 136 lb/yd (67.5 kg/m) section of steel rail are additionally installed atop the model concrete crosstie. The model does not incorporate a polyurethane pad nor steel rail line. Triangular markers denote temperature value from KTIP weather station, square markers denote measured temperature values from ballast, and circular markers denote measured temperature values inside concrete.

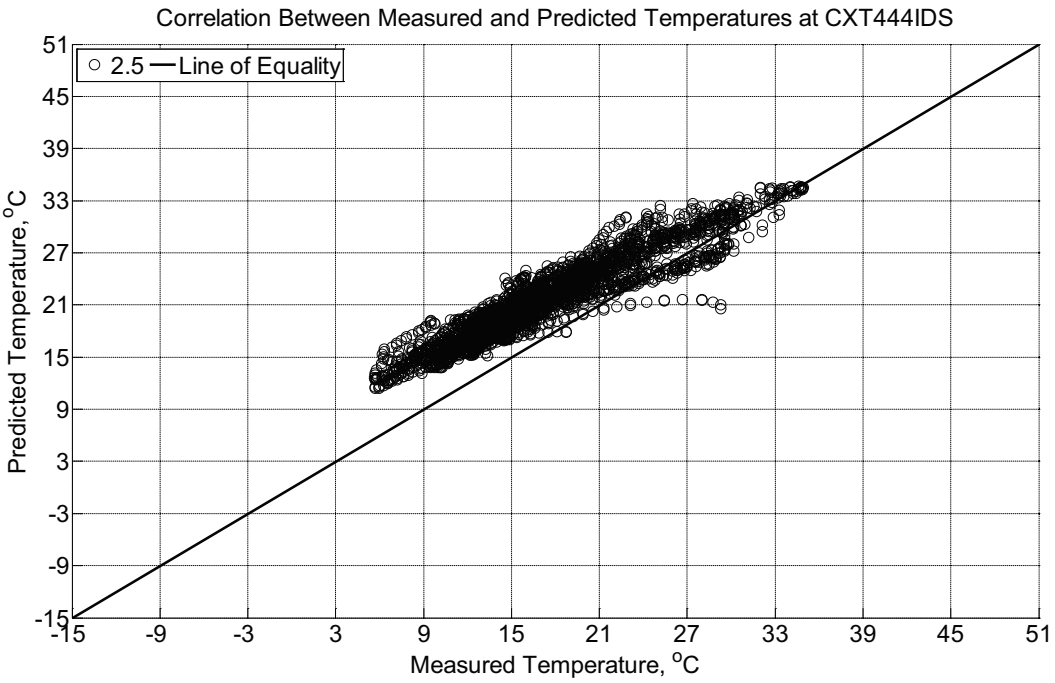

Figure B-620 Correlation between measured and predicted temperature values 2.5 inches (63.5 mm) from the surface of a concrete crosstie (labeled CXT444IDS) without a polyurethane pad nor rail installed in ballast in Rantoul, IL, between September 8, 2014, through October 20, 2014.

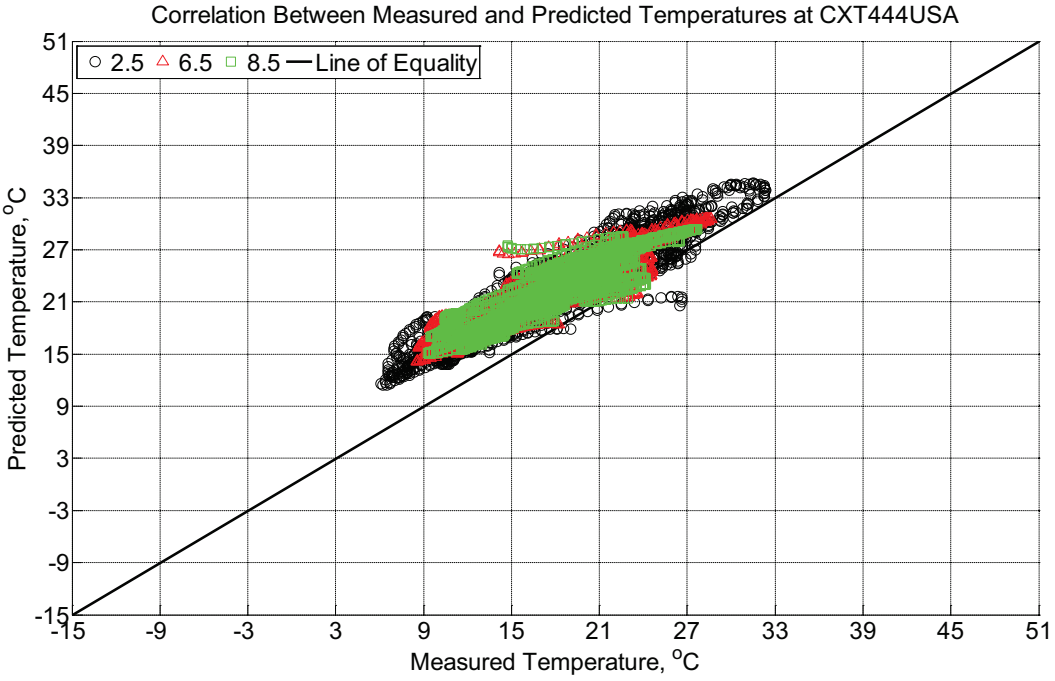

Figure B-621 Correlation between measured and predicted temperature values 2.5 inches (63.5 mm), 6.5 inches (139.7 mm), and 8.5 inches (215.9 mm) from the surface of a concrete

crosstie (labeled CXT444USA) installed in ballast in Rantoul, IL, between September 8, 2014, through October 20, 2014. An 8 mm thick polyurethane pad and 12 in (30.48 cm) length 136 lb/yd (67.5 kg/m) section of steel rail are additionally installed atop the concrete crosstie. The model does not incorporate a polyurethane pad nor steel rail line.

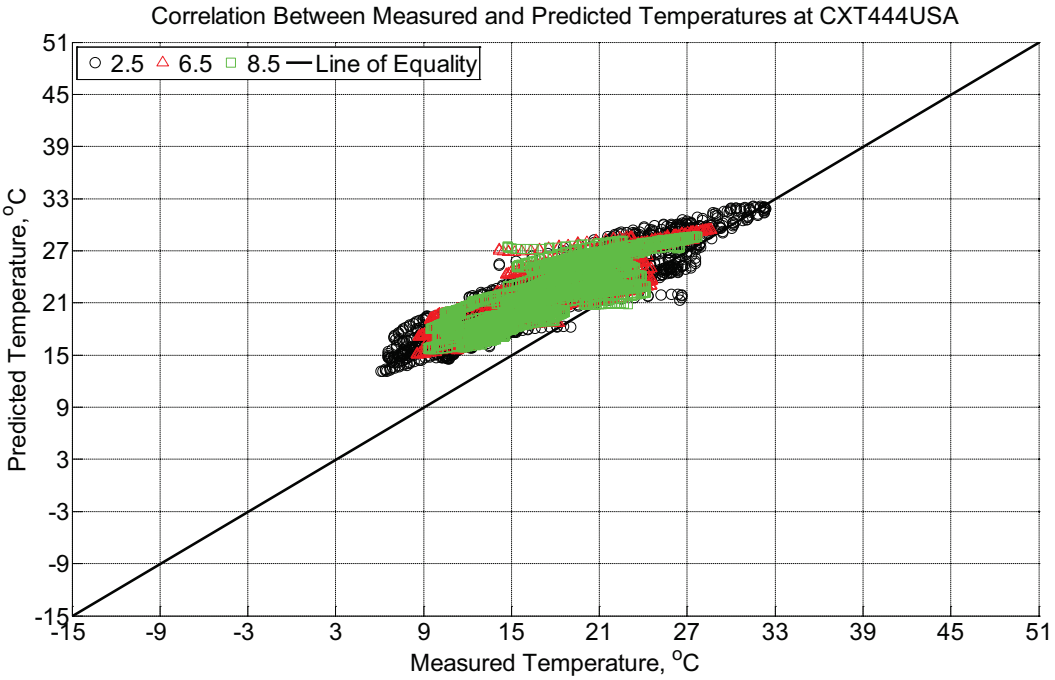

Figure B-622 Correlation between measured and predicted temperature values 2.5 inches (63.5 mm), 6.5 inches (139.7 mm), and 8.5 inches (215.9 mm) from the surface of a concrete crosstie (labeled CXT444USA) installed in ballast in Rantoul, IL, between September 8, 2014, through October 20, 2014. An 8 mm thick polyurethane pad and 12 in (30.48 cm) length 136 lb/yd (67.5 kg/m) section of steel rail are additionally installed atop the concrete crosstie. The model incorporates a 1 mm thick polyurethane pad and 1 mm thick steel rail line.

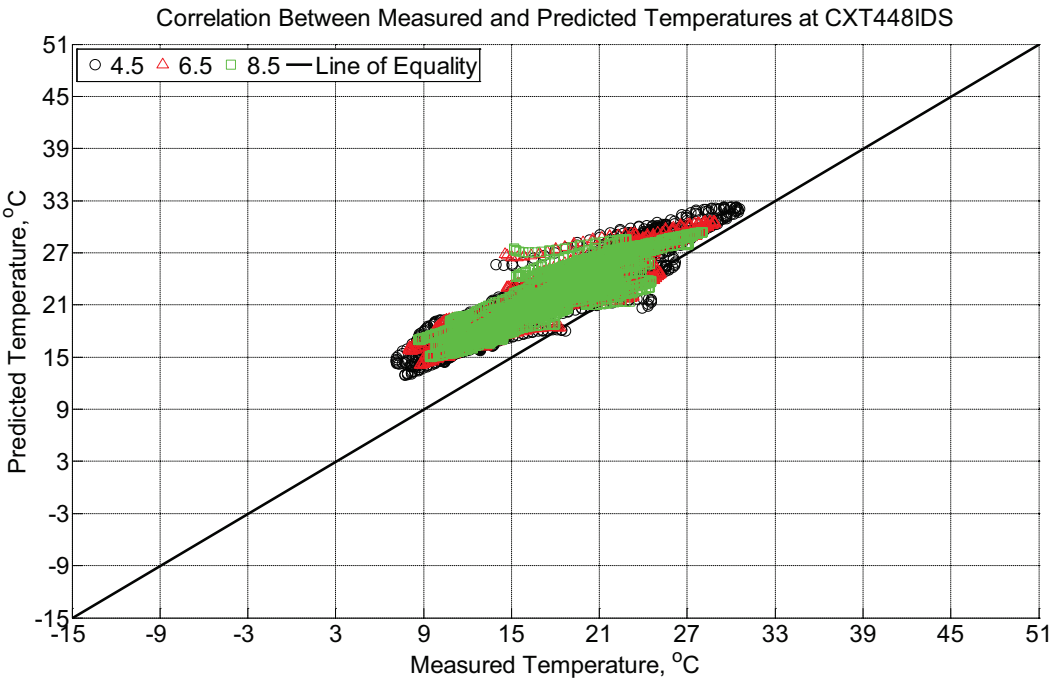

Figure B-623 Correlation between measured and predicted temperature values 4.5 inches (114.3 mm), 6.5 inches (139.7 mm), and 8.5 inches (215.9 mm) from the surface of a concrete crosstie (labeled CXT448IDS) installed in ballast in Rantoul, IL, between September 8, 2014, through October 20, 2014. An 8 mm thick polyurethane pad and 12 in (30.48 cm) length 136 lb/yd (67.5 kg/m) section of steel rail are additionally installed atop the concrete crosstie. The model does not incorporate a polyurethane pad nor steel rail line.

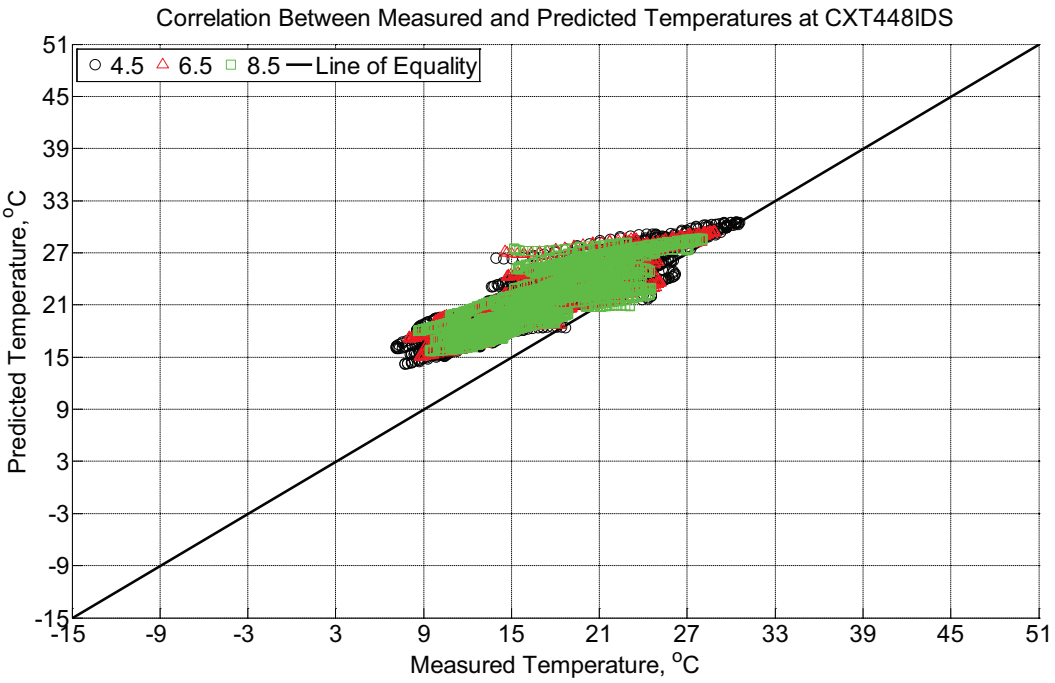

Figure B-624 Correlation between measured and predicted temperature values 4.5 inches (114.3 mm), 6.5 inches (139.7 mm), and 8.5 inches (215.9 mm) from the surface of a concrete crosstie (labeled CXT448IDS) installed in ballast in Rantoul, IL, between September 8, 2014, through October 20, 2014. An 8 mm thick polyurethane pad and 12 in (30.48 cm) length 136 lb/yd (67.5 kg/m) section of steel rail are additionally installed atop the concrete crosstie. The model incorporates a 1 mm thick polyurethane pad and 1 mm thick steel rail line.

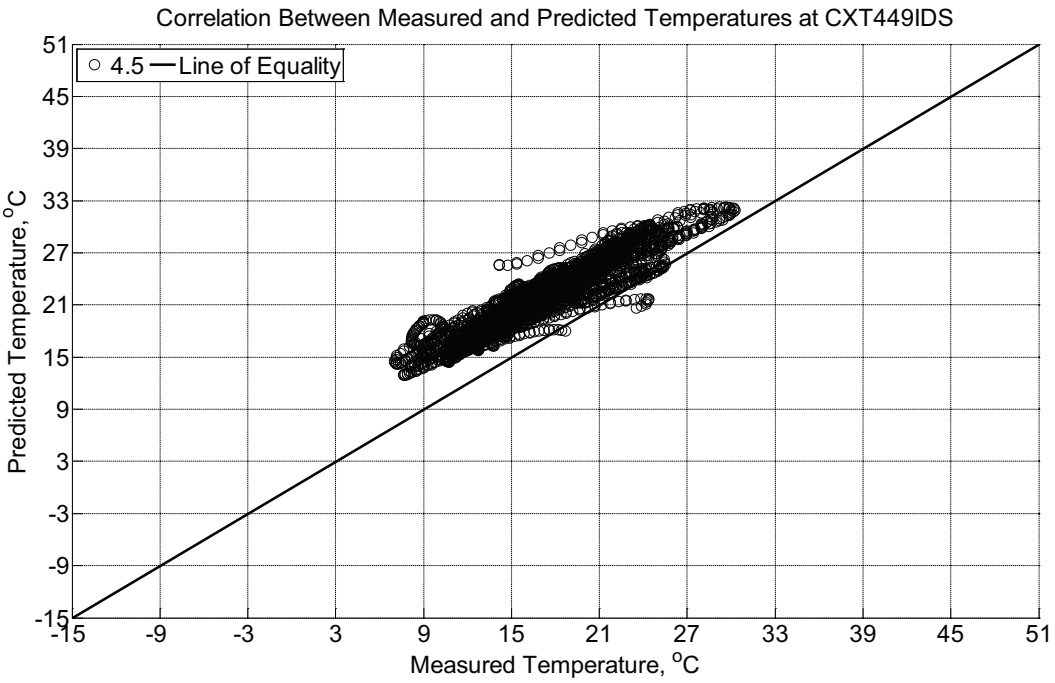

Figure B-625 Correlation between measured and predicted temperature values 4.5 inches (114.3 mm) from the surface of a concrete crosstie (labeled CXT449IDS) installed in ballast in Rantoul, IL, between September 8, 2014, through October 20, 2014. An 8 mm thick polyurethane pad and 12 in (30.48 cm) length 136 lb/yd (67.5 kg/m) section of steel rail are additionally installed atop the concrete crosstie. The model does not incorporate a polyurethane pad nor steel rail line.

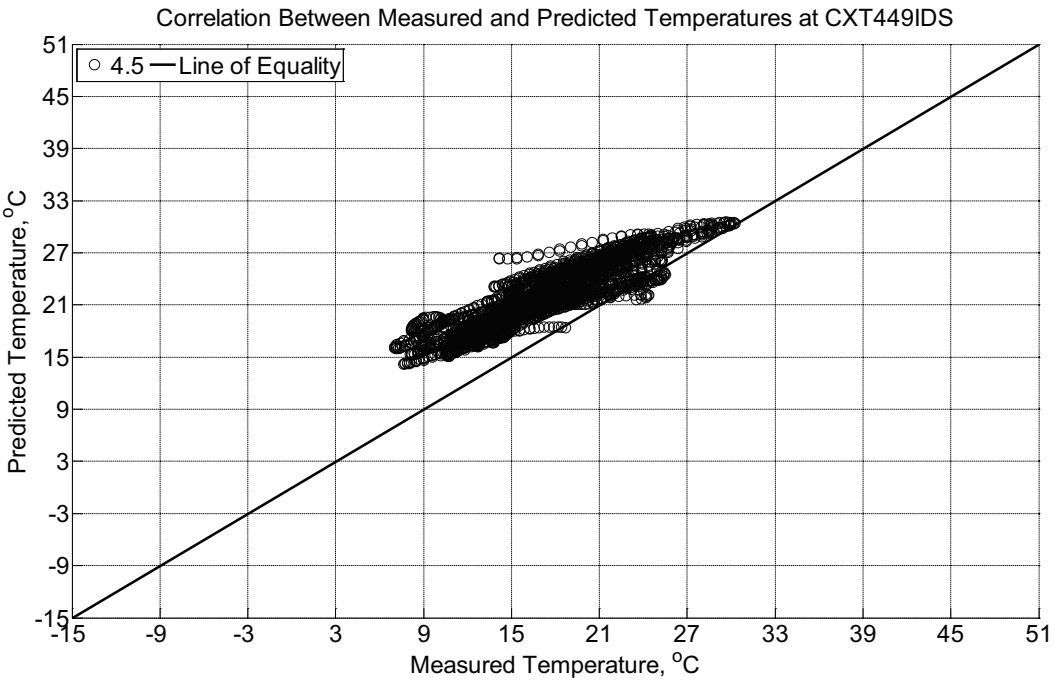

Figure B-626 Correlation between measured and predicted temperature values 4.5 inches (114.3 mm) from the surface of a concrete crosstie (labeled CXT449IDS) installed in ballast in Rantoul, IL, between September 8, 2014, through October 20, 2014. An 8 mm thick polyurethane pad and 12 in (30.48 cm) length 136 lb/yd (67.5 kg/m) section of steel rail are additionally installed atop the concrete crosstie. The model incorporates a 1 mm thick polyurethane pad and 1 mm thick steel rail line.

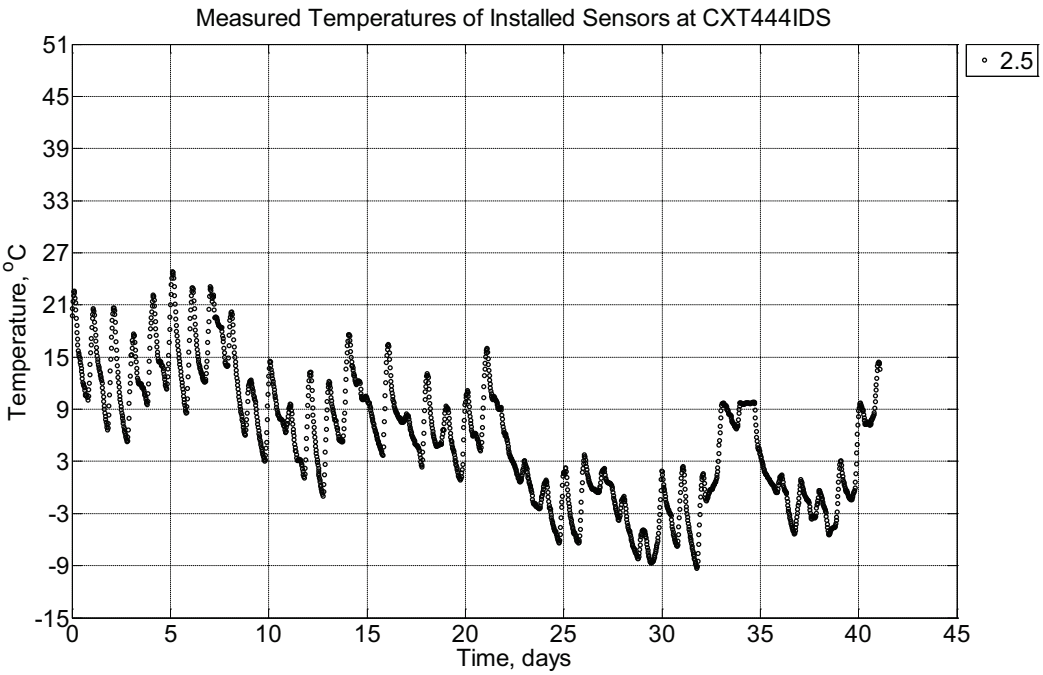

Figure B-627 Measured temperature at a depth of 2.5 inches (63.5 mm) from the surface of a concrete crosstie (labeled CXT444IDS) without a polyurethane pad nor rail installed in ballast in Rantoul, IL, between October 20, 2014, through November 30, 2014.

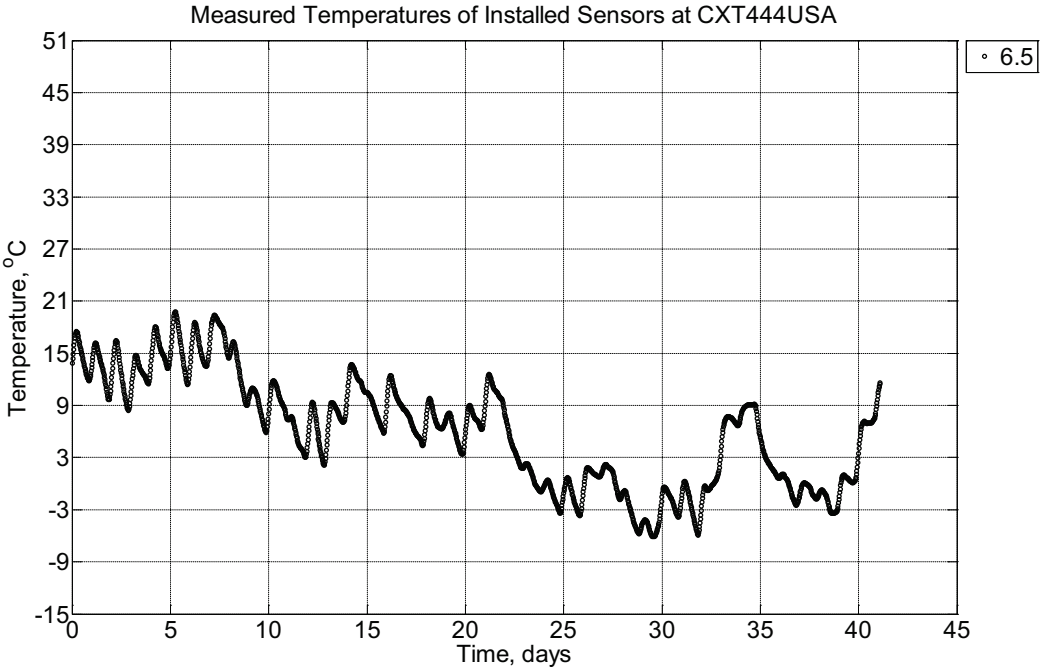

Figure B-628 Measured temperature at a depth of 6.5 inches (139.7 mm) from the surface of a concrete crosstie (labeled CXT444USA) installed in ballast in Rantoul, IL, between October 20, 2014, through November 30, 2014. An 8 mm thick polyurethane pad and 12 in

(30.48 cm) length 136 lb/yd (67.5 kg/m) section of steel rail are additionally installed atop the concrete crosstie.

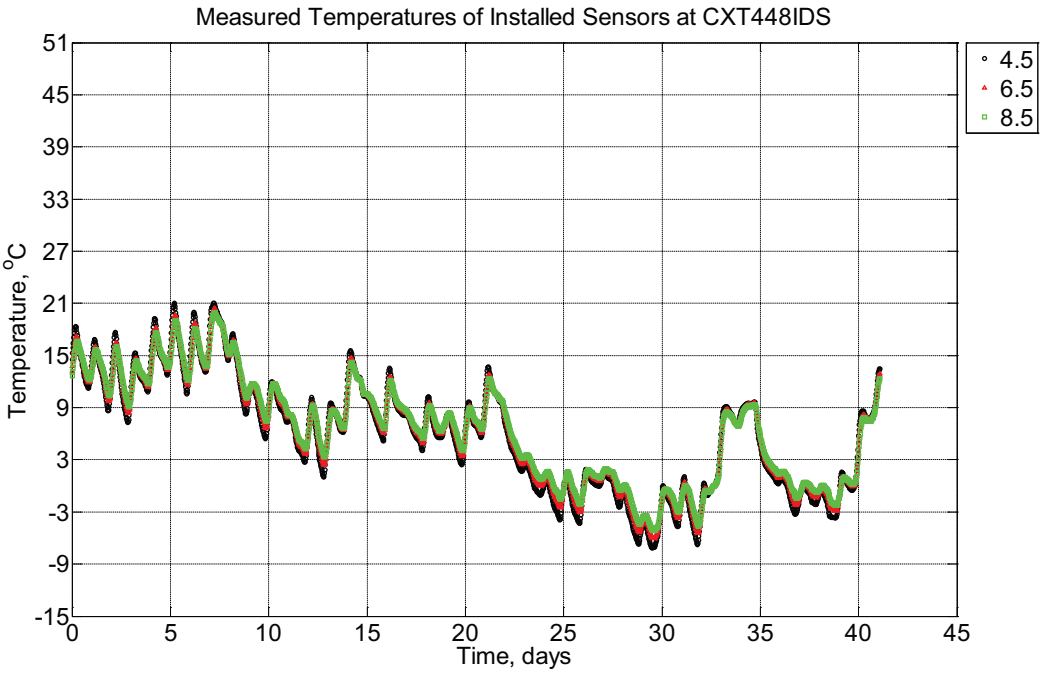

Figure B-629 Measured temperature at depths of 4.5 inches (114.3 mm), 6.5 inches (139.7 mm), and 8.5 inches (215.9 mm) from the surface of a concrete crosstie (labeled CXT448IDS) installed in ballast in Rantoul, IL, between October 20, 2014, through November 30, 2014. An 8 mm thick polyurethane pad and 12 in (30.48 cm) length 136 lb/yd (67.5 kg/m) section of steel rail are additionally installed atop the concrete crosstie.

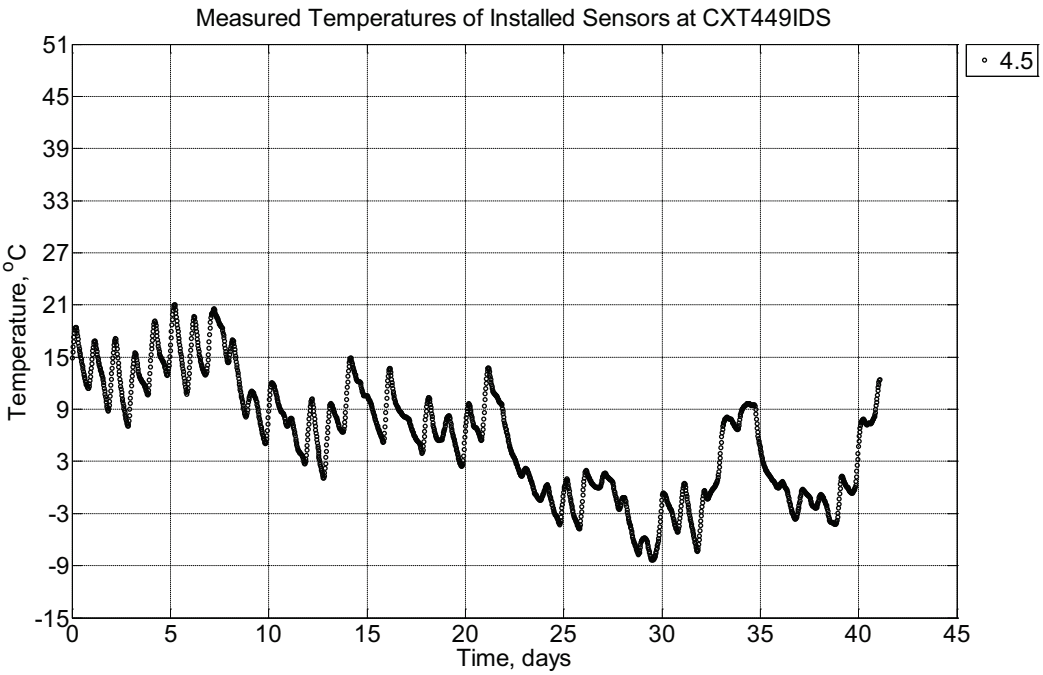

Figure B-630 Measured temperature at a depth of 4.5 inches (114.3 mm) from the surface of a concrete crosstie (labeled CXT449IDS) installed in ballast in Rantoul, IL, between October 20, 2014, through November 30, 2014. An 8 mm thick polyurethane pad and 12 in (30.48 cm) length 136 lb/yd (67.5 kg/m) section of steel rail are additionally installed atop the concrete crosstie.

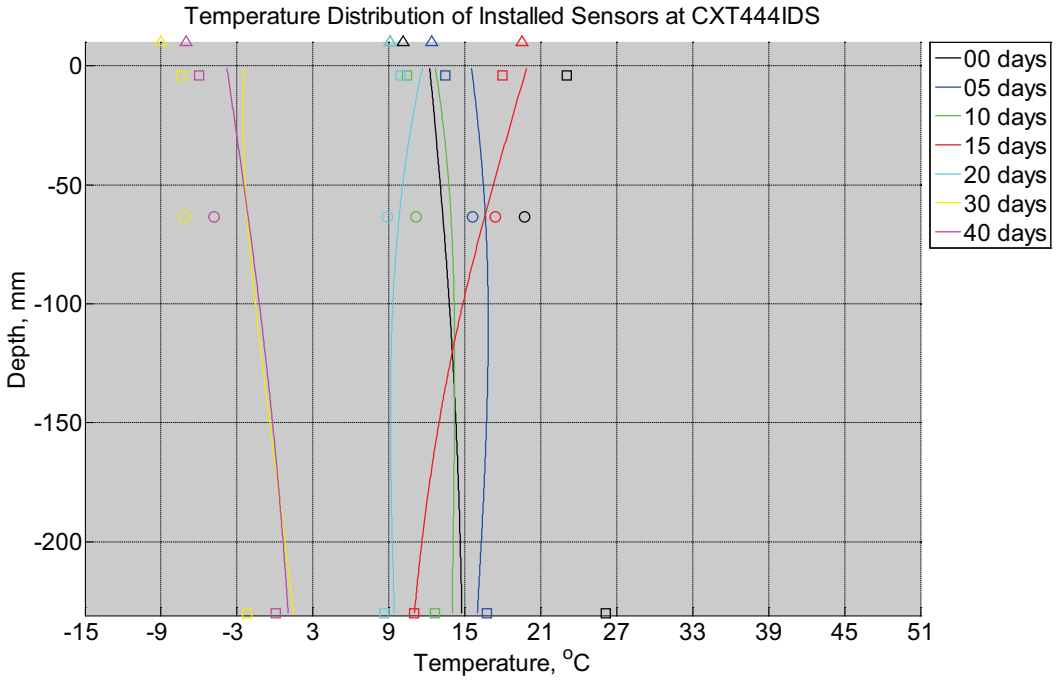

Figure B-631 Measured (markers) and modeled (continuous line) temperature profile

distribution as a function of depth inside a concrete crosstie (labeled CXT444IDS) without a polyurethane pad nor rail installed in ballast in Rantoul, IL, between October 20, 2014, through November 30, 2014. Triangular markers denote temperature value from KTIP weather station, square markers denote measured temperature values from ballast, and circular markers denote measured temperature values inside concrete.

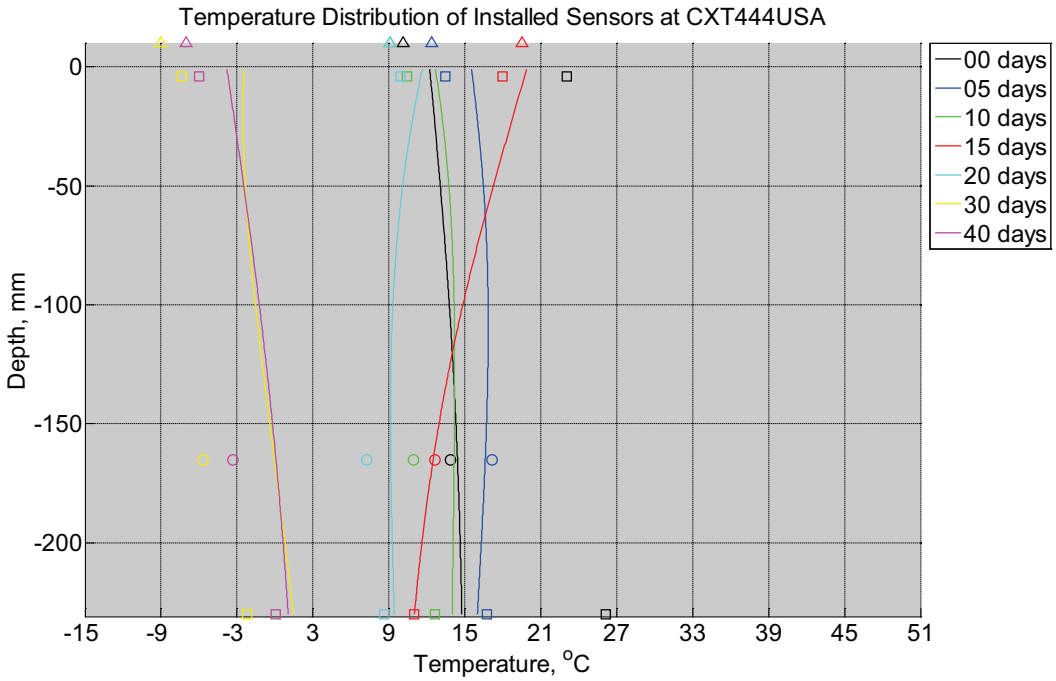

Figure B-632 Measured (markers) and modeled (continuous line) temperature profile distribution as a function of depth inside a concrete crosstie (labeled CXT444USA) installed in ballast in Rantoul, IL, between October 20, 2014, through November 30, 2014. An 8 mm thick polyurethane pad and 12 in (30.48 cm) length 136 lb/yd (67.5 kg/m) section of steel rail are additionally installed atop the model concrete crosstie. The model does not incorporate a polyurethane pad nor steel rail line. Triangular markers denote temperature value from KTIP weather station, square markers denote measured temperature values from ballast, and circular markers denote measured temperature values inside concrete.

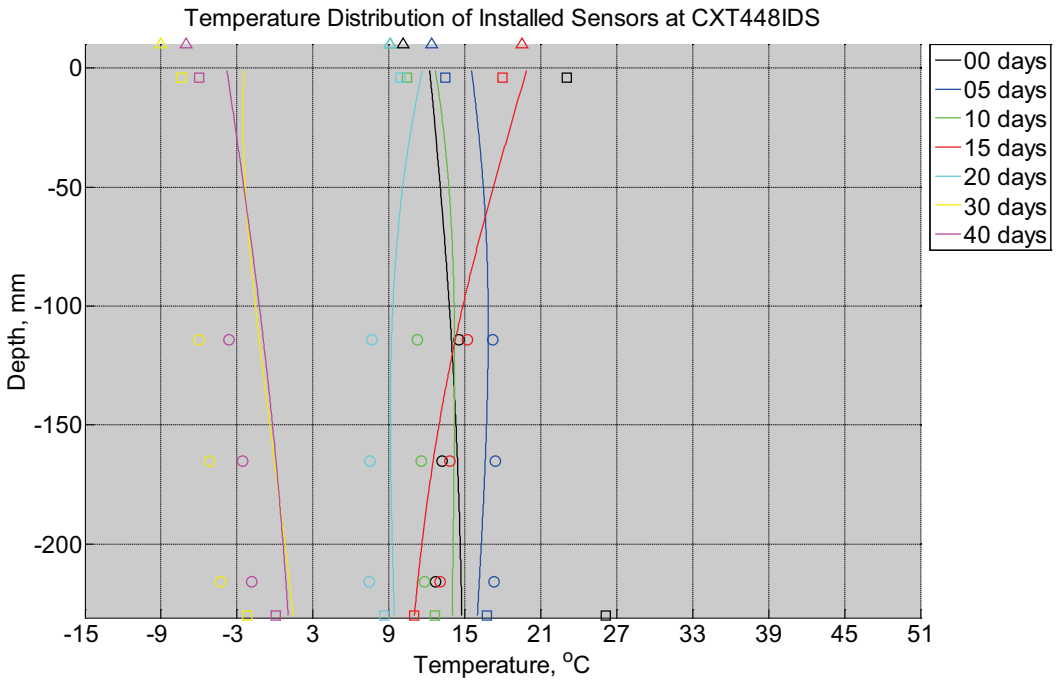

Figure B-633 Measured (markers) and modeled (continuous line) temperature profile distribution as a function of depth inside a concrete crosstie (labeled CXT448IDS) installed in ballast in Rantoul, IL, between October 20, 2014, through November 30, 2014. An 8 mm thick polyurethane pad and 12 in (30.48 cm) length 136 lb/yd (67.5 kg/m) section of steel rail are additionally installed atop the model concrete crosstie. The model does not incorporate a polyurethane pad nor steel rail line. Triangular markers denote temperature value from KTIP weather station, square markers denote measured temperature values from ballast, and circular markers denote measured temperature values inside concrete.

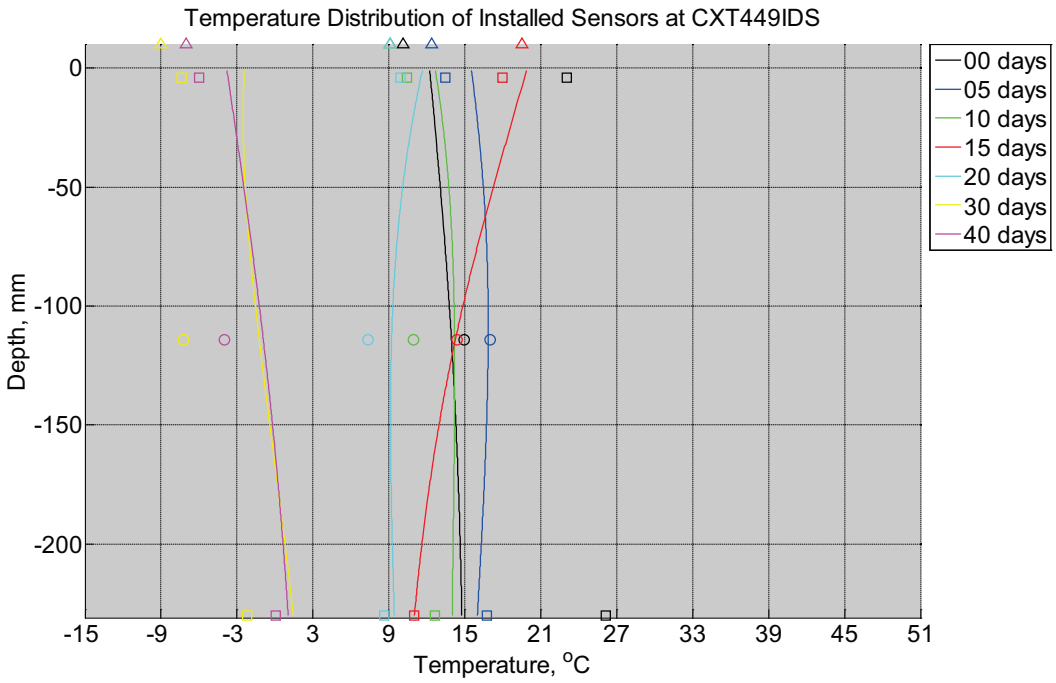

Figure B-634 Measured (markers) and modeled (continuous line) temperature profile distribution as a function of depth inside a concrete crosstie (labeled CXT449IDS) installed in ballast in Rantoul, IL, between October 20, 2014, through November 30, 2014. An 8 mm thick polyurethane pad and 12 in (30.48 cm) length 136 lb/yd (67.5 kg/m) section of steel rail are additionally installed atop the model concrete crosstie. The model does not incorporate a polyurethane pad nor steel rail line. Triangular markers denote temperature value from KTIP weather station, square markers denote measured temperature values from ballast, and circular markers denote measured temperature values inside concrete.

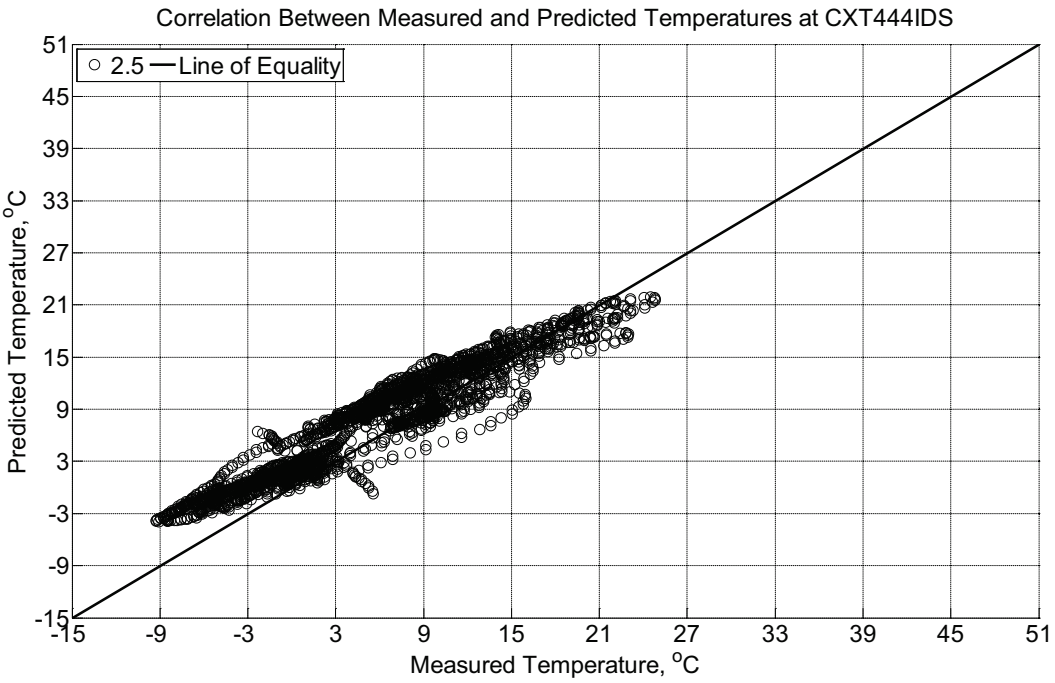

Figure B-635 Correlation between measured and predicted temperature values 2.5 inches (63.5 mm) from the surface of a concrete crosstie (labeled CXT444IDS) without a polyurethane pad nor rail installed in ballast in Rantoul, IL, between October 20, 2014, through November 30, 2014.

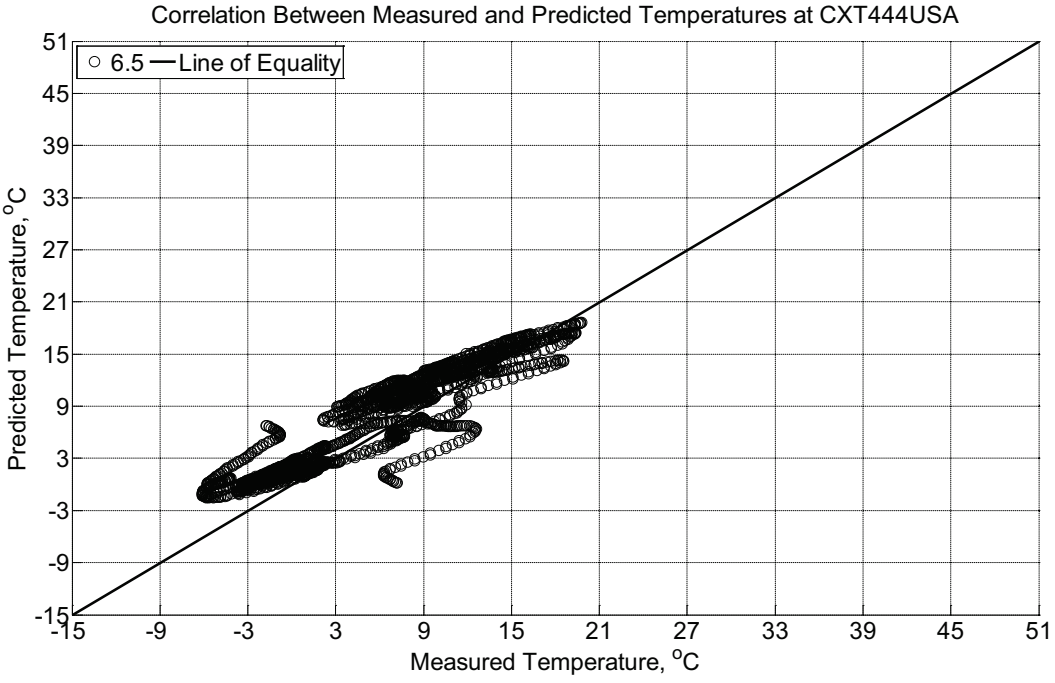

Figure B-636 Correlation between measured and predicted temperature values 6.5 inches (139.7 mm) from the surface of a concrete crosstie (labeled CXT444USA) installed in

ballast in Rantoul, IL, between October 20, 2014, through November 30, 2014. An 8 mm thick polyurethane pad and 12 in (30.48 cm) length 136 lb/yd (67.5 kg/m) section of steel rail are additionally installed atop the concrete crosstie. The model does not incorporate a polyurethane pad nor steel rail line.

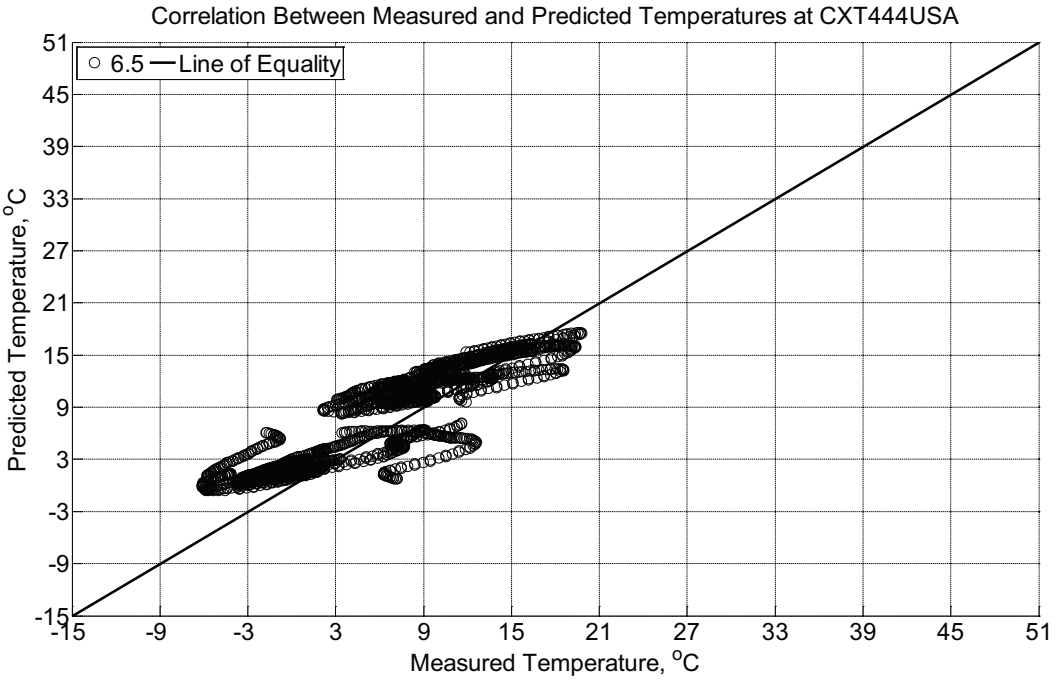

Figure B-637 Correlation between measured and predicted temperature values 6.5 inches (139.7 mm) from the surface of a concrete crosstie (labeled CXT444USA) installed in ballast in Rantoul, IL, between October 20, 2014, through November 30, 2014. An 8 mm thick polyurethane pad and 12 in (30.48 cm) length 136 lb/yd (67.5 kg/m) section of steel rail are additionally installed atop the concrete crosstie. The model incorporates a 1 mm thick polyurethane pad and 1 mm thick steel rail line.

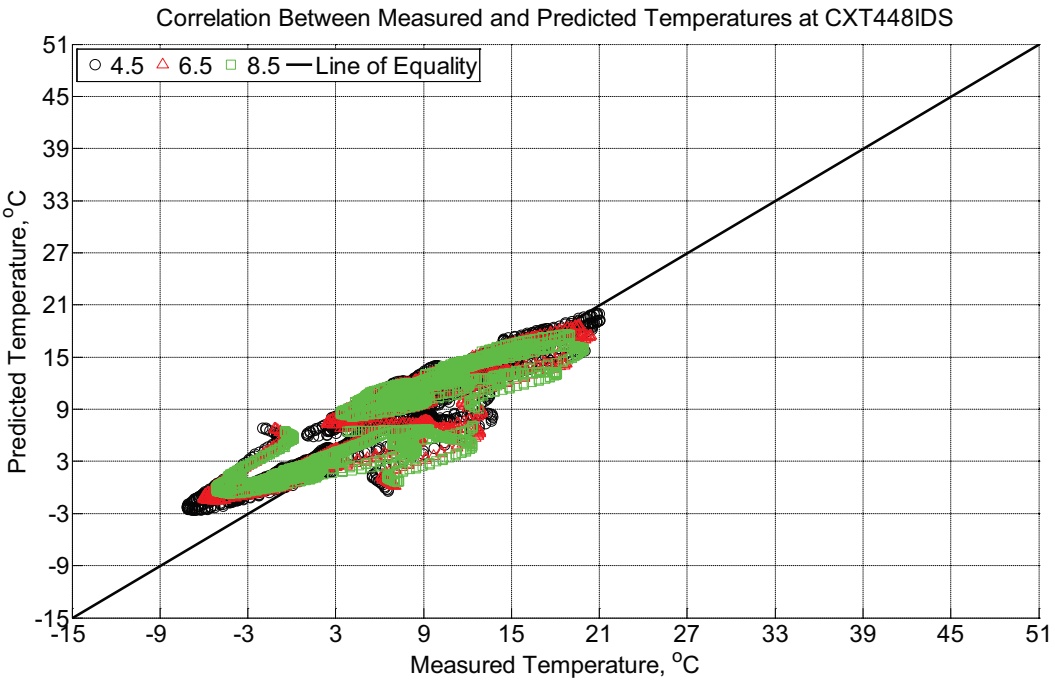

Figure B-638 Correlation between measured and predicted temperature values 4.5 inches (114.3 mm), 6.5 inches (139.7 mm), and 8.5 inches (215.9 mm) from the surface of a concrete crosstie (labeled CXT448IDS) installed in ballast in Rantoul, IL, between October 20, 2014, through November 30, 2014. An 8 mm thick polyurethane pad and 12 in (30.48 cm) length 136 lb/yd (67.5 kg/m) section of steel rail are additionally installed atop the concrete crosstie. The model does not incorporate a polyurethane pad nor steel rail line.

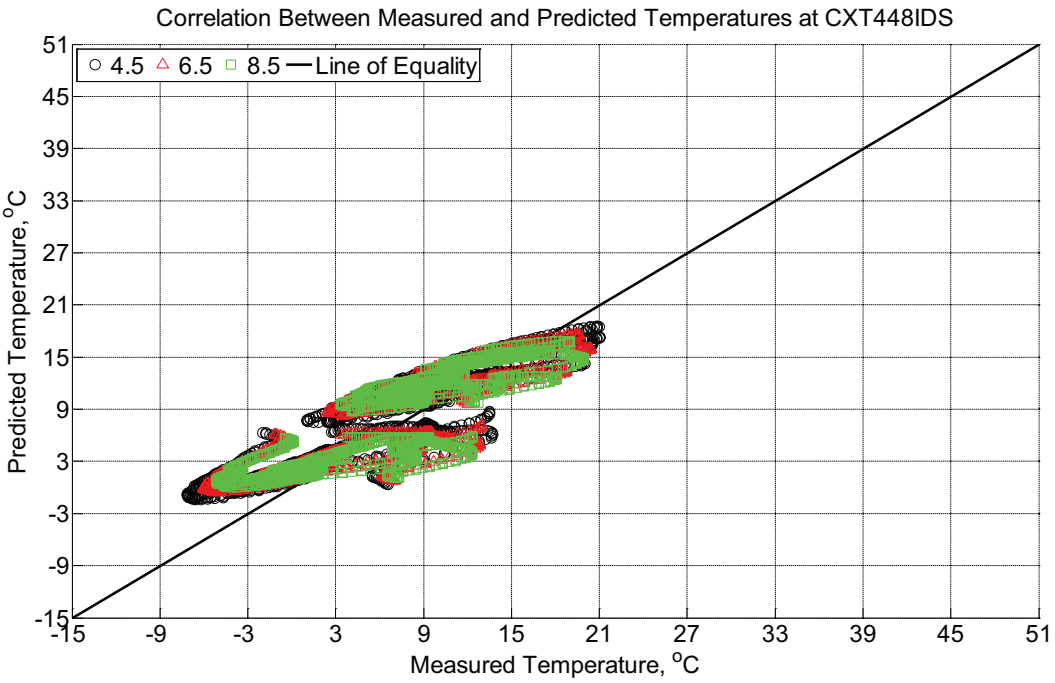

Figure B-639 Correlation between measured and predicted temperature values 4.5 inches (114.3 mm), 6.5 inches (139.7 mm), and 8.5 inches (215.9 mm) from the surface of a concrete crosstie (labeled CXT448IDS) installed in ballast in Rantoul, IL, between October 20, 2014, through November 30, 2014. An 8 mm thick polyurethane pad and 12 in (30.48 cm) length 136 lb/yd (67.5 kg/m) section of steel rail are additionally installed atop the concrete crosstie. The model incorporates a 1 mm thick polyurethane pad and 1 mm thick steel rail line.

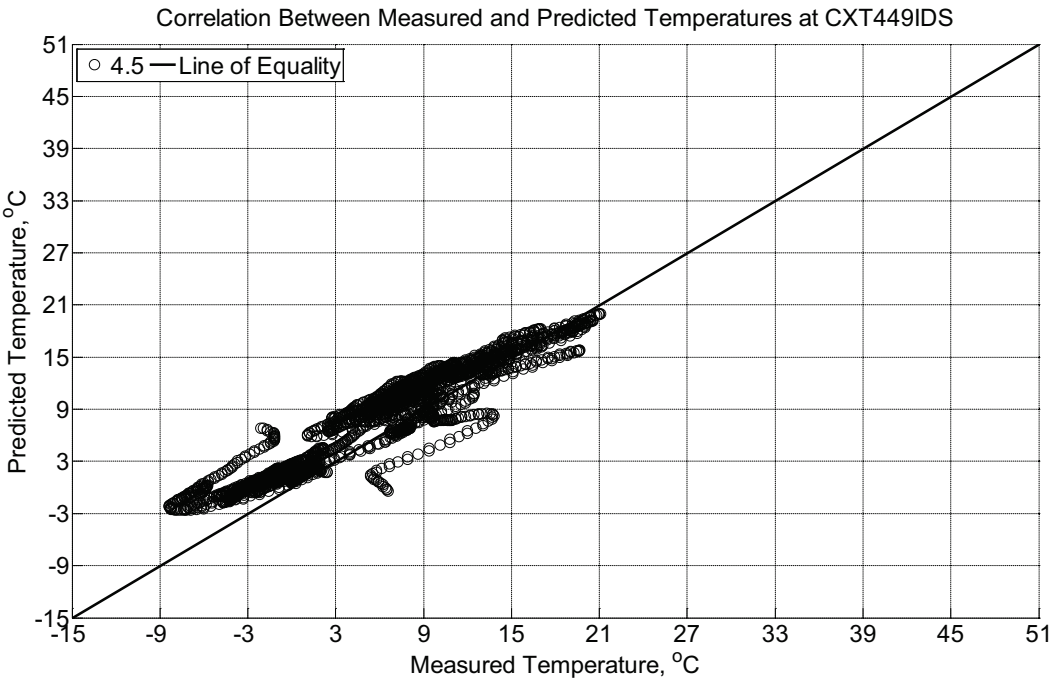

Figure B-640 Correlation between measured and predicted temperature values 4.5 inches (114.3 mm) from the surface of a concrete crosstie (labeled CXT449IDS) installed in ballast in Rantoul, IL, between October 20, 2014, through November 30, 2014. An 8 mm thick polyurethane pad and 12 in (30.48 cm) length 136 lb/yd (67.5 kg/m) section of steel rail are additionally installed atop the concrete crosstie. The model does not incorporate a polyurethane pad nor steel rail line.

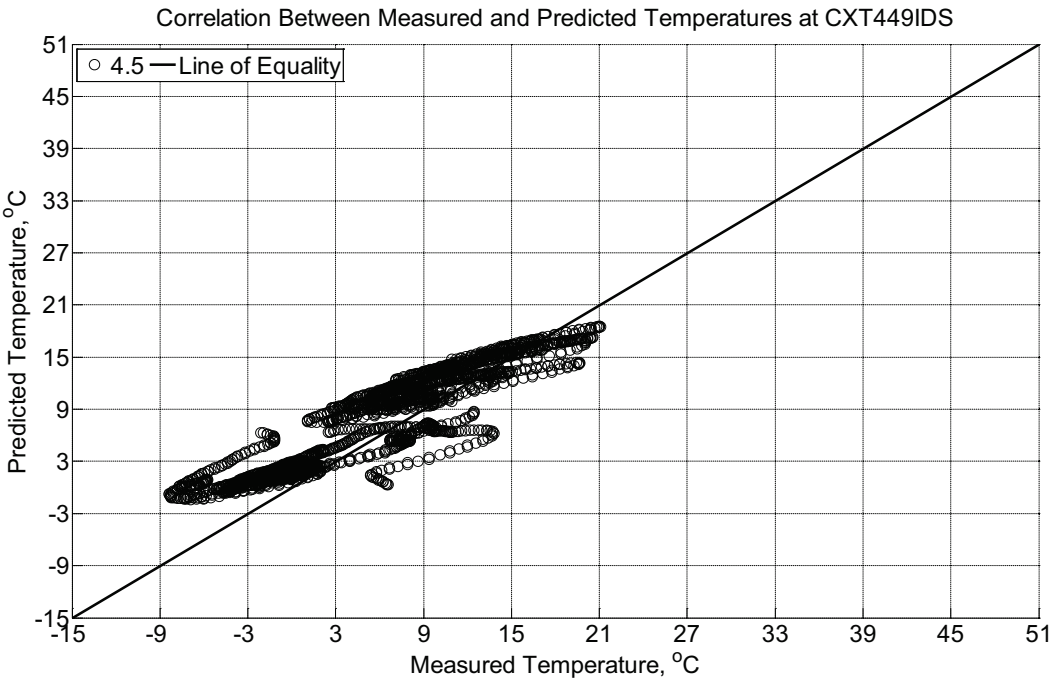

Figure B-641 Correlation between measured and predicted temperature values 4.5 inches (114.3 mm) from the surface of a concrete crosstie (labeled CXT449IDS) installed in ballast in Rantoul, IL, between October 20, 2014, through November 30, 2014. An 8 mm thick polyurethane pad and 12 in (30.48 cm) length 136 lb/yd (67.5 kg/m) section of steel rail are additionally installed atop the concrete crosstie. The model incorporates a 1 mm thick polyurethane pad and 1 mm thick steel rail line.

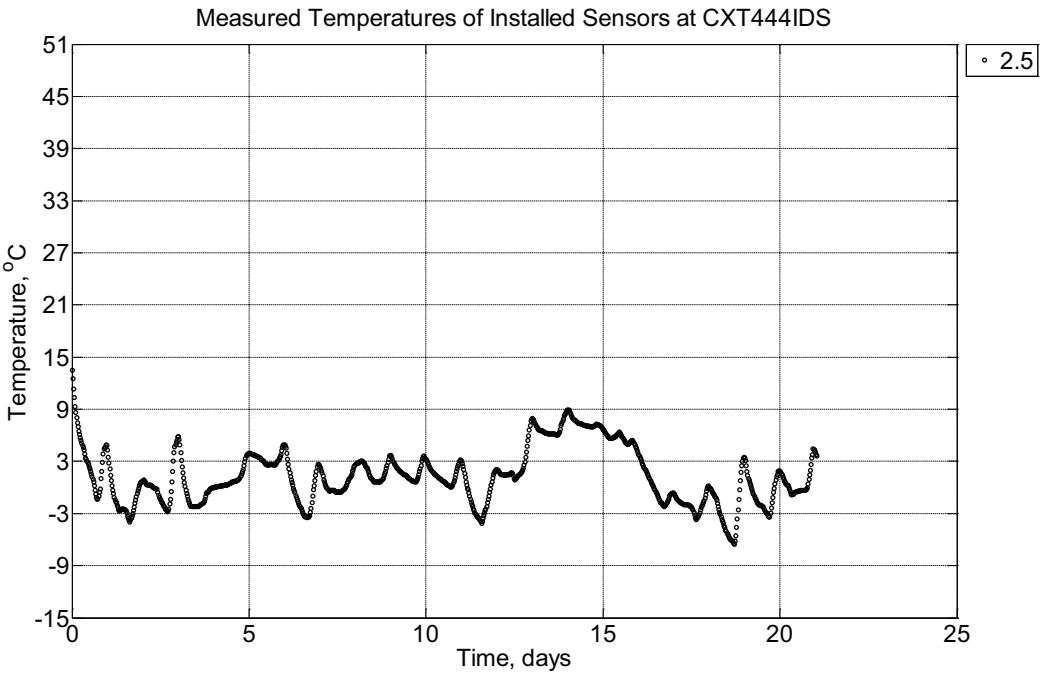

Figure B-642 Measured temperature at a depth of 2.5 inches (63.5 mm) from the surface of a concrete crosstie (labeled CXT444IDS) without a polyurethane pad nor rail installed in ballast in Rantoul, IL, between November 30, 2014, through December 21, 2014.

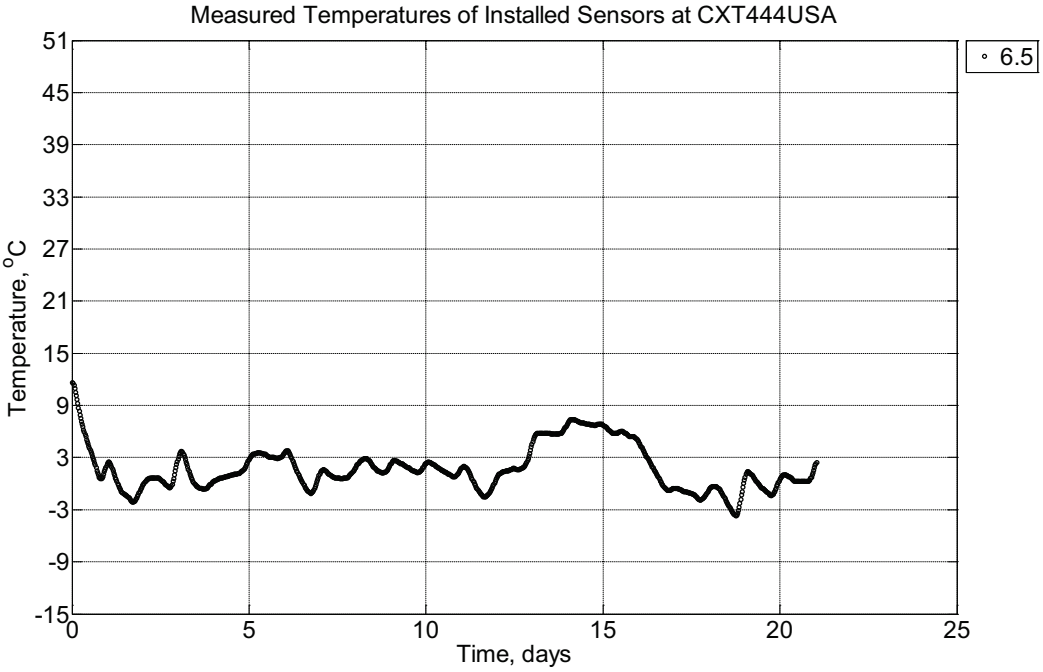

Figure B-643 Measured temperature at a depth of 6.5 inches (139.7 mm) from the surface of a concrete crosstie (labeled CXT444USA) installed in ballast in Rantoul, IL, between November 30, 2014, through December 21, 2014. An 8 mm thick polyurethane pad and 12

in (30.48 cm) length 136 lb/yd (67.5 kg/m) section of steel rail are additionally installed atop the concrete crosstie.

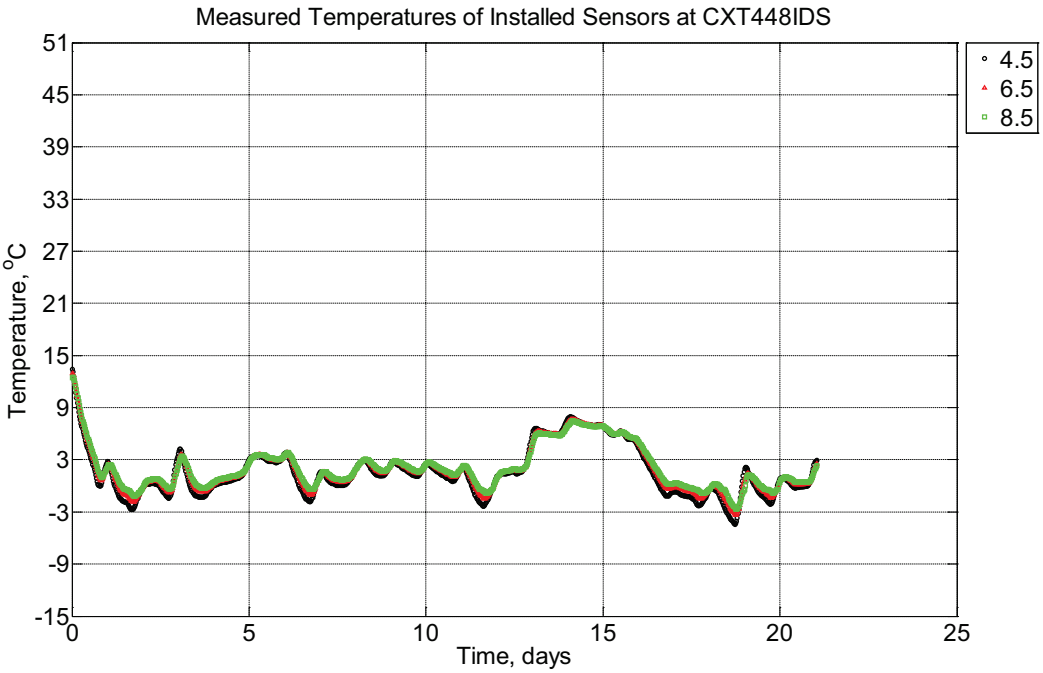

Figure B-644 Measured temperature at depths of 4.5 inches (114.3 mm), 6.5 inches (139.7 mm), and 8.5 inches (215.9 mm) from the surface of a concrete crosstie (labeled CXT448IDS) installed in ballast in Rantoul, IL, between November 30, 2014, through December 21, 2014. An 8 mm thick polyurethane pad and 12 in (30.48 cm) length 136 lb/yd (67.5 kg/m) section of steel rail are additionally installed atop the concrete crosstie.

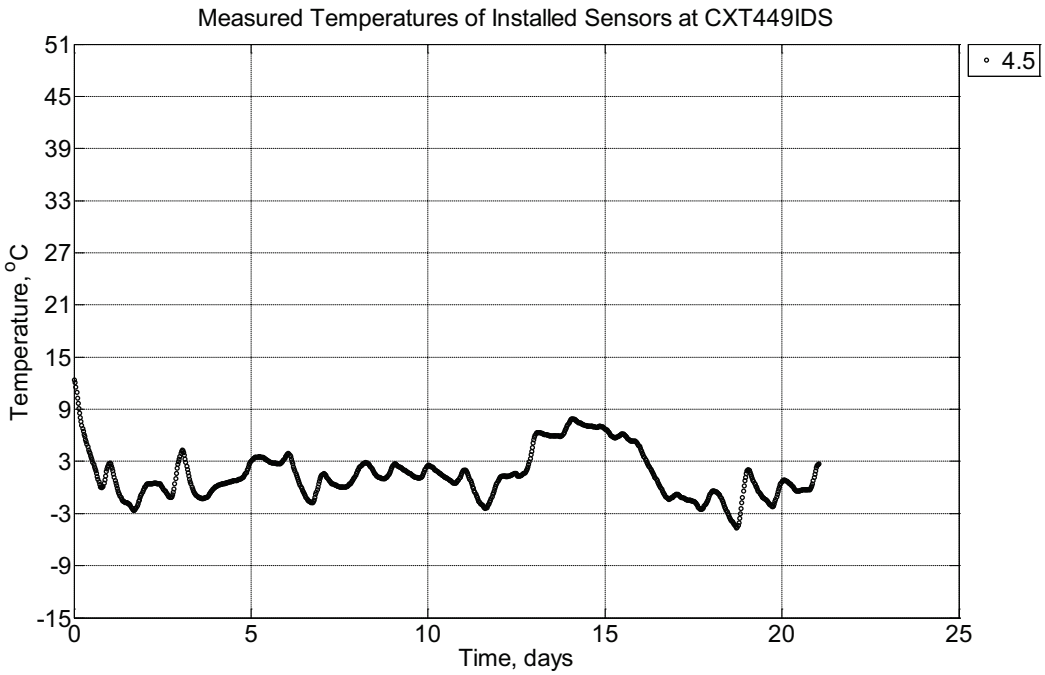

Figure B-645 Measured temperature at a depth of 4.5 inches (114.3 mm) from the surface of a concrete crosstie (labeled CXT449IDS) installed in ballast in Rantoul, IL, between November 30, 2014, through December 21, 2014. An 8 mm thick polyurethane pad and 12 in (30.48 cm) length 136 lb/yd (67.5 kg/m) section of steel rail are additionally installed atop the concrete crosstie.

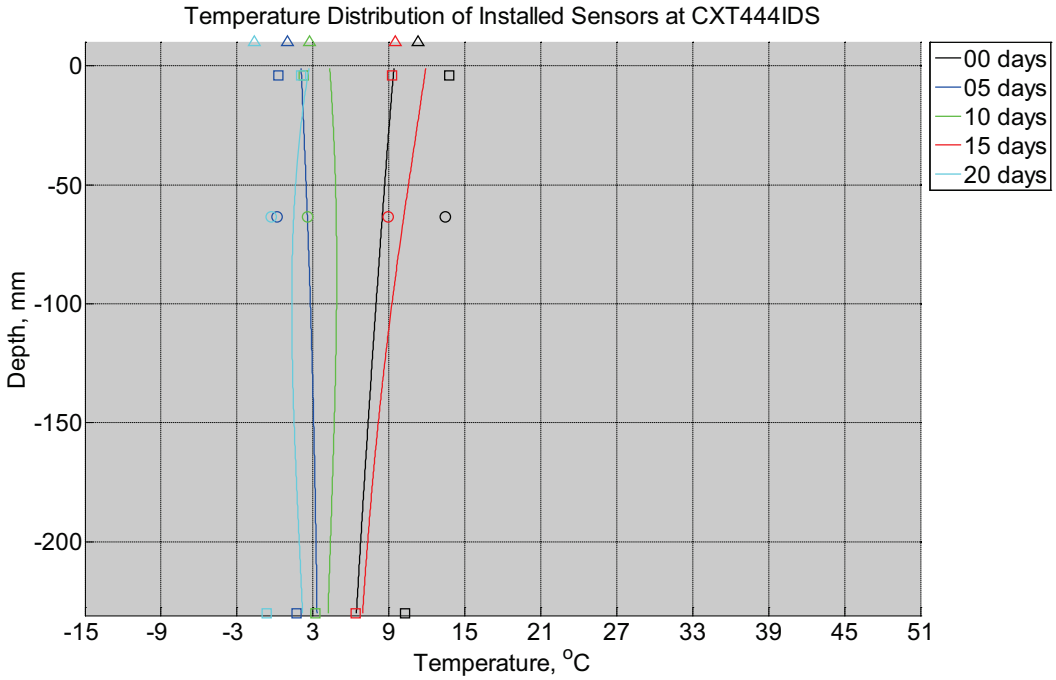

Figure B-646 Measured (markers) and modeled (continuous line) temperature profile

distribution as a function of depth inside a concrete crosstie (labeled CXT444IDS) without a polyurethane pad nor rail installed in ballast in Rantoul, IL, between November 30, 2014, through December 21, 2014. Triangular markers denote temperature value from KTIP weather station, square markers denote measured temperature values from ballast, and circular markers denote measured temperature values inside concrete.

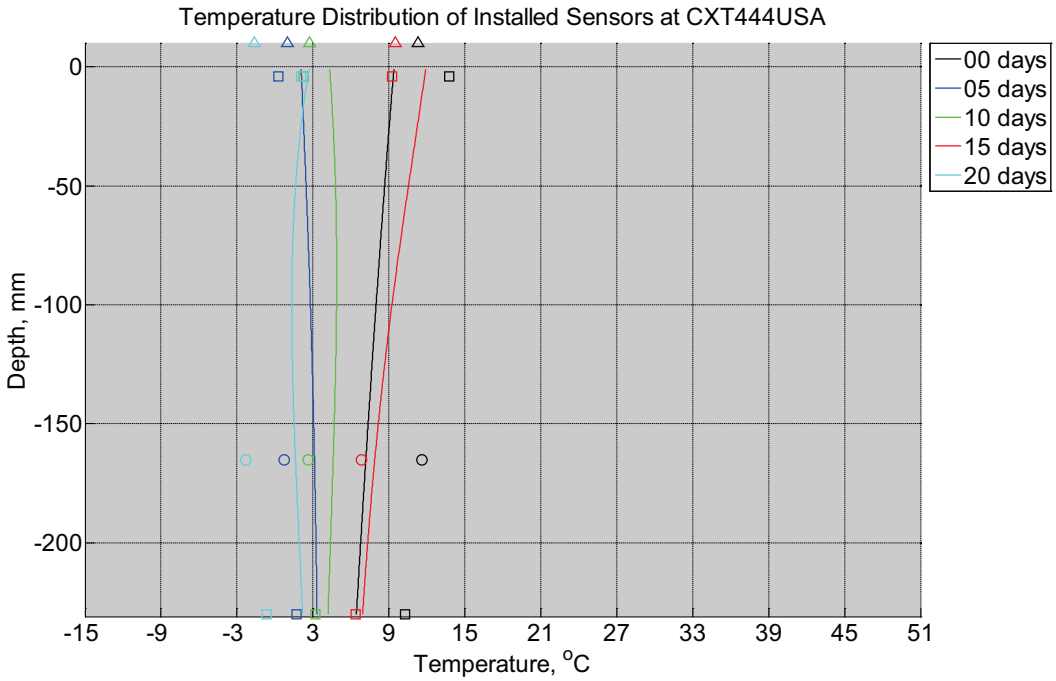

Figure B-647 Measured (markers) and modeled (continuous line) temperature profile distribution as a function of depth inside a concrete crosstie (labeled CXT444USA) installed in ballast in Rantoul, IL, between November 30, 2014, through December 21, 2014. An 8 mm thick polyurethane pad and 12 in (30.48 cm) length 136 lb/yd (67.5 kg/m) section of steel rail are additionally installed atop the model concrete crosstie. The model does not incorporate a polyurethane pad nor steel rail line. Triangular markers denote temperature value from KTIP weather station, square markers denote measured temperature values from ballast, and circular markers denote measured temperature values inside concrete.

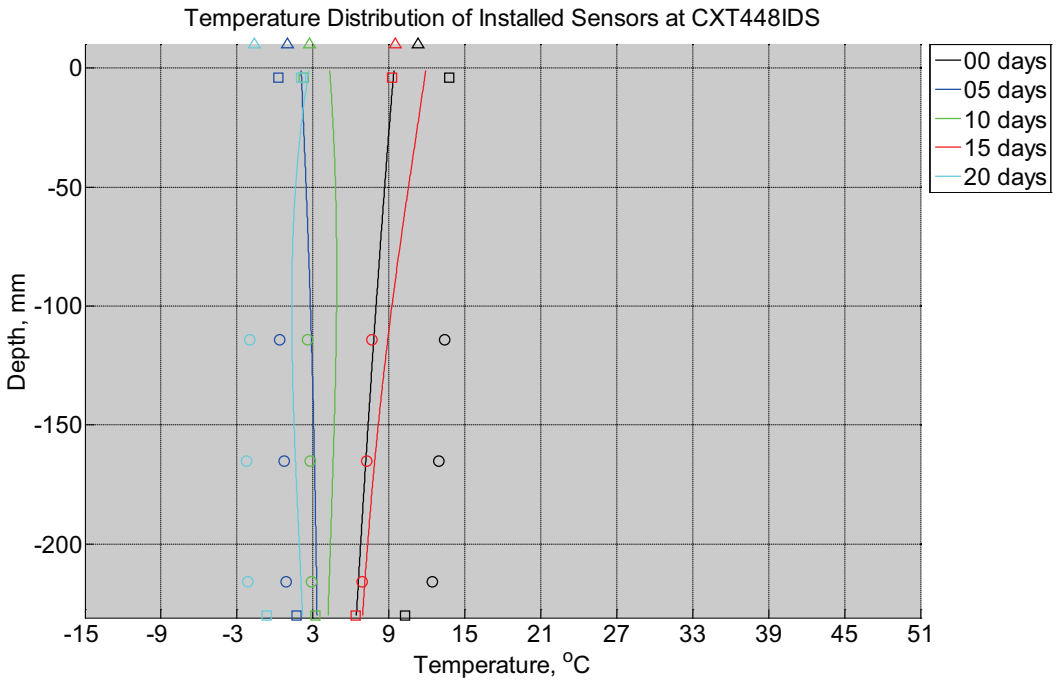

Figure B-648 Measured (markers) and modeled (continuous line) temperature profile distribution as a function of depth inside a concrete crosstie (labeled CXT448IDS) installed in ballast in Rantoul, IL, between November 30, 2014, through December 21, 2014. An 8 mm thick polyurethane pad and 12 in (30.48 cm) length 136 lb/yd (67.5 kg/m) section of steel rail are additionally installed atop the model concrete crosstie. The model does not incorporate a polyurethane pad nor steel rail line. Triangular markers denote temperature value from KTIP weather station, square markers denote measured temperature values from ballast, and circular markers denote measured temperature values inside concrete.

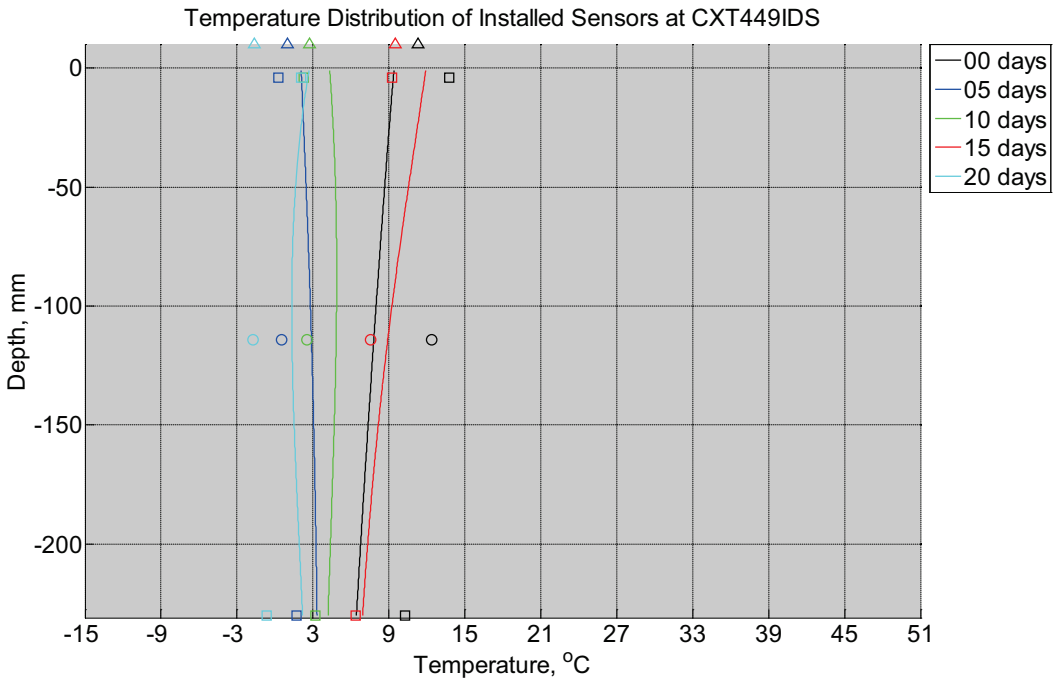

Figure B-649 Measured (markers) and modeled (continuous line) temperature profile distribution as a function of depth inside a concrete crosstie (labeled CXT449IDS) installed in ballast in Rantoul, IL, between November 30, 2014, through December 21, 2014. An 8 mm thick polyurethane pad and 12 in (30.48 cm) length 136 lb/yd (67.5 kg/m) section of steel rail are additionally installed atop the model concrete crosstie. The model does not incorporate a polyurethane pad nor steel rail line. Triangular markers denote temperature value from KTIP weather station, square markers denote measured temperature values from ballast, and circular markers denote measured temperature values inside concrete.

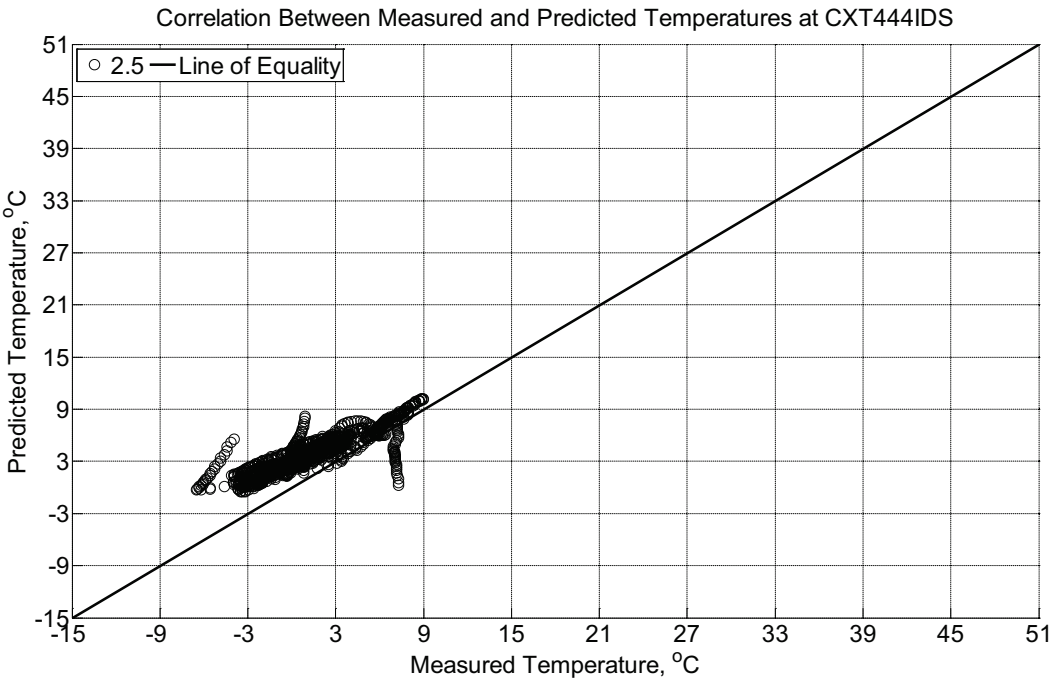

Figure B-650 Correlation between measured and predicted temperature values 2.5 inches (63.5 mm) from the surface of a concrete crosstie (labeled CXT444IDS) without a polyurethane pad nor rail installed in ballast in Rantoul, IL, between November 30, 2014, through December 21, 2014.

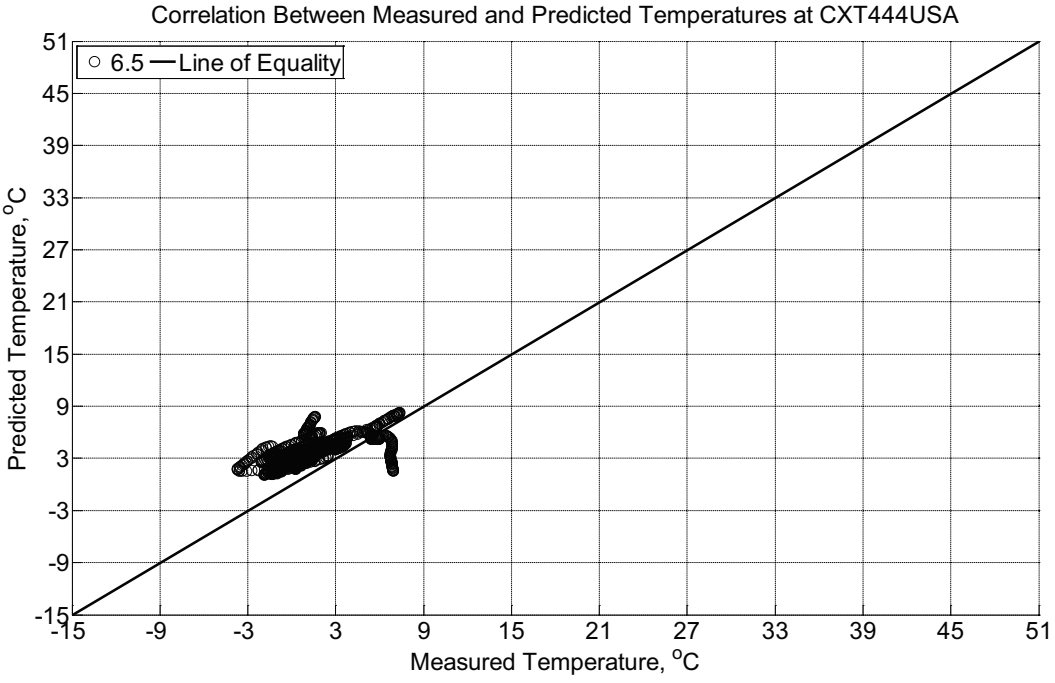

Figure B-651 Correlation between measured and predicted temperature values 6.5 inches (139.7 mm) from the surface of a concrete crosstie (labeled CXT444USA) installed in

ballast in Rantoul, IL, between November 30, 2014, through December 21, 2014. An 8 mm thick polyurethane pad and 12 in (30.48 cm) length 136 lb/yd (67.5 kg/m) section of steel rail are additionally installed atop the concrete crosstie. The model does not incorporate a polyurethane pad nor steel rail line.

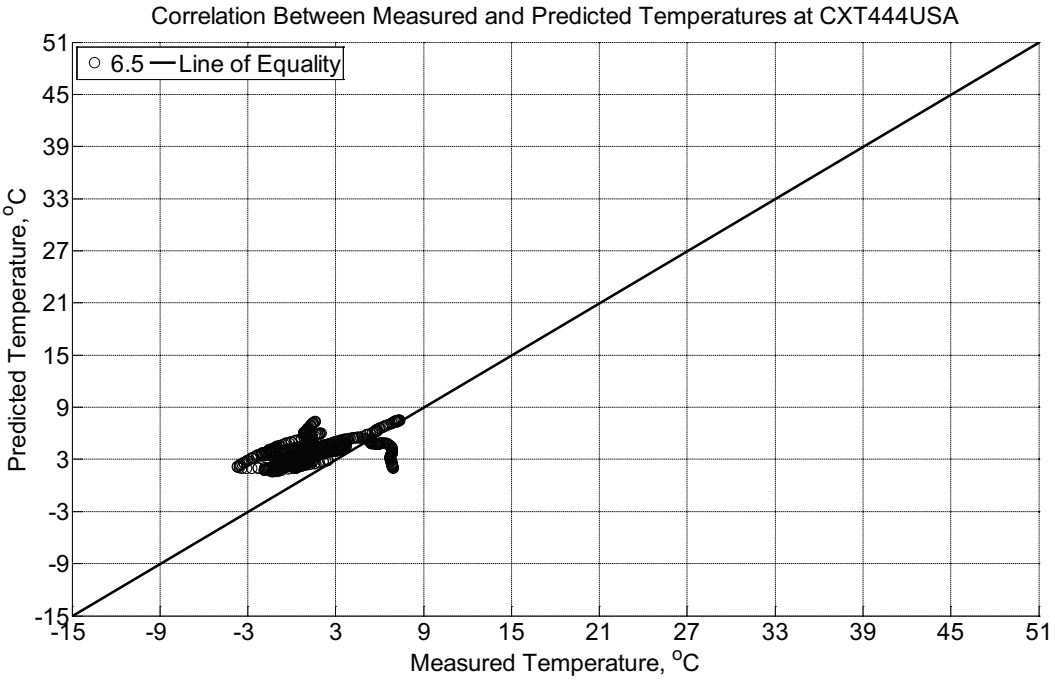

Figure B-652 Correlation between measured and predicted temperature values 6.5 inches (139.7 mm) from the surface of a concrete crosstie (labeled CXT444USA) installed in ballast in Rantoul, IL, between November 30, 2014, through December 21, 2014. An 8 mm thick polyurethane pad and 12 in (30.48 cm) length 136 lb/yd (67.5 kg/m) section of steel rail are additionally installed atop the concrete crosstie. The model incorporates a 1 mm thick polyurethane pad and 1 mm thick steel rail line.

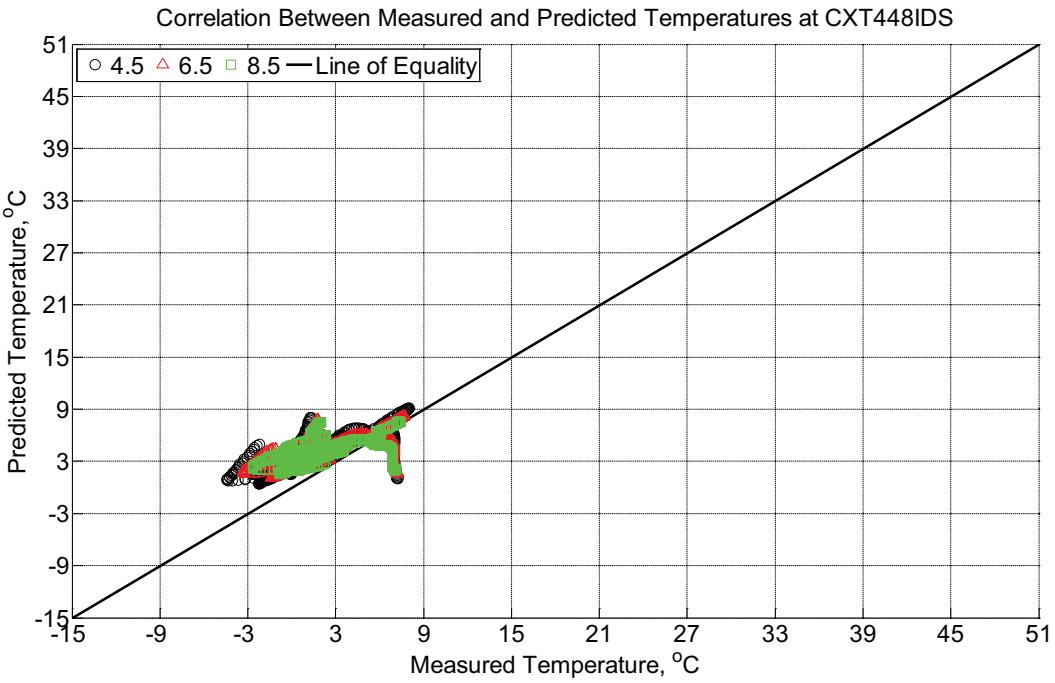

Figure B-653 Correlation between measured and predicted temperature values 4.5 inches (114.3 mm), 6.5 inches (139.7 mm), and 8.5 inches (215.9 mm) from the surface of a concrete crosstie (labeled CXT448IDS) installed in ballast in Rantoul, IL, between November 30, 2014, through December 21, 2014. An 8 mm thick polyurethane pad and 12 in (30.48 cm) length 136 lb/yd (67.5 kg/m) section of steel rail are additionally installed atop the concrete crosstie. The model does not incorporate a polyurethane pad nor steel rail line.

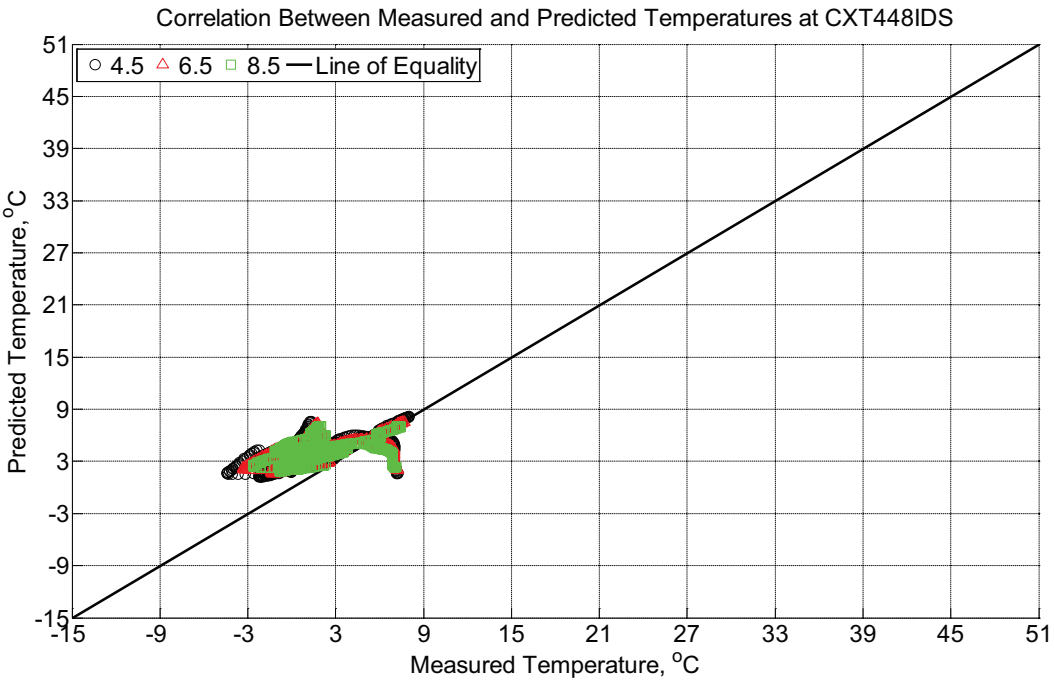

Figure B-654 Correlation between measured and predicted temperature values 4.5 inches (114.3 mm), 6.5 inches (139.7 mm), and 8.5 inches (215.9 mm) from the surface of a concrete crosstie (labeled CXT448IDS) installed in ballast in Rantoul, IL, between November 30, 2014, through December 21, 2014. An 8 mm thick polyurethane pad and 12 in (30.48 cm) length 136 lb/yd (67.5 kg/m) section of steel rail are additionally installed atop the concrete crosstie. The model incorporates a 1 mm thick polyurethane pad and 1 mm thick steel rail line.

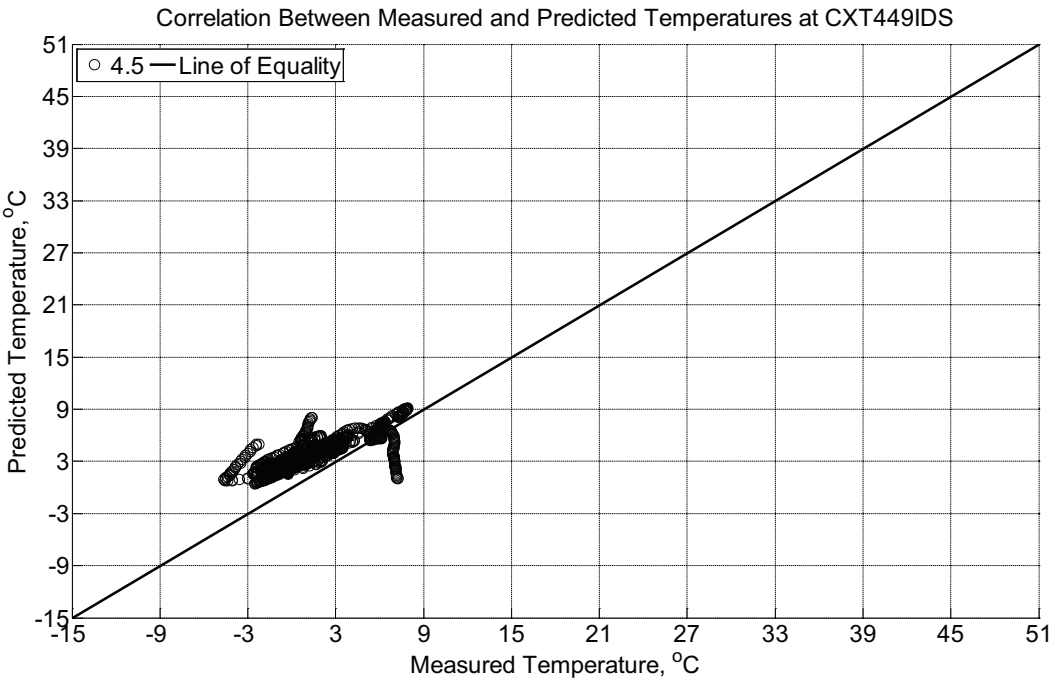

Figure B-655 Correlation between measured and predicted temperature values 4.5 inches (114.3 mm) from the surface of a concrete crosstie (labeled CXT449IDS) installed in ballast in Rantoul, IL, between November 30, 2014, through December 21, 2014. An 8 mm thick polyurethane pad and 12 in (30.48 cm) length 136 lb/yd (67.5 kg/m) section of steel rail are additionally installed atop the concrete crosstie. The model does not incorporate a polyurethane pad nor steel rail line.

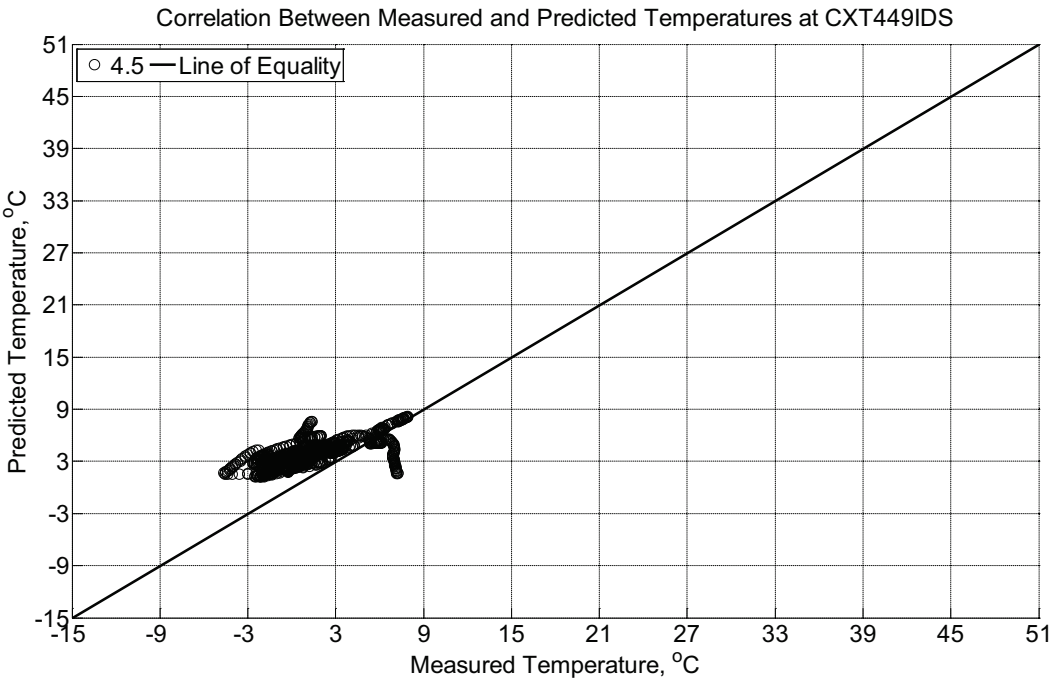

Figure B-656 Correlation between measured and predicted temperature values 4.5 inches (114.3 mm) from the surface of a concrete crosstie (labeled CXT449IDS) installed in ballast in Rantoul, IL, between November 30, 2014, through December 21, 2014. An 8 mm thick polyurethane pad and 12 in (30.48 cm) length 136 lb/yd (67.5 kg/m) section of steel rail are additionally installed atop the concrete crosstie. The model incorporates a 1 mm thick polyurethane pad and 1 mm thick steel rail line.

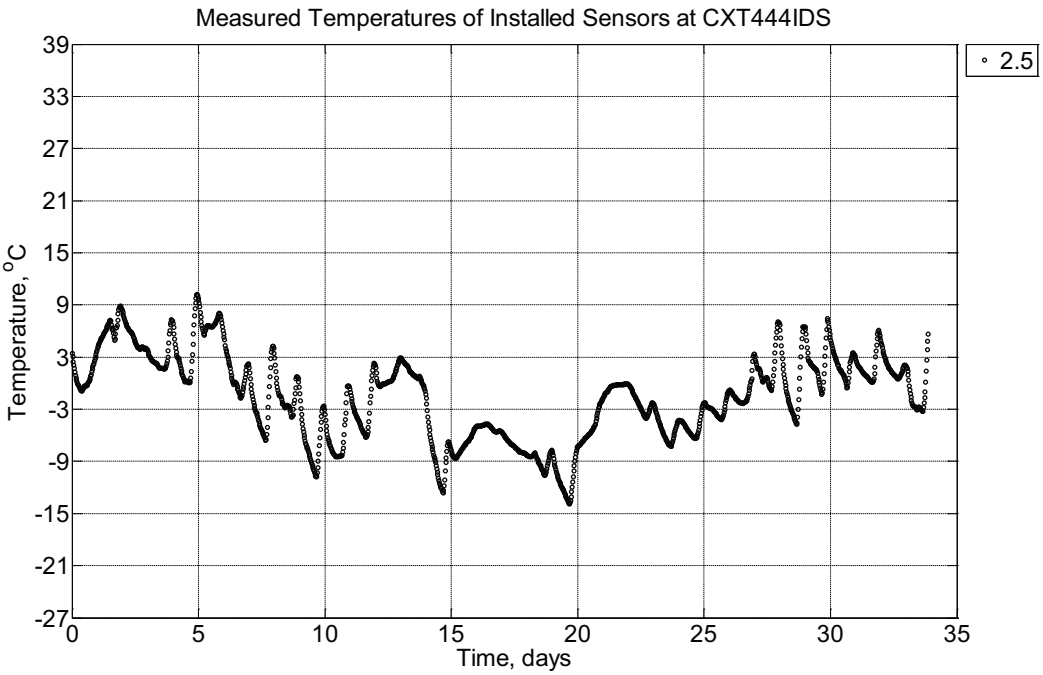

Figure B-657 Measured temperature at a depth of 2.5 inches (63.5 mm) from the surface of a concrete crosstie (labeled CXT444IDS) without a polyurethane pad nor rail installed in ballast in Rantoul, IL, between December 21, 2014, through January 24, 2015.

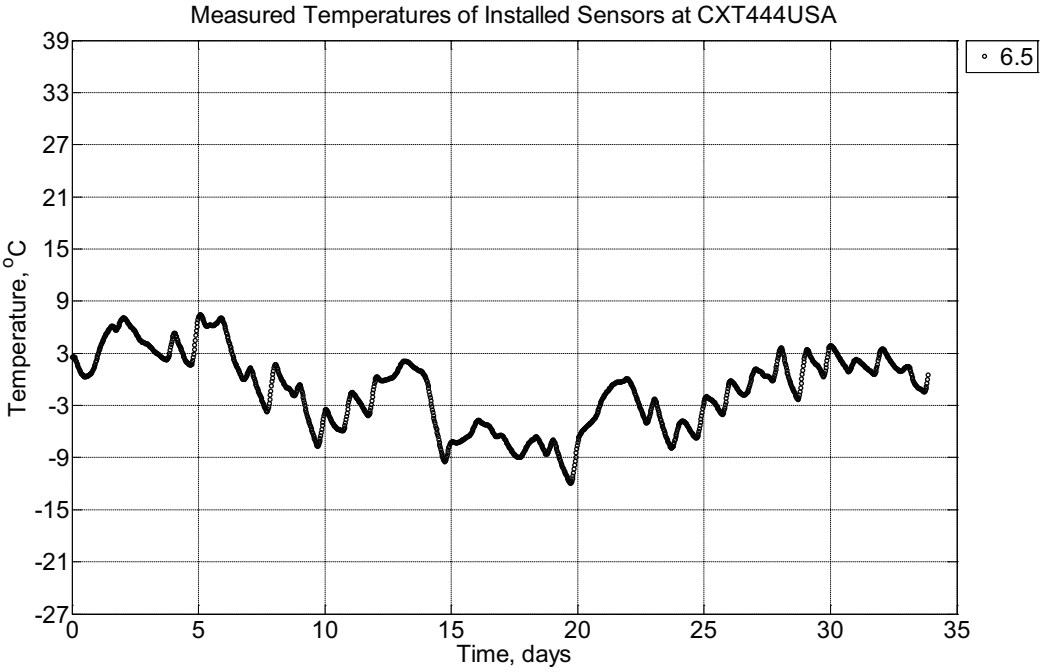

Figure B-658 Measured temperature at a depth of 6.5 inches (139.7 mm) from the surface of a concrete crosstie (labeled CXT444USA) installed in ballast in Rantoul, IL, between December 21, 2014, through January 24, 2015. An 8 mm thick polyurethane pad and 12 in

(30.48 cm) length 136 lb/yd (67.5 kg/m) section of steel rail are additionally installed atop the concrete crosstie.

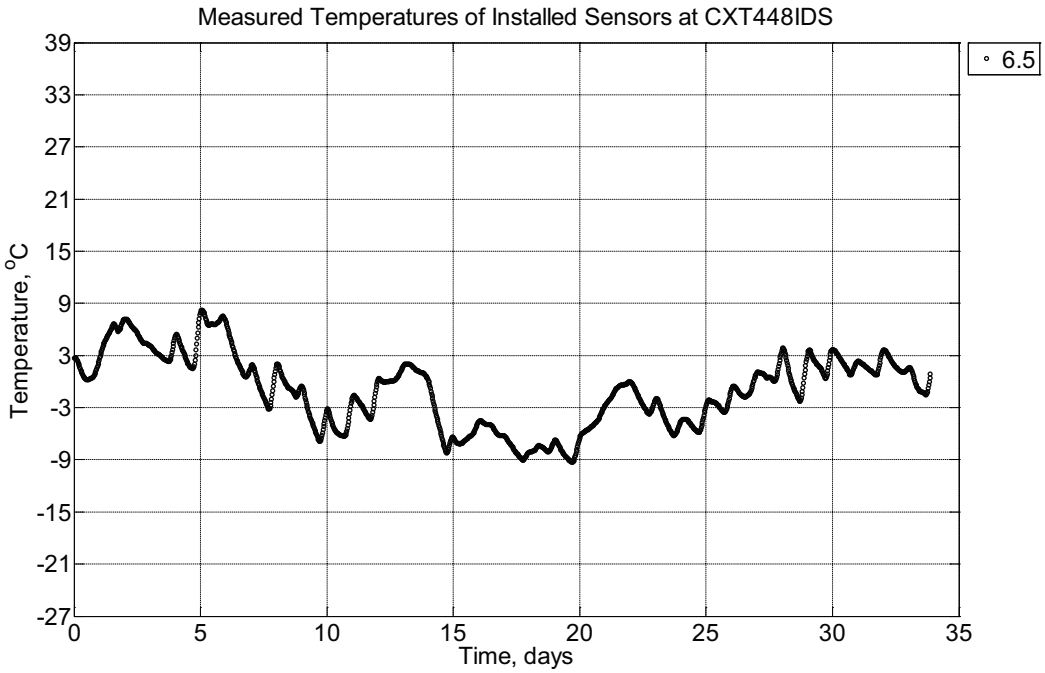

Figure B-659 Measured temperature at depths of 6.5 inches (139.7 mm) from the surface of a concrete crosstie (labeled CXT448IDS) installed in ballast in Rantoul, IL, between December 21, 2014, through January 24, 2015. An 8 mm thick polyurethane pad and 12 in (30.48 cm) length 136 lb/yd (67.5 kg/m) section of steel rail are additionally installed atop the concrete crosstie.

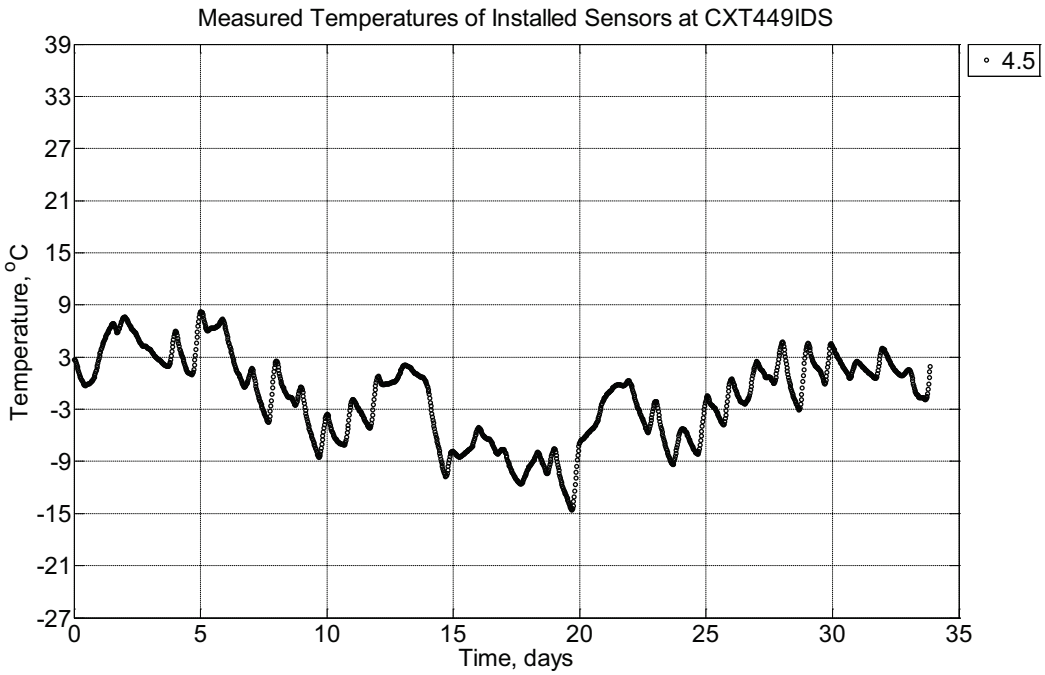

Figure B-660 Measured temperature at a depth of 4.5 inches (114.3 mm) from the surface of a concrete crosstie (labeled CXT449IDS) installed in ballast in Rantoul, IL, between December 21, 2014, through January 24, 2015. An 8 mm thick polyurethane pad and 12 in (30.48 cm) length 136 lb/yd (67.5 kg/m) section of steel rail are additionally installed atop the concrete crosstie.

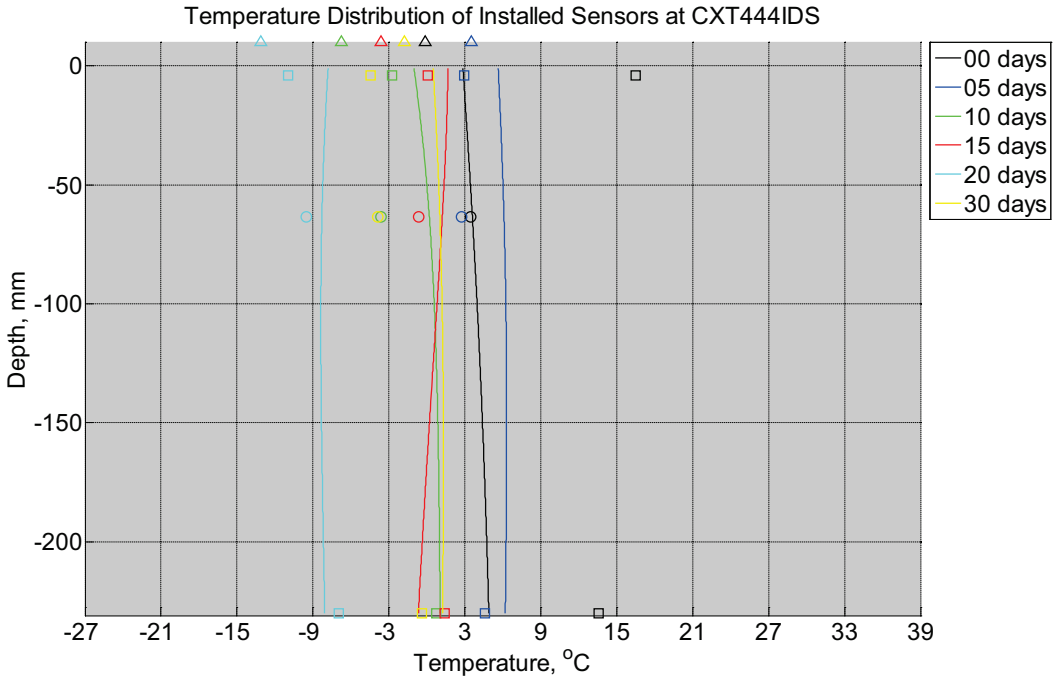

Figure B-661 Measured (markers) and modeled (continuous line) temperature profile

distribution as a function of depth inside a concrete crosstie (labeled CXT444IDS) without a polyurethane pad nor rail installed in ballast in Rantoul, IL, between December 21, 2014, through January 24, 2015. Triangular markers denote temperature value from KTIP weather station, square markers denote measured temperature values from ballast, and circular markers denote measured temperature values inside concrete.

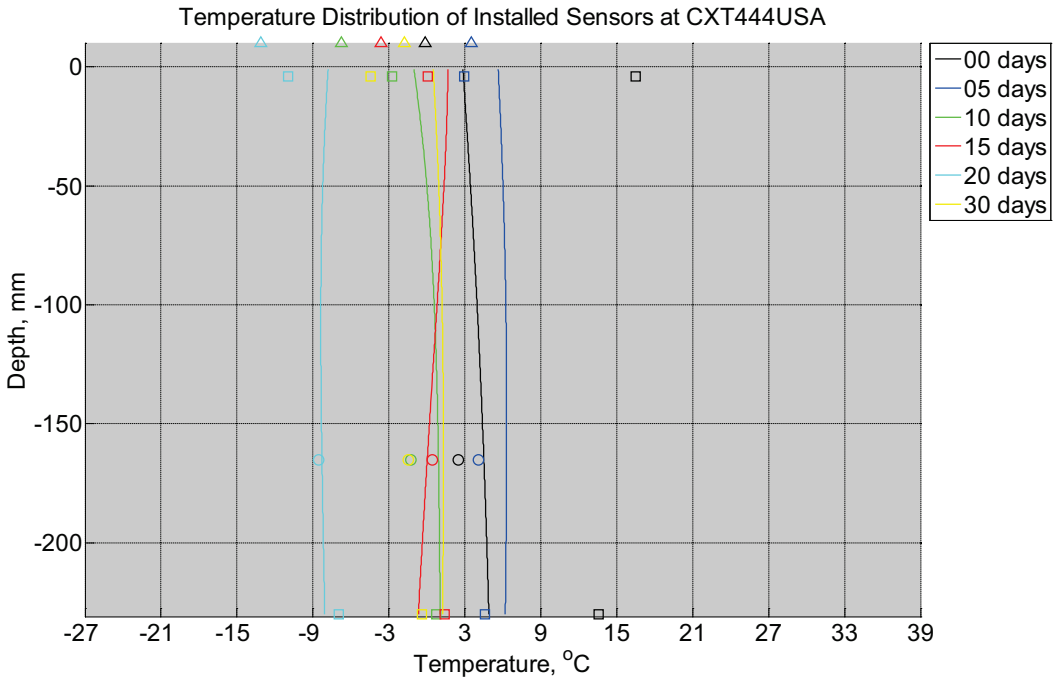

Figure B-662 Measured (markers) and modeled (continuous line) temperature profile distribution as a function of depth inside a concrete crosstie (labeled CXT444USA) installed in ballast in Rantoul, IL, between December 21, 2014, through January 24, 2015. An 8 mm thick polyurethane pad and 12 in (30.48 cm) length 136 lb/yd (67.5 kg/m) section of steel rail are additionally installed atop the model concrete crosstie. The model does not incorporate a polyurethane pad nor steel rail line. Triangular markers denote temperature value from KTIP weather station, square markers denote measured temperature values from ballast, and circular markers denote measured temperature values inside concrete.

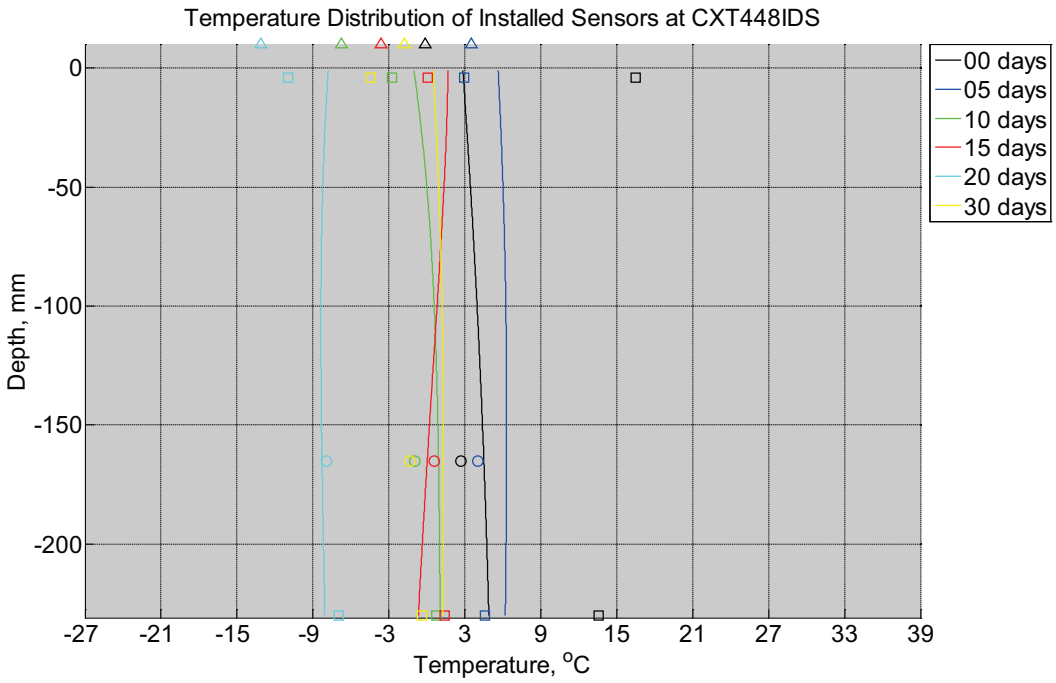

Figure B-663 Measured (markers) and modeled (continuous line) temperature profile distribution as a function of depth inside a concrete crosstie (labeled CXT448IDS) installed in ballast in Rantoul, IL, between December 21, 2014, through January 24, 2015. An 8 mm thick polyurethane pad and 12 in (30.48 cm) length 136 lb/yd (67.5 kg/m) section of steel rail are additionally installed atop the model concrete crosstie. The model does not incorporate a polyurethane pad nor steel rail line. Triangular markers denote temperature value from KTIP weather station, square markers denote measured temperature values from ballast, and circular markers denote measured temperature values inside concrete.

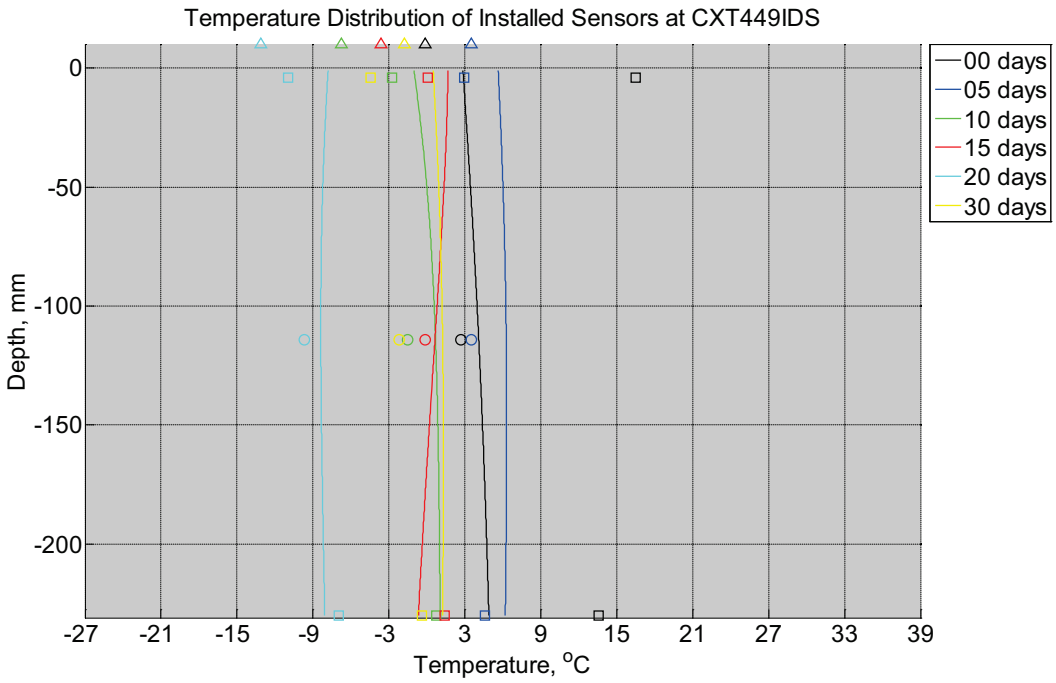

Figure B-664 Measured (markers) and modeled (continuous line) temperature profile distribution as a function of depth inside a concrete crosstie (labeled CXT449IDS) installed in ballast in Rantoul, IL, between December 21, 2014, through January 24, 2015. An 8 mm thick polyurethane pad and 12 in (30.48 cm) length 136 lb/yd (67.5 kg/m) section of steel rail are additionally installed atop the model concrete crosstie. The model does not incorporate a polyurethane pad nor steel rail line. Triangular markers denote temperature value from KTIP weather station, square markers denote measured temperature values from ballast, and circular markers denote measured temperature values inside concrete.

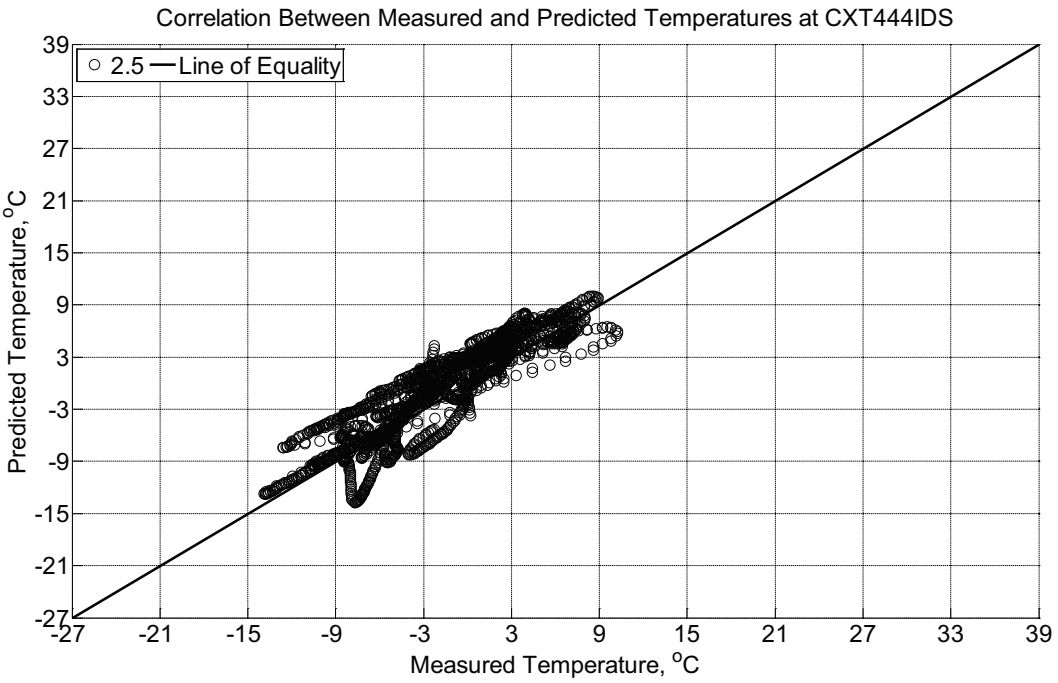

Figure B-665 Correlation between measured and predicted temperature values 2.5 inches (63.5 mm) from the surface of a concrete crosstie (labeled CXT444IDS) without a polyurethane pad nor rail installed in ballast in Rantoul, IL, between December 21, 2014, through January 24, 2015.

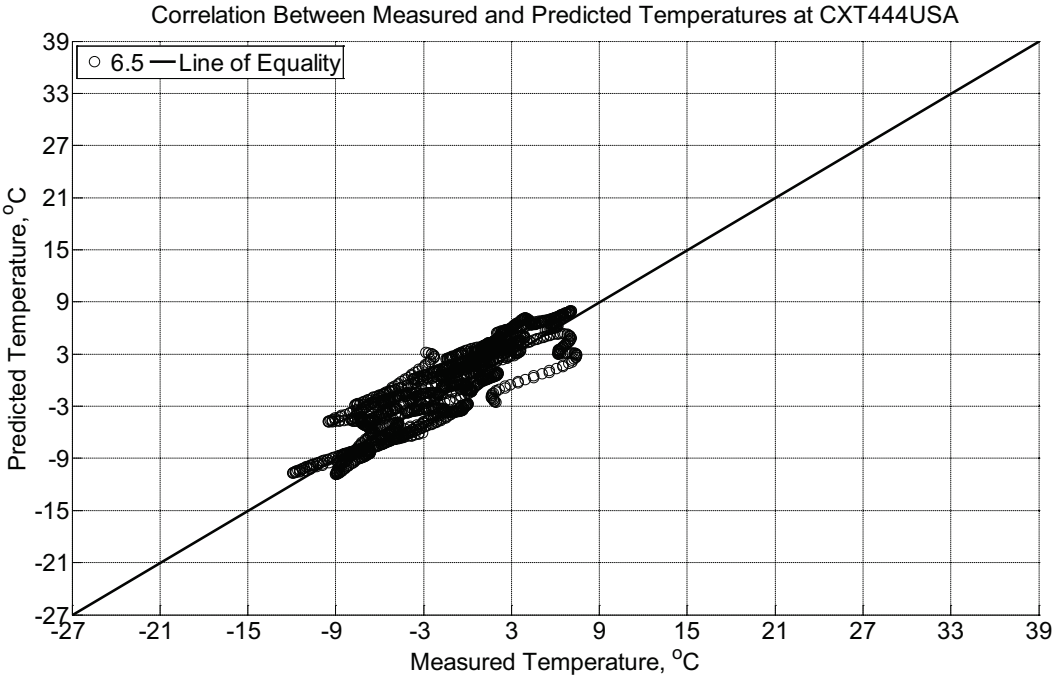

Figure B-666 Correlation between measured and predicted temperature values 6.5 inches (139.7 mm) from the surface of a concrete crosstie (labeled CXT444USA) installed in

ballast in Rantoul, IL, between December 21, 2014, through January 24, 2015. An 8 mm thick polyurethane pad and 12 in (30.48 cm) length 136 lb/yd (67.5 kg/m) section of steel rail are additionally installed atop the concrete crosstie. The model does not incorporate a polyurethane pad nor steel rail line.

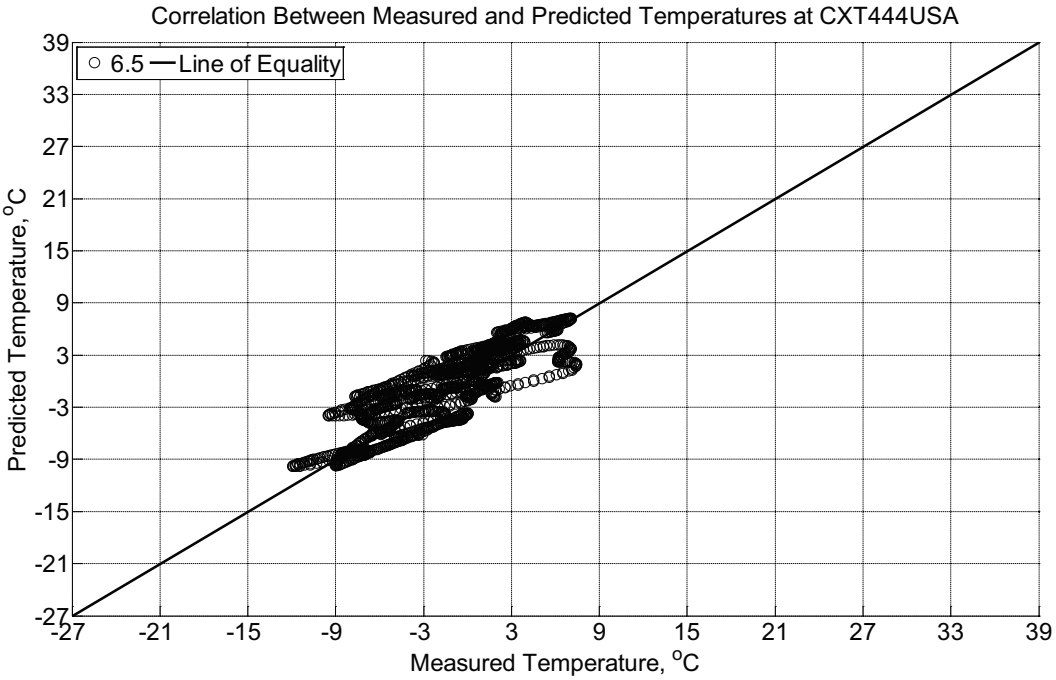

Figure B-667 Correlation between measured and predicted temperature values 6.5 inches (139.7 mm) from the surface of a concrete crosstie (labeled CXT444USA) installed in ballast in Rantoul, IL, between December 21, 2014, through January 24, 2015. An 8 mm thick polyurethane pad and 12 in (30.48 cm) length 136 lb/yd (67.5 kg/m) section of steel rail are additionally installed atop the concrete crosstie. The model incorporates a 1 mm thick polyurethane pad and 1 mm thick steel rail line.

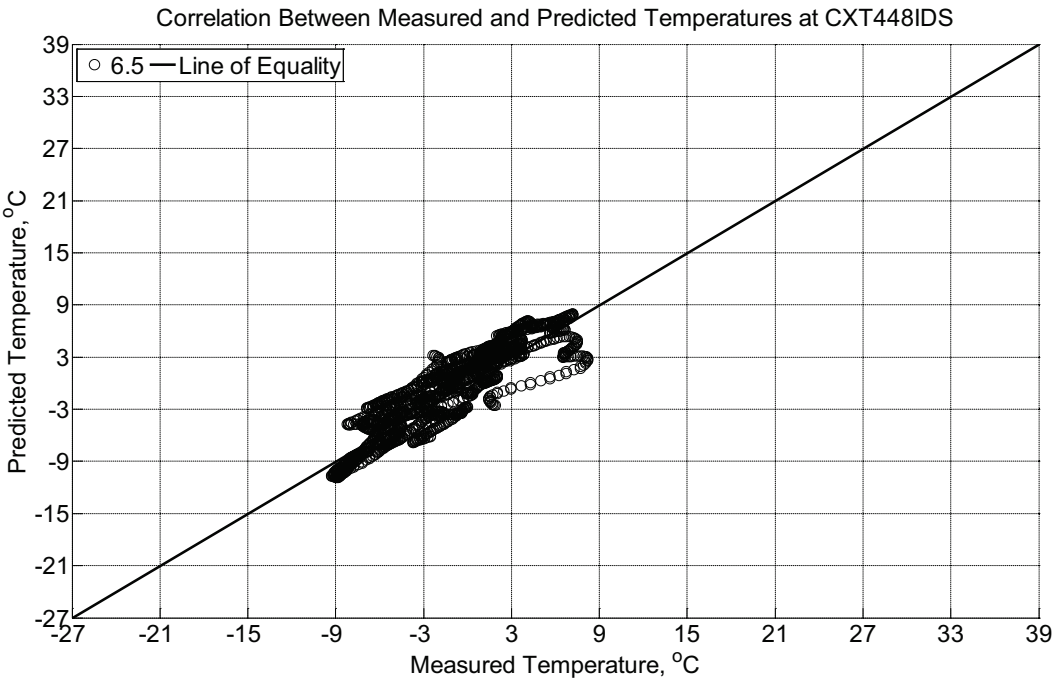

Figure B-668 Correlation between measured and predicted temperature values 6.5 inches (139.7 mm) from the surface of a concrete crosstie (labeled CXT448IDS) installed in ballast in Rantoul, IL, between December 21, 2014, through January 24, 2015. An 8 mm thick polyurethane pad and 12 in (30.48 cm) length 136 lb/yd (67.5 kg/m) section of steel rail are additionally installed atop the concrete crosstie. The model does not incorporate a polyurethane pad nor steel rail line.

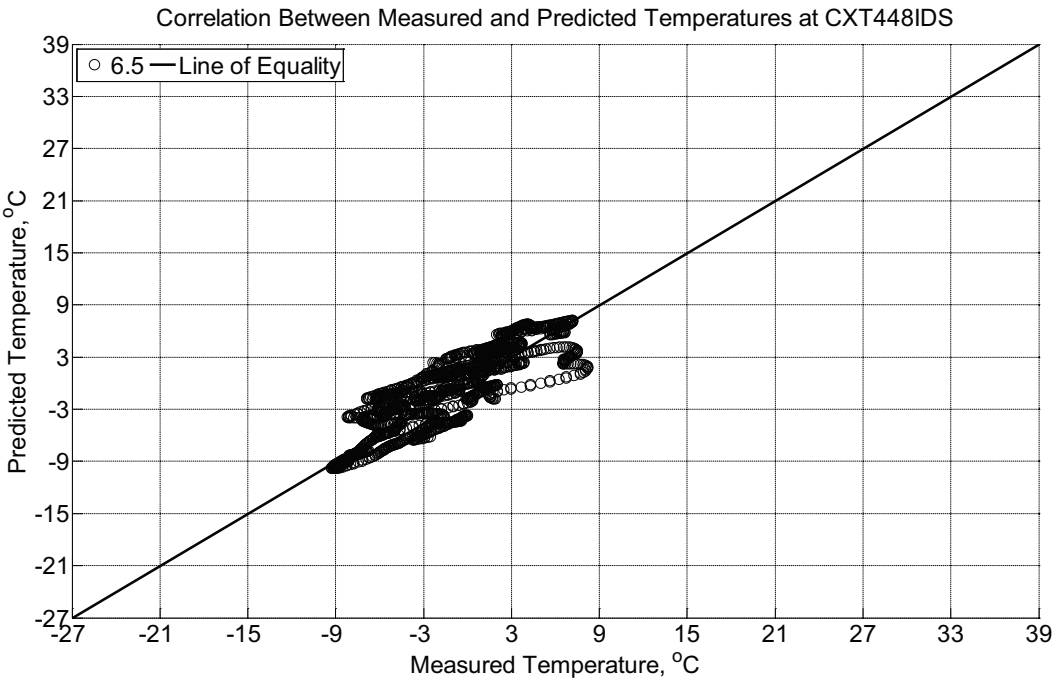

Figure B-669 Correlation between measured and predicted temperature values 6.5 inches (139.7 mm) from the surface of a concrete crosstie (labeled CXT448IDS) installed in ballast in Rantoul, IL, between December 21, 2014, through January 24, 2015. An 8 mm thick polyurethane pad and 12 in (30.48 cm) length 136 lb/yd (67.5 kg/m) section of steel rail are additionally installed atop the concrete crosstie. The model incorporates a 1 mm thick polyurethane pad and 1 mm thick steel rail line.

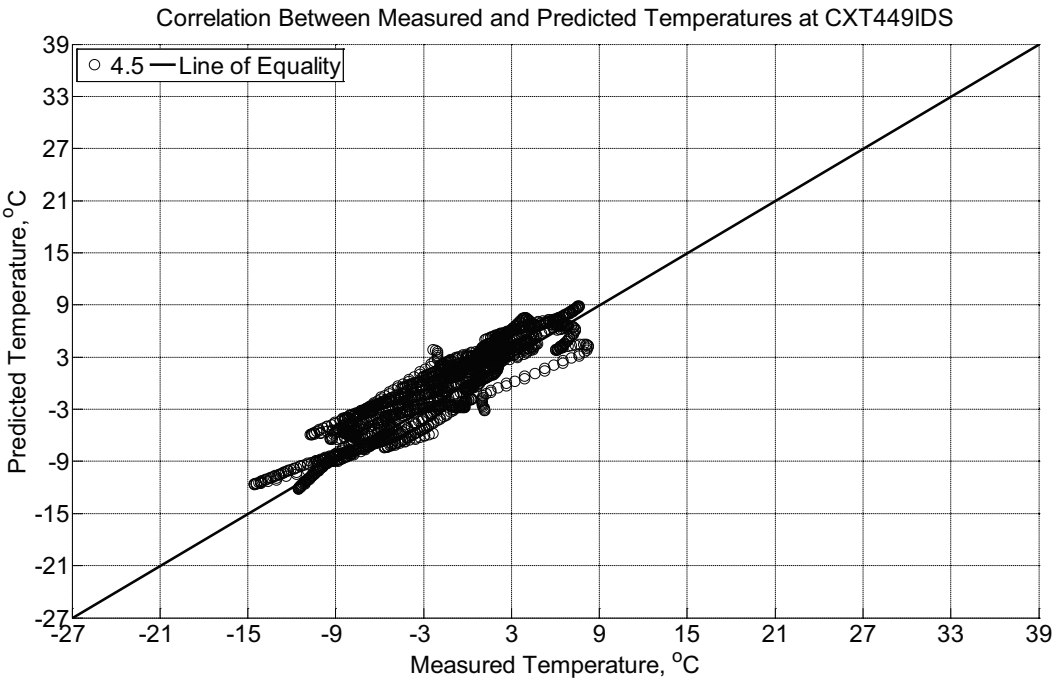

Figure B-670 Correlation between measured and predicted temperature values 4.5 inches (114.3 mm) from the surface of a concrete crosstie (labeled CXT449IDS) installed in ballast in Rantoul, IL, between December 21, 2014, through January 24, 2015. An 8 mm thick polyurethane pad and 12 in (30.48 cm) length 136 lb/yd (67.5 kg/m) section of steel rail are additionally installed atop the concrete crosstie. The model does not incorporate a polyurethane pad nor steel rail line.

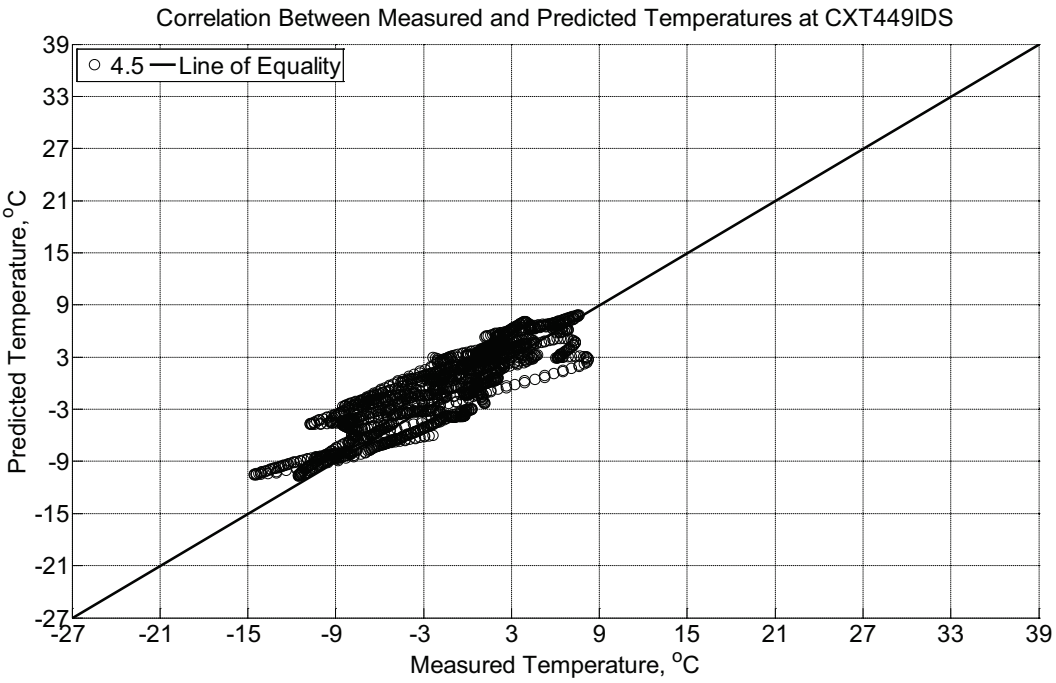

Figure B-671 Correlation between measured and predicted temperature values 4.5 inches (114.3 mm) from the surface of a concrete crosstie (labeled CXT449IDS) installed in ballast in Rantoul, IL, between December 21, 2014, through January 24, 2015. An 8 mm thick polyurethane pad and 12 in (30.48 cm) length 136 lb/yd (67.5 kg/m) section of steel rail are additionally installed atop the concrete crosstie. The model incorporates a 1 mm thick polyurethane pad and 1 mm thick steel rail line.

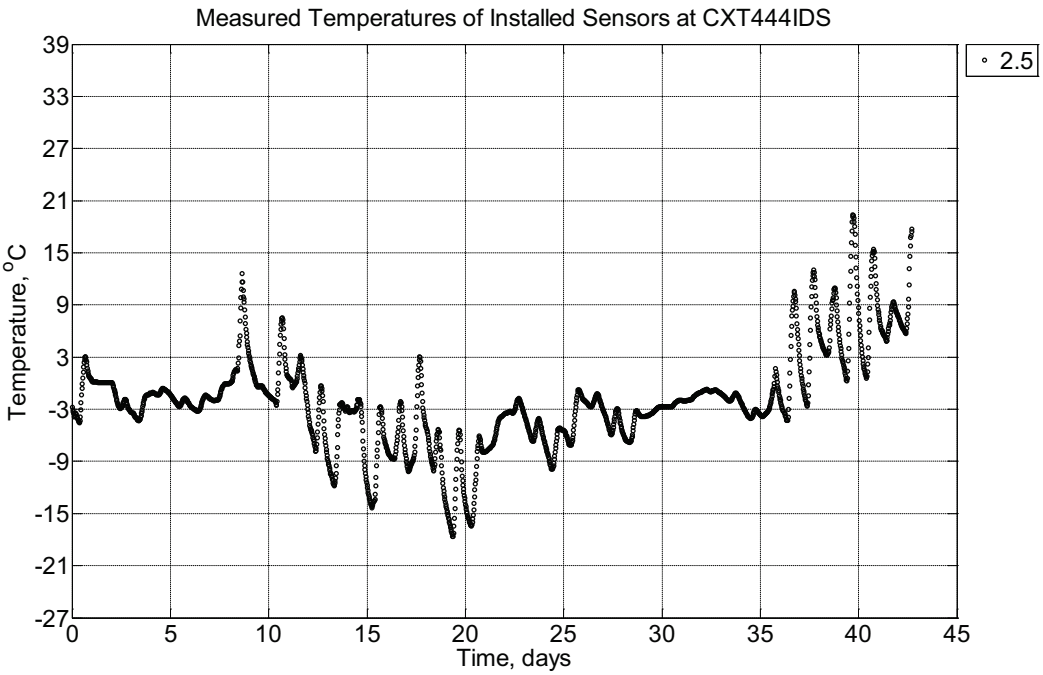

Figure B-672 Measured temperature at a depth of 2.5 inches (63.5 mm) from the surface of a concrete crosstie (labeled CXT444IDS) without a polyurethane pad nor rail installed in ballast in Rantoul, IL, between January 30, 2015, through March 14, 2015.

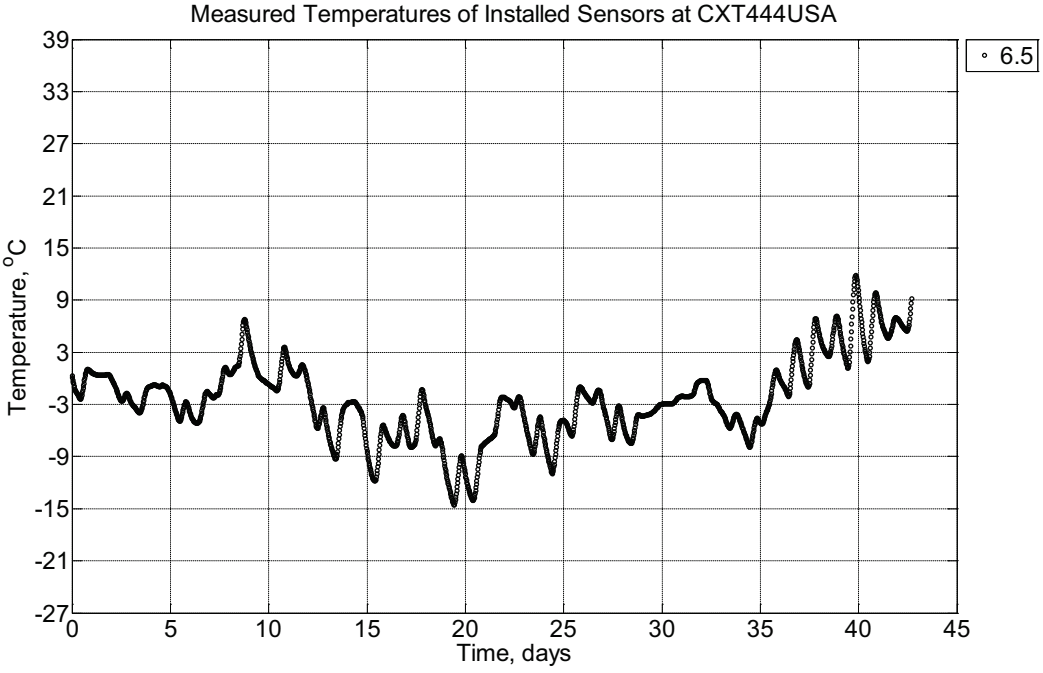

Figure B-673 Measured temperature at a depth of 6.5 inches (139.7 mm) from the surface of a concrete crosstie (labeled CXT444USA) installed in ballast in Rantoul, IL, between January 30, 2015, through March 14, 2015. An 8 mm thick polyurethane pad and 12 in

(30.48 cm) length 136 lb/yd (67.5 kg/m) section of steel rail are additionally installed atop the concrete crosstie.

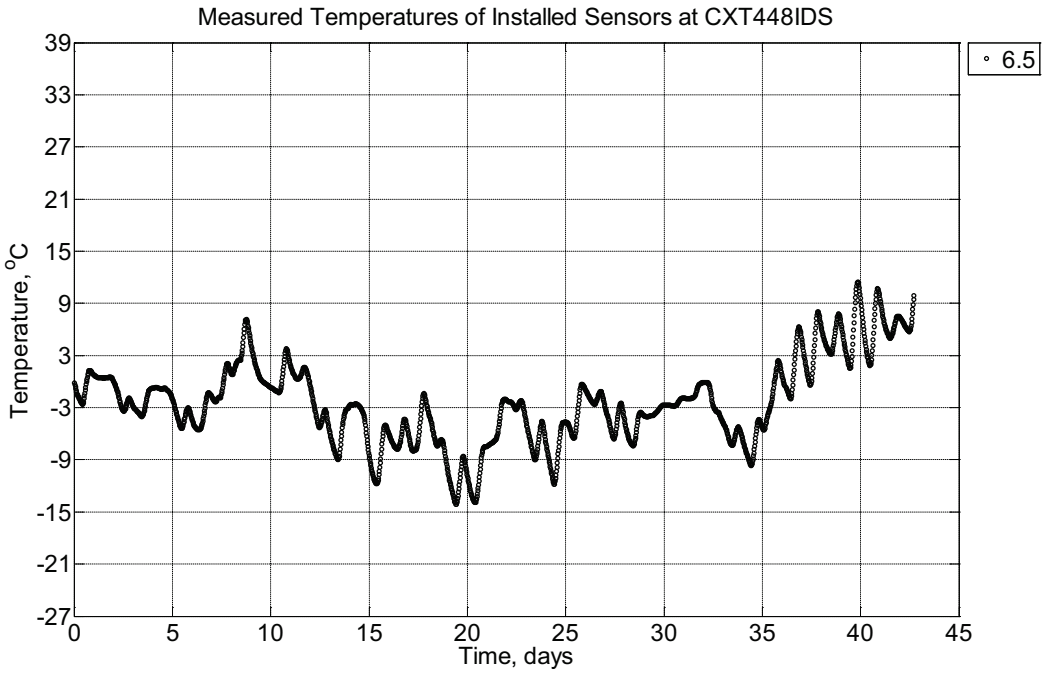

Figure B-674 Measured temperature at depths of 6.5 inches (139.7 mm) from the surface of a concrete crosstie (labeled CXT448IDS) installed in ballast in Rantoul, IL, between January 30, 2015, through March 14, 2015. An 8 mm thick polyurethane pad and 12 in (30.48 cm) length 136 lb/yd (67.5 kg/m) section of steel rail are additionally installed atop the concrete crosstie.

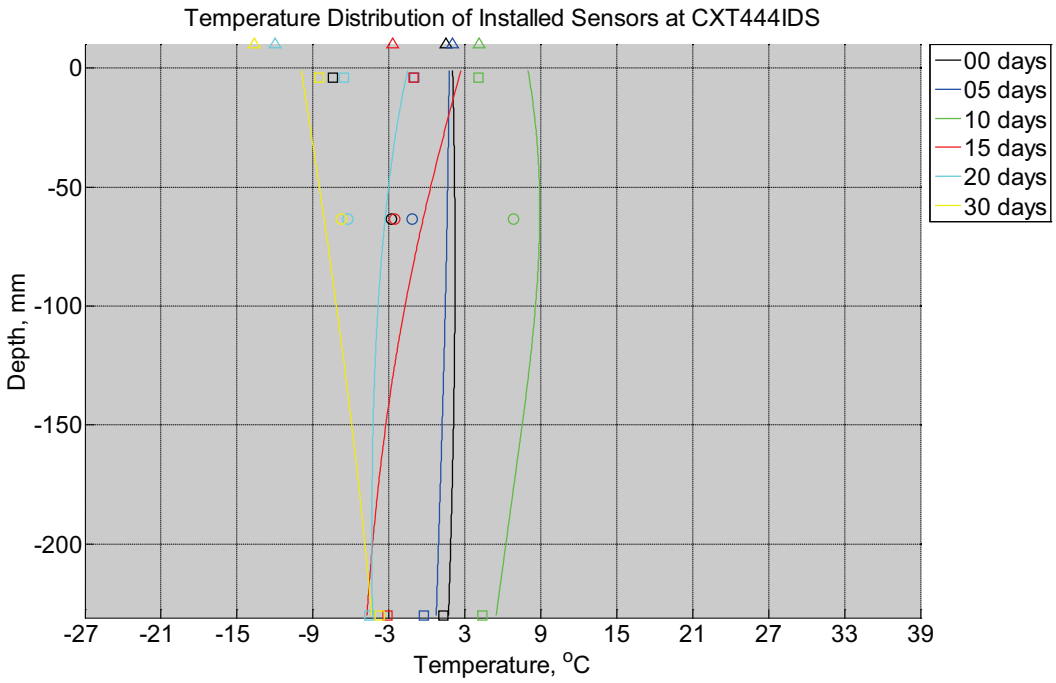

Figure B-675 Measured (markers) and modeled (continuous line) temperature profile distribution as a function of depth inside a concrete crosstie (labeled CXT444IDS) without a polyurethane pad nor rail installed in ballast in Rantoul, IL, between January 30, 2015, through March 14, 2015. Triangular markers denote temperature value from KTIP weather station, square markers denote measured temperature values from ballast, and circular markers denote measured temperature values inside concrete.

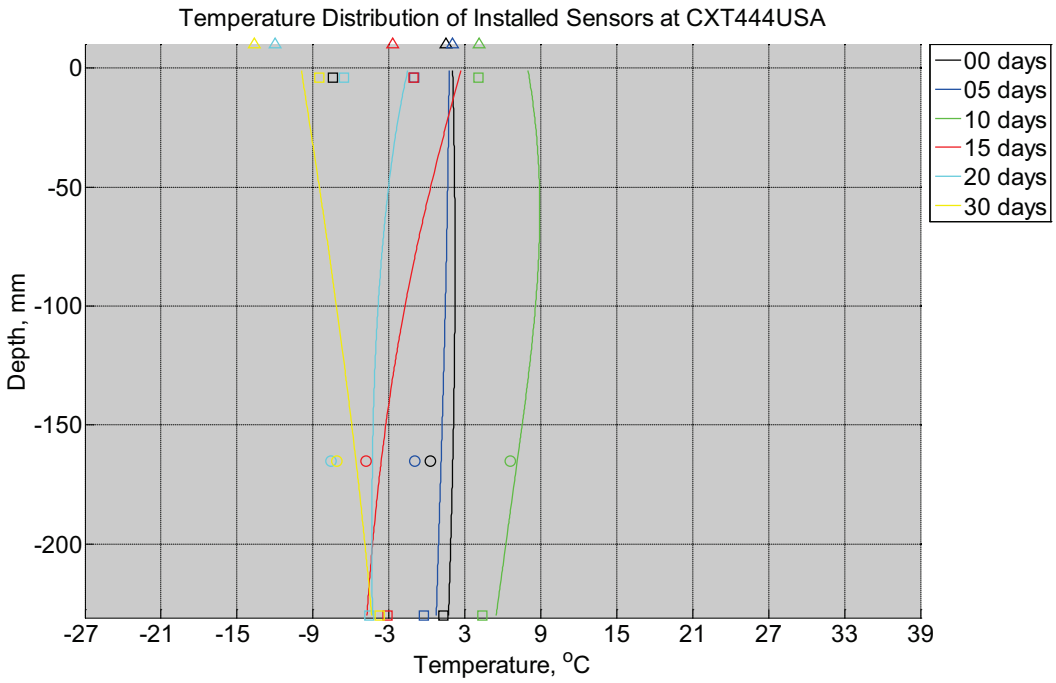

Figure B-676 Measured (markers) and modeled (continuous line) temperature profile distribution as a function of depth inside a concrete crosstie (labeled CXT444USA) installed in ballast in Rantoul, IL, between January 30, 2015, through March 14, 2015. An 8 mm thick polyurethane pad and 12 in (30.48 cm) length 136 lb/yd (67.5 kg/m) section of steel rail are additionally installed atop the model concrete crosstie. The model does not incorporate a polyurethane pad nor steel rail line. Triangular markers denote temperature value from KTIP weather station, square markers denote measured temperature values from ballast, and circular markers denote measured temperature values inside concrete.

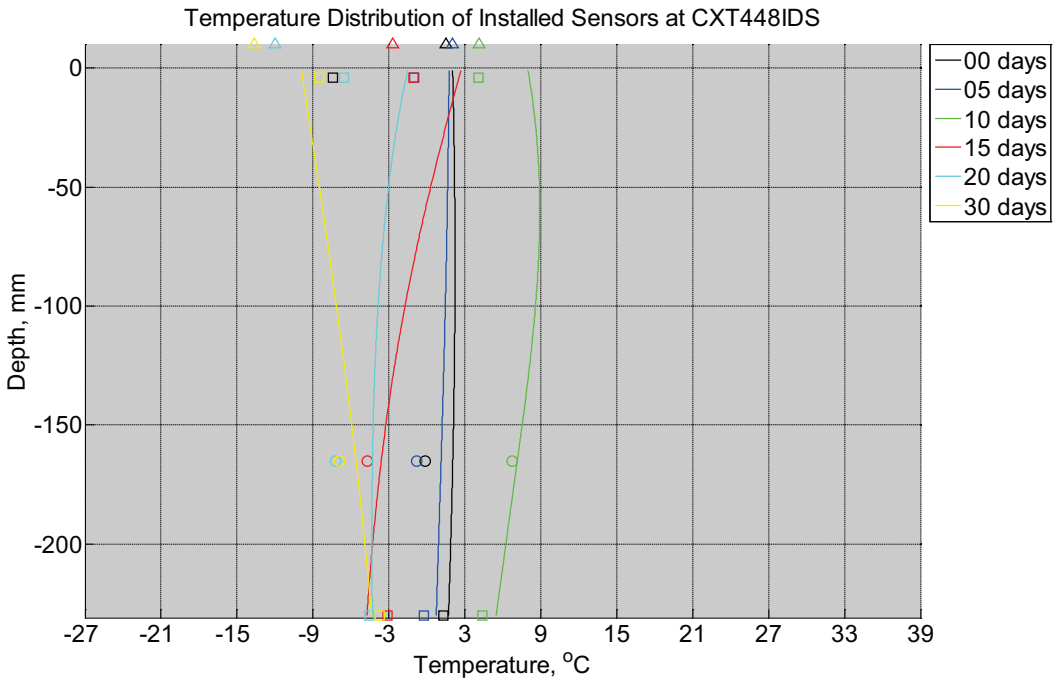

Figure B-677 Measured (markers) and modeled (continuous line) temperature profile distribution as a function of depth inside a concrete crosstie (labeled CXT448IDS) installed in ballast in Rantoul, IL, between January 30, 2015, through March 14, 2015. An 8 mm thick polyurethane pad and 12 in (30.48 cm) length 136 lb/yd (67.5 kg/m) section of steel rail are additionally installed atop the model concrete crosstie. The model does not incorporate a polyurethane pad nor steel rail line. Triangular markers denote temperature value from KTIP weather station, square markers denote measured temperature values from ballast, and circular markers denote measured temperature values inside concrete.

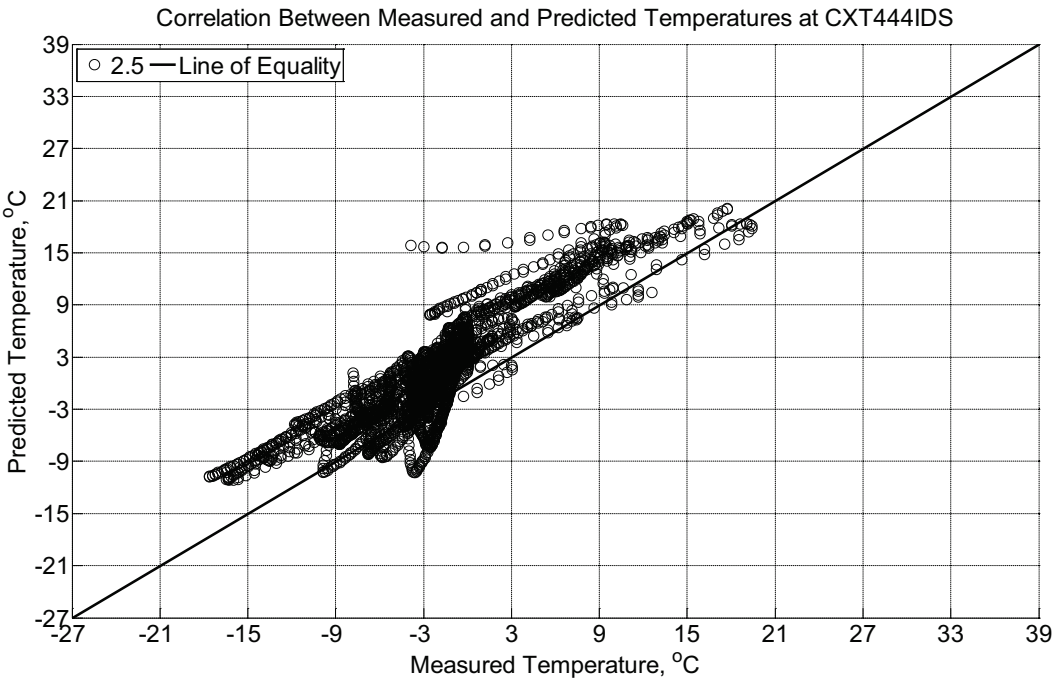

Figure B-678 Correlation between measured and predicted temperature values 2.5 inches (63.5 mm) from the surface of a concrete crosstie (labeled CXT444IDS) without a polyurethane pad nor rail installed in ballast in Rantoul, IL, between January 30, 2015, through March 14, 2015.

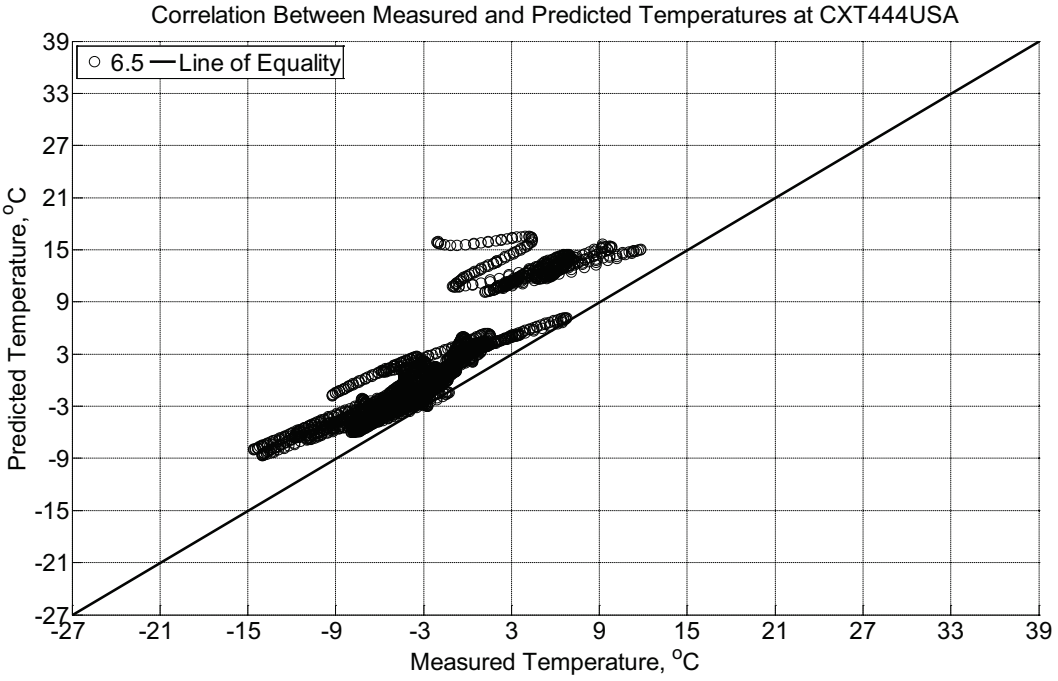

Figure B-679 Correlation between measured and predicted temperature values 6.5 inches (139.7 mm) from the surface of a concrete crosstie (labeled CXT444USA) installed in

ballast in Rantoul, IL, between January 30, 2015, through March 14, 2015. An 8 mm thick polyurethane pad and 12 in (30.48 cm) length 136 lb/yd (67.5 kg/m) section of steel rail are additionally installed atop the concrete crosstie. The model does not incorporate a polyurethane pad nor steel rail line.

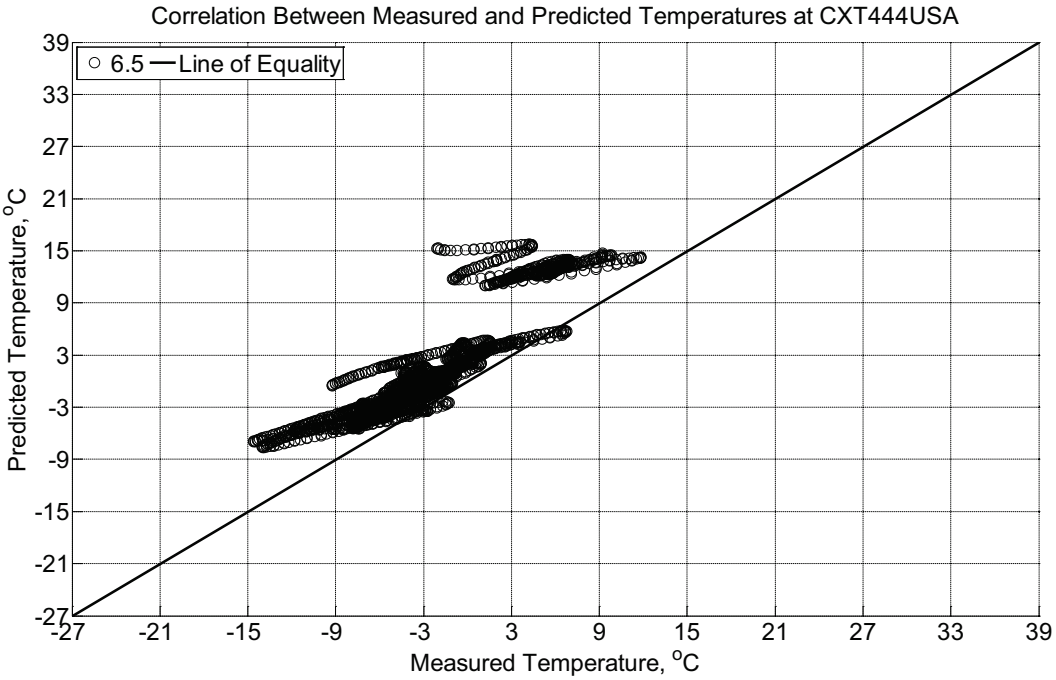

Figure B-680 Correlation between measured and predicted temperature values 6.5 inches (139.7 mm) from the surface of a concrete crosstie (labeled CXT444USA) installed in ballast in Rantoul, IL, between January 30, 2015, through March 14, 2015. An 8 mm thick polyurethane pad and 12 in (30.48 cm) length 136 lb/yd (67.5 kg/m) section of steel rail are additionally installed atop the concrete crosstie. The model incorporates a 1 mm thick polyurethane pad and 1 mm thick steel rail line.

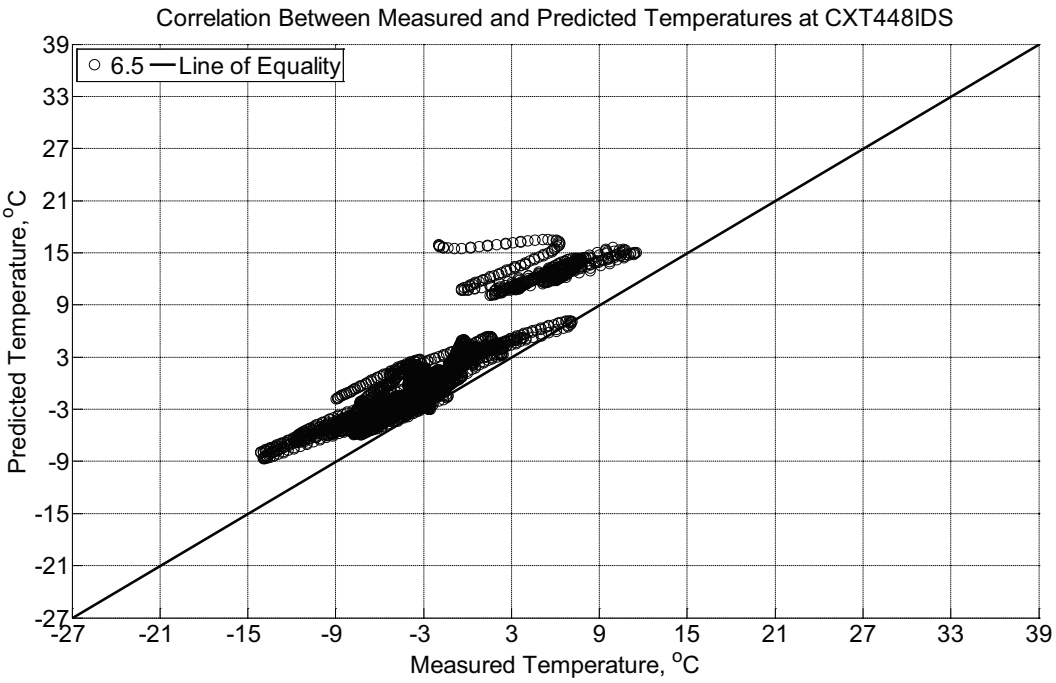

Figure B-681 Correlation between measured and predicted temperature values 6.5 inches (139.7 mm) from the surface of a concrete crosstie (labeled CXT448IDS) installed in ballast in Rantoul, IL, between January 30, 2015, through March 14, 2015. An 8 mm thick polyurethane pad and 12 in (30.48 cm) length 136 lb/yd (67.5 kg/m) section of steel rail are additionally installed atop the concrete crosstie. The model does not incorporate a polyurethane pad nor steel rail line.

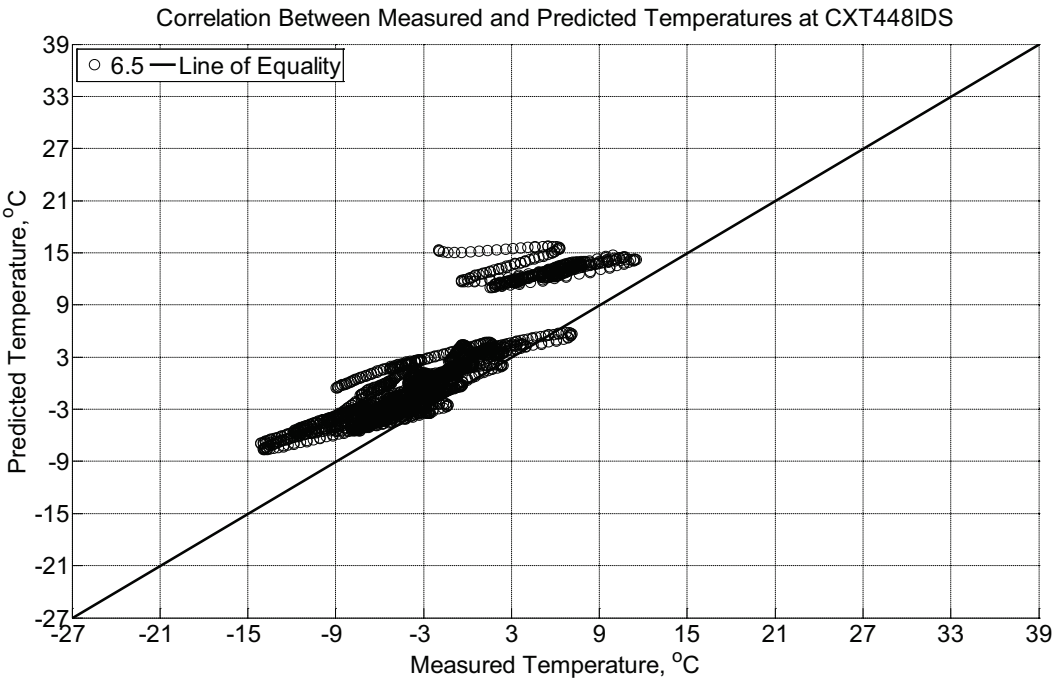

Figure B-682 Correlation between measured and predicted temperature values 6.5 inches (139.7 mm) from the surface of a concrete crosstie (labeled CXT448IDS) installed in ballast in Rantoul, IL, between January 30, 2015, through March 14, 2015. An 8 mm thick polyurethane pad and 12 in (30.48 cm) length 136 lb/yd (67.5 kg/m) section of steel rail are additionally installed atop the concrete crosstie. The model incorporates a 1 mm thick polyurethane pad and 1 mm thick steel rail line.

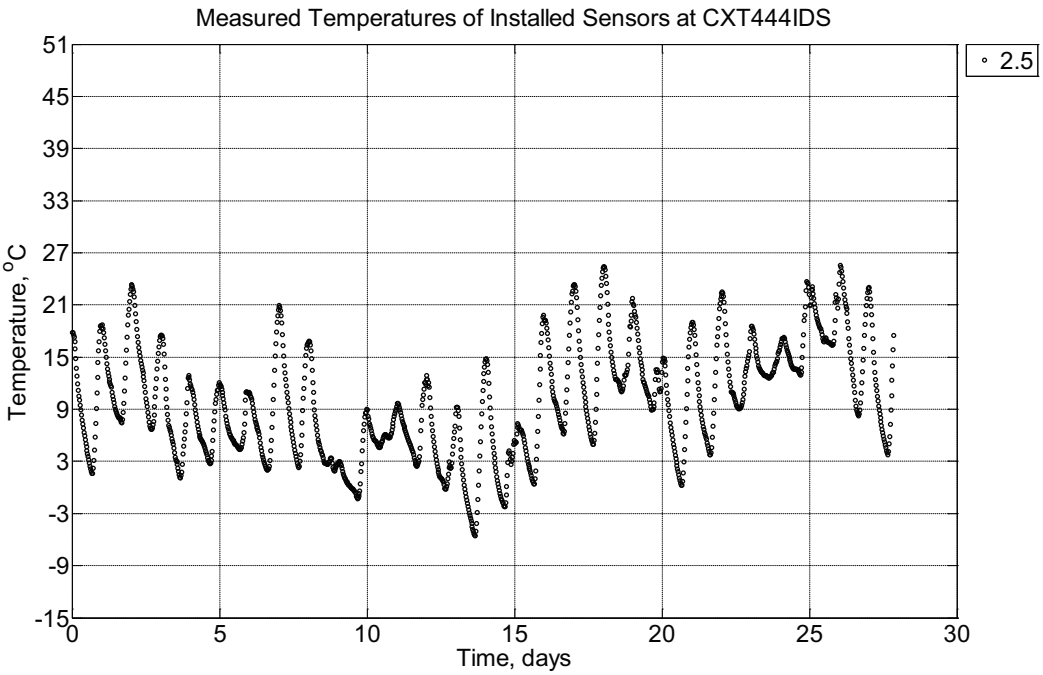

Figure B-683 Measured temperature at a depth of 2.5 inches (63.5 mm) from the surface of a concrete crosstie (labeled CXT444IDS) without a polyurethane pad nor rail installed in ballast in Rantoul, IL, between March 14, 2015, through April 11, 2015.

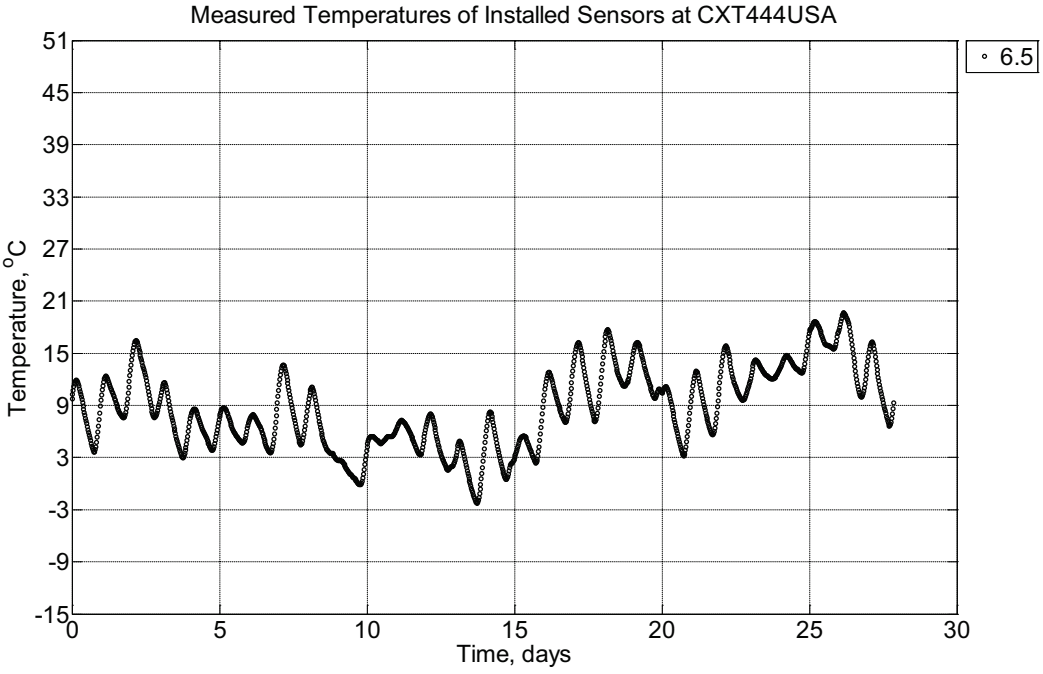

Figure B-684 Measured temperature at a depth of 6.5 inches (139.7 mm) from the surface of a concrete crosstie (labeled CXT444USA) installed in ballast in Rantoul, IL, between March 14, 2015, through April 11, 2015. An 8 mm thick polyurethane pad and 12 in (30.48

cm) length 136 lb/yd (67.5 kg/m) section of steel rail are additionally installed atop the concrete crosstie.

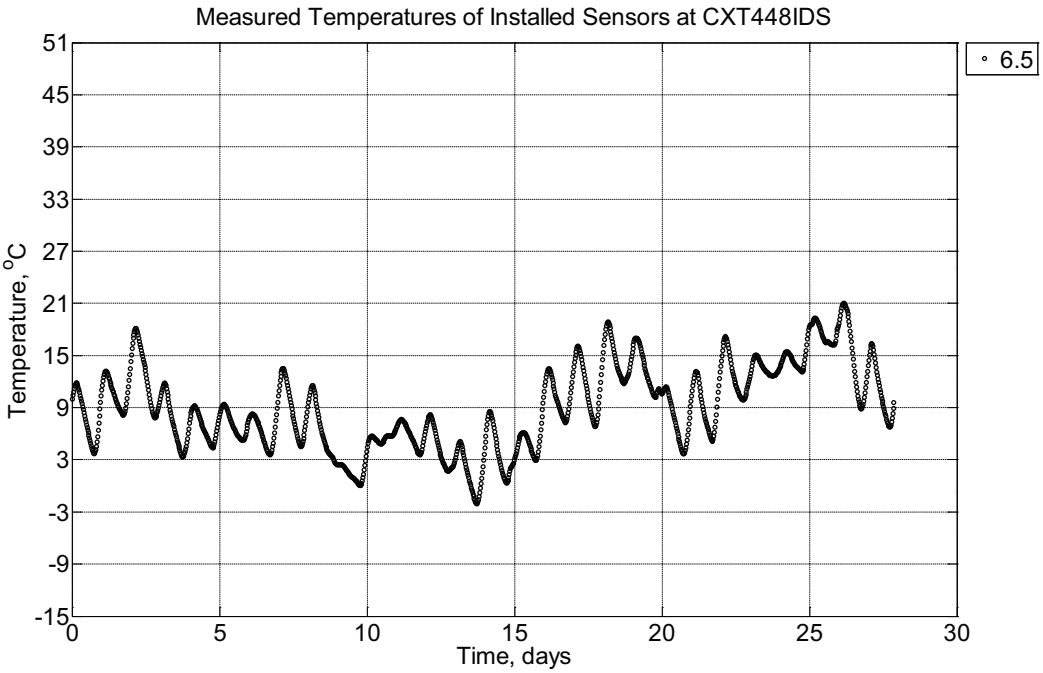

Figure B-685 Measured temperature at depths of 6.5 inches (139.7 mm) from the surface of a concrete crosstie (labeled CXT448IDS) installed in ballast in Rantoul, IL, between March 14, 2015, through April 11, 2015. An 8 mm thick polyurethane pad and 12 in (30.48 cm) length 136 lb/yd (67.5 kg/m) section of steel rail are additionally installed atop the concrete crosstie.

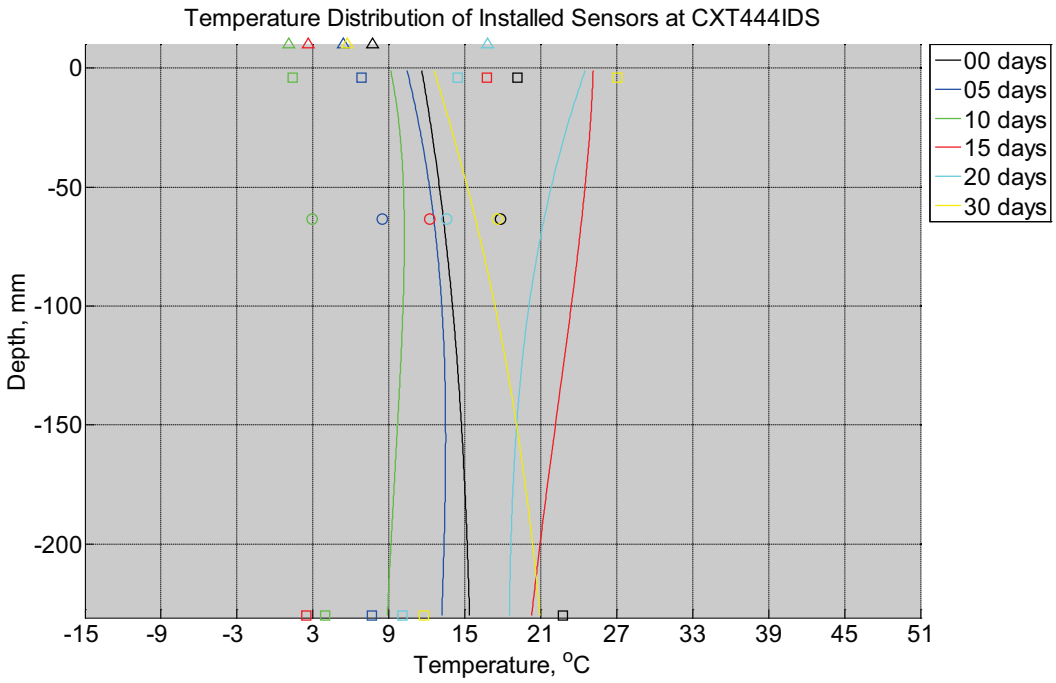

Figure B-686 Measured (markers) and modeled (continuous line) temperature profile distribution as a function of depth inside a concrete crosstie (labeled CXT444IDS) without a polyurethane pad nor rail installed in ballast in Rantoul, IL, between March 14, 2015, through April 11, 2015. Triangular markers denote temperature value from KTIP weather station, square markers denote measured temperature values from ballast, and circular markers denote measured temperature values inside concrete.

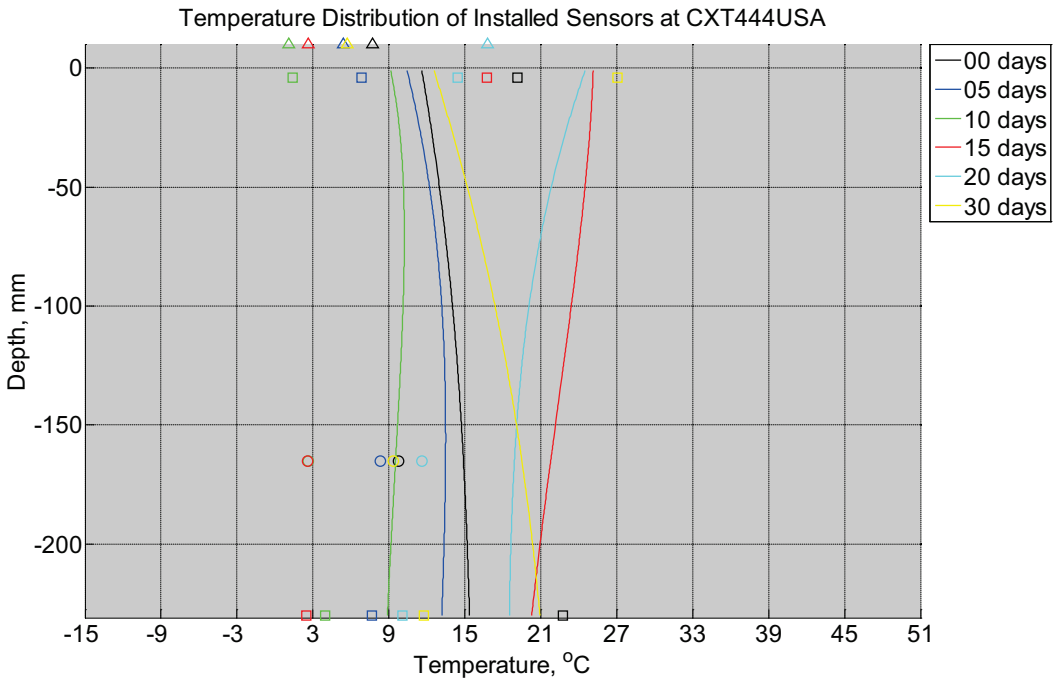

Figure B-687 Measured (markers) and modeled (continuous line) temperature profile distribution as a function of depth inside a concrete crosstie (labeled CXT444USA) installed in ballast in Rantoul, IL, between March 14, 2015, through April 11, 2015. An 8 mm thick polyurethane pad and 12 in (30.48 cm) length 136 lb/yd (67.5 kg/m) section of steel rail are additionally installed atop the model concrete crosstie. The model does not incorporate a polyurethane pad nor steel rail line. Triangular markers denote temperature value from KTIP weather station, square markers denote measured temperature values from ballast, and circular markers denote measured temperature values inside concrete.

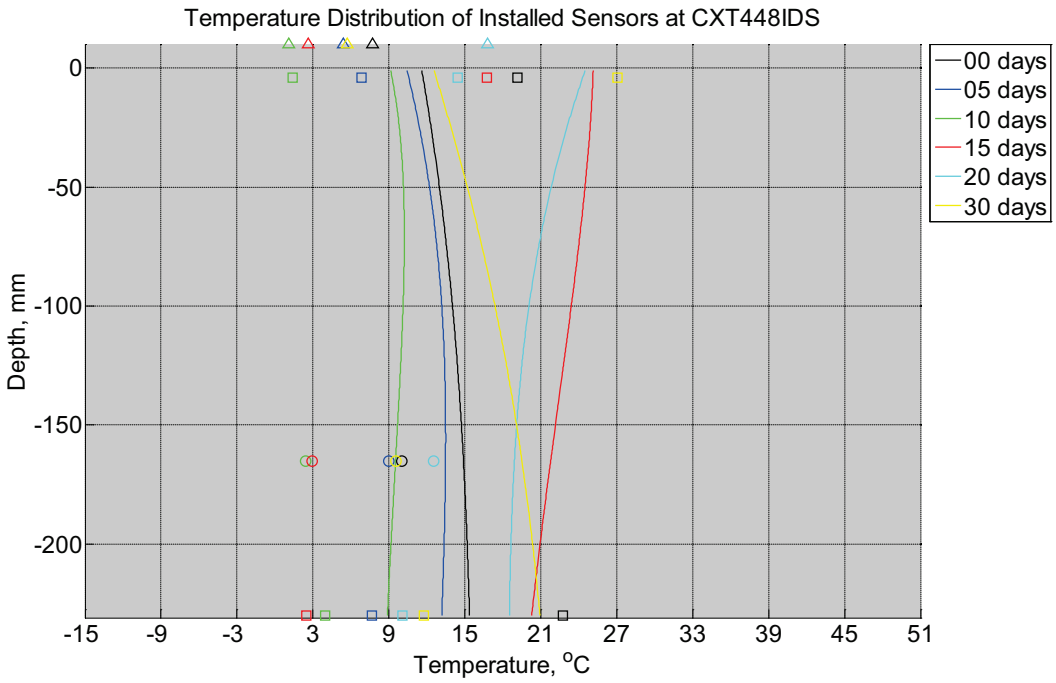

Figure B-688 Measured (markers) and modeled (continuous line) temperature profile distribution as a function of depth inside a concrete crosstie (labeled CXT448IDS) installed in ballast in Rantoul, IL, between March 14, 2015, through April 11, 2015. An 8 mm thick polyurethane pad and 12 in (30.48 cm) length 136 lb/yd (67.5 kg/m) section of steel rail are additionally installed atop the model concrete crosstie. The model does not incorporate a polyurethane pad nor steel rail line. Triangular markers denote temperature value from KTIP weather station, square markers denote measured temperature values from ballast, and circular markers denote measured temperature values inside concrete.

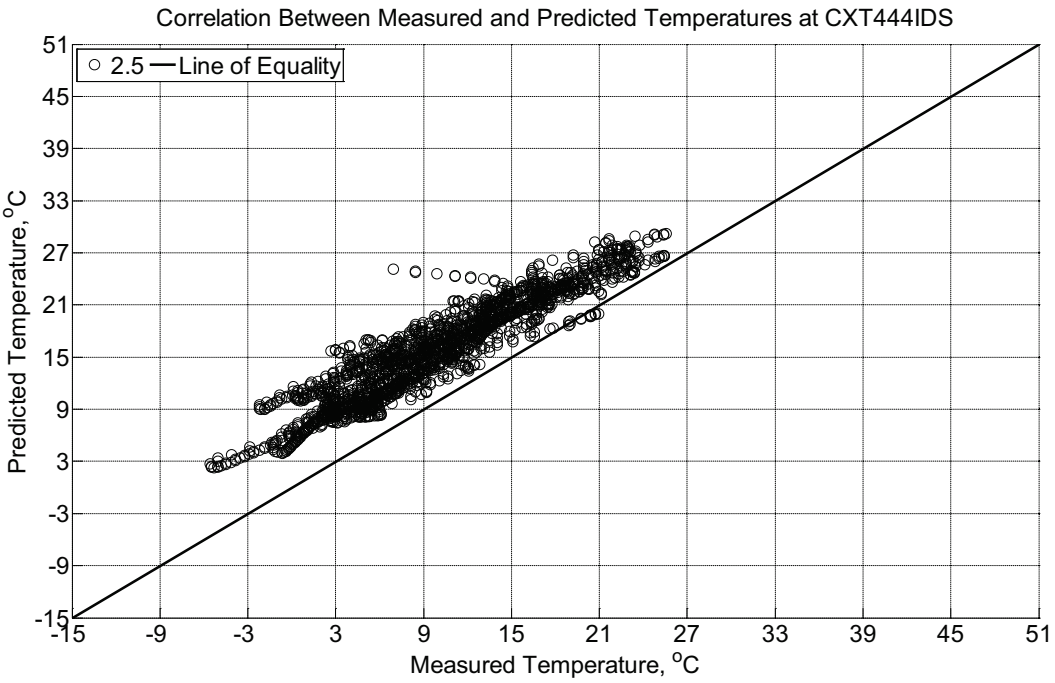

Figure B-689 Correlation between measured and predicted temperature values 2.5 inches (63.5 mm) from the surface of a concrete crosstie (labeled CXT444IDS) without a polyurethane pad nor rail installed in ballast in Rantoul, IL, between March 14, 2015, through April 11, 2015.

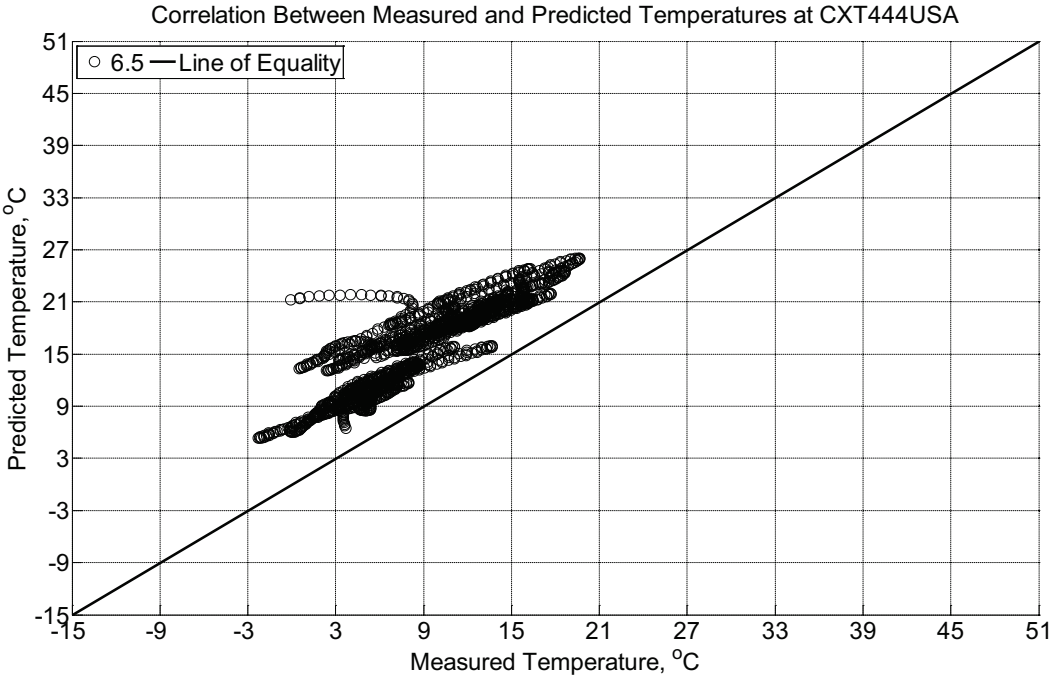

Figure B-690 Correlation between measured and predicted temperature values 6.5 inches (139.7 mm) from the surface of a concrete crosstie (labeled CXT444USA) installed in

ballast in Rantoul, IL, between March 14, 2015, through April 11, 2015. An 8 mm thick polyurethane pad and 12 in (30.48 cm) length 136 lb/yd (67.5 kg/m) section of steel rail are additionally installed atop the concrete crosstie. The model does not incorporate a polyurethane pad nor steel rail line.

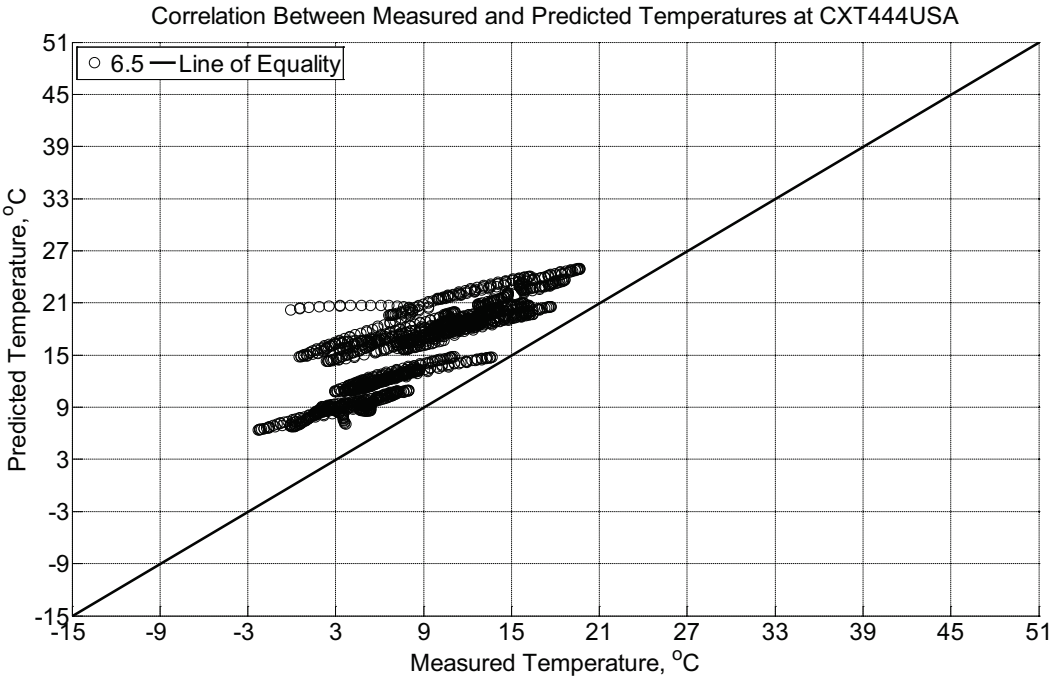

Figure B-691 Correlation between measured and predicted temperature values 6.5 inches (139.7 mm) from the surface of a concrete crosstie (labeled CXT444USA) installed in ballast in Rantoul, IL, between March 14, 2015, through April 11, 2015. An 8 mm thick polyurethane pad and 12 in (30.48 cm) length 136 lb/yd (67.5 kg/m) section of steel rail are additionally installed atop the concrete crosstie. The model incorporates a 1 mm thick polyurethane pad and 1 mm thick steel rail line.

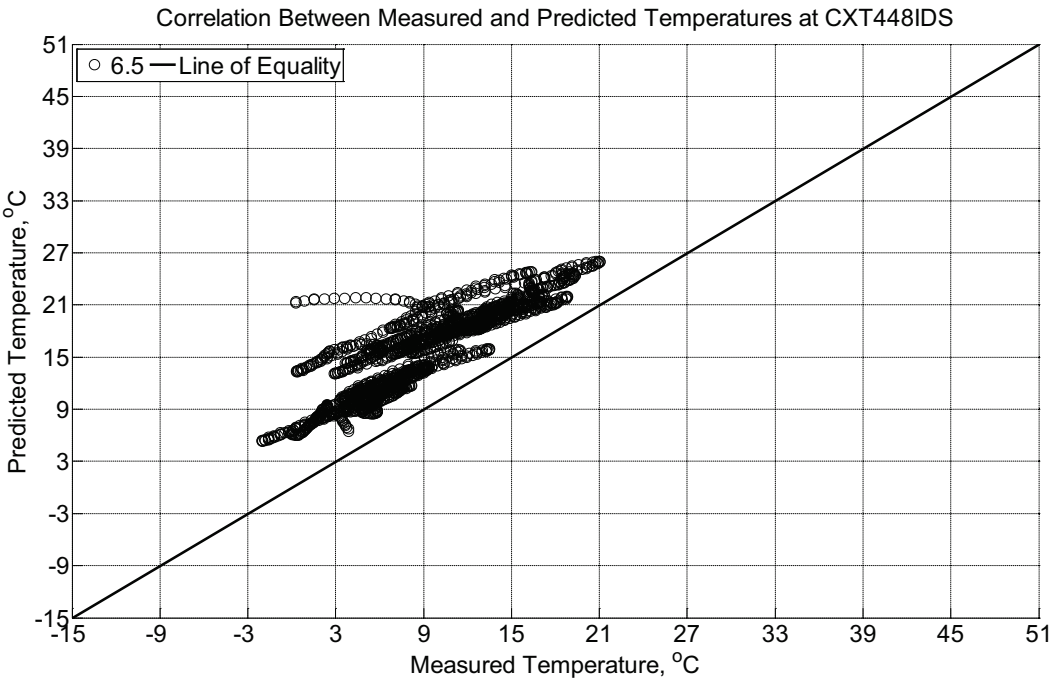

Figure B-692 Correlation between measured and predicted temperature values 6.5 inches (139.7 mm) from the surface of a concrete crosstie (labeled CXT448IDS) installed in ballast in Rantoul, IL, between March 14, 2015, through April 11, 2015. An 8 mm thick polyurethane pad and 12 in (30.48 cm) length 136 lb/yd (67.5 kg/m) section of steel rail are additionally installed atop the concrete crosstie. The model does not incorporate a polyurethane pad nor steel rail line.

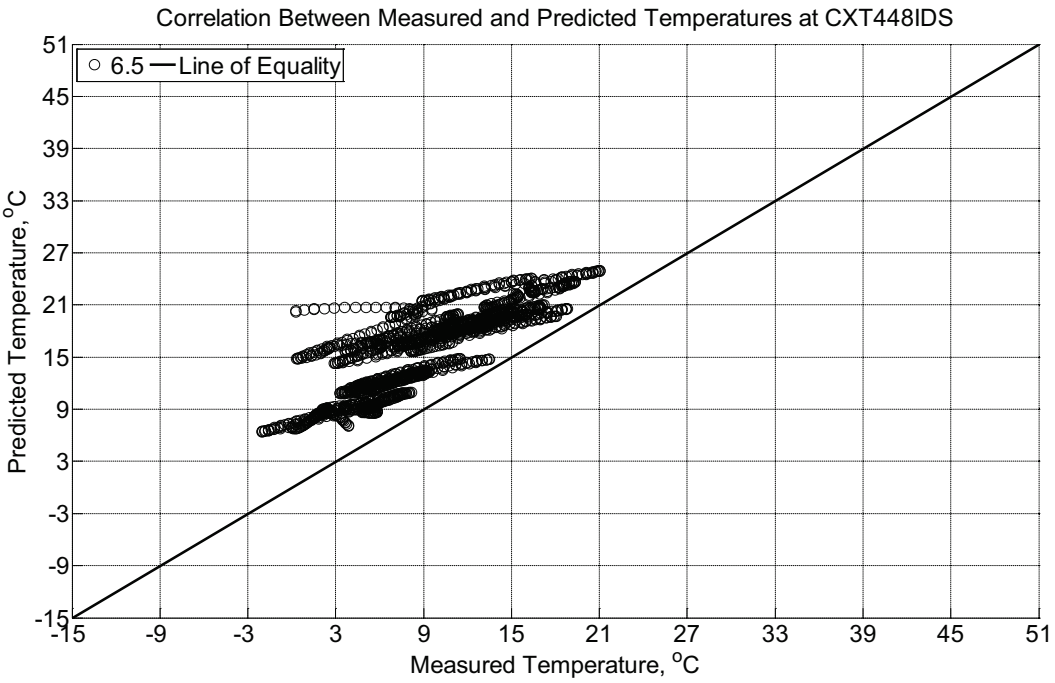

Figure B-693 Correlation between measured and predicted temperature values 6.5 inches (139.7 mm) from the surface of a concrete crosstie (labeled CXT448IDS) installed in ballast in Rantoul, IL, between March 14, 2015, through April 11, 2015. An 8 mm thick polyurethane pad and 12 in (30.48 cm) length 136 lb/yd (67.5 kg/m) section of steel rail are additionally installed atop the concrete crosstie. The model incorporates a 1 mm thick polyurethane pad and 1 mm thick steel rail line.

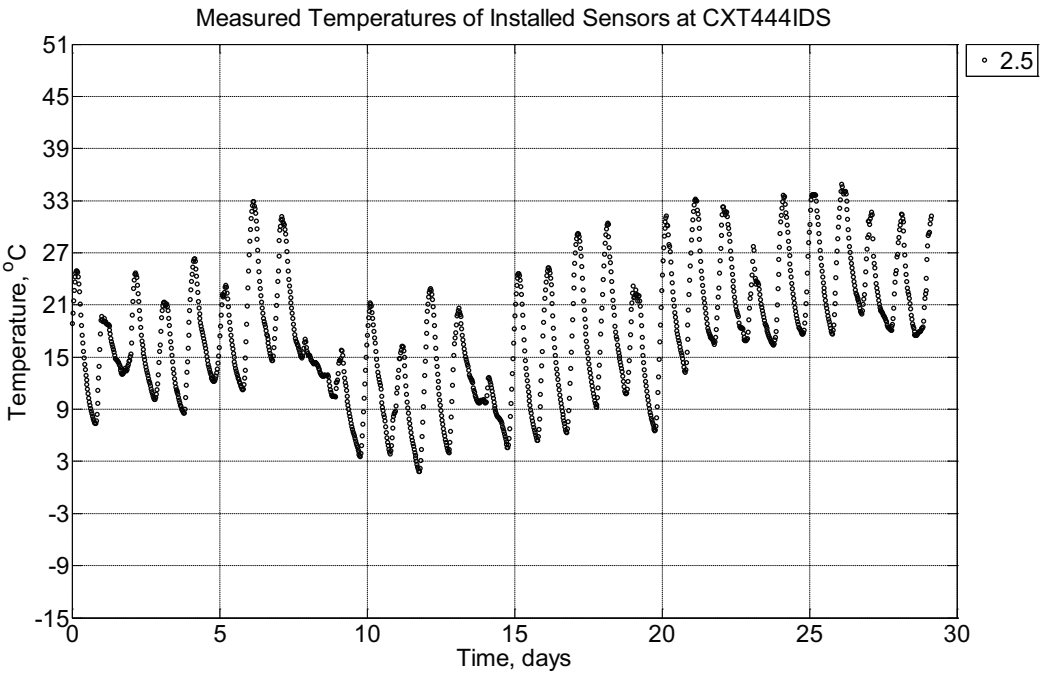

Figure B-694 Measured temperature at a depth of 2.5 inches (63.5 mm) from the surface of a concrete crosstie (labeled CXT444IDS) without a polyurethane pad nor rail installed in ballast in Rantoul, IL, between April 11, 2015, through May 10, 2015.

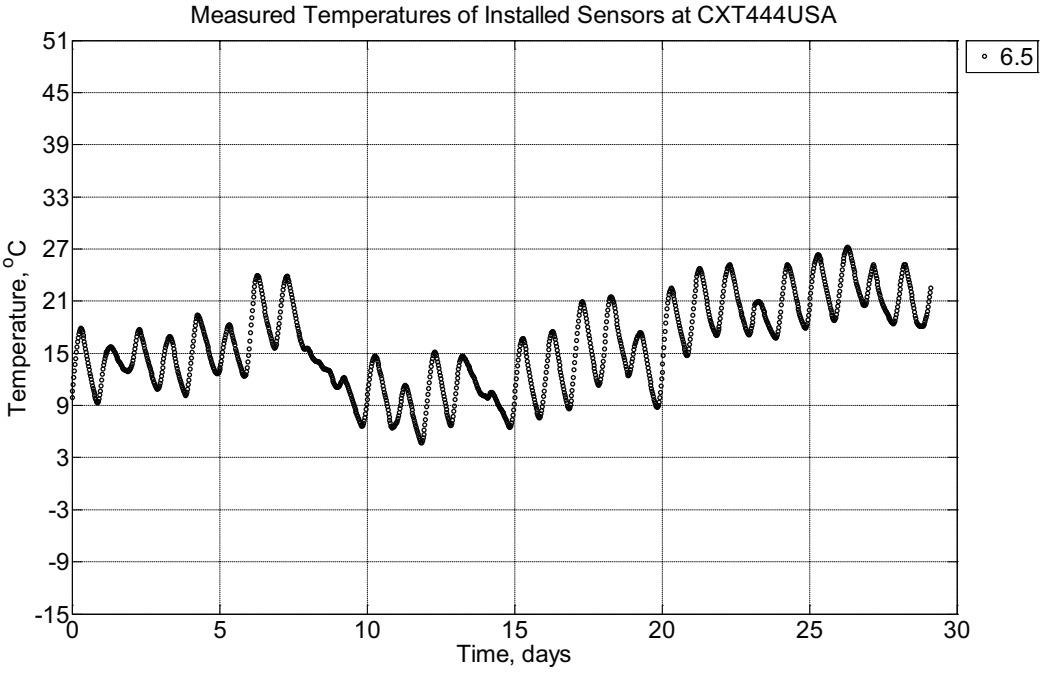

Figure B-695 Measured temperature at a depth of 6.5 inches (139.7 mm) from the surface of a concrete crosstie (labeled CXT444USA) installed in ballast in Rantoul, IL, between April 11, 2015, through May 10, 2015. An 8 mm thick polyurethane pad and 12 in (30.48

cm) length 136 lb/yd (67.5 kg/m) section of steel rail are additionally installed atop the concrete crosstie.

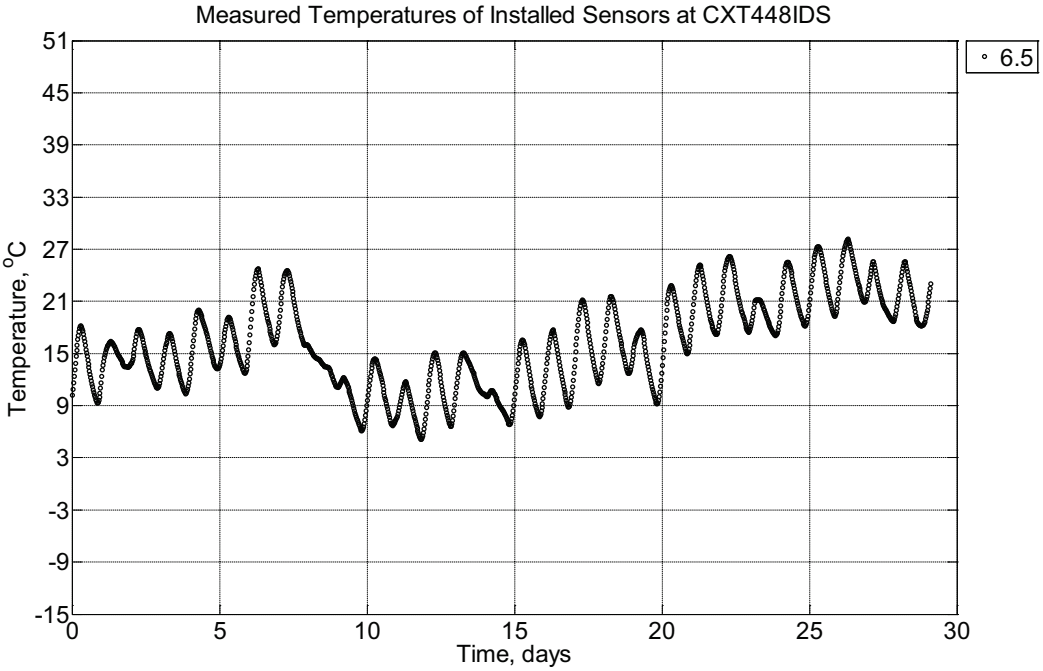

Figure B-696 Measured temperature at depths of 6.5 inches (139.7 mm) from the surface of a concrete crosstie (labeled CXT448IDS) installed in ballast in Rantoul, IL, between April 11, 2015, through May 10, 2015. An 8 mm thick polyurethane pad and 12 in (30.48 cm) length 136 lb/yd (67.5 kg/m) section of steel rail are additionally installed atop the concrete crosstie.

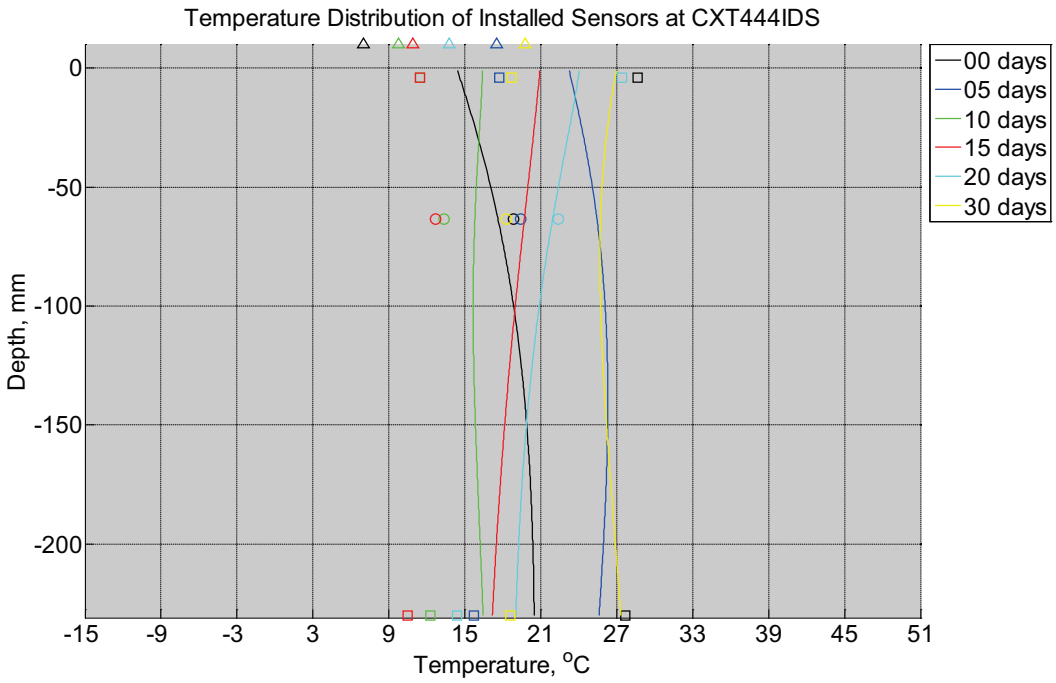

Figure B-697 Measured (markers) and modeled (continuous line) temperature profile distribution as a function of depth inside a concrete crosstie (labeled CXT444IDS) without a polyurethane pad nor rail installed in ballast in Rantoul, IL, between April 11, 2015, through May 10, 2015. Triangular markers denote temperature value from KTIP weather station, square markers denote measured temperature values from ballast, and circular markers denote measured temperature values inside concrete.

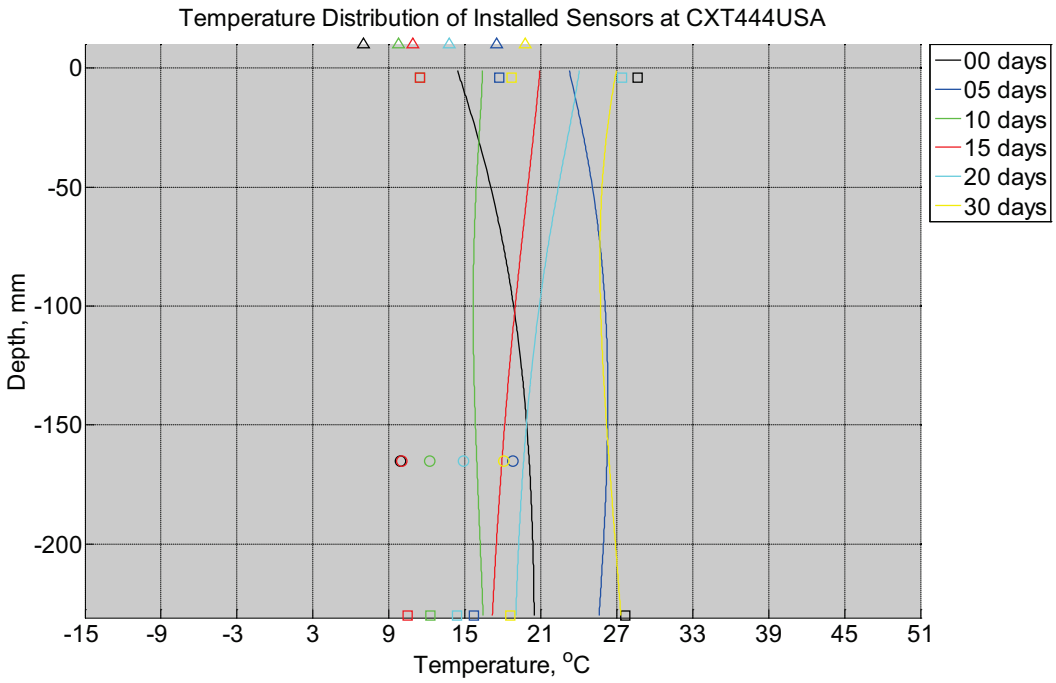

Figure B-698 Measured (markers) and modeled (continuous line) temperature profile distribution as a function of depth inside a concrete crosstie (labeled CXT444USA) installed in ballast in Rantoul, IL, between April 11, 2015, through May 10, 2015. An 8 mm thick polyurethane pad and 12 in (30.48 cm) length 136 lb/yd (67.5 kg/m) section of steel rail are additionally installed atop the model concrete crosstie. The model does not incorporate a polyurethane pad nor steel rail line. Triangular markers denote temperature value from KTIP weather station, square markers denote measured temperature values from ballast, and circular markers denote measured temperature values inside concrete.

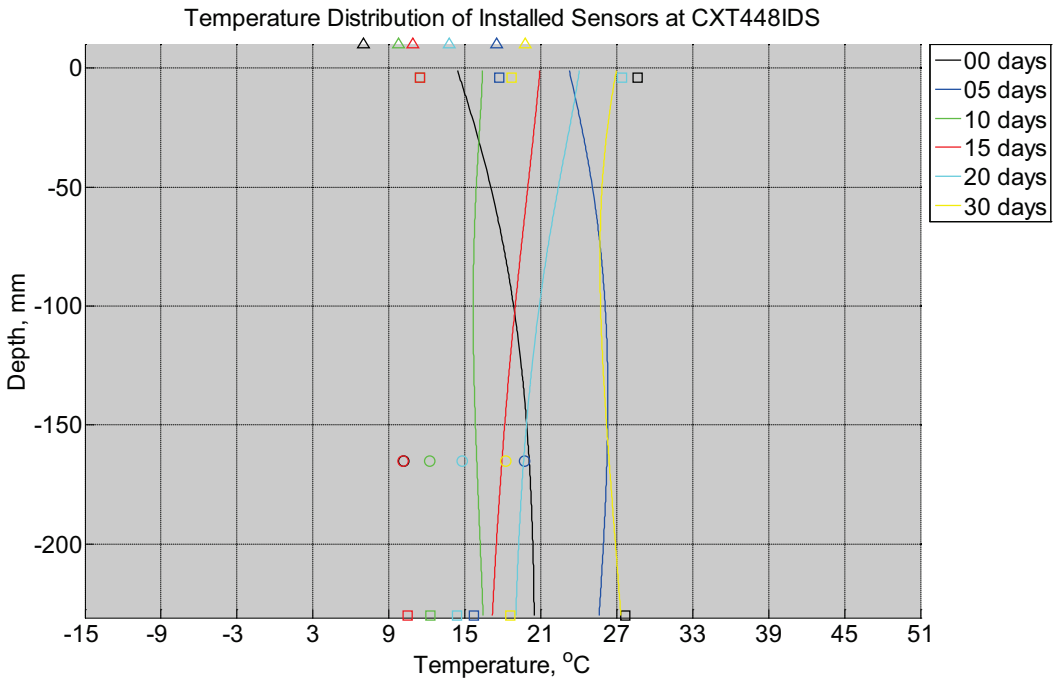

Figure B-699 Measured (markers) and modeled (continuous line) temperature profile distribution as a function of depth inside a concrete crosstie (labeled CXT448IDS) installed in ballast in Rantoul, IL, between April 11, 2015, through May 10, 2015. An 8 mm thick polyurethane pad and 12 in (30.48 cm) length 136 lb/yd (67.5 kg/m) section of steel rail are additionally installed atop the model concrete crosstie. The model does not incorporate a polyurethane pad nor steel rail line. Triangular markers denote temperature value from KTIP weather station, square markers denote measured temperature values from ballast, and circular markers denote measured temperature values inside concrete.

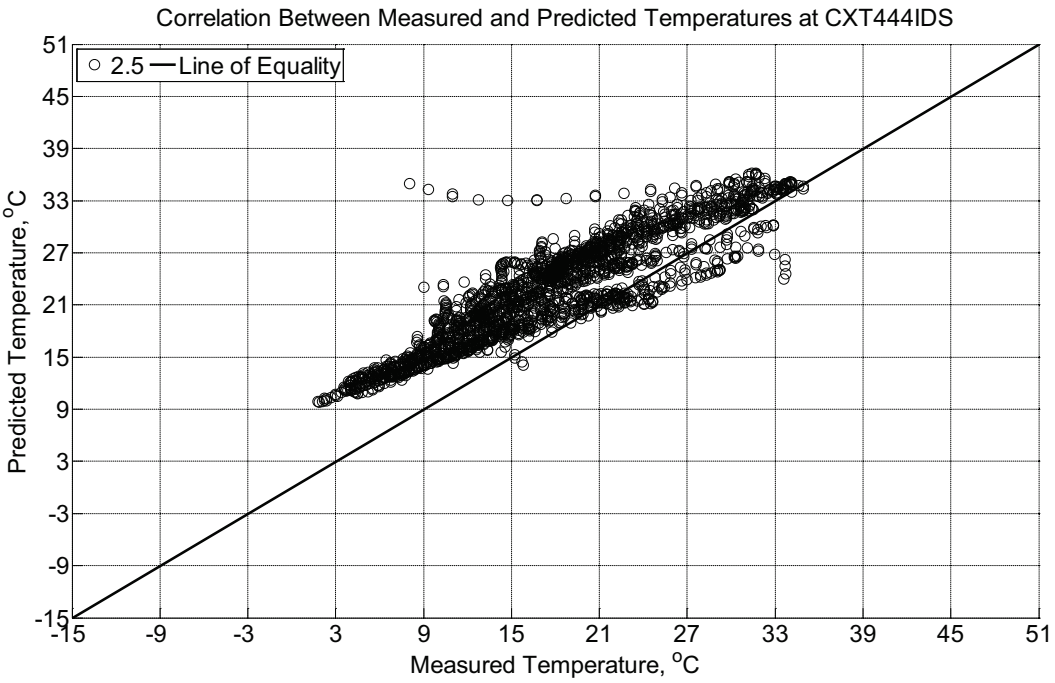

Figure B-700 Correlation between measured and predicted temperature values 2.5 inches (63.5 mm) from the surface of a concrete crosstie (labeled CXT444IDS) without a polyurethane pad nor rail installed in ballast in Rantoul, IL, between April 11, 2015, through May 10, 2015.

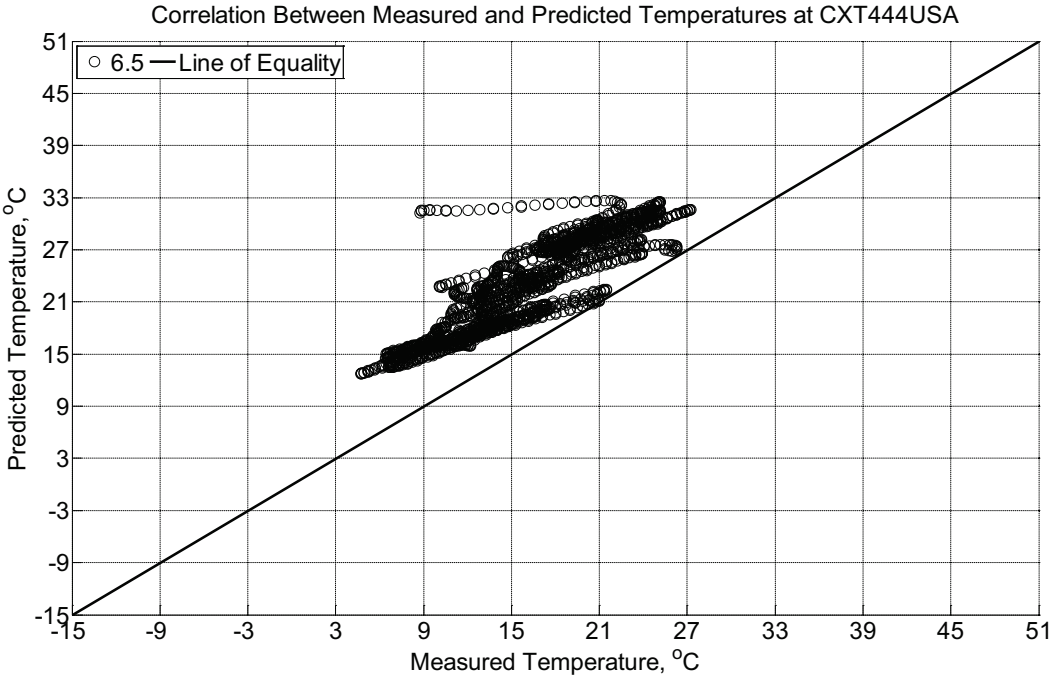

Figure B-701 Correlation between measured and predicted temperature values 6.5 inches (139.7 mm) from the surface of a concrete crosstie (labeled CXT444USA) installed in

ballast in Rantoul, IL, between April 11, 2015, through May 10, 2015. An 8 mm thick polyurethane pad and 12 in (30.48 cm) length 136 lb/yd (67.5 kg/m) section of steel rail are additionally installed atop the concrete crosstie. The model does not incorporate a polyurethane pad nor steel rail line.

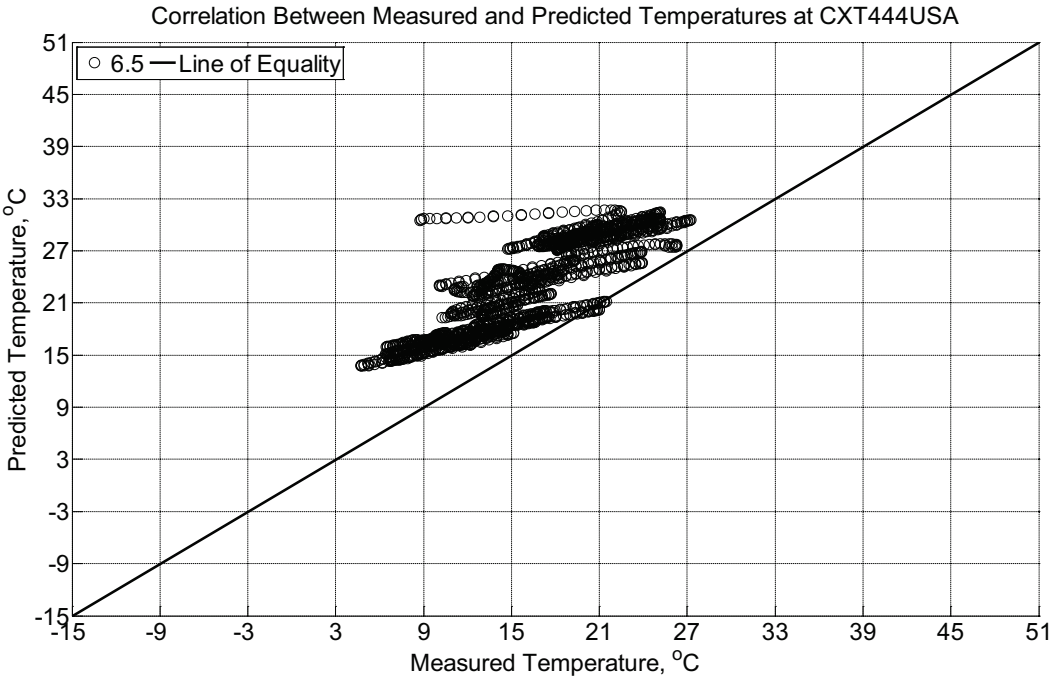

Figure B-702 Correlation between measured and predicted temperature values 6.5 inches (139.7 mm) from the surface of a concrete crosstie (labeled CXT444USA) installed in ballast in Rantoul, IL, between April 11, 2015, through May 10, 2015. An 8 mm thick polyurethane pad and 12 in (30.48 cm) length 136 lb/yd (67.5 kg/m) section of steel rail are additionally installed atop the concrete crosstie. The model incorporates a 1 mm thick polyurethane pad and 1 mm thick steel rail line.

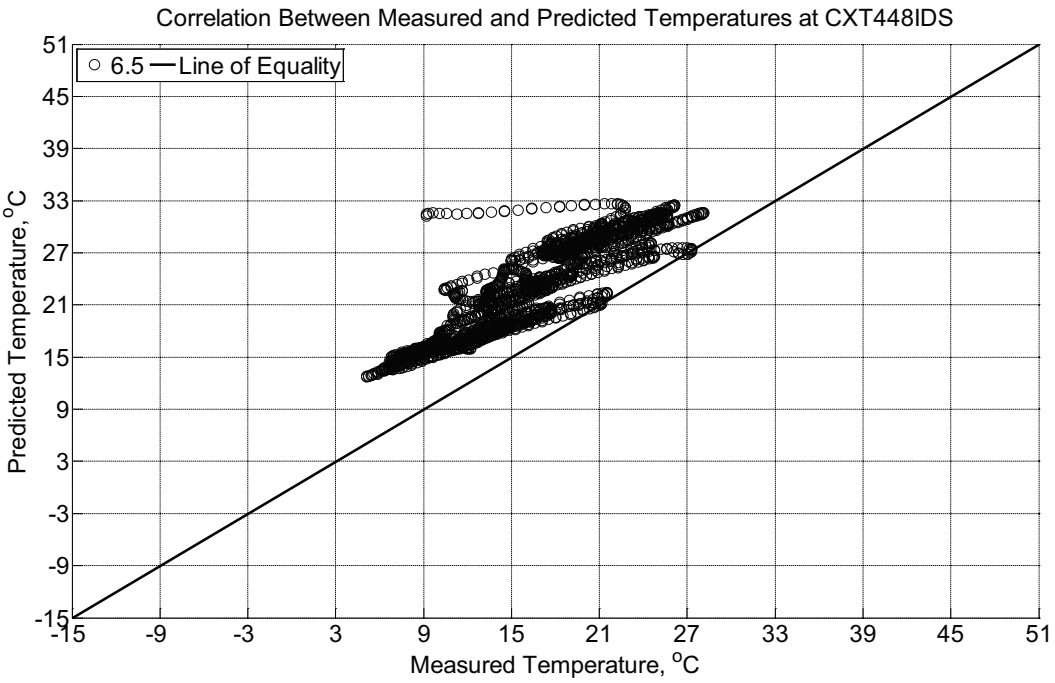

Figure B-703 Correlation between measured and predicted temperature values 6.5 inches (139.7 mm) from the surface of a concrete crosstie (labeled CXT448IDS) installed in ballast in Rantoul, IL, between April 11, 2015, through May 10, 2015. An 8 mm thick polyurethane pad and 12 in (30.48 cm) length 136 lb/yd (67.5 kg/m) section of steel rail are additionally installed atop the concrete crosstie. The model does not incorporate a polyurethane pad nor steel rail line.

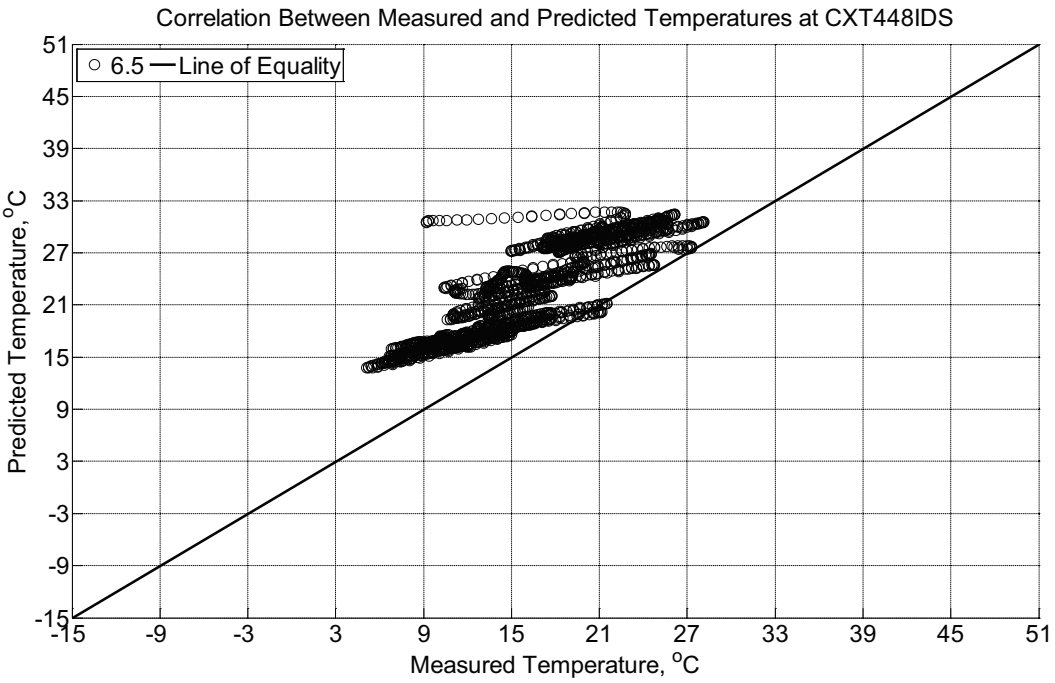

Figure B-704 Correlation between measured and predicted temperature values 6.5 inches (139.7 mm) from the surface of a concrete crosstie (labeled CXT448IDS) installed in ballast in Rantoul, IL, between April 11, 2015, through May 10, 2015. An 8 mm thick polyurethane pad and 12 in (30.48 cm) length 136 lb/yd (67.5 kg/m) section of steel rail are additionally installed atop the concrete crosstie. The model incorporates a 1 mm thick polyurethane pad and 1 mm thick steel rail line.

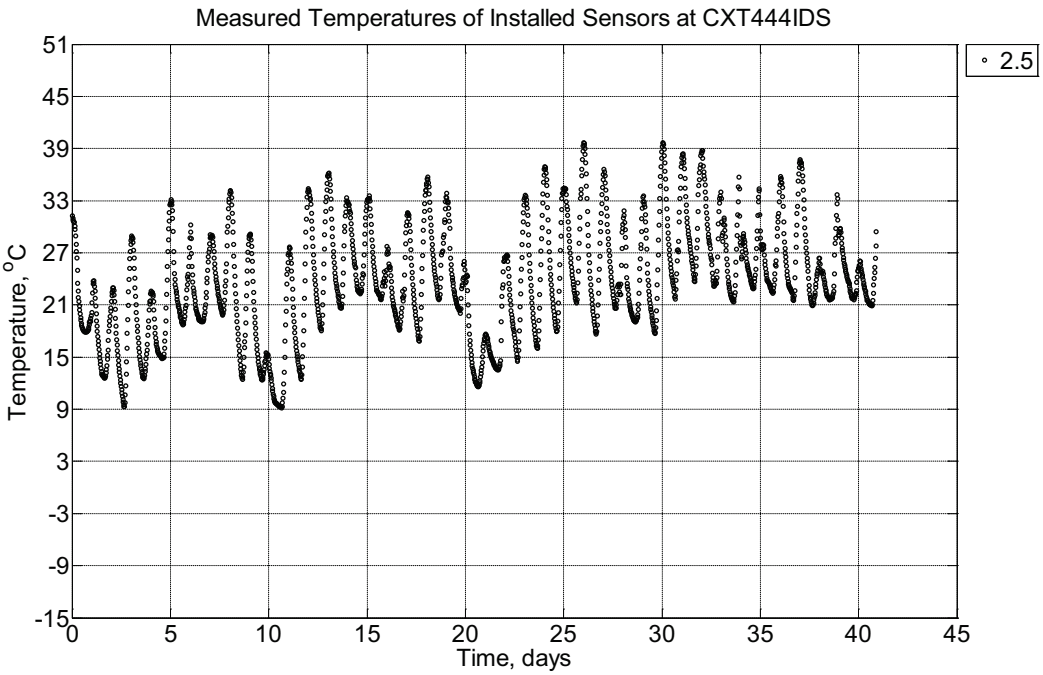

Figure B-705 Measured temperature at a depth of 2.5 inches (63.5 mm) from the surface of a concrete crosstie (labeled CXT444IDS) without a polyurethane pad nor rail installed in ballast in Rantoul, IL, between May 10, 2015, through June 20, 2015.

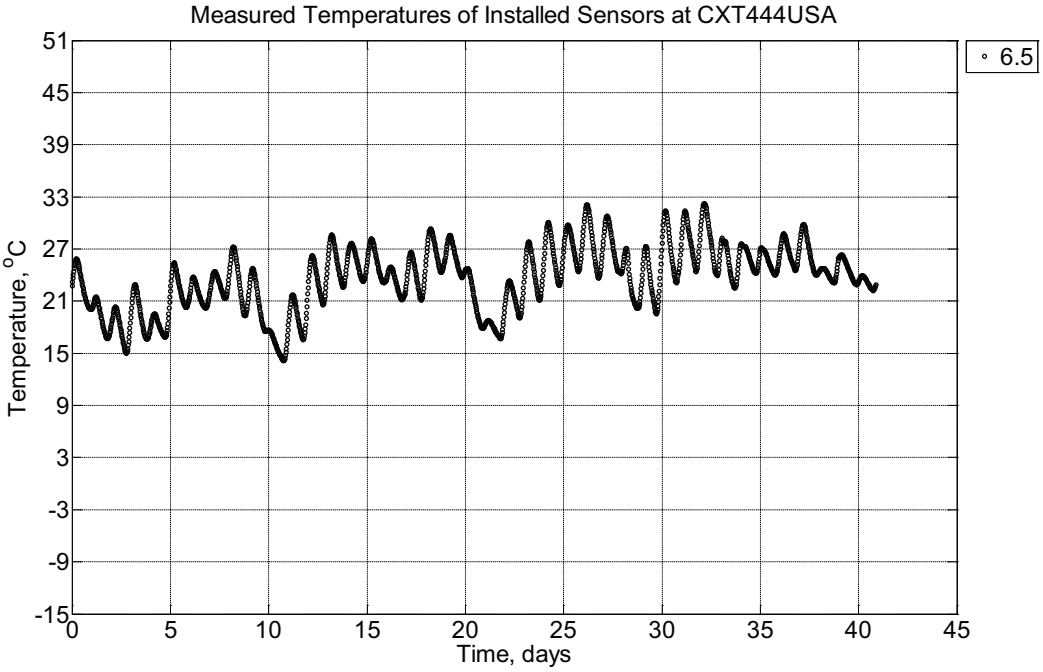

Figure B-706 Measured temperature at a depth of 6.5 inches (139.7 mm) from the surface of a concrete crosstie (labeled CXT444USA) installed in ballast in Rantoul, IL, between May 10, 2015, through June 20, 2015. An 8 mm thick polyurethane pad and 12 in (30.48

cm) length 136 lb/yd (67.5 kg/m) section of steel rail are additionally installed atop the concrete crosstie. A breathable water-resistant canvas tarp is additionally installed over the concrete crosstie and immediate ballast area.

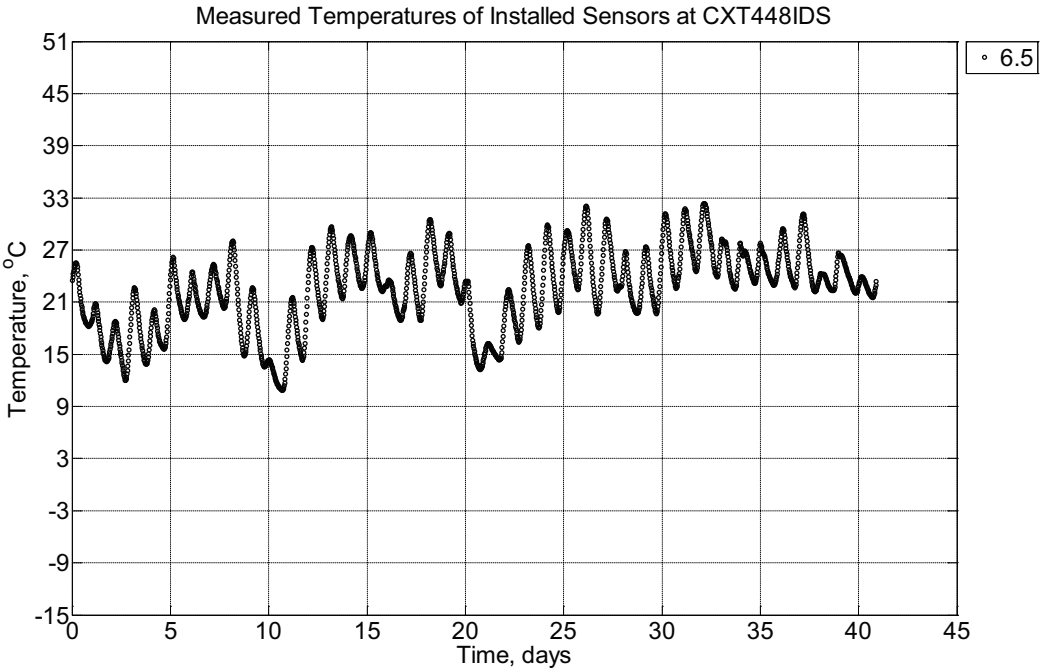

Figure B-707 Measured temperature at depths of 6.5 inches (139.7 mm) from the surface of a concrete crosstie (labeled CXT448IDS) installed in ballast in Rantoul, IL, between May 10, 2015, through June 20, 2015. An 8 mm thick polyurethane pad and 12 in (30.48 cm) length 136 lb/yd (67.5 kg/m) section of steel rail are additionally installed atop the concrete crosstie.

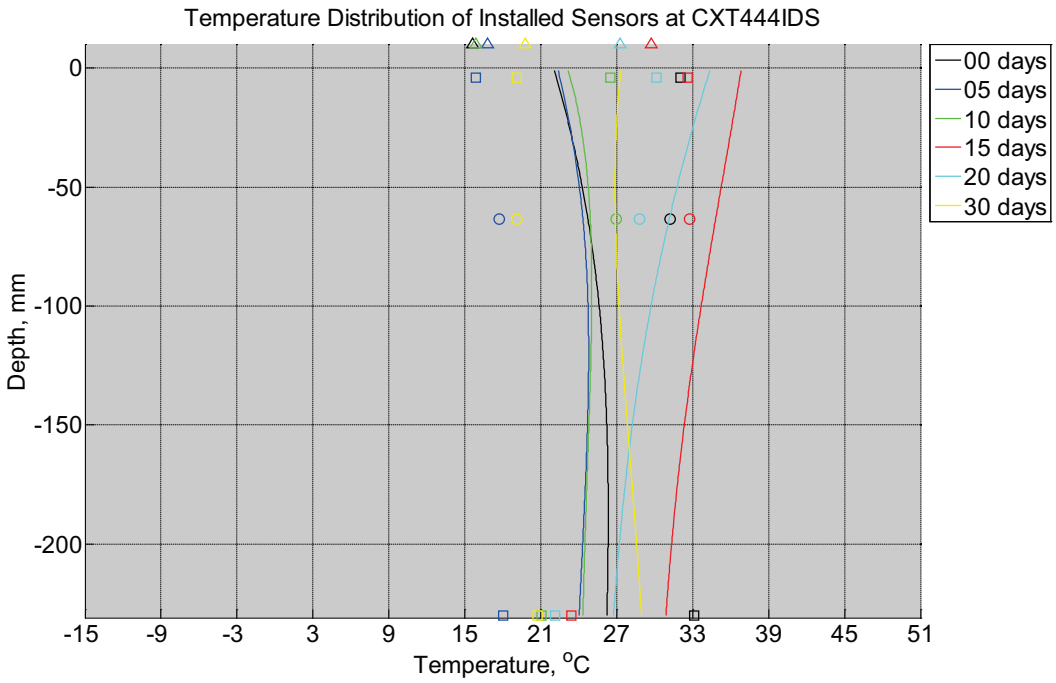

Figure B-708 Measured (markers) and modeled (continuous line) temperature profile distribution as a function of depth inside a concrete crosstie (labeled CXT444IDS) without a polyurethane pad nor rail installed in ballast in Rantoul, IL, between May 10, 2015, through June 20, 2015. Triangular markers denote temperature value from KTIP weather station, square markers denote measured temperature values from ballast, and circular markers denote measured temperature values inside concrete.

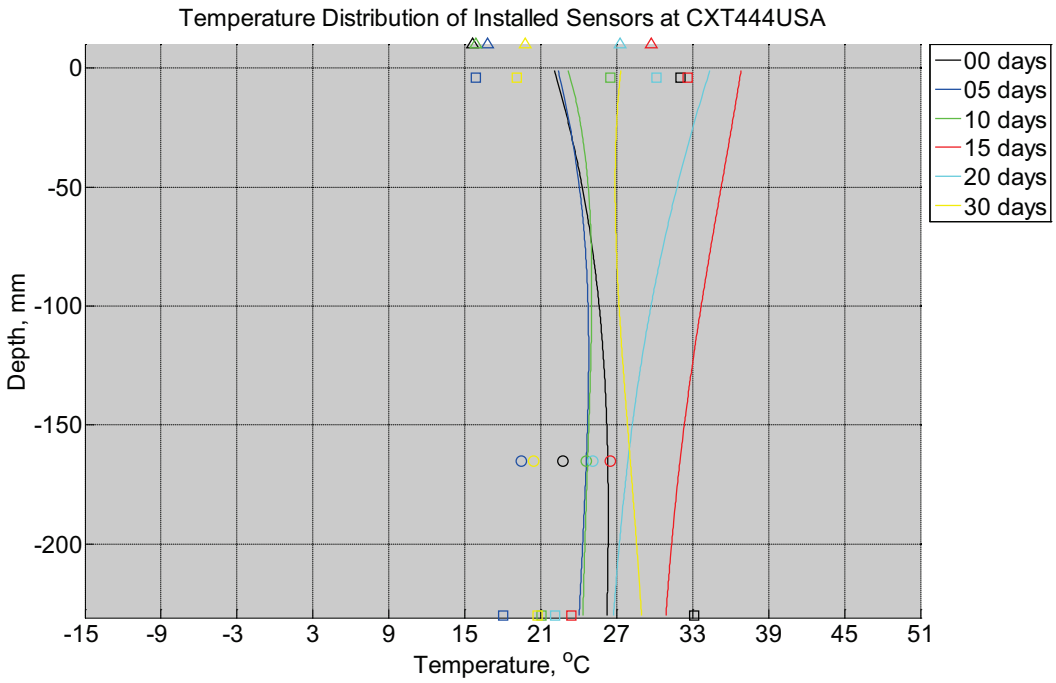

Figure B-709 Measured (markers) and modeled (continuous line) temperature profile distribution as a function of depth inside a concrete crosstie (labeled CXT444USA) installed in ballast in Rantoul, IL, between May 10, 2015, through June 20, 2015. An 8 mm thick polyurethane pad and 12 in (30.48 cm) length 136 lb/yd (67.5 kg/m) section of steel rail are additionally installed atop the model concrete crosstie. A breathable water-resistant canvas tarp is additionally installed over the concrete crosstie and immediate ballast area. The model does not incorporate a polyurethane pad nor steel rail line. Triangular markers denote temperature value from KTIP weather station, square markers denote measured temperature values from ballast, and circular markers denote measured temperature values inside concrete.

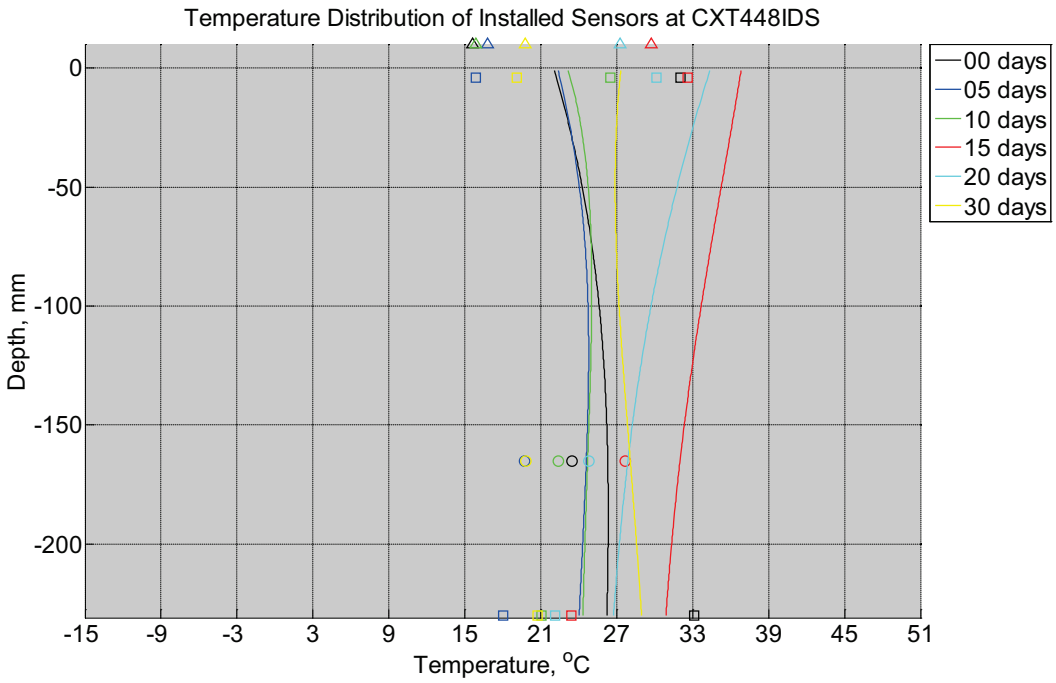

Figure B-710 Measured (markers) and modeled (continuous line) temperature profile distribution as a function of depth inside a concrete crosstie (labeled CXT448IDS) installed in ballast in Rantoul, IL, between May 10, 2015, through June 20, 2015. An 8 mm thick polyurethane pad and 12 in (30.48 cm) length 136 lb/yd (67.5 kg/m) section of steel rail are additionally installed atop the model concrete crosstie. The model does not incorporate a polyurethane pad nor steel rail line. Triangular markers denote temperature value from KTIP weather station, square markers denote measured temperature values from ballast, and circular markers denote measured temperature values inside concrete.

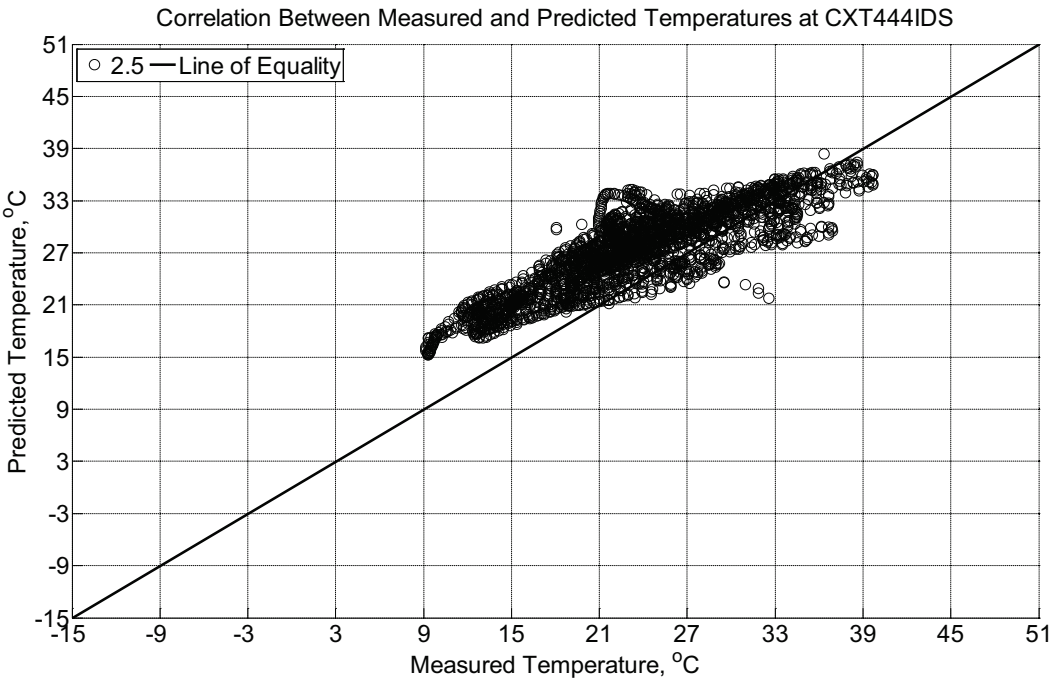

Figure B-711 Correlation between measured and predicted temperature values 2.5 inches (63.5 mm) from the surface of a concrete crosstie (labeled CXT444IDS) without a polyurethane pad nor rail installed in ballast in Rantoul, IL, between May 10, 2015, through June 20, 2015.

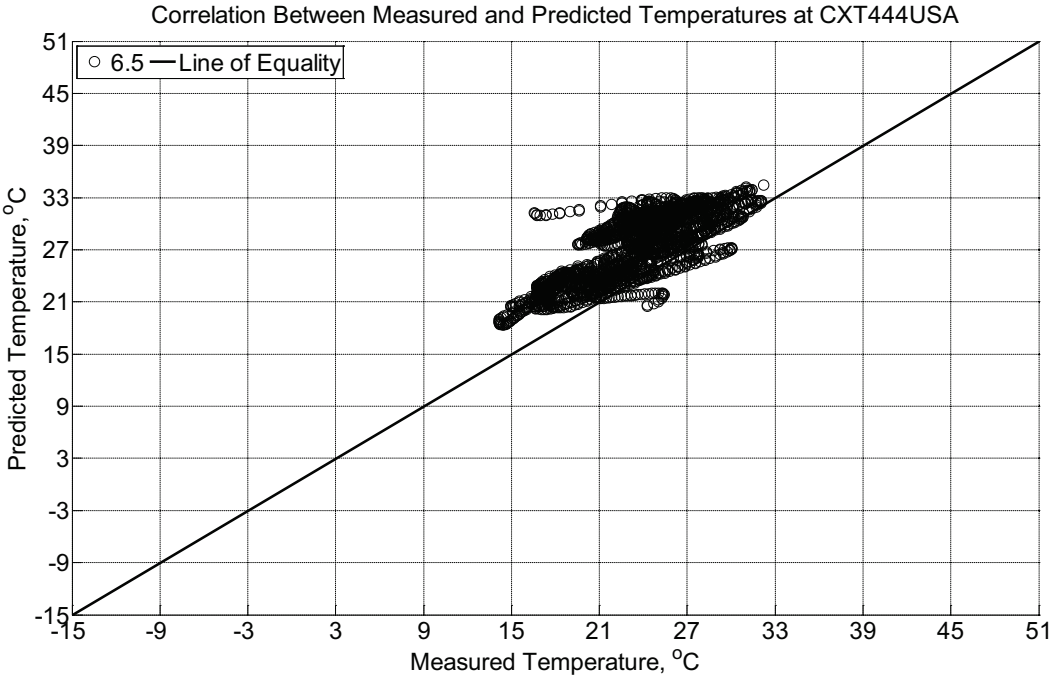

Figure B-712 Correlation between measured and predicted temperature values 6.5 inches (139.7 mm) from the surface of a concrete crosstie (labeled CXT444USA) installed in

ballast in Rantoul, IL, between May 10, 2015, through June 20, 2015. An 8 mm thick polyurethane pad and 12 in (30.48 cm) length 136 lb/yd (67.5 kg/m) section of steel rail are additionally installed atop the concrete crosstie. A breathable water-resistant canvas tarp is additionally installed over the concrete crosstie and immediate ballast area. The model does not incorporate a polyurethane pad nor steel rail line.

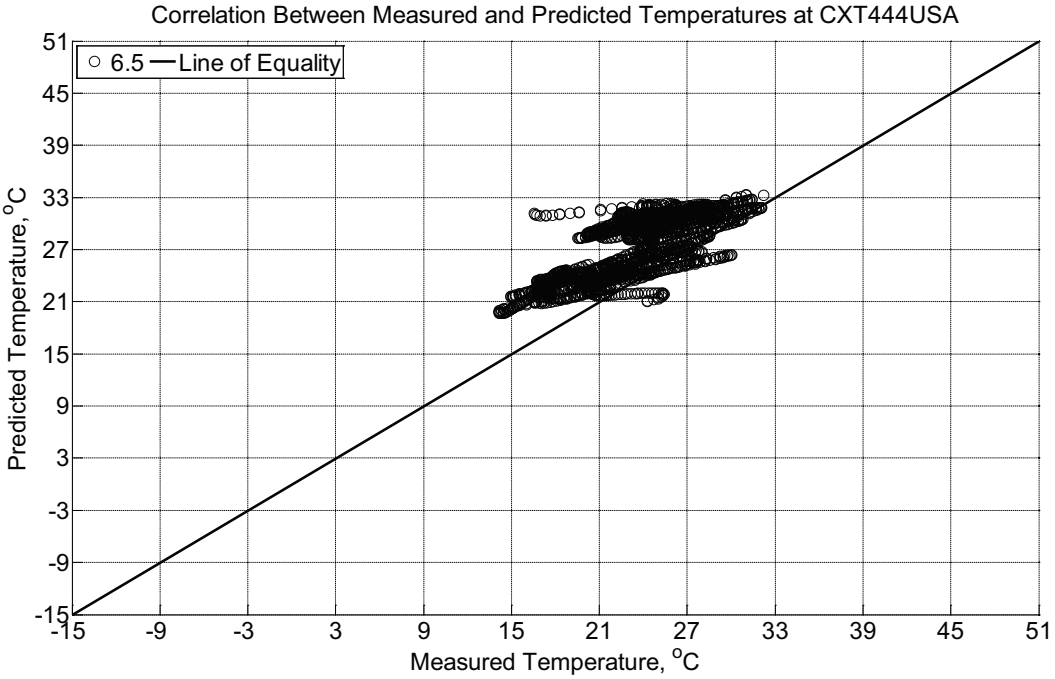

Figure B-713 Correlation between measured and predicted temperature values 6.5 inches (139.7 mm) from the surface of a concrete crosstie (labeled CXT444USA) installed in ballast in Rantoul, IL, between May 10, 2015, through June 20, 2015. An 8 mm thick polyurethane pad and 12 in (30.48 cm) length 136 lb/yd (67.5 kg/m) section of steel rail are additionally installed atop the concrete crosstie. A breathable water-resistant canvas tarp is additionally installed over the concrete crosstie and immediate ballast area. The model incorporates a 1 mm thick polyurethane pad and 1 mm thick steel rail line.

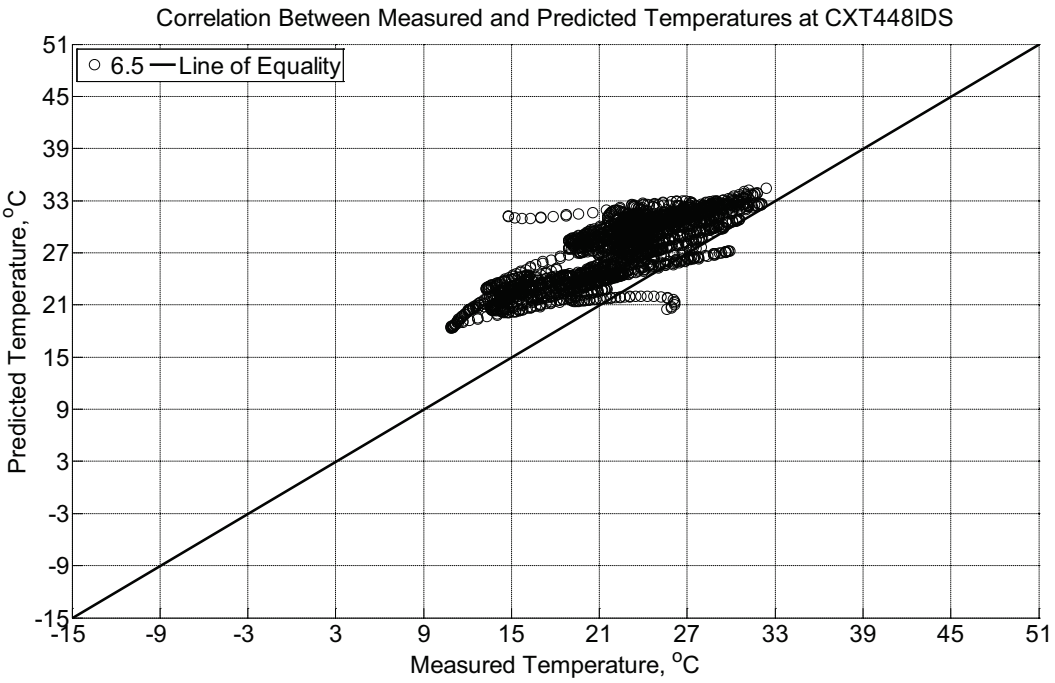

Figure B-714 Correlation between measured and predicted temperature values 6.5 inches (139.7 mm) from the surface of a concrete crosstie (labeled CXT448IDS) installed in ballast in Rantoul, IL, between May 10, 2015, through June 20, 2015. An 8 mm thick polyurethane pad and 12 in (30.48 cm) length 136 lb/yd (67.5 kg/m) section of steel rail are additionally installed atop the concrete crosstie. The model does not incorporate a polyurethane pad nor steel rail line.

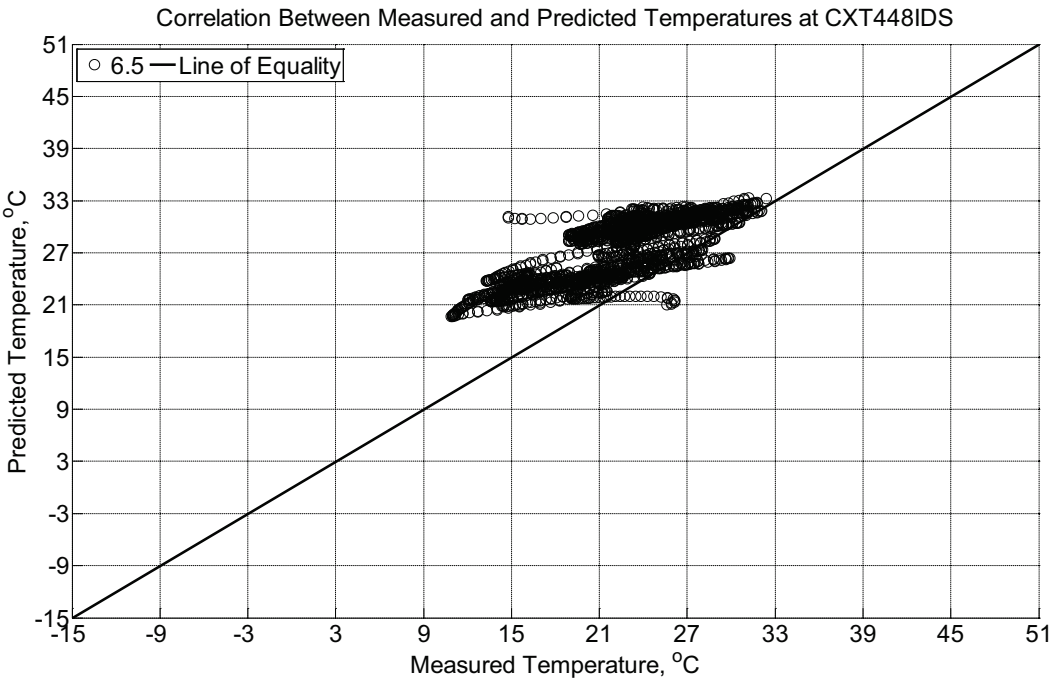

Figure B-715 Correlation between measured and predicted temperature values 6.5 inches (139.7 mm) from the surface of a concrete crosstie (labeled CXT448IDS) installed in ballast in Rantoul, IL, between May 10, 2015, through June 20, 2015. An 8 mm thick polyurethane pad and 12 in (30.48 cm) length 136 lb/yd (67.5 kg/m) section of steel rail are additionally installed atop the concrete crosstie. The model incorporates a 1 mm thick polyurethane pad and 1 mm thick steel rail line.

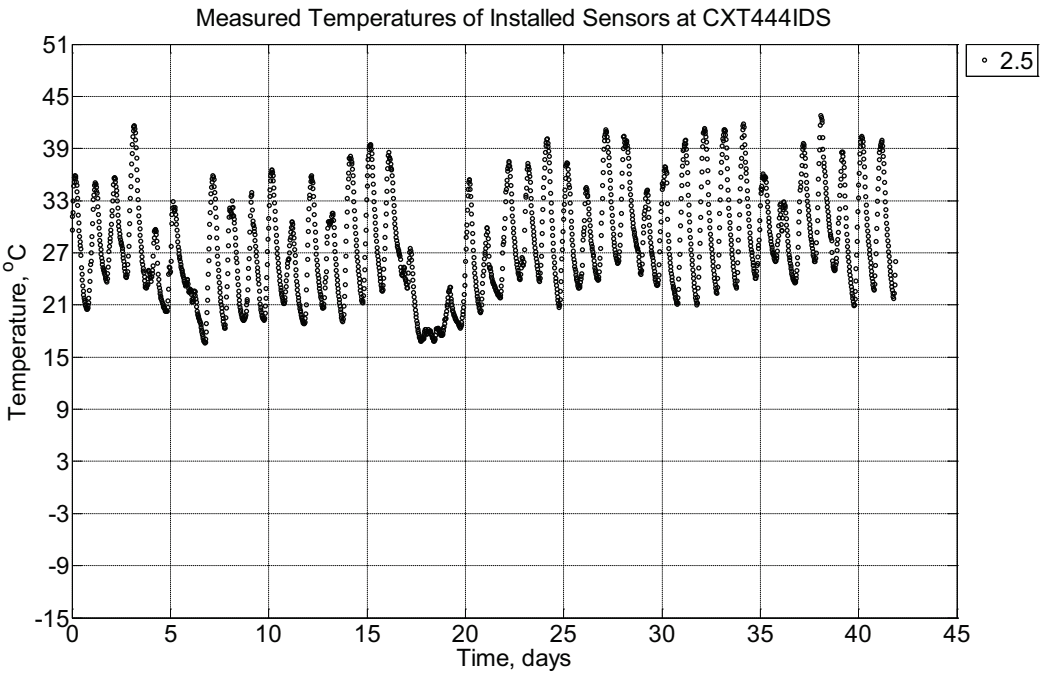

Figure B-716 Measured temperature at a depth of 2.5 inches (63.5 mm) from the surface of a concrete crosstie (labeled CXT444IDS) without a polyurethane pad nor rail installed in ballast in Rantoul, IL, between June 20, 2015, through August 1, 2015.

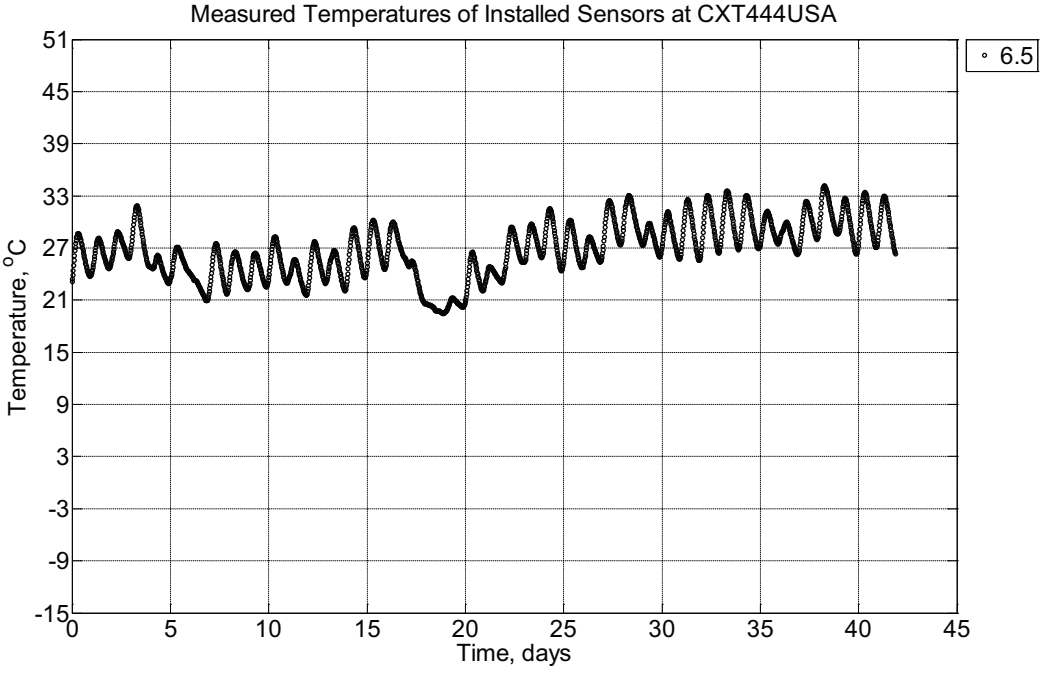

Figure B-717 Measured temperature at a depth of 6.5 inches (139.7 mm) from the surface of a concrete crosstie (labeled CXT444USA) installed in ballast in Rantoul, IL, between June 20, 2015, through August 1, 2015. An 8 mm thick polyurethane pad and 12 in (30.48

cm) length 136 lb/yd (67.5 kg/m) section of steel rail are additionally installed atop the concrete crosstie. A breathable water-resistant canvas tarp is additionally installed over the concrete crosstie and immediate ballast area.

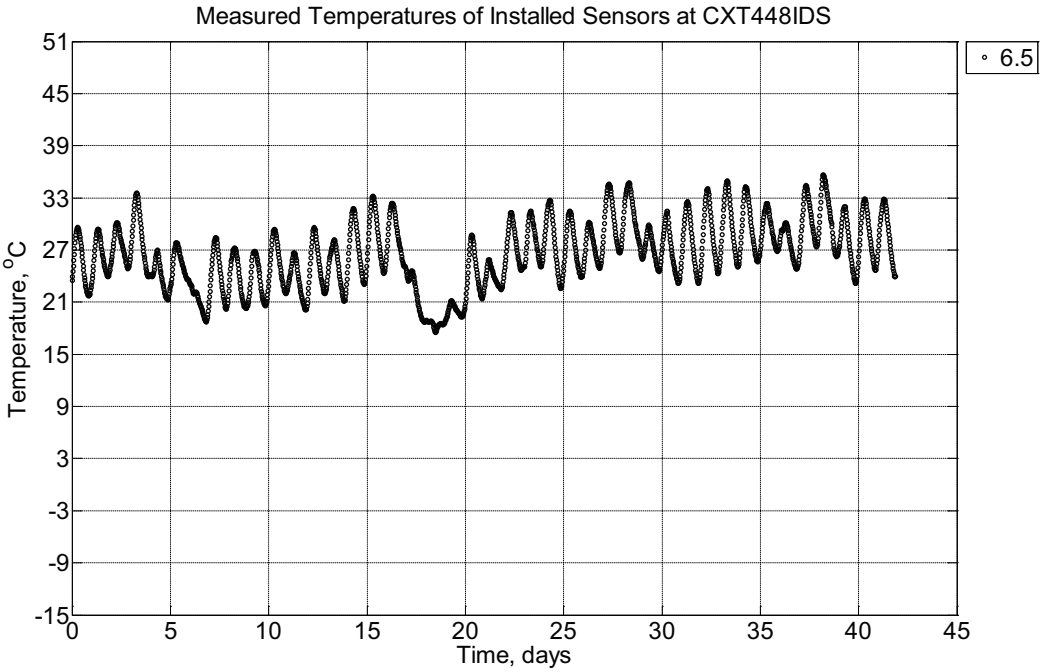

Figure B-718 Measured temperature at depths of 6.5 inches (139.7 mm) from the surface of a concrete crosstie (labeled CXT448IDS) installed in ballast in Rantoul, IL, between June 20, 2015, through August 1, 2015. An 8 mm thick polyurethane pad and 12 in (30.48 cm) length 136 lb/yd (67.5 kg/m) section of steel rail are additionally installed atop the concrete crosstie.

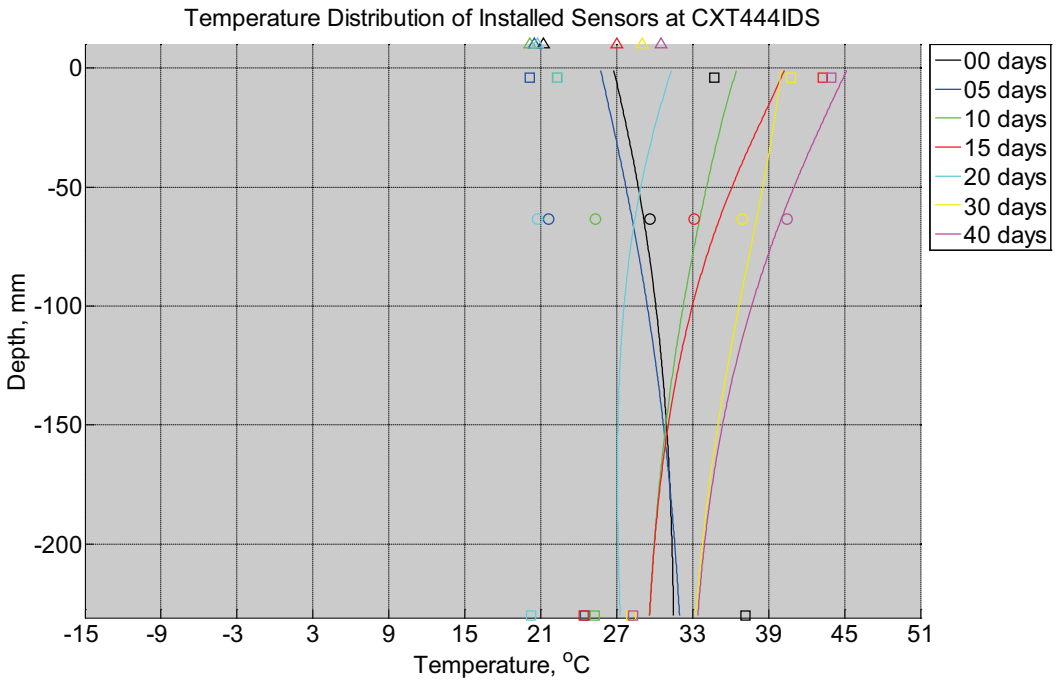

Figure B-719 Measured (markers) and modeled (continuous line) temperature profile distribution as a function of depth inside a concrete crosstie (labeled CXT444IDS) without a polyurethane pad nor rail installed in ballast in Rantoul, IL, between June 20, 2015, through August 1, 2015. Triangular markers denote temperature value from KTIP weather station, square markers denote measured temperature values from ballast, and circular markers denote measured temperature values inside concrete.

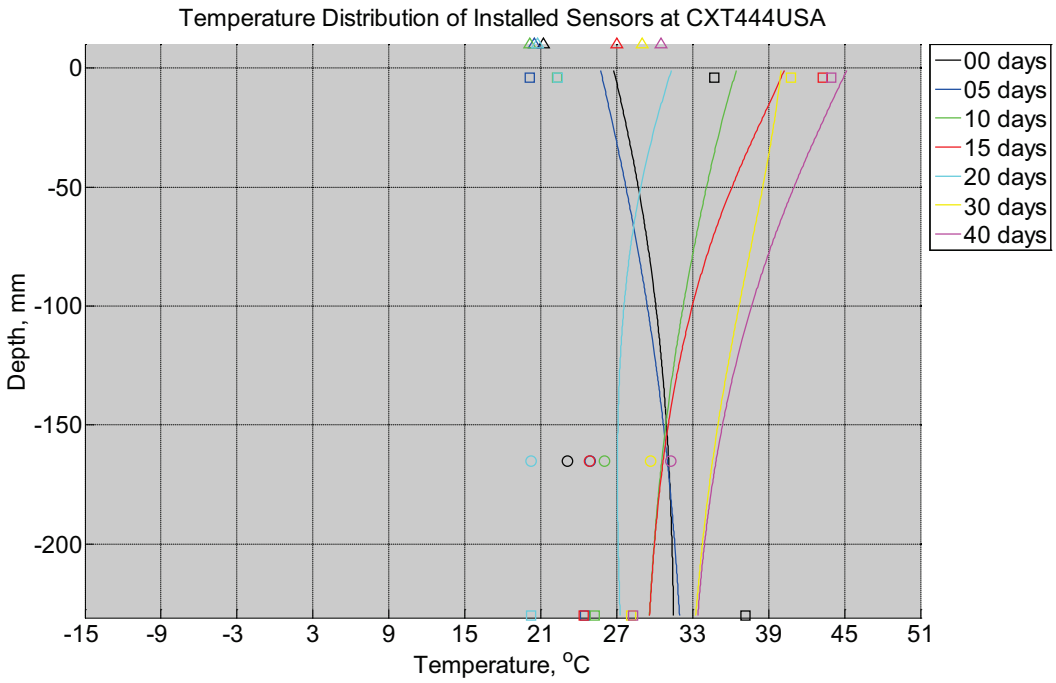

Figure B-720 Measured (markers) and modeled (continuous line) temperature profile distribution as a function of depth inside a concrete crosstie (labeled CXT444USA) installed in ballast in Rantoul, IL, between June 20, 2015, through August 1, 2015. An 8 mm thick polyurethane pad and 12 in (30.48 cm) length 136 lb/yd (67.5 kg/m) section of steel rail are additionally installed atop the model concrete crosstie. A breathable water-resistant canvas tarp is additionally installed over the concrete crosstie and immediate ballast area. The model does not incorporate a polyurethane pad nor steel rail line. Triangular markers denote temperature value from KTIP weather station, square markers denote measured temperature values from ballast, and circular markers denote measured temperature values inside concrete.

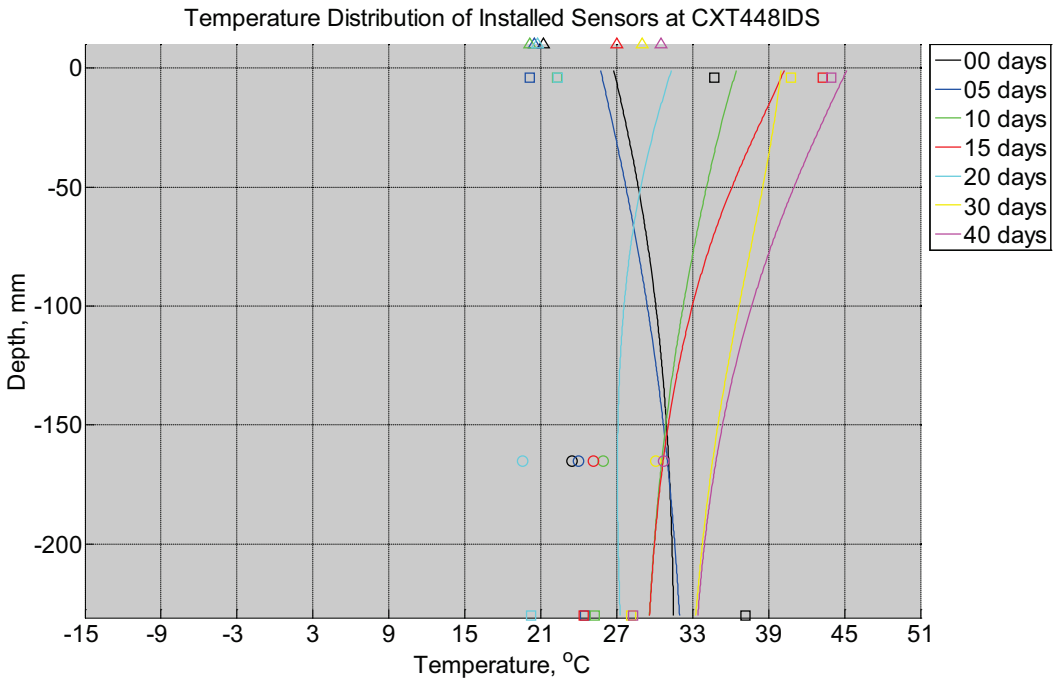

Figure B-721 Measured (markers) and modeled (continuous line) temperature profile distribution as a function of depth inside a concrete crosstie (labeled CXT448IDS) installed in ballast in Rantoul, IL, between June 20, 2015, through August 1, 2015. An 8 mm thick polyurethane pad and 12 in (30.48 cm) length 136 lb/yd (67.5 kg/m) section of steel rail are additionally installed atop the model concrete crosstie. The model does not incorporate a polyurethane pad nor steel rail line. Triangular markers denote temperature value from KTIP weather station, square markers denote measured temperature values from ballast, and circular markers denote measured temperature values inside concrete.

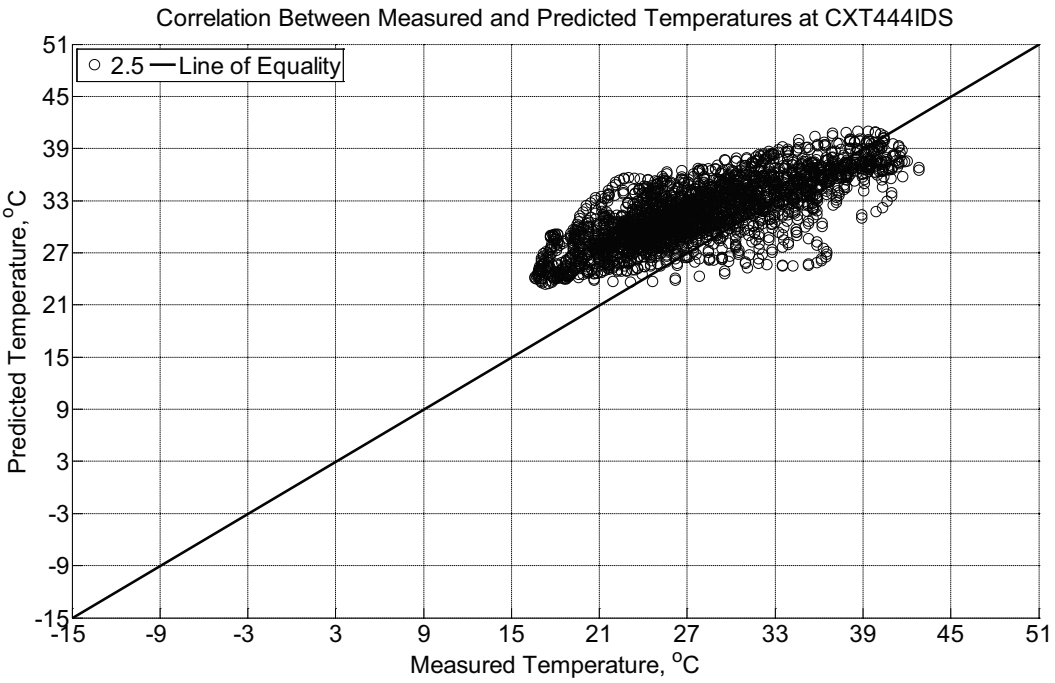

Figure B-722 Correlation between measured and predicted temperature values 2.5 inches (63.5 mm) from the surface of a concrete crosstie (labeled CXT444IDS) without a polyurethane pad nor rail installed in ballast in Rantoul, IL, between June 20, 2015, through August 1, 2015.

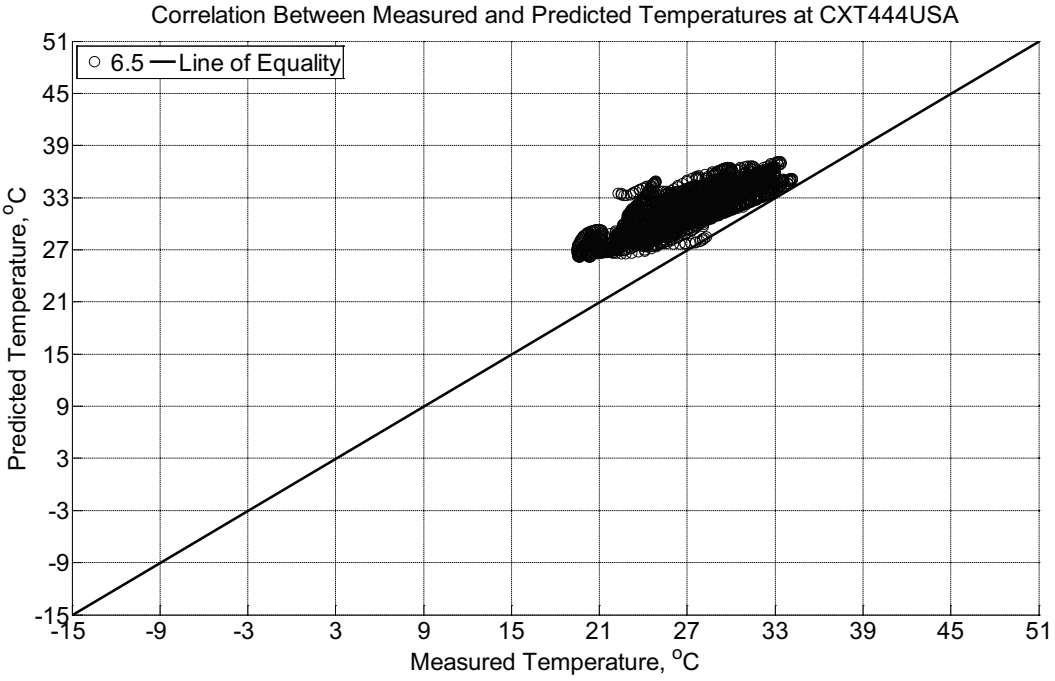

Figure B-723 Correlation between measured and predicted temperature values 6.5 inches (139.7 mm) from the surface of a concrete crosstie (labeled CXT444USA) installed in

ballast in Rantoul, IL, between June 20, 2015, through August 1, 2015. An 8 mm thick polyurethane pad and 12 in (30.48 cm) length 136 lb/yd (67.5 kg/m) section of steel rail are additionally installed atop the concrete crosstie. A breathable water-resistant canvas tarp is additionally installed over the concrete crosstie and immediate ballast area. The model does not incorporate a polyurethane pad nor steel rail line.

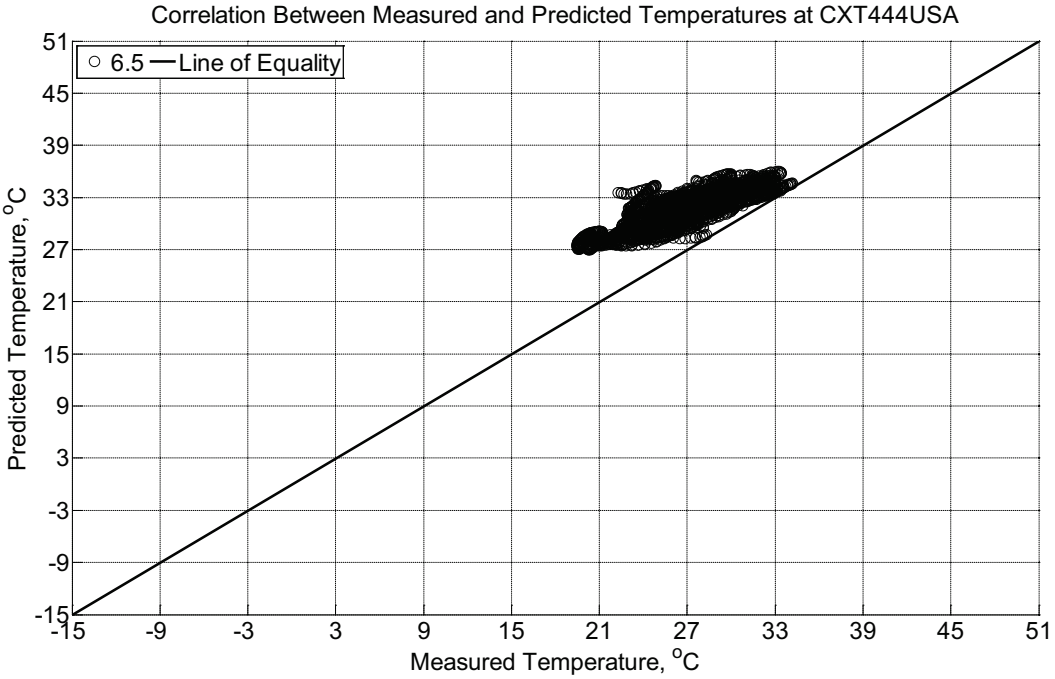

Figure B-724 Correlation between measured and predicted temperature values 6.5 inches (139.7 mm) from the surface of a concrete crosstie (labeled CXT444USA) installed in ballast in Rantoul, IL, between June 20, 2015, through August 1, 2015. An 8 mm thick polyurethane pad and 12 in (30.48 cm) length 136 lb/yd (67.5 kg/m) section of steel rail are additionally installed atop the concrete crosstie. A breathable water-resistant canvas tarp is additionally installed over the concrete crosstie and immediate ballast area. The model incorporates a 1 mm thick polyurethane pad and 1 mm thick steel rail line.

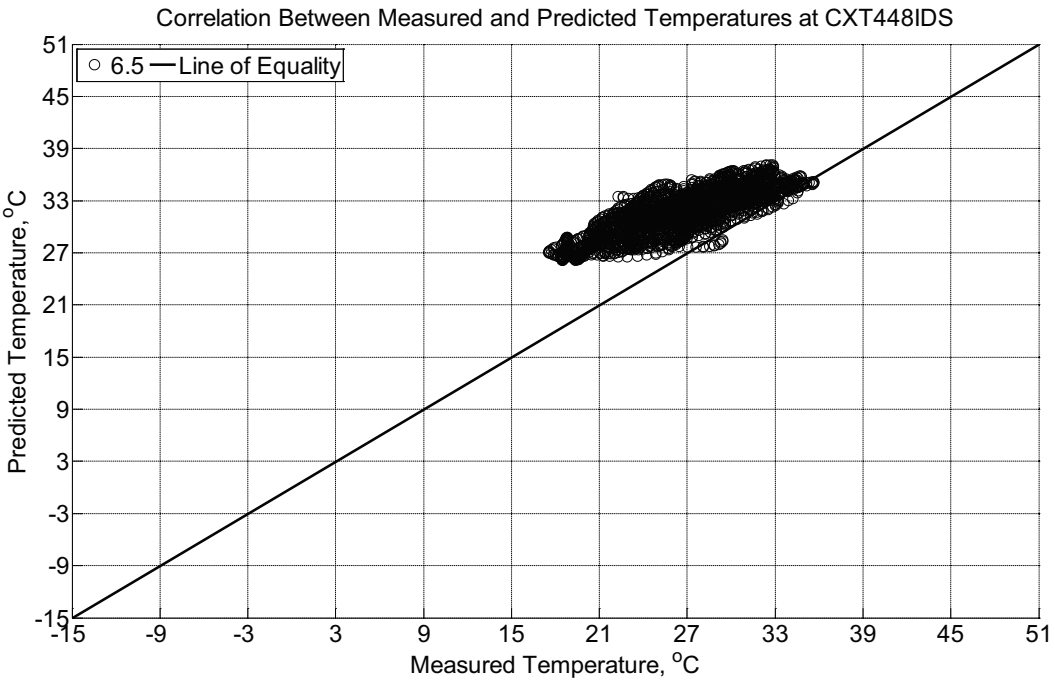

Figure B-725 Correlation between measured and predicted temperature values 6.5 inches (139.7 mm) from the surface of a concrete crosstie (labeled CXT448IDS) installed in ballast in Rantoul, IL, between June 20, 2015, through August 1, 2015. An 8 mm thick polyurethane pad and 12 in (30.48 cm) length 136 lb/yd (67.5 kg/m) section of steel rail are additionally installed atop the concrete crosstie. The model does not incorporate a polyurethane pad nor steel rail line.

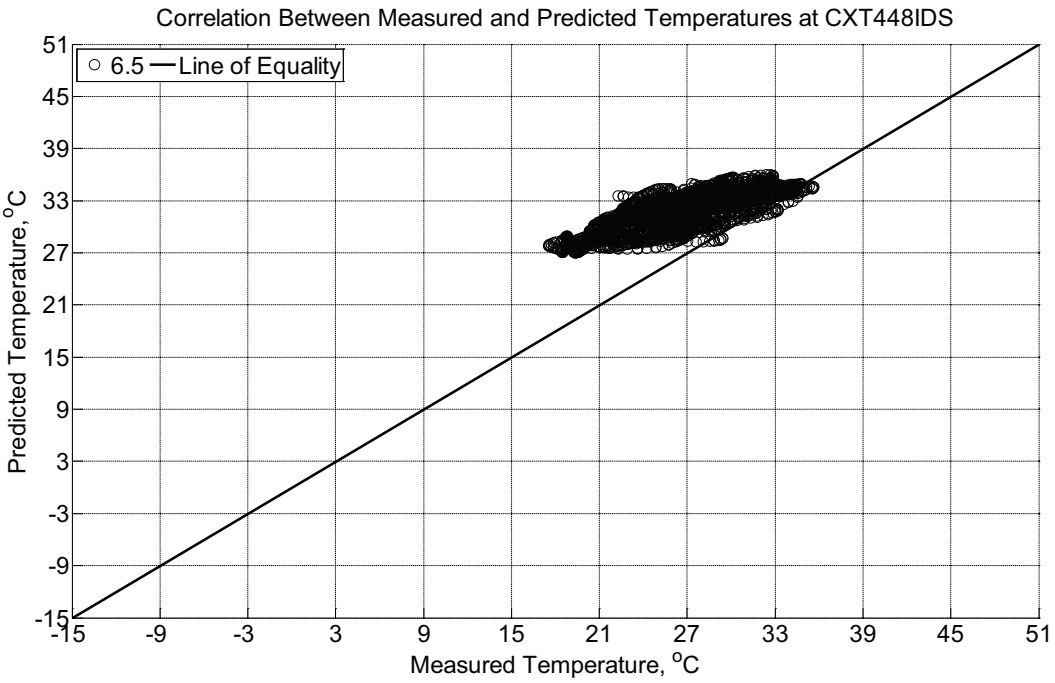

Figure B-726 Correlation between measured and predicted temperature values 6.5 inches (139.7 mm) from the surface of a concrete crosstie (labeled CXT448IDS) installed in ballast in Rantoul, IL, between June 20, 2015, through August 1, 2015. An 8 mm thick polyurethane pad and 12 in (30.48 cm) length 136 lb/yd (67.5 kg/m) section of steel rail are additionally installed atop the concrete crosstie. The model incorporates a 1 mm thick polyurethane pad and 1 mm thick steel rail line.

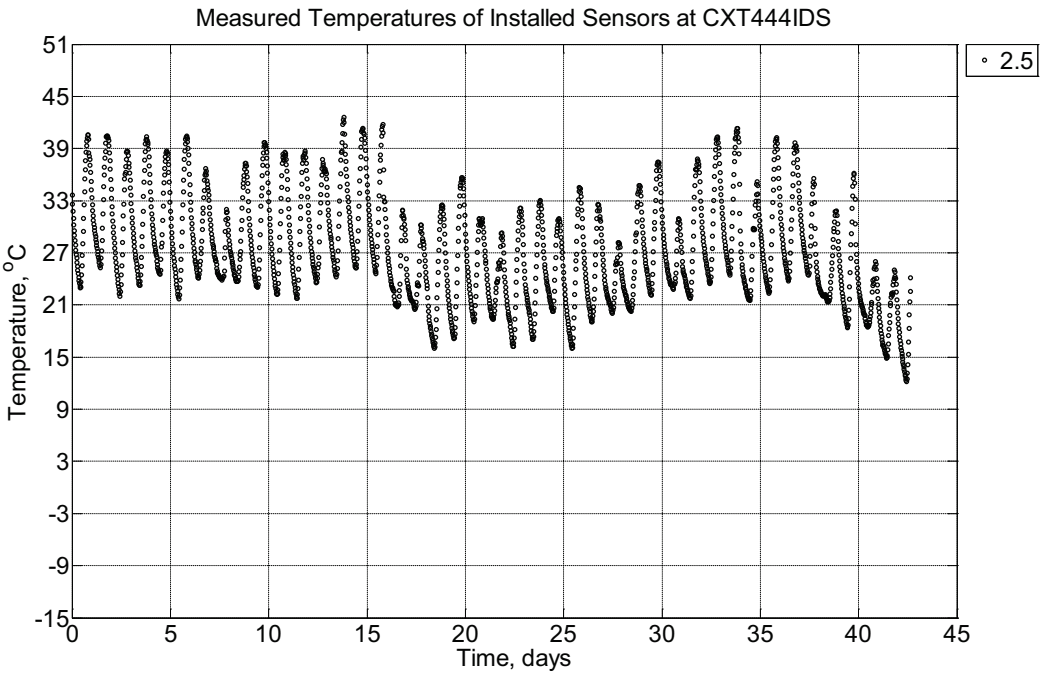

Figure B-727 Measured temperature at a depth of 2.5 inches (63.5 mm) from the surface of a concrete crosstie (labeled CXT444IDS) without a polyurethane pad nor rail installed in ballast in Rantoul, IL, between August 1, 2015, through September 13, 2015.

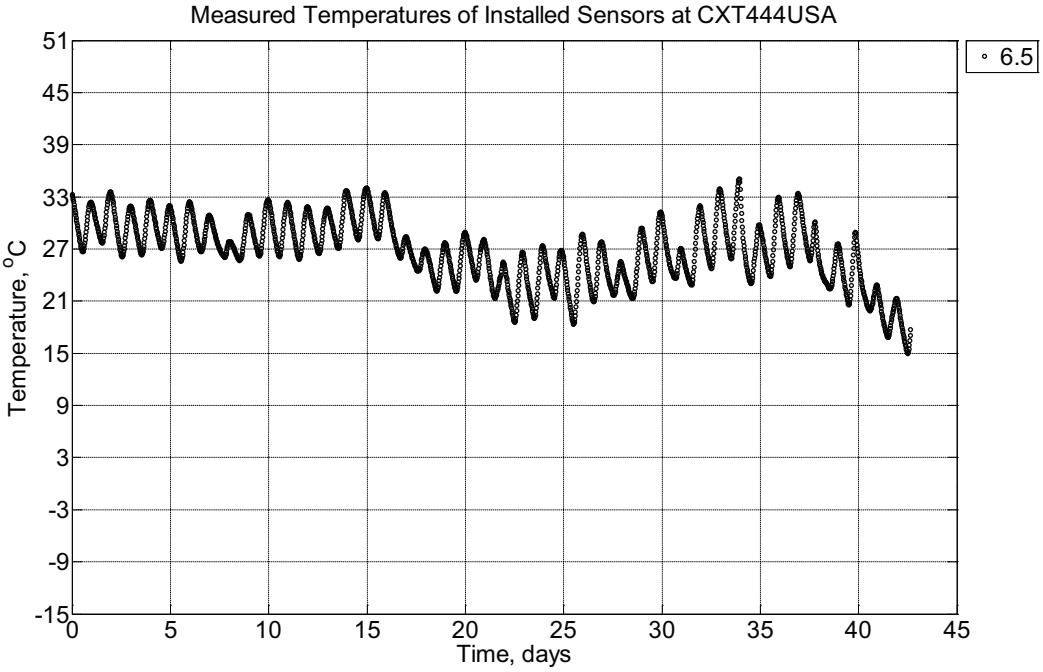

Figure B-728 Measured temperature at a depth of 6.5 inches (139.7 mm) from the surface of a concrete crosstie (labeled CXT444USA) installed in ballast in Rantoul, IL, between August 1, 2015, through September 13, 2015. An 8 mm thick polyurethane pad and 12 in

(30.48 cm) length 136 lb/yd (67.5 kg/m) section of steel rail are additionally installed atop the concrete crosstie. A breathable water-resistant canvas tarp is additionally installed over the concrete crosstie and immediate ballast area.

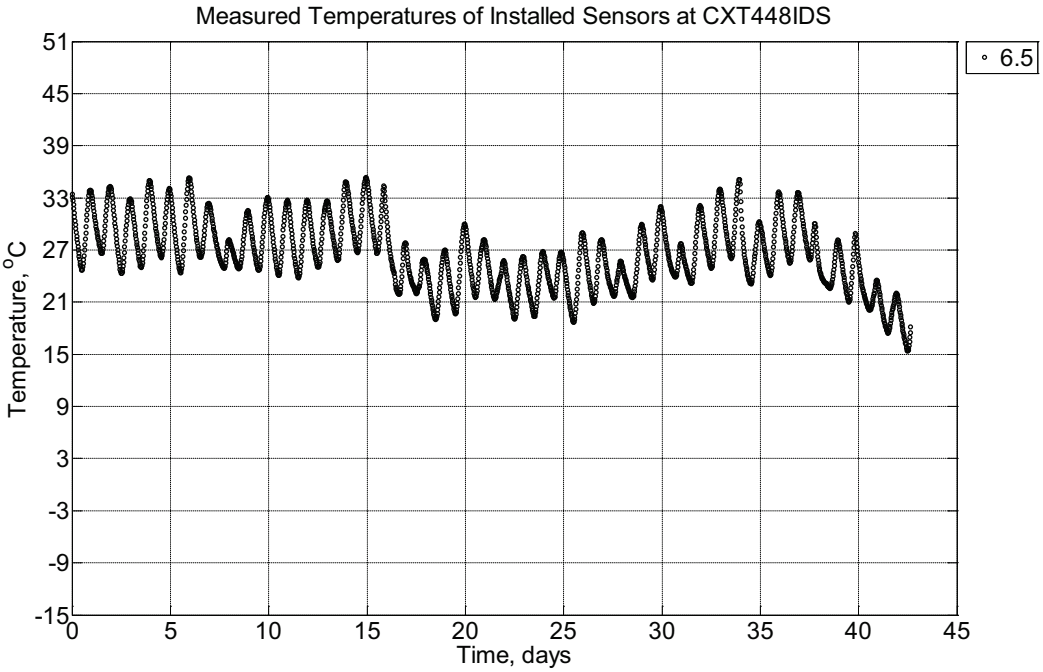

Figure B-729 Measured temperature at depths of 6.5 inches (139.7 mm) from the surface of a concrete crosstie (labeled CXT448IDS) installed in ballast in Rantoul, IL, between August 1, 2015, through September 13, 2015. An 8 mm thick polyurethane pad and 12 in (30.48 cm) length 136 lb/yd (67.5 kg/m) section of steel rail are additionally installed atop the concrete crosstie.

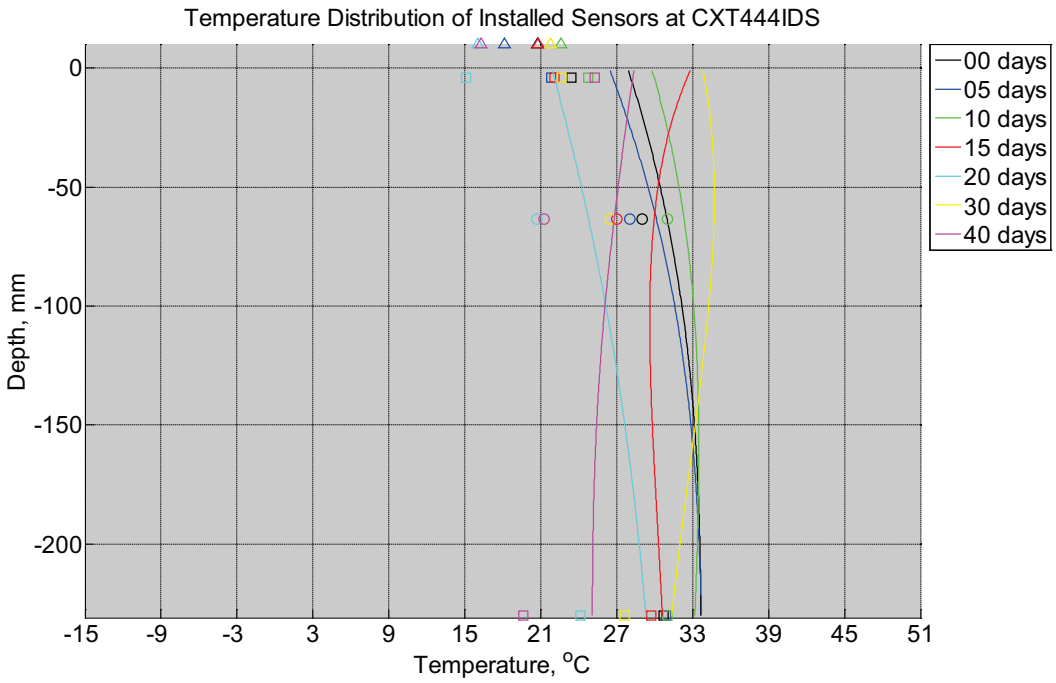

Figure B-730 Measured (markers) and modeled (continuous line) temperature profile distribution as a function of depth inside a concrete crosstie (labeled CXT444IDS) without a polyurethane pad nor rail installed in ballast in Rantoul, IL, between August 1, 2015, through September 13, 2015. Triangular markers denote temperature value from KTIP weather station, square markers denote measured temperature values from ballast, and circular markers denote measured temperature values inside concrete.

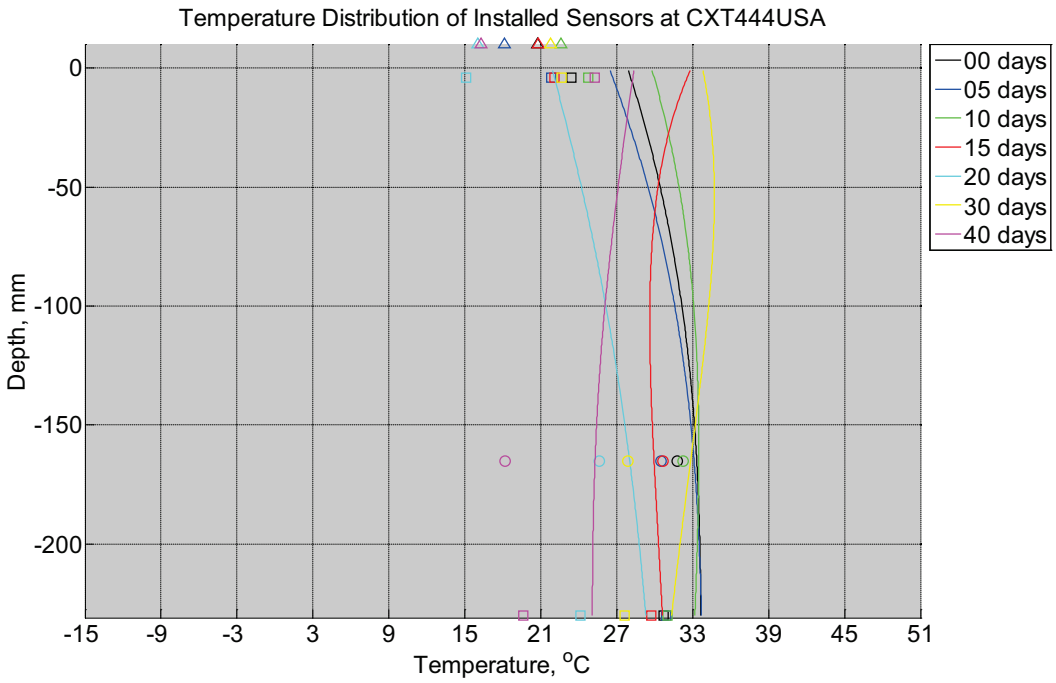

Figure B-731 Measured (markers) and modeled (continuous line) temperature profile distribution as a function of depth inside a concrete crosstie (labeled CXT444USA) installed in ballast in Rantoul, IL, between August 1, 2015, through September 13, 2015. An 8 mm thick polyurethane pad and 12 in (30.48 cm) length 136 lb/yd (67.5 kg/m) section of steel rail are additionally installed atop the model concrete crosstie. A breathable water-resistant canvas tarp is additionally installed over the concrete crosstie and immediate ballast area. The model does not incorporate a polyurethane pad nor steel rail line. Triangular markers denote temperature value from KTIP weather station, square markers denote measured temperature values from ballast, and circular markers denote measured temperature values inside concrete.

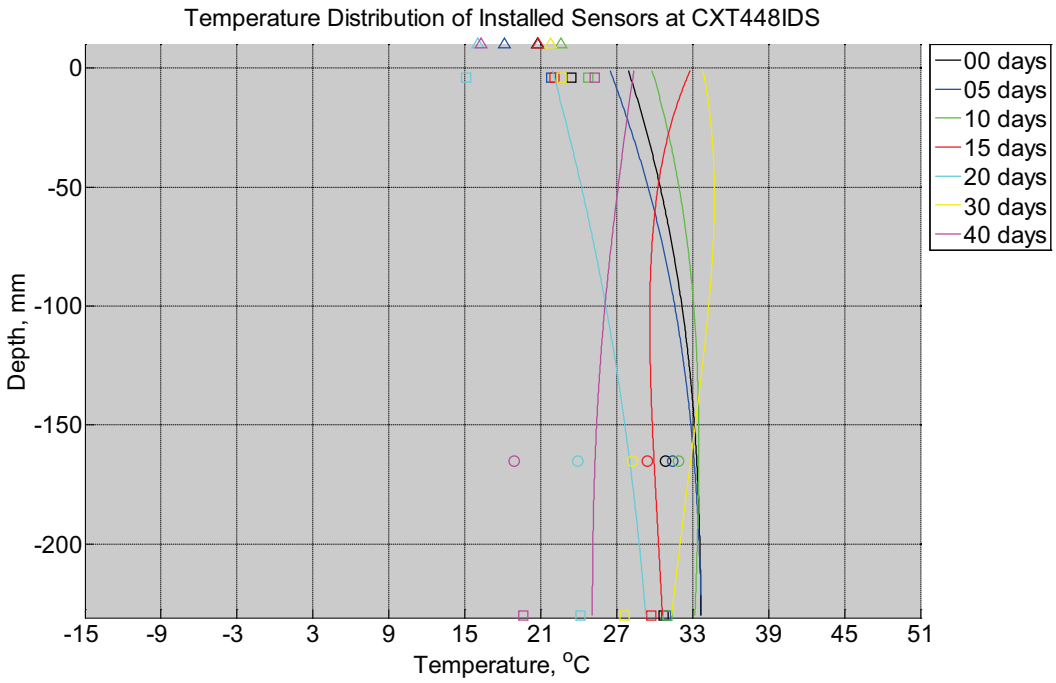

Figure B-732 Measured (markers) and modeled (continuous line) temperature profile distribution as a function of depth inside a concrete crosstie (labeled CXT448IDS) installed in ballast in Rantoul, IL, between August 1, 2015, through September 13, 2015. An 8 mm thick polyurethane pad and 12 in (30.48 cm) length 136 lb/yd (67.5 kg/m) section of steel rail are additionally installed atop the model concrete crosstie. The model does not incorporate a polyurethane pad nor steel rail line. Triangular markers denote temperature value from KTIP weather station, square markers denote measured temperature values from ballast, and circular markers denote measured temperature values inside concrete.

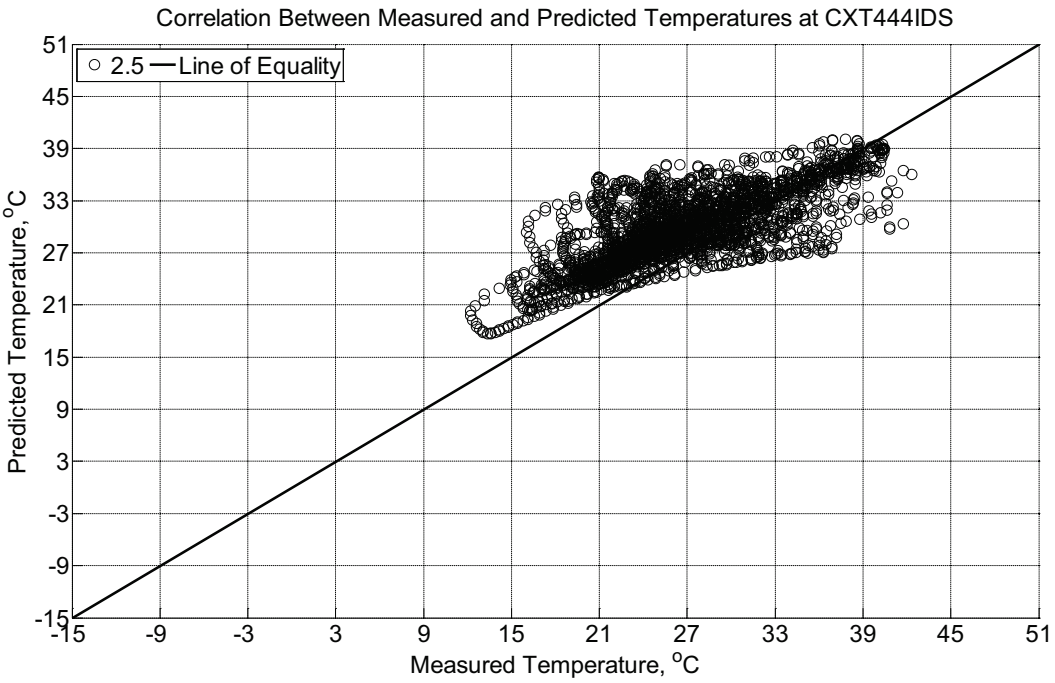

Figure B-733 Correlation between measured and predicted temperature values 2.5 inches (63.5 mm) from the surface of a concrete crosstie (labeled CXT444IDS) without a polyurethane pad nor rail installed in ballast in Rantoul, IL, between August 1, 2015, through September 13, 2015.

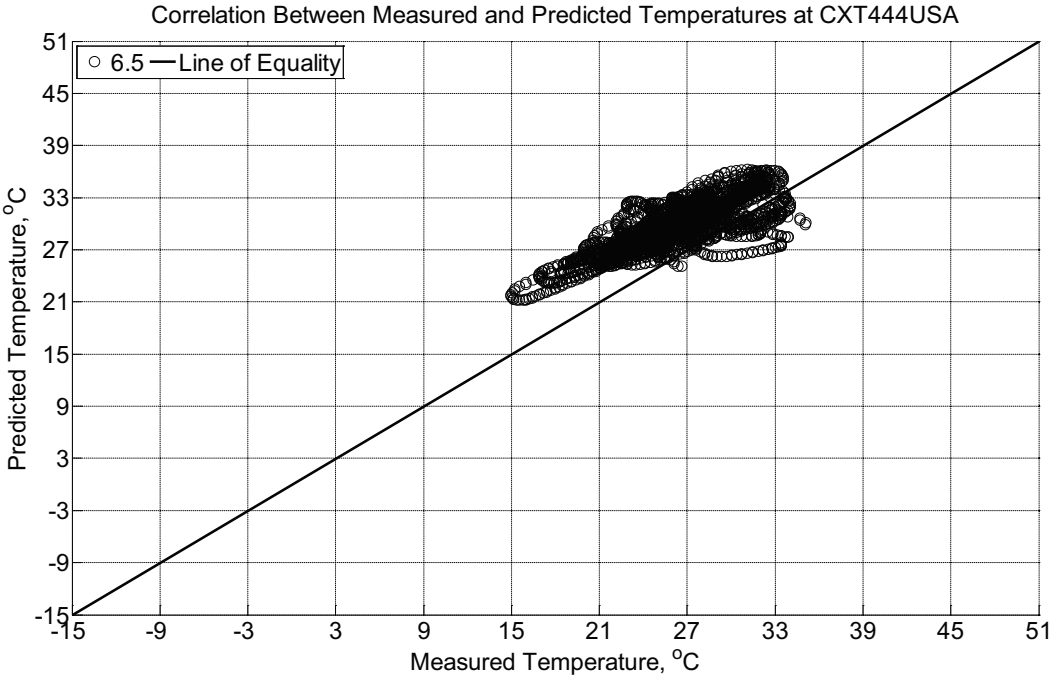

Figure B-734 Correlation between measured and predicted temperature values 6.5 inches (139.7 mm) from the surface of a concrete crosstie (labeled CXT444USA) installed in

ballast in Rantoul, IL, between August 1, 2015, through September 13, 2015. An 8 mm thick polyurethane pad and 12 in (30.48 cm) length 136 lb/yd (67.5 kg/m) section of steel rail are additionally installed atop the concrete crosstie. A breathable water-resistant canvas tarp is additionally installed over the concrete crosstie and immediate ballast area. The model does not incorporate a polyurethane pad nor steel rail line.

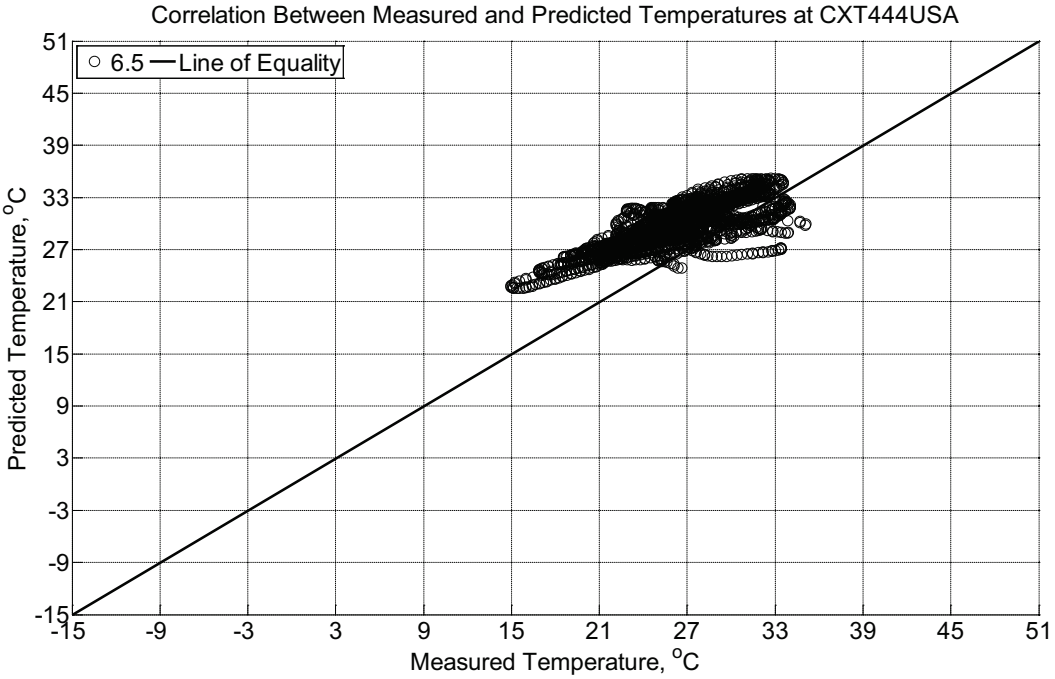

Figure B-735 Correlation between measured and predicted temperature values 6.5 inches (139.7 mm) from the surface of a concrete crosstie (labeled CXT444USA) installed in ballast in Rantoul, IL, between August 1, 2015, through September 13, 2015. An 8 mm thick polyurethane pad and 12 in (30.48 cm) length 136 lb/yd (67.5 kg/m) section of steel rail are additionally installed atop the concrete crosstie. A breathable water-resistant canvas tarp is additionally installed over the concrete crosstie and immediate ballast area. The model incorporates a 1 mm thick polyurethane pad and 1 mm thick steel rail line.

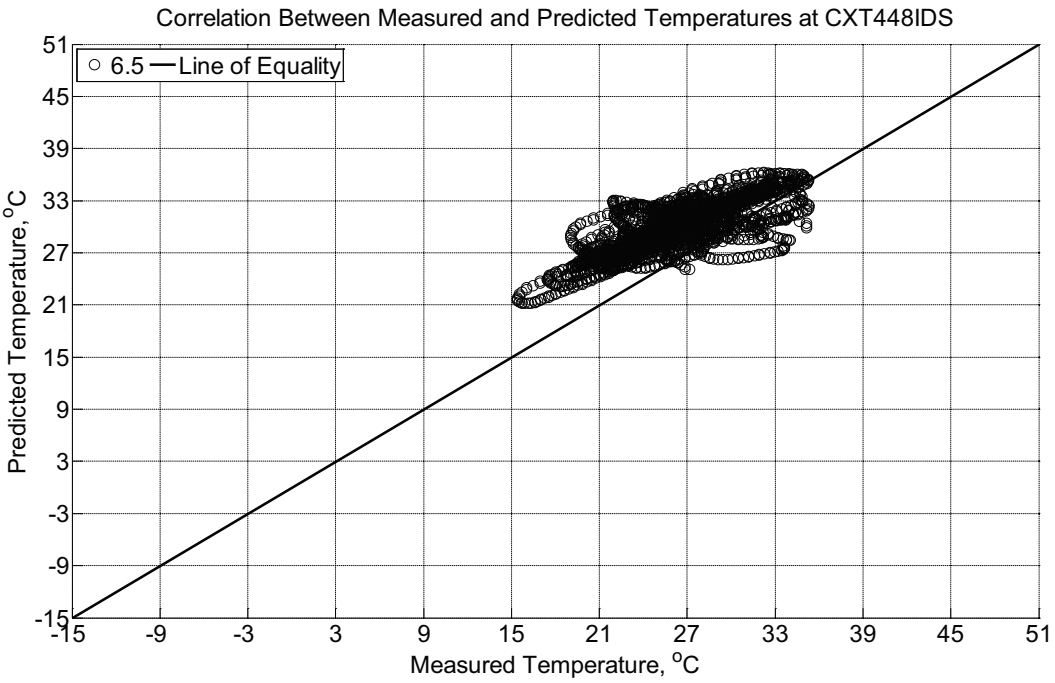

Figure B-736 Correlation between measured and predicted temperature values 6.5 inches (139.7 mm) from the surface of a concrete crosstie (labeled CXT448IDS) installed in ballast in Rantoul, IL, between August 1, 2015, through September 13, 2015. An 8 mm thick polyurethane pad and 12 in (30.48 cm) length 136 lb/yd (67.5 kg/m) section of steel rail are additionally installed atop the concrete crosstie. The model does not incorporate a polyurethane pad nor steel rail line.

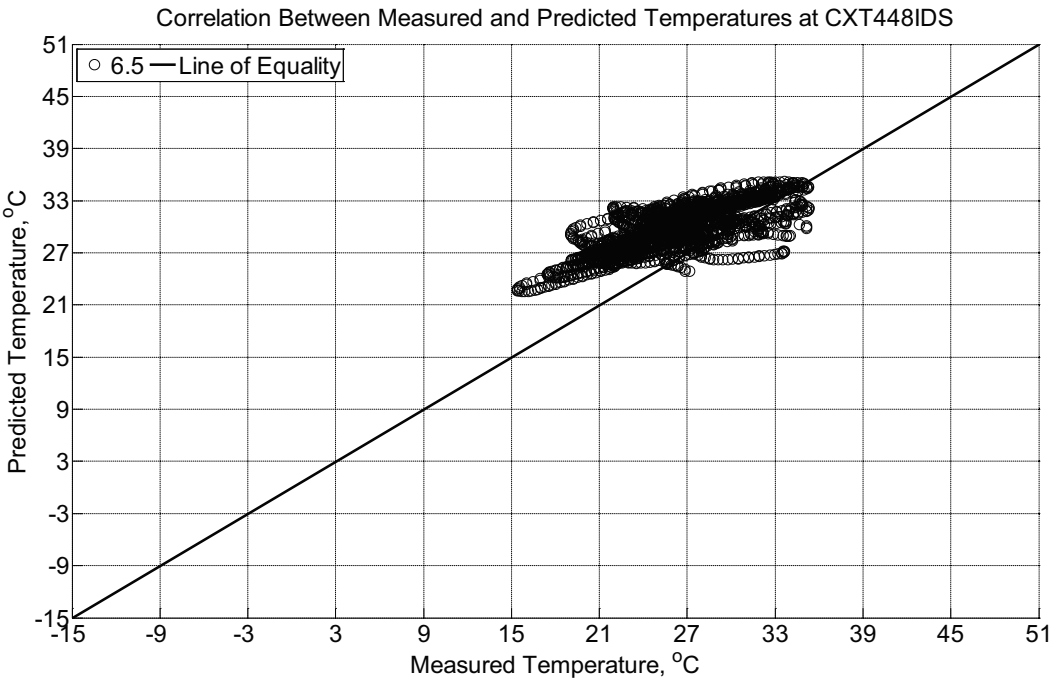

Figure B-737 Correlation between measured and predicted temperature values 6.5 inches (139.7 mm) from the surface of a concrete crosstie (labeled CXT448IDS) installed in ballast in Rantoul, IL, between August 1, 2015, through September 13, 2015. An 8 mm thick polyurethane pad and 12 in (30.48 cm) length 136 lb/yd (67.5 kg/m) section of steel rail are additionally installed atop the concrete crosstie. The model incorporates a 1 mm thick polyurethane pad and 1 mm thick steel rail line.

Measured and predicted internal relative humidity of instrumented concrete crossties located near Lytton, BC

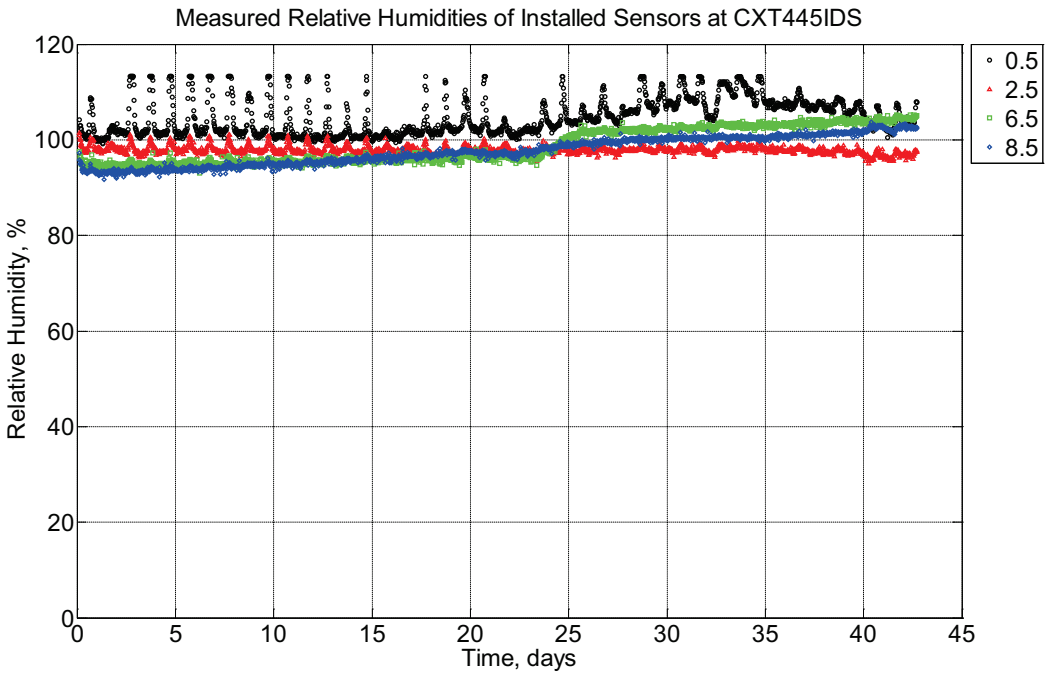

Figure B-738 Measured relative humidity at depths of 0.5 inches (12.7 mm), 2.5 inches (63.5 mm), 6.5 inches (139.7 mm), and 8.5 inches (215.9 mm) from the surface of a concrete crosstie (labeled CXT445IDS) installed in track near Lytton, BC, between October 11, 2013, through November 22, 2013. An 8 mm thick polyurethane pad and steel rail are additionally installed atop the concrete crosstie.

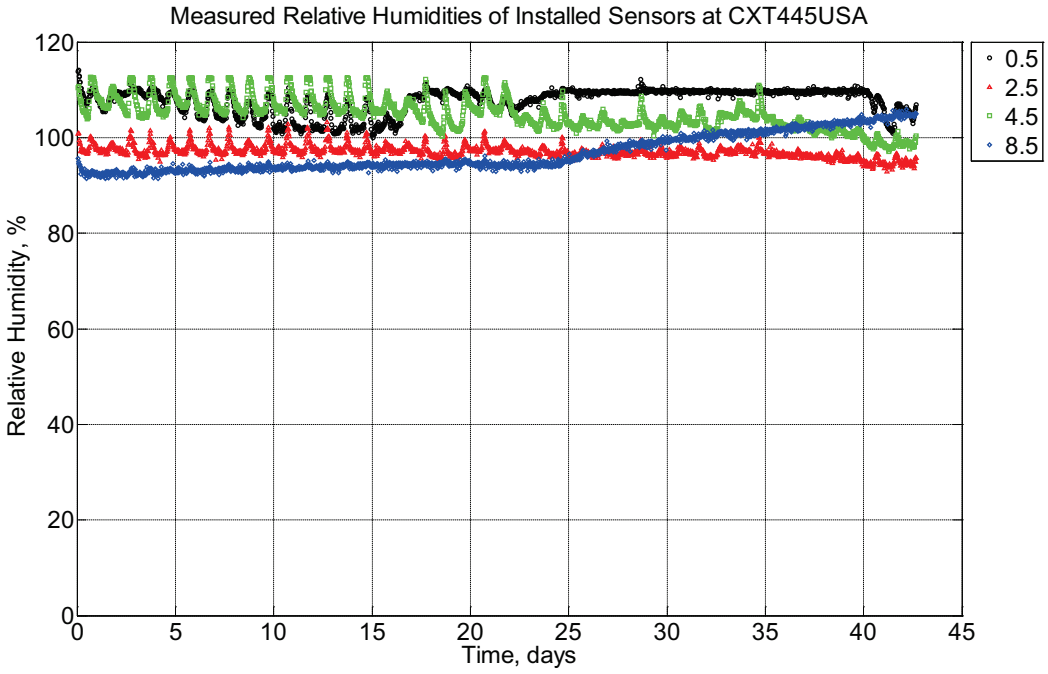

Figure B-739 Measured relative humidity at depths of 0.5 inches (12.7 mm), 2.5 inches (63.5

mm), 4.5 inches (114.3 mm), and 8.5 inches (215.9 mm) from the surface of a concrete crosstie (labeled CXT445USA) installed in track near Lytton, BC, between October 11, 2013, through November 22, 2013. An 8 mm thick polyurethane pad and steel rail are additionally installed atop the concrete crosstie.

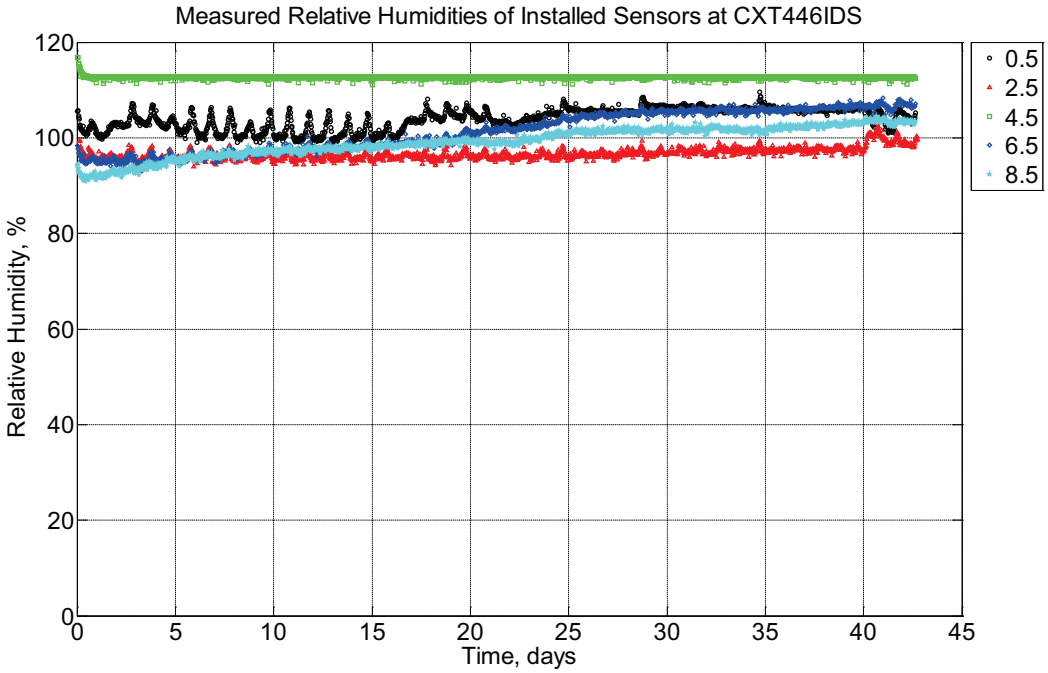

Figure B-740 Measured relative humidity at depths of 0.5 inches (12.7 mm), 2.5 inches (63.5 mm), 4.5 inches (114.3 mm), 6.5 inches (139.7 mm), and 8.5 inches (215.9 mm) from the surface of a concrete crosstie (labeled CXT446IDS) installed in track near Lytton, BC, between October 11, 2013, through November 22, 2013. An 8 mm thick polyurethane pad and steel rail are additionally installed atop the concrete crosstie.

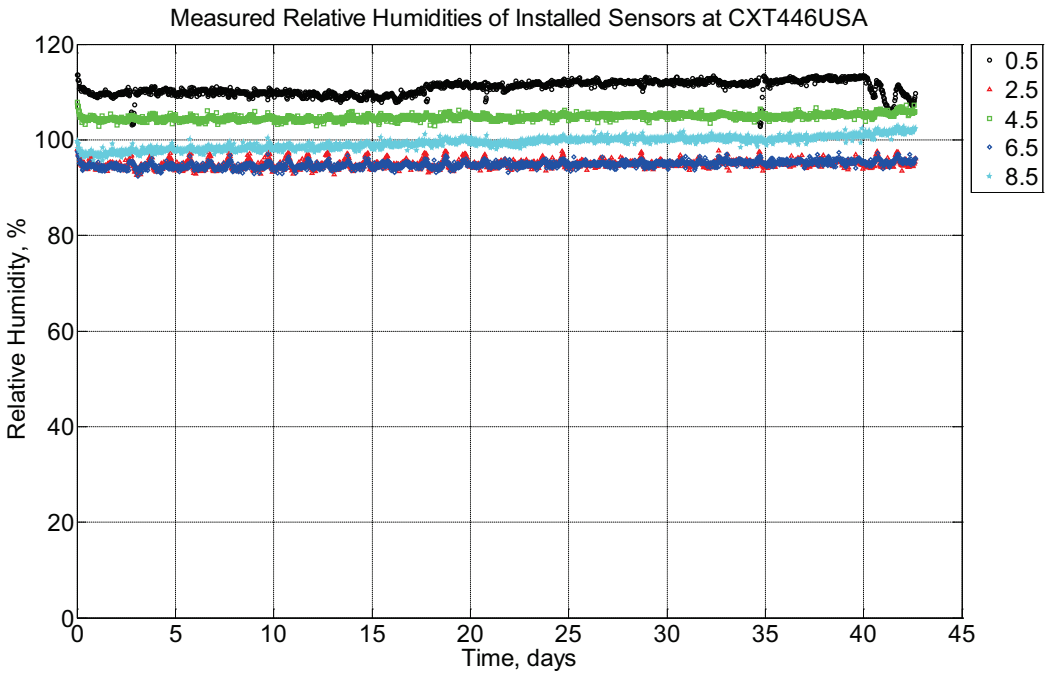

Figure B-741 Measured relative humidity at depths of 0.5 inches (12.7 mm), 2.5 inches (63.5 mm), 4.5 inches (114.3 mm), 6.5 inches (139.7 mm), and 8.5 inches (215.9 mm) from the surface of a concrete crosstie (labeled CXT446USA) installed in track near Lytton, BC, between October 11, 2013, through November 22, 2013. An 8 mm thick polyurethane pad and steel rail are additionally installed atop the concrete crosstie.

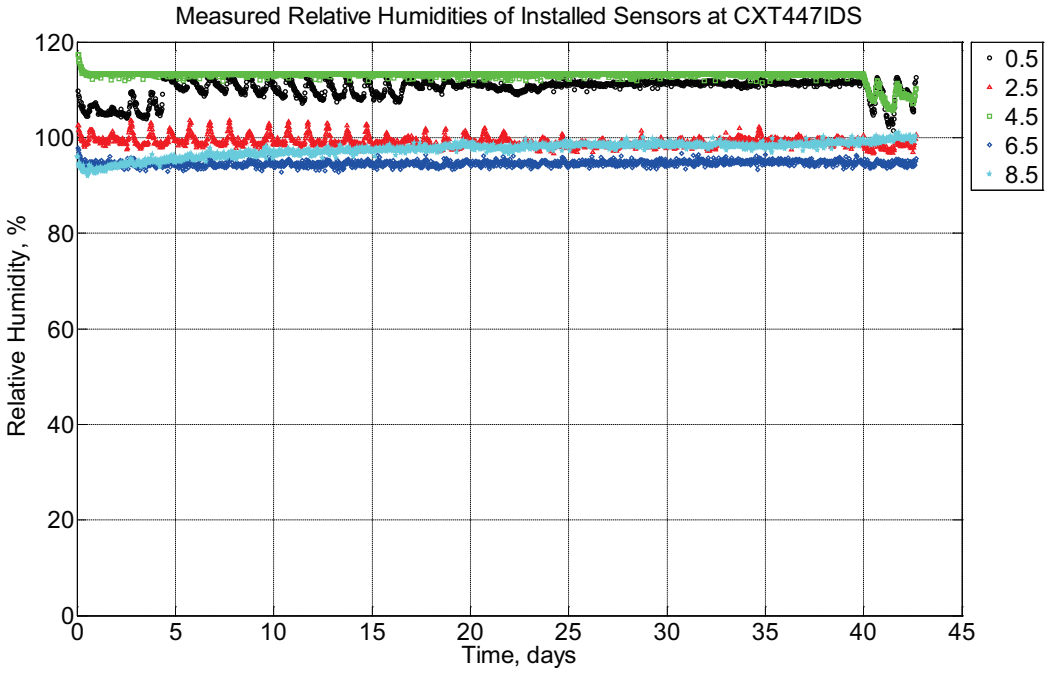

Figure B-742 Measured relative humidity at depths of 0.5 inches (12.7 mm), 2.5 inches (63.5

mm), 4.5 inches (114.3 mm), 6.5 inches (139.7 mm), and 8.5 inches (215.9 mm) from the surface of a concrete crosstie (labeled CXT447IDS) installed in track near Lytton, BC, between October 11, 2013, through November 22, 2013. An 8 mm thick polyurethane pad and steel rail are additionally installed atop the concrete crosstie.

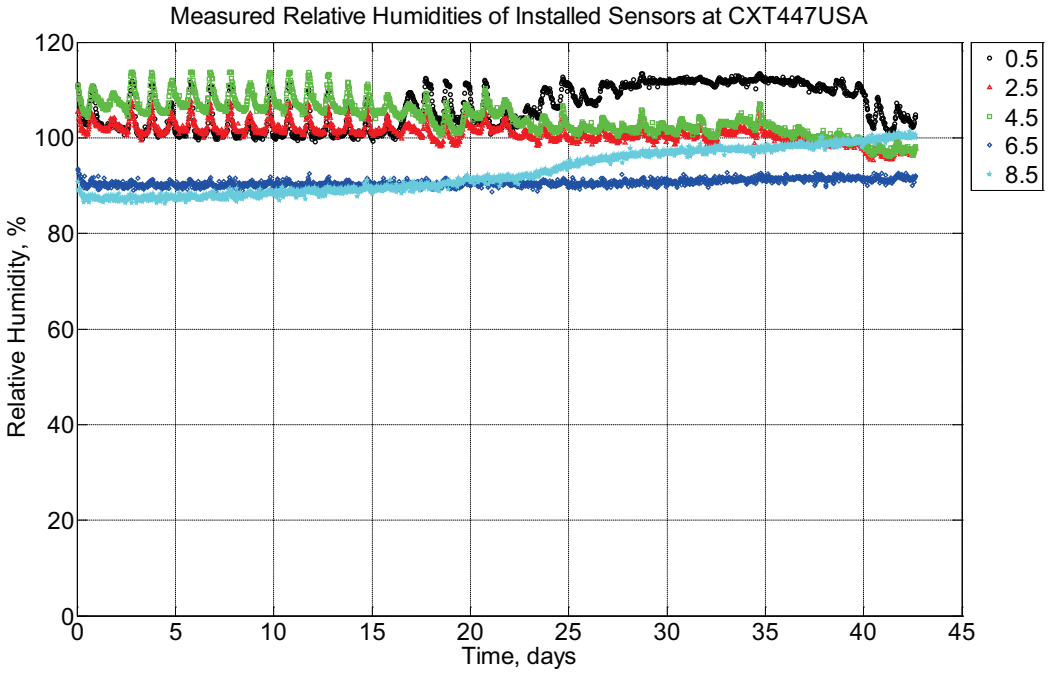

Figure B-743 Measured relative humidity at depths of 0.5 inches (12.7 mm), 2.5 inches (63.5 mm), 4.5 inches (114.3 mm), 6.5 inches (139.7 mm), and 8.5 inches (215.9 mm) from the surface of a concrete crosstie (labeled CXT447USA) installed in track near Lytton, BC, between October 11, 2013, through November 22, 2013. An 8 mm thick polyurethane pad and steel rail are additionally installed atop the concrete crosstie.

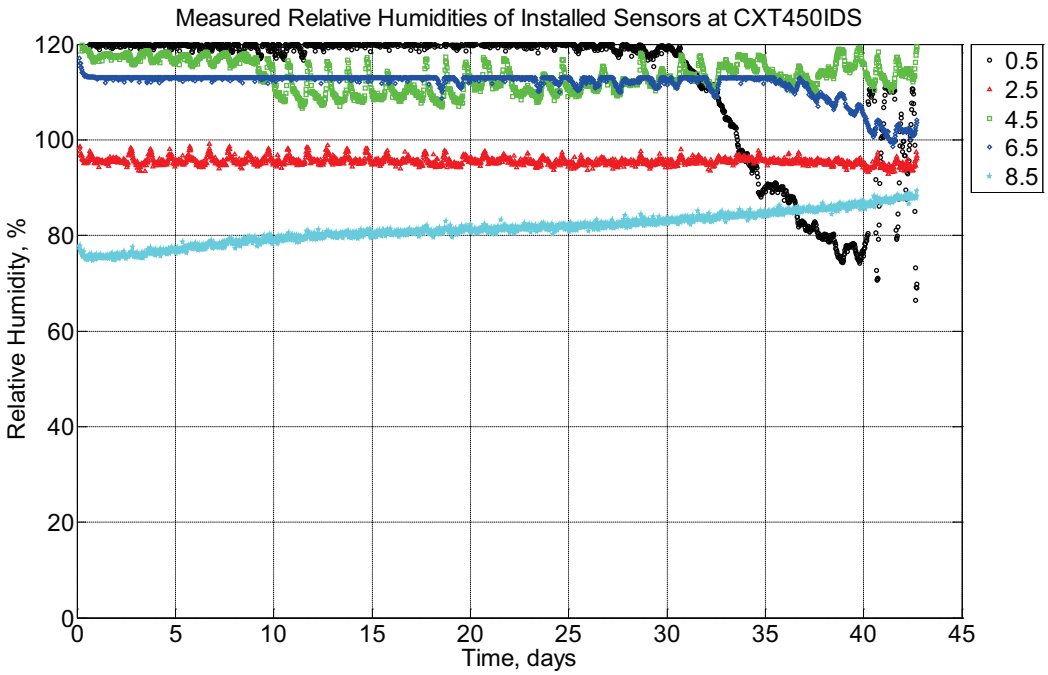

Figure B-744 Measured relative humidity at depths of 0.5 inches (12.7 mm), 2.5 inches (63.5 mm), 4.5 inches (114.3 mm), 6.5 inches (139.7 mm), and 8.5 inches (215.9 mm) from the surface of a concrete crosstie (labeled CXT450IDS) installed in track near Lytton, BC, between October 11, 2013, through November 22, 2013. An 8 mm thick polyurethane pad and steel rail are additionally installed atop the concrete crosstie.

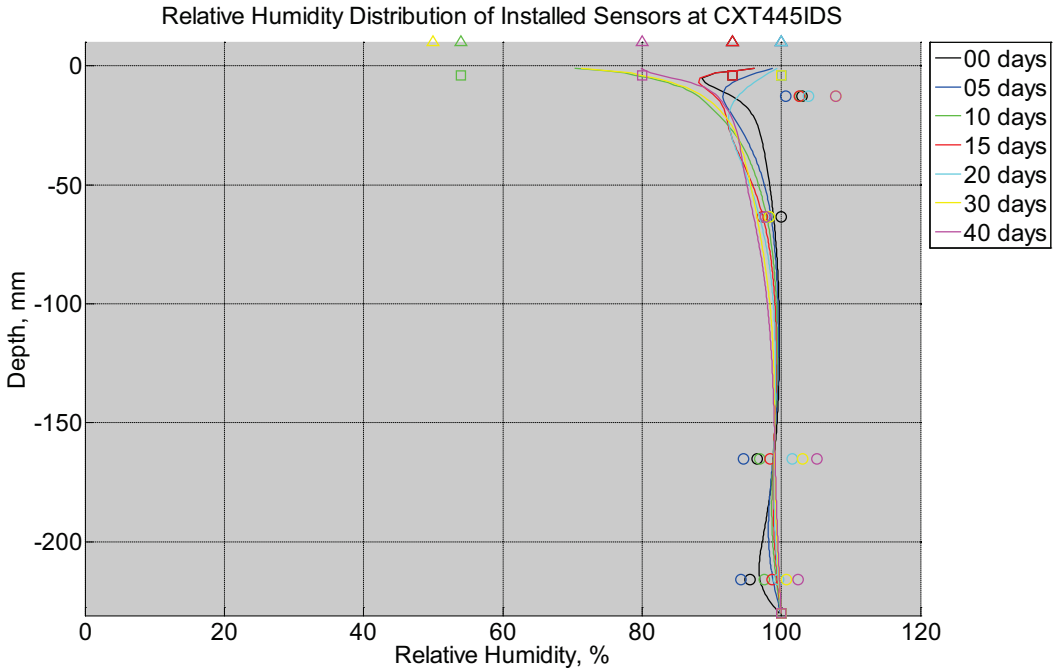

Figure B-745 Measured (markers) and modeled (continuous line) relative humidity profile

distribution as a function of depth inside a concrete crosstie (labeled CXT445IDS) installed in track near Lytton, BC, between October 11, 2013, through November 22, 2013. An 8 mm thick polyurethane pad and steel rail are additionally installed atop the concrete crosstie. The model does not incorporate a polyurethane pad nor steel rail line. Triangular markers denote relative humidity value from CWLY weather station, square markers denote assumed relative humidity values in ballast, and circular markers denote measured relative humidity values inside concrete.

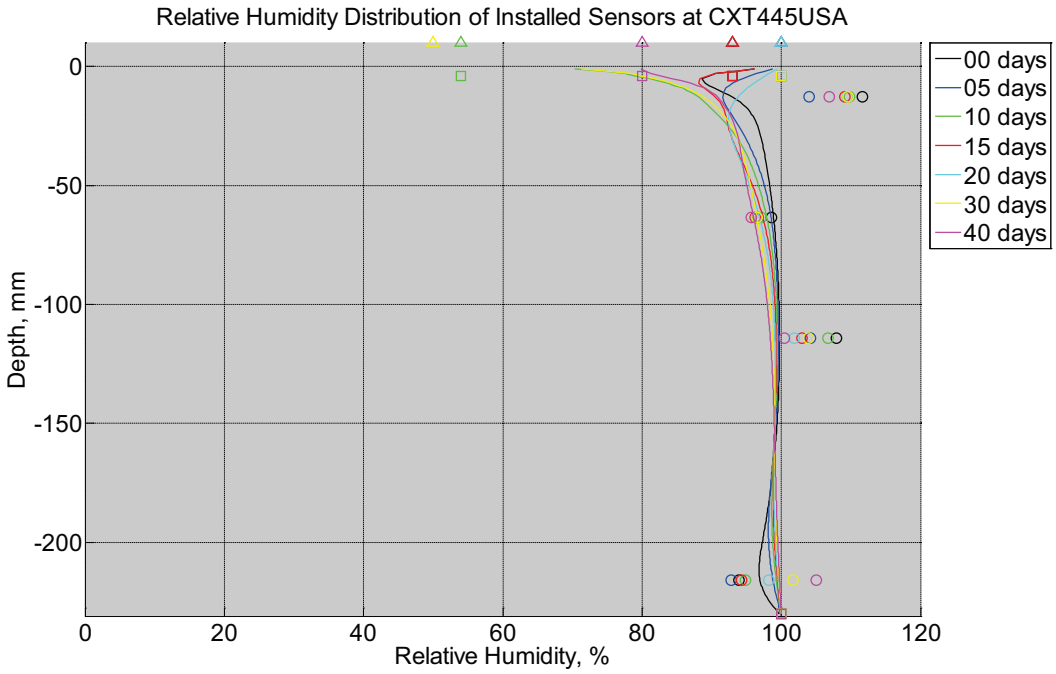

Figure B-746 Measured (markers) and modeled (continuous line) relative humidity profile distribution as a function of depth inside a concrete crosstie (labeled CXT445USA) installed in track near Lytton, BC, between October 11, 2013, through November 22, 2013. An 8 mm thick polyurethane pad and steel rail are additionally installed atop the concrete crosstie. The model does not incorporate a polyurethane pad nor steel rail line. Triangular markers denote relative humidity value from CWLY weather station, square markers denote assumed relative humidity values in ballast, and circular markers denote measured relative humidity values inside concrete.

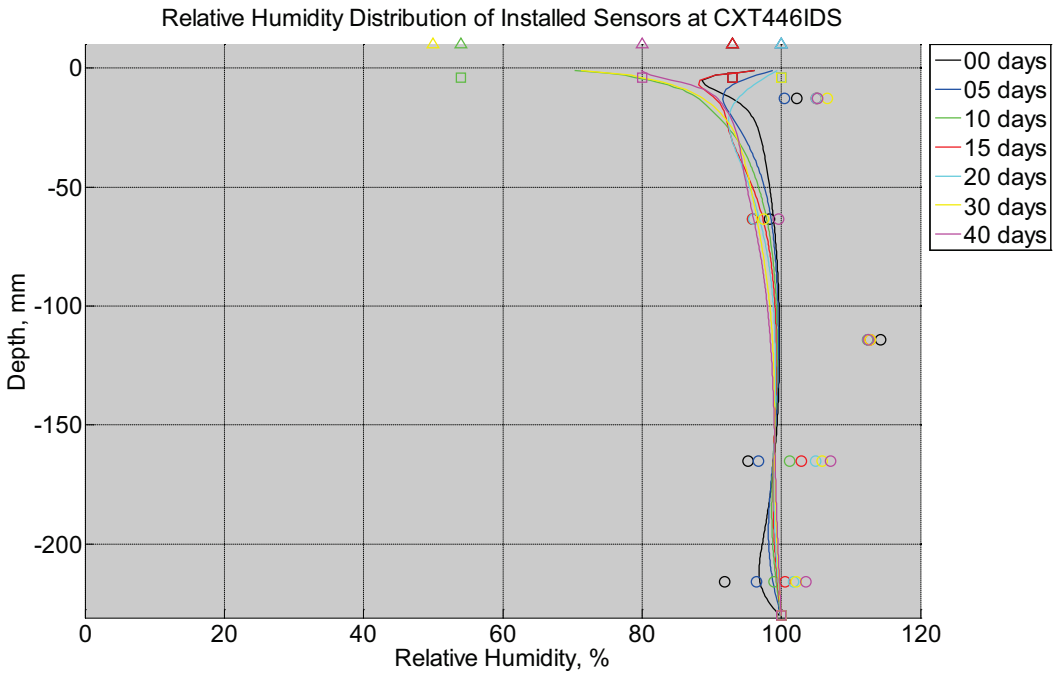

Figure B-747 Measured (markers) and modeled (continuous line) relative humidity profile distribution as a function of depth inside a concrete crosstie (labeled CXT446IDS) installed in track near Lytton, BC, between October 11, 2013, through November 22, 2013. An 8 mm thick polyurethane pad and steel rail are additionally installed atop the concrete crosstie. The model does not incorporate a polyurethane pad nor steel rail line. Triangular markers denote relative humidity value from CWLY weather station, square markers denote assumed relative humidity values in ballast, and circular markers denote measured relative humidity values inside concrete.

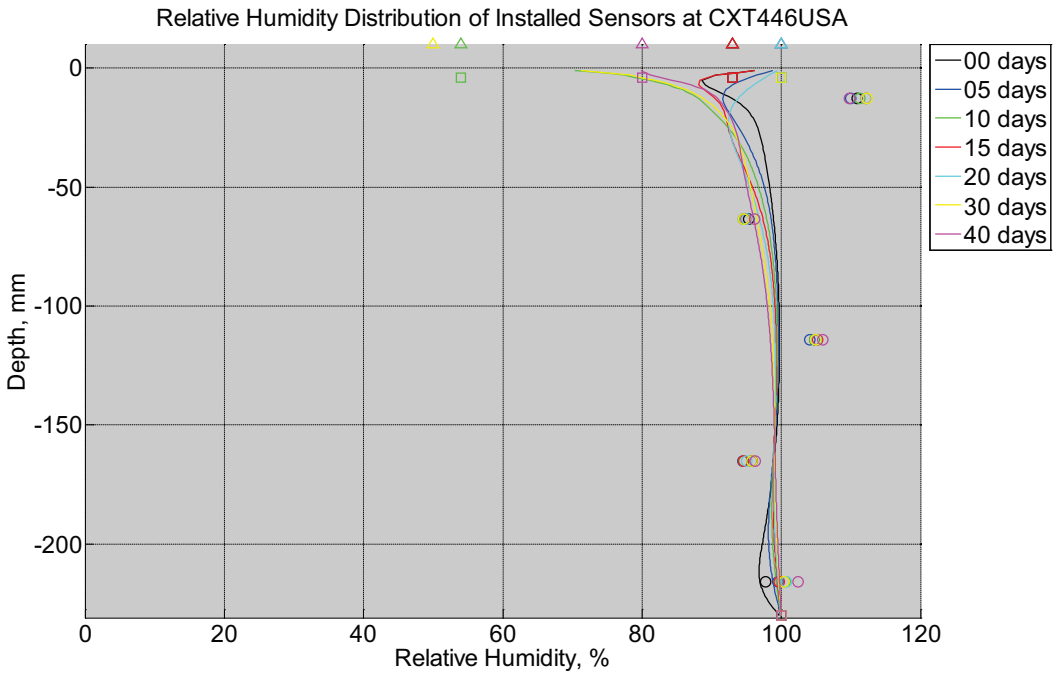

Figure B-748 Measured (markers) and modeled (continuous line) relative humidity profile distribution as a function of depth inside a concrete crosstie (labeled CXT446USA) installed in track near Lytton, BC, between October 11, 2013, through November 22, 2013. An 8 mm thick polyurethane pad and steel rail are additionally installed atop the concrete crosstie. The model does not incorporate a polyurethane pad nor steel rail line. Triangular markers denote relative humidity value from CWLY weather station, square markers denote assumed relative humidity values in ballast, and circular markers denote measured relative humidity values inside concrete.

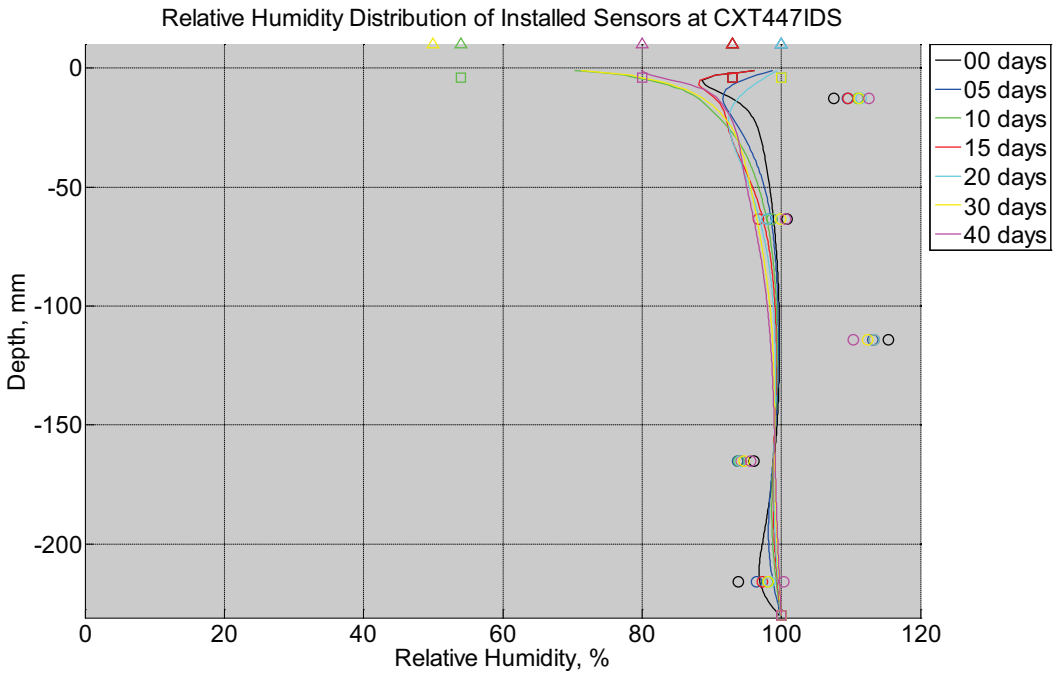

Figure B-749 Measured (markers) and modeled (continuous line) relative humidity profile distribution as a function of depth inside a concrete crosstie (labeled CXT447IDS) installed in track near Lytton, BC, between October 11, 2013, through November 22, 2013. An 8 mm thick polyurethane pad and steel rail are additionally installed atop the concrete crosstie. The model does not incorporate a polyurethane pad nor steel rail line. Triangular markers denote relative humidity value from CWLY weather station, square markers denote assumed relative humidity values in ballast, and circular markers denote measured relative humidity values inside concrete.

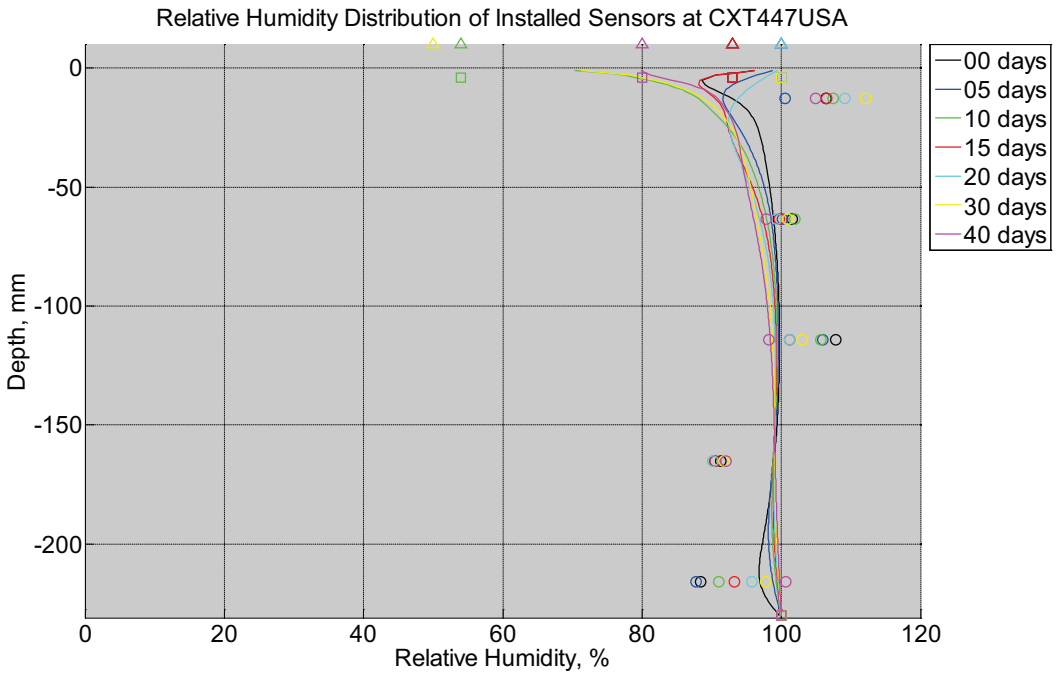

Figure B-750 Measured (markers) and modeled (continuous line) relative humidity profile distribution as a function of depth inside a concrete crosstie (labeled CXT447USA) installed in track near Lytton, BC, between October 11, 2013, through November 22, 2013. An 8 mm thick polyurethane pad and steel rail are additionally installed atop the concrete crosstie. The model does not incorporate a polyurethane pad nor steel rail line. Triangular markers denote relative humidity value from CWLY weather station, square markers denote assumed relative humidity values in ballast, and circular markers denote measured relative humidity values inside concrete.

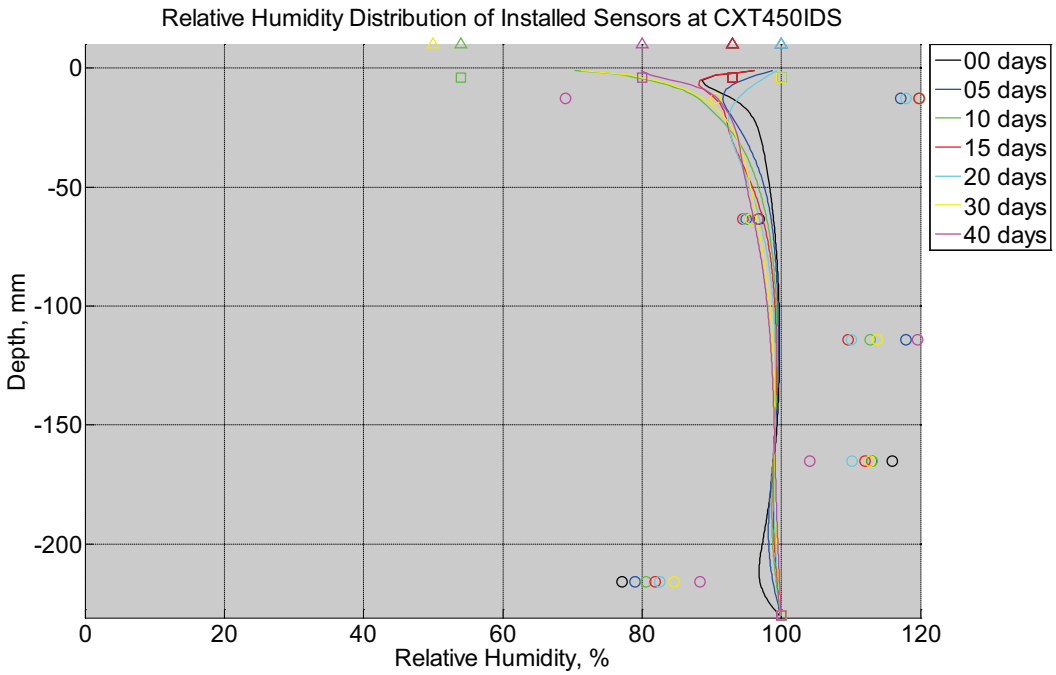

Figure B-751 Measured (markers) and modeled (continuous line) relative humidity profile distribution as a function of depth inside a concrete crosstie (labeled CXT450IDS) installed in track near Lytton, BC, between October 11, 2013, through November 22, 2013. An 8 mm thick polyurethane pad and steel rail are additionally installed atop the concrete crosstie. The model does not incorporate a polyurethane pad nor steel rail line. Triangular markers denote relative humidity value from CWLY weather station, square markers denote assumed relative humidity values in ballast, and circular markers denote measured relative humidity values inside concrete.

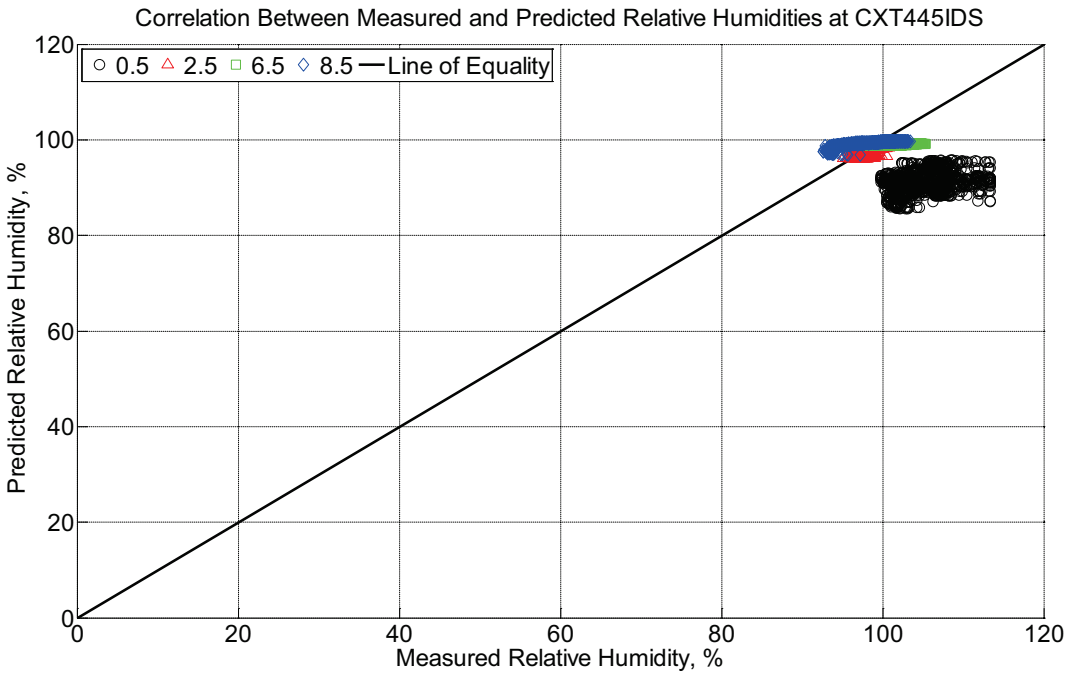

Figure B-752 Correlation between measured and predicted relative humidity values 0.5 inches (12.7 mm), 2.5 inches (63.5 mm), 6.5 inches (139.7 mm), and 8.5 inches (215.9 mm) from the surface of a concrete crosstie (labeled CXT445IDS) installed in track near Lytton, BC, between October 11, 2013, through November 22, 2013. An 8 mm thick polyurethane pad and steel rail are additionally installed atop the concrete crosstie. The model does not incorporate a polyurethane pad nor steel rail line.

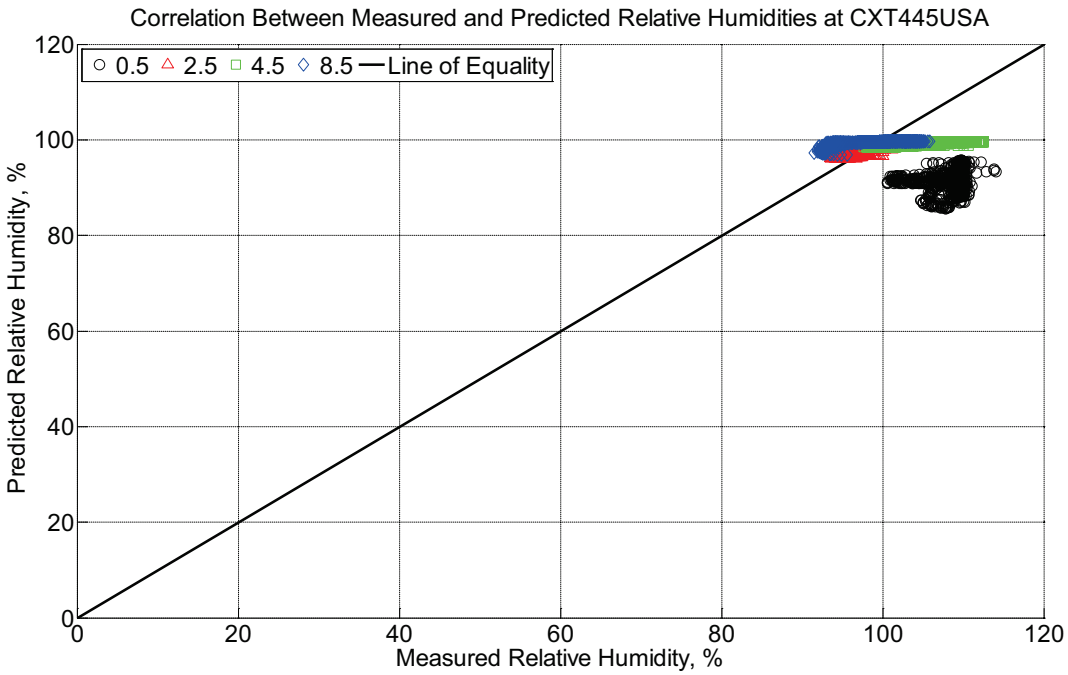

Figure B-753 Correlation between measured and predicted relative humidity values 0.5 inches (12.7 mm), 2.5 inches (63.5 mm), 4.5 inches (114.3 mm), and 8.5 inches (215.9 mm) from the surface of a concrete crosstie (labeled CXT445USA) installed in track near Lytton, BC, between October 11, 2013, through November 22, 2013. An 8 mm thick polyurethane pad and steel rail are additionally installed atop the concrete crosstie. The model does not incorporate a polyurethane pad nor steel rail line.

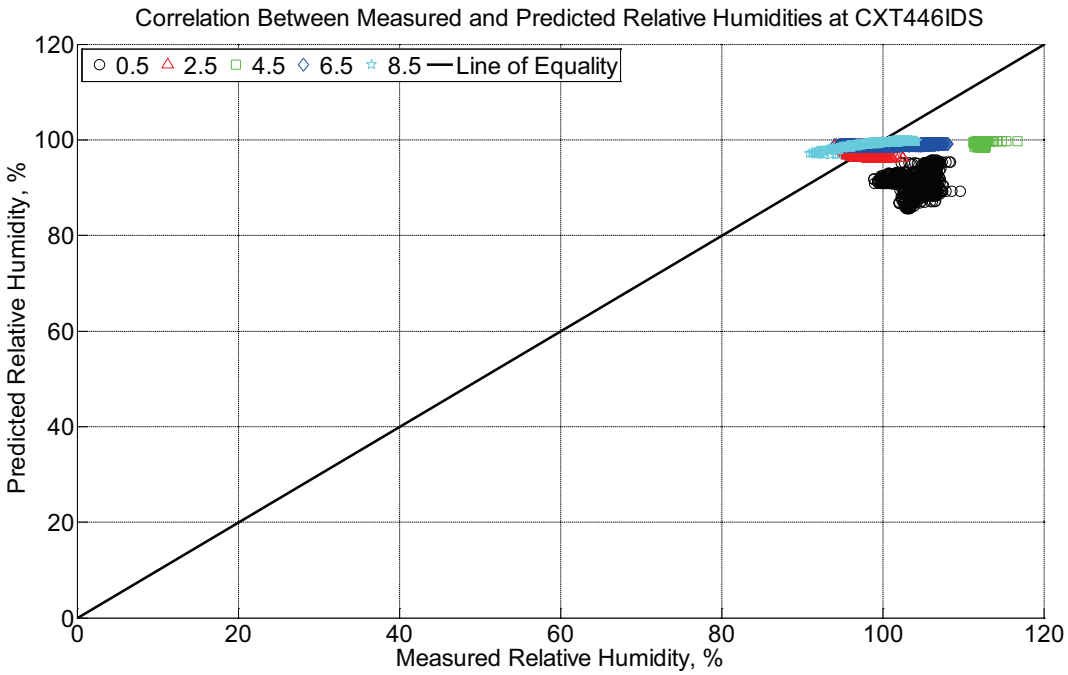

Figure B-754 Correlation between measured and predicted relative humidity values 0.5 inches (12.7 mm), 2.5 inches (63.5 mm), 4.5 inches (114.3 mm), 6.5 inches (139.7 mm), and 8.5 inches (215.9 mm) from the surface of a concrete crosstie (labeled CXT446IDS) installed in track near Lytton, BC, between October 11, 2013, through November 22, 2013. An 8 mm thick polyurethane pad and steel rail are additionally installed atop the concrete crosstie. The model does not incorporate a polyurethane pad nor steel rail line.

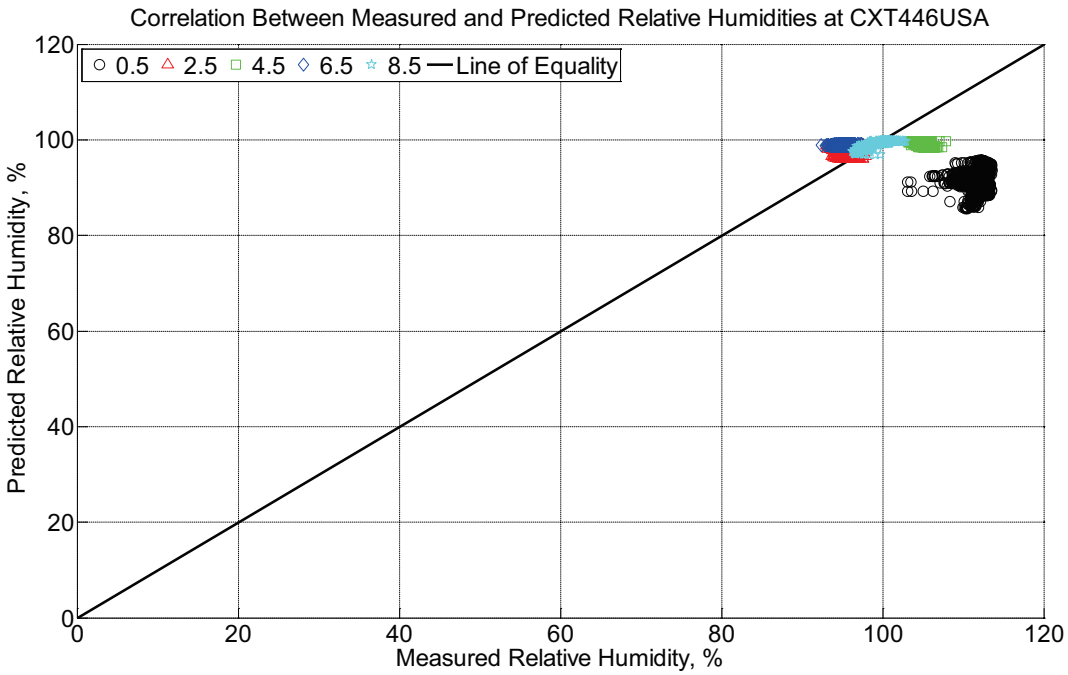

Figure B-755 Correlation between measured and predicted relative humidity values 0.5 inches (12.7 mm), 2.5 inches (63.5 mm), 4.5 inches (114.3 mm), 6.5 inches (139.7 mm), and 8.5 inches (215.9 mm) from the surface of a concrete crosstie (labeled CXT446USA) installed in track near Lytton, BC, between October 11, 2013, through November 22, 2013. An 8 mm thick polyurethane pad and steel rail are additionally installed atop the concrete crosstie. The model does not incorporate a polyurethane pad nor steel rail line.

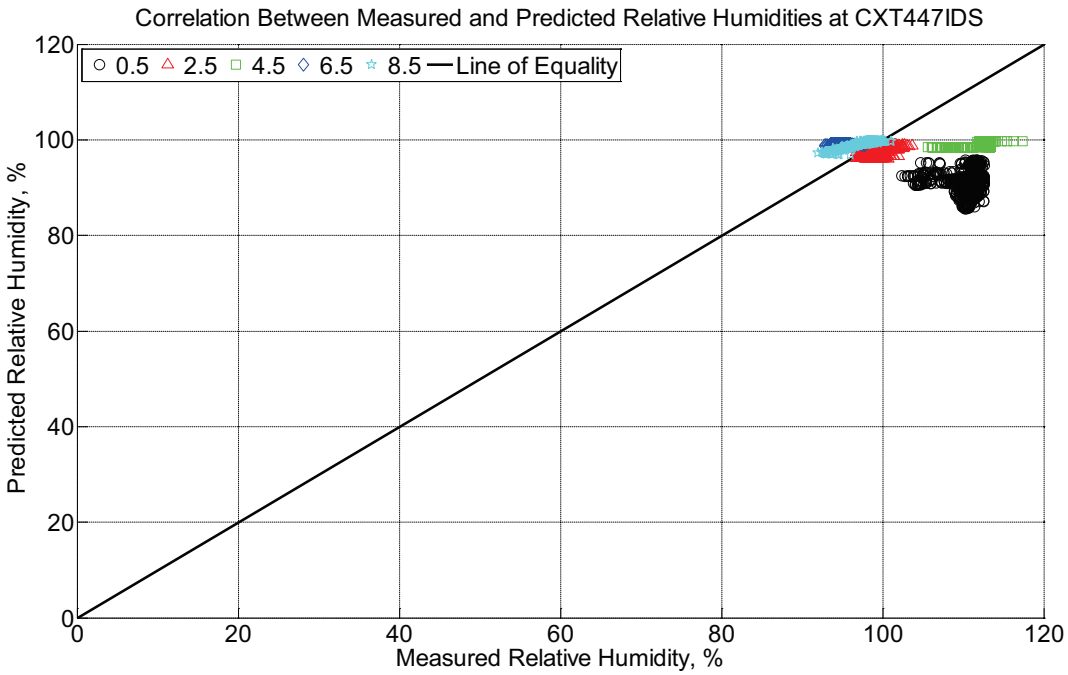

Figure B-756 Correlation between measured and predicted relative humidity values 0.5 inches (12.7 mm), 2.5 inches (63.5 mm), 4.5 inches (114.3 mm), 6.5 inches (139.7 mm), and 8.5 inches (215.9 mm) from the surface of a concrete crosstie (labeled CXT447IDS) installed in track near Lytton, BC, between October 11, 2013, through November 22, 2013. An 8 mm thick polyurethane pad and steel rail are additionally installed atop the concrete crosstie. The model does not incorporate a polyurethane pad nor steel rail line.

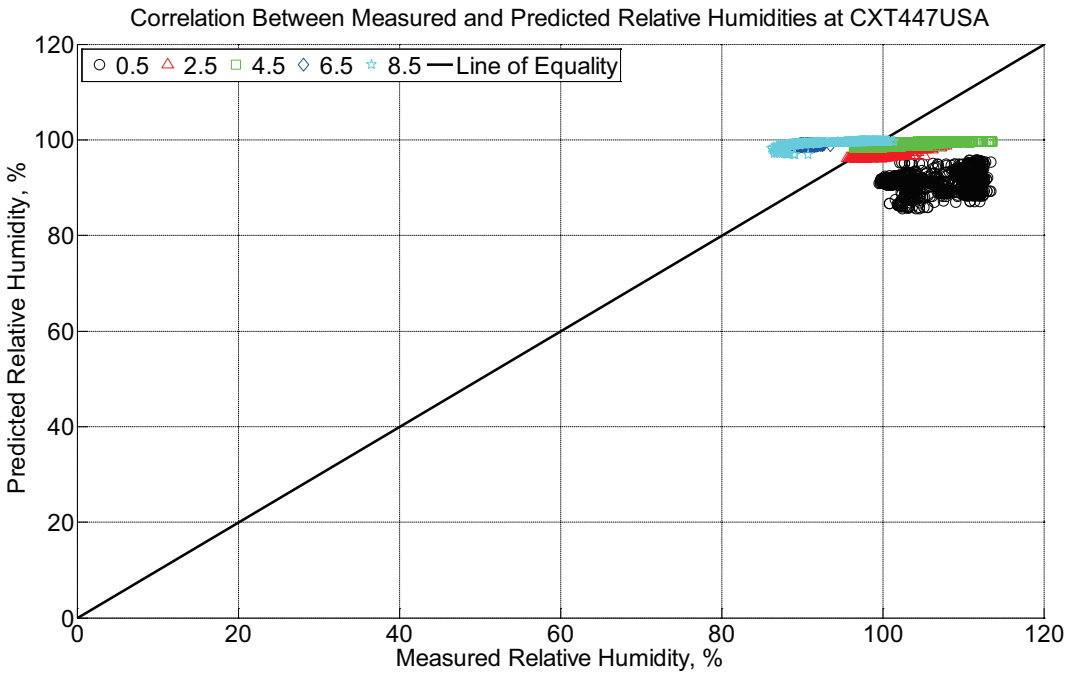

Figure B-757 Correlation between measured and predicted relative humidity values 0.5 inches (12.7 mm), 2.5 inches (63.5 mm), 4.5 inches (114.3 mm), 6.5 inches (139.7 mm), and 8.5 inches (215.9 mm) from the surface of a concrete crosstie (labeled CXT447USA) installed in track near Lytton, BC, between October 11, 2013, through November 22, 2013. An 8 mm thick polyurethane pad and steel rail are additionally installed atop the concrete crosstie. The model does not incorporate a polyurethane pad nor steel rail line.

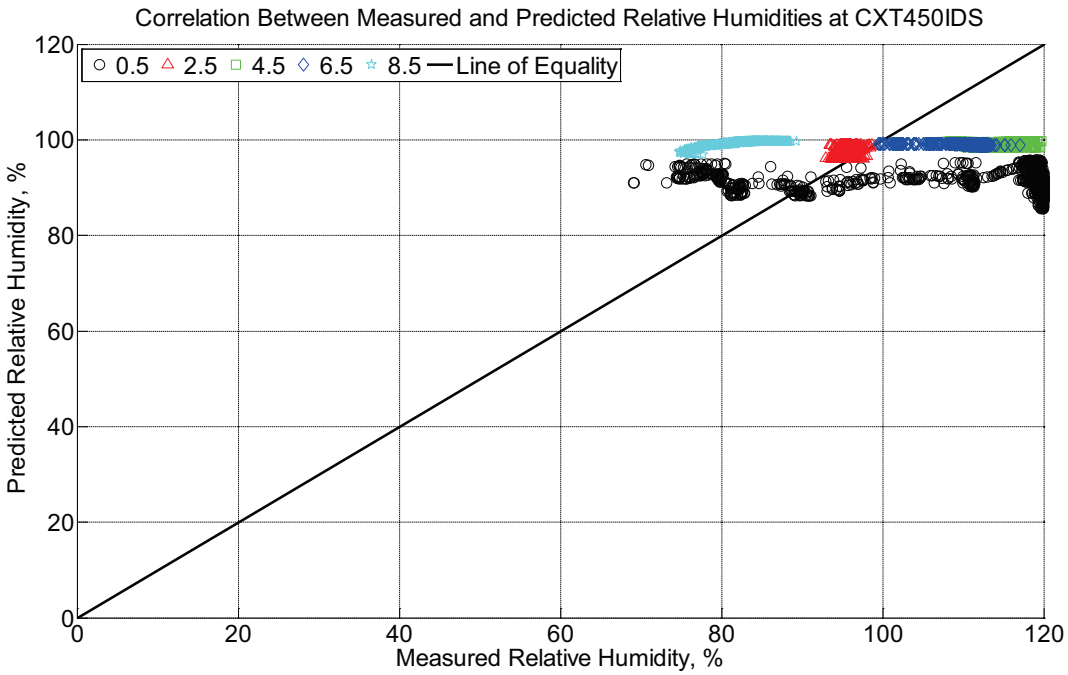

Figure B-758 Correlation between measured and predicted relative humidity values 0.5 inches (12.7 mm), 2.5 inches (63.5 mm), 4.5 inches (114.3 mm), 6.5 inches (139.7 mm), and 8.5 inches (215.9 mm) from the surface of a concrete crosstie (labeled CXT450IDS) installed in track near Lytton, BC, between October 11, 2013, through November 22, 2013. An 8 mm thick polyurethane pad and steel rail are additionally installed atop the concrete crosstie. The model does not incorporate a polyurethane pad nor steel rail line.

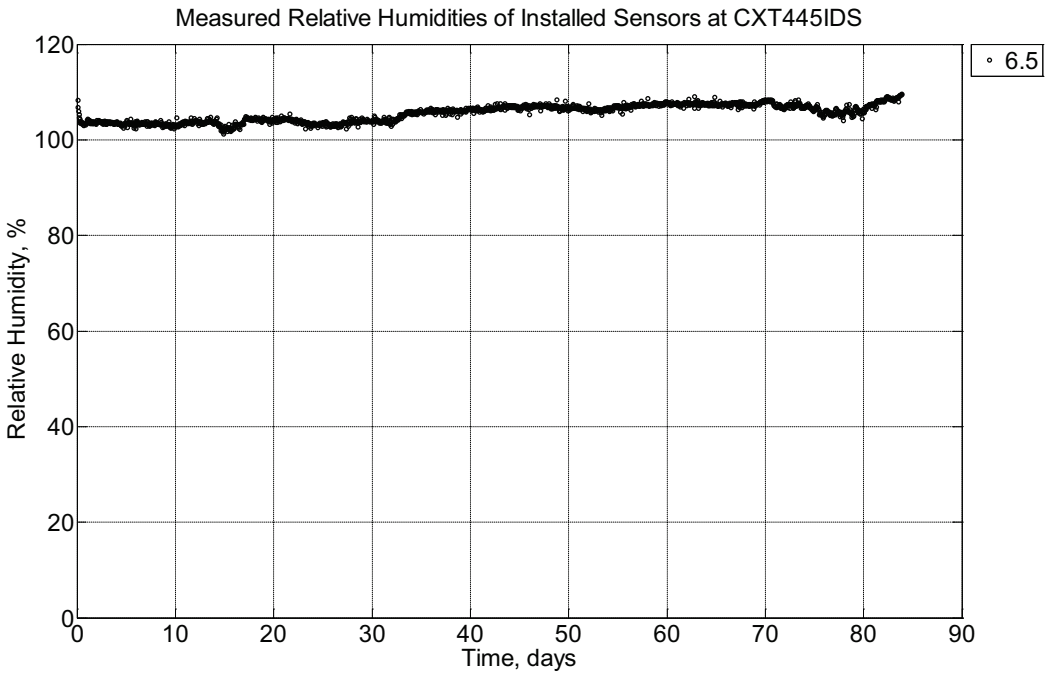

Figure B-759 Measured relative humidity at a depth of 6.5 inches (139.7 mm) from the surface of a concrete crosstie (labeled CXT445IDS) installed in track near Lytton, BC, between November 22, 2013, through February 14, 2014. An 8 mm thick polyurethane pad and steel rail are additionally installed atop the concrete crosstie.

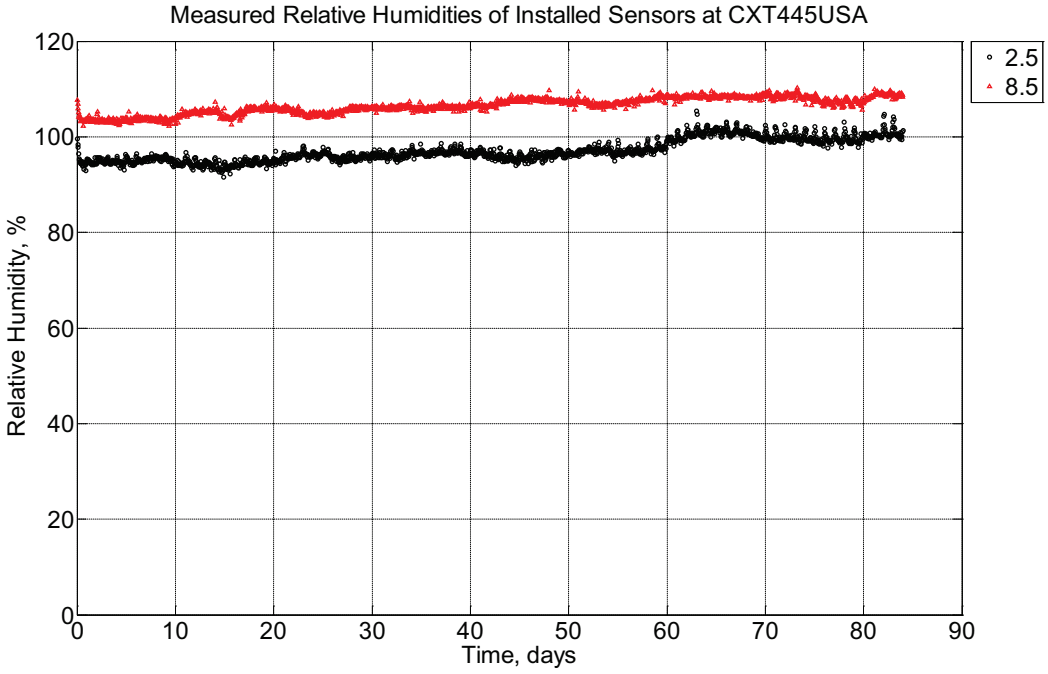

Figure B-760 Measured relative humidity at depths of 2.5 inches (63.5 mm) and 8.5 inches (215.9 mm) from the surface of a concrete crosstie (labeled CXT445USA) installed in track

near Lytton, BC, between November 22, 2013, through February 14, 2014. An 8 mm thick polyurethane pad and steel rail are additionally installed atop the concrete crosstie.

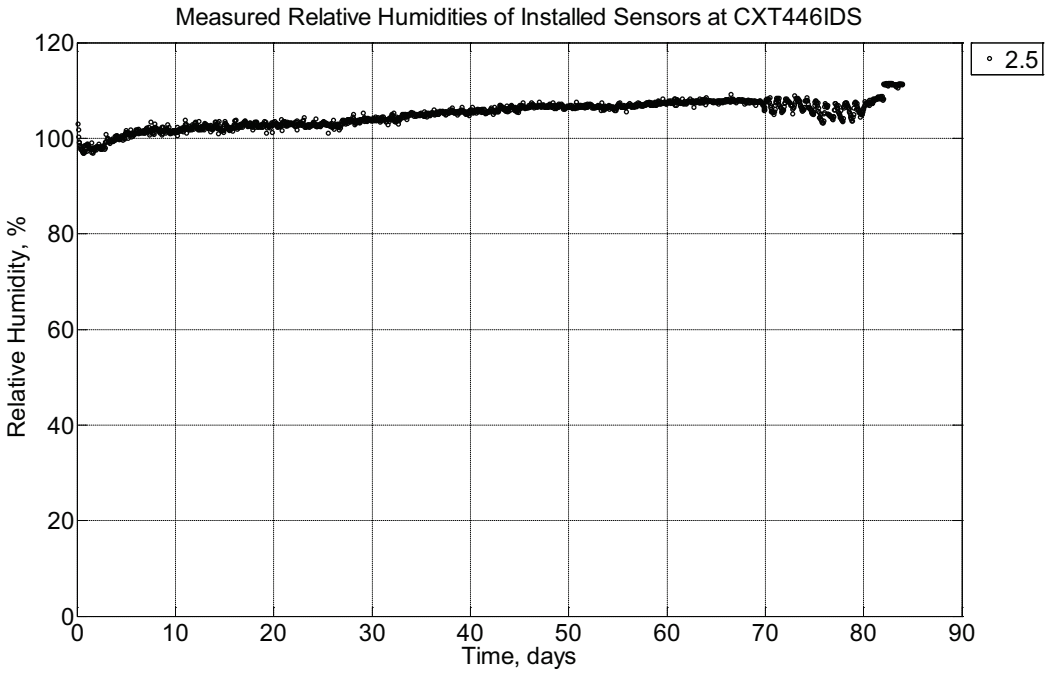

Figure B-761 Measured relative humidity at a depth of 2.5 inches (63.5 mm) from the surface of a concrete crosstie (labeled CXT446IDS) installed in track near Lytton, BC, between November 22, 2013, through February 14, 2014. An 8 mm thick polyurethane pad and steel rail are additionally installed atop the concrete crosstie.

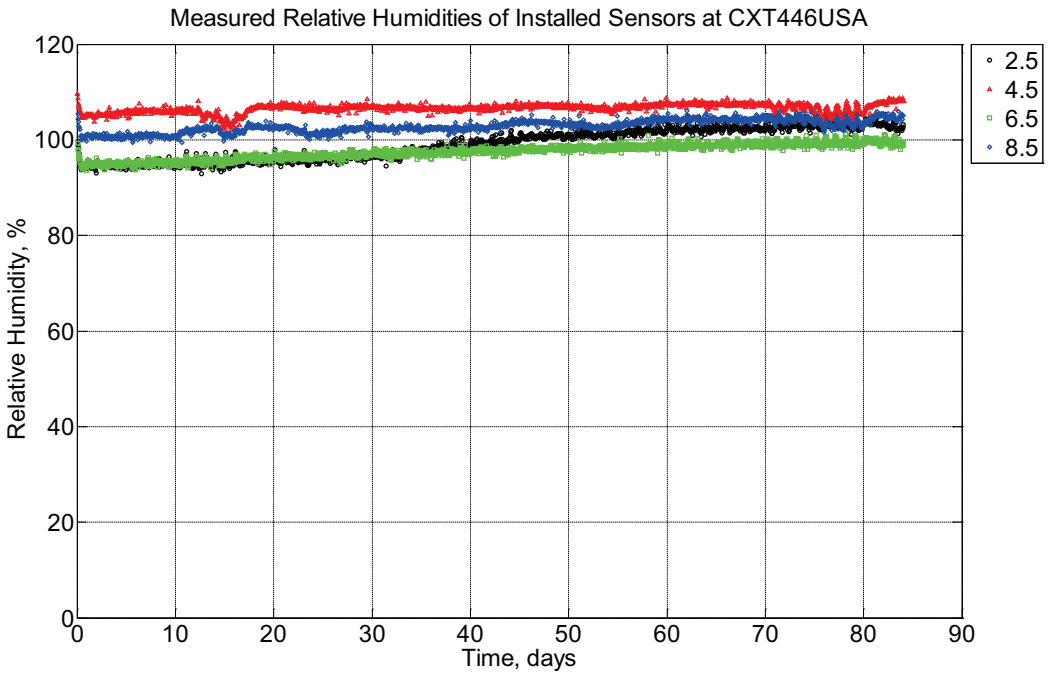

Figure B-762 Measured relative humidity at depths of 2.5 inches (63.5 mm), 4.5 inches (114.3 mm), 6.5 inches (139.7 mm), and 8.5 inches (215.9 mm) from the surface of a concrete crosstie (labeled CXT446USA) installed in track near Lytton, BC, between November 22, 2013, through February 14, 2014. An 8 mm thick polyurethane pad and steel rail are additionally installed atop the concrete crosstie.

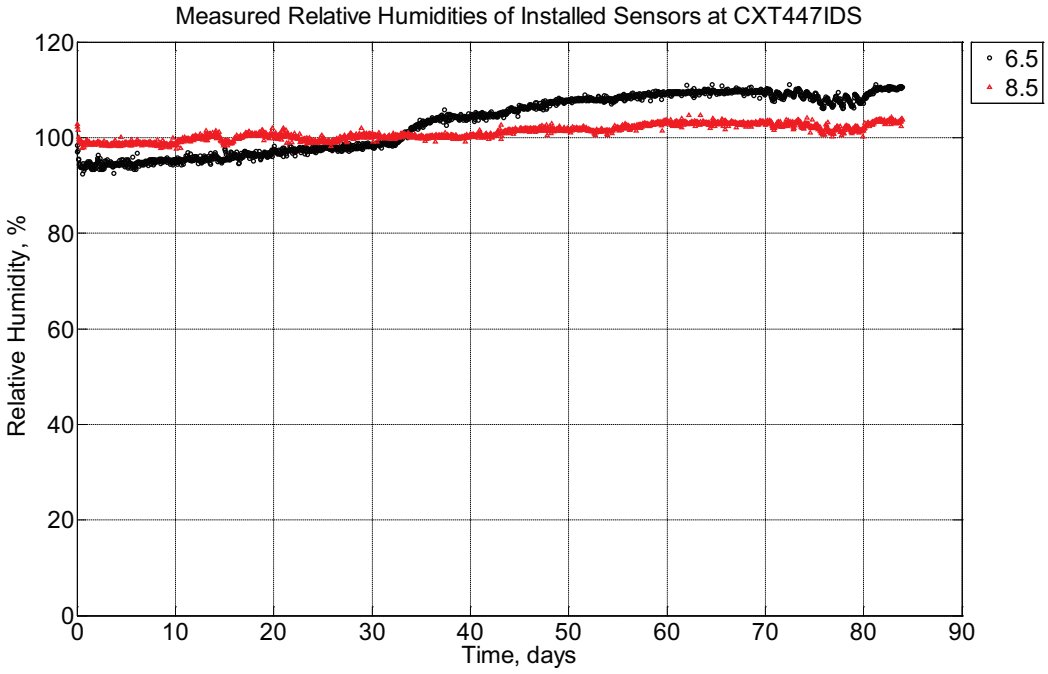

Figure B-763 Measured relative humidity at depths of 6.5 inches (139.7 mm) and 8.5 inches

(215.9 mm) from the surface of a concrete crosstie (labeled CXT447IDS) installed in track near Lytton, BC, between November 22, 2013, through February 14, 2014. An 8 mm thick polyurethane pad and steel rail are additionally installed atop the concrete crosstie.

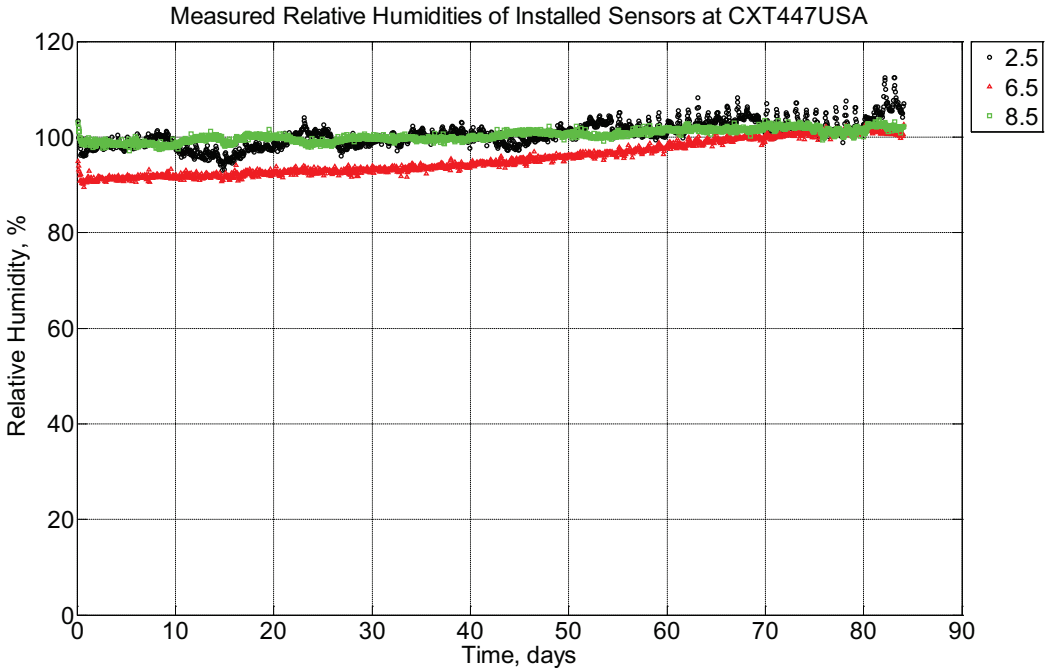

Figure B-764 Measured relative humidity at depths of 2.5 inches (63.5 mm), 6.5 inches (139.7 mm), and 8.5 inches (215.9 mm) from the surface of a concrete crosstie (labeled CXT447USA) installed in track near Lytton, BC, between November 22, 2013, through February 14, 2014. An 8 mm thick polyurethane pad and steel rail are additionally installed atop the concrete crosstie.

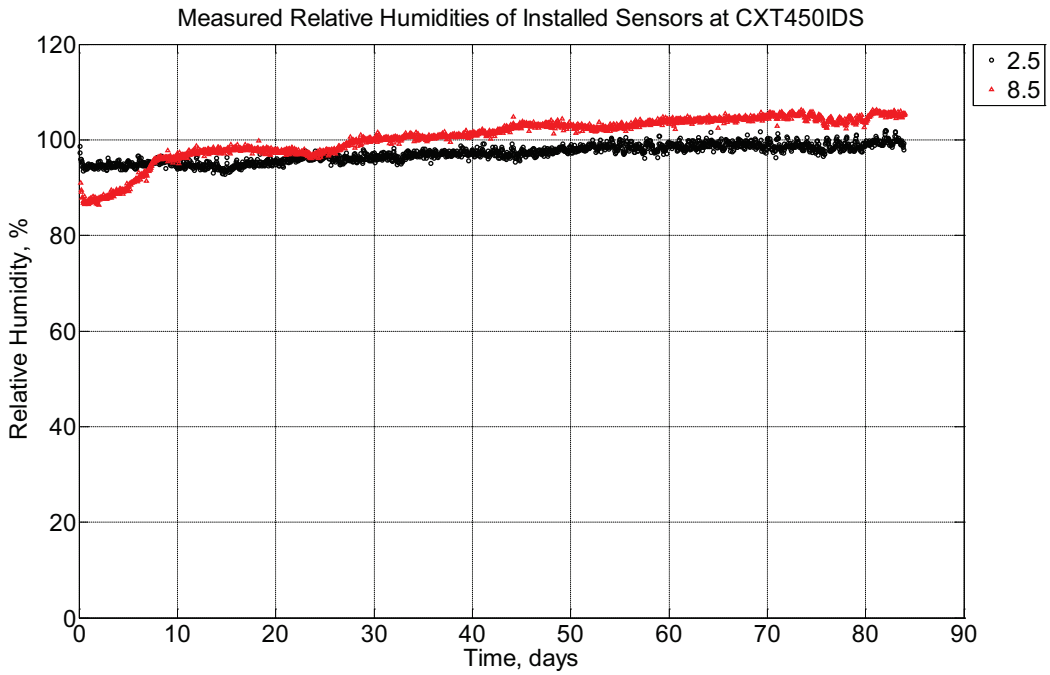

Figure B-765 Measured relative humidity at depths of 2.5 inches (63.5 mm) and 8.5 inches (215.9 mm) from the surface of a concrete crosstie (labeled CXT450IDS) installed in track near Lytton, BC, between November 22, 2013, through February 14, 2014. An 8 mm thick polyurethane pad and steel rail are additionally installed atop the concrete crosstie.

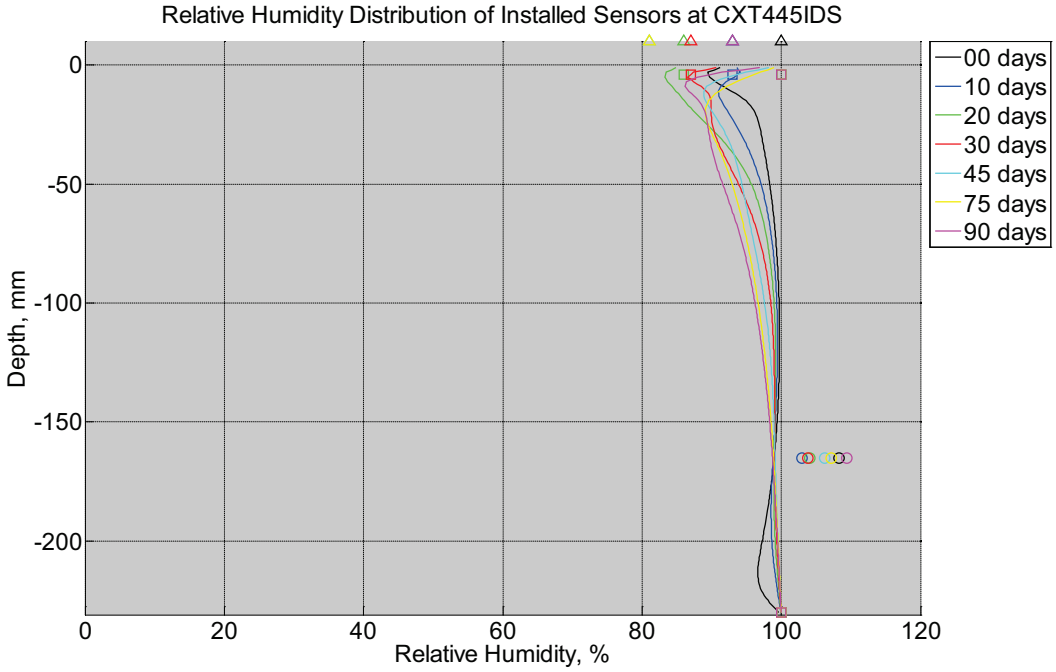

Figure B-766 Measured (markers) and modeled (continuous line) relative humidity profile distribution as a function of depth inside a concrete crosstie (labeled CXT445IDS) installed

in track near Lytton, BC, between November 22, 2013, through February 14, 2014. An 8 mm thick polyurethane pad and steel rail are additionally installed atop the concrete crosstie. The model does not incorporate a polyurethane pad nor steel rail line. Triangular markers denote relative humidity value from CWLY weather station, square markers denote assumed relative humidity values in ballast, and circular markers denote measured relative humidity values inside concrete.

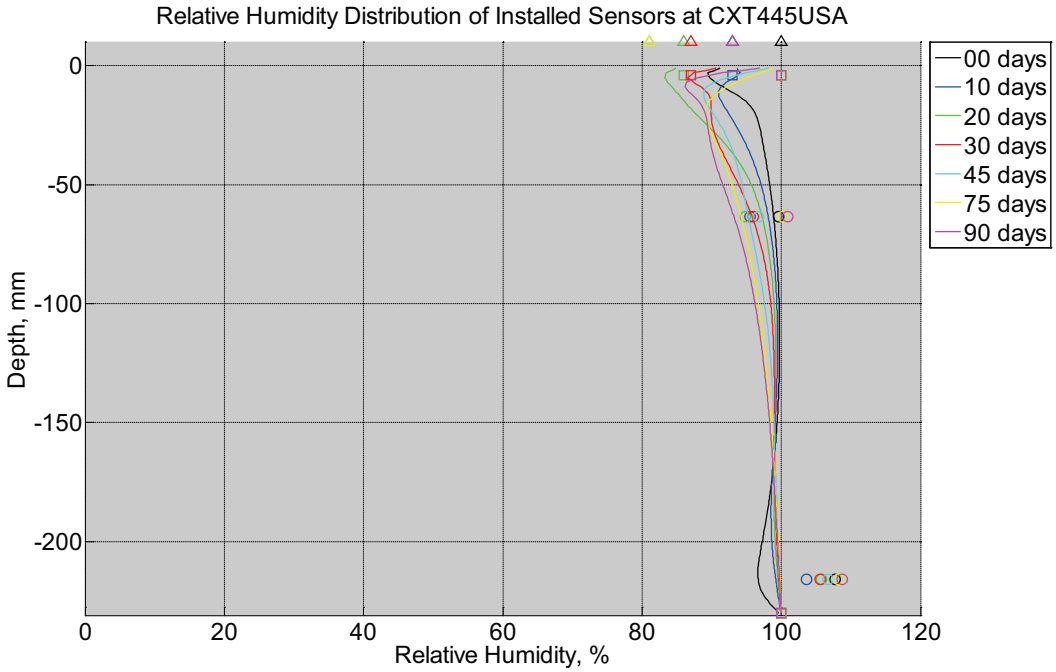

Figure B-767 Measured (markers) and modeled (continuous line) relative humidity profile distribution as a function of depth inside a concrete crosstie (labeled CXT445USA) installed in track near Lytton, BC, between November 22, 2013, through February 14, 2014. An 8 mm thick polyurethane pad and steel rail are additionally installed atop the concrete crosstie. The model does not incorporate a polyurethane pad nor steel rail line. Triangular markers denote relative humidity value from CWLY weather station, square markers denote assumed relative humidity values in ballast, and circular markers denote measured relative humidity values inside concrete.

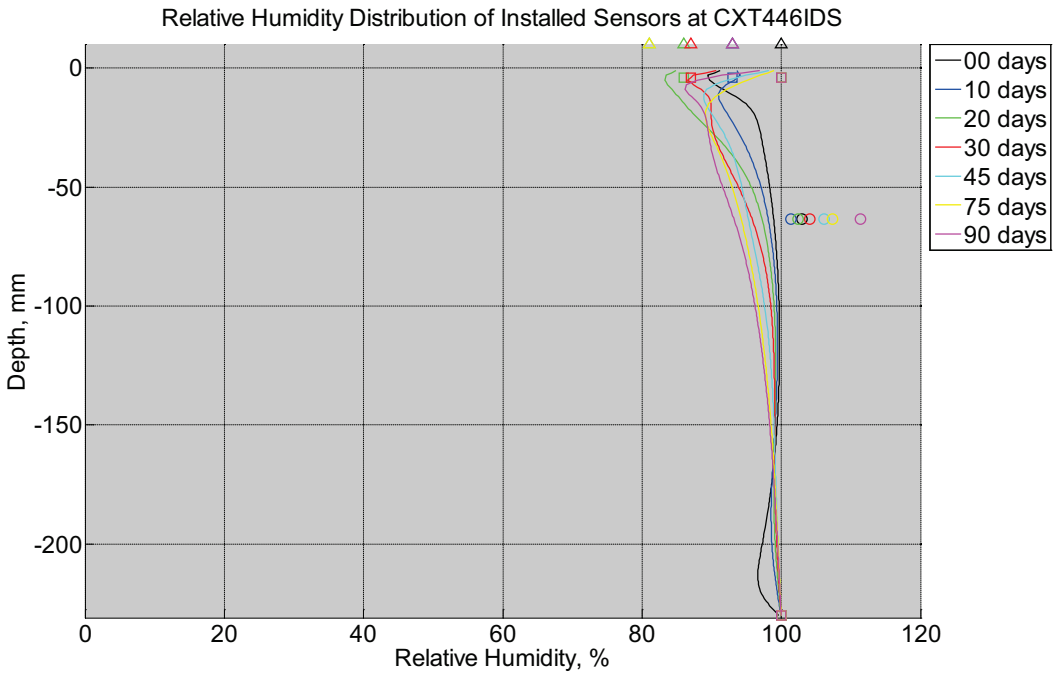

Figure B-768 Measured (markers) and modeled (continuous line) relative humidity profile distribution as a function of depth inside a concrete crosstie (labeled CXT446IDS) installed in track near Lytton, BC, between November 22, 2013, through February 14, 2014. An 8 mm thick polyurethane pad and steel rail are additionally installed atop the concrete crosstie. The model does not incorporate a polyurethane pad nor steel rail line. Triangular markers denote relative humidity value from CWLY weather station, square markers denote assumed relative humidity values in ballast, and circular markers denote measured relative humidity values inside concrete.

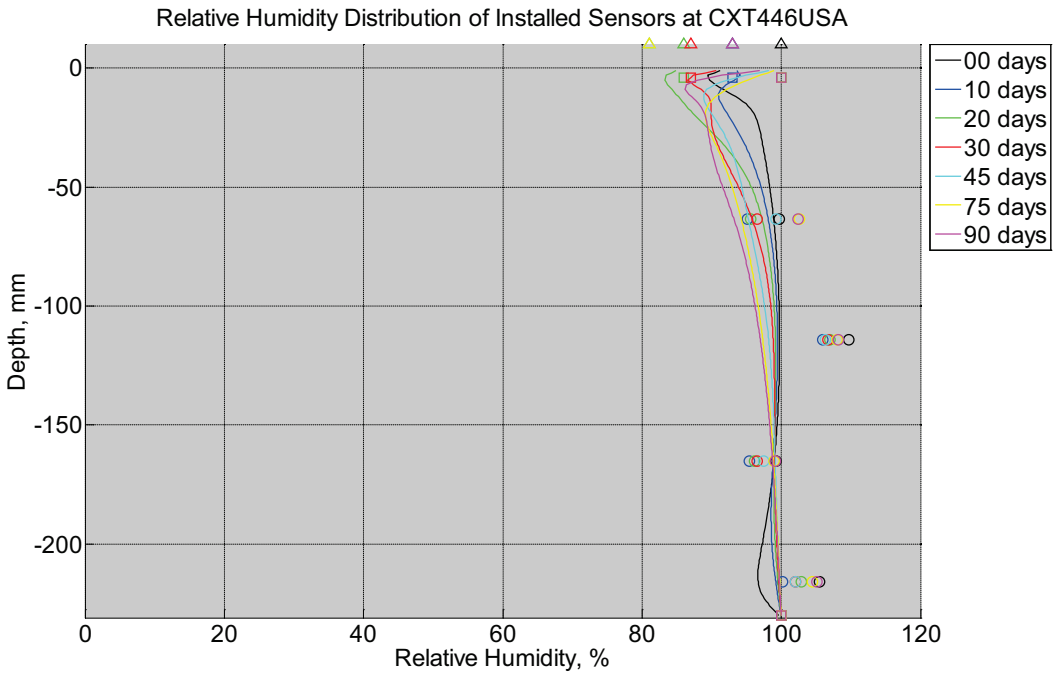

Figure B-769 Measured (markers) and modeled (continuous line) relative humidity profile distribution as a function of depth inside a concrete crosstie (labeled CXT446IDS) installed in track near Lytton, BC, between November 22, 2013, through February 14, 2014. An 8 mm thick polyurethane pad and steel rail are additionally installed atop the concrete crosstie. The model does not incorporate a polyurethane pad nor steel rail line. Triangular markers denote relative humidity value from CWLY weather station, square markers denote assumed relative humidity values in ballast, and circular markers denote measured relative humidity values inside concrete.

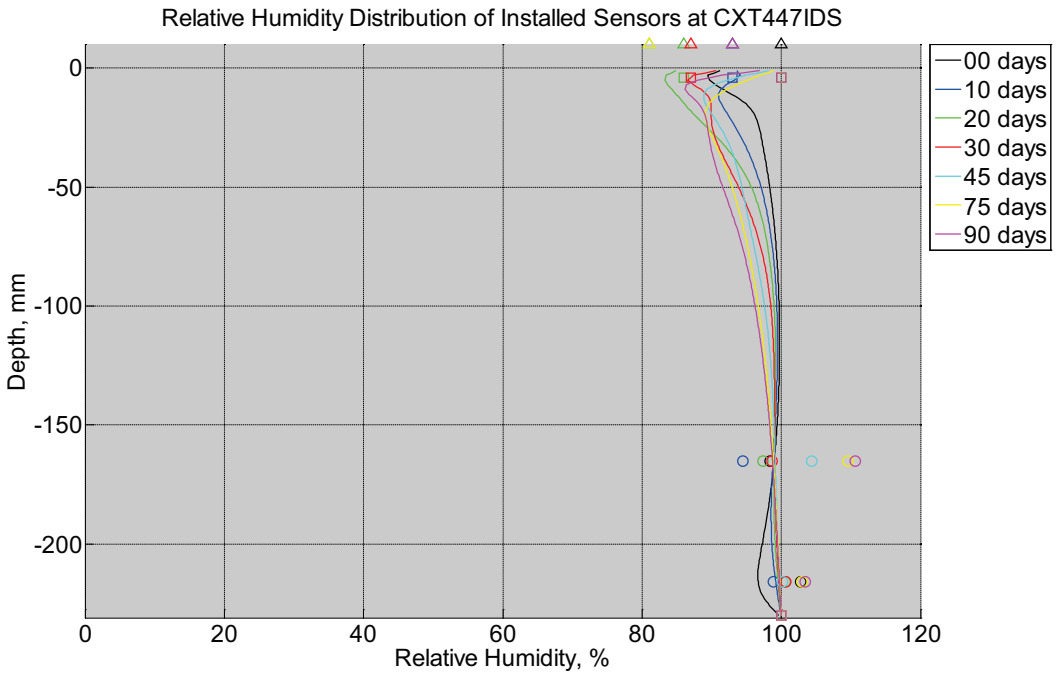

Figure B-770 Measured (markers) and modeled (continuous line) relative humidity profile distribution as a function of depth inside a concrete crosstie (labeled CXT447IDS) installed in track near Lytton, BC, between November 22, 2013, through February 14, 2014. An 8 mm thick polyurethane pad and steel rail are additionally installed atop the concrete crosstie. The model does not incorporate a polyurethane pad nor steel rail line. Triangular markers denote relative humidity value from CWLY weather station, square markers denote assumed relative humidity values in ballast, and circular markers denote measured relative humidity values inside concrete.

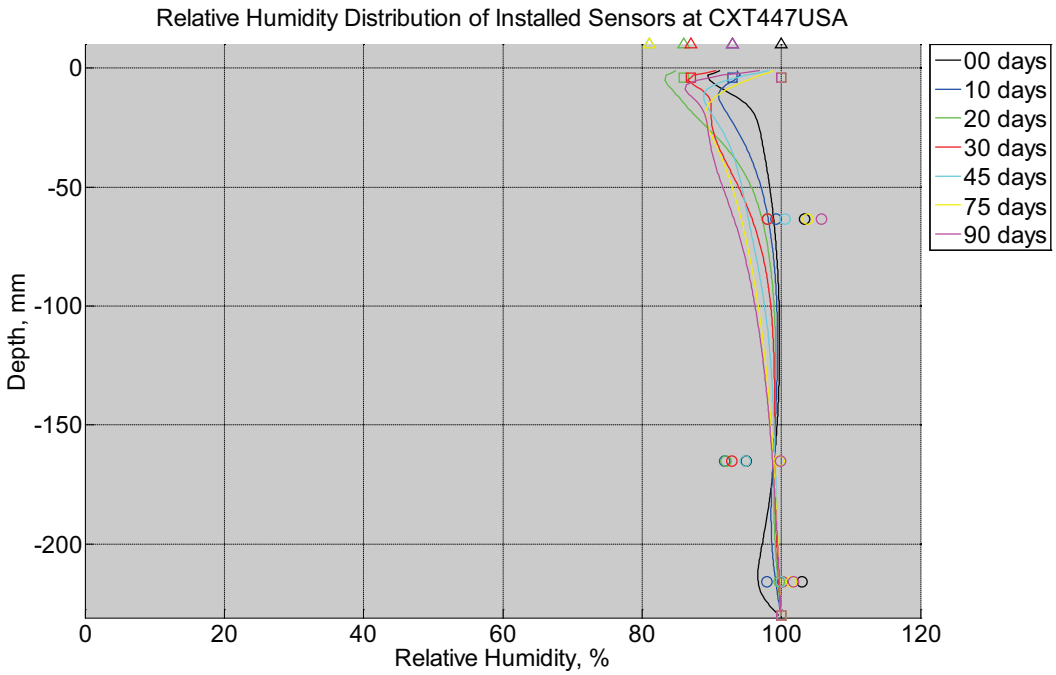

Figure B-771 Measured (markers) and modeled (continuous line) relative humidity profile distribution as a function of depth inside a concrete crosstie (labeled CXT447USA) installed in track near Lytton, BC, between November 22, 2013, through February 14, 2014. An 8 mm thick polyurethane pad and steel rail are additionally installed atop the concrete crosstie. The model does not incorporate a polyurethane pad nor steel rail line. Triangular markers denote relative humidity value from CWLY weather station, square markers denote assumed relative humidity values in ballast, and circular markers denote measured relative humidity values inside concrete.

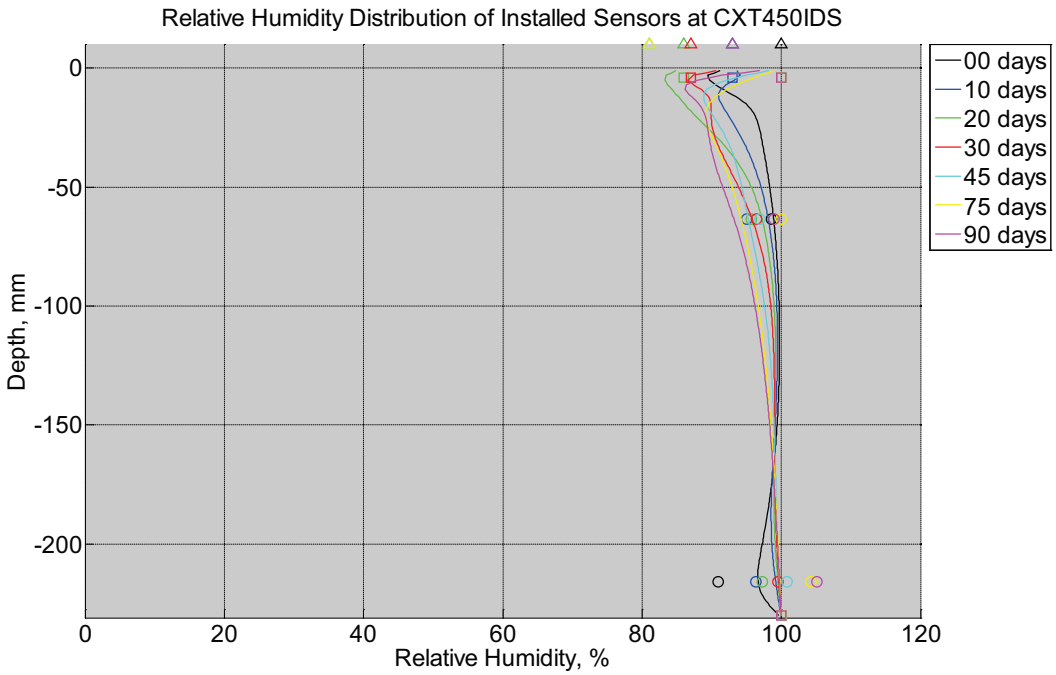

Figure B-772 Measured (markers) and modeled (continuous line) relative humidity profile distribution as a function of depth inside a concrete crosstie (labeled CXT450IDS) installed in track near Lytton, BC, between November 22, 2013, through February 14, 2014. An 8 mm thick polyurethane pad and steel rail are additionally installed atop the concrete crosstie. The model does not incorporate a polyurethane pad nor steel rail line. Triangular markers denote relative humidity value from CWLY weather station, square markers denote assumed relative humidity values in ballast, and circular markers denote measured relative humidity values inside concrete.

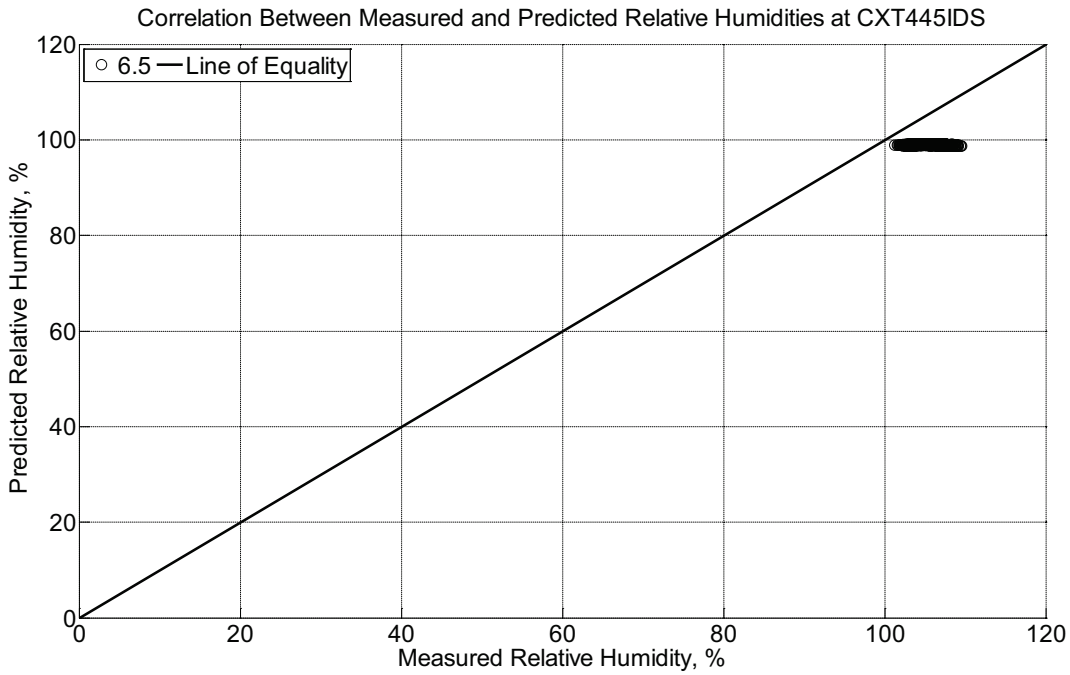

Figure B-773 Correlation between measured and predicted relative humidity values 6.5 inches (139.7 mm) from the surface of a concrete crosstie (labeled CXT445IDS) installed in track near Lytton, BC, between November 22, 2013, through February 14, 2014. An 8 mm thick polyurethane pad and steel rail are additionally installed atop the concrete crosstie. The model does not incorporate a polyurethane pad nor steel rail line.

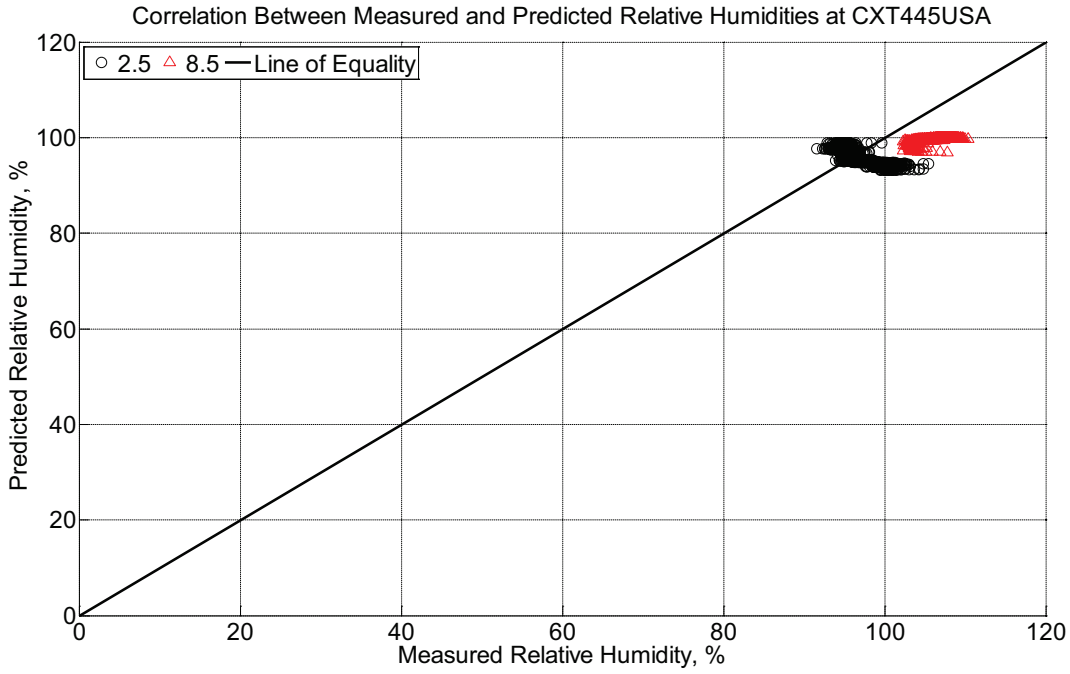

Figure B-774 Correlation between measured and predicted relative humidity values 2.5

inches (63.5 mm) and 8.5 inches (215.9 mm) from the surface of a concrete crosstie (labeled CXT445USA) installed in track near Lytton, BC, between November 22, 2013, through February 14, 2014. An 8 mm thick polyurethane pad and steel rail are additionally installed atop the concrete crosstie. The model does not incorporate a polyurethane pad nor steel rail line.

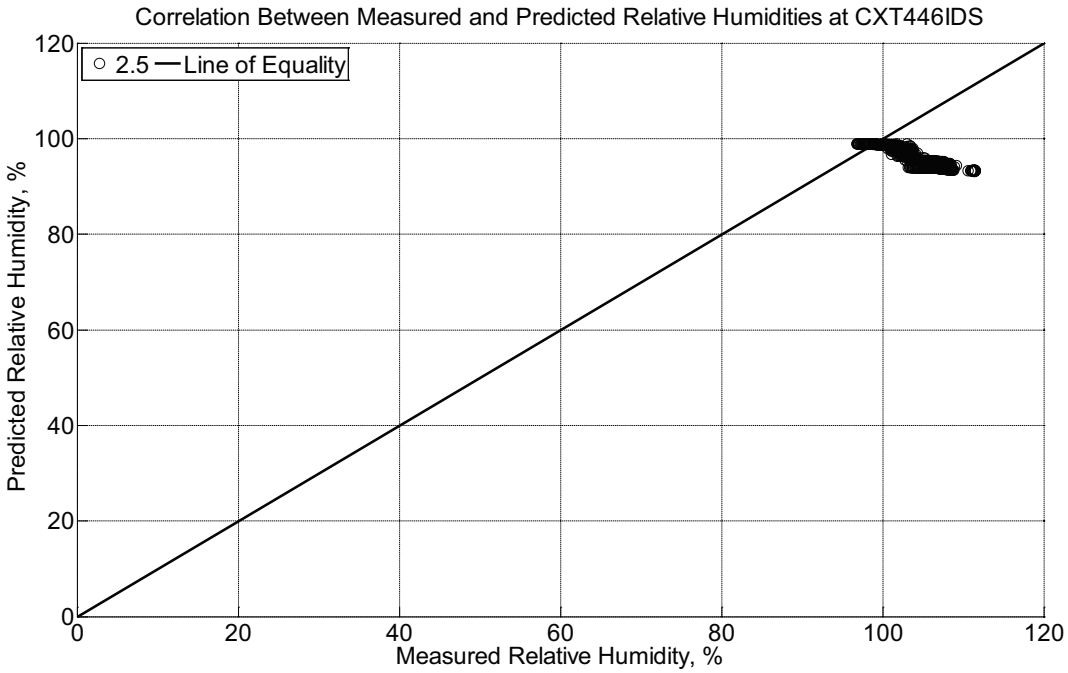

Figure B-775 Correlation between measured and predicted relative humidity values 2.5 inches (63.5 mm) from the surface of a concrete crosstie (labeled CXT446IDS) installed in track near Lytton, BC, between November 22, 2013, through February 14, 2014. An 8 mm thick polyurethane pad and steel rail are additionally installed atop the concrete crosstie. The model does not incorporate a polyurethane pad nor steel rail line.

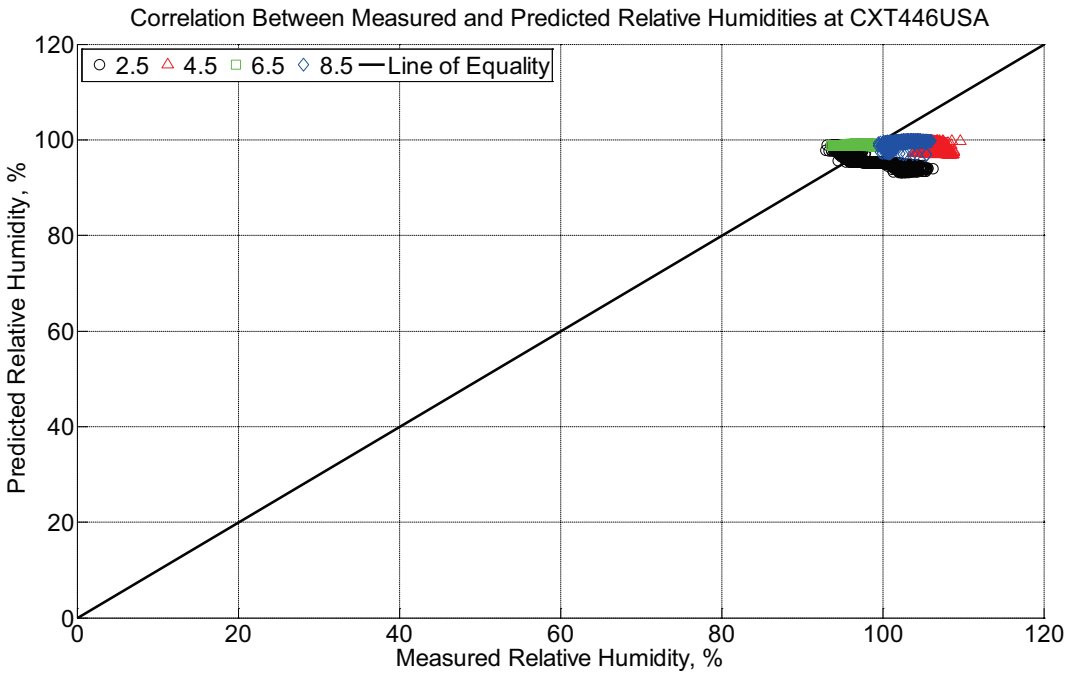

Figure B-776 Correlation between measured and predicted relative humidity values 2.5 inches (63.5 mm), 4.5 inches (114.3 mm), 6.5 inches (139.7 mm), and 8.5 inches (215.9 mm) from the surface of a concrete crosstie (labeled CXT446USA) installed in track near Lytton, BC, between November 22, 2013, through February 14, 2014. An 8 mm thick polyurethane pad and steel rail are additionally installed atop the concrete crosstie. The model does not incorporate a polyurethane pad nor steel rail line.

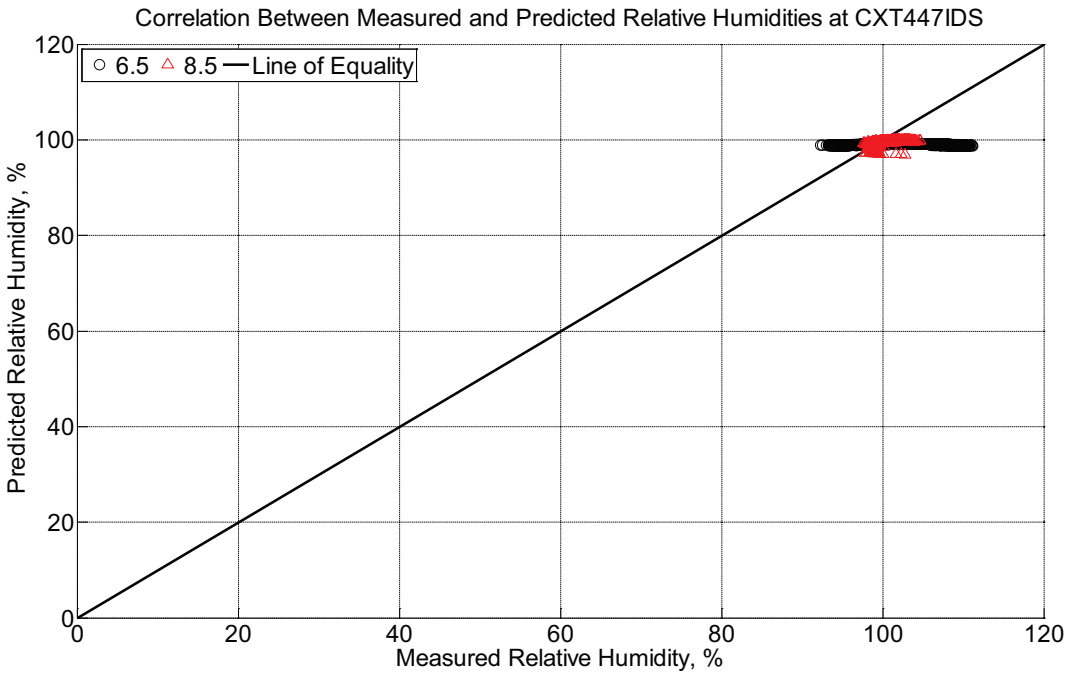

Figure B-777 Correlation between measured and predicted relative humidity values 6.5 inches (139.7 mm) and 8.5 inches (215.9 mm) from the surface of a concrete crosstie (labeled CXT447IDS) installed in track near Lytton, BC, between November 22, 2013, through February 14, 2014. An 8 mm thick polyurethane pad and steel rail are additionally installed atop the concrete crosstie. The model does not incorporate a polyurethane pad nor steel rail line.

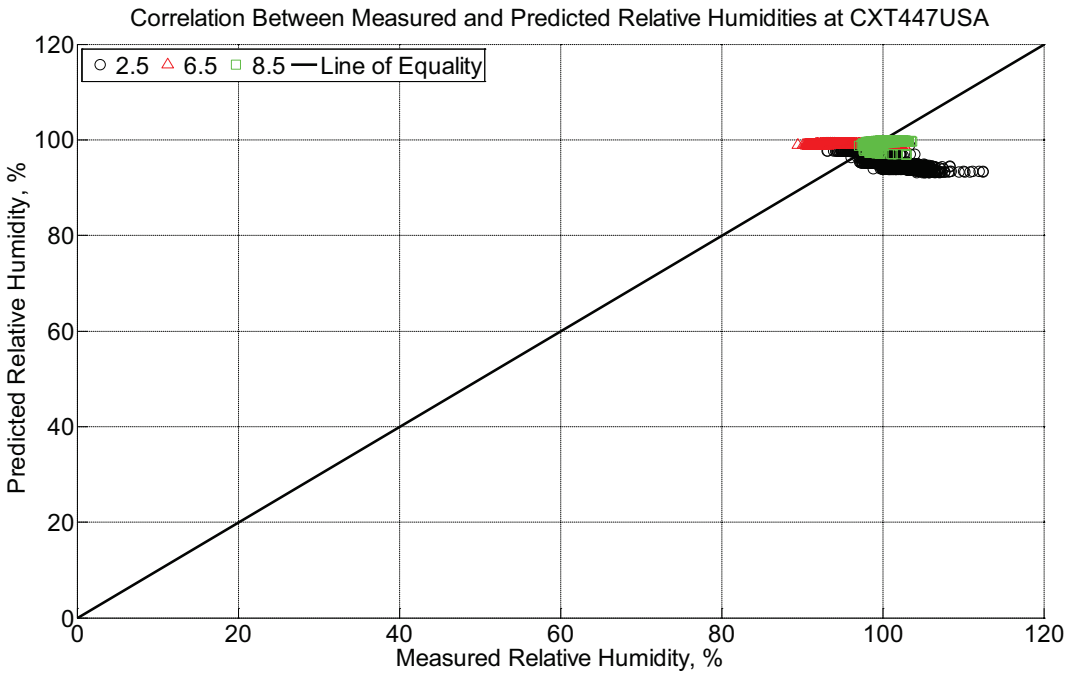

Figure B-778 Correlation between measured and predicted relative humidity values 2.5 inches (63.5 mm), 6.5 inches (139.7 mm), and 8.5 inches (215.9 mm) from the surface of a concrete crosstie (labeled CXT447USA) installed in track near Lytton, BC, between November 22, 2013, through February 14, 2014. An 8 mm thick polyurethane pad and steel rail are additionally installed atop the concrete crosstie. The model does not incorporate a polyurethane pad nor steel rail line.

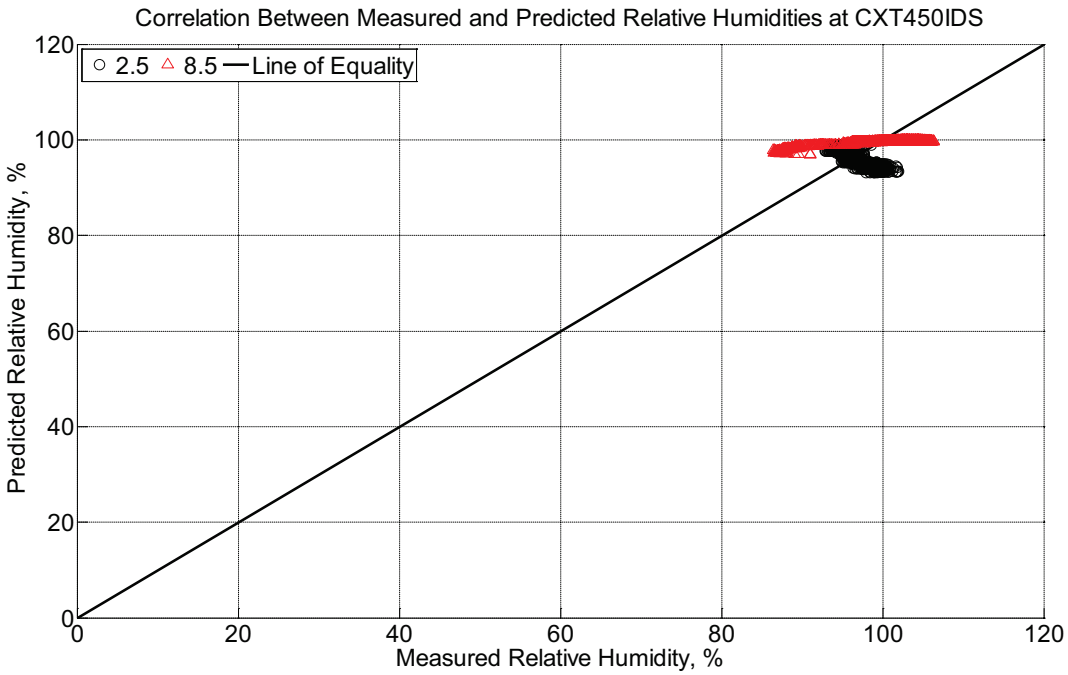

Figure B-779 Correlation between measured and predicted relative humidity values 2.5 inches (63.5 mm) and 8.5 inches (215.9 mm) from the surface of a concrete crosstie (labeled CXT450IDS) installed in track near Lytton, BC, between November 22, 2013, through February 14, 2014. An 8 mm thick polyurethane pad and steel rail are additionally installed atop the concrete crosstie. The model does not incorporate a polyurethane pad nor steel rail line.

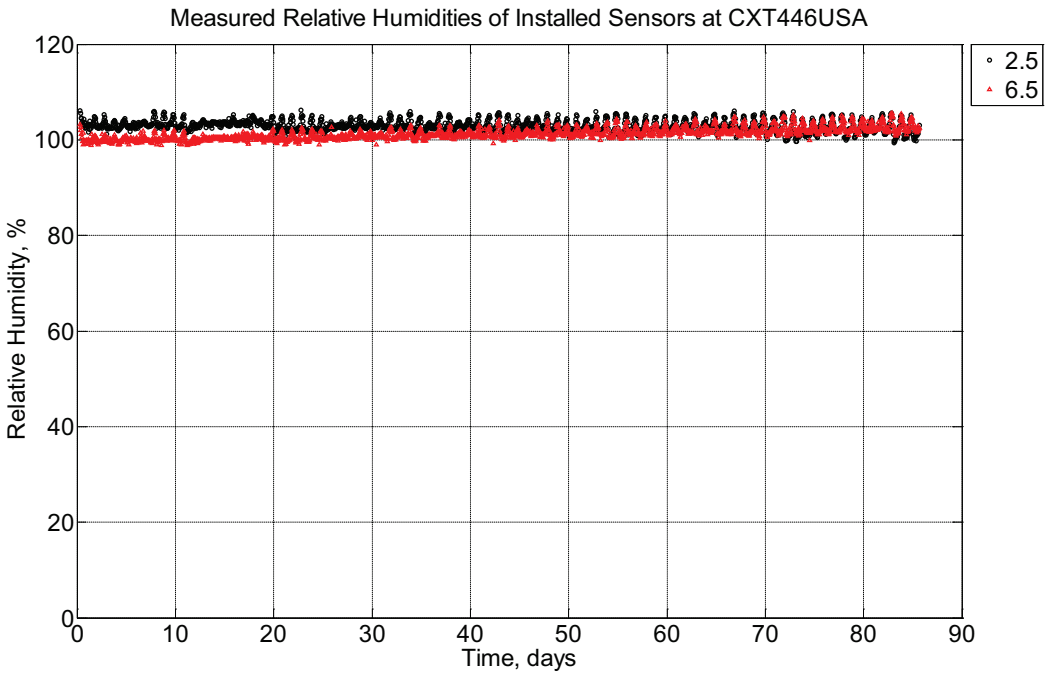

Figure B-780 Measured relative humidity at depths of 2.5 inches (63.5 mm) and 6.5 inches (139.7 mm) from the surface of a concrete crosstie (labeled CXT446USA) installed in track near Lytton, BC, between February 18, 2014, through May 14, 2014. An 8 mm thick polyurethane pad and steel rail are additionally installed atop the concrete crosstie.

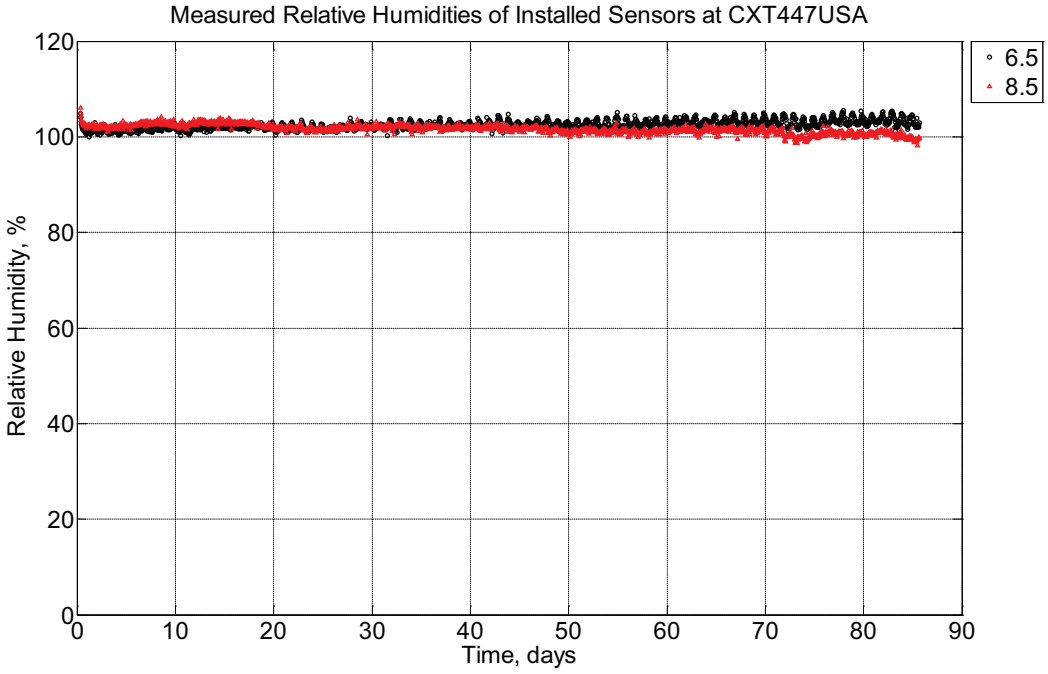

Figure B-781 Measured relative humidity at depths of 6.5 inches (139.7 mm) and 8.5 inches (215.9 mm) from the surface of a concrete crosstie (labeled CXT447USA) installed in track

near Lytton, BC, between February 18, 2014, through May 14, 2014. An 8 mm thick polyurethane pad and steel rail are additionally installed atop the concrete crosstie.

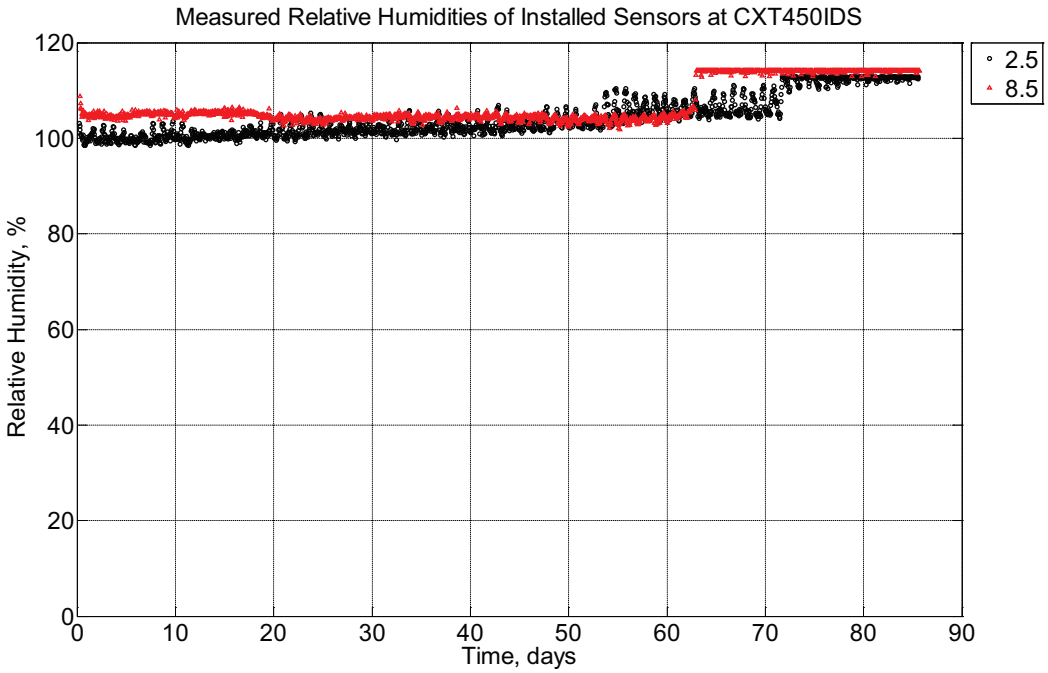

Figure B-782 Measured relative humidity at depths of 2.5 inches (63.5 mm) and 8.5 inches (215.9 mm) from the surface of a concrete crosstie (labeled CXT450IDS) installed in track near Lytton, BC, between February 18, 2014, through May 14, 2014. An 8 mm thick polyurethane pad and steel rail are additionally installed atop the concrete crosstie.

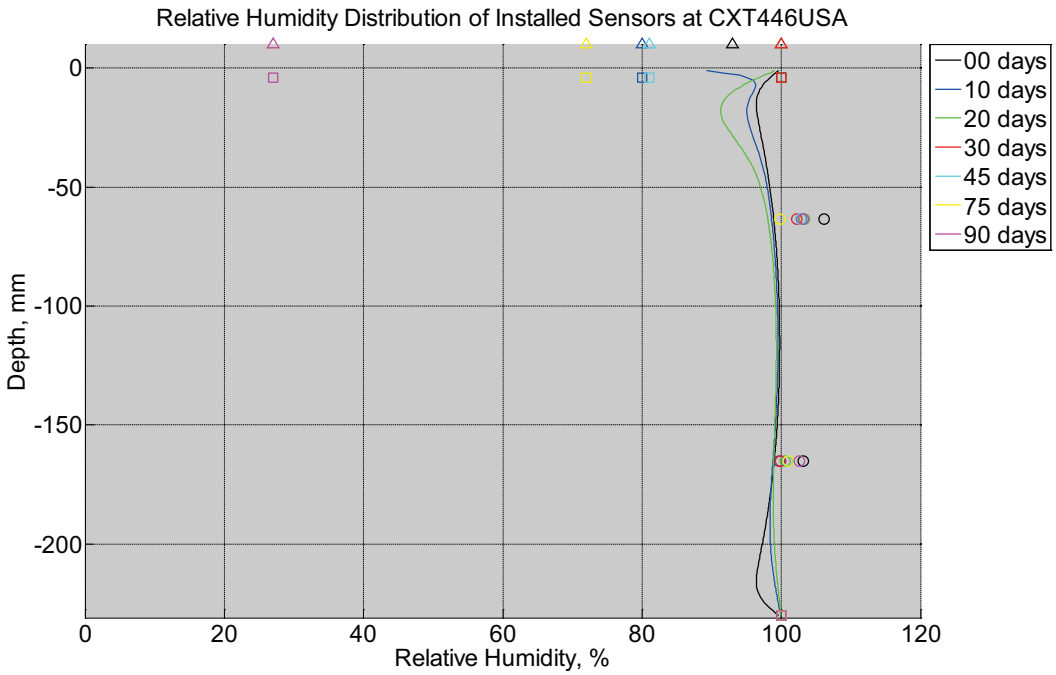

Figure B-783 Measured (markers) and modeled (continuous line) relative humidity profile distribution as a function of depth inside a concrete crosstie (labeled CXT446USA) installed in track near Lytton, BC, between February 18, 2014, through May 14, 2014. An 8 mm thick polyurethane pad and steel rail are additionally installed atop the concrete crosstie. The model does not incorporate a polyurethane pad nor steel rail line. Triangular markers denote relative humidity value from CWLY weather station, square markers denote assumed relative humidity values in ballast, and circular markers denote measured relative humidity values inside concrete.

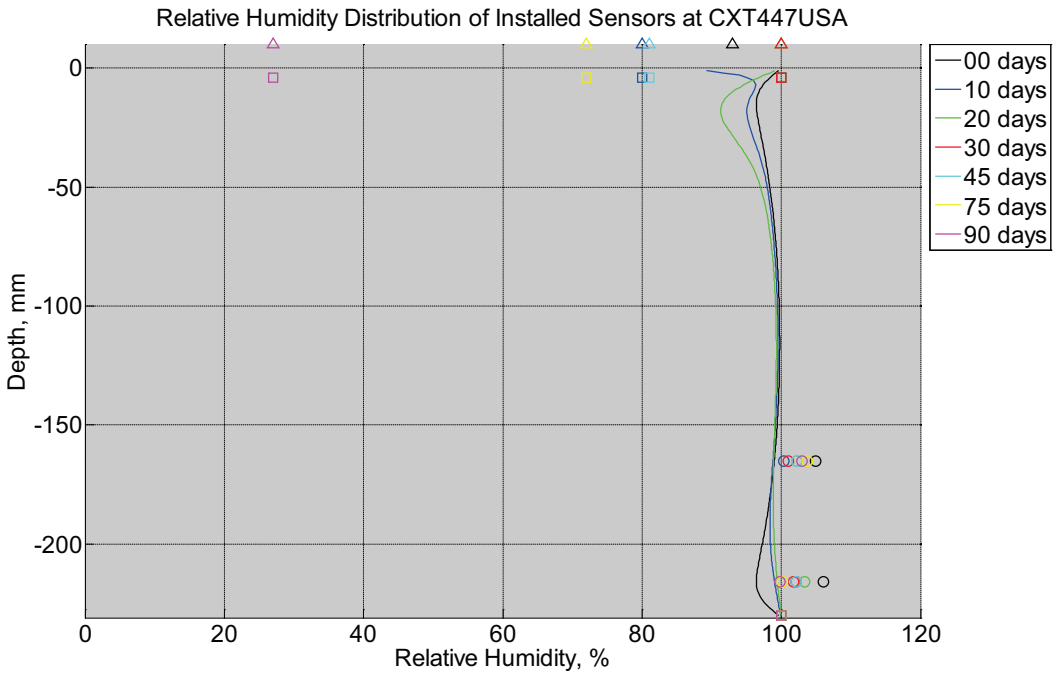

Figure B-784 Measured (markers) and modeled (continuous line) relative humidity profile distribution as a function of depth inside a concrete crosstie (labeled CXT447USA) installed in track near Lytton, BC, between February 18, 2014, through May 14, 2014. An 8 mm thick polyurethane pad and steel rail are additionally installed atop the concrete crosstie. The model does not incorporate a polyurethane pad nor steel rail line. Triangular markers denote relative humidity value from CWLY weather station, square markers denote assumed relative humidity values in ballast, and circular markers denote measured relative humidity values inside concrete.

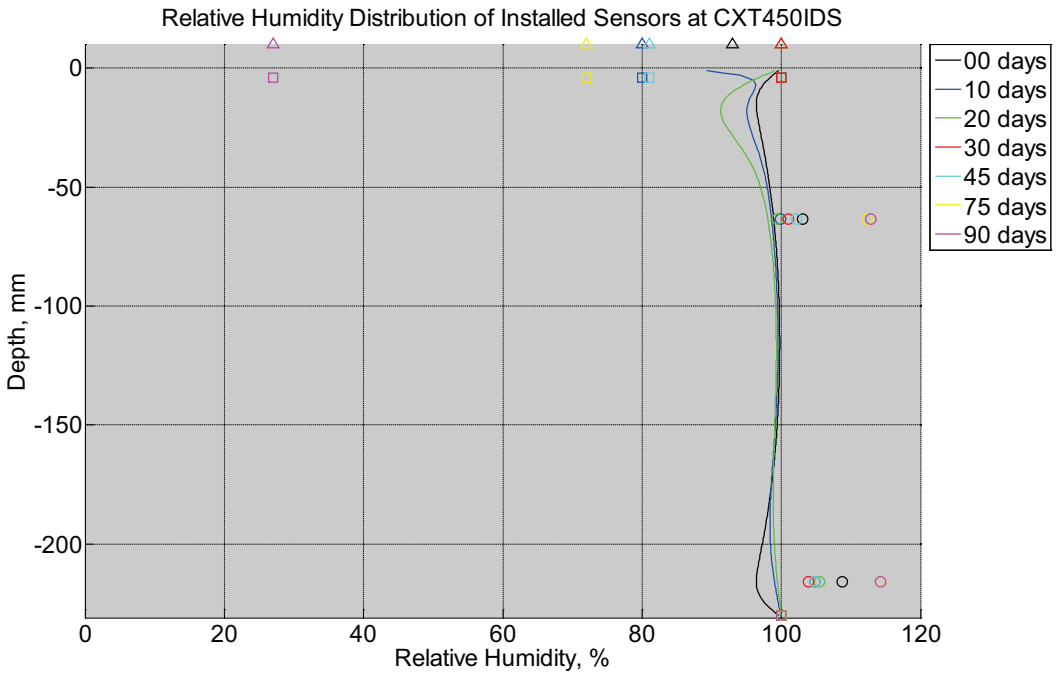

Figure B-785 Measured (markers) and modeled (continuous line) relative humidity profile distribution as a function of depth inside a concrete crosstie (labeled CXT450IDS) installed in track near Lytton, BC, between February 18, 2014, through May 14, 2014. An 8 mm thick polyurethane pad and steel rail are additionally installed atop the concrete crosstie. The model does not incorporate a polyurethane pad nor steel rail line. Triangular markers denote relative humidity value from CWLY weather station, square markers denote assumed relative humidity values in ballast, and circular markers denote measured relative humidity values inside concrete.

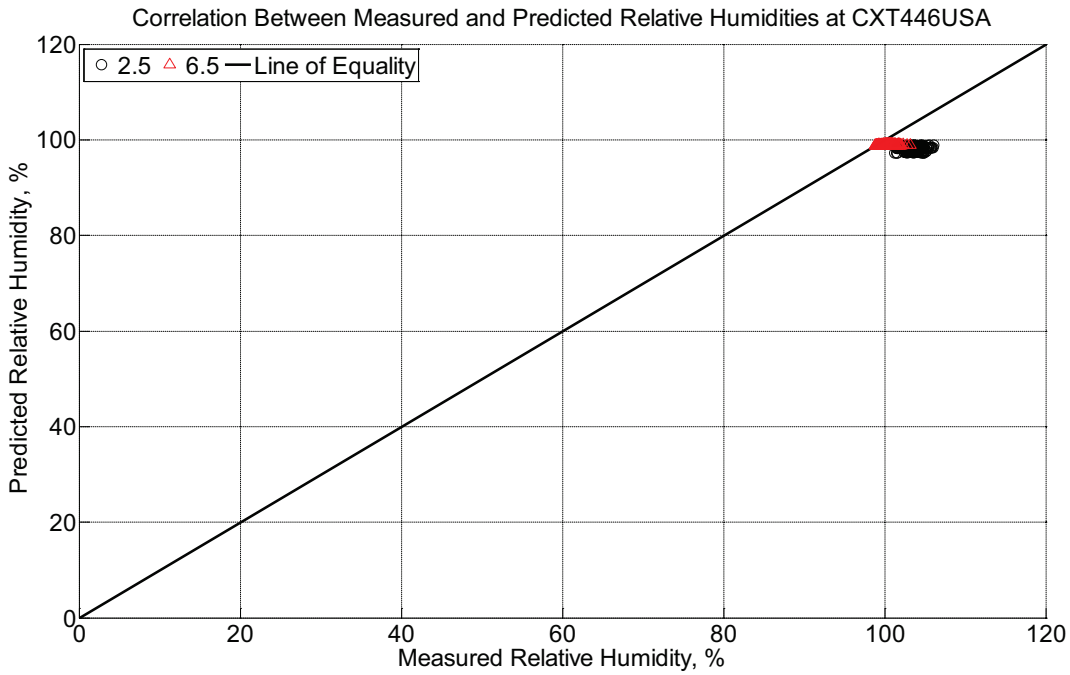

Figure B-786 Correlation between measured and predicted relative humidity values 2.5 inches (63.5 mm) and 6.5 inches (139.7 mm) from the surface of a concrete crosstie (labeled CXT446USA) installed in track near Lytton, BC, between February 18, 2014, through May 14, 2014. An 8 mm thick polyurethane pad and steel rail are additionally installed atop the concrete crosstie. The model does not incorporate a polyurethane pad nor steel rail line.

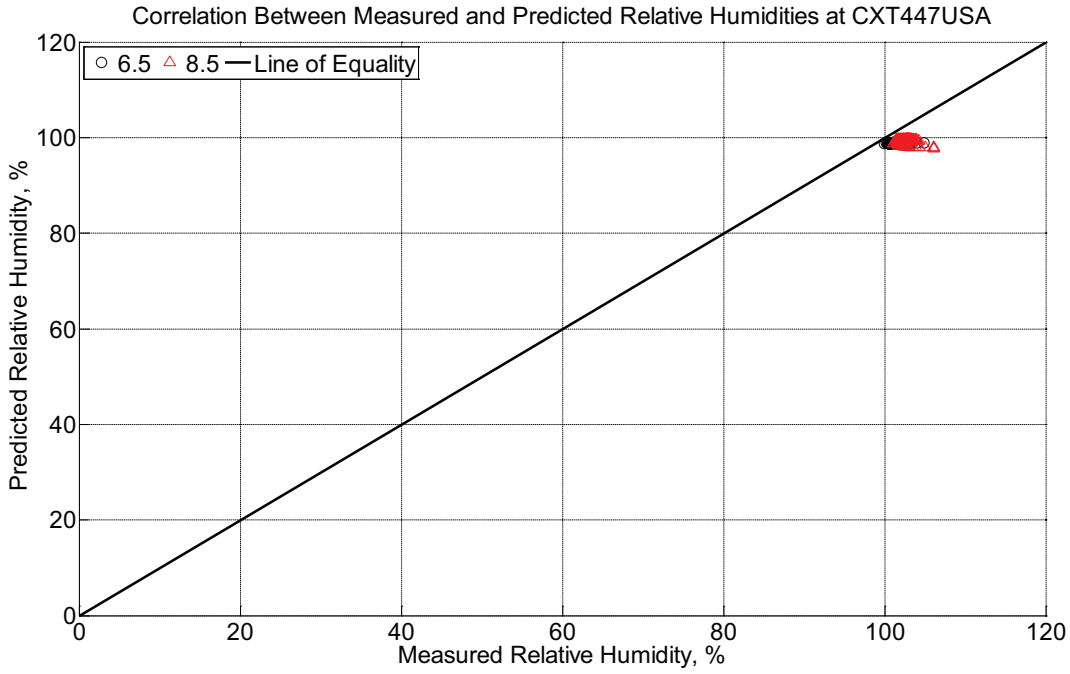

Figure B-787 Correlation between measured and predicted relative humidity values 6.5

inches (139.7 mm) and 8.5 inches (215.9 mm) from the surface of a concrete crosstie (labeled CXT447USA) installed in track near Lytton, BC, between February 18, 2014, through May 14, 2014. An 8 mm thick polyurethane pad and steel rail are additionally installed atop the concrete crosstie. The model does not incorporate a polyurethane pad nor steel rail line.

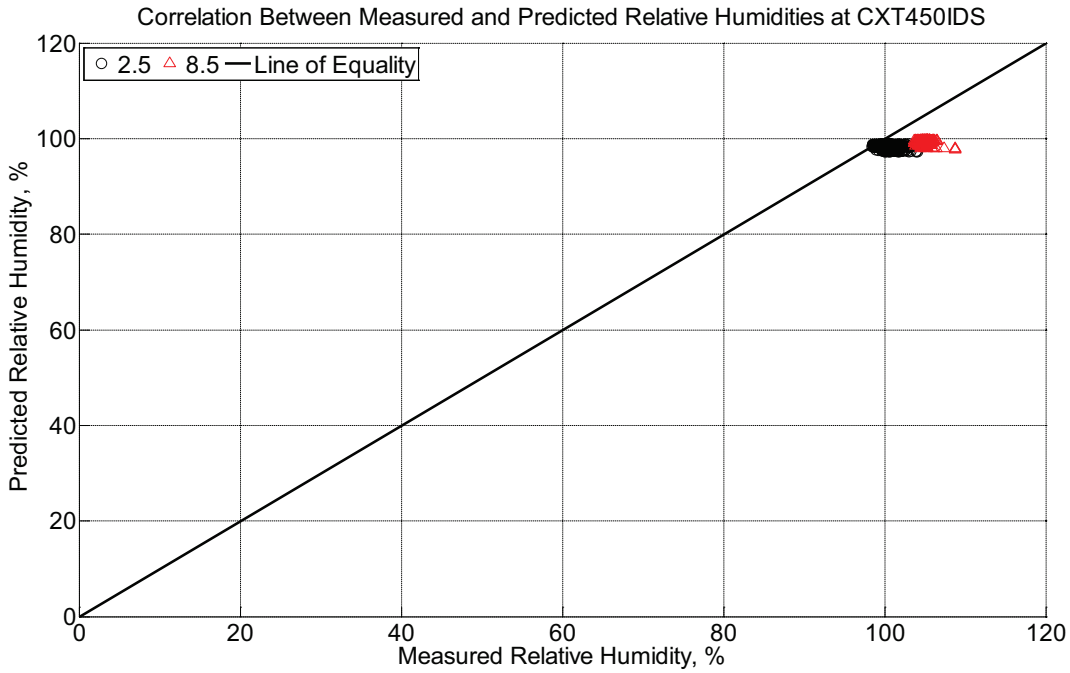

Figure B-788 Correlation between measured and predicted relative humidity values 2.5 inches (63.5 mm) and 8.5 inches (215.9 mm) from the surface of a concrete crosstie (labeled CXT450IDS) installed in track near Lytton, BC, between February 18, 2014, through May 14, 2014. An 8 mm thick polyurethane pad and steel rail are additionally installed atop the concrete crosstie. The model does not incorporate a polyurethane pad nor steel rail line.

Measured and predicted internal temperature of instrumented concrete crossties located near Lytton, BC

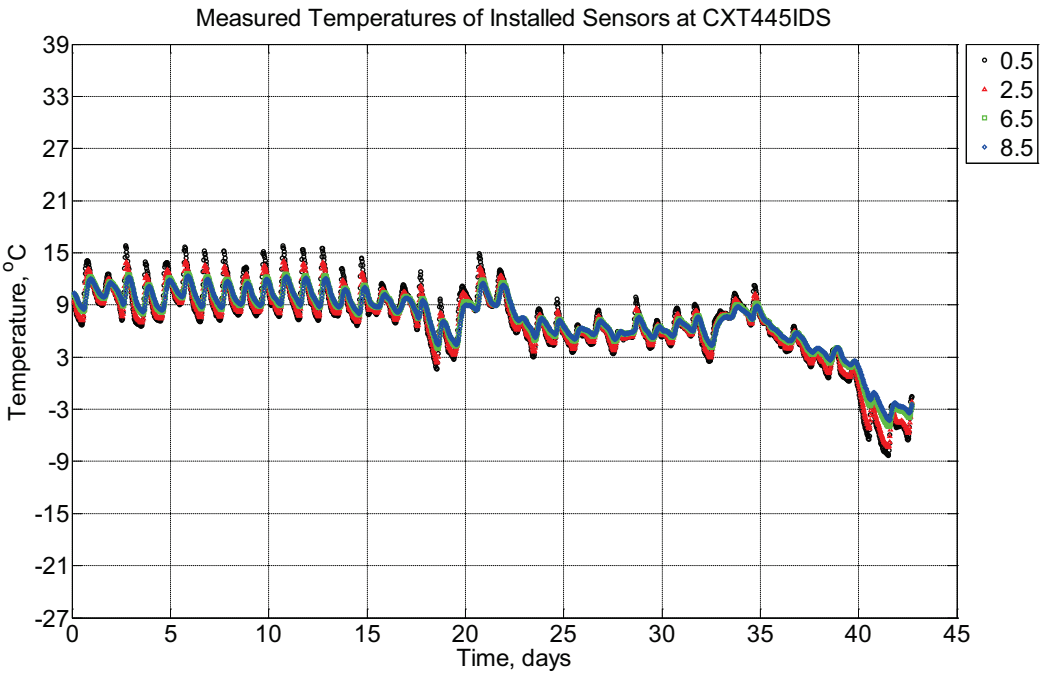

Figure B-789 Measured temperature at depths of 0.5 inches (12.7 mm), 2.5 inches (63.5 mm), 6.5 inches (139.7 mm), and 8.5 inches (215.9 mm) from the surface of a concrete crosstie (labeled CXT445IDS) installed in track near Lytton, BC, between October 11, 2013, through November 22, 2013. An 8 mm thick polyurethane pad and steel rail are additionally installed atop the concrete crosstie.

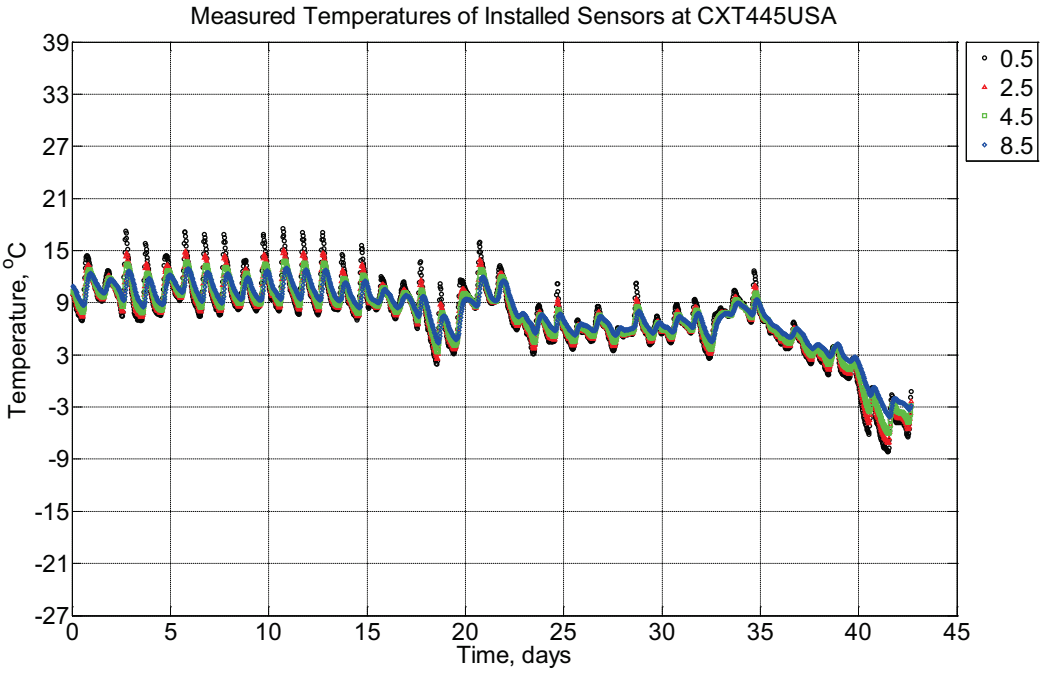

Figure B-790 Measured temperature at depths of 0.5 inches (12.7 mm), 2.5 inches (63.5

mm), 4.5 inches (114.3 mm), and 8.5 inches (215.9 mm) from the surface of a concrete crosstie (labeled CXT445USA) installed in track near Lytton, BC, between October 11, 2013, through November 22, 2013. An 8 mm thick polyurethane pad and steel rail are additionally installed atop the concrete crosstie.

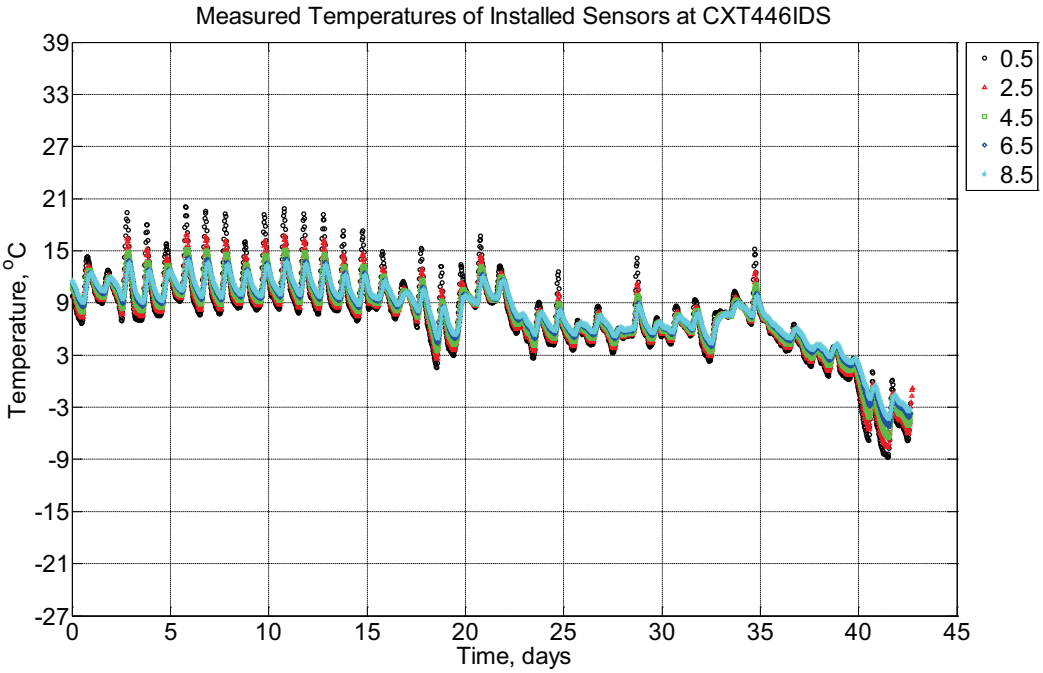

Figure B-791 Measured temperature at depths of 0.5 inches (12.7 mm), 2.5 inches (63.5 mm), 4.5 inches (114.3 mm), 6.5 inches (139.7 mm), and 8.5 inches (215.9 mm) from the surface of a concrete crosstie (labeled CXT446IDS) installed in track near Lytton, BC, between October 11, 2013, through November 22, 2013. An 8 mm thick polyurethane pad and steel rail are additionally installed atop the concrete crosstie.

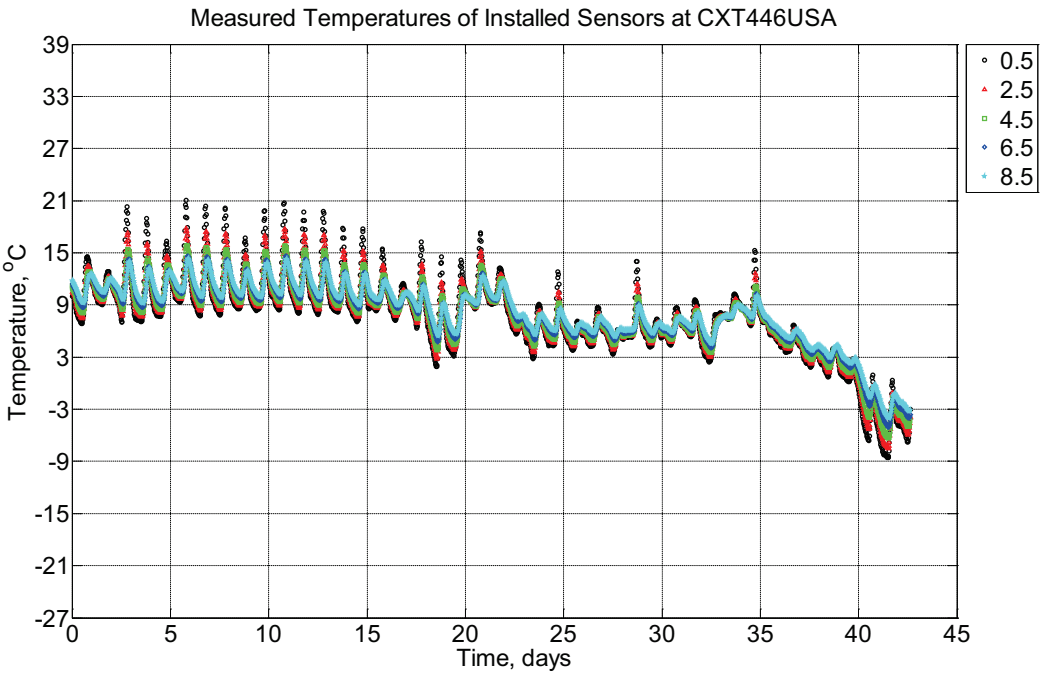

Figure B-792 Measured temperature at depths of 0.5 inches (12.7 mm), 2.5 inches (63.5 mm), 4.5 inches (114.3 mm), 6.5 inches (139.7 mm), and 8.5 inches (215.9 mm) from the surface of a concrete crosstie (labeled CXT446USA) installed in track near Lytton, BC, between October 11, 2013, through November 22, 2013. An 8 mm thick polyurethane pad and steel rail are additionally installed atop the concrete crosstie.

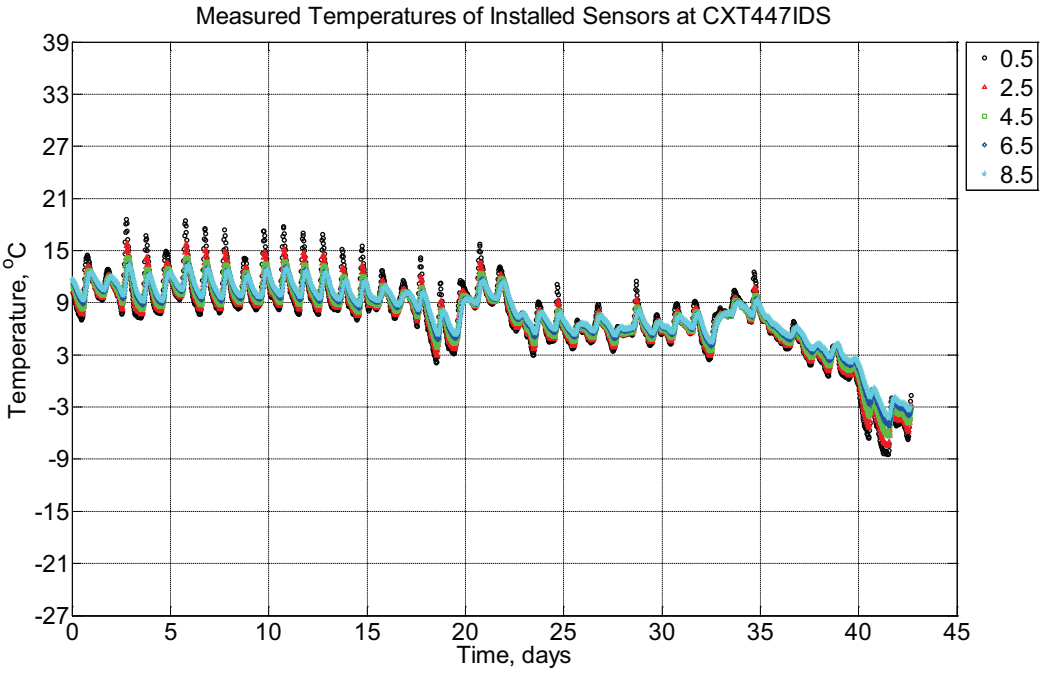

Figure B-793 Measured temperature at depths of 0.5 inches (12.7 mm), 2.5 inches (63.5

mm), 4.5 inches (114.3 mm), 6.5 inches (139.7 mm), and 8.5 inches (215.9 mm) from the surface of a concrete crosstie (labeled CXT447IDS) installed in track near Lytton, BC, between October 11, 2013, through November 22, 2013. An 8 mm thick polyurethane pad and steel rail are additionally installed atop the concrete crosstie.

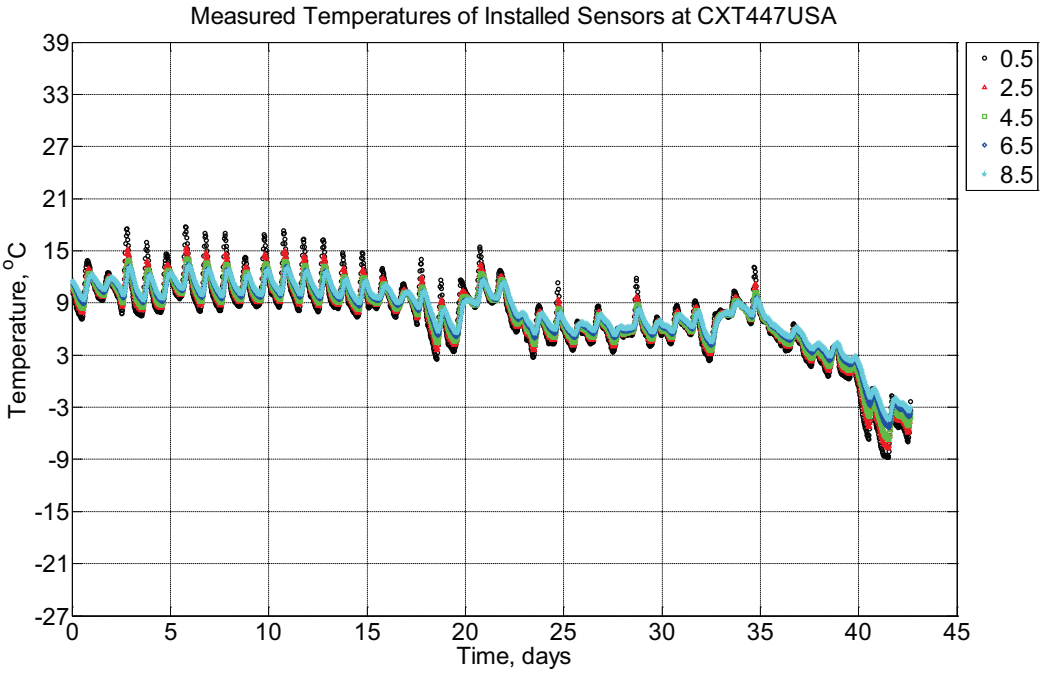

Figure B-794 Measured temperature at depths of 0.5 inches (12.7 mm), 2.5 inches (63.5 mm), 4.5 inches (114.3 mm), 6.5 inches (139.7 mm), and 8.5 inches (215.9 mm) from the surface of a concrete crosstie (labeled CXT447USA) installed in track near Lytton, BC, between October 11, 2013, through November 22, 2013. An 8 mm thick polyurethane pad and steel rail are additionally installed atop the concrete crosstie.

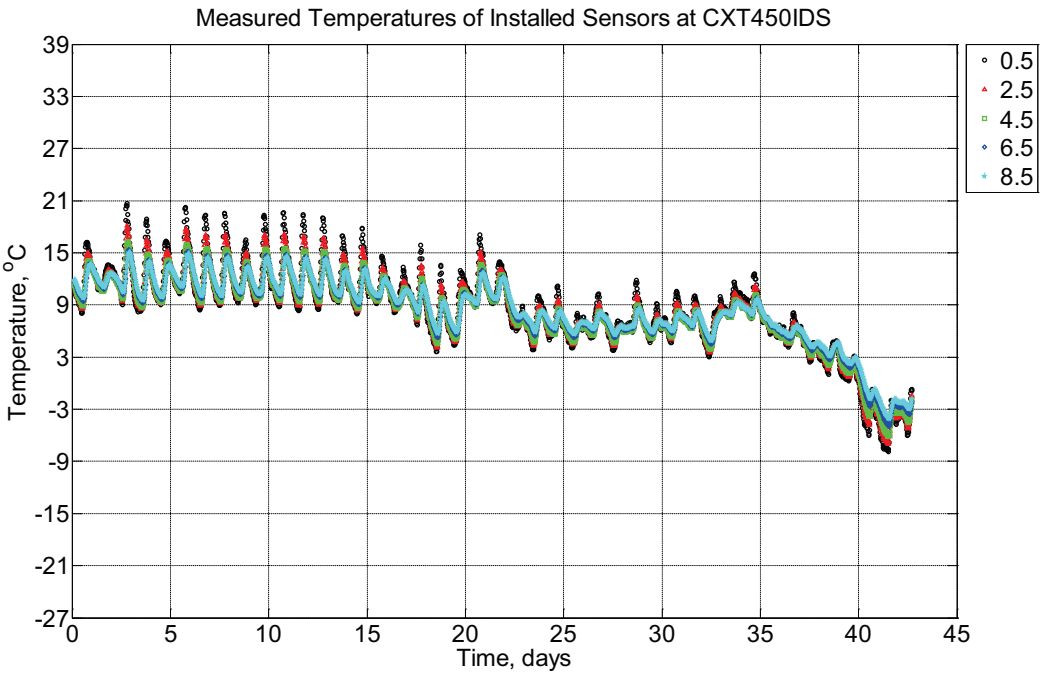

Figure B-795 Measured temperature at depths of 0.5 inches (12.7 mm), 2.5 inches (63.5 mm), 4.5 inches (114.3 mm), 6.5 inches (139.7 mm), and 8.5 inches (215.9 mm) from the surface of a concrete crosstie (labeled CXT450IDS) installed in track near Lytton, BC, between October 11, 2013, through November 22, 2013. An 8 mm thick polyurethane pad and steel rail are additionally installed atop the concrete crosstie.

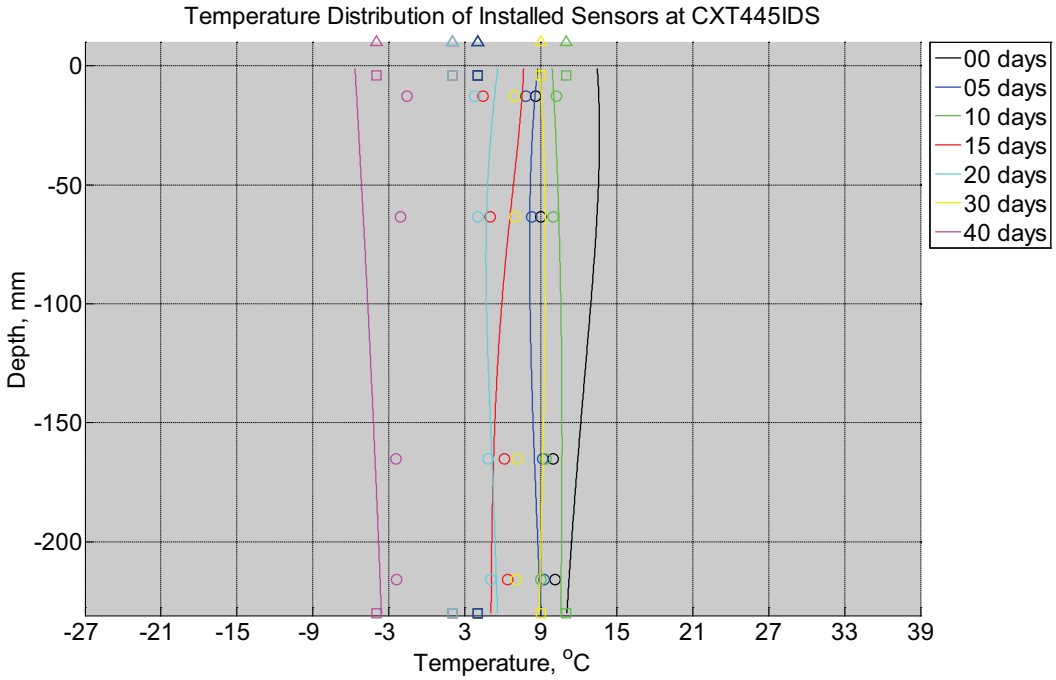

Figure B-796 Measured (markers) and modeled (continuous line) temperature profile

distribution as a function of depth inside a concrete crosstie (labeled CXT445IDS) installed in track near Lytton, BC, between October 11, 2013, through November 22, 2013. An 8 mm thick polyurethane pad and steel rail are additionally installed atop the concrete crosstie. The model does not incorporate a polyurethane pad nor steel rail line. Triangular markers denote temperature value from CWLY weather station, square markers denote assumed temperature values in ballast, and circular markers denote measured temperature values inside concrete.

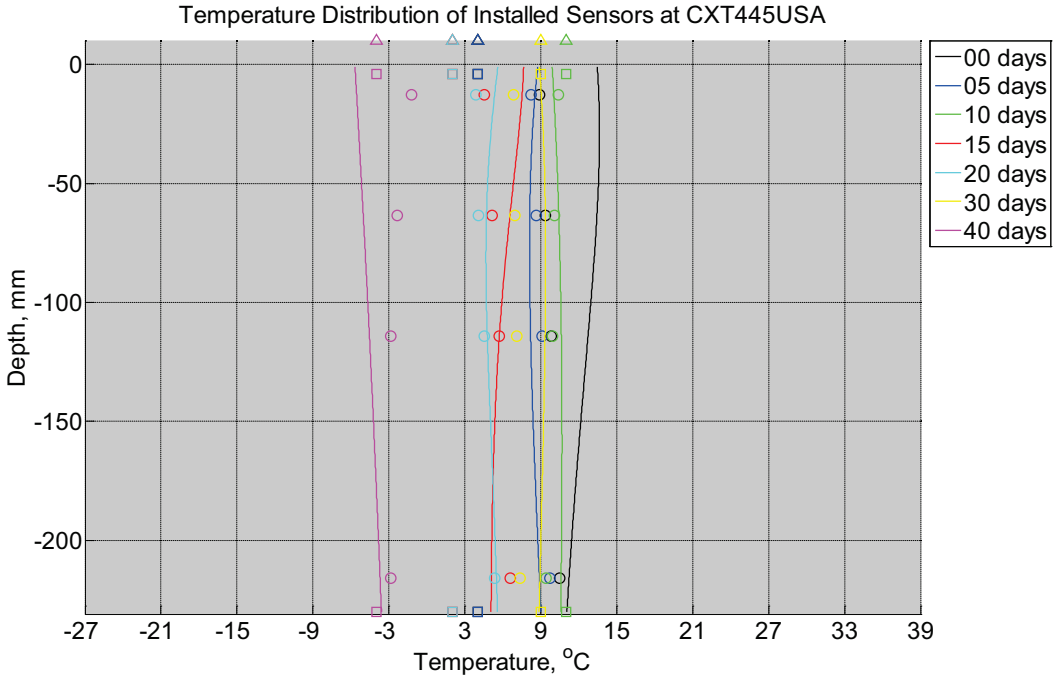

Figure B-797 Measured (markers) and modeled (continuous line) temperature profile distribution as a function of depth inside a concrete crosstie (labeled CXT445USA) installed in track near Lytton, BC, between October 11, 2013, through November 22, 2013. An 8 mm thick polyurethane pad and steel rail are additionally installed atop the concrete crosstie. The model does not incorporate a polyurethane pad nor steel rail line. Triangular markers denote temperature value from CWLY weather station, square markers denote assumed temperature values in ballast, and circular markers denote measured temperature values inside concrete.

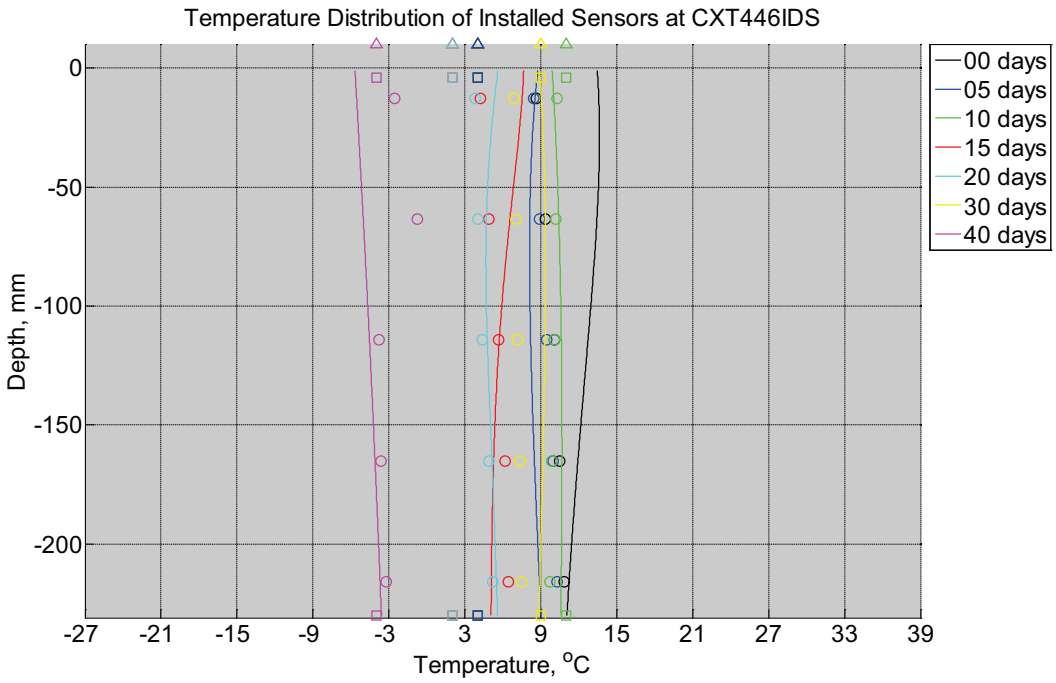

Figure B-798 Measured (markers) and modeled (continuous line) temperature profile distribution as a function of depth inside a concrete crosstie (labeled CXT446IDS) installed in track near Lytton, BC, between October 11, 2013, through November 22, 2013. An 8 mm thick polyurethane pad and steel rail are additionally installed atop the concrete crosstie. The model does not incorporate a polyurethane pad nor steel rail line. Triangular markers denote temperature value from CWLY weather station, square markers denote assumed temperature values in ballast, and circular markers denote measured temperature values inside concrete.

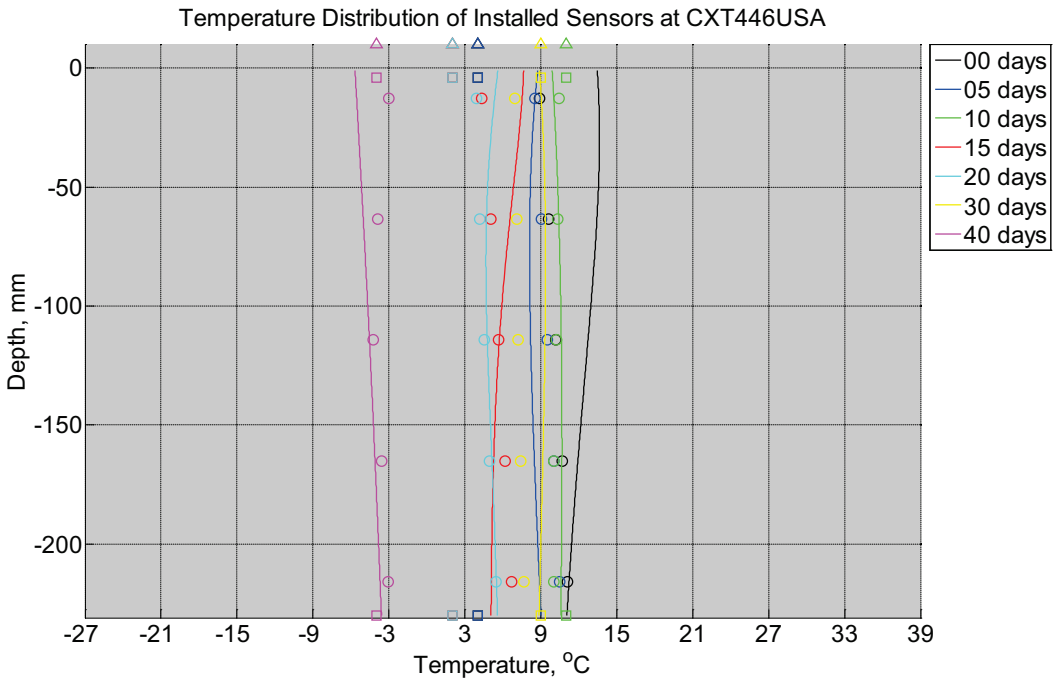

Figure B-799 Measured (markers) and modeled (continuous line) temperature profile distribution as a function of depth inside a concrete crosstie (labeled CXT446USA) installed in track near Lytton, BC, between October 11, 2013, through November 22, 2013. An 8 mm thick polyurethane pad and steel rail are additionally installed atop the concrete crosstie. The model does not incorporate a polyurethane pad nor steel rail line. Triangular markers denote temperature value from CWLY weather station, square markers denote assumed temperature values in ballast, and circular markers denote measured temperature values inside concrete.

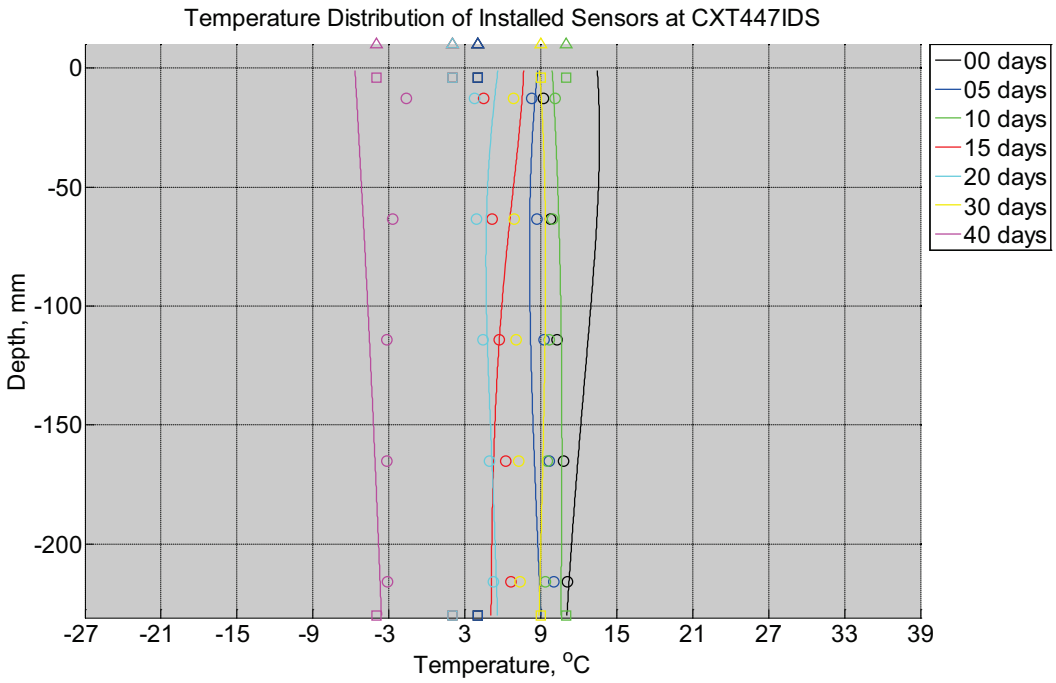

Figure B-800 Measured (markers) and modeled (continuous line) temperature profile distribution as a function of depth inside a concrete crosstie (labeled CXT447IDS) installed in track near Lytton, BC, between October 11, 2013, through November 22, 2013. An 8 mm thick polyurethane pad and steel rail are additionally installed atop the concrete crosstie. The model does not incorporate a polyurethane pad nor steel rail line. Triangular markers denote temperature value from CWLY weather station, square markers denote assumed temperature values in ballast, and circular markers denote measured temperature values inside concrete.

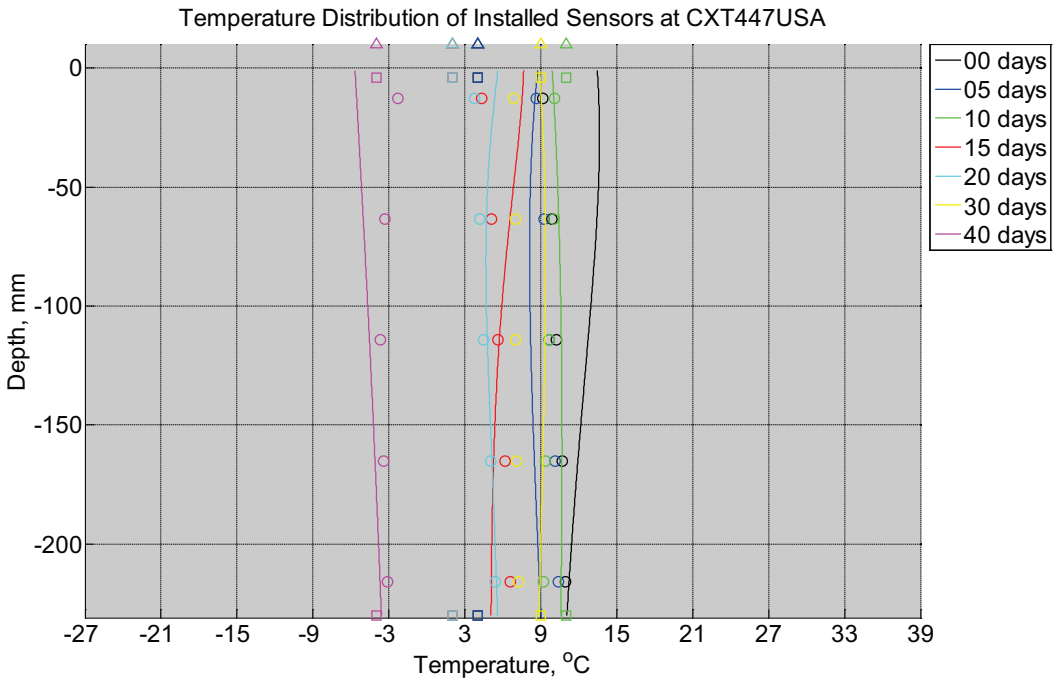

Figure B-801 Measured (markers) and modeled (continuous line) temperature profile distribution as a function of depth inside a concrete crosstie (labeled CXT447USA) installed in track near Lytton, BC, between October 11, 2013, through November 22, 2013. An 8 mm thick polyurethane pad and steel rail are additionally installed atop the concrete crosstie. The model does not incorporate a polyurethane pad nor steel rail line. Triangular markers denote temperature value from CWLY weather station, square markers denote assumed temperature values in ballast, and circular markers denote measured temperature values inside concrete.

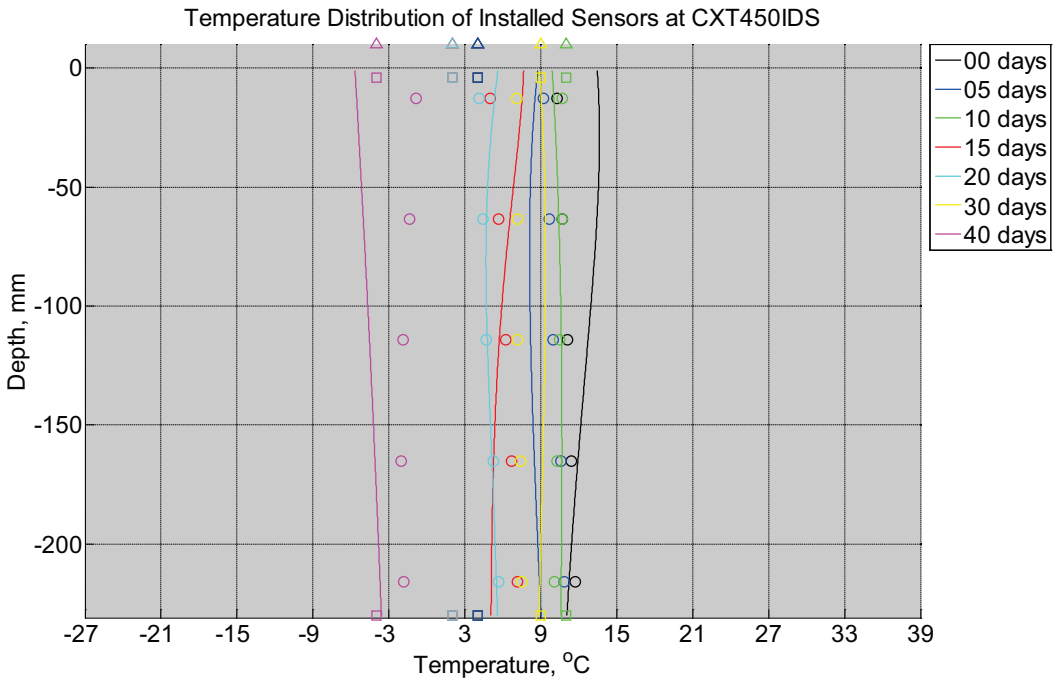

Figure B-802 Measured (markers) and modeled (continuous line) temperature profile distribution as a function of depth inside a concrete crosstie (labeled CXT450IDS) installed in track near Lytton, BC, between October 11, 2013, through November 22, 2013. An 8 mm thick polyurethane pad and steel rail are additionally installed atop the concrete crosstie. The model does not incorporate a polyurethane pad nor steel rail line. Triangular markers denote temperature value from CWLY weather station, square markers denote assumed temperature values in ballast, and circular markers denote measured temperature values inside concrete.

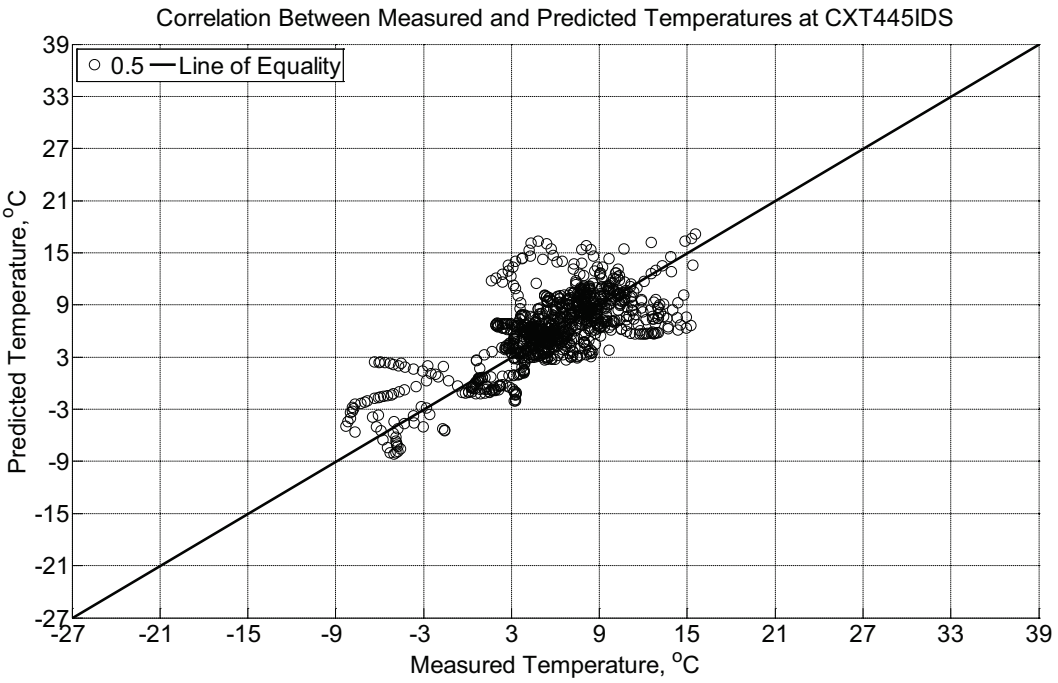

Figure B-803 Correlation between measured and predicted temperature values 0.5 inches (12.7 mm) from the surface of a concrete crosstie (labeled CXT445IDS) installed in track near Lytton, BC, between October 11, 2013, through November 22, 2013. An 8 mm thick polyurethane pad and steel rail are additionally installed atop the concrete crosstie. The model does not incorporate a polyurethane pad nor steel rail line.

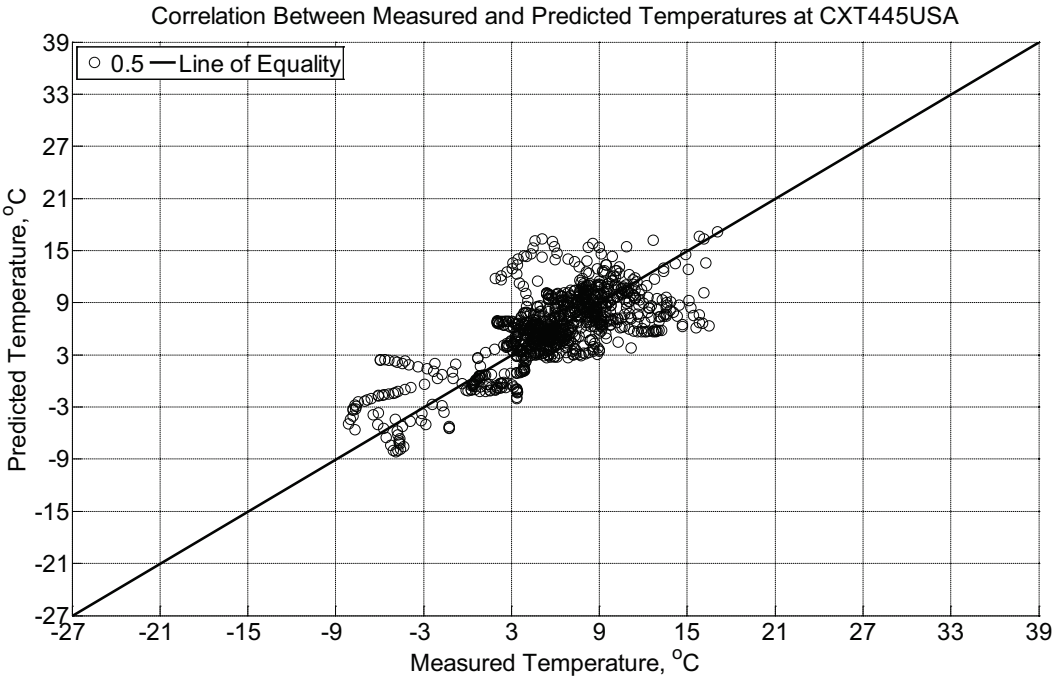

Figure B-804 Correlation between measured and predicted temperature values 0.5 inches

(12.7 mm) from the surface of a concrete crosstie (labeled CXT445USA) installed in track near Lytton, BC, between October 11, 2013, through November 22, 2013. An 8 mm thick polyurethane pad and steel rail are additionally installed atop the concrete crosstie. The model does not incorporate a polyurethane pad nor steel rail line.

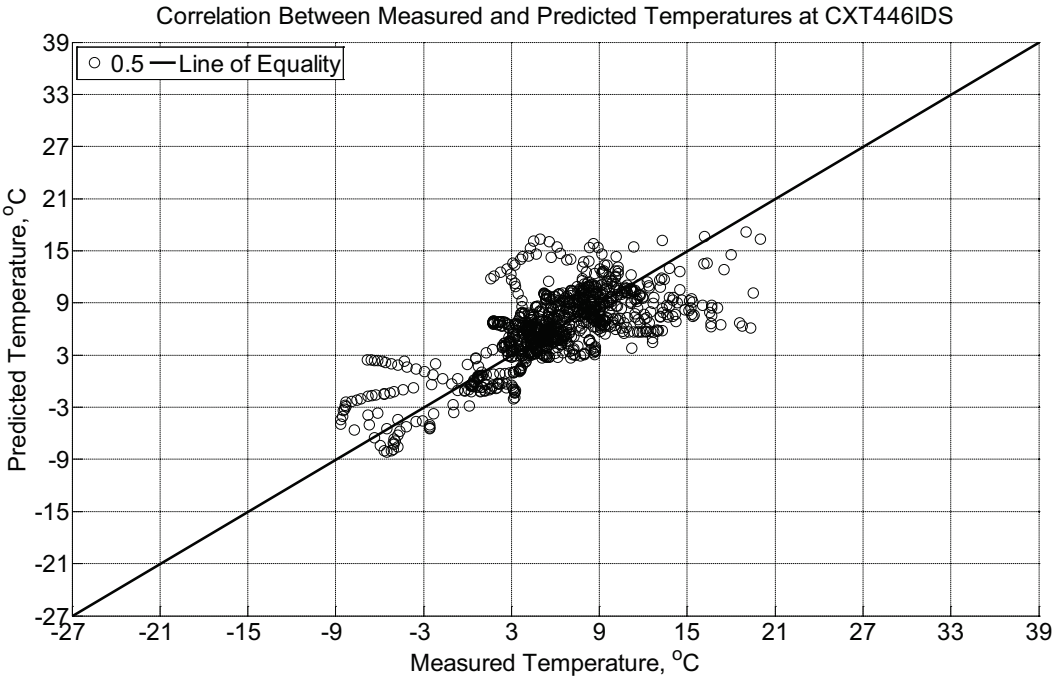

Figure B-805 Correlation between measured and predicted temperature values 0.5 inches (12.7 mm) from the surface of a concrete crosstie (labeled CXT446IDS) installed in track near Lytton, BC, between October 11, 2013, through November 22, 2013. An 8 mm thick polyurethane pad and steel rail are additionally installed atop the concrete crosstie. The model does not incorporate a polyurethane pad nor steel rail line.

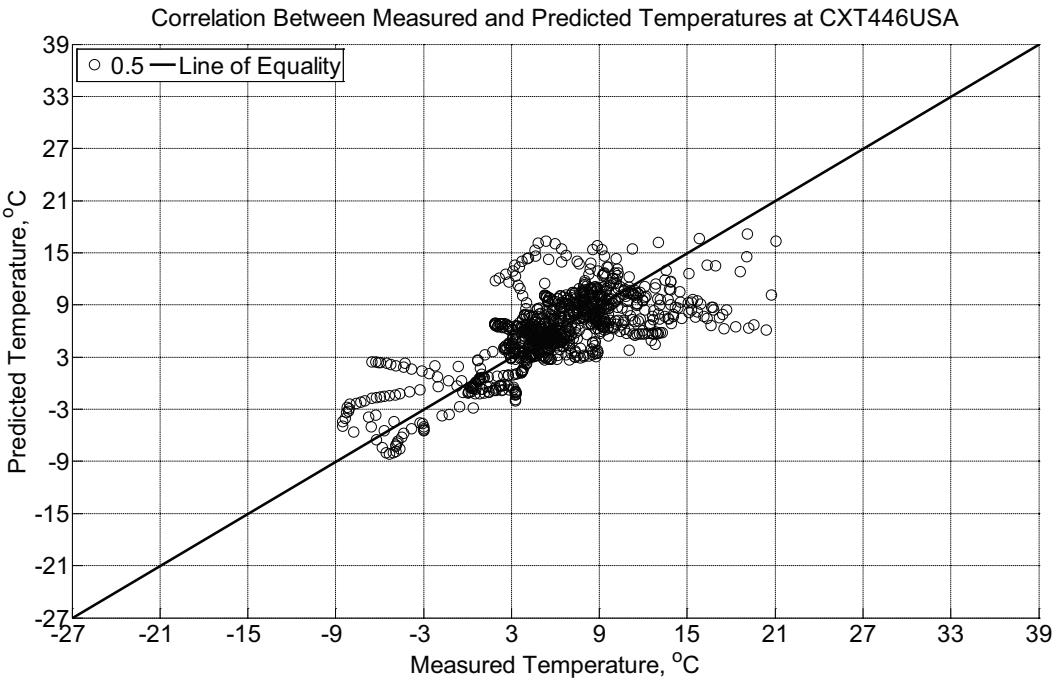

Figure B-806 Correlation between measured and predicted temperature values 0.5 inches (12.7 mm) from the surface of a concrete crosstie (labeled CXT446USA) installed in track near Lytton, BC, between October 11, 2013, through November 22, 2013. An 8 mm thick polyurethane pad and steel rail are additionally installed atop the concrete crosstie. The model does not incorporate a polyurethane pad nor steel rail line.

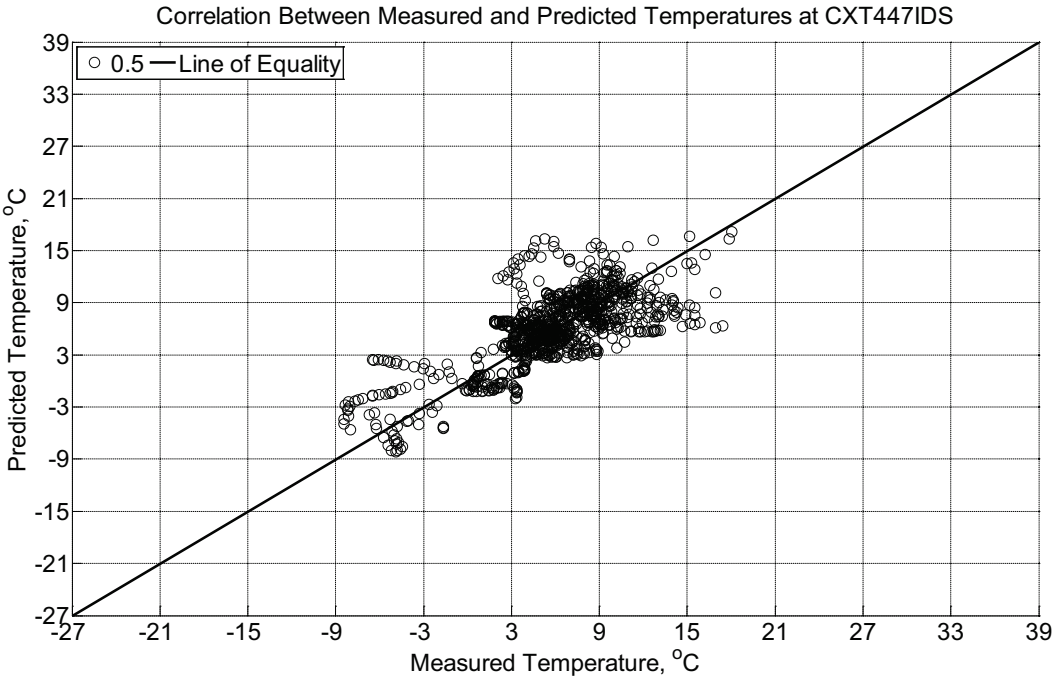

Figure B-807 Correlation between measured and predicted temperature values 0.5 inches

(12.7 mm) from the surface of a concrete crosstie (labeled CXT447IDS) installed in track near Lytton, BC, between October 11, 2013, through November 22, 2013. An 8 mm thick polyurethane pad and steel rail are additionally installed atop the concrete crosstie. The model does not incorporate a polyurethane pad nor steel rail line.

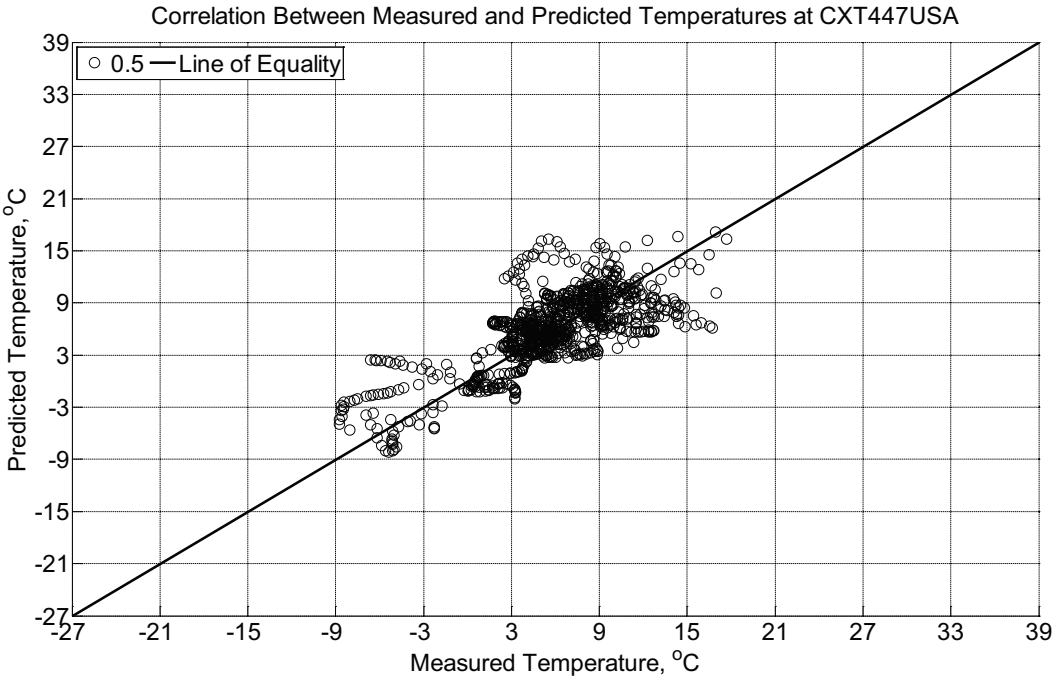

Figure B-808 Correlation between measured and predicted temperature values 0.5 inches (12.7 mm) from the surface of a concrete crosstie (labeled CXT447USA) installed in track near Lytton, BC, between October 11, 2013, through November 22, 2013. An 8 mm thick polyurethane pad and steel rail are additionally installed atop the concrete crosstie. The model does not incorporate a polyurethane pad nor steel rail line.

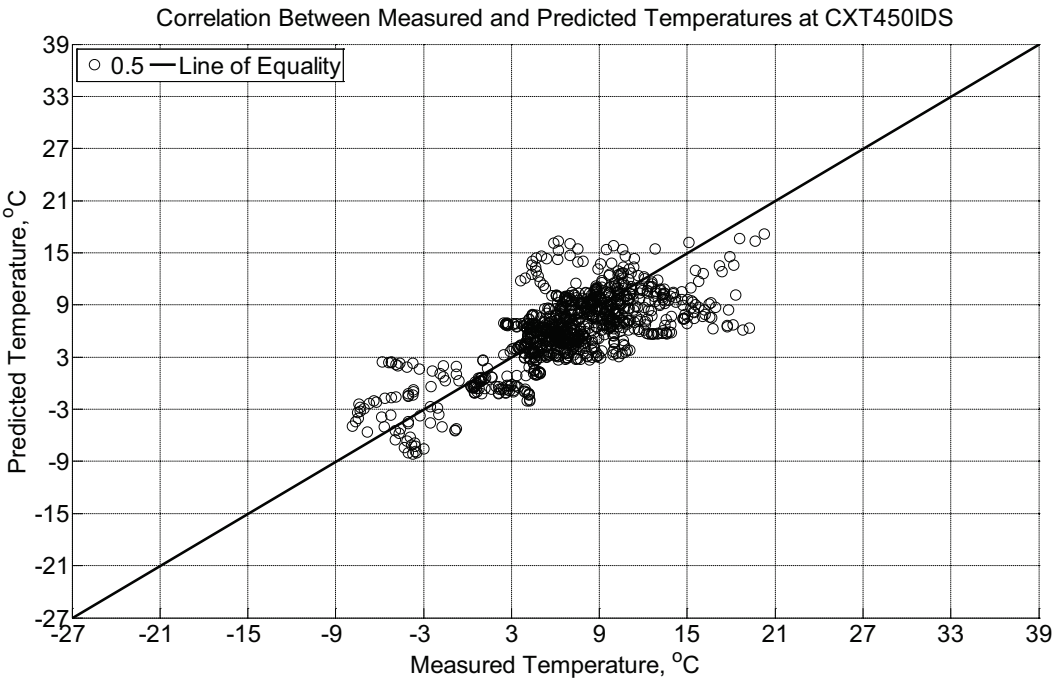

Figure B-809 Correlation between measured and predicted temperature values 0.5 inches (12.7 mm) from the surface of a concrete crosstie (labeled CXT450IDS) installed in track near Lytton, BC, between October 11, 2013, through November 22, 2013. An 8 mm thick polyurethane pad and steel rail are additionally installed atop the concrete crosstie. The model does not incorporate a polyurethane pad nor steel rail line.

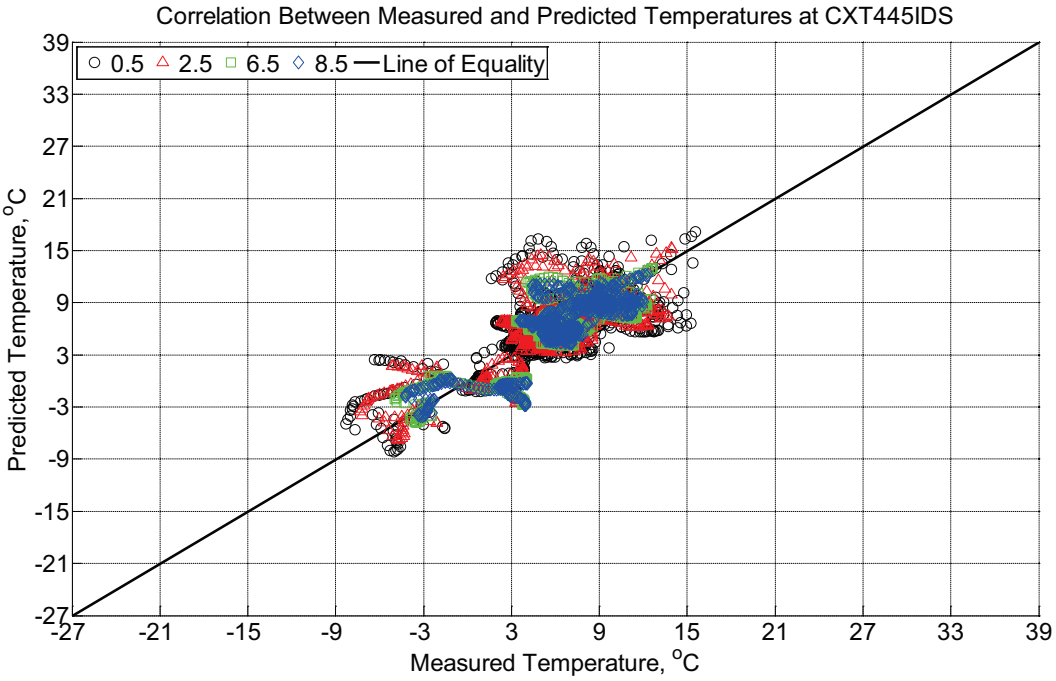

Figure B-810 Correlation between measured and predicted temperature values 0.5 inches

(12.7 mm), 2.5 inches (63.5 mm), 6.5 inches (139.7 mm), and 8.5 inches (215.9 mm) from the surface of a concrete crosstie (labeled CXT445IDS) installed in track near Lytton, BC, between October 11, 2013, through November 22, 2013. An 8 mm thick polyurethane pad and steel rail are additionally installed atop the concrete crosstie. The model does not incorporate a polyurethane pad nor steel rail line.

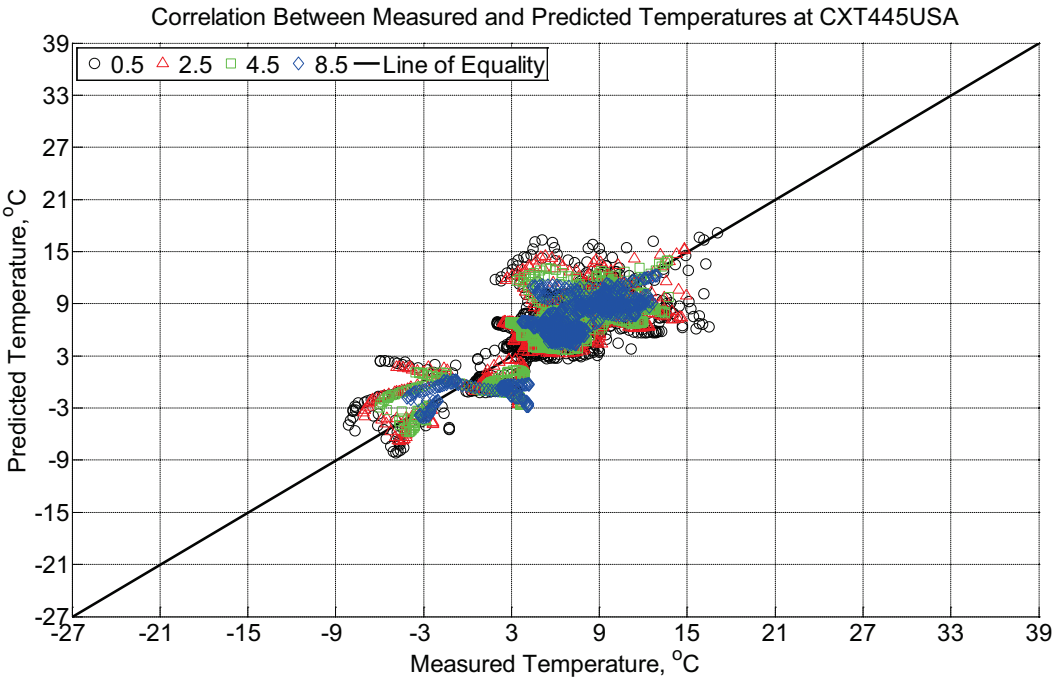

Figure B-811 Correlation between measured and predicted temperature values 0.5 inches (12.7 mm), 2.5 inches (63.5 mm), 4.5 inches (114.3 mm), and 8.5 inches (215.9 mm) from the surface of a concrete crosstie (labeled CXT445USA) installed in track near Lytton, BC, between October 11, 2013, through November 22, 2013. An 8 mm thick polyurethane pad and steel rail are additionally installed atop the concrete crosstie. The model does not incorporate a polyurethane pad nor steel rail line.

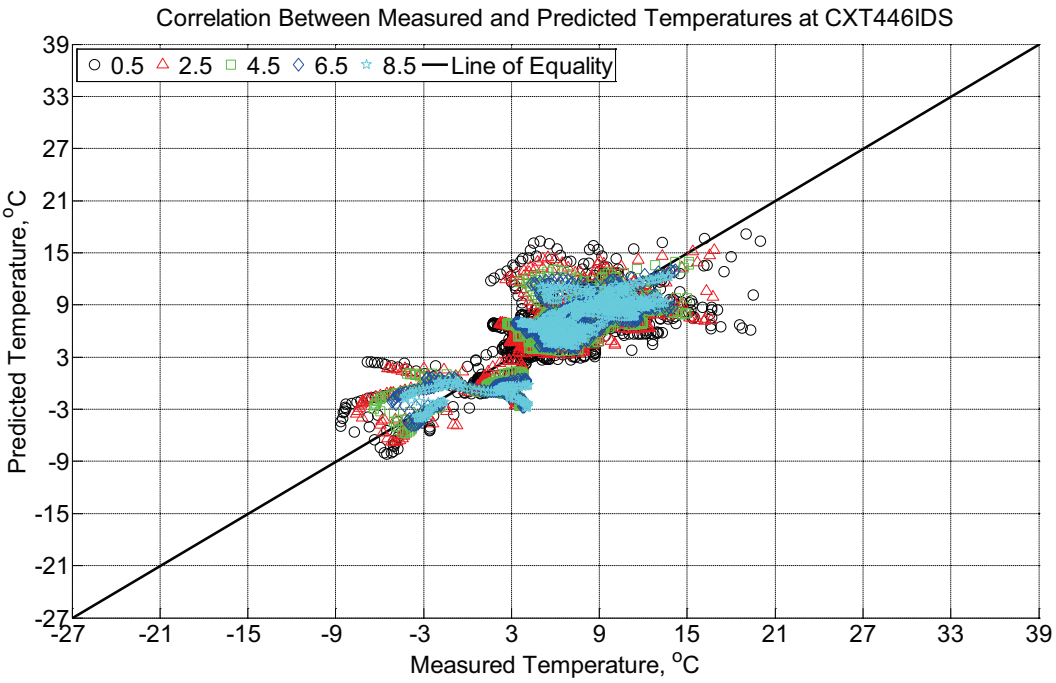

Figure B-812 Correlation between measured and predicted temperature values 0.5 inches (12.7 mm), 2.5 inches (63.5 mm), 4.5 inches (114.3 mm), 6.5 inches (139.7 mm), and 8.5 inches (215.9 mm) from the surface of a concrete crosstie (labeled CXT446IDS) installed in track near Lytton, BC, between October 11, 2013, through November 22, 2013. An 8 mm thick polyurethane pad and steel rail are additionally installed atop the concrete crosstie. The model does not incorporate a polyurethane pad nor steel rail line.

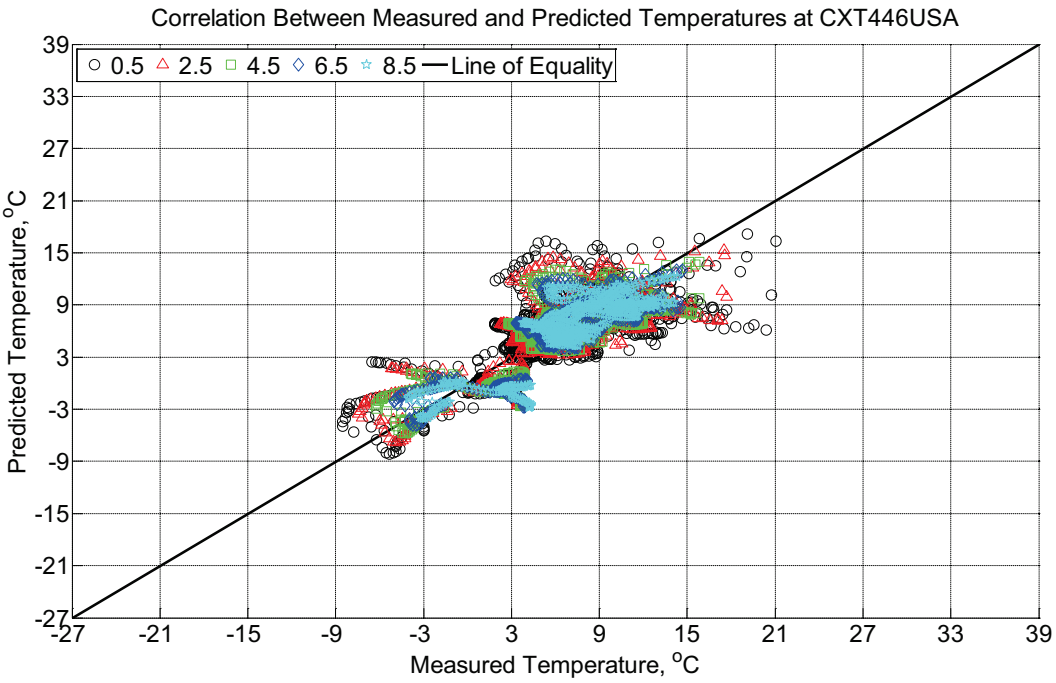

Figure B-813 Correlation between measured and predicted temperature values 0.5 inches (12.7 mm), 2.5 inches (63.5 mm), 4.5 inches (114.3 mm), 6.5 inches (139.7 mm), and 8.5 inches (215.9 mm) from the surface of a concrete crosstie (labeled CXT446USA) installed in track near Lytton, BC, between October 11, 2013, through November 22, 2013. An 8 mm thick polyurethane pad and steel rail are additionally installed atop the concrete crosstie. The model does not incorporate a polyurethane pad nor steel rail line.

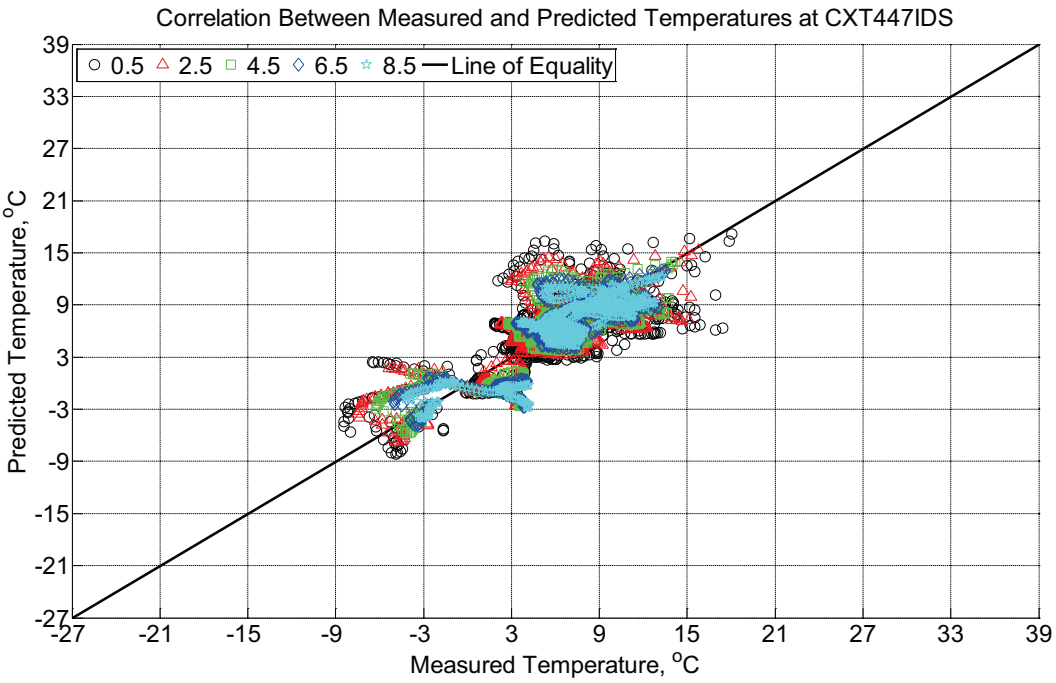

Figure B-814 Correlation between measured and predicted temperature values 0.5 inches (12.7 mm), 2.5 inches (63.5 mm), 4.5 inches (114.3 mm), 6.5 inches (139.7 mm), and 8.5 inches (215.9 mm) from the surface of a concrete crosstie (labeled CXT447IDS) installed in track near Lytton, BC, between October 11, 2013, through November 22, 2013. An 8 mm thick polyurethane pad and steel rail are additionally installed atop the concrete crosstie. The model does not incorporate a polyurethane pad nor steel rail line.

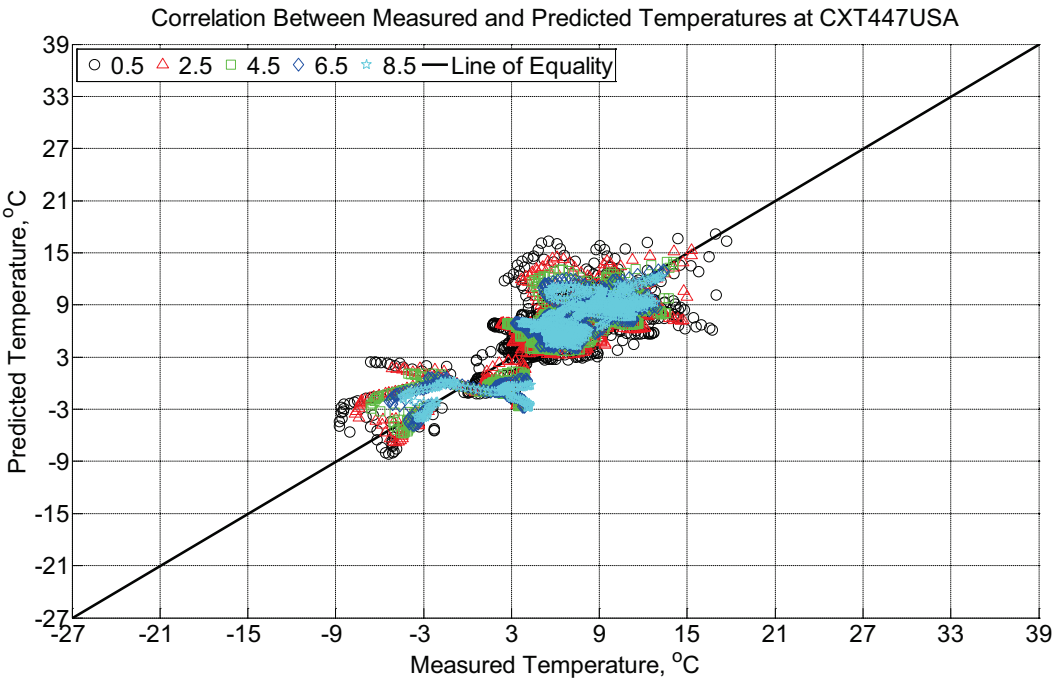

Figure B-815 Correlation between measured and predicted temperature values 0.5 inches (12.7 mm), 2.5 inches (63.5 mm), 4.5 inches (114.3 mm), 6.5 inches (139.7 mm), and 8.5 inches (215.9 mm) from the surface of a concrete crosstie (labeled CXT447USA) installed in track near Lytton, BC, between October 11, 2013, through November 22, 2013. An 8 mm thick polyurethane pad and steel rail are additionally installed atop the concrete crosstie. The model does not incorporate a polyurethane pad nor steel rail line.

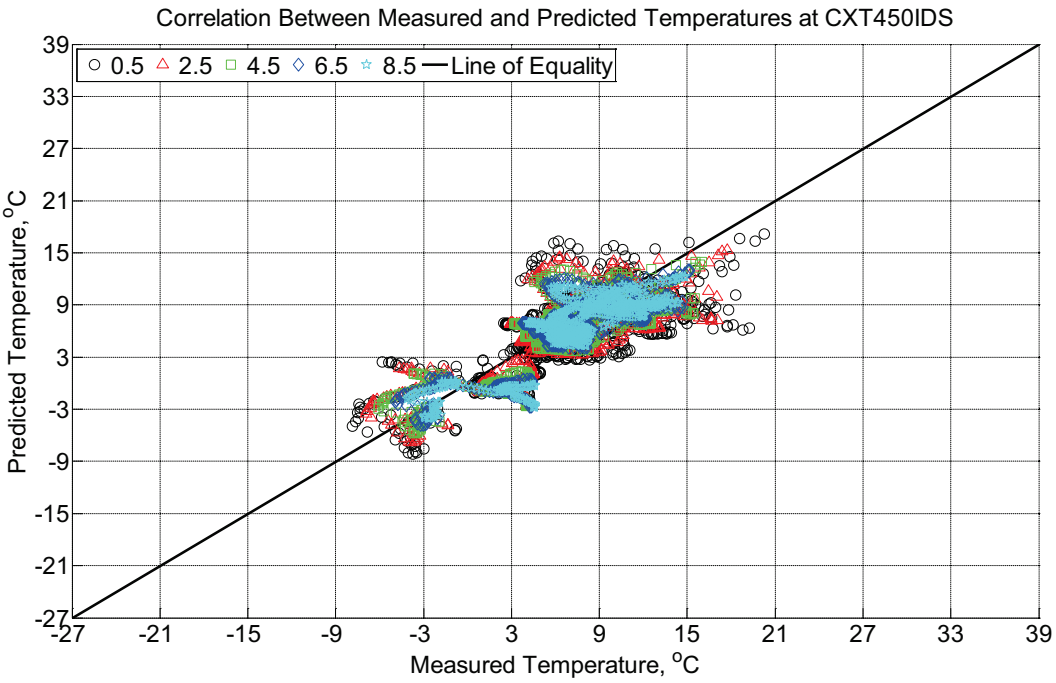

Figure B-816 Correlation between measured and predicted temperature values 0.5 inches (12.7 mm), 2.5 inches (63.5 mm), 4.5 inches (114.3 mm), 6.5 inches (139.7 mm), and 8.5 inches (215.9 mm) from the surface of a concrete crosstie (labeled CXT450IDS) installed in track near Lytton, BC, between October 11, 2013, through November 22, 2013. An 8 mm thick polyurethane pad and steel rail are additionally installed atop the concrete crosstie. The model does not incorporate a polyurethane pad nor steel rail line.

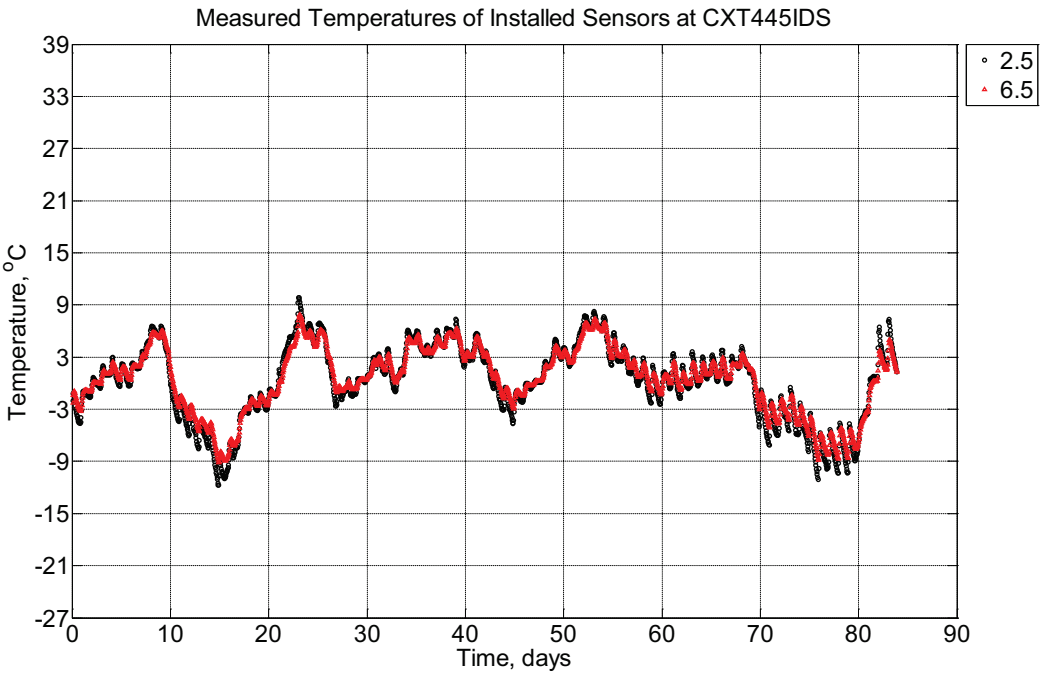

Figure B-817 Measured temperature at depths of 2.5 inches (63.5 mm) and 6.5 inches (139.7 mm) from the surface of a concrete crosstie (labeled CXT445IDS) installed in track near Lytton, BC, between November 22, 2013, through February 14, 2014. An 8 mm thick polyurethane pad and steel rail are additionally installed atop the concrete crosstie.

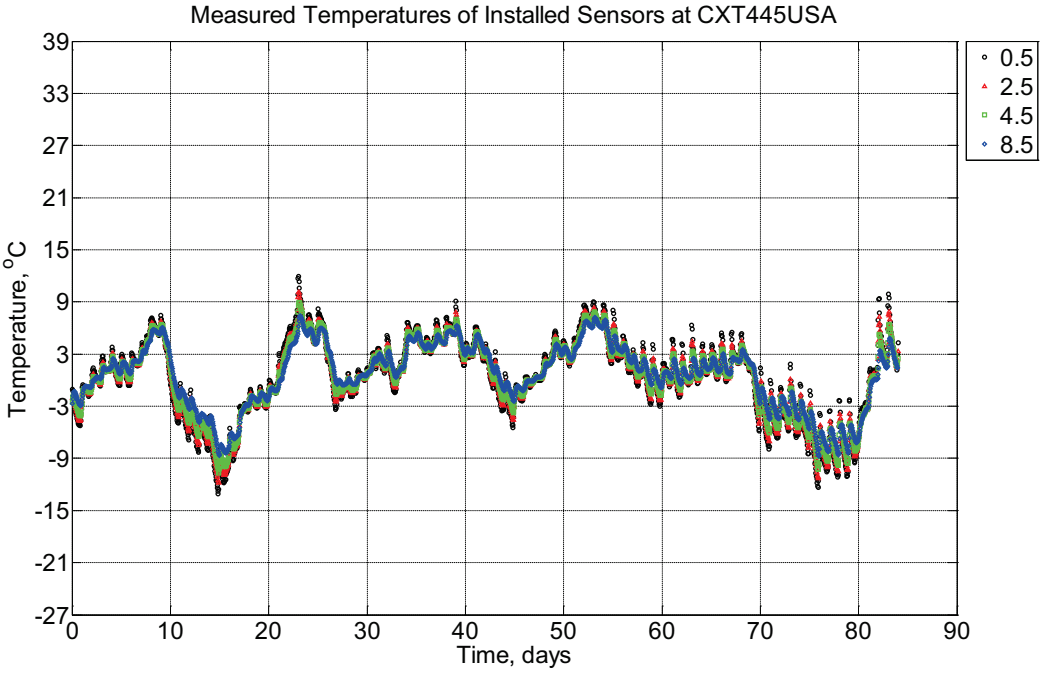

Figure B-818 Measured temperature at depths of 0.5 inches (12.7 mm), 2.5 inches (63.5 mm), 4.5 inches (114.3 mm), and 8.5 inches (215.9 mm) from the surface of a concrete

crosstie (labeled CXT445USA) installed in track near Lytton, BC, between November 22, 2013, through February 14, 2014. An 8 mm thick polyurethane pad and steel rail are additionally installed atop the concrete crosstie.

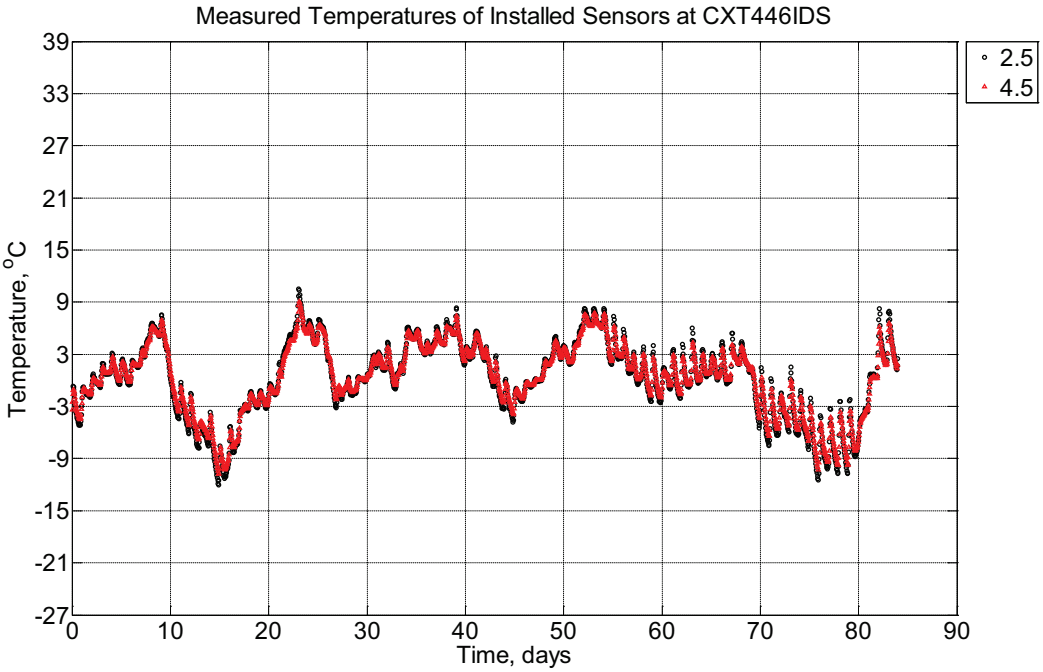

Figure B-819 Measured temperature at depths of 2.5 inches (63.5 mm) and 4.5 inches (114.3 mm) from the surface of a concrete crosstie (labeled CXT446IDS) installed in track near Lytton, BC, between November 22, 2013, through February 14, 2014. An 8 mm thick polyurethane pad and steel rail are additionally installed atop the concrete crosstie.

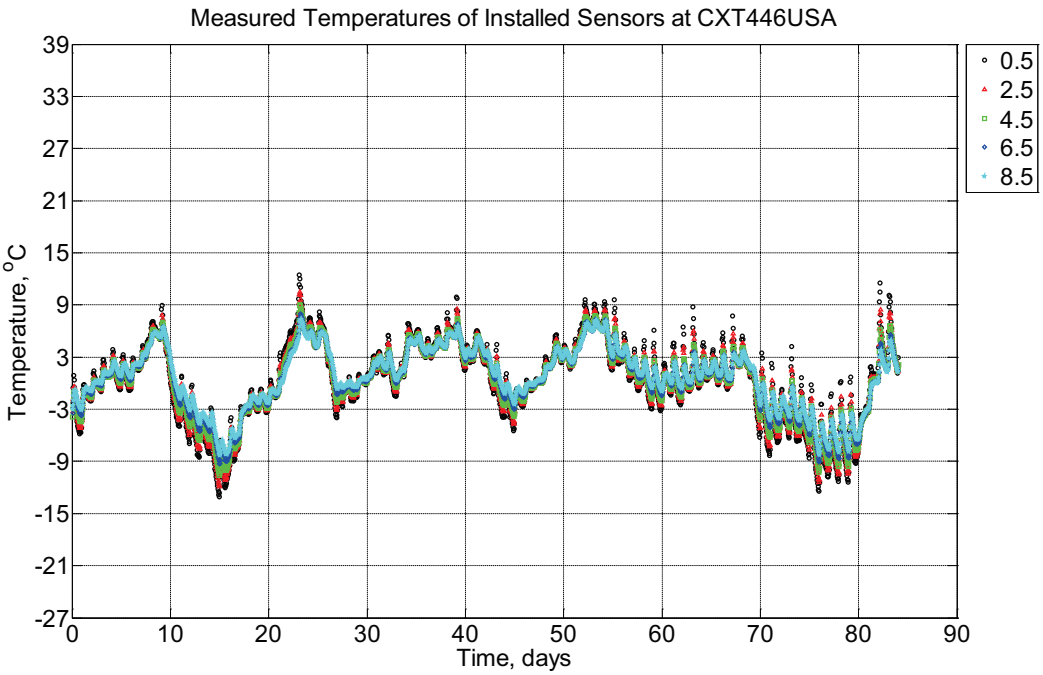

Figure B-820 Measured temperature at depths of 0.5 inches (12.7 mm), 2.5 inches (63.5 mm), 4.5 inches (114.3 mm), 6.5 inches (139.7 mm), and 8.5 inches (215.9 mm) from the surface of a concrete crosstie (labeled CXT446USA) installed in track near Lytton, BC, between November 22, 2013, through February 14, 2014. An 8 mm thick polyurethane pad and steel rail are additionally installed atop the concrete crosstie.

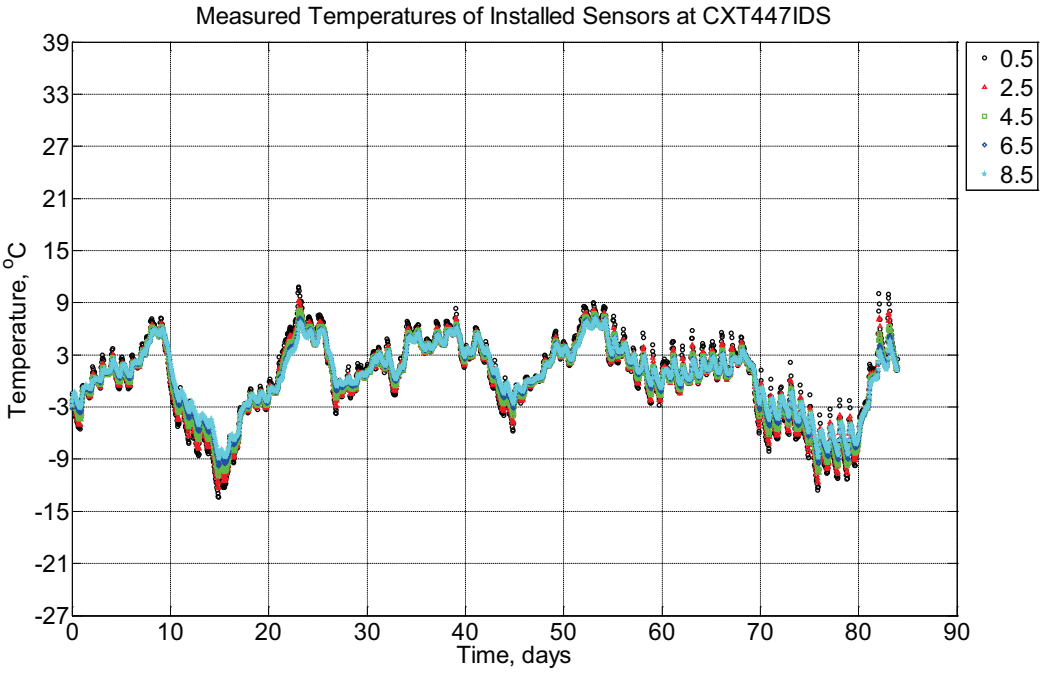

Figure B-821 Measured temperature at depths of 0.5 inches (12.7 mm), 2.5 inches (63.5

mm), 4.5 inches (114.3 mm), 6.5 inches (139.7 mm), and 8.5 inches (215.9 mm) from the surface of a concrete crosstie (labeled CXT447IDS) installed in track near Lytton, BC, between November 22, 2013, through Febraury 14, 2014. An 8 mm thick polyurethane pad and steel rail are additionally installed atop the concrete crosstie.

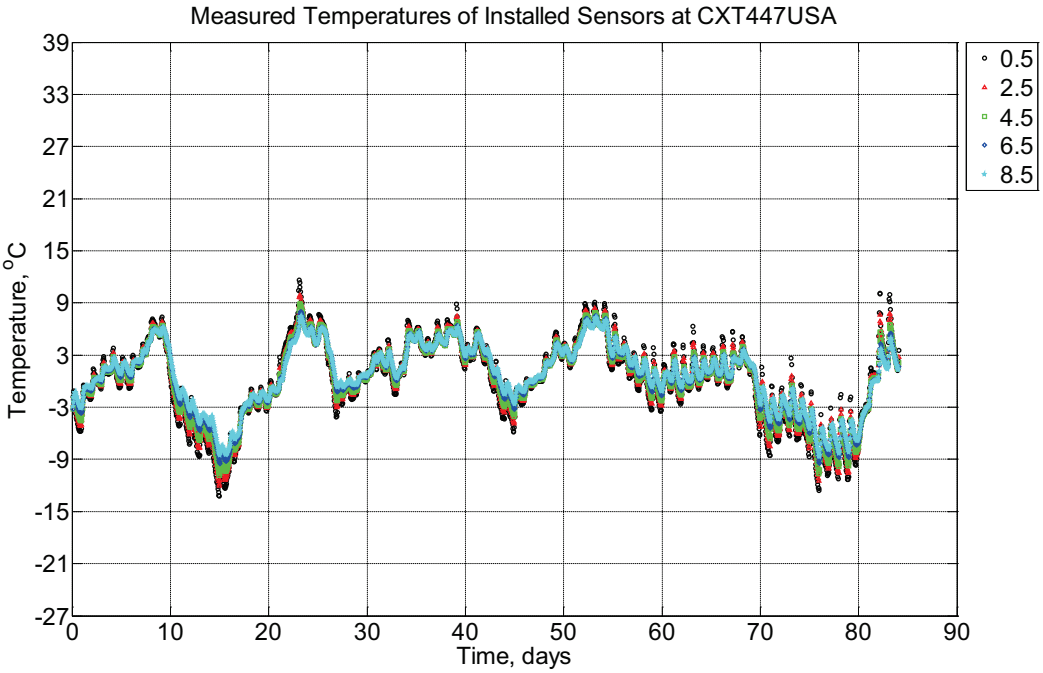

Figure B-822 Measured temperature at depths of 0.5 inches (12.7 mm), 2.5 inches (63.5 mm), 4.5 inches (114.3 mm), 6.5 inches (139.7 mm), and 8.5 inches (215.9 mm) from the surface of a concrete crosstie (labeled CXT447USA) installed in track near Lytton, BC, between November 22, 2013, through February 14, 2014. An 8 mm thick polyurethane pad and steel rail are additionally installed atop the concrete crosstie.

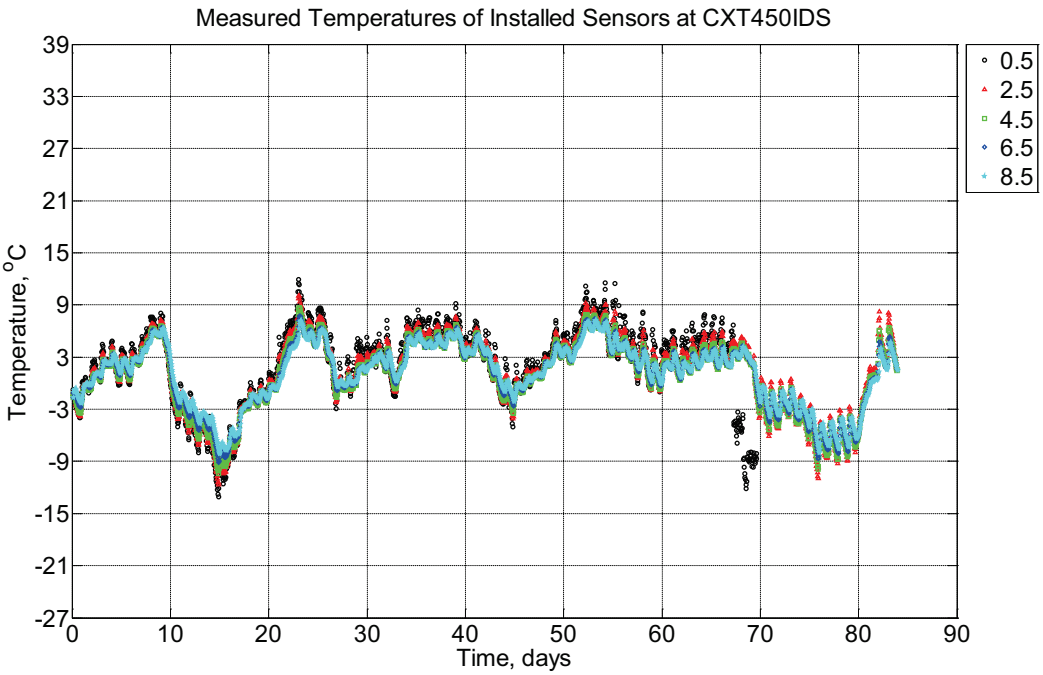

Figure B-823 Measured temperature at depths of 0.5 inches (12.7 mm), 2.5 inches (63.5 mm), 4.5 inches (114.3 mm), 6.5 inches (139.7 mm), and 8.5 inches (215.9 mm) from the surface of a concrete crosstie (labeled CXT450IDS) installed in track near Lytton, BC, between November 22, 2013, through February 14, 2014. An 8 mm thick polyurethane pad and steel rail are additionally installed atop the concrete crosstie.

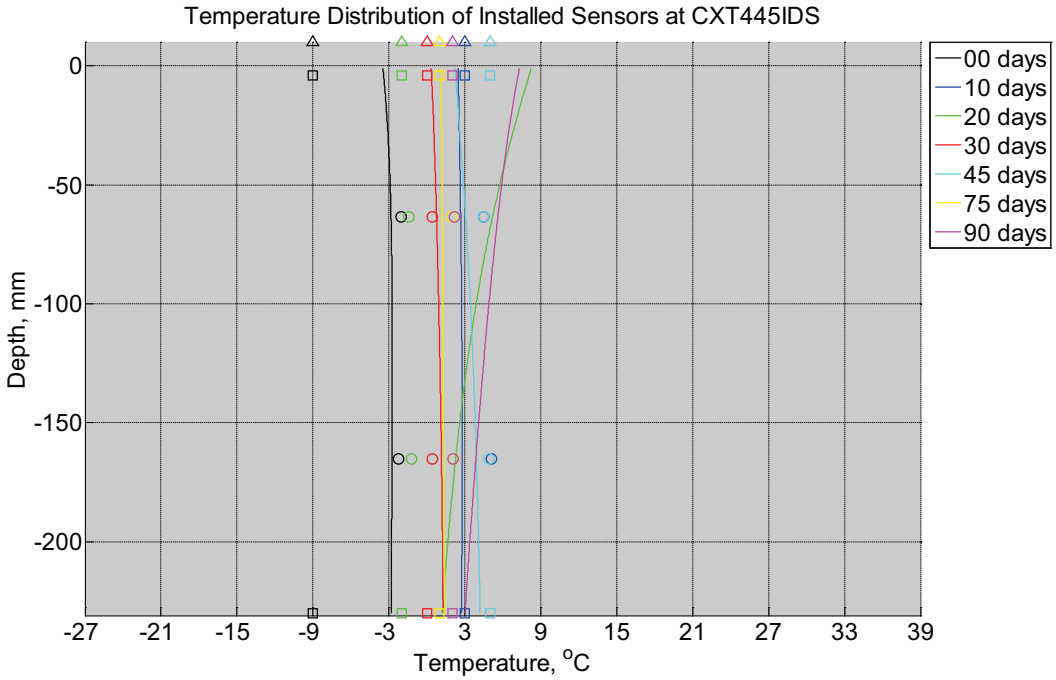

Figure B-824 Measured (markers) and modeled (continuous line) temperature profile

distribution as a function of depth inside a concrete crosstie (labeled CXT445IDS) installed in track near Lytton, BC, between November 22, 2013, through February 14, 2014. An 8 mm thick polyurethane pad and steel rail are additionally installed atop the concrete crosstie. The model does not incorporate a polyurethane pad nor steel rail line. Triangular markers denote temperature value from CWLY weather station, square markers denote assumed temperature values in ballast, and circular markers denote measured temperature values inside concrete.

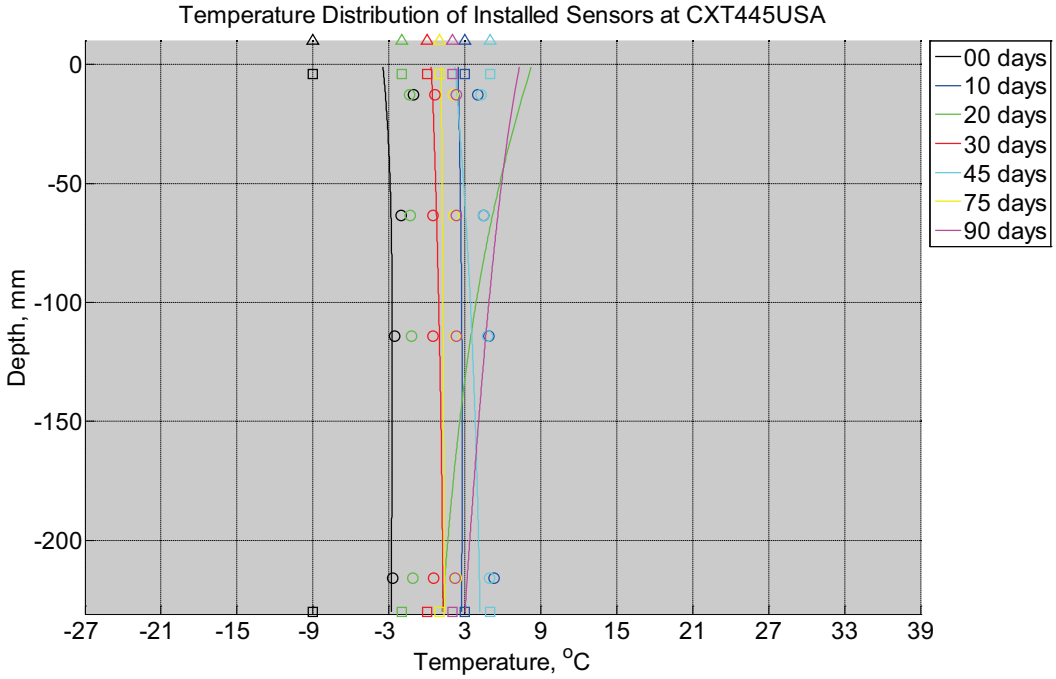

Figure B-825 Measured (markers) and modeled (continuous line) temperature profile distribution as a function of depth inside a concrete crosstie (labeled CXT445USA) installed in track near Lytton, BC, between November 22, 2013, through February 14, 2014. An 8 mm thick polyurethane pad and steel rail are additionally installed atop the concrete crosstie. The model does not incorporate a polyurethane pad nor steel rail line. Triangular markers denote temperature value from CWLY weather station, square markers denote assumed temperature values in ballast, and circular markers denote measured temperature values inside concrete.

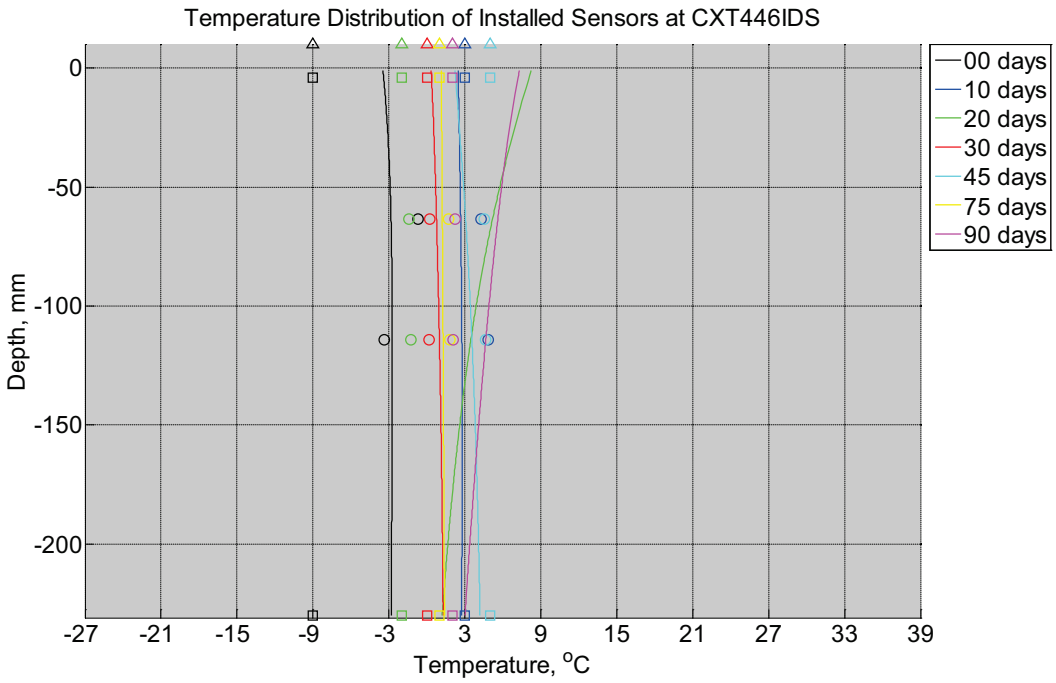

Figure B-826 Measured (markers) and modeled (continuous line) temperature profile distribution as a function of depth inside a concrete crosstie (labeled CXT446IDS) installed in track near Lytton, BC, between November 22, 2013, through February 14, 2014. An 8 mm thick polyurethane pad and steel rail are additionally installed atop the concrete crosstie. The model does not incorporate a polyurethane pad nor steel rail line. Triangular markers denote temperature value from CWLY weather station, square markers denote assumed temperature values in ballast, and circular markers denote measured temperature values inside concrete.

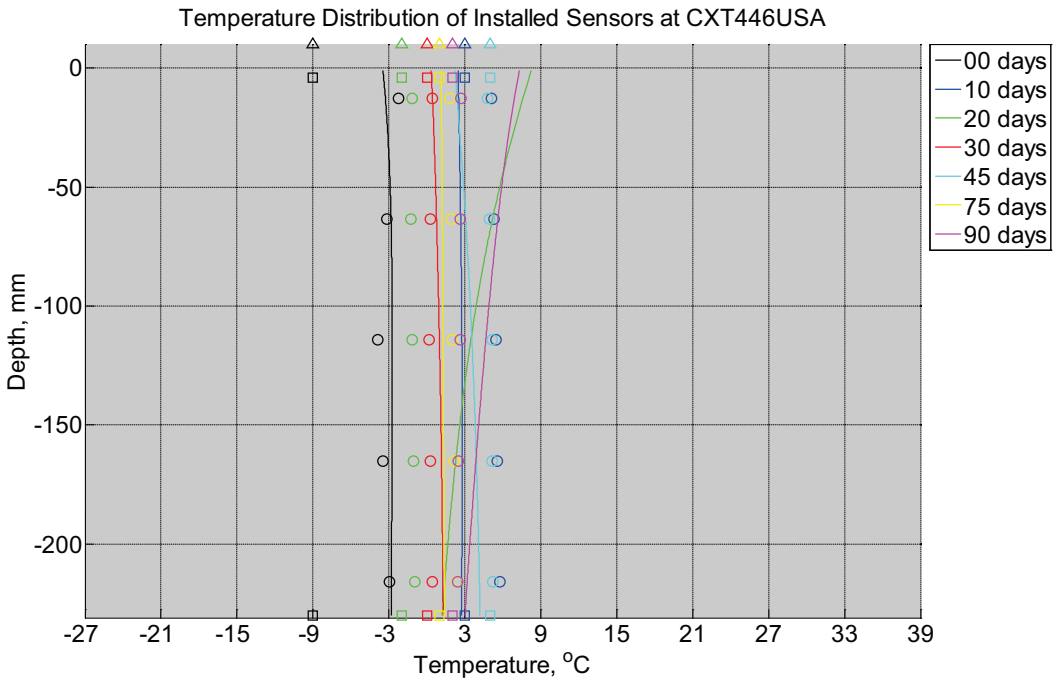

Figure B-827 Measured (markers) and modeled (continuous line) temperature profile distribution as a function of depth inside a concrete crosstie (labeled CXT446USA) installed in track near Lytton, BC, between November 22, 2013, through February 14, 2014. An 8 mm thick polyurethane pad and steel rail are additionally installed atop the concrete crosstie. The model does not incorporate a polyurethane pad nor steel rail line. Triangular markers denote temperature value from CWLY weather station, square markers denote assumed temperature values in ballast, and circular markers denote measured temperature values inside concrete.

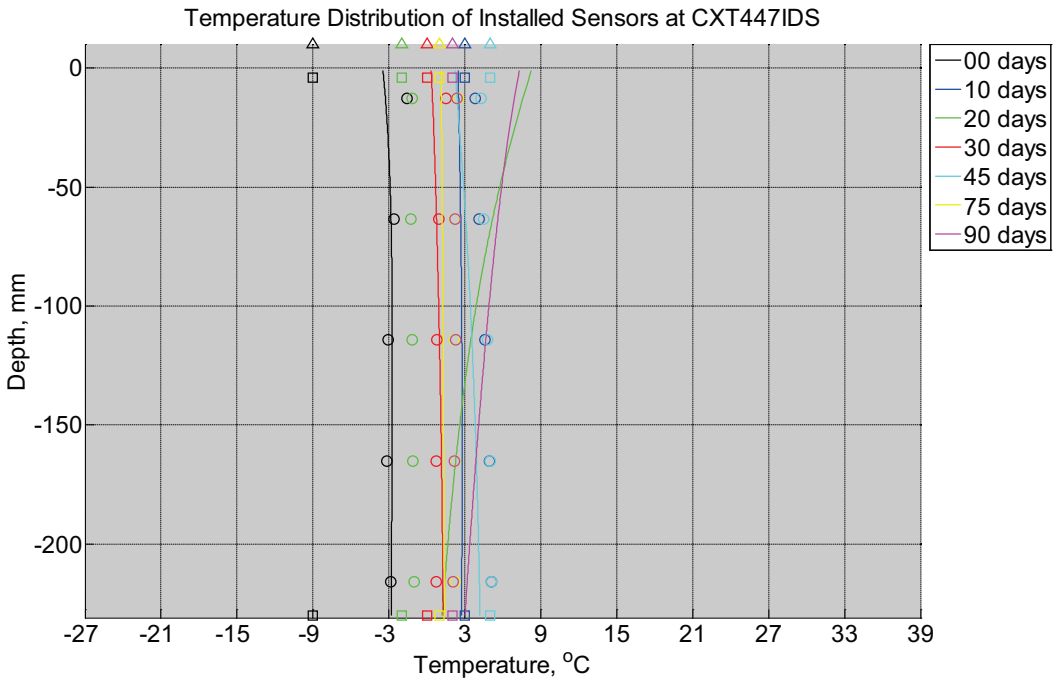

Figure B-828 Measured (markers) and modeled (continuous line) temperature profile distribution as a function of depth inside a concrete crosstie (labeled CXT447IDS) installed in track near Lytton, BC, between November 22, 2013, through February 14, 2014. An 8 mm thick polyurethane pad and steel rail are additionally installed atop the concrete crosstie. The model does not incorporate a polyurethane pad nor steel rail line. Triangular markers denote temperature value from CWLY weather station, square markers denote assumed temperature values in ballast, and circular markers denote measured temperature values inside concrete.

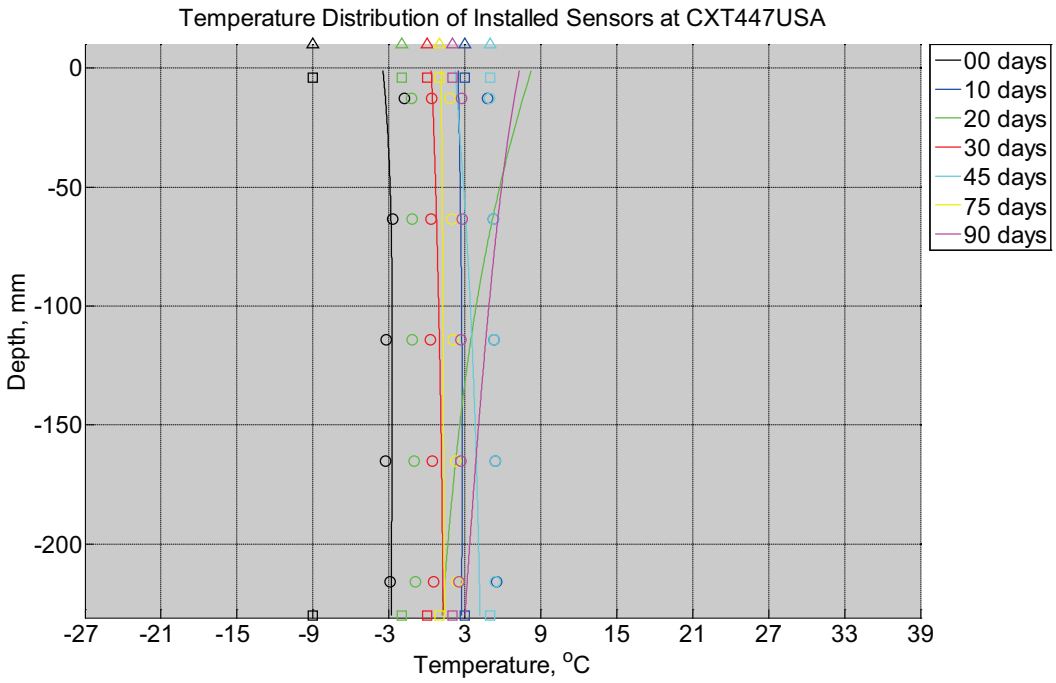

Figure B-829 Measured (markers) and modeled (continuous line) temperature profile distribution as a function of depth inside a concrete crosstie (labeled CXT447USA) installed in track near Lytton, BC, between November 22, 2013, through February 14, 2014. An 8 mm thick polyurethane pad and steel rail are additionally installed atop the concrete crosstie. The model does not incorporate a polyurethane pad nor steel rail line. Triangular markers denote temperature value from CWLY weather station, square markers denote assumed temperature values in ballast, and circular markers denote measured temperature values inside concrete.

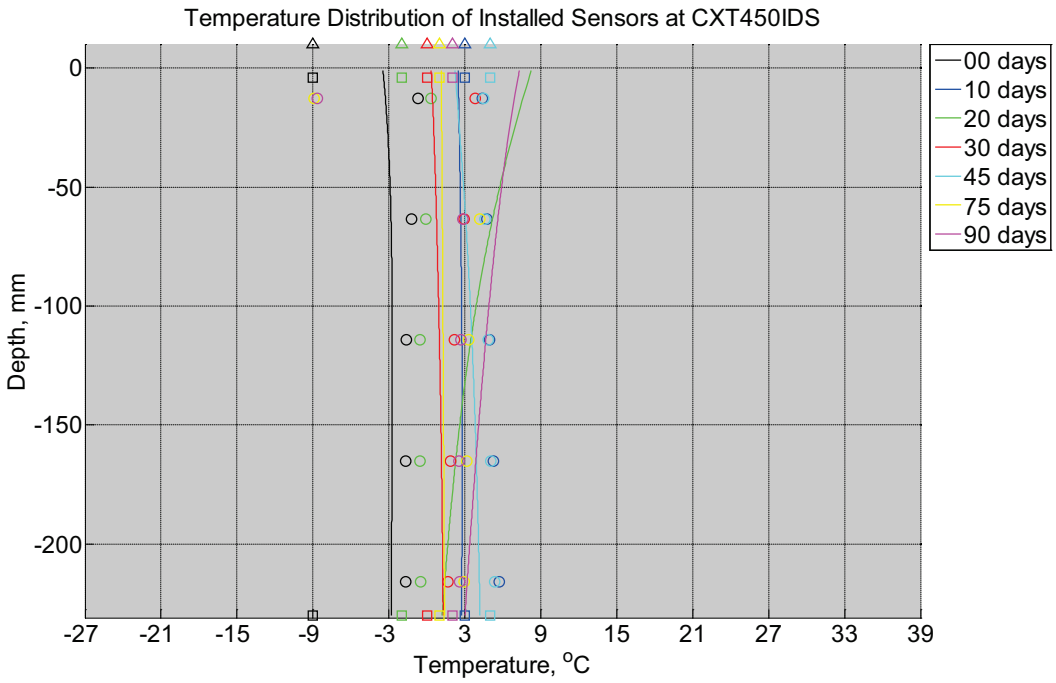

Figure B-830 Measured (markers) and modeled (continuous line) temperature profile distribution as a function of depth inside a concrete crosstie (labeled CXT450IDS) installed in track near Lytton, BC, between November 22, 2013, through February 14, 2014. An 8 mm thick polyurethane pad and steel rail are additionally installed atop the concrete crosstie. The model does not incorporate a polyurethane pad nor steel rail line. Triangular markers denote temperature value from CWLY weather station, square markers denote assumed temperature values in ballast, and circular markers denote measured temperature values inside concrete.

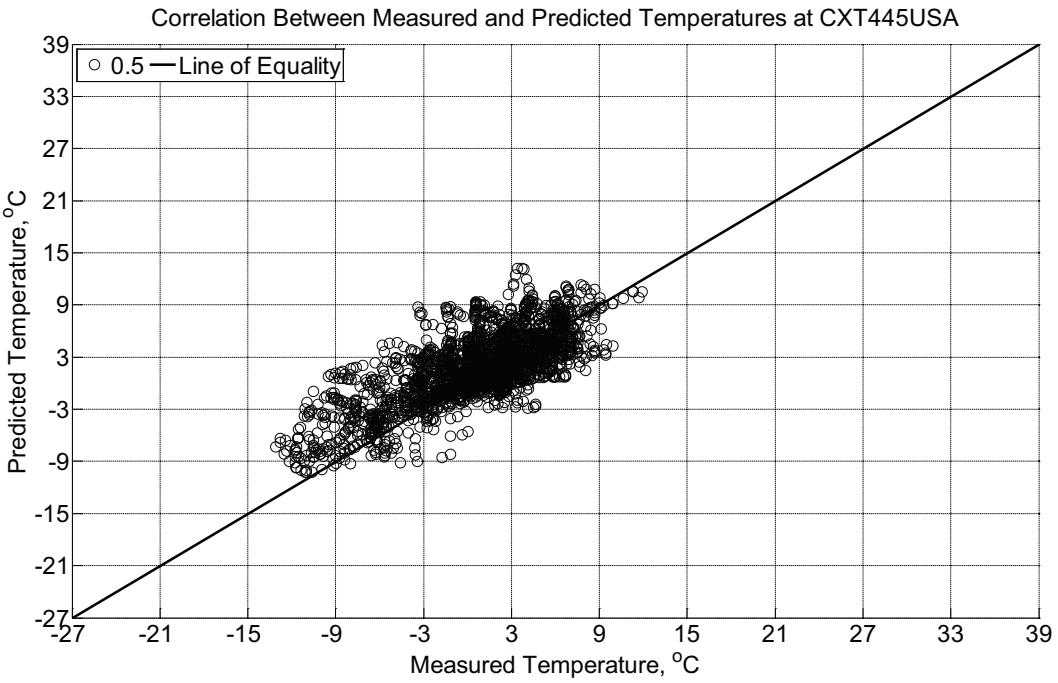

Figure B-831 Correlation between measured and predicted temperature values 0.5 inches (12.7 mm) from the surface of a concrete crosstie (labeled CXT445USA) installed in track near Lytton, BC, between November 22, 2013, through February 14, 2014. An 8 mm thick polyurethane pad and steel rail are additionally installed atop the concrete crosstie. The model does not incorporate a polyurethane pad nor steel rail line.

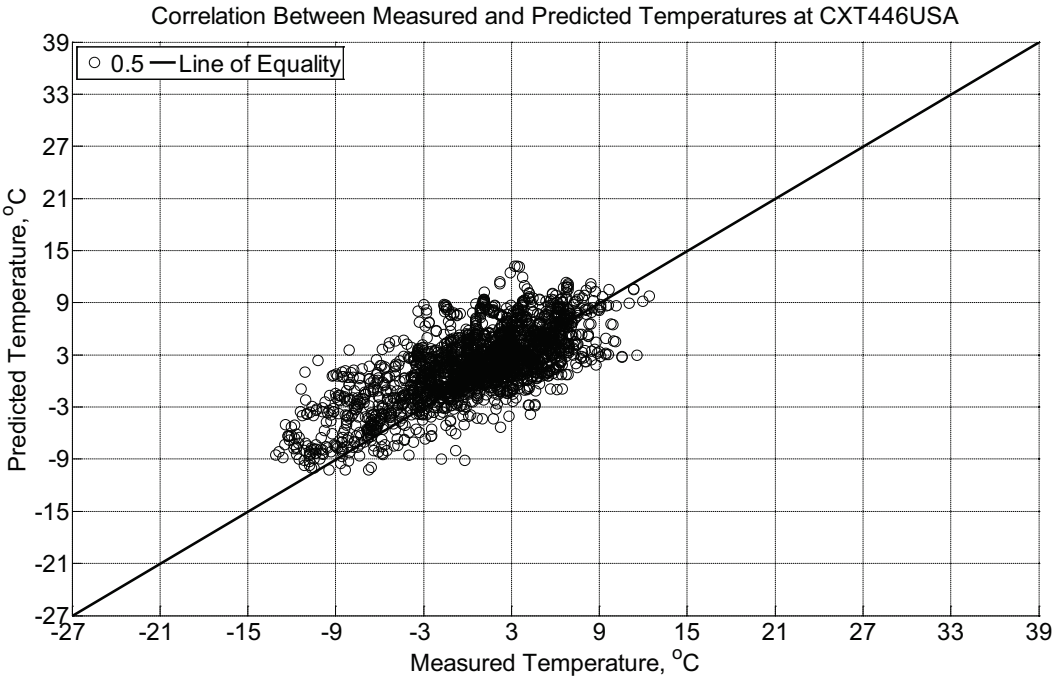

Figure B-832 Correlation between measured and predicted temperature values 0.5 inches

(12.7 mm) from the surface of a concrete crosstie (labeled CXT446USA) installed in track near Lytton, BC, between November 22, 2013, through February 14, 2014. An 8 mm thick polyurethane pad and steel rail are additionally installed atop the concrete crosstie. The model does not incorporate a polyurethane pad nor steel rail line.

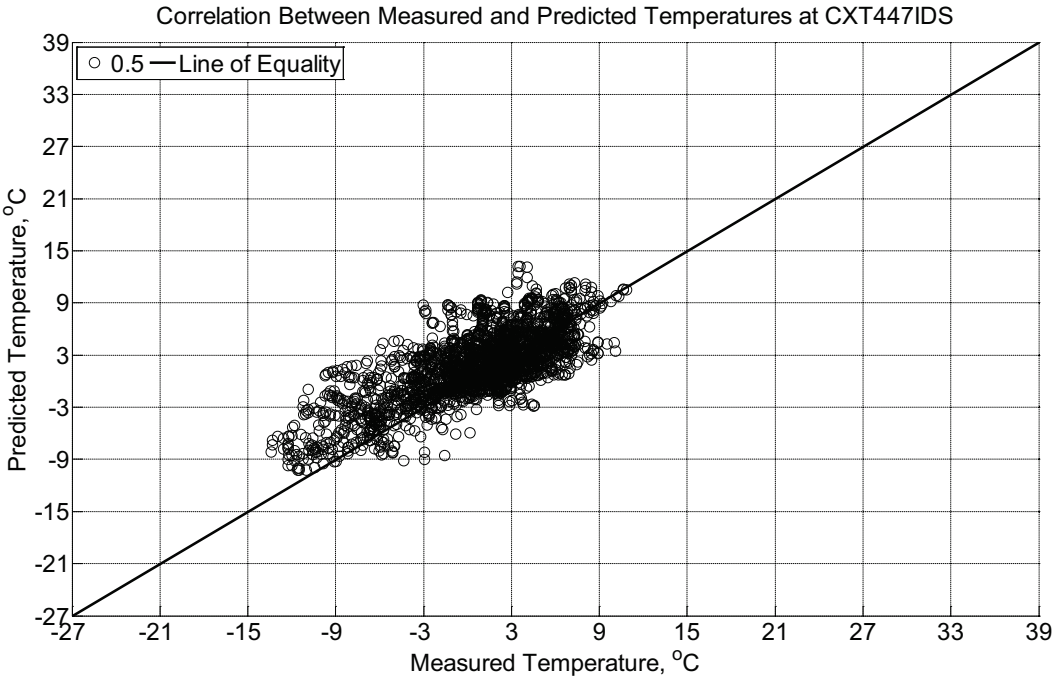

Figure B-833 Correlation between measured and predicted temperature values 0.5 inches (12.7 mm) from the surface of a concrete crosstie (labeled CXT447IDS) installed in track near Lytton, BC, between November 22, 2013, through February 14, 2014. An 8 mm thick polyurethane pad and steel rail are additionally installed atop the concrete crosstie. The model does not incorporate a polyurethane pad nor steel rail line.

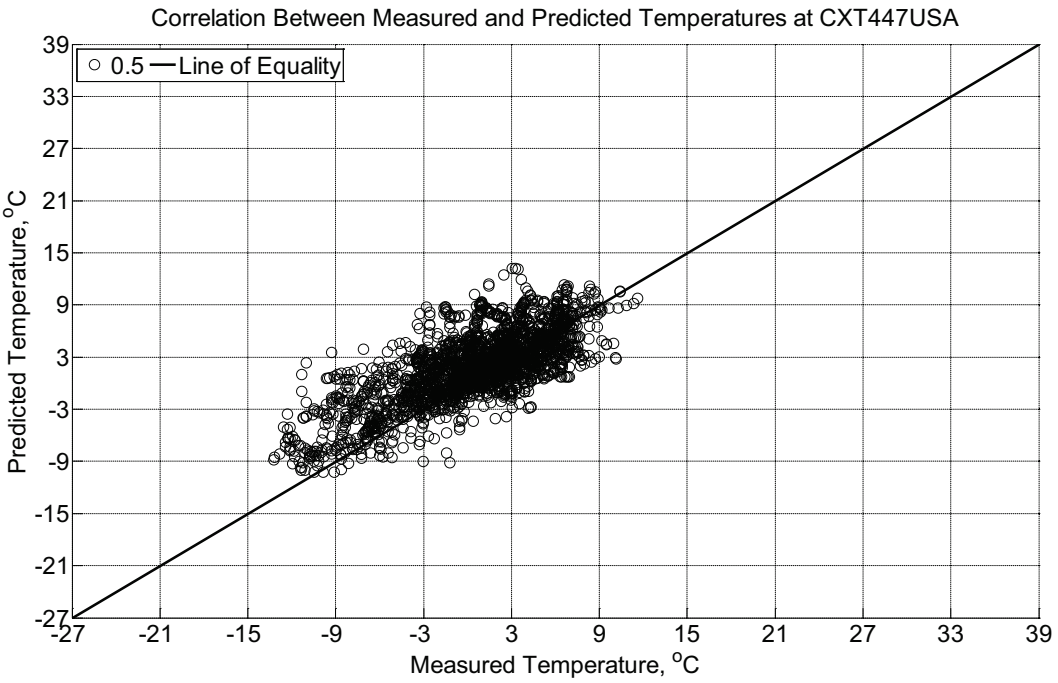

Figure B-834 Correlation between measured and predicted temperature values 0.5 inches (12.7 mm) from the surface of a concrete crosstie (labeled CXT447USA) installed in track near Lytton, BC, between November 22, 2013, through February 14, 2014. An 8 mm thick polyurethane pad and steel rail are additionally installed atop the concrete crosstie. The model does not incorporate a polyurethane pad nor steel rail line.

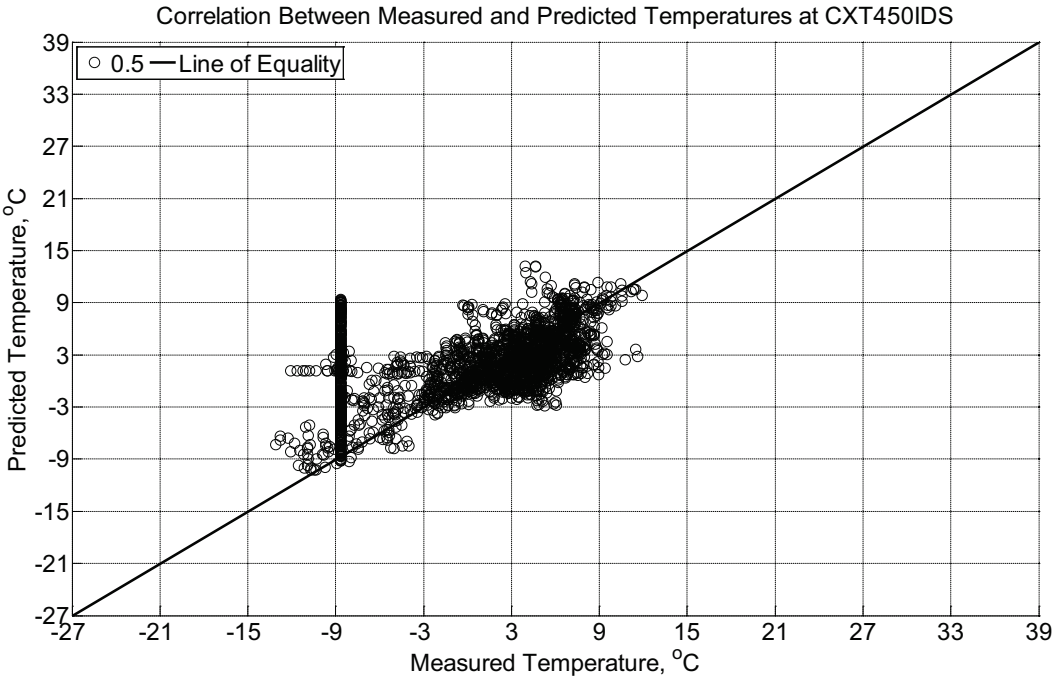

Figure B-835 Correlation between measured and predicted temperature values 0.5 inches

(12.7 mm) from the surface of a concrete crosstie (labeled CXT450IDS) installed in track near Lytton, BC, between November 22, 2013, through February 14, 2014. An 8 mm thick polyurethane pad and steel rail are additionally installed atop the concrete crosstie. The model does not incorporate a polyurethane pad nor steel rail line.

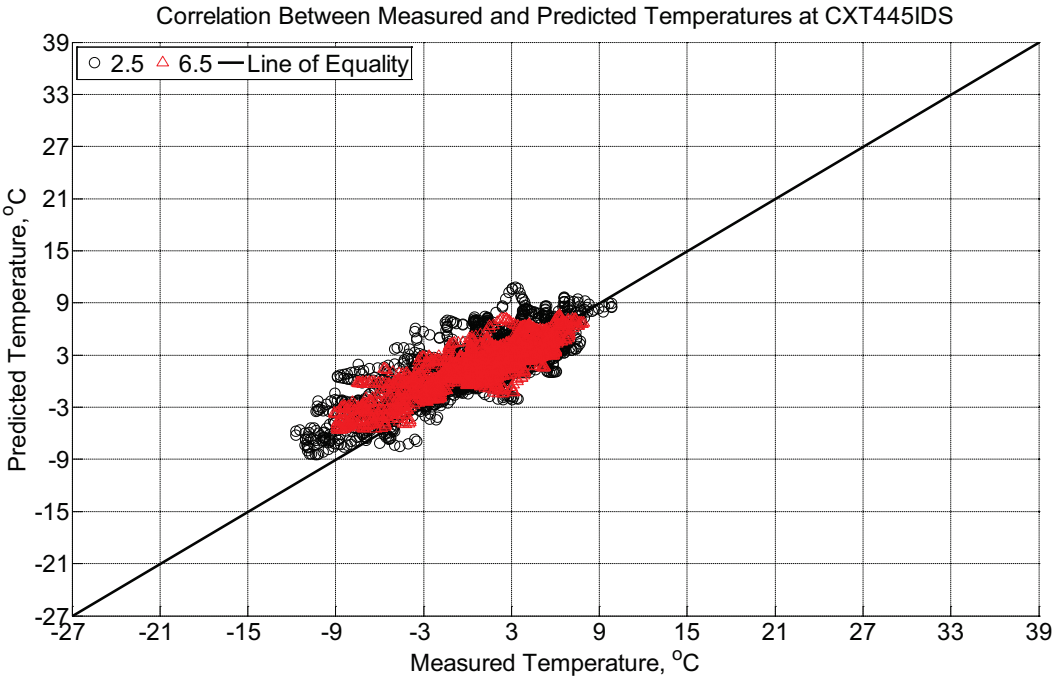

Figure B-836 Correlation between measured and predicted temperature values 2.5 inches (63.5 mm) and 6.5 inches (139.7 mm) from the surface of a concrete crosstie (labeled CXT446IDS) installed in track near Lytton, BC, between November 22, 2013, through February 14, 2014. An 8 mm thick polyurethane pad and steel rail are additionally installed atop the concrete crosstie. The model does not incorporate a polyurethane pad nor steel rail line.

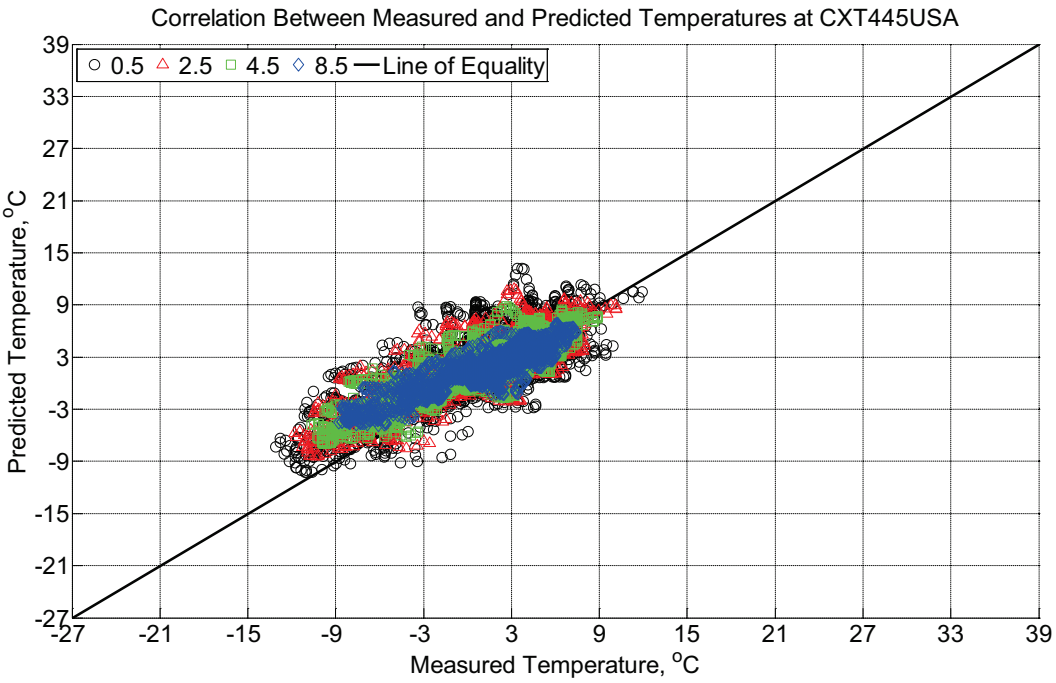

Figure B-837 Correlation between measured and predicted temperature values 0.5 inches (12.7 mm), 2.5 inches (63.5 mm), 4.5 inches (114.3 mm), and 8.5 inches (215.9 mm) from the surface of a concrete crosstie (labeled CXT445USA) installed in track near Lytton, BC, between November 22, 2013, through February 14, 2014. An 8 mm thick polyurethane pad and steel rail are additionally installed atop the concrete crosstie. The model does not incorporate a polyurethane pad nor steel rail line.

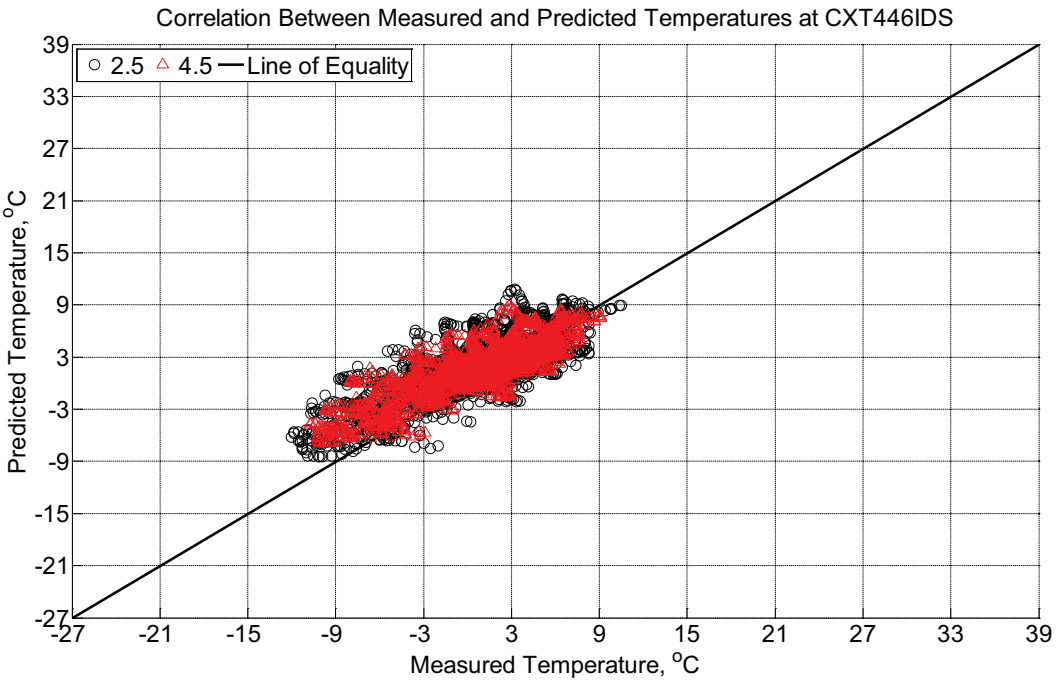

Figure B-838 Correlation between measured and predicted temperature values 2.5 inches (63.5 mm) and 4.5 inches (114.3 mm) from the surface of a concrete crosstie (labeled CXT446IDS) installed in track near Lytton, BC, between November 22, 2013, through February 14, 2014. An 8 mm thick polyurethane pad and steel rail are additionally installed atop the concrete crosstie. The model does not incorporate a polyurethane pad nor steel rail line.

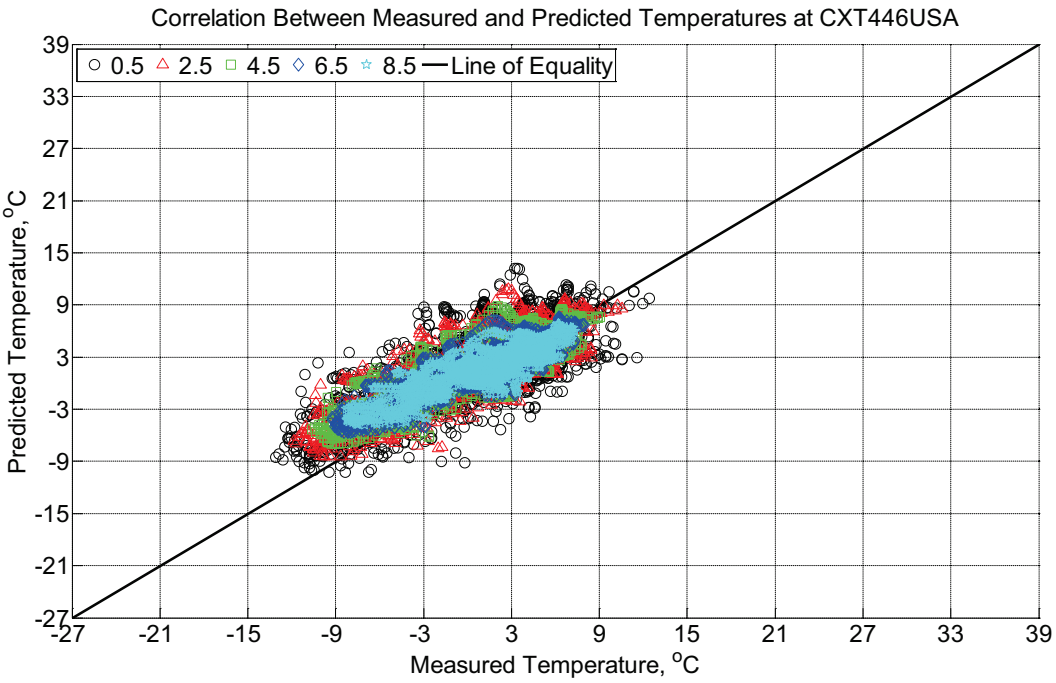

Figure B-839 Correlation between measured and predicted temperature values 0.5 inches (12.7 mm), 2.5 inches (63.5 mm), 4.5 inches (114.3 mm), 6.5 inches (139.7 mm), and 8.5 inches (215.9 mm) from the surface of a concrete crosstie (labeled CXT446USA) installed in track near Lytton, BC, between November 22, 2013, through February 14, 2014. An 8 mm thick polyurethane pad and steel rail are additionally installed atop the concrete crosstie. The model does not incorporate a polyurethane pad nor steel rail line.

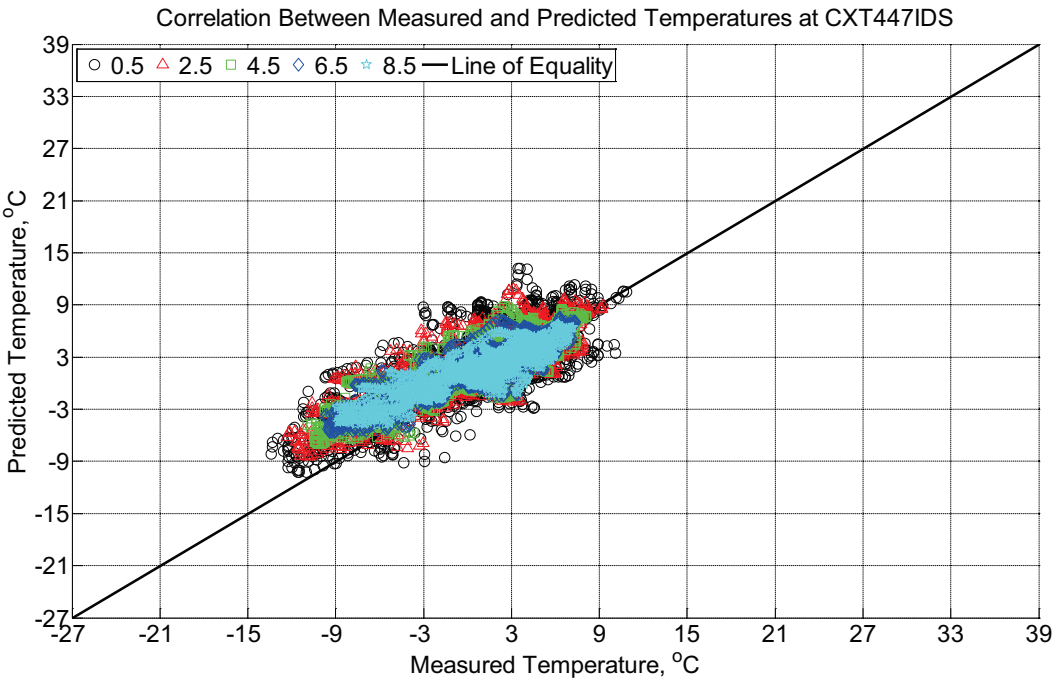

Figure B-840 Correlation between measured and predicted temperature values 0.5 inches (12.7 mm), 2.5 inches (63.5 mm), 4.5 inches (114.3 mm), 6.5 inches (139.7 mm), and 8.5 inches (215.9 mm) from the surface of a concrete crosstie (labeled CXT447IDS) installed in track near Lytton, BC, between November 22, 2013, through February 14, 2014. An 8 mm thick polyurethane pad and steel rail are additionally installed atop the concrete crosstie. The model does not incorporate a polyurethane pad nor steel rail line.

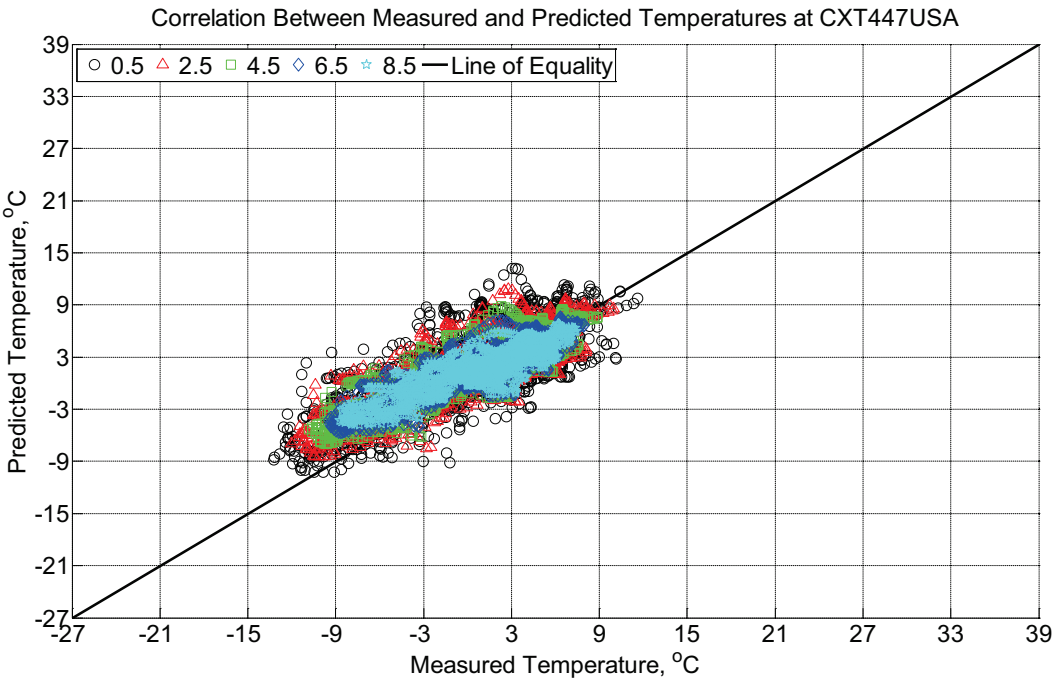

Figure B-841 Correlation between measured and predicted temperature values 0.5 inches (12.7 mm), 2.5 inches (63.5 mm), 4.5 inches (114.3 mm), 6.5 inches (139.7 mm), and 8.5 inches (215.9 mm) from the surface of a concrete crosstie (labeled CXT447USA) installed in track near Lytton, BC, between November 22, 2013, through February 14, 2014. An 8 mm thick polyurethane pad and steel rail are additionally installed atop the concrete crosstie. The model does not incorporate a polyurethane pad nor steel rail line.

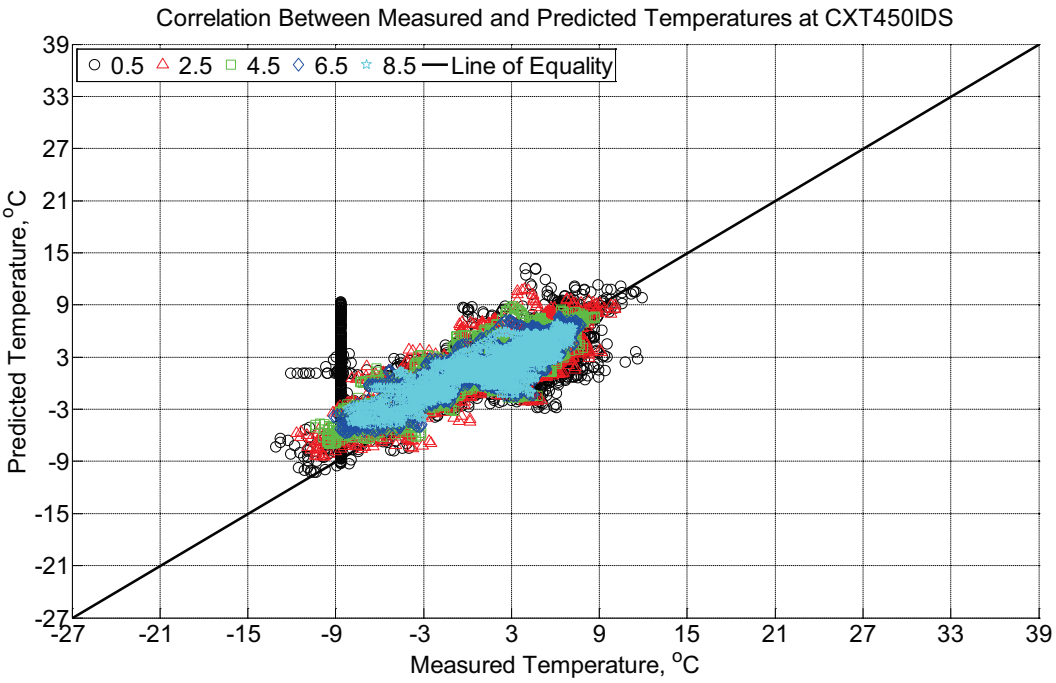

Figure B-842 Correlation between measured and predicted temperature values 0.5 inches (12.7 mm), 2.5 inches (63.5 mm), 4.5 inches (114.3 mm), 6.5 inches (139.7 mm), and 8.5 inches (215.9 mm) from the surface of a concrete crosstie (labeled CXT450IDS) installed in track near Lytton, BC, between November 22, 2013, through February 14, 2014. An 8 mm thick polyurethane pad and steel rail are additionally installed atop the concrete crosstie. The model does not incorporate a polyurethane pad nor steel rail line.

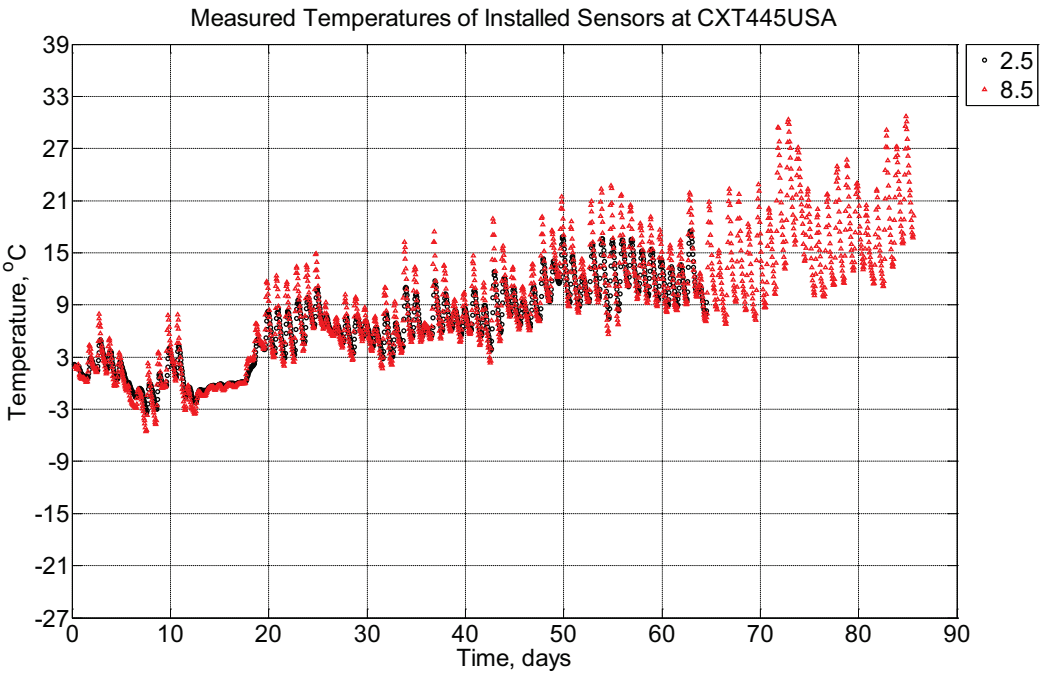

Figure B-843 Measured temperature at depths 2.5 inches (63.5 mm) and 8.5 inches (215.9 mm) from the surface of a concrete crosstie (labeled CXT445USA) installed in track near Lytton, BC, between February 18, 2014, through Mayy 14, 2014. An 8 mm thick polyurethane pad and steel rail are additionally installed atop the concrete crosstie.

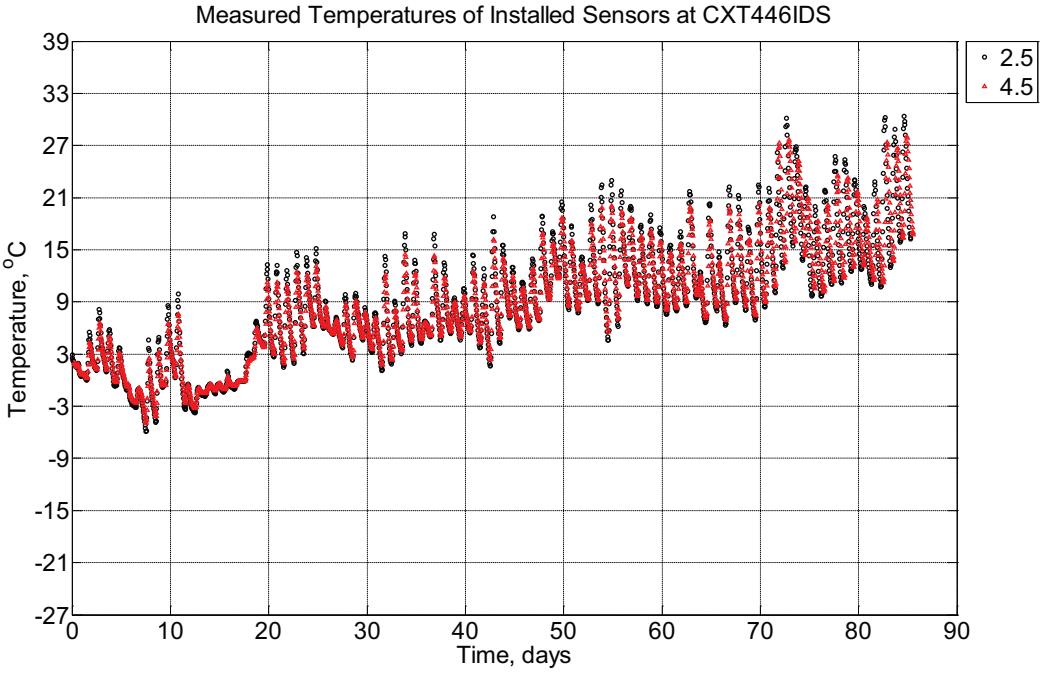

Figure B-844 Measured temperature at depths of 2.5 inches (63.5 mm) and 4.5 inches (114.3 mm) from the surface of a concrete crosstie (labeled CXT446IDS) installed in track

near Lytton, BC, between February 18, 2014, through May 14, 2014. An 8 mm thick polyurethane pad and steel rail are additionally installed atop the concrete crosstie.

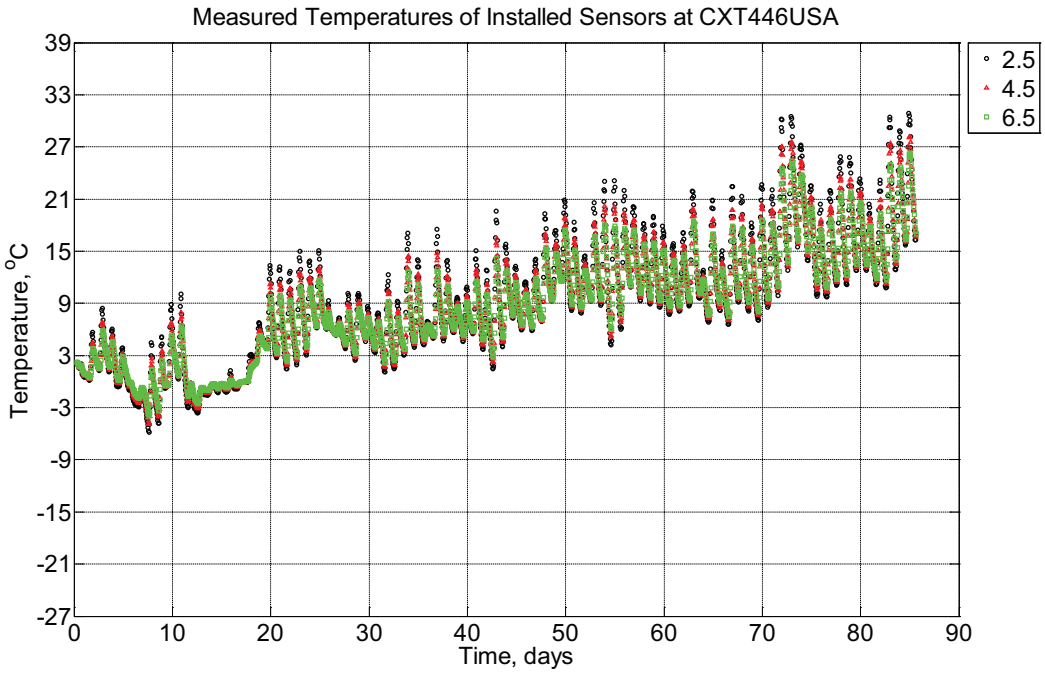

Figure B-845 Measured temperature at depths of 2.5 inches (63.5 mm), 4.5 inches (114.3 mm), and 6.5 inches (139.7 mm) from the surface of a concrete crosstie (labeled CXT446USA) installed in track near Lytton, BC, between February 18, 2014, through May 14, 2014. An 8 mm thick polyurethane pad and steel rail are additionally installed atop the concrete crosstie.

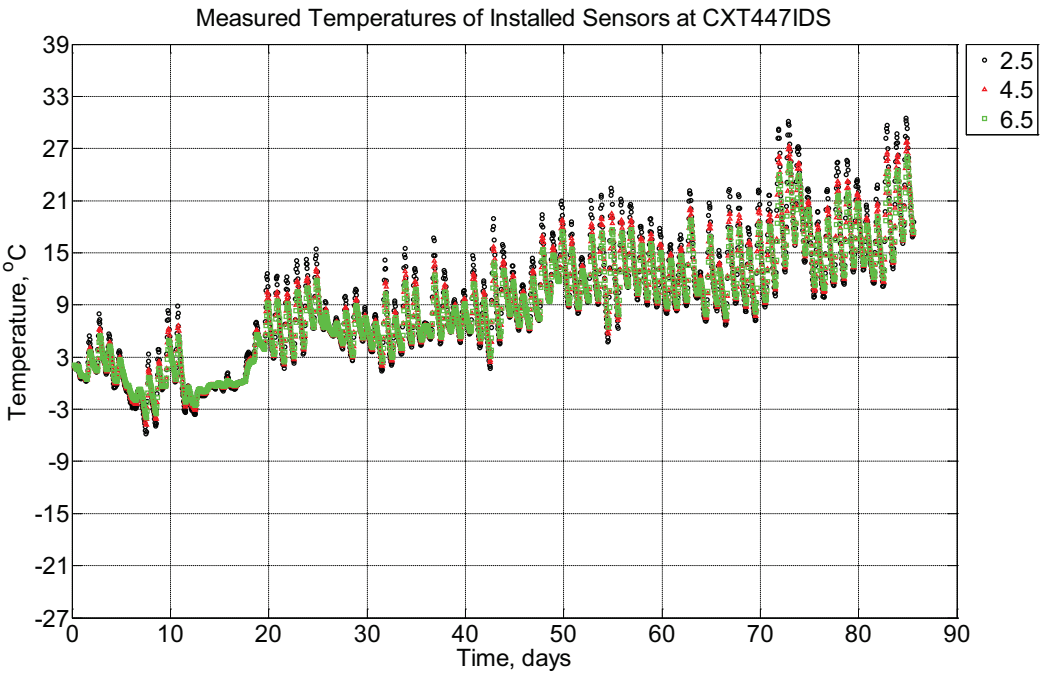

Figure B-846 Measured temperature at depths of 2.5 inches (63.5 mm), 4.5 inches (114.3 mm), and 6.5 inches (139.7 mm) from the surface of a concrete crosstie (labeled CXT447IDS) installed in track near Lytton, BC, between February 18, 2014, through May 14, 2014. An 8 mm thick polyurethane pad and steel rail are additionally installed atop the concrete crosstie.

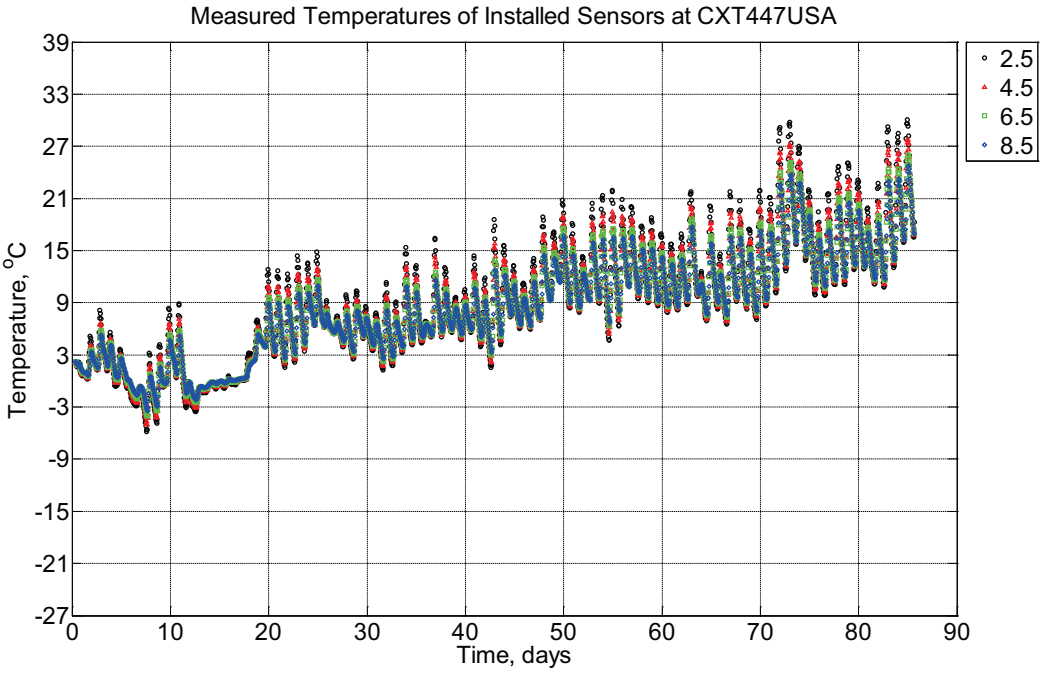

Figure B-847 Measured temperature at depths of 2.5 inches (63.5 mm), 4.5 inches (114.3

mm), 6.5 inches (139.7 mm), and 8.5 inches (215.9 mm) from the surface of a concrete crosstie (labeled CXT447USA) installed in track near Lytton, BC, between February 18, 2014, through May 14, 2014. An 8 mm thick polyurethane pad and steel rail are additionally installed atop the concrete crosstie.

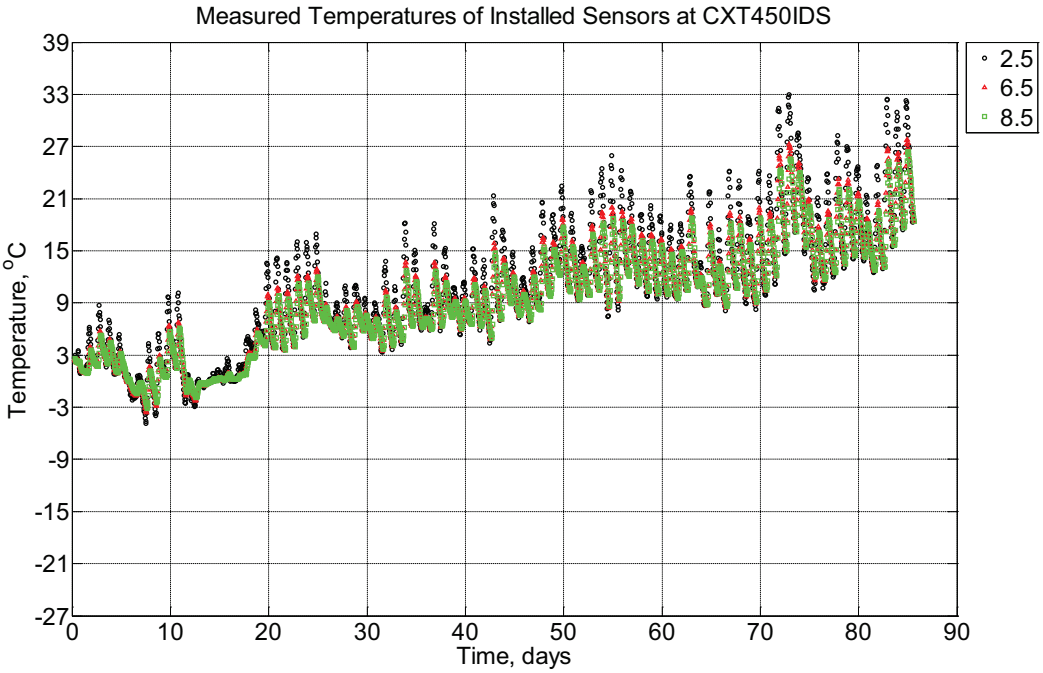

Figure B-848 Measured temperature at depths of 2.5 inches (63.5 mm), 6.5 inches (139.7 mm), and 8.5 inches (215.9 mm) from the surface of a concrete crosstie (labeled CXT450IDS) installed in track near Lytton, BC, between February 18, 2014, through May 14, 2014. An 8 mm thick polyurethane pad and steel rail are additionally installed atop the concrete crosstie.

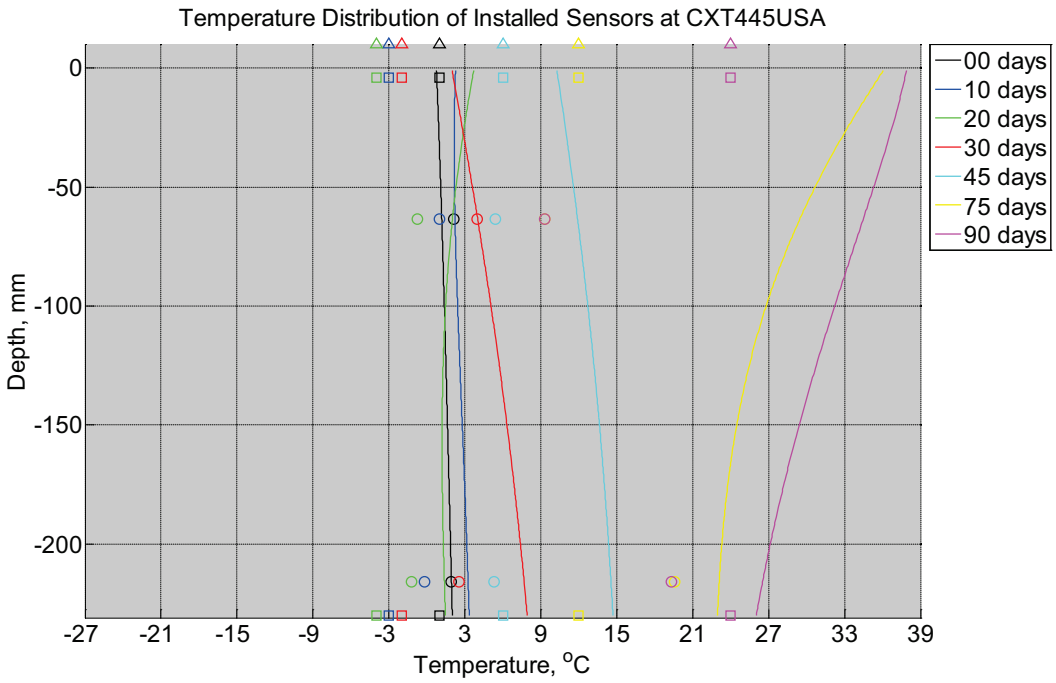

Figure B-849 Measured (markers) and modeled (continuous line) temperature profile distribution as a function of depth inside a concrete crosstie (labeled CXT445USA) installed in track near Lytton, BC, between February 18, 2014, through May 14, 2014. An 8 mm thick polyurethane pad and steel rail are additionally installed atop the concrete crosstie. The model does not incorporate a polyurethane pad nor steel rail line. Triangular markers denote temperature value from CWLY weather station, square markers denote assumed temperature values in ballast, and circular markers denote measured temperature values inside concrete.

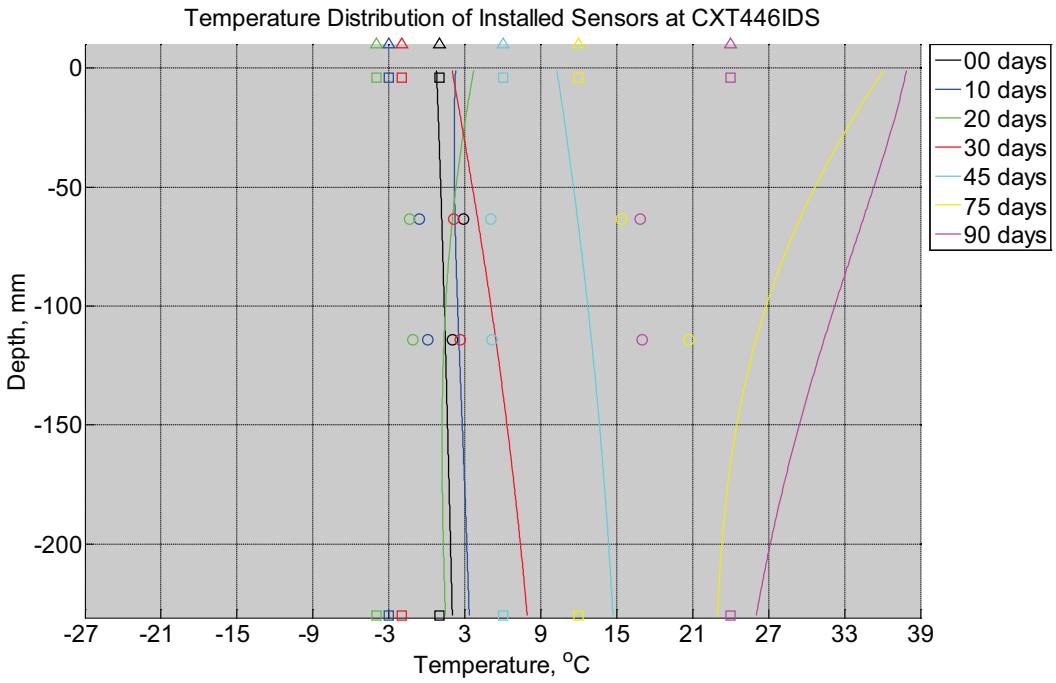

Figure B-850 Measured (markers) and modeled (continuous line) temperature profile distribution as a function of depth inside a concrete crosstie (labeled CXT446IDS) installed in track near Lytton, BC, between February 18, 2014, through May 14, 2014. An 8 mm thick polyurethane pad and steel rail are additionally installed atop the concrete crosstie. The model does not incorporate a polyurethane pad nor steel rail line. Triangular markers denote temperature value from CWLY weather station, square markers denote assumed temperature values in ballast, and circular markers denote measured temperature values inside concrete.

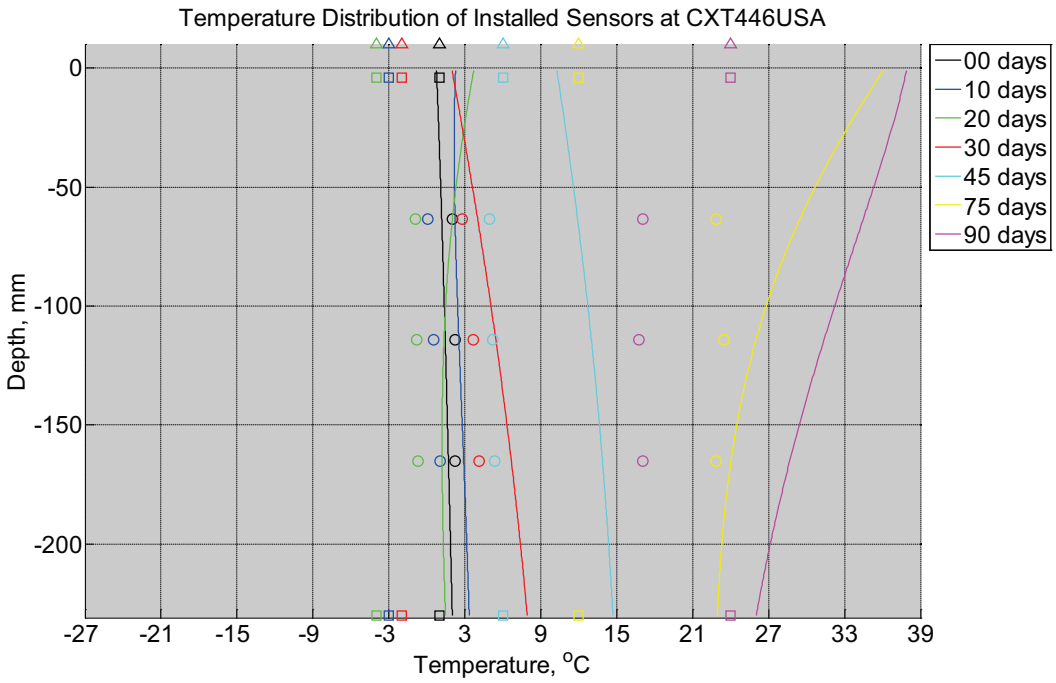

Figure B-851 Measured (markers) and modeled (continuous line) temperature profile distribution as a function of depth inside a concrete crosstie (labeled CXT446USA) installed in track near Lytton, BC, between February 18, 2014, through May 14, 2014. An 8 mm thick polyurethane pad and steel rail are additionally installed atop the concrete crosstie. The model does not incorporate a polyurethane pad nor steel rail line. Triangular markers denote temperature value from CWLY weather station, square markers denote assumed temperature values in ballast, and circular markers denote measured temperature values inside concrete.

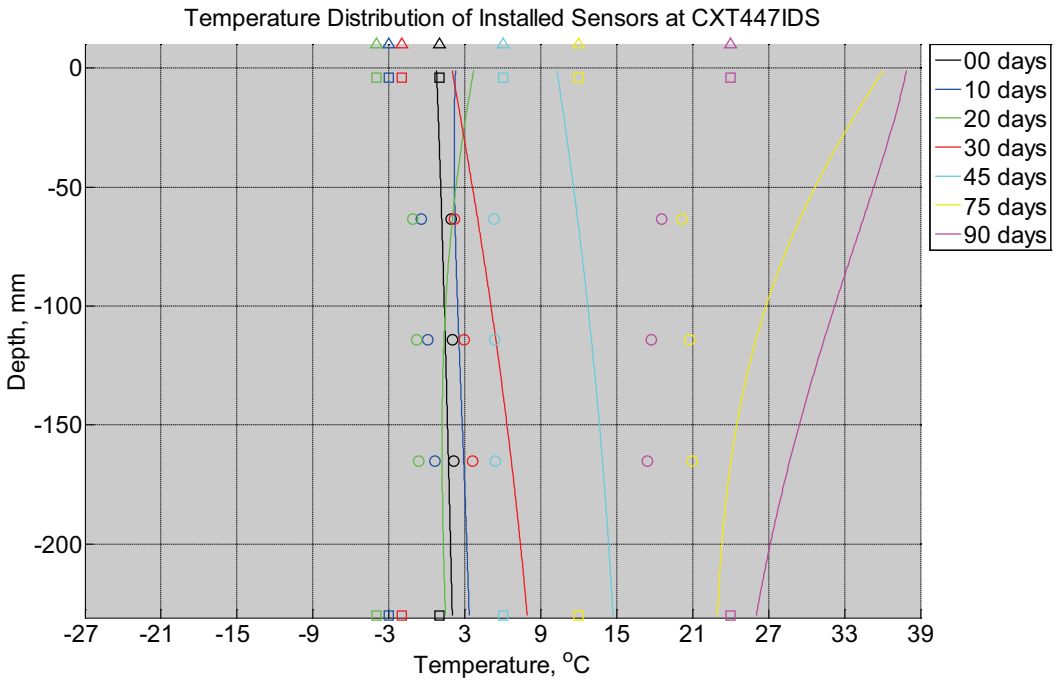

Figure B-852 Measured (markers) and modeled (continuous line) temperature profile distribution as a function of depth inside a concrete crosstie (labeled CXT447IDS) installed in track near Lytton, BC, between February 18, 2014, through May 14, 2014. An 8 mm thick polyurethane pad and steel rail are additionally installed atop the concrete crosstie. The model does not incorporate a polyurethane pad nor steel rail line. Triangular markers denote temperature value from CWLY weather station, square markers denote assumed temperature values in ballast, and circular markers denote measured temperature values inside concrete.

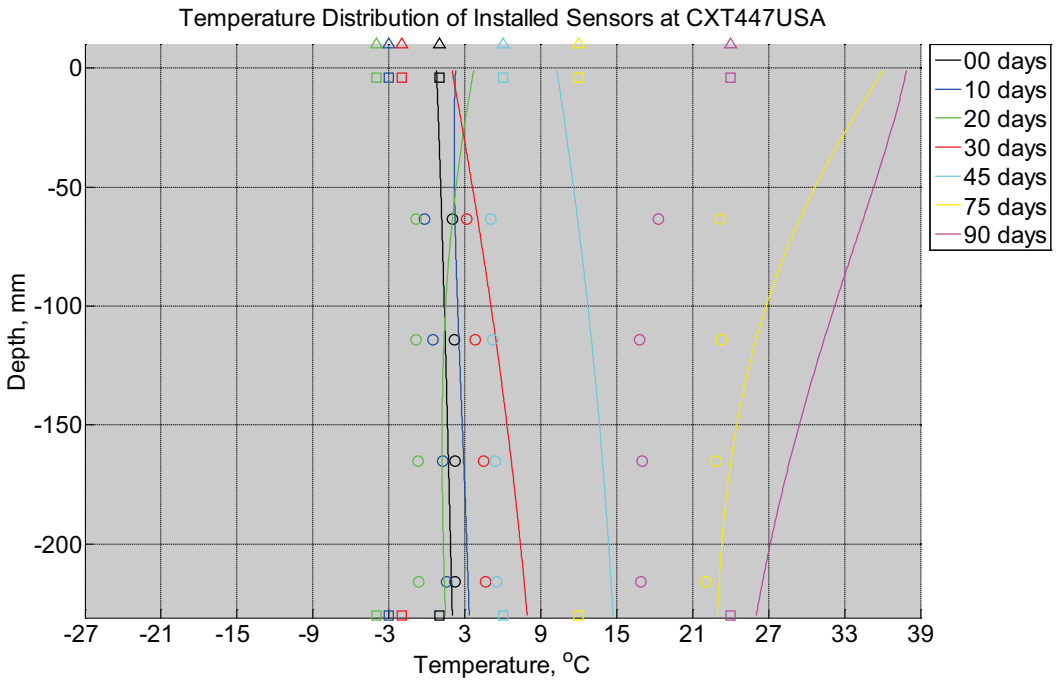

Figure B-853 Measured (markers) and modeled (continuous line) temperature profile distribution as a function of depth inside a concrete crosstie (labeled CXT447USA) installed in track near Lytton, BC, between February 18, 2014, through May 14, 2014. An 8 mm thick polyurethane pad and steel rail are additionally installed atop the concrete crosstie. The model does not incorporate a polyurethane pad nor steel rail line. Triangular markers denote temperature value from CWLY weather station, square markers denote assumed temperature values in ballast, and circular markers denote measured temperature values inside concrete.

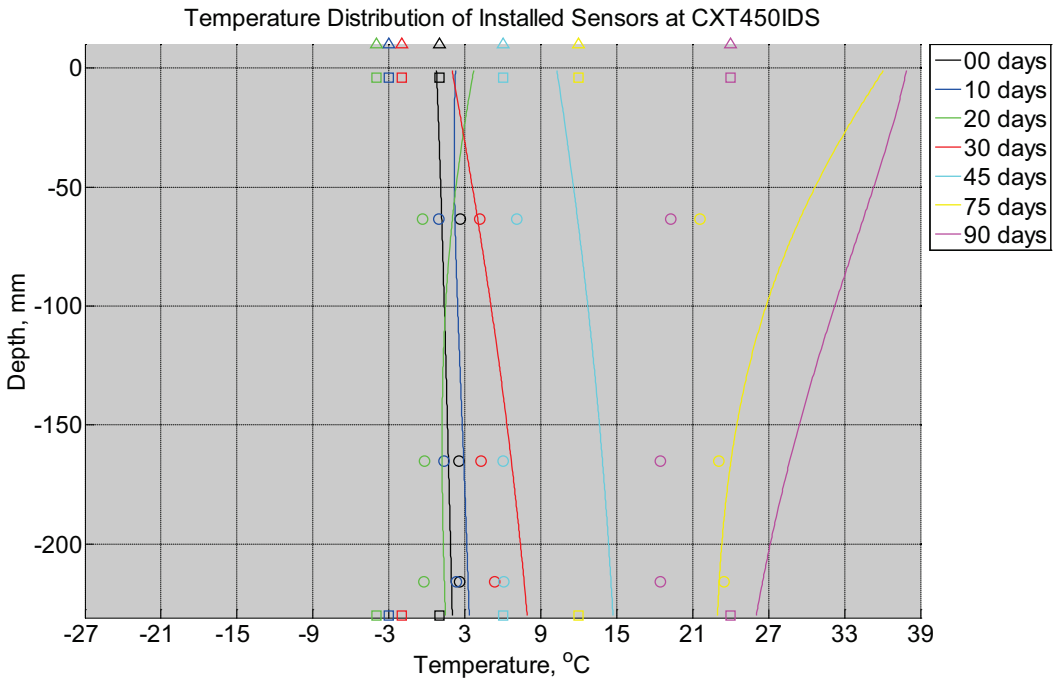

Figure B-854 Measured (markers) and modeled (continuous line) temperature profile distribution as a function of depth inside a concrete crosstie (labeled CXT450IDS) installed in track near Lytton, BC, between February 18, 2014, through May 14, 2014. An 8 mm thick polyurethane pad and steel rail are additionally installed atop the concrete crosstie. The model does not incorporate a polyurethane pad nor steel rail line. Triangular markers denote temperature value from CWLY weather station, square markers denote assumed temperature values in ballast, and circular markers denote measured temperature values inside concrete.

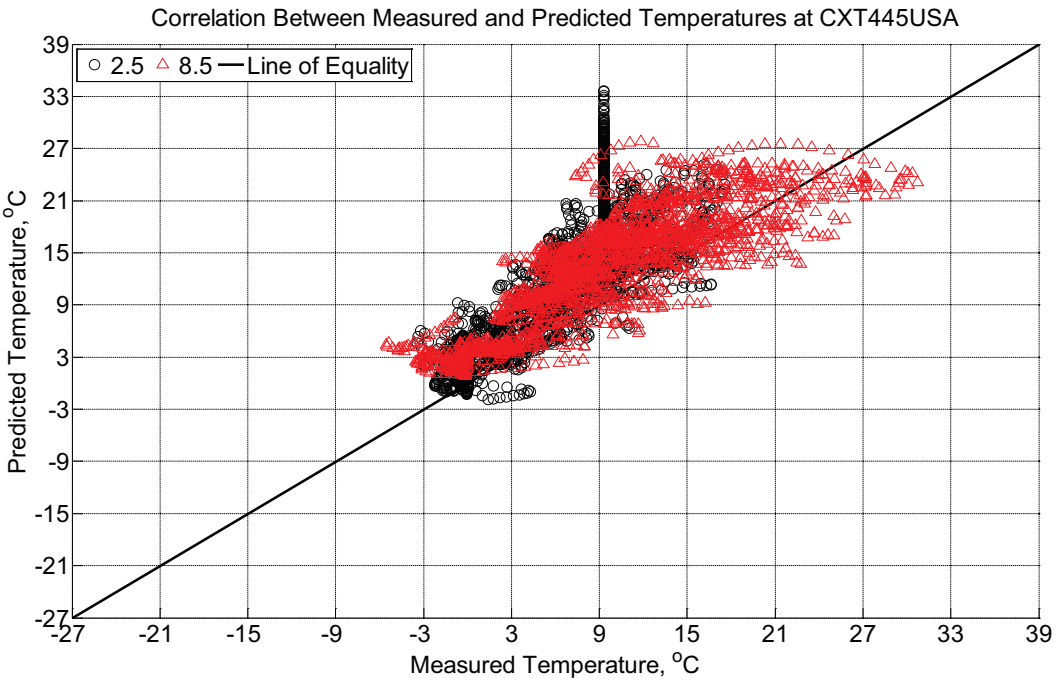

Figure B-855 Correlation between measured and predicted temperature values 2.5 inches (63.5 mm), 4.5 inches (114.3 mm) and 8.5 inches (215.9 mm) from the surface of a concrete crosstie (labeled CXT445USA) installed in track near Lytton, BC, between February 18, 2014, through May 14, 2014. An 8 mm thick polyurethane pad and steel rail are additionally installed atop the concrete crosstie. The model does not incorporate a polyurethane pad nor steel rail line.

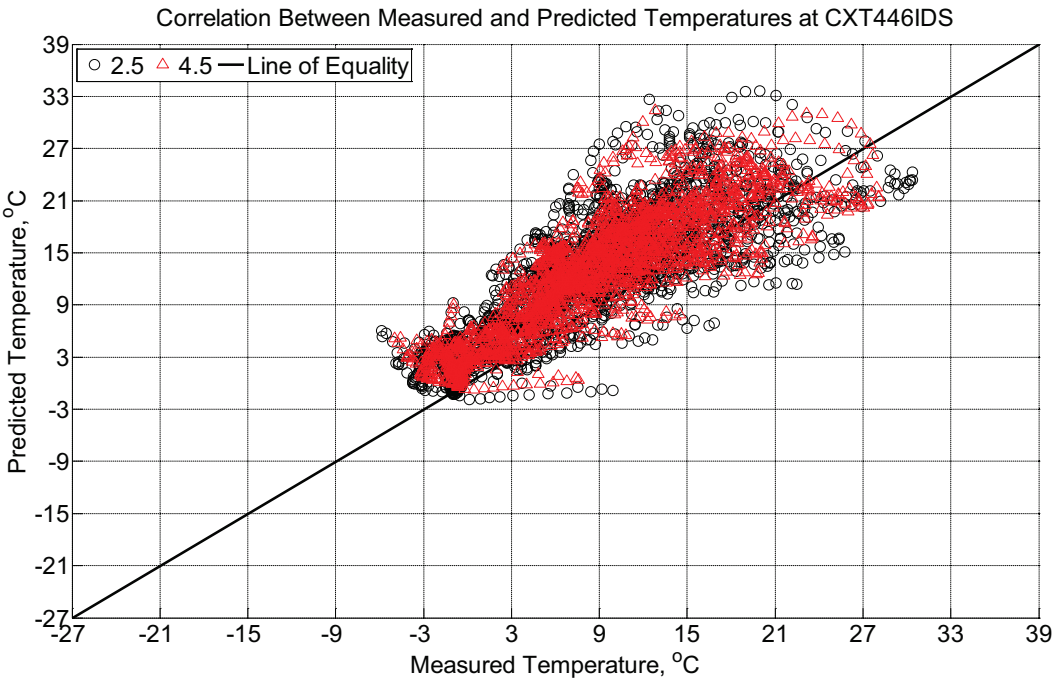

Figure B-856 Correlation between measured and predicted temperature values 2.5 inches (63.5 mm) and 4.5 inches (114.3 mm, from the surface of a concrete crosstie (labeled CXT446IDS) installed in track near Lytton, BC, between February 18, 2014, through May 14, 2014. An 8 mm thick polyurethane pad and steel rail are additionally installed atop the concrete crosstie. The model does not incorporate a polyurethane pad nor steel rail line.

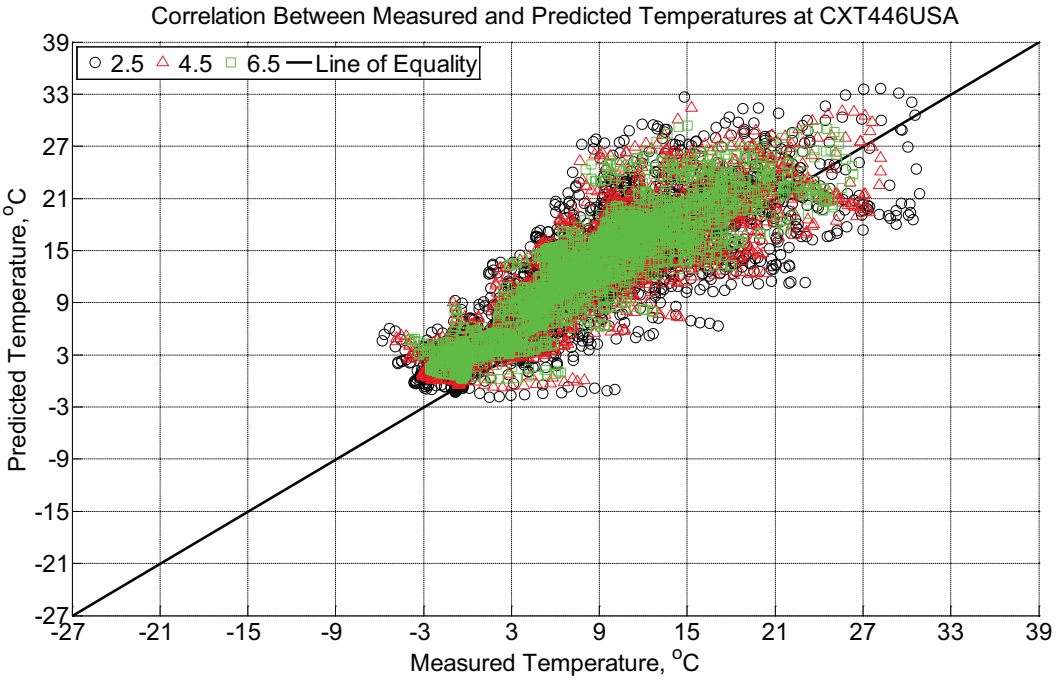

Figure B-857 Correlation between measured and predicted temperature values 2.5 inches

(63.5 mm), 4.5 inches (114.3 mm), and 6.5 inches (139.7 mm) from the surface of a concrete crosstie (labeled CXT446USA) installed in track near Lytton, BC, between February 18, 2014, through May 14, 2014. An 8 mm thick polyurethane pad and steel rail are additionally installed atop the concrete crosstie. The model does not incorporate a polyurethane pad nor steel rail line.

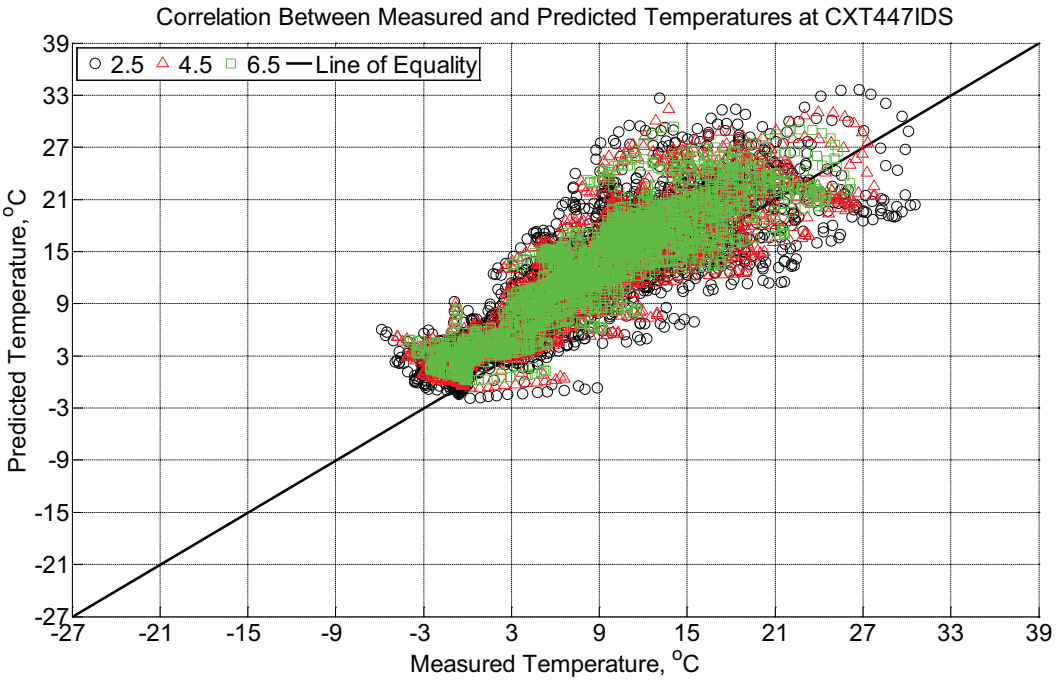

Figure B-858 Correlation between measured and predicted temperature values 2.5 inches (63.5 mm), 4.5 inches (114.3 mm), and 6.5 inches (139.7 mm) from the surface of a concrete crosstie (labeled CXT447IDS) installed in track near Lytton, BC, between February 18, 2013, through May 14, 2014. An 8 mm thick polyurethane pad and steel rail are additionally installed atop the concrete crosstie. The model does not incorporate a polyurethane pad nor steel rail line.

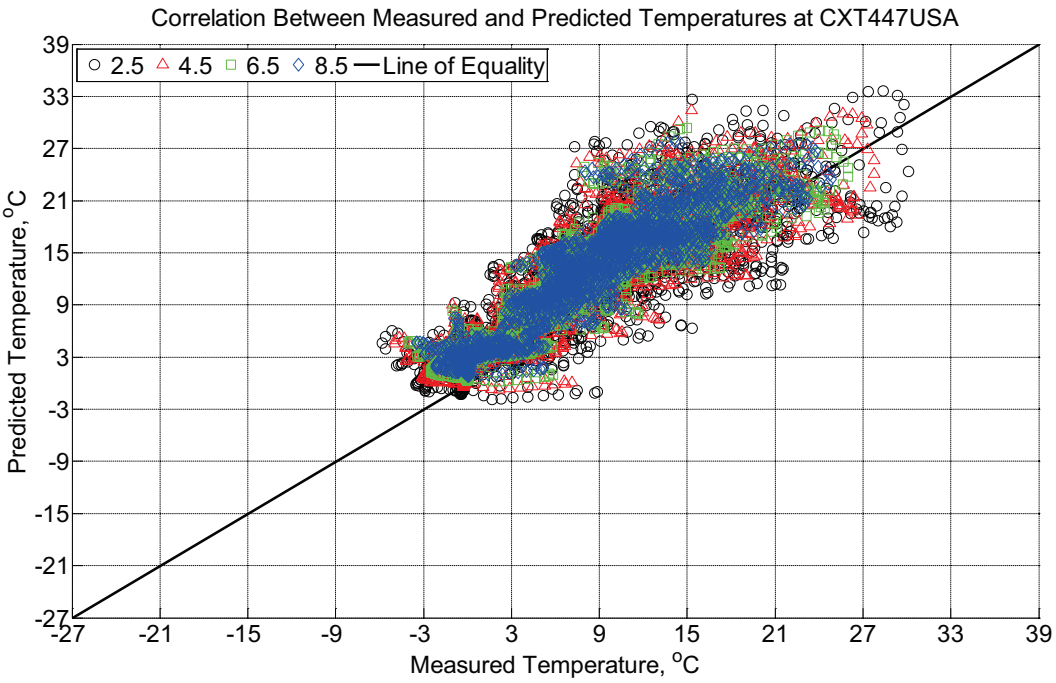

Figure B-859 Correlation between measured and predicted temperature values 2.5 inches (63.5 mm), 4.5 inches (114.3 mm), 6.5 inches (139.7 mm), and 8.5 inches (215.9 mm) from the surface of a concrete crosstie (labeled CXT447USA) installed in track near Lytton, BC, between February 18, 2014, through May 14, 2014. An 8 mm thick polyurethane pad and steel rail are additionally installed atop the concrete crosstie. The model does not incorporate a polyurethane pad nor steel rail line.

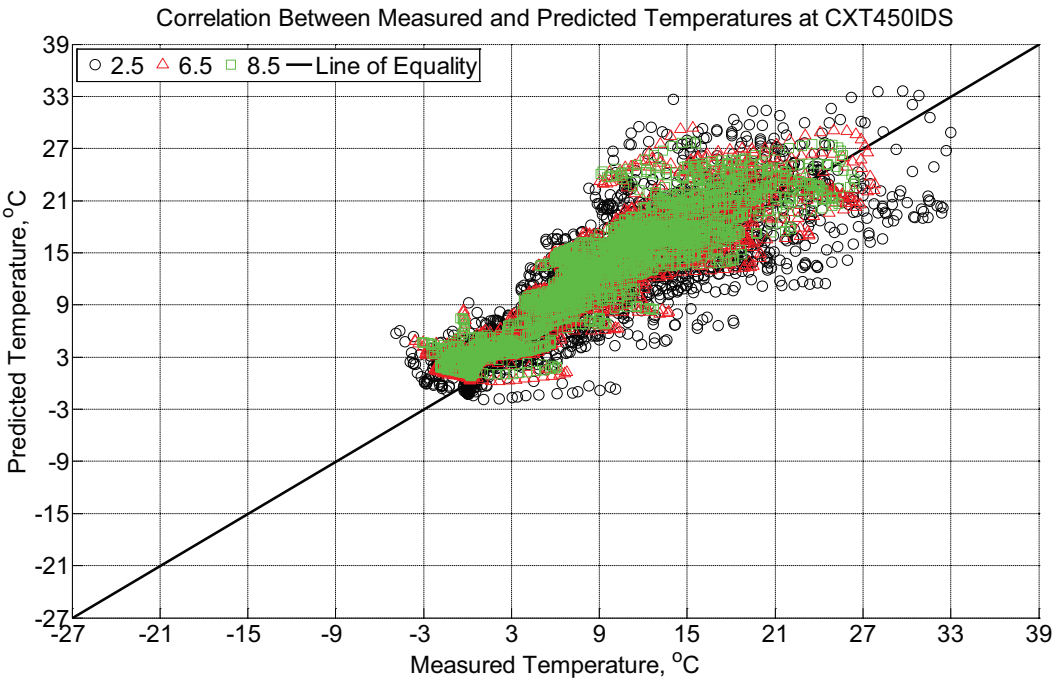

Figure B-860 Correlation between measured and predicted temperature values 2.5 inches (63.5 mm), 6.5 inches (139.7 mm), and 8.5 inches (215.9 mm) from the surface of a concrete crosstie (labeled CXT450IDS) installed in track near Lytton, BC, between February 18, 2014, through May 14, 2014. An 8 mm thick polyurethane pad and steel rail are additionally installed atop the concrete crosstie. The model does not incorporate a polyurethane pad nor steel rail line.

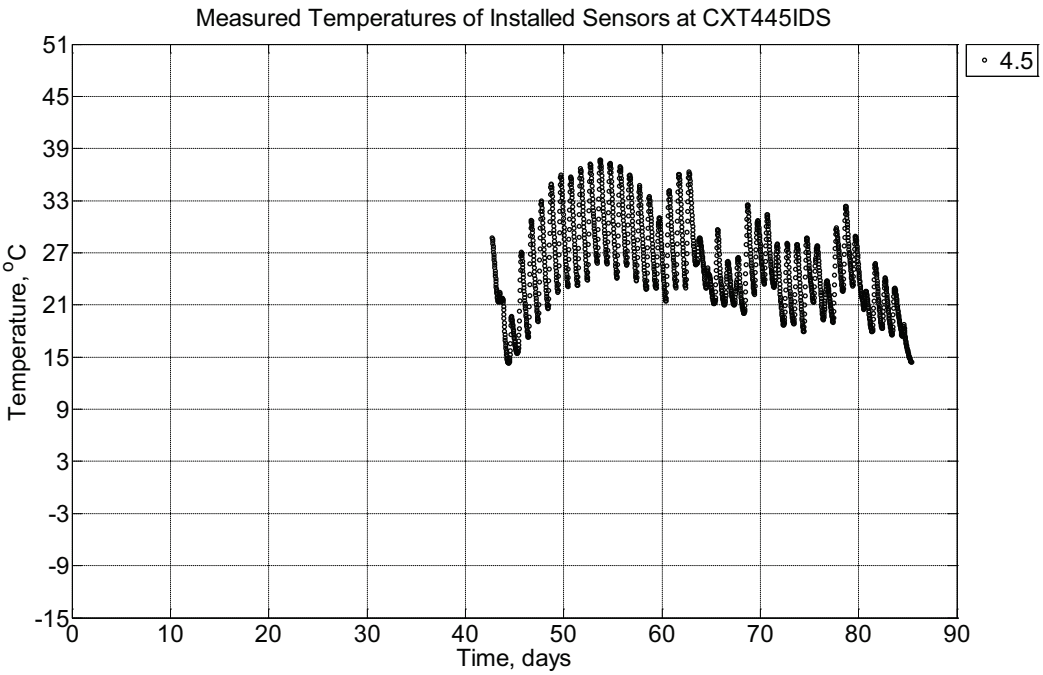

Figure B-861 Measured temperature at a depth of 4.5 inches (114.3 mm) from the surface of a concrete crosstie (labeled CXT445IDS) installed in track near Lytton, BC, between June 10, 2014, through September 3, 2014. An 8 mm thick polyurethane pad and steel rail are additionally installed atop the concrete crosstie.

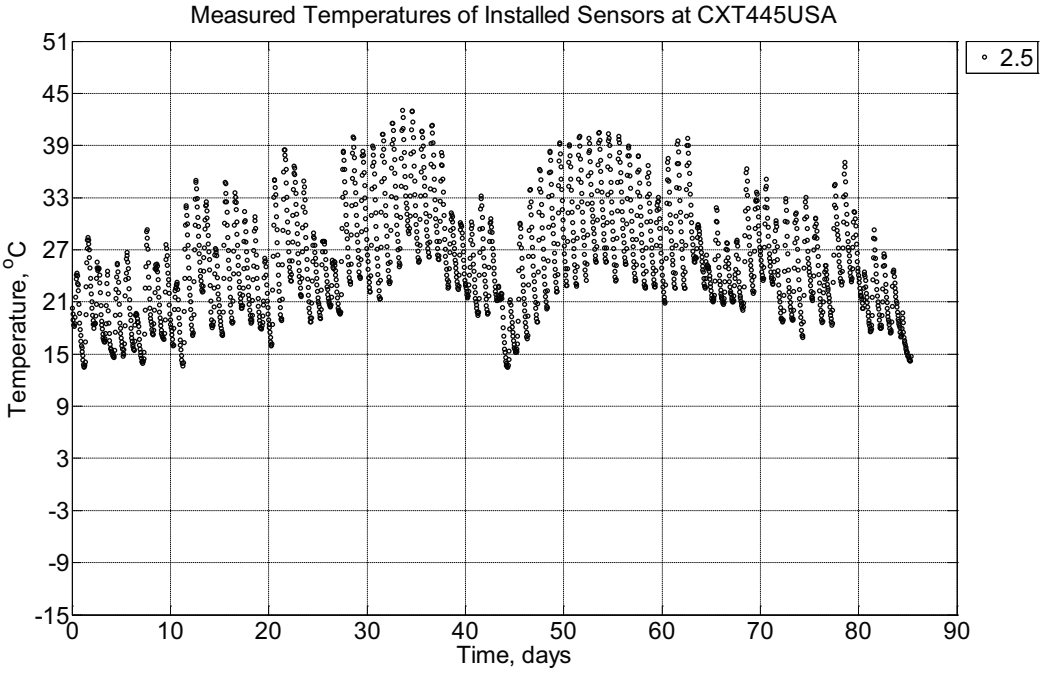

Figure B-862 Measured temperature at a depth of 2.5 inches (63.5 mm) from the surface of a concrete crosstie (labeled CXT445USA) installed in track near Lytton, BC, between June

10, 2014, through September 3, 2014. An 8 mm thick polyurethane pad and steel rail are additionally installed atop the concrete crosstie.

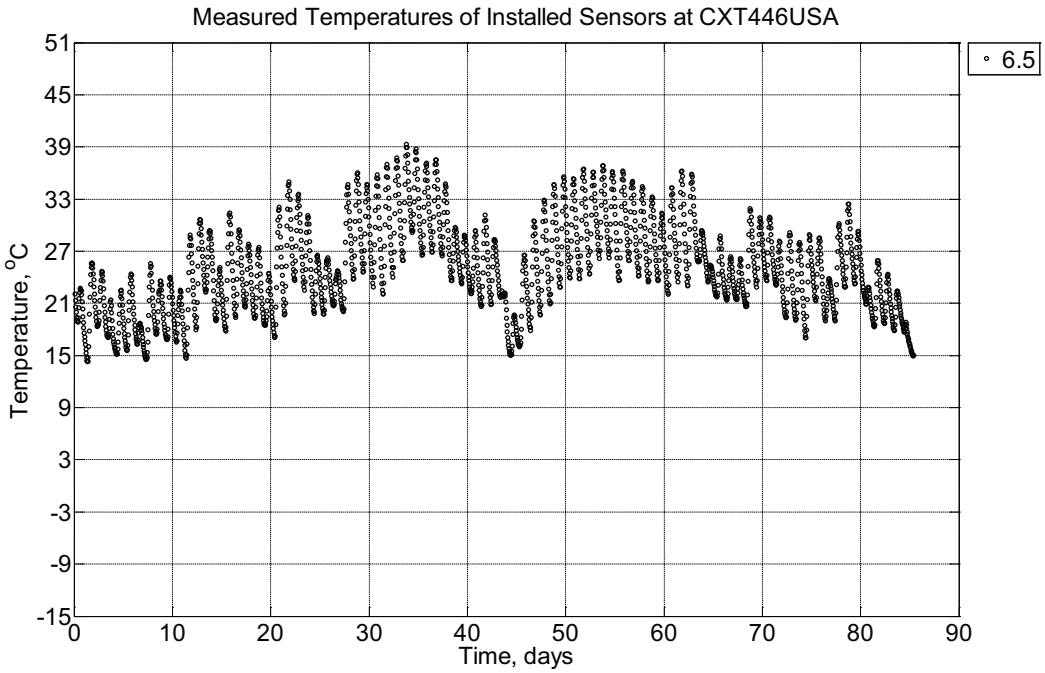

Figure B-863 Measured temperature at a depth of 6.5 inches (139.7 mm) from the surface of a concrete crosstie (labeled CXT446USA) installed in track near Lytton, BC, between June 10, 2014, through September 3, 2014. An 8 mm thick polyurethane pad and steel rail are additionally installed atop the concrete crosstie.

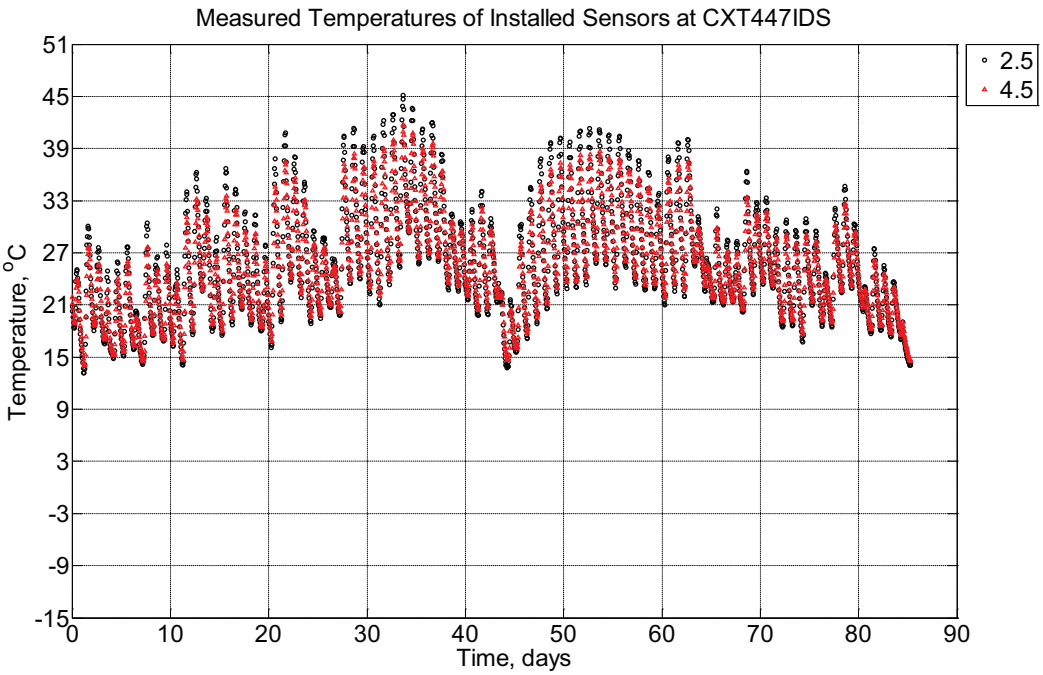

Figure B-864 Measured temperature at depths of 2.5 inches (63.5 mm) and 4.5 inches (114.3 mm) from the surface of a concrete crosstie (labeled CXT447IDS) installed in track near Lytton, BC, between June 10, 2014, through September 3, 2014. An 8 mm thick polyurethane pad and steel rail are additionally installed atop the concrete crosstie.

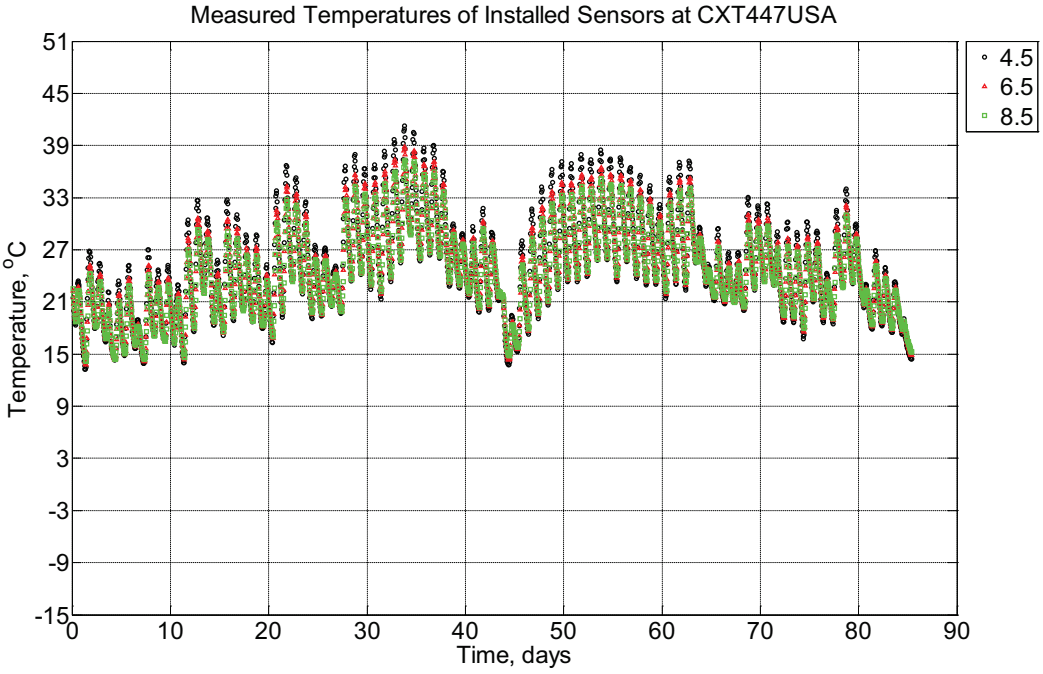

Figure B-865 Measured temperature at depths 4.5 inches (114.3 mm), 6.5 inches (139.7 mm), and 8.5 inches (215.9 mm) from the surface of a concrete crosstie (labeled

CXT447USA) installed in track near Lytton, BC, between June 10, 2014, through September 3, 2014. An 8 mm thick polyurethane pad and steel rail are additionally installed atop the concrete crosstie.

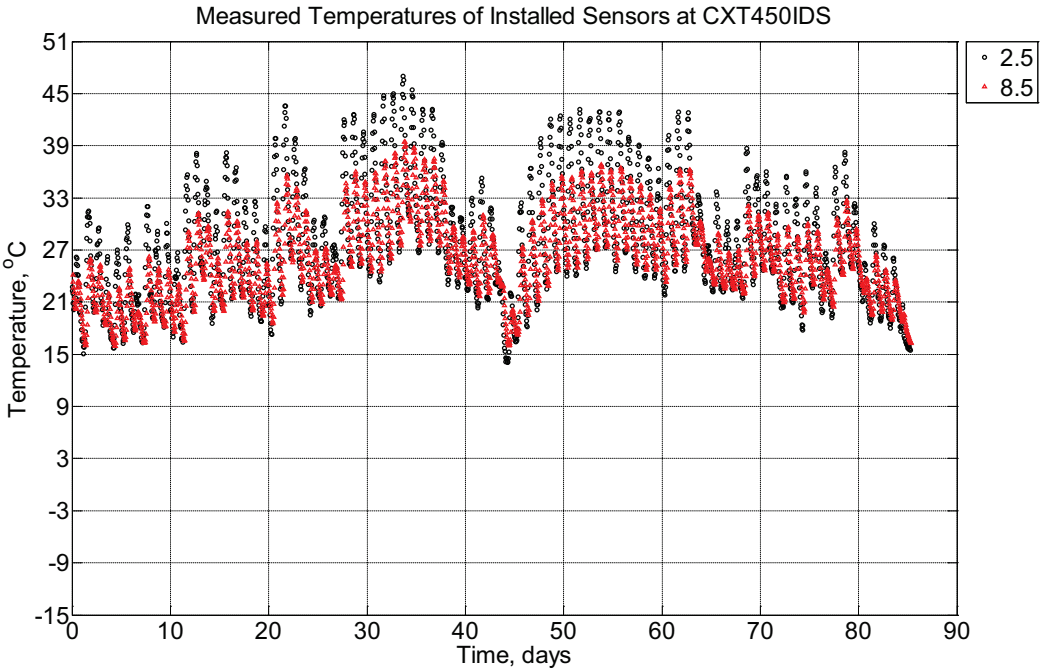

Figure B-866 Measured temperature at depths of 2.5 inches (63.5 mm) and 8.5 inches (215.9 mm) from the surface of a concrete crosstie (labeled CXT450IDS) installed in track near Lytton, BC, between June 10, 2014, through September 3, 2014. An 8 mm thick polyurethane pad and steel rail are additionally installed atop the concrete crosstie.

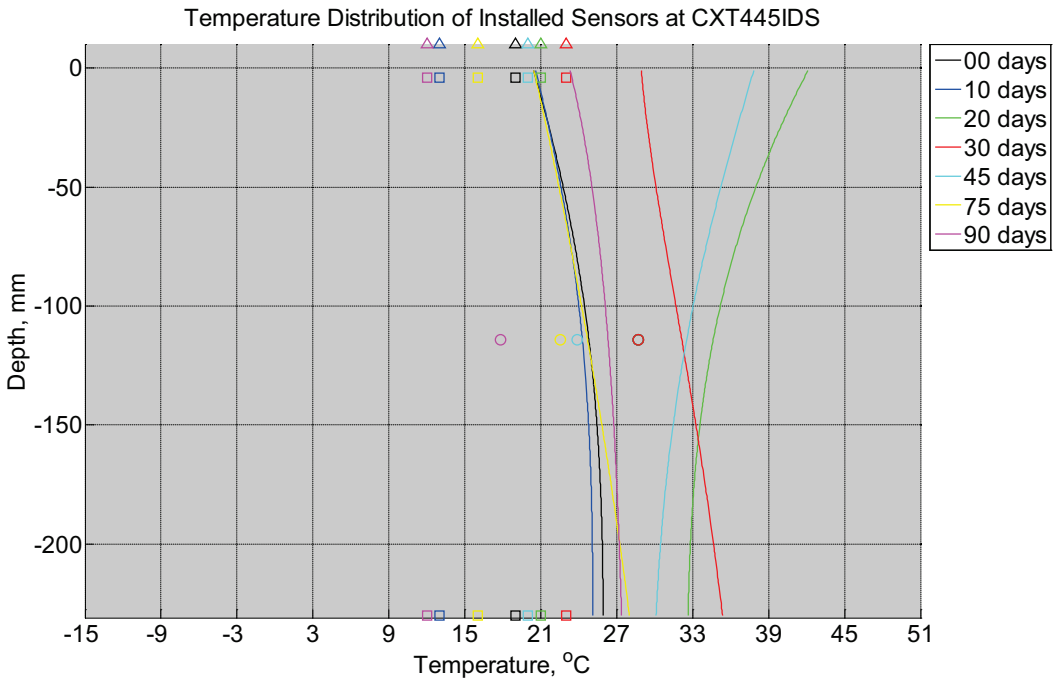

Figure B-867 Measured (markers) and modeled (continuous line) temperature profile distribution as a function of depth inside a concrete crosstie (labeled CXT445IDS) installed in track near Lytton, BC, between June 10, 2014, through September 3, 2014. An 8 mm thick polyurethane pad and steel rail are additionally installed atop the concrete crosstie. The model does not incorporate a polyurethane pad nor steel rail line. Triangular markers denote temperature value from CWLY weather station, square markers denote assumed temperature values in ballast, and circular markers denote measured temperature values inside concrete.

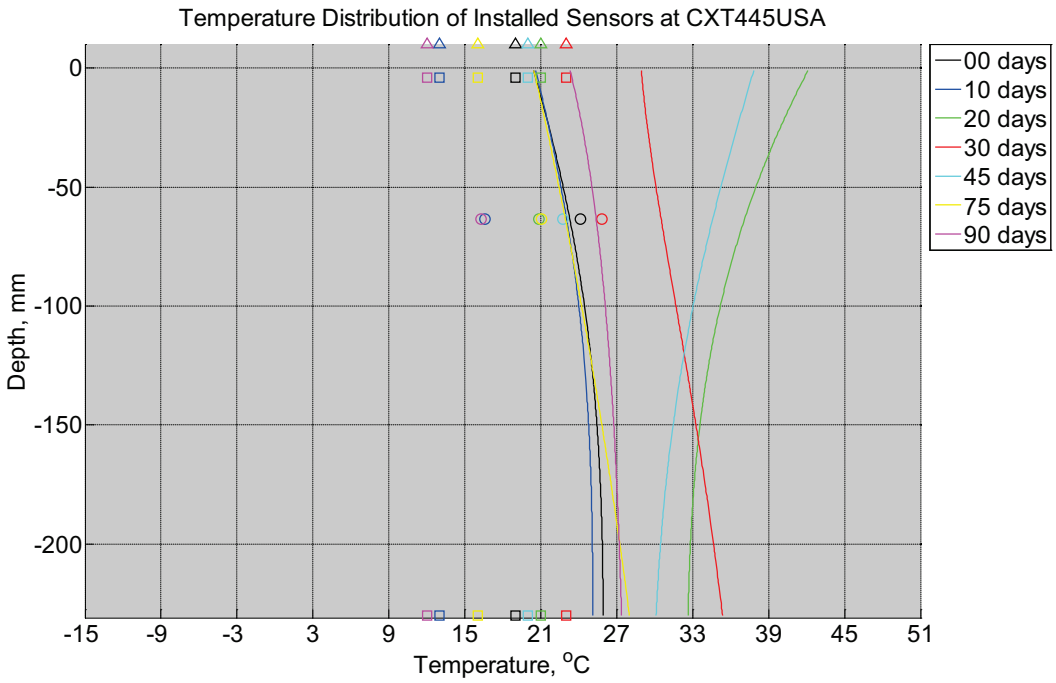

Figure B-868 Measured (markers) and modeled (continuous line) temperature profile distribution as a function of depth inside a concrete crosstie (labeled CXT445USA) installed in track near Lytton, BC, between June 10, 2014, through September 3, 2014. An 8 mm thick polyurethane pad and steel rail are additionally installed atop the concrete crosstie. The model does not incorporate a polyurethane pad nor steel rail line. Triangular markers denote temperature value from CWLY weather station, square markers denote assumed temperature values in ballast, and circular markers denote measured temperature values inside concrete.

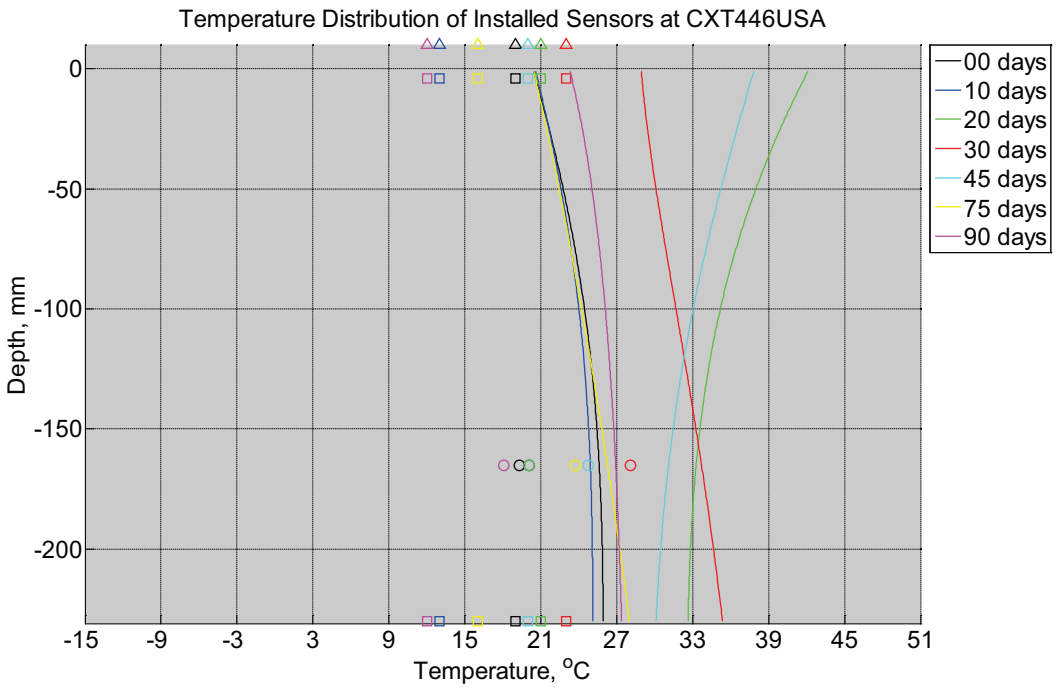

Figure B-869 Measured (markers) and modeled (continuous line) temperature profile distribution as a function of depth inside a concrete crosstie (labeled CXT446USA) installed in track near Lytton, BC, between June 10, 2014, through September 3, 2014. An 8 mm thick polyurethane pad and steel rail are additionally installed atop the concrete crosstie. The model does not incorporate a polyurethane pad nor steel rail line. Triangular markers denote temperature value from CWLY weather station, square markers denote assumed temperature values in ballast, and circular markers denote measured temperature values inside concrete.

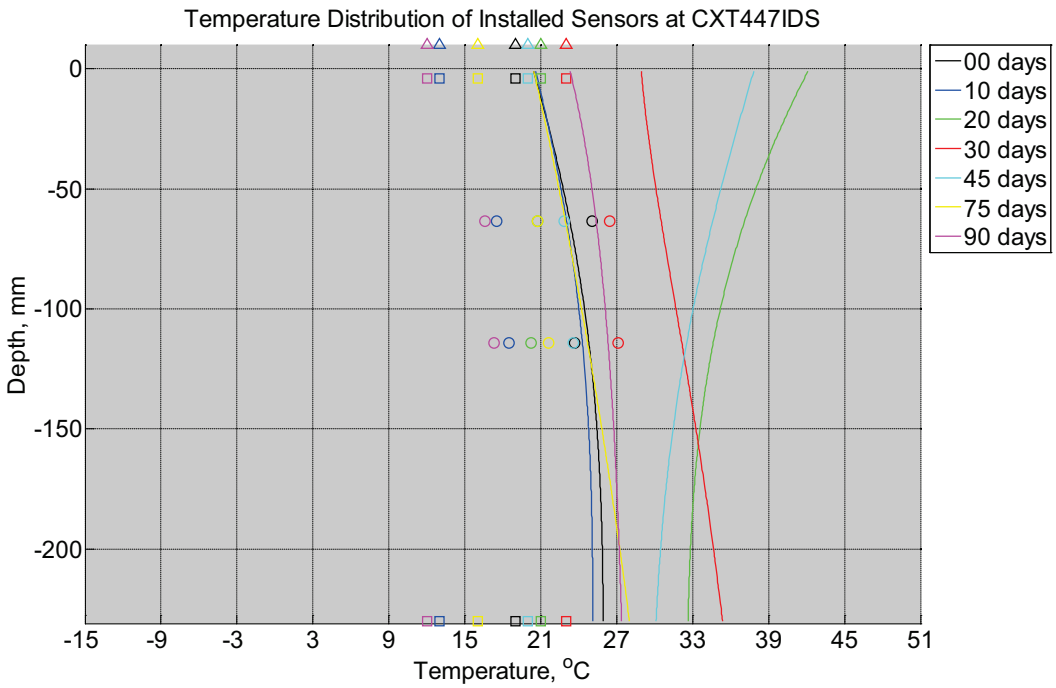

Figure B-870 Measured (markers) and modeled (continuous line) temperature profile distribution as a function of depth inside a concrete crosstie (labeled CXT447IDS) installed in track near Lytton, BC, between June 10, 2014, through September 3, 2014. An 8 mm thick polyurethane pad and steel rail are additionally installed atop the concrete crosstie. The model does not incorporate a polyurethane pad nor steel rail line. Triangular markers denote temperature value from CWLY weather station, square markers denote assumed temperature values in ballast, and circular markers denote measured temperature values inside concrete.

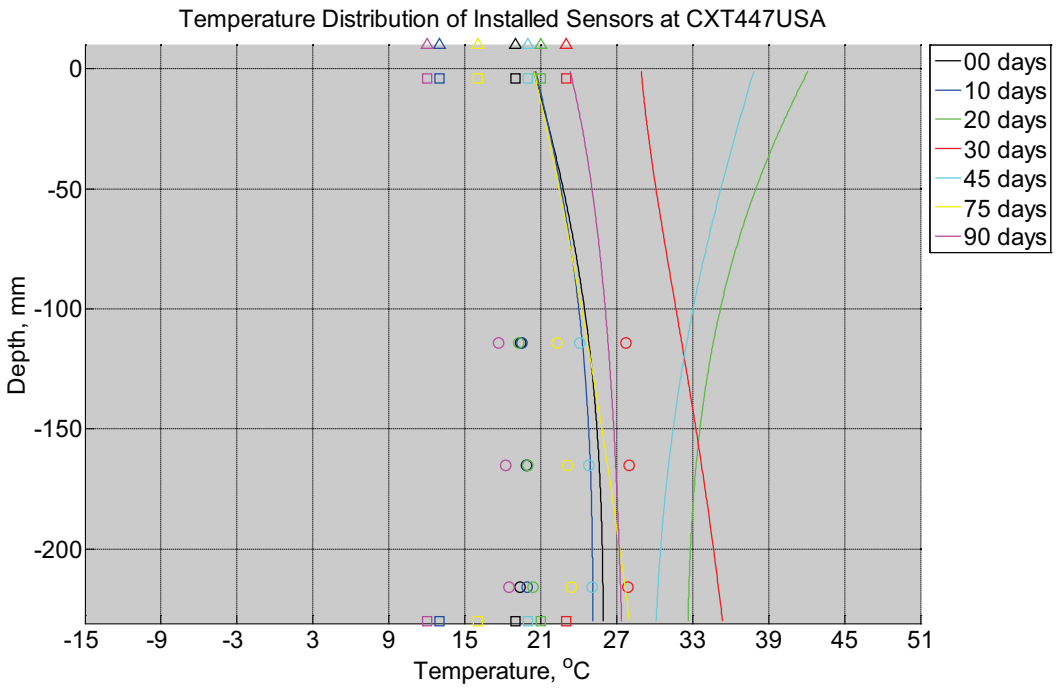

Figure B-871 Measured (markers) and modeled (continuous line) temperature profile distribution as a function of depth inside a concrete crosstie (labeled CXT447USA) installed in track near Lytton, BC, between June 10, 2014, through September 3, 2014. An 8 mm thick polyurethane pad and steel rail are additionally installed atop the concrete crosstie. The model does not incorporate a polyurethane pad nor steel rail line. Triangular markers denote temperature value from CWLY weather station, square markers denote assumed temperature values in ballast, and circular markers denote measured temperature values inside concrete.

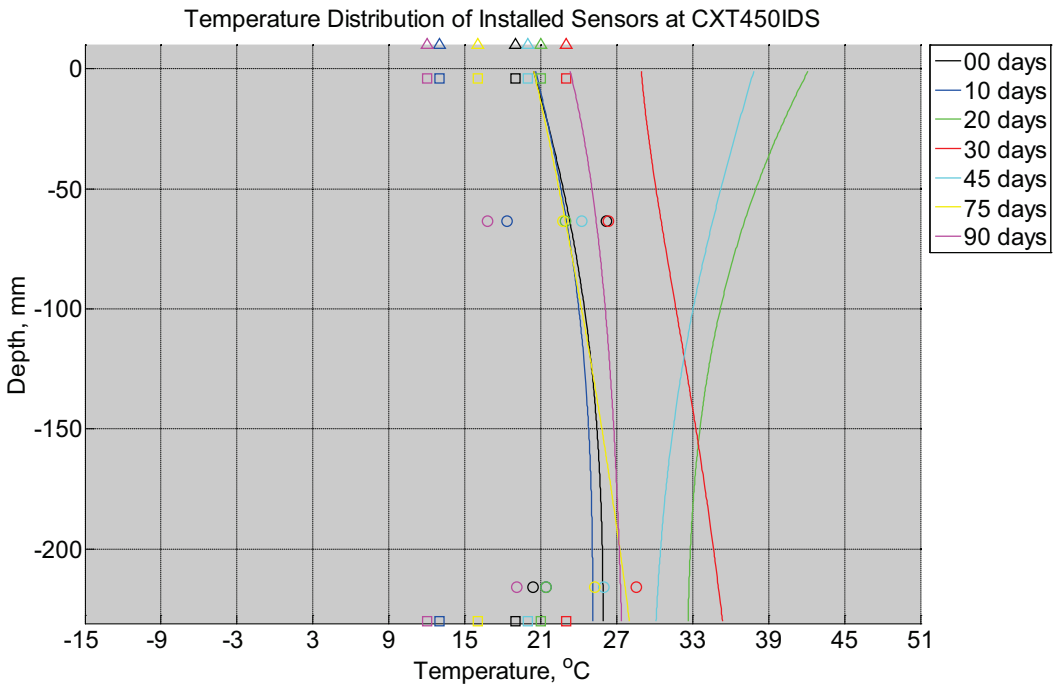

Figure B-872 Measured (markers) and modeled (continuous line) temperature profile distribution as a function of depth inside a concrete crosstie (labeled CXT450IDS) installed in track near Lytton, BC, between June 10, 2014, through September 3, 2014. An 8 mm thick polyurethane pad and steel rail are additionally installed atop the concrete crosstie. The model does not incorporate a polyurethane pad nor steel rail line. Triangular markers denote temperature value from CWLY weather station, square markers denote assumed temperature values in ballast, and circular markers denote measured temperature values inside concrete.

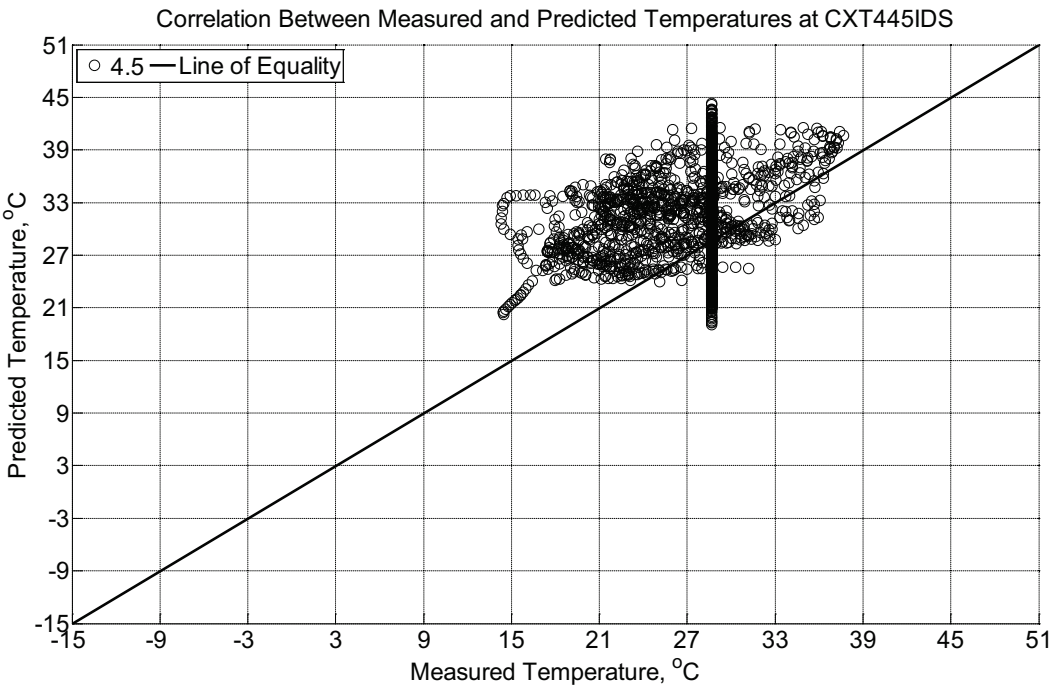

Figure B-873 Correlation between measured and predicted temperature values 4.5 inches (114.3 mm) from the surface of a concrete crosstie (labeled CXT445IDS) installed in track near Lytton, BC, between June 10, 2014, through September 3, 2014. An 8 mm thick polyurethane pad and steel rail are additionally installed atop the concrete crosstie. The model does not incorporate a polyurethane pad nor steel rail line.

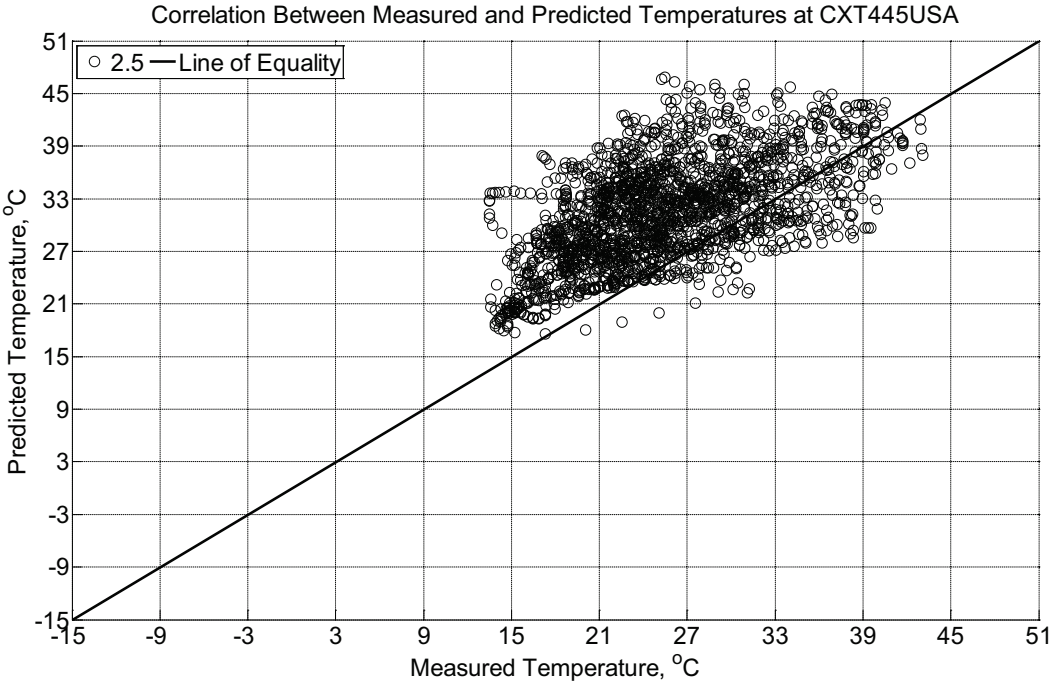

Figure B-874 Correlation between measured and predicted temperature values 2.5 inches

(63.5 mm) from the surface of a concrete crosstie (labeled CXT445USA) installed in track near Lytton, BC, between June 10, 2014, through September 3, 2014. An 8 mm thick polyurethane pad and steel rail are additionally installed atop the concrete crosstie. The model does not incorporate a polyurethane pad nor steel rail line.

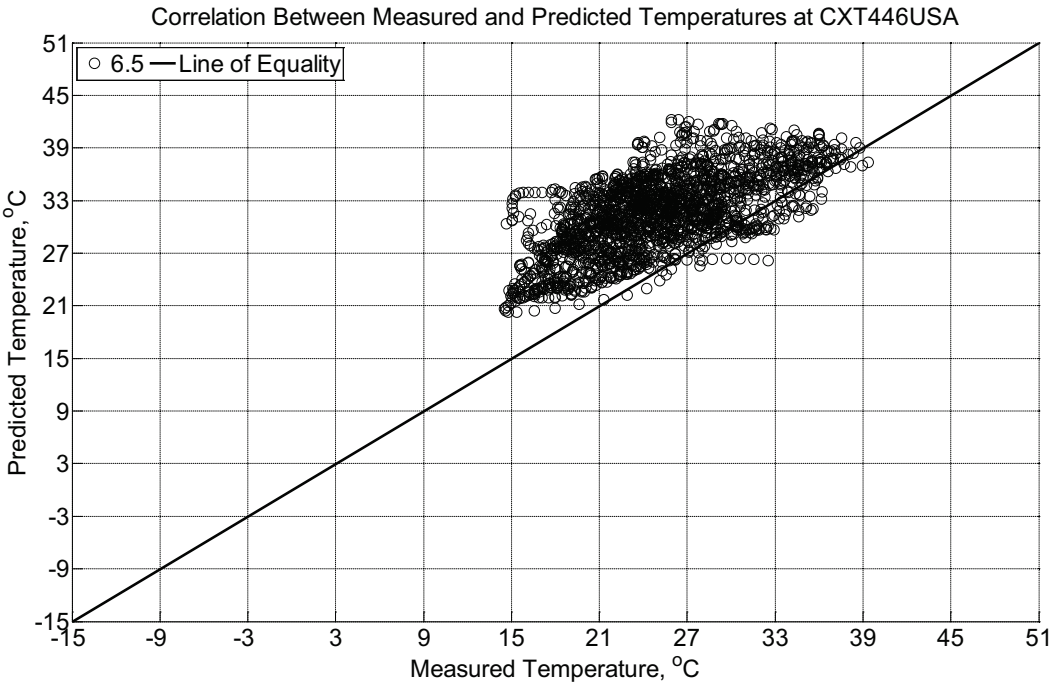

Figure B-875 Correlation between measured and predicted temperature values 6.5 inches (139.7 mm) from the surface of a concrete crosstie (labeled CXT446USA) installed in track near Lytton, BC, between June 10, 2014, through September 3, 2014. An 8 mm thick polyurethane pad and steel rail are additionally installed atop the concrete crosstie. The model does not incorporate a polyurethane pad nor steel rail line.

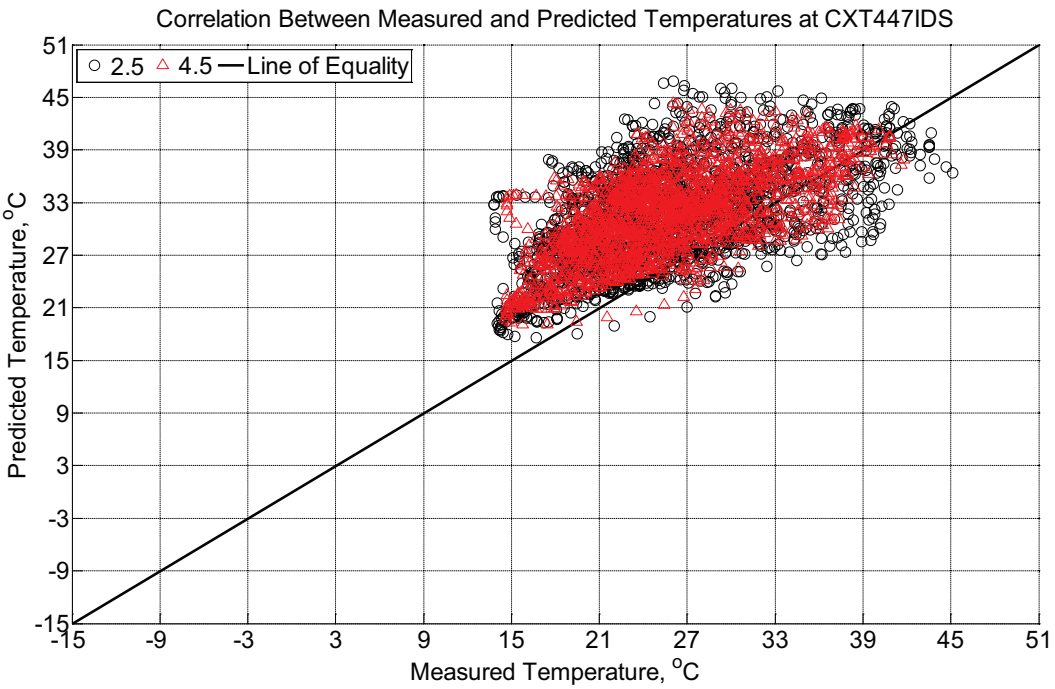

Figure B-876 Correlation between measured and predicted temperature values 2.5 inches (63.5 mm) and 4.5 inches (114.3 mm) from the surface of a concrete crosstie (labeled CXT447IDS) installed in track near Lytton, BC, between June 10, 2014, through September 3, 2014. An 8 mm thick polyurethane pad and steel rail are additionally installed atop the concrete crosstie. The model does not incorporate a polyurethane pad nor steel rail line.

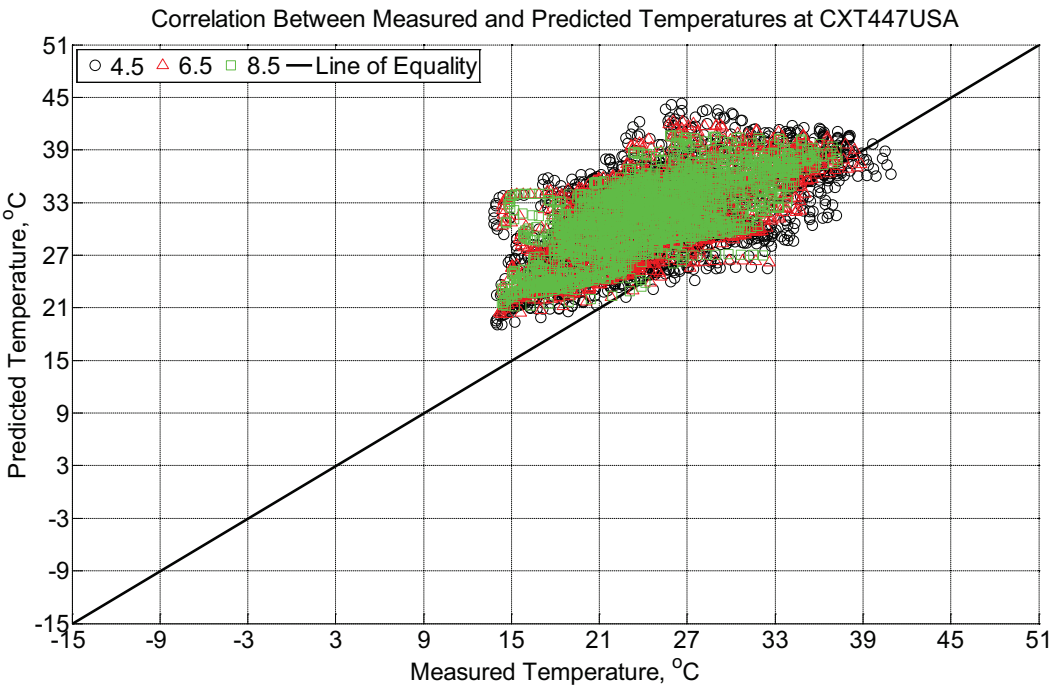

Figure B-877 Correlation between measured and predicted temperature 4.5 inches (114.3 mm), 6.5 inches (139.7 mm), and 8.5 inches (215.9 mm) from the surface of a concrete crosstie (labeled CXT447USA) installed in track near Lytton, BC, between June 10, 2014, through September 3, 2014. An 8 mm thick polyurethane pad and steel rail are additionally installed atop the concrete crosstie. The model does not incorporate a polyurethane pad nor steel rail line.

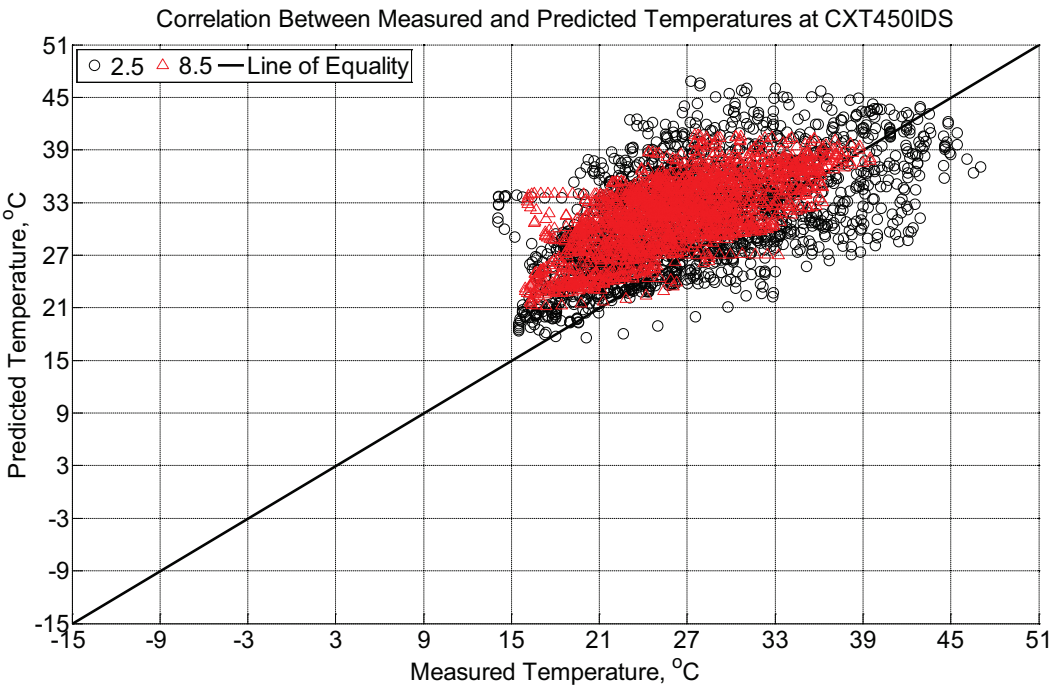

Figure B-878 Correlation between measured and predicted temperature values 2.5 inches (63.5 mm) and 8.5 inches (215.9 mm) from the surface of a concrete crosstie (labeled CXT450IDS) installed in track near Lytton, BC, between June 10, 2014, through September 3, 2014. An 8 mm thick polyurethane pad and steel rail are additionally installed atop the concrete crosstie. The model does not incorporate a polyurethane pad nor steel rail line.

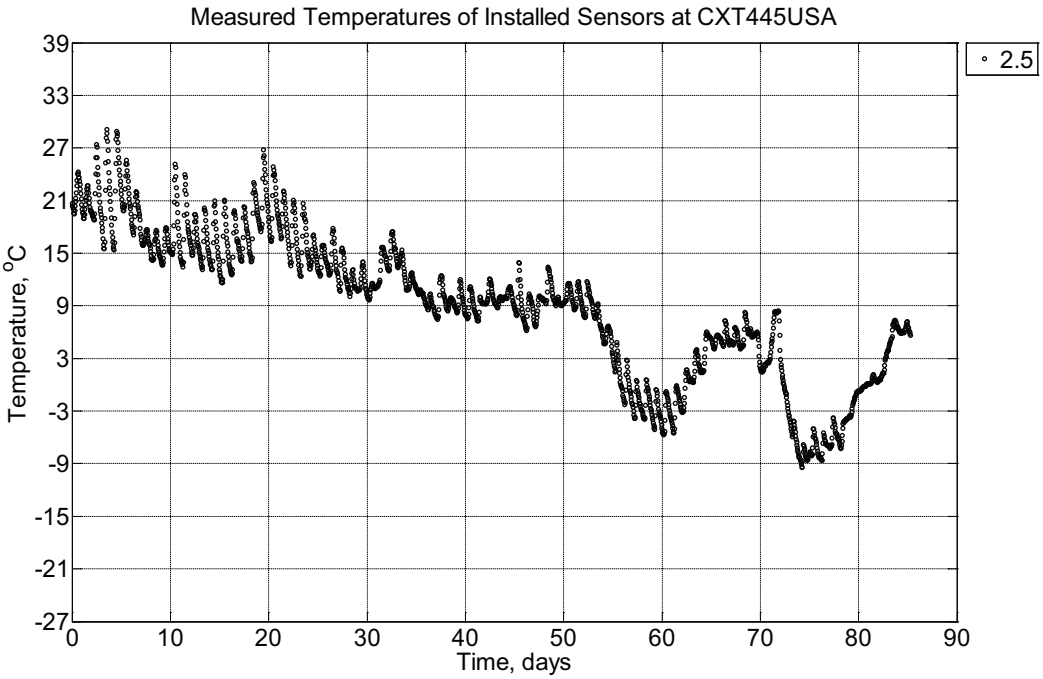

Figure B-879 Measured temperature at a depth of 2.5 inches (63.5 mm) from the surface of a concrete crosstie (labeled CXT445USA) installed in track near Lytton, BC, between September 17, 2014, through December 11, 2014. An 8 mm thick polyurethane pad and steel rail are additionally installed atop the concrete crosstie.

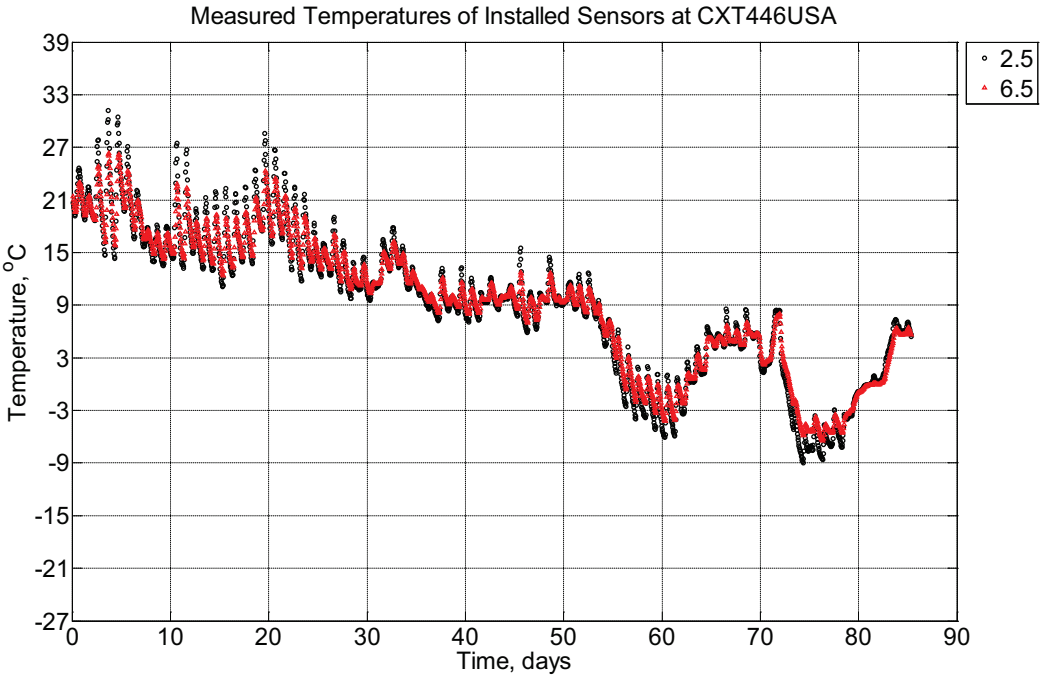

Figure B-880 Measured temperature at depths of 2.5 inches (63.5 mm) and 6.5 inches (139.7 mm) from the surface of a concrete crosstie (labeled CXT446USA) installed in track

near Lytton, BC, between September 17, 2014, through December 11, 2014. An 8 mm thick polyurethane pad and steel rail are additionally installed atop the concrete crosstie.

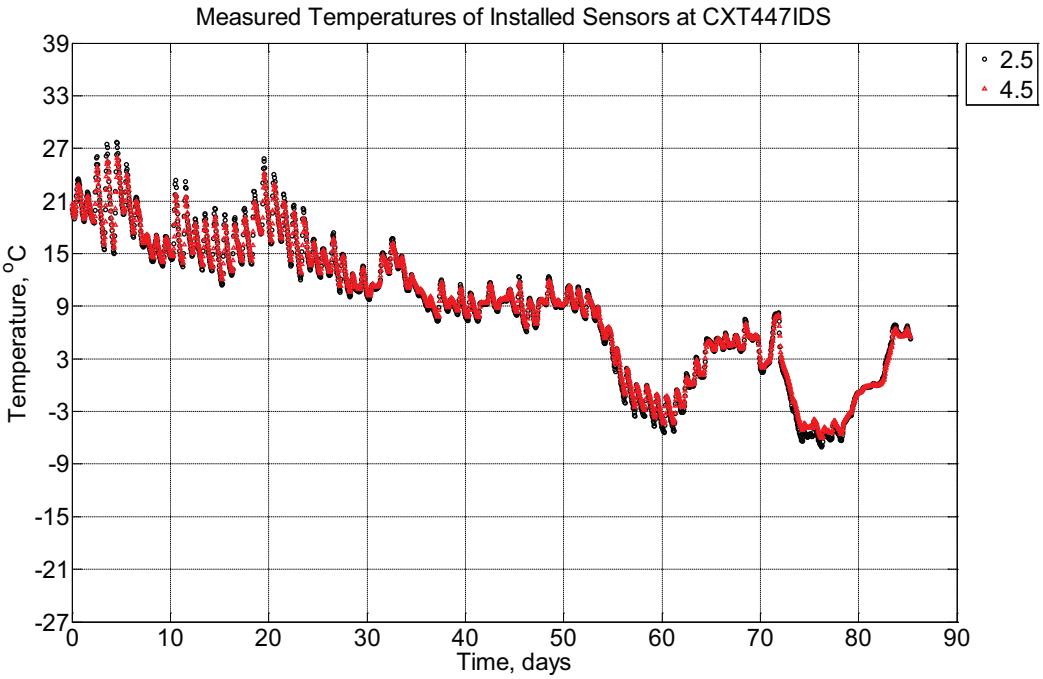

Figure B-881 Measured temperature at depths of 0.5 2.5 inches (63.5 mm) and 4.5 inches (114.3 mm) from the surface of a concrete crosstie (labeled CXT447IDS) installed in track near Lytton, BC, between September 17, 2014, through December 11, 2014. An 8 mm thick polyurethane pad and steel rail are additionally installed atop the concrete crosstie.

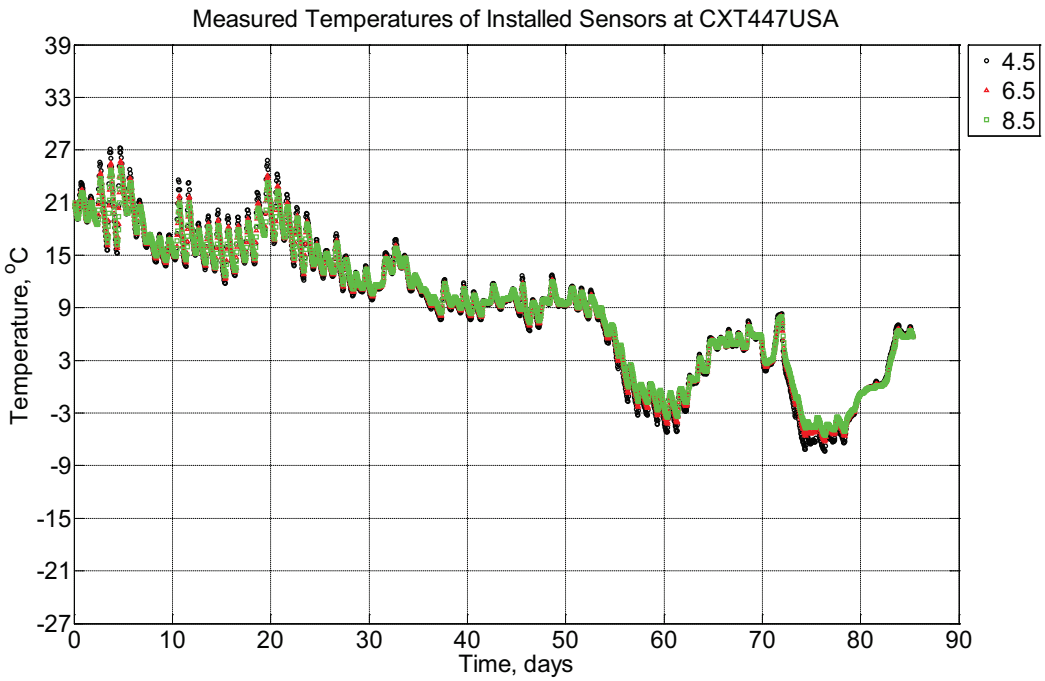

Figure B-882 Measured temperature at depths of 4.5 inches (114.3 mm), 6.5 inches (139.7 mm), and 8.5 inches (215.9 mm) from the surface of a concrete crosstie (labeled CXT447USA) installed in track near Lytton, BC, between September 17, 2014, through December 11, 2014. An 8 mm thick polyurethane pad and steel rail are additionally installed atop the concrete crosstie.

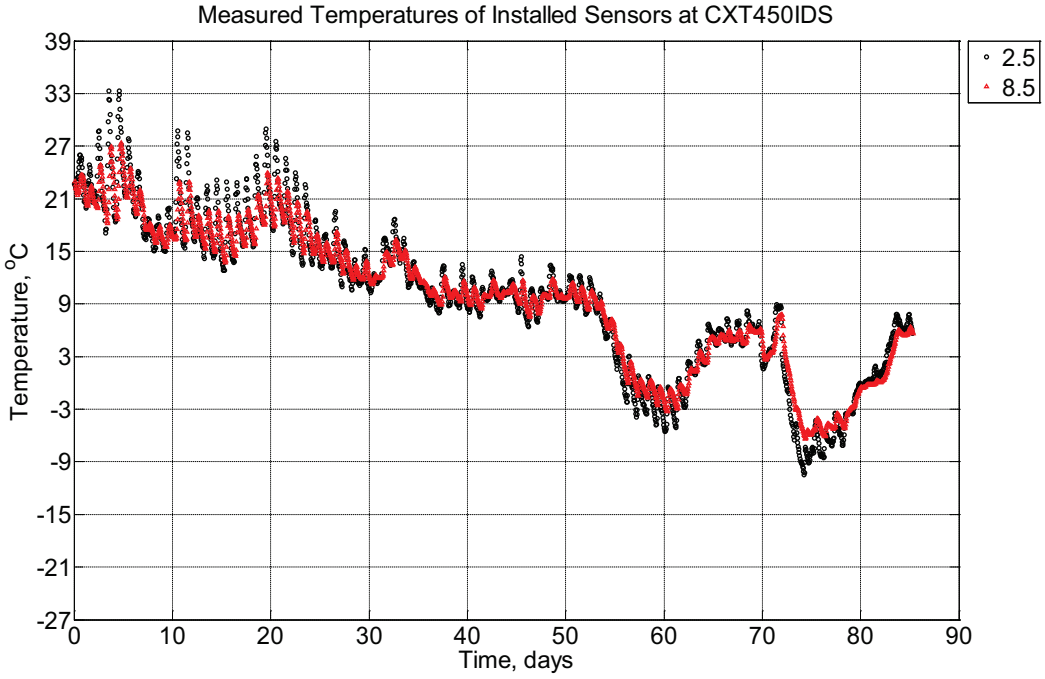

Figure B-883 Measured temperature at depths of 2.5 inches (63.5 mm), and 8.5 inches

(215.9 mm) from the surface of a concrete crosstie (labeled CXT450IDS) installed in track near Lytton, BC, between September 17, 2014, through December 11, 2014. An 8 mm thick polyurethane pad and steel rail are additionally installed atop the concrete crosstie.

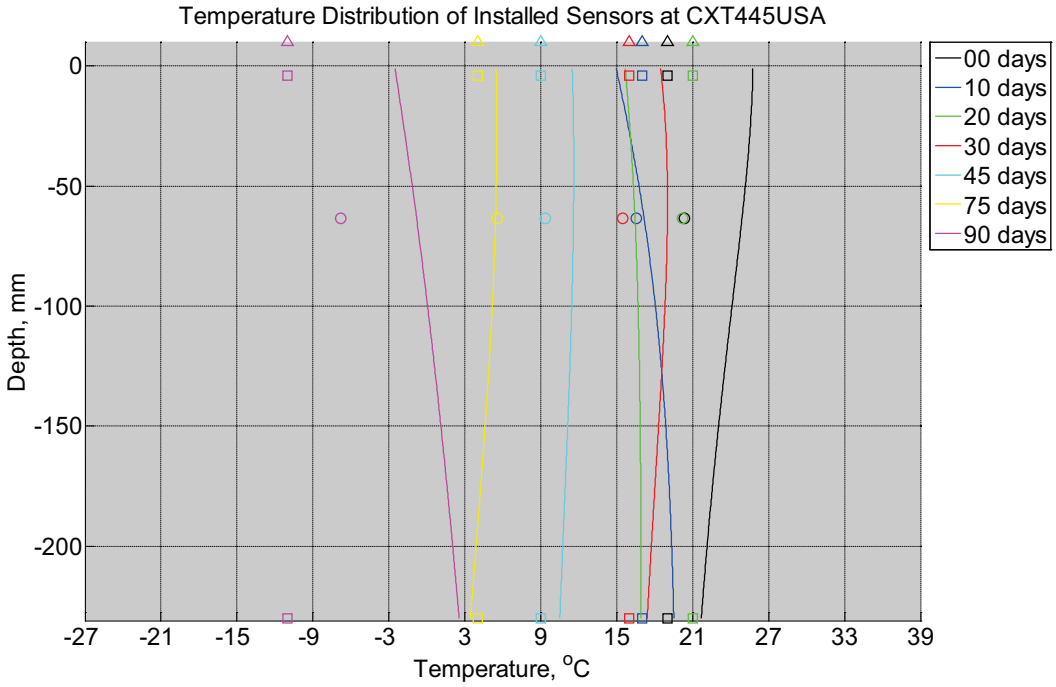

Figure B-884 Measured (markers) and modeled (continuous line) temperature profile distribution as a function of depth inside a concrete crosstie (labeled CXT445USA) installed in track near Lytton, BC, between September 17, 2014, through December 11, 2014. An 8 mm thick polyurethane pad and steel rail are additionally installed atop the concrete crosstie. The model does not incorporate a polyurethane pad nor steel rail line. Triangular markers denote temperature value from CWLY weather station, square markers denote assumed temperature values in ballast, and circular markers denote measured temperature values inside concrete.

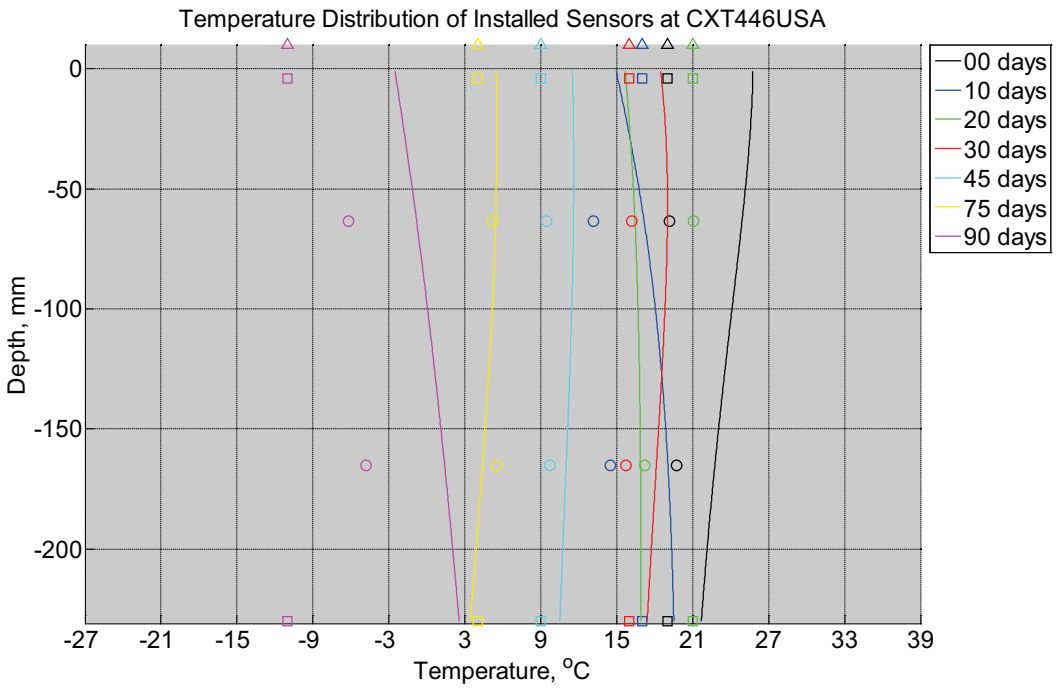

Figure B-885 Measured (markers) and modeled (continuous line) temperature profile distribution as a function of depth inside a concrete crosstie (labeled CXT446USA) installed in track near Lytton, BC, between September 17, 2014, through December 11, 2014. An 8 mm thick polyurethane pad and steel rail are additionally installed atop the concrete crosstie. The model does not incorporate a polyurethane pad nor steel rail line. Triangular markers denote temperature value from CWLY weather station, square markers denote assumed temperature values in ballast, and circular markers denote measured temperature values inside concrete.

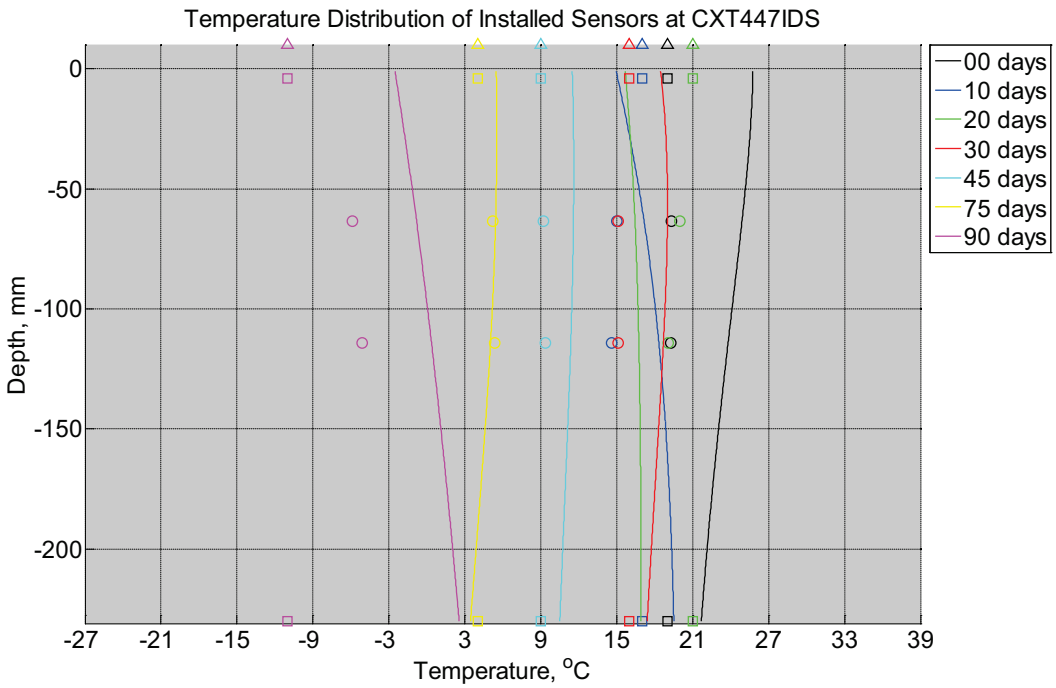

Figure B-886 Measured (markers) and modeled (continuous line) temperature profile distribution as a function of depth inside a concrete crosstie (labeled CXT447IDS) installed in track near Lytton, BC, between September 17, 2014, through December 11, 2014. An 8 mm thick polyurethane pad and steel rail are additionally installed atop the concrete crosstie. The model does not incorporate a polyurethane pad nor steel rail line. Triangular markers denote temperature value from CWLY weather station, square markers denote assumed temperature values in ballast, and circular markers denote measured temperature values inside concrete.

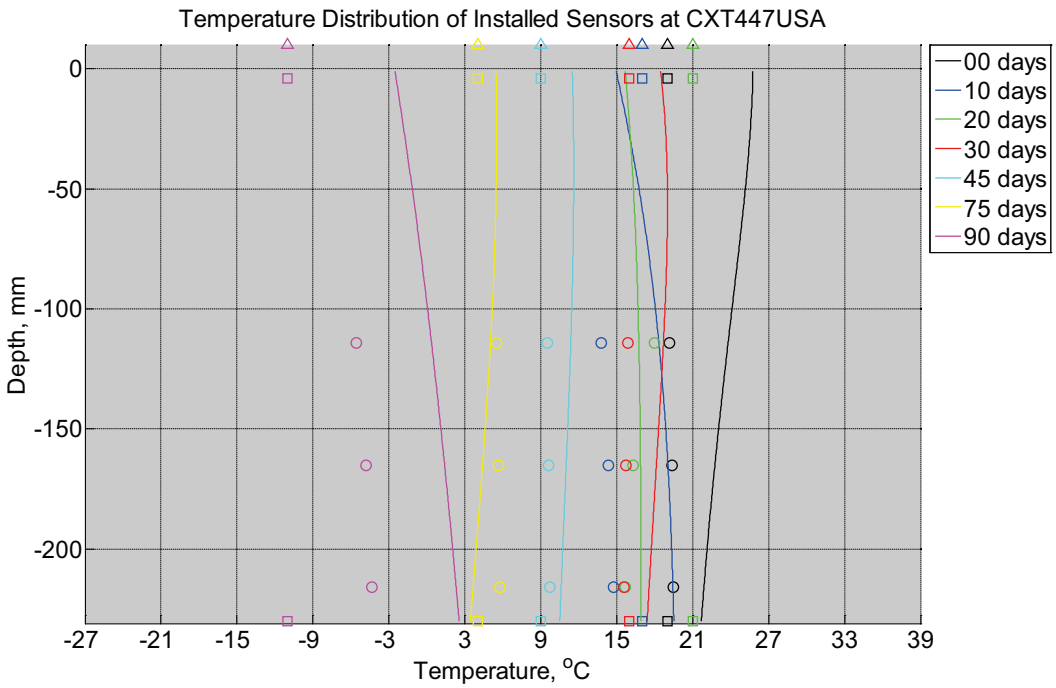

Figure B-887 Measured (markers) and modeled (continuous line) temperature profile distribution as a function of depth inside a concrete crosstie (labeled CXT447USA) installed in track near Lytton, BC, between September 17, 2014, through December 11, 2014. An 8 mm thick polyurethane pad and steel rail are additionally installed atop the concrete crosstie. The model does not incorporate a polyurethane pad nor steel rail line. Triangular markers denote temperature value from CWLY weather station, square markers denote assumed temperature values in ballast, and circular markers denote measured temperature values inside concrete.

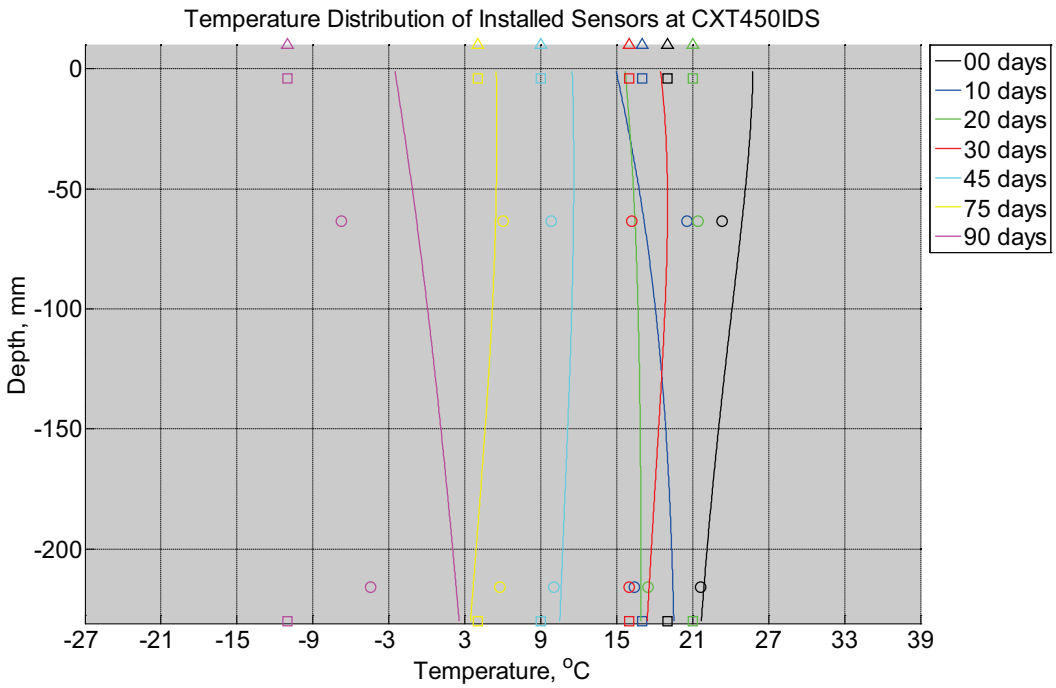

Figure B-888 Measured (markers) and modeled (continuous line) temperature profile distribution as a function of depth inside a concrete crosstie (labeled CXT450IDS) installed in track near Lytton, BC, between September 17, 2014, through December 11, 2014. An 8 mm thick polyurethane pad and steel rail are additionally installed atop the concrete crosstie. The model does not incorporate a polyurethane pad nor steel rail line. Triangular markers denote temperature value from CWLY weather station, square markers denote assumed temperature values in ballast, and circular markers denote measured temperature values inside concrete.

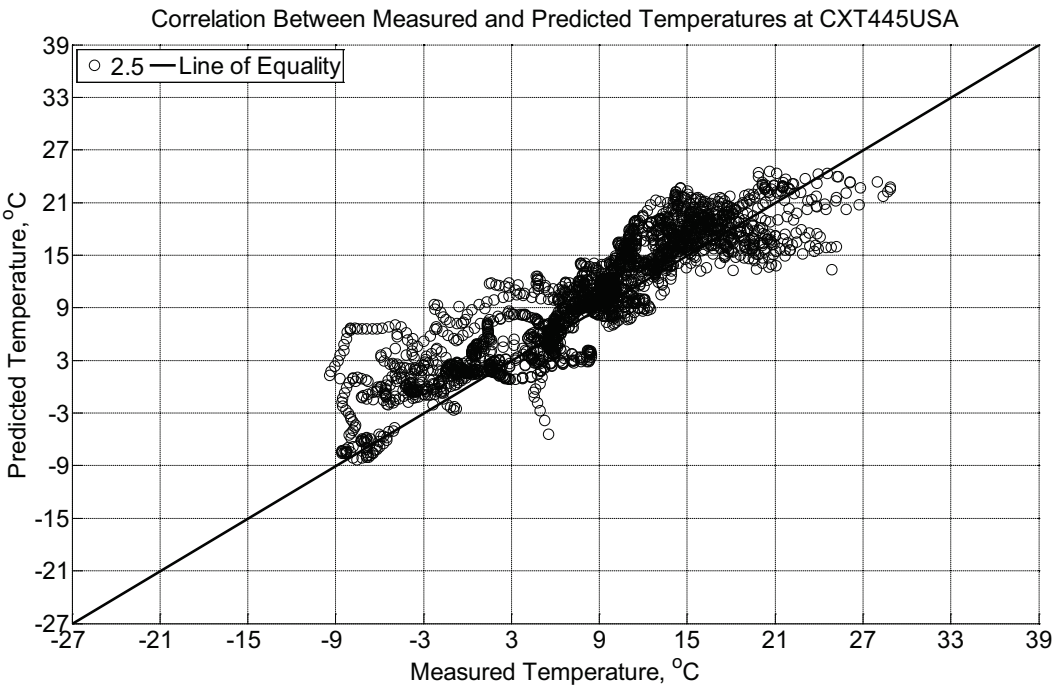

Figure B-889 Correlation between measured and predicted temperature values 2.5 inches (63.5 mm) from the surface of a concrete crosstie (labeled CXT445USA) installed in track near Lytton, BC, between September 17, 2014, through December 11, 2014. An 8 mm thick polyurethane pad and steel rail are additionally installed atop the concrete crosstie. The model does not incorporate a polyurethane pad nor steel rail line.

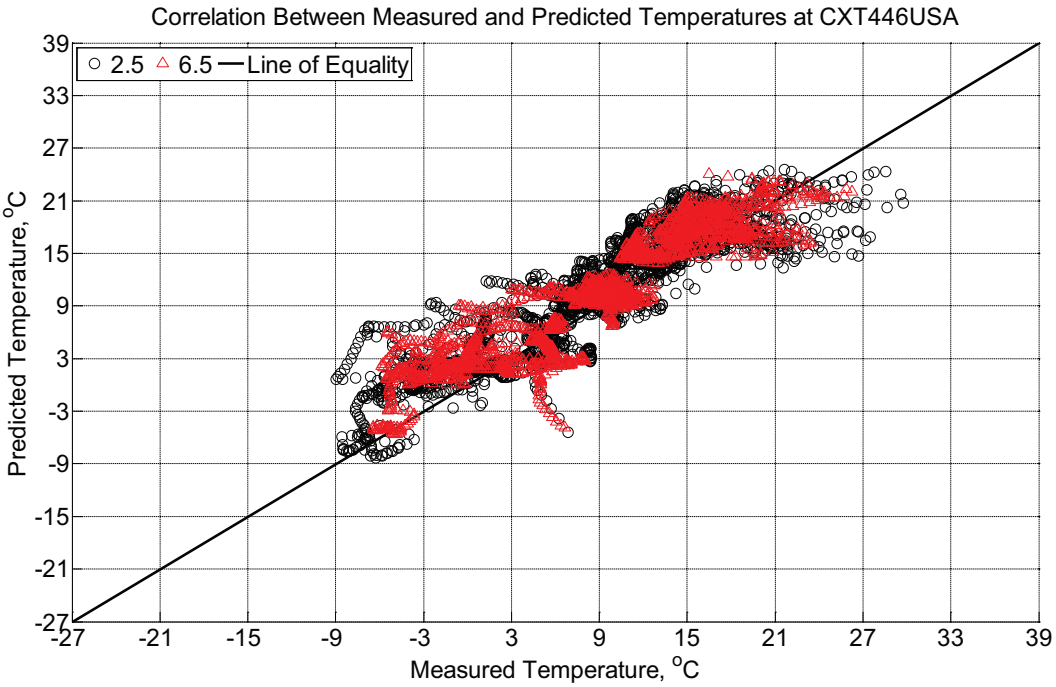

Figure B-890 Correlation between measured and predicted temperature values 2.5 inches

(63.5 mm) and 6.5 inches (139.7 mm) from the surface of a concrete crosstie (labeled CXT446USA) installed in track near Lytton, BC, between September 17, 2014, through December 11, 2014. An 8 mm thick polyurethane pad and steel rail are additionally installed atop the concrete crosstie. The model does not incorporate a polyurethane pad nor steel rail line.

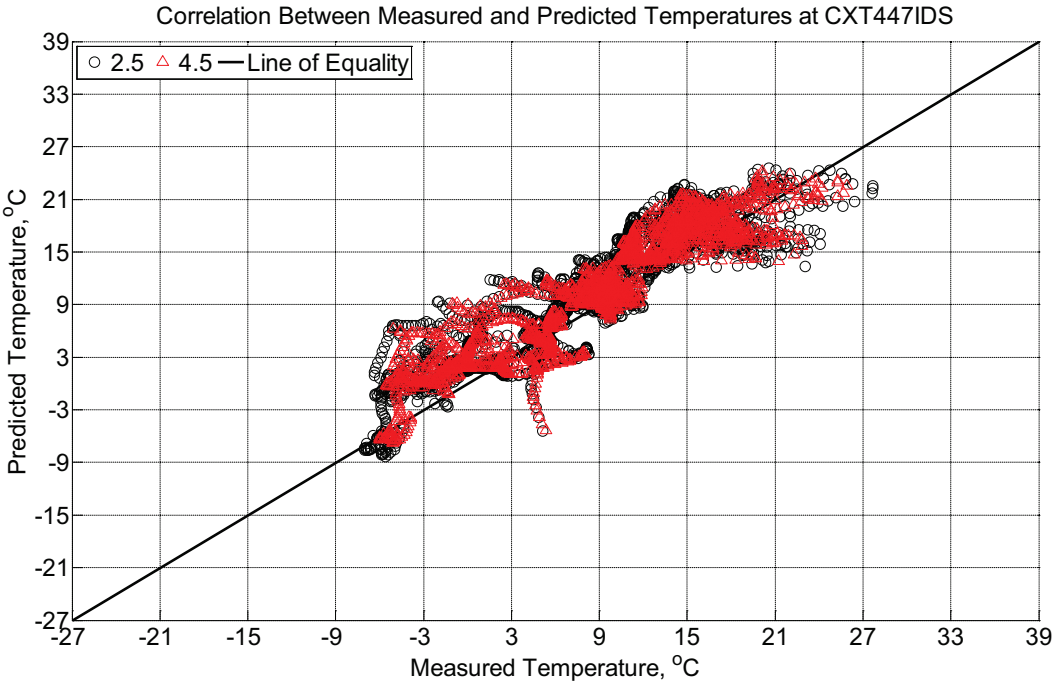

Figure B-891 Correlation between measured and predicted temperature values 2.5 inches (63.5 mm) and 4.5 inches (114.3 mm) from the surface of a concrete crosstie (labeled CXT447IDS) installed in track near Lytton, BC, between September 17, 2014, through December 11, 2014. An 8 mm thick polyurethane pad and steel rail are additionally installed atop the concrete crosstie. The model does not incorporate a polyurethane pad nor steel rail line.

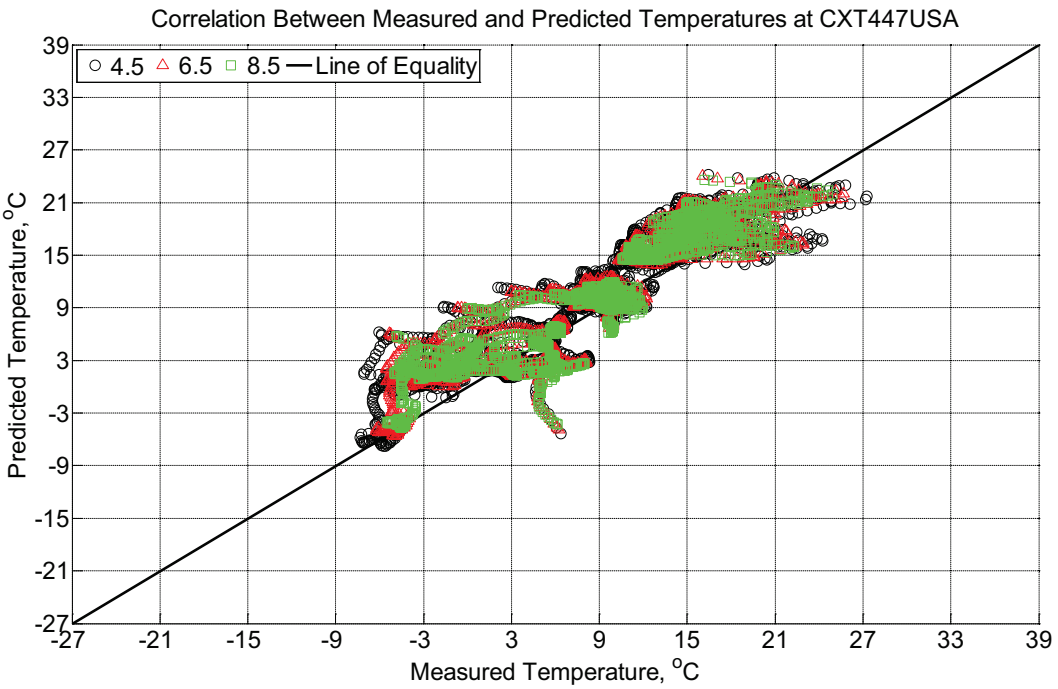

Figure B-892 Correlation between measured and predicted temperature values 4.5 inches (114.3 mm), 6.5 inches (139.7 mm), and 8.5 inches (215.9 mm) from the surface of a concrete crosstie (labeled CXT447USA) installed in track near Lytton, BC, between September 17, 2014, through December 11, 2014. An 8 mm thick polyurethane pad and steel rail are additionally installed atop the concrete crosstie. The model does not incorporate a polyurethane pad nor steel rail line.

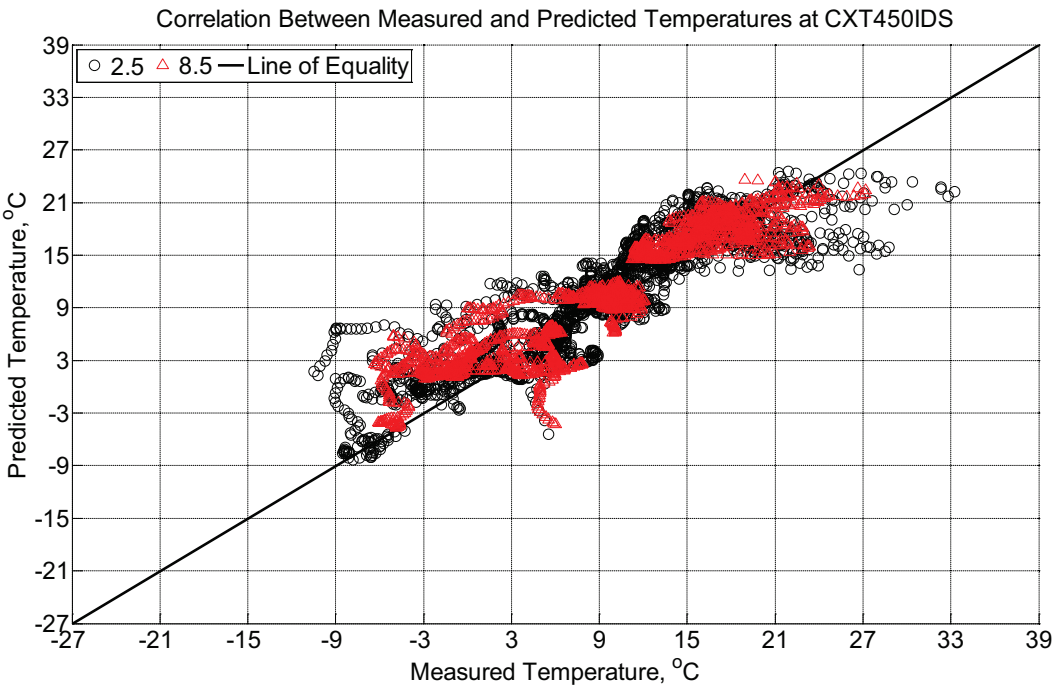

Figure B-893 Correlation between measured and predicted temperature values 2.5 inches (63.5 mm) and 8.5 inches (215.9 mm) from the surface of a concrete crosstie (labeled CXT450IDS) installed in track near Lytton, BC, between September 17, 2014, through December 11, 2014. An 8 mm thick polyurethane pad and steel rail are additionally installed atop the concrete crosstie. The model does not incorporate a polyurethane pad nor steel rail line.

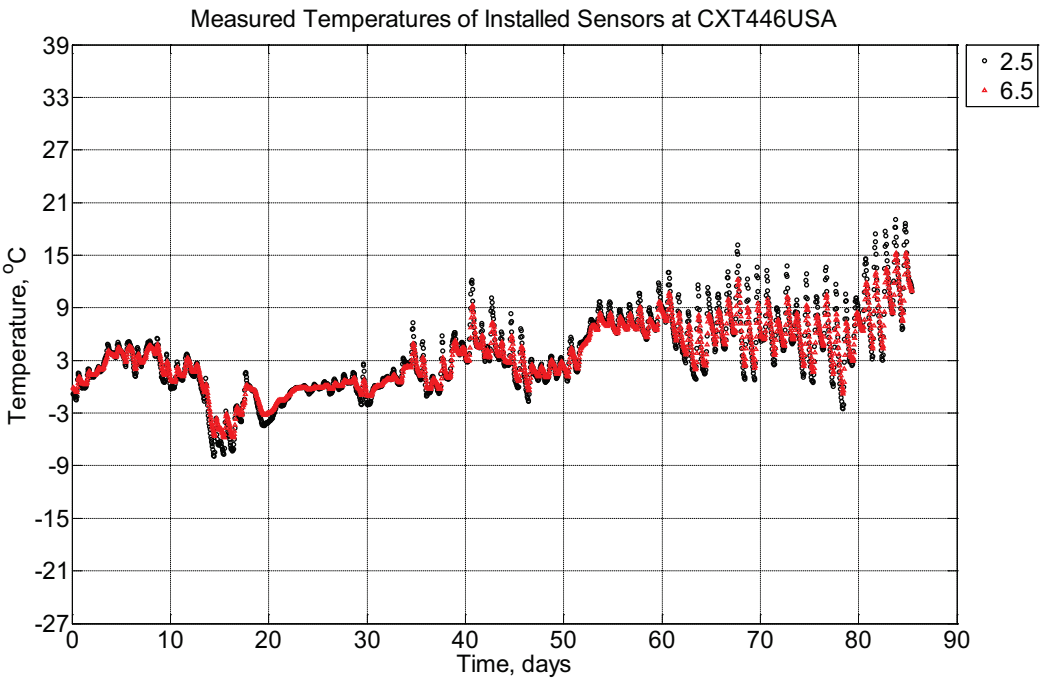

Figure B-894 Measured temperature at depths 2.5 inches (63.5 mm) and 6.5 inches (139.7 mm) from the surface of a concrete crosstie (labeled CXT446USA) installed in track near Lytton, BC, between December 16, 2014, through March 11, 2015. An 8 mm thick polyurethane pad and steel rail are additionally installed atop the concrete crosstie.

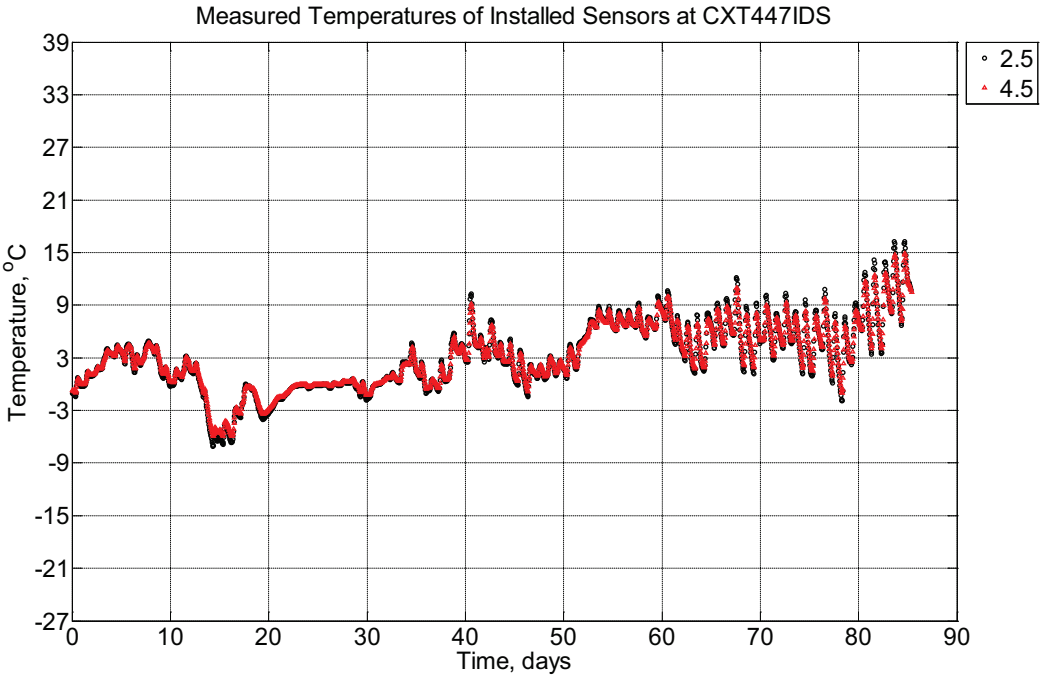

Figure B-895 Measured temperature at depths of 2.5 inches (63.5 mm) and 4.5 inches (114.3 mm) from the surface of a concrete crosstie (labeled CXT447IDS) installed in track

near Lytton, BC, between December 16, 2014, through March 11, 2015. An 8 mm thick polyurethane pad and steel rail are additionally installed atop the concrete crosstie.

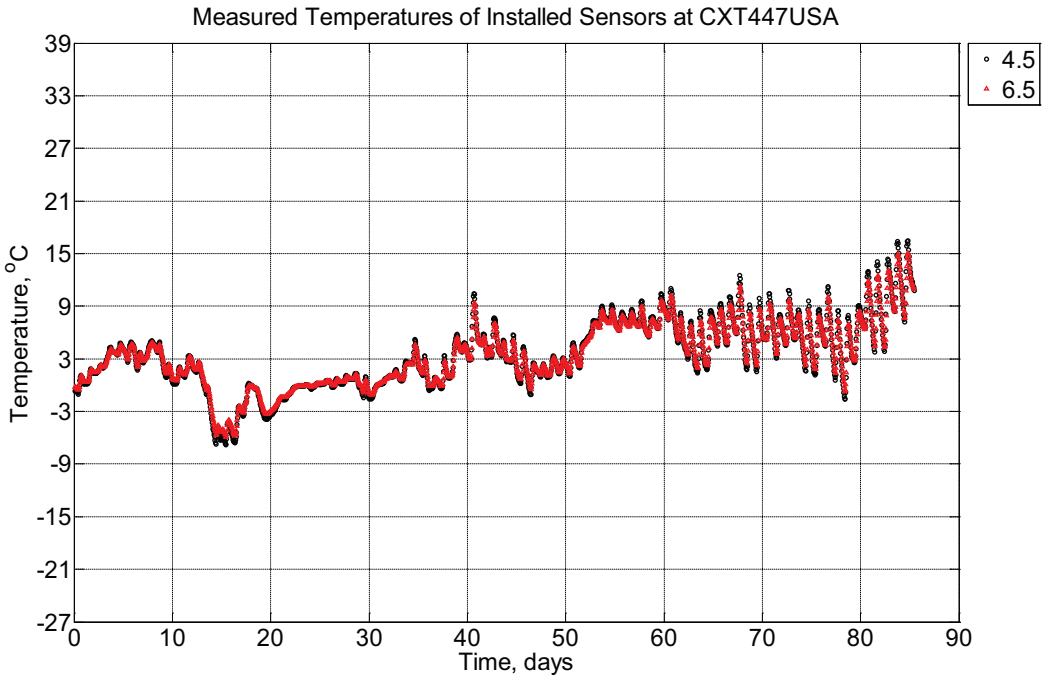

Figure B-896 Measured temperature at depths of 4.5 inches (114.3 mm) and 6.5 inches (139.7 mm) from the surface of a concrete crosstie (labeled CXT447USA) installed in track near Lytton, BC, between December 16, 2014, through March 11, 2015. An 8 mm thick polyurethane pad and steel rail are additionally installed atop the concrete crosstie.

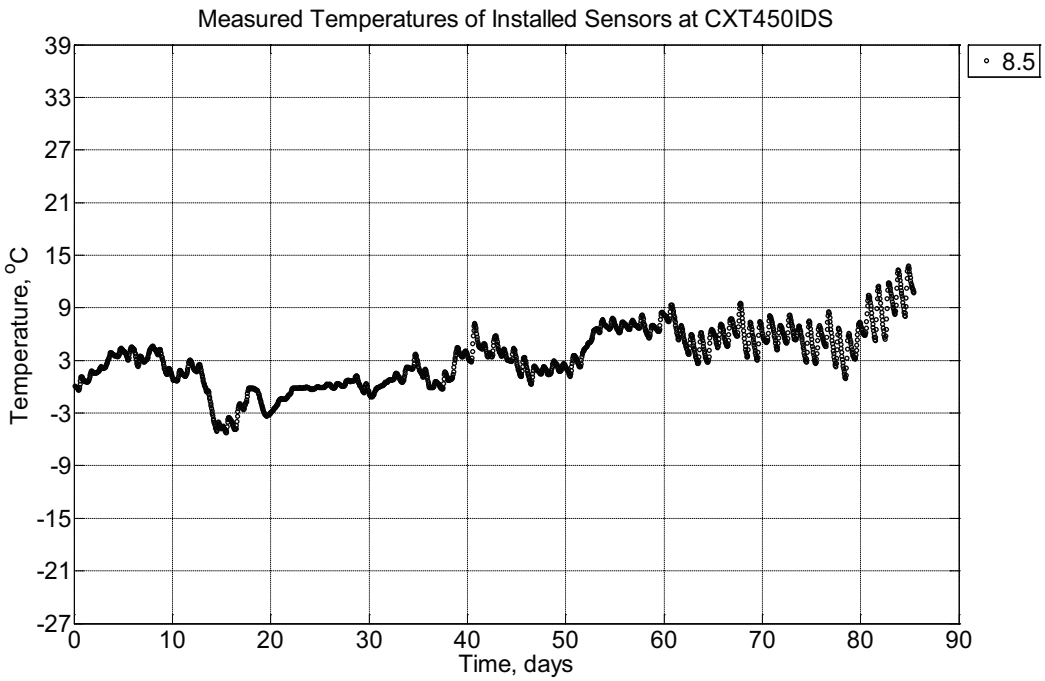

Figure B-897 Measured temperature at a depth 8.5 inches (215.9 mm) from the surface of a concrete crosstie (labeled CXT450IDS) installed in track near Lytton, BC, between December 16, 2014, through March 11, 2015. An 8 mm thick polyurethane pad and steel rail are additionally installed atop the concrete crosstie.

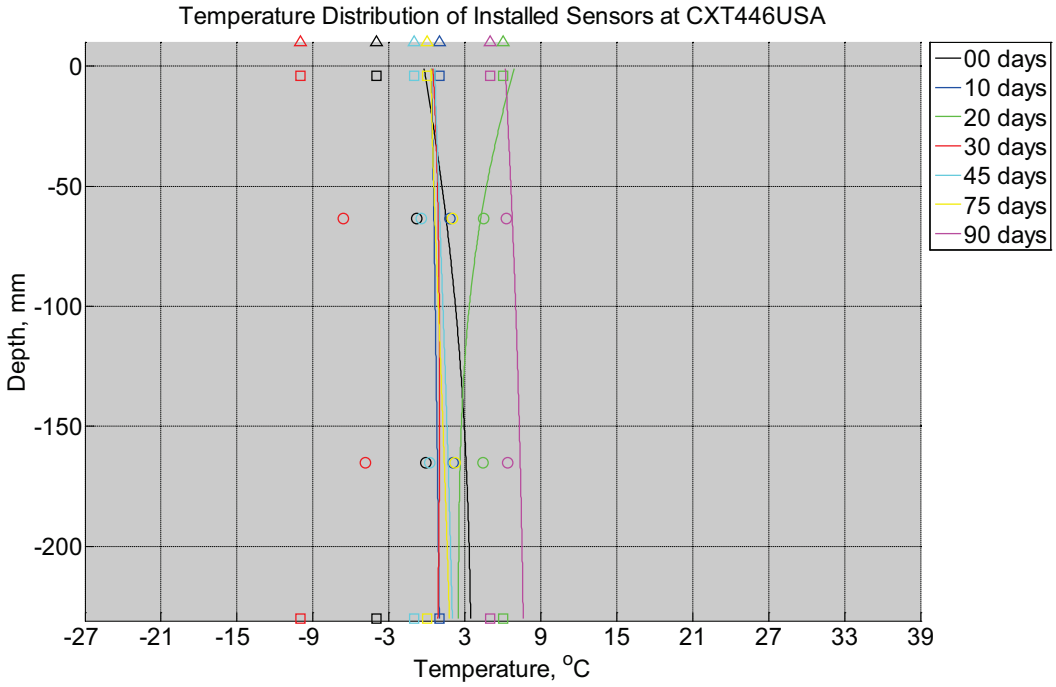

Figure B-898 Measured (markers) and modeled (continuous line) temperature profile distribution as a function of depth inside a concrete crosstie (labeled CXT446USA)

installed in track near Lytton, BC, between December 16, 2014, through March 11, 2015. An 8 mm thick polyurethane pad and steel rail are additionally installed atop the concrete crosstie. The model does not incorporate a polyurethane pad nor steel rail line. Triangular markers denote temperature value from CWLY weather station, square markers denote assumed temperature values in ballast, and circular markers denote measured temperature values inside concrete.

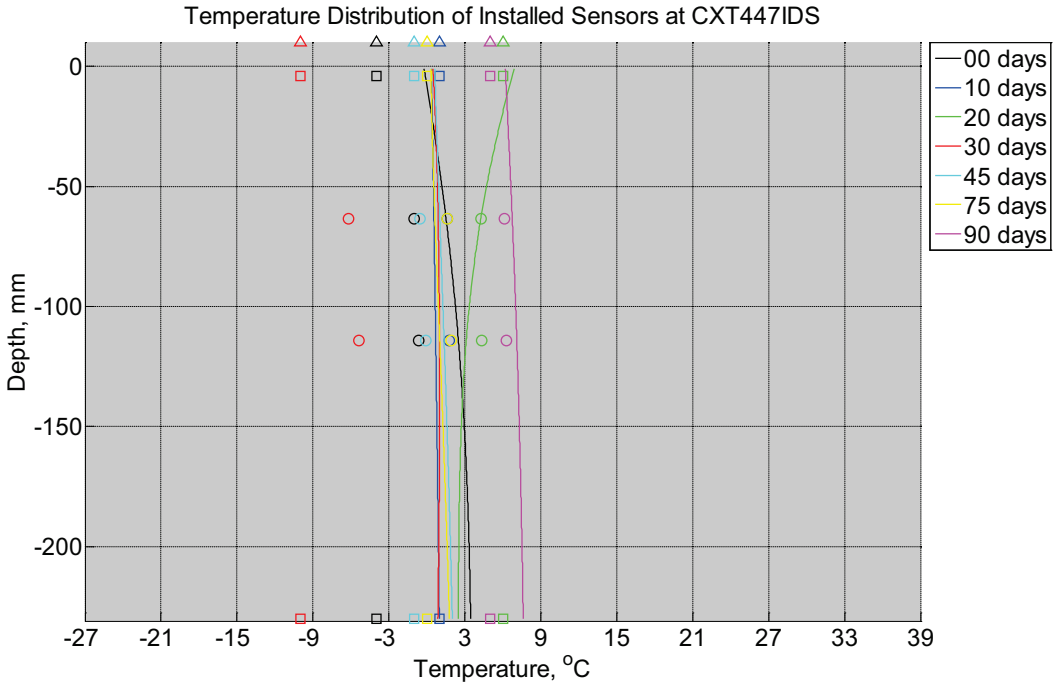

Figure B-899 Measured (markers) and modeled (continuous line) temperature profile distribution as a function of depth inside a concrete crosstie (labeled CXT446USA) installed in track near Lytton, BC, between December 16, 2014, through March 11, 2015. An 8 mm thick polyurethane pad and steel rail are additionally installed atop the concrete crosstie. The model does not incorporate a polyurethane pad nor steel rail line. Triangular markers denote temperature value from CWLY weather station, square markers denote assumed temperature values in ballast, and circular markers denote measured temperature values inside concrete.

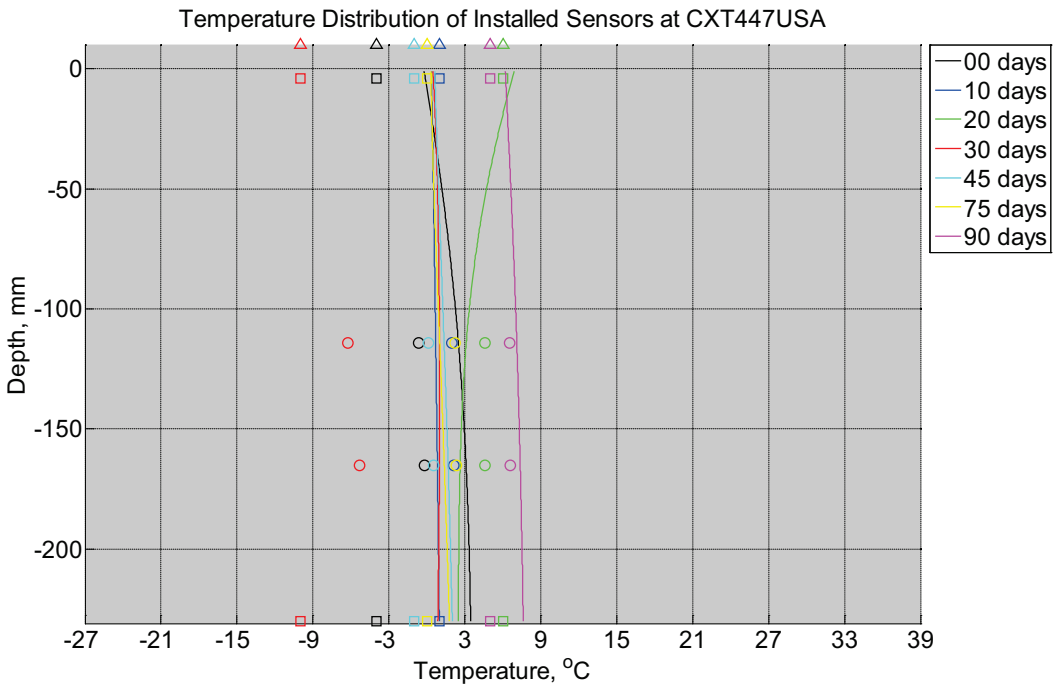

Figure B-900 Measured (markers) and modeled (continuous line) temperature profile distribution as a function of depth inside a concrete crosstie (labeled CXT446USA) installed in track near Lytton, BC, between December 16, 2014, through March 11, 2015. An 8 mm thick polyurethane pad and steel rail are additionally installed atop the concrete crosstie. The model does not incorporate a polyurethane pad nor steel rail line. Triangular markers denote temperature value from CWLY weather station, square markers denote assumed temperature values in ballast, and circular markers denote measured temperature values inside concrete.

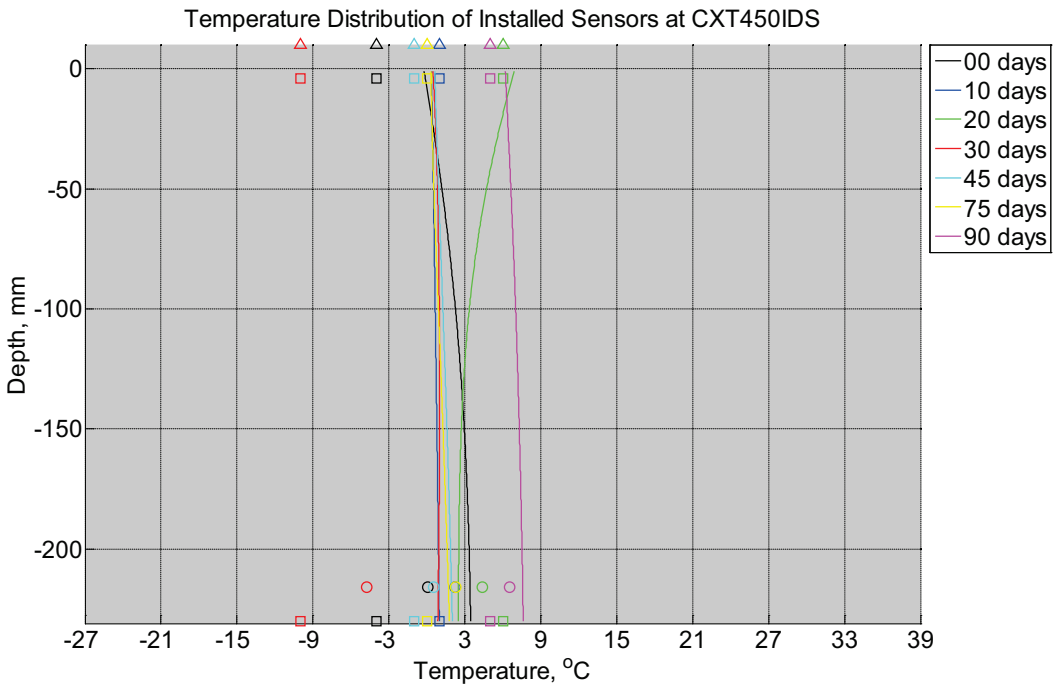

Figure B-901 Measured (markers) and modeled (continuous line) temperature profile distribution as a function of depth inside a concrete crosstie (labeled CXT446USA) installed in track near Lytton, BC, between December 16, 2014, through March 11, 2015. An 8 mm thick polyurethane pad and steel rail are additionally installed atop the concrete crosstie. The model does not incorporate a polyurethane pad nor steel rail line. Triangular markers denote temperature value from CWLY weather station, square markers denote assumed temperature values in ballast, and circular markers denote measured temperature values inside concrete.

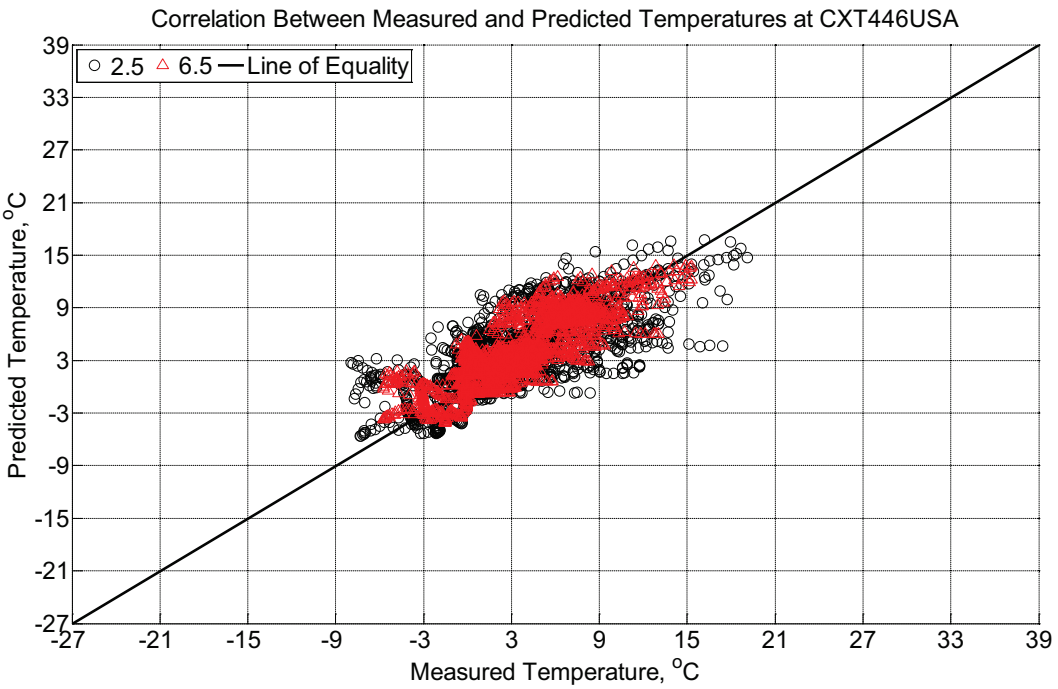

Figure B-902 Correlation between measured and predicted temperature values 2.5 inches (63.5 mm) and 6.5 inches (139.7 mm) from the surface of a concrete crosstie (labeled CXT446USA) installed in track near Lytton, BC, between December 16, 2014, through March 11, 2015. An 8 mm thick polyurethane pad and steel rail are additionally installed atop the concrete crosstie. The model does not incorporate a polyurethane pad nor steel rail line.

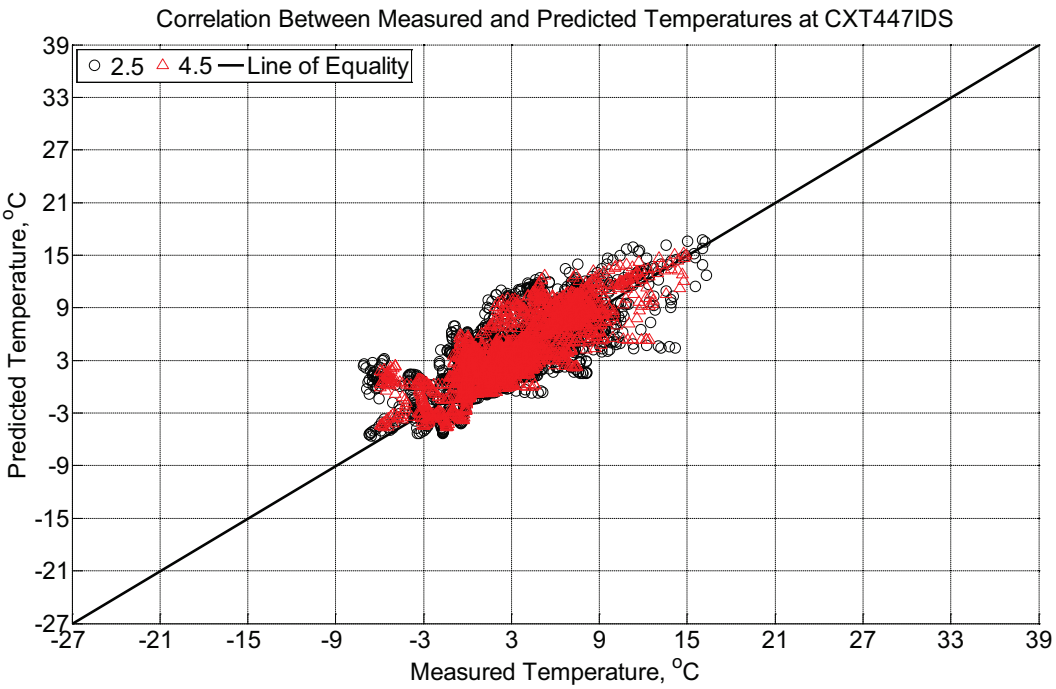

Figure B-903 Correlation between measured and predicted temperature values 2.5 inches (63.5 mm) and 4.5 inches (114.3 mm) from the surface of a concrete crosstie (labeled CXT447IDS) installed in track near Lytton, BC, between December 16, 2014, through March 11, 2015. An 8 mm thick polyurethane pad and steel rail are additionally installed atop the concrete crosstie. The model does not incorporate a polyurethane pad nor steel rail line.

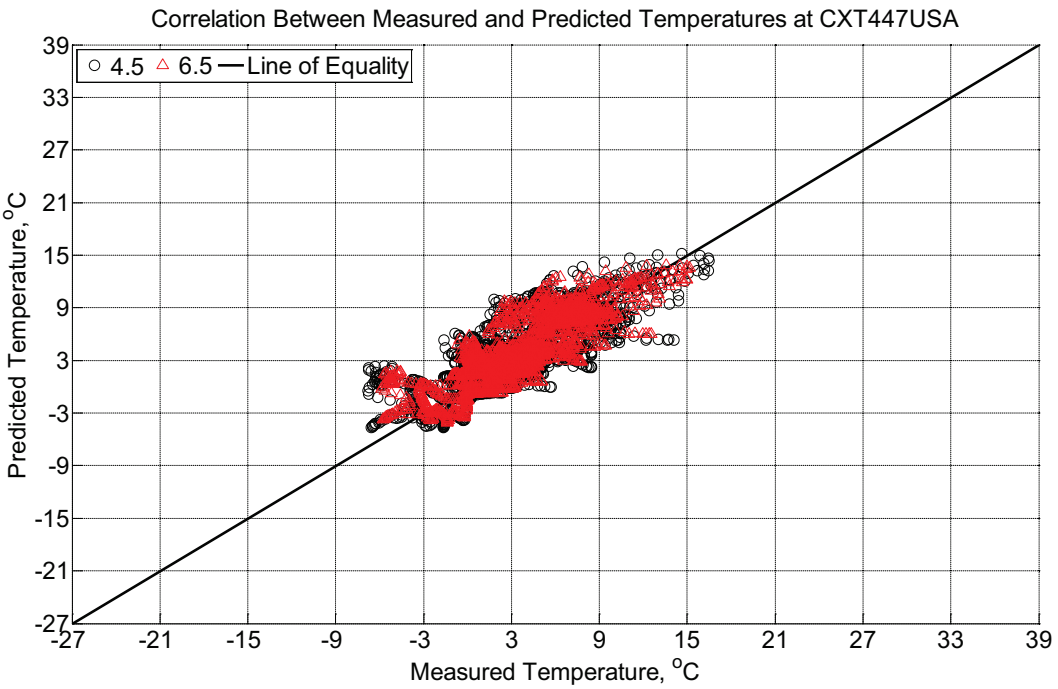

Figure B-904 Correlation between measured and predicted temperature values 4.5 inches (114.3 mm) and 6.5 inches (139.7 mm) from the surface of a concrete crosstie (labeled CXT447USA) installed in track near Lytton, BC, between December 16, 2014, through March 11, 2015. An 8 mm thick polyurethane pad and steel rail are additionally installed atop the concrete crosstie. The model does not incorporate a polyurethane pad nor steel rail line.

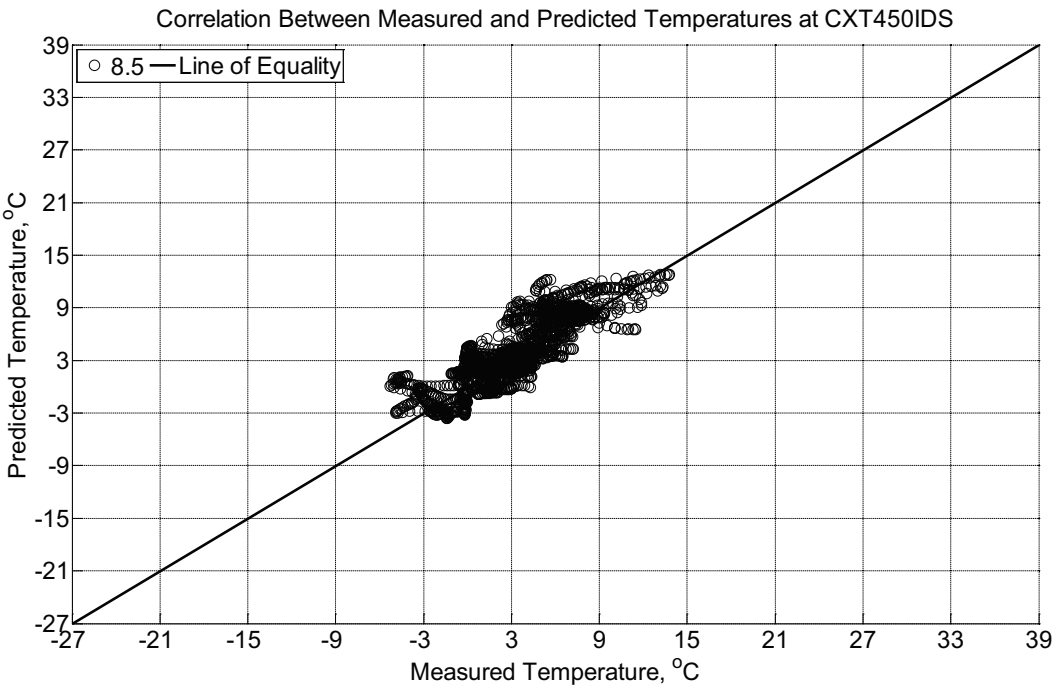

Figure B-905 Correlation between measured and predicted temperature values 8.5 inches (215.9 mm) from the surface of a concrete crosstie (labeled CXT450IDS) installed in track near Lytton, BC, between December 16, 2014, through March 11, 2015. An 8 mm thick polyurethane pad and steel rail are additionally installed atop the concrete crosstie. The model does not incorporate a polyurethane pad nor steel rail line.

Measured and predicted internal relative humidity of instrumented model concrete crossties located in Rantoul, IL.

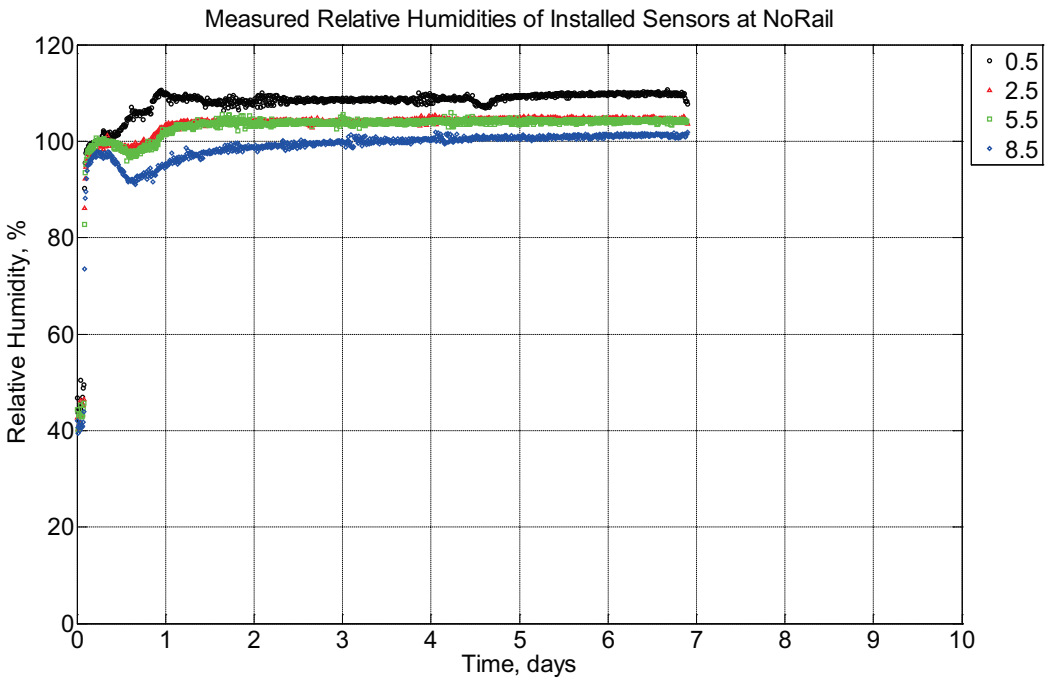

Figure B-906 Measured relative humidity at depths of 0.5 inches (12.7 mm), 2.5 inches (63.5 mm), 5.5 inches (139.7 mm), and 8.5 inches (215.9 mm) from the surface of a model concrete crosstie (labeled NoRail) without a polyurethane pad nor rail curing inside an environmentally controlled room (50% RH, 23 ºC) between October 8, 2014, through October 15, 2014.

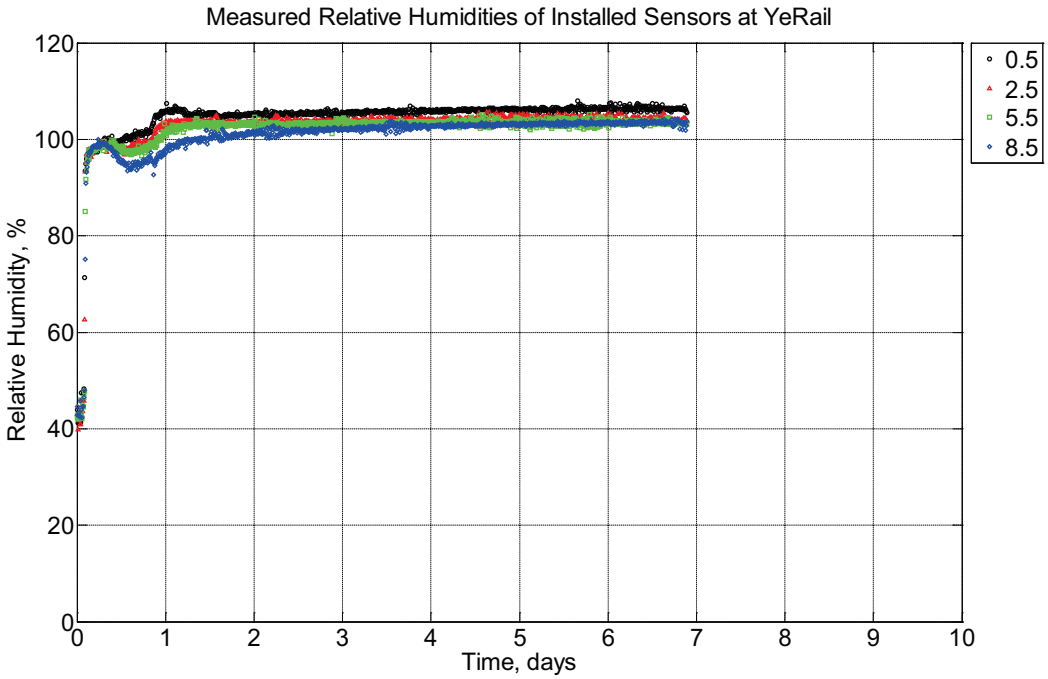

Figure B-907 Measured relative humidity at depths of 0.5 inches (12.7 mm), 2.5 inches

(63.5 mm), 5.5 inches (139.7 mm), and 8.5 inches (215.9 mm) from the surface of a model concrete crosstie (labeled YeRail) without a polyurethane pad nor rail curing inside an environmentally controlled room (50% RH, 23 ºC) between October 8, 2014, through October 15, 2014.

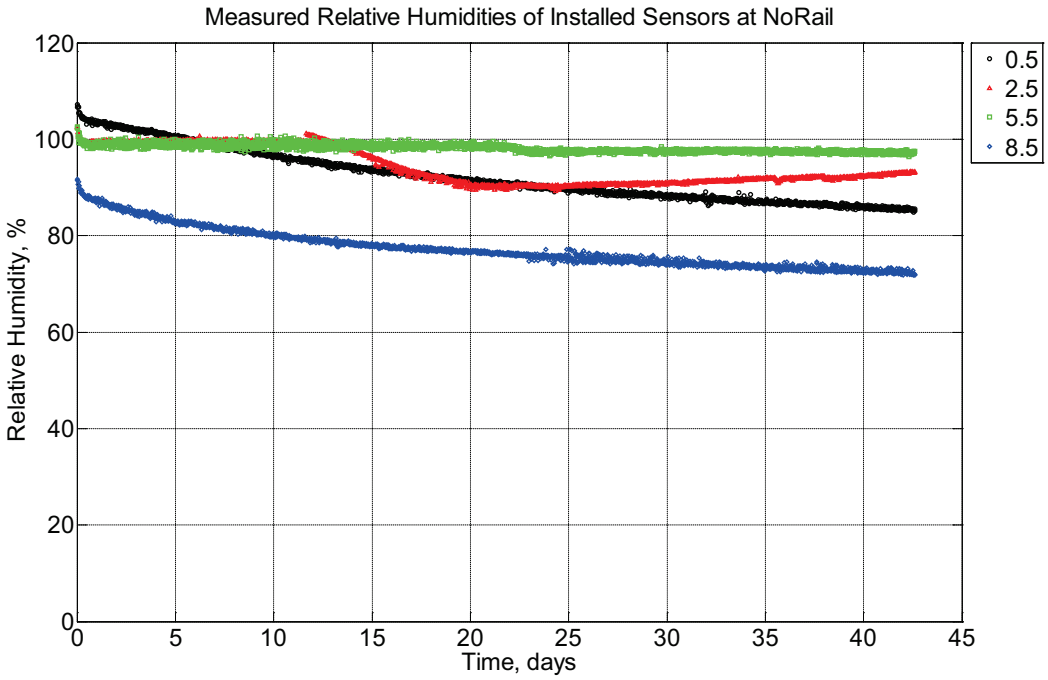

Figure B-908 Measured relative humidity at depths of 0.5 inches (12.7 mm), 2.5 inches (63.5 mm), 5.5 inches (139.7 mm), and 8.5 inches (215.9 mm) from the surface of a model concrete crosstie (labeled NoRail) without a polyurethane pad nor rail curing inside an environmentally controlled room (50% RH, 23 ºC) between October 18, 2014, through November 29, 2014.

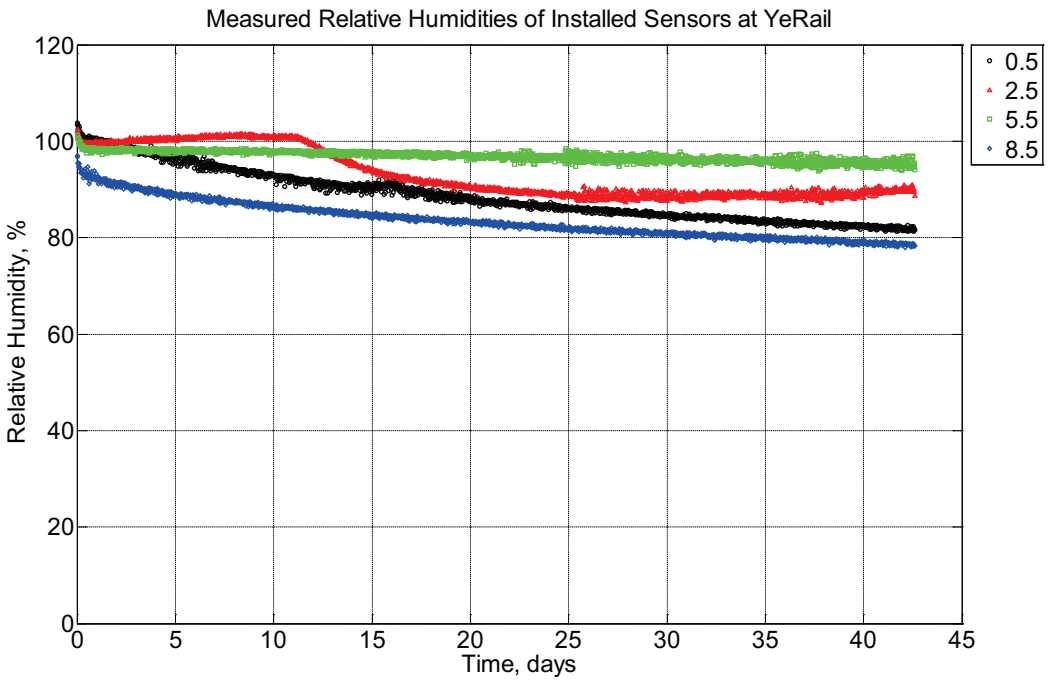

Figure B-909 Measured relative humidity at depths of 0.5 inches (12.7 mm), 2.5 inches (63.5 mm), 5.5 inches (139.7 mm), and 8.5 inches (215.9 mm) from the surface of a model concrete crosstie (labeled YeRail) without a polyurethane pad nor rail curing inside an environmentally controlled room (50% RH, 23 ºC) between October 18, 2014, through November 29, 2014.

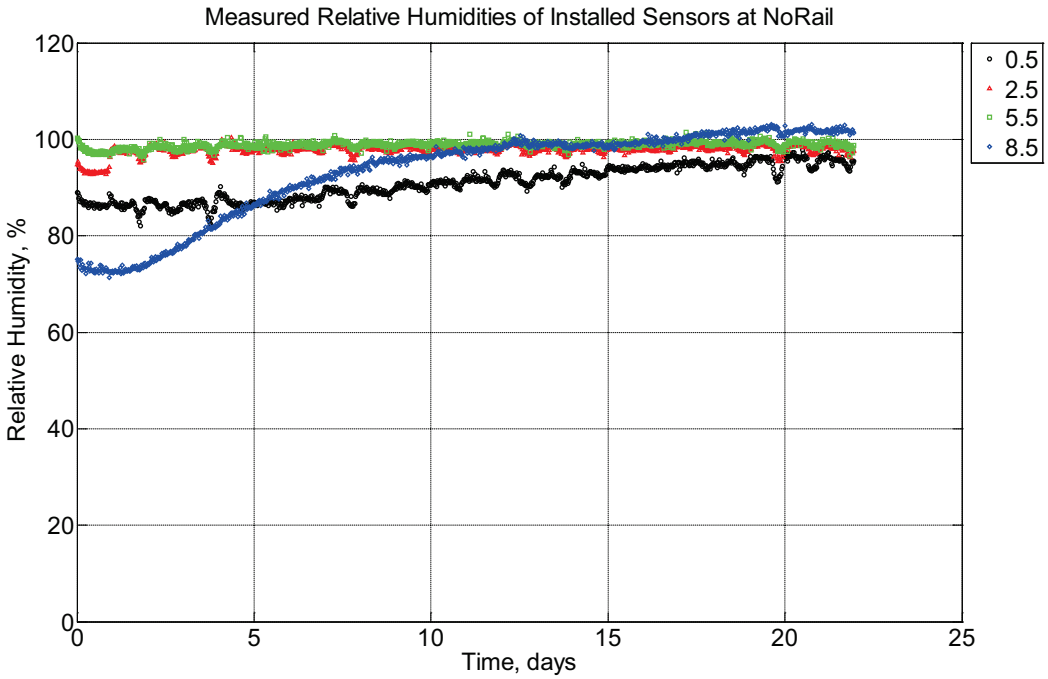

Figure B-910 Measured relative humidity at depths of 0.5 inches (12.7 mm), 2.5 inches

(63.5 mm), 5.5 inches (139.7 mm), and 8.5 inches (215.9 mm) from the surface of a model concrete crosstie (labeled NoRail) without a polyurethane pad nor rail installed in ballast in Rantoul, IL, between November 29, 2014, through December 21, 2014.

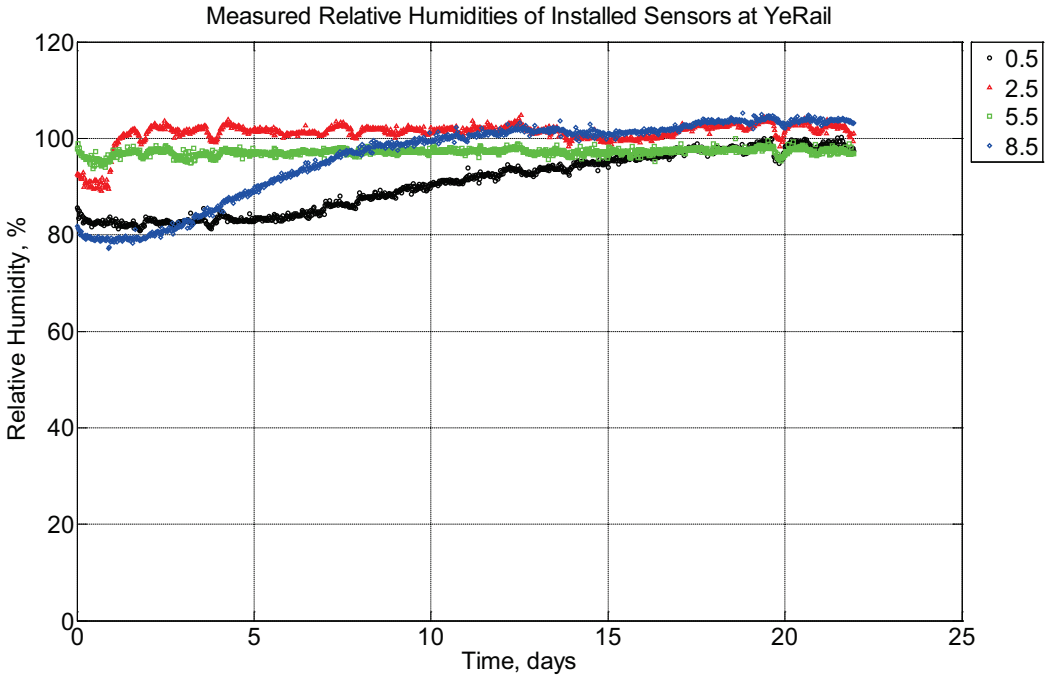

Figure B-911 Measured relative humidity at depths of 0.5 inches (12.7 mm), 2.5 inches (63.5 mm), 5.5 inches (139.7 mm), and 8.5 inches (215.9 mm) from the surface of a model concrete crosstie (labeled YeRail) installed in ballast in Rantoul, IL, between November 29, 2014, through December 21, 2014. An 8 mm thick polyurethane pad and 12 in (30.48 cm) length 136 lb/yd (67.5 kg/m) section of steel rail are additionally installed atop the model concrete crosstie.

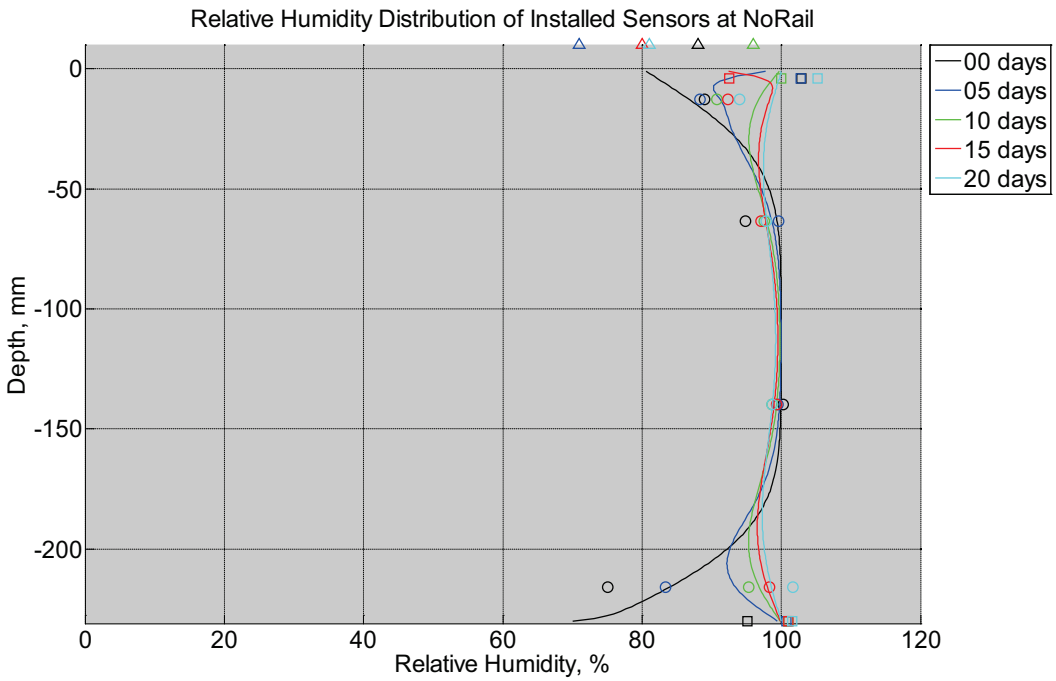

Figure B-912 Measured (markers) and modeled (continuous line) relative humidity profile distribution as a function of depth inside a model concrete crosstie (labeled NoRail) without a polyurethane pad nor rail installed in ballast in Rantoul, IL, between November 29, 2014, through December 21, 2014. Triangular markers denote relative humidity value from KTIP weather station, square markers denote measured relative humidity values from ballast, and circular markers denote measured relative humidity values inside concrete.

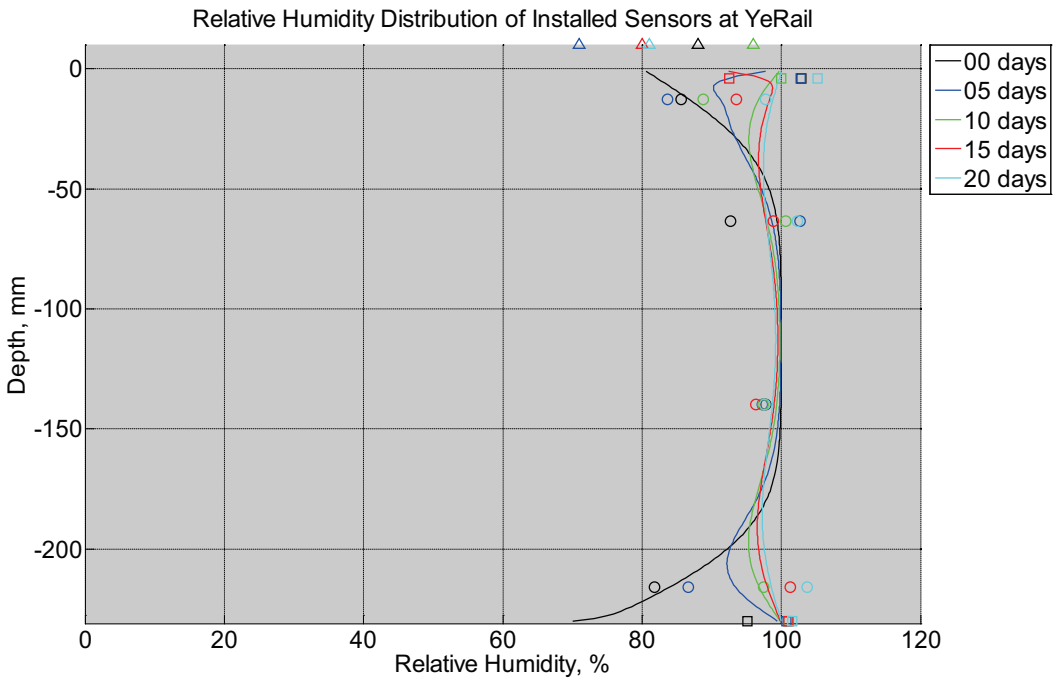

Figure B-913 Measured (markers) and modeled (continuous line) relative humidity profile distribution as a function of depth inside a model concrete crosstie (labeled YeRail) installed in ballast in Rantoul, IL, between November 29, 2014, through December 21, 2014. An 8 mm thick polyurethane pad and 12 in (30.48 cm) length 136 lb/yd (67.5 kg/m) section of steel rail are additionally installed atop the model concrete crosstie. The model does not incorporate a polyurethane pad nor steel rail line. Triangular markers denote relative humidity value from KTIP weather station, square markers denote measured relative humidity values from ballast, and circular markers denote measured relative humidity values inside concrete.

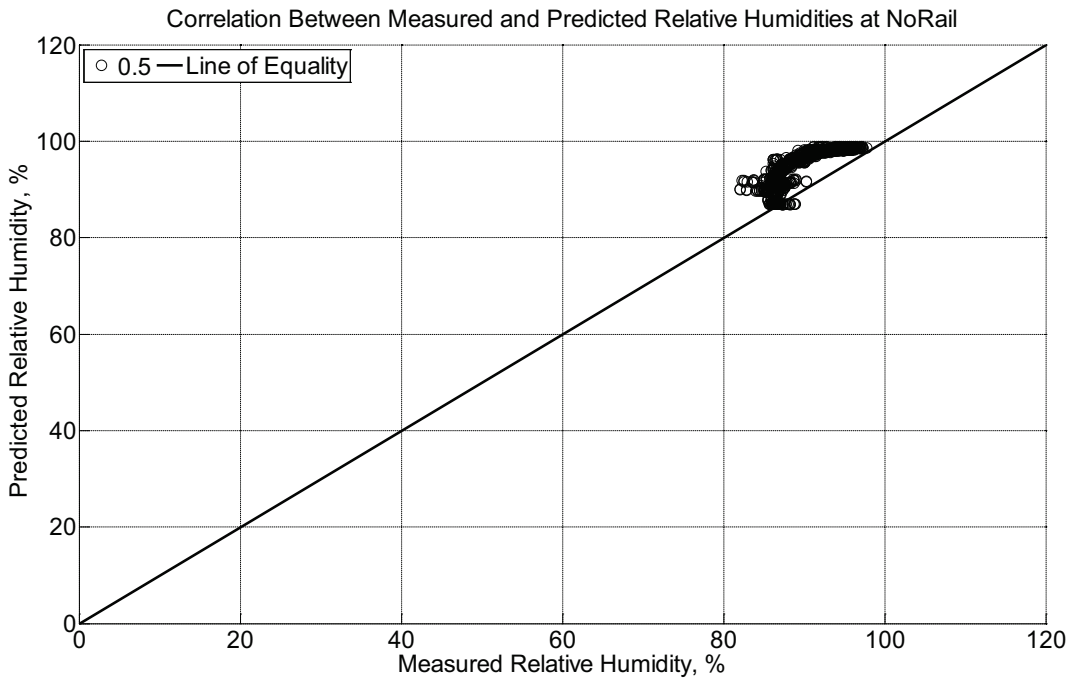

Figure B-914 Correlation between measured and predicted relative humidity values 0.5 inches (12.7 mm) from the surface of a model concrete crosstie (labeled NoRail) without a polyurethane pad nor rail installed in ballast in Rantoul, IL, between November 29, 2014, through December 21, 2014.

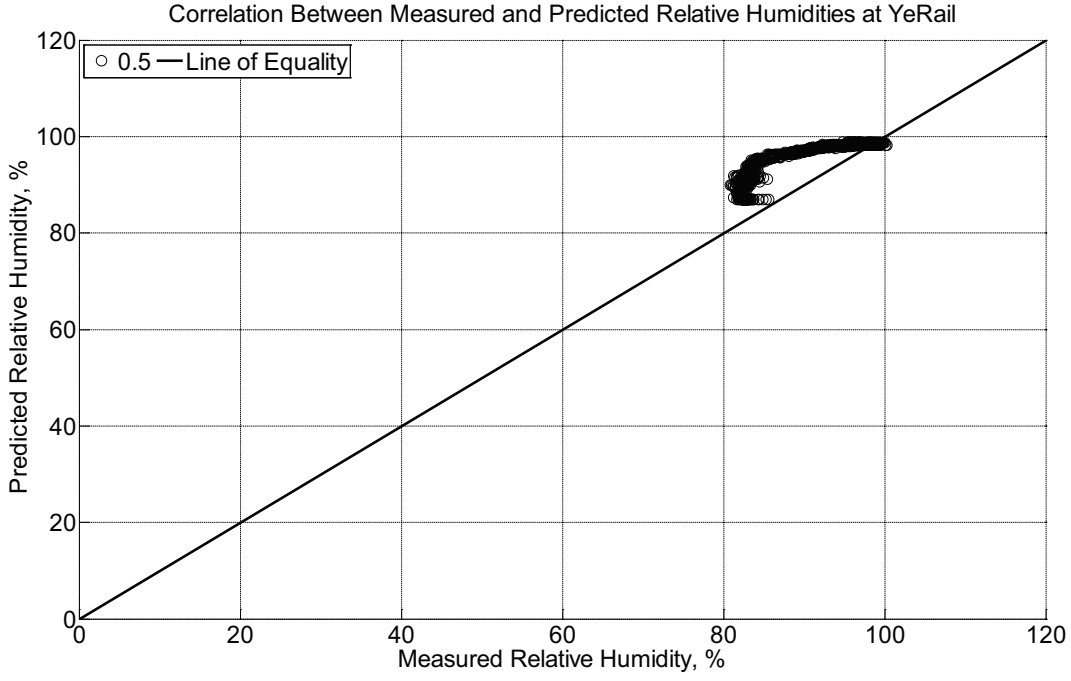

Figure B-915 Correlation between measured and predicted relative humidity values 0.5 inches (12.7 mm) from the surface of a model concrete crosstie (labeled YeRail)

installed in ballast in Rantoul, IL, between November 29, 2014, through December 21, 2014. An 8 mm thick polyurethane pad and 12 in (30.48 cm) length 136 lb/yd (67.5 kg/m) section of steel rail are additionally installed atop the model concrete crosstie. The model does not incorporate a polyurethane pad nor steel rail line.

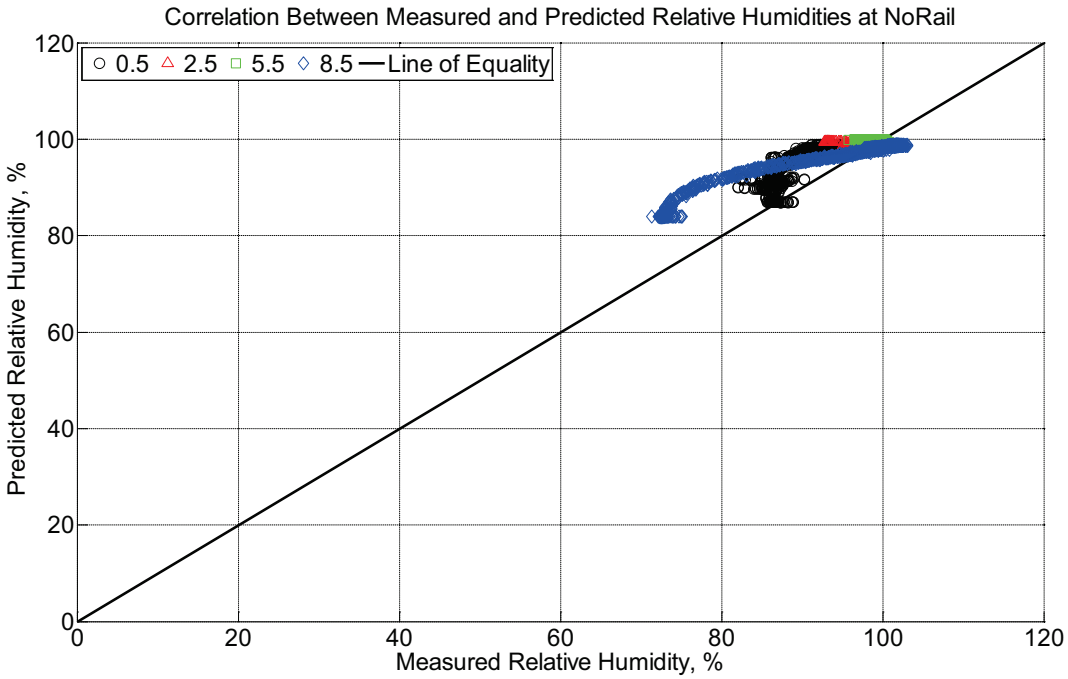

Figure B-916 Correlation between measured and predicted relative humidity values 0.5 inches (12.7 mm), 2.5 inches (63.5 mm), 5.5 inches (139.7 mm), and 8.5 inches (215.9 mm) from the surface of a model concrete crosstie (labeled NoRail) without a polyurethane pad nor rail installed in ballast in Rantoul, IL, between November 29, 2014, through December 21, 2014.

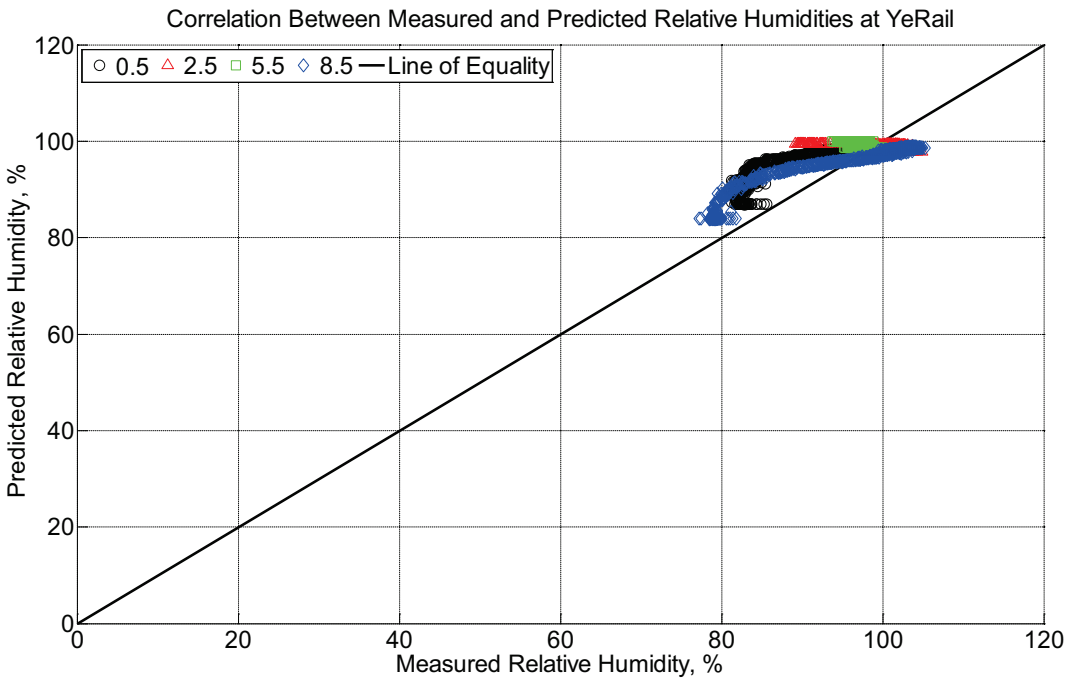

Figure B-917 Correlation between measured and predicted relative humidity values 0.5 inches (12.7 mm), 2.5 inches (63.5 mm), 5.5 inches (139.7 mm), and 8.5 inches (215.9 mm) from the surface of a model concrete crosstie (labeled YeRail) installed in ballast in Rantoul, IL, between November 29, 2014, through December 21, 2014. An 8 mm thick polyurethane pad and 12 in (30.48 cm) length 136 lb/yd (67.5 kg/m) section of steel rail are additionally installed atop the model concrete crosstie. The model does not incorporate a polyurethane pad nor steel rail line.

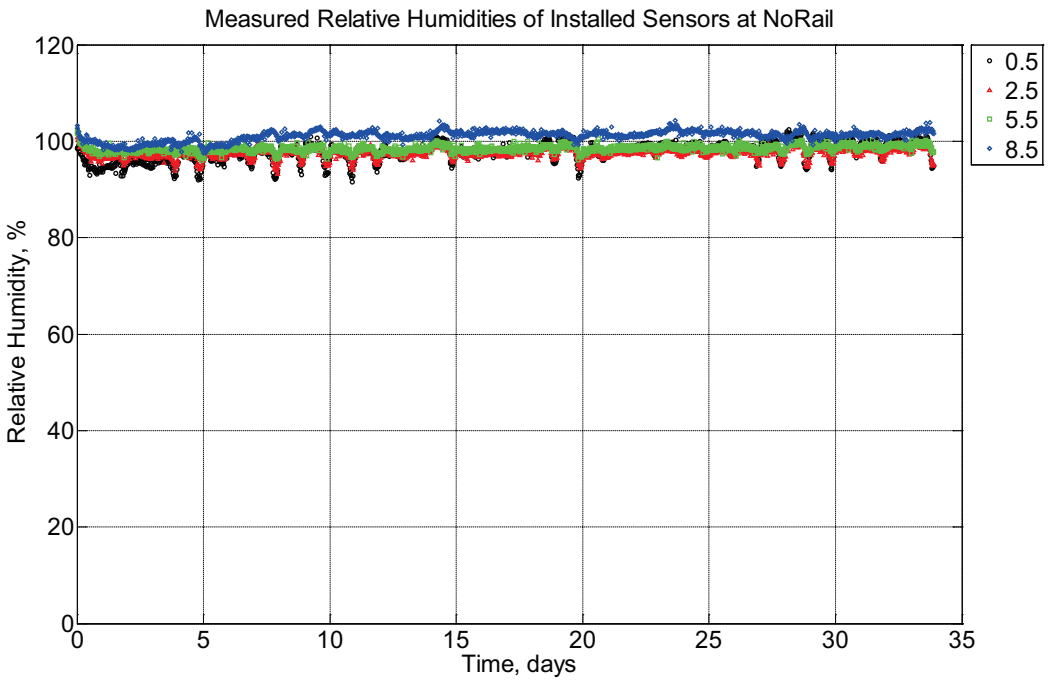

Figure B-918 Measured relative humidity at depths of 0.5 inches (12.7 mm), 2.5 inches (63.5 mm), 5.5 inches (139.7 mm), and 8.5 inches (215.9 mm) from the surface of a model concrete crosstie (labeled NoRail) without a polyurethane pad nor rail installed in ballast in Rantoul, IL, between December 21, 2014, through January 24, 2015.

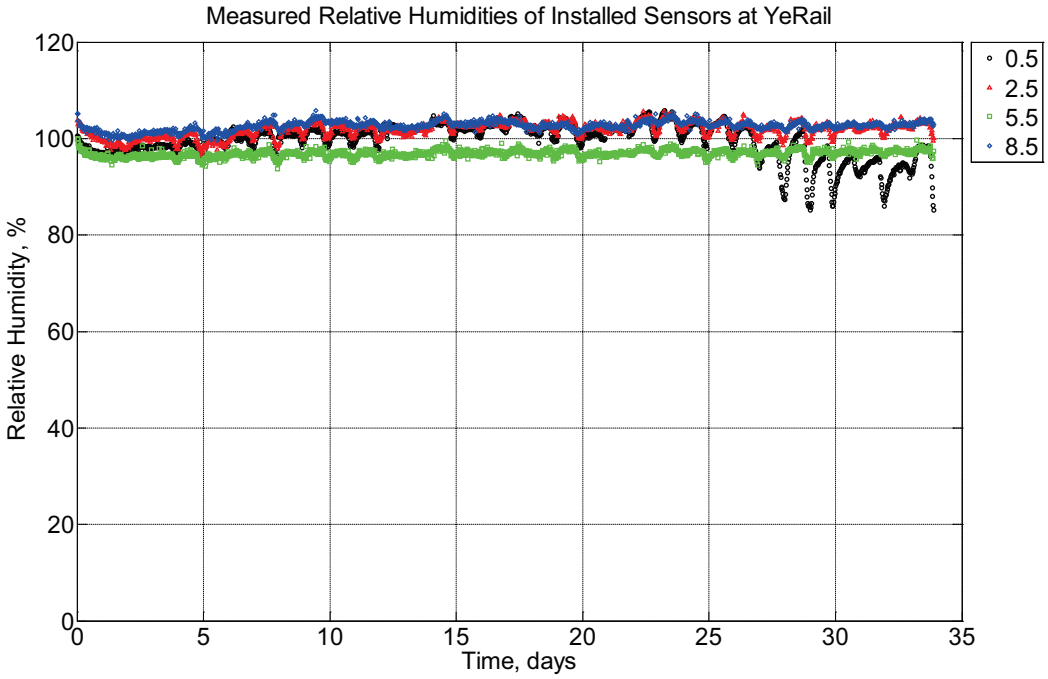

Figure B-919 Measured relative humidity at depths of 0.5 inches (12.7 mm), 2.5 inches (63.5 mm), 5.5 inches (139.7 mm), and 8.5 inches (215.9 mm) from the surface of a model

concrete crosstie (labeled YeRail) installed in ballast in Rantoul, IL, between December 21, 2014, through January 24, 2015. An 8 mm thick polyurethane pad and 12 in (30.48 cm) length 136 lb/yd (67.5 kg/m) section of steel rail are additionally installed atop the model concrete crosstie.

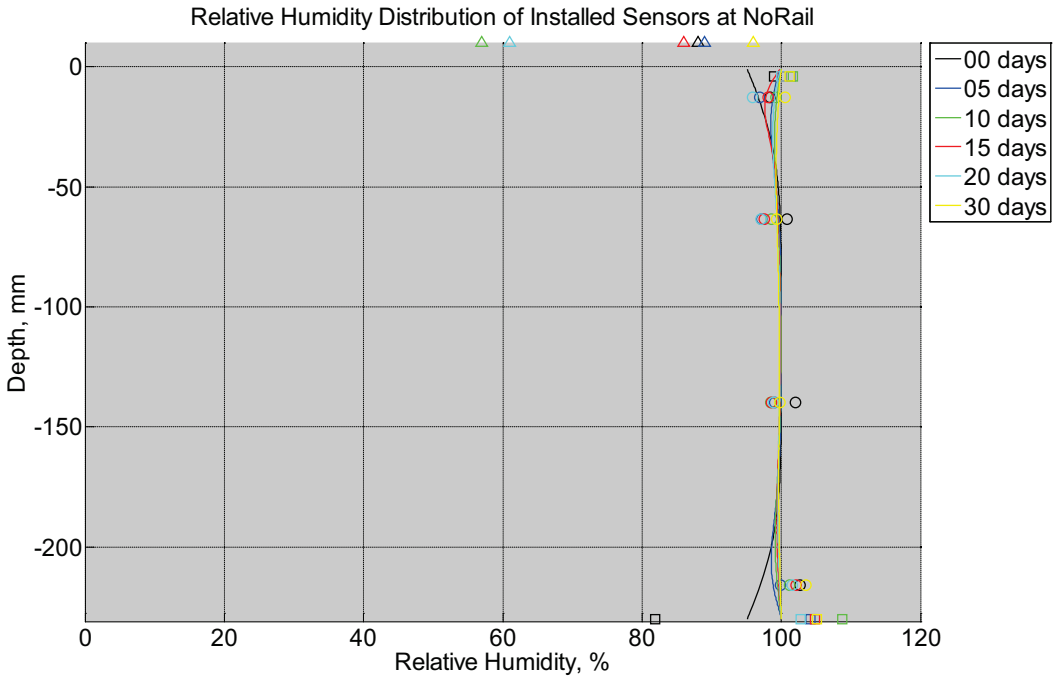

Figure B-920 Measured (markers) and modeled (continuous line) relative humidity profile distribution as a function of depth inside a model concrete crosstie (labeled NoRail) without a polyurethane pad nor rail installed in ballast in Rantoul, IL, between December 21, 2014, through January 24, 2015. Triangular markers denote relative humidity value from KTIP weather station, square markers denote measured relative humidity values from ballast, and circular markers denote measured relative humidity values inside concrete.

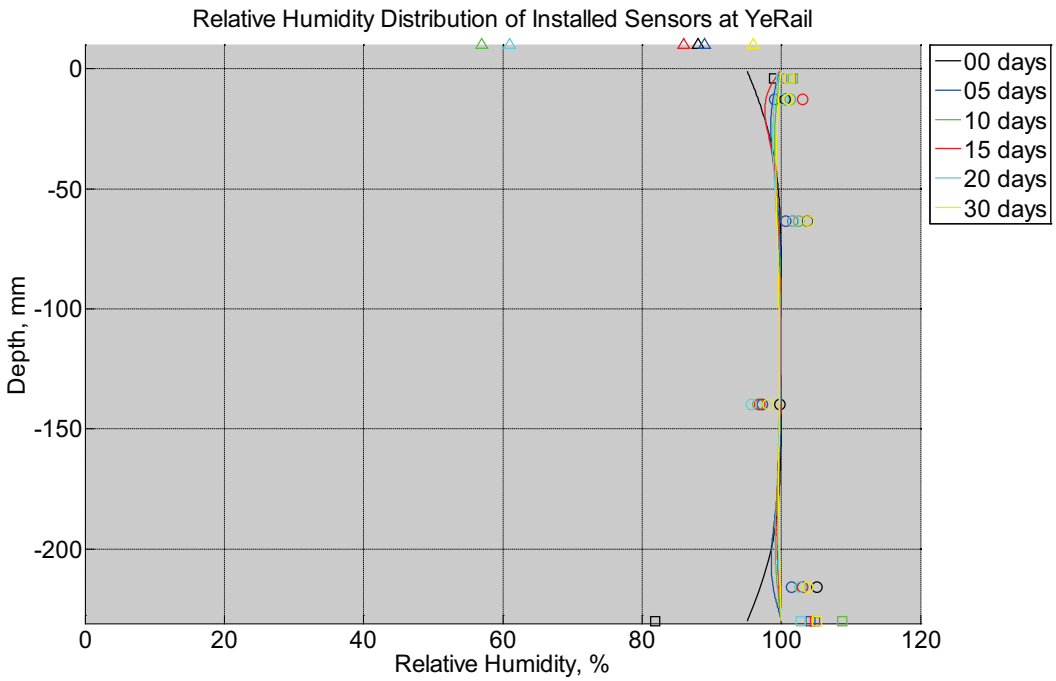

Figure B-921 Measured (markers) and modeled (continuous line) relative humidity profile distribution as a function of depth inside a model concrete crosstie (labeled YeRail) installed in ballast in Rantoul, IL, between December 21, 2014, through January 24, 2015. An 8 mm thick polyurethane pad and 12 in (30.48 cm) length 136 lb/yd (67.5 kg/m) section of steel rail are additionally installed atop the model concrete crosstie. The model does not incorporate a polyurethane pad nor steel rail line. Triangular markers denote relative humidity value from KTIP weather station, square markers denote measured relative humidity values from ballast, and circular markers denote measured relative humidity values inside concrete.

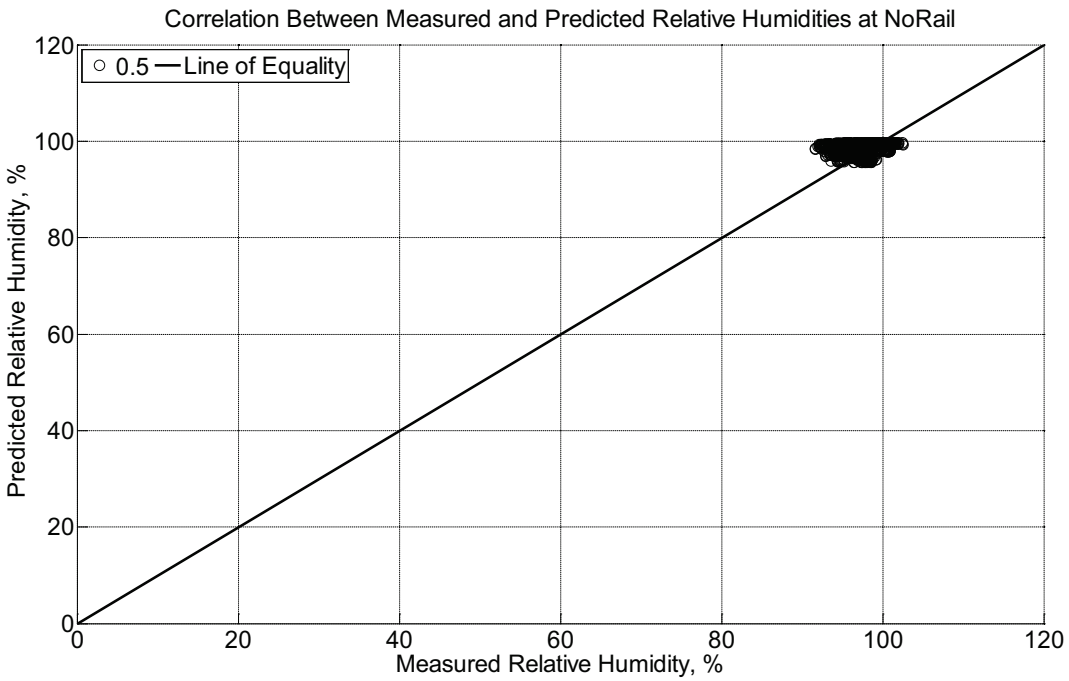

Figure B-922 Correlation between measured and predicted relative humidity values 0.5 inches (12.7 mm) from the surface of a model concrete crosstie (labeled NoRail) without a polyurethane pad nor rail installed in ballast in Rantoul, IL, between December 21, 2014, through January 24, 2015.

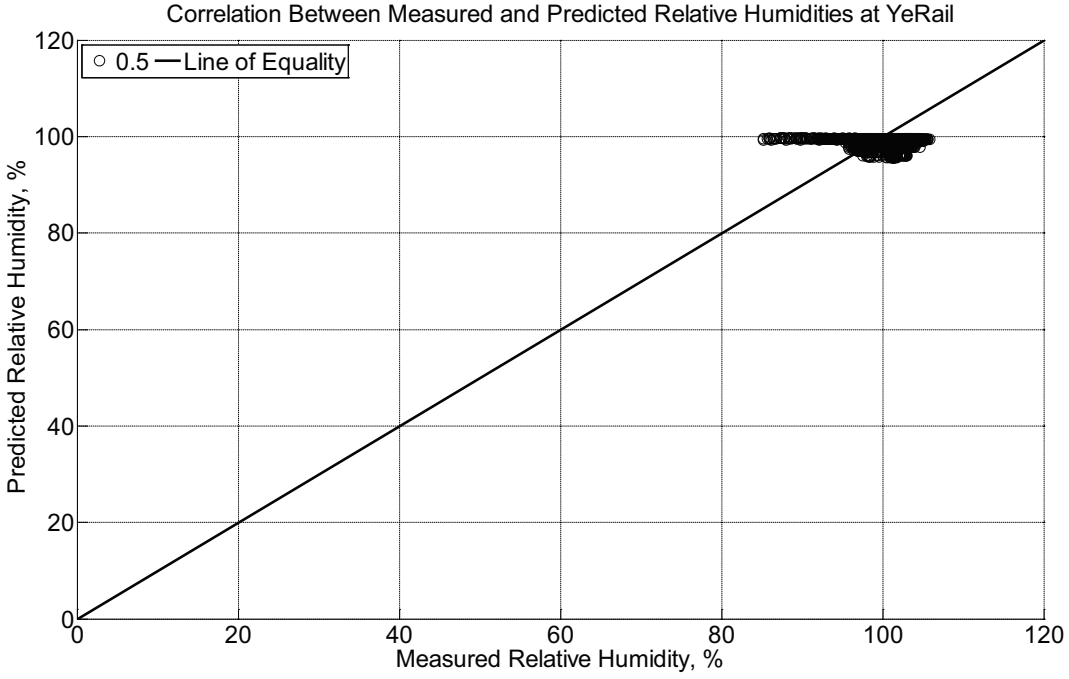

Figure B-923 Correlation between measured and predicted relative humidity values 0.5 inches (12.7 mm) from the surface of a model concrete crosstie (labeled YeRail) installed in

ballast in Rantoul, IL, between December 21, 2014, through January 24, 2015. An 8 mm thick polyurethane pad and 12 in (30.48 cm) length 136 lb/yd (67.5 kg/m) section of steel rail are additionally installed atop the model concrete crosstie. The model does not incorporate a polyurethane pad nor steel rail line.

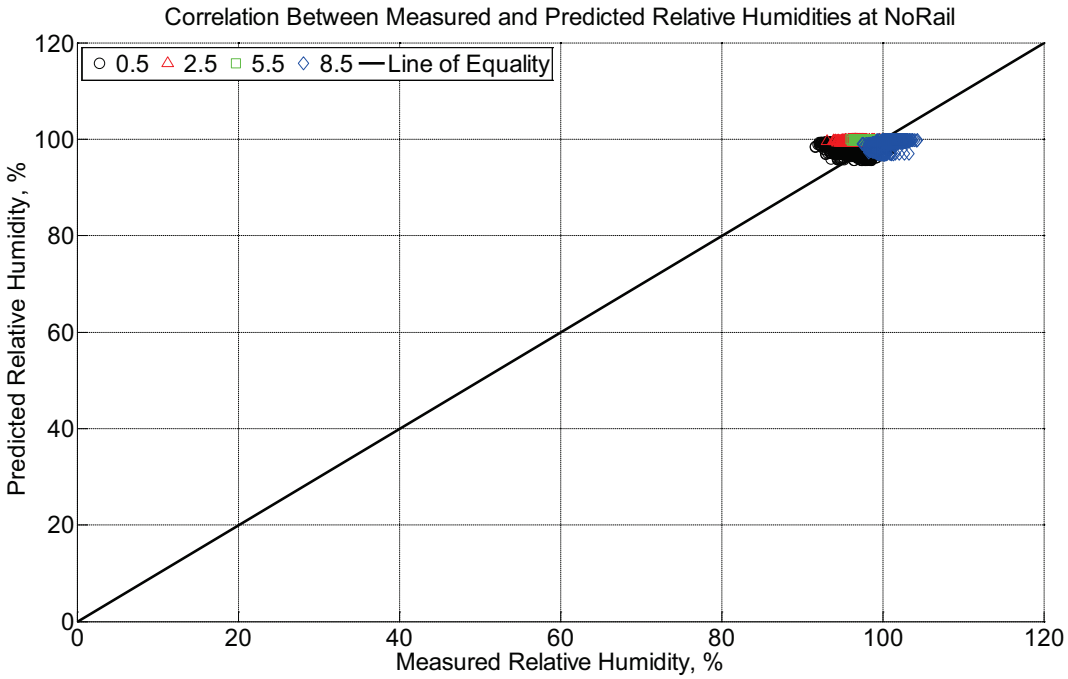

Figure B-924 Correlation between measured and predicted relative humidity values 0.5 inches (12.7 mm), 2.5 inches (63.5 mm), 5.5 inches (139.7 mm), and 8.5 inches (215.9 mm) from the surface of a model concrete crosstie (labeled NoRail) without a polyurethane pad nor rail installed in ballast in Rantoul, IL, between December 21, 2014, through January 24, 2015.

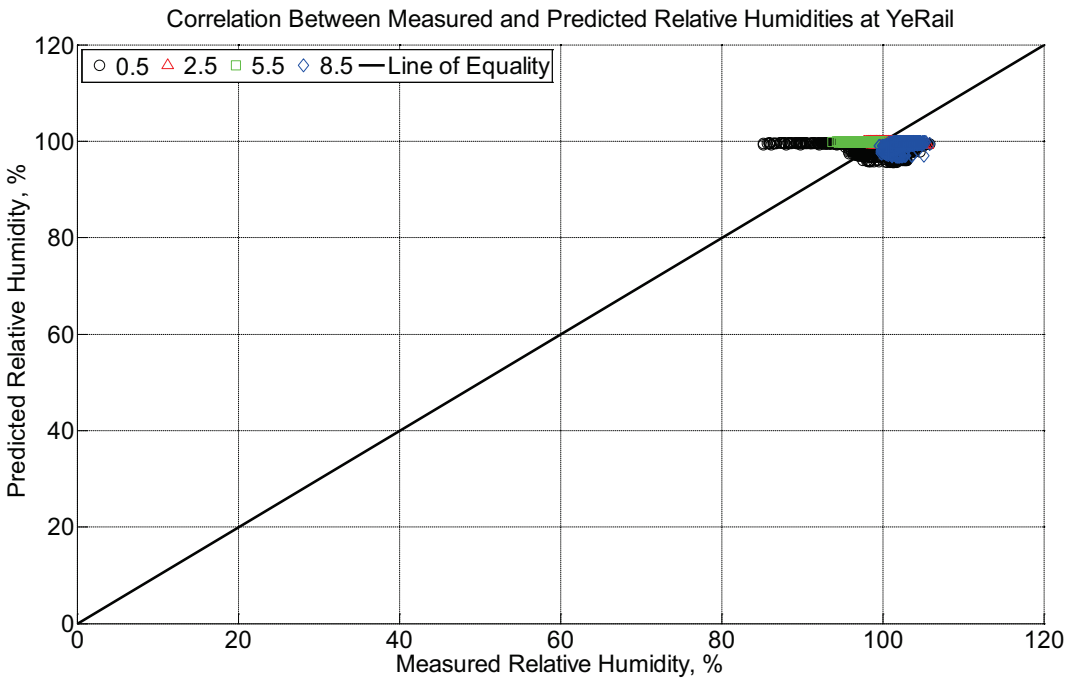

Figure B-925 Correlation between measured and predicted relative humidity values 0.5 inches (12.7 mm), 2.5 inches (63.5 mm), 5.5 inches (139.7 mm), and 8.5 inches (215.9 mm) from the surface of a model concrete crosstie (labeled YeRail) installed in ballast in Rantoul, IL, between December 21, 2014, through January 24, 2015. An 8 mm thick polyurethane pad and 12 in (30.48 cm) length 136 lb/yd (67.5 kg/m) section of steel rail are additionally installed atop the model concrete crosstie. The model does not incorporate a polyurethane pad nor steel rail line.

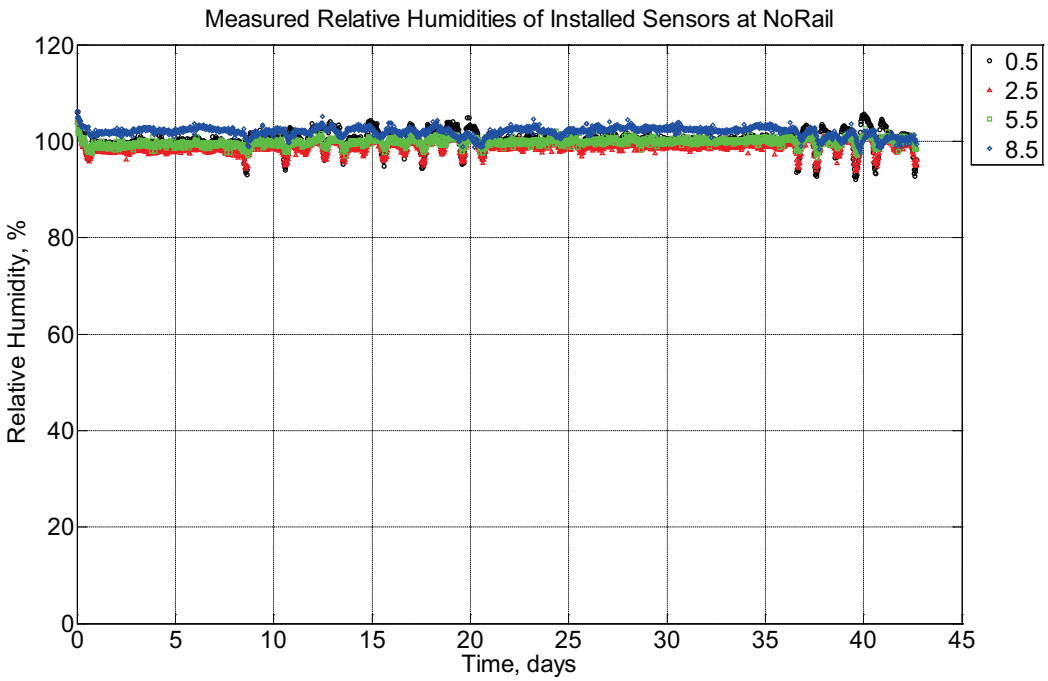

Figure B-926 Measured relative humidity at depths of 0.5 inches (12.7 mm), 2.5 inches (63.5 mm), 5.5 inches (139.7 mm), and 8.5 inches (215.9 mm) from the surface of a model concrete crosstie (labeled NoRail) without a polyurethane pad nor rail installed in ballast in Rantoul, IL, between January 30, 2015, through March 14, 2015.

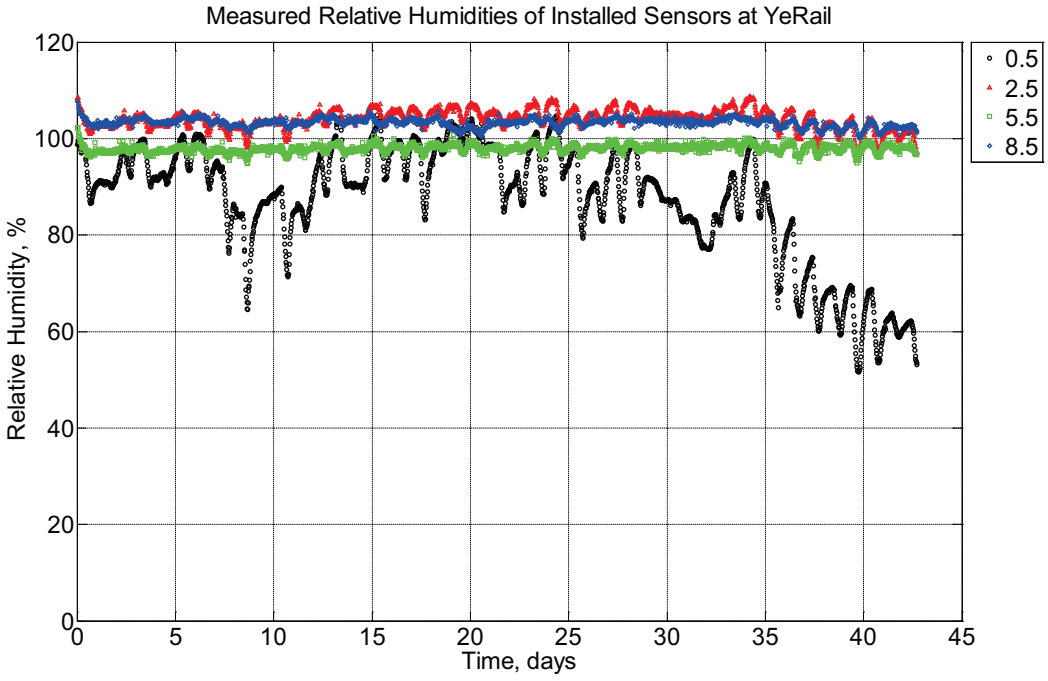

Figure B-927 Measured relative humidity at depths of 0.5 inches (12.7 mm), 2.5 inches (63.5 mm), 5.5 inches (139.7 mm), and 8.5 inches (215.9 mm) from the surface of a model

concrete crosstie (labeled YeRail) installed in ballast in Rantoul, IL, between January 30, 2015, through March 14, 2015. An 8 mm thick polyurethane pad and 12 in (30.48 cm) length 136 lb/yd (67.5 kg/m) section of steel rail are additionally installed atop the model concrete crosstie.

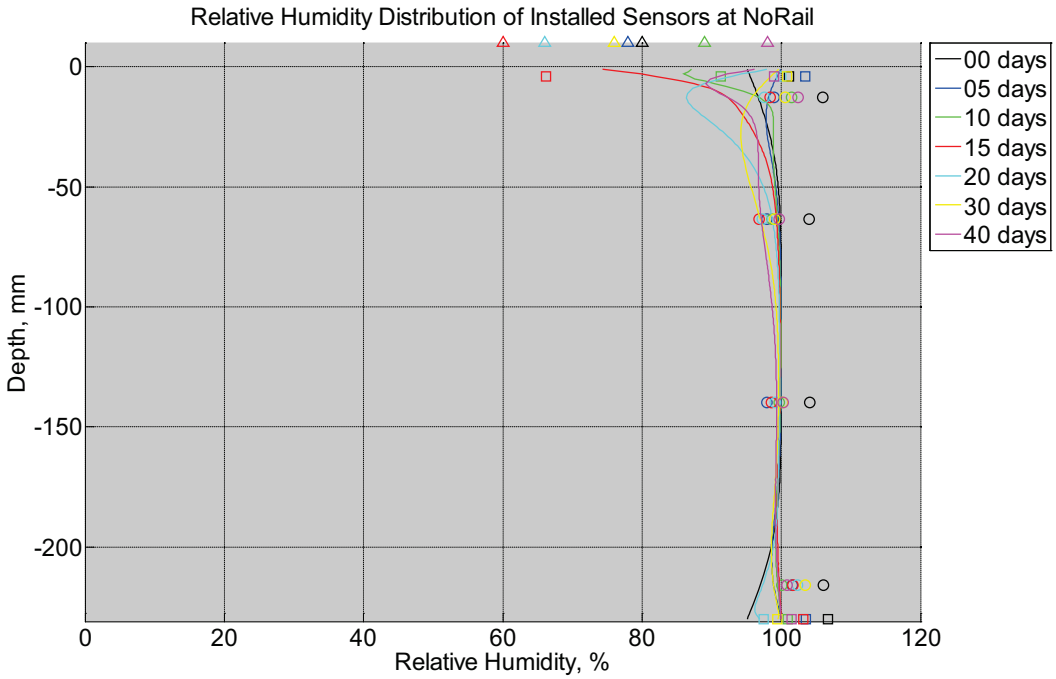

Figure B-928 Measured (markers) and modeled (continuous line) relative humidity profile distribution as a function of depth inside a model concrete crosstie (labeled NoRail) without a polyurethane pad nor rail installed in ballast in Rantoul, IL, between January 30, 2015, through March 14, 2015. Triangular markers denote relative humidity value from KTIP weather station, square markers denote measured relative humidity values from ballast, and circular markers denote measured relative humidity values inside concrete.

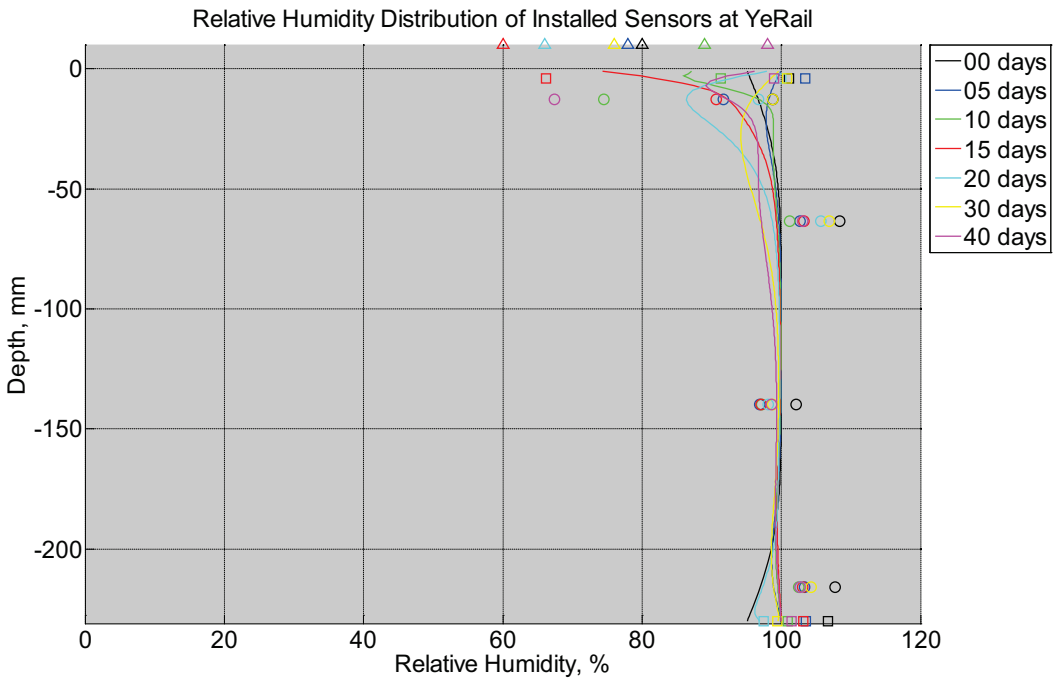

Figure B-929 Measured (markers) and modeled (continuous line) relative humidity profile distribution as a function of depth inside a model concrete crosstie (labeled YeRail) installed in ballast in Rantoul, IL, between January 30, 2015, through March 14, 2015. An 8 mm thick polyurethane pad and 12 in (30.48 cm) length 136 lb/yd (67.5 kg/m) section of steel rail are additionally installed atop the model concrete crosstie. The model does not incorporate a polyurethane pad nor steel rail line. Triangular markers denote relative humidity value from KTIP weather station, square markers denote measured relative humidity values from ballast, and circular markers denote measured relative humidity values inside concrete.

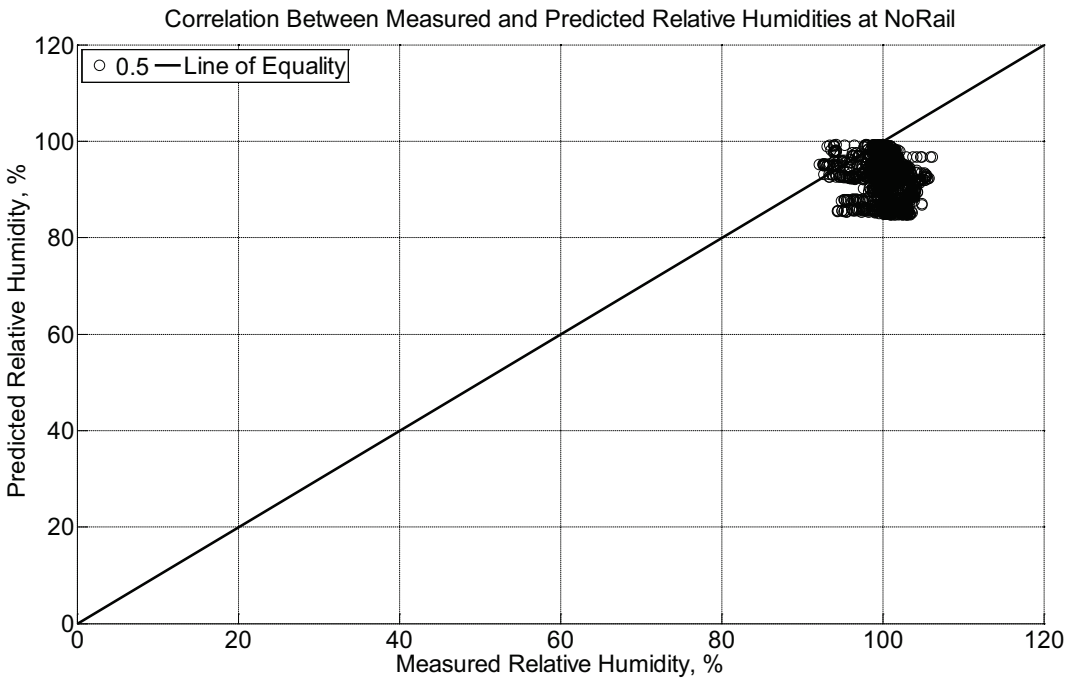

Figure B-930 Correlation between measured and predicted relative humidity values 0.5 inches (12.7 mm) from the surface of a model concrete crosstie (labeled NoRail) without a polyurethane pad nor rail installed in ballast in Rantoul, IL, between January 30, 2015, through March 14, 2015.

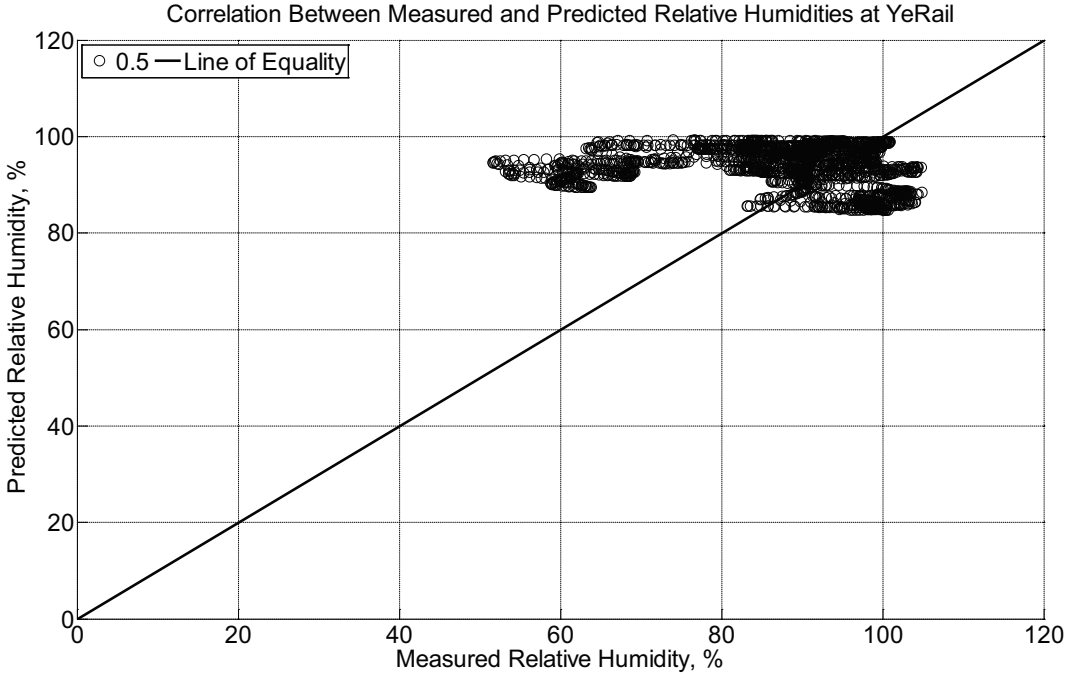

Figure B-931 Correlation between measured and predicted relative humidity values 0.5 inches (12.7 mm) from the surface of a model concrete crosstie (labeled YeRail) installed in

ballast in Rantoul, IL, between January 30, 2015, through March 14, 2015. An 8 mm thick polyurethane pad and 12 in (30.48 cm) length 136 lb/yd (67.5 kg/m) section of steel rail are additionally installed atop the model concrete crosstie. The model does not incorporate a polyurethane pad nor steel rail line.

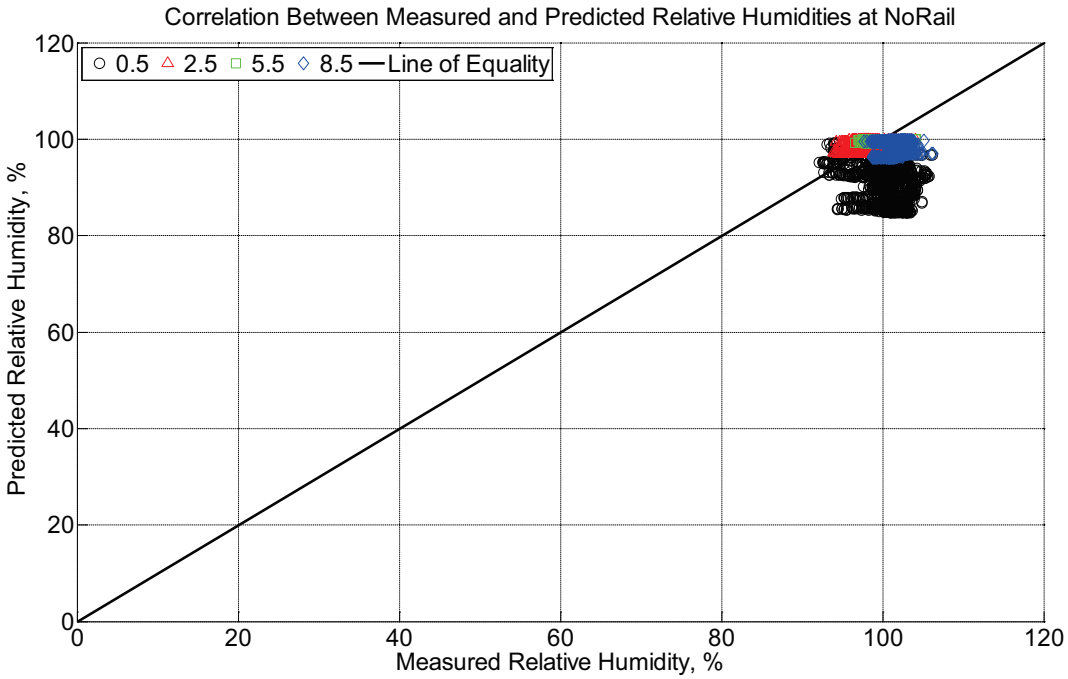

Figure B-932 Correlation between measured and predicted relative humidity values 0.5 inches (12.7 mm), 2.5 inches (63.5 mm), 5.5 inches (139.7 mm), and 8.5 inches (215.9 mm) from the surface of a model concrete crosstie (labeled NoRail) without a polyurethane pad nor rail installed in ballast in Rantoul, IL, between January 30, 2015, through March 14, 2015.

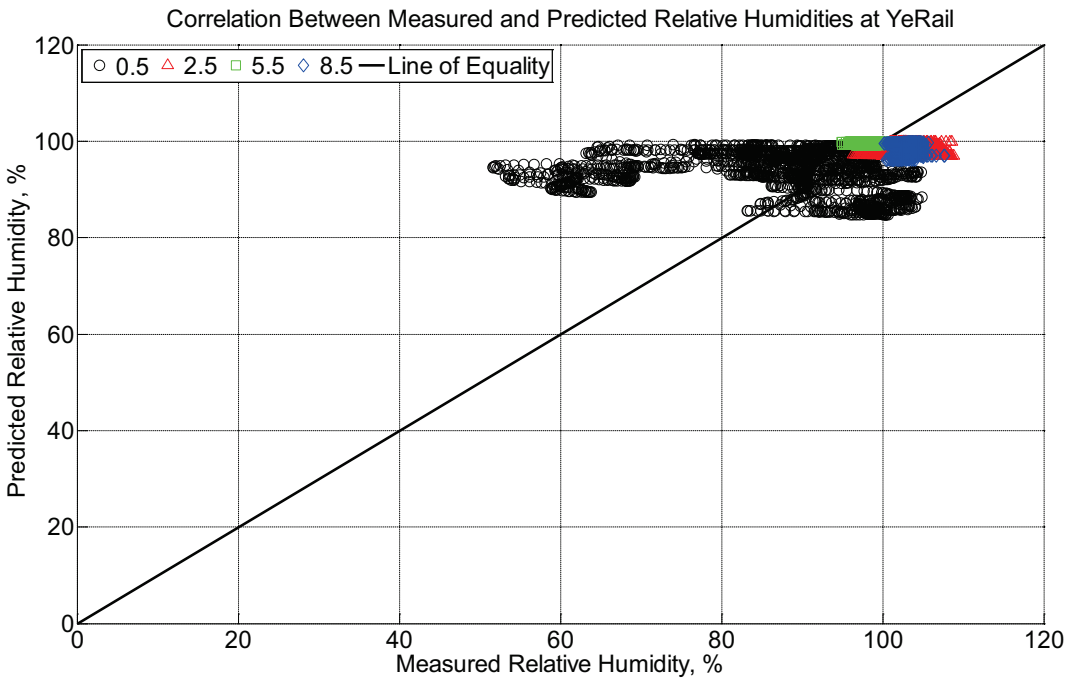

Figure B-933 Correlation between measured and predicted relative humidity values 0.5 inches (12.7 mm), 2.5 inches (63.5 mm), 5.5 inches (139.7 mm), and 8.5 inches (215.9 mm) from the surface of a model concrete crosstie (labeled YeRail) installed in ballast in Rantoul, IL, between January 30, 2015, through March 14, 2015. An 8 mm thick polyurethane pad and 12 in (30.48 cm) length 136 lb/yd (67.5 kg/m) section of steel rail are additionally installed atop the model concrete crosstie. The model does not incorporate a polyurethane pad nor steel rail line.

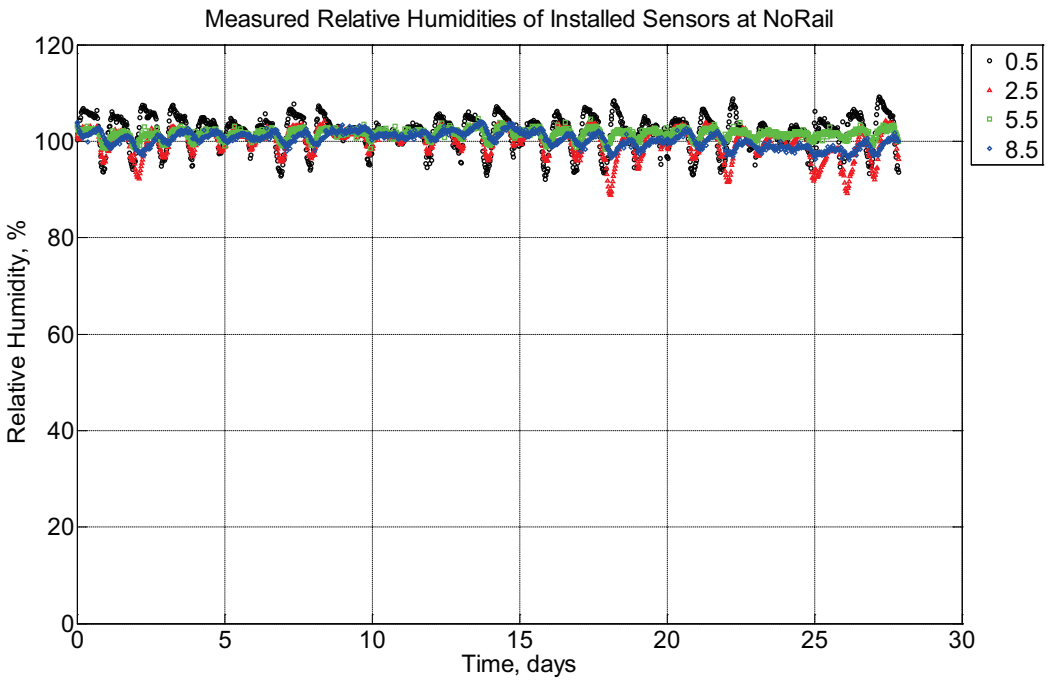

Figure B-934 Measured relative humidity at depths of 0.5 inches (12.7 mm), 2.5 inches (63.5 mm), 5.5 inches (139.7 mm), and 8.5 inches (215.9 mm) from the surface of a model concrete crosstie (labeled NoRail) without a polyurethane pad nor rail installed in ballast in Rantoul, IL, between March 14, 2015, through April 11, 2015.

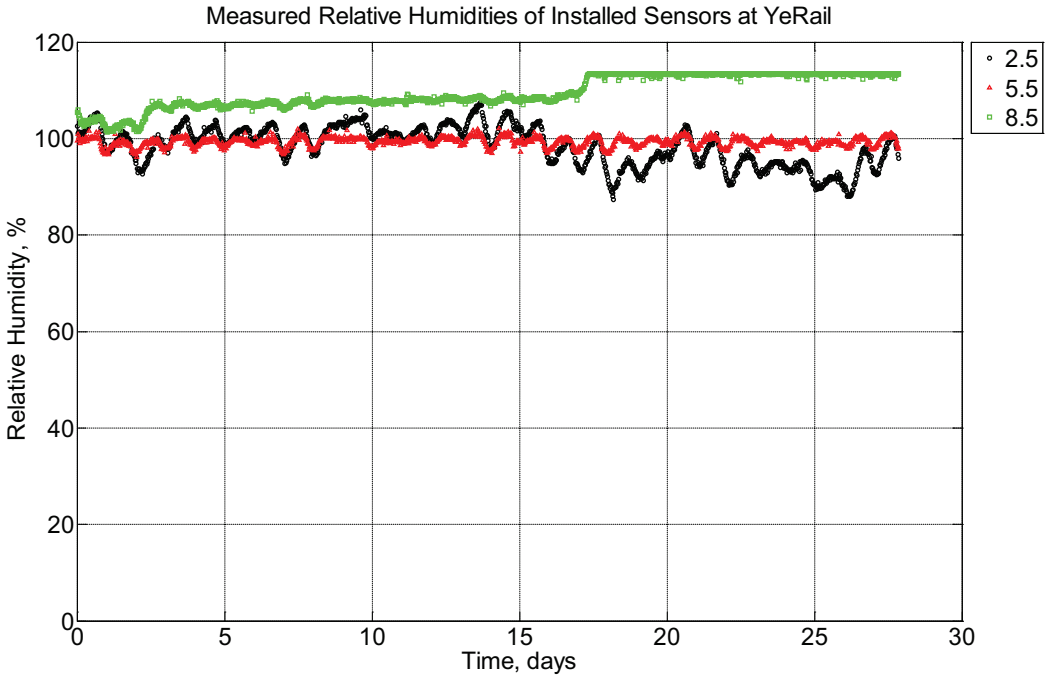

Figure B-935 Measured relative humidity at depths of 2.5 inches (63.5 mm), 5.5 inches (139.7 mm), and 8.5 inches (215.9 mm) from the surface of a model concrete crosstie

(labeled YeRail) installed in ballast in Rantoul, IL, between March 14, 2015, through April 11, 2015. An 8 mm thick polyurethane pad and 12 in (30.48 cm) length 136 lb/yd (67.5 kg/m) section of steel rail are additionally installed atop the model concrete crosstie.

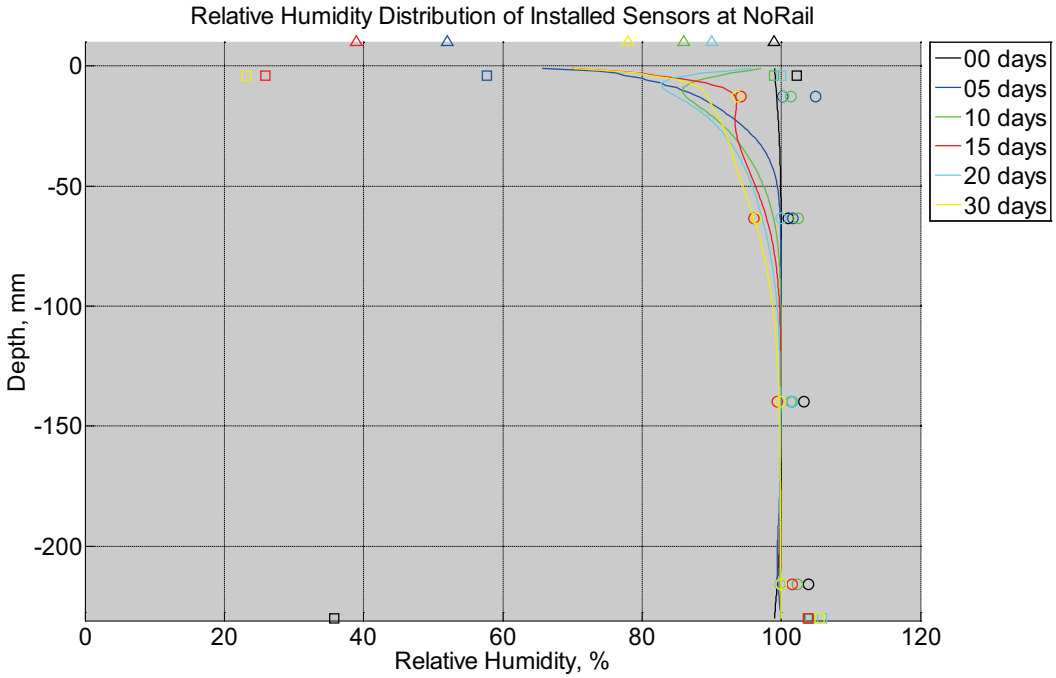

Figure B-936 Measured (markers) and modeled (continuous line) relative humidity profile distribution as a function of depth inside a model concrete crosstie (labeled NoRail) without a polyurethane pad nor rail installed in ballast in Rantoul, IL, between March 14, 2015, through April 11, 2015. Triangular markers denote relative humidity value from KTIP weather station, square markers denote measured relative humidity values from ballast, and circular markers denote measured relative humidity values inside concrete.

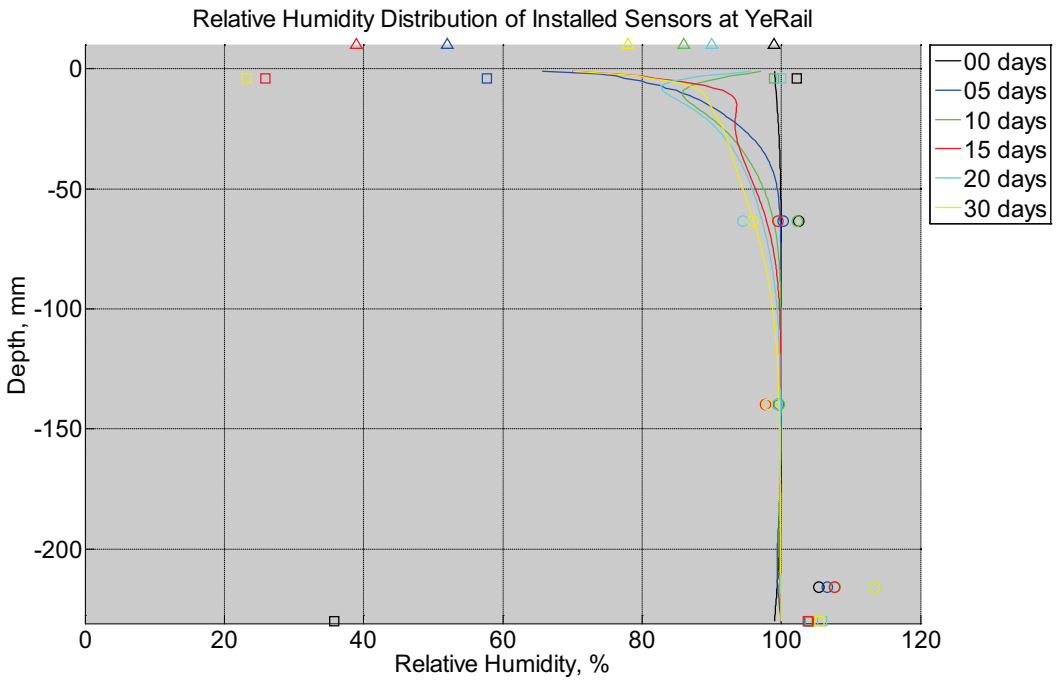

Figure B-937 Measured (markers) and modeled (continuous line) relative humidity profile distribution as a function of depth inside a model concrete crosstie (labeled YeRail) installed in ballast in Rantoul, IL, between March 14, 2015, through April 11, 2015. An 8 mm thick polyurethane pad and 12 in (30.48 cm) length 136 lb/yd (67.5 kg/m) section of steel rail are additionally installed atop the model concrete crosstie. The model does not incorporate a polyurethane pad nor steel rail line. Triangular markers denote relative humidity value from KTIP weather station, square markers denote measured relative humidity values from ballast, and circular markers denote measured relative humidity values inside concrete.

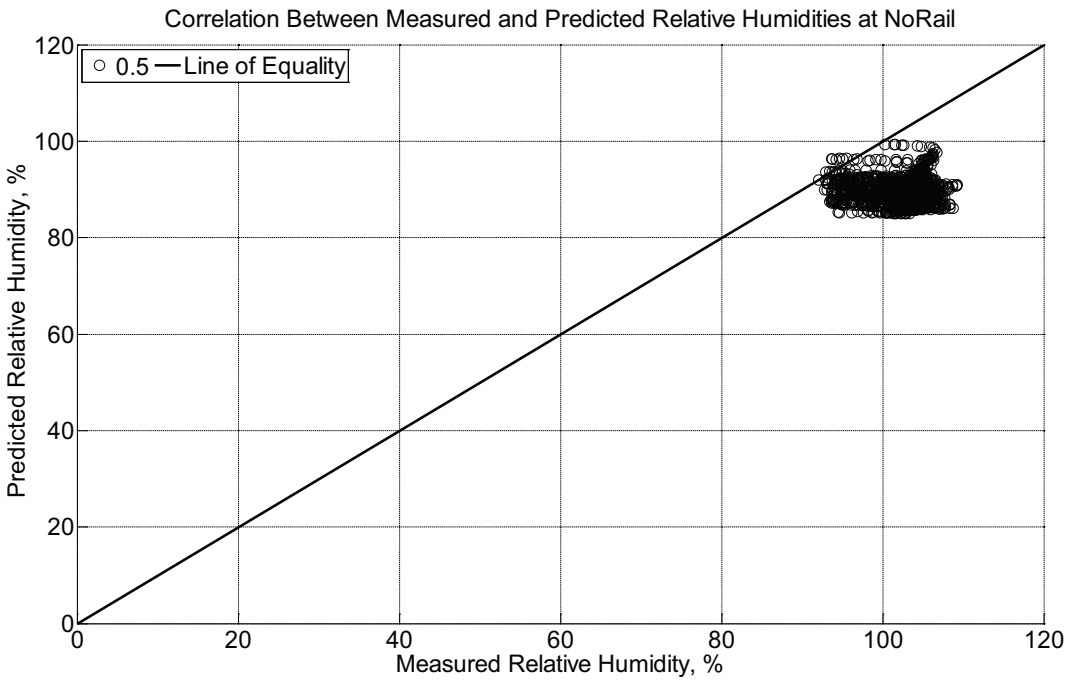

Figure B-938 Correlation between measured and predicted relative humidity values 0.5 inches (12.7 mm) from the surface of a model concrete crosstie (labeled NoRail) without a polyurethane pad nor rail installed in ballast in Rantoul, IL, between March 14, 2015, through April 11, 2015.

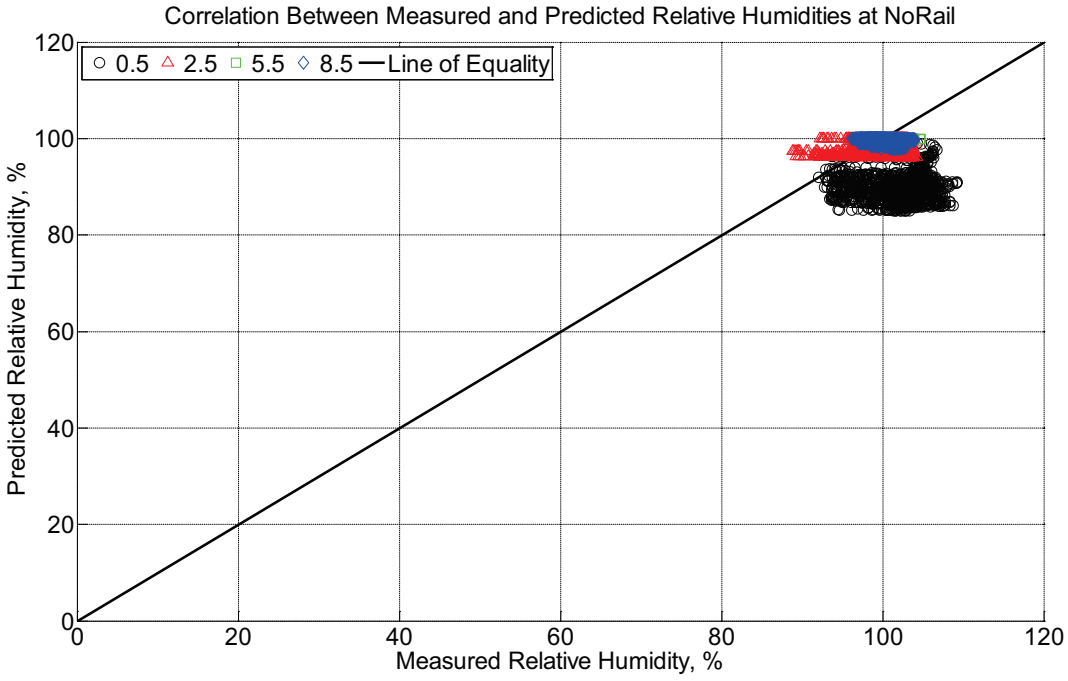

Figure B-939 Correlation between measured and predicted relative humidity values 0.5 inches (12.7 mm), 2.5 inches (63.5 mm), 5.5 inches (139.7 mm), and 8.5 inches (215.9 mm)

from the surface of a model concrete crosstie (labeled NoRail) without a polyurethane pad nor rail installed in ballast in Rantoul, IL, between March 14, 2015, through April 11, 2015.

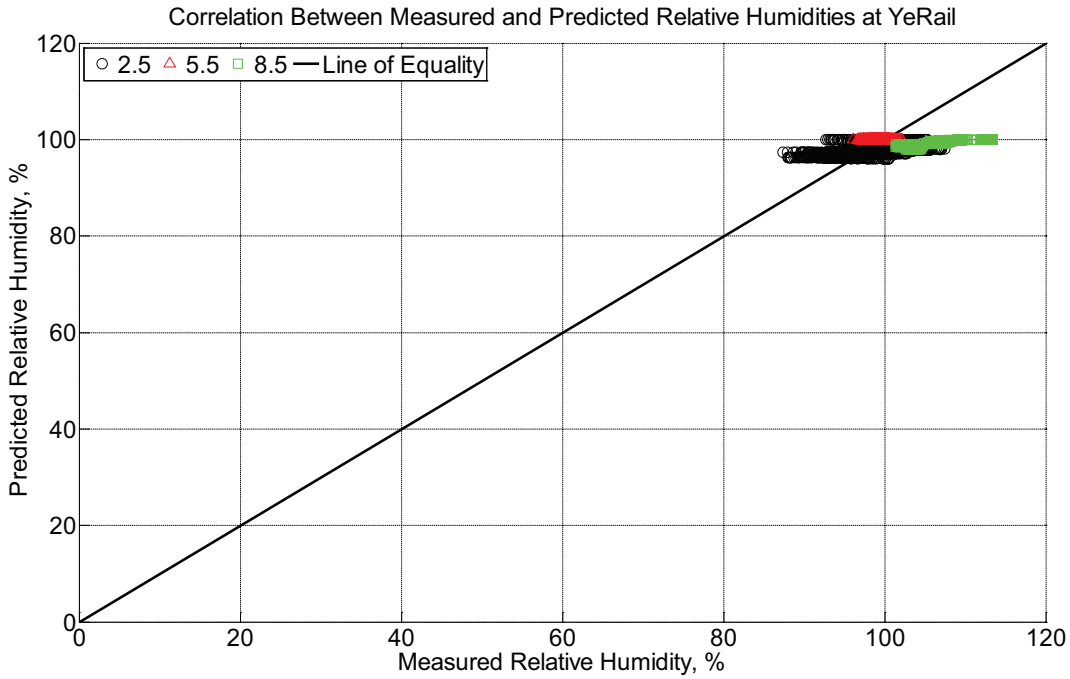

Figure B-940 Correlation between measured and predicted relative humidity values 2.5 inches (63.5 mm), 5.5 inches (139.7 mm), and 8.5 inches (215.9 mm) from the surface of a model concrete crosstie (labeled YeRail) installed in ballast in Rantoul, IL, between March 14, 2015, through April 11, 2015. An 8 mm thick polyurethane pad and 12 in (30.48 cm) length 136 lb/yd (67.5 kg/m) section of steel rail are additionally installed atop the model concrete crosstie. The model does not incorporate a polyurethane pad nor steel rail line.

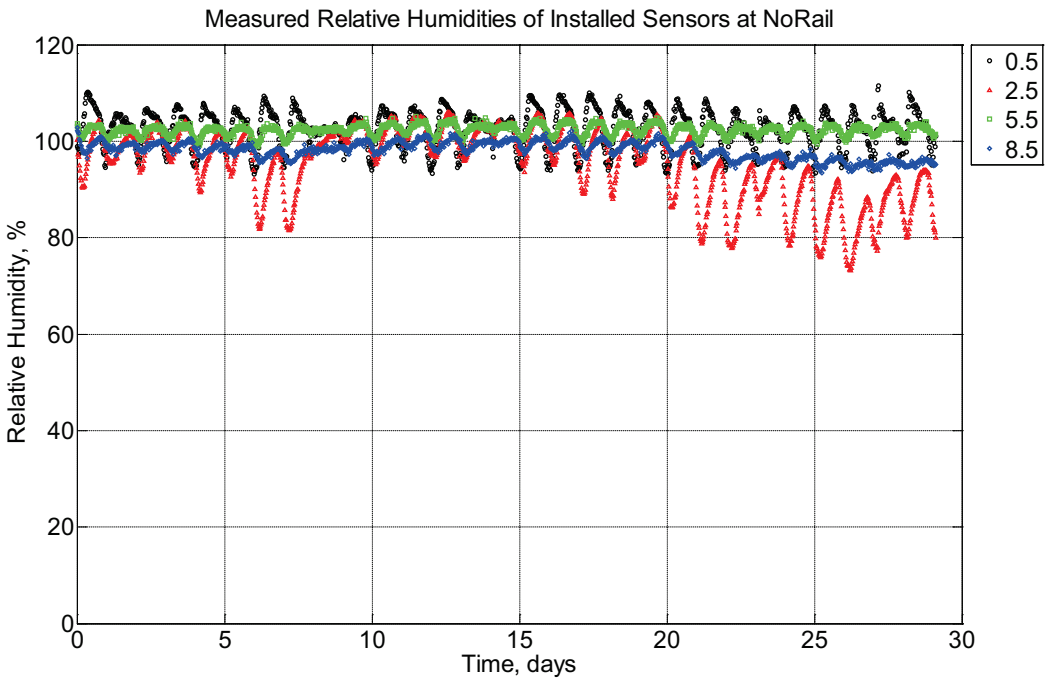

Figure B-941 Measured relative humidity at depths of 0.5 inches (12.7 mm), 2.5 inches (63.5 mm), 5.5 inches (139.7 mm), and 8.5 inches (215.9 mm) from the surface of a model concrete crosstie (labeled NoRail) without a polyurethane pad nor rail installed in ballast in Rantoul, IL, between April 11, 2015, through May 10, 2015.

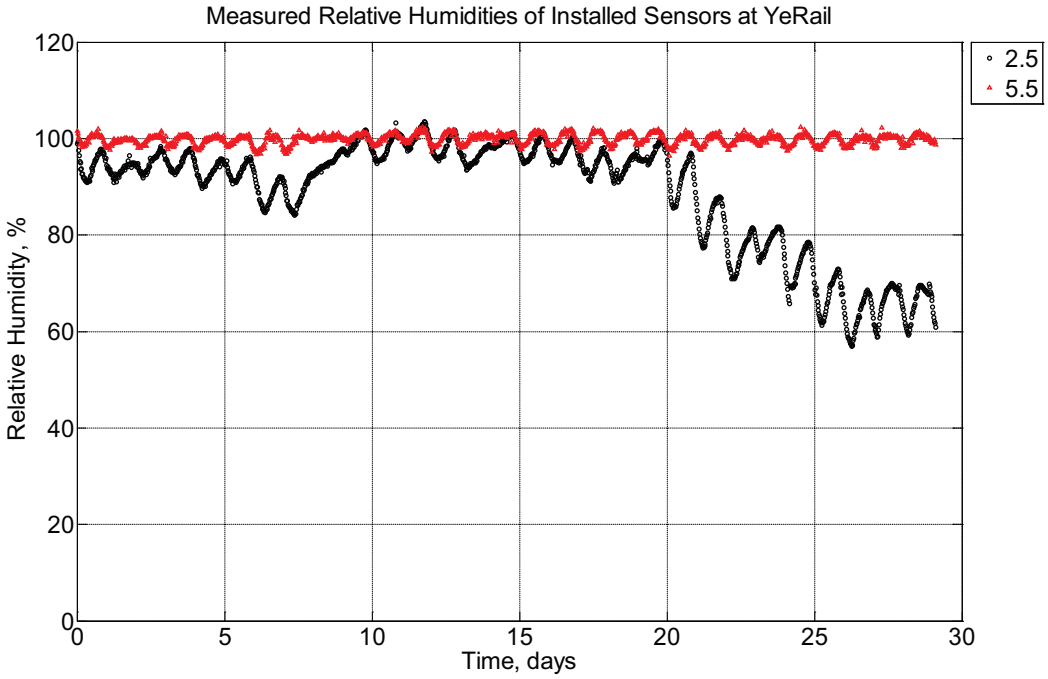

Figure B-942 Measured relative humidity at depths of 2.5 inches (63.5 mm) and 5.5 inches (139.7 mm) from the surface of a model concrete crosstie (labeled YeRail) installed in

ballast in Rantoul, IL, between April 11, 2015, through May 10, 2015. An 8 mm thick polyurethane pad and 12 in (30.48 cm) length 136 lb/yd (67.5 kg/m) section of steel rail are additionally installed atop the model concrete crosstie.

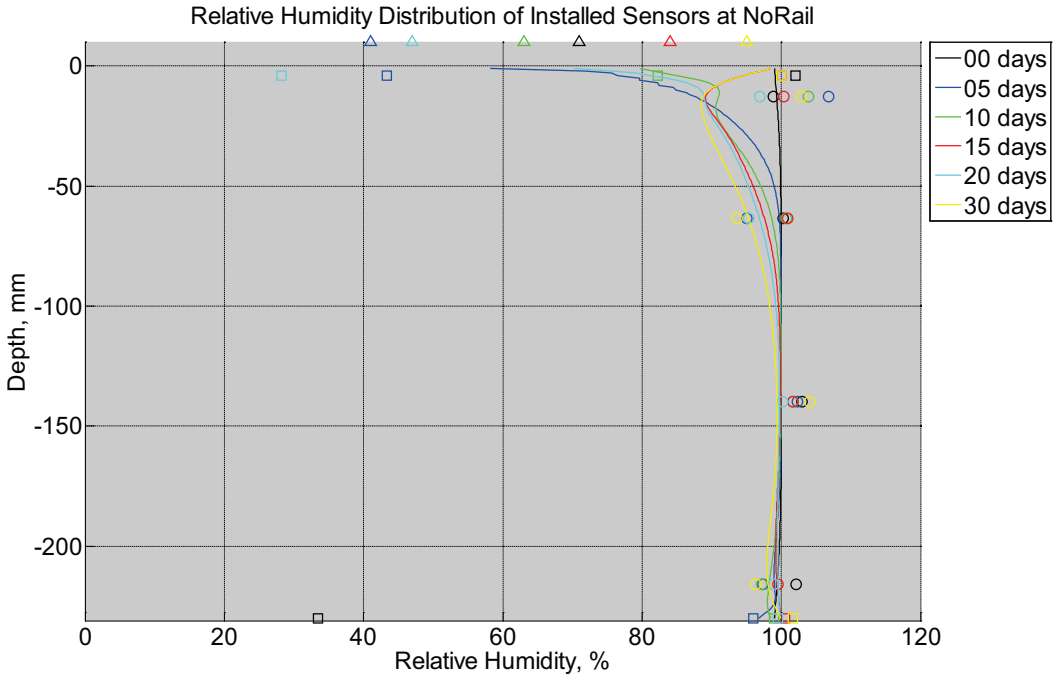

Figure B-943 Measured (markers) and modeled (continuous line) relative humidity profile distribution as a function of depth inside a model concrete crosstie (labeled NoRail) without a polyurethane pad nor rail installed in ballast in Rantoul, IL, between April 11, 2015, through May 10, 2015. Triangular markers denote relative humidity value from KTIP weather station, square markers denote measured relative humidity values from ballast, and circular markers denote measured relative humidity values inside concrete.

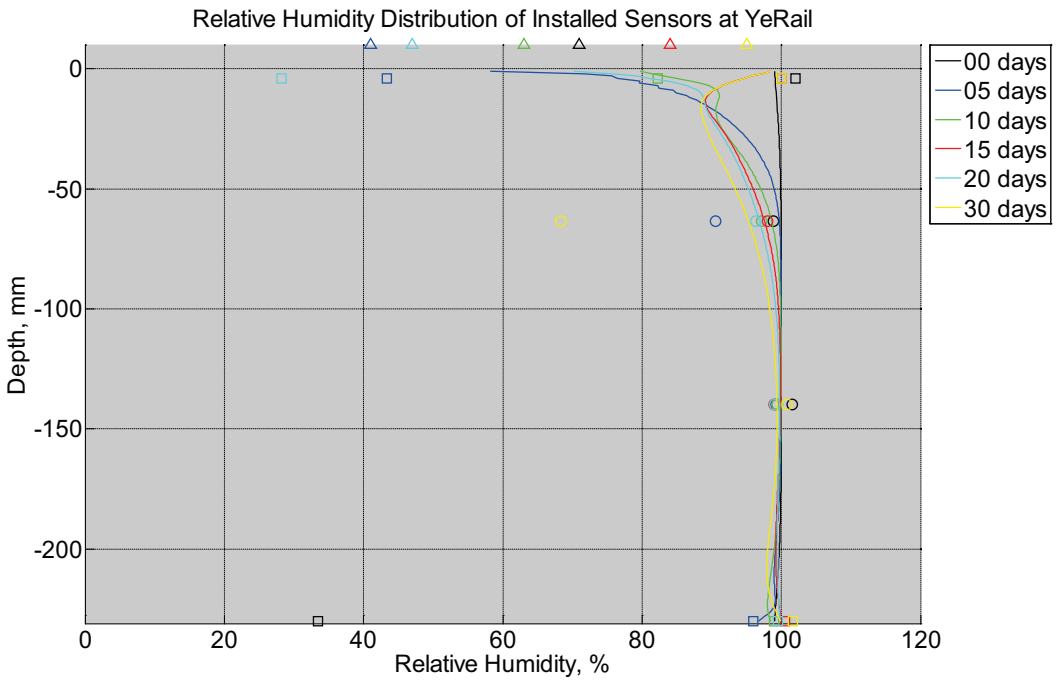

Figure B-944 Measured (markers) and modeled (continuous line) relative humidity profile distribution as a function of depth inside a model concrete crosstie (labeled YeRail) installed in ballast in Rantoul, IL, between April 11, 2015, through May 10, 2015. An 8 mm thick polyurethane pad and 12 in (30.48 cm) length 136 lb/yd (67.5 kg/m) section of steel rail are additionally installed atop the model concrete crosstie. The model does not incorporate a polyurethane pad nor steel rail line. Triangular markers denote relative humidity value from KTIP weather station, square markers denote measured relative humidity values from ballast, and circular markers denote measured relative humidity values inside concrete.

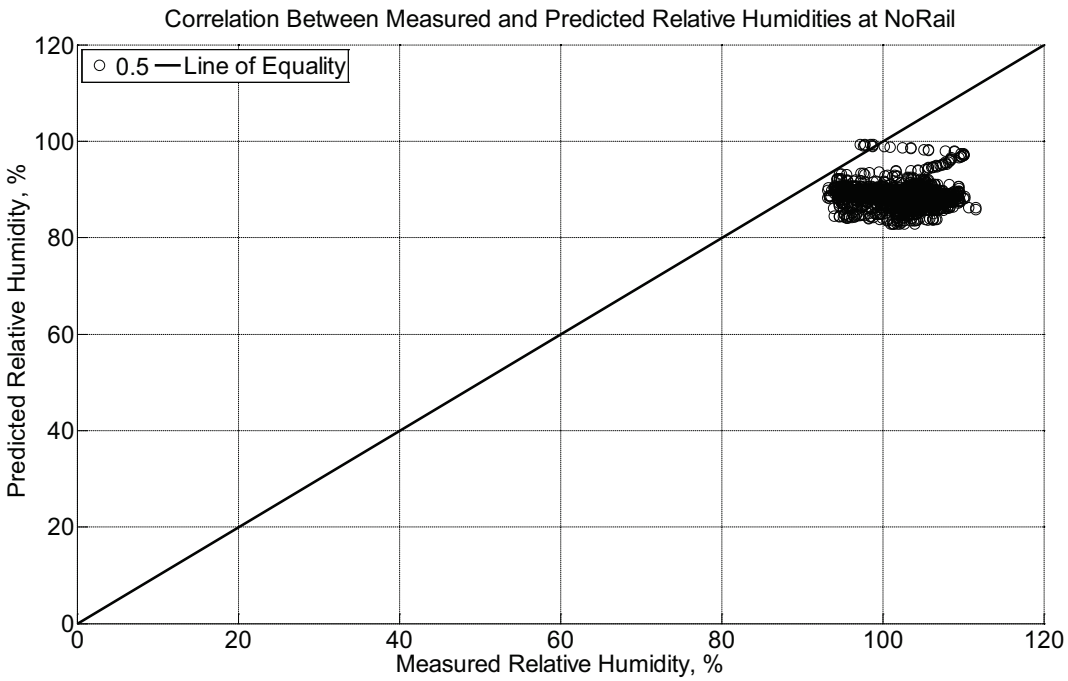

Figure B-945 Correlation between measured and predicted relative humidity values 0.5 inches (12.7 mm) from the surface of a model concrete crosstie (labeled NoRail) without a polyurethane pad nor rail installed in ballast in Rantoul, IL, between April 11, 2015, through May 10, 2015.

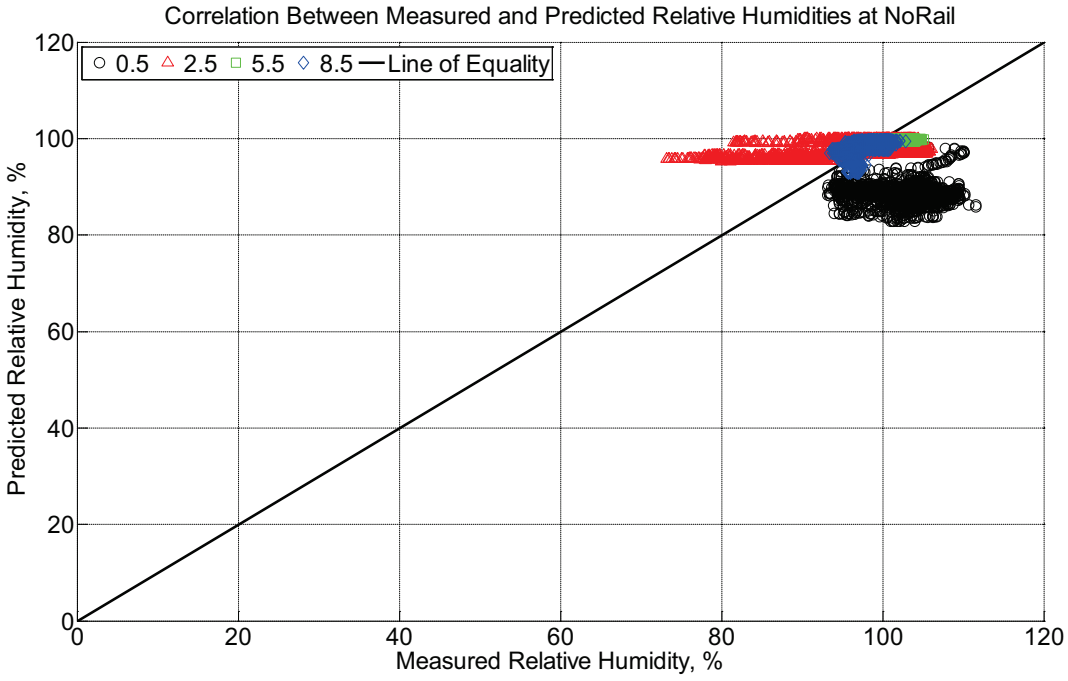

Figure B-946 Correlation between measured and predicted relative humidity values 0.5 inches (12.7 mm), 2.5 inches (63.5 mm), 5.5 inches (139.7 mm), and 8.5 inches (215.9 mm)

from the surface of a model concrete crosstie (labeled NoRail) without a polyurethane pad nor rail installed in ballast in Rantoul, IL, between April 11, 2015, through May 10, 2015.

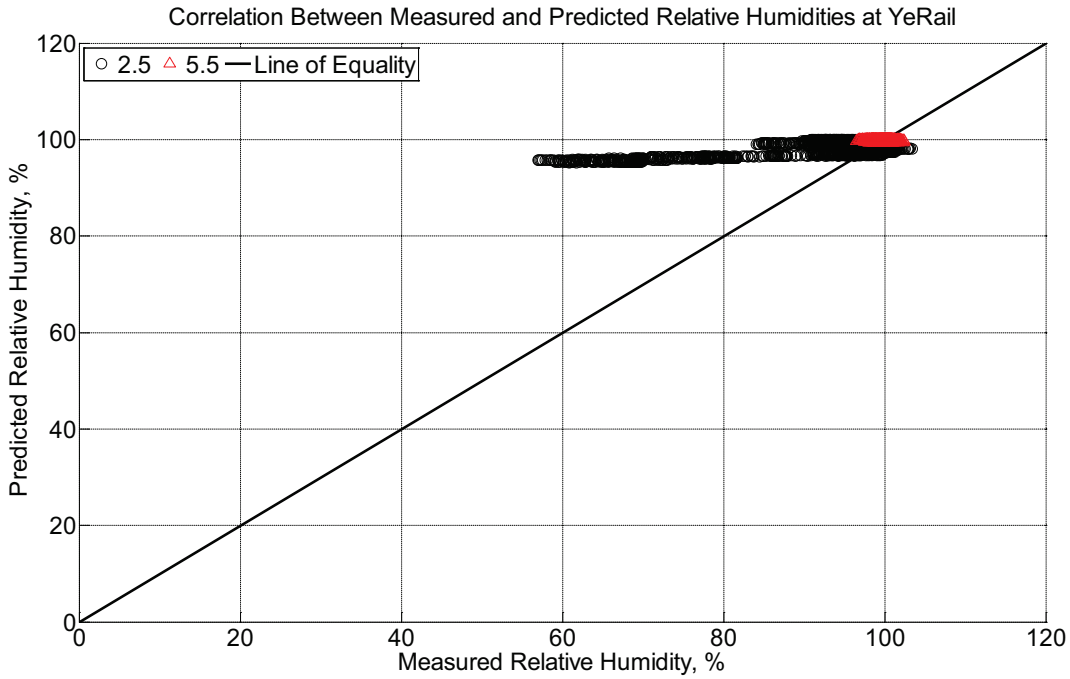

Figure B-947 Correlation between measured and predicted relative humidity values 2.5 inches (63.5 mm) and 5.5 inches (139.7 mm) from the surface of a model concrete crosstie (labeled YeRail) installed in ballast in Rantoul, IL, between April 11, 2015, through May 10, 2015. An 8 mm thick polyurethane pad and 12 in (30.48 cm) length 136 lb/yd (67.5 kg/m) section of steel rail are additionally installed atop the model concrete crosstie. The model does not incorporate a polyurethane pad nor steel rail line.

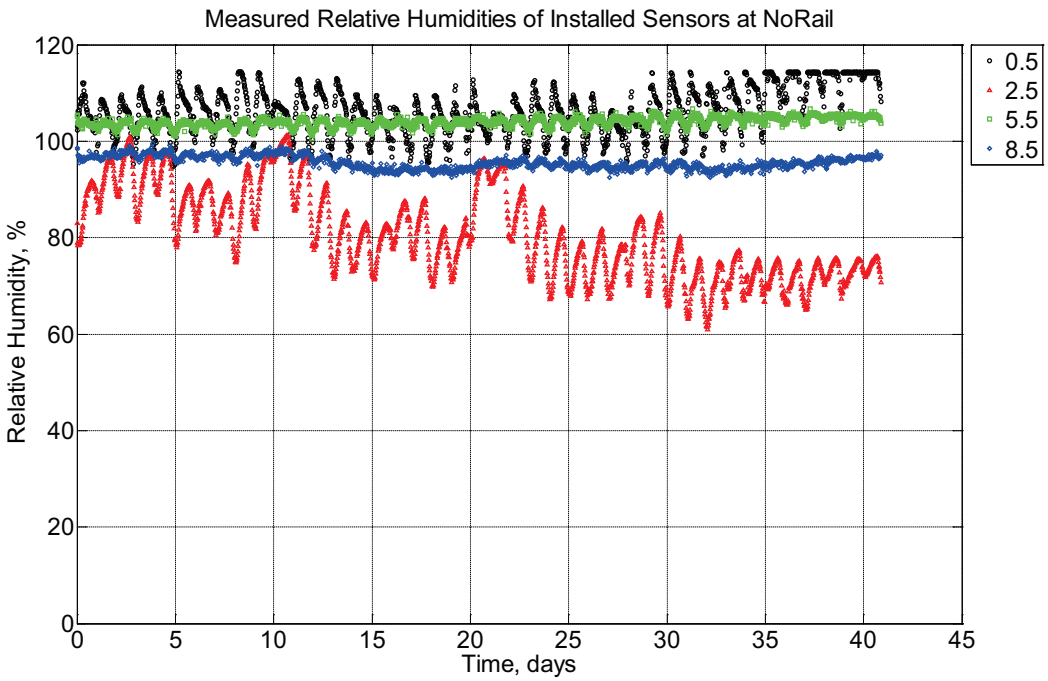

Figure B-948 Measured relative humidity at depths of 0.5 inches (12.7 mm), 2.5 inches (63.5 mm), 5.5 inches (139.7 mm), and 8.5 inches (215.9 mm) from the surface of a model concrete crosstie (labeled NoRail) without a polyurethane pad nor rail installed in ballast in Rantoul, IL, between May 10, 2015, through June 20, 2015. A breathable water-resistant canvas tarp is additionally installed over the model crosstie and immediate ballast area.

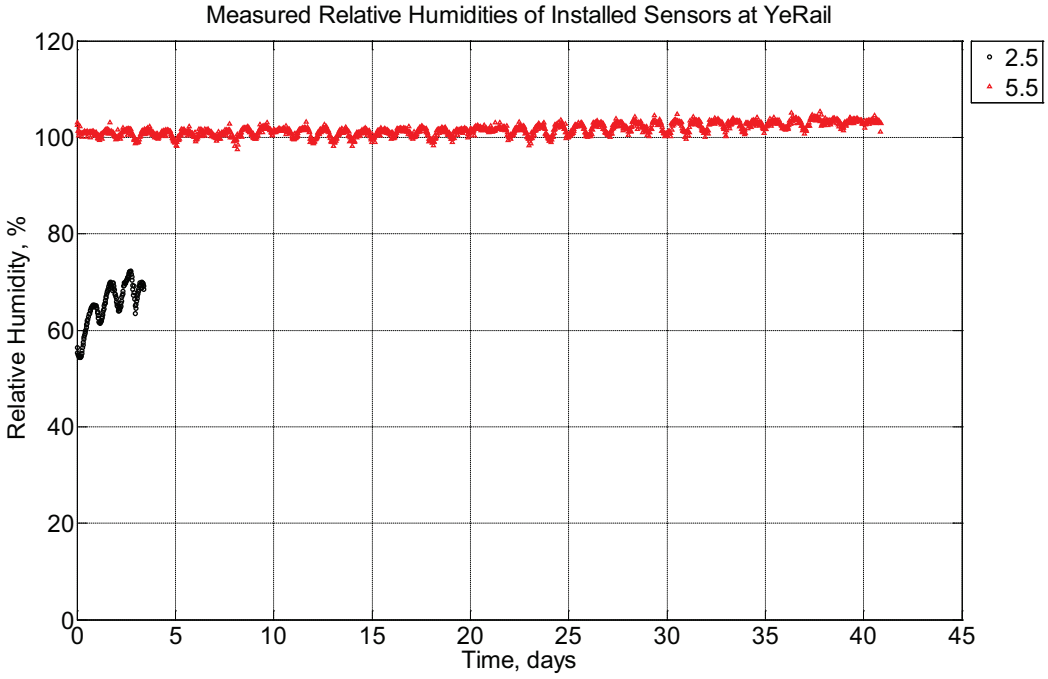

Figure B-949 Measured relative humidity at depths of 2.5 inches (63.5 mm) and 5.5 inches

(139.7 mm) from the surface of a model concrete crosstie (labeled YeRail) installed in ballast in Rantoul, IL, between May 10, 2015, through June 20, 2015. An 8 mm thick polyurethane pad and 12 in (30.48 cm) length 136 lb/yd (67.5 kg/m) section of steel rail are additionally installed atop the model concrete crosstie. A breathable water-resistant canvas tarp is additionally installed over the model crosstie and immediate ballast area.

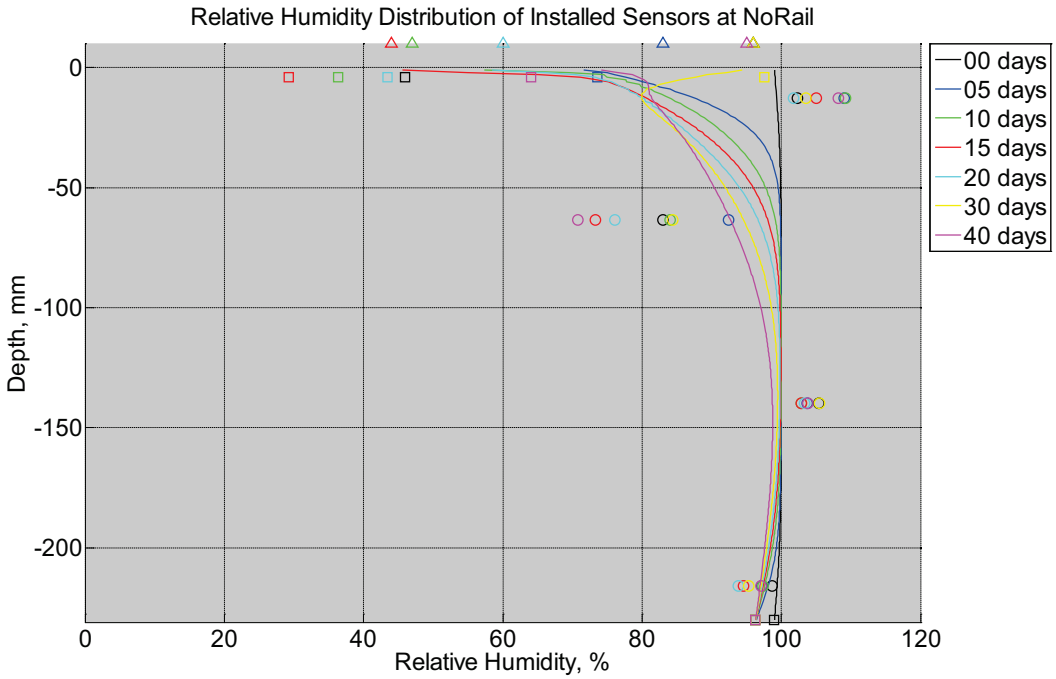

Figure B-950 Measured (markers) and modeled (continuous line) relative humidity profile distribution as a function of depth inside a model concrete crosstie (labeled NoRail) without a polyurethane pad nor rail installed in ballast in Rantoul, IL, between May 10, 2015, through June 20, 2015. A breathable water-resistant canvas tarp is additionally installed over the model crosstie and immediate ballast area. Triangular markers denote relative humidity value from KTIP weather station, square markers denote measured relative humidity values from ballast, and circular markers denote measured relative humidity values inside concrete.

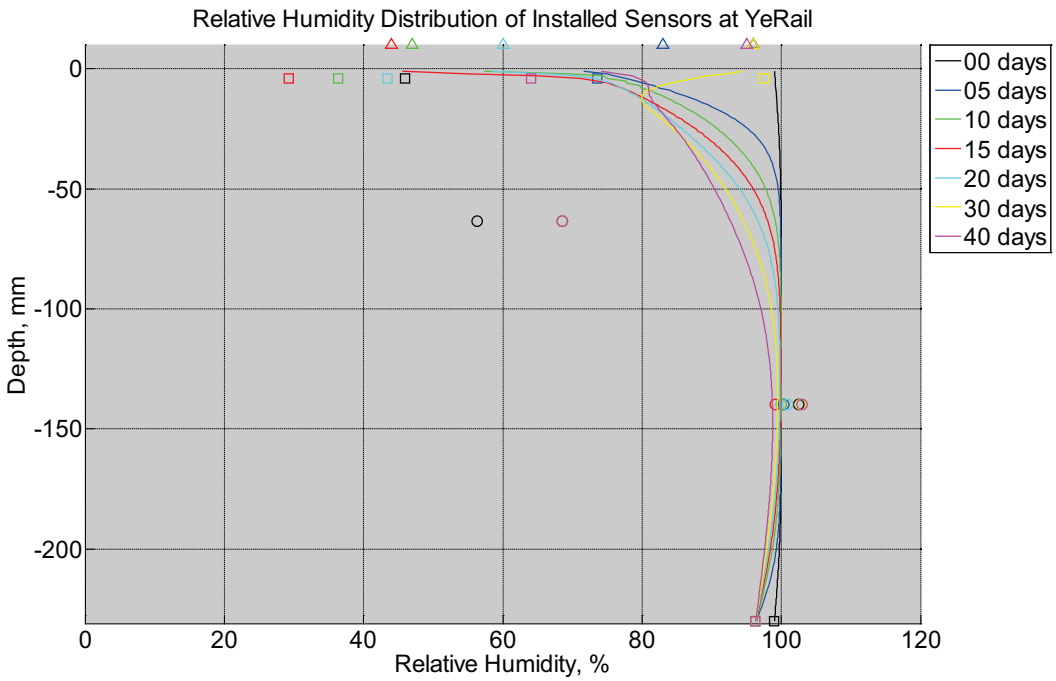

Figure B-951 Measured (markers) and modeled (continuous line) relative humidity profile distribution as a function of depth inside a model concrete crosstie (labeled YeRail) installed in ballast in Rantoul, IL, between May 10, 2015, through June 20, 2015. An 8 mm thick polyurethane pad and 12 in (30.48 cm) length 136 lb/yd (67.5 kg/m) section of steel rail are additionally installed atop the model concrete crosstie. A breathable water-resistant canvas tarp is additionally installed over the model crosstie and immediate ballast area. The model does not incorporate a polyurethane pad nor steel rail line. Triangular markers denote relative humidity value from KTIP weather station, square markers denote measured relative humidity values from ballast, and circular markers denote measured relative humidity values inside concrete.

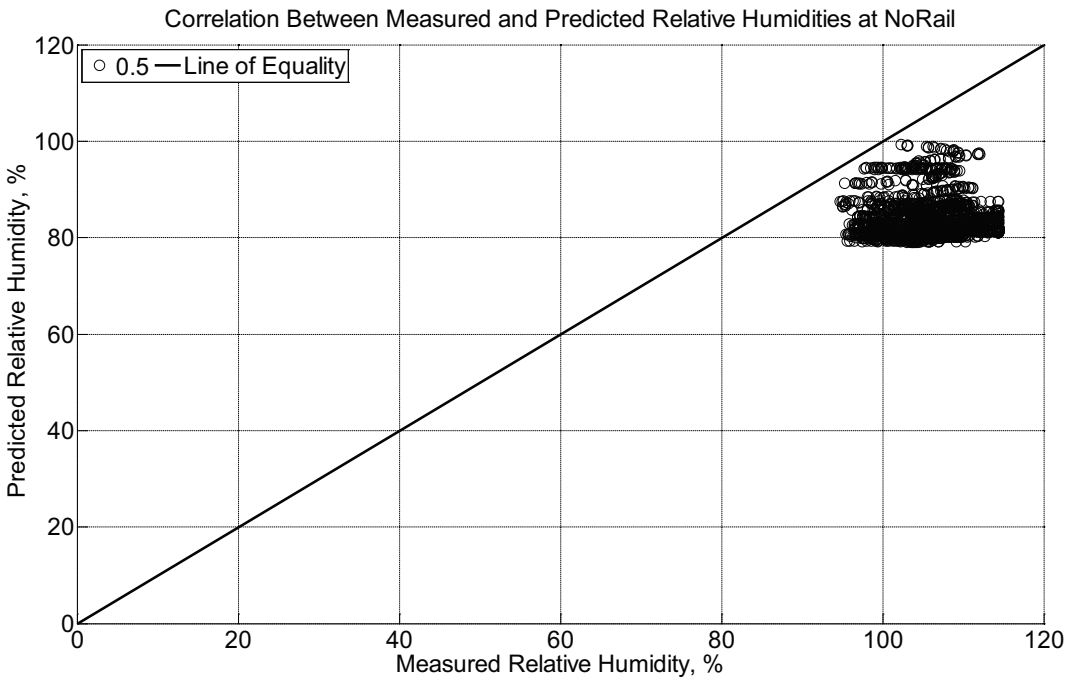

Figure B-952 Correlation between measured and predicted relative humidity values 0.5 inches (12.7 mm) from the surface of a model concrete crosstie (labeled NoRail) without a polyurethane pad nor rail installed in ballast in Rantoul, IL, between May 10, 2015, through June 20, 2015. A breathable water-resistant canvas tarp is additionally installed over the model crosstie and immediate ballast area.

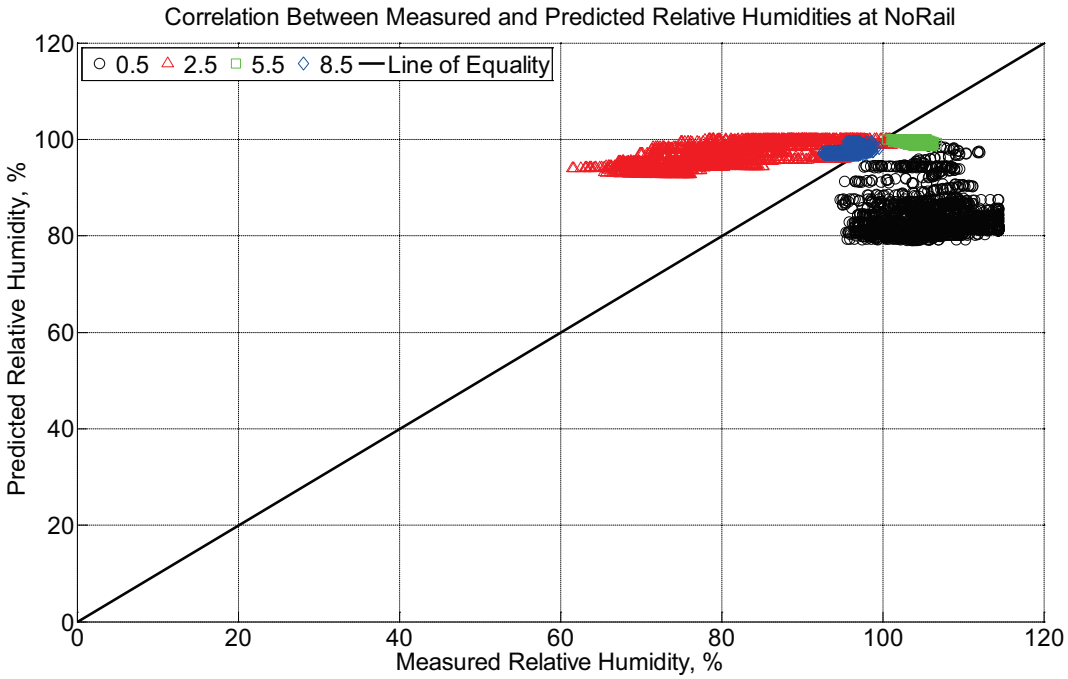

Figure B-953 Correlation between measured and predicted relative humidity values 0.5

inches (12.7 mm), 2.5 inches (63.5 mm), 5.5 inches (139.7 mm), and 8.5 inches (215.9 mm) from the surface of a model concrete crosstie (labeled NoRail) without a polyurethane pad nor rail installed in ballast in Rantoul, IL, between May 10, 2015, through June 20, 2015. A breathable water-resistant canvas tarp is additionally installed over the model crosstie and immediate ballast area.

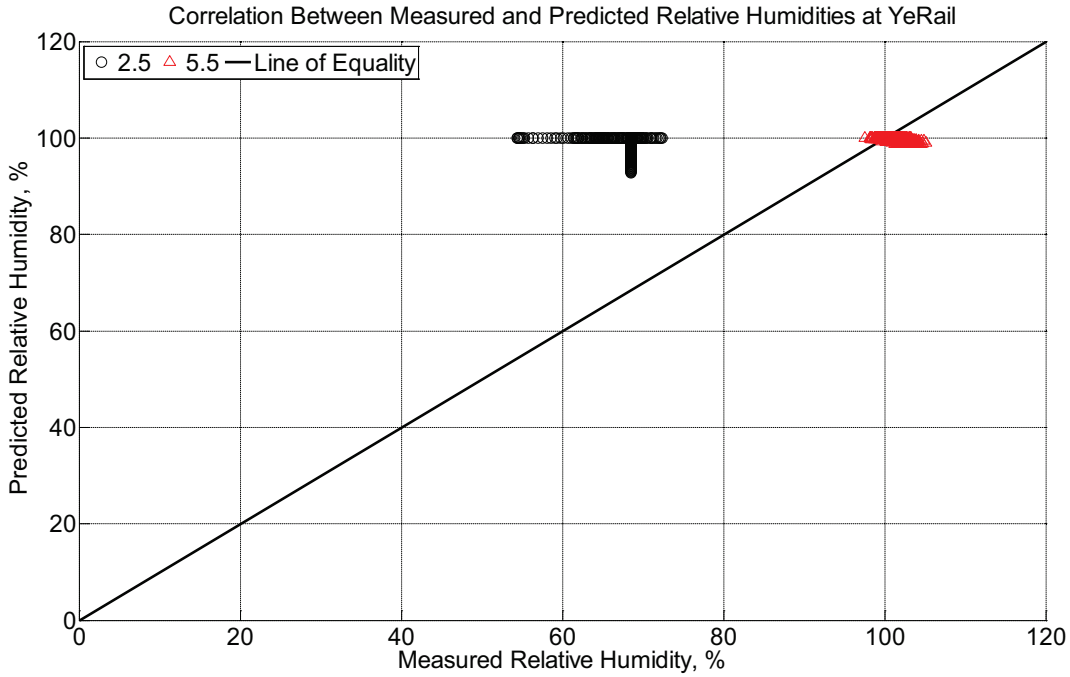

Figure B-954 Correlation between measured and predicted relative humidity values 2.5 inches (63.5 mm) and 5.5 inches (139.7 mm) from the surface of a model concrete crosstie (labeled YeRail) installed in ballast in Rantoul, IL, between May 10, 2015, through June 20, 2015. An 8 mm thick polyurethane pad and 12 in (30.48 cm) length 136 lb/yd (67.5 kg/m) section of steel rail are additionally installed atop the model concrete crosstie. A breathable water-resistant canvas tarp is additionally installed over the model crosstie and immediate ballast area. The model does not incorporate a polyurethane pad nor steel rail line.

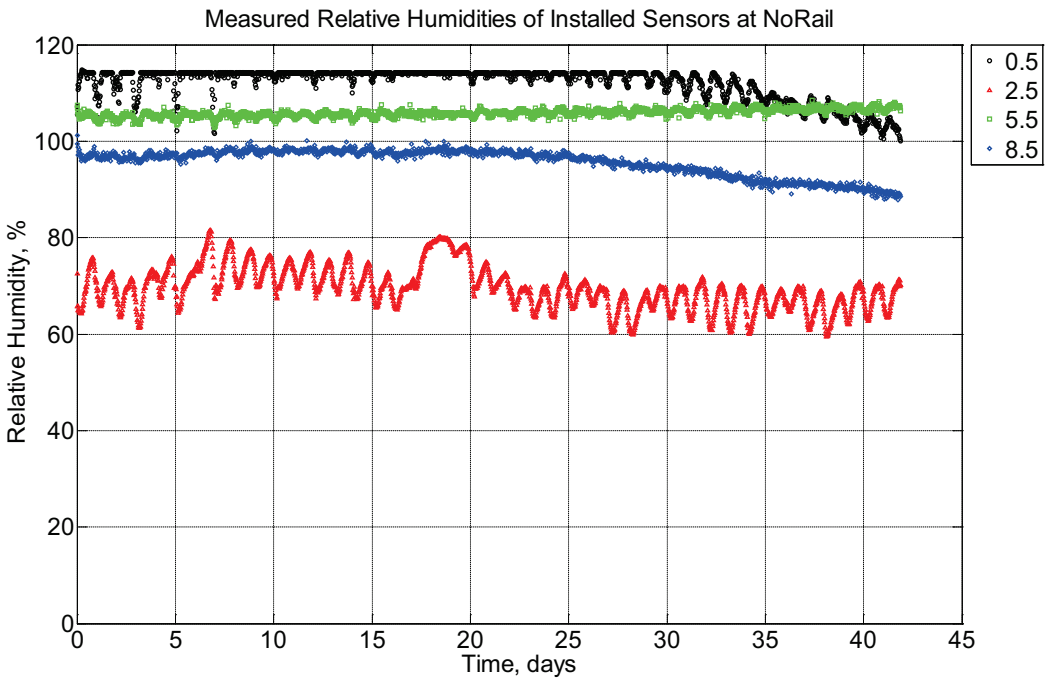

Figure B-955 Measured relative humidity at depths of 0.5 inches (12.7 mm), 2.5 inches (63.5 mm), 5.5 inches (139.7 mm), and 8.5 inches (215.9 mm) from the surface of a model concrete crosstie (labeled NoRail) without a polyurethane pad nor rail installed in ballast in Rantoul, IL, between June 20, 2015, through August 1, 2015. A breathable water-resistant canvas tarp is additionally installed over the model crosstie and immediate ballast area.

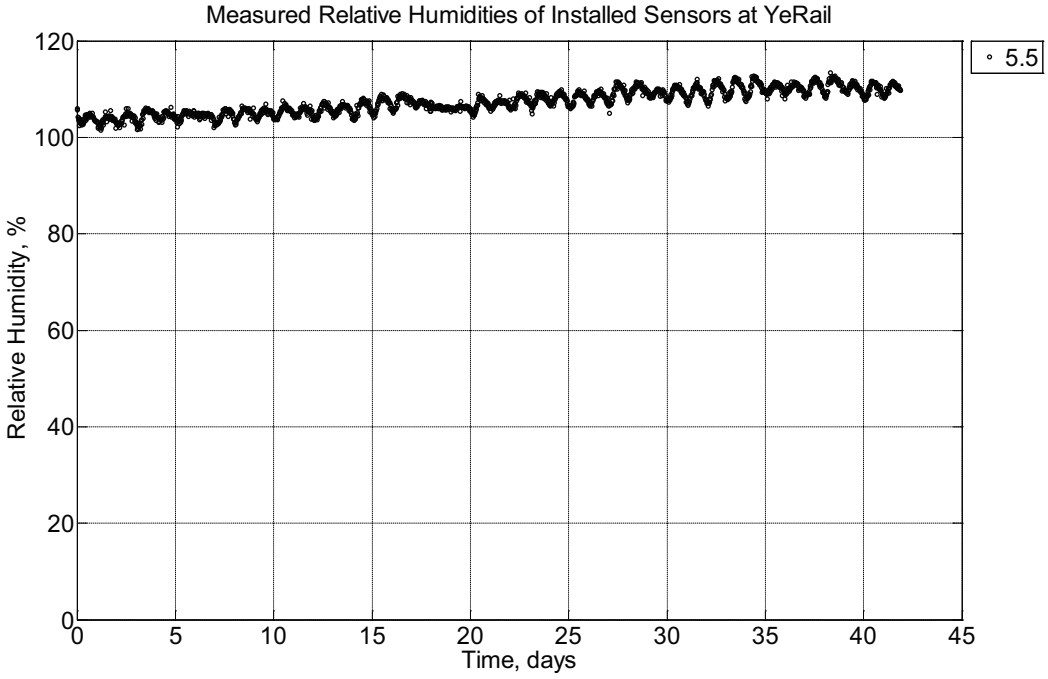

Figure B-956 Measured relative humidity at depths of 2.5 inches (63.5 mm) and 5.5 inches

(139.7 mm) from the surface of a model concrete crosstie (labeled YeRail) installed in ballast in Rantoul, IL, between June 20, 2015, through August 1, 2015. An 8 mm thick polyurethane pad and 12 in (30.48 cm) length 136 lb/yd (67.5 kg/m) section of steel rail are additionally installed atop the model concrete crosstie. A breathable water-resistant canvas tarp is additionally installed over the model crosstie and immediate ballast area.

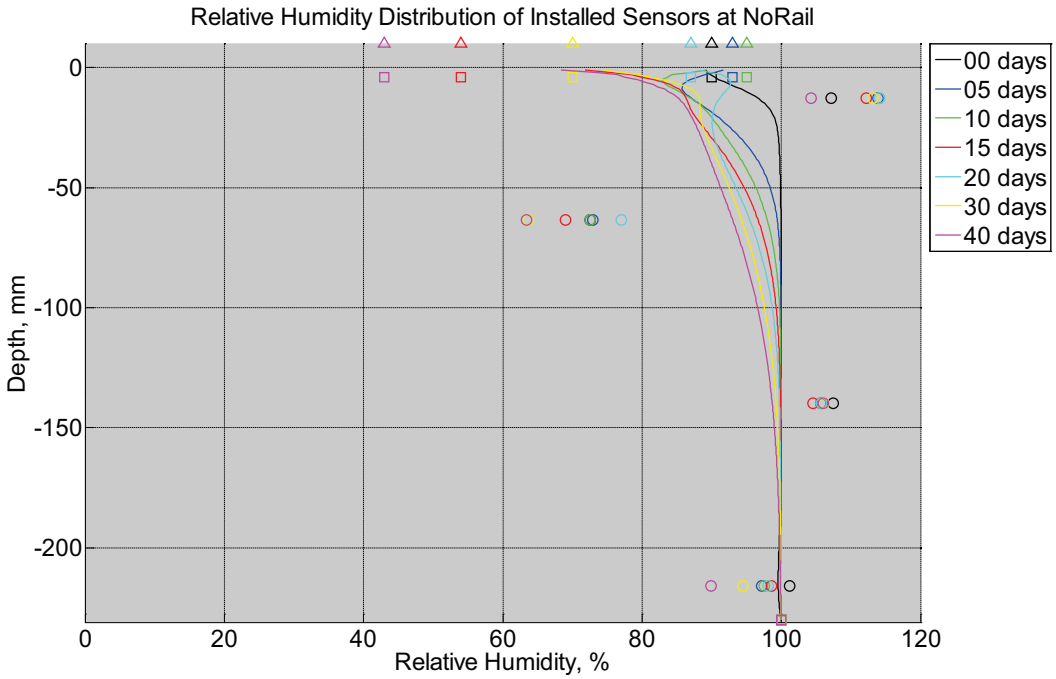

Figure B-957 Measured (markers) and modeled (continuous line) relative humidity profile distribution as a function of depth inside a model concrete crosstie (labeled NoRail) without a polyurethane pad nor rail installed in ballast in Rantoul, IL, between June 20, 2015, through August 1, 2015. A breathable water-resistant canvas tarp is additionally installed over the model crosstie and immediate ballast area. Triangular markers denote relative humidity value from KTIP weather station, square markers denote measured relative humidity values from ballast, and circular markers denote measured relative humidity values inside concrete.

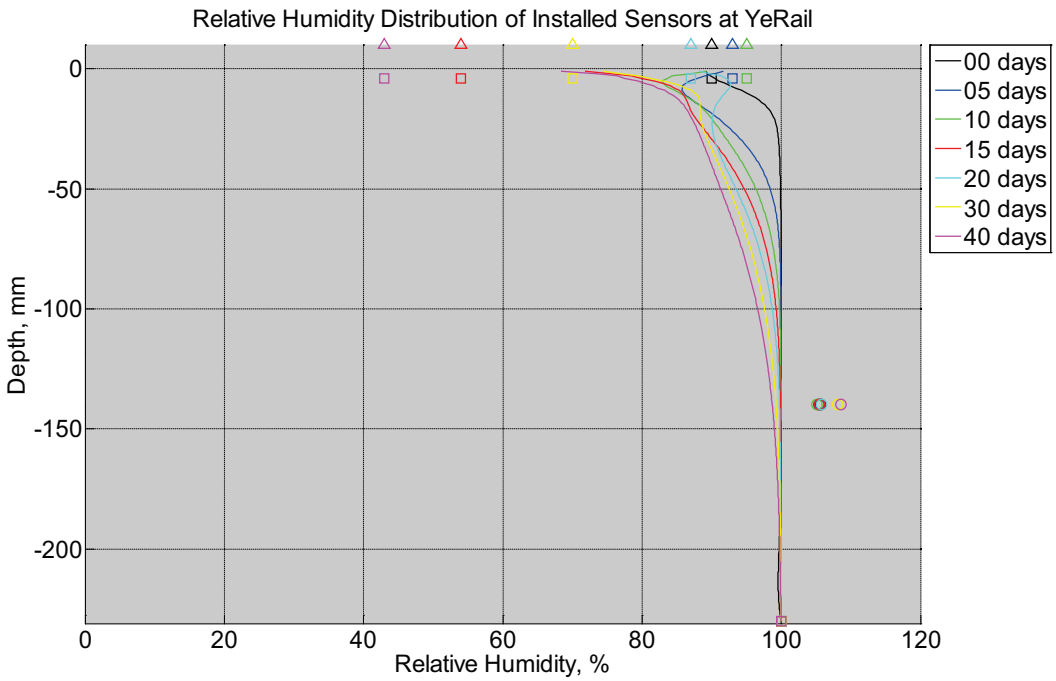

Figure B-958 Measured (markers) and modeled (continuous line) relative humidity profile distribution as a function of depth inside a model concrete crosstie (labeled YeRail) installed in ballast in Rantoul, IL, between June 20, 2015, through August 1, 2015. An 8 mm thick polyurethane pad and 12 in (30.48 cm) length 136 lb/yd (67.5 kg/m) section of steel rail are additionally installed atop the model concrete crosstie. A breathable water-resistant canvas tarp is additionally installed over the model crosstie and immediate ballast area. The model does not incorporate a polyurethane pad nor steel rail line. Triangular markers denote relative humidity value from KTIP weather station, square markers denote measured relative humidity values from ballast, and circular markers denote measured relative humidity values inside concrete.

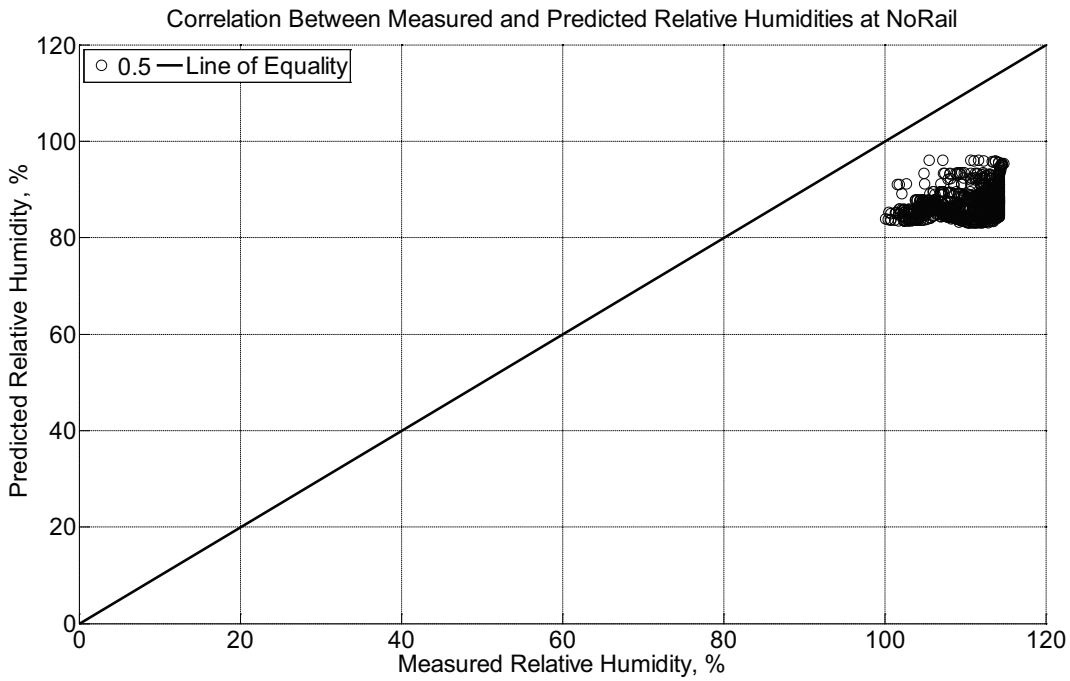

Figure B-959 Correlation between measured and predicted relative humidity values 0.5 inches (12.7 mm) from the surface of a model concrete crosstie (labeled NoRail) without a polyurethane pad nor rail installed in ballast in Rantoul, IL, between June 20, 2015, through August 1, 2015. A breathable water-resistant canvas tarp is additionally installed over the model crosstie and immediate ballast area.

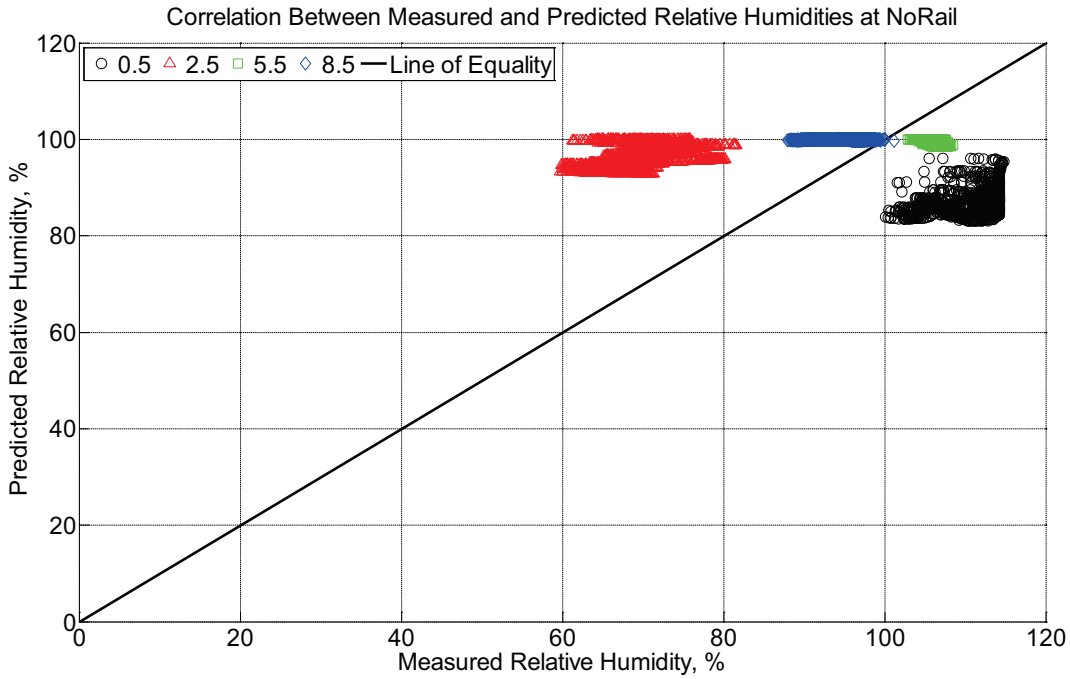

Figure B-960 Correlation between measured and predicted relative humidity values 0.5

inches (12.7 mm), 2.5 inches (63.5 mm), 5.5 inches (139.7 mm), and 8.5 inches (215.9 mm) from the surface of a model concrete crosstie (labeled NoRail) without a polyurethane pad nor rail installed in ballast in Rantoul, IL, between June 20, 2015, through August 1, 2015. A breathable water-resistant canvas tarp is additionally installed over the model crosstie and immediate ballast area.

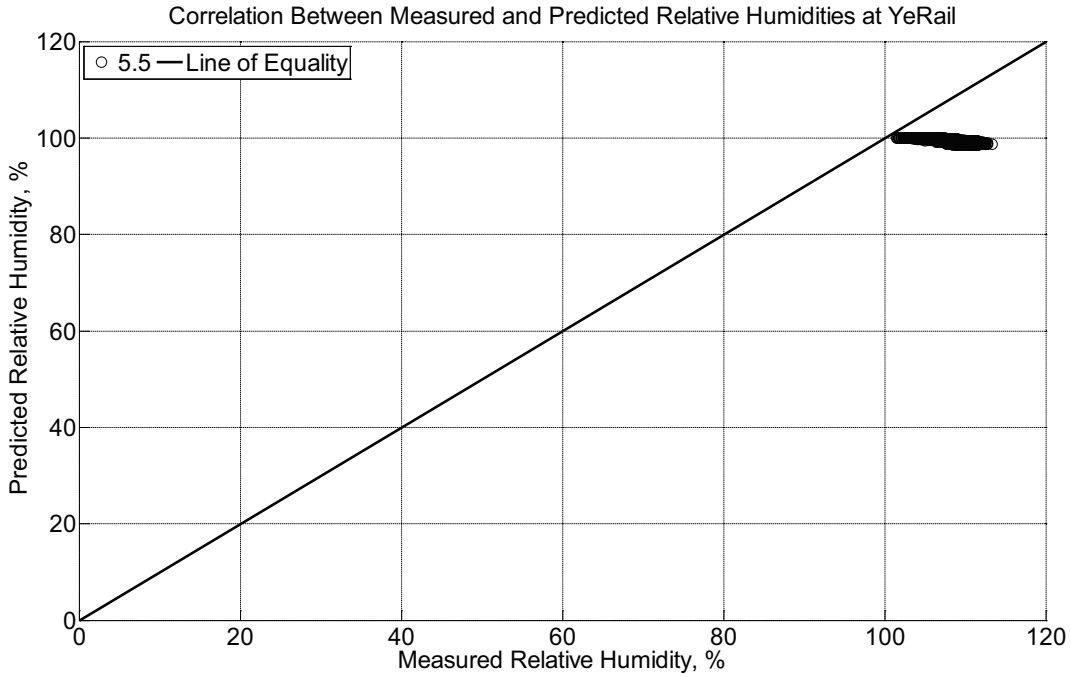

Figure B-961 Correlation between measured and predicted relative humidity values 2.5 inches (63.5 mm) and 5.5 inches (139.7 mm) from the surface of a model concrete crosstie (labeled YeRail) installed in ballast in Rantoul, IL, between June 20, 2015, through August 1, 2015. An 8 mm thick polyurethane pad and 12 in (30.48 cm) length 136 lb/yd (67.5 kg/m) section of steel rail are additionally installed atop the model concrete crosstie. A breathable water-resistant canvas tarp is additionally installed over the model crosstie and immediate ballast area. The model does not incorporate a polyurethane pad nor steel rail line.

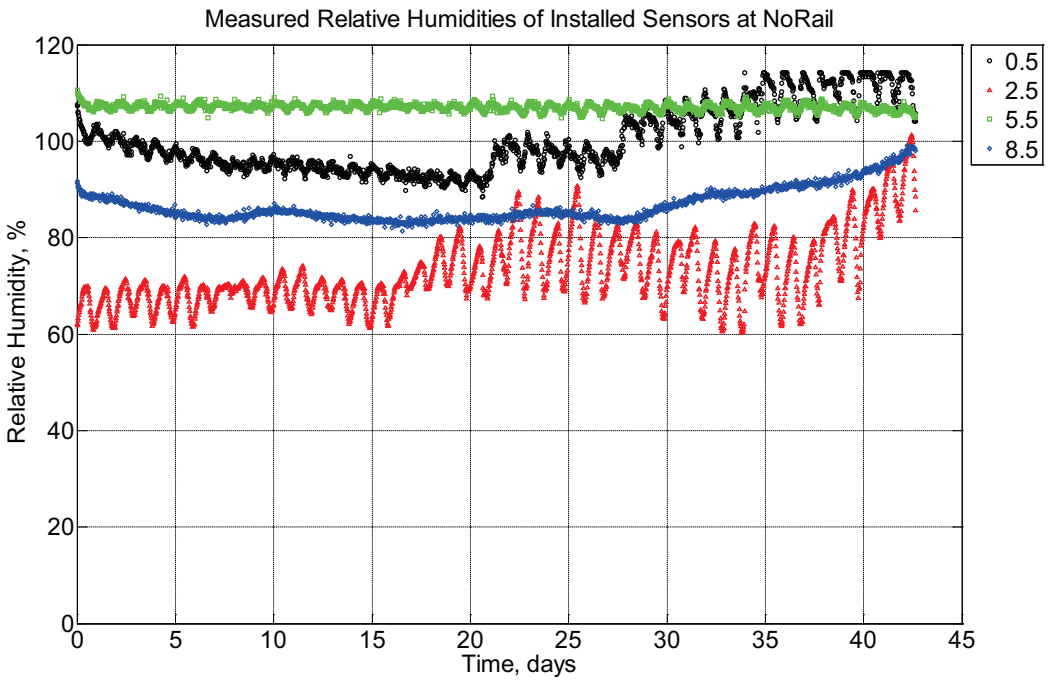

Figure B-962 Measured relative humidity at depths of 0.5 inches (12.7 mm), 2.5 inches (63.5 mm), 5.5 inches (139.7 mm), and 8.5 inches (215.9 mm) from the surface of a model concrete crosstie (labeled NoRail) without a polyurethane pad nor rail installed in ballast in Rantoul, IL, between August 1, 2015, through September 13, 2015. A breathable water-resistant canvas tarp is additionally installed over the model crosstie and immediate ballast area and removed on day 22.

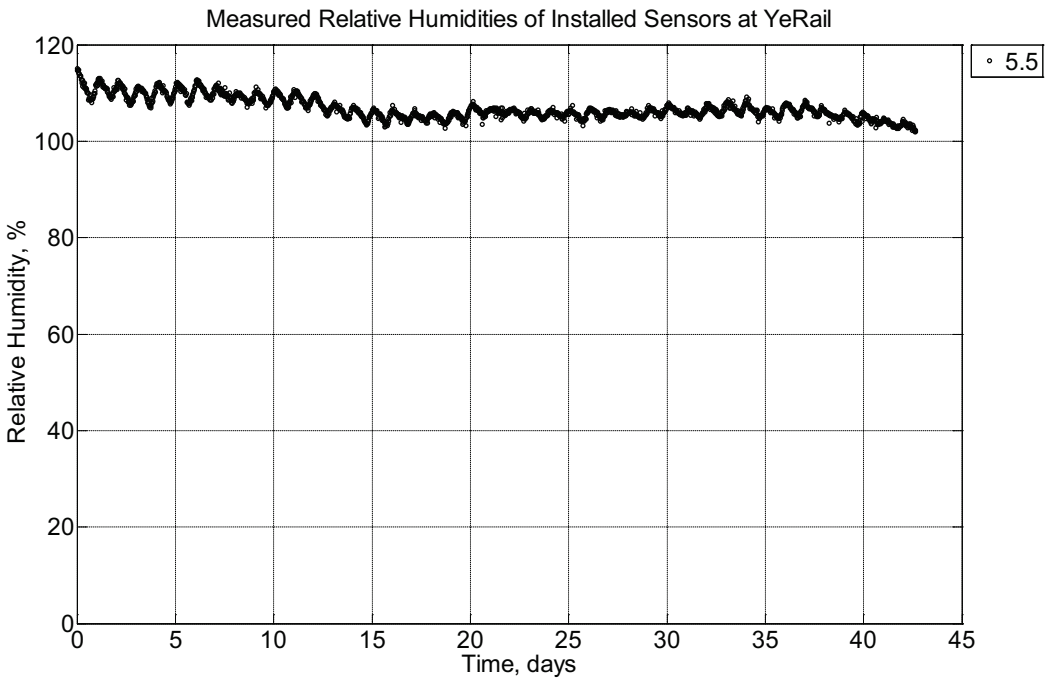

Figure B-963 Measured relative humidity at depths of 2.5 inches (63.5 mm) and 5.5 inches (139.7 mm) from the surface of a model concrete crosstie (labeled YeRail) installed in ballast in Rantoul, IL, between August 1, 2015, through September 13, 2015. An 8 mm thick polyurethane pad and 12 in (30.48 cm) length 136 lb/yd (67.5 kg/m) section of steel rail are additionally installed atop the model concrete crosstie. A breathable water-resistant canvas tarp is additionally installed over the model crosstie and immediate ballast area.

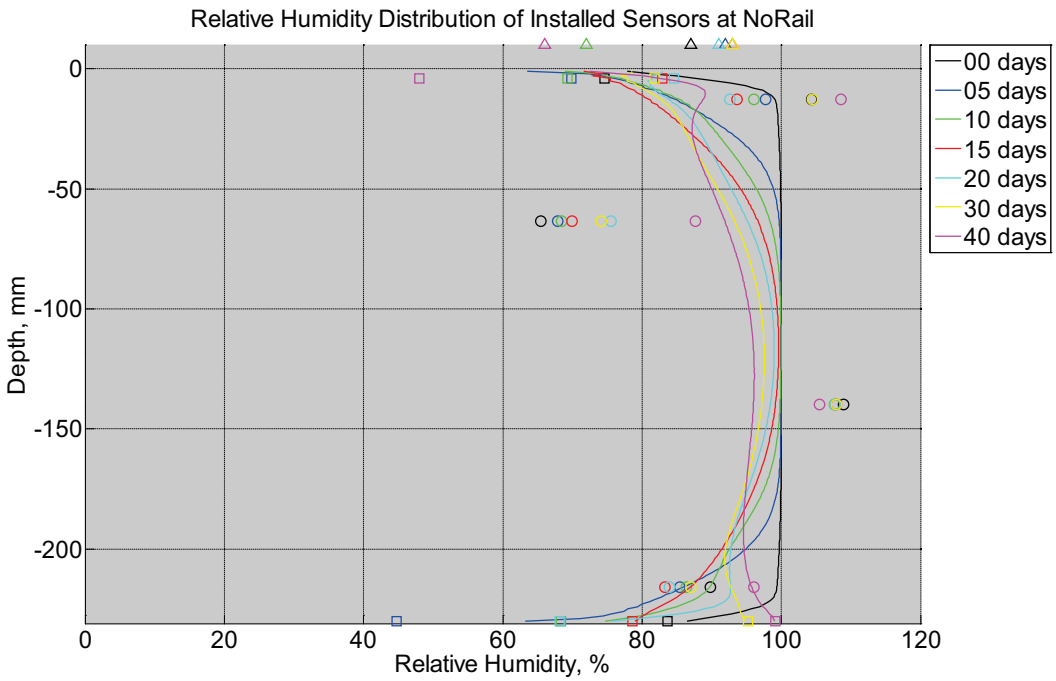

Figure B-964 Measured (markers) and modeled (continuous line) relative humidity profile distribution as a function of depth inside a model concrete crosstie (labeled NoRail) without a polyurethane pad nor rail installed in ballast in Rantoul, IL, between August 1, 2015, through September 13, 2015. A breathable water-resistant canvas tarp is additionally installed over the model crosstie and immediate ballast area and removed on day 22. Triangular markers denote relative humidity value from KTIP weather station, square markers denote measured relative humidity values from ballast, and circular markers denote measured relative humidity values inside concrete.

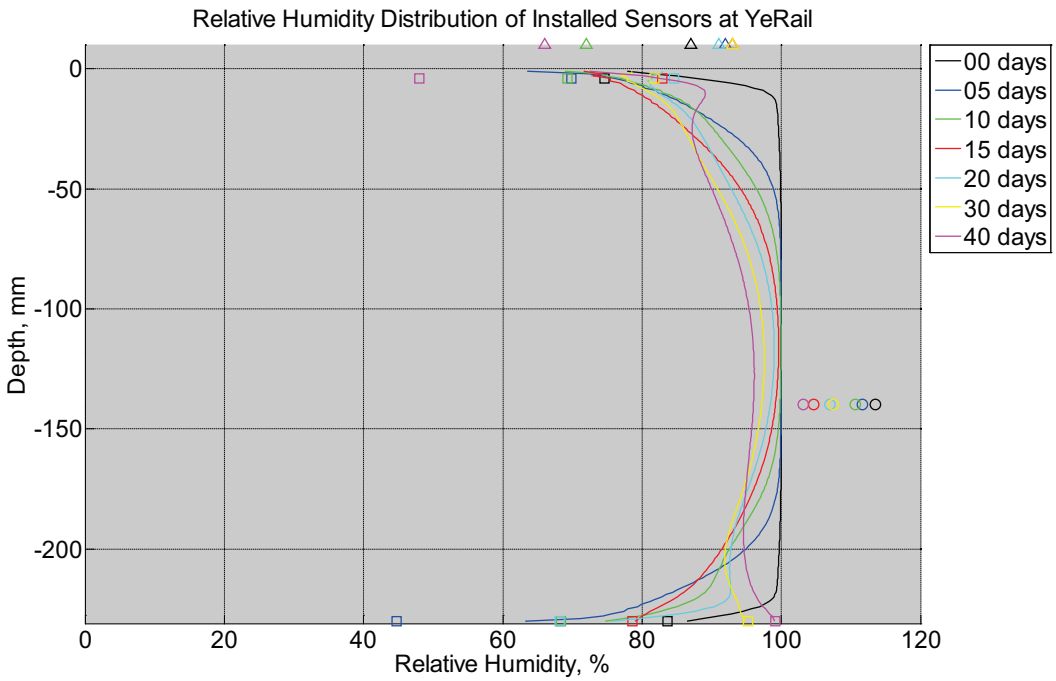

Figure B-965 Measured (markers) and modeled (continuous line) relative humidity profile distribution as a function of depth inside a model concrete crosstie (labeled YeRail) installed in ballast in Rantoul, IL, between August 1, 2015, through September 13, 2015. An 8 mm thick polyurethane pad and 12 in (30.48 cm) length 136 lb/yd (67.5 kg/m) section of steel rail are additionally installed atop the model concrete crosstie. A breathable water-resistant canvas tarp is additionally installed over the model crosstie and immediate ballast area. The model does not incorporate a polyurethane pad nor steel rail line. Triangular markers denote relative humidity value from KTIP weather station, square markers denote measured relative humidity values from ballast, and circular markers denote measured relative humidity values inside concrete.

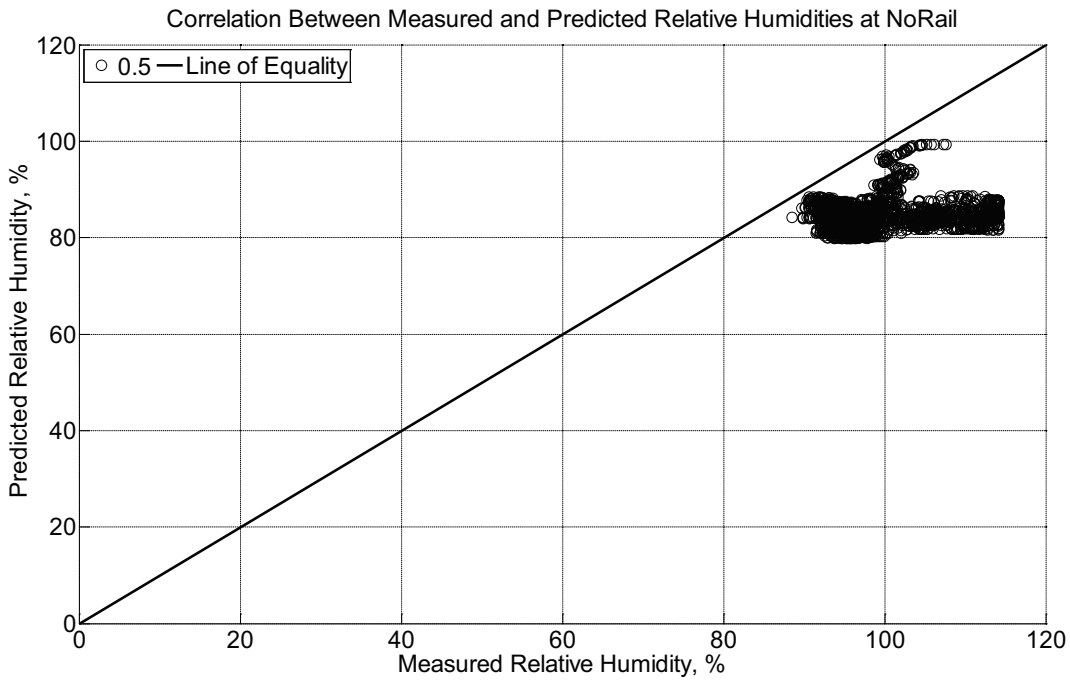

Figure B-966 Correlation between measured and predicted relative humidity values 0.5 inches (12.7 mm) from the surface of a model concrete crosstie (labeled NoRail) without a polyurethane pad nor rail installed in ballast in Rantoul, IL, between August 1, 2015, through September 13, 2015. A breathable water-resistant canvas tarp is additionally installed over the model crosstie and immediate ballast area and removed on day 22.

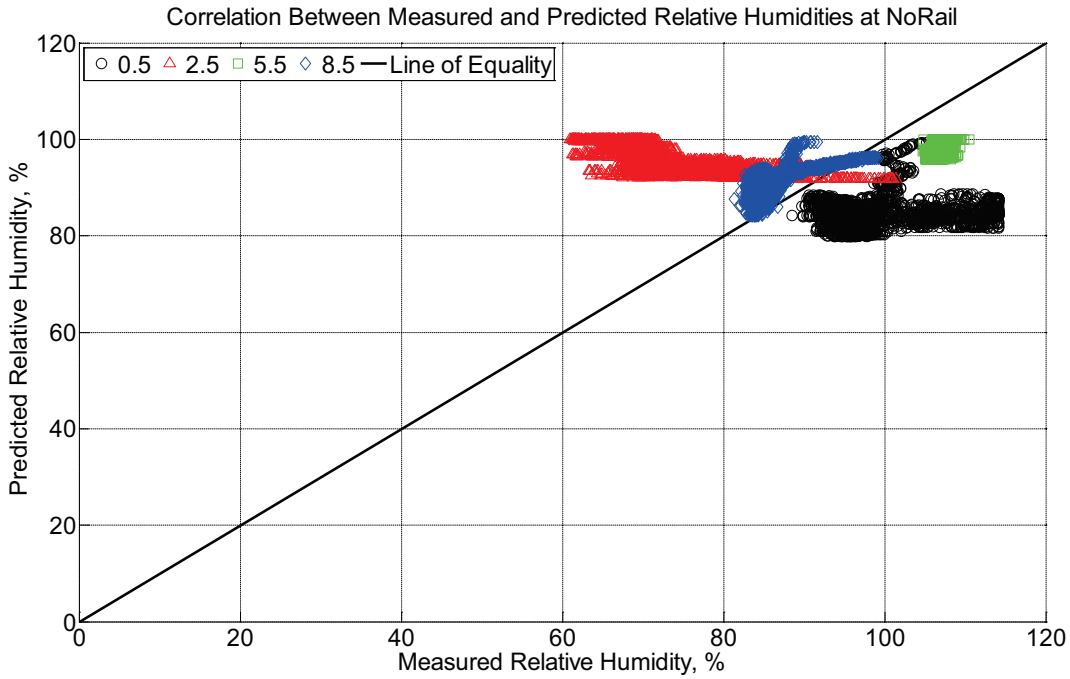

Figure B-967 Correlation between measured and predicted relative humidity values 0.5

inches (12.7 mm), 2.5 inches (63.5 mm), 5.5 inches (139.7 mm), and 8.5 inches (215.9 mm) from the surface of a model concrete crosstie (labeled NoRail) without a polyurethane pad nor rail installed in ballast in Rantoul, IL, between August 1, 2015, through September 13, 2015. A breathable water-resistant canvas tarp is additionally installed over the model crosstie and immediate ballast area and removed on day 22.

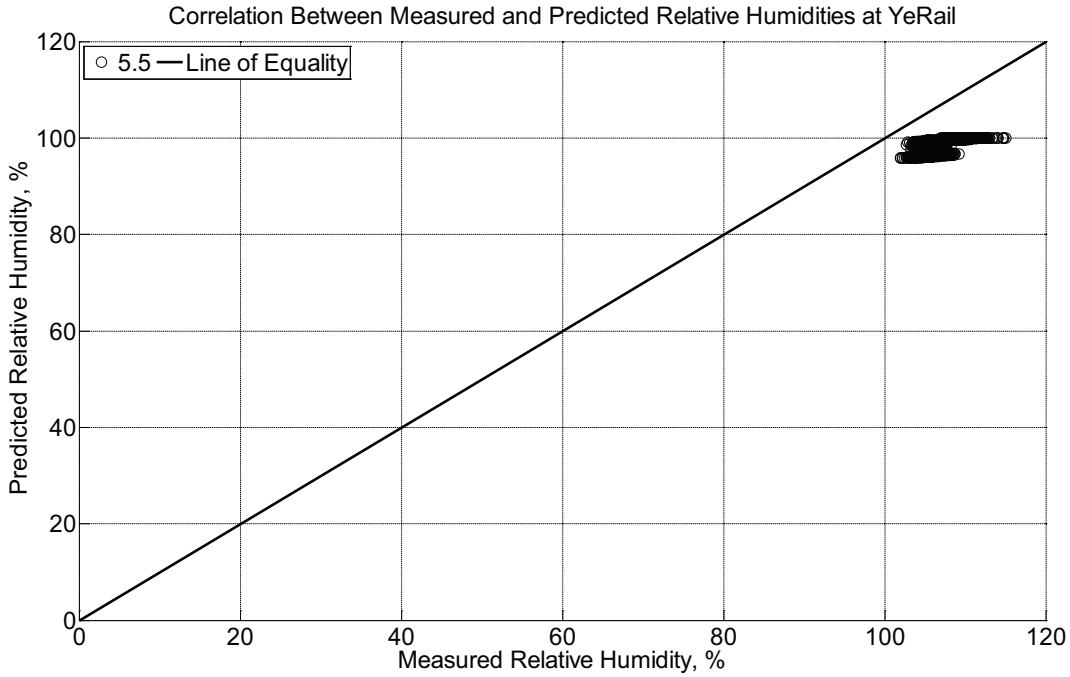

Figure B-968 Correlation between measured and predicted relative humidity values 2.5 inches (63.5 mm) and 5.5 inches (139.7 mm) from the surface of a model concrete crosstie (labeled YeRail) installed in ballast in Rantoul, IL, between August 1, 2015, through September 13, 2015. An 8 mm thick polyurethane pad and 12 in (30.48 cm) length 136 lb/yd (67.5 kg/m) section of steel rail are additionally installed atop the model concrete crosstie. A breathable water-resistant canvas tarp is additionally installed over the model crosstie and immediate ballast area. The model does not incorporate a polyurethane pad nor steel rail line.

Measured and predicted internal temperature of instrumented model concrete crossties located in Rantoul, IL

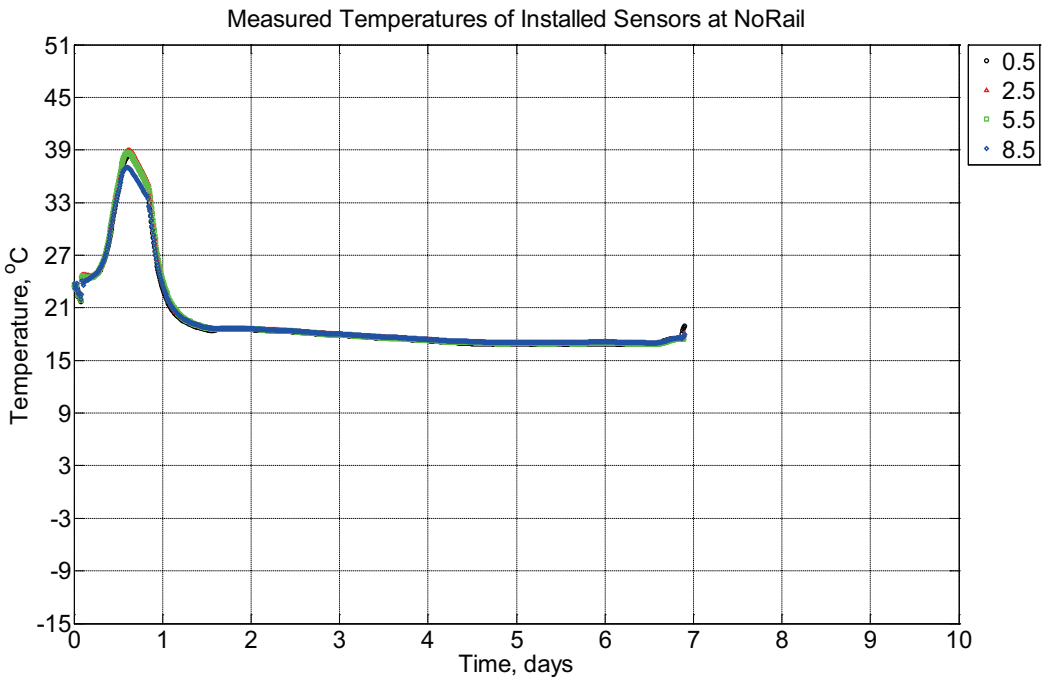

Figure B-969 Measured temperature at depths of 0.5 inches (12.7 mm), 2.5 inches (63.5 mm), 5.5 inches (139.7 mm), and 8.5 inches (215.9 mm) from the surface of a model concrete crosstie (labeled NoRail) without a polyurethane pad nor rail curing inside an environmentally controlled room (50% RH, 23 ºC) between October 8, 2014, through October 15, 2014.

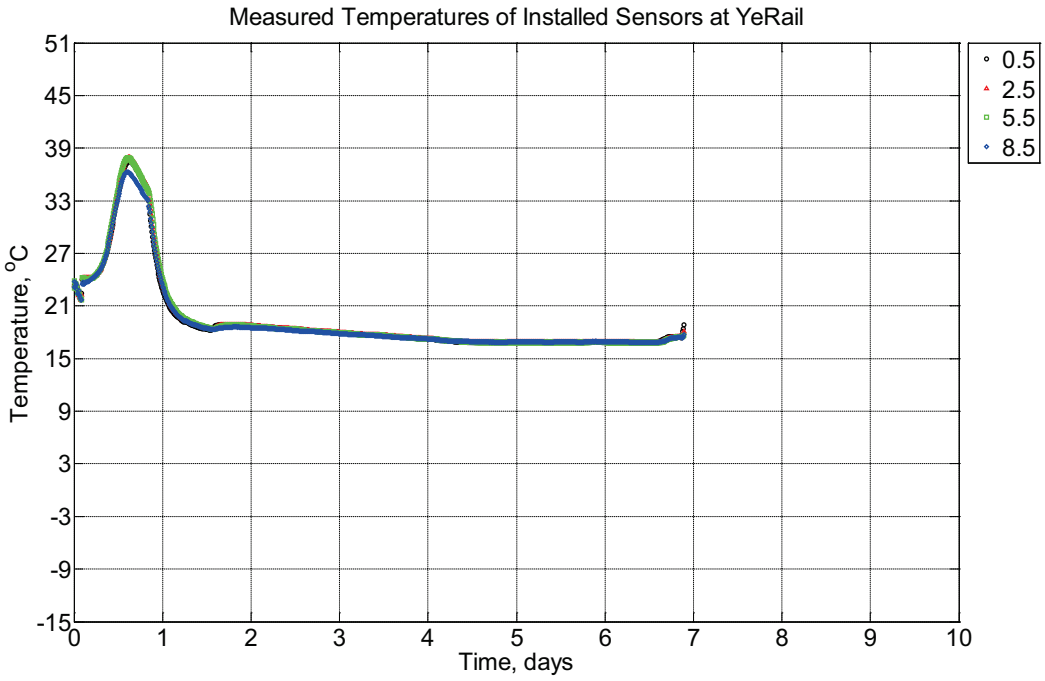

Figure B-970 Measured temperature at depths of 0.5 inches (12.7 mm), 2.5 inches (63.5

mm), 5.5 inches (139.7 mm), and 8.5 inches (215.9 mm) from the surface of a model concrete crosstie (labeled YeRail) without a polyurethane pad nor rail curing inside an environmentally controlled room (50% RH, 23 ºC) between October 8, 2014, through October 15, 2014.

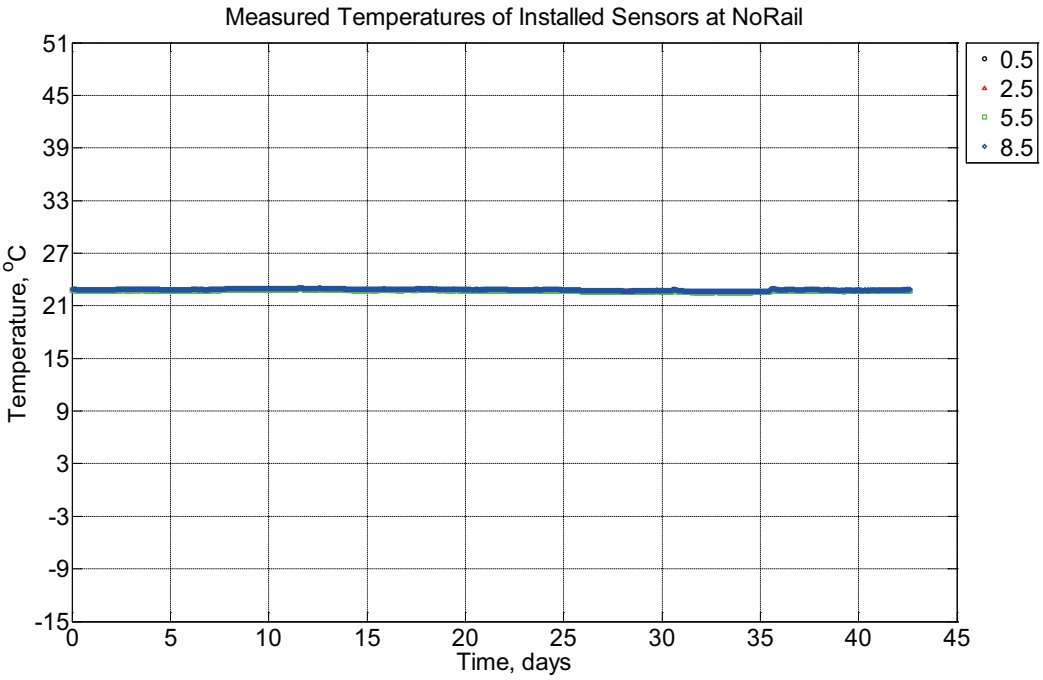

Figure B-971 Measured temperature at depths of 0.5 inches (12.7 mm), 2.5 inches (63.5 mm), 5.5 inches (139.7 mm), and 8.5 inches (215.9 mm) from the surface of a model concrete crosstie (labeled NoRail) without a polyurethane pad nor rail curing inside an environmentally controlled room (50% RH, 23 ºC) between October 18, 2014, through November 29, 2014.

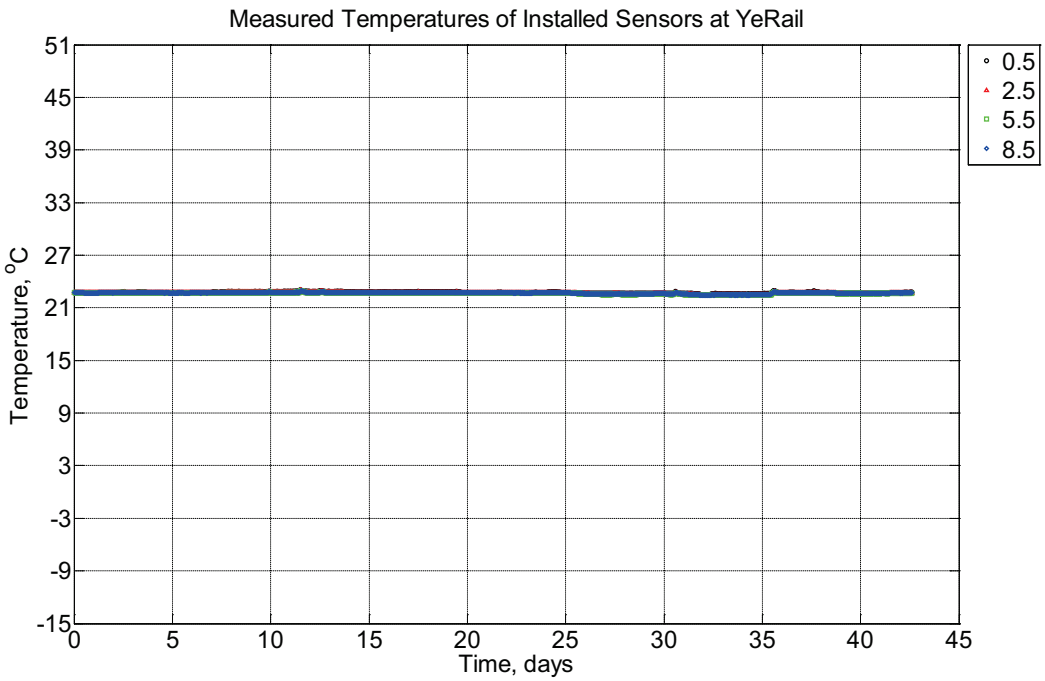

Figure B-972 Measured temperature at depths of 0.5 inches (12.7 mm), 2.5 inches (63.5 mm), 5.5 inches (139.7 mm), and 8.5 inches (215.9 mm) from the surface of a model concrete crosstie (labeled YeRail) without a polyurethane pad nor rail curing inside an environmentally controlled room (50% RH, 23 °C) between October 18, 2014, through November 29, 2014.

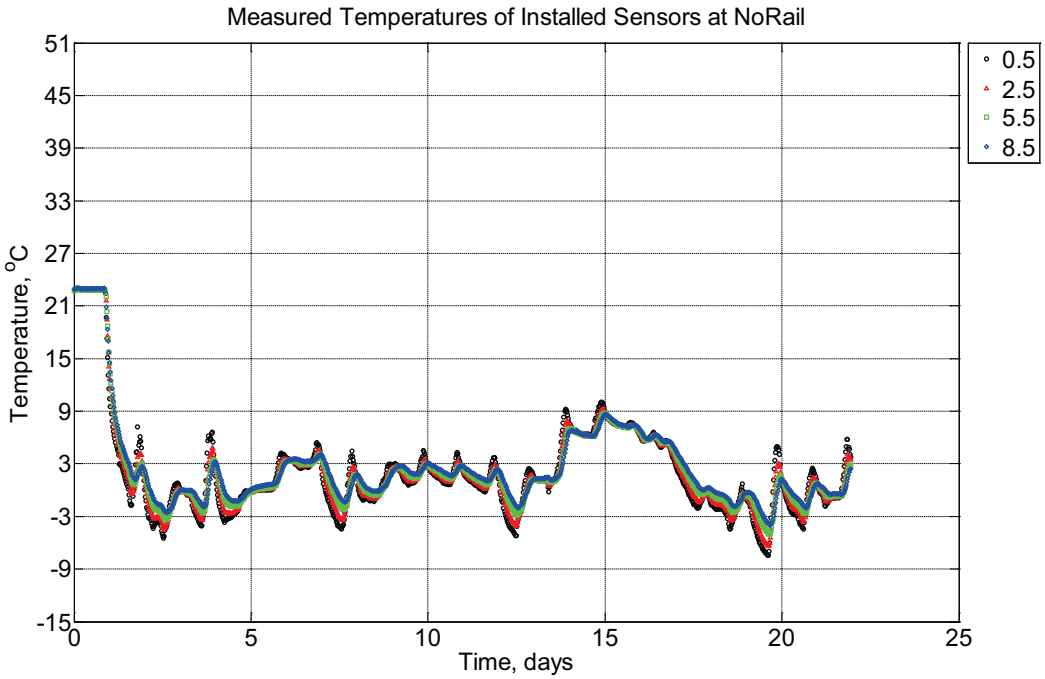

Figure B-973 Measured temperature at depths of 0.5 inches (12.7 mm), 2.5 inches (63.5

mm), 5.5 inches (139.7 mm), and 8.5 inches (215.9 mm) from the surface of a model concrete crosstie (labeled NoRail) without a polyurethane pad nor rail installed in ballast in Rantoul, IL, between November 29, 2014, through December 21, 2014.

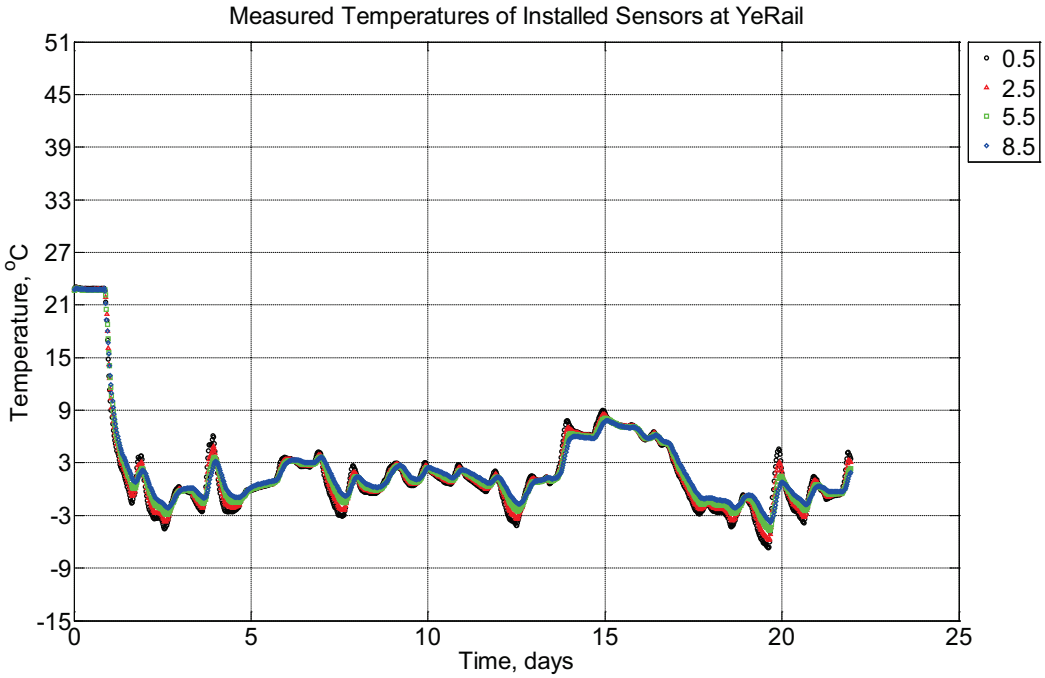

Figure B-974 Measured temperature at depths of 0.5 inches (12.7 mm), 2.5 inches (63.5 mm), 5.5 inches (139.7 mm), and 8.5 inches (215.9 mm) from the surface of a model concrete crosstie (labeled YeRail) installed in ballast in Rantoul, IL, between November 29, 2014, through December 21, 2014. An 8 mm thick polyurethane pad and 12 in (30.48 cm) length 136 lb/yd (67.5 kg/m) section of steel rail are additionally installed atop the model concrete crosstie.

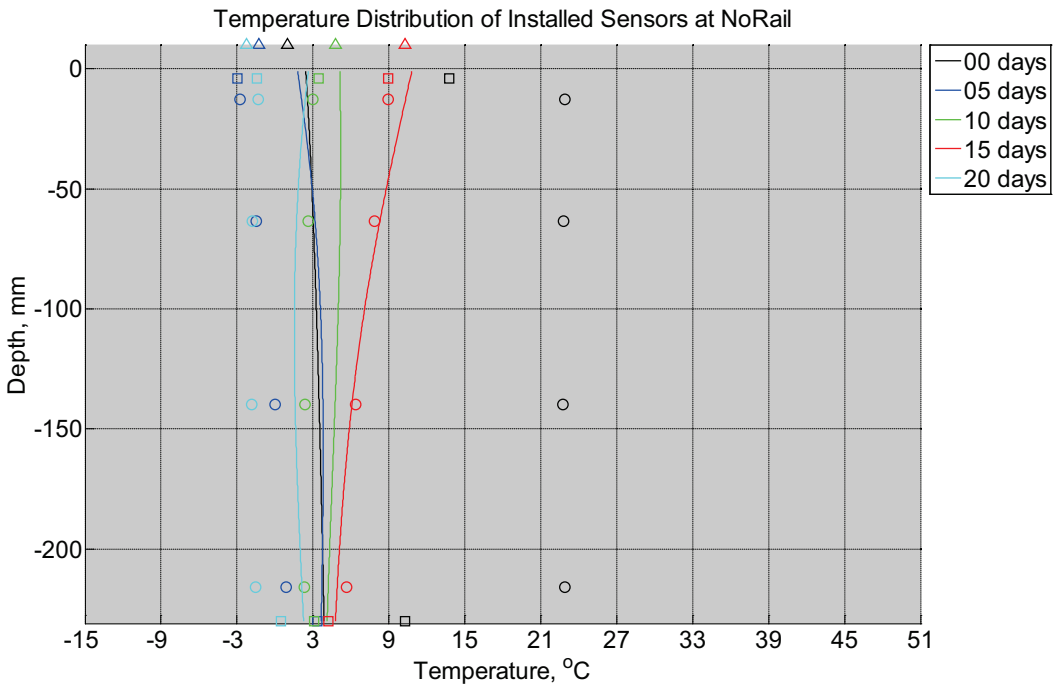

Figure B-975 Measured (markers) and modeled (continuous line) temperature profile distribution as a function of depth inside a model concrete crosstie (labeled NoRail) without a polyurethane pad nor rail installed in ballast in Rantoul, IL, between November 29, 2014, through December 21, 2014. Triangular markers denote temperature value from KTIP weather station, square markers denote measured temperature values from ballast, and circular markers denote measured temperature values inside concrete.

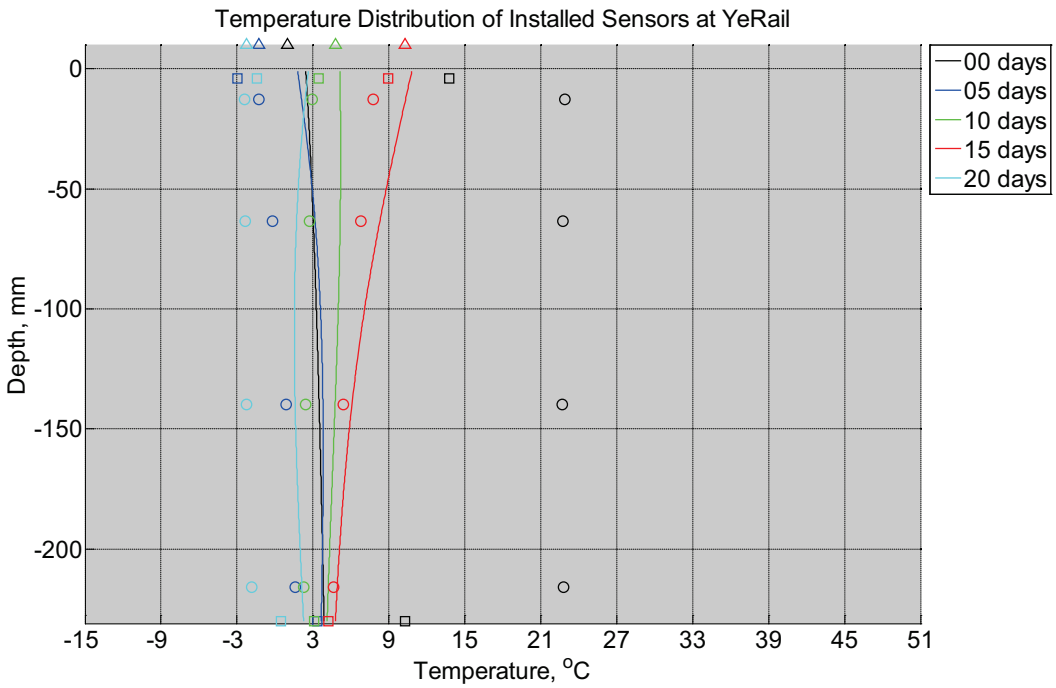

Figure B-976 Measured (markers) and modeled (continuous line) temperature profile distribution as a function of depth inside a model concrete crosstie (labeled YeRail) installed in ballast in Rantoul, IL, between November 29, 2014, through December 21, 2014. An 8 mm thick polyurethane pad and 12 in (30.48 cm) length 136 lb/yd (67.5 kg/m) section of steel rail are additionally installed atop the model concrete crosstie. The model does not incorporate a polyurethane pad nor steel rail line. Triangular markers denote temperature value from KTIP weather station, square markers denote measured temperature values from ballast, and circular markers denote measured temperature values inside concrete.

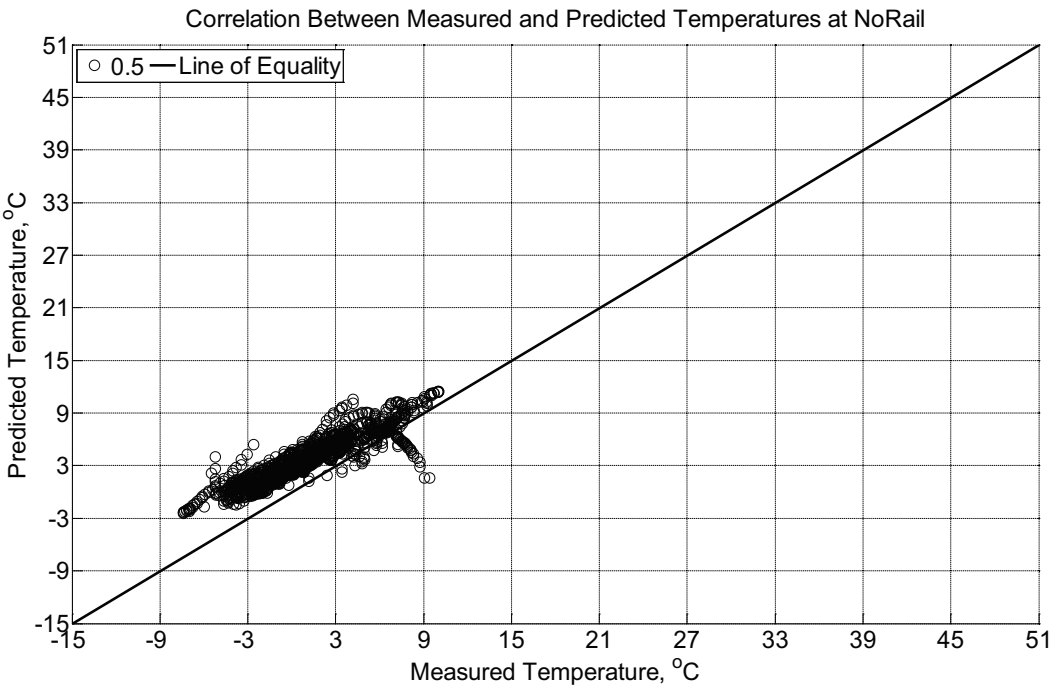

Figure B-977 Correlation between measured and predicted temperature values 0.5 inches (12.7 mm) from the surface of a model concrete crosstie (labeled NoRail) without a polyurethane pad nor rail installed in ballast in Rantoul, IL, between November 29, 2014, through December 21, 2014.

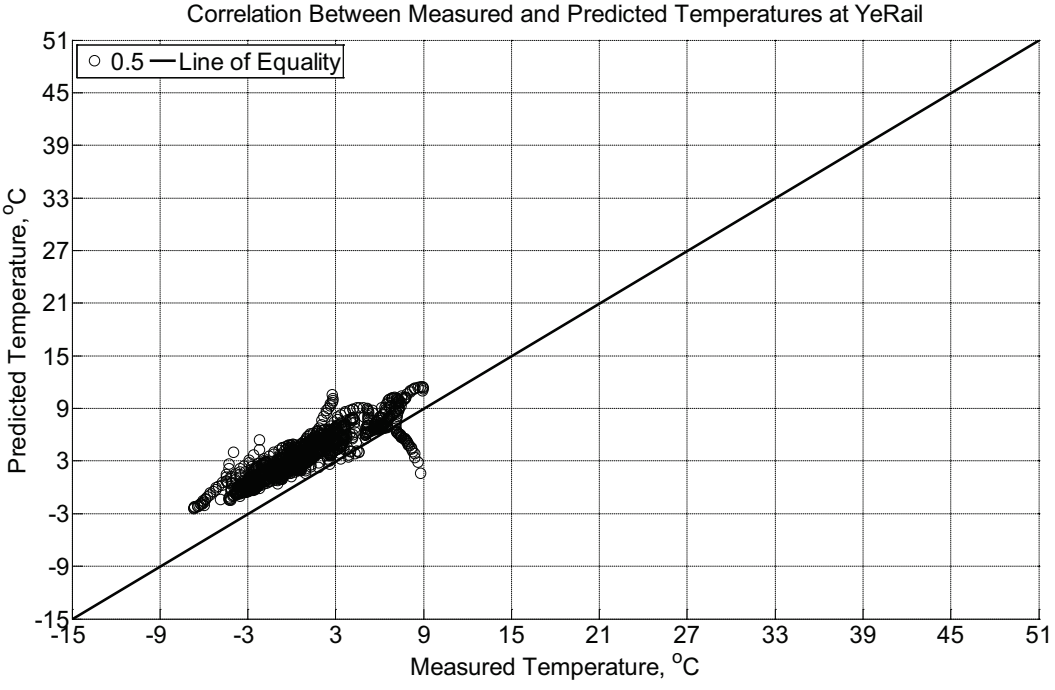

Figure B-978 Correlation between measured and predicted temperature values 0.5 inches (12.7 mm) from the surface of a model concrete crosstie (labeled YeRail) installed in ballast

in Rantoul, IL, between November 29, 2014, through December 21, 2014. An 8 mm thick polyurethane pad and 12 in (30.48 cm) length 136 lb/yd (67.5 kg/m) section of steel rail are additionally installed atop the model concrete crosstie. The model does not incorporate a polyurethane pad nor steel rail line.

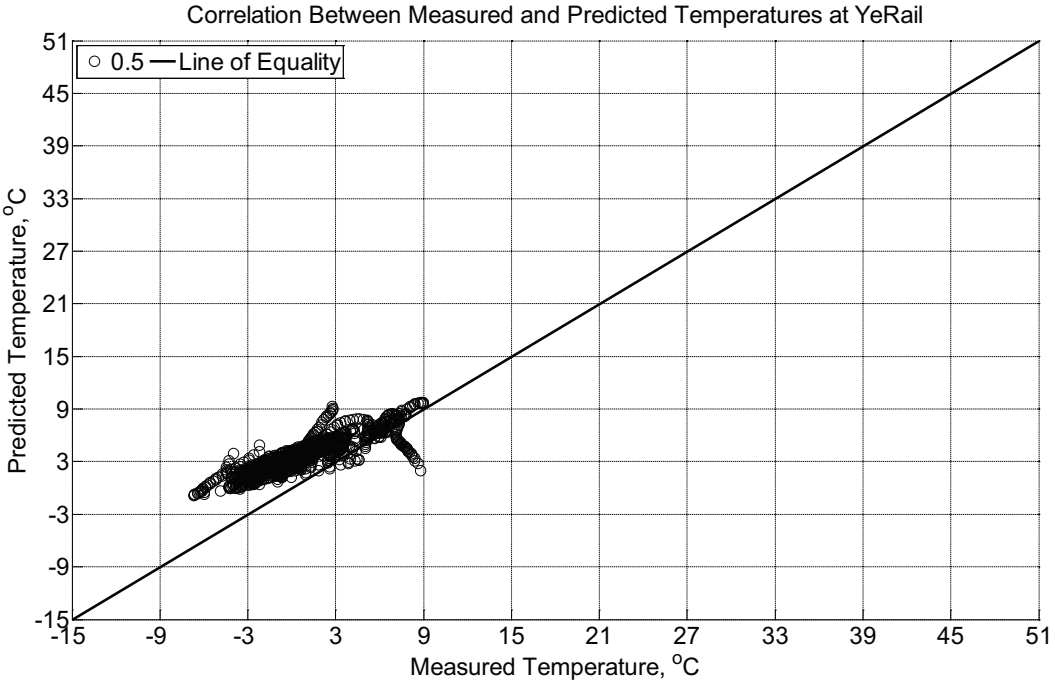

Figure B-979 Correlation between measured and predicted temperature values 0.5 inches (12.7 mm) from the surface of a model concrete crosstie (labeled YeRail) installed in ballast in Rantoul, IL, between November 29, 2014, through December 21, 2014. An 8 mm thick polyurethane pad and 12 in (30.48 cm) length 136 lb/yd (67.5 kg/m) section of steel rail are additionally installed atop the model concrete crosstie. The model incorporates a 1 mm thick polyurethane pad and 1 mm thick steel rail line.

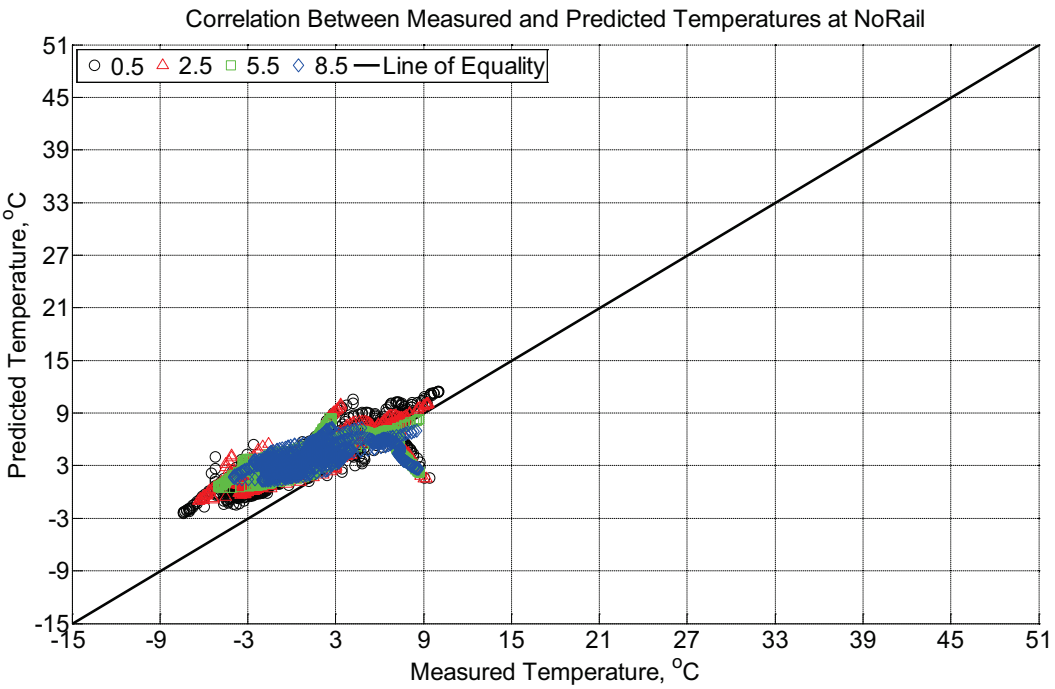

Figure B-980 Correlation between measured and predicted temperature values 0.5 inches (12.7 mm), 2.5 inches (63.5 mm), 5.5 inches (139.7 mm), and 8.5 inches (215.9 mm) from the surface of a model concrete crosstie (labeled NoRail) without a polyurethane pad nor rail installed in ballast in Rantoul, IL, between November 29, 2014, through December 21, 2014.

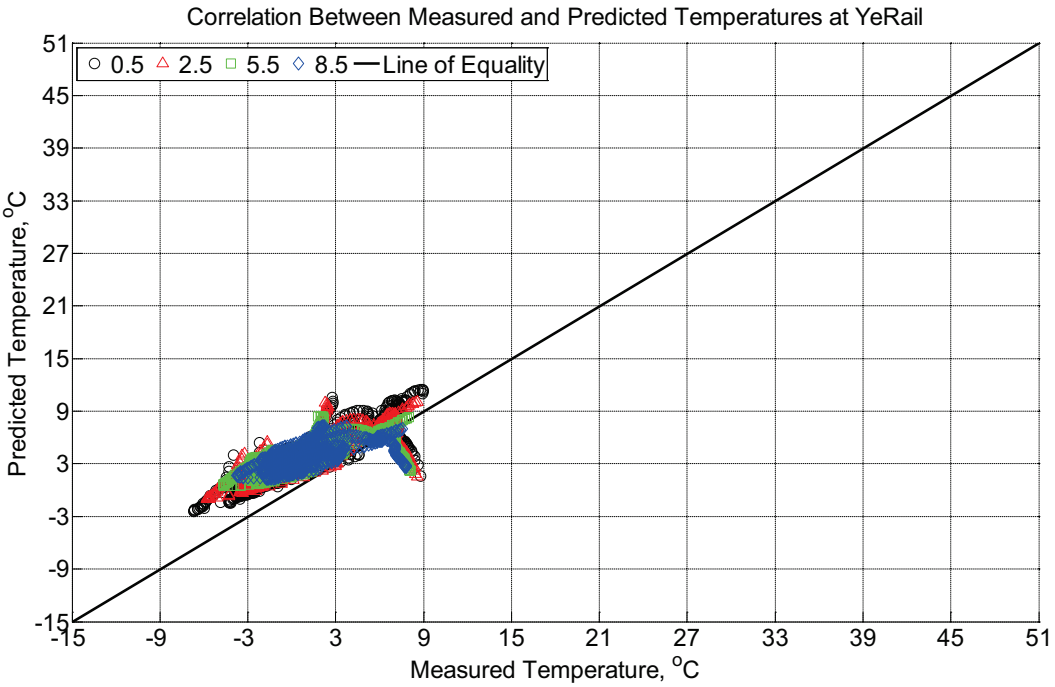

Figure B-981 Correlation between measured and predicted temperature values 0.5 inches

(12.7 mm), 2.5 inches (63.5 mm), 5.5 inches (139.7 mm), and 8.5 inches (215.9 mm) from the surface of a model concrete crosstie (labeled YeRail) installed in ballast in Rantoul, IL, between November 29, 2014, through December 21, 2014. An 8 mm thick polyurethane pad and 12 in (30.48 cm) length 136 lb/yd (67.5 kg/m) section of steel rail are additionally installed atop the model concrete crosstie. The model does not incorporate a polyurethane pad nor steel rail line.

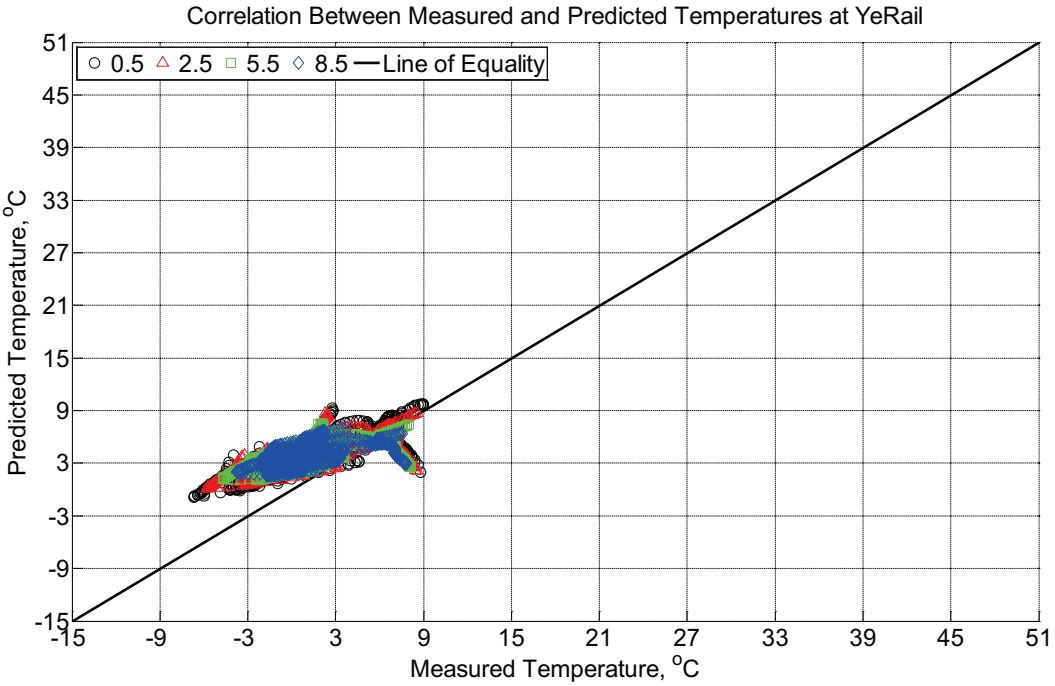

Figure B-982 Correlation between measured and predicted temperature values 0.5 inches (12.7 mm), 2.5 inches (63.5 mm), 5.5 inches (139.7 mm), and 8.5 inches (215.9 mm) from the surface of a model concrete crosstie (labeled YeRail) installed in ballast in Rantoul, IL, between November 29, 2014, through December 21, 2014. An 8 mm thick polyurethane pad and 12 in (30.48 cm) length 136 lb/yd (67.5 kg/m) section of steel rail are additionally installed atop the model concrete crosstie. The model incorporates a 1 mm thick polyurethane pad and 1 mm thick steel rail line.

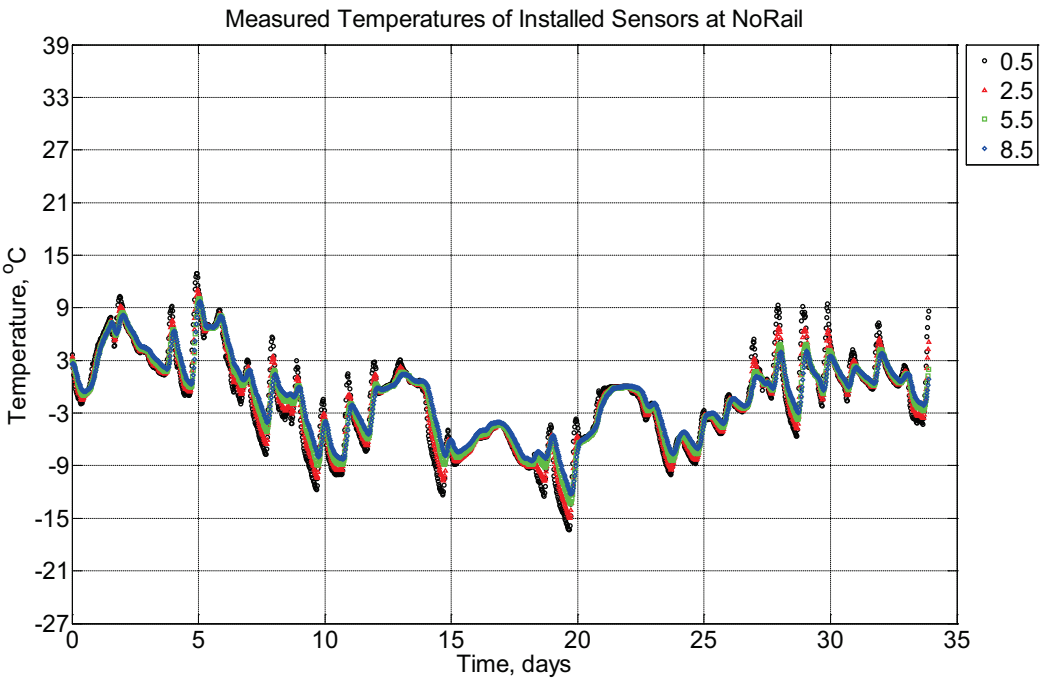

Figure B-983 Measured temperature at depths of 0.5 inches (12.7 mm), 2.5 inches (63.5 mm), 5.5 inches (139.7 mm), and 8.5 inches (215.9 mm) from the surface of a model concrete crosstie (labeled NoRail) without a polyurethane pad nor rail installed in ballast in Rantoul, IL, between December 21, 2014, through January 24, 2015.

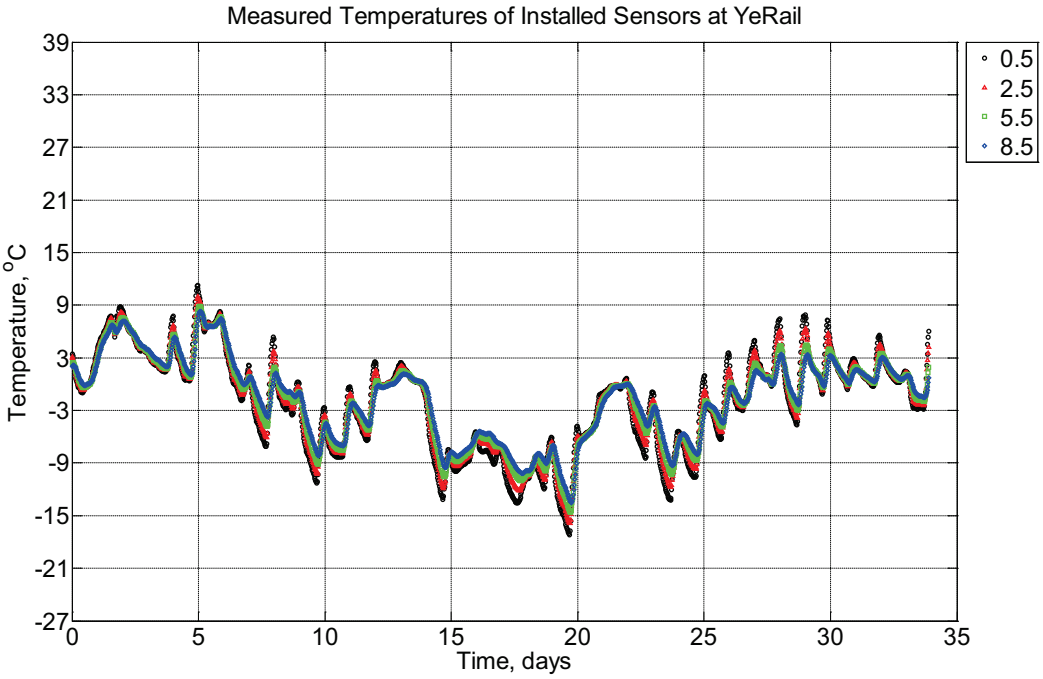

Figure B-984 Measured temperature at depths of 0.5 inches (12.7 mm), 2.5 inches (63.5 mm), 5.5 inches (139.7 mm), and 8.5 inches (215.9 mm) from the surface of a model

concrete crosstie (labeled YeRail) installed in ballast in Rantoul, IL, between December 21, 2014, through January 24, 2015. An 8 mm thick polyurethane pad and 12 in (30.48 cm) length 136 lb/yd (67.5 kg/m) section of steel rail are additionally installed atop the model concrete crosstie.

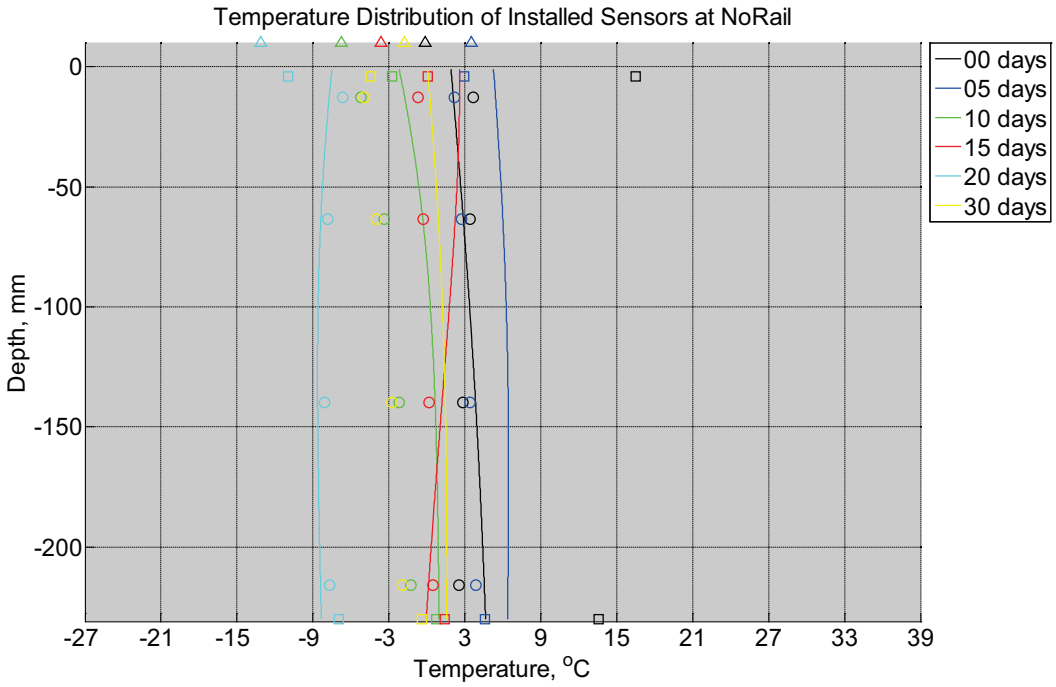

Figure B-985 Measured (markers) and modeled (continuous line) temperature profile distribution as a function of depth inside a model concrete crosstie (labeled NoRail) without a polyurethane pad nor rail installed in ballast in Rantoul, IL, between December 21, 2014, through January 24, 2015. Triangular markers denote temperature value from KTIP weather station, square markers denote measured temperature values from ballast, and circular markers denote measured temperature values inside concrete.

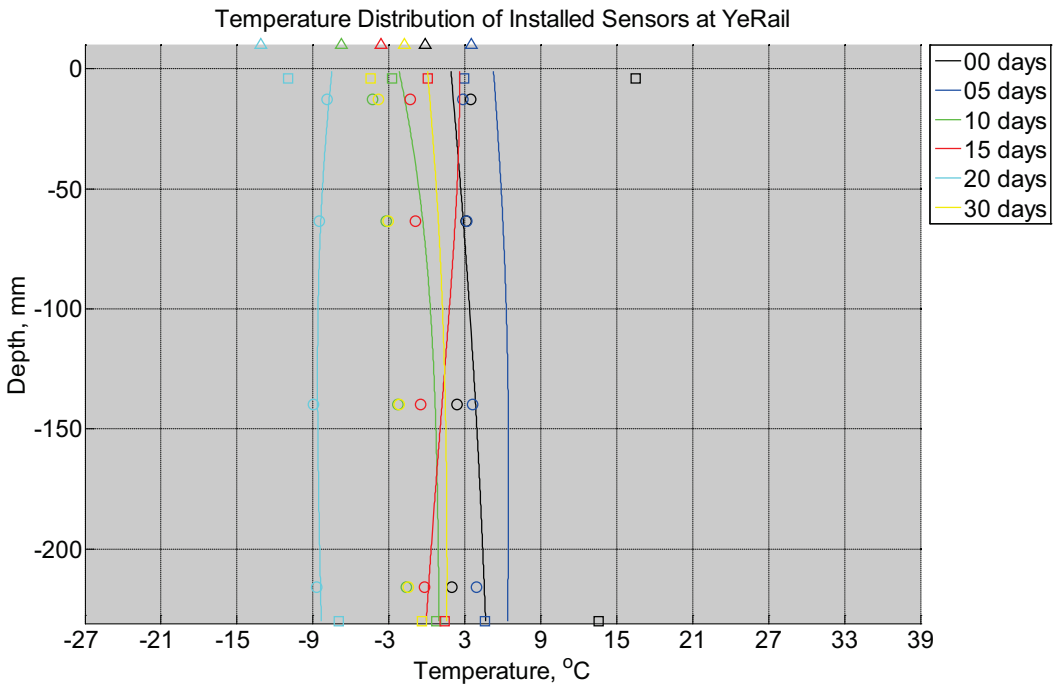

Figure B-986 Measured (markers) and modeled (continuous line) temperature profile distribution as a function of depth inside a model concrete crosstie (labeled YeRail) installed in ballast in Rantoul, IL, between December 21, 2014, through January 24, 2015. An 8 mm thick polyurethane pad and 12 in (30.48 cm) length 136 lb/yd (67.5 kg/m) section of steel rail are additionally installed atop the model concrete crosstie. The model does not incorporate a polyurethane pad nor steel rail line. Triangular markers denote temperature value from KTIP weather station, square markers denote measured temperature values from ballast, and circular markers denote measured temperature values inside concrete.

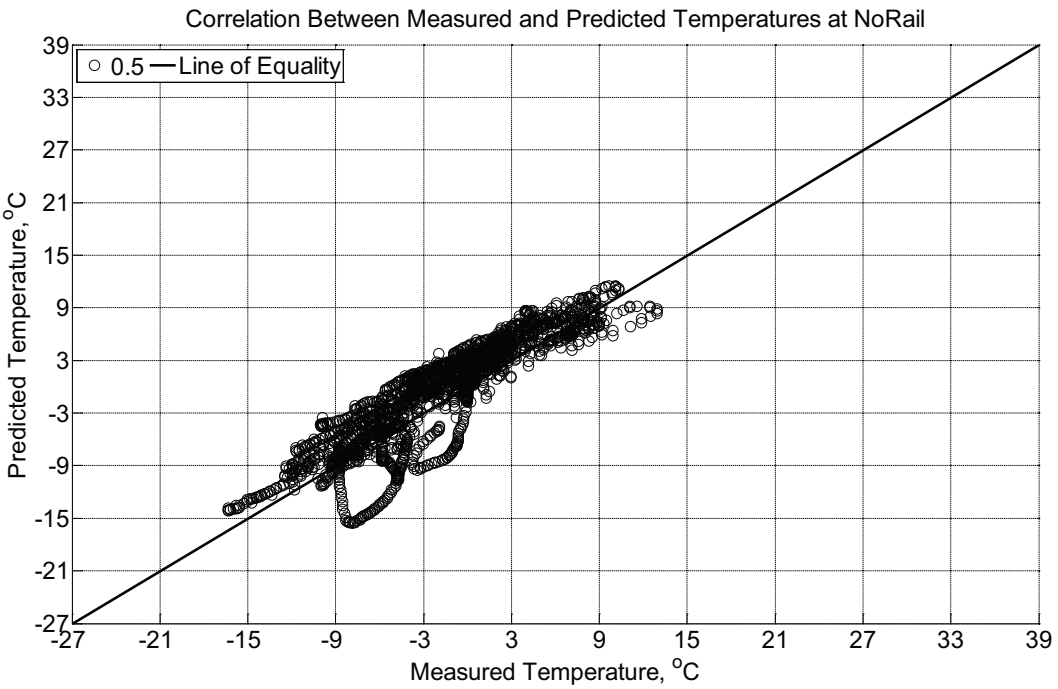

Figure B-987 Correlation between measured and predicted temperature values 0.5 inches (12.7 mm) from the surface of a model concrete crosstie (labeled NoRail) without a polyurethane pad nor rail installed in ballast in Rantoul, IL, between December 21, 2014, through January 24, 2015.

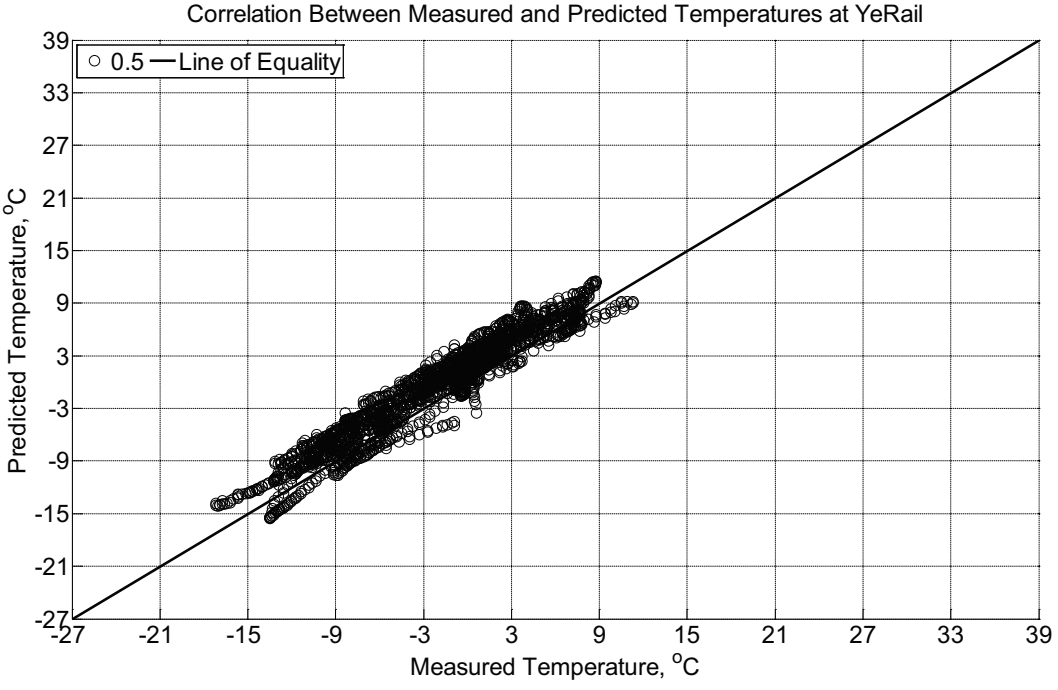

Figure B-988 Correlation between measured and predicted temperature values 0.5 inches (12.7 mm) from the surface of a model concrete crosstie (labeled YeRail) installed in ballast

in Rantoul, IL, between December 21, 2014, through January 24, 2015. An 8 mm thick polyurethane pad and 12 in (30.48 cm) length 136 lb/yd (67.5 kg/m) section of steel rail are additionally installed atop the model concrete crosstie. The model does not incorporate a polyurethane pad nor steel rail line.

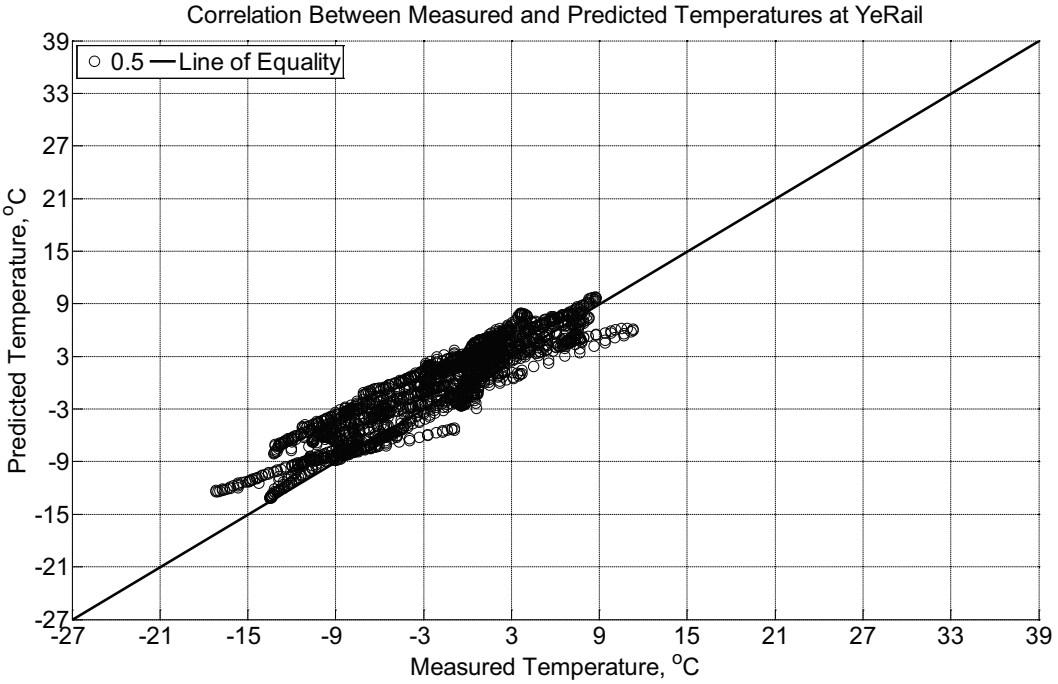

Figure B-989 Correlation between measured and predicted temperature values 0.5 inches (12.7 mm) from the surface of a model concrete crosstie (labeled YeRail) installed in ballast in Rantoul, IL, between December 21, 2014, through January 24, 2015. An 8 mm thick polyurethane pad and 12 in (30.48 cm) length 136 lb/yd (67.5 kg/m) section of steel rail are additionally installed atop the model concrete crosstie. The model incorporates a 1 mm thick polyurethane pad and 1 mm thick steel rail line.

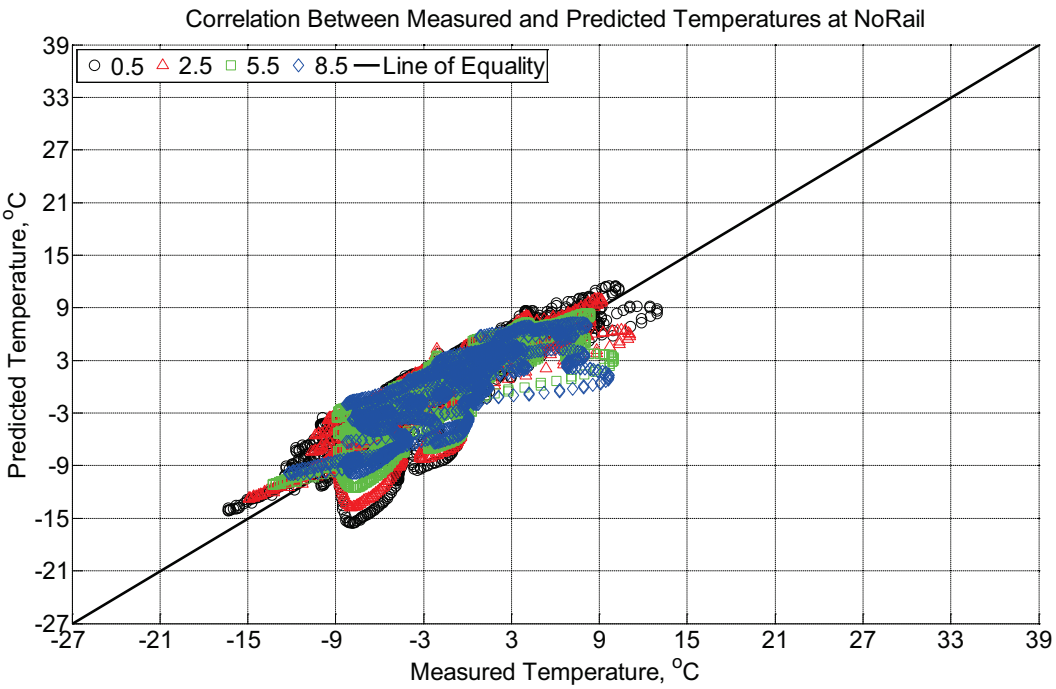

Figure B-990 Correlation between measured and predicted temperature values 0.5 inches (12.7 mm), 2.5 inches (63.5 mm), 5.5 inches (139.7 mm), and 8.5 inches (215.9 mm) from the surface of a model concrete crosstie (labeled NoRail) without a polyurethane pad nor rail installed in ballast in Rantoul, IL, between December 21, 2014, through January 24, 2015.

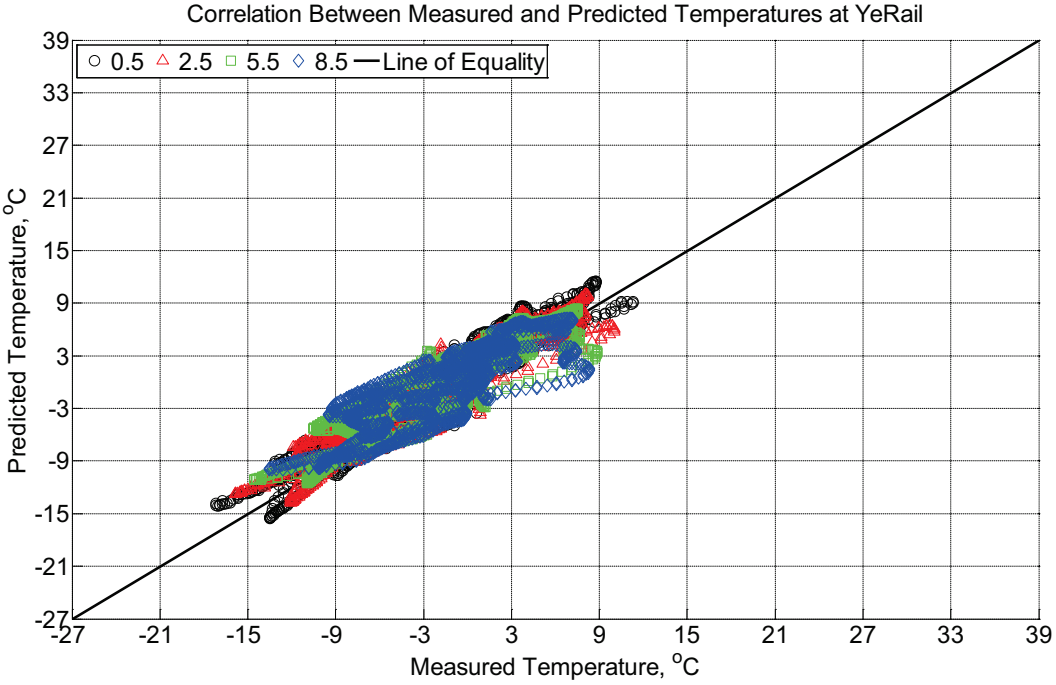

Figure B-991 Correlation between measured and predicted temperature values 0.5 inches (12.7 mm), 2.5 inches (63.5 mm), 5.5 inches (139.7 mm), and 8.5 inches (215.9 mm) from the

surface of a model concrete crosstie (labeled YeRail) installed in ballast in Rantoul, IL, between December 21, 2014, through January 24, 2015. An 8 mm thick polyurethane pad and 12 in (30.48 cm) length 136 lb/yd (67.5 kg/m) section of steel rail are additionally installed atop the model concrete crosstie. The model does not incorporate a polyurethane pad nor steel rail line.

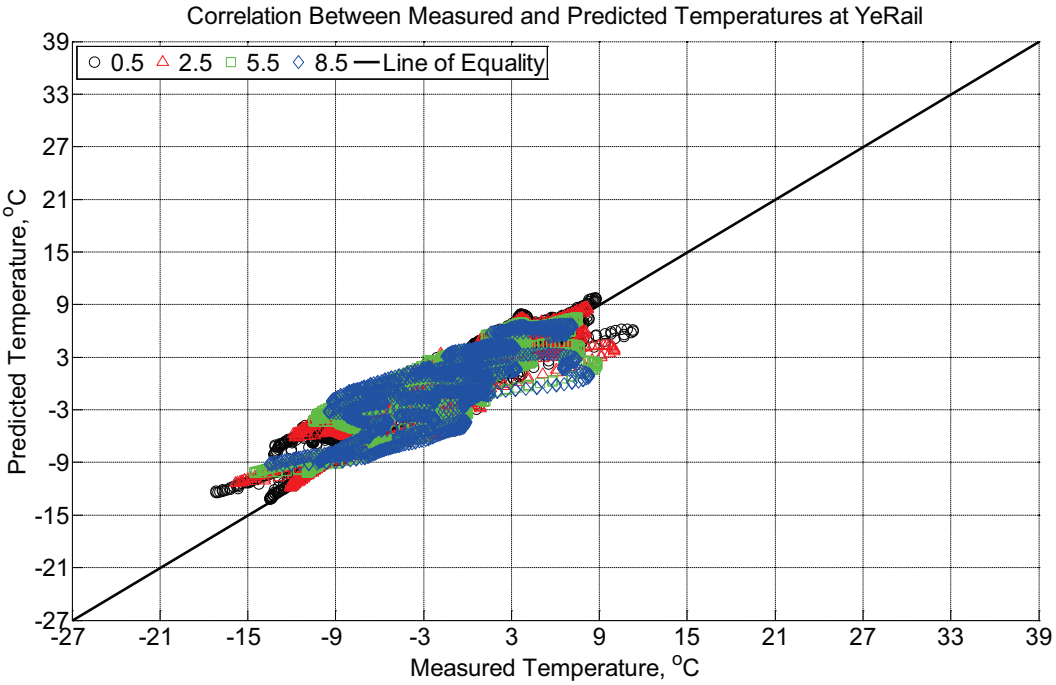

Figure B-992 Correlation between measured and predicted temperature values 0.5 inches (12.7 mm), 2.5 inches (63.5 mm), 5.5 inches (139.7 mm), and 8.5 inches (215.9 mm) from the surface of a model concrete crosstie (labeled YeRail) installed in ballast in Rantoul, IL, between December 21, 2014, through January 24, 2015. An 8 mm thick polyurethane pad and 12 in (30.48 cm) length 136 lb/yd (67.5 kg/m) section of steel rail are additionally installed atop the model concrete crosstie. The model incorporates a 1 mm thick polyurethane pad and 1 mm thick steel rail line.

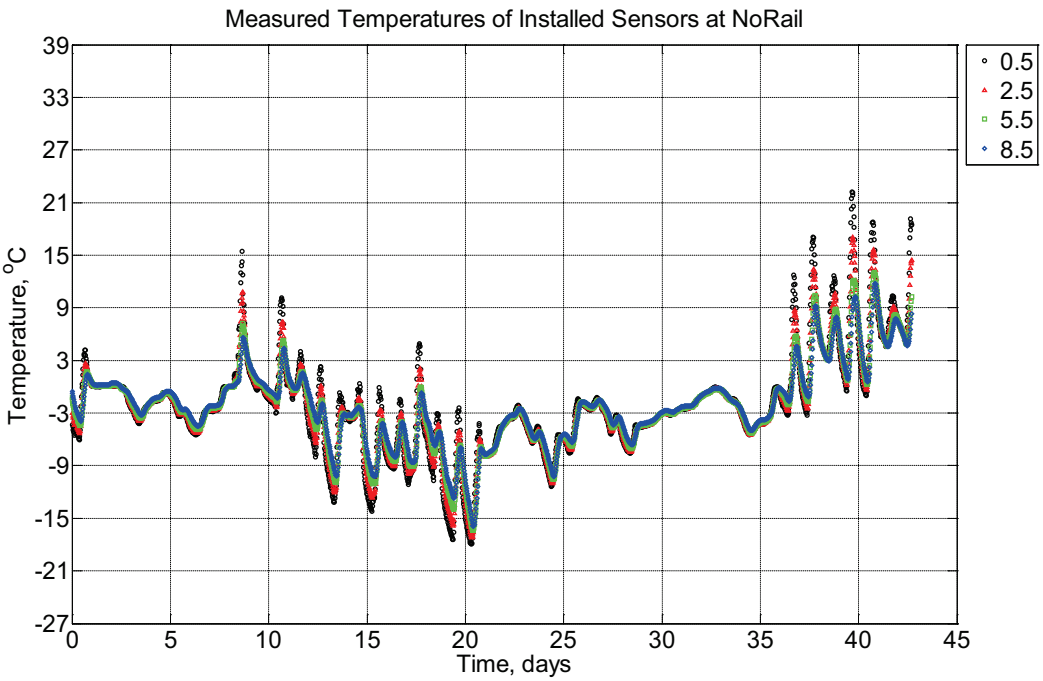

Figure B-993 Measured temperature at depths of 0.5 inches (12.7 mm), 2.5 inches (63.5 mm), 5.5 inches (139.7 mm), and 8.5 inches (215.9 mm) from the surface of a model concrete crosstie (labeled NoRail) without a polyurethane pad nor rail installed in ballast in Rantoul, IL, between January 30, 2015, through March 14, 2015.

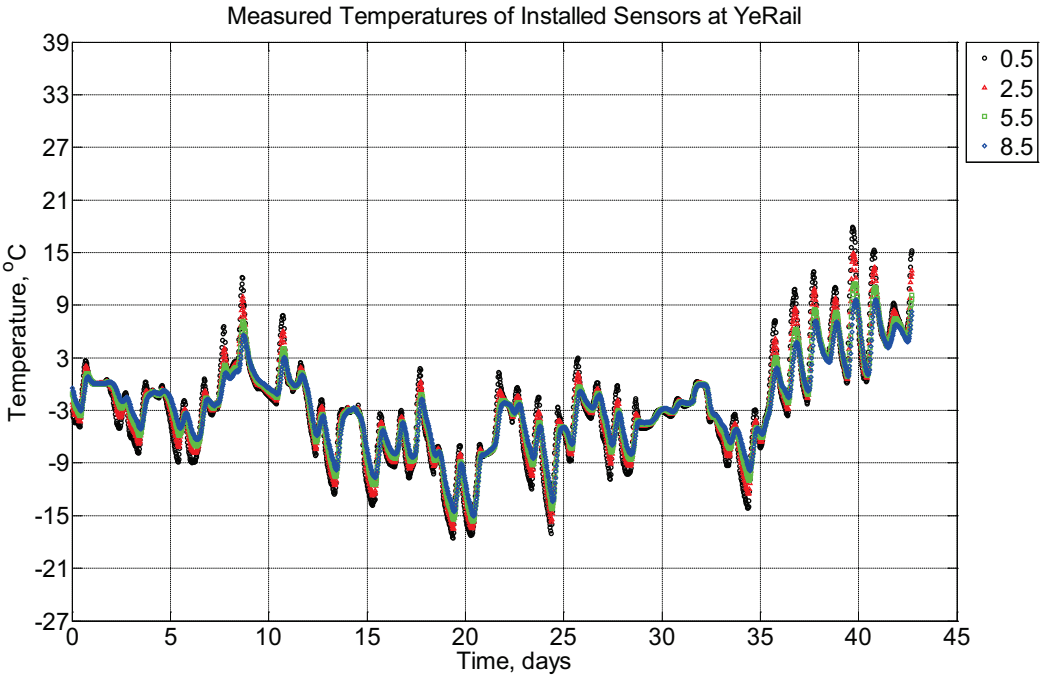

Figure B-994 Measured temperature at depths of 0.5 inches (12.7 mm), 2.5 inches (63.5 mm), 5.5 inches (139.7 mm), and 8.5 inches (215.9 mm) from the surface of a model

concrete crosstie (labeled YeRail) installed in ballast in Rantoul, IL, between January 30, 2015, through March 14, 2015. An 8 mm thick polyurethane pad and 12 in (30.48 cm) length 136 lb/yd (67.5 kg/m) section of steel rail are additionally installed atop the model concrete crosstie.

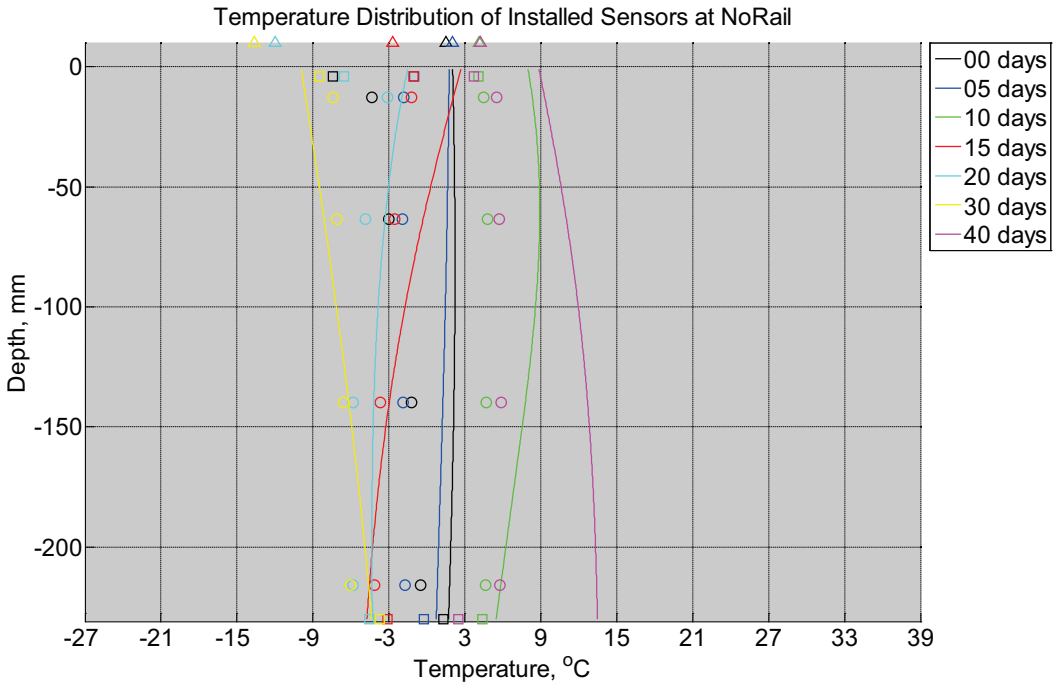

Figure B-995 Measured (markers) and modeled (continuous line) temperature profile distribution as a function of depth inside a model concrete crosstie (labeled NoRail) without a polyurethane pad nor rail installed in ballast in Rantoul, IL, between January 30, 2015, through March 14, 2015. Triangular markers denote temperature value from KTIP weather station, square markers denote measured temperature values from ballast, and circular markers denote measured temperature values inside concrete.

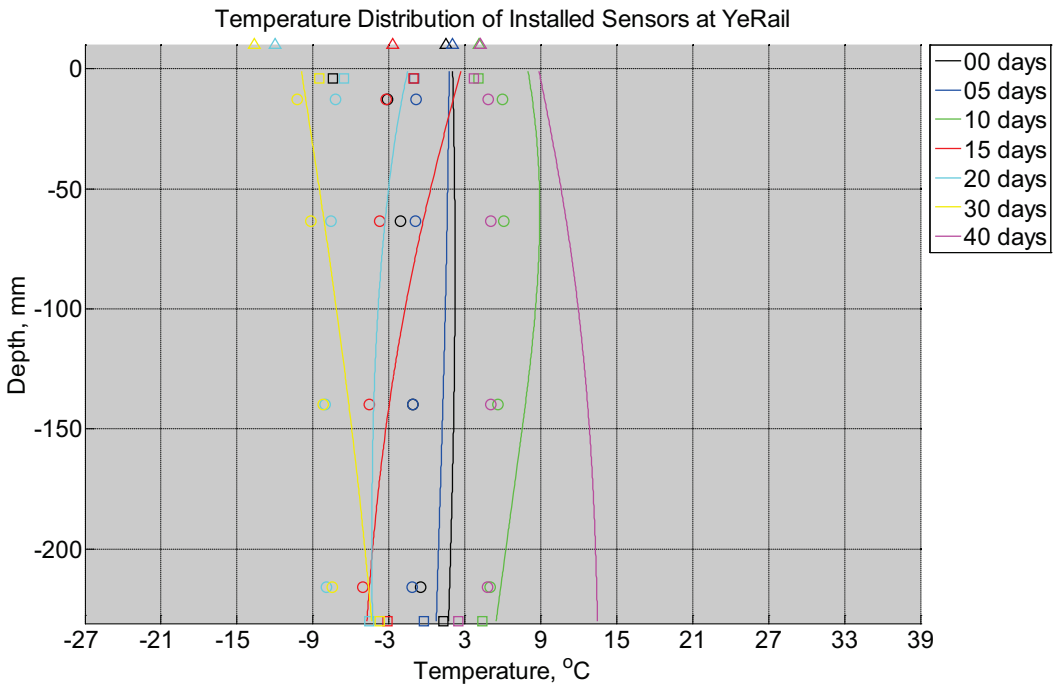

Figure B-996 Measured (markers) and modeled (continuous line) temperature profile distribution as a function of depth inside a model concrete crosstie (labeled YeRail) installed in ballast in Rantoul, IL, between January 30, 2015, through March 14, 2015. An 8 mm thick polyurethane pad and 12 in (30.48 cm) length 136 lb/yd (67.5 kg/m) section of steel rail are additionally installed atop the model concrete crosstie. The model does not incorporate a polyurethane pad nor steel rail line. Triangular markers denote temperature value from KTIP weather station, square markers denote measured temperature values from ballast, and circular markers denote measured temperature values inside concrete.

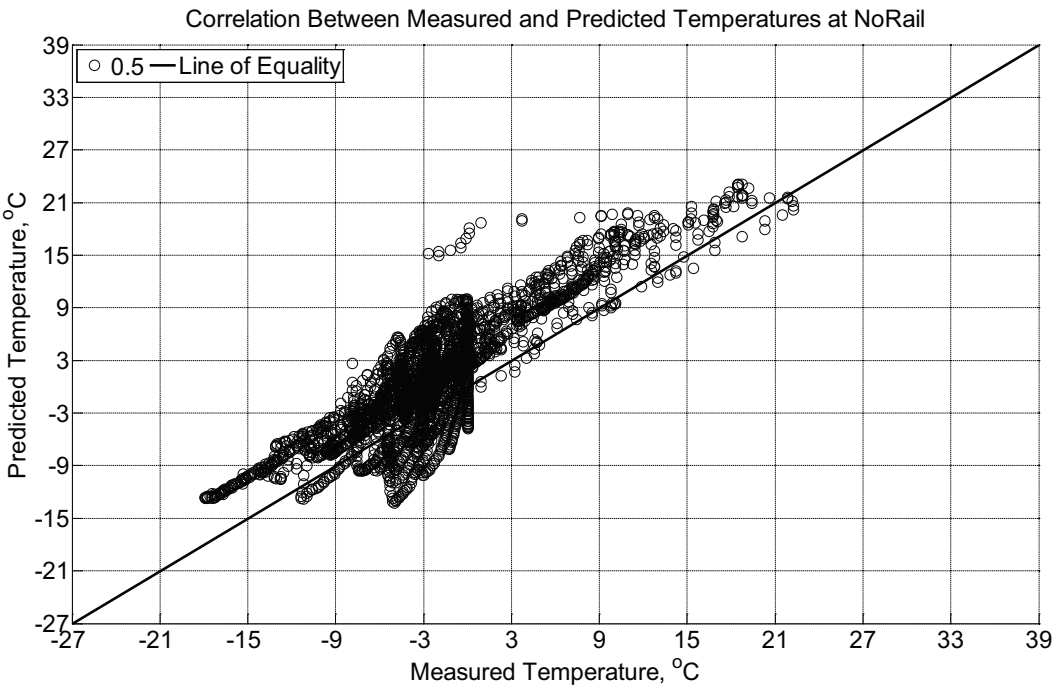

Figure B-997 Correlation between measured and predicted temperature values 0.5 inches (12.7 mm) from the surface of a model concrete crosstie (labeled NoRail) without a polyurethane pad nor rail installed in ballast in Rantoul, IL, between January 30, 2015, through March 14, 2015.

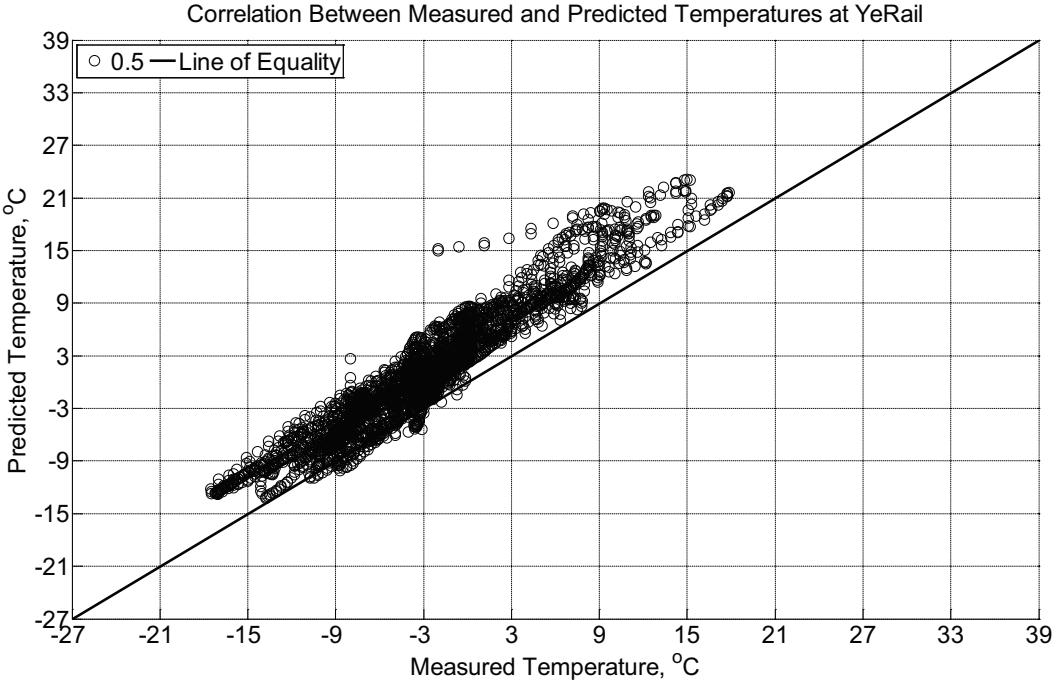

Figure B-998 Correlation between measured and predicted temperature values 0.5 inches (12.7 mm) from the surface of a model concrete crosstie (labeled YeRail) installed in ballast

in Rantoul, IL, between January 30, 2015, through March 14, 2015. An 8 mm thick polyurethane pad and 12 in (30.48 cm) length 136 lb/yd (67.5 kg/m) section of steel rail are additionally installed atop the model concrete crosstie. The model does not incorporate a polyurethane pad nor steel rail line.

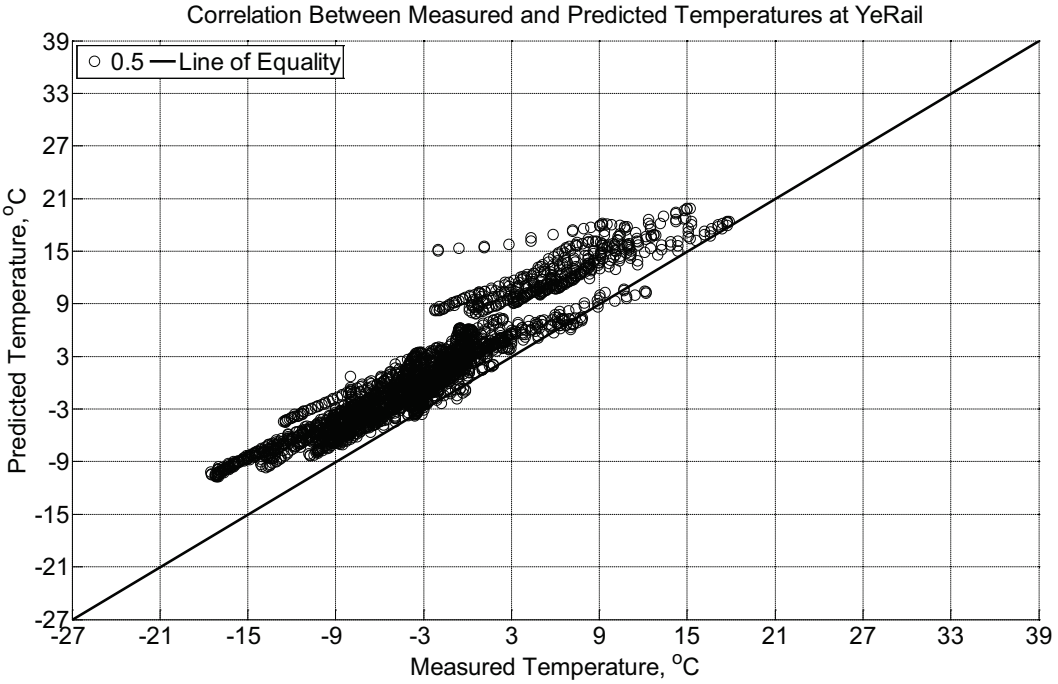

Figure B-999 Correlation between measured and predicted temperature values 0.5 inches (12.7 mm) from the surface of a model concrete crosstie (labeled YeRail) installed in ballast in Rantoul, IL, between January 30, 2015, through March 14, 2015. An 8 mm thick polyurethane pad and 12 in (30.48 cm) length 136 lb/yd (67.5 kg/m) section of steel rail are additionally installed atop the model concrete crosstie. The model incorporates a 1 mm thick polyurethane pad and 1 mm thick steel rail line.

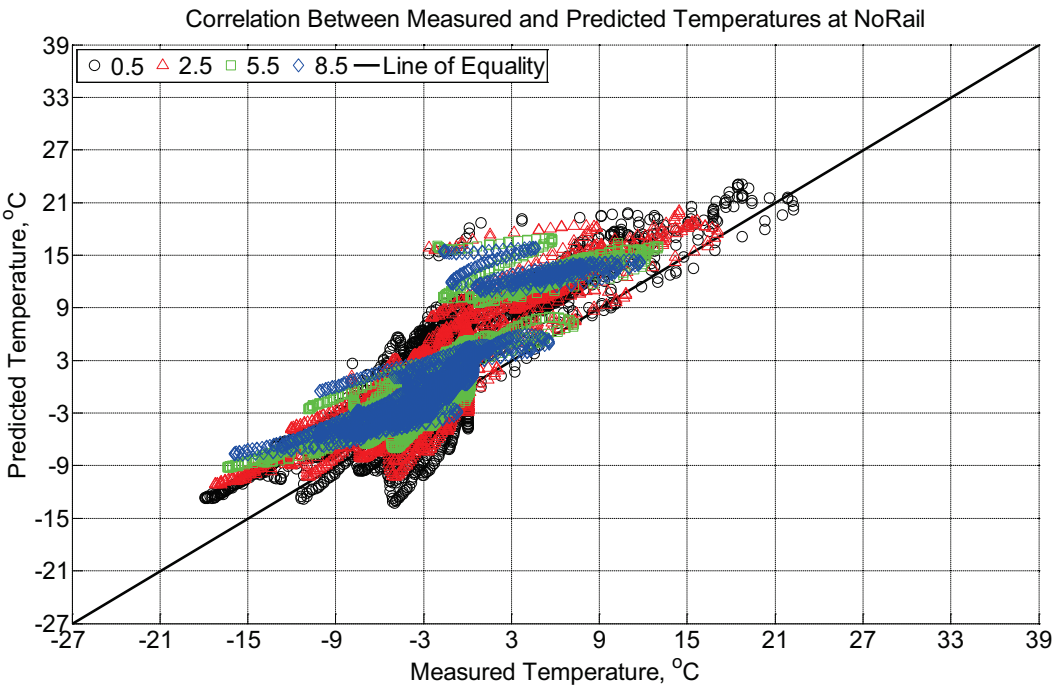

Figure B-1000 Correlation between measured and predicted temperature values 0.5 inches (12.7 mm), 2.5 inches (63.5 mm), 5.5 inches (139.7 mm), and 8.5 inches (215.9 mm) from the surface of a model concrete crosstie (labeled NoRail) without a polyurethane pad nor rail installed in ballast in Rantoul, IL, between January 30, 2015, through March 14, 2015.

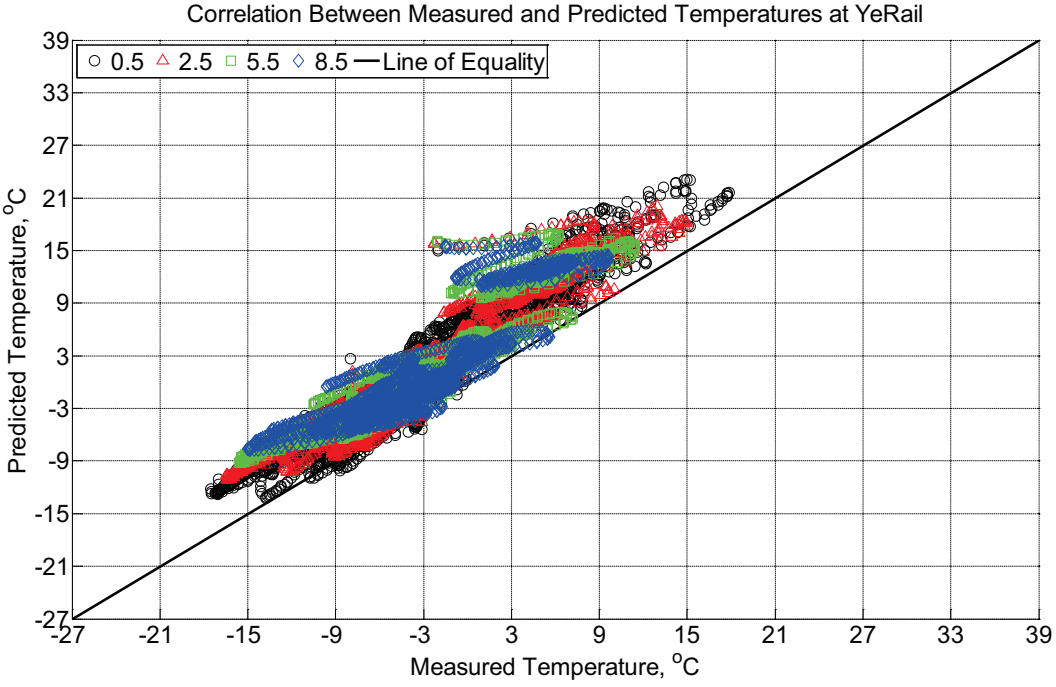

Figure B-1001 Correlation between measured and predicted temperature values 0.5 inches (12.7 mm), 2.5 inches (63.5 mm), 5.5 inches (139.7 mm), and 8.5 inches (215.9 mm) from the

surface of a model concrete crosstie (labeled YeRail) installed in ballast in Rantoul, IL, between January 30, 2015, through March 14, 2015. An 8 mm thick polyurethane pad and 12 in (30.48 cm) length 136 lb/yd (67.5 kg/m) section of steel rail are additionally installed atop the model concrete crosstie. The model does not incorporate a polyurethane pad nor steel rail line.

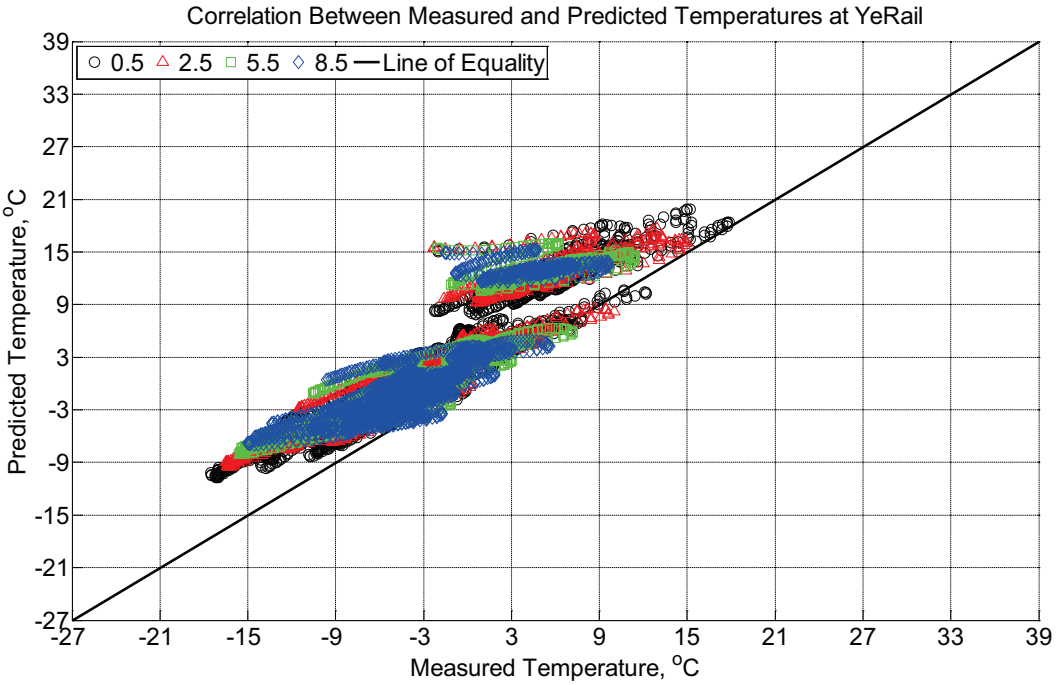

Figure B-1002 Correlation between measured and predicted temperature values 0.5 inches (12.7 mm), 2.5 inches (63.5 mm), 5.5 inches (139.7 mm), and 8.5 inches (215.9 mm) from the surface of a model concrete crosstie (labeled YeRail) installed in ballast in Rantoul, IL, between January 30, 2015, through March 14, 2015. An 8 mm thick polyurethane pad and 12 in (30.48 cm) length 136 lb/yd (67.5 kg/m) section of steel rail are additionally installed atop the model concrete crosstie. The model incorporates a 1 mm thick polyurethane pad and 1 mm thick steel rail line.

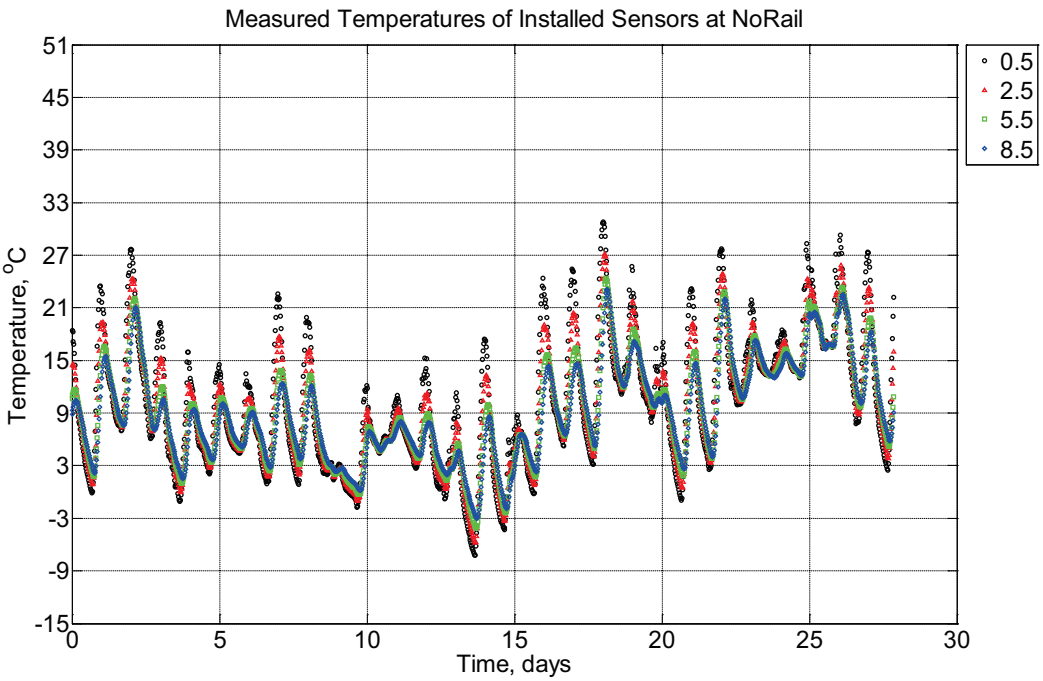

Figure B-1003 Measured temperature at depths of 0.5 inches (12.7 mm), 2.5 inches (63.5 mm), 5.5 inches (139.7 mm), and 8.5 inches (215.9 mm) from the surface of a model concrete crosstie (labeled NoRail) without a polyurethane pad nor rail installed in ballast in Rantoul, IL, between March 14, 2015, through April 11, 2015.

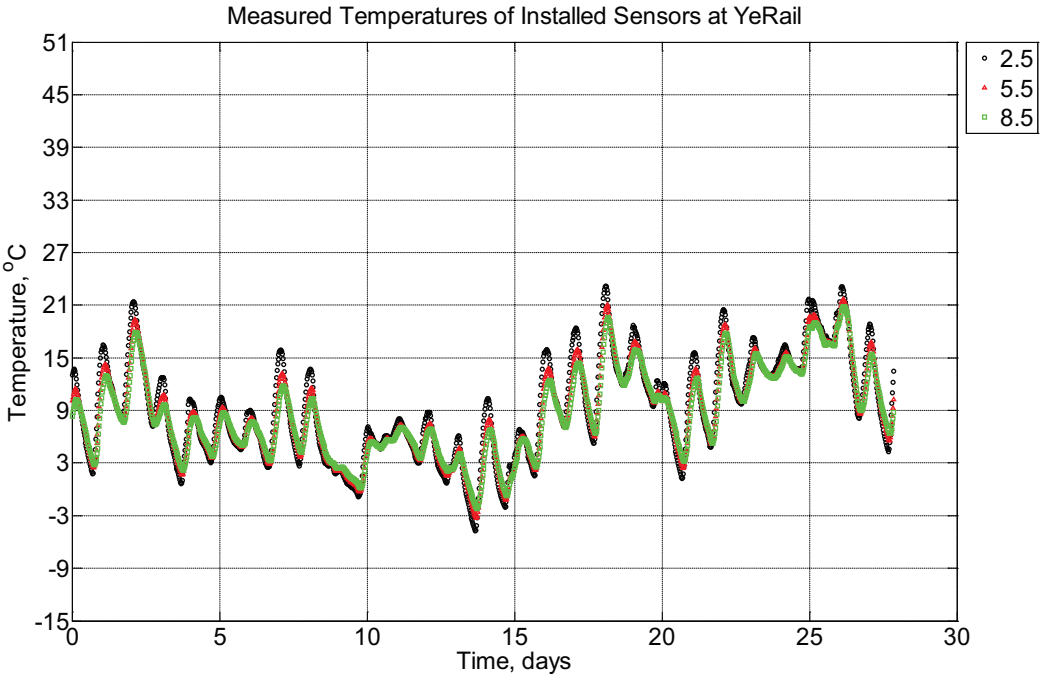

Figure B-1004 Measured temperature at depths of 2.5 inches (63.5 mm), 5.5 inches (139.7 mm), and 8.5 inches (215.9 mm) from the surface of a model concrete crosstie (labeled

YeRail) installed in ballast in Rantoul, IL, between March 14, 2015, through April 11, 2015. An 8 mm thick polyurethane pad and 12 in (30.48 cm) length 136 lb/yd (67.5 kg/m) section of steel rail are additionally installed atop the model concrete crosstie.

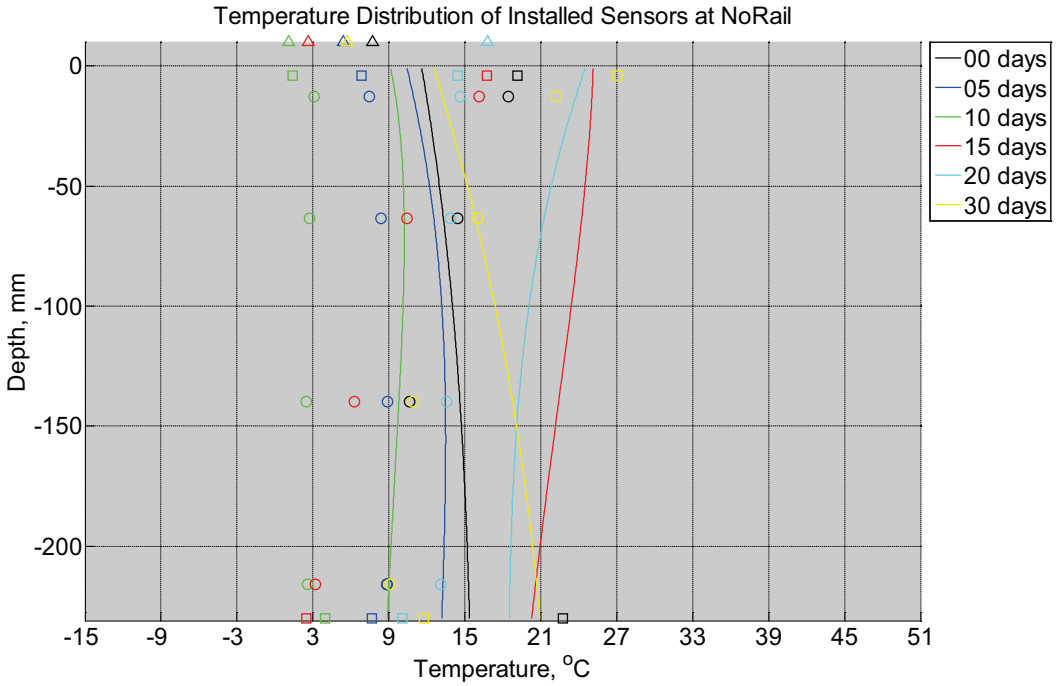

Figure B-1005 Measured (markers) and modeled (continuous line) temperature profile distribution as a function of depth inside a model concrete crosstie (labeled NoRail) without a polyurethane pad nor rail installed in ballast in Rantoul, IL, between March 14, 2015, through April 11, 2015. Triangular markers denote temperature value from KTIP weather station, square markers denote measured temperature values from ballast, and circular markers denote measured temperature values inside concrete.

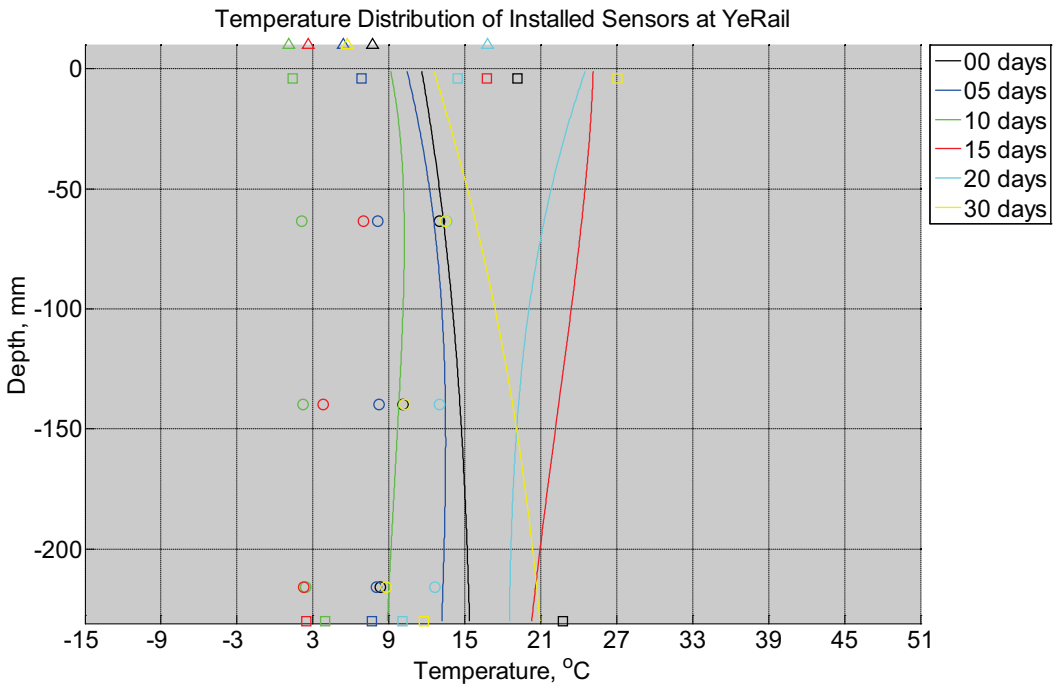

Figure B-1006 Measured (markers) and modeled (continuous line) temperature profile distribution as a function of depth inside a model concrete crosstie (labeled YeRail) installed in ballast in Rantoul, IL, between March 14, 2015, through April 11, 2015. An 8 mm thick polyurethane pad and 12 in (30.48 cm) length 136 lb/yd (67.5 kg/m) section of steel rail are additionally installed atop the model concrete crosstie. The model does not incorporate a polyurethane pad nor steel rail line. Triangular markers denote temperature value from KTIP weather station, square markers denote measured temperature values from ballast, and circular markers denote measured temperature values inside concrete.

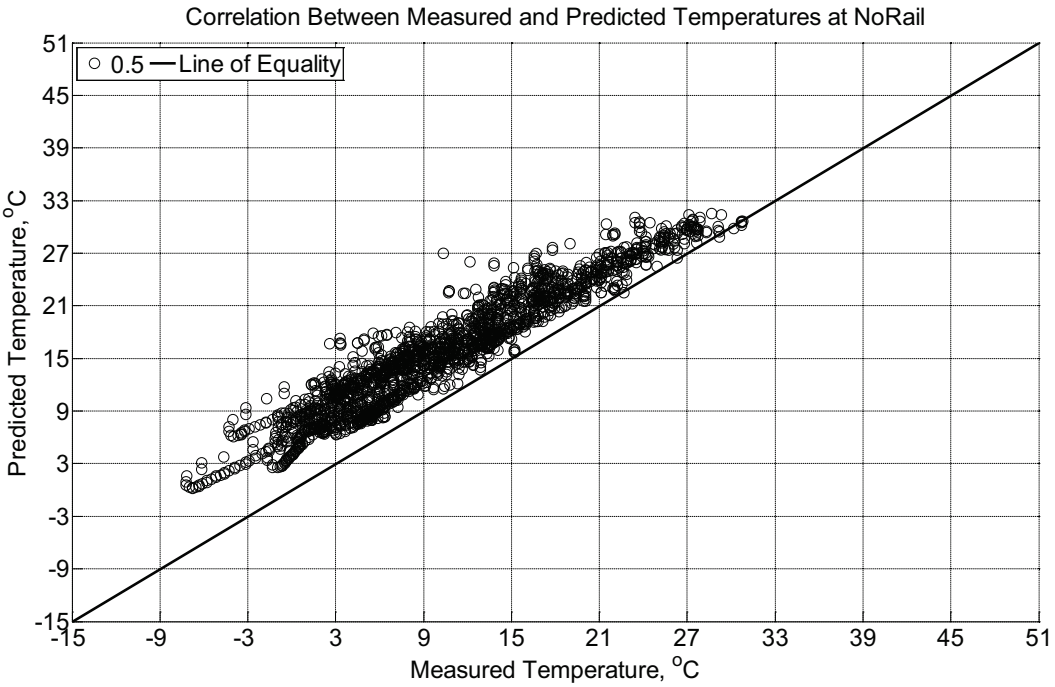

Figure B-1007 Correlation between measured and predicted temperature values 0.5 inches (12.7 mm) from the surface of a model concrete crosstie (labeled NoRail) without a polyurethane pad nor rail installed in ballast in Rantoul, IL, between March 14, 2015, through April 11, 2015.

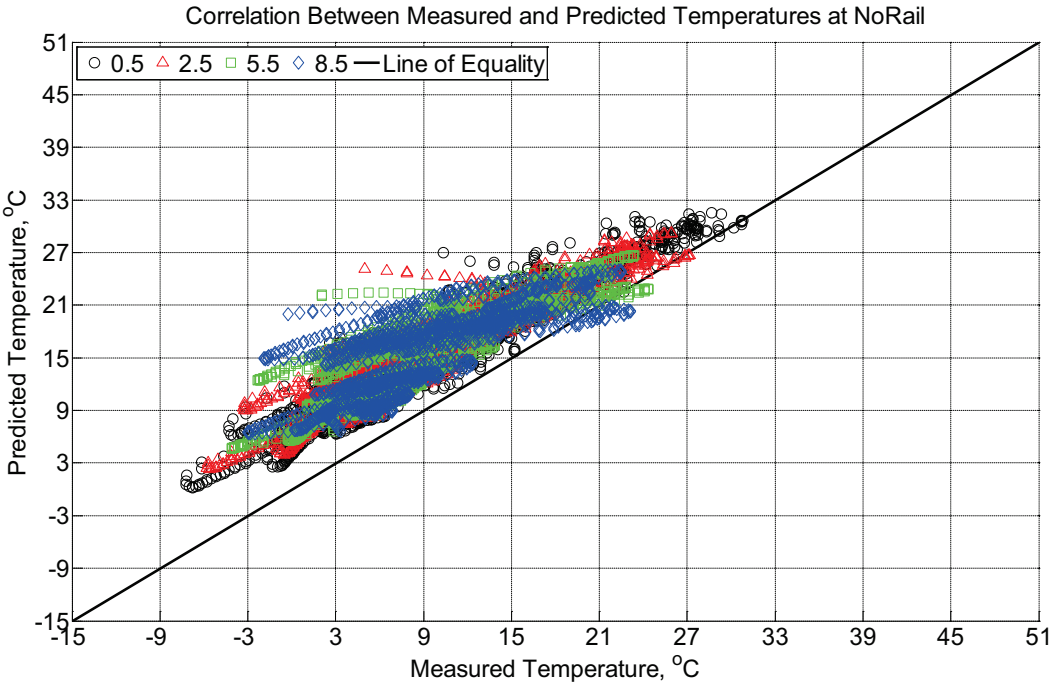

Figure B-1008 Correlation between measured and predicted temperature values 0.5 inches (12.7 mm), 2.5 inches (63.5 mm), 5.5 inches (139.7 mm), and 8.5 inches (215.9 mm) from the

surface of a model concrete crosstie (labeled NoRail) without a polyurethane pad nor rail installed in ballast in Rantoul, IL, between March 14, 2015, through April 11, 2015.

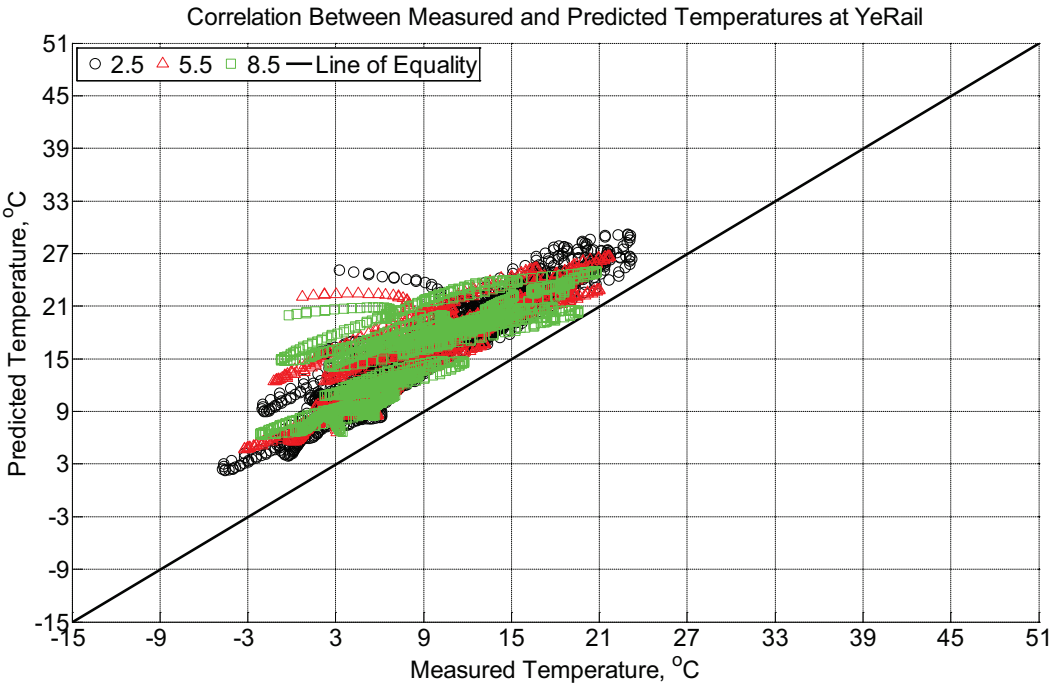

Figure B-1009 Correlation between measured and predicted temperature values 2.5 inches (63.5 mm), 5.5 inches (139.7 mm), and 8.5 inches (215.9 mm) from the surface of a model concrete crosstie (labeled YeRail) installed in ballast in Rantoul, IL, between March 14, 2015, through April 11, 2015. An 8 mm thick polyurethane pad and 12 in (30.48 cm) length 136 lb/yd (67.5 kg/m) section of steel rail are additionally installed atop the model concrete crosstie. The model does not incorporate a polyurethane pad nor steel rail line.

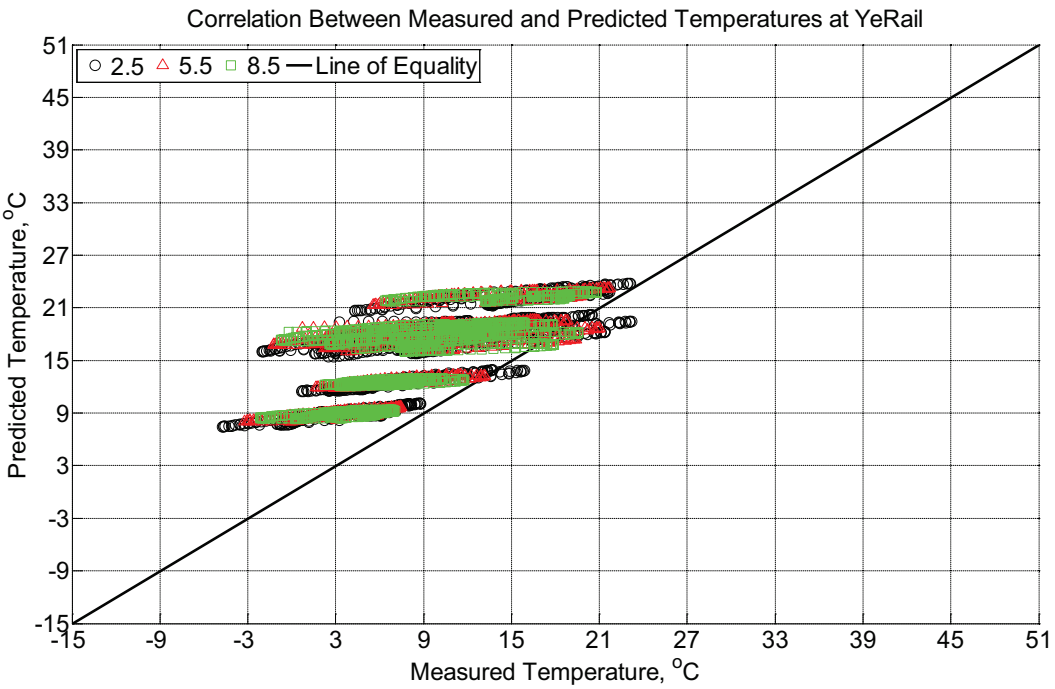

Figure B-1010 Correlation between measured and predicted temperature values 2.5 inches (63.5 mm), 5.5 inches (139.7 mm), and 8.5 inches (215.9 mm) from the surface of a model concrete crosstie (labeled YeRail) installed in ballast in Rantoul, IL, between March 14, 2015, through April 11, 2015. An 8 mm thick polyurethane pad and 12 in (30.48 cm) length 136 lb/yd (67.5 kg/m) section of steel rail are additionally installed atop the model concrete crosstie. The model incorporates an 8 mm thick polyurethane pad and 10 mm thick steel rail line.

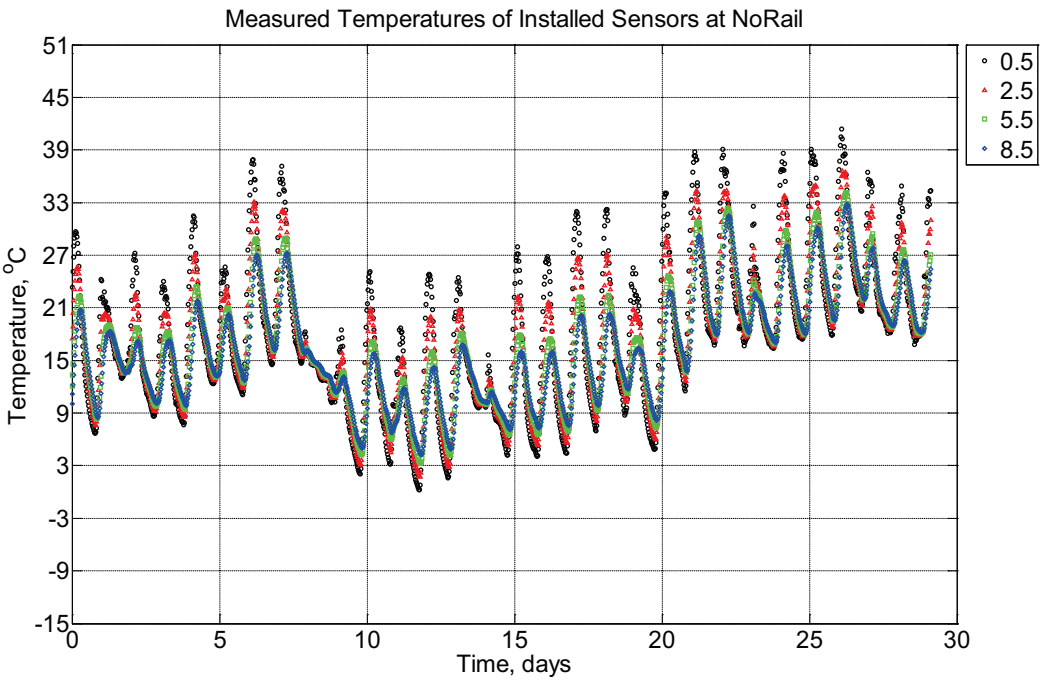

Figure B-1011 Measured temperature at depths of 0.5 inches (12.7 mm), 2.5 inches (63.5 mm), 5.5 inches (139.7 mm), and 8.5 inches (215.9 mm) from the surface of a model concrete crosstie (labeled NoRail) without a polyurethane pad nor rail installed in ballast in Rantoul, IL, between April 11, 2015, through May 10, 2015.

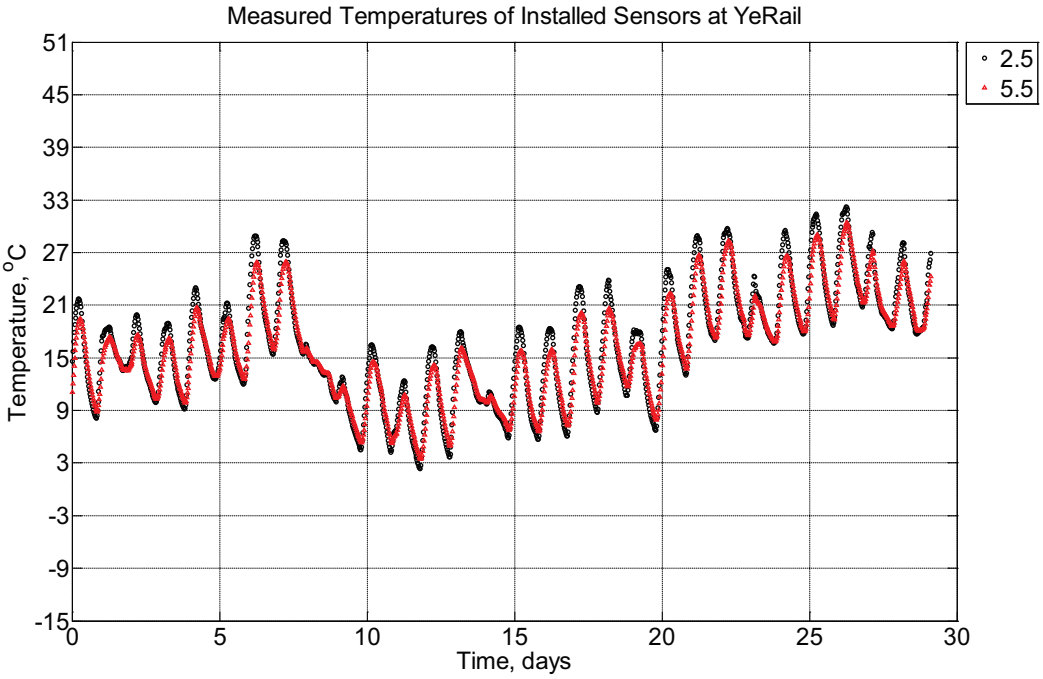

Figure B-1012 Measured temperature at depths of 2.5 inches (63.5 mm) and 5.5 inches (139.7 mm) from the surface of a model concrete crosstie (labeled YeRail) installed in

ballast in Rantoul, IL, between April 11, 2015, through May 10, 2015. An 8 mm thick polyurethane pad and 12 in (30.48 cm) length 136 lb/yd (67.5 kg/m) section of steel rail are additionally installed atop the model concrete crosstie.

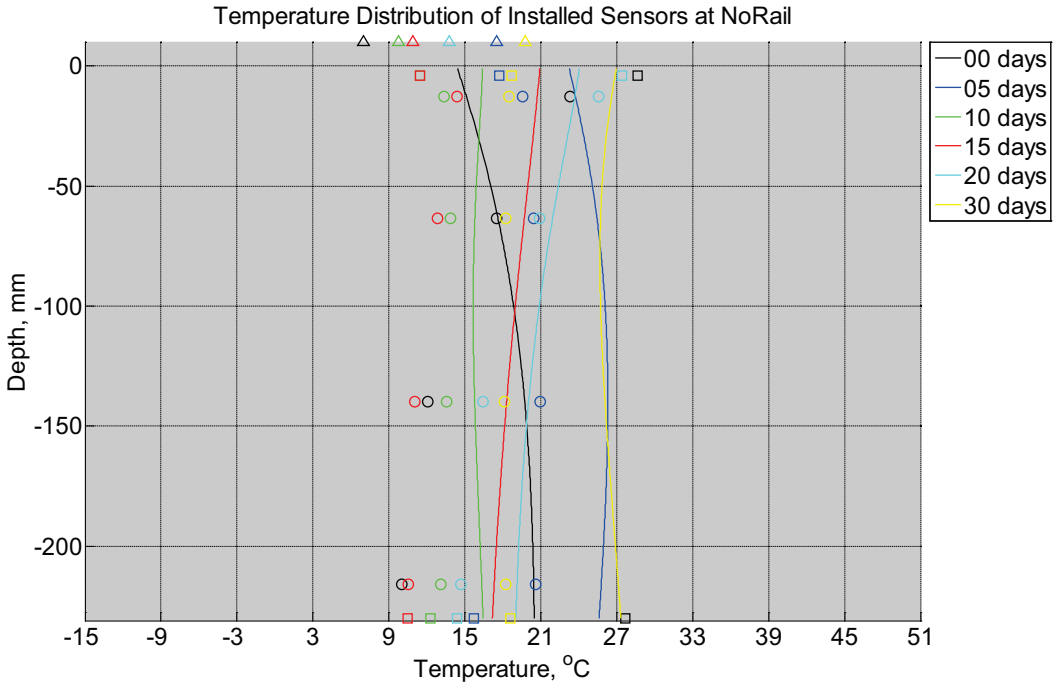

Figure B-1013 Measured (markers) and modeled (continuous line) temperature profile distribution as a function of depth inside a model concrete crosstie (labeled NoRail) without a polyurethane pad nor rail installed in ballast in Rantoul, IL, between April 11, 2015, through May 10, 2015. Triangular markers denote temperature value from KTIP weather station, square markers denote measured temperature values from ballast, and circular markers denote measured temperature values inside concrete.

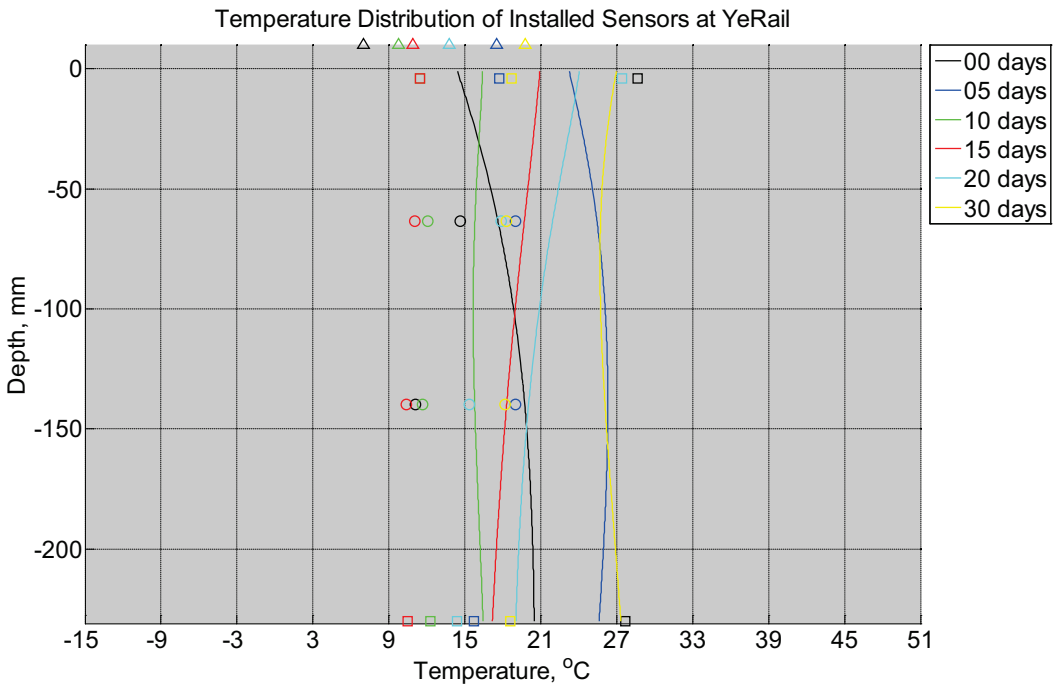

Figure B-1014 Measured (markers) and modeled (continuous line) temperature profile distribution as a function of depth inside a model concrete crosstie (labeled YeRail) installed in ballast in Rantoul, IL, between April 11, 2015, through May 10, 2015. An 8 mm thick polyurethane pad and 12 in (30.48 cm) length 136 lb/yd (67.5 kg/m) section of steel rail are additionally installed atop the model concrete crosstie. The model does not incorporate a polyurethane pad nor steel rail line. Triangular markers denote temperature value from KTIP weather station, square markers denote measured temperature values from ballast, and circular markers denote measured temperature values inside concrete.

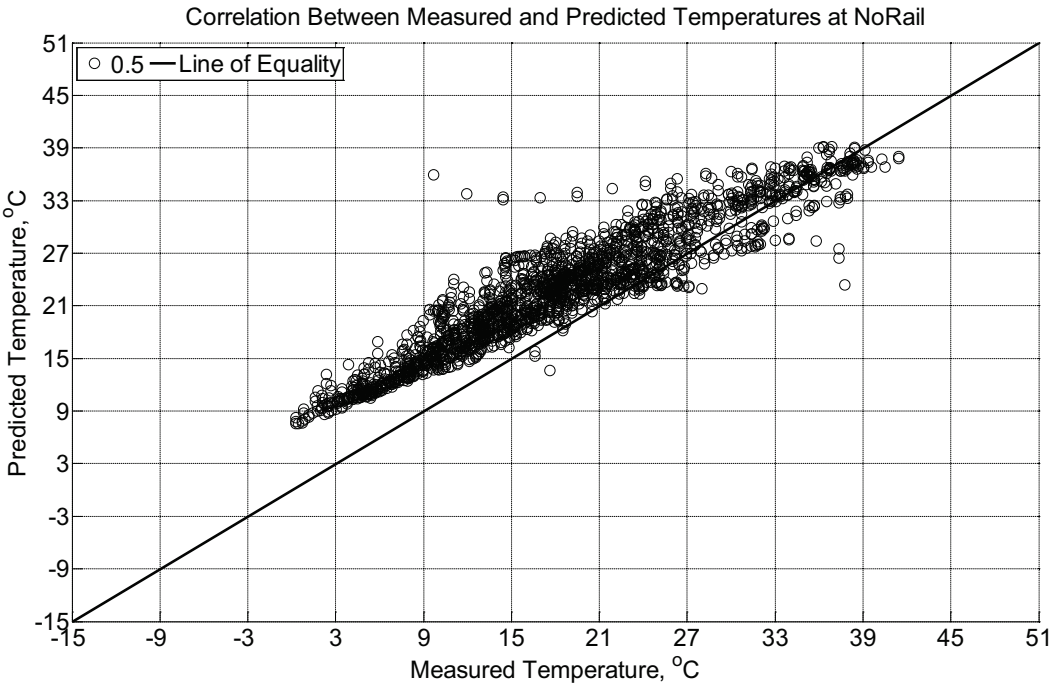

Figure B-1015 Correlation between measured and predicted temperature values 0.5 inches (12.7 mm) from the surface of a model concrete crosstie (labeled NoRail) without a polyurethane pad nor rail installed in ballast in Rantoul, IL, between April 11, 2015, through May 10, 2015.

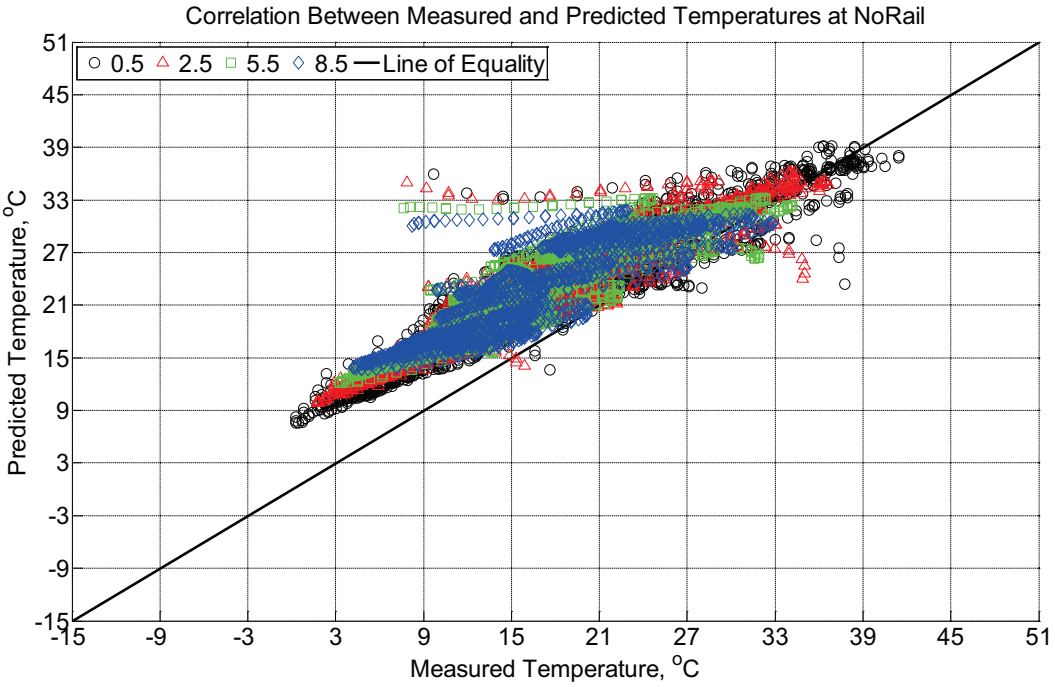

Figure B-1016 Correlation between measured and predicted temperature values 0.5 inches (12.7 mm), 2.5 inches (63.5 mm), 5.5 inches (139.7 mm), and 8.5 inches (215.9 mm) from the

surface of a model concrete crosstie (labeled NoRail) without a polyurethane pad nor rail installed in ballast in Rantoul, IL, between April 11, 2015, through May 10, 2015.

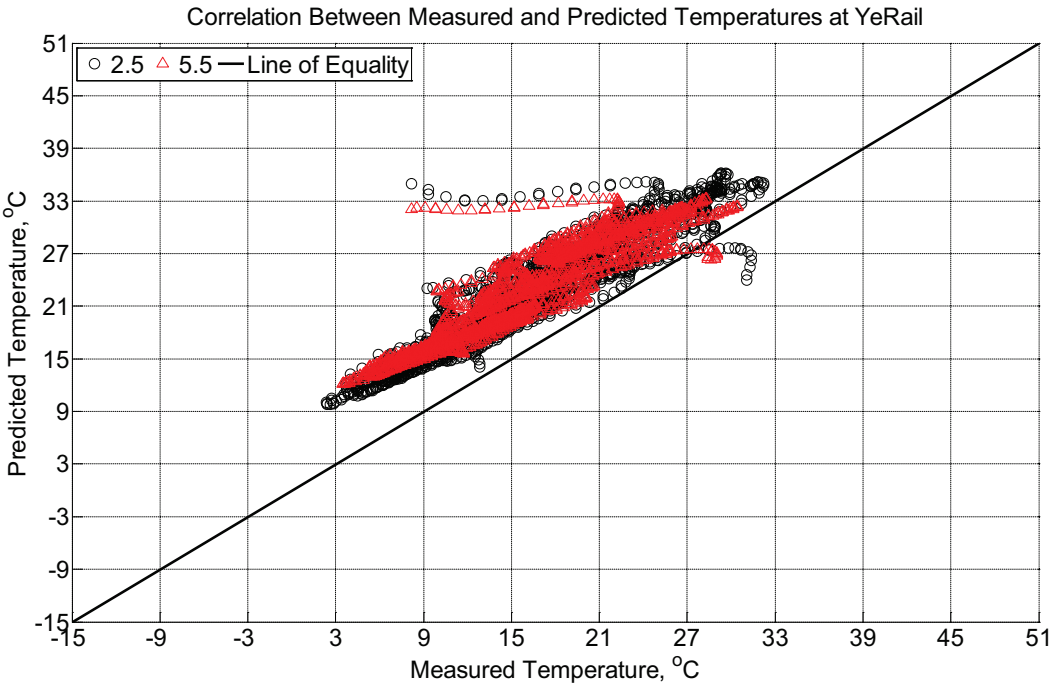

Figure B-1017 Correlation between measured and predicted temperature values 2.5 inches (63.5 mm) and 5.5 inches (139.7 mm) from the surface of a model concrete crosstie (labeled YeRail) installed in ballast in Rantoul, IL, between April 11, 2015, through May 10, 2015. An 8 mm thick polyurethane pad and 12 in (30.48 cm) length 136 lb/yd (67.5 kg/m) section of steel rail are additionally installed atop the model concrete crosstie. The model does not incorporate a polyurethane pad nor steel rail line.

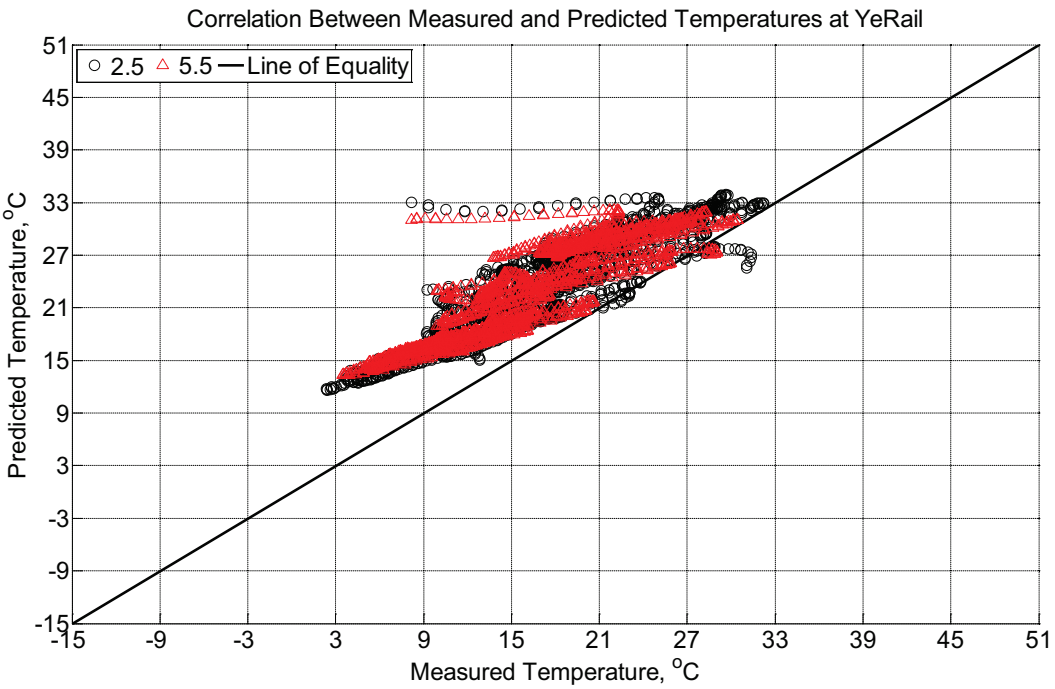

Figure B-1018 Correlation between measured and predicted temperature values 2.5 inches (63.5 mm) and 5.5 inches (139.7 mm) from the surface of a model concrete crosstie (labeled YeRail) installed in ballast in Rantoul, IL, between April 11, 2015, through May 10, 2015. An 8 mm thick polyurethane pad and 12 in (30.48 cm) length 136 lb/yd (67.5 kg/m) section of steel rail are additionally installed atop the model concrete crosstie. The model incorporates an 8 mm thick polyurethane pad and 10 mm thick steel rail line.

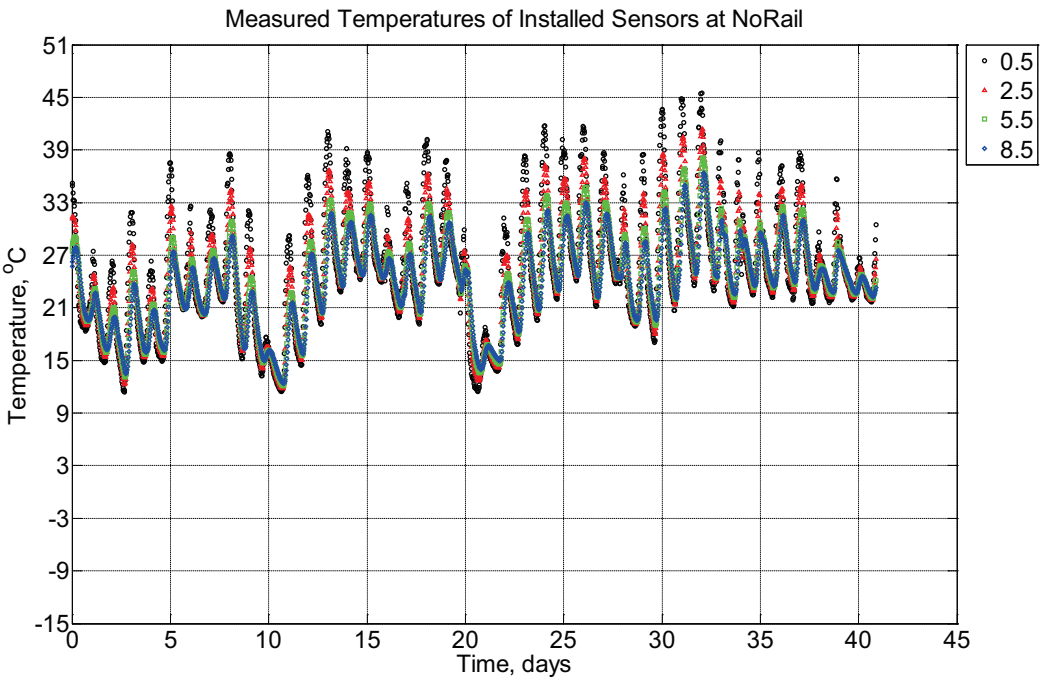

Figure B-1019 Measured temperature at depths of 0.5 inches (12.7 mm), 2.5 inches (63.5 mm), 5.5 inches (139.7 mm), and 8.5 inches (215.9 mm) from the surface of a model concrete crosstie (labeled NoRail) without a polyurethane pad nor rail installed in ballast in Rantoul, IL, between May 10, 2015, through June 20, 2015. A breathable water-resistant canvas tarp is additionally installed over the model crosstie and immediate ballast area.

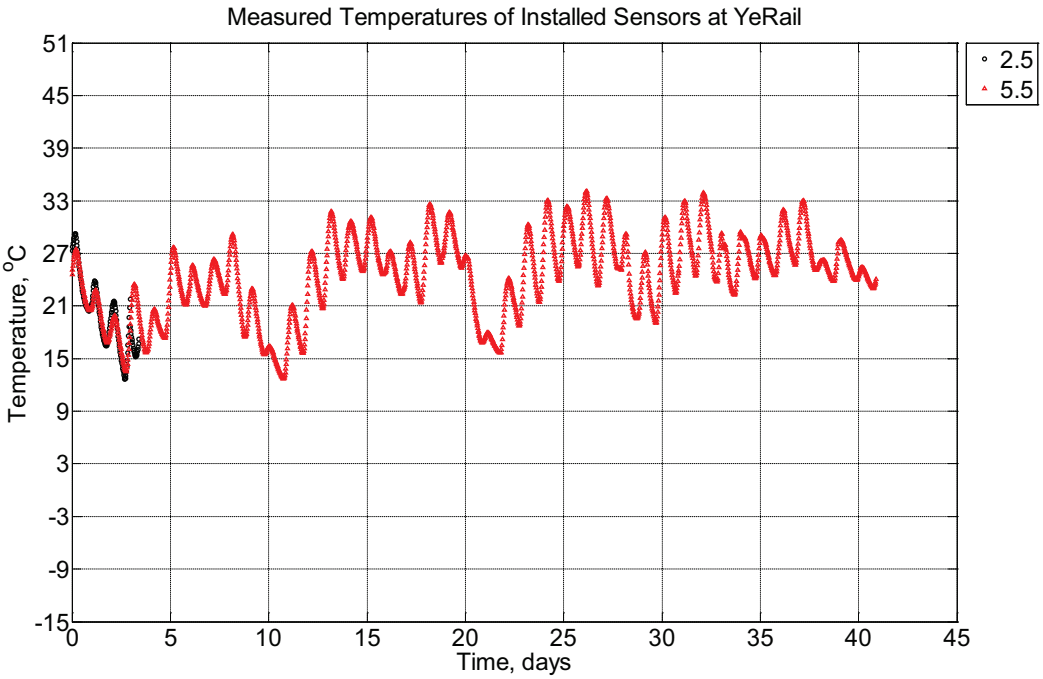

Figure B-1020 Measured temperature at depths of 2.5 inches (63.5 mm) and 5.5 inches

(139.7 mm) from the surface of a model concrete crosstie (labeled YeRail) installed in ballast in Rantoul, IL, between May 10, 2015, through June 20, 2015. An 8 mm thick polyurethane pad and 12 in (30.48 cm) length 136 lb/yd (67.5 kg/m) section of steel rail are additionally installed atop the model concrete crosstie. A breathable water-resistant canvas tarp is additionally installed over the model crosstie and immediate ballast area.

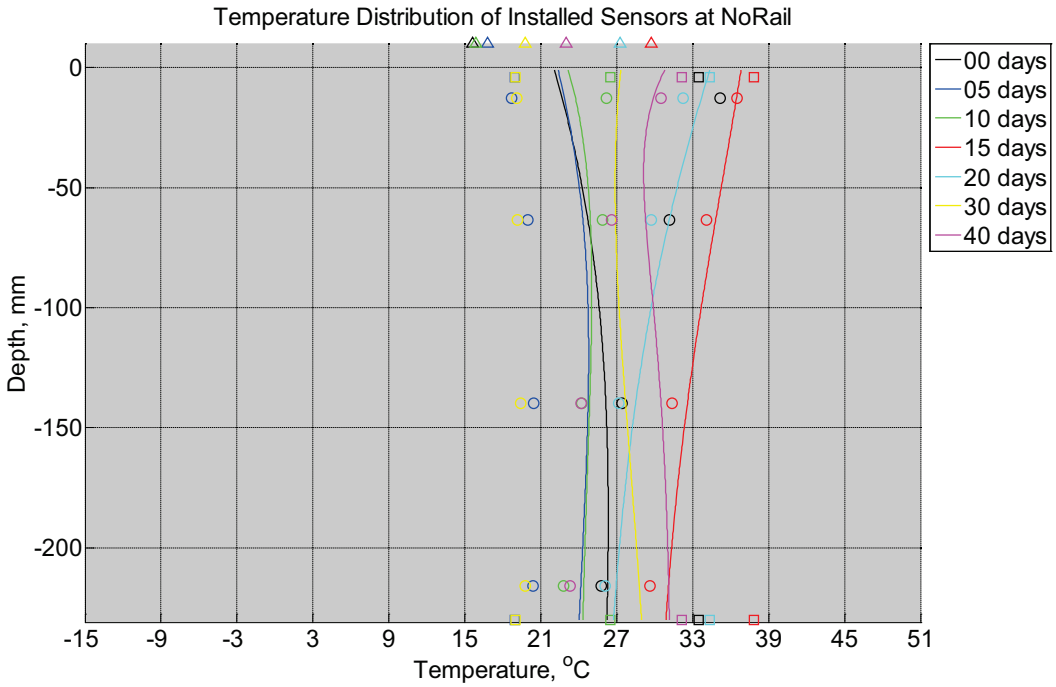

Figure B-1021 Measured (markers) and modeled (continuous line) temperature profile distribution as a function of depth inside a model concrete crosstie (labeled NoRail) without a polyurethane pad nor rail installed in ballast in Rantoul, IL, between May 10, 2015, through June 20, 2015. A breathable water-resistant canvas tarp is additionally installed over the model crosstie and immediate ballast area. Triangular markers denote temperature value from KTIP weather station, square markers denote measured temperature values from ballast, and circular markers denote measured temperature values inside concrete.

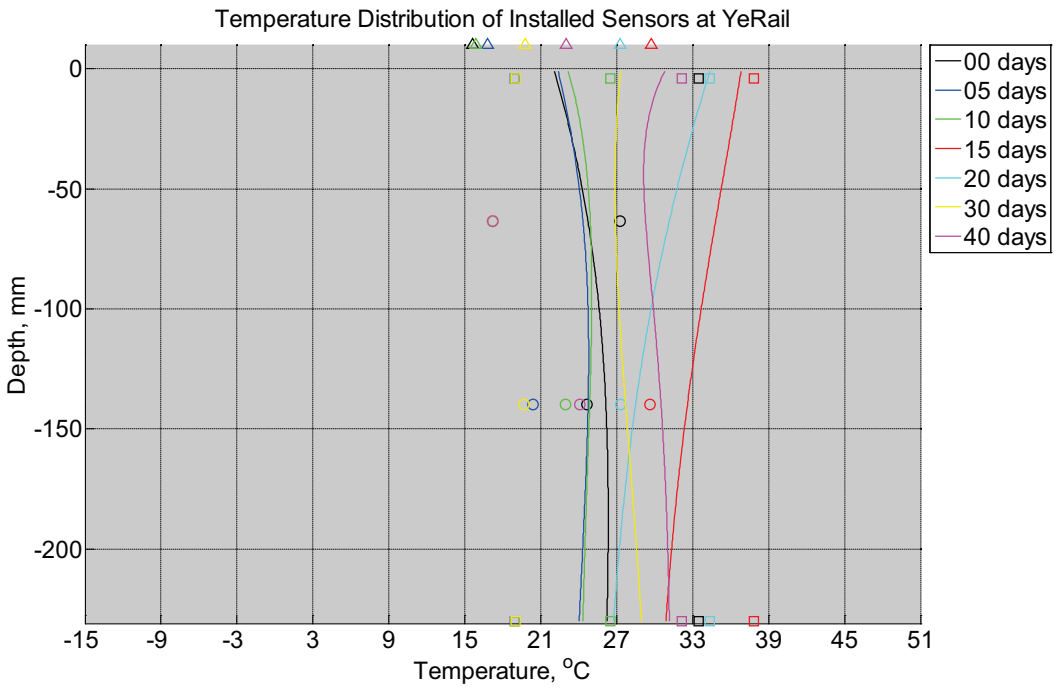

Figure B-1022 Measured (markers) and modeled (continuous line) temperature profile distribution as a function of depth inside a model concrete crosstie (labeled YeRail) installed in ballast in Rantoul, IL, between May 10, 2015, through June 20, 2015. An 8 mm thick polyurethane pad and 12 in (30.48 cm) length 136 lb/yd (67.5 kg/m) section of steel rail are additionally installed atop the model concrete crosstie. A breathable water-resistant canvas tarp is additionally installed over the model crosstie and immediate ballast area. The model does not incorporate a polyurethane pad nor steel rail line. Triangular markers denote temperature value from KTIP weather station, square markers denote measured temperature values from ballast, and circular markers denote measured temperature values inside concrete.

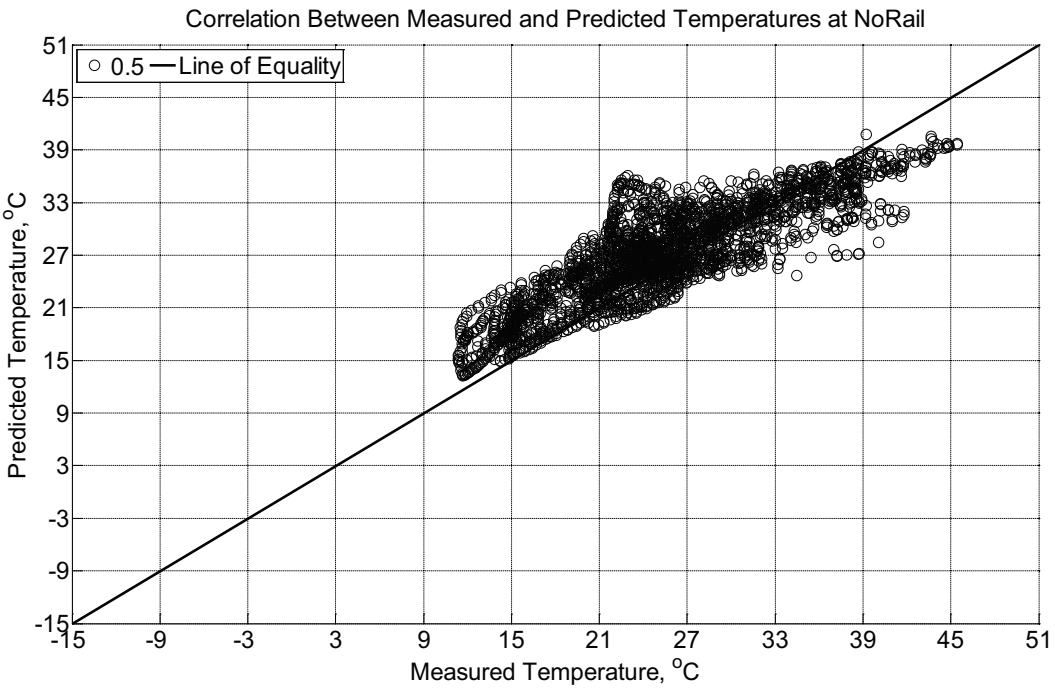

Figure B-1023 Correlation between measured and predicted temperature values 0.5 inches (12.7 mm) from the surface of a model concrete crosstie (labeled NoRail) without a polyurethane pad nor rail installed in ballast in Rantoul, IL, between May 10, 2015, through June 20, 2015. A breathable water-resistant canvas tarp is additionally installed over the model crosstie and immediate ballast area.

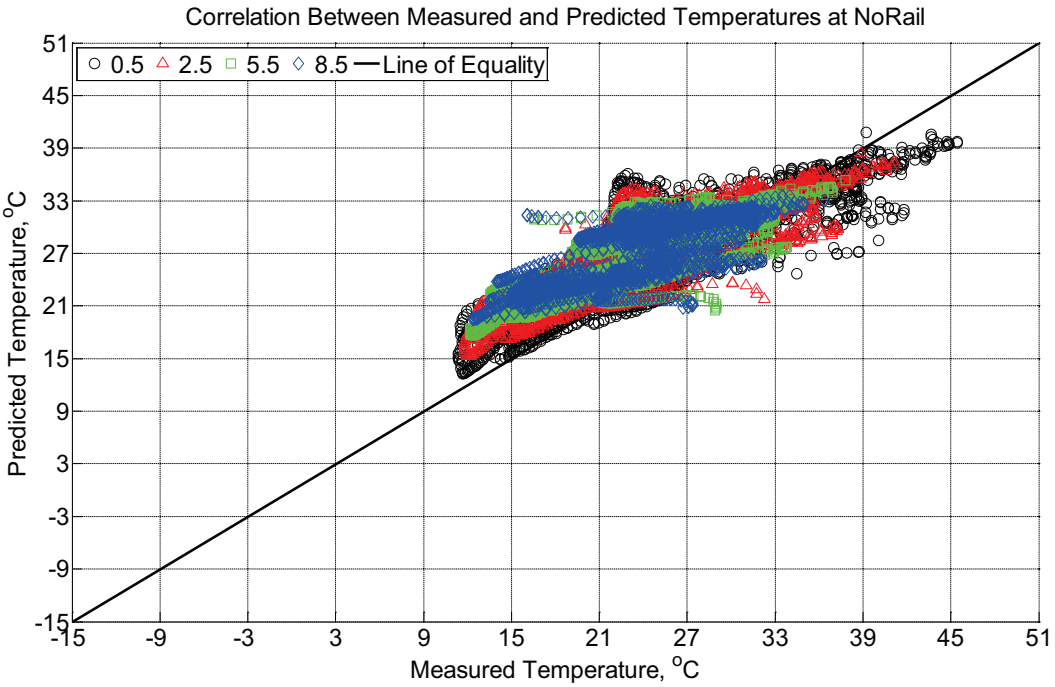

Figure B-1024 Correlation between measured and predicted temperature values 0.5 inches

(12.7 mm), 2.5 inches (63.5 mm), 5.5 inches (139.7 mm), and 8.5 inches (215.9 mm) from the surface of a model concrete crosstie (labeled NoRail) without a polyurethane pad nor rail installed in ballast in Rantoul, IL, between May 10, 2015, through June 20, 2015. A breathable water-resistant canvas tarp is additionally installed over the model crosstie and immediate ballast area.

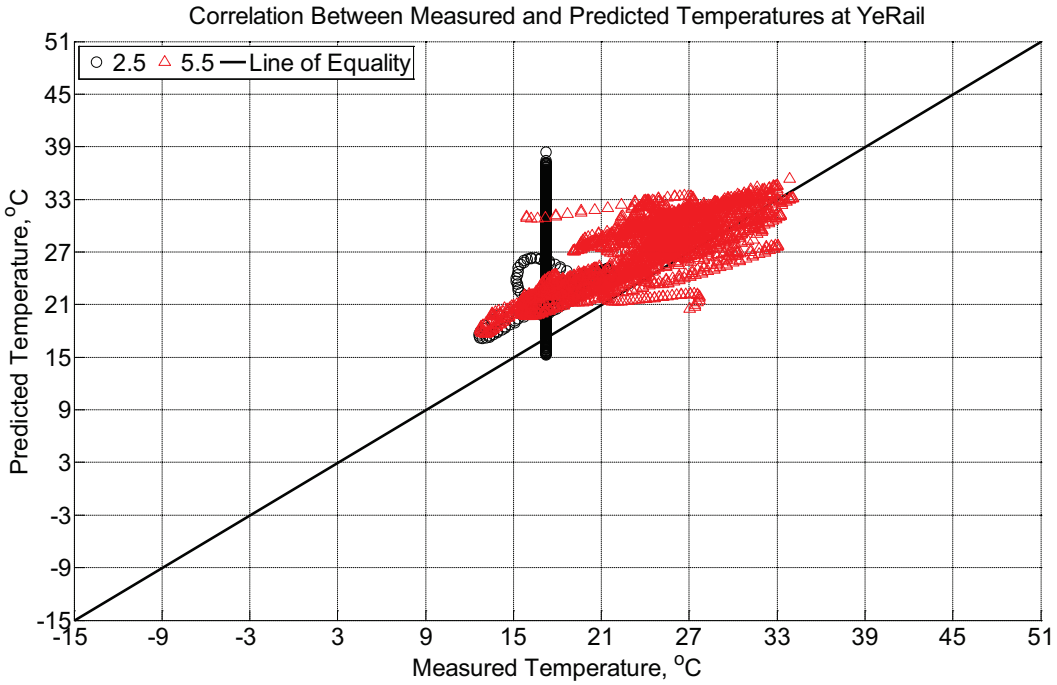

Figure B-1025 Correlation between measured and predicted temperature values 2.5 inches (63.5 mm) and 5.5 inches (139.7 mm) from the surface of a model concrete crosstie (labeled YeRail) installed in ballast in Rantoul, IL, between May 10, 2015, through June 20, 2015. An 8 mm thick polyurethane pad and 12 in (30.48 cm) length 136 lb/yd (67.5 kg/m) section of steel rail are additionally installed atop the model concrete crosstie. A breathable water-resistant canvas tarp is additionally installed over the model crosstie and immediate ballast area. The model does not incorporate a polyurethane pad nor steel rail line.

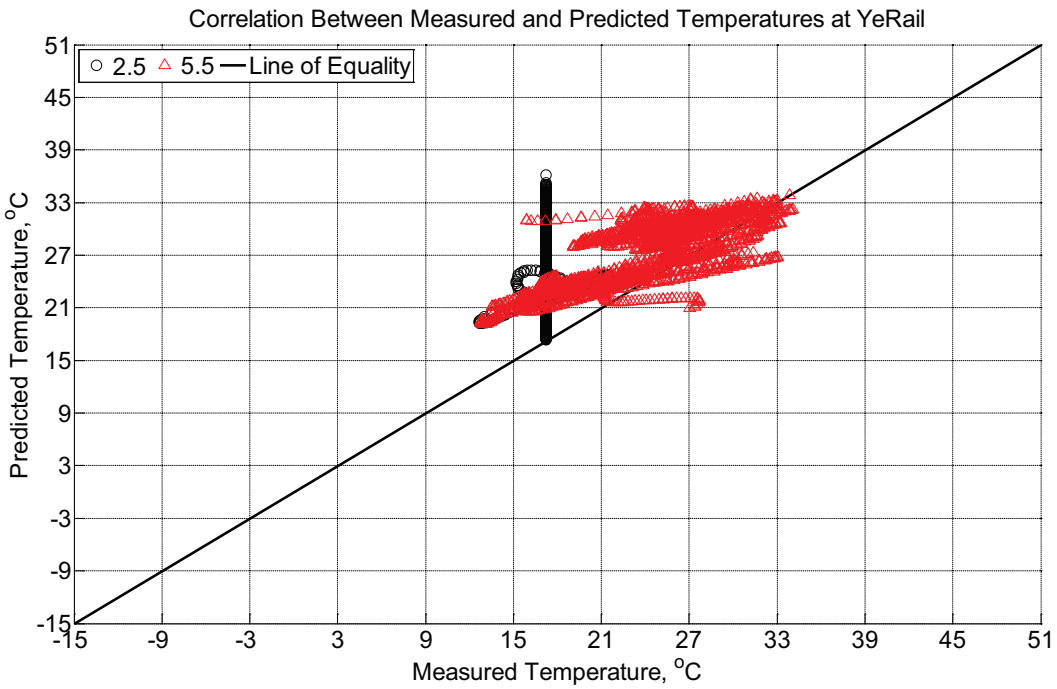

Figure B-1026 Correlation between measured and predicted temperature values 2.5 inches (63.5 mm) and 5.5 inches (139.7 mm) from the surface of a model concrete crosstie (labeled YeRail) installed in ballast in Rantoul, IL, between May 10, 2015, through June 20, 2015. An 8 mm thick polyurethane pad and 12 in (30.48 cm) length 136 lb/yd (67.5 kg/m) section of steel rail are additionally installed atop the model concrete crosstie. A breathable water-resistant canvas tarp is additionally installed over the model crosstie and immediate ballast area. The model incorporates an 8 mm thick polyurethane pad and 10 mm thick steel rail line.

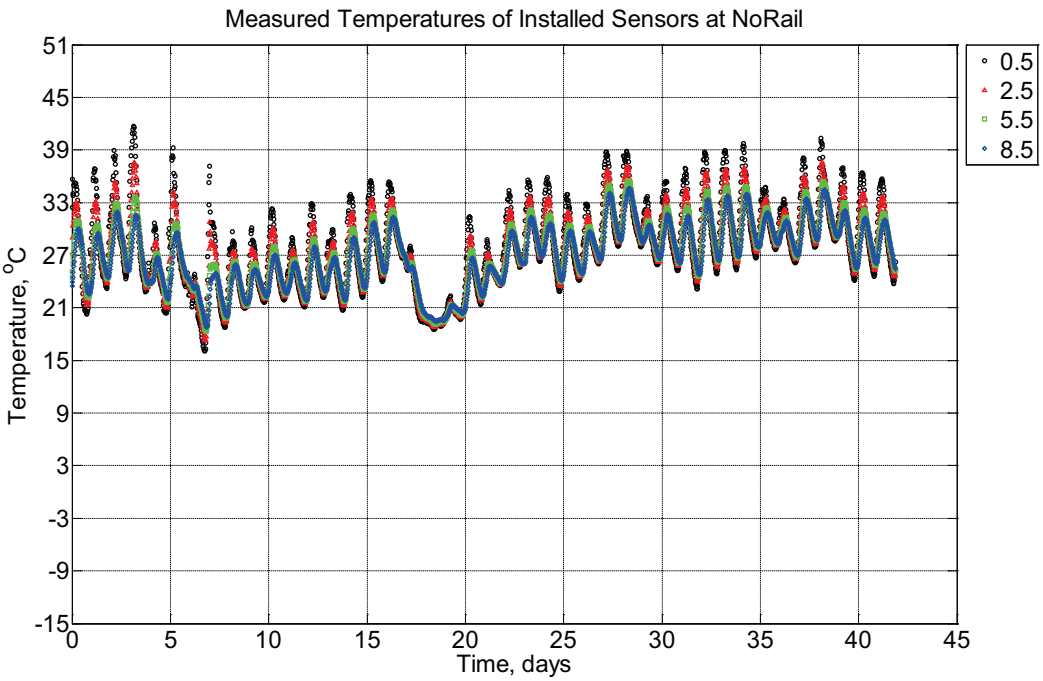

Figure B-1027 Measured temperature at depths of 0.5 inches (12.7 mm), 2.5 inches (63.5 mm), 5.5 inches (139.7 mm), and 8.5 inches (215.9 mm) from the surface of a model concrete crosstie (labeled NoRail) without a polyurethane pad nor rail installed in ballast in Rantoul, IL, between June 20, 2015, through August 1, 2015. A breathable water-resistant canvas tarp is additionally installed over the model crosstie and immediate ballast area.

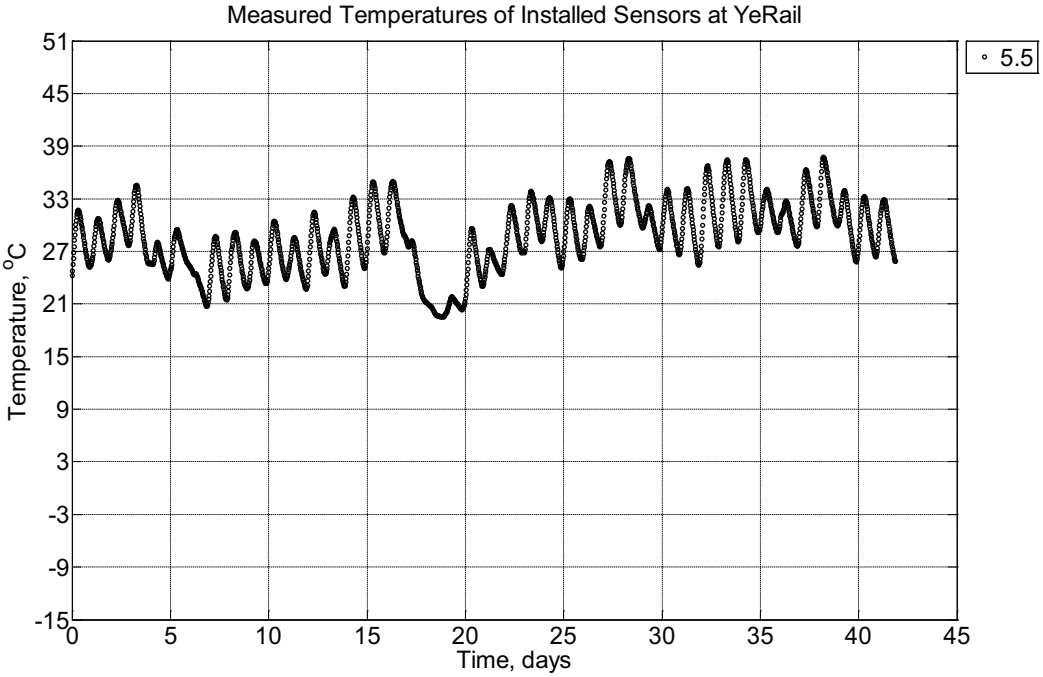

Figure B-1028 Measured temperature at a depth of 5.5 inches (139.7 mm) from the surface

of a model concrete crosstie (labeled YeRail) installed in ballast in Rantoul, IL, between June 20, 2015, through August 1, 2015. An 8 mm thick polyurethane pad and 12 in (30.48 cm) length 136 lb/yd (67.5 kg/m) section of steel rail are additionally installed atop the model concrete crosstie. A breathable water-resistant canvas tarp is additionally installed over the model crosstie and immediate ballast area.

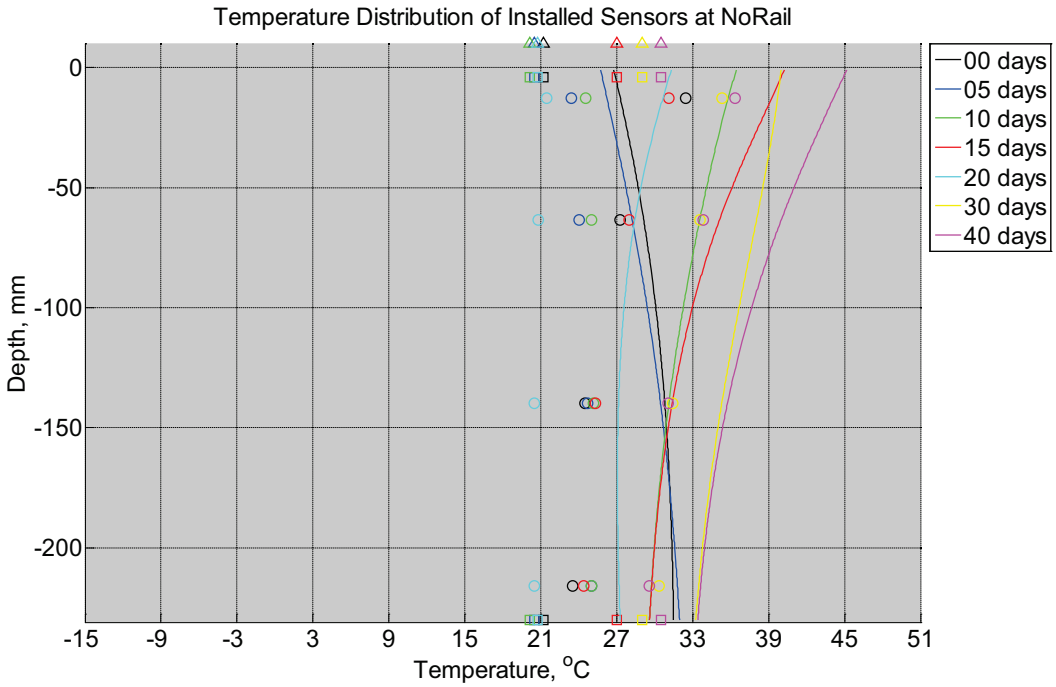

Figure B-1029 Measured (markers) and modeled (continuous line) temperature profile distribution as a function of depth inside a model concrete crosstie (labeled NoRail) without a polyurethane pad nor rail installed in ballast in Rantoul, IL, between June 20, 2015, through August 1, 2015. A breathable water-resistant canvas tarp is additionally installed over the model crosstie and immediate ballast area. Triangular markers denote temperature value from KTIP weather station, square markers denote measured temperature values from ballast, and circular markers denote measured temperature values inside concrete.

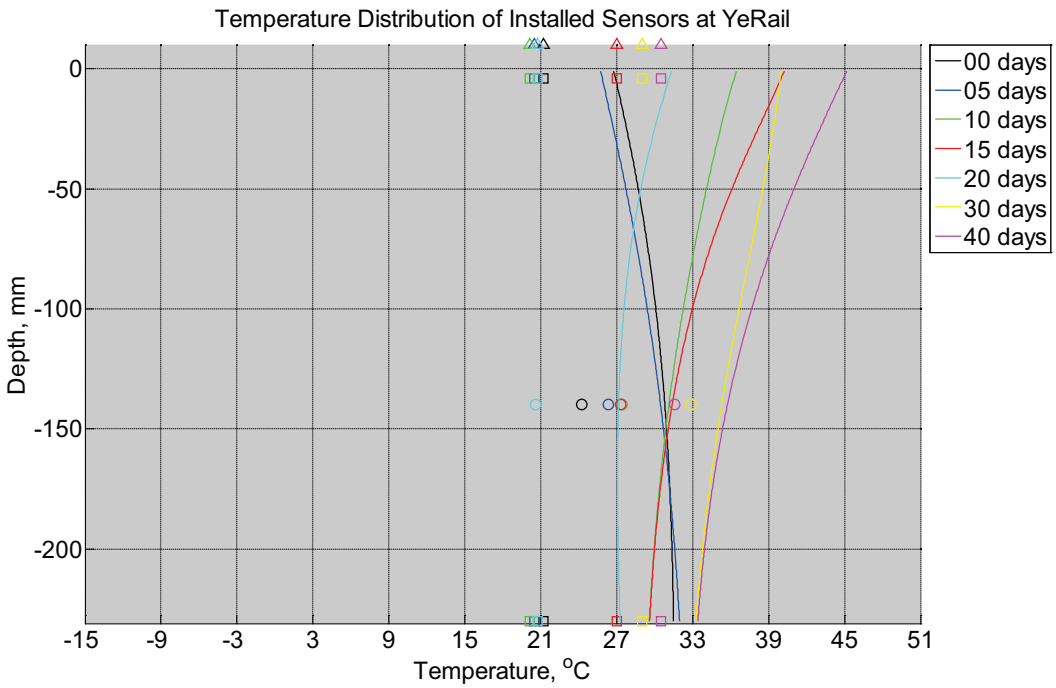

Figure B-1030 Measured (markers) and modeled (continuous line) temperature profile distribution as a function of depth inside a model concrete crosstie (labeled YeRail) installed in ballast in Rantoul, IL, between June 20, 2015, through August 1, 2015. An 8 mm thick polyurethane pad and 12 in (30.48 cm) length 136 lb/yd (67.5 kg/m) section of steel rail are additionally installed atop the model concrete crosstie. A breathable water-resistant canvas tarp is additionally installed over the model crosstie and immediate ballast area. The model does not incorporate a polyurethane pad nor steel rail line. Triangular markers denote temperature value from KTIP weather station, square markers denote measured temperature values from ballast, and circular markers denote measured temperature values inside concrete.

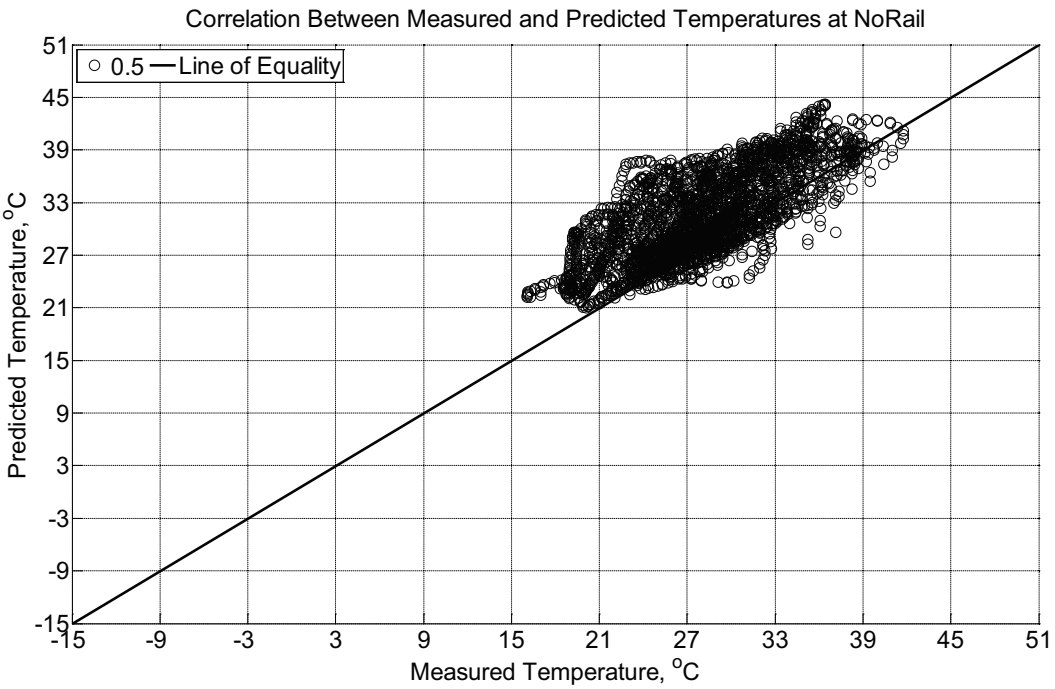

Figure B-1031 Correlation between measured and predicted temperature values 0.5 inches (12.7 mm) from the surface of a model concrete crosstie (labeled NoRail) without a polyurethane pad nor rail installed in ballast in Rantoul, IL, between June 20, 2015, through August 1, 2015. A breathable water-resistant canvas tarp is additionally installed over the model crosstie and immediate ballast area.

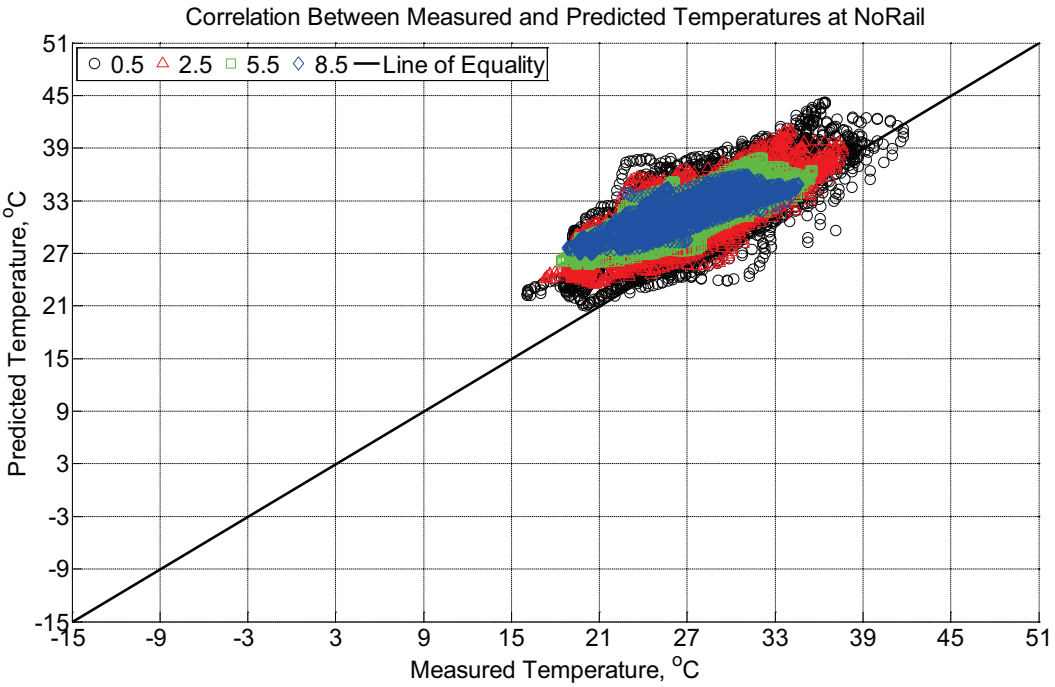

Figure B-1032 Correlation between measured and predicted temperature values 0.5 inches

(12.7 mm), 2.5 inches (63.5 mm), 5.5 inches (139.7 mm), and 8.5 inches (215.9 mm) from the surface of a model concrete crosstie (labeled NoRail) without a polyurethane pad nor rail installed in ballast in Rantoul, IL, between June 20, 2015, through August 1, 2015. A breathable water-resistant canvas tarp is additionally installed over the model crosstie and immediate ballast area.

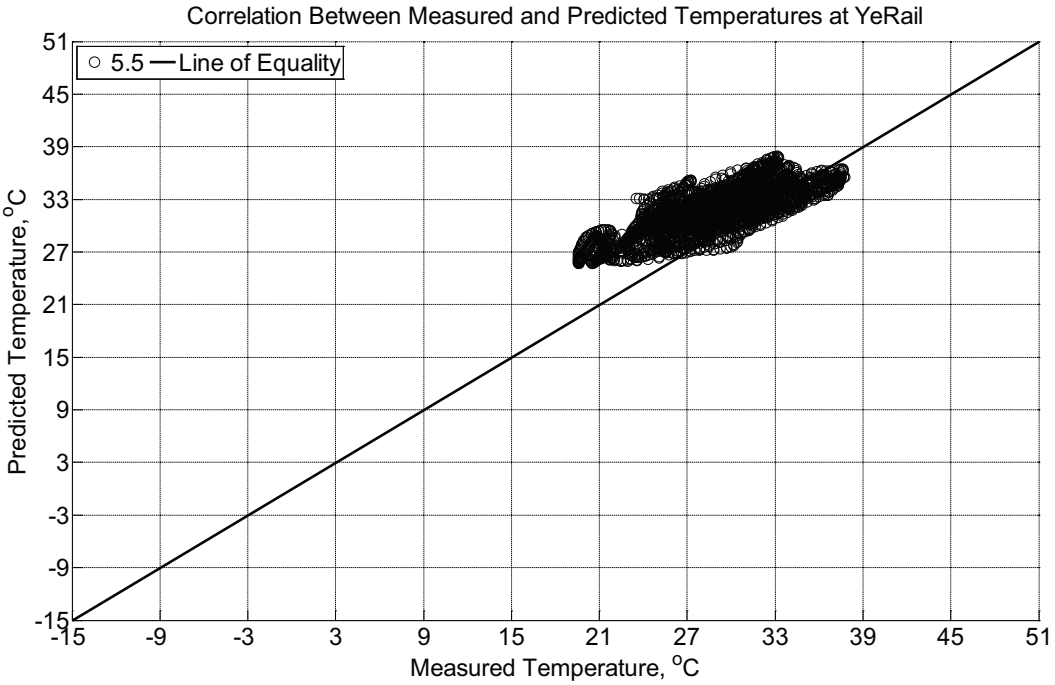

Figure B-1033 Correlation between measured and predicted temperature values 5.5 inches (139.7 mm) from the surface of a model concrete crosstie (labeled YeRail) installed in ballast in Rantoul, IL, between June 20, 2015, through August 1, 2015. An 8 mm thick polyurethane pad and 12 in (30.48 cm) length 136 lb/yd (67.5 kg/m) section of steel rail are additionally installed atop the model concrete crosstie. A breathable water-resistant canvas tarp is additionally installed over the model crosstie and immediate ballast area. The model does not incorporate a polyurethane pad nor steel rail line.

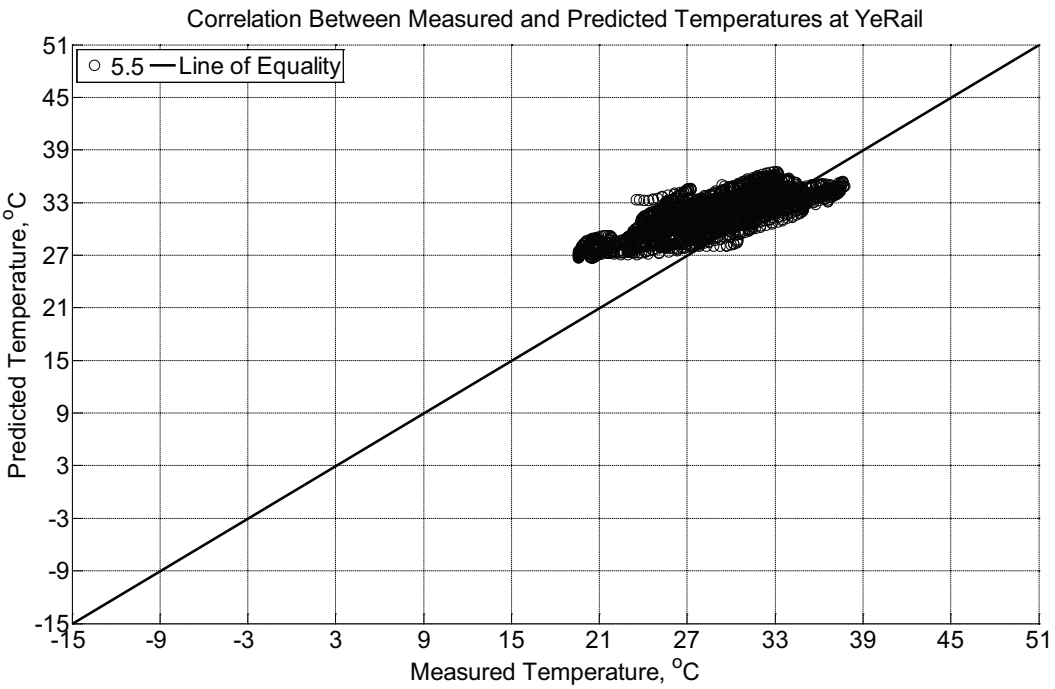

Figure B-1034 Correlation between measured and predicted temperature values 5.5 inches (139.7 mm) from the surface of a model concrete crosstie (labeled YeRail) installed in ballast in Rantoul, IL, between June 20, 2015, through August 1, 2015. An 8 mm thick polyurethane pad and 12 in (30.48 cm) length 136 lb/yd (67.5 kg/m) section of steel rail are additionally installed atop the model concrete crosstie. A breathable water-resistant canvas tarp is additionally installed over the model crosstie and immediate ballast area. The model incorporates an 8 mm thick polyurethane pad and 10 mm thick steel rail line.

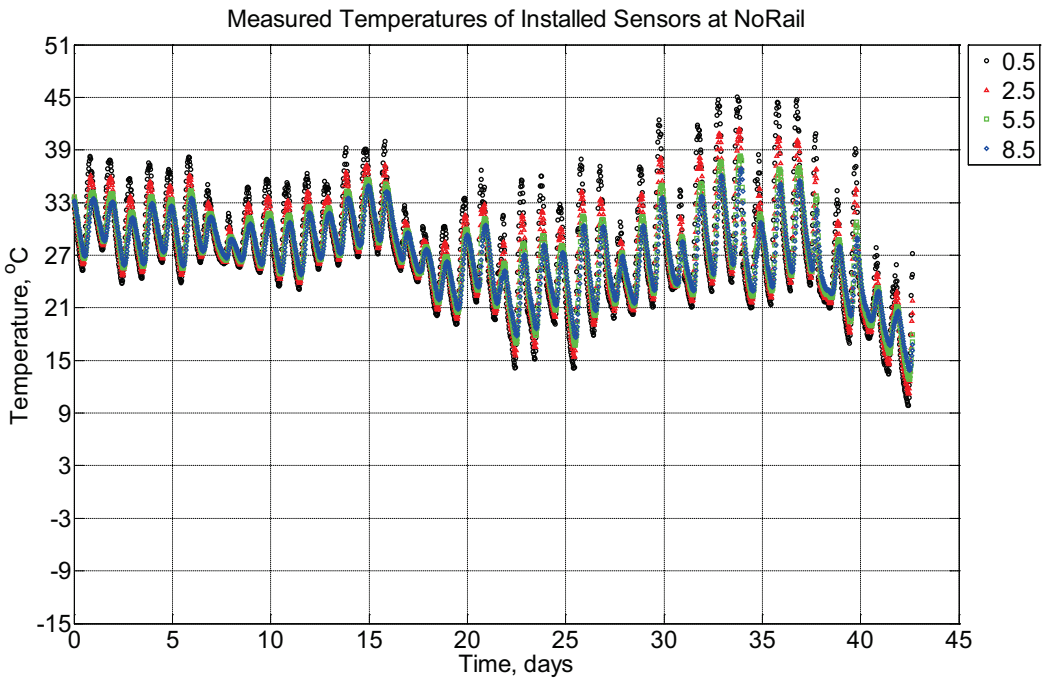

Figure B-1035 Measured temperature at depths of 0.5 inches (12.7 mm), 2.5 inches (63.5 mm), 5.5 inches (139.7 mm), and 8.5 inches (215.9 mm) from the surface of a model concrete crosstie (labeled NoRail) without a polyurethane pad nor rail installed in ballast in Rantoul, IL, between August 1, 2015, through September 13, 2015. A breathable water-resistant canvas tarp is additionally installed over the model crosstie and immediate ballast area and removed on day 20.

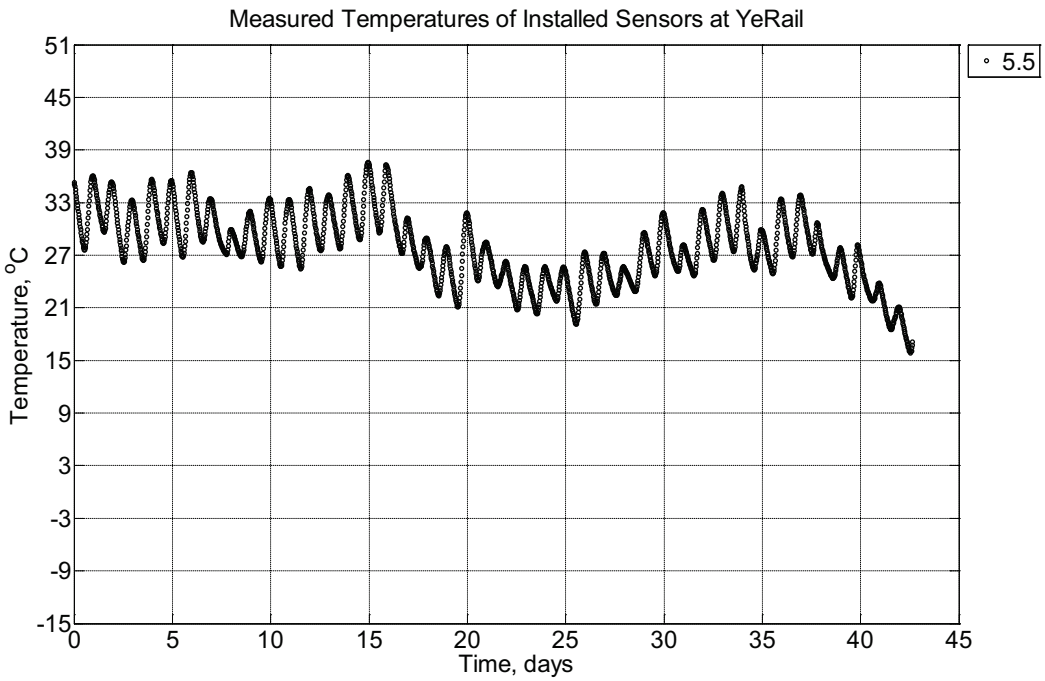

Figure B-1036 Measured temperature at a depth of 5.5 inches (139.7 mm) from the surface of a model concrete crosstie (labeled YeRail) installed in ballast in Rantoul, IL, between August 1, 2015, through September 13, 2015. An 8 mm thick polyurethane pad and 12 in (30.48 cm) length 136 lb/yd (67.5 kg/m) section of steel rail are additionally installed atop the model concrete crosstie. A breathable water-resistant canvas tarp is additionally installed over the model crosstie and immediate ballast area.

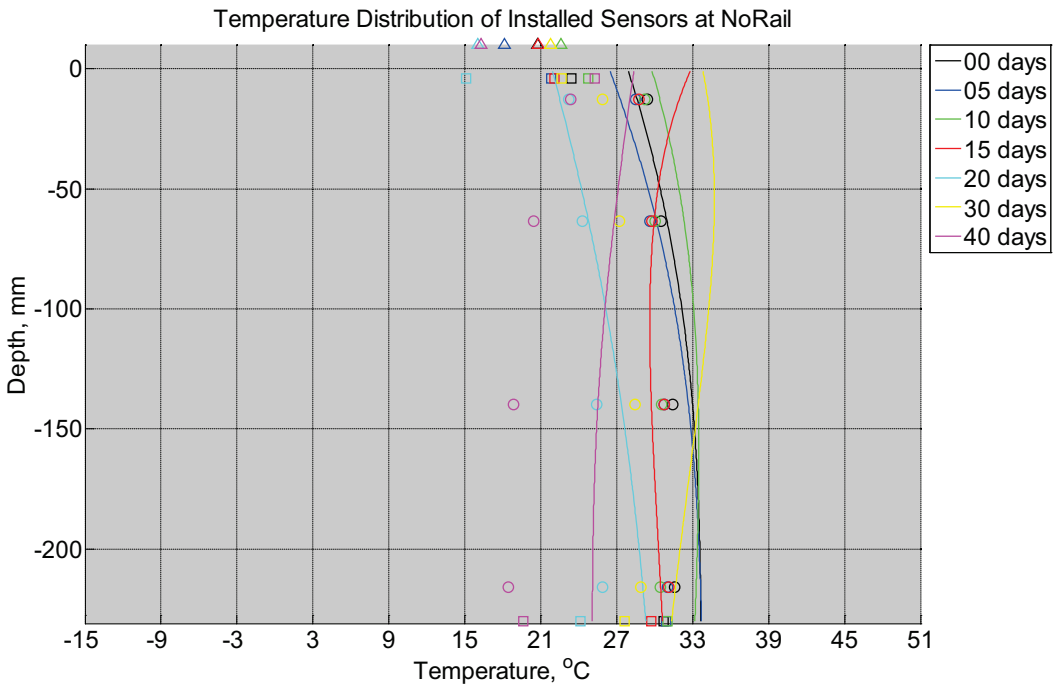

Figure B-1037 Measured (markers) and modeled (continuous line) temperature profile distribution as a function of depth inside a model concrete crosstie (labeled NoRail) without a polyurethane pad nor rail installed in ballast in Rantoul, IL, between August 1, 2015, through September 13, 2015. A breathable water-resistant canvas tarp is additionally installed over the model crosstie and immediate ballast area and removed on day 20. Triangular markers denote temperature value from KTIP weather station, square markers denote measured temperature values from ballast, and circular markers denote measured temperature values inside concrete.

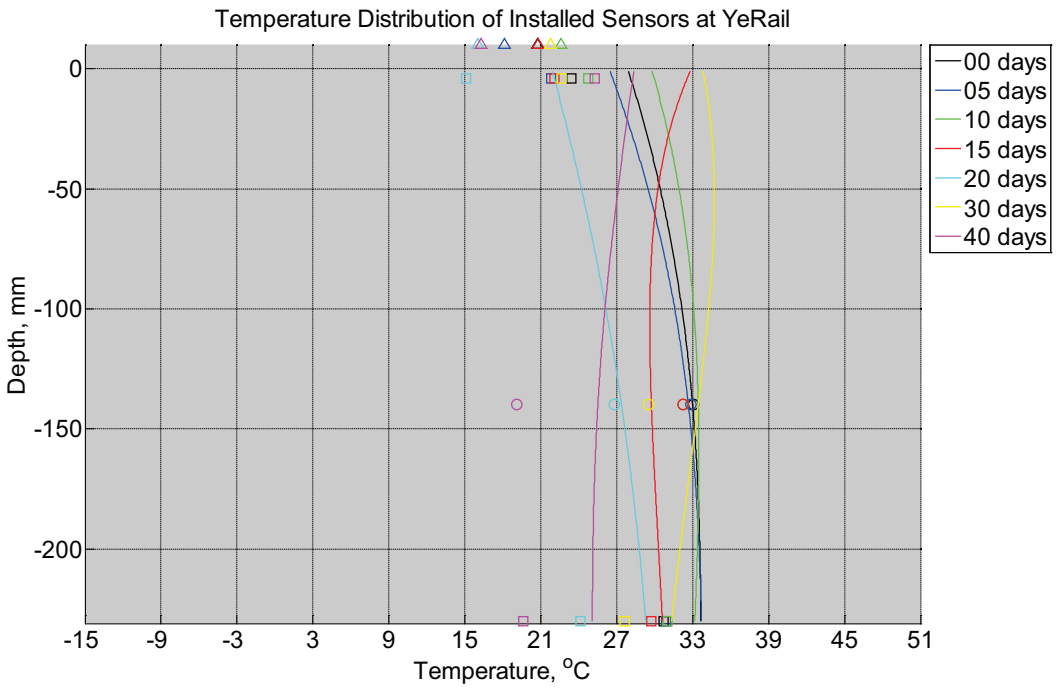

Figure B-1038 Measured (markers) and modeled (continuous line) temperature profile distribution as a function of depth inside a model concrete crosstie (labeled YeRail) installed in ballast in Rantoul, IL, between August 1, 2015, through September 13, 2015. An 8 mm thick polyurethane pad and 12 in (30.48 cm) length 136 lb/yd (67.5 kg/m) section of steel rail are additionally installed atop the model concrete crosstie. A breathable water-resistant canvas tarp is additionally installed over the model crosstie and immediate ballast area. The model does not incorporate a polyurethane pad nor steel rail line. Triangular markers denote temperature value from KTIP weather station, square markers denote measured temperature values from ballast, and circular markers denote measured temperature values inside concrete.

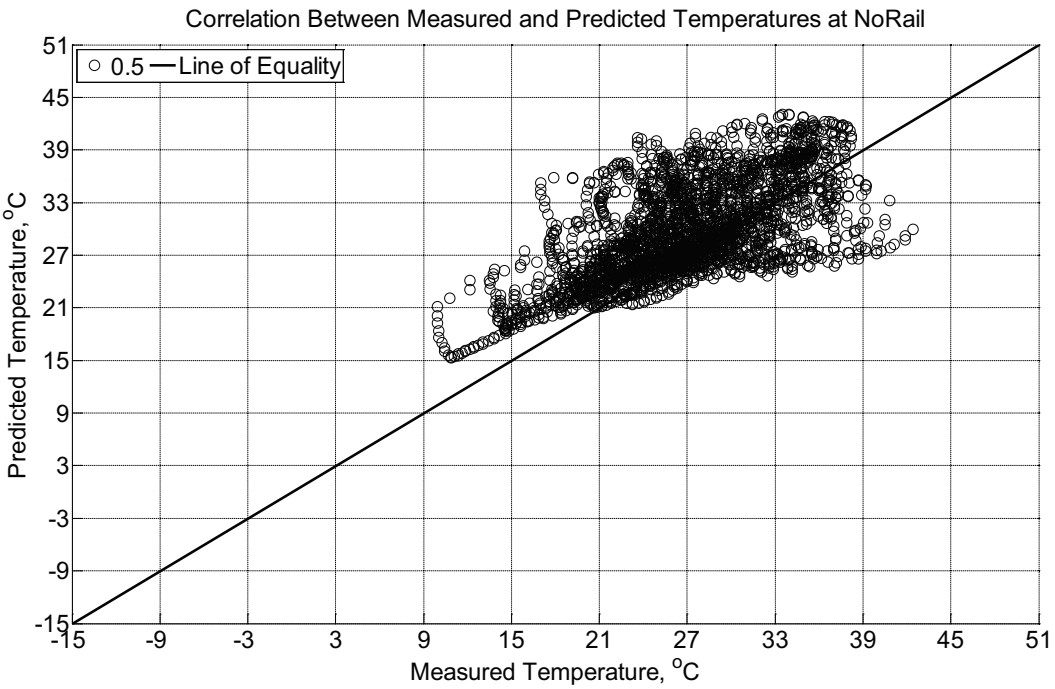

Figure B-1039 Correlation between measured and predicted temperature values 0.5 inches (12.7 mm) from the surface of a model concrete crosstie (labeled NoRail) without a polyurethane pad nor rail installed in ballast in Rantoul, IL, between August 1, 2015, through September 13, 2015. A breathable water-resistant canvas tarp is additionally installed over the model crosstie and immediate ballast area and removed on day 20.

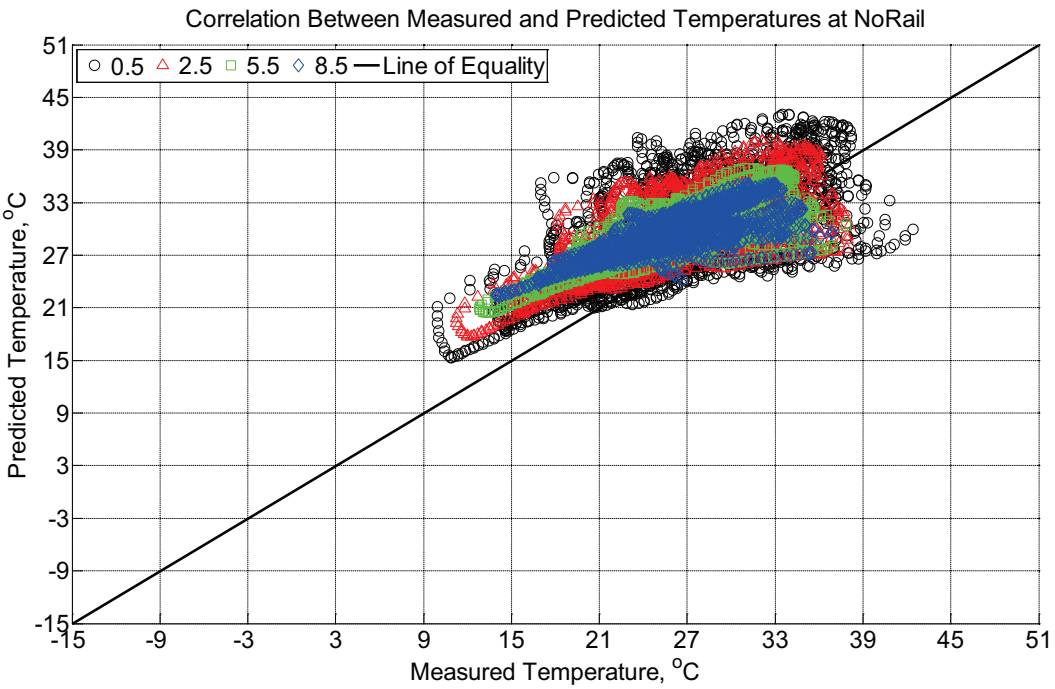

Figure B-1040 Correlation between measured and predicted temperature values 0.5 inches (12.7 mm), 2.5 inches (63.5 mm), 5.5 inches (139.7 mm), and 8.5 inches (215.9 mm) from the surface of a model concrete crosstie (labeled NoRail) without a polyurethane pad nor rail installed in ballast in Rantoul, IL, between August 1, 2015, through September 13, 2015. A breathable water-resistant canvas tarp is additionally installed over the model crosstie and immediate ballast area and removed on day 20.

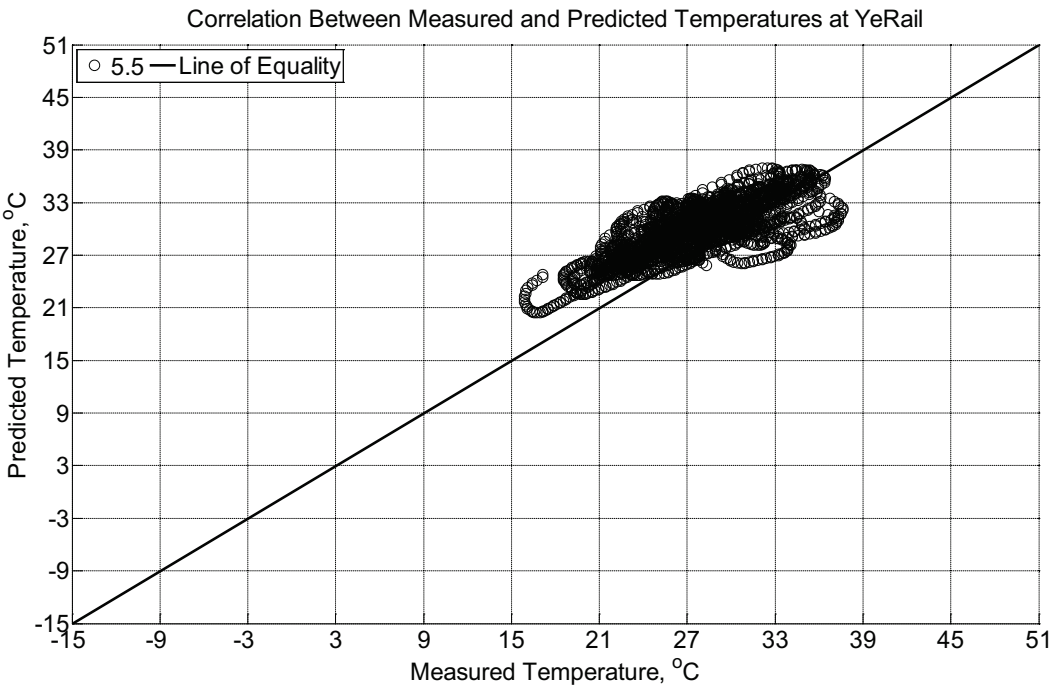

Figure B-1041 Correlation between measured and predicted temperature values 5.5 inches (139.7 mm) from the surface of a model concrete crosstie (labeled YeRail) installed in ballast in Rantoul, IL, between August 1, 2015, through September 13, 2015. An 8 mm thick polyurethane pad and 12 in (30.48 cm) length 136 lb/yd (67.5 kg/m) section of steel rail are additionally installed atop the model concrete crosstie. A breathable water-resistant canvas tarp is additionally installed over the model crosstie and immediate ballast area. The model does not incorporate a polyurethane pad nor steel rail line.

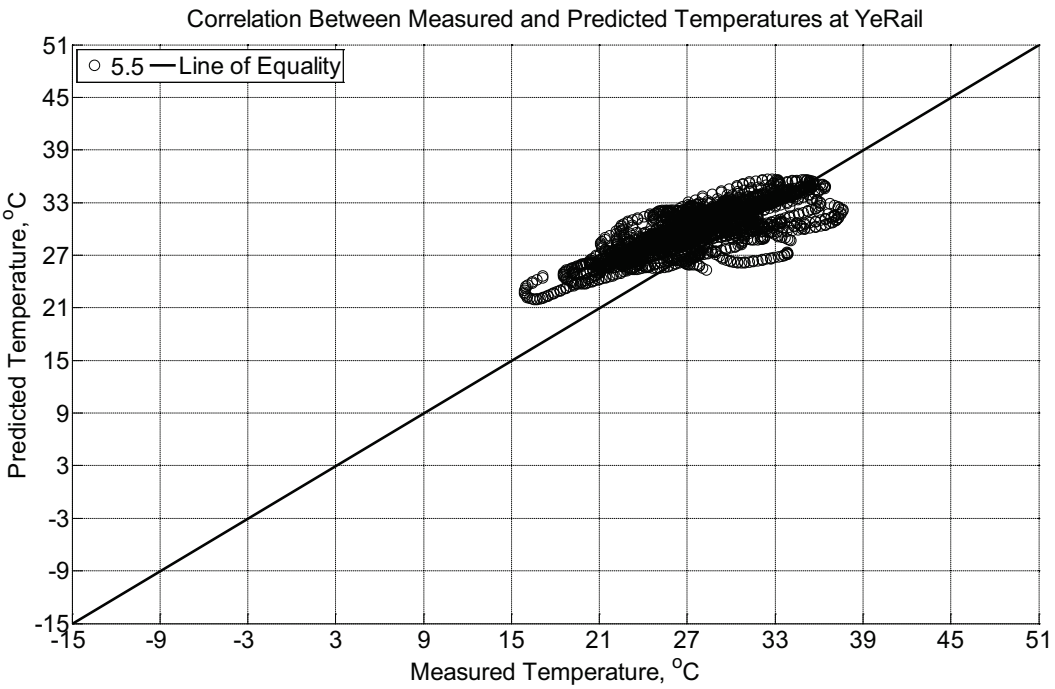

Figure B-1042 Correlation between measured and predicted temperature values 5.5 inches (139.7 mm) from the surface of a model concrete crosstie (labeled YeRail) installed in ballast in Rantoul, IL, between August 1, 2015, through September 13, 2015. An 8 mm thick polyurethane pad and 12 in (30.48 cm) length 136 lb/yd (67.5 kg/m) section of steel rail are additionally installed atop the model concrete crosstie. A breathable water-resistant canvas tarp is additionally installed over the model crosstie and immediate ballast area. The model incorporates an 8 mm thick polyurethane pad and 10 mm thick steel rail line.

Appendix C Predicted Number of Freeze-Thaw Cycles in Concrete as a Function of Depth and Concrete Quality

Modeled freeze-thaw cycles of concrete in Rantoul, IL, due to temperature fluctuations

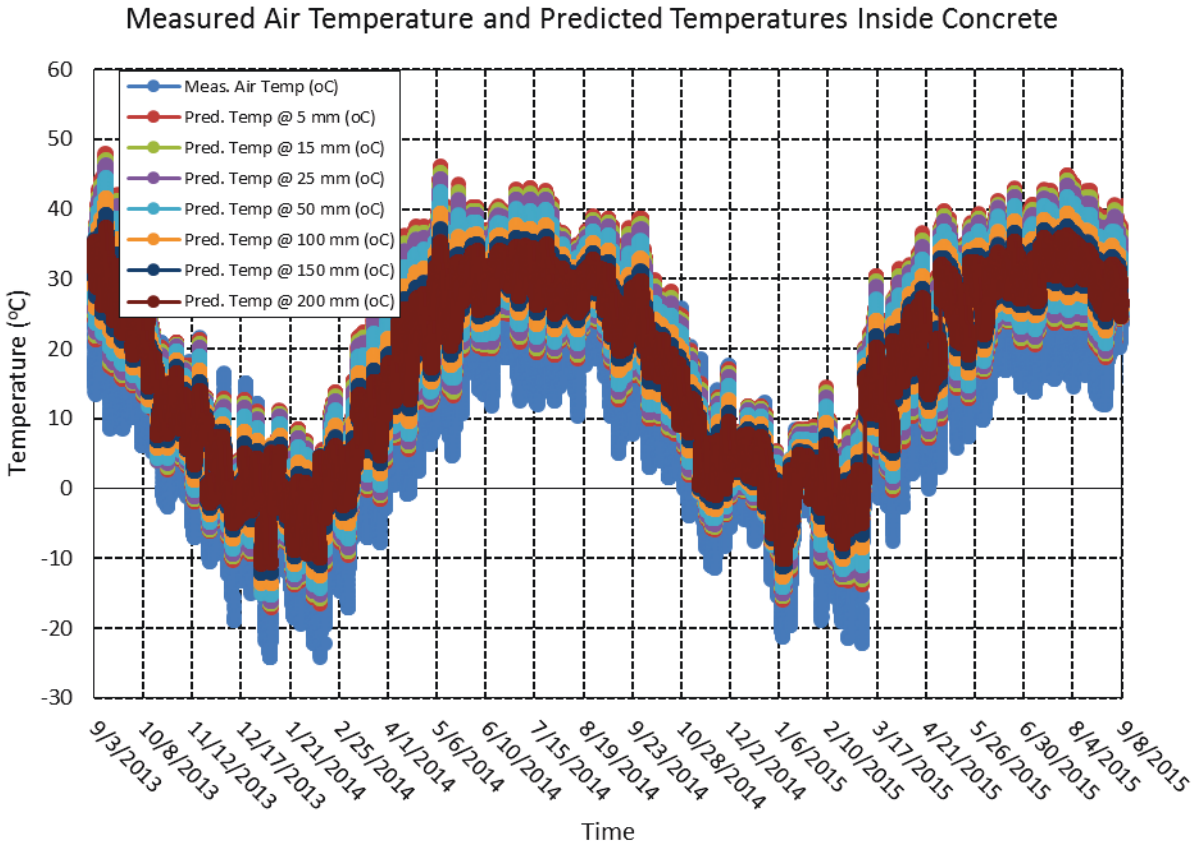

Figure C-1 Measured air temperature and predicted temperature inside model concrete in Rantoul, IL, from September 3, 2013, through September 8, 2015. Predicted internal temperature values are computed using a 2-layered system whose upper concrete layer is defined by a thermal conductivity, λ, value of 1.85 kcal/hmC^{o} and a thermal diffusivity, α, value of 0.0025 m^2/h. The underlying aggregate ballast layer is defined by a thermal conductivity, λ, value of 2.58 kcal/hmC^{o} and a thermal diffusivity, α, value of 0.0030 m^2/h.

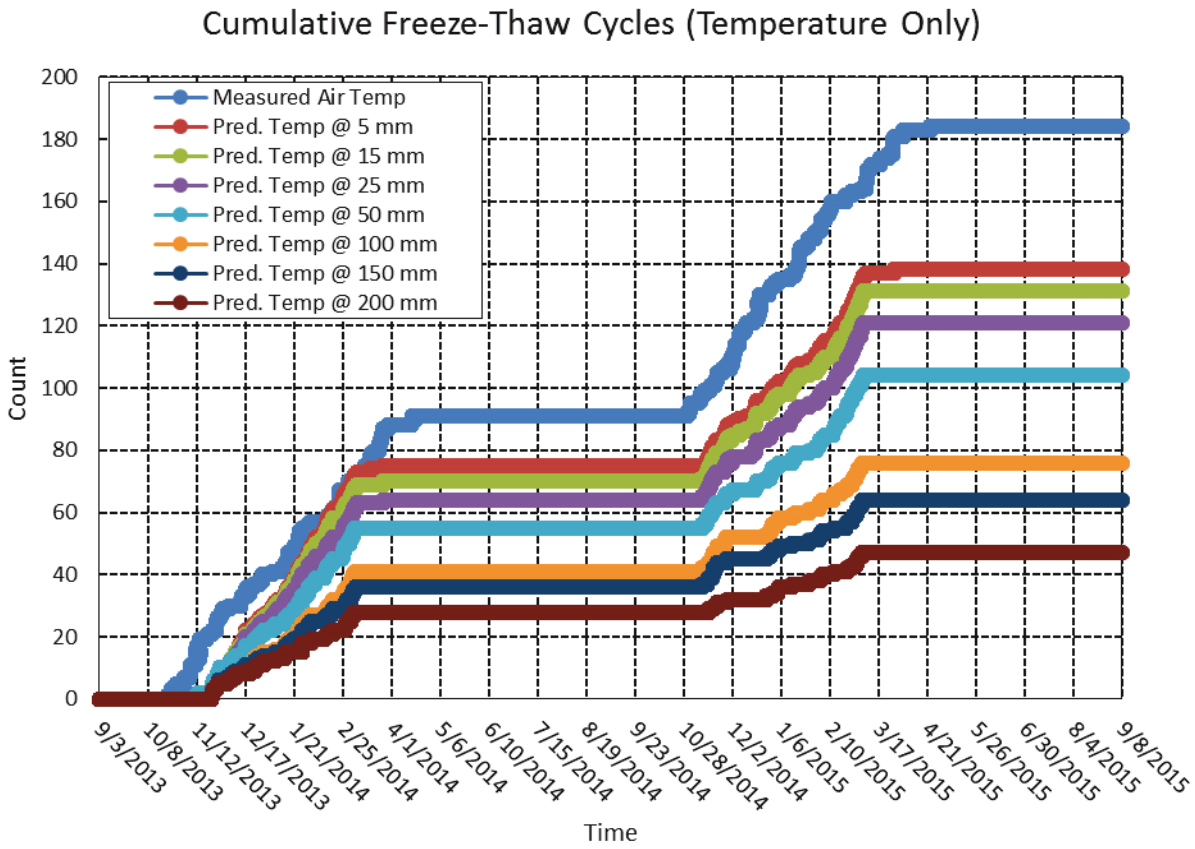

Figure C-2 Cumulative number of freeze-thaw cycles in Rantoul, IL, from September 3, 2013, through September 8, 2015. Predicted internal temperature values are computed using a 2-layered system whose upper concrete layer is defined by a thermal conductivity, λ, value of 1.85 kcal/hmC^{o} and a thermal diffusivity, α, value of 0.0025 m^2/h. The underlying aggregate ballast layer is defined by a thermal conductivity, λ, value of 2.58 kcal/hmC^{o} and a thermal diffusivity, α, value of 0.0030 m^2/h.

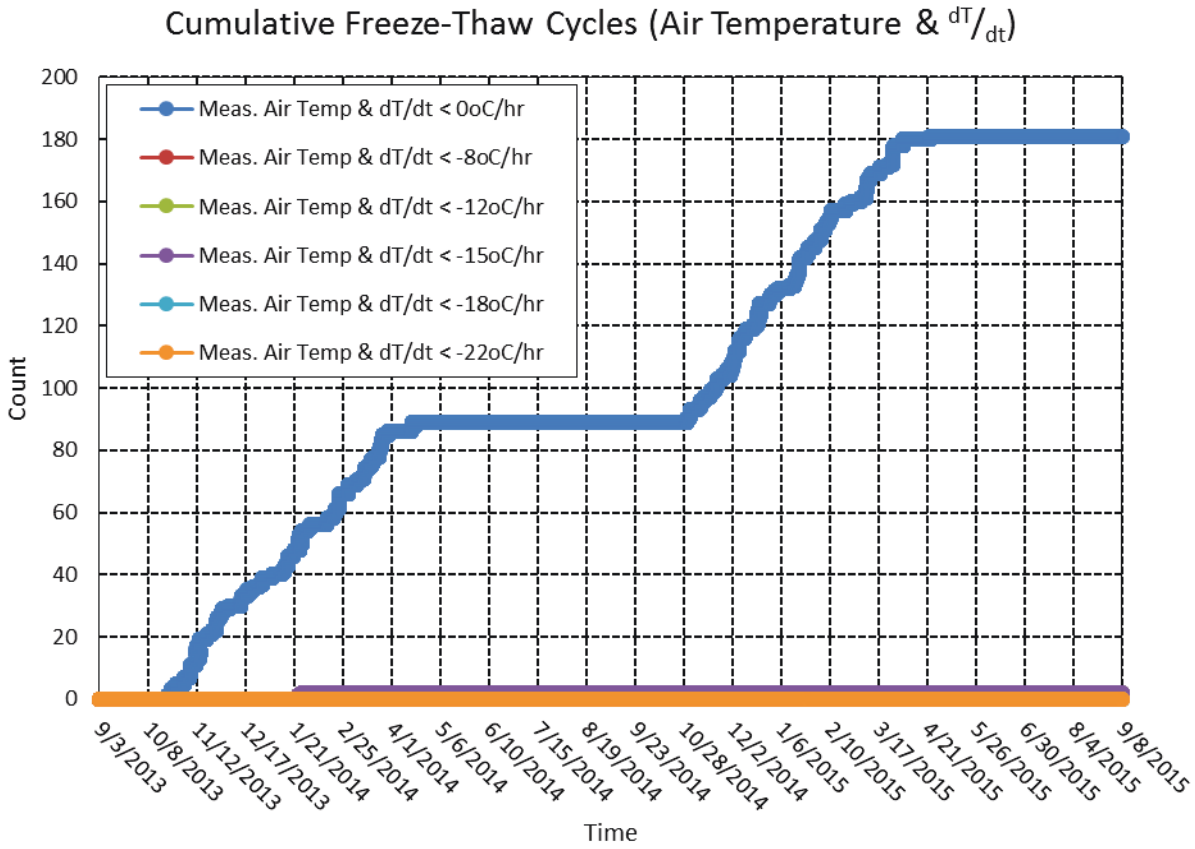

Figure C-3 Cumulative number of freeze-thaw cycles in Rantoul, IL, from September 3, 2013, through September 8, 2015, when both freezing air temperatures and minimum rate of freezing is achieved at time of freezing.

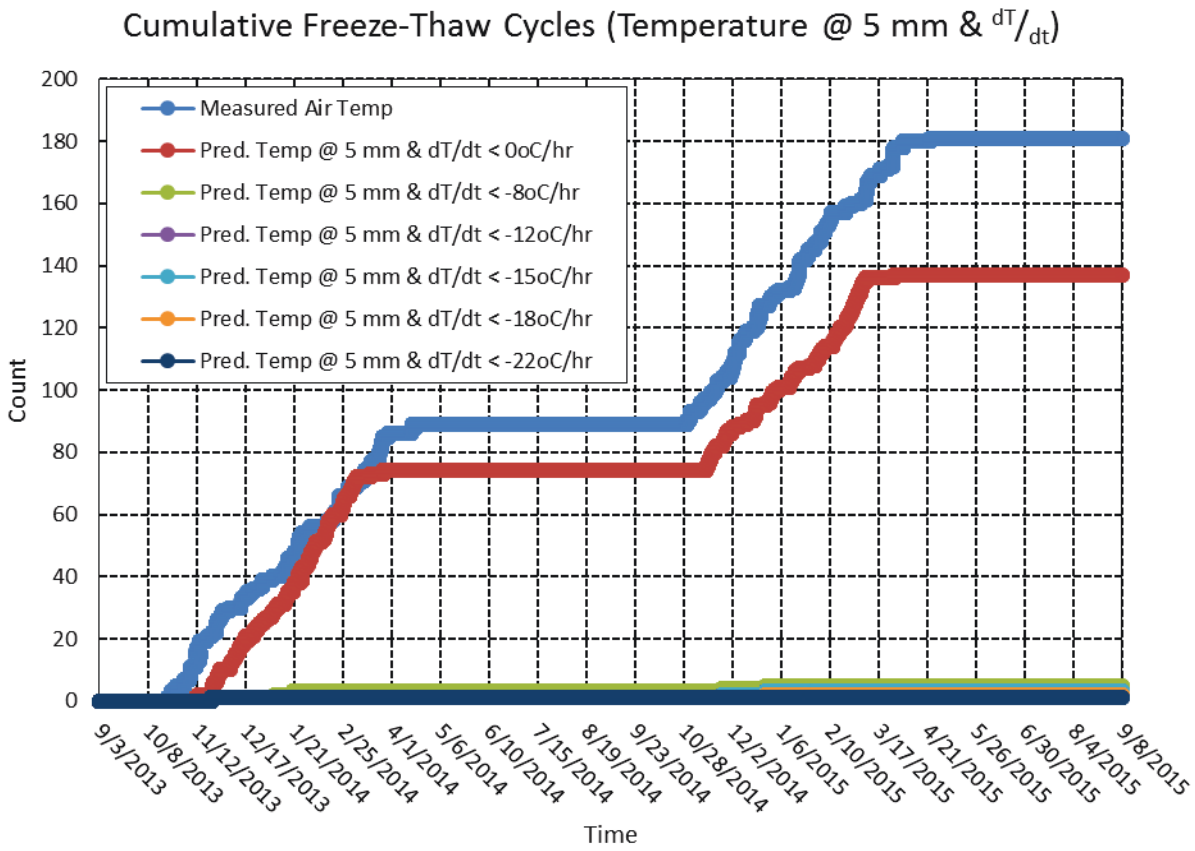

Figure C-4 Cumulative number of freeze-thaw cycles in Rantoul, IL, from September 3, 2013, through September 8, 2015, when both freezing temperatures at a depth of 5 mm and minimum rate of freezing is achieved at time of freezing. Predicted internal temperature values are computed using a 2-layered system whose upper concrete layer is defined by a thermal conductivity, λ, value of 1.85 kcal/hmC^o and a thermal diffusivity, α, value of 0.0025 m^2/h. The underlying aggregate ballast layer is defined by a thermal conductivity, λ, value of 2.58 kcal/hmC^o and a thermal diffusivity, α, value of 0.0030 m^2/h.

Modeled freeze-thaw cycles of concrete in Lytton, BC, due to temperature fluctuations

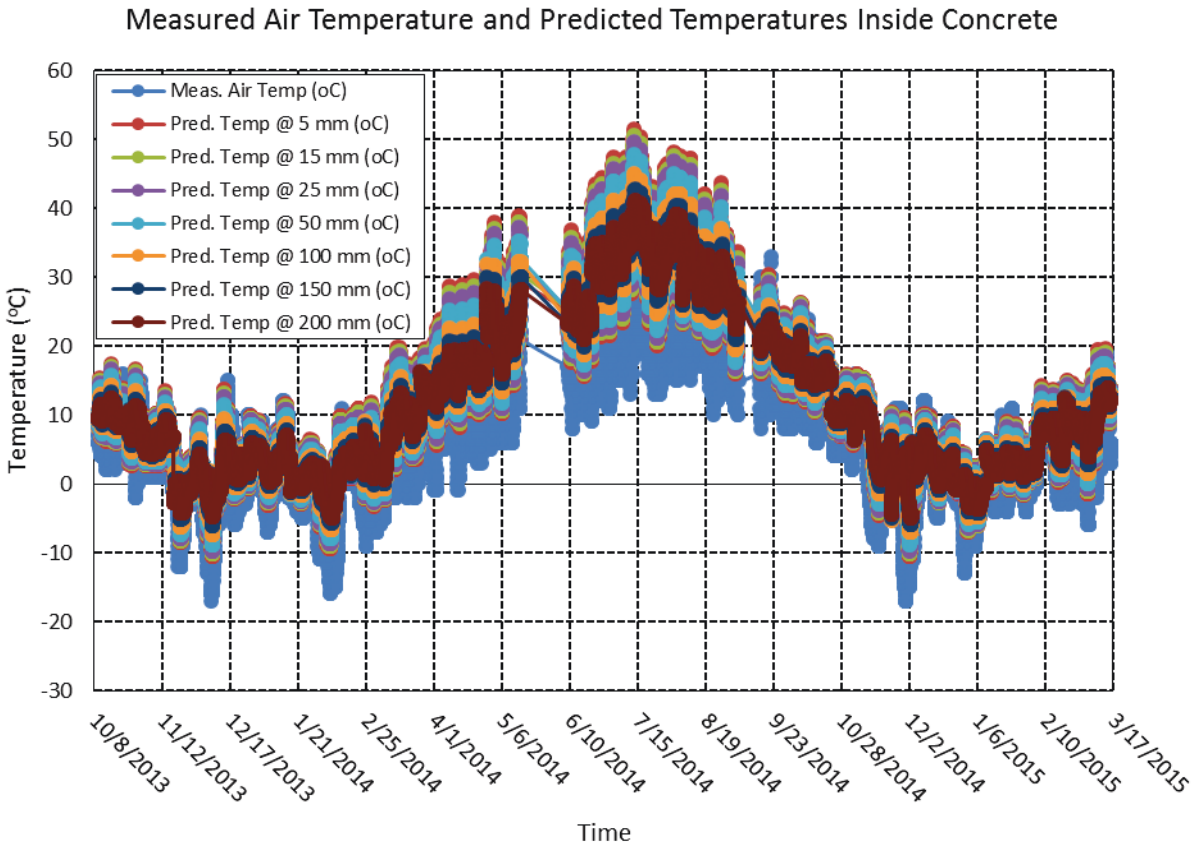

Figure C-5 Measured air temperatures and predicted temperature inside model concrete in Lytton, BC, from October 8, 2013, through March 17, 2015. Predicted internal temperature values are computed using a 2-layered system whose upper concrete layer is defined by a thermal conductivity, λ, value of 1.85 kcal/hmC^{o} and a thermal diffusivity, α, value of 0.0025 m^2/h. The underlying aggregate ballast layer is defined by a thermal conductivity, λ, value of 2.58 kcal/hmC^{o} and a thermal diffusivity, α, value of 0.0030 m^2/h.

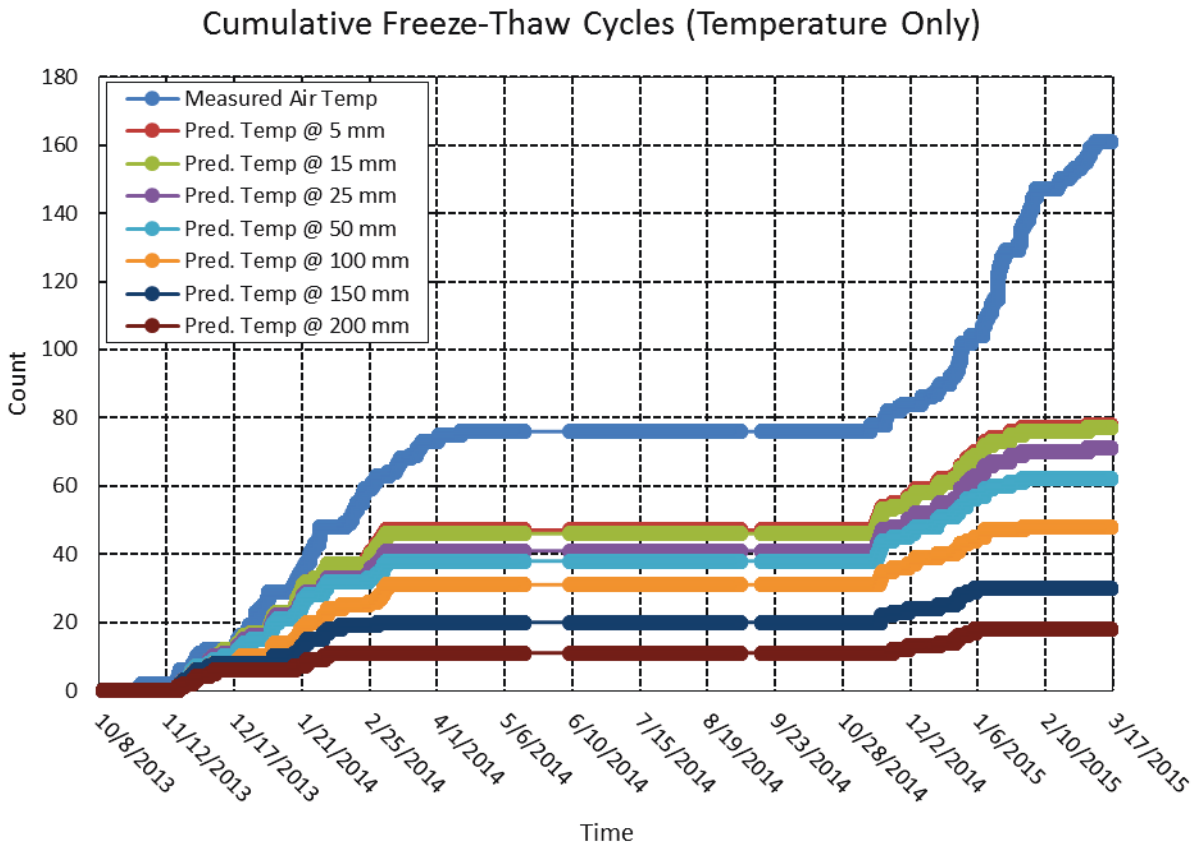

Figure C-6 Cumulative number of freeze-thaw cycles in Lytton, BC, from October 8, 2013, through March 17, 2015. Predicted internal temperature values are computed using a 2-layered system whose upper concrete layer is defined by a thermal conductivity, λ, value of 1.85 kcal/hmC^o and a thermal diffusivity, α, value of 0.0025 m^2/h. The underlying aggregate ballast layer is defined by a thermal conductivity, λ, value of 2.58 kcal/hmC^o and a thermal diffusivity, α, value of 0.0030 m^2/h.

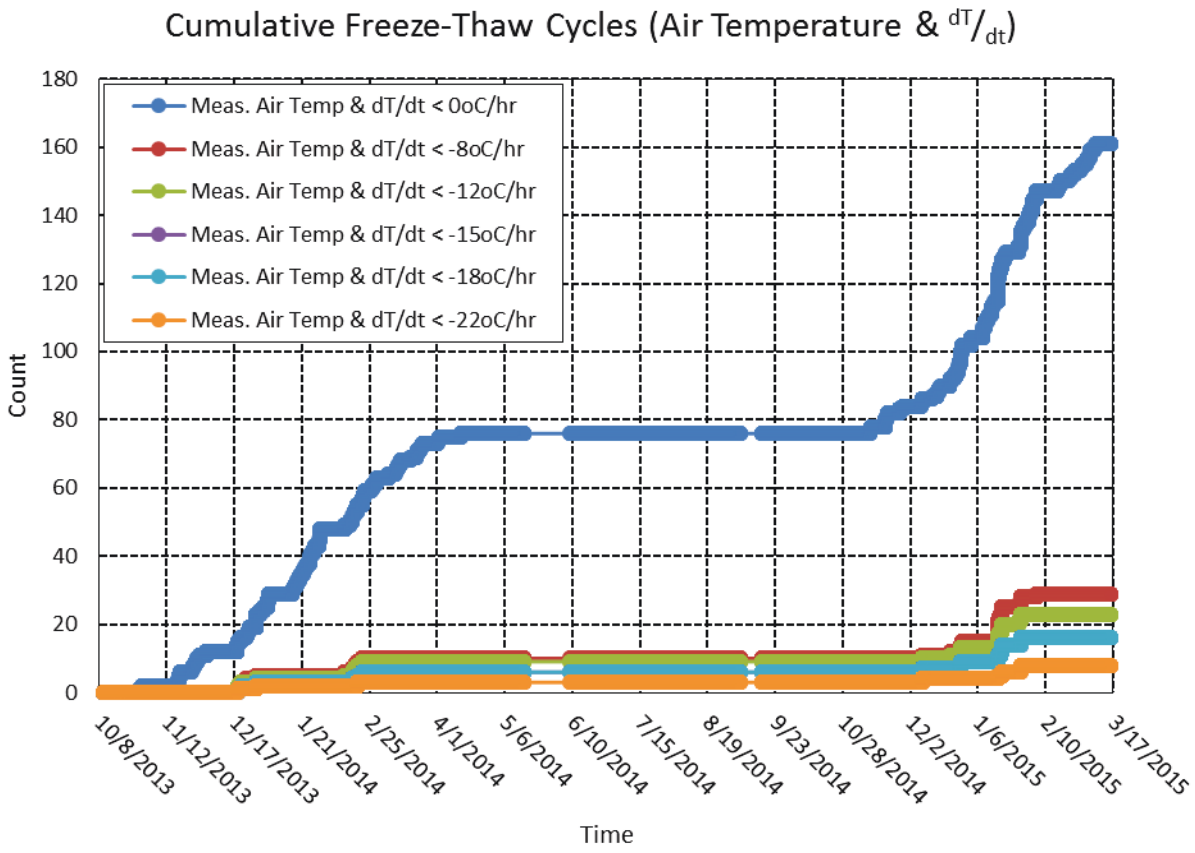

Figure C-7 Cumulative number of freeze-thaw cycles in Lytton, BC, from October 8, 2013, through March 17, 2015, when both freezing air temperatures and minimum rate of freezing is achieved at time of freezing.

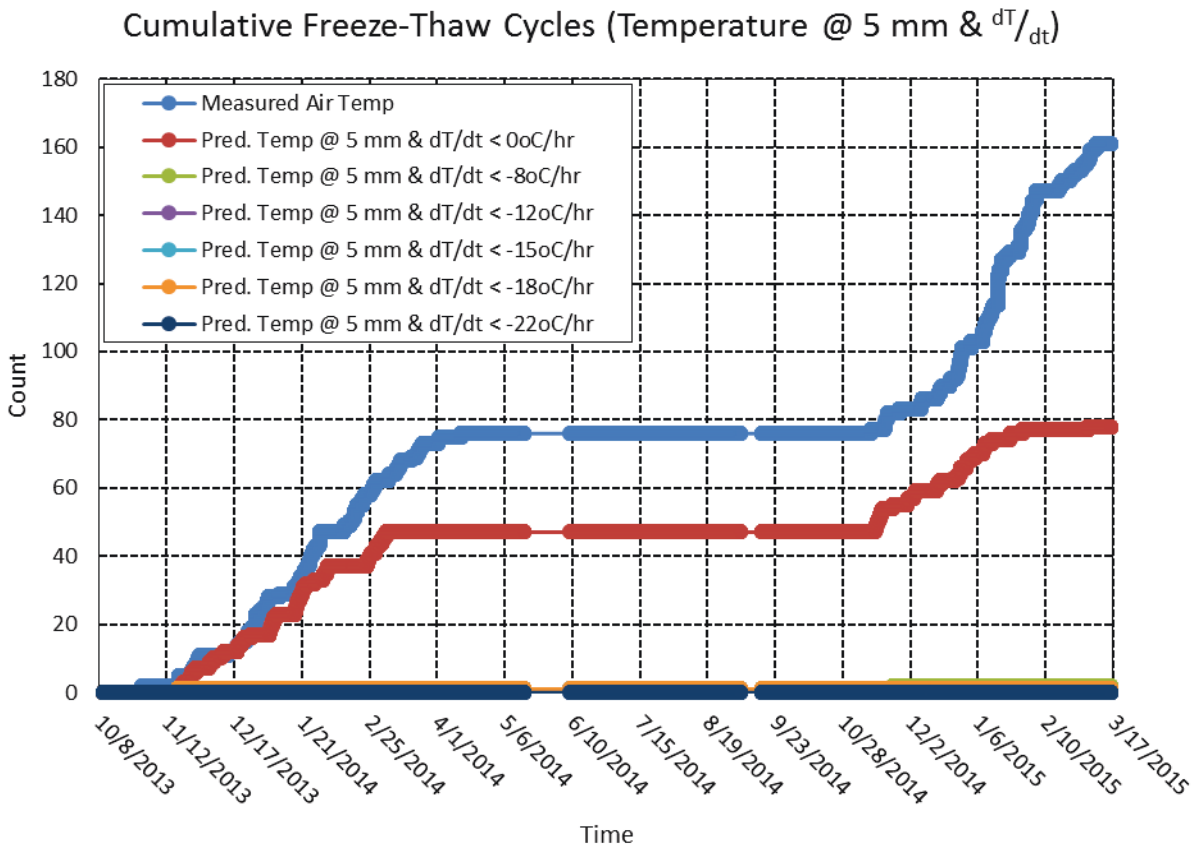

Figure C-8 Cumulative number of freeze-thaw cycles in Rantoul, IL, from September 3, 2013, through September 8, 2015, when both freezing temperatures at a depth of 5 mm and minimum rate of freezing is achieved at time of freezing. Predicted internal temperature values are computed using a 2-layered system whose upper concrete layer is defined by a thermal conductivity, λ, value of 1.85 kcal/hmC^o and a thermal diffusivity, α, value of 0.0025 m^2/h. The underlying aggregate ballast layer is defined by a thermal conductivity, λ, value of 2.58 kcal/hmC^o and a thermal diffusivity, α, value of 0.0030 m^2/h.

Modeled freeze-thaw cycles of concrete in Rantoul, IL, due to saturation (modeled with D = 0.86 and initial RH = 85%)

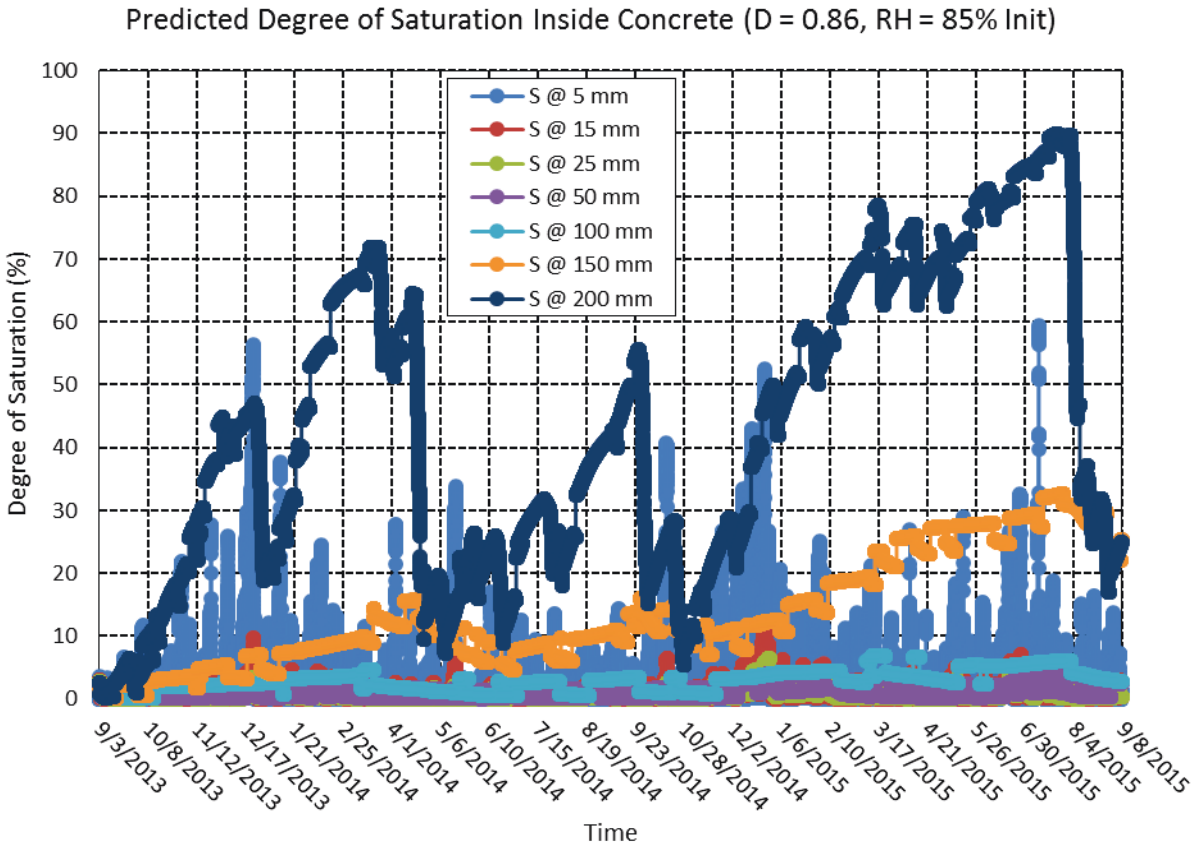

Figure C-9 Predicted degree of saturation inside a 1-layered concrete system in Rantoul, IL, from September 3, 2013, through September 8, 2015. The concrete is defined by a diffusivity (at S = 100%) value of 0.86×10^{-6} m^2/hr, a regression coefficient, *n*, of 15, α value of 0.05, and an empirical correlation between relative humidity and degree of saturation. The simulation is initialized with an even distribution of 85 %RH throughout the depth of the concrete.

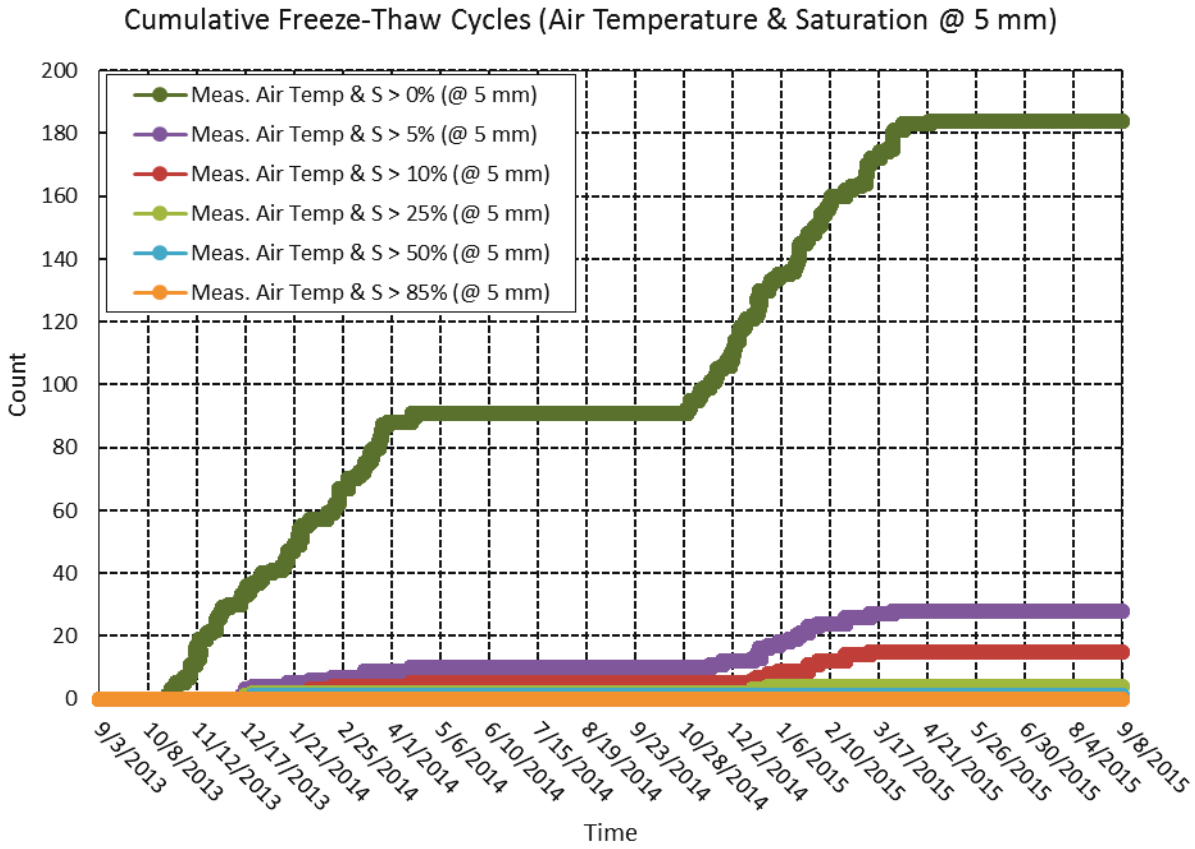

Figure C-10 Cumulative number of freeze-thaw cycles in Rantoul, IL, from September 3, 2013, through September 8, 2015, at a depth of 5 mm when both freezing air temperatures and minimum degree of saturation is achieved at time of freezing. Predicted degree of saturation is defined by a diffusivity (at S = 100%) value of 0.86×10^{-6} m^2/hr, a regression coefficient, *n*, of 15, α value of 0.05, and an empirical correlation between relative humidity and degree of saturation. The simulation is initialized with an even distribution of 85 %RH throughout the depth of the concrete.

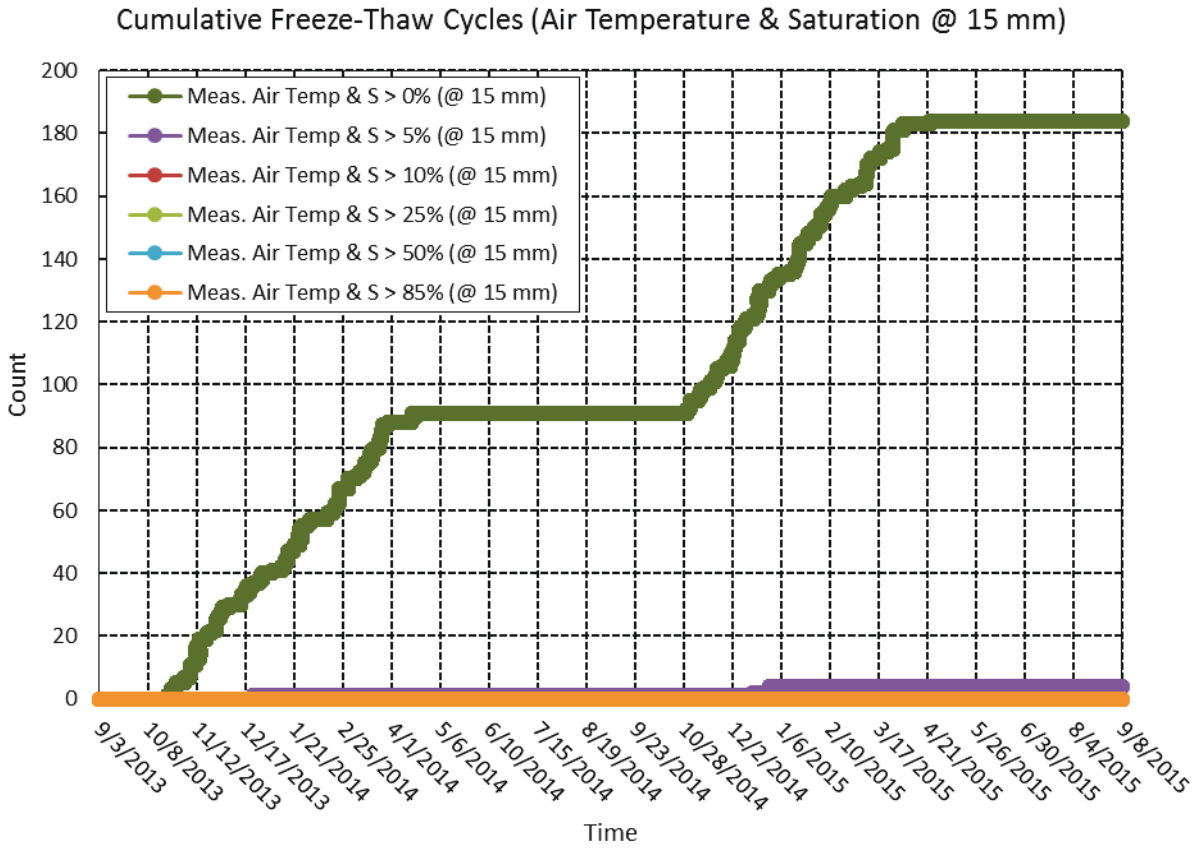

Figure C-11 Cumulative number of freeze-thaw cycles in Rantoul, IL, from September 3, 2013, through September 8, 2015, at a depth of 15 mm when both freezing air temperatures and minimum degree of saturation is achieved at time of freezing. Predicted degree of saturation is defined by a diffusivity (at S = 100%) value of 0.86×10^{-6} m^2/hr, a regression coefficient, *n*, of 15, α value of 0.05, and an empirical correlation between relative humidity and degree of saturation. The simulation is initialized with an even distribution of 85 %RH throughout the depth of the concrete.

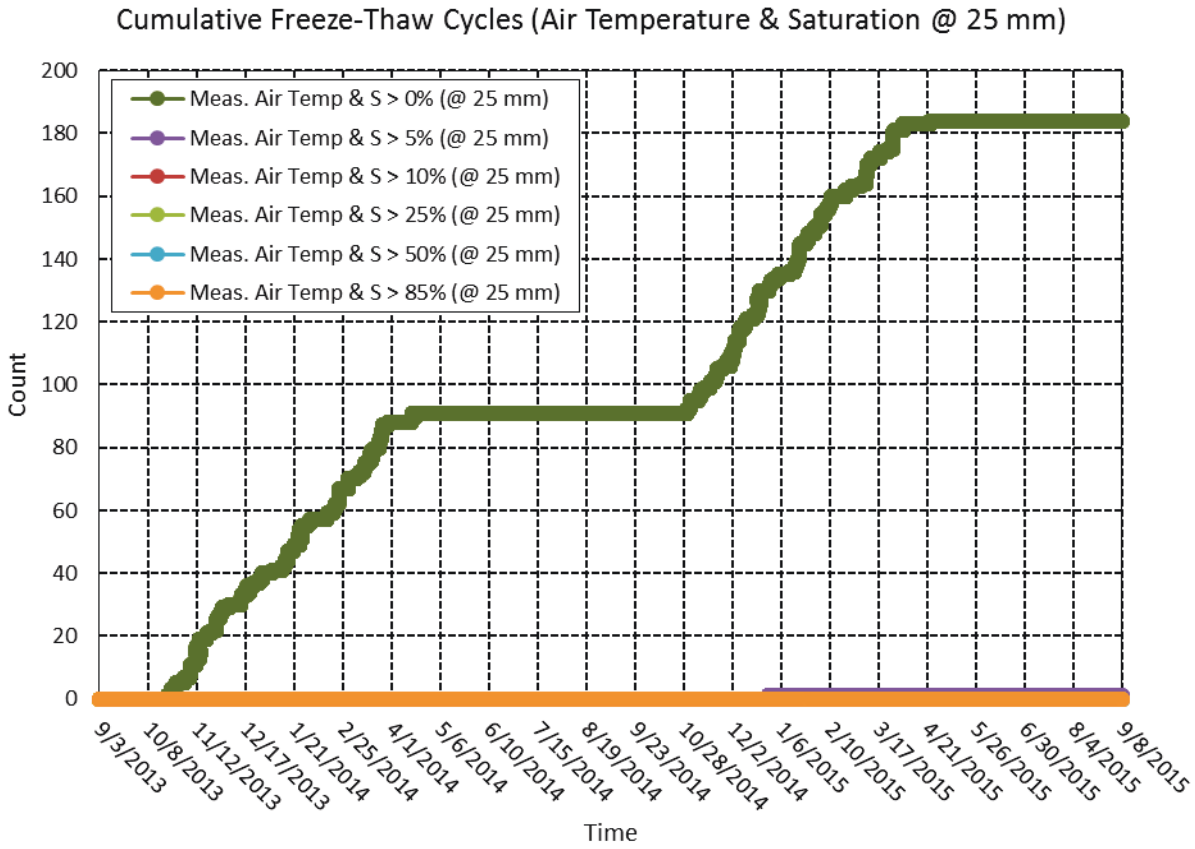

Figure C-12 Cumulative number of freeze-thaw cycles in Rantoul, IL, from September 3, 2013, through September 8, 2015, at a depth of 25 mm when both freezing air temperatures and minimum degree of saturation is achieved at time of freezing. Predicted degree of saturation is defined by a diffusivity (at S = 100%) value of 0.86×10^{-6} m^2/hr, a regression coefficient, *n*, of 15, α value of 0.05, and an empirical correlation between relative humidity and degree of saturation. The simulation is initialized with an even distribution of 85 %RH throughout the depth of the concrete.

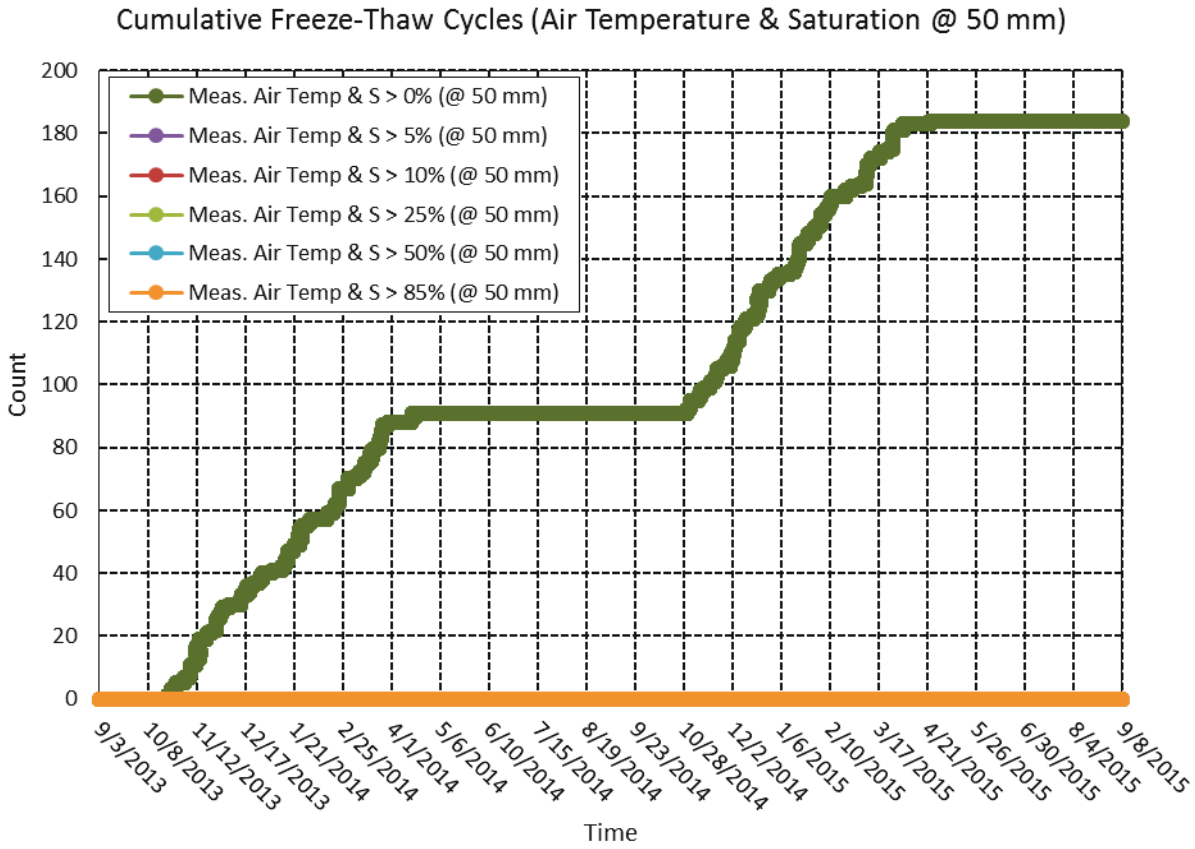

Figure C-13 Cumulative number of freeze-thaw cycles in Rantoul, IL, from September 3, 2013, through September 8, 2015, at a depth of 50 mm when both freezing air temperatures and minimum degree of saturation is achieved at time of freezing. Predicted degree of saturation is defined by a diffusivity (at S = 100%) value of 0.86×10^{-6} m^2/hr, a regression coefficient, *n*, of 15, α value of 0.05, and an empirical correlation between relative humidity and degree of saturation. The simulation is initialized with an even distribution of 85 %RH throughout the depth of the concrete.

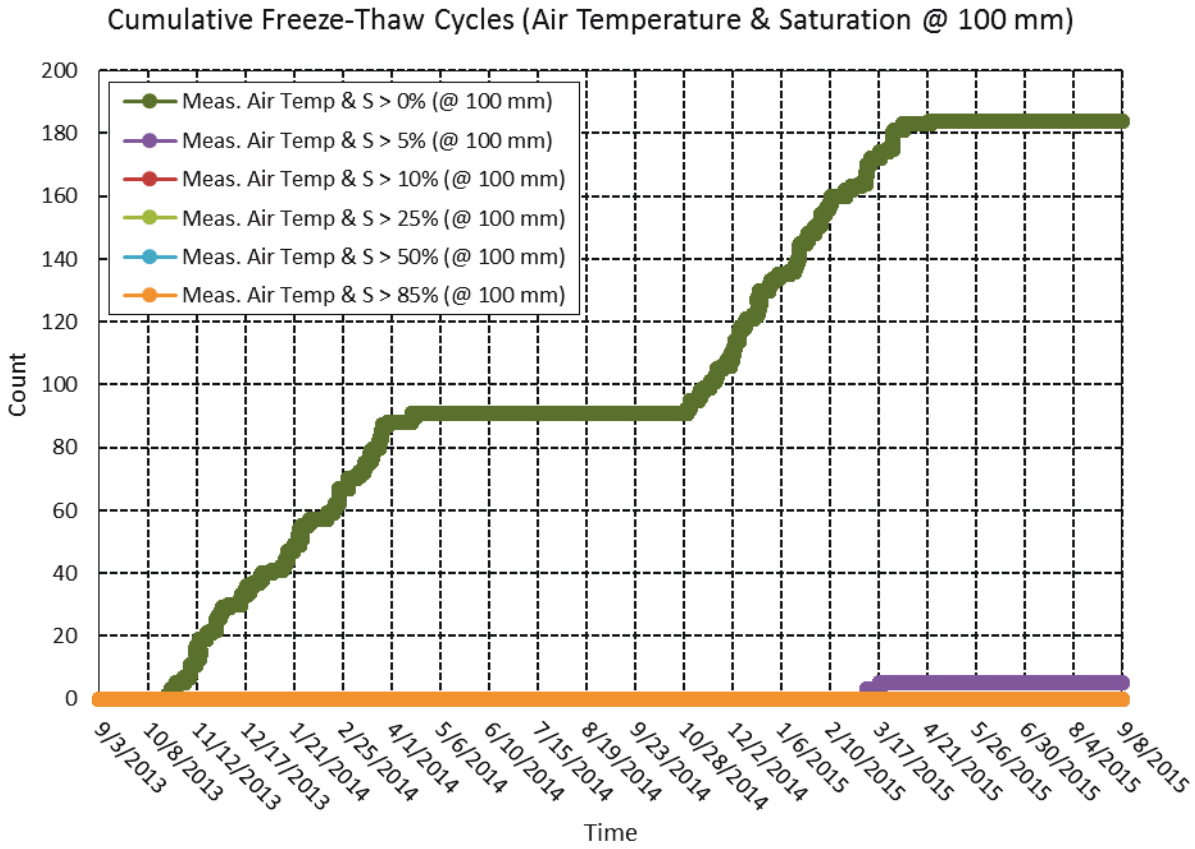

Figure C-14 Cumulative number of freeze-thaw cycles in Rantoul, IL, from September 3, 2013, through September 8, 2015, at a depth of 100 mm when both freezing air temperatures and minimum degree of saturation is achieved at time of freezing. Predicted degree of saturation is defined by a diffusivity (at S = 100%) value of 0.86×10^{-6} m^2/hr, a regression coefficient, *n*, of 15, α value of 0.05, and an empirical correlation between relative humidity and degree of saturation. The simulation is initialized with an even distribution of 85 %RH throughout the depth of the concrete.

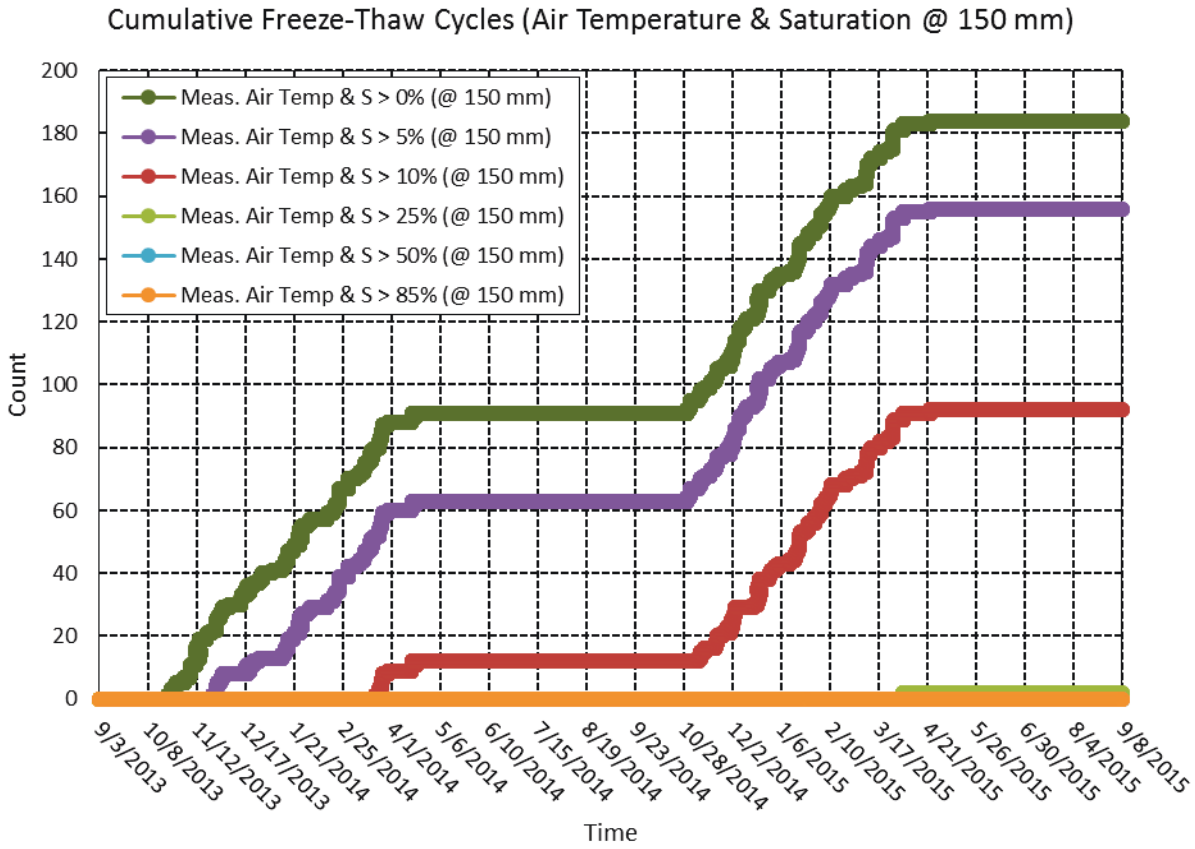

Figure C-15 Cumulative number of freeze-thaw cycles in Rantoul, IL, from September 3, 2013, through September 8, 2015, at a depth of 150 mm when both freezing air temperatures and minimum degree of saturation is achieved at time of freezing. Predicted degree of saturation is defined by a diffusivity (at S = 100%) value of 0.86×10^{-6} m^2/hr, a regression coefficient, *n*, of 15, α value of 0.05, and an empirical correlation between relative humidity and degree of saturation. The simulation is initialized with an even distribution of 85 %RH throughout the depth of the concrete.

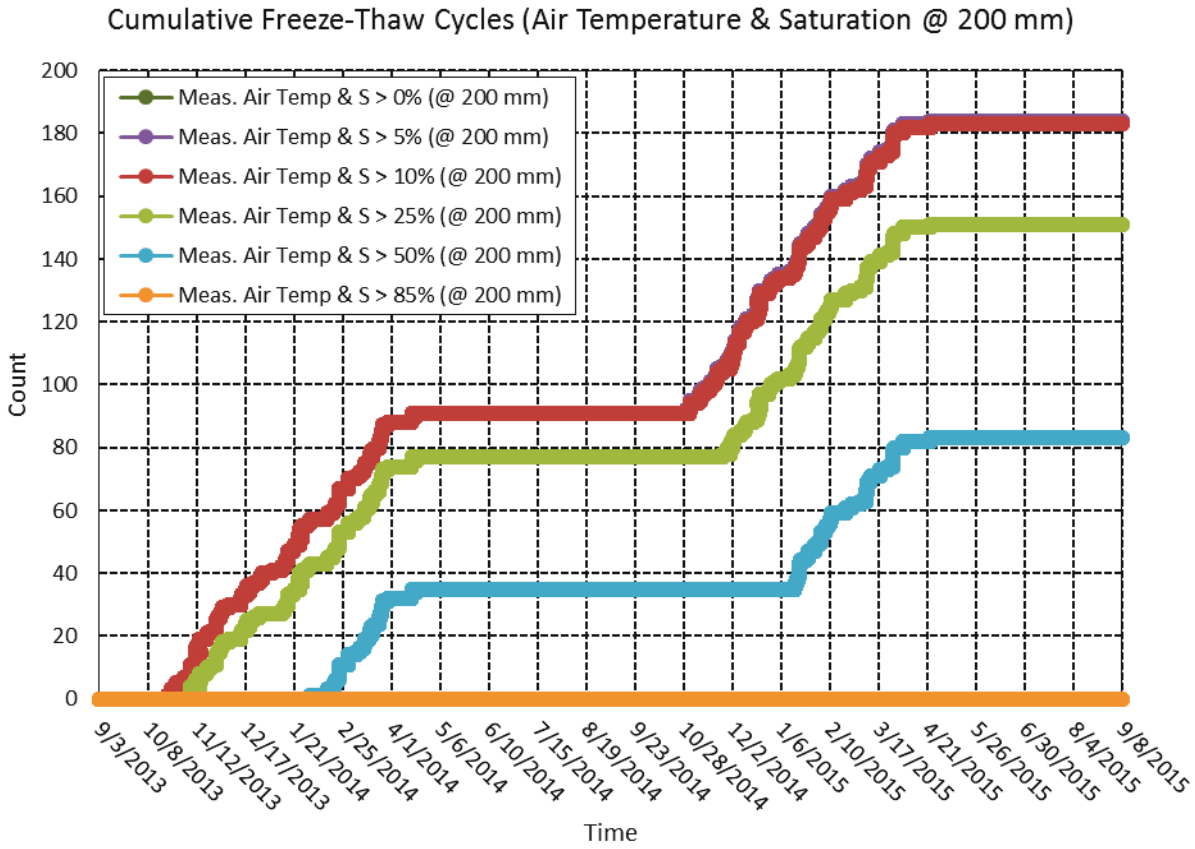

Figure C-16 Cumulative number of freeze-thaw cycles in Rantoul, IL, from September 3, 2013, through September 8, 2015, at a depth of 200 mm when both freezing air temperatures and minimum degree of saturation is achieved at time of freezing. Predicted degree of saturation is defined by a diffusivity (at S = 100%) value of 0.86×10^{-6} m^2/hr, a regression coefficient, *n*, of 15, α value of 0.05, and an empirical correlation between relative humidity and degree of saturation. The simulation is initialized with an even distribution of 85 %RH throughout the depth of the concrete.

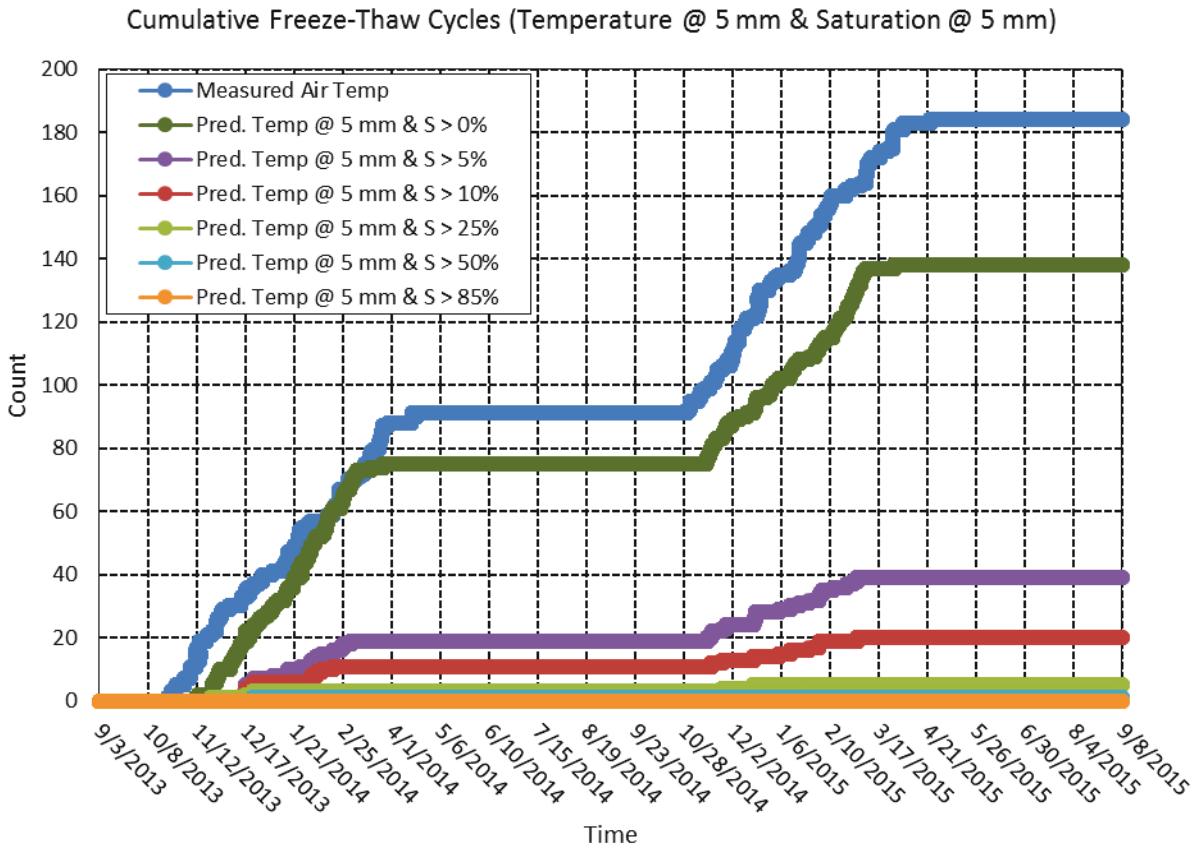

Figure C-17 Cumulative number of freeze-thaw cycles in Rantoul, IL, from September 3, 2013, through September 8, 2015, at a depth of 5 mm when both freezing temperatures and minimum degree of saturation is achieved at time of freezing. Predicted internal temperature values are computed using a 2-layered system whose upper concrete layer is defined by a thermal conductivity, λ, value of 1.85 kcal/hmC^o and a thermal diffusivity, α, value of 0.0025 m^2/h. The underlying aggregate ballast layer is defined by a thermal conductivity, λ, value of 2.58 kcal/hmC^o and a thermal diffusivity, α, value of 0.0030 m^2/h. Predicted degree of saturation is defined by a diffusivity (at S = 100%) value of 0.86x10^{-6} m^2/hr, a regression coefficient, n, of 15, α value of 0.05, and an empirical correlation between relative humidity and degree of saturation. The simulation is initialized with an even distribution of 85 %RH throughout the depth of the concrete.

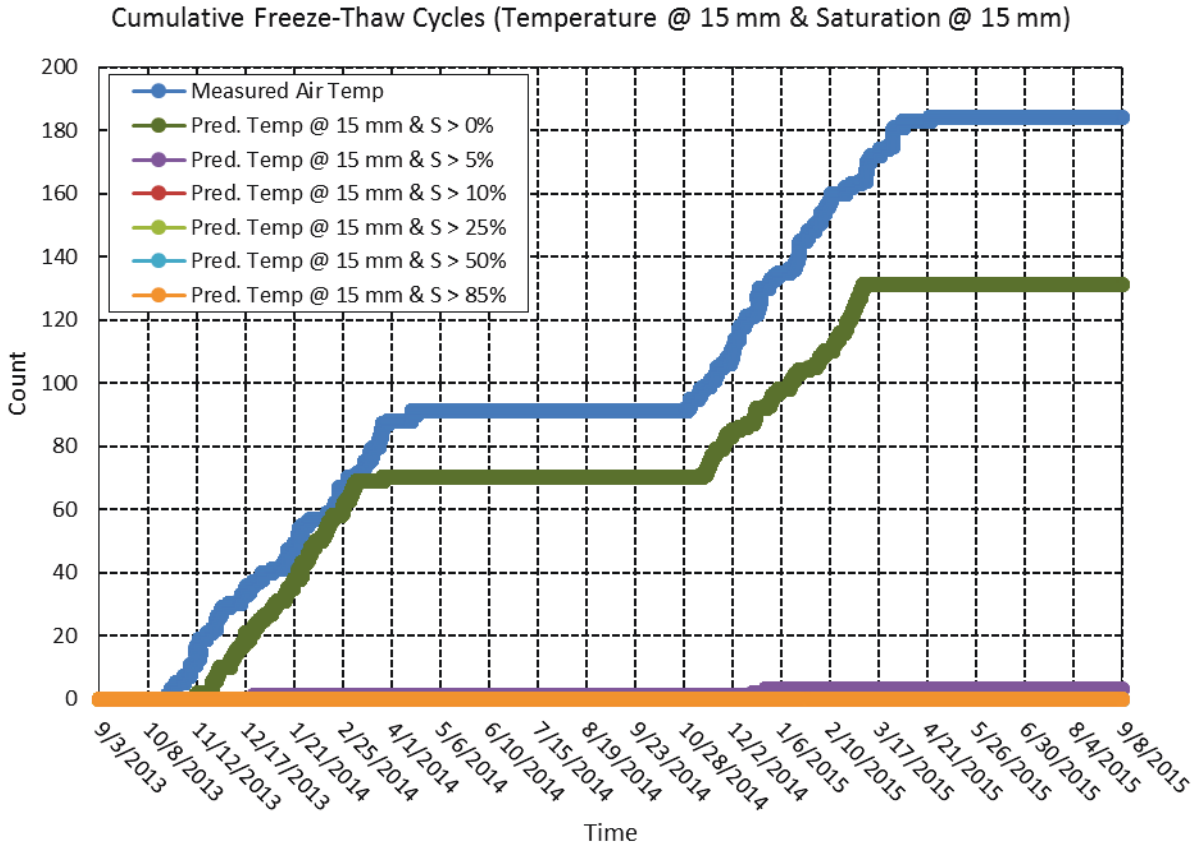

Figure C-18 Cumulative number of freeze-thaw cycles in Rantoul, IL, from September 3, 2013, through September 8, 2015, at a depth of 15 mm when both freezing temperatures and minimum degree of saturation is achieved at time of freezing. Predicted internal temperature values are computed using a 2-layered system whose upper concrete layer is defined by a thermal conductivity, λ, value of 1.85 kcal/hmC^o and a thermal diffusivity, α, value of 0.0025 m^2/h. The underlying aggregate ballast layer is defined by a thermal conductivity, λ, value of 2.58 kcal/hmC^o and a thermal diffusivity, α, value of 0.0030 m^2/h. Predicted degree of saturation is defined by a diffusivity (at S = 100%) value of 0.86x10^{-6} m^2/hr, a regression coefficient, n, of 15, α value of 0.05, and an empirical correlation between relative humidity and degree of saturation. The simulation is initialized with an even distribution of 85 %RH throughout the depth of the concrete.

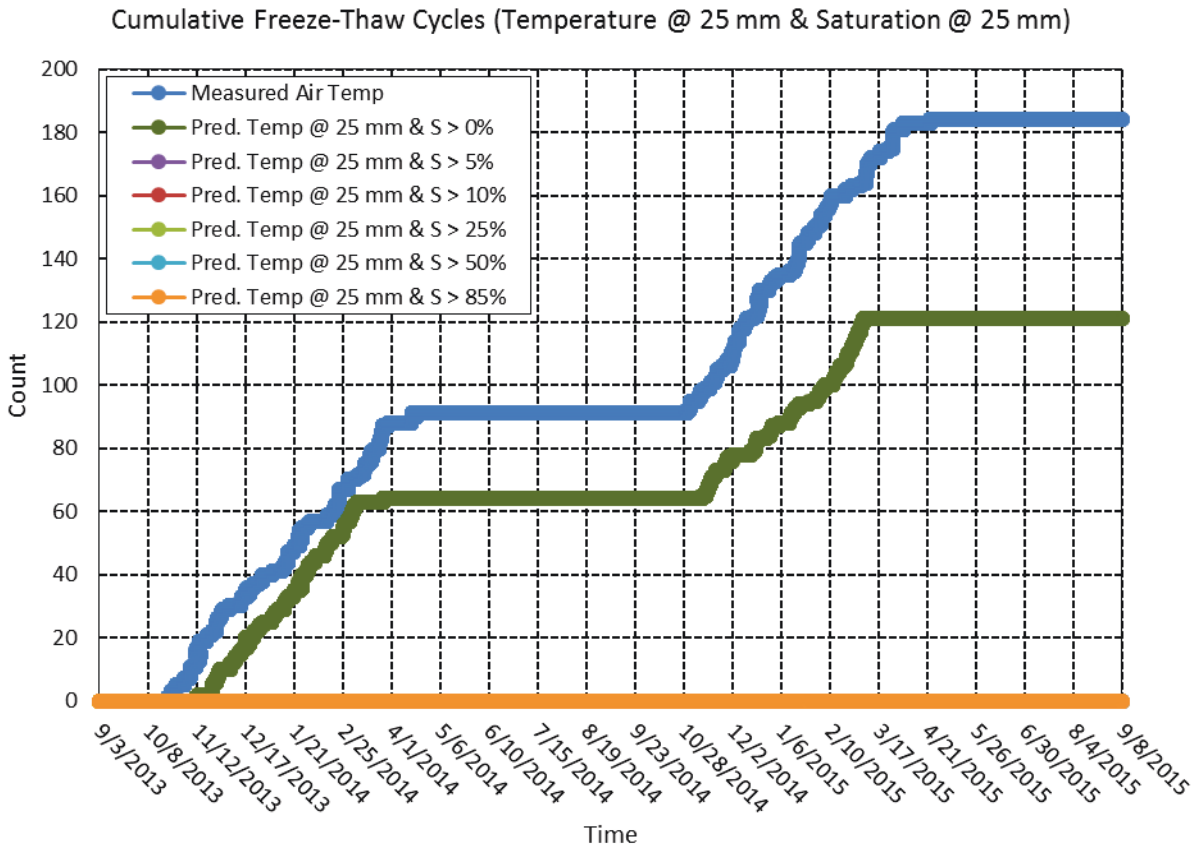

Figure C-19 Cumulative number of freeze-thaw cycles in Rantoul, IL, from September 3, 2013, through September 8, 2015, at a depth of 25 mm when both freezing temperatures and minimum degree of saturation is achieved at time of freezing. Predicted internal temperature values are computed using a 2-layered system whose upper concrete layer is defined by a thermal conductivity, λ, value of 1.85 kcal/hmC^o and a thermal diffusivity, α, value of 0.0025 m^2/h. The underlying aggregate ballast layer is defined by a thermal conductivity, λ, value of 2.58 kcal/hmC^o and a thermal diffusivity, α, value of 0.0030 m^2/h. Predicted degree of saturation is defined by a diffusivity (at S = 100%) value of 0.86x10^{-6} m^2/hr, a regression coefficient, n, of 15, α value of 0.05, and an empirical correlation between relative humidity and degree of saturation. The simulation is initialized with an even distribution of 85 %RH throughout the depth of the concrete.

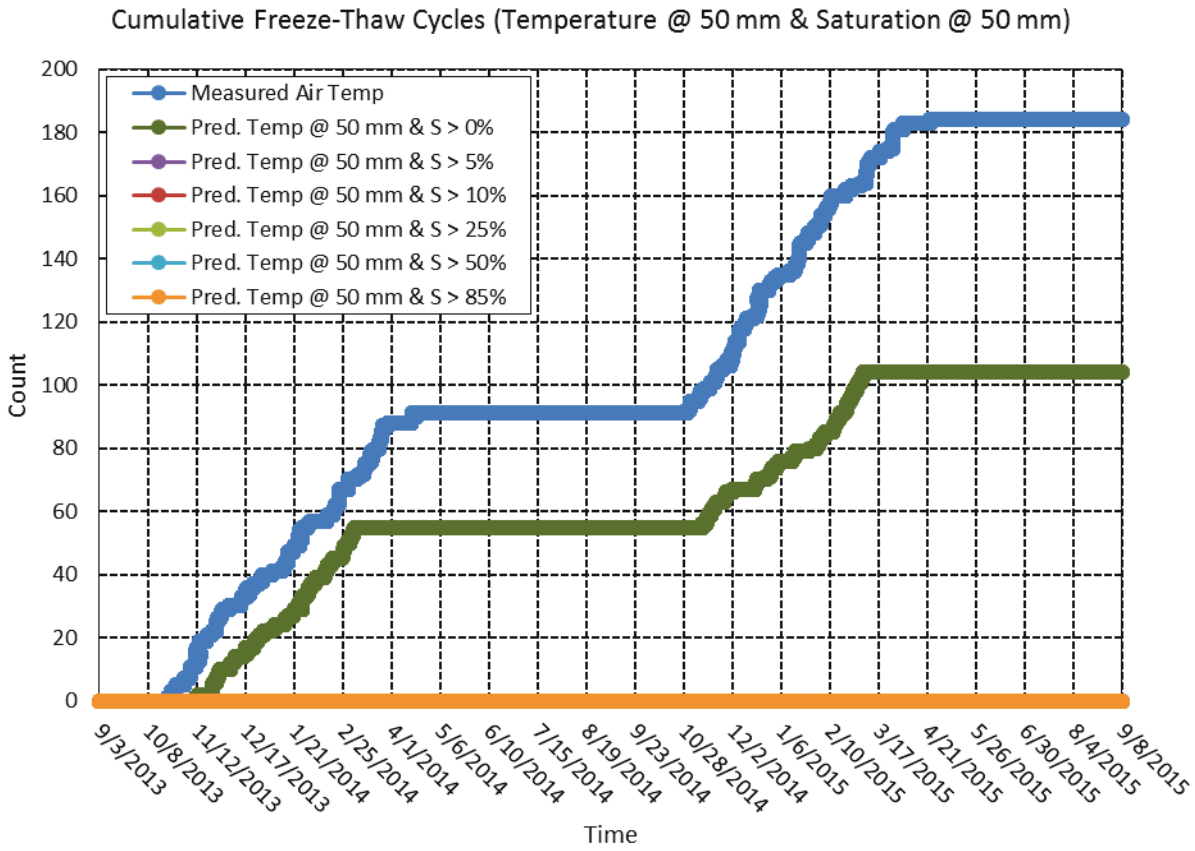

Figure C-20 Cumulative number of freeze-thaw cycles in Rantoul, IL, from September 3, 2013, through September 8, 2015, at a depth of 50 mm when both freezing temperatures and minimum degree of saturation is achieved at time of freezing. Predicted internal temperature values are computed using a 2-layered system whose upper concrete layer is defined by a thermal conductivity, λ, value of 1.85 kcal/hmC^o and a thermal diffusivity, α, value of 0.0025 m^2/h. The underlying aggregate ballast layer is defined by a thermal conductivity, λ, value of 2.58 kcal/hmC^o and a thermal diffusivity, α, value of 0.0030 m^2/h. Predicted degree of saturation is defined by a diffusivity (at S = 100%) value of 0.86x10^{-6} m^2/hr, a regression coefficient, n, of 15, α value of 0.05, and an empirical correlation between relative humidity and degree of saturation. The simulation is initialized with an even distribution of 85 %RH throughout the depth of the concrete.

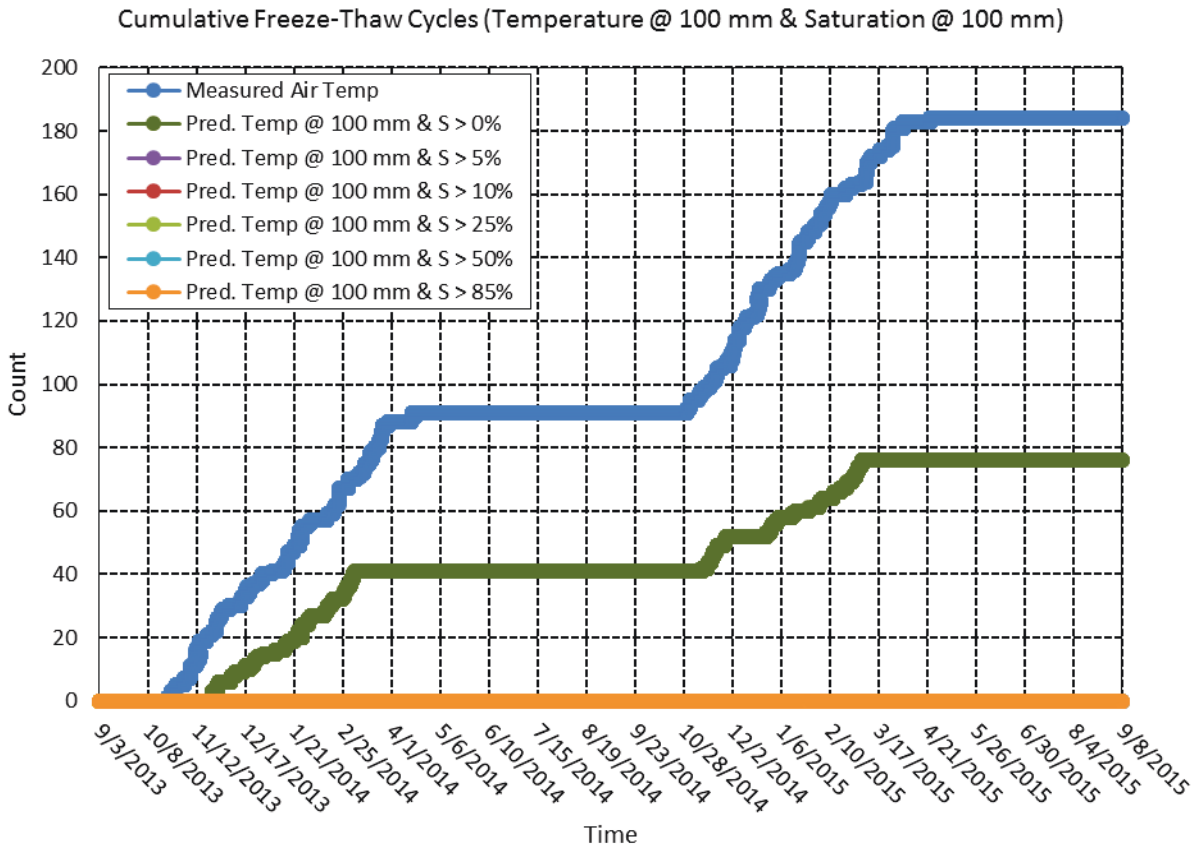

Figure C-21 Cumulative number of freeze-thaw cycles in Rantoul, IL, from September 3, 2013, through September 8, 2015, at a depth of 100 mm when both freezing temperatures and minimum degree of saturation is achieved at time of freezing. Predicted internal temperature values are computed using a 2-layered system whose upper concrete layer is defined by a thermal conductivity, λ, value of 1.85 kcal/hmC^o and a thermal diffusivity, α, value of 0.0025 m^2/h. The underlying aggregate ballast layer is defined by a thermal conductivity, λ, value of 2.58 kcal/hmC^o and a thermal diffusivity, α, value of 0.0030 m^2/h. Predicted degree of saturation is defined by a diffusivity (at S = 100%) value of 0.86x10^{-6} m^2/hr, a regression coefficient, n, of 15, α value of 0.05, and an empirical correlation between relative humidity and degree of saturation. The simulation is initialized with an even distribution of 85 %RH throughout the depth of the concrete.

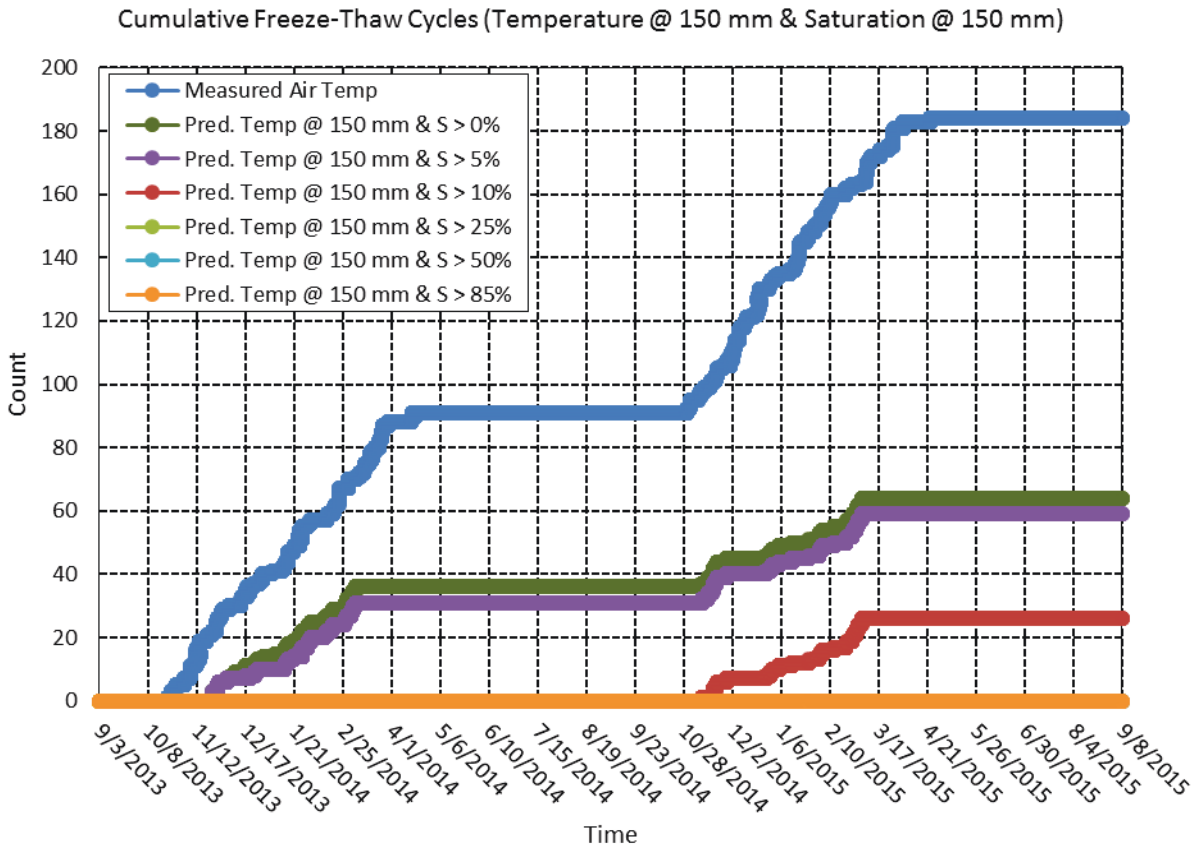

Figure C-22 Cumulative number of freeze-thaw cycles in Rantoul, IL, from September 3, 2013, through September 8, 2015, at a depth of 150 mm when both freezing temperatures and minimum degree of saturation is achieved at time of freezing. Predicted internal temperature values are computed using a 2-layered system whose upper concrete layer is defined by a thermal conductivity, λ, value of 1.85 kcal/hmC^o and a thermal diffusivity, α, value of 0.0025 m^2/h. The underlying aggregate ballast layer is defined by a thermal conductivity, λ, value of 2.58 kcal/hmC^o and a thermal diffusivity, α, value of 0.0030 m^2/h. Predicted degree of saturation is defined by a diffusivity (at S = 100%) value of 0.86x10^{-6} m^2/hr, a regression coefficient, n, of 15, α value of 0.05, and an empirical correlation between relative humidity and degree of saturation. The simulation is initialized with an even distribution of 85 %RH throughout the depth of the concrete.

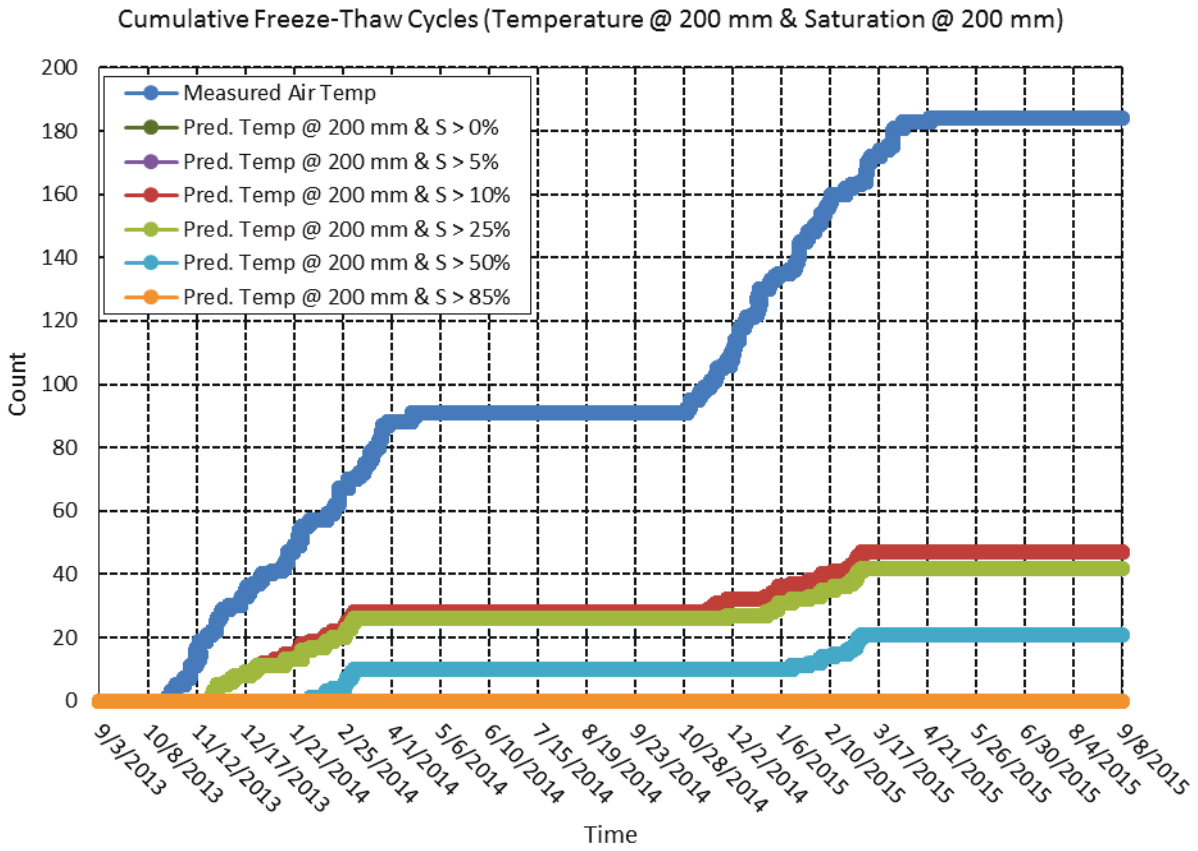

Figure C-23 Cumulative number of freeze-thaw cycles in Rantoul, IL, from September 3, 2013, through September 8, 2015, at a depth of 200 mm when both freezing temperatures and minimum degree of saturation is achieved at time of freezing. Predicted internal temperature values are computed using a 2-layered system whose upper concrete layer is defined by a thermal conductivity, λ, value of 1.85 kcal/hmC^o and a thermal diffusivity, α, value of 0.0025 m^2/h. The underlying aggregate ballast layer is defined by a thermal conductivity, λ, value of 2.58 kcal/hmC^o and a thermal diffusivity, α, value of 0.0030 m^2/h. Predicted degree of saturation is defined by a diffusivity (at S = 100%) value of 0.86x10^{-6} m^2/hr, a regression coefficient, n, of 15, α value of 0.05, and an empirical correlation between relative humidity and degree of saturation. The simulation is initialized with an even distribution of 85 %RH throughout the depth of the concrete.

Modeled freeze-thaw cycles of concrete in Rantoul, IL, due to saturation (modeled with D = 1.29 and initial RH = 85%)

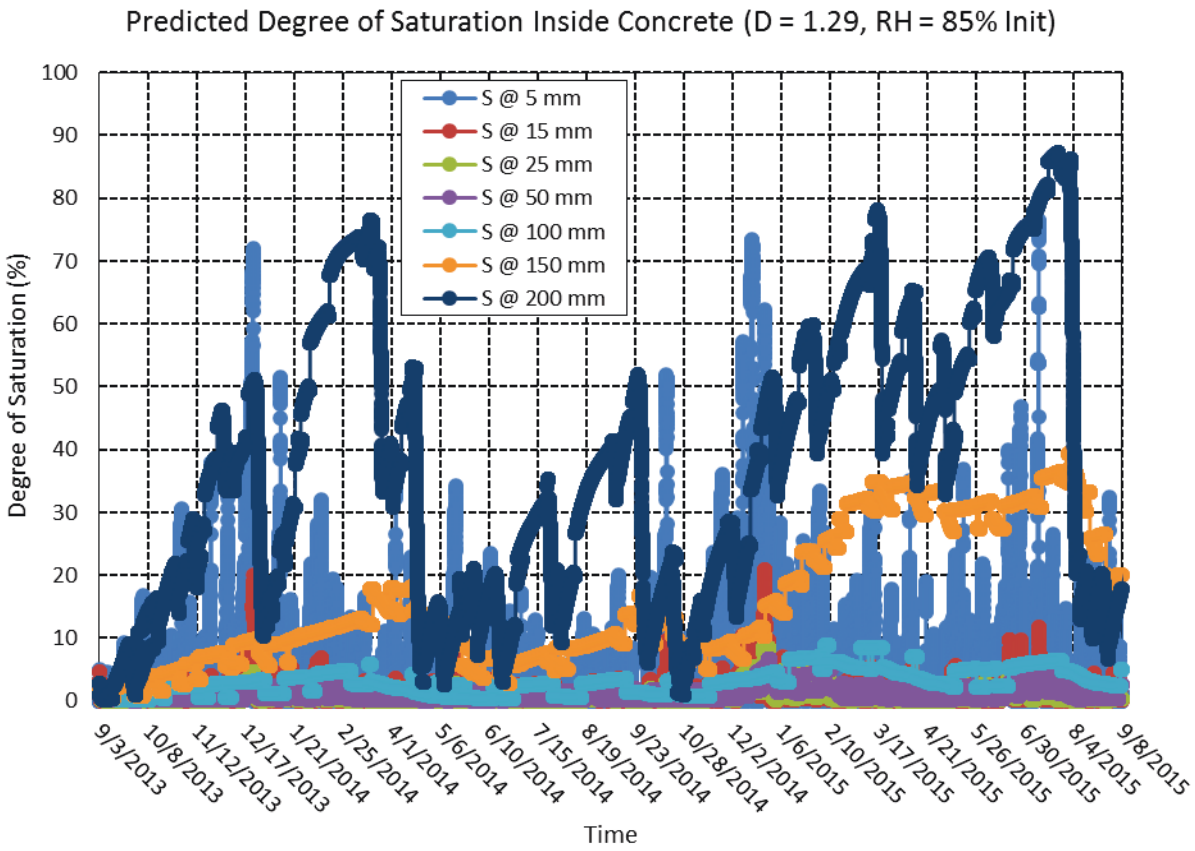

Figure C-24 Predicted degree of saturation inside a 1-layered concrete system in Rantoul, IL, from September 3, 2013, through September 8, 2015. The concrete is defined by a diffusivity (at S = 100%) value of 1.29×10^{-6} m^2/hr, a regression coefficient, *n*, of 15, α value of 0.05, and an empirical correlation between relative humidity and degree of saturation. The simulation is initialized with an even distribution of 85 %RH throughout the depth of the concrete.

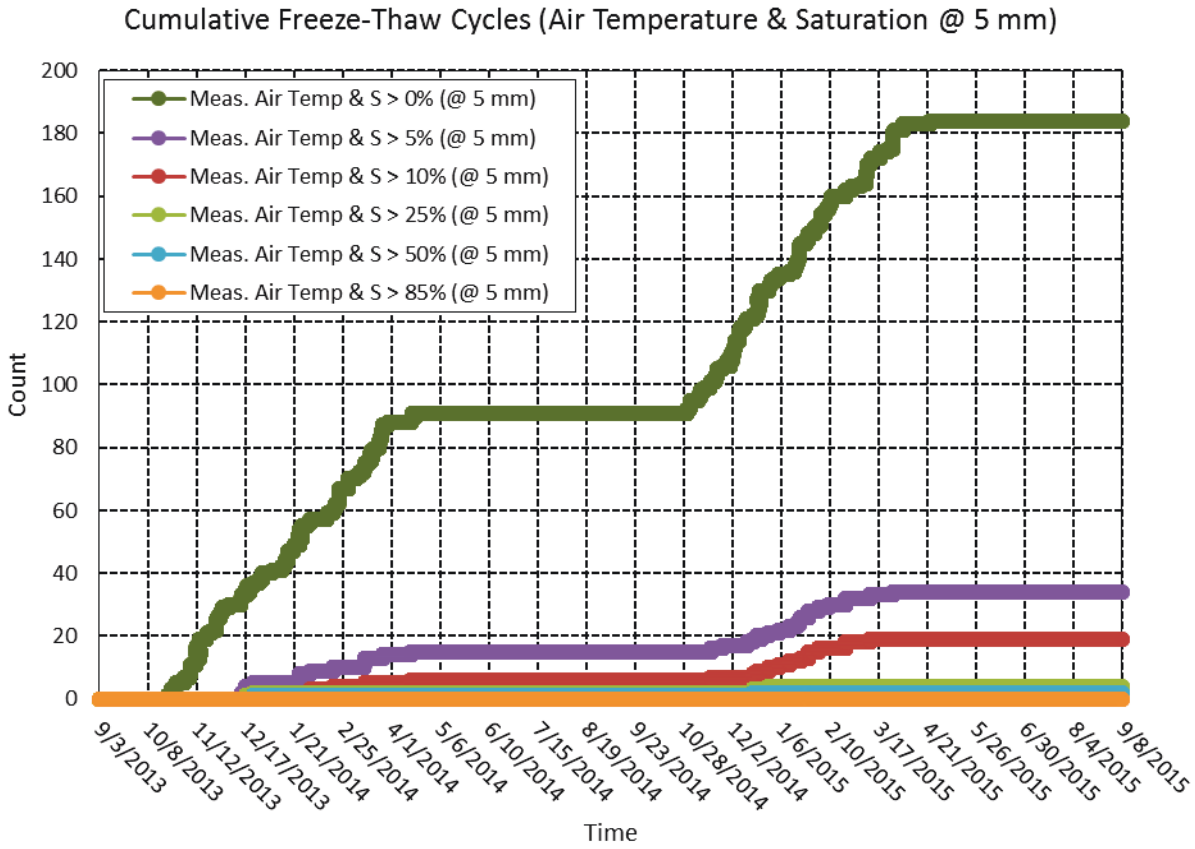

Figure C-25 Cumulative number of freeze-thaw cycles in Rantoul, IL, from September 3, 2013, through September 8, 2015, at a depth of 5 mm when both freezing air temperatures and minimum degree of saturation is achieved at time of freezing. Predicted degree of saturation is defined by a diffusivity (at S = 100%) value of 1.29×10^{-6} m^2/hr, a regression coefficient, *n*, of 15, α value of 0.05, and an empirical correlation between relative humidity and degree of saturation. The simulation is initialized with an even distribution of 85 %RH throughout the depth of the concrete.

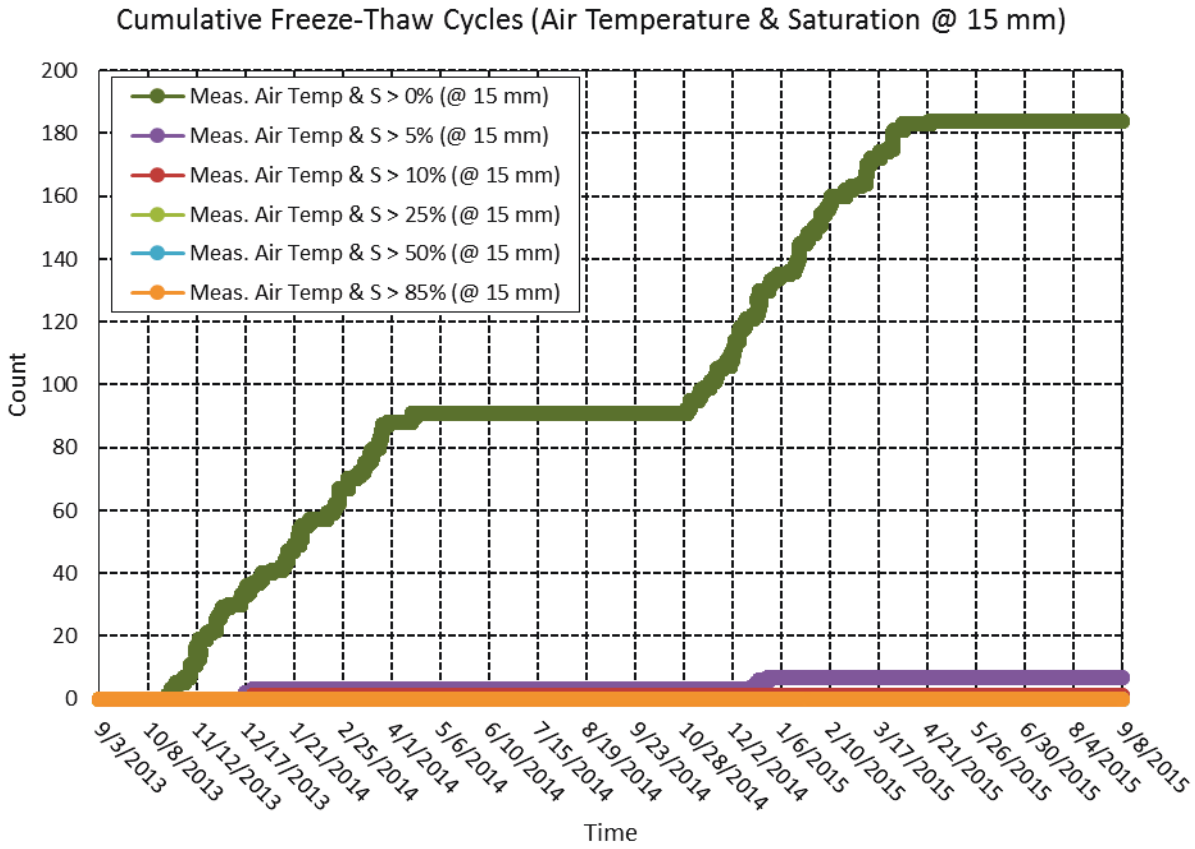

Figure C-26 Cumulative number of freeze-thaw cycles in Rantoul, IL, from September 3, 2013, through September 8, 2015, at a depth of 15 mm when both freezing air temperatures and minimum degree of saturation is achieved at time of freezing. Predicted degree of saturation is defined by a diffusivity (at S = 100%) value of 1.29×10^{-6} m^2/hr, a regression coefficient, *n*, of 15, α value of 0.05, and an empirical correlation between relative humidity and degree of saturation. The simulation is initialized with an even distribution of 85 %RH throughout the depth of the concrete.

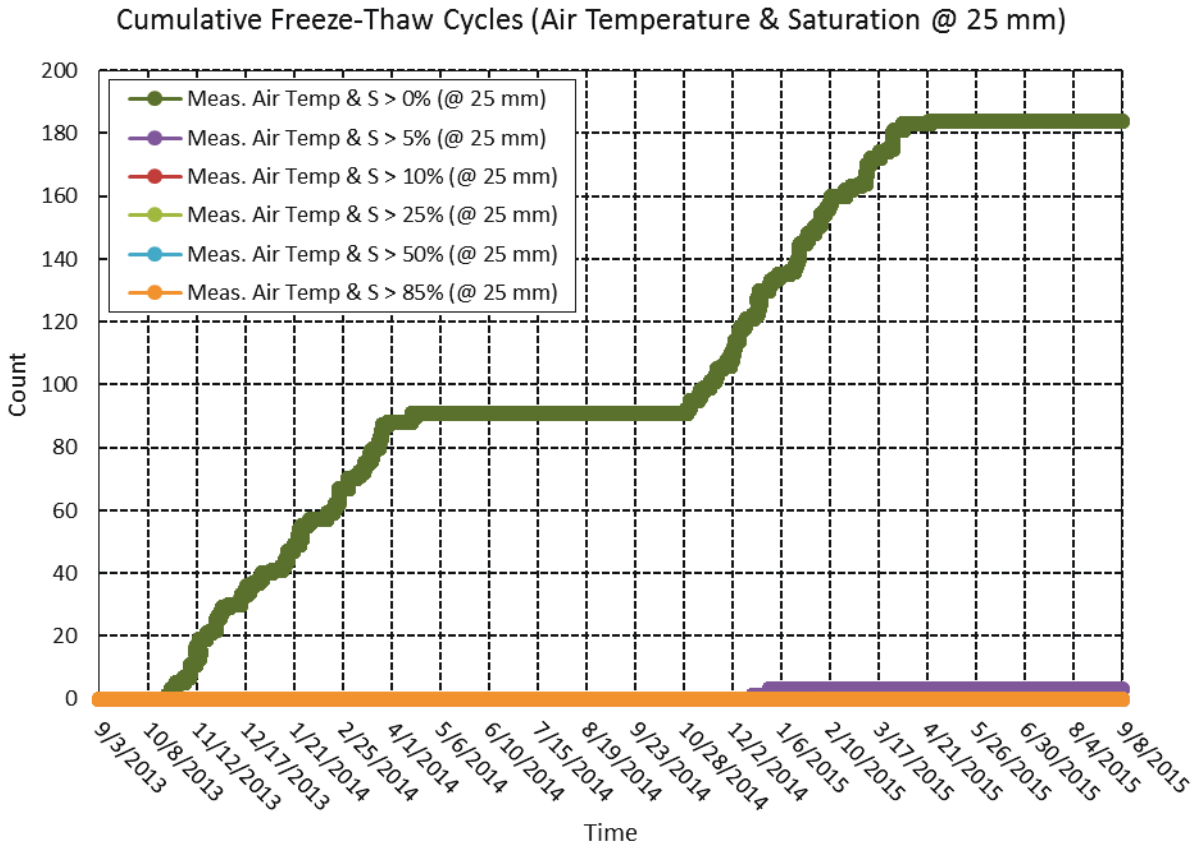

Figure C-27 Cumulative number of freeze-thaw cycles in Rantoul, IL, from September 3, 2013, through September 8, 2015, at a depth of 25 mm when both freezing air temperatures and minimum degree of saturation is achieved at time of freezing. Predicted degree of saturation is defined by a diffusivity (at S = 100%) value of 1.29×10^{-6} m^2/hr, a regression coefficient, *n*, of 15, α value of 0.05, and an empirical correlation between relative humidity and degree of saturation. The simulation is initialized with an even distribution of 85 %RH throughout the depth of the concrete.

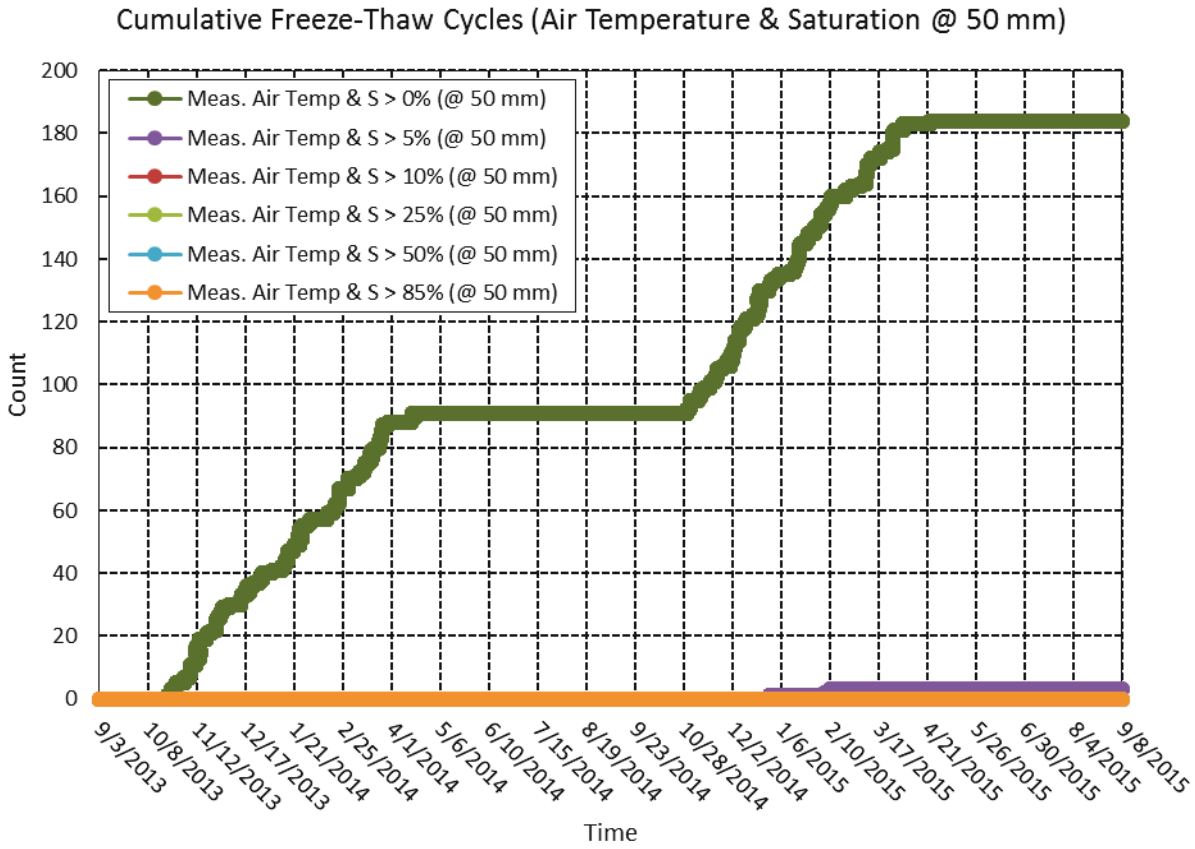

Figure C-28 Cumulative number of freeze-thaw cycles in Rantoul, IL, from September 3, 2013, through September 8, 2015, at a depth of 50 mm when both freezing air temperatures and minimum degree of saturation is achieved at time of freezing. Predicted degree of saturation is defined by a diffusivity (at S = 100%) value of 1.29×10^{-6} m^2/hr, a regression coefficient, *n*, of 15, α value of 0.05, and an empirical correlation between relative humidity and degree of saturation. The simulation is initialized with an even distribution of 85 %RH throughout the depth of the concrete.

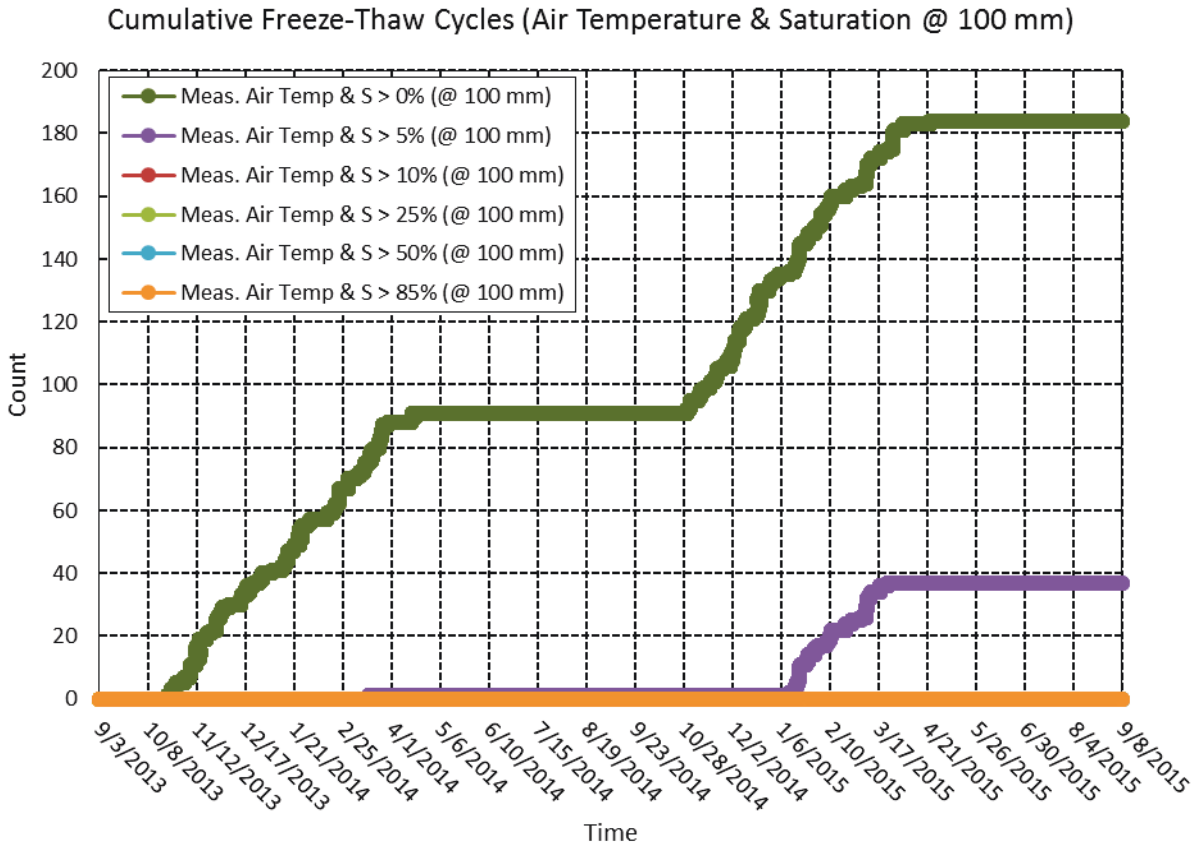

Figure C-29 Cumulative number of freeze-thaw cycles in Rantoul, IL, from September 3, 2013, through September 8, 2015, at a depth of 100 mm when both freezing air temperatures and minimum degree of saturation is achieved at time of freezing. Predicted degree of saturation is defined by a diffusivity (at S = 100%) value of 1.29×10^{-6} m^2/hr, a regression coefficient, *n*, of 15, α value of 0.05, and an empirical correlation between relative humidity and degree of saturation. The simulation is initialized with an even distribution of 85 %RH throughout the depth of the concrete.

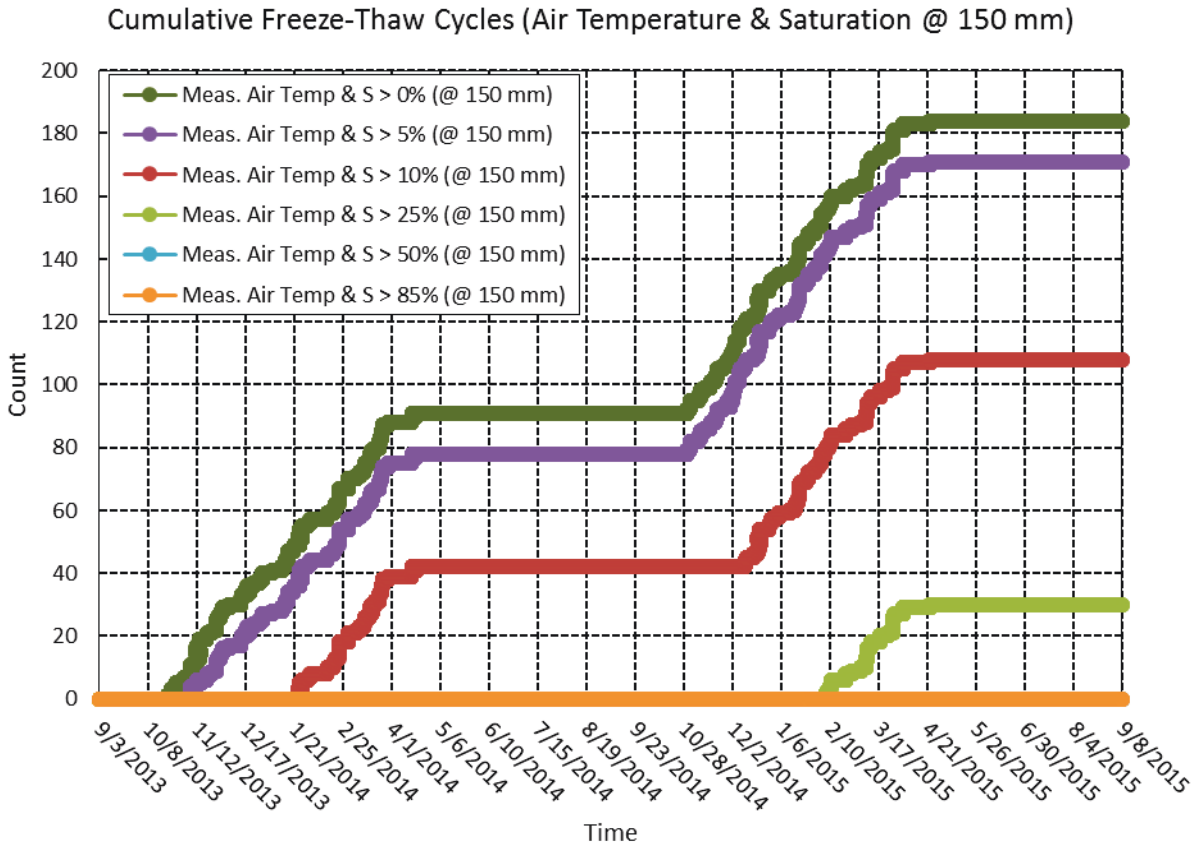

Figure C-30 Cumulative number of freeze-thaw cycles in Rantoul, IL, from September 3, 2013, through September 8, 2015, at a depth of 150 mm when both freezing air temperatures and minimum degree of saturation is achieved at time of freezing. Predicted degree of saturation is defined by a diffusivity (at S = 100%) value of 1.29×10^{-6} m^2/hr, a regression coefficient, *n*, of 15, α value of 0.05, and an empirical correlation between relative humidity and degree of saturation. The simulation is initialized with an even distribution of 85 %RH throughout the depth of the concrete.

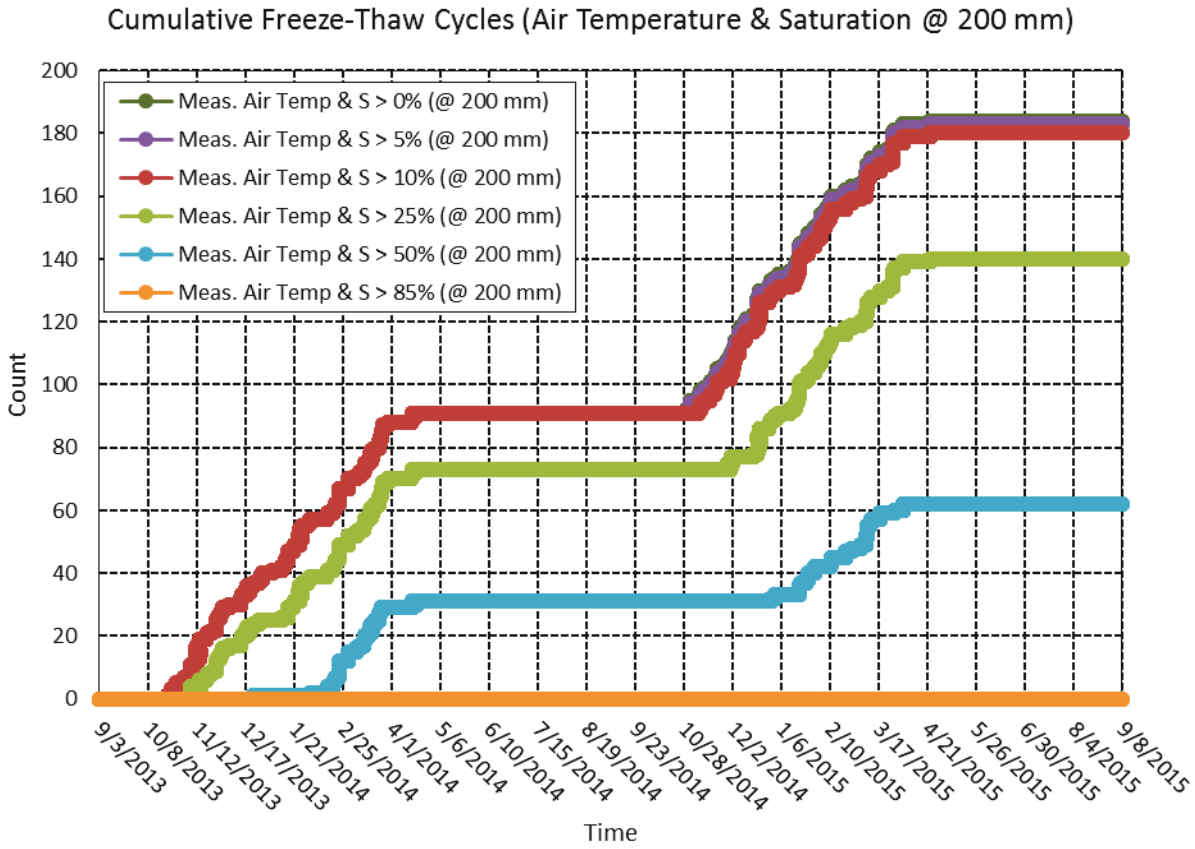

Figure C-31 Cumulative number of freeze-thaw cycles in Rantoul, IL, from September 3, 2013, through September 8, 2015, at a depth of 200 mm when both freezing air temperatures and minimum degree of saturation is achieved at time of freezing. Predicted degree of saturation is defined by a diffusivity (at S = 100%) value of 1.29×10^{-6} m^2/hr, a regression coefficient, *n*, of 15, α value of 0.05, and an empirical correlation between relative humidity and degree of saturation. The simulation is initialized with an even distribution of 85 %RH throughout the depth of the concrete.

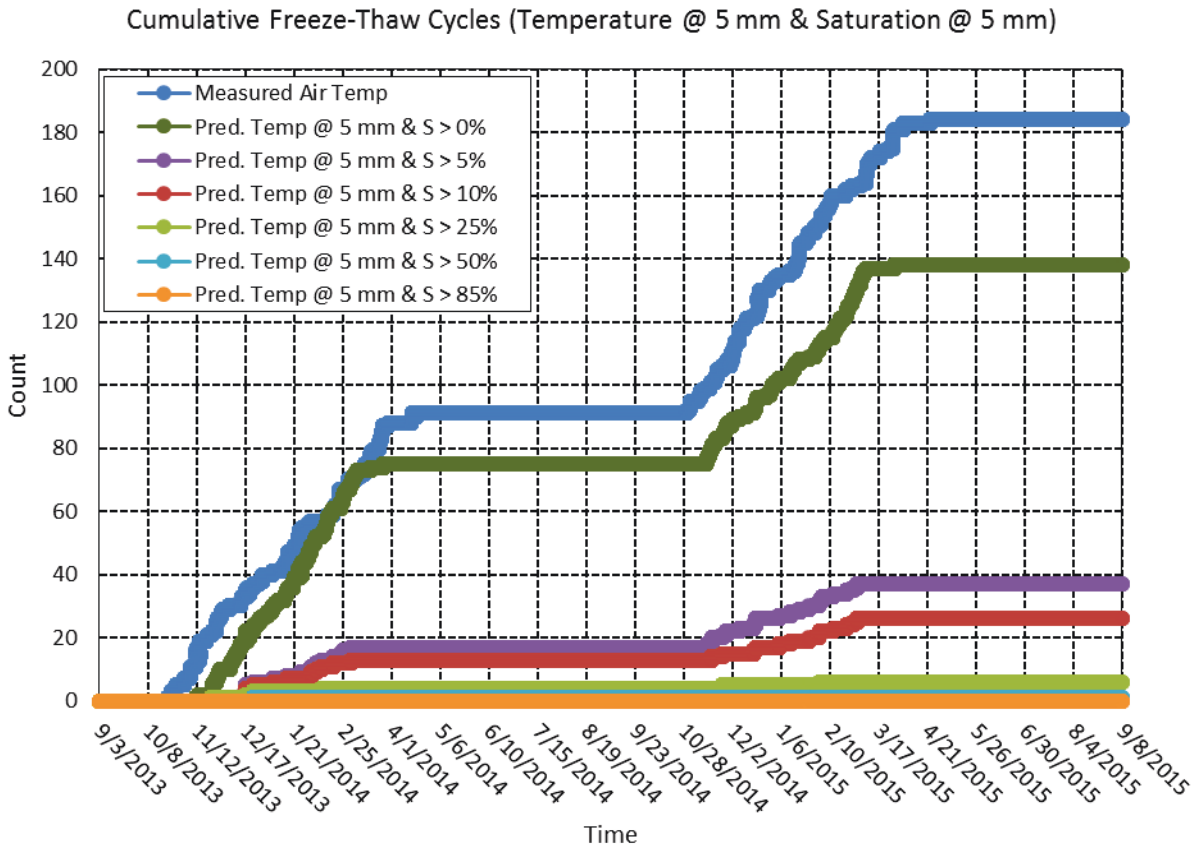

Figure C-32 Cumulative number of freeze-thaw cycles in Rantoul, IL, from September 3, 2013, through September 8, 2015, at a depth of 5 mm when both freezing temperatures and minimum degree of saturation is achieved at time of freezing. Predicted internal temperature values are computed using a 2-layered system whose upper concrete layer is defined by a thermal conductivity, λ, value of 1.85 kcal/hmC^o and a thermal diffusivity, α, value of 0.0025 m^2/h. The underlying aggregate ballast layer is defined by a thermal conductivity, λ, value of 2.58 kcal/hmC^o and a thermal diffusivity, α, value of 0.0030 m^2/h. Predicted degree of saturation is defined by a diffusivity (at S = 100%) value of 1.29x10^{-6} m^2/hr, a regression coefficient, n, of 15, α value of 0.05, and an empirical correlation between relative humidity and degree of saturation. The simulation is initialized with an even distribution of 85 %RH throughout the depth of the concrete.

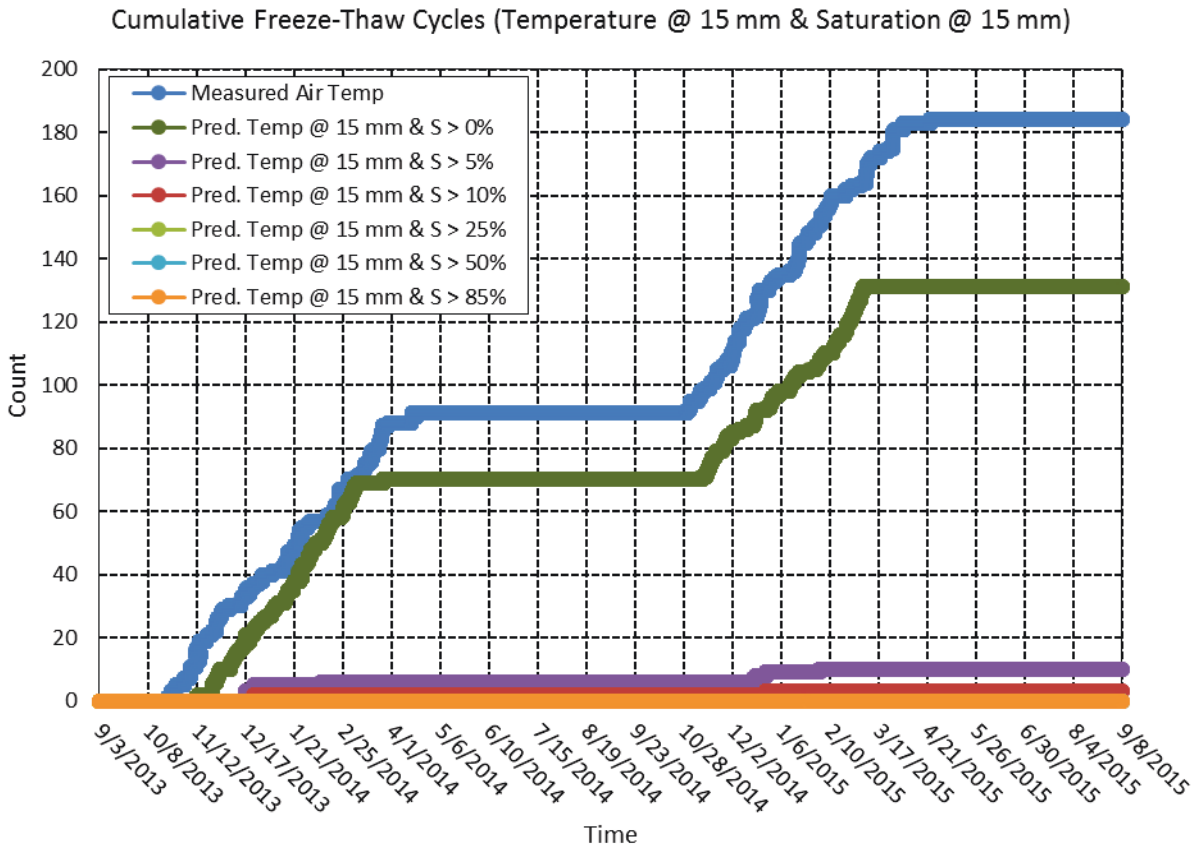

Figure C-33 Cumulative number of freeze-thaw cycles in Rantoul, IL, from September 3, 2013, through September 8, 2015, at a depth of 15 mm when both freezing temperatures and minimum degree of saturation is achieved at time of freezing. Predicted internal temperature values are computed using a 2-layered system whose upper concrete layer is defined by a thermal conductivity, λ, value of 1.85 kcal/hmC^o and a thermal diffusivity, α, value of 0.0025 m^2/h. The underlying aggregate ballast layer is defined by a thermal conductivity, λ, value of 2.58 kcal/hmC^o and a thermal diffusivity, α, value of 0.0030 m^2/h. Predicted degree of saturation is defined by a diffusivity (at S = 100%) value of 1.29x10^{-6} m^2/hr, a regression coefficient, n, of 15, α value of 0.05, and an empirical correlation between relative humidity and degree of saturation. The simulation is initialized with an even distribution of 85 %RH throughout the depth of the concrete.

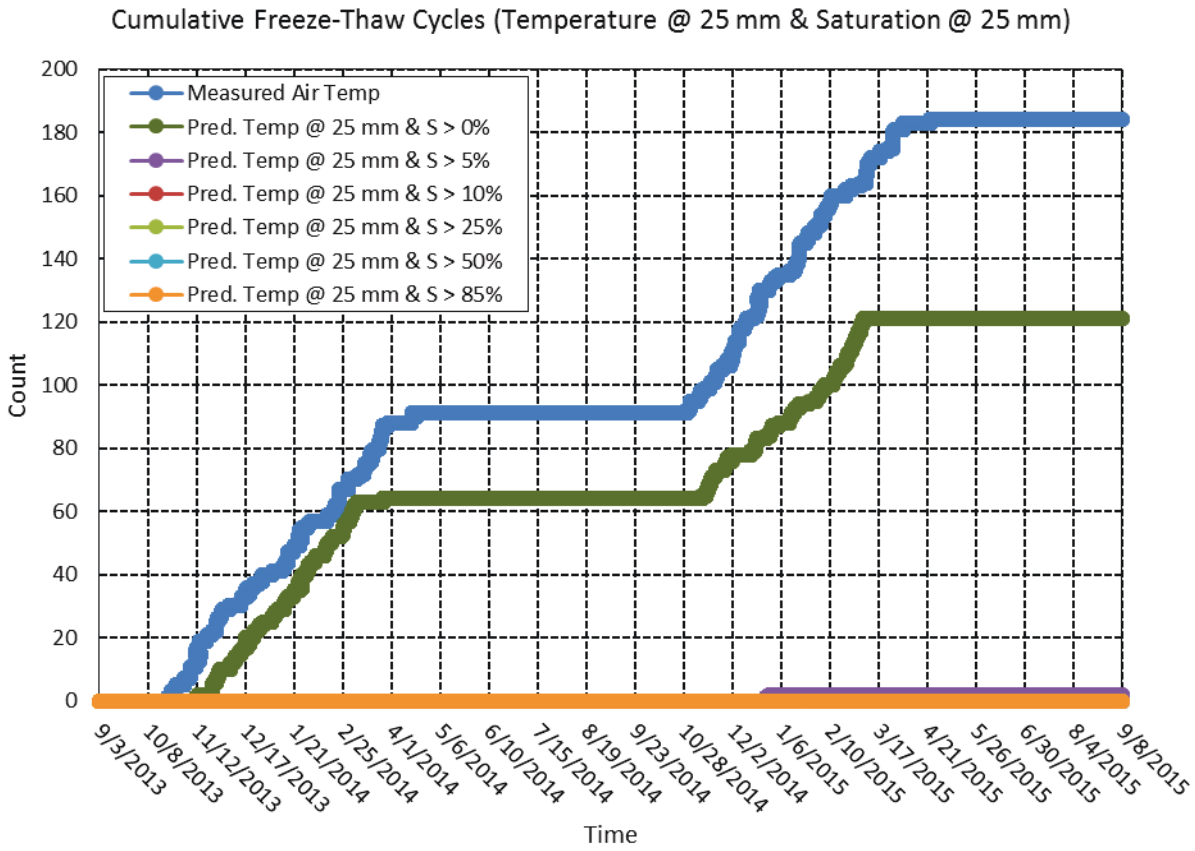

Figure C-34 Cumulative number of freeze-thaw cycles in Rantoul, IL, from September 3, 2013, through September 8, 2015, at a depth of 25 mm when both freezing temperatures and minimum degree of saturation is achieved at time of freezing. Predicted internal temperature values are computed using a 2-layered system whose upper concrete layer is defined by a thermal conductivity, λ, value of 1.85 kcal/hmC^o and a thermal diffusivity, α, value of 0.0025 m^2/h. The underlying aggregate ballast layer is defined by a thermal conductivity, λ, value of 2.58 kcal/hmC^o and a thermal diffusivity, α, value of 0.0030 m^2/h. Predicted degree of saturation is defined by a diffusivity (at S = 100%) value of 1.29x10^{-6} m^2/hr, a regression coefficient, n, of 15, α value of 0.05, and an empirical correlation between relative humidity and degree of saturation. The simulation is initialized with an even distribution of 85 %RH throughout the depth of the concrete.

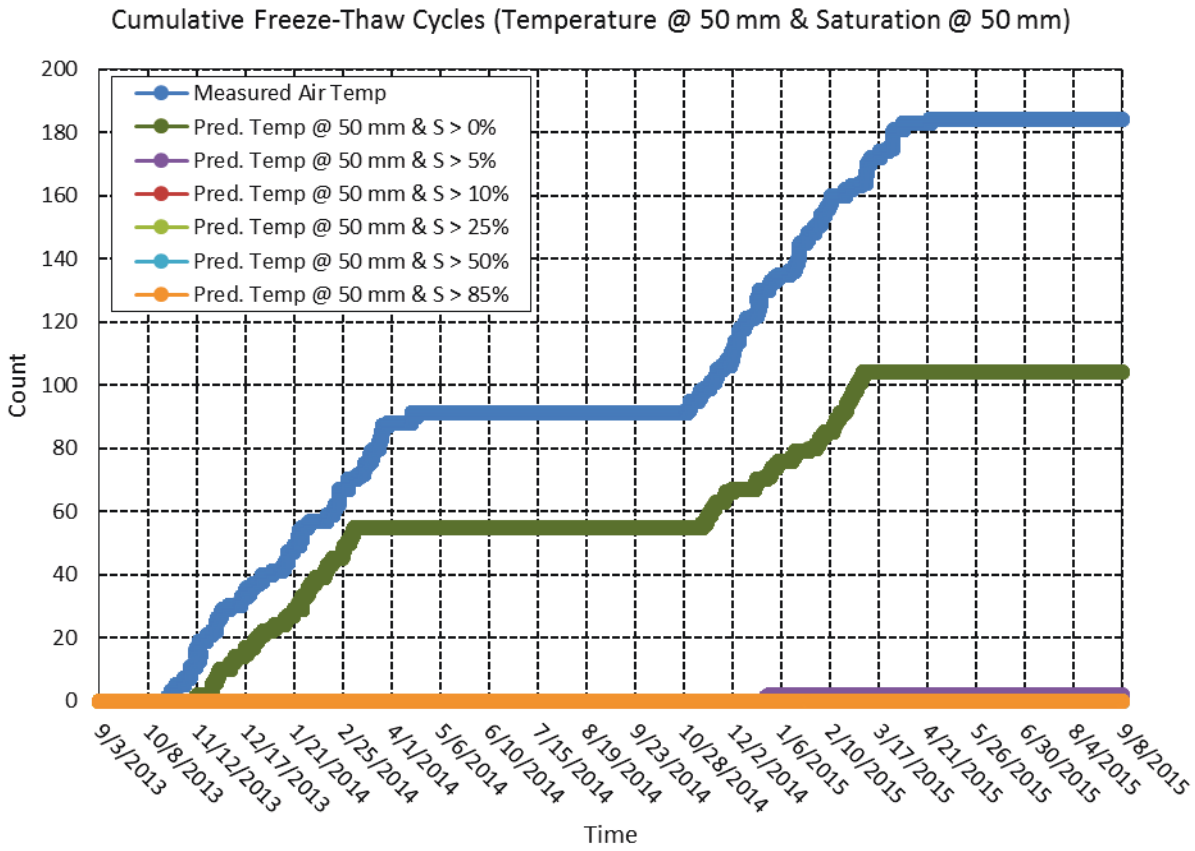

Figure C-35 Cumulative number of freeze-thaw cycles in Rantoul, IL, from September 3, 2013, through September 8, 2015, at a depth of 50 mm when both freezing temperatures and minimum degree of saturation is achieved at time of freezing. Predicted internal temperature values are computed using a 2-layered system whose upper concrete layer is defined by a thermal conductivity, λ, value of 1.85 kcal/hmC^o and a thermal diffusivity, α, value of 0.0025 m^2/h. The underlying aggregate ballast layer is defined by a thermal conductivity, λ, value of 2.58 kcal/hmC^o and a thermal diffusivity, α, value of 0.0030 m^2/h. Predicted degree of saturation is defined by a diffusivity (at S = 100%) value of 1.29x10^{-6} m^2/hr, a regression coefficient, n, of 15, α value of 0.05, and an empirical correlation between relative humidity and degree of saturation. The simulation is initialized with an even distribution of 85 %RH throughout the depth of the concrete.

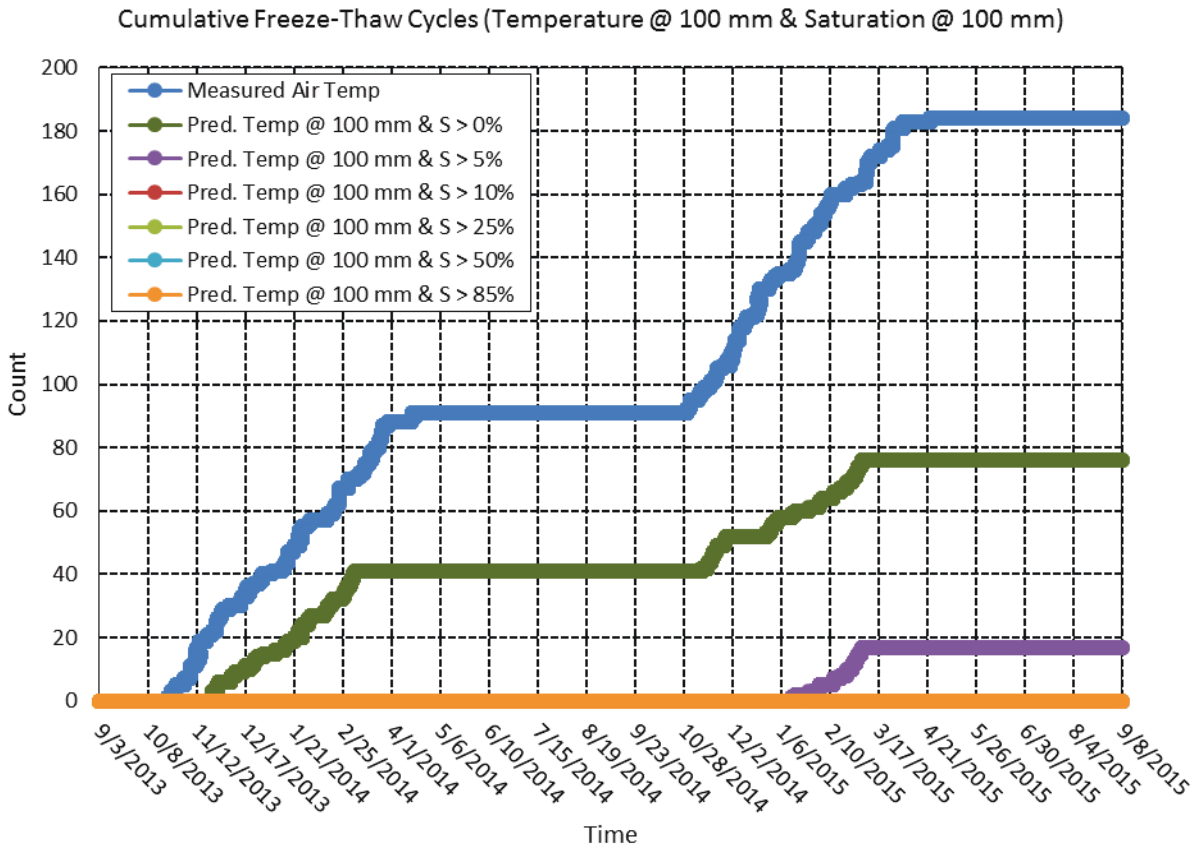

Figure C-36 Cumulative number of freeze-thaw cycles in Rantoul, IL, from September 3, 2013, through September 8, 2015, at a depth of 100 mm when both freezing temperatures and minimum degree of saturation is achieved at time of freezing. Predicted internal temperature values are computed using a 2-layered system whose upper concrete layer is defined by a thermal conductivity, λ, value of 1.85 kcal/hmC^o and a thermal diffusivity, α, value of 0.0025 m^2/h. The underlying aggregate ballast layer is defined by a thermal conductivity, λ, value of 2.58 kcal/hmC^o and a thermal diffusivity, α, value of 0.0030 m^2/h. Predicted degree of saturation is defined by a diffusivity (at S = 100%) value of 1.29x10^{-6} m^2/hr, a regression coefficient, n, of 15, α value of 0.05, and an empirical correlation between relative humidity and degree of saturation. The simulation is initialized with an even distribution of 85 %RH throughout the depth of the concrete.

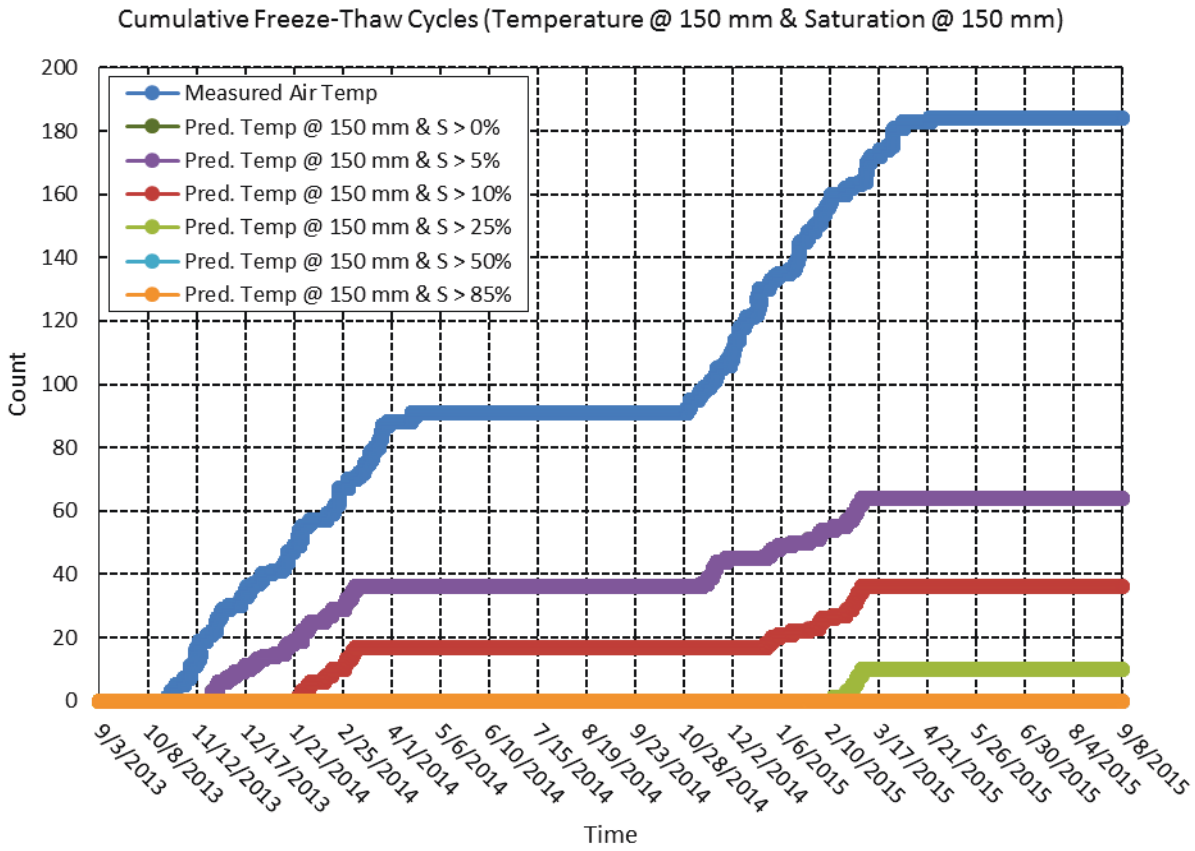

Figure C-37 Cumulative number of freeze-thaw cycles in Rantoul, IL, from September 3, 2013, through September 8, 2015, at a depth of 150 mm when both freezing temperatures and minimum degree of saturation is achieved at time of freezing. Predicted internal temperature values are computed using a 2-layered system whose upper concrete layer is defined by a thermal conductivity, λ, value of 1.85 kcal/hmC^o and a thermal diffusivity, α, value of 0.0025 m^2/h. The underlying aggregate ballast layer is defined by a thermal conductivity, λ, value of 2.58 kcal/hmC^o and a thermal diffusivity, α, value of 0.0030 m^2/h. Predicted degree of saturation is defined by a diffusivity (at S = 100%) value of 1.29x10^{-6} m^2/hr, a regression coefficient, n, of 15, α value of 0.05, and an empirical correlation between relative humidity and degree of saturation. The simulation is initialized with an even distribution of 85 %RH throughout the depth of the concrete.

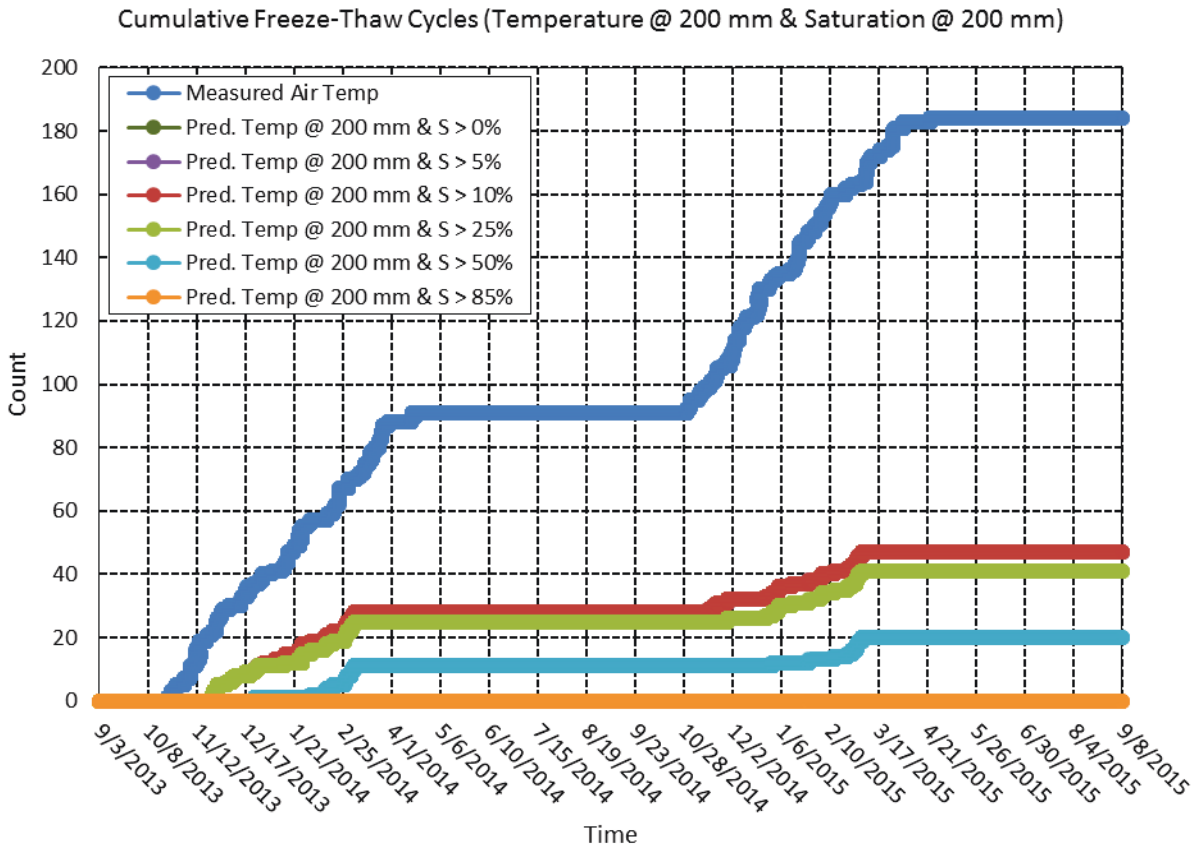

Figure C-38 Cumulative number of freeze-thaw cycles in Rantoul, IL, from September 3, 2013, through September 8, 2015, at a depth of 200 mm when both freezing temperatures and minimum degree of saturation is achieved at time of freezing. Predicted internal temperature values are computed using a 2-layered system whose upper concrete layer is defined by a thermal conductivity, λ, value of 1.85 kcal/hmC^o and a thermal diffusivity, α, value of 0.0025 m^2/h. The underlying aggregate ballast layer is defined by a thermal conductivity, λ, value of 2.58 kcal/hmC^o and a thermal diffusivity, α, value of 0.0030 m^2/h. Predicted degree of saturation is defined by a diffusivity (at S = 100%) value of 1.29x10^{-6} m^2/hr, a regression coefficient, n, of 15, α value of 0.05, and an empirical correlation between relative humidity and degree of saturation. The simulation is initialized with an even distribution of 85 %RH throughout the depth of the concrete.

Modeled freeze-thaw cycles of concrete in Lytton, BC, due to saturation (modeled with D = 0.86 and initial RH = 50%)

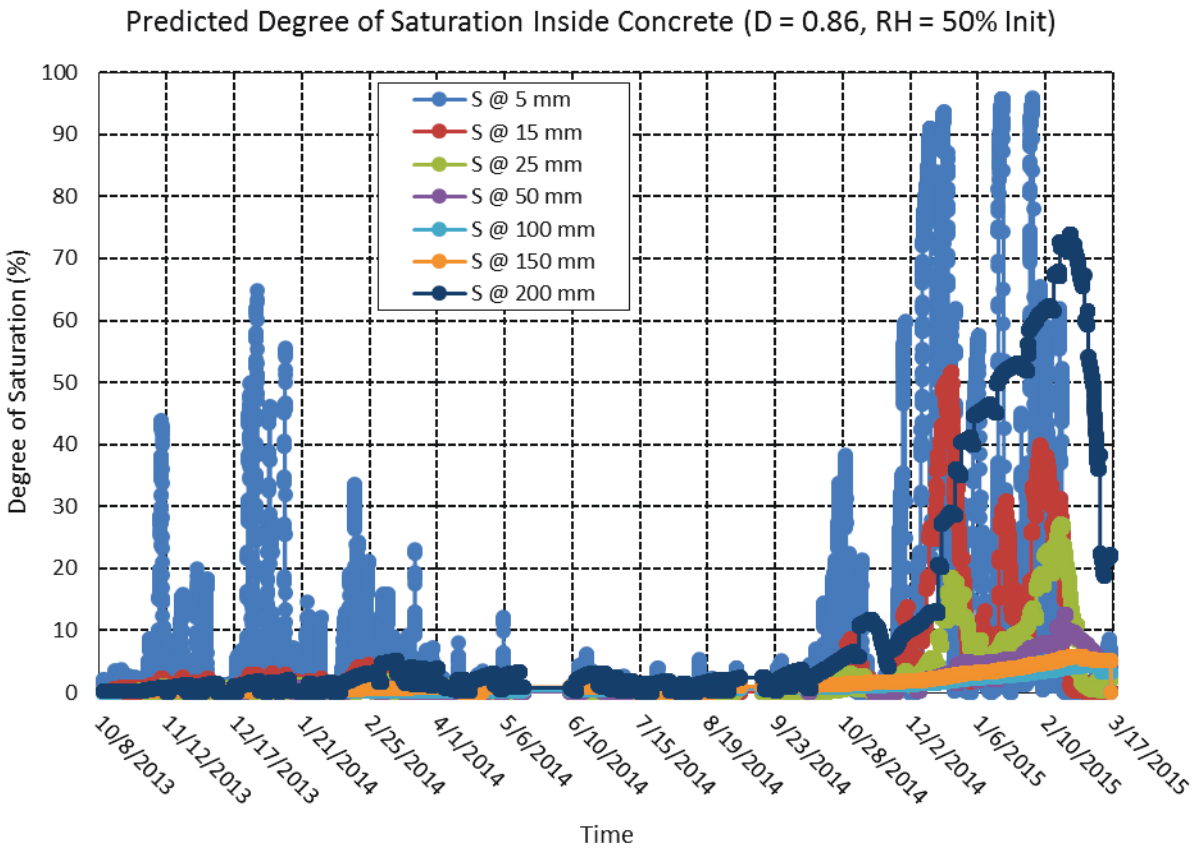

Figure C-39 Predicted degree of saturation inside a 1-layered concrete system in Lytton, BC, from October 8, 2013, through March 17, 2015. The concrete is defined by a diffusivity (at S = 100%) value of 0.86×10^{-6} m^2/hr, a regression coefficient, *n*, of 15, α value of 0.05, and an empirical correlation between relative humidity and degree of saturation. The simulation is initialized with an even distribution of 50 %RH throughout the depth of the concrete.

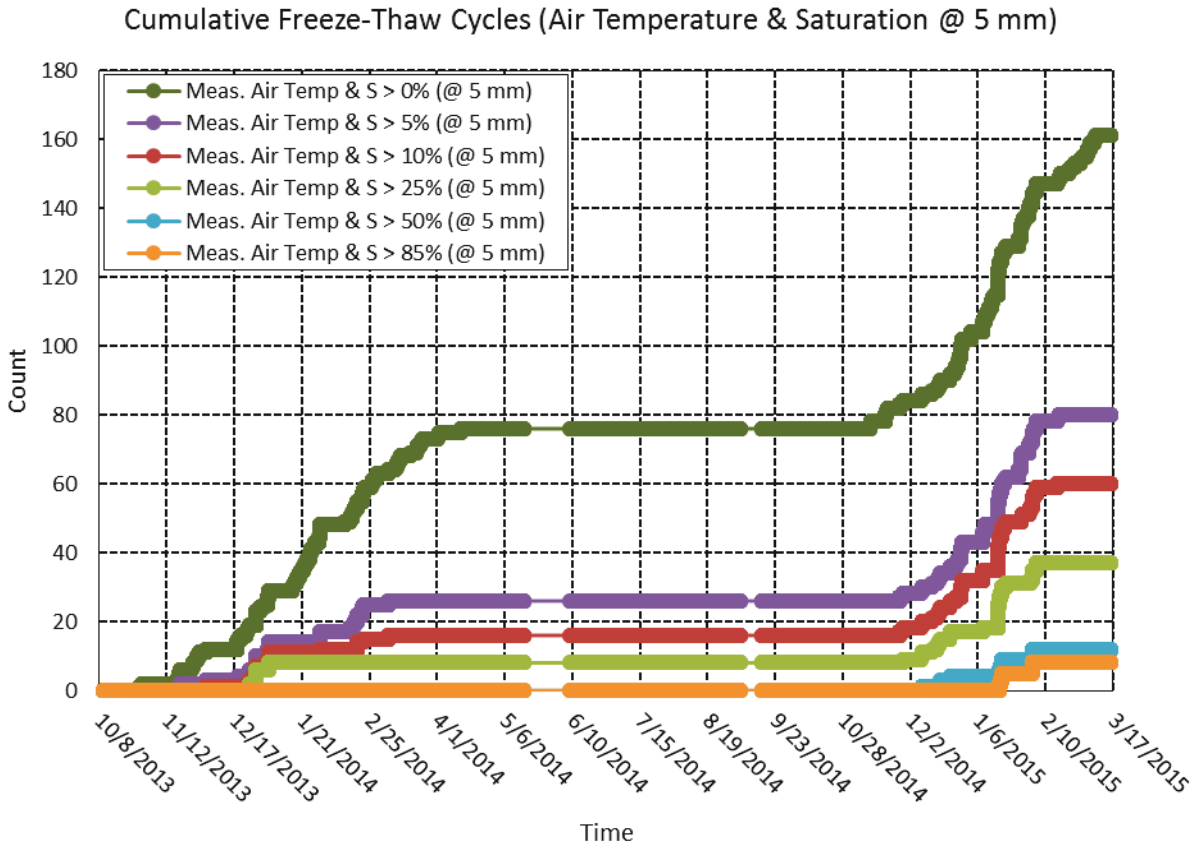

Figure C-40 Cumulative number of freeze-thaw cycles in Lytton, BC, from October 8, 2013, through March 17, 2015, at a depth of 5 mm when both freezing air temperatures and minimum degree of saturation is achieved at time of freezing. Predicted degree of saturation is defined by a diffusivity (at S = 100%) value of 0.86×10^{-6} m^2/hr, a regression coefficient, *n*, of 15, α value of 0.05, and an empirical correlation between relative humidity and degree of saturation. The simulation is initialized with an even distribution of 50 %RH throughout the depth of the concrete.

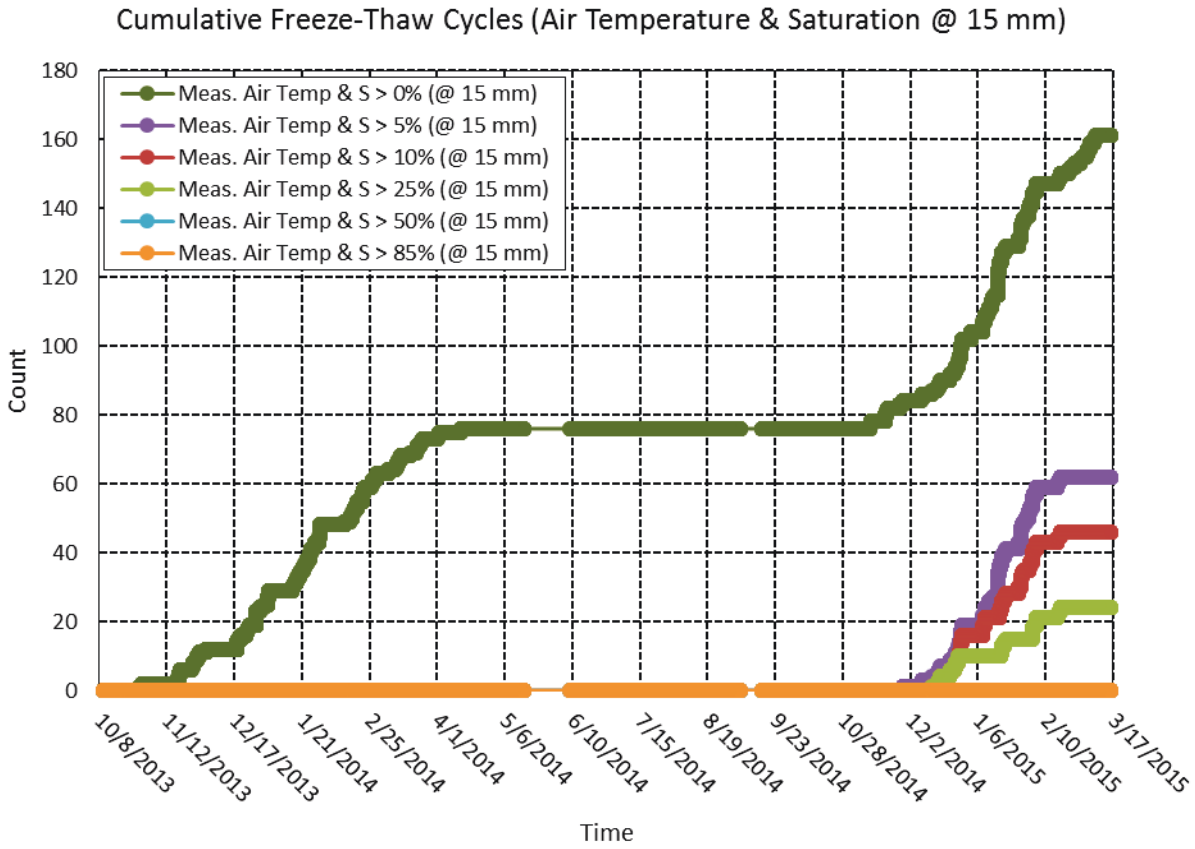

Figure C-41 Cumulative number of freeze-thaw cycles in Lytton, BC, from October 8, 2013, through March 17, 2015, at a depth of 15 mm when both freezing air temperatures and minimum degree of saturation is achieved at time of freezing. Predicted degree of saturation is defined by a diffusivity (at S = 100%) value of 0.86×10^{-6} m^2/hr, a regression coefficient, *n*, of 15, α value of 0.05, and an empirical correlation between relative humidity and degree of saturation. The simulation is initialized with an even distribution of 50 %RH throughout the depth of the concrete.

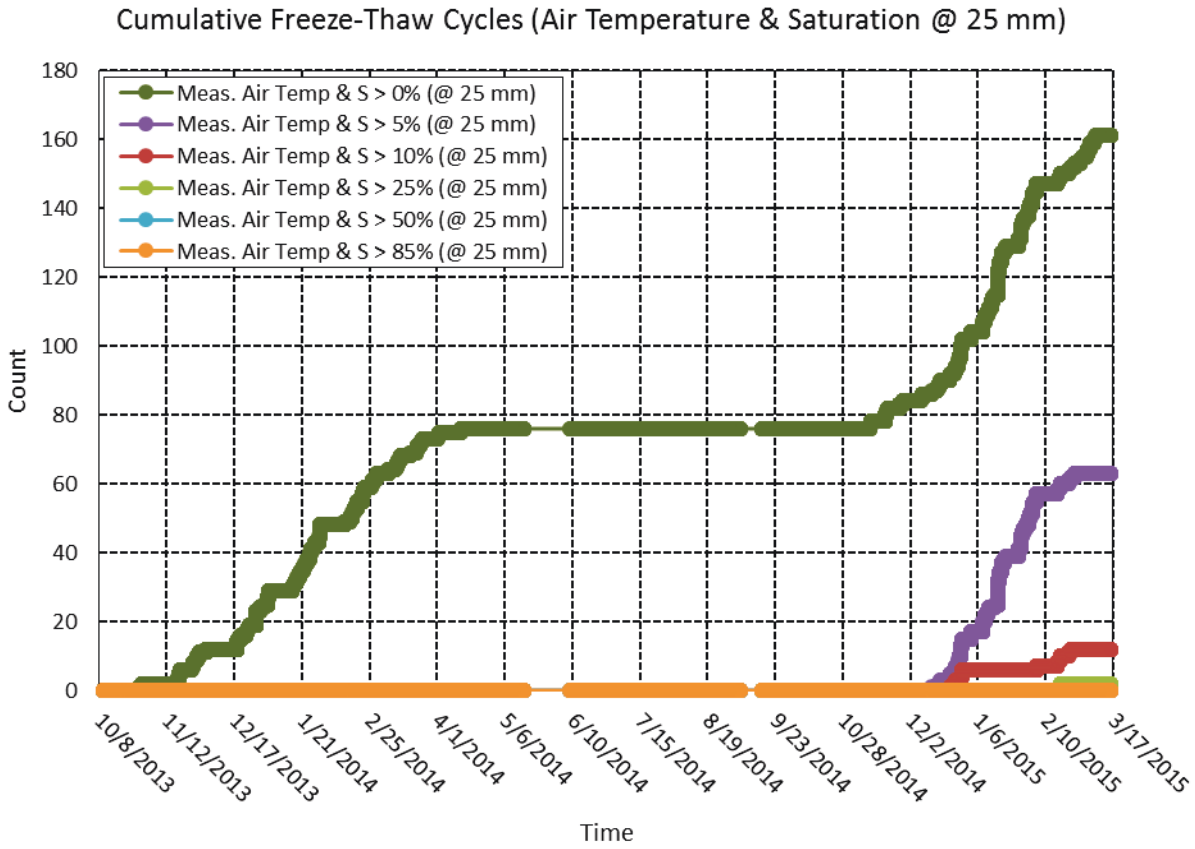

Figure C-42 Cumulative number of freeze-thaw cycles in Lytton, BC, from October 8, 2013, through March 17, 2015, at a depth of 25 mm when both freezing air temperatures and minimum degree of saturation is achieved at time of freezing. Predicted degree of saturation is defined by a diffusivity (at S = 100%) value of 0.86×10^{-6} m^2/hr, a regression coefficient, *n*, of 15, α value of 0.05, and an empirical correlation between relative humidity and degree of saturation. The simulation is initialized with an even distribution of 50 %RH throughout the depth of the concrete.

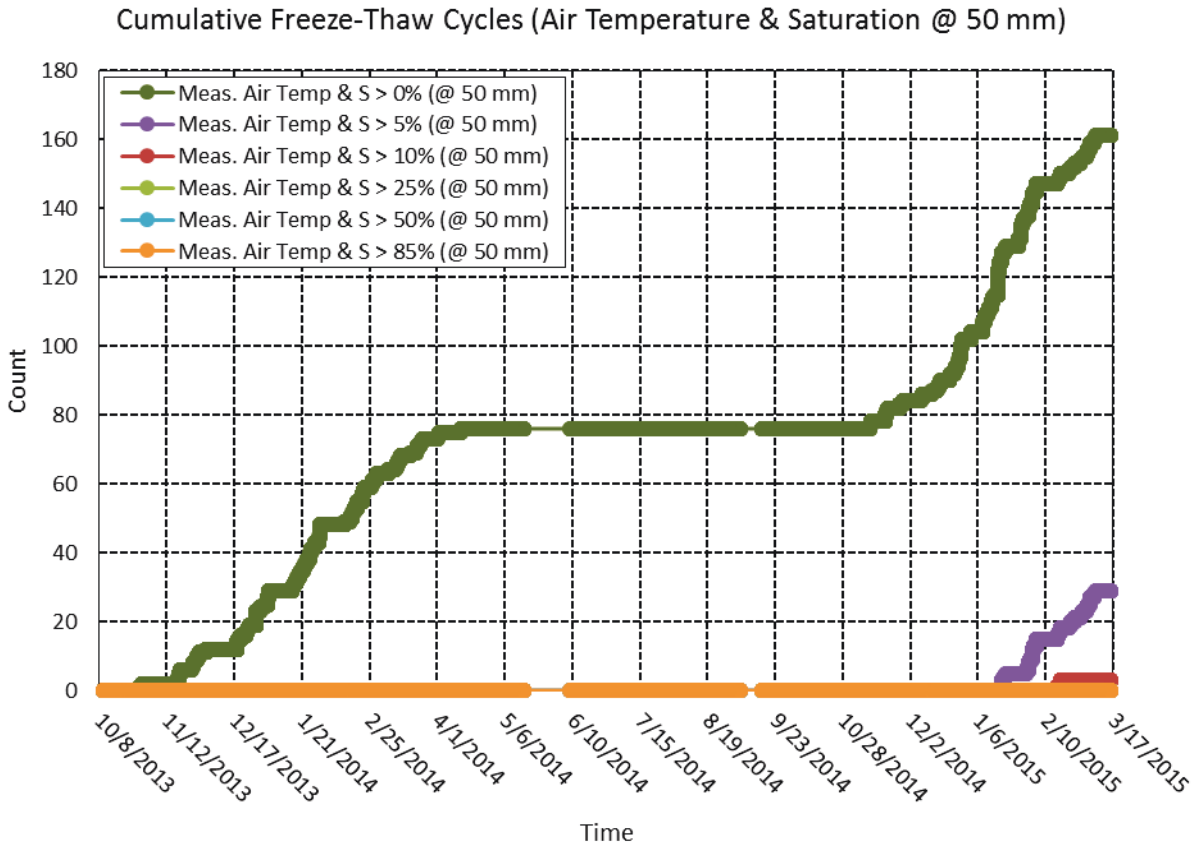

Figure C-43 Cumulative number of freeze-thaw cycles in Lytton, BC, from October 8, 2013, through March 17, 2015, at a depth of 50 mm when both freezing air temperatures and minimum degree of saturation is achieved at time of freezing. Predicted degree of saturation is defined by a diffusivity (at S = 100%) value of 0.86×10^{-6} m^2/hr, a regression coefficient, *n*, of 15, α value of 0.05, and an empirical correlation between relative humidity and degree of saturation. The simulation is initialized with an even distribution of 50 %RH throughout the depth of the concrete.

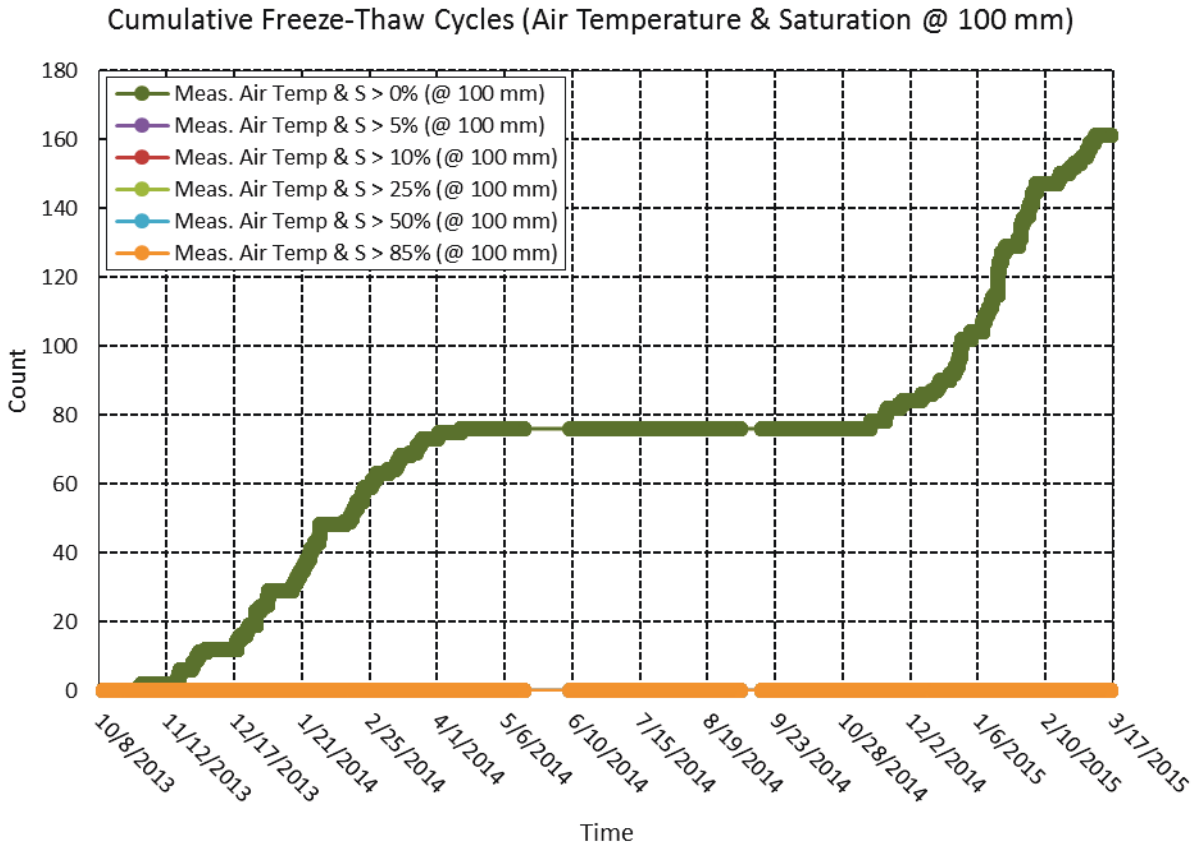

Figure C-44 Cumulative number of freeze-thaw cycles in Lytton, BC, from October 8, 2013, through March 17, 2015, at a depth of 100 mm when both freezing air temperatures and minimum degree of saturation is achieved at time of freezing. Predicted degree of saturation is defined by a diffusivity (at S = 100%) value of 0.86×10^{-6} m^2/hr, a regression coefficient, *n*, of 15, α value of 0.05, and an empirical correlation between relative humidity and degree of saturation. The simulation is initialized with an even distribution of 50 %RH throughout the depth of the concrete.

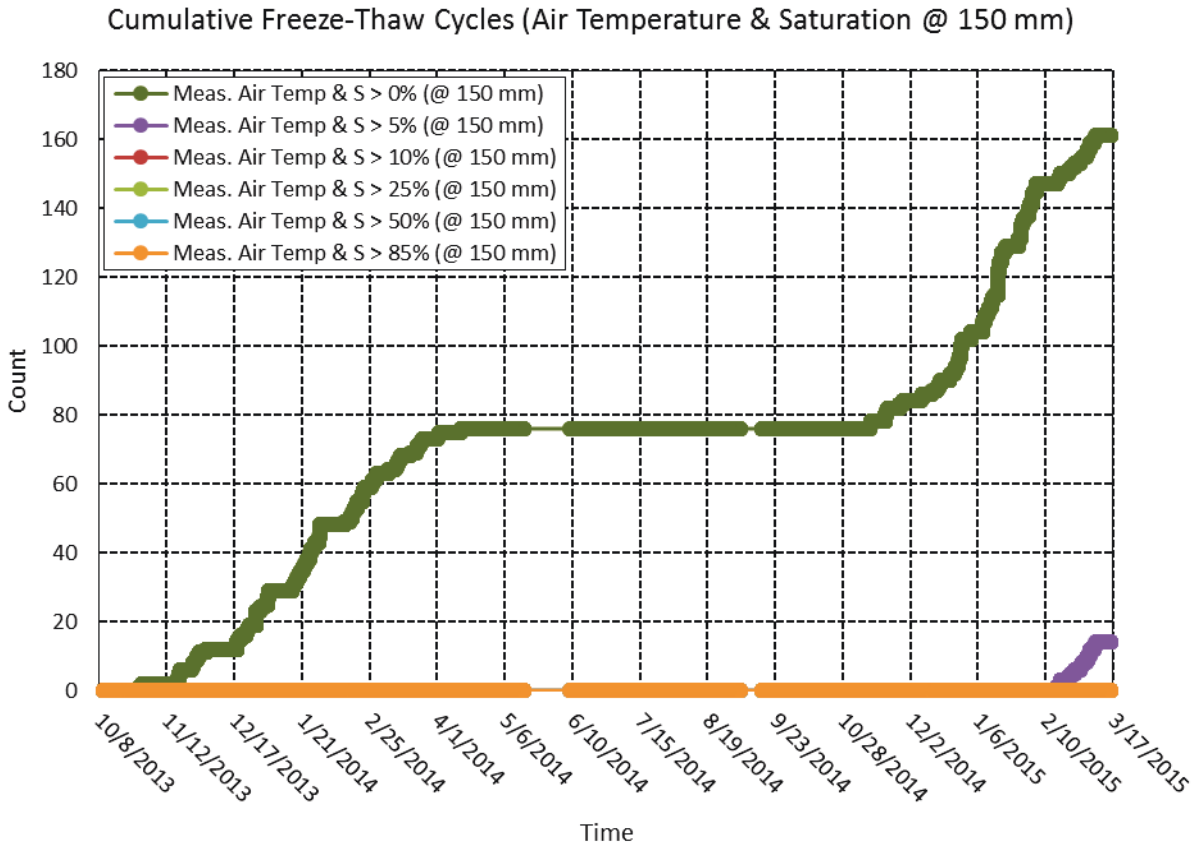

Figure C-45 Cumulative number of freeze-thaw cycles in Lytton, BC, from October 8, 2013, through March 17, 2015, at a depth of 150 mm when both freezing air temperatures and minimum degree of saturation is achieved at time of freezing. Predicted degree of saturation is defined by a diffusivity (at S = 100%) value of 0.86×10^{-6} m^2/hr, a regression coefficient, *n*, of 15, α value of 0.05, and an empirical correlation between relative humidity and degree of saturation. The simulation is initialized with an even distribution of 50 %RH throughout the depth of the concrete.

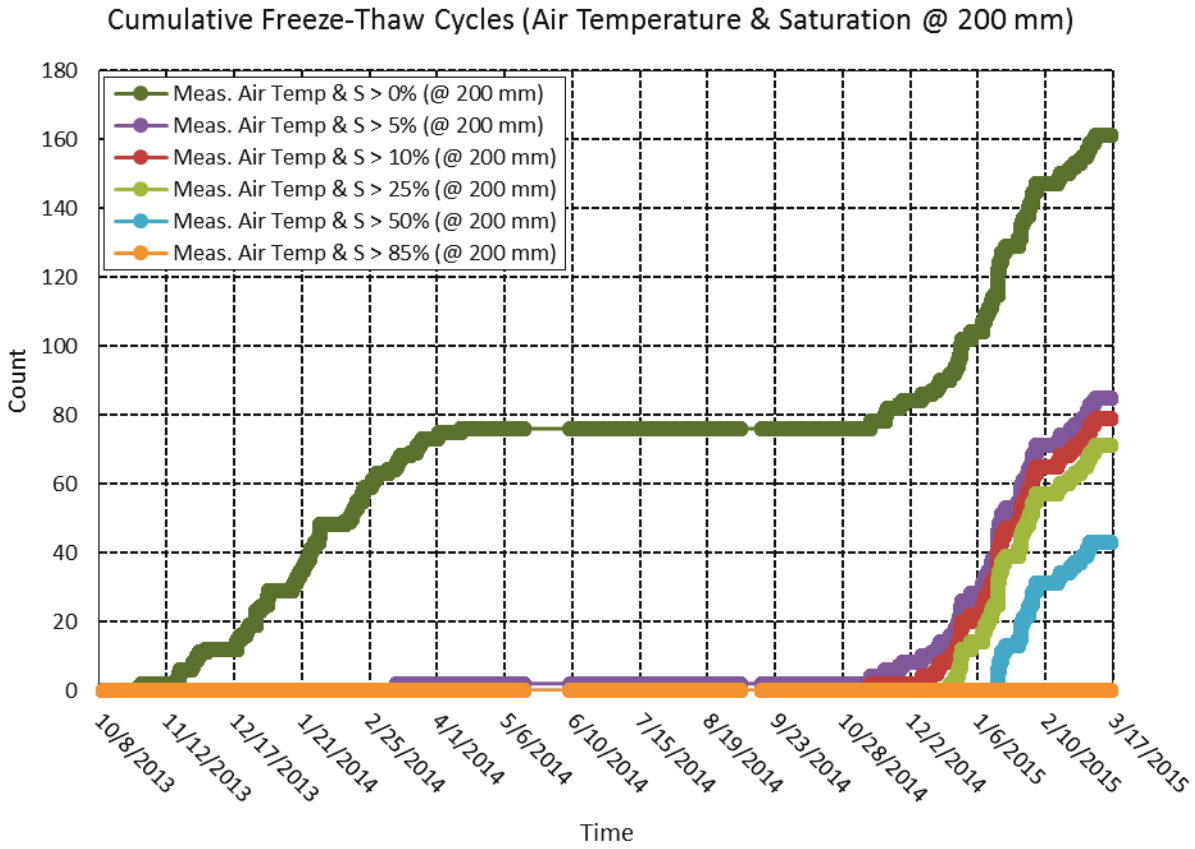

Figure C-46 Cumulative number of freeze-thaw cycles in Lytton, BC, from October 8, 2013, through March 17, 2015, at a depth of 200 mm when both freezing air temperatures and minimum degree of saturation is achieved at time of freezing. Predicted degree of saturation is defined by a diffusivity (at S = 100%) value of 0.86×10^{-6} m^2/hr, a regression coefficient, *n*, of 15, α value of 0.05, and an empirical correlation between relative humidity and degree of saturation. The simulation is initialized with an even distribution of 50 %RH throughout the depth of the concrete.

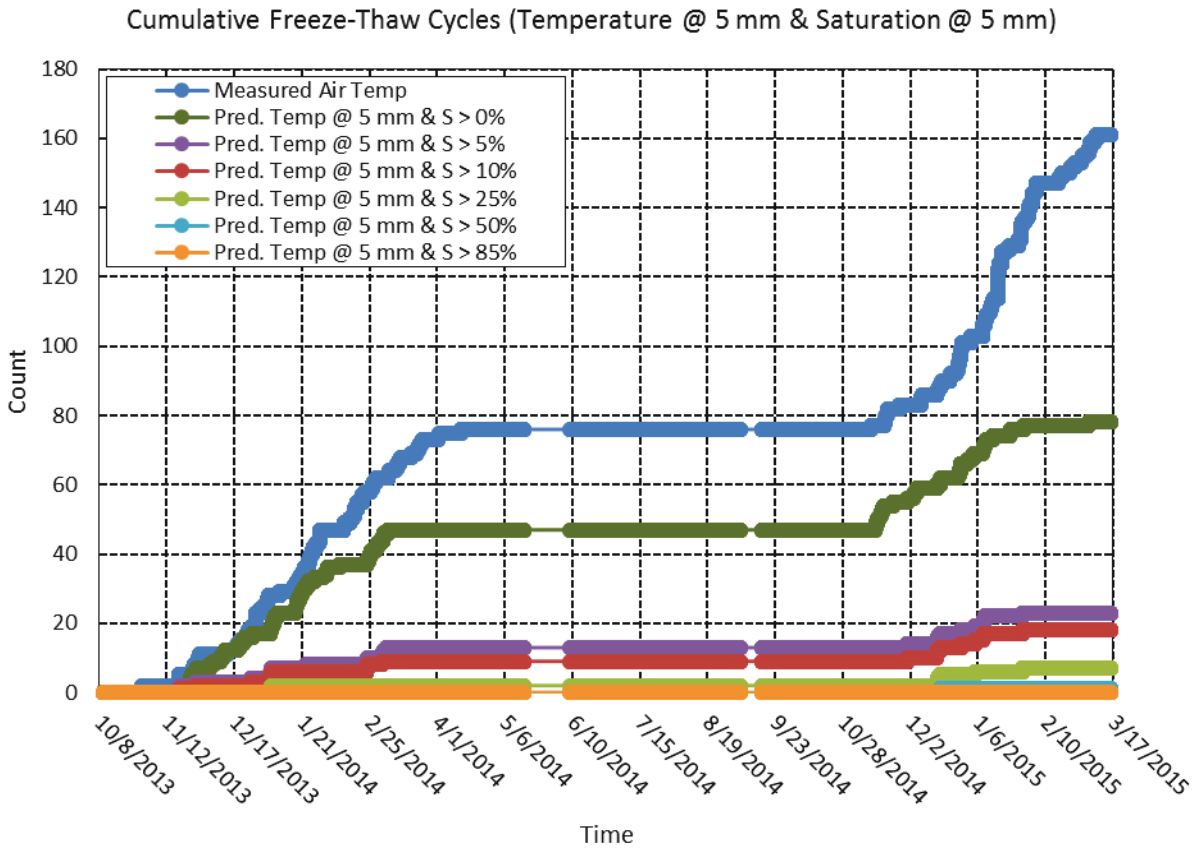

Figure C-47 Cumulative number of freeze-thaw cycles in Lytton, BC, from October 8, 2013, through March 17, 2015, at a depth of 5 mm when both freezing temperatures and minimum degree of saturation is achieved at time of freezing. Predicted internal temperature values are computed using a 2-layered system whose upper concrete layer is defined by a thermal conductivity, λ, value of 1.85 kcal/hmC^{o} and a thermal diffusivity, α, value of 0.0025 m^2/h. The underlying aggregate ballast layer is defined by a thermal conductivity, λ, value of 2.58 kcal/hmC^{o} and a thermal diffusivity, α, value of 0.0030 m^2/h. Predicted degree of saturation is defined by a diffusivity (at S = 100%) value of 0.86x10^{-6} m^2/hr, a regression coefficient, n, of 15, α value of 0.05, and an empirical correlation between relative humidity and degree of saturation. The simulation is initialized with an even distribution of 50 %RH throughout the depth of the concrete.

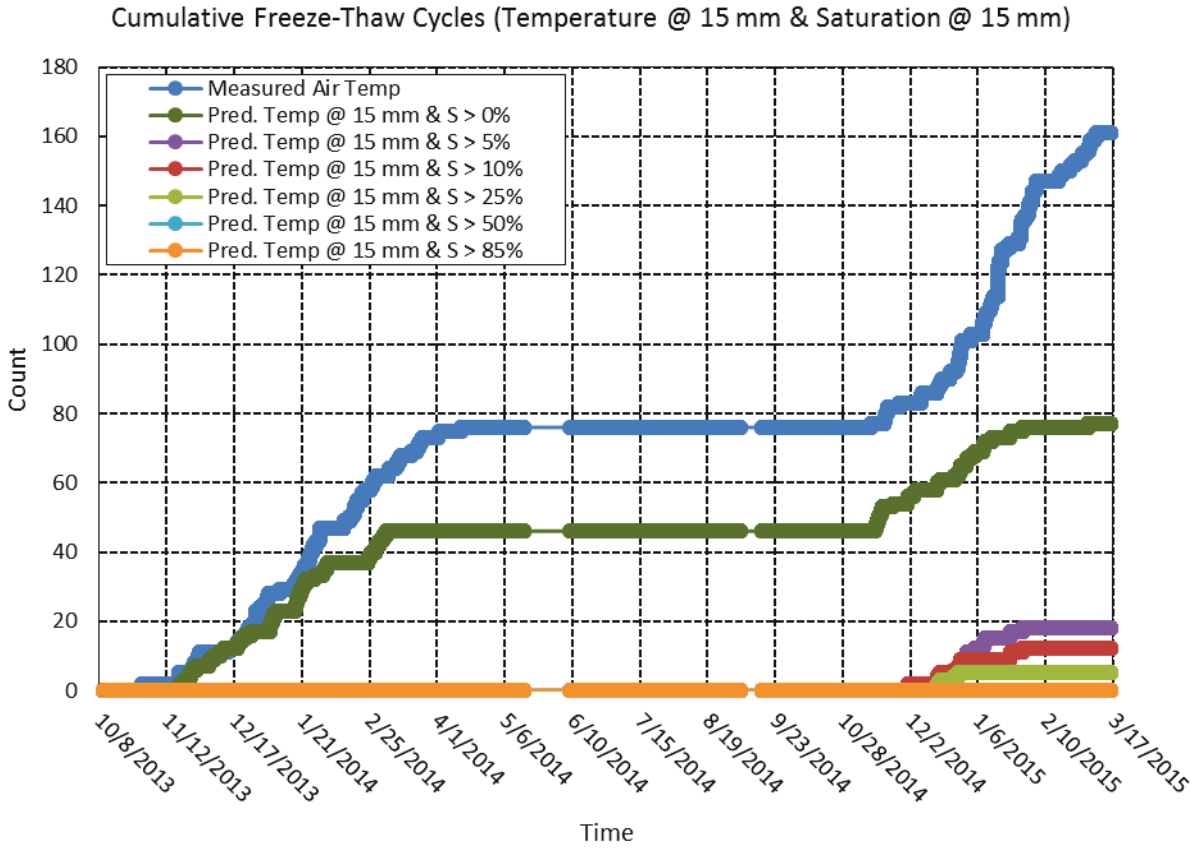

Figure C-48 Cumulative number of freeze-thaw cycles in Lytton, BC, from October 8, 2013, through March 17, 2015, at a depth of 15 mm when both freezing temperatures and minimum degree of saturation is achieved at time of freezing. Predicted internal temperature values are computed using a 2-layered system whose upper concrete layer is defined by a thermal conductivity, λ, value of 1.85 kcal/hmC^{o} and a thermal diffusivity, α, value of 0.0025 m^2/h. The underlying aggregate ballast layer is defined by a thermal conductivity, λ, value of 2.58 kcal/hmC^{o} and a thermal diffusivity, α, value of 0.0030 m^2/h. Predicted degree of saturation is defined by a diffusivity (at S = 100%) value of 0.86x10^{-6} m^2/hr, a regression coefficient, n, of 15, α value of 0.05, and an empirical correlation between relative humidity and degree of saturation. The simulation is initialized with an even distribution of 50 %RH throughout the depth of the concrete.

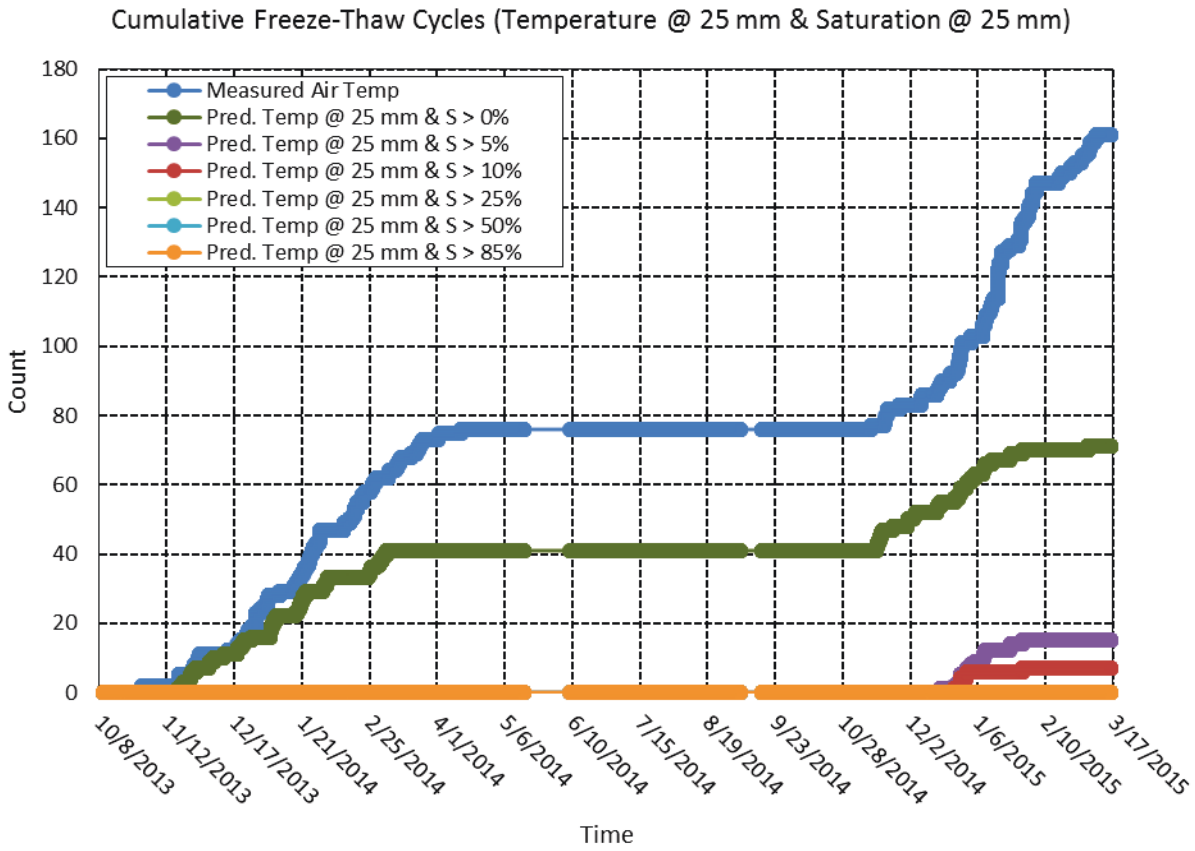

Figure C-49 Cumulative number of freeze-thaw cycles in Lytton, BC, from October 8, 2013, through March 17, 2015, at a depth of 25 mm when both freezing temperatures and minimum degree of saturation is achieved at time of freezing. Predicted internal temperature values are computed using a 2-layered system whose upper concrete layer is defined by a thermal conductivity, λ, value of 1.85 kcal/hmC^{o} and a thermal diffusivity, α, value of 0.0025 m^2/h. The underlying aggregate ballast layer is defined by a thermal conductivity, λ, value of 2.58 kcal/hmC^{o} and a thermal diffusivity, α, value of 0.0030 m^2/h. Predicted degree of saturation is defined by a diffusivity (at S = 100%) value of 0.86x10^{-6} m^2/hr, a regression coefficient, n, of 15, α value of 0.05, and an empirical correlation between relative humidity and degree of saturation. The simulation is initialized with an even distribution of 50 %RH throughout the depth of the concrete.

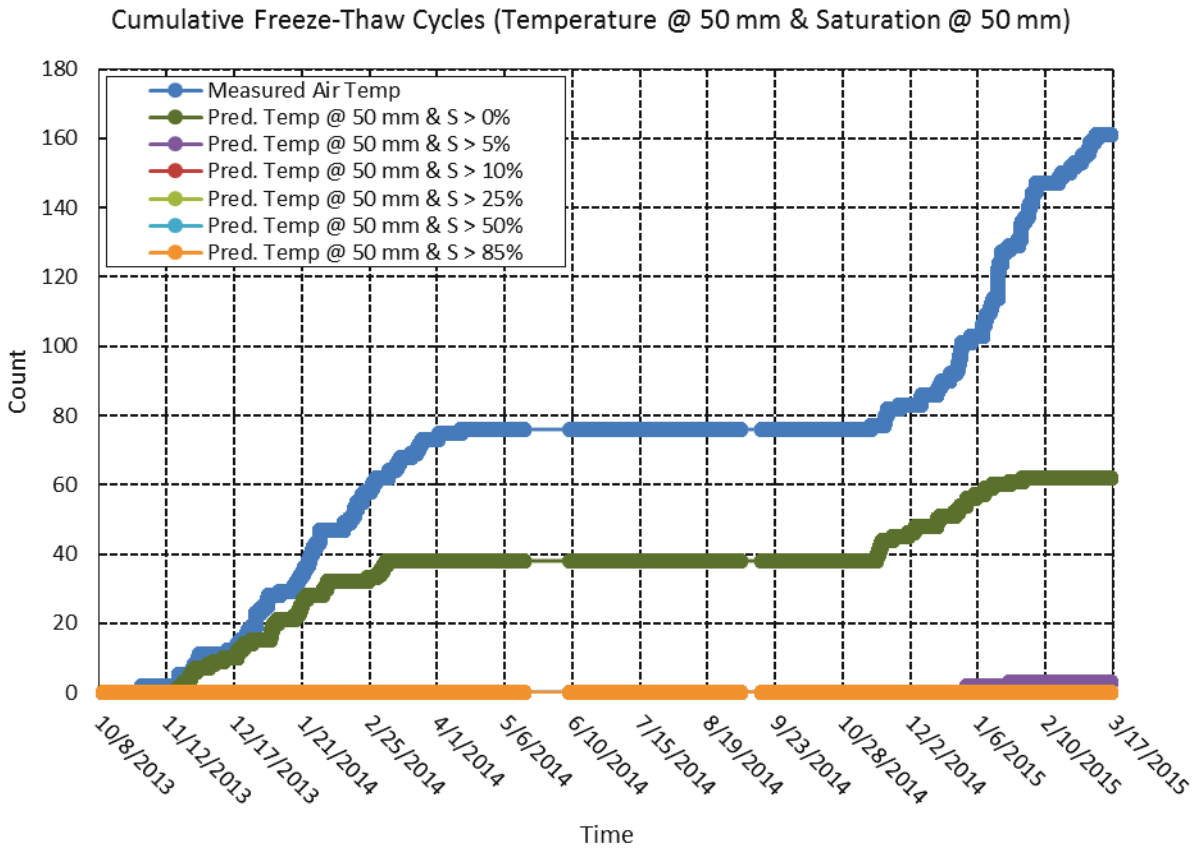

Figure C-50 Cumulative number of freeze-thaw cycles in Lytton, BC, from October 8, 2013, through March 17, 2015, at a depth of 50 mm when both freezing temperatures and minimum degree of saturation is achieved at time of freezing. Predicted internal temperature values are computed using a 2-layered system whose upper concrete layer is defined by a thermal conductivity, λ, value of 1.85 kcal/hmC^{o} and a thermal diffusivity, α, value of 0.0025 m^2/h. The underlying aggregate ballast layer is defined by a thermal conductivity, λ, value of 2.58 kcal/hmC^{o} and a thermal diffusivity, α, value of 0.0030 m^2/h. Predicted degree of saturation is defined by a diffusivity (at S = 100%) value of 0.86x10^{-6} m^2/hr, a regression coefficient, n, of 15, α value of 0.05, and an empirical correlation between relative humidity and degree of saturation. The simulation is initialized with an even distribution of 50 %RH throughout the depth of the concrete.

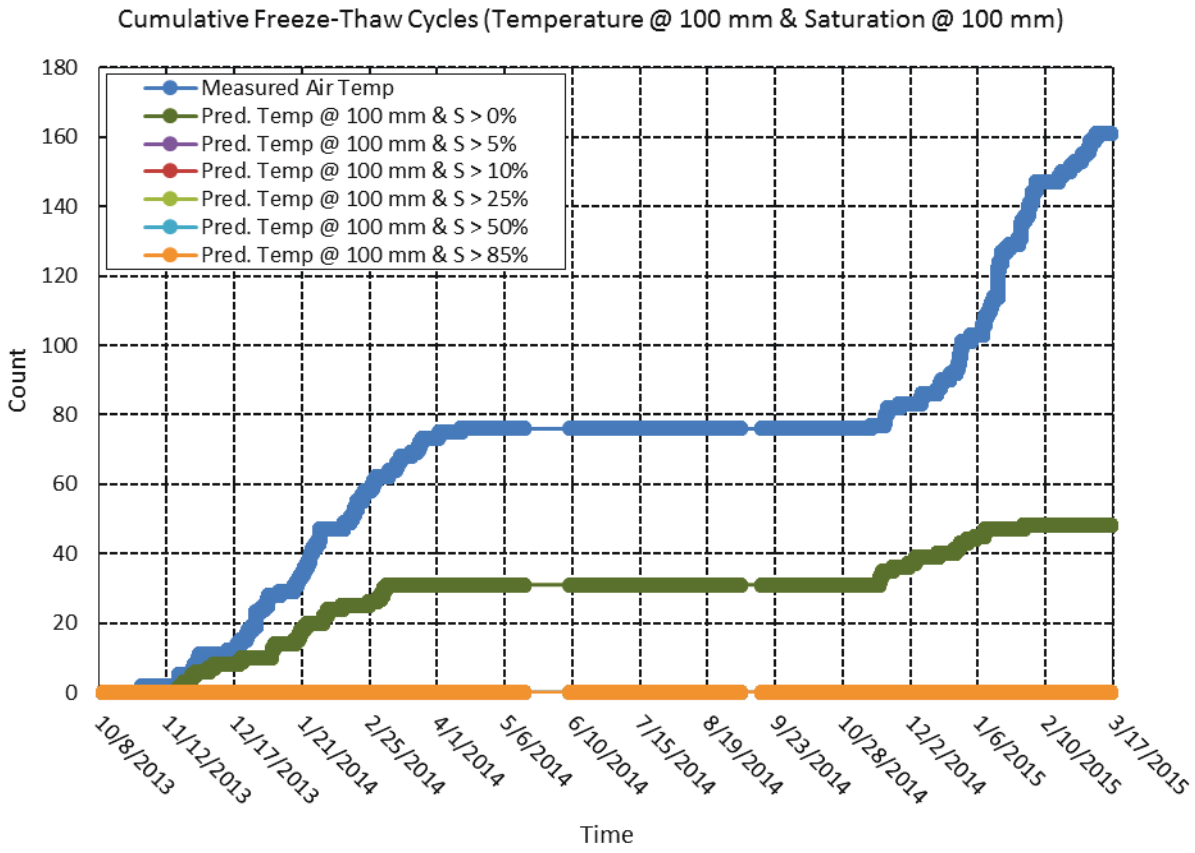

Figure C-51 Cumulative number of freeze-thaw cycles in Lytton, BC, from October 8, 2013, through March 17, 2015, at a depth of 100 mm when both freezing temperatures and minimum degree of saturation is achieved at time of freezing. Predicted internal temperature values are computed using a 2-layered system whose upper concrete layer is defined by a thermal conductivity, λ, value of 1.85 kcal/hmC^o and a thermal diffusivity, α, value of 0.0025 m^2/h. The underlying aggregate ballast layer is defined by a thermal conductivity, λ, value of 2.58 kcal/hmC^o and a thermal diffusivity, α, value of 0.0030 m^2/h. Predicted degree of saturation is defined by a diffusivity (at S = 100%) value of 0.86x10^{-6} m^2/hr, a regression coefficient, n, of 15, α value of 0.05, and an empirical correlation between relative humidity and degree of saturation. The simulation is initialized with an even distribution of 50 %RH throughout the depth of the concrete.

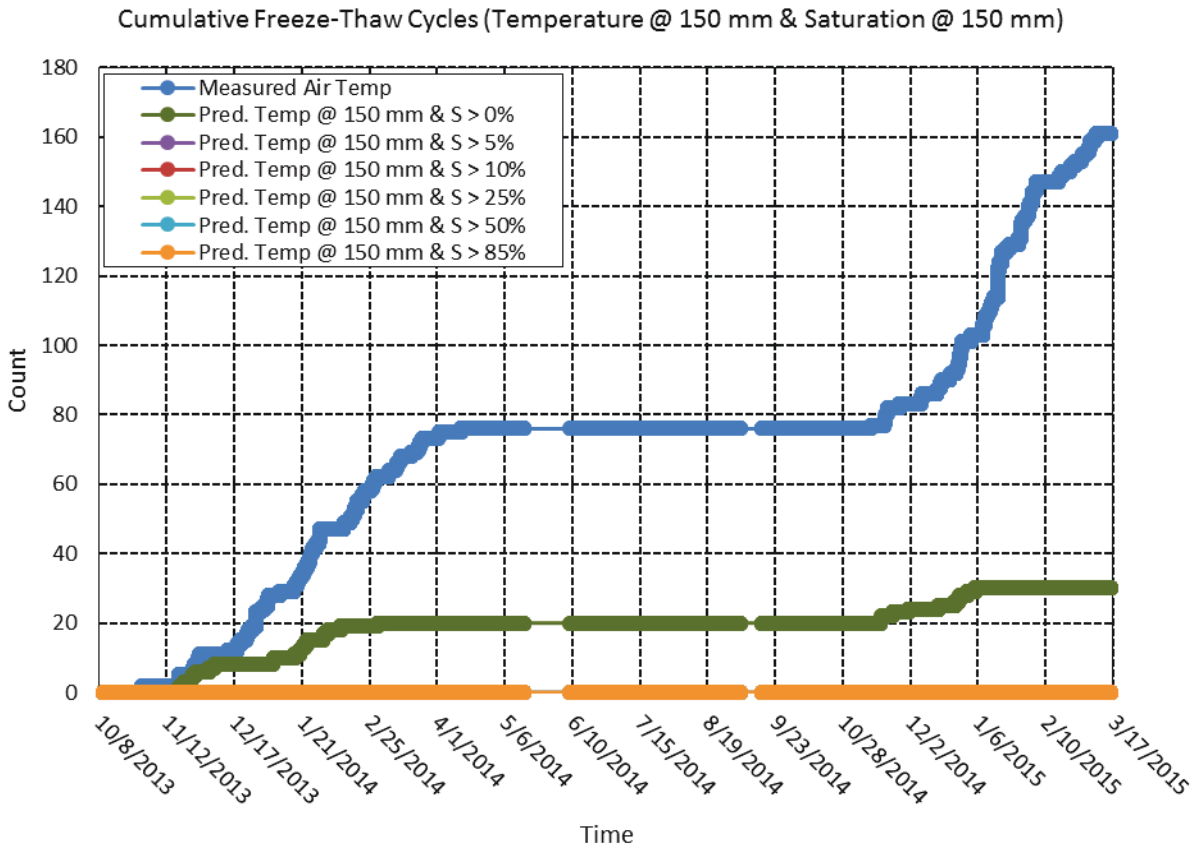

Figure C-52 Cumulative number of freeze-thaw cycles in Lytton, BC, from October 8, 2013, through March 17, 2015, at a depth of 150 mm when both freezing temperatures and minimum degree of saturation is achieved at time of freezing. Predicted internal temperature values are computed using a 2-layered system whose upper concrete layer is defined by a thermal conductivity, λ, value of 1.85 kcal/hmC^{o} and a thermal diffusivity, α, value of 0.0025 m^2/h. The underlying aggregate ballast layer is defined by a thermal conductivity, λ, value of 2.58 kcal/hmC^{o} and a thermal diffusivity, α, value of 0.0030 m^2/h. Predicted degree of saturation is defined by a diffusivity (at S = 100%) value of 0.86x10^{-6} m^2/hr, a regression coefficient, n, of 15, α value of 0.05, and an empirical correlation between relative humidity and degree of saturation. The simulation is initialized with an even distribution of 50 %RH throughout the depth of the concrete.

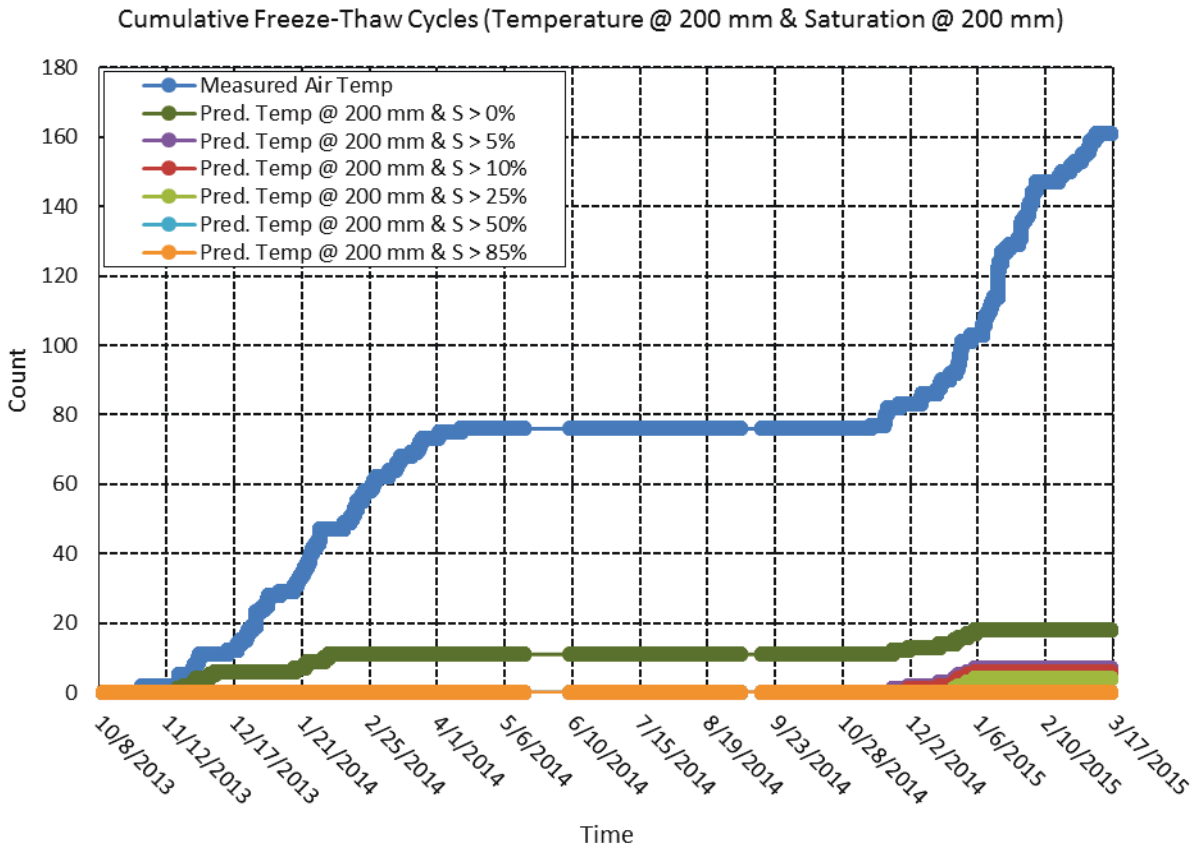

Figure C-53 Cumulative number of freeze-thaw cycles in Lytton, BC, from October 8, 2013, through March 17, 2015, at a depth of 200 mm when both freezing temperatures and minimum degree of saturation is achieved at time of freezing. Predicted internal temperature values are computed using a 2-layered system whose upper concrete layer is defined by a thermal conductivity, λ, value of 1.85 kcal/hmC^{o} and a thermal diffusivity, α, value of 0.0025 m^2/h. The underlying aggregate ballast layer is defined by a thermal conductivity, λ, value of 2.58 kcal/hmC^{o} and a thermal diffusivity, α, value of 0.0030 m^2/h. Predicted degree of saturation is defined by a diffusivity (at S = 100%) value of 0.86x10^{-6} m^2/hr, a regression coefficient, n, of 15, α value of 0.05, and an empirical correlation between relative humidity and degree of saturation. The simulation is initialized with an even distribution of 50 %RH throughout the depth of the concrete.

Modeled freeze-thaw cycles of concrete in Lytton, BC, due to saturation (modeled with D = 1.29 and initial RH = 50%)

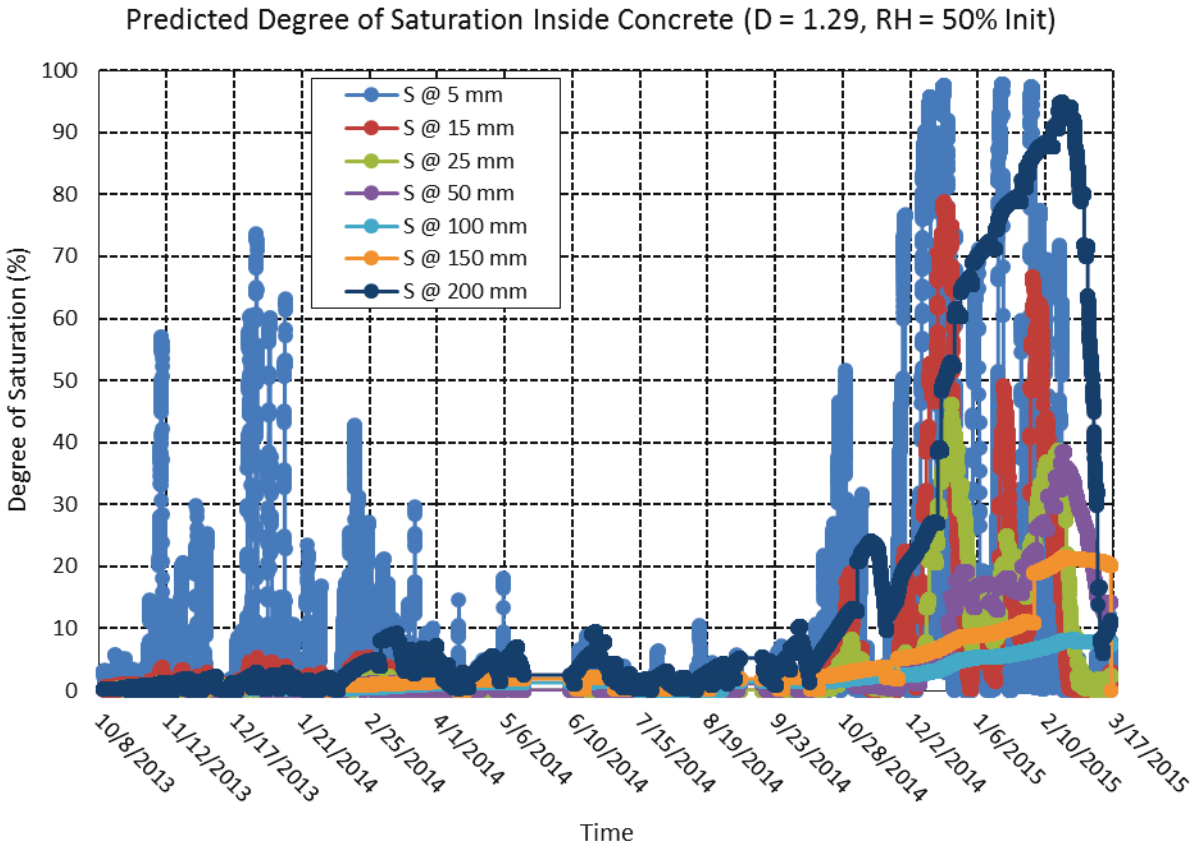

Figure C-54 redicted degree of saturation inside a 1-layered concrete system in Lytton, BC, from October 8, 2013, through March 17, 2015. The concrete is defined by a diffusivity (at S = 100%) value of 1.29×10^{-6} m^2/hr, a regression coefficient, *n*, of 15, α value of 0.05, and an empirical correlation between relative humidity and degree of saturation. The simulation is initialized with an even distribution of 50 %RH throughout the depth of the concrete.

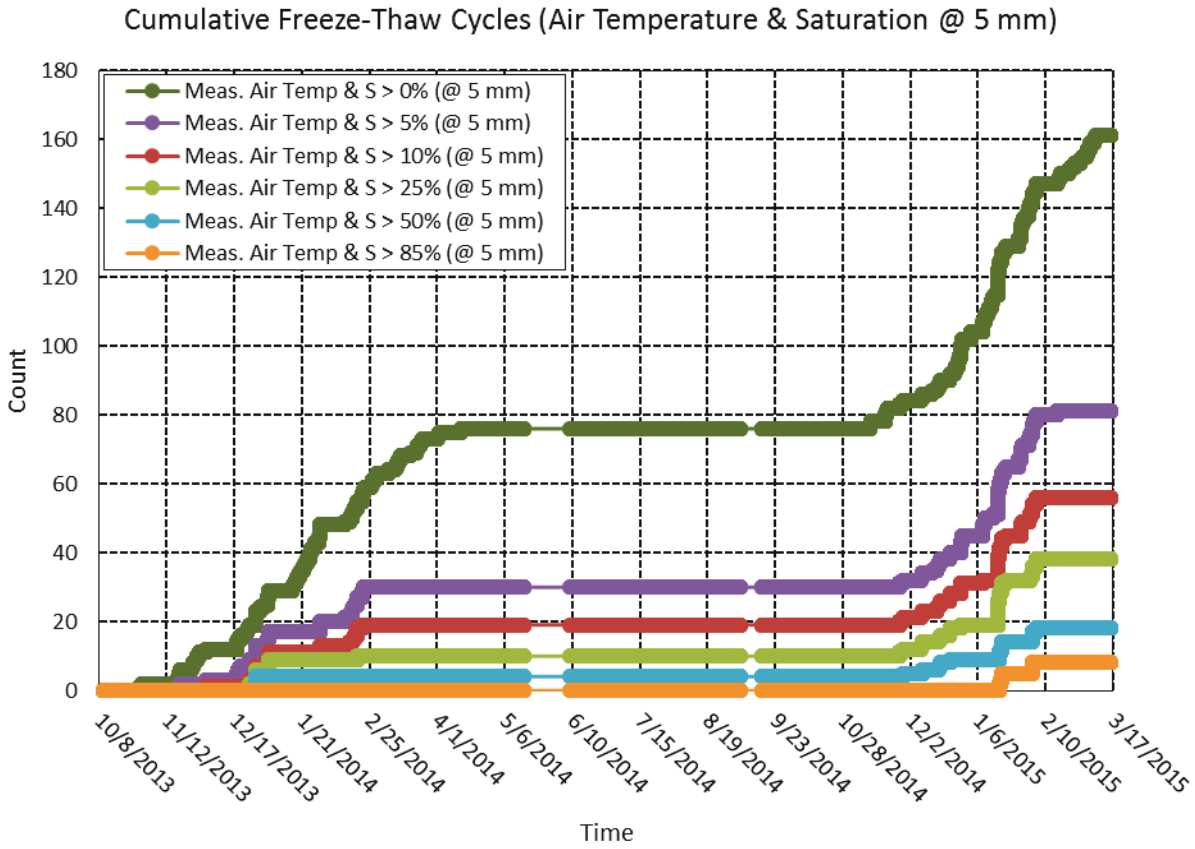

Figure C-55 Cumulative number of freeze-thaw cycles in Lytton, BC, from October 8, 2013, through March 17, 2015, at a depth of 5 mm when both freezing air temperatures and minimum degree of saturation is achieved at time of freezing. Predicted degree of saturation is defined by a diffusivity (at S = 100%) value of 1.29×10^{-6} m^2/hr, a regression coefficient, *n*, of 15, α value of 0.05, and an empirical correlation between relative humidity and degree of saturation. The simulation is initialized with an even distribution of 50 %RH throughout the depth of the concrete.

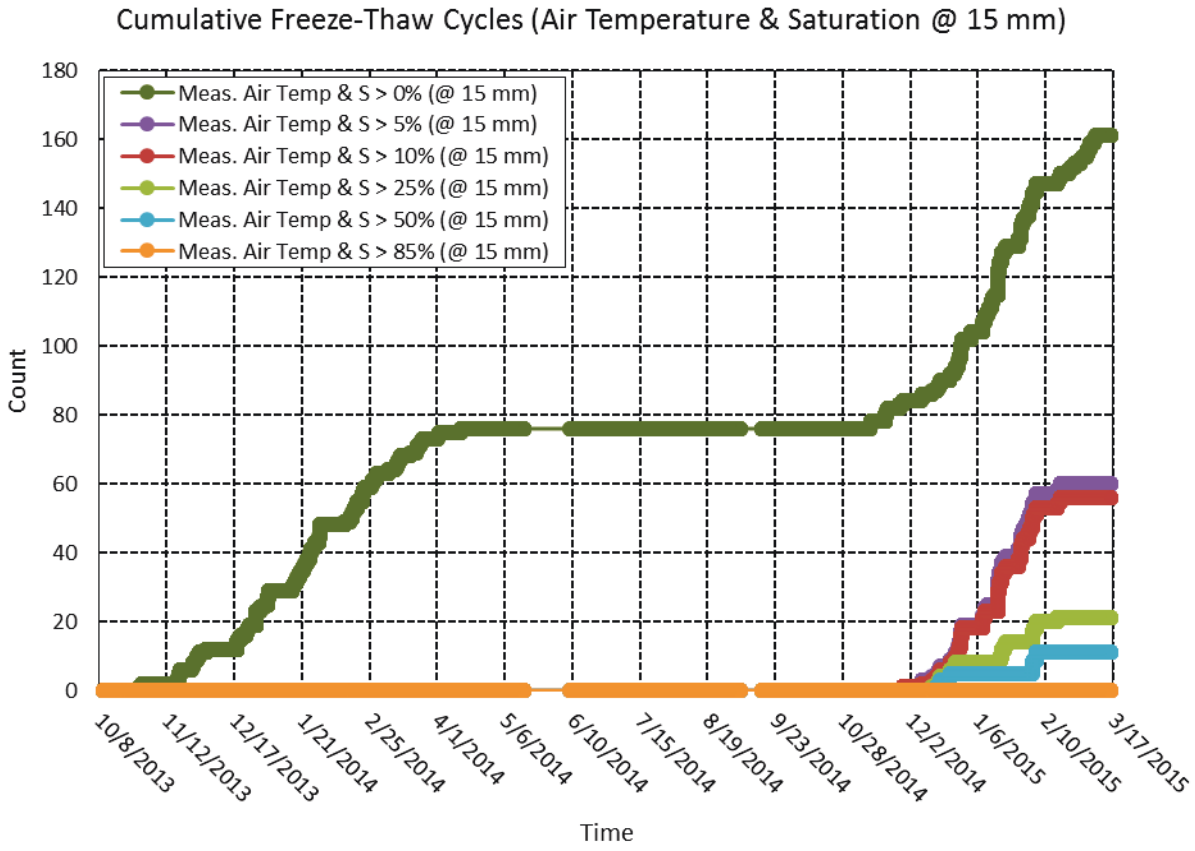

Figure C-56 Cumulative number of freeze-thaw cycles in Lytton, BC, from October 8, 2013, through March 17, 2015, at a depth of 15 mm when both freezing air temperatures and minimum degree of saturation is achieved at time of freezing. Predicted degree of saturation is defined by a diffusivity (at S = 100%) value of 1.29×10^{-6} m^2/hr, a regression coefficient, *n*, of 15, α value of 0.05, and an empirical correlation between relative humidity and degree of saturation. The simulation is initialized with an even distribution of 50 %RH throughout the depth of the concrete.

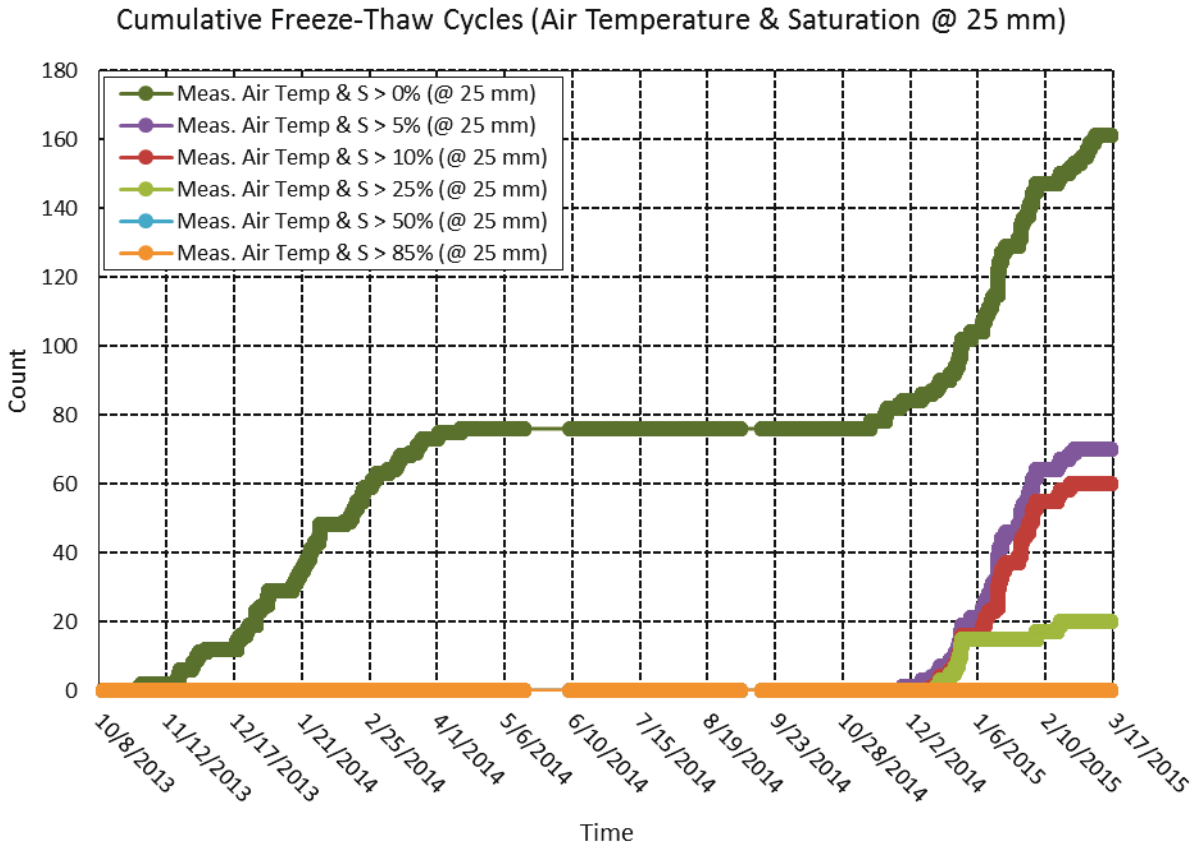

Figure C-57 Cumulative number of freeze-thaw cycles in Lytton, BC, from October 8, 2013, through March 17, 2015, at a depth of 25 mm when both freezing air temperatures and minimum degree of saturation is achieved at time of freezing. Predicted degree of saturation is defined by a diffusivity (at S = 100%) value of 1.29×10^{-6} m^2/hr, a regression coefficient, *n*, of 15, α value of 0.05, and an empirical correlation between relative humidity and degree of saturation. The simulation is initialized with an even distribution of 50 %RH throughout the depth of the concrete.

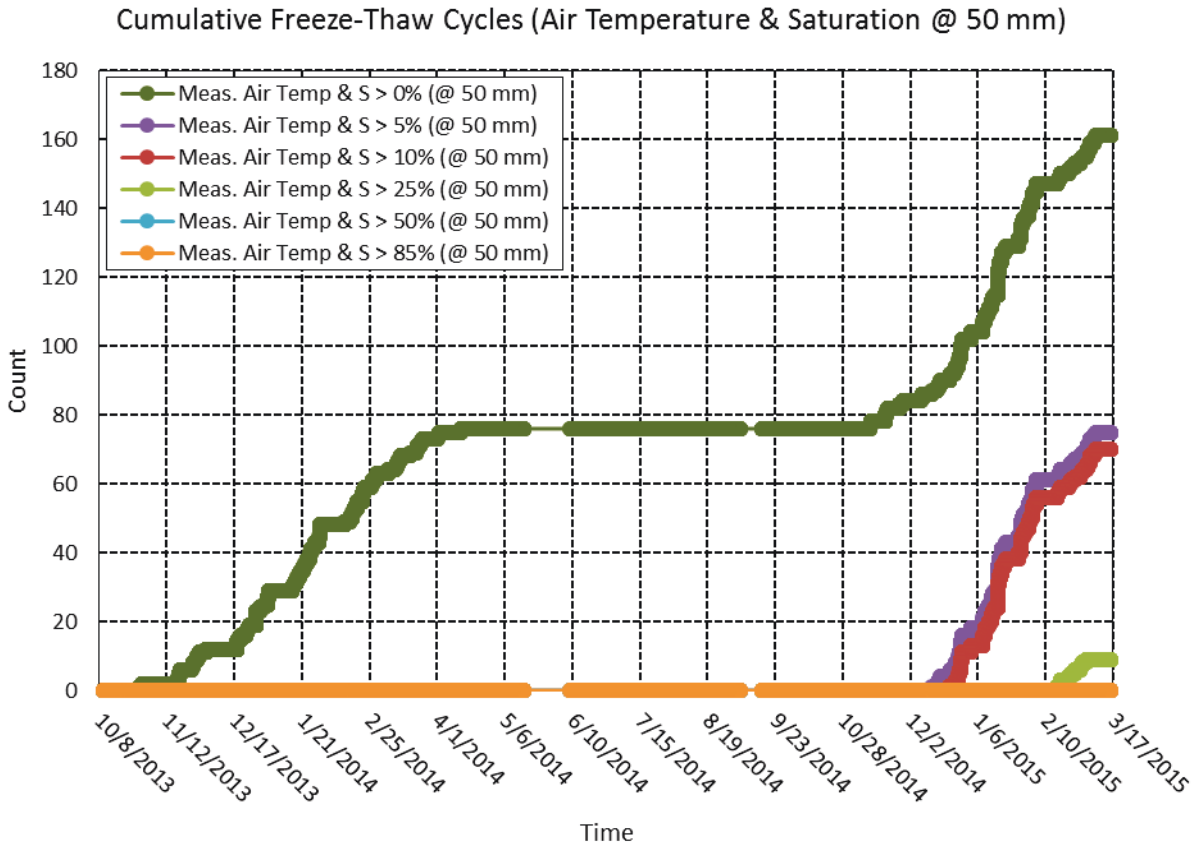

Figure C-58 Cumulative number of freeze-thaw cycles in Lytton, BC, from October 8, 2013, through March 17, 2015, at a depth of 50 mm when both freezing air temperatures and minimum degree of saturation is achieved at time of freezing. Predicted degree of saturation is defined by a diffusivity (at S = 100%) value of 1.29×10^{-6} m^2/hr, a regression coefficient, *n*, of 15, α value of 0.05, and an empirical correlation between relative humidity and degree of saturation. The simulation is initialized with an even distribution of 50 %RH throughout the depth of the concrete.

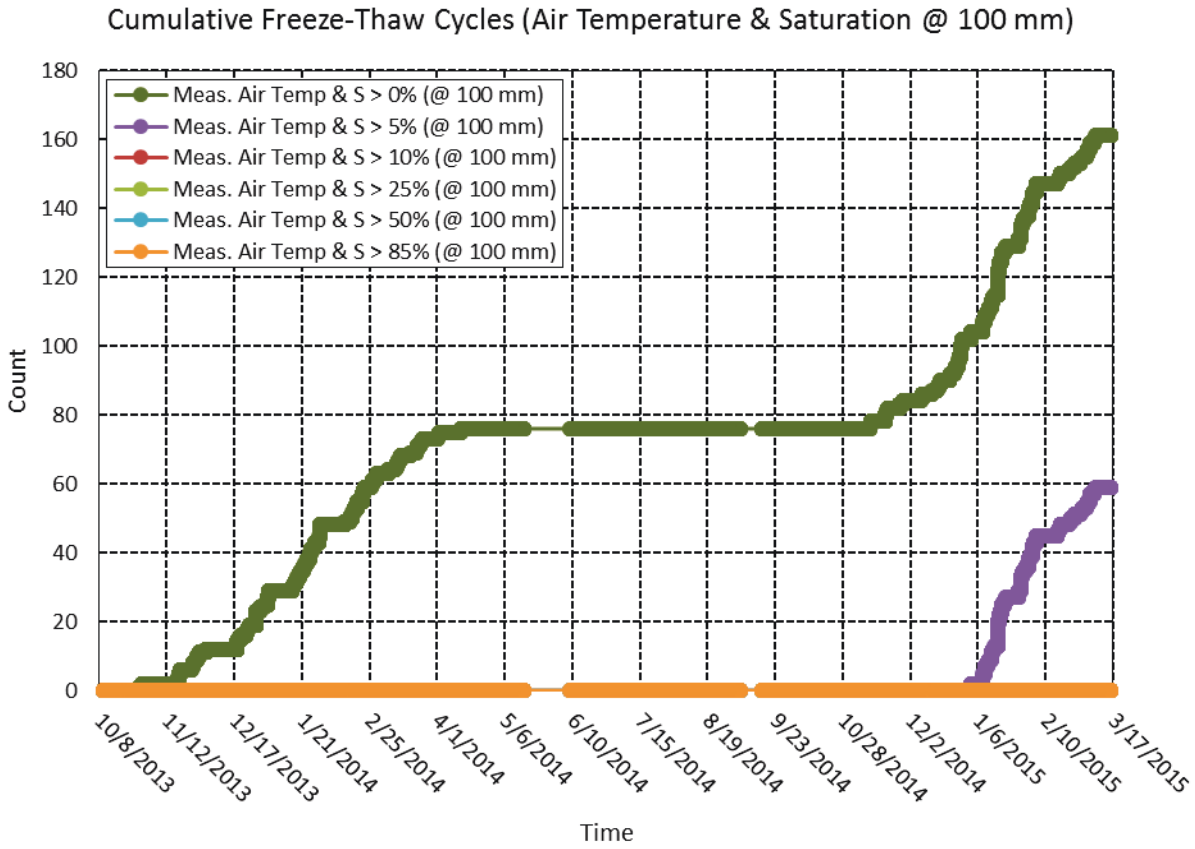

Figure C-59 Cumulative number of freeze-thaw cycles in Lytton, BC, from October 8, 2013, through March 17, 2015, at a depth of 100 mm when both freezing air temperatures and minimum degree of saturation is achieved at time of freezing. Predicted degree of saturation is defined by a diffusivity (at S = 100%) value of 1.29×10^{-6} m^2/hr, a regression coefficient, *n*, of 15, α value of 0.05, and an empirical correlation between relative humidity and degree of saturation. The simulation is initialized with an even distribution of 50 %RH throughout the depth of the concrete.

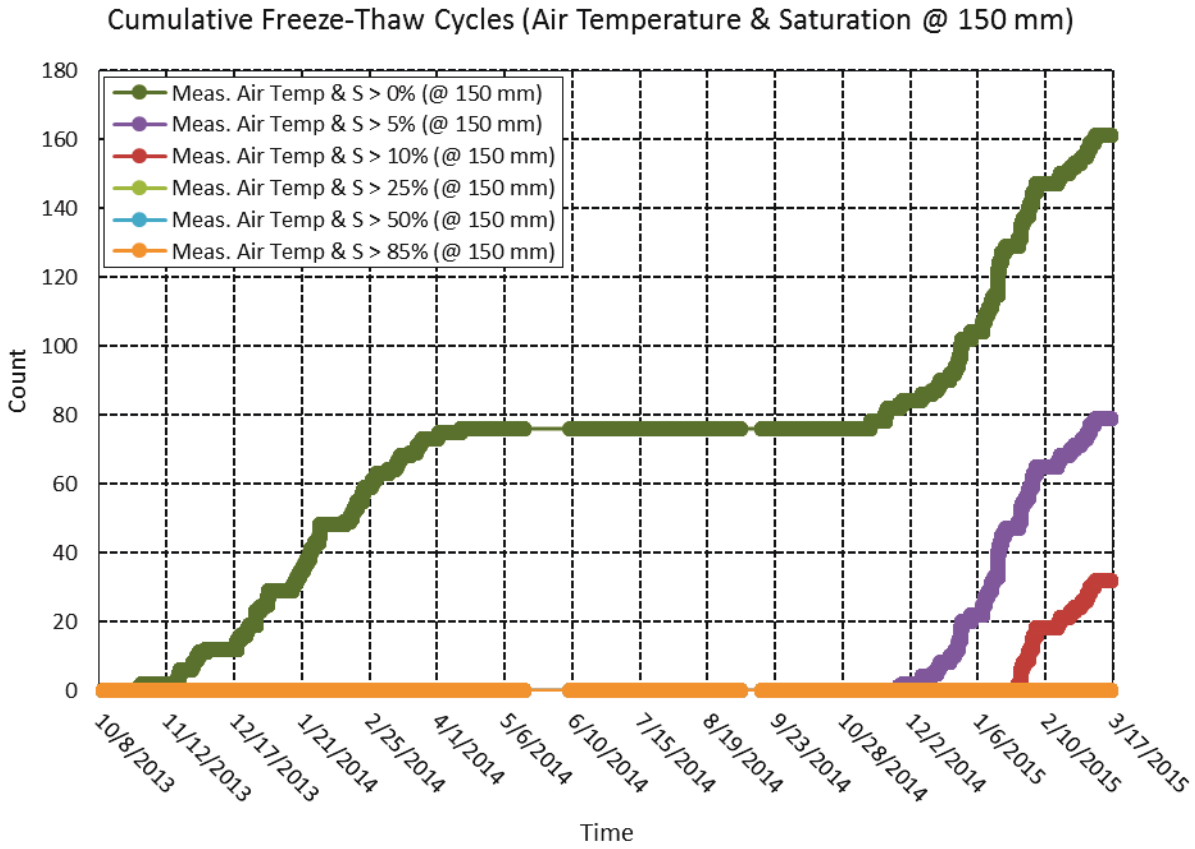

Figure C-60 Cumulative number of freeze-thaw cycles in Lytton, BC, from October 8, 2013, through March 17, 2015, at a depth of 150 mm when both freezing air temperatures and minimum degree of saturation is achieved at time of freezing. Predicted degree of saturation is defined by a diffusivity (at S = 100%) value of 1.29×10^{-6} m^2/hr, a regression coefficient, *n*, of 15, α value of 0.05, and an empirical correlation between relative humidity and degree of saturation. The simulation is initialized with an even distribution of 50 %RH throughout the depth of the concrete.

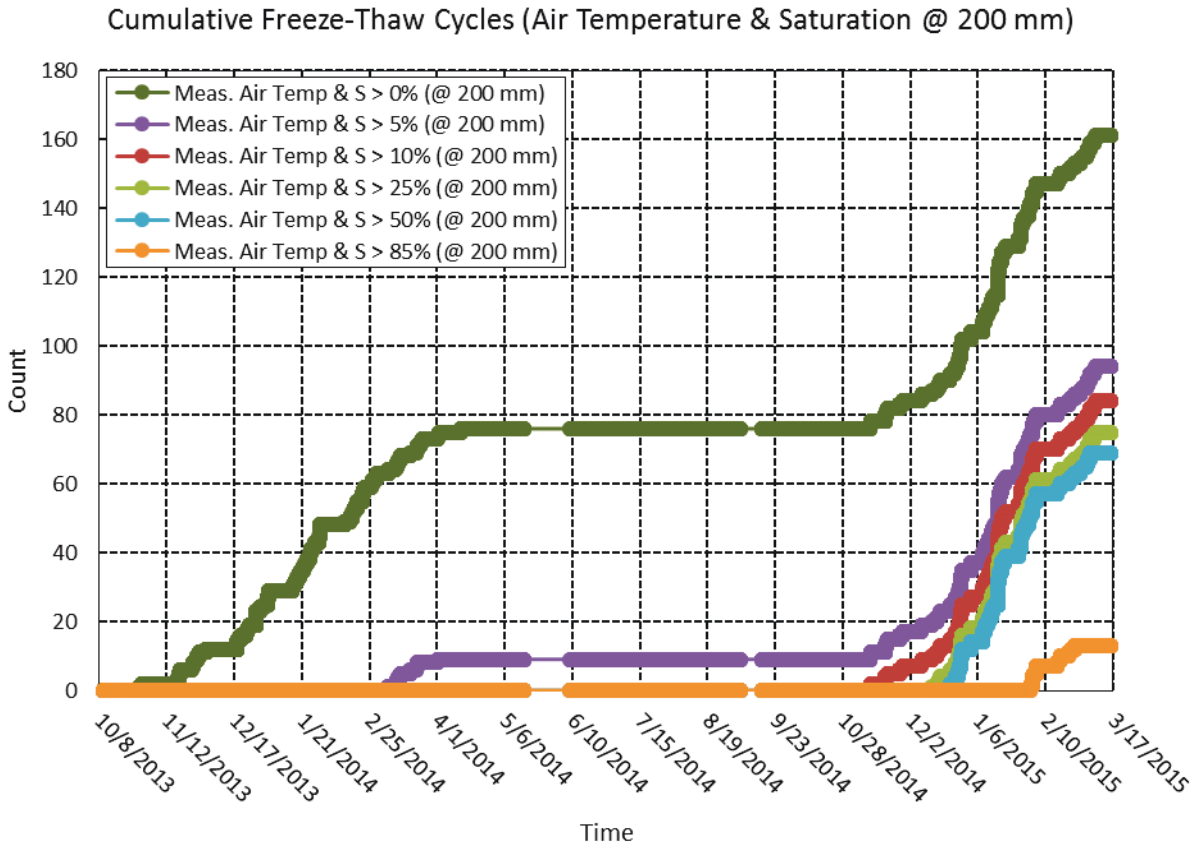

Figure C-61 Cumulative number of freeze-thaw cycles in Lytton, BC, from October 8, 2013, through March 17, 2015, at a depth of 200 mm when both freezing air temperatures and minimum degree of saturation is achieved at time of freezing. Predicted degree of saturation is defined by a diffusivity (at S = 100%) value of 1.29×10^{-6} m^2/hr, a regression coefficient, *n*, of 15, α value of 0.05, and an empirical correlation between relative humidity and degree of saturation. The simulation is initialized with an even distribution of 50 %RH throughout the depth of the concrete.

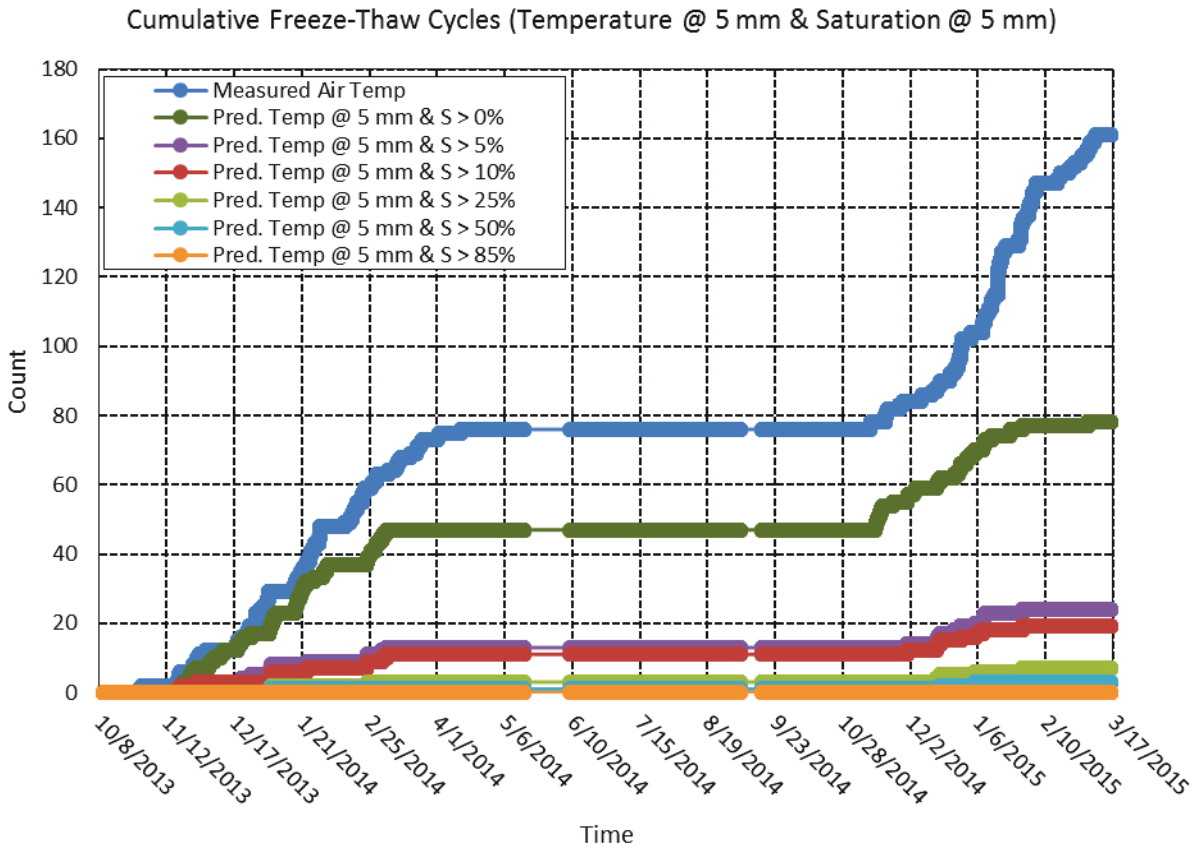

Figure C-62 Cumulative number of freeze-thaw cycles in Lytton, BC, from October 8, 2013, through March 17, 2015, at a depth of 5 mm when both freezing temperatures and minimum degree of saturation is achieved at time of freezing. Predicted internal temperature values are computed using a 2-layered system whose upper concrete layer is defined by a thermal conductivity, λ, value of 1.85 kcal/hmC^{o} and a thermal diffusivity, α, value of 0.0025 m^2/h. The underlying aggregate ballast layer is defined by a thermal conductivity, λ, value of 2.58 kcal/hmC^{o} and a thermal diffusivity, α, value of 0.0030 m^2/h. Predicted degree of saturation is defined by a diffusivity (at S = 100%) value of 1.29x10^{-6} m^2/hr, a regression coefficient, n, of 15, α value of 0.05, and an empirical correlation between relative humidity and degree of saturation. The simulation is initialized with an even distribution of 50 %RH throughout the depth of the concrete.

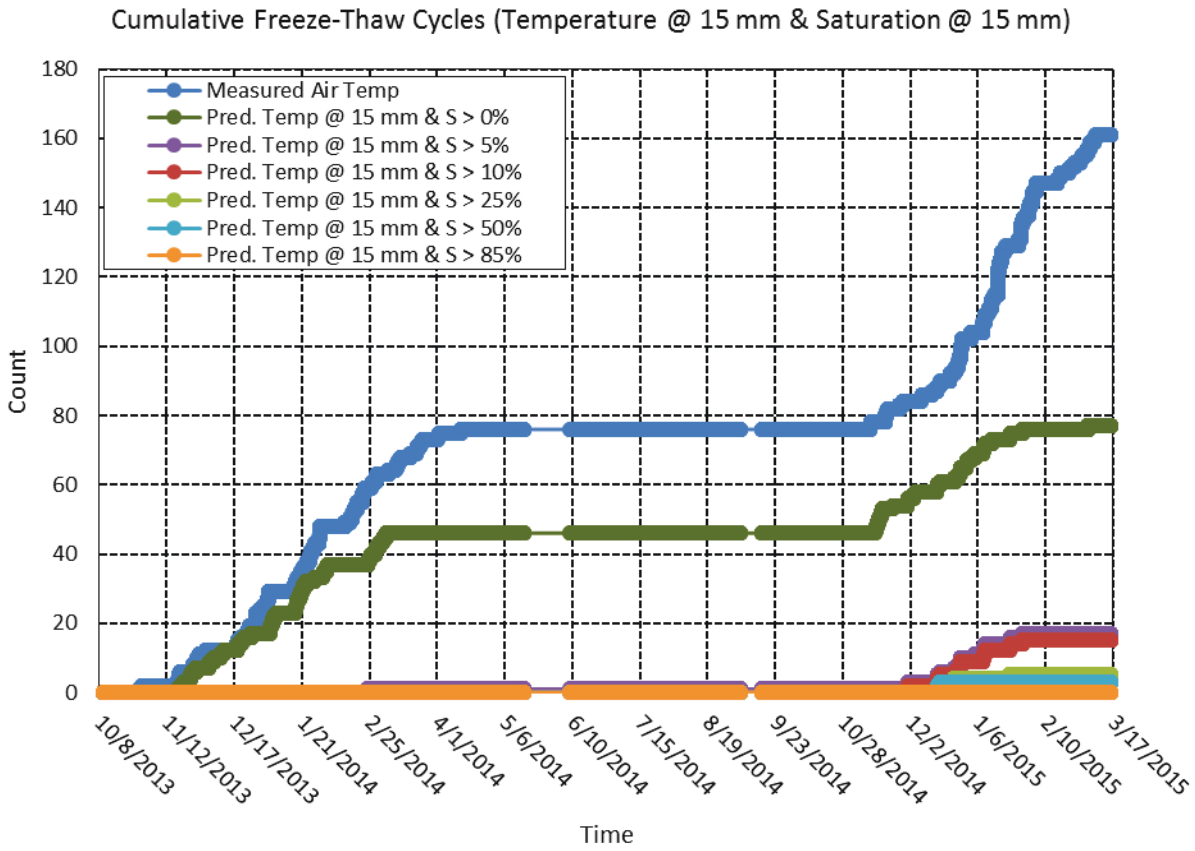

Figure C-63 Cumulative number of freeze-thaw cycles in Lytton, BC, from October 8, 2013, through March 17, 2015, at a depth of 15 mm when both freezing temperatures and minimum degree of saturation is achieved at time of freezing. Predicted internal temperature values are computed using a 2-layered system whose upper concrete layer is defined by a thermal conductivity, λ, value of 1.85 kcal/hmC^{o} and a thermal diffusivity, α, value of 0.0025 m^2/h. The underlying aggregate ballast layer is defined by a thermal conductivity, λ, value of 2.58 kcal/hmC^{o} and a thermal diffusivity, α, value of 0.0030 m^2/h. Predicted degree of saturation is defined by a diffusivity (at S = 100%) value of 1.29x10^{-6} m^2/hr, a regression coefficient, n, of 15, α value of 0.05, and an empirical correlation between relative humidity and degree of saturation. The simulation is initialized with an even distribution of 50 %RH throughout the depth of the concrete.

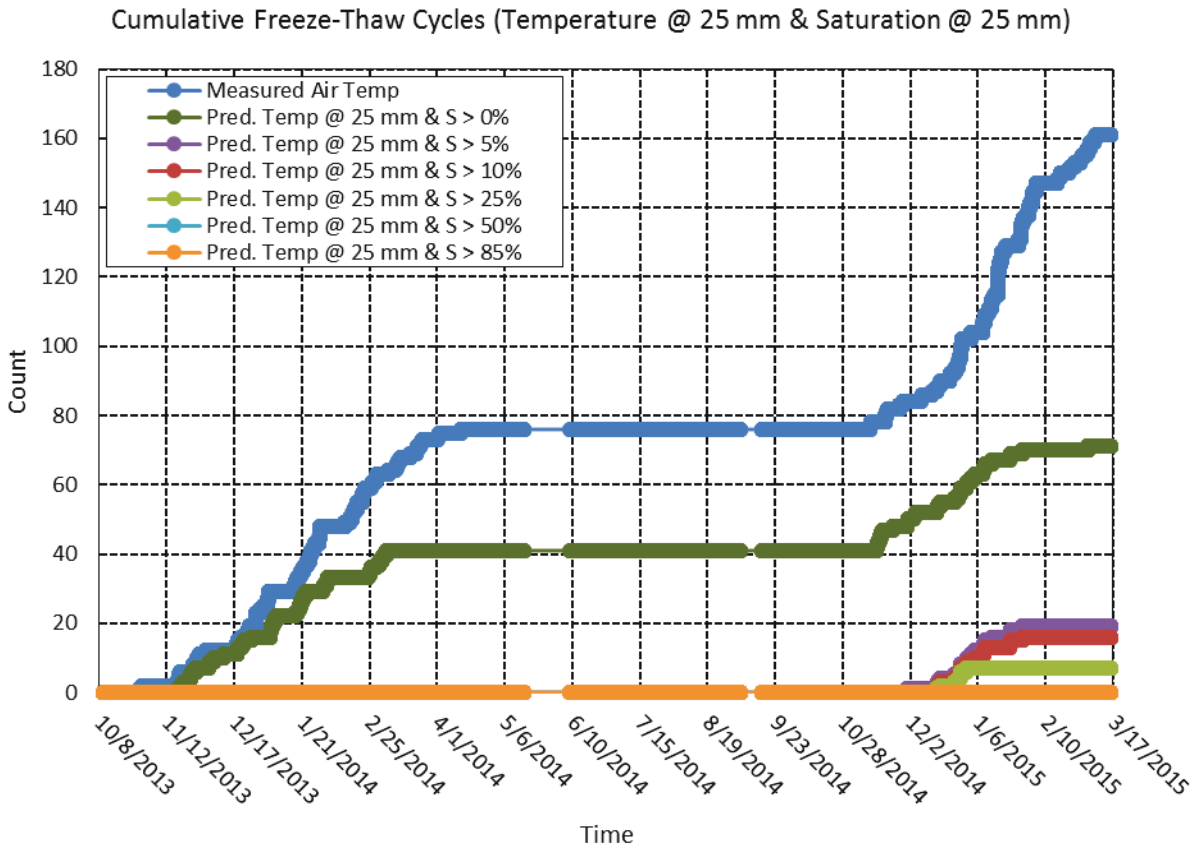

Figure C-64 Cumulative number of freeze-thaw cycles in Lytton, BC, from October 8, 2013, through March 17, 2015, at a depth of 25 mm when both freezing temperatures and minimum degree of saturation is achieved at time of freezing. Predicted internal temperature values are computed using a 2-layered system whose upper concrete layer is defined by a thermal conductivity, λ, value of 1.85 kcal/hmC^{o} and a thermal diffusivity, α, value of 0.0025 m^2/h. The underlying aggregate ballast layer is defined by a thermal conductivity, λ, value of 2.58 kcal/hmC^{o} and a thermal diffusivity, α, value of 0.0030 m^2/h. Predicted degree of saturation is defined by a diffusivity (at S = 100%) value of 1.29x10^{-6} m^2/hr, a regression coefficient, n, of 15, α value of 0.05, and an empirical correlation between relative humidity and degree of saturation. The simulation is initialized with an even distribution of 50 %RH throughout the depth of the concrete.

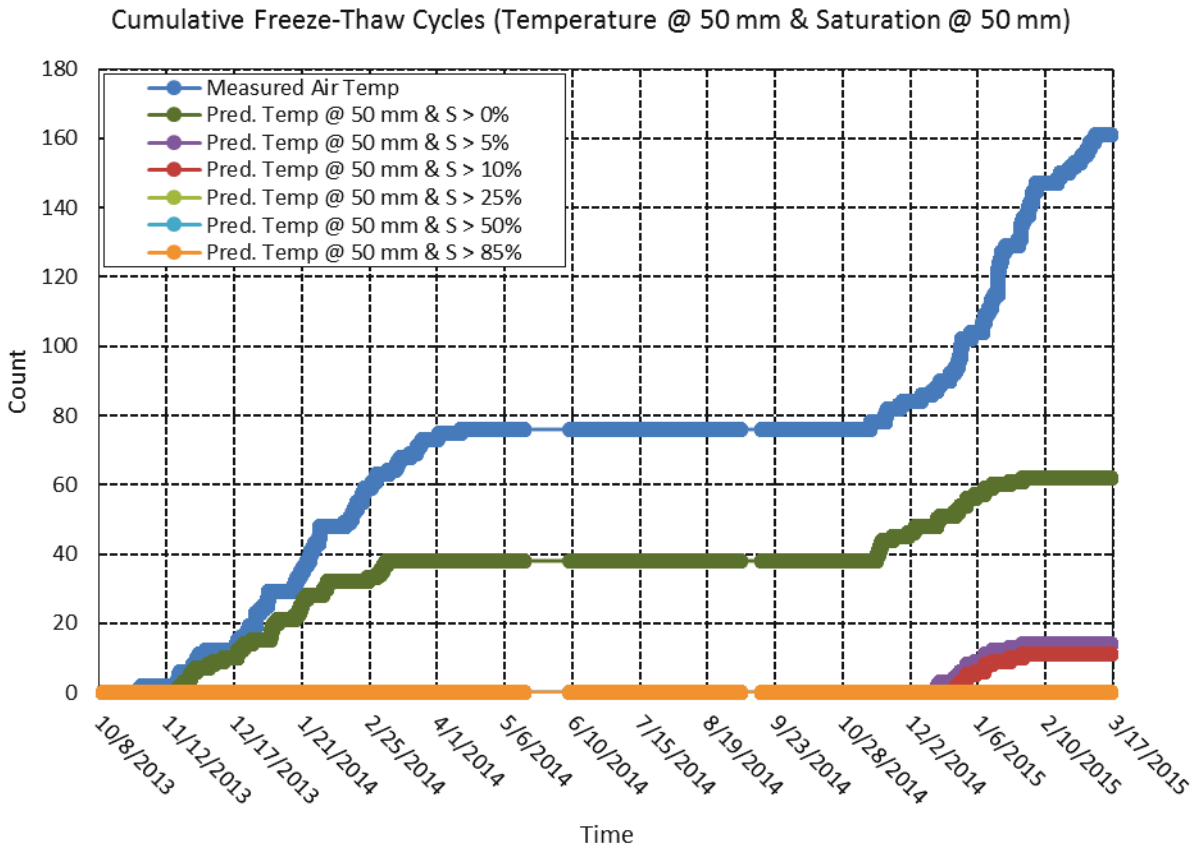

Figure C-65 Cumulative number of freeze-thaw cycles in Lytton, BC, from October 8, 2013, through March 17, 2015, at a depth of 50 mm when both freezing temperatures and minimum degree of saturation is achieved at time of freezing. Predicted internal temperature values are computed using a 2-layered system whose upper concrete layer is defined by a thermal conductivity, λ, value of 1.85 kcal/hmC^{o} and a thermal diffusivity, α, value of 0.0025 m^2/h. The underlying aggregate ballast layer is defined by a thermal conductivity, λ, value of 2.58 kcal/hmC^{o} and a thermal diffusivity, α, value of 0.0030 m^2/h. Predicted degree of saturation is defined by a diffusivity (at S = 100%) value of 1.29x10^{-6} m^2/hr, a regression coefficient, n, of 15, α value of 0.05, and an empirical correlation between relative humidity and degree of saturation. The simulation is initialized with an even distribution of 50 %RH throughout the depth of the concrete.

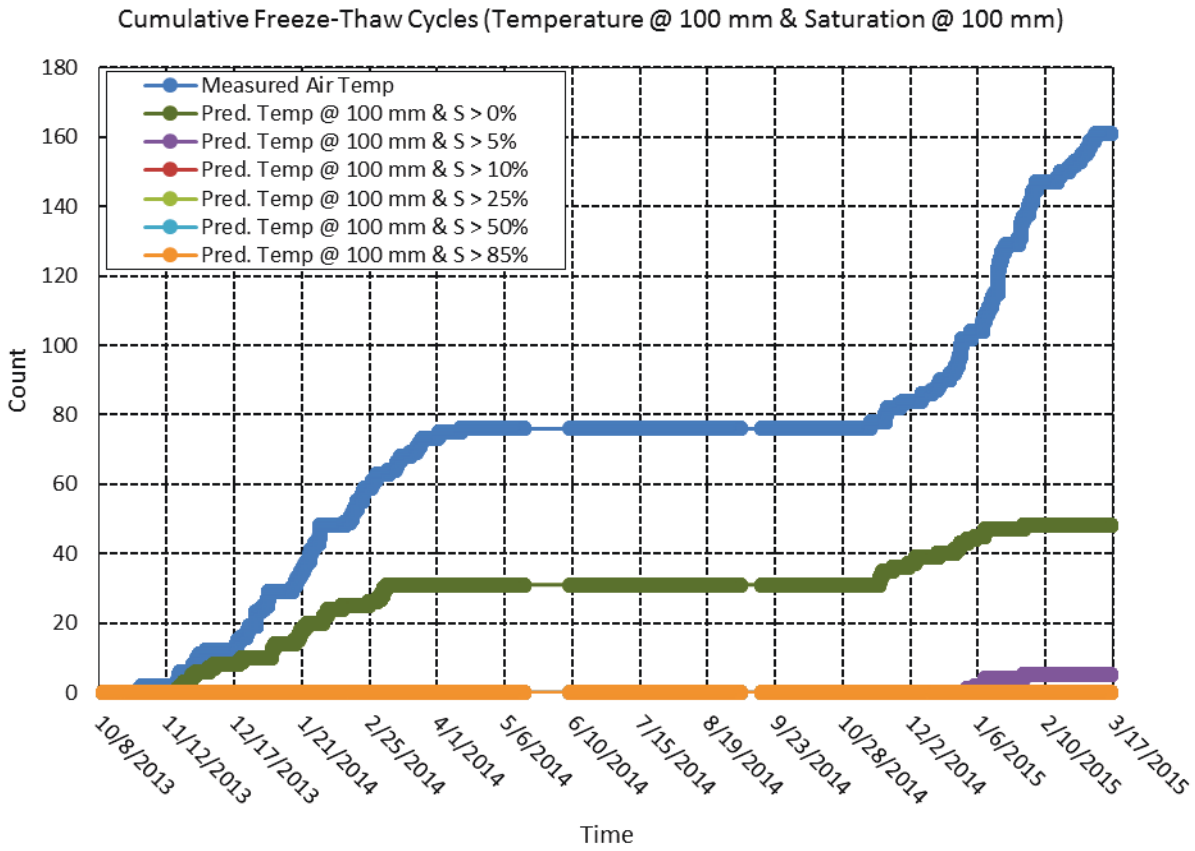

Figure C-66 Cumulative number of freeze-thaw cycles in Lytton, BC, from October 8, 2013, through March 17, 2015, at a depth of 100 mm when both freezing temperatures and minimum degree of saturation is achieved at time of freezing. Predicted internal temperature values are computed using a 2-layered system whose upper concrete layer is defined by a thermal conductivity, λ, value of 1.85 kcal/hmC^{o} and a thermal diffusivity, α, value of 0.0025 m^2/h. The underlying aggregate ballast layer is defined by a thermal conductivity, λ, value of 2.58 kcal/hmC^{o} and a thermal diffusivity, α, value of 0.0030 m^2/h. Predicted degree of saturation is defined by a diffusivity (at S = 100%) value of 1.29x10^{-6} m^2/hr, a regression coefficient, n, of 15, α value of 0.05, and an empirical correlation between relative humidity and degree of saturation. The simulation is initialized with an even distribution of 50 %RH throughout the depth of the concrete.

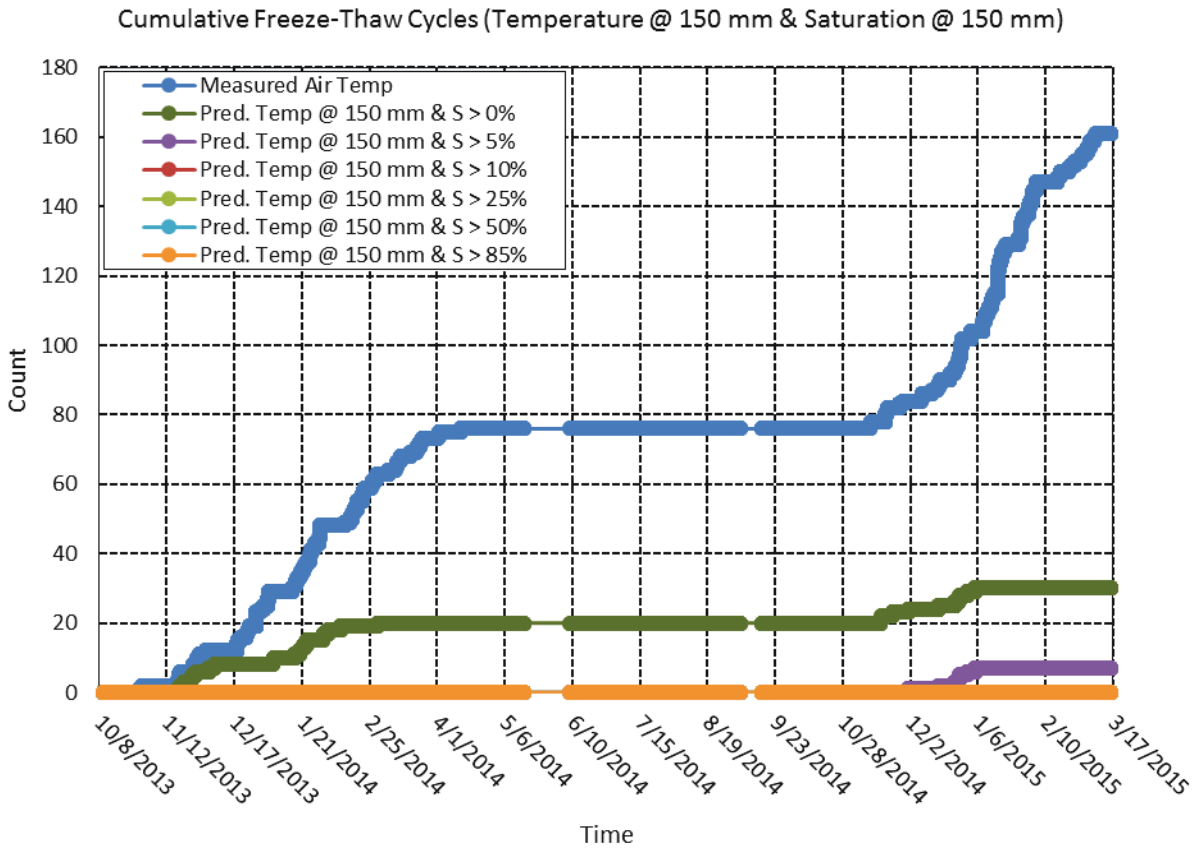

Figure C-67 Cumulative number of freeze-thaw cycles in Lytton, BC, from October 8, 2013, through March 17, 2015, at a depth of 150 mm when both freezing temperatures and minimum degree of saturation is achieved at time of freezing. Predicted internal temperature values are computed using a 2-layered system whose upper concrete layer is defined by a thermal conductivity, λ, value of 1.85 kcal/hmC^{o} and a thermal diffusivity, α, value of 0.0025 m^2/h. The underlying aggregate ballast layer is defined by a thermal conductivity, λ, value of 2.58 kcal/hmC^{o} and a thermal diffusivity, α, value of 0.0030 m^2/h. Predicted degree of saturation is defined by a diffusivity (at S = 100%) value of 1.29x10^{-6} m^2/hr, a regression coefficient, n, of 15, α value of 0.05, and an empirical correlation between relative humidity and degree of saturation. The simulation is initialized with an even distribution of 50 %RH throughout the depth of the concrete.

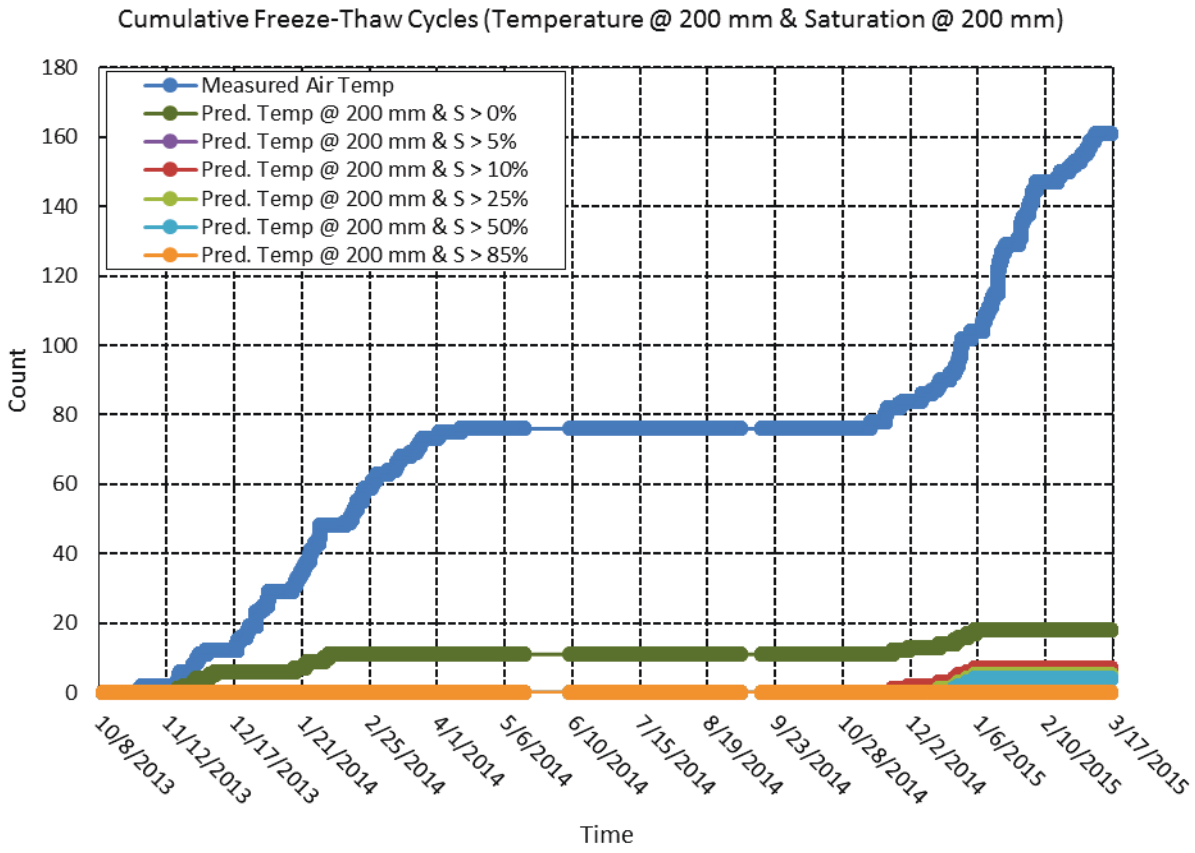

Figure C-68 Cumulative number of freeze-thaw cycles in Lytton, BC, from October 8, 2013, through March 17, 2015, at a depth of 200 mm when both freezing temperatures and minimum degree of saturation is achieved at time of freezing. Predicted internal temperature values are computed using a 2-layered system whose upper concrete layer is defined by a thermal conductivity, λ, value of 1.85 kcal/hmC^{o} and a thermal diffusivity, α, value of 0.0025 m^2/h. The underlying aggregate ballast layer is defined by a thermal conductivity, λ, value of 2.58 kcal/hmC^{o} and a thermal diffusivity, α, value of 0.0030 m^2/h. Predicted degree of saturation is defined by a diffusivity (at S = 100%) value of 1.29x10^{-6} m^2/hr, a regression coefficient, n, of 15, α value of 0.05, and an empirical correlation between relative humidity and degree of saturation. The simulation is initialized with an even distribution of 50 %RH throughout the depth of the concrete.

Modeled freeze-thaw cycles of concrete in Rantoul, IL, due to saturation (modeled with D = 0.86 and initial RH = 85%)

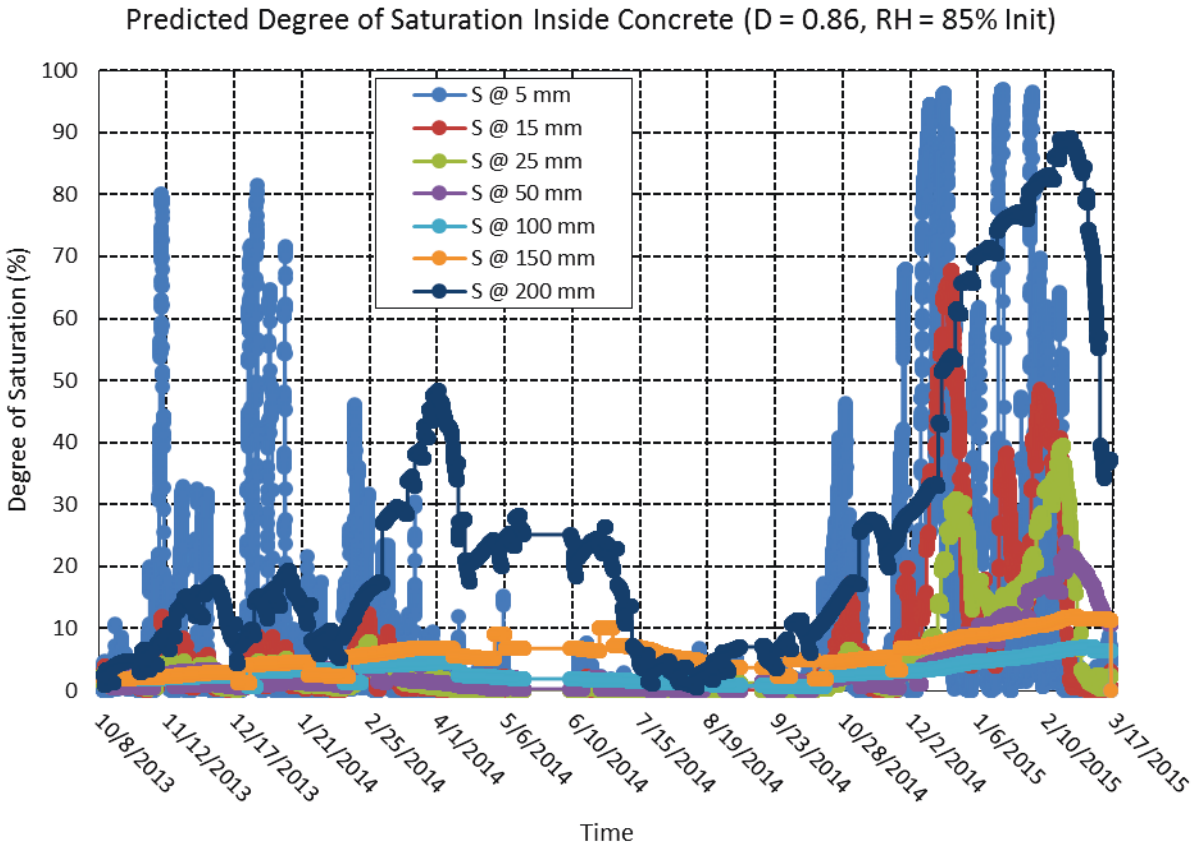

Figure C-69 Predicted degree of saturation inside a 1-layered concrete system in Lytton, BC, from October 8, 2013, through March 17, 2015. The concrete is defined by a diffusivity (at S = 100%) value of 0.86×10^{-6} m^2/hr, a regression coefficient, *n*, of 15, α value of 0.05, and an empirical correlation between relative humidity and degree of saturation. The simulation is initialized with an even distribution of 85 %RH throughout the depth of the concrete.

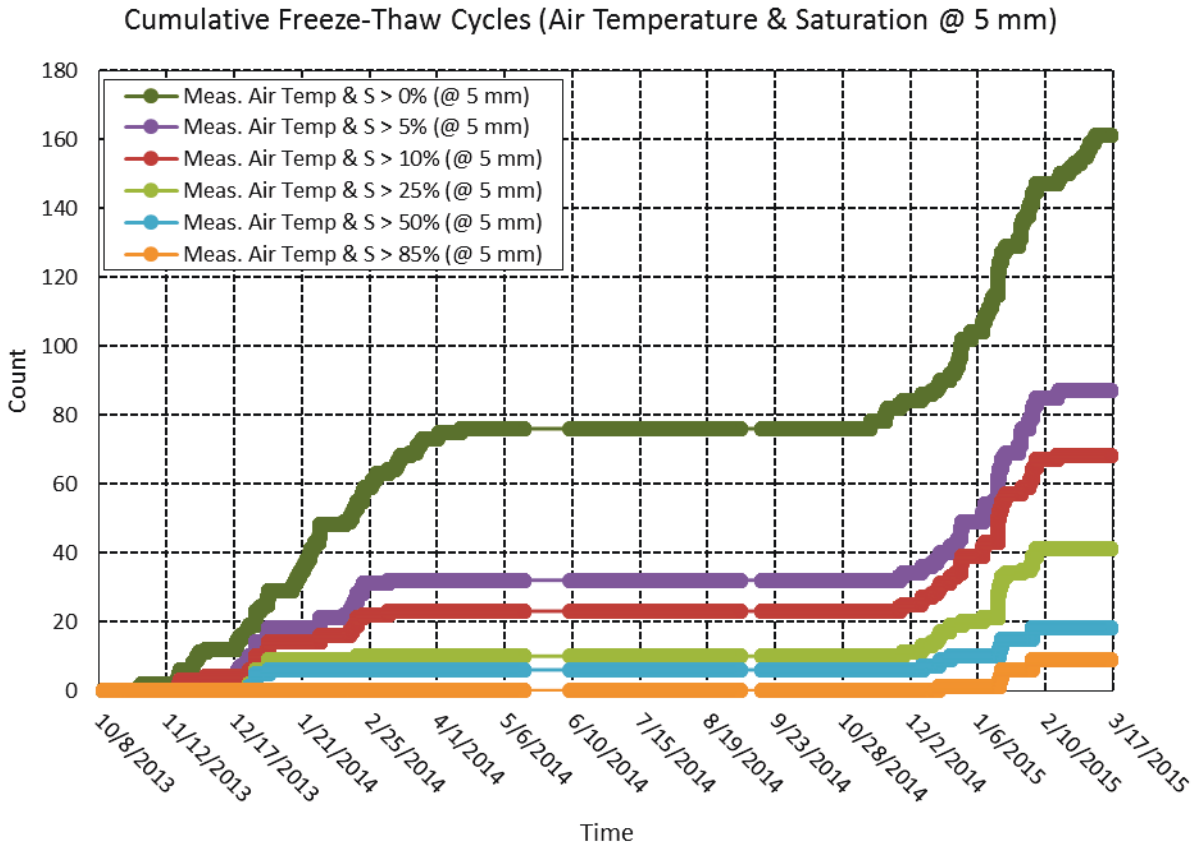

Figure C-70 Cumulative number of freeze-thaw cycles in Lytton, BC, from October 8, 2013, through March 17, 2015, at a depth of 5 mm when both freezing air temperatures and minimum degree of saturation is achieved at time of freezing. Predicted degree of saturation is defined by a diffusivity (at S = 100%) value of 0.86×10^{-6} m^2/hr, a regression coefficient, *n*, of 15, α value of 0.05, and an empirical correlation between relative humidity and degree of saturation. The simulation is initialized with an even distribution of 85 %RH throughout the depth of the concrete.

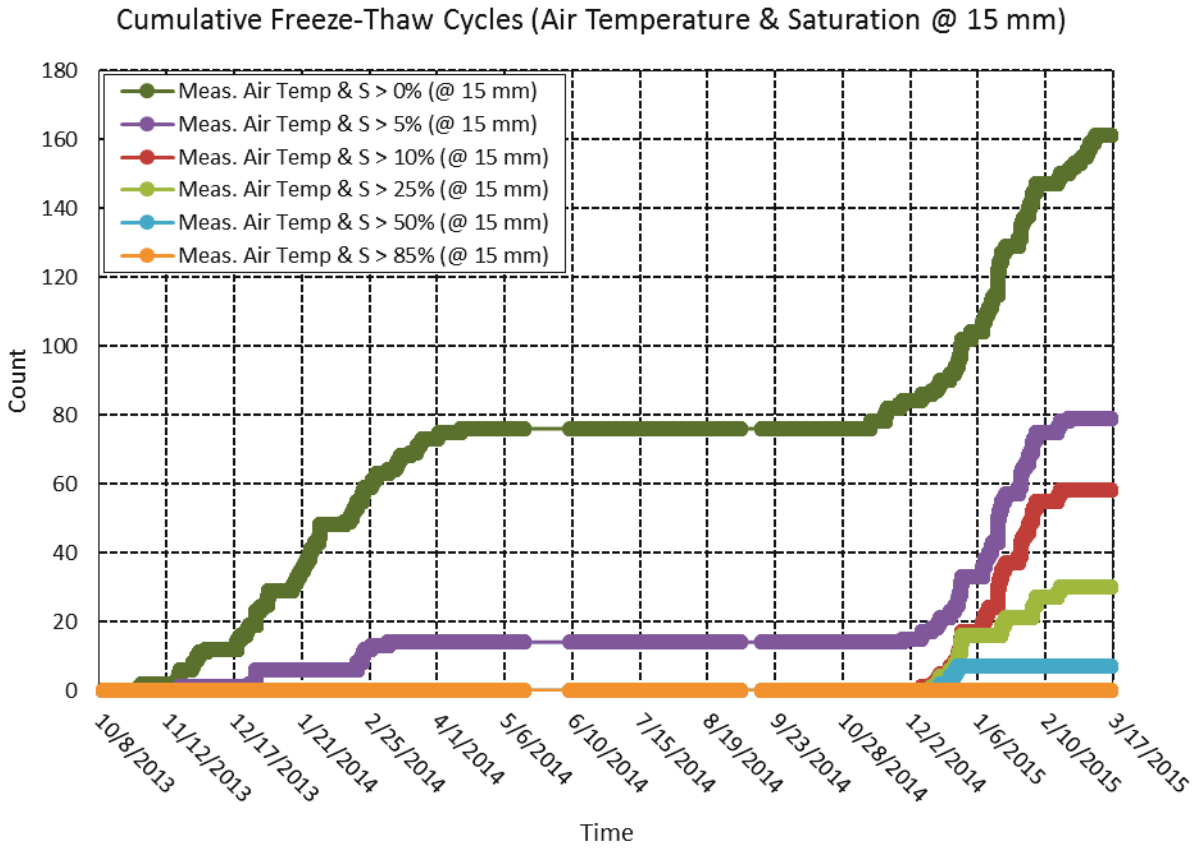

Figure C-71 Cumulative number of freeze-thaw cycles in Lytton, BC, from October 8, 2013, through March 17, 2015, at a depth of 15 mm when both freezing air temperatures and minimum degree of saturation is achieved at time of freezing. Predicted degree of saturation is defined by a diffusivity (at S = 100%) value of 0.86×10^{-6} m^2/hr, a regression coefficient, *n*, of 15, α value of 0.05, and an empirical correlation between relative humidity and degree of saturation. The simulation is initialized with an even distribution of 85 %RH throughout the depth of the concrete.

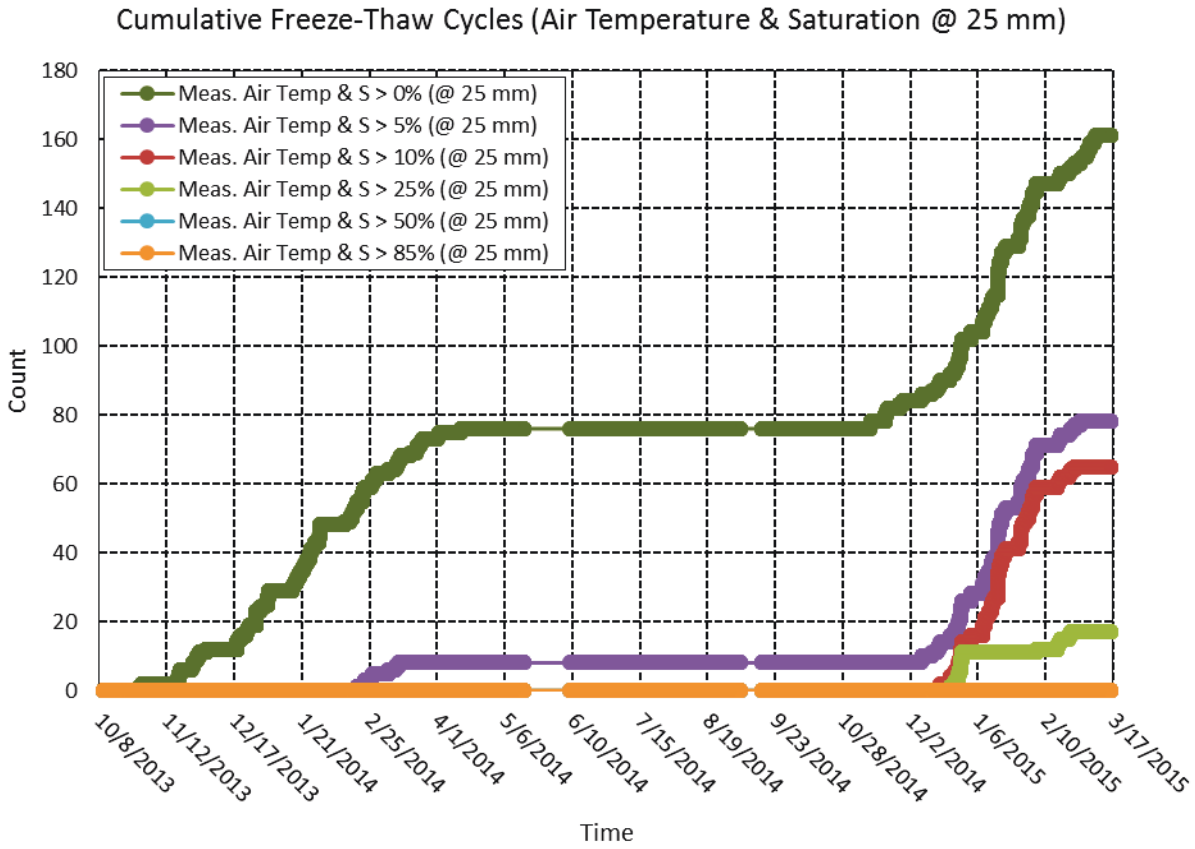

Figure C-72 Cumulative number of freeze-thaw cycles in Lytton, BC, from October 8, 2013, through March 17, 2015, at a depth of 25 mm when both freezing air temperatures and minimum degree of saturation is achieved at time of freezing. Predicted degree of saturation is defined by a diffusivity (at S = 100%) value of 0.86×10^{-6} m^2/hr, a regression coefficient, *n*, of 15, α value of 0.05, and an empirical correlation between relative humidity and degree of saturation. The simulation is initialized with an even distribution of 85 %RH throughout the depth of the concrete.

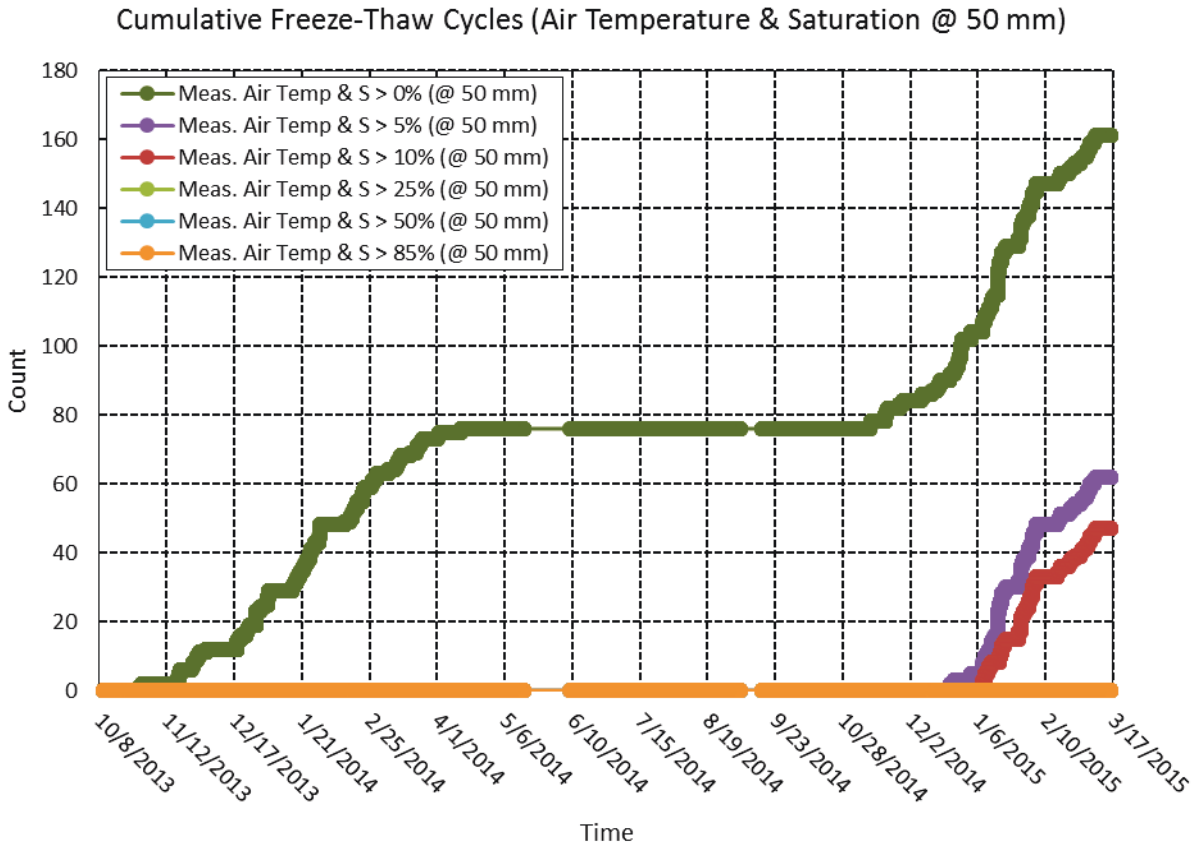

Figure C-73 Cumulative number of freeze-thaw cycles in Lytton, BC, from October 8, 2013, through March 17, 2015, at a depth of 50 mm when both freezing air temperatures and minimum degree of saturation is achieved at time of freezing. Predicted degree of saturation is defined by a diffusivity (at S = 100%) value of 0.86×10^{-6} m^2/hr, a regression coefficient, *n*, of 15, α value of 0.05, and an empirical correlation between relative humidity and degree of saturation. The simulation is initialized with an even distribution of 85 %RH throughout the depth of the concrete.

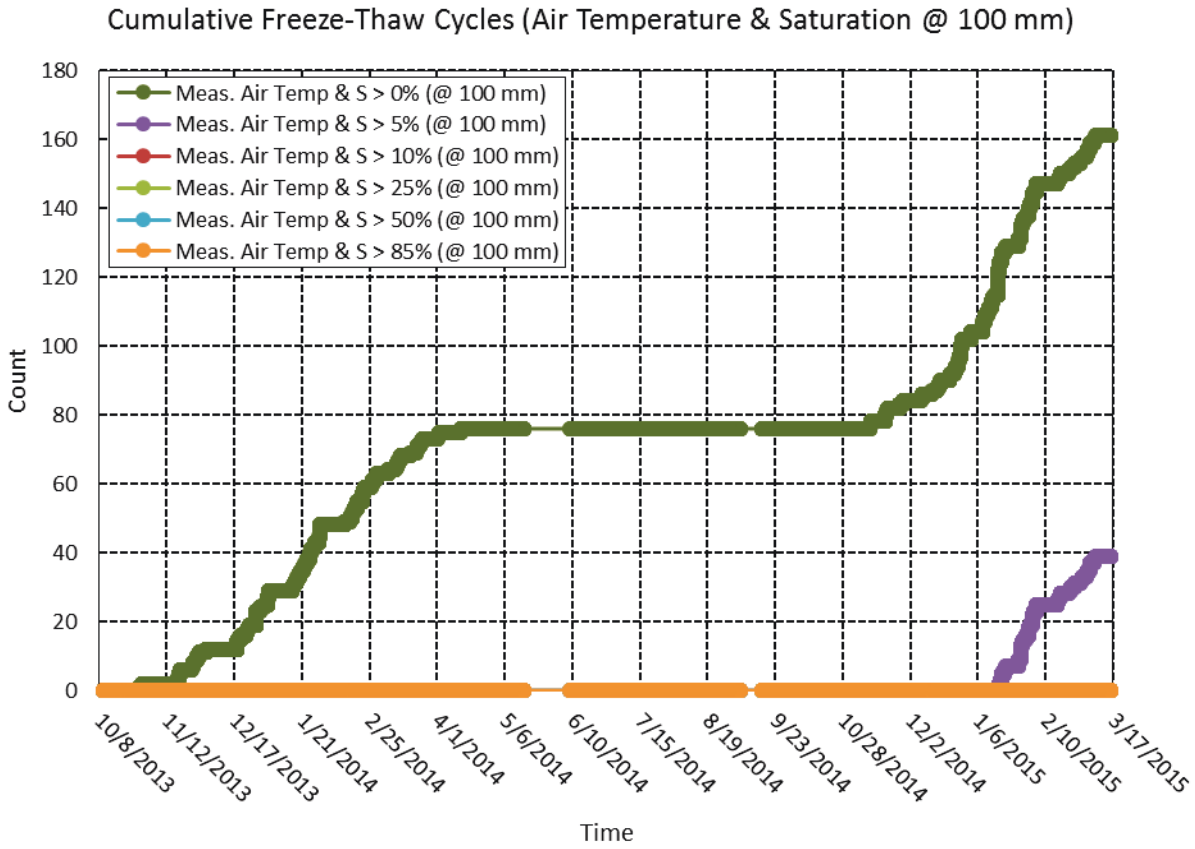

Figure C-74 Cumulative number of freeze-thaw cycles in Lytton, BC, from October 8, 2013, through March 17, 2015, at a depth of 100 mm when both freezing air temperatures and minimum degree of saturation is achieved at time of freezing. Predicted degree of saturation is defined by a diffusivity (at S = 100%) value of 0.86×10^{-6} m^2/hr, a regression coefficient, *n*, of 15, α value of 0.05, and an empirical correlation between relative humidity and degree of saturation. The simulation is initialized with an even distribution of 85 %RH throughout the depth of the concrete.

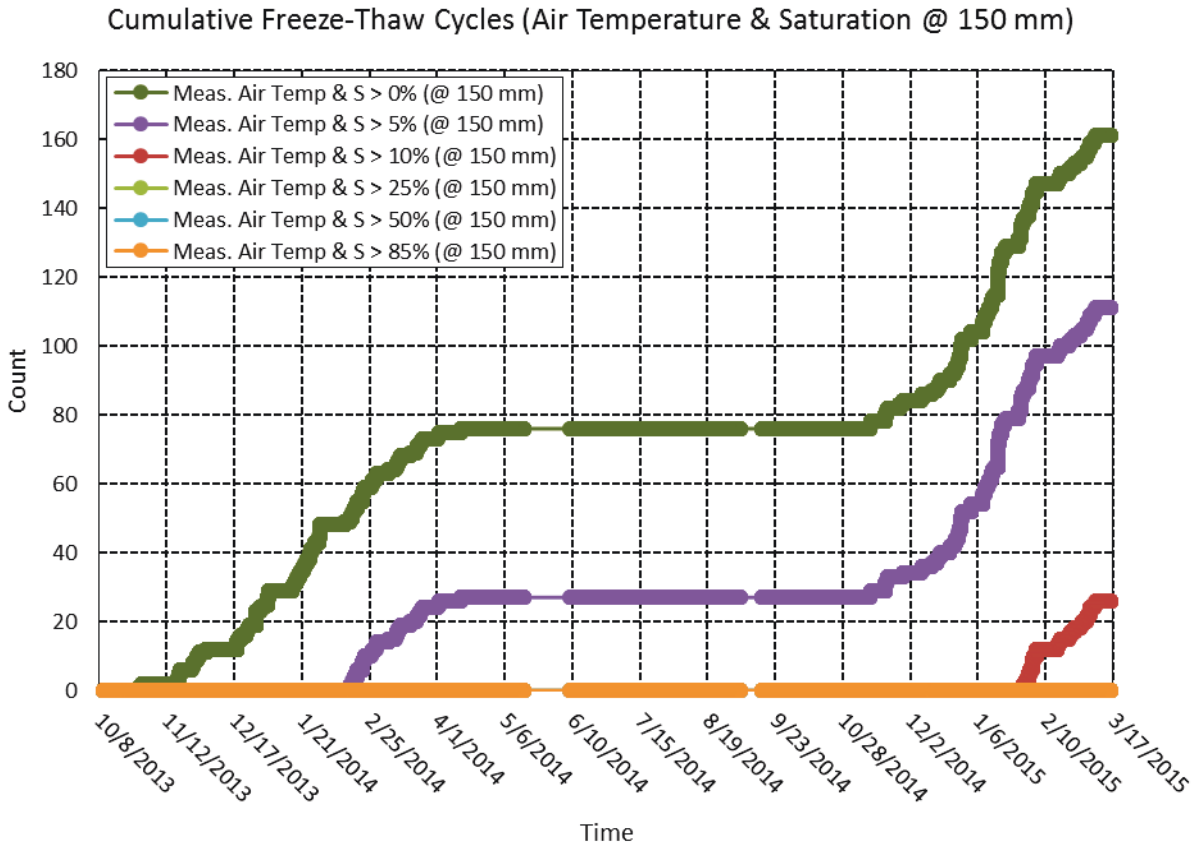

Figure C-75 Cumulative number of freeze-thaw cycles in Lytton, BC, from October 8, 2013, through March 17, 2015, at a depth of 150 mm when both freezing air temperatures and minimum degree of saturation is achieved at time of freezing. Predicted degree of saturation is defined by a diffusivity (at S = 100%) value of 0.86×10^{-6} m^2/hr, a regression coefficient, *n*, of 15, α value of 0.05, and an empirical correlation between relative humidity and degree of saturation. The simulation is initialized with an even distribution of 85 %RH throughout the depth of the concrete.

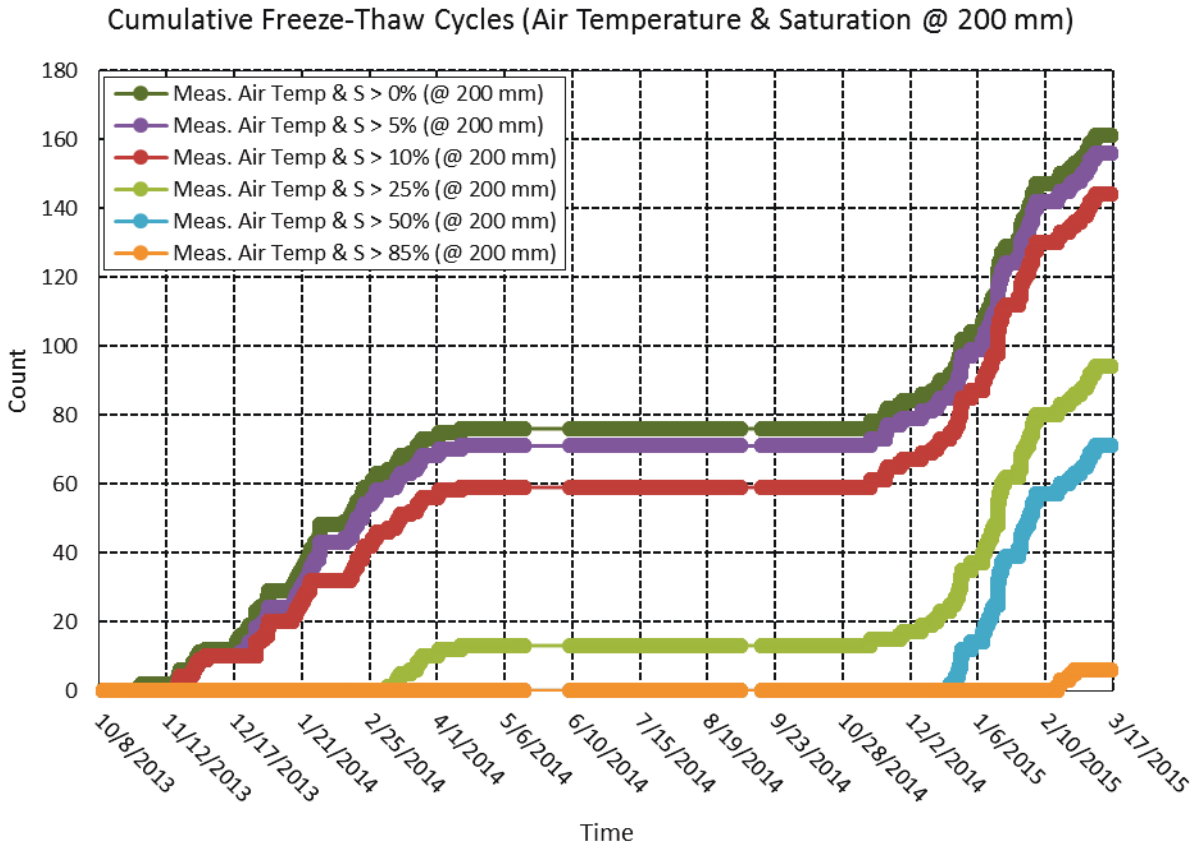

Figure C-76 Cumulative number of freeze-thaw cycles in Lytton, BC, from October 8, 2013, through March 17, 2015, at a depth of 200 mm when both freezing air temperatures and minimum degree of saturation is achieved at time of freezing. Predicted degree of saturation is defined by a diffusivity (at S = 100%) value of 0.86×10^{-6} m^2/hr, a regression coefficient, *n*, of 15, α value of 0.05, and an empirical correlation between relative humidity and degree of saturation. The simulation is initialized with an even distribution of 85 %RH throughout the depth of the concrete.

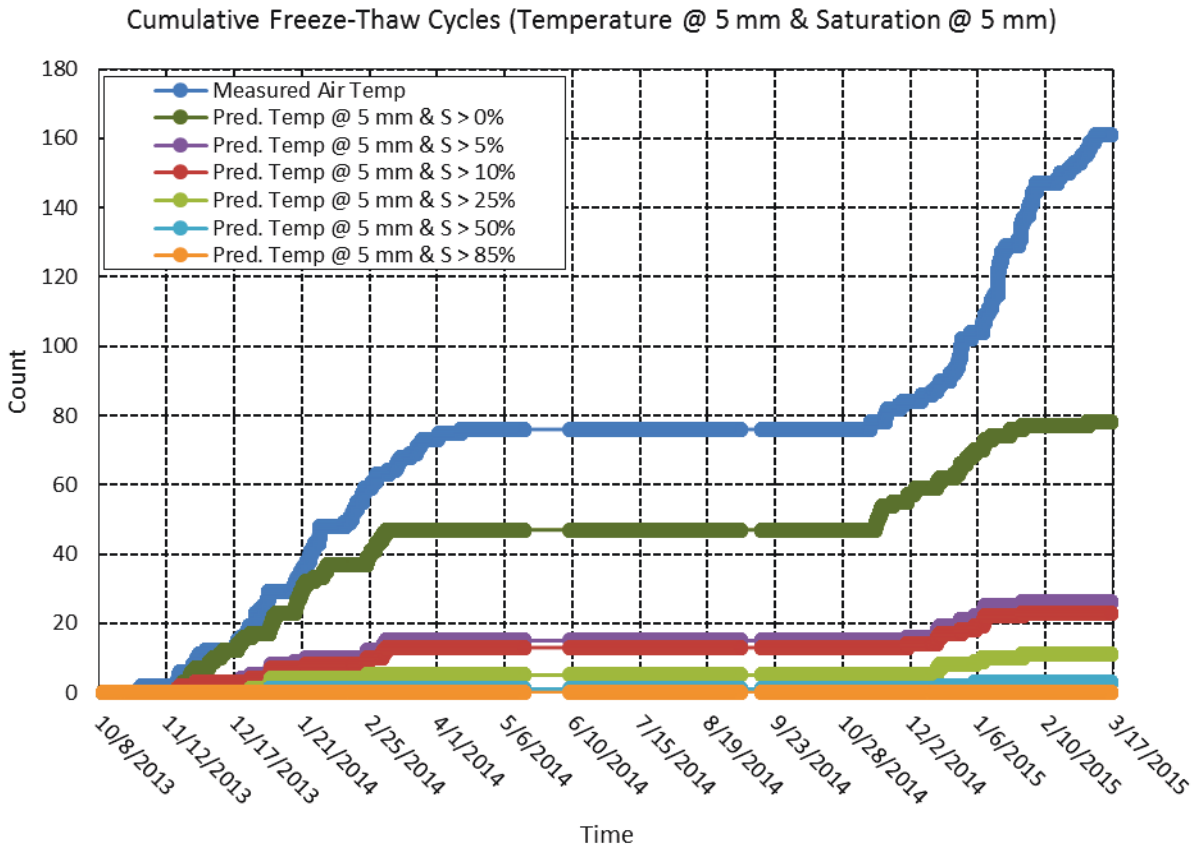

Figure C-77 Cumulative number of freeze-thaw cycles in Lytton, BC, from October 8, 2013, through March 17, 2015, at a depth of 5 mm when both freezing temperatures and minimum degree of saturation is achieved at time of freezing. Predicted internal temperature values are computed using a 2-layered system whose upper concrete layer is defined by a thermal conductivity, λ, value of 1.85 kcal/hmC^{o} and a thermal diffusivity, α, value of 0.0025 m^2/h. The underlying aggregate ballast layer is defined by a thermal conductivity, λ, value of 2.58 kcal/hmC^{o} and a thermal diffusivity, α, value of 0.0030 m^2/h. Predicted degree of saturation is defined by a diffusivity (at S = 100%) value of 0.86x10^{-6} m^2/hr, a regression coefficient, n, of 15, α value of 0.05, and an empirical correlation between relative humidity and degree of saturation. The simulation is initialized with an even distribution of 85 %RH throughout the depth of the concrete.

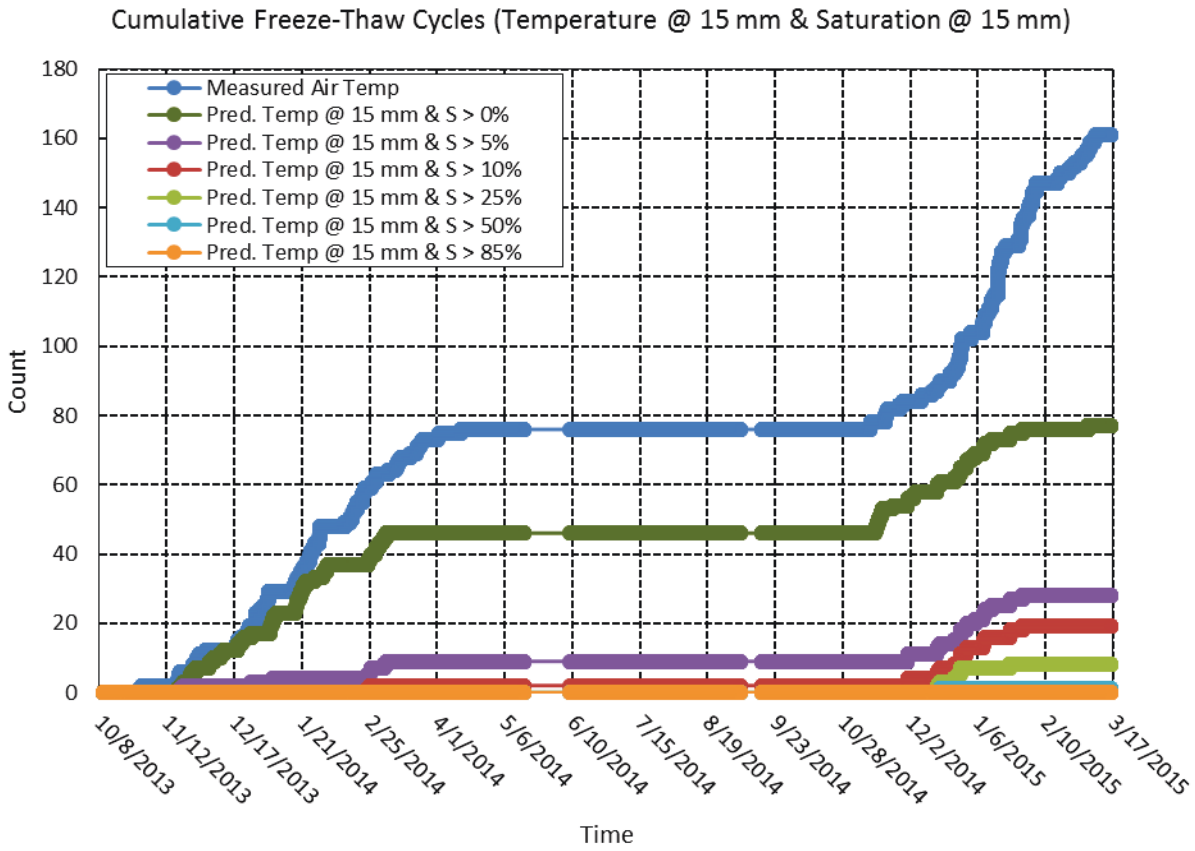

Figure C-78 Cumulative number of freeze-thaw cycles in Lytton, BC, from October 8, 2013, through March 17, 2015, at a depth of 15 mm when both freezing temperatures and minimum degree of saturation is achieved at time of freezing. Predicted internal temperature values are computed using a 2-layered system whose upper concrete layer is defined by a thermal conductivity, λ, value of 1.85 kcal/hmC^{o} and a thermal diffusivity, α, value of 0.0025 m^2/h. The underlying aggregate ballast layer is defined by a thermal conductivity, λ, value of 2.58 kcal/hmC^{o} and a thermal diffusivity, α, value of 0.0030 m^2/h. Predicted degree of saturation is defined by a diffusivity (at S = 100%) value of 0.86x10^{-6} m^2/hr, a regression coefficient, n, of 15, α value of 0.05, and an empirical correlation between relative humidity and degree of saturation. The simulation is initialized with an even distribution of 85 %RH throughout the depth of the concrete.

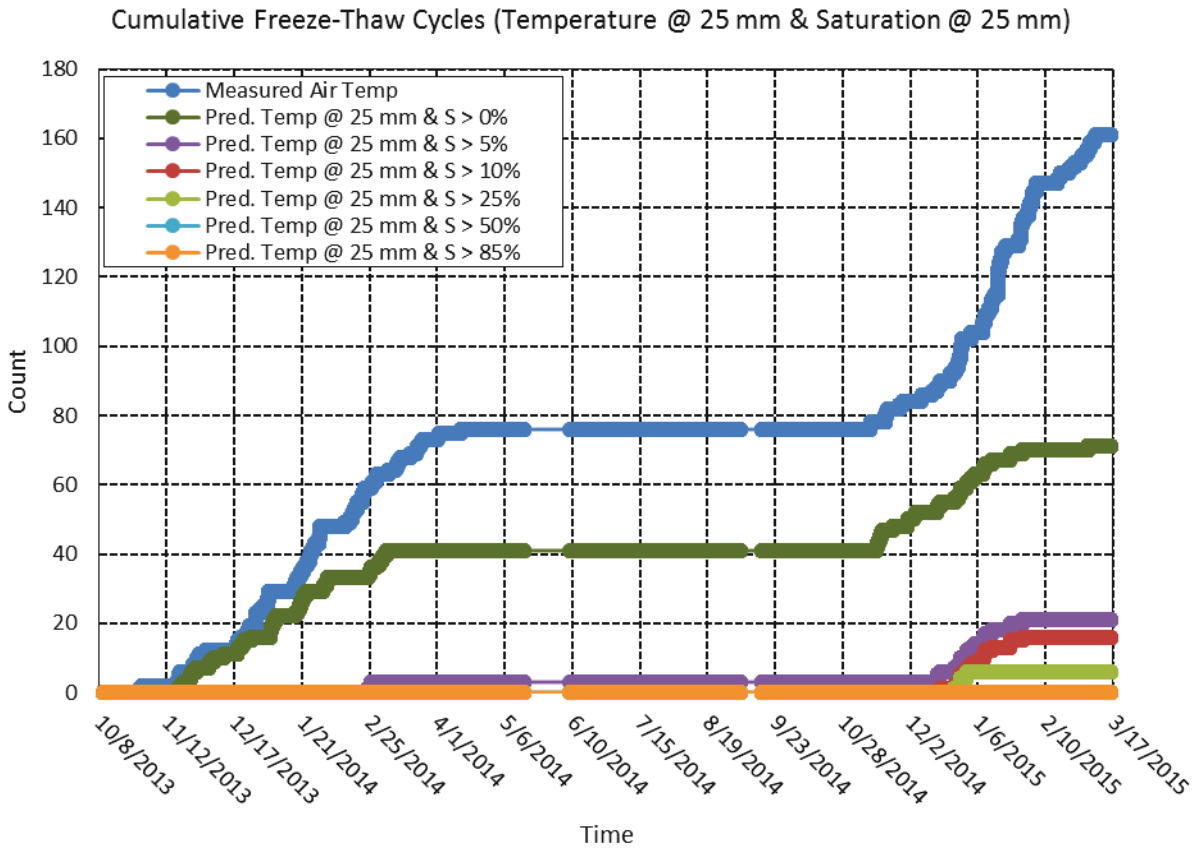

Figure C-79 Cumulative number of freeze-thaw cycles in Lytton, BC, from October 8, 2013, through March 17, 2015, at a depth of 25 mm when both freezing temperatures and minimum degree of saturation is achieved at time of freezing. Predicted internal temperature values are computed using a 2-layered system whose upper concrete layer is defined by a thermal conductivity, λ, value of 1.85 kcal/hmC^{o} and a thermal diffusivity, α, value of 0.0025 m^2/h. The underlying aggregate ballast layer is defined by a thermal conductivity, λ, value of 2.58 kcal/hmC^{o} and a thermal diffusivity, α, value of 0.0030 m^2/h. Predicted degree of saturation is defined by a diffusivity (at S = 100%) value of 0.86x10^{-6} m^2/hr, a regression coefficient, n, of 15, α value of 0.05, and an empirical correlation between relative humidity and degree of saturation. The simulation is initialized with an even distribution of 85 %RH throughout the depth of the concrete.

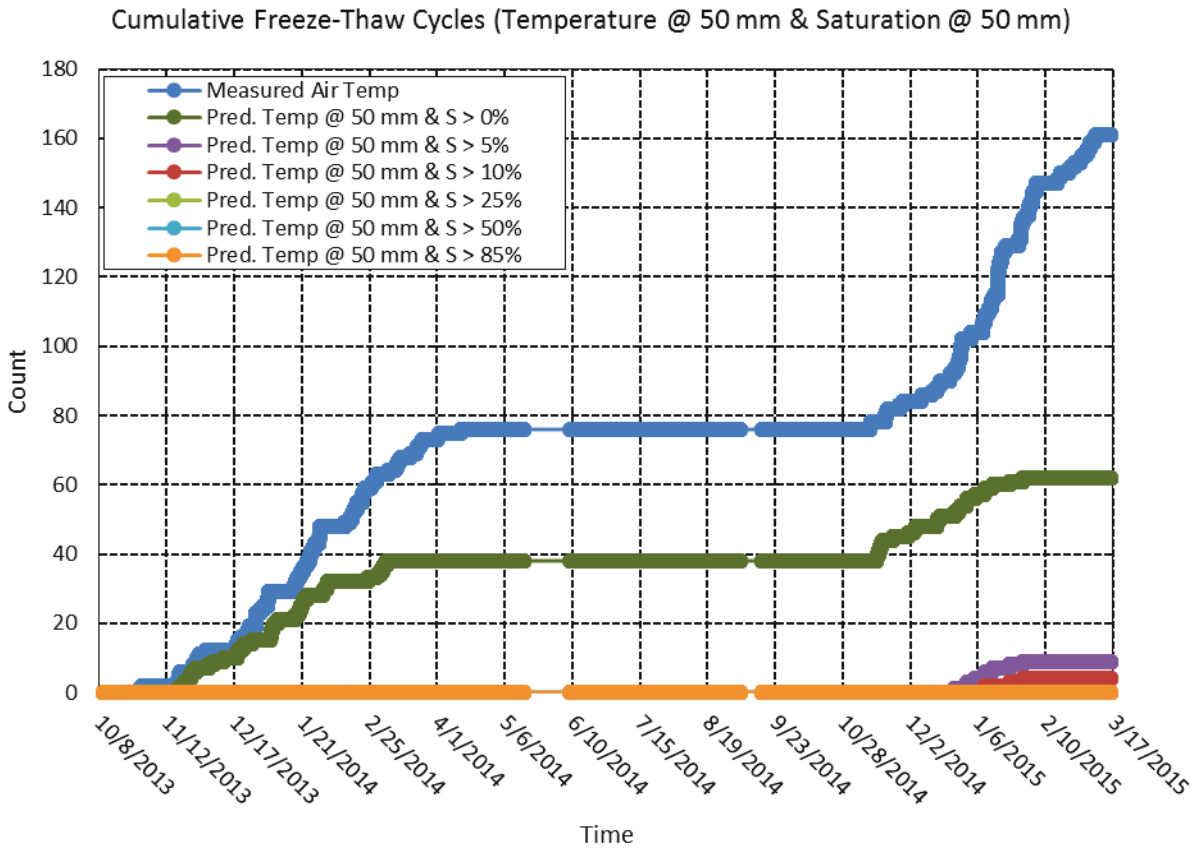

Figure C-80 Cumulative number of freeze-thaw cycles in Lytton, BC, from October 8, 2013, through March 17, 2015, at a depth of 50 mm when both freezing temperatures and minimum degree of saturation is achieved at time of freezing. Predicted internal temperature values are computed using a 2-layered system whose upper concrete layer is defined by a thermal conductivity, λ, value of 1.85 kcal/hmC^{o} and a thermal diffusivity, α, value of 0.0025 m^2/h. The underlying aggregate ballast layer is defined by a thermal conductivity, λ, value of 2.58 kcal/hmC^{o} and a thermal diffusivity, α, value of 0.0030 m^2/h. Predicted degree of saturation is defined by a diffusivity (at S = 100%) value of 0.86x10^{-6} m^2/hr, a regression coefficient, n, of 15, α value of 0.05, and an empirical correlation between relative humidity and degree of saturation. The simulation is initialized with an even distribution of 85 %RH throughout the depth of the concrete.

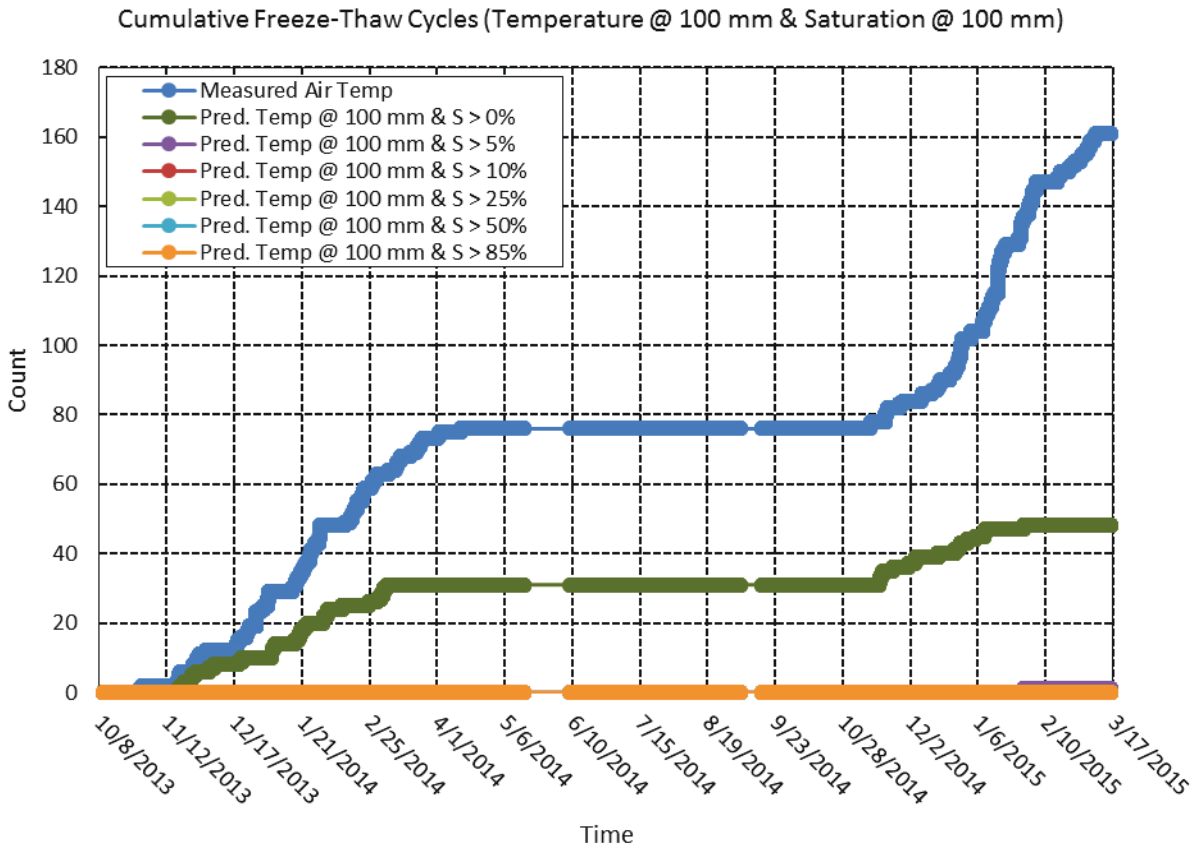

Figure C-81 Cumulative number of freeze-thaw cycles in Lytton, BC, from October 8, 2013, through March 17, 2015, at a depth of 100 mm when both freezing temperatures and minimum degree of saturation is achieved at time of freezing. Predicted internal temperature values are computed using a 2-layered system whose upper concrete layer is defined by a thermal conductivity, λ, value of 1.85 kcal/hmC^o and a thermal diffusivity, α, value of 0.0025 m^2/h. The underlying aggregate ballast layer is defined by a thermal conductivity, λ, value of 2.58 kcal/hmC^o and a thermal diffusivity, α, value of 0.0030 m^2/h. Predicted degree of saturation is defined by a diffusivity (at S = 100%) value of 0.86x10^{-6} m^2/hr, a regression coefficient, n, of 15, α value of 0.05, and an empirical correlation between relative humidity and degree of saturation. The simulation is initialized with an even distribution of 85 %RH throughout the depth of the concrete.

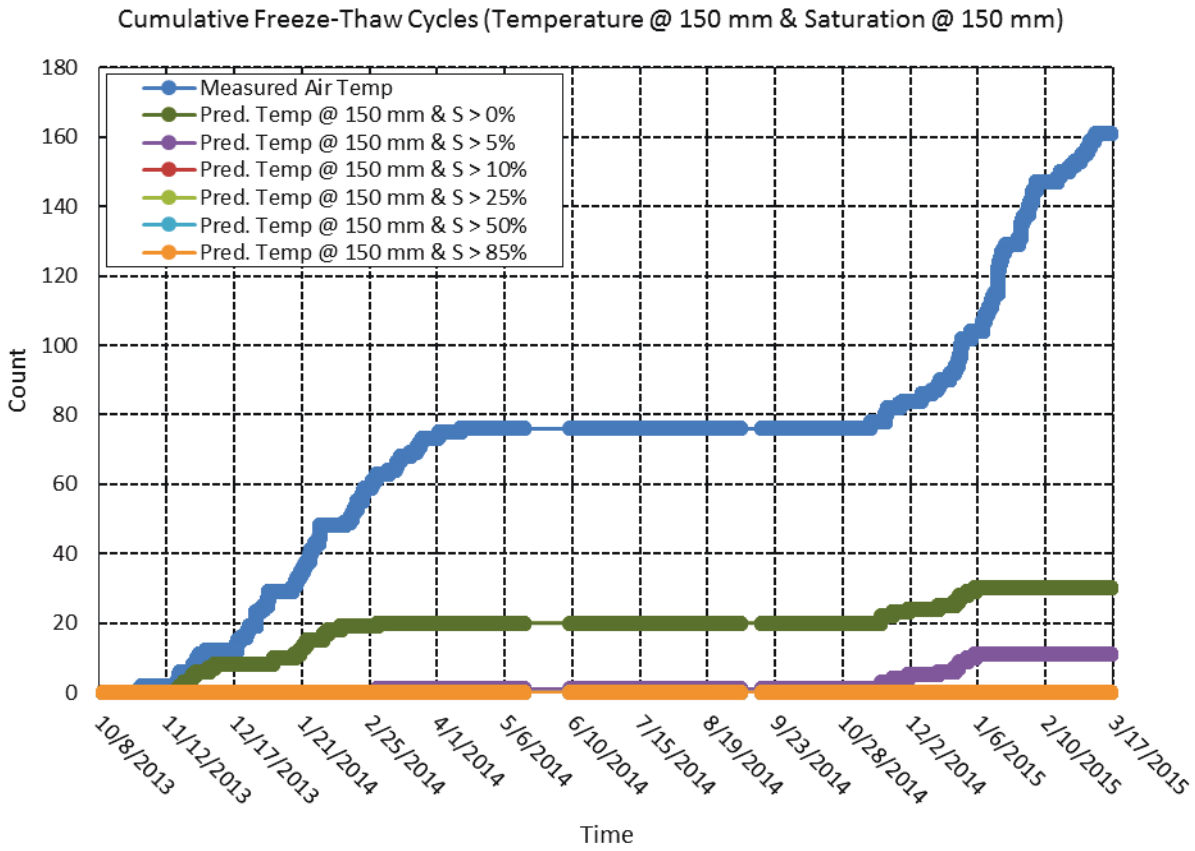

Figure C-82 Cumulative number of freeze-thaw cycles in Lytton, BC, from October 8, 2013, through March 17, 2015, at a depth of 150 mm when both freezing temperatures and minimum degree of saturation is achieved at time of freezing. Predicted internal temperature values are computed using a 2-layered system whose upper concrete layer is defined by a thermal conductivity, λ, value of 1.85 kcal/hmC^{o} and a thermal diffusivity, α, value of 0.0025 m^2/h. The underlying aggregate ballast layer is defined by a thermal conductivity, λ, value of 2.58 kcal/hmC^{o} and a thermal diffusivity, α, value of 0.0030 m^2/h. Predicted degree of saturation is defined by a diffusivity (at S = 100%) value of 0.86x10^{-6} m^2/hr, a regression coefficient, n, of 15, α value of 0.05, and an empirical correlation between relative humidity and degree of saturation. The simulation is initialized with an even distribution of 85 %RH throughout the depth of the concrete.

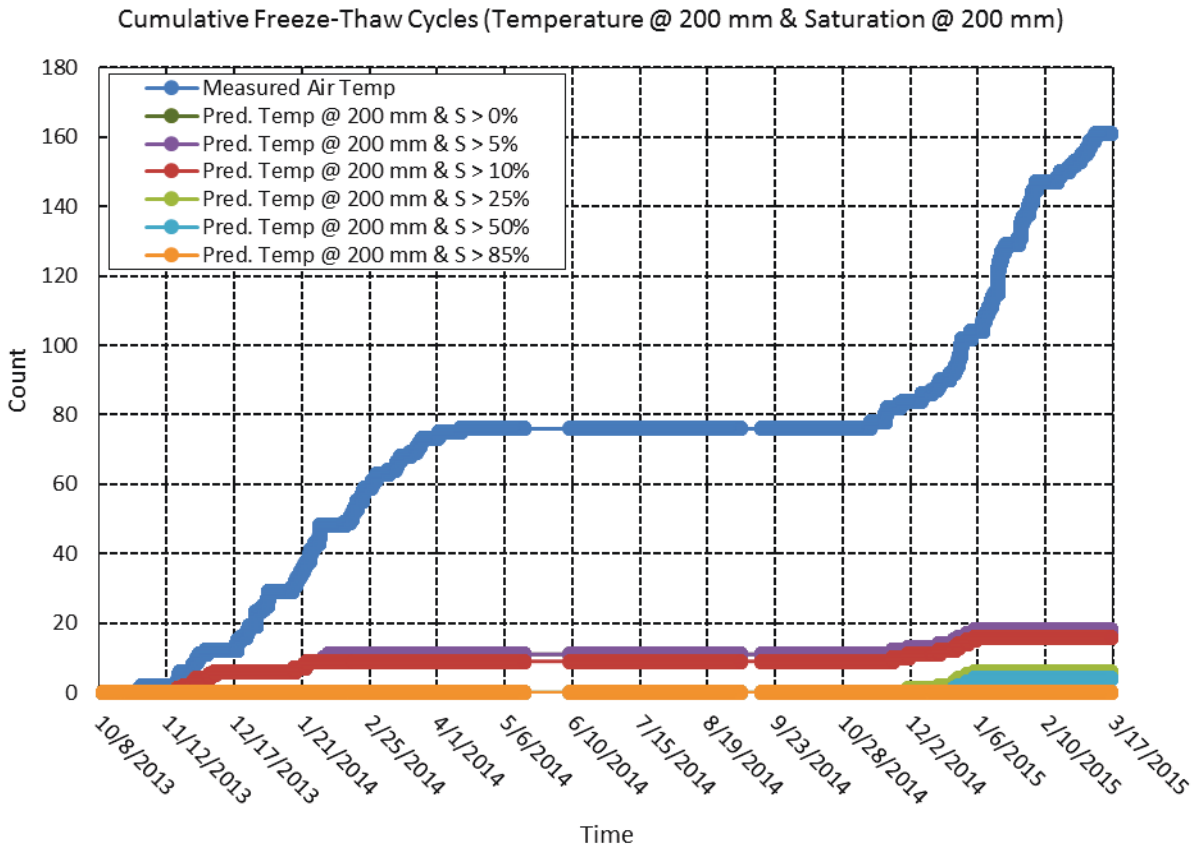

Figure C-83 Cumulative number of freeze-thaw cycles in Lytton, BC, from October 8, 2013, through March 17, 2015, at a depth of 200 mm when both freezing temperatures and minimum degree of saturation is achieved at time of freezing. Predicted internal temperature values are computed using a 2-layered system whose upper concrete layer is defined by a thermal conductivity, λ, value of 1.85 kcal/hmC^o and a thermal diffusivity, α, value of 0.0025 m^2/h. The underlying aggregate ballast layer is defined by a thermal conductivity, λ, value of 2.58 kcal/hmC^o and a thermal diffusivity, α, value of 0.0030 m^2/h. Predicted degree of saturation is defined by a diffusivity (at S = 100%) value of 0.86x10^{-6} m^2/hr, a regression coefficient, n, of 15, α value of 0.05, and an empirical correlation between relative humidity and degree of saturation. The simulation is initialized with an even distribution of 85 %RH throughout the depth of the concrete.

Modeled freeze-thaw cycles of concrete in Lytton, BC, due to saturation (modeled with D = 1.29 and initial RH = 85%)

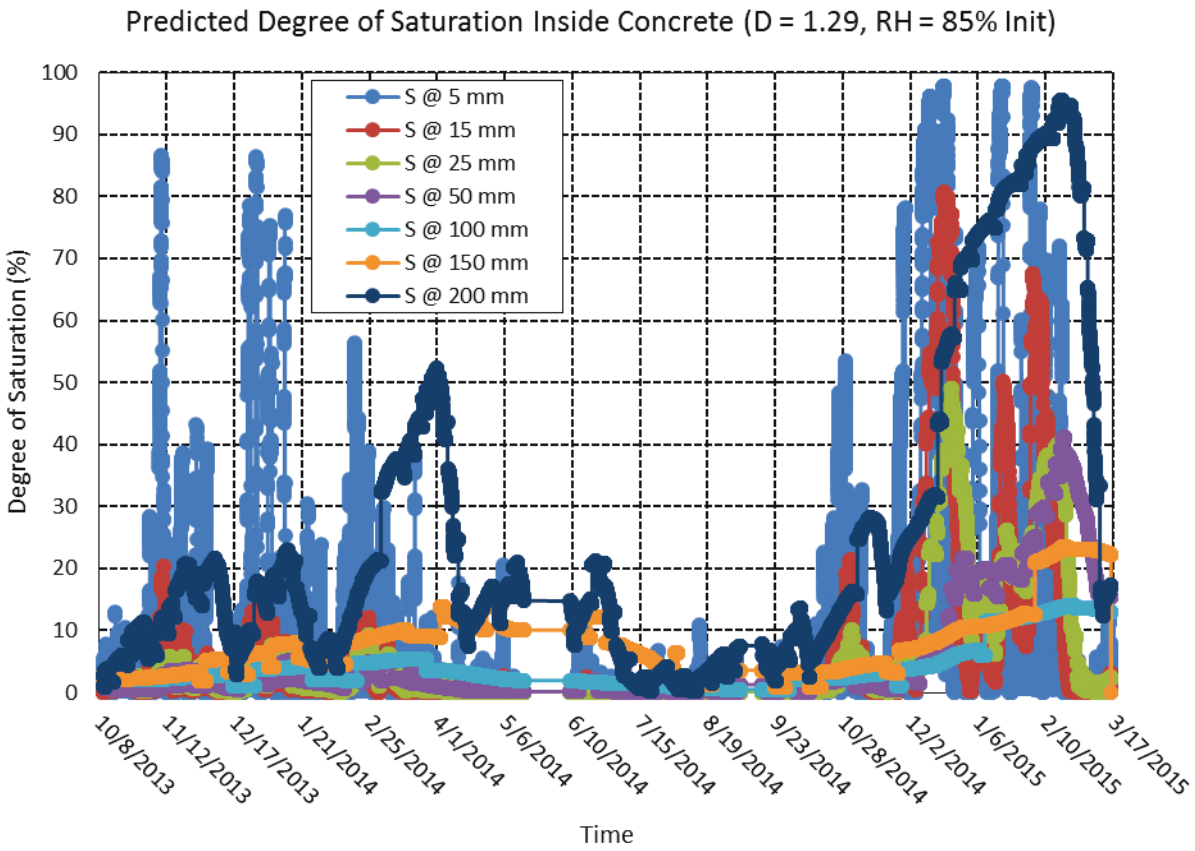

Figure C-84 Predicted degree of saturation inside a 1-layered concrete system in Lytton, BC, from October 8, 2013, through March 17, 2015. The concrete is defined by a diffusivity (at S = 100%) value of 1.29×10^{-6} m^2/hr, a regression coefficient, *n*, of 15, α value of 0.05, and an empirical correlation between relative humidity and degree of saturation. The simulation is initialized with an even distribution of 85 %RH throughout the depth of the concrete.

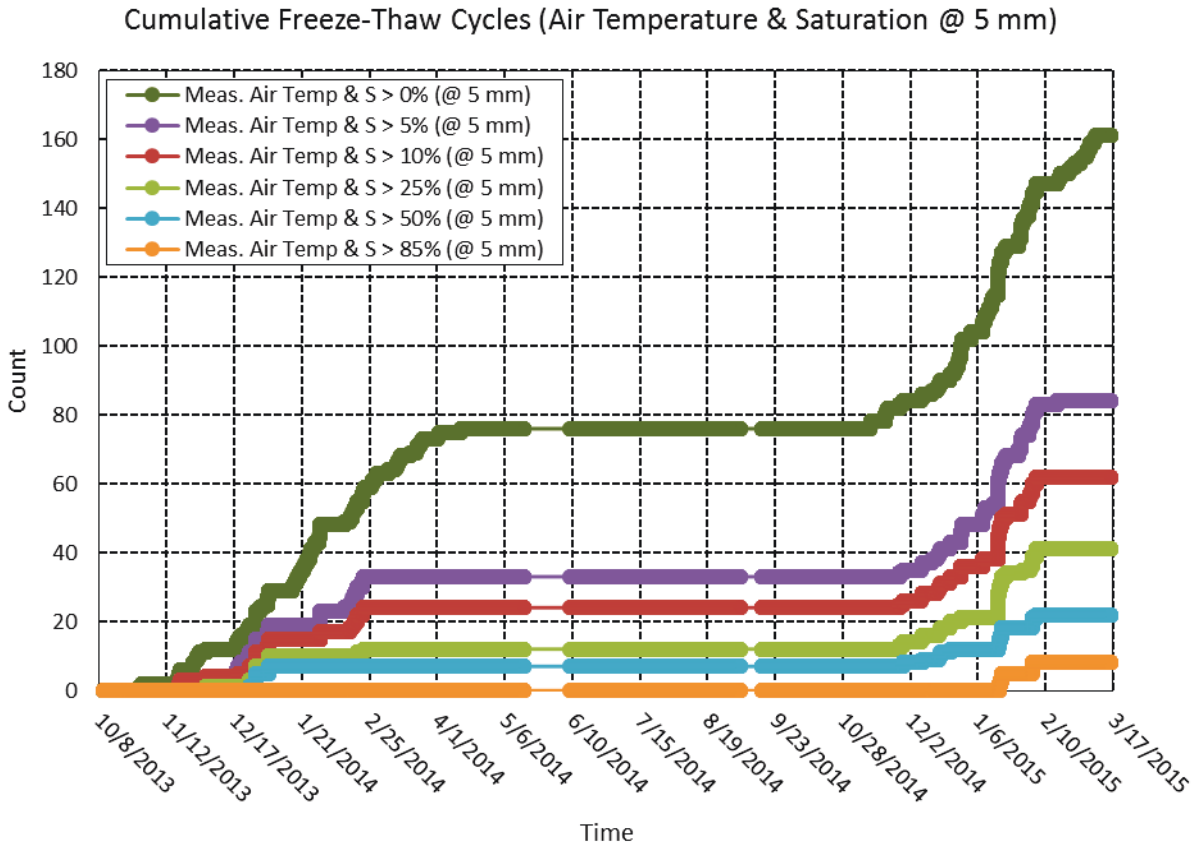

Figure C-85 Cumulative number of freeze-thaw cycles in Lytton, BC, from October 8, 2013, through March 17, 2015, at a depth of 5 mm when both freezing air temperatures and minimum degree of saturation is achieved at time of freezing. Predicted degree of saturation is defined by a diffusivity (at S = 100%) value of 1.29×10^{-6} m^2/hr, a regression coefficient, *n*, of 15, α value of 0.05, and an empirical correlation between relative humidity and degree of saturation. The simulation is initialized with an even distribution of 85 %RH throughout the depth of the concrete.

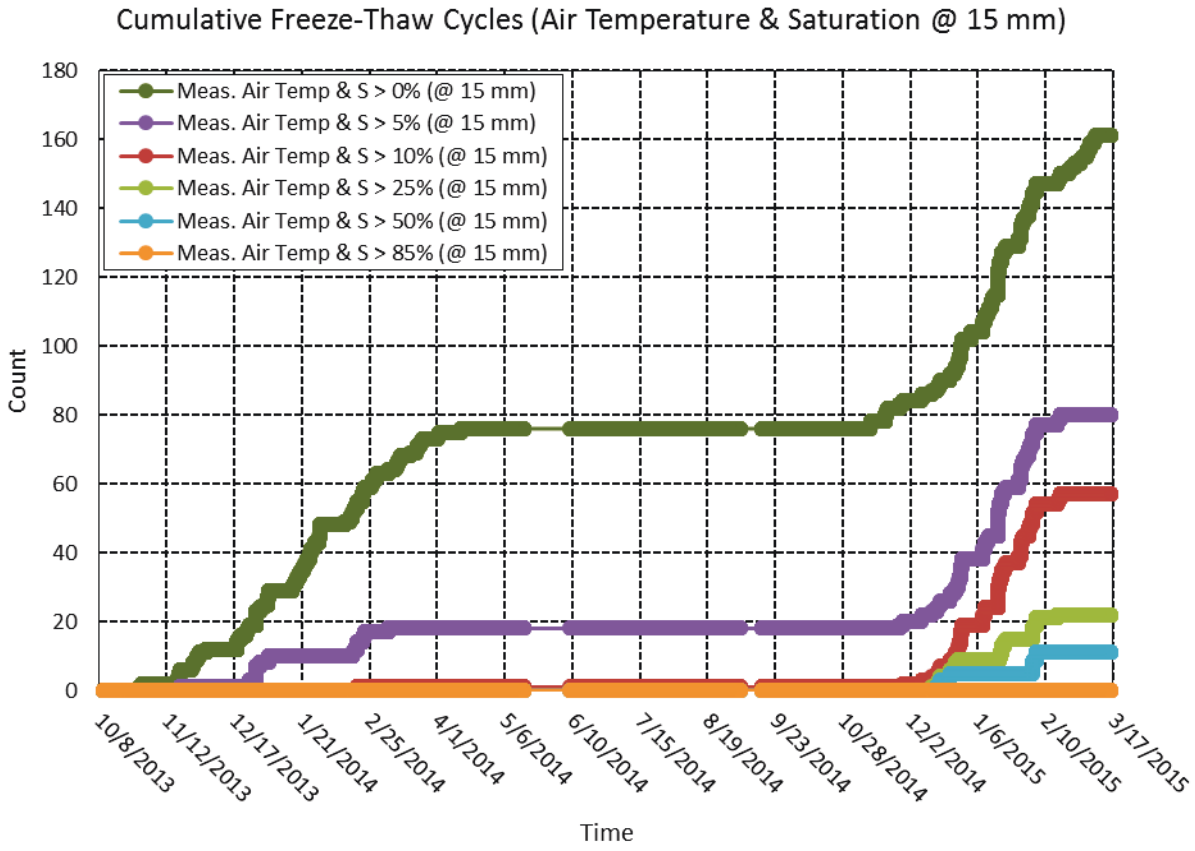

Figure C-86 Cumulative number of freeze-thaw cycles in Lytton, BC, from October 8, 2013, through March 17, 2015, at a depth of 15 mm when both freezing air temperatures and minimum degree of saturation is achieved at time of freezing. Predicted degree of saturation is defined by a diffusivity (at S = 100%) value of 1.29×10^{-6} m^2/hr, a regression coefficient, *n*, of 15, α value of 0.05, and an empirical correlation between relative humidity and degree of saturation. The simulation is initialized with an even distribution of 85 %RH throughout the depth of the concrete.

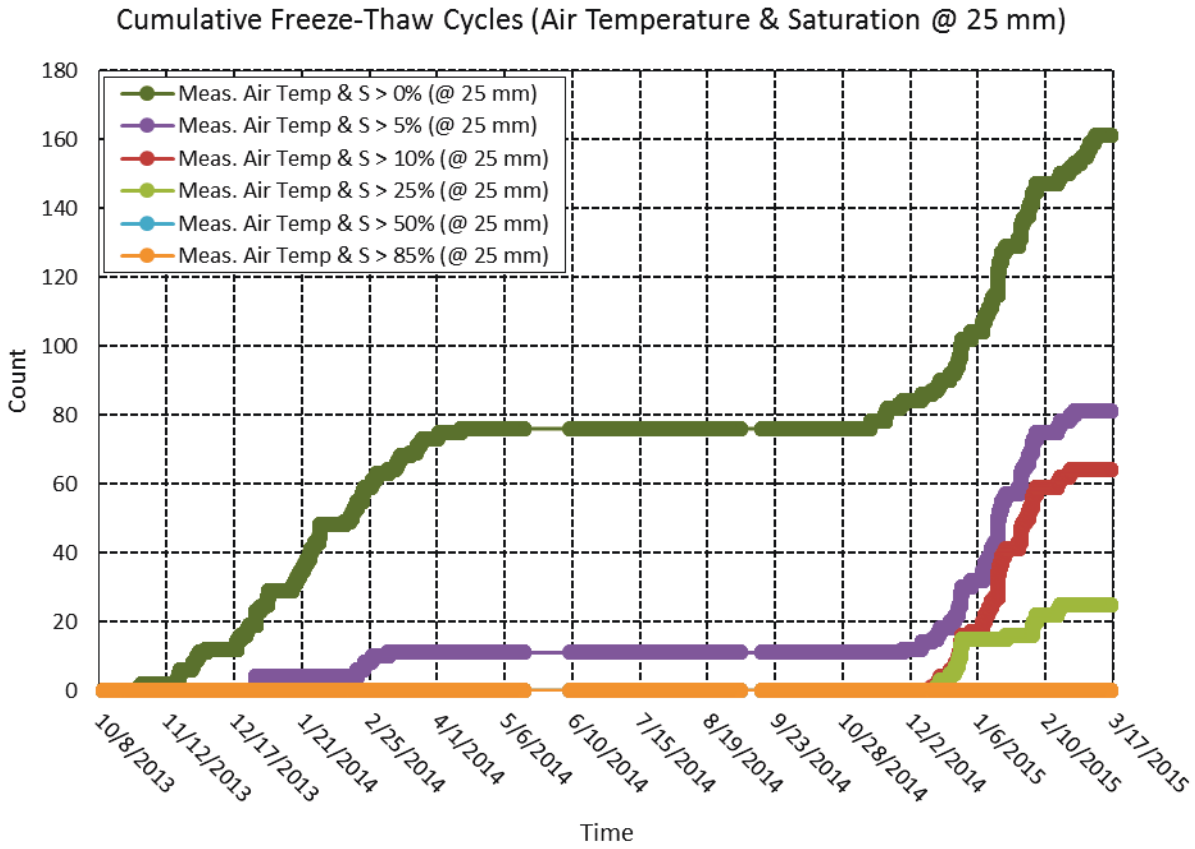

Figure C-87 Cumulative number of freeze-thaw cycles in Lytton, BC, from October 8, 2013, through March 17, 2015, at a depth of 25 mm when both freezing air temperatures and minimum degree of saturation is achieved at time of freezing. Predicted degree of saturation is defined by a diffusivity (at S = 100%) value of 1.29×10^{-6} m^2/hr, a regression coefficient, *n*, of 15, α value of 0.05, and an empirical correlation between relative humidity and degree of saturation. The simulation is initialized with an even distribution of 85 %RH throughout the depth of the concrete.

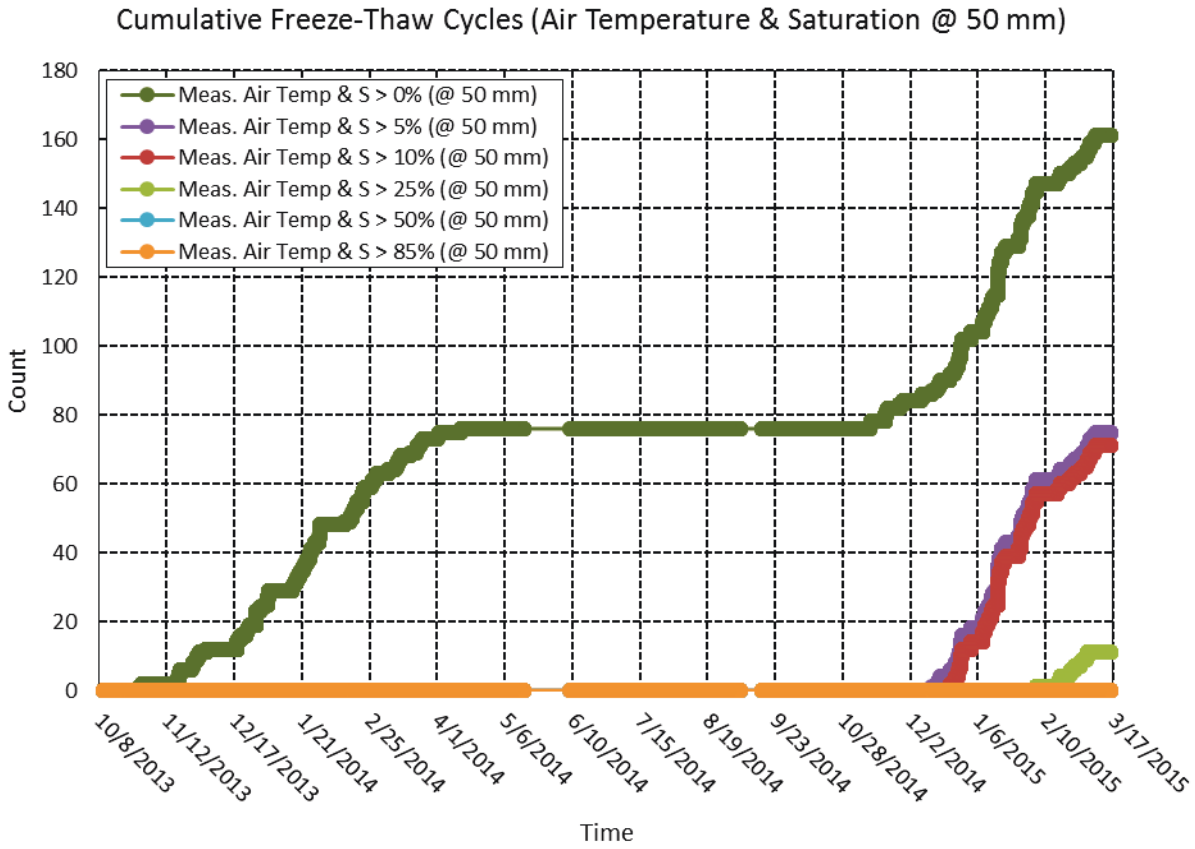

Figure C-88 Cumulative number of freeze-thaw cycles in Lytton, BC, from October 8, 2013, through March 17, 2015, at a depth of 50 mm when both freezing air temperatures and minimum degree of saturation is achieved at time of freezing. Predicted degree of saturation is defined by a diffusivity (at S = 100%) value of 1.29×10^{-6} m^2/hr, a regression coefficient, *n*, of 15, α value of 0.05, and an empirical correlation between relative humidity and degree of saturation. The simulation is initialized with an even distribution of 85 %RH throughout the depth of the concrete.

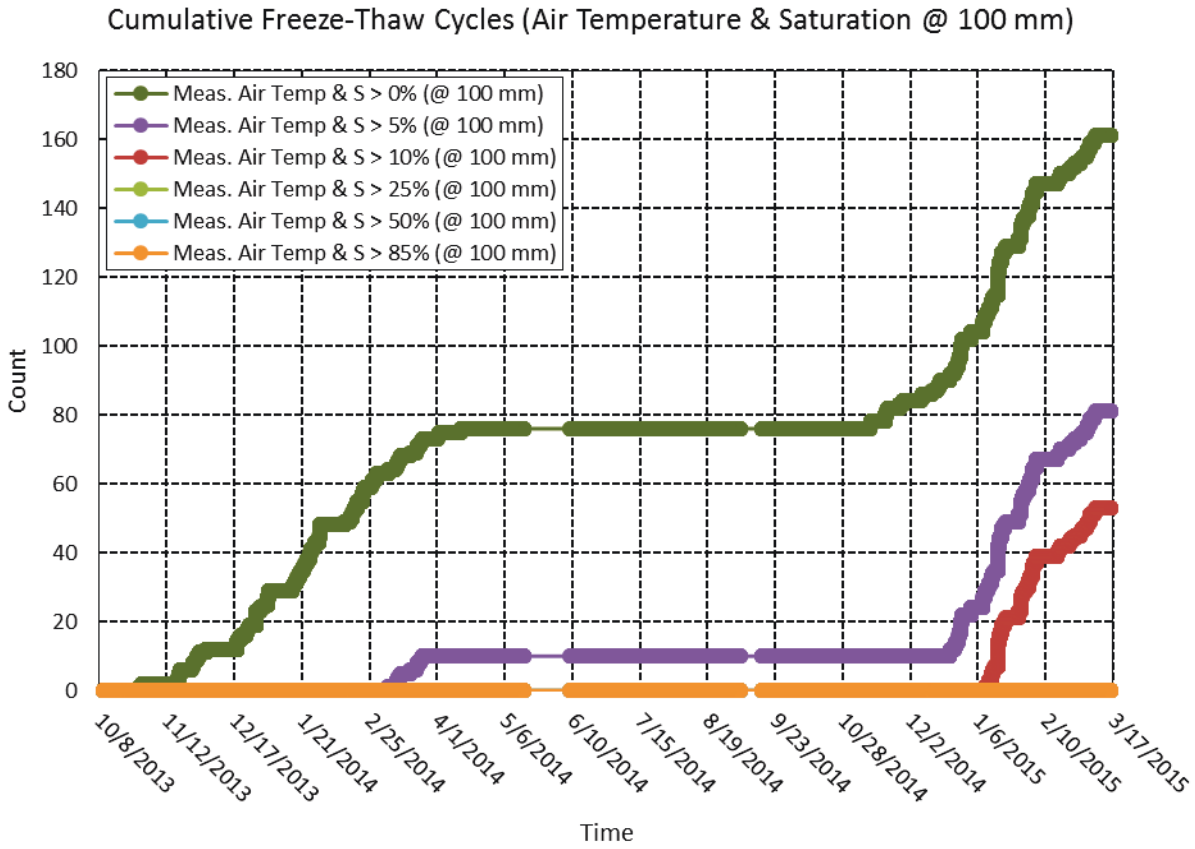

Figure C-89 Cumulative number of freeze-thaw cycles in Lytton, BC, from October 8, 2013, through March 17, 2015, at a depth of 100 mm when both freezing air temperatures and minimum degree of saturation is achieved at time of freezing. Predicted degree of saturation is defined by a diffusivity (at S = 100%) value of 1.29×10^{-6} m^2/hr, a regression coefficient, *n*, of 15, α value of 0.05, and an empirical correlation between relative humidity and degree of saturation. The simulation is initialized with an even distribution of 85 %RH throughout the depth of the concrete.

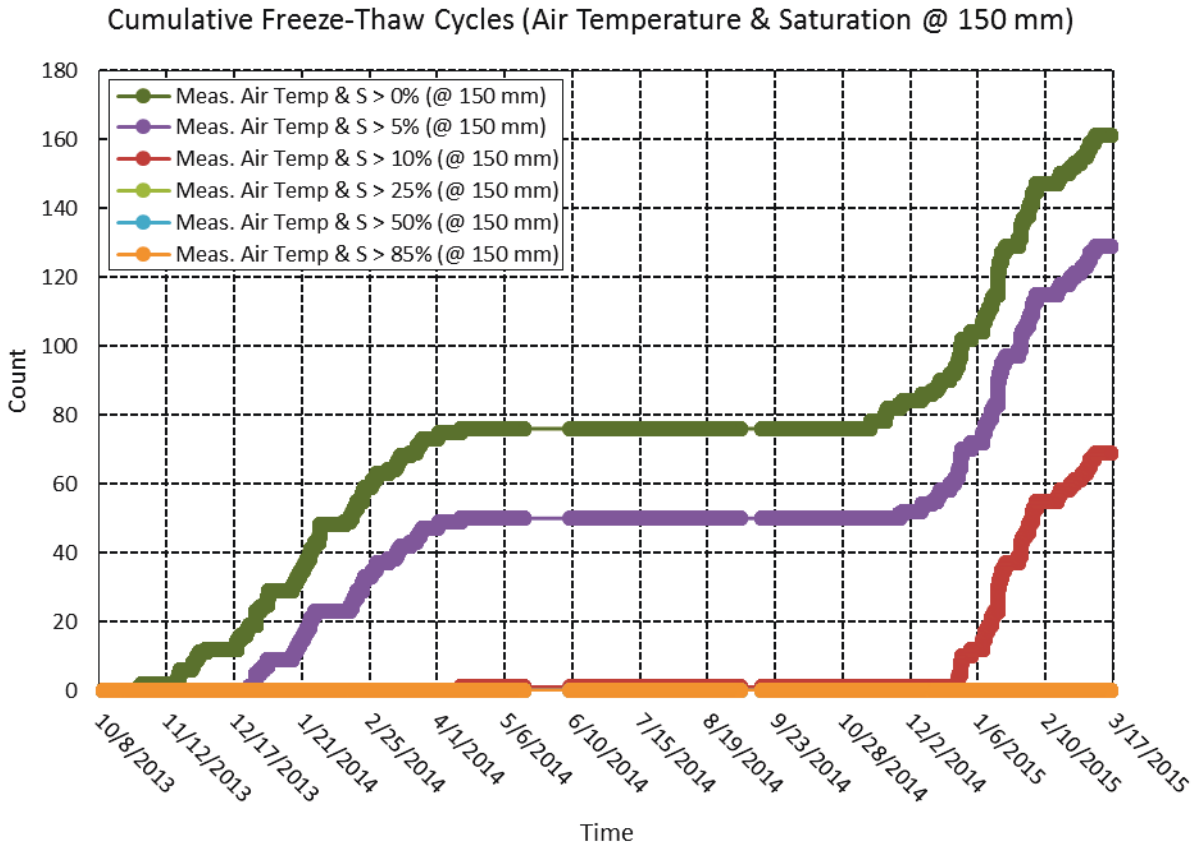

Figure C-90 Cumulative number of freeze-thaw cycles in Lytton, BC, from October 8, 2013, through March 17, 2015, at a depth of 150 mm when both freezing air temperatures and minimum degree of saturation is achieved at time of freezing. Predicted degree of saturation is defined by a diffusivity (at S = 100%) value of 1.29×10^{-6} m^2/hr, a regression coefficient, *n*, of 15, α value of 0.05, and an empirical correlation between relative humidity and degree of saturation. The simulation is initialized with an even distribution of 85 %RH throughout the depth of the concrete.

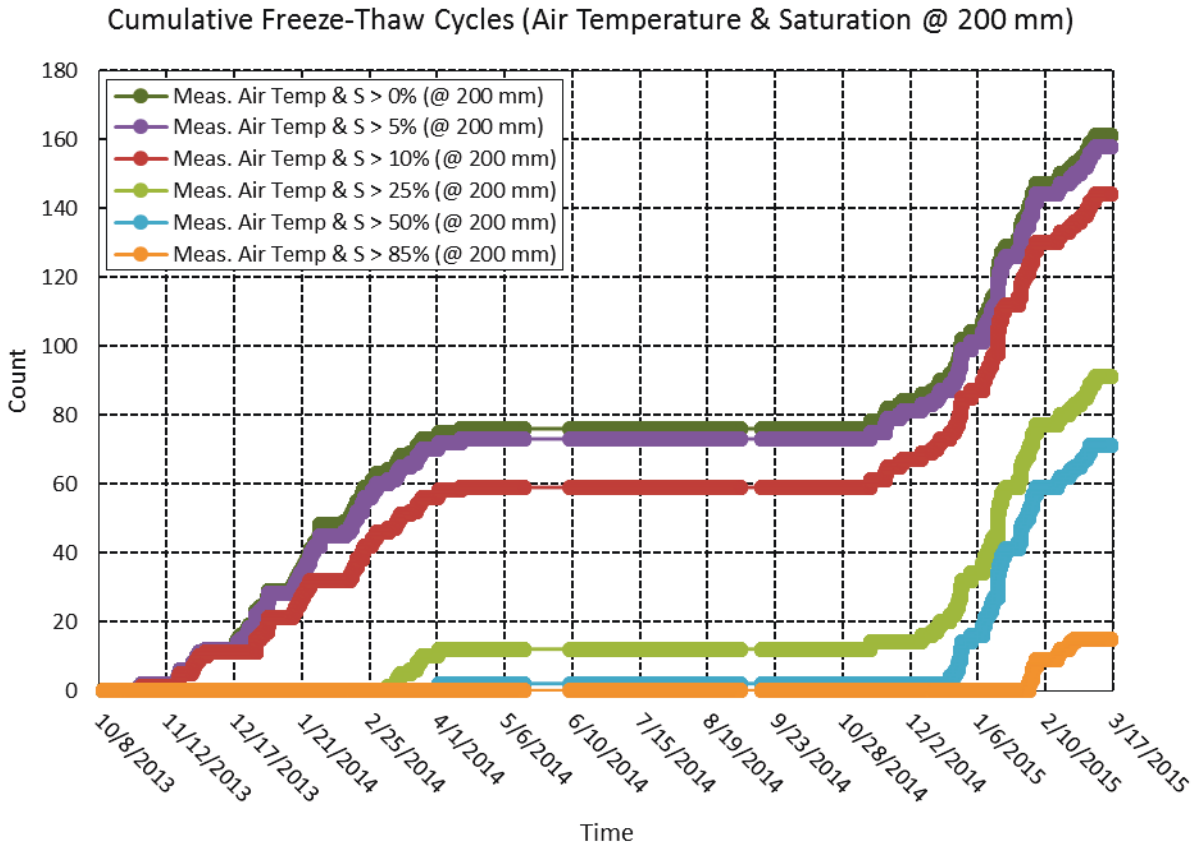

Figure C-91 Cumulative number of freeze-thaw cycles in Lytton, BC, from October 8, 2013, through March 17, 2015, at a depth of 200 mm when both freezing air temperatures and minimum degree of saturation is achieved at time of freezing. Predicted degree of saturation is defined by a diffusivity (at S = 100%) value of 1.29×10^{-6} m^2/hr, a regression coefficient, *n*, of 15, α value of 0.05, and an empirical correlation between relative humidity and degree of saturation. The simulation is initialized with an even distribution of 85 %RH throughout the depth of the concrete.

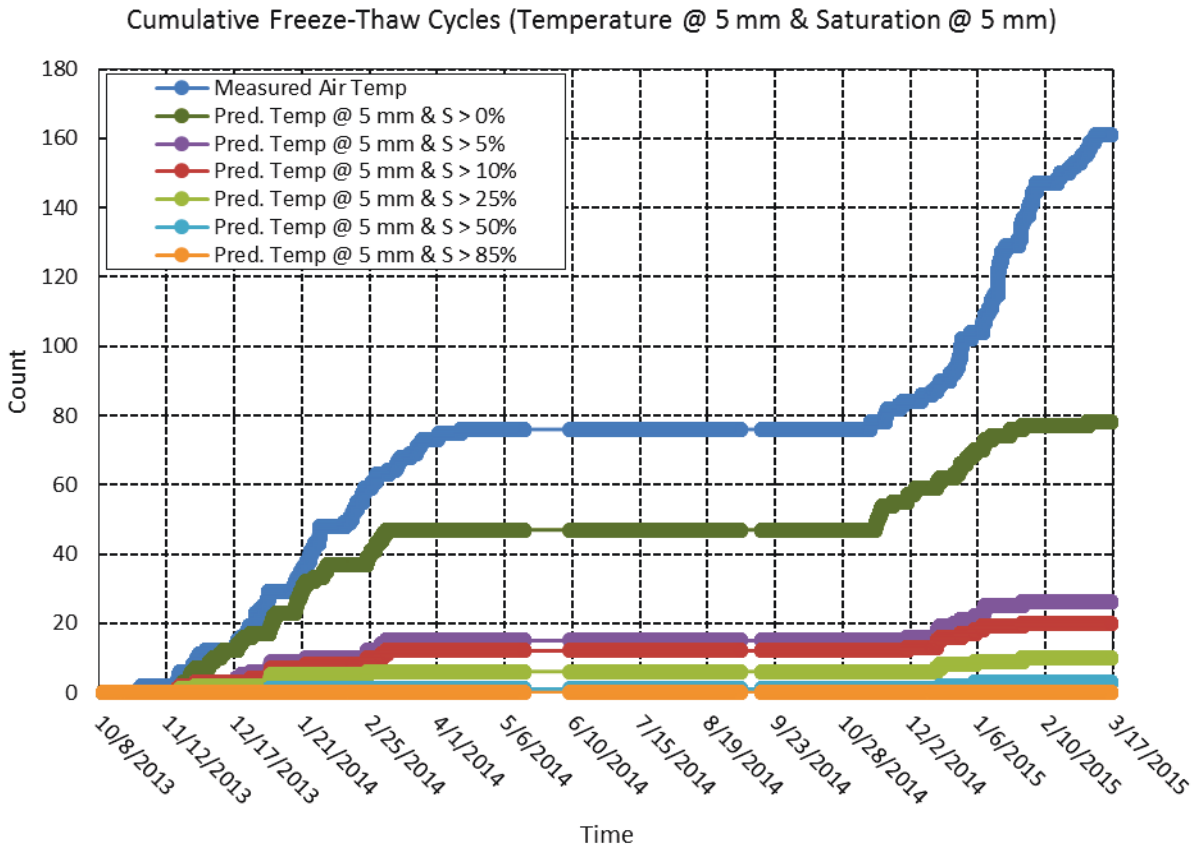

Figure C-92 Cumulative number of freeze-thaw cycles in Lytton, BC, from October 8, 2013, through March 17, 2015, at a depth of 5 mm when both freezing temperatures and minimum degree of saturation is achieved at time of freezing. Predicted internal temperature values are computed using a 2-layered system whose upper concrete layer is defined by a thermal conductivity, λ, value of 1.85 kcal/hmC^{o} and a thermal diffusivity, α, value of 0.0025 m^2/h. The underlying aggregate ballast layer is defined by a thermal conductivity, λ, value of 2.58 kcal/hmC^{o} and a thermal diffusivity, α, value of 0.0030 m^2/h. Predicted degree of saturation is defined by a diffusivity (at S = 100%) value of 1.29x10^{-6} m^2/hr, a regression coefficient, n, of 15, α value of 0.05, and an empirical correlation between relative humidity and degree of saturation. The simulation is initialized with an even distribution of 85 %RH throughout the depth of the concrete.

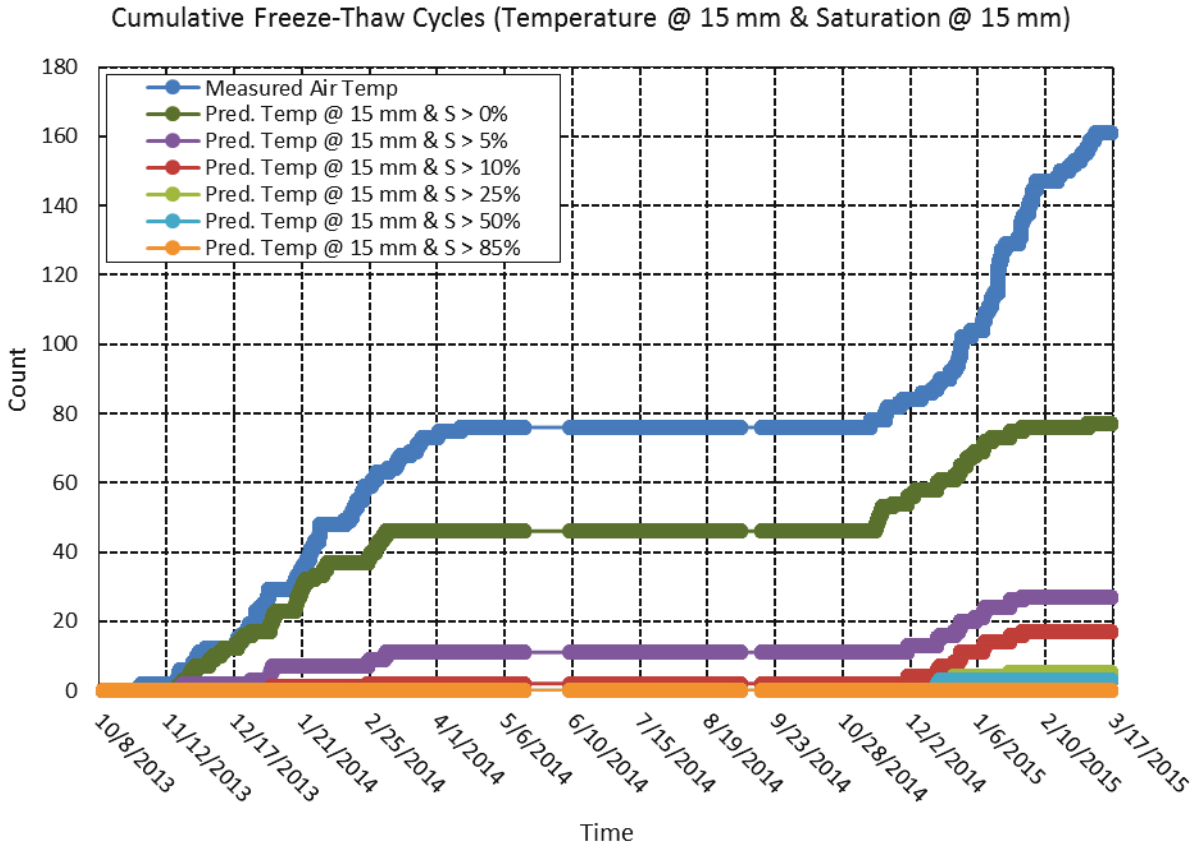

Figure C-93 Cumulative number of freeze-thaw cycles in Lytton, BC, from October 8, 2013, through March 17, 2015, at a depth of 15 mm when both freezing temperatures and minimum degree of saturation is achieved at time of freezing. Predicted internal temperature values are computed using a 2-layered system whose upper concrete layer is defined by a thermal conductivity, λ, value of 1.85 kcal/hmC^{o} and a thermal diffusivity, α, value of 0.0025 m^2/h. The underlying aggregate ballast layer is defined by a thermal conductivity, λ, value of 2.58 kcal/hmC^{o} and a thermal diffusivity, α, value of 0.0030 m^2/h. Predicted degree of saturation is defined by a diffusivity (at S = 100%) value of 1.29x10^{-6} m^2/hr, a regression coefficient, n, of 15, α value of 0.05, and an empirical correlation between relative humidity and degree of saturation. The simulation is initialized with an even distribution of 85 %RH throughout the depth of the concrete.

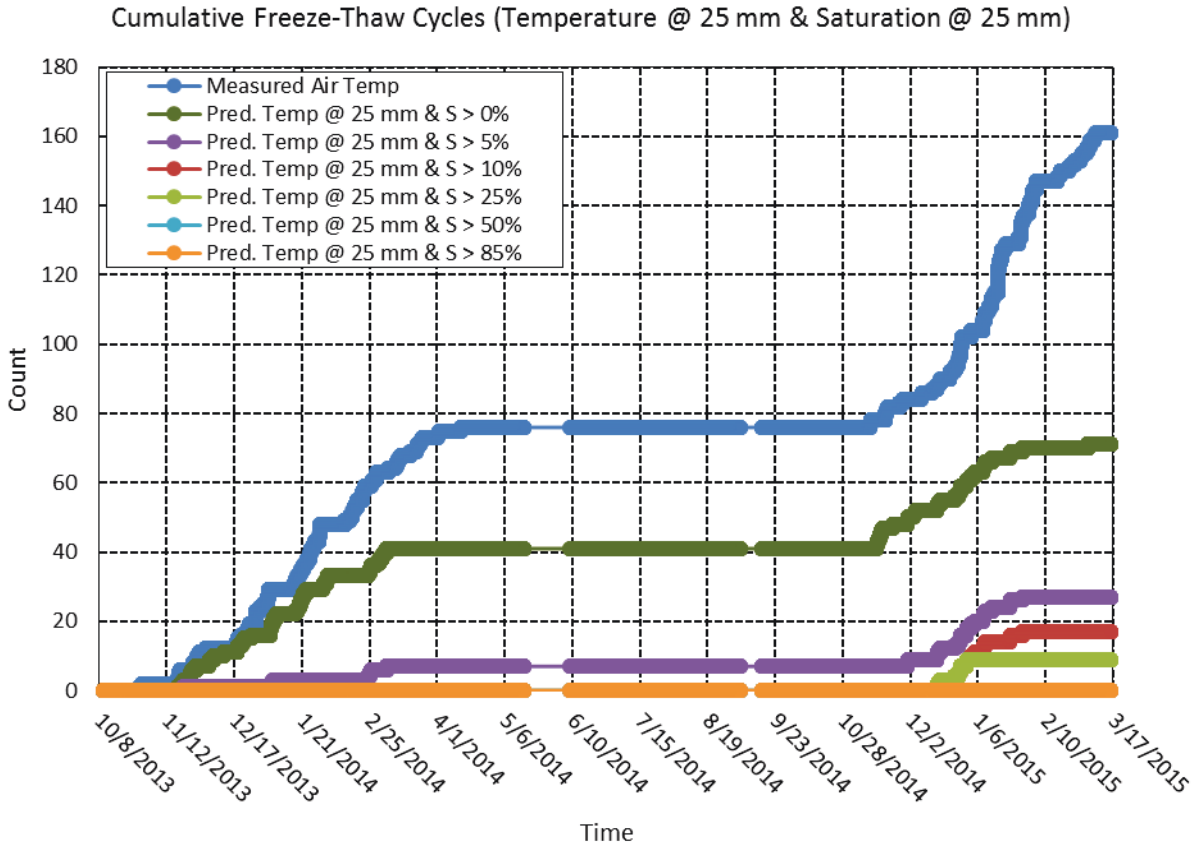

Figure C-94 Cumulative number of freeze-thaw cycles in Lytton, BC, from October 8, 2013, through March 17, 2015, at a depth of 25 mm when both freezing temperatures and minimum degree of saturation is achieved at time of freezing. Predicted internal temperature values are computed using a 2-layered system whose upper concrete layer is defined by a thermal conductivity, λ, value of 1.85 kcal/hmC^{o} and a thermal diffusivity, α, value of 0.0025 m^2/h. The underlying aggregate ballast layer is defined by a thermal conductivity, λ, value of 2.58 kcal/hmC^{o} and a thermal diffusivity, α, value of 0.0030 m^2/h. Predicted degree of saturation is defined by a diffusivity (at S = 100%) value of 1.29x10^{-6} m^2/hr, a regression coefficient, n, of 15, α value of 0.05, and an empirical correlation between relative humidity and degree of saturation. The simulation is initialized with an even distribution of 85 %RH throughout the depth of the concrete.

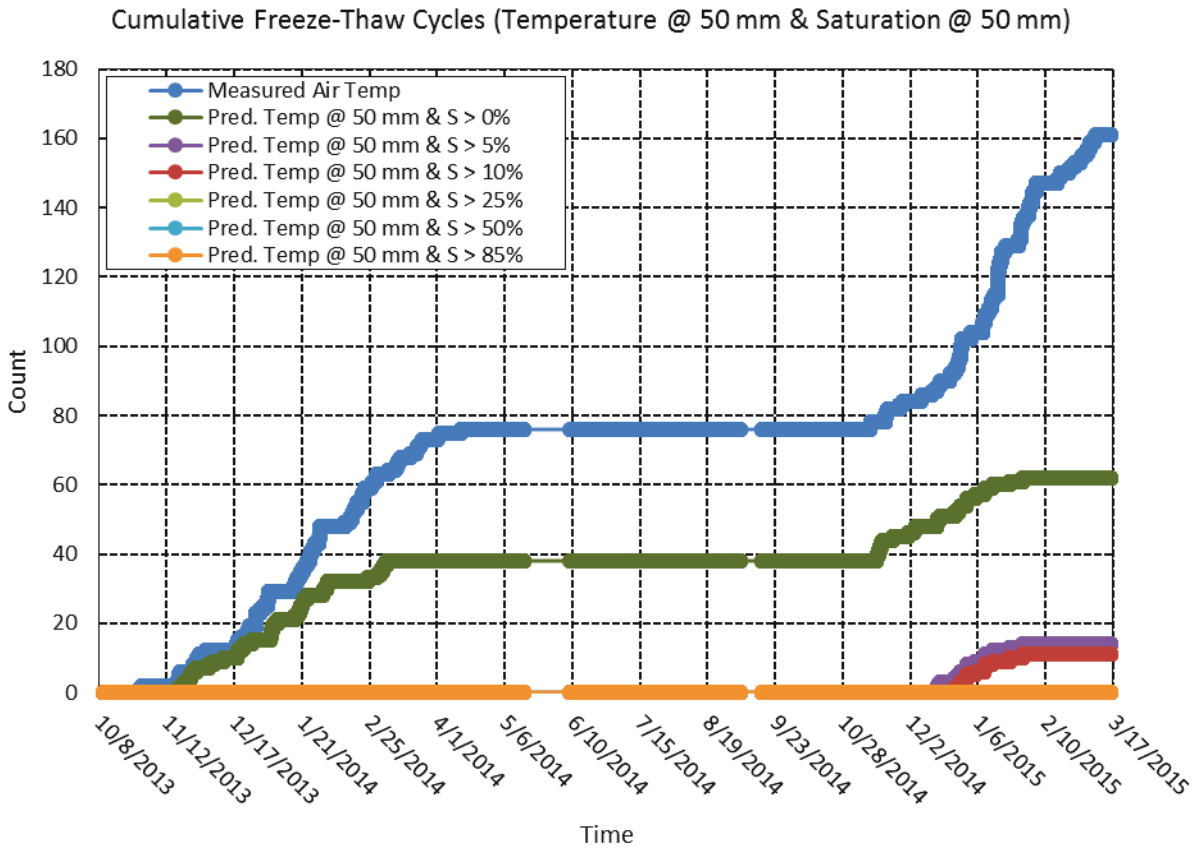

Figure C-95 Cumulative number of freeze-thaw cycles in Lytton, BC, from October 8, 2013, through March 17, 2015, at a depth of 50 mm when both freezing temperatures and minimum degree of saturation is achieved at time of freezing. Predicted internal temperature values are computed using a 2-layered system whose upper concrete layer is defined by a thermal conductivity, λ, value of 1.85 kcal/hmC^{o} and a thermal diffusivity, α, value of 0.0025 m^2/h. The underlying aggregate ballast layer is defined by a thermal conductivity, λ, value of 2.58 kcal/hmC^{o} and a thermal diffusivity, α, value of 0.0030 m^2/h. Predicted degree of saturation is defined by a diffusivity (at S = 100%) value of 1.29x10^{-6} m^2/hr, a regression coefficient, n, of 15, α value of 0.05, and an empirical correlation between relative humidity and degree of saturation. The simulation is initialized with an even distribution of 85 %RH throughout the depth of the concrete.

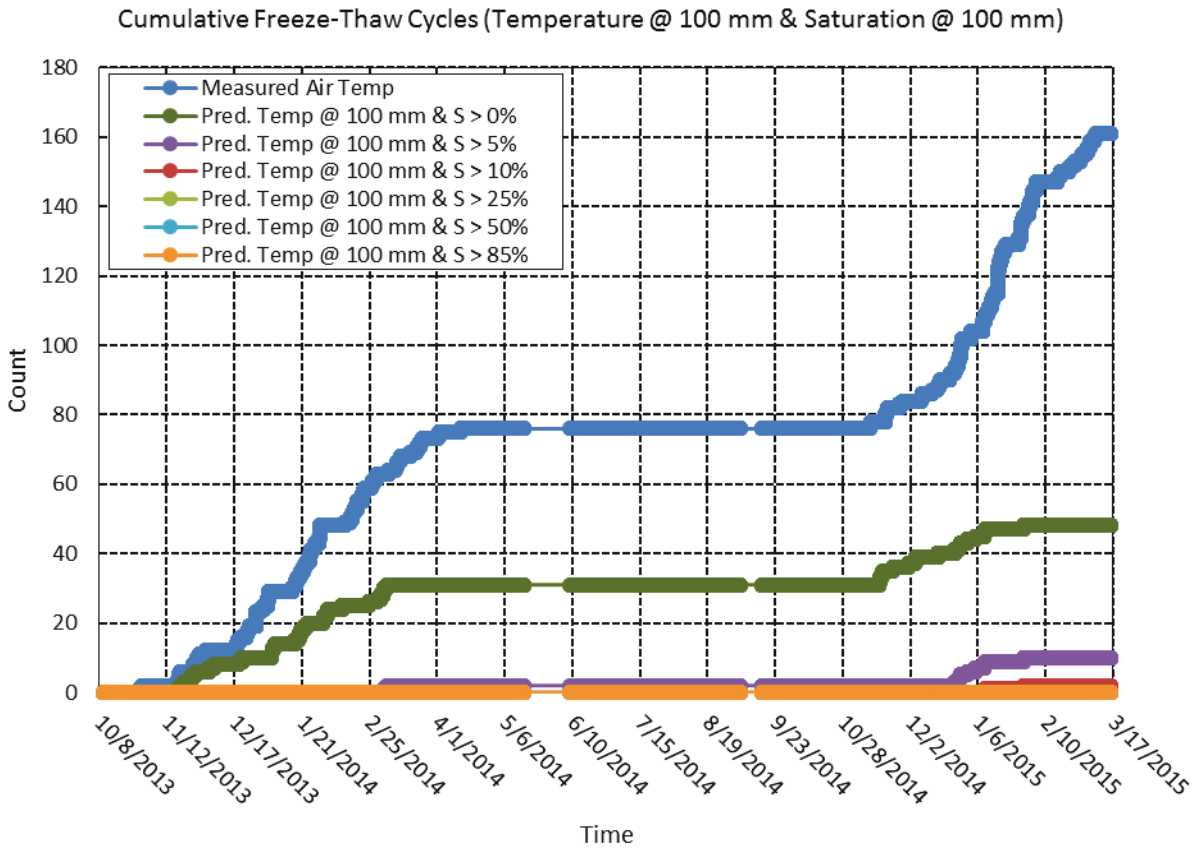

Figure C-96 Cumulative number of freeze-thaw cycles in Lytton, BC, from October 8, 2013, through March 17, 2015, at a depth of 100 mm when both freezing temperatures and minimum degree of saturation is achieved at time of freezing. Predicted internal temperature values are computed using a 2-layered system whose upper concrete layer is defined by a thermal conductivity, λ, value of 1.85 kcal/hmC^{o} and a thermal diffusivity, α, value of 0.0025 m^2/h. The underlying aggregate ballast layer is defined by a thermal conductivity, λ, value of 2.58 kcal/hmC^{o} and a thermal diffusivity, α, value of 0.0030 m^2/h. Predicted degree of saturation is defined by a diffusivity (at S = 100%) value of 1.29x10^{-6} m^2/hr, a regression coefficient, n, of 15, α value of 0.05, and an empirical correlation between relative humidity and degree of saturation. The simulation is initialized with an even distribution of 85 %RH throughout the depth of the concrete.

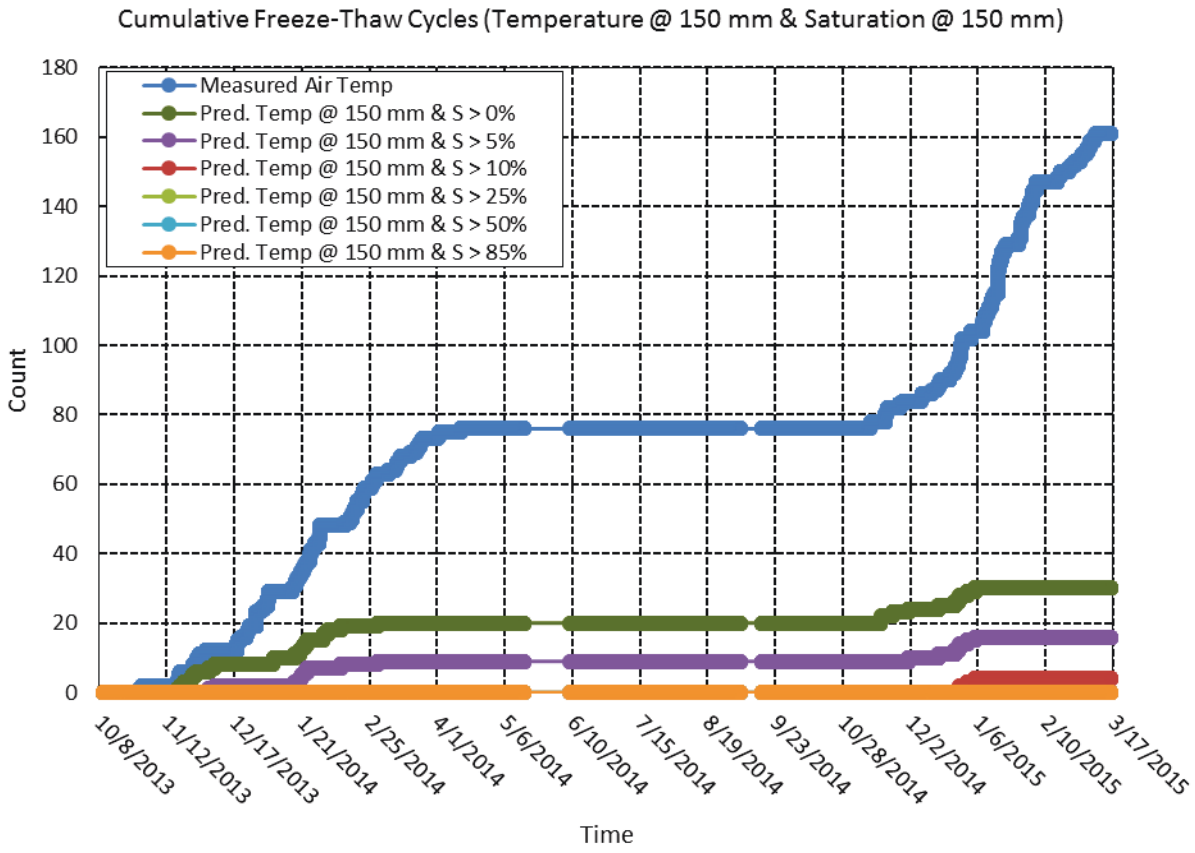

Figure C-97 Cumulative number of freeze-thaw cycles in Lytton, BC, from October 8, 2013, through March 17, 2015, at a depth of 150 mm when both freezing temperatures and minimum degree of saturation is achieved at time of freezing. Predicted internal temperature values are computed using a 2-layered system whose upper concrete layer is defined by a thermal conductivity, λ, value of 1.85 kcal/hmC^{o} and a thermal diffusivity, α, value of 0.0025 m^2/h. The underlying aggregate ballast layer is defined by a thermal conductivity, λ, value of 2.58 kcal/hmC^{o} and a thermal diffusivity, α, value of 0.0030 m^2/h. Predicted degree of saturation is defined by a diffusivity (at S = 100%) value of 1.29x10^{-6} m^2/hr, a regression coefficient, n, of 15, α value of 0.05, and an empirical correlation between relative humidity and degree of saturation. The simulation is initialized with an even distribution of 85 %RH throughout the depth of the concrete.

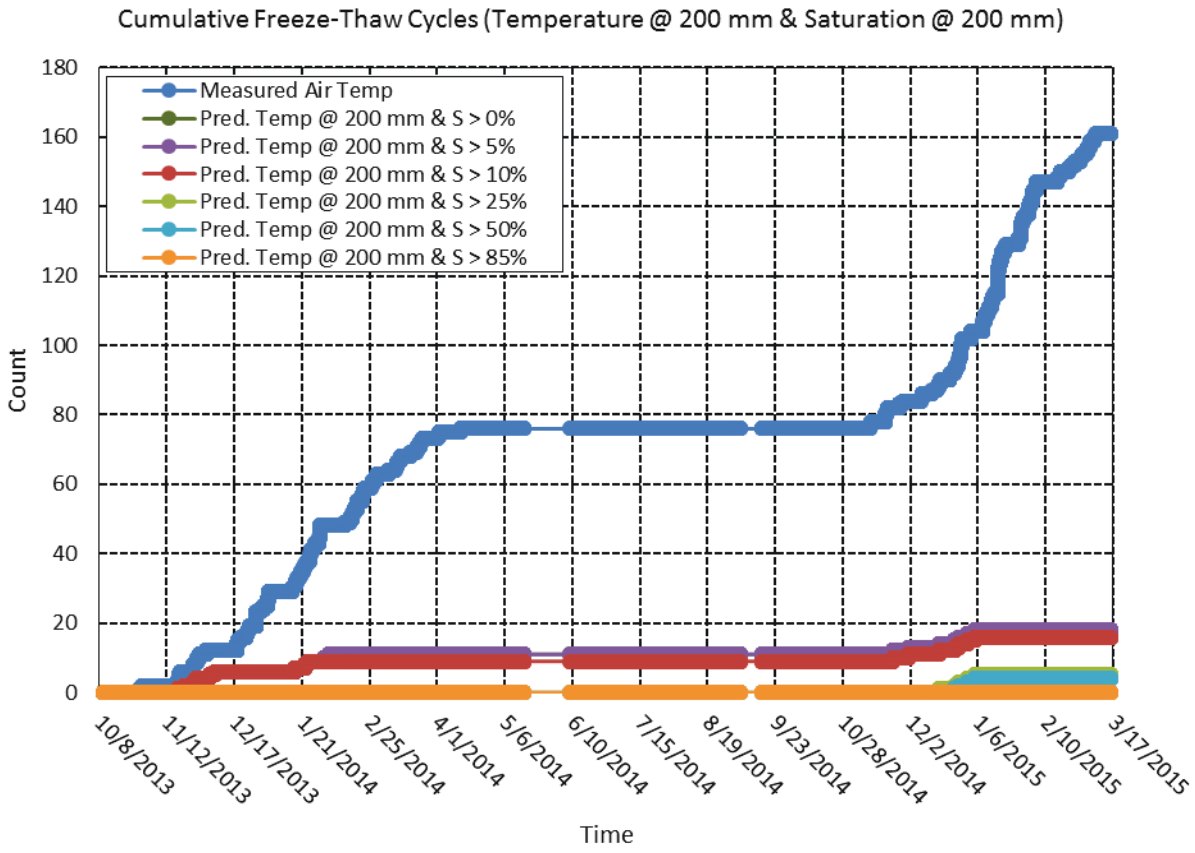

Figure C-98 Cumulative number of freeze-thaw cycles in Lytton, BC, from October 8, 2013, through March 17, 2015, at a depth of 200 mm when both freezing temperatures and minimum degree of saturation is achieved at time of freezing. Predicted internal temperature values are computed using a 2-layered system whose upper concrete layer is defined by a thermal conductivity, λ, value of 1.85 kcal/hmC^{o} and a thermal diffusivity, α, value of 0.0025 m^2/h. The underlying aggregate ballast layer is defined by a thermal conductivity, λ, value of 2.58 kcal/hmC^{o} and a thermal diffusivity, α, value of 0.0030 m^2/h. Predicted degree of saturation is defined by a diffusivity (at S = 100%) value of 1.29x10^{-6} m^2/hr, a regression coefficient, n, of 15, α value of 0.05, and an empirical correlation between relative humidity and degree of saturation. The simulation is initialized with an even distribution of 85 %RH throughout the depth of the concrete.

Abbreviations and Acronyms

ACI	American Concrete Institute
AEA	Air-Entraining Agent
ASTM	American Society for Testing and Materials
AV	After Vibration
BV	Before Vibration
CA	Coarse aggregate
CP	Cement paste
CSH	Calcium silicate hydrate
DF	Durability factor
FA	Fine aggregate
FFT	Fast Fourier Transform
F-T	Freeze-Thaw
HRWR	High-Range Water Reducer
ICAR	International Center for Aggregates Research
IDOT	Illinois Department of Transportation
IE	Impact Echo
ITZ	Interfacial Transition Zone
LRWR	Low-Range Water Reducer
MOR	Modulus of rupture
PVC	Polyvinyl chloride
RDME	Relative Dynamic Modulus of Elasticity
RF	Resonance Frequency
RH	Relative humidty
SAM	Super Air Meter
SCC	Self-Consolidating Concrete
SF	Spacing Factor
SSD	Saturated Surface Dry
UPRR	Union Pacific Railroad
UPV	Ultrasonic Pulse Velocity
VMA	Viscosity-Modifying Admixture
w/c	water-cement ratio
w/cm	Water-Cementitious Material Ratio
WR	Water Reducer